Metabolic Flux Analysis of *Streptomyces fradiae* C373-10

Christopher Michael Wells

Submitted for the degree of Doctor of Philosophy at the University of Strathclyde, Department of Biosciences, Royal College.

Supervisor Professor Iain Hunter

The research in this thesis is my own original work except where otherwise stated and has not been submitted for any other degree.

Christopher Michael Wells, 23 rd April 2004

This thesis is dedicated to my grandmother, Peggy Netherton, and my brother Tim Wells, the memory of whom gave me the courage and determination to finish.

Contents

Appendices (found in compendium CD)

List of Figures & Tables

Chapter 1: Comprehensive Models for Cellular Reactions: A review

Chapter 2: A review of Cellular Metabolism: Streptomycetes

ABBREVIATIONS

Below is a list of symbols most frequently used throughout this text (Zubay, 1998; Merck Index, 2002). The units specified is the most typically applied unit or abbreviation, in some cases the symbols may have another unit or abbreviation.

Metabolites & General abbreviations

aa/s	Amino acid/s
ABC	ATP binding cassette
5A4CRN	5-Aminoimidazole-4-carboxamide ribonucleotide
AcCoA	Acetyl-CoA
AcetylP	acetyl phosphate
ACP	Acyl carrier protein
AMM	Atom mapping matrix
AT	Acyl tranferase
ATC	Actinorhodin
OGA / AKG	Oxo-glutarate
ADP	Adenosine-5'-monophosphate
AQC	6-aminoquinolyl-N-hydroxysuccinimidyl carbamate
ALA	Alanine
AMP	Adenosine monophosphate
ARG	Arginine
ASN	Asparagine
ATP	Adenosine triphosphate
F_1F_0-ATPase	ATP synthase
BCA	Bicinchoninic acid
BRNE	Bioreaction network
BSA	Bovine serum albumin
BST	Biochemical systems theory
BT	Benzylthiocyanate
cAMP	Adenosine 3'-5' cyclic monophosphate

CIT	Citrate
CC/s	Control coefficient/s
CCC/s	Concentration control coefficient/s
CDC	Carbon dioxide concentration
CCR	Carbon catabolite repression
CFU	Colony forming units
CER	Carbon dioxide evolution rate
CHO/s	Carbohydrate/s
CHOR	Chorismate
CIT	Citrate
CMP	Cytidine monophosphate
CMPs	Central metabolic pathways
CN	Condition number
COSY	Correlation spectroscopy
CO2 / CO_2	Carbon dioxide
CoA	Coenzyme A
CR	Catabolite repression
CCR	Carbon catabolite repression
CRP	cAMP receptor protein
CYS	Cysteine
d	2'-deoxyribo-
dH_2O	Distilled water
tH_2O	Tap water
DH	Dehydrogenase
DHAP	Dihydroxyacetone phosphate
DNA	Deoxyribonucleic acid
DO	Dissolved oxygen
DOC	Deoxycholic acid
ds	Double stranded
DW / dry wt	Dry weight
2'3-DPG	2,3-diphosphoglycerate
Ea	Exhaust air
EC	Elasticity coefficients
EDTA	Ethylene diamine tetra-acetic acid
ER	Enoyl reductase
E4P	Erythrose-5-phosphate
F6P/fructose6P	Fructose-6-phosphate
FBA	Flux balance analysis
FCC	Flux control coefficient
EMP	Embden-Meyerhof pathway
FA / FAs	Fatty acid/s
FAD	Flavin adenine nucleotide (oxidised form)
FADH	Flavin adenine nucleotide (reduced form)
$FADH_2$	Flavin adenine nucleotide (reduced form)
Ferm	Fermentation
FMOC-Cl	9-fluorenylmethyl chloroformate
FRU	Fructose
Fru16dP/fructose6bisP	Fructose-1,6-bisphosphate
FTHF	Formyl tetrahydrofolate
F-1,6-P2	Fructose-1,6-bisphosphate

FUM	Fumarate
GABA	4-amino-butyrate
GAP/3PGlycerate	Glyceraldehyde-3-phosphate
G6P/glucose6P	Glucose6-phosphate
GBP	Glyoxylate bypass pathway
GC	Gas chromatography
GFP	Green fluorescent protein
G/G	Glucose glutamate defined medium
GLC	Glucose
GYLC	Glycerol
GLYOX	Glyoxylate
GLN	Glutamine
GLU	Glutamate
GLX	Glutamate + Glutamine
GMP	Guanosine monophosphate
G/O	Glucose oxo-glutarate defined medium
GTP	Guanine triphosphate
~H	Hydrogen/available hydrogen atoms
HGU	Hyphal growth unit
HIS	Histidine
HPLC	High performance liquid chromatography
Ia	Incoming air
IC	Inorganic carbon / ion chromatography
ICP	Inductively coupled plasma
ILE	Isoleucine
IMP	Inosine-5- monophosphate
INT	Iodonitrotetrazolium chloride
IPA	Propan-2-ol
ISOCIT	Isocitrate
ISE/s	Isoenzyme/s
KR	Ketoreductase
KS	Polyketide synthase
LAT	Lysine-6-amino transferase
LL-A_2PM	LL-diaminopimelic acid
LL-DAP	diaminopimelic acid
LEU	Leucine
LYS	Lysine
M	*Pseudo* element for metals
MAL	Malate
MCA	Metabolic control analysis
MCT	Metabolic control theory
MES	4-morphollineethltenesulphonic
MESH	2-hydroxy mercapto-β-mercaptoethanol
MET	Methionine
MFA	Metabolic flux analysis
MGU	Correlation between metabolic costs and synonymous codon usage
MIT	Massachusetts Institute of Technology
MS	Mass spectrometry
MTHF	Methylene tetrahydrofolate

MO	Methyl oleate
MOPS	3-[N-morpholino]propansulfonic acid
N	Nitrogen / normalisation factor
NA/s	Nucleic acid/s
NAD	Nicotinamide adenine dinucleotide (oxidised)
NADH	Nicotinamide adenine dinucleotide (reduced)
NADP	Nicotinamide adenine dinucleotide phosphate (oxidised)
NADPH	Nicotinamide adenine dinucleotide phosphate (reduced)
NAG	N-acetyl glucosamine
NAM	N-acetylmuramic acid
NDIR	Infra red gas analyser
NH3 / NH_3	Ammonium
NH4 / NH_4	Ammonia
NMR	Nuclear magnetic resonance
NVFA	Non volatile fatty acids
O	Oxygen
O2 / O_2	Oxygen (diatomic)
OAA	Oxaloacetate
OD	Extinction coefficient
OGA	Oxo-glutarate
OPA	o-phthalaldehyde
ORF	Open reading frame
OUR	Oxygen uptake rate
meso-DAP	*meso*-diaminopimelic acid
MMCT	Methylmalonyl-CoA carboxyltransferase
P / ~P	Phosphorus / phosphate high energy bond
PABAS	p-Aminobenzoic acid synthase
PCA	Perchloric acid
PEP/ Penolpyruvate	Phosphoenolpyruvate
PEP-PTS	Phosphoenolpyruvate phosphotransferase system
PG	Phosphoglycerate
2PG	2-Phosphoglycerate
3PG	3-Phosphoglycerate
PHE	Phenylalanine
Pi	Inorganic phosphate
PPi	Pyrophosphate
PITC	Phenylisothiocyanate
PL	Pentalenolactone
PolyPn	Polyphosphate
PP pathway/PPP	Pentose phosphate pathway
ppGpp	Guanosine-3-diphosphate 5’ diphosphate
pppGpp	Guanosine-3-diphosphate 5’ triphosphate
P/O	The ratio of the number of ATP's produced to the number of atmospheric oxygen atoms converted to water
6PGL	6-phosphoglucone-1,3-lactone
6PG	6-phosphogluconate
q	Specific production rate
PRO	Proline
PROT	Protein
PRPP	5-Phosphoribosyl-1-pyrophosphate

PSS	*Pseudo*-steady-state
PTS	Phosphotransferase system
PYR	Pyruvate
RC/s	Response coefficient/s
RED	Undecylprodigiosin
RNA	Ribonucleic acid
mRNA	Messenger ribonucleic acid
rRNA	Ribosomal ribonucleic acid
tRNA	Transfer ribonucleic acid
R5P	Ribose-5-phosphate
RQ	Respiratory quotient
Ru5P	Ribulose-5-phosphate
S	Sulphur
S7P	Seduheptulose-7-phosphate
SARP	Streptomyces antibiotic regulatory protein family
SC/s	Stoichiometric coefficient/s
SER	Serine
SP	Sample point
SUC	Succinate
SUCCOA	Succinyl-CoA
SWR	Standard working reagent
t_n	Specified normalised time
$t_{limitation}$	Specified limitation time period
$t_{normalised}$	Specified normalised time period
t_{actual}	Actual specified time
TA/s	Teichoic acid/s
TC	Total carbon
TCA	Tricarboxylic acid cycle
TH	Pyridine dinucleotide transhydrogenase
Th.In	Thermodynamic inefficiency
THR	Threonine
TMP	Thymidine monophosphate
TOC	Total organic carbon
TOCA	Total organic carbon analysis
TON	Total organic nitrogen
TONA	Total organic nitrogen analysis
TP/triose6P	Triose phosphate
Tris	Tris(hydroxymethyl)aminoethane
TrCA	Trichloroacetic acid
TRP	Tryptophan
TYR	Tyrosine
UMP	Uridine monophosphate
UTP	Uridine triphosphate
VAL	Valine
VFA	Volatile fatty acids
XC	Oxygen concentration
X5P	Xylulose-5-phosphate
Yo/x	Cell yield mmoles O_2 consumed per gram cell
wet wt	Wet weight
Y_x	Maximum production of NADPH

Y_{PPP}	The TCA cycles NADPH producing capacity
Y_{TCA}	The PP pathway NADPH producing capacity

Enzymes

ADH	Alanine dehydrogenase
AHAS	Acetohydroxy acid synthase
ASAT	Aspartate aminotransferase
CS	Citrate synthase
GAPDH	Glyceraldehyde-3-phosphate dehydrogenase
G6PDH	Glucose-6-phosphate dehydrogenase
6PGDH	6-phosphogluconate dehydrogenase
GK	Glycerol kinase
GlkA	Glucose kinase
GDH	Glutamate dehydrogenase
GOGAT	Glutamate synthase
GS	Glutamine synthetase
GOD	Glucose oxidase
FBA	Fructose-1,6-bisphospahte aldolase
FGD	F_{420} dependent glucose-6-phosphate dehydrogenase
HK	Hexokinase
IDH	Isocitrate dehydrogenase
ICL	Isocitrate lyase
LAT	Lysine-6-minotransferase
LDH	Lactate dehydrogenase
MDH	Malate dehydrogenase
ME/MDH(dc)	Malic enzyme / malate dehydrogenase decarboxylating
MMCT	Methylmalonyl-CoA carboxyltransferase
MS	Malate synthase
OGDH	Oxo-glutarate dehydrogenase
PC	Pyruvate carboxylase
PDC/PDH	Pyruvate dehydrogenase complex
PEC	Phosphoenolpyruvate carboxytransphosphorylase
PEPC	Phosphoenolpyruvate carboxylase
PEPCK	Phosphoenolpyruvate carboxykinase
PGM	phosphoglycerate mutase
PPDK	pyruvate orthophosphate dikinase
PFK	Phosphofructokinase
PK	Pyruvate kinase
PKS	Polyketide synthases
TDT	Threonine dehydratase
TA	Transaldolase
TK	Transketolase
VDH	Valine dehydrogenase

Gene annotation

*ace*A	Isocitrate lyase
*ace*B	Malate synthase A
*ace*E	Pyruvate dehydrogenase
ccr	Crotonyl-CoA reductase
crea	carbon catabolite repressor

eno	Enolase
fda	Fructose-bisphosphate aldolase
gap	Glyceraldehyde-3-phosphate dehydrogenase
glk	Glucose kinase
icl	Isocitrate lyase
*ilv*BN	acetohydroxy acid synthase
*mea*A	vitamin B_{12}–dependent mutase
*pcc*A	propionyl-CoA carboxylase
pfkA	6-phosphofructokinase
pgi	Glucosephosphate isomerase
pgk	Phosphoglycerate
pgm	Phosphoglucomutase
*pnc*B	Nicotinamidase
*pnc*A	Nicotinate phosphoribosyltransferase
*pnt*B	Pyridine nucleotide transhydrogenase
*ty*II	Cytochrome P450
*tyl*AI	NADP-glucose reductase
*tyl*AII	NADP-glucose-4,6-dehydratase
*tyl*B	3-aminotransferase
*tyl*CII	2,3-enoyl reductase
*tyl*CIII	3-C-methyl transferase
*tyl*CIV	4-ketoreductase
*tyl*CV	Mycarosyltransferase
*tyl*CVI	2,3-dehydratase
*tyl*CVII	5-(or 3,5-) epimerase
*tyl*D	4-keto reductase
*tyl*E	2”-O-methytransferase
*tyl*F	3”-O-methyltransferase
*tyl*GI	Polyketide synthase
*tyl*GII	Polyketide synthase
*tyl*GIII	Polyketide synthase
*tyl*GIV	Polyketide synthase
*tyl*GV	Polyketide synthase
*tyl*HI	Cytochrome P450
*tyl*HII	Tylodoxin
*tyl*J	Epimerase
*tyl*MI	3-N-methyl transferase
*tyl*MII	Mycaminosyltransferase
*tyl*MIII	3,4-isomerase
*tyl*N	Deoxyallosyltransferase
*trp*C	N-(5-phosphoribosyl)anthranilate isomerase
*trp*D	glutamine amidotransferase-phosphoribosyl anthranilate transferase
*trp*BA	tryptophan synthase
*trp*EG	anthranilate synthase

Units of measurement (SI units)

^{o} C	Temperature/ celsius
sec	Second
min	Minutes

hr / hrs	Hours
t / T	Temperature (^{o} C)
KJ	Kilojoule
g	gramme / gravimetric force (g = 10^{-3} kg)
mg	Milligramme (mg = 10^{-3} g = 10^{-6} kg)
µg	Microgramme (µg = 10^{-6} g = 10^{-9} kg)
ng	Nanogramme
l / L	Litre (l = dm^3 = 10^{-3} m^3)
ml	Millilitre (ml = cm^3 = 10^{-6} m^3)
µl	Microlitre (µl = 10^{-3} cm^3)
cm	Centimetre (cm = 10^{-2} m)
nm	Nanometre (nm = 10^{-9} m)
M	mole (mol.l^{-1} = mol dm^{-3})
mM	Millimole
µM	Micromole
FW	Formula weight
Mb	Million base pairs
MW	Molecular weight
N	Normality / Normalisation factor
Pa	Pascal
PI	pH is termed the isoelectric point or pI
PSI	Pound per square inch
ppm	Parts per million (ppm = µg.g^{-1} = 10^{-6} g.g^{-1})
%	Percentage
STDEV/s	Standard deviation/s

Symbols

A	Matrix containing coefficient for the ith substrate in the jth reaction.
B	Matrix containing the stoichiometric coefficients for the metabolic products.
c	Concentration (mmole.l^{-1})
c_i	Concentration of the ith compound (mmole.l^{-1})
C^{ji}_i	Flux control coefficient for the ith enzyme on the jth steady state flux J_j
$*C^{ji}_i$	Group flux control coefficient for the ith enzyme on the jth metabolite concentration.
C^J	Matrix containing flux control coefficients.
C^X	Matrix containing concentration control coefficients.
exp(x)	exponential of x.
E_i	Activity (or concentration) of the ith enzyme.
E	Elemental composition matrix or matrix containing elasticity coefficients.
E_c	Elemental composition matrix for non-measured compounds.
E_m	Elemental composition matrix for measured compounds.
F	Degree of freedom
g_{ij}	Stoichiometric coefficient for the ith intracellular metabolite in the jth reaction.
G	Gibbs function (kJ $mole^{-1}$)
ΔG	Gibbs free energy change (kJ $mole^{-1}$)
ΔG^o	Gibbs free energy change with all reactants and products at their standard states (kJ $mole^{-1}$).
G	Matrix containing the stoichiometric coefficients for intracellular metabolites.
G_c	Matrix containing the stoichiometric coefficients for intracellular metabolites in reactions for which fluxes are not measured.

G_m	Matrix containing the stoichiometric coefficients for intracellular metabolites in reactions for which fluxes are measured.
G_{ex}	Stoichiometric matrix for a metabolic model containing the stoichiometry for all reactions both in a forward and in a reverse direction.
J_i	Steady state flux through the ith pathway branch (mmoles (g.dry wt.h)$^{-1}$).
J	Vector of steady state fluxes (mmoles (g. dry wt.h)$^{-1}$).
J_{dep}	Vector of dependent fluxes (mmoles (g. dry wt.h)$^{-1}$).
J_{in}	Vector of independent fluxes (mmoles (g. dry wt.h)$^{-1}$).
K	The number of intracellular metabolites considered in the analysis.
k_{cat}	Enzyme turn over number / catalytic constant
K_m	Michaelis-Menten constant (or saturation constant) (mmole.l^{-1}).
IU	The specific activity of the relevant enzyme.
ln x	natural logarithm of x.
log x	common logarithm of x.
M	The number of metabolic products considered in the analysis.
nkat	One katal (kat) is the amount of enzyme that converts one mole of substrate per second.
N	The number of substrates considered in the analysis.
P	Cuvette protein concentration in mg protein.ml^{-1}.
r	Specific rate (mmoles (g. dry wt.h)$^{-1}$).
$r_{macro,i}$	Specific rate of formation of the ith macromolecular pool (mmoles (g.dry wt.h)$^{-1}$).
$r_{met,I}$	Specific rate of formation of the ith intracellular metabolite pool (mmoles (g. dry wt.h)$^{-1}$).
r_p	Specific product formation rate (mmoles (g. dry wt.h)$^{-1}$).
r_s	Specific substrate uptake rate (mmoles (g. dry wt.h)$^{-1}$).
r_c	Vector of non-measured specific rates (mmoles (g. dry wt.h)$^{-1}$).
r_m	Vector of measured specific rates (mmoles (g. dry wt.h)$^{-1}$).
r_{macro}	Vector containing the specific rates of macromolecular formation (mmoles (g. dry wt.h)$^{-1}$).
r_{met}	Vector containing the specific rates of intracellular metabolite formation (mmoles (g. dry wt.h)$^{-1}$).
r_p	Vector containing the specific rates of metabolic product formation (mmoles (g. dry wt.h)$^{-1}$).
r_s	Vector containing the specific rates of substrate uptake (mmoles (g. dry wt .h)$^{-1}$).
R^{Ji}_{Xi}	Response coefficient.
s	Standard deviation.
S_i	The ith substrate.
T	Matrix containing stoichiometric coefficients.
v_j	Specific rate of the jth relation (mmoles (g. dry wt.h)$^{-1}$).
*v	Overall specific rate (or activity) of the ith reaction group (mmoles (g. dry wt.h)$^{-1}$).
v_{max}	Maximum specific rate of an enzyme catalysed reaction (mmole.h^{-1}).
v	Vector of reaction rates [or intracellular steady state fluxes] (mmoles (g. dry wt.h)$^{-1}$).
v_c	Vector of non-measured reaction rates (mmoles (g. dry wt.h)$^{-1}$).
v_m	Vector of measured reaction rates (mmoles (g. dry wt.h)$^{-1}$).
x	Biomass concentration (g.l^{-1}).
$X_{macro,i}$	Concentration of the ith macromolecular pool (g (g. dry wt)$^{-1}$).
$X_{met,i}$	Concentration of ith intracellular metabolite.

Greek Letters

α_{ji}	Stoichiometric coefficient for the ith substrate in the jth reaction.
β_{ji}	Stoichiometric coefficient for the ith metabolic product in the jth reaction.
ε^{i}_{xj}	Elasticity coefficient.
ε	The number of absorbance units that are equivalent to 1 μmole NADH in a 1 ml cuvette with a 1 cm path length.
γ_{ji}	Stoichiometric coefficient for the ith macromolecular pool in the jth reaction.
Γ	Matrix containing the stoichiometric coefficients for the macromolecular pools.
μ/s	Specific growth rate (h^{-1}).
γ	Degree of reduction.
ϕ	Degree of dispersion.
$\| \|$	Indicates any matrix norm

Abstract

Metabolic flux analysis of *Streptomyces fradiae*

The main aim of this project was to prepare a material balance of a *Streptomyces fradiae* fermentation using metabolic flux analysis (MFA). MFA is a theoretical methodology used to determine fluxes through metabolic pathways, in terms of specific rates of reactions through a stoichiometric model of cellular reactions, using mass balances for the intracellular metabolites. Two approaches have generally been used; (1) the monomeric composition (amino acids, lipids, carbohydrates, RNA & DNA) and extracellular measurements of the cell are used to build a simple arithmetic model of cellular metabolism, (2) differential equations are used to model metabolism from extracellular metabolites only.

It was necessary to develop an adequate defined medium, to acquire all of the compositional data. A number of different medium formulations were tested for their ability to produce tylosin. That have been previously used to produce tylosin, tetracycline, actinorhodin and physostigmine. The only media that significantly produced tylosin were ones that were cultured with a rich fatty acid source or complex polysaccharides. When betaine was an addition to the medium there was a considerable increase in biomass yield and the degree of dispersion. No significant improvement in tylosin yields was obtained, with the medium optimisation strategy used in this work.

The biomass composition of *S. fradiae* grown in batch culture under nitrogen limitation was analysed for its elemental and for its molecular composition. Both descriptions

initially resulted in conflicting results concerning the elemental composition, molecular weight, and degrees of reduction. Repeated measurements and critical analysis of the sample handling and analysis did not provide a satisfactory explanation for the difference. The difference in carbon, nitrogen, sulphur and phosphorus would indicate a considerable proportion of the biomass was not accounted for, possibly cell wall material. Phosphorus was likely to be accounted for as teichoic acid.

The average relative amounts and order of requirement of several of the amino acids was very similar compared to the expected order of requirement calculated from genomic codon usage tables. By contrast the costs of amino acid biosynthesis vs. codon usage showed a preference for low cost amino acids with the exception of arginine. The sequence of the order of requirement for the amino acid families for *S. fradiae* and *E. coli* showed no differences. It may be the case to reduce metabolic disruption codon bias does not necessitate a change in the order of requirement of amino acid families. The amino acid composition of the industrial complex medium and whole biomass showed a similar trend in composition.

Difficulties arose in constructing a MFA model due to the poor knowledge of primary metabolic pathways in streptomycetes. An initial sensitivity analysis would indicate that the biomass composition is relatively unimportant to a flux analysis, but accounting for the considerable number of isoenzymes in streptomycete metabolism has a considerable effect on fluxes. The main recommendation of this work is the need to use continuous culture to obtain increasingly more accurate metabolite profiling, elemental and macromolecular analysis to further increase the accuracy of flux-based strategies.

Acknowledgements

'And it is also said,' answered Frodo: '*Go not to the Elves for counsel, for they will say both no and Yes*.'
'Is it indeed?' laughed Gildor. '*Elves seldom give unguarded advice, for advice is a dangerous gift, even from the wise to the wise, and all courses may run ill.*'

-JRR Tolkein, 1954-The lord of the rings-The fellowship of the ring

This thesis is the culmination of three years of research, and as such, many people have contributed to it. Some have directly assisted and are easily acknowledged, while many others have contributed in more subtle ways to the development of new ideas or the maintenance of my sanity. Although it is not possible to acknowledge everyone, to whom I am indebted, I will attempt to scratch the surface.

First of all, I would like to express my gratitude to Professor Iain Hunter, my supervisor, for allowing me the freedom, with a dash of guidance, to formulate my own research objectives and approaches. Although such freedom can often extend ones tenure, and send one off in a tangent to the ultimate objective; it is an experience, I feel, that will prove invaluable in the future. Appreciation also goes to Dr Neil Rowan for the use of his fermentation equipment, and to Mrs. Vera Gill for her invaluable advice and expertise in operating this equipment. To Dr David Mousdale & Dr Jill Melville for the use of all the facilities in the Bioflux Ltd (Beocarta) laboratories. My thanks also go to Dr James McIntyre and everyone at Eli Lilly Ltd Speke, without whose help, academic discussions and expertise this project would not have been possible; and for making a six month stay at their facility most enjoyable.

If it were not for my parents and grandparents, I may never have returned to education and achieved so much. To them I can only say, “so you think it’s easy…”.

This work was supported by funding from the BBSRC, a case studentship with supplementary funding from Eli Lilly LTD and the University of Strathclyde Glasgow.

Project Aims

In order to obtain high yields of antibiotics, the flow of carbon through the primary metabolic pathways (i.e., glycolysis, the TCA cycle, pentose phosphate pathway, etc) must be radically redirected from the pathways that normally support balanced growth, towards pathways that support antibiotic synthesis. Such metabolic flux alterations directly oppose the enzyme level control mechanisms that are responsible for maintaining flux distributions optimal for growth. This enzyme resistance is referred to, as metabolic or network rigidity, which must be removed in order to attain improvements in product yield. Although modifications of the primary metabolism can be achieved through molecular biology, the choice of enzymes to be amplified or attenuated to mitigate network rigidity remains uncertain, and yield enhancements via metabolic modifications are largely pursued by trial and error. Hence, there is a clear need to develop a robust technique to identify limitations in the primary metabolism.

To this end, Metabolic Flux Analysis (MFA) has been used to map the flow of carbon through primary metabolic pathways of *Streptomyces fradiae* C373-10 during batch cultures grown on a number of different carbon sources. MFA has been researched synergistically by a number of researchers, who have employed vastly different mathematical styles. Metabolic flux analysis (MFA) is a theoretical methodology used to determine fluxes through metabolic pathways, in terms of specific rates of reactions through a stoichiometric model of cellular reactions, using mass balances for the intracellular metabolites. Two approaches have generally been used; (1) the monomeric composition (amino acids, lipids, carbohydrates, RNA & DNA) and extracellular

measurements of the cell are used to build a simple arithmetic model of cellular metabolism, (2) differential equations are used to model metabolism from extracellular metabolites only. In essence they are trying to achieve the same objectives. The alternative approach of Harry Holms (1986) has been adopted by this laboratory in the past. It offers a logical place to start, building compositional tables that need to be constructed to undertake any form of flux analysis.

The main aim of this project was to prepare such a theoretical material balance of *Streptomyces fradiae* fermentations in batch culture. It would be of interest to see which of the approaches could be best applied to a *Streptomyces* fermentations, in the same way as MFA has been applied, to well defined bacteria such as *E. coli* (Holms, 1986, 1991, 1996, 1997, 2001; Aristidou *et al*., 1998; Varma *et al.*, 1993a, 1993b, Varma & Palsson, 1994a, 1994b, 1995; Van Gulik & Heijnen, 1995; Pramanik & Keasling, 1997; Yang, 1999; Yang *et al.*, 1999a, b) & *Corynebacterium glutamicum* (Vallino & Stephanopoulos, 1993, 1994a, b). It was therefore necessary to develop an adequate defined medium, to acquire all of the data for *S. fradiae* biomass required to calculate these fluxes. Additional information that was needed to achieve this objective is listed below.

(1) A number of different medium compositions were tested for their suitability, optimised, and stepped up to bench top fermentation. To undertake a flux analysis, the main requirements are simple nitrogen and carbon sources that produce, reasonable antibiotic yields (Chapter 4).
(2) Determine the macromolecular composition of *S. fradiae* C373-10 & *S. coelicolor* 1147 during exponential growth phase.
(3) Investigate methods for the fractionation of biomass into its macromolecular and monomeric contents. Previous workers have shown considerable analytical error and reproducibility of standard assay techniques to collect bacterial compositional data. The intension was to reduce the inconsistencies in calculating compositional data by applying a number of analytical protocols and reconciling the data (see Chapter 8, discussion).
(4) Determine the elemental composition of *S. fradiae* C373-10. Although this was not required for calculation of the fluxes, it would give an overall view of the composition of the biomass.

(5) Investigate the differences between the elemental, monomeric, and macromolecular content of the biomass; inaccuracies of 20 % or more are commonly accepted in the literature. Since the molecular composition should directly define the elemental composition further investigation is needed. One theory is that metabolites such as shunt metabolites or cell wall material are not adequately accounted for.

(6) The monomeric composition of *S. coelicolor* 1147, *S. fradiae* C373-10, and *E. coli* ML308 will be converted to compositional tables as Holms (1986)[see Chapter 6 and Appendix B]. Where appropriate the monomeric composition will be used to determine the (monomeric) composition of *S. fradiae* & *S. coelicolor*. In addition macromolecular data will be used where monomeric data analysis was not feasible, i.e., monomer content for DNA may be obtained from the macromolecular content; for example, approximately 70 % of *Streptomyces* DNA is comprised of guanine and cytosine bases (Pridham & Tresner, 1974). The DNA content may be expressed in terms of its bases. However, not all monomer amounts can be calculated from the macromolecular composition. For example, for the monomeric content of amino acids; high pressure liquid chromatography (HPLC) was undertaken.

(7) Investigate the amino acid composition of *S. fradiae* C373-10 & *S. coelicolor* 1147; it will be of interest to see, how the amino acid contents of these streptomycetes differ due to the consequences of codon bias.

(8) Collect the following information throughout the fermentations. specific rates of substrate uptake, specific growth rate, specific oxygen uptake and specific carbon dioxide evolution.

(9) Identify and quantify the excretion rates of organic acids of *S. fradiae* C373-10 & *S. coelicolor* 1147 under different growth conditions.

(10) Identify and quantify secondary metabolites excreted by *S. fradiae* C373-10 through out the fermentation, to allow for the determination of fluxes to these metabolites.

(11) Determine the throughputs and fluxes through the central metabolic pathways of *S. fradiae* C373-10 & *S. coelicolor* 1147 to biomass. The throughputs would be calculated from the monomeric compositional data using the Holms (1986) approach. Assumptions were made, that central metabolic pathways were similar to *E. coli*, when there was no literature available to prove otherwise.

(12) Compare the fluxes through the central metabolic pathways of *S. fradiae* C373-10 & *S. coelicolor* 1147 to biomass and to antibiotic production. Although the magnitude of

fluxes in batch culture will be significantly different even between similar cultures. It should be possible to compare the ratio of flux to biosynthesis, to identify alterations in fluxes with the view of highlighting possible sites of regulation.

(13) To investigate and develop on existing matrix algebra flux based techniques to the analysis of the fluxes through the central metabolic pathways of *S. fradiae* C373-10 & *S. coelicolor* 1147. The ultimate goal being to compare the strategies for flux analysis and undertake a further investigation in sensitivity analysis. With the main emphasis on defining how differences in compositional data and isoenzymes may affect the overall partitioning of flux.

The above research has been undertaken; to investigate whether observations on specific rates of substrate uptake, the fate of individual medium components, specific growth rate, antibiotic production, shunt metabolites, oxygen uptake and carbon dioxide evolution could identify the enzymes or metabolic pathways most responsible for the overall reaction rate. This could result in the identification of areas concerned with regulation of these fluxes. Identification of such areas by flux determination would provide a foundation upon which further physiological and genetic studies could be based, thus contributing to a further understanding of the switch from primary to secondary metabolism in *Streptomyces*.

Thesis Organisation

Chapter 1, is a theoretical review of kinetic based techniques, material balancing techniques, and tracer studies employed for metabolic flux estimation and analysis; Appendices A - C offer practical examples of these techniques, to give templates for the applications. Although most of these techniques presented in these sections were not employed in this study, they represent alternative methods; hence, the review provides the background by which the techniques employed in Chapter's 6 & 7 may be gauged. Chapter 2 undertakes an extensive literature review of *Streptomyces* biochemistry, taking into account primary and secondary metabolism, & early microbial physiological studies. This review was considered essential in undertaking any flux analysis of a relatively ill-defined bacterial system; such as a *Streptomyces*. In Chapter 3, lists the analytical techniques used and developed to undertake this research. Chapter 4 gives an introductory review of media used to date to produce tylosin and undertake physiological growth studies to date; and suitable minimal and defined media for this study were developed, from a base medium used for tylosin production in continuous culture by Eli Lilly Ltd, and optimised at shake flask level (All Tables can be found in the companion CD; Appendices O Chapter 4). Further work entailed basic growth studies undertaken in bench top fermenters [All fermentation numbers relate to the same cultures throughout Chapter 4, 5, 6 & 7; *S. fradiae* C373-10 cultures for glucose (Ferm 1 & 2); fructose (Ferm 1); glycerol (Ferm 1 & 2); oxo-glutarate (Ferm 1); glucose glutamate (Ferm 1 - 4); glucose oxo-glutarate (Ferm 1 & 2); methyl oleate medium (Ferm 1 - 3); Industrial complex (Ferm 1 & 2); *S. coelicolor* cultures

for glucose (Ferm 1 & 2)], to determine the suitability of the latter media for flux based analysis. In Chapter 5 (All Tables can be found in the companion CD; Appendices O Chapter 5), the biomass composition of *Streptomyces fradiae* C373-10 grown in batch culture under different carbon sources was analysed for its elemental and its molecular composition utilising a number of analytical & statistical techniques to reduce errors in the construction of monomeric compositional tables. In Chapter 6, Flux based diagrams were constructed to identify branch point restrictions and rigidity in the primary pathways of *S. fradiae* (All summary Tables can be found in the companion CD; Appendices O Chapter 6). The compendium (companion CD; Appendices P - U) contains the detailed workings for this approach which were summarised in Chapter 6 and the Appendices. In Chapter 7, matrix algebra approaches and sensitivity issues were investigated (All Tables can be found in the companion CD; Appendices O Chapter 7). In Chapter 8, the discussion and conclusion; discusses points that arose from the direction taken to achieve this project (All Tables can be found in the companion CD; Appendices O Chapter 8).

Chapter 1

Comprehensive Models For Cellular Reactions: A Review

1.0 Introduction

There are two general techniques employed to estimate flux distributions in metabolic networks. The first technique relies on kinetic expressions to represent the enzymatic reactions that comprise the metabolic pathways. These expressions, coupled with reaction stoichiometry, are used to construct a kinetic-based model of cellular metabolism, which can be solved numerically for the flux distributions (Fell, 1997; Stephanopoulos *et al*., 1998). The advantage of a kinetic-based description of metabolism is that it can be analysed for control architecture, as well as rate limiting reactions. Such analysis techniques are reviewed in section 1.3. The obvious disadvantage to the kinetic-based approach is that detailed kinetic expressions for enzymatic reactions are often unavailable. Furthermore, the analysis of large kinetic models can tax numerical techniques and are usually unsolvable by current analytical techniques. To circumvent such constraints, mass balance techniques can be employed (which are reviewed in section 1.2) to attempt to simplify the kinetic models so that the overall dynamics of metabolism can be analysed (Vallino & Stephanopoulos, 1990; Stephanopoulos & Vallino, 1991; Stephanopoulos *et al*., 1998; Stephanopoulos, 1999; Holms, 1986, 1991, 1996, 1997, 2001). These techniques only require knowledge of the biochemistry; however, they cannot be used to predict metabolic responses to enzymatic perturbations. Although not all of the techniques discussed in the following Chapter are employed in this thesis, they represent alternative methodologies for network analysis to that employed in this thesis.

1.1 The steady state

One of the characteristic features of living organisms is their ability to maintain a relatively constant composition whilst continually taking in nutrients from the environment and returning excretory products. The organism can only maintain their internal state constant by this flux of matter and energy through the metabolic pathways of the cell. This is termed dynamic equilibrium (Fell, 1997).

The concept of a steady state corresponds to a perfect dynamic equilibrium; suppose that a metabolic pathway starts with a source of material that is derived at constant concentration from the environment and finishes with an end product (Fell, 1997) the sink (intracellular metabolites), between the source and the product kept at constant concentration, by direct or indirect excretion into the environment. In most cases this will lead to the development of a steady-state, where the concentration of the intermediates remain constant because their rates of formation have come to be in exact balance with their rates of degradation (Fell, 1997). This also requires that the flow through the pathway remains constant.

It is not inconceivable that any sequence of successive enzymatic reactions will always be able to reach steady state in these circumstances, but the consequences of not reaching a steady state would be that one or more intermediate metabolites would continue to accumulate in ever increasing amounts. Such an increase would start to give; a cell severe osmotic problems, and would be at odds with the general impression of dynamic equilibrium (Fell, 1997).

It must be recognised that an exact steady state is a mathematical abstraction. One reason for this is that as a pathway becomes closer and closer to a steady state, its rate of approach becomes ever slower, so that in theory it will only arrive there after an infinite amount of time. In practice this does not matter, because the limited accuracy of methods of biochemical measurement mean that a system that is more than 95 % of the way to steady state is virtually indistinguishable from the steady state itself.

The primary inputs required for the determination of intracellular fluxes, as discussed in the following section (1.2), are fluxes of extracellular metabolites, namely, rates of substrate uptake and rates of product secretion. These rates can best be obtained from steady state chemostat experiments, in which concentrations of all metabolites are measured at steady state. The corresponding rates of specific secretion/uptake can then be calculated by multiplying these concentrations by the chemostat dilution rate. Because chemostat experiments are very long in duration, often batch experiments are employed for the determination of fluxes. Batch cultivation of microorganisms can generate large amounts of data in a relatively short period of time; however, the determination of extracellular metabolite rates is significantly more involved as it requires calculation of the derivative of the corresponding concentrations with respect to time, an operation that

usually introduces large errors. Furthermore the identification of fermentation period that has achieved a *pseudo*-steady-state [PSS](*pseudo* Latin for False), can complicate the interpretation of the experimental data (Goel *et al*. (1993); for experimental evidence of the difficulties of using batch culture against continuous culture).

1.2 Metabolic flux analysis (MFA)

The use of elemental mass balance constraints on the growth of a micro-organism became popular in estimation and control of processes after it was observed that the elemental composition of the biomass remains relatively constant during growth (Minkevich & Eroshin, 1973). This permits one to construct a general equation of stoichiometric growth, for carbon & nitrogen source utilisation and production of biomass, such as

$$\underset{\text{Carbon source}}{C_wH_xO_yN_z} + aO_2 + bNH_3 \rightarrow \underset{\text{Biomass}}{cCH_\alpha O_\beta N_\delta} + dCO_2 + eH_2O + \underset{\text{Product}}{fC_jH_kO_lN_m}$$

In this equation (as presented by Doran, 1997) the only unknowns are the seven (*a* - *f*) stoichiometric coefficients (SCs), since four elemental balance equations can be constructed around carbon, hydrogen, nitrogen, and oxygen. Consequently, if production or consumption rates of three compounds, such as glucose, O_2, and CO_2, are measured, then the production or consumption rates of the remaining four compounds can be estimated (see Case study 1; Appendix A for a worked example). The classic example of such stoichiometric based control is that for the production of Yeast (Cooney *et al*., 1977, 1979; Wang *et al*., 1979)[Darlington, 1964; Johnson, 1964; Righelato *et al*., 1968; Mateles, 1971 for further examples of use of stoichiometric equations], where it was demonstrated that controlling the respiratory quotient at 1.04 would minimise ethanol synthesis and thereby maximise biomass production (Roubos *et al*. (2001) and Bushell & Fryday (1983) applied this technique to *S. cattleya* and *S. clavuligerus*). Around the same period it was demonstrated that the elemental balance constraints could be used to estimate flux distributions in the TCA cycle during citric acid production by *Aspergillus niger* and *Candida lipolytica* (Verhoff & Spradlin, 1976; Guebel & Torres Darias, 2001; Aiba and Matsuoka, 1979)[see Case study 3; Appendix C for a worked example]; a number of reviews led to the development of this technique (Holms, 1986; Bailey, 1991; Stephanopoulos & Vallino, 1991).

Flux-based Analysis can be broken into two basic concepts metabolic flux analysis (MFA) and flux balance analysis (FBA). MFA characterises the flux distribution in more experimental detail, estimating internal fluxes based on a combination of analytical techniques and mathematical analysis (Christensen & Nielsen, 2000). Where FBA examines the metabolic network from a performance perspective, using matrix algebra to determine optimal cellular behaviour, under changing environments and genetic condition. It is simply a computer representation of cellular constraints (Edwards *et al*., 1999).

MFA is a sophisticated mathematical methodology that provides a way of determining steady state fluxes in a metabolic network, just by measuring some external (and independent) key fluxes (Vallino & Stephanopoulos, 1990; Stephanopoulos & Vallino, 1991; Nielsen & Villadsen, 1994; Stephanopoulos *et al*., 1998; Varma & Palsson, 1994a,b; Stephanopoulos, 1999 for in depth reviews of this technique)[see Case study 3; Appendix C for a worked example]. Or a more straightforward arithmetical method can be applied (Holms, 1986, 1991, 1996, 1997, 2001) (see Case Study 2; Appendix B for a worked example). These key fluxes can be steady state uptake rates of substrates, e.g. glucose, ammonia and oxygen, and formation rates of various products, e.g. carbon dioxide (CO_2) and product (e.g., penicillin), but also fluxes representing growth, e.g. the formation rates of macromolecular components like proteins, carbohydrates, lipids, DNA and RNA. The quantification of metabolic fluxes is very important when studying microbial physiology, especially when the aim is to redirect as much substrate as possible into a desired metabolic product (Vallino and Stephanopoulos, 1993). By determination of the metabolic flux distribution in a metabolic network, it is possible to identify rigid and flexible nodes (branch points) in the biochemical pathways (Stephanopoulos & Vallino, 1991). A node is classified as being flexible when the participating enzymes show similar affinities for the node substrate, and where the flux partitioning into each branch readily changes to meet the metabolic demands. A node is classified as being rigid if the flux split-ratio (carbon flux channeled through that branch, normalised by the flux into the node) is tightly regulated. The identification of rigid and flexible nodes by MFA gives helpful information when one is trying to increase the carbon flow through a specific pathway (Vallino and Stephanopoulos, 1993; Bailey, 1991; for more up to date reviews see Stephanopoulos *et al.,* 1998; Yang *et al.,* 1998).

There are basically three different measurement techniques that can be used to estimate metabolic flux distributions in metabolic pathways: 1) tracer based techniques in which elements of a substrate are labelled with a stable or radioactive isotope; 2) nuclear magnetic resonance (NMR) techniques in which magnetised nuclei serve as the label; and 3) metabolite balance techniques in which the consumption and accumulation rates of substrates, monomers and products are used to estimate the metabolic flux distributions. Metabolite balances and tracers are indirect techniques in the sense that a flux supported by a particular enzyme is not actually measured.

1.2.1 Metabolic flux analysis: the approach

As can be seen from case study 2 & 3 (Appendices B & C), there are considerably different mathematical techniques to undertake flux analysis. The approach used by Holms (1986, 1991, 1996, 1997, 2001) is more simplistic in nature, compared to the rigid structural architecture of the matrix algebra. Realistically this is a good base to start any flux analysis, as the compositional tables that are required are a necessity to build up better metabolic modelling architectures such as Metabolic Control Analysis [see Section 1.3 & El Mansi & Stephanopoulos, 1999; for worked example] and matrix algebra flux-based techniques. The approach requires considerable analytical analysis (see Case study 2 Appendix B). Although Holms (1986) strategy is not versatile enough to undertake network sensitivity analysis, e.g., condition, & redundancy analysis (discussed by Stephanopoulos and Vallino, 1991; Stephanopoulos *et al*., 1998; see Appendix N; sensitivity analysis).

The matrix annotation approach [Aiba & Matsuoka (1979); Case study 3; Appendix C] offers a flux-based approach that can incorporate further data such as micro-array technology; leading to the ultimate goal of flux analysis *in silico*. When genome sequences, and regulatory (Covert *et al*, 2001; Varner & Ramkrishna, 1999; Schuster *et al*., 1999; Edwards & Palsson, 2000a,b; Schilling *et al*., 1999a,b, 2001 for articles that advocate the use of these techniques in conjunction with proteome modelling, micro-array analysis and genomic research) information becomes readily available, computational approaches such as flux analysis could be used to decipher the information (i.e., Edwards & Palsson, 2000 a,b; where MFA and *in silico* (FBA) analysis has been applied to *E. coli*

K12, where the metabolic capabilities have been analysed through various gene deletions).

1.2.2 Metabolic Flux Analysis: the theory

From an intense literature search it can be ascertained that, with the exception of one group, in almost all cases matrix algebra is used for flux-based strategies; the following section, shows the only differences between the differing approaches is where they diverge from the SCs obtained in the following section (the following section is constructed from Stephanopoulos *et al*., 1998; the most up to date unifying text of the methods discussed in this Chapter).

In the following example (1) the uptake of glucose by phosphotransferase system (PTS) is used to illustrate the preceding approach to flux analysis. The actual PTS transport mechanism involves a number of enzymes (see Chapter 2; Section 2.5); however, for the purpose of this discussion, the PTS is summarised through the overall stoichiometry:

(1) - glucose - PEP + glucose-6-phosphate + Pyruvate = 0

In the preceding reactions, the stoichiometry is written such that a compound **used** in the forward reaction (reactant) has a negative SC, and a compound **formed** in the forward reaction (product) has a positive SC, whereas SCs for intracellular metabolites may be either positive or negative (Stephanopoulos *et al*., 1998). The sign is irrelevant, what is important is that SCs in these reactions supply information, for e.g., 1 mol of phosphoenolpyruvate (PEP) is used in the uptake and phosphorylation of 1 mol of glucose, and at the same time 1 mol of pyruvate (PYR) and 1 mol of glucose-6-phosphate (G6P) is formed.

$$\textbf{(2)}\quad \sum_{i=1}^{N} \alpha_{ji} S_i + \sum_{i=1}^{M} \beta_{ji} P_i + \sum_{i=1}^{\varphi} \gamma_{ji} Xmacro_i + \sum_{i=1}^{K} g_{ji} Xmet_i = 0$$

The SCs are represented in the following manner; for substrates α, the SCs for metabolic products β, the SCs for intracellular metabolites g, and the SCs for biomass γ. This is formulated into a general stoichiometry for cellular reactions (2). For this purpose a system is constructed where N substrates are converted to M metabolic products and φ biomass

constituents. The conversions are carried out in J reactions in which K intracellular metabolites also participate as pathway intermediates (Stephanopoulos *et al*., 1998). A two-numbered index on the SCs will indicate the reaction number and the compound e.g., α_{ji} is the SC for the ith substrate in the jth reaction. The substrates are termed S_i, the metabolic products P_i and the biomass constituents $X_{macro,i}$, the K pathway intermediates are termed $X_{met,i}$. With these definitions, the stoichiometry for the jth cellular reaction can be specified as equation (2)[Stephanopoulos *et al*., 1998]. In a metabolic model there will be an equation like (2) for each of the J cellular reactions. In a generalised stoichiometry, the SCs; for all substrates, metabolic products, intracellular metabolites, and the biomass constituents in each of the reactions, is introduced. Many of the SCs therefore become zero, as the corresponding compound does not participate in a reaction, e.g., the SC for glucose in reaction (3) is zero.

(3) - oxo-glutarate - NH_3 - NADPH + glutamate + NADP = 0

The stoichiometry specified in equation 2 defines the relative amounts of the compounds produced or consumed in each of the intracellular reactions, but does not allow the calculation of the rates or relative amounts at which metabolic products are secreted in the medium. This can be done by introducing the rates of the individual reactions and further coupling them to determine the overall rates of product secretion (Stephanopoulos *et al*., 1998). The rate of a chemical reaction is defined as the forward rate (or velocity) ν, which specifies that a compound that has a SC β is formed at the rate $\beta\nu$. Thus the forward reaction rates of the J reactions in Equation (2) are collected in a rate vector ν. Thus, $\beta_{ji}\nu_j$ specifies the specific rate of formation of the ith metabolic product in the jth reaction. Because the SCs for the substrates are generally negative, the specific conversion rate of the ith substrate in the jth reaction is given by $-\alpha_{ji}\nu_j$ (Stephanopoulos *et al*., 1998). To calculate the overall production or consumption of a compound, the contribution from the different reactions have to be summed together (El Mansi & Stephanopoulos, 1999). This can be illustrated by considering Case study 3 (Appendix C), where CO_2 is formed in a number of reactions and used in another reaction (PEP carboxylase). The total production rate of CO_2 is obviously determined by the relative rates of the sum of these reactions. The net specific uptake rate for the ith substrate is the sum of its consumption rate in all J reactions (Stephanopoulos *et al*., 1998):

(4) $$r_{s,i} = \sum_{j=1}^{j} \alpha_{ji} v_j$$

And similarly for the net specific rate of formation of the ith metabolic product (Stephanopoulos *et al*., 1998):

(5) $$r_{p,i} = \sum_{j=1}^{j} \beta_{ji} v_j$$

Equations (4) & (5) specify very important relationships between what can be measured directly, namely the specific uptake rates of substrates and specific formation rate of products on one hand and the rates of the various intracellular reactions on the other. The term *fluxes,* is used to indicate that they are rates through pathways rather than rates of single reactions. Similar to equations, (4) & (5), it is possible to write equations for the biomass constituents and the intracellular metabolites (Equations 6 & 7) [Stephanopoulos *et al*., 1998]:

(6) $$r macro_i = \sum_{j=1}^{j} \gamma_{ji} v_j$$

(7) $$r met_{,i} = \sum_{j=1}^{j} g_{ji} v_j$$

These rates are not determined experimentally as easily as the specific substrate uptake rates and the specific product formation rates. Holms (1986, 1996, 1997, 2001)[see Case study 2; Appendix B] considers biomass components in a similar way as product formation. Stephanopoulos *et al*. (1998) uses an overall stoichiometry for the synthesis of macromolecular constituents of biomass. The rates in equations, (6) & (7) are net specific formation rates and can be quantified from measurements of intracellular components. Thus, a compound may be consumed in one reaction and produced in another, and the rates specified on the left-hand sides of equations, (6) & (7) are the net result of consumption and production of that compound in all J intracellular reactions. If the rate $r_{met,i}$ is positive there is a net formation of the ith intracellular metabolite, and if it is negative there is a net consumption of this metabolite. If the rate is zero, the rates of formation in the J reactions exactly balance the rates of consumption, and this balancing is the basis of flux analysis (Stephanopoulos *et al*., 1998). It is convenient to write the stoichiometry for all J cellular reactions in a compact form using matrix annotation. The

summation equations (4) – (7) can be formulated in matrix notation as (Stephanopoulos *et al*., 1998; El Mansi & Stephanopoulos, 1999):

(8) $\mathbf{r_s} = -\mathbf{A^T v}$

(9) $\mathbf{r_p} = \mathbf{B^T v}$

(10) $\mathbf{r_{macro}} = \mathbf{\Gamma^T v}$

(11) $\mathbf{r_{met}} = \mathbf{G^T v}$

Where the specific rate vector r_s contains the N specific substrate uptake rates, r_p the M specific product formation rates, etc (Stephanopoulos *et al*., 1998; El Mansi & Stephanopoulos, 1999).

Equation. (11) forms the basis for MFA, i.e., the determination of the unknown pathway fluxes in the intracellular rate vector v. This vector equation represents K linear algebraic balances for the K metabolites with J unknowns (the pathway fluxes)[Stephanopoulos *et al*., 1998; El Mansi & Stephanopoulos, 1999]. The number of reactions (J) is always greater than the number of pathway metabolites (K), there is a certain degree of freedom (F) in the set of algebraic equations given by F = J – K or F = M – N (Stephanopoulos *et al*., 1998; El Mansi & Stephanopoulos, 1999). Alternatively the number of degrees of freedom is the number of fluxes that can be manipulated independently.

A typical example of a reaction rate that can be measured is the conversion of glucose to G6P if a PTS uptake system is being used, which may be taken to be equal to the glucose uptake rate. If exactly F fluxes (or reaction rates) in v are measured, the system becomes determined and the solution is simple to obtain. In the event that more than F fluxes are measured, the system is over determined, meaning that extra equations exist that can be used for testing the consistency of the overall balances, the accuracy of the flux measurements, the validity of the *pseudo*-steady state assumption, and, ultimately, the calculation of more accurate values for the unknown intracellular fluxes. If fewer than F fluxes are measured, the system is undetermined and unknown fluxes cannot be determined (Stephanopoulos *et al*., 1998).

In a determined system, that is one for which exactly F fluxes (or reaction rates in v) are measured, the remaining fluxes can be calculated by solving the linear system (11). It is

convenient to introduce matrix algebra to describe the various steps. To this end the solution to equation (11), is found by collecting the measured rates in a new vector, v_m, and the remaining elements of vector v (which are the rates to be calculated) in another vector, v_c. Similarly, the SCs in matrix G are partitioned by collecting those of the measured reactions in G_m and the remaining in matrix G_c. Equation (11) may then be rewritten as (12) [Stephanopoulos *et al*., 1998]:

(12) $\mathbf{G^T v = G^T_m v_m + G^T_c v_c = 0}$

Then if F = J – K fluxes are measured, G_c is a square matrix (Dimension K × K) and, if this matrix can be inverted then the elements of v_c can be found from (13)[Stephanopoulos *et al*., 1998]:

(13) $\mathbf{v_c = -(G^T_c)^{-1} G^T_m v_m}$

Case study 3 (Appendix C), demonstrates the application of matrix algebra to flux determination. The case studies are detailed to provide templates to undertake such analysis and demonstrate the pros and cons of the different techniques. It must be remembered that matrix algebra brings to flux analysis the mathematical techniques that can test hypotheses systematically and apply strict protocols to the understanding of flux-based analysis.

1.2.3 Methods for the experimental determination of metabolic fluxes

Figure 1.1 presents a simplified biosynthetic reaction network for growth of a bacteria on glucose as sole carbon source. The estimation of the carbon flux through each reaction is the desired goal with the minimum number of experimental measurements. Although this simplified network is used to represent cellular metabolism, it is quite obvious that not all the biosynthetic reactions have been incorporated. There are thousands of such reactions, to include all would be impractical. The construction and conversion of Fig 1.1 to a stoichiometric written sequence of reactions is termed the bioreaction network (BRNE)[see Appendices I to M for examples of streptomycete metabolism]. This sequence of reactions can then be converted to matrix algebra using computer packages such as BioNet (see Case study 3 Appendix C). The main fuelling and metabolite-generating bioreaction, such as the Embden-Meyerhof-Parnas pathway (EMP), Pentose Phosphate

pathway (PP pathway) and the TCA cycle (see Chapter 2 for discussion of streptomycete biochemistry) are assembled. In order to maintain observability of the overall network from the extracellular measurements, the pathways that couple extracellular metabolites (including the product) to the fuelling reactions must be included. Since a PSS (see section 1.1) approximation will be used for intracellular metabolites, regenerating reactions such as those for ATP and NAD via the respiratory chain are included to ensure that no intracellular metabolite has a net production or consumption. Elaborate or ill-defined pathways, such as biomass synthesis or maintenance requirements, must be expressed as lumped reactions. Finally, to minimise the dimensionality of the system, only metabolites that are involved at branch points in the biosynthetic pathways are considered in the network. The BRNEs used for *S. fradiae* fermentation are presented in Appendices L & M and analysed and discussed in Chapter 7.

The extent to which metabolic networks can be elucidated by using concentration measurements of extracellular metabolites alone is limited. At most, such measurements provide information about the distribution of carbon flux at a small number of branch points in the metabolic network. This point may be obscured with the use matrix algebra methods as, formulating the equations of the BRNE can be complex. Stephanopoulos *et al*. (1998); illustrated the reduction of rather complex sets of biochemical reactions to their simple network equivalents. In particular, extracellular measurements have limited potential in elucidating aspects of metabolic networks, such as:

(a) Flux distribution at split points that converge at another point of the network.
(b) Metabolic cycles (futile cycles).
(c) Unravelling network structure to a finer biochemical resolution.

These points are illustrated in Fig 1.2 which shows the split of a primary compound A between two competing pathways 1 and 2 proceeding at net rates v_1 and v_2. Measurements of the consumption rate of A and the secretion rates of F and G are sufficient to determine the distribution of fluxes at branch points D and H and the independent calculation of another secreted metabolite, K.

However, the flux split ratio at metabolite A between the two pathways 1 and 2 or, equivalently, the flux through the cycle A $\rightarrow$ B $\rightarrow$ C $\leftrightarrow$ A is indeterminable. Similarly, if

more reactions are involved in the conversion of C to 2D, they must all be lumped into a single reaction. If more information about the split ratio between pathways 1 & 2 are required additional constraints are required; for e.g., the use of mass balances of co-metabolites such, as ATP or NADPH. This is explained in Figure 1.3A & B. The mass balances of metabolites A & B yield the same information, as a result fluxes 1 and 2 cannot be determined; here, the solution space that contains all permissible solutions for both fluxes can be represented as a single line. In contrast, when a co-metabolite is produced or consumed in either flux 1 or 2 the three mass balances A, C, and E yield one unique solution (Fig 1.3 B) [Bonarius, 1998].

In reality however, the addition of mass balances of co-metabolites is generally not sufficient (Bonarius, 1998). Inclusion of NADH and NADPH balances, are subject to controversial debate (e.g., transhydrogenation [TH] reactions, & maintenance energy is difficult to account for)[However, it is the NADPH balance that, to a large extent, determines the calculated flux through the PP pathway; hence, wrong assumptions on the presence or activity of TH reactions will result in wrong estimations of intracellular flux distribution]{Bonarius, 1998}. In complex networks, co-metabolites are either produced in more than one cyclic pathway, or are not balanceable. For example CO_2 is co-produced in the pentose cycle, the TCA cycle, glyoxylate pathway, and can be utilised by enzymes e.g. PEP carboxylase (see Chapter 2; Section 2.5). The addition of the CO_2 balance to the metabolite methods will therefore, not bring further resolution (Daae and Ison, 1999). However useful information can be obtained from the CO_2 evolution rate as it provides additional information on the total flow in the three cycles mentioned alone (Stephanopoulos *et al*., 1998). If a finer biochemical resolution of the depicted steps is desirable, different methods must be applied.

One class of such methods is the use of compounds labelled with ^{13}C or ^{14}C at specific carbon locations (Stephanopoulos *et al*., 1998). Through the use of such compounds, pathways that introduce asymmetries in the distribution of carbon atoms of intermediary metabolites may be distinguished from one another, even though they lead to the formation of the same final product (Stephanopoulos *et al*., 1998). This asymmetry leads to fundamentally different patterns of label enrichment in one or more metabolites, the measurement of which provides the necessary information for the determination of the

rates of the competing reactions. ^{13}C or ^{14}C-labeled compounds are used in connection with the measurement of label enrichment in extracellular or intracellular metabolites (Stephanopoulos *et al*., 1998). Furthermore, the type of information that can be obtained from the applications of such methods depends greatly on the type of labelled substrate used, the particular carbon atoms that are labelled, and the particular metabolite (intracellular or extracellular) whose degree of enrichment is measured.

Although the basic idea of labelling experiments is similar, they can in general be categorised into three types of analysis, primarily depending on the size and complexity of the network that is being analysed. The first case is applicable to situations with directly measurable metabolites or simple networks that are usually amenable to analytical solutions where transient intensity measurements of radiolabelled compounds can be used to probe a specific metabolic pathway directly. For metabolic networks involving cycles, straightforward accounting of label transfer is adequate. An alternative method based on the enumeration of all possible metabolite isotopomers, is the method of choice for MFA [Stephanopoulos *et al*., 1998; Chapter 9, example 9.2, for worked example; adapted from Blum & Stein, 1982]. In addition to facilitating the exact determination of the degree of label enrichment of specific metabolites, isotopomer enumeration also allows the estimation of molecular weight distributions of specific metabolites, measurable by gas chromatography-mass spectrometry instruments (GC-MS). Because molecular weight distributions depend on metabolic fluxes, GC-MS combined with ^{13}C-NMR spectrometry is another source of valuable information regarding intracellular metabolic fluxes. Finally, for complex situations of large networks, numerical solutions are required. For such cases, the concept of atom mapping matrixes (AMMs) provides a convenient framework for carrying out efficiently the label distribution calculations especially when iterative procedures are needed. The analysis of such networks involves a fair amount of trial and error in order to ensure consistency of the large number of measurements possible through the application of NMR spectrometry. These calculations are facilitated by the use of AMMs, a technique introduced by Zupke & Stephanopoulos, (1994). See Stephanopoulos *et al*., 1998; Christiansen *et al*. 2002, for examples of the technique.

1.2.4 Tracer experiments Vs metabolite balancing for metabolic flux analysis

Using tracer experiments, flux analysis can be performed on the basis of only well established stoichiometric equations and measurements of the labelling state of intracellular metabolites. Neither NADH/NADPH balancing nor assumptions on energy yields need to be included to determine the intracellular fluxes. Because metabolite balancing methods and the use of tracer labelling measurements are two different approaches to the determination of intracellular fluxes, both methods can be used to verify each other or to discuss the origin and significance of deviations in the results (Schmidt *et al*., 1998; Stephanopoulos *et al*., 1998).

Sauer *et al*. (1997) used an approach based on biosynthetically directed fractionation of ^{13}C-labelling of proteinogenic amino acids with glucose (Neri *et al*., 1989; Senn *et al*., 1989); which allows determination of the relative abundance of contiguous carbon fragments originating from the same source molecule (Wuthrich *et al*., 1992; Szyperski, 1995). This enables estimation of the relative contribution of alternative primary pathways in the generation of precursor molecules; specifically, it is possible to obtain reliable estimates on the fluxes of both the reaction catalysed by the malate dehydrogenase decarboxylating enzyme, and futile cycles through consecutive reactions catalysed by PEP carboxylase, PEP carboxykinase, PYR kinase and PYR carboxylase. The relative abundance can be determined by NMR spectroscopy, specifically by analysis of ^{13}C - ^{13}C scalar couplings and fine structures observed with two dimensional protein detected [^{13}C,^{1}H]-correlation spectroscopy (2D[^{13}C,^{1}H]-COSY) of the hydrolysed biomass.

The main two disadvantages of radio-labelled tracer based studies are, the demanding procedures and high costs (Walsh & Koshland, 1985; Longacre *et al*., 1997; for good examples of the demanding experimental detail needed). Likewise, ^{13}C NMR strategies can be illuminating although there are difficulties in maintaining a cell suspension in a desired physiological state during an experiment (Goel *et al*., 1993); although this has in general been overcome by the use of amino acid biomass hydrolysates (Schmidt & Norregaard, 1999 for one of the most up to date attempts with complete NMR isotopomer modelling in *E. coli*; also see Abel *et al*., 1999; for initial trials of on-line NMR analysis of *Streptomyces citricolor*).

1.2.5 Applications of metabolic flux analysis

The goal of this modelling effort is to determine how mass and energy are calculated within the network of metabolic reactions. Metabolic fluxes constitute a fundamental determinant of cell physiology, primarily because they provide a measure of the degree of engagement of various pathways (Stephanopoulos *et al.*, 1998). Accurate quantification of the magnitude of the pathway fluxes *in vivo* is, therefore, an important goal of cell physiology. The real value of such metabolic flux maps lies in the flux differences that are observed, when flux maps obtained with different strains or under different conditions are compared with one another. It is through such comparisons that the impact of genetic and environmental perturbations can be fully described and the importance of specific pathways, and reactions within such pathways, assessed accurately. In addition to quantification of pathway fluxes, MFA can provide additional insights about other important aspects of cell physiological characteristics, described below:

(1) **The calculation of non-measured fluxes**; normally the number fluxes that can be measured is larger than needed for the calculation of the intracellular fluxes (Nielson, 1998; Stephanopoulos *et al.*, 1998). In this case it is possible to calculate some of the intracellular fluxes, e.g. the production of various by-products, by use of the stoichiometric model and the measured rates.

(2) **The calculation of maximum theoretical yields**; from a stoichiometric model it is possible to calculate the maximum theoretical yield of a given metabolite, if a set of constants is specified. This has been illustrated by Stephanopoulos & Vallino (1991); who calculated the maximum theoretical yield of lysine from glucose by *Corynebacterium glutamicum*; and by Jorgensen *et al*. (1995a, b), who calculated the maximum theoretical yield of penicillin from glucose by *Penicillium chrysogenum.*

(3) **The identification of the existence of different pathways**; formulation of the stoichiometric matrix that is the basis for MFA requires detailed information on the biochemistry. However, for many microorganisms certain details about the pathway stoichiometries are not known (i.e. function of different isoenzymes [ISEs]), and it may not be known whether a given pathway is active. By calculating the metabolic fluxes with different sets of cellular pathways, it may be possible to identify the set of pathways which

is most likely to be active, or to deduce indications of the function of different ISEs and\or pathways. This approach is illustrated in one of the first applications of MFA, where Aiba & Matsuoka. (1979) examined various optimisation pathways in citrate producing *C. lipolytica* (see Case study 3; Appendix C). In the analysis of *Saccharomyces cerevisiae*, it was found that alcohol dehydrogenase, a mitochondrial enzyme whose physiological function has not been determined, plays an important role in monitoring the redox level inside the mitochondria (Nissen *et al.,* 1997; Nielson, 1998). Santosh *et al*. (2000) used material balancing and kinetic modelling (very similar in nature to Vallino (1991), one of the best examples of MFA) to measure the fate of glutamate and evaluation of the flux through the 4-amino-butyrate (GABA) shunt in *A. niger*.

(4) **Examination of the influence of alternative pathways on the distribution of fluxes**; in connection with optimisation of metabolite production it may be possible to identify one or several constraints for increasing the yield of a particular metabolite on the substrate or for increasing the flux leading to the desired metabolite. Thus various scenarios can be compared to examine whether insertion of a new pathway or an ISE (or perhaps deletion of an ISE) can help to remove the constraints and thereby lead to an increased flux towards the desired metabolite. In a study undertaken by Jorgensen *et al.*, (1995a, b); of penicillin production, the calculated yield of penicillin from glucose is likely to be higher if cysteine, one the precursors for penicillin production is synthesised by direct sulphylhydrylation rather than by the transulphuration pathway claimed to exist in *P. chrysogenum* (Jorgensen *et al.,* 1995a, b; Nielsen, 1998).

(5) **Identification of possible rigid branch points (or nodes) in the cellular pathway**; through comparison of the distribution of fluxes at different operating conditions it is possible to identify whether a pathway node is rigid or flexible (Stephanopoulos & Vallino, 1991). Thus in lysine producing *C. glutamicum* it was found that the nodes at G6P, PYR and oxaloacetate are flexible, whereas the PEP node is rigid (Stephanopoulos & Sinskey, 1993; Vallino & Stephanopoulos, 1993, 1994a, 1994b) [Shimizu *et al*., 1999; Hua *et al*., 1999; for further work in this area].

1.2.6 Examples & applications of MFA

It is possible to find many examples of MFA while undertaking a literature search, for

example:

1.2.6.1 Penicillin production by the filamentous fungus *Penicillium chrysogenum*; this system has been analysed by Jorgensen *et al.* (1995a,b) and Henriksen *et al.* (1996), who used MFA to calculate metabolic flux distributions during fed-batch and continuous cultures. Furthermore, they used MFA to calculate the maximum theoretical yields for different biosynthetic pathways leading to cysteine (which is a precursor for penicillin biosynthesis). In their analysis, they found a correlation between the flux through the PP pathway and penicillin production. Their model is the first example of a consideration of intracellular compartmentation, i.e., it distinguishes between cytosolic and mitochondrial reactions. Other applications have been detailed for *C. glutamicum,* (Vallino & Stephanopoulos, 1993; 1994a, b); Van Gulik *et al*. (2000) indicate potential bottlenecks in primary metabolism with respect to penicillin production, around co-factor supply/regeneration (NADPH) and not so much around the supply of carbon precursors.

1.2.6.2 A flux-based stoichiometric model for enhanced biological phosphorus removal (EBPR) in water treatment; this system has been analysed by Pramanik *et al*. (1998a, 1999) where the overall aim was to decrease biomass and maximise commission of the materials to CO_2, (Van Dam, 1986); the fluxes in this model were calculated using matrix algebra.

1.2.6.3 Applications of this approach to the metabolism of Hybridoma cell lines. (Savinell *et al.*, 1989, 1992a; Savinell & Palsson, 1992b; Xie & Wang, 1994a, 1994b, 1994c, 1996a, b; for an example see Fell & Small, 1986; where it was shown how fat synthesis constrains other metabolic pathways in adipose tissue). Another application was the determination; of an ATP balance to model energy metabolism. Xie & Wang (1996b) developed a method for the estimation of the stoichiometric production of ATP.

1.2.6.4 Growth of *Escherichia coli*; this system has been studied extensively (Holms, 1986, 1991, 1996, 1997, 2001; Aristidou *et al*., 1998; Varma *et al.*, 1993a, 1993b, Varma & Palsson, 1994a, 1994b, 1995; Van Gulik & Heijnen, 1995; Pramanik & Keasling, 1997; Yang, 1999; Yang *et al.*, 1999a, b). Holms (1986, 1996, 1991 1997, 2001) application of MFA has been used to ascertain the excretion of acetate, when *E. coli* was growing on minimal medium components such as glucose, PYR, glycerol & acetate as the sole carbon

source. Acetate accumulation has been reported to be a common problem that hampers the production of heterologous proteins and metabolites in *E. coli* (Holms, 1986; Majewski & Domach, 1990). The reason is considered to be an imbalance between glucose uptake and utilization in addition to the uncoupling of oxidative phosphorylation.

1.2.6.5 MFA has also been profitably applied to studies of; *C. glutamicum,* (Vallino & Stephanopoulos, 1993, 1994a, b); *Rhizopus oryzae,* (Longacre, 1997); *Klebsiella pneumonia*, (Zeng *et al.*, 1996a, b); *Phaffia rhodozyma*, (Yamane *et al.*, 1997); *Streptoverticillium mobaraense*, (Zha *et al.*, 1996); *Bacillus licheniformis*, (Calik & Ozdamar, 1999; Calik *et al*., 1999); *Candida milleri*, (Cranstrom *et al*., 2000); *Bacillus subtilis*, (Sauer *et al*., 1996, 1997, 1998; Goel *et al., 1993*); *Alcaligenes eutrophus*, (Shi *et al*., 1997) for the biosynthesis of poly (β-hydroxybutyric acid); *Torulopsis glabrata*, (Hua & Shimizu, 1999; Hua & Shimizu, 1999; Hua *et al*., 2001); *Corynebacterium melassecola* (Pons *et al*., 1996); *Clostridium acetobutylicum*, (Desai *et al*., 1999; Desai & Harris, 1999) where non-linear constraints were solved by correlating calculated production rates with measured intracellular pH profiles, among many others.

1.2.6.6 Metabolic flux analysis in *Streptomyces*; the first MFA of streptomycetes were undertaken on *S. clavuligerus* (Holms, 1986); which was undertaken by Bioflux Ltd and has only come into the academic arena in part (see Case study 2; Appendix C); and *S. coelicolor* (Davidson, 1992), which used Holms (1986) strategy to calculate metabolic fluxes. Later attempts at flux analysis on *S. lividans* (Daae & Ison, 1998; Daae & Ison, 1999) [see Appendix L, for bio-reaction network], *S. coelicolor* (Naeimpoor & Mavituna, 2000), and for *S. lividans* producing, actinorhodin and tripyrrole undecylprodigiosin (Avignone-Rossa *et al*., 2002). These have entered straight into the realms of matrix algebra and lack a great deal of experimental detail & detailed mathematical workings. Flux analysis has been attempted on *S. clavuligerus* by Kirk *et al*. (2000) [see Appendix K for bio-reaction network]. That is good in nature. Initial studies of where the majority of carbon sinks are was not undertaken and after viewing this work it is unlikely that an accurate carbon balance was achieved. Early strains of *S. clavuligerus* produced β–lactams as well as clavulanic acid; when β–lactam pathways were initially disrupted, a lot of carbon flowed into the medium as β–lactam intermediates. It can only be ascertained from this work that certain parameters were not calibrated i.e., CO_2 analysis. King (1997) and

King & Budenbender (1997), constructed a mathematical model for *Streptomyces tendae*; which also reports the difficulties of formulating a general model for *Streptomyces.*

1.2.6.7 Strategies for MFA in plants. Steady-state isotope labelling experiments offer several powerful methods for measuring metabolic fluxes in plants (Roscher *et al*., 2000). However, in contrast to microorganisms and animal cell cultures, it is necessary to make due allowance for the effects arising from the compartmentation and greater complexity of the primary metabolism in plant material. A combination of ^{13}C-labelling and NMR analysis has become the preferred analytical approach in many cases, and with suitable precautions it is possible to generate quantitative metabolic models that highlight the integration of plant metabolism.

It should be emphasised that flux estimates based on metabolite balances are no less accurate or prone to error than those based on radio or stable isotope tracers. Since accumulation rates of extracellular metabolites are readily measured under normal fermentation conditions, metabolite balance techniques are the first choice. If flux distribution cannot be completely observed from metabolite accumulation rates only, then tracers or further compositional data can supplement the measurements. In any case, flux estimation based on tracer methods can always be improved by utilising mass balance constraints as well. It is also important to realise that the metabolite balance techniques can also be used in conjunction with kinetic-based models. Since both models involve the same biochemical pathways, the steady state flux distributions obtained from the kinetic simulations must match that obtained experimentally from the metabolite-based model (El-Mansi & Stephanopoulos, 1999; Chapter 6 & 7 for a for discussion).

1.3 Metabolic Control and Biochemical Systems Theory

Metabolic control theory (MCT), was independently developed by Kacser & Burns (1973a, b) and Heinrich & Rapoport (1974) to identify the kinetic constraints in a biochemical network, which were both building on ideas initially developed by Higgins (1963, 1965). It has many similarities with two other frameworks developed to quantify metabolic control: Biochemical Systems Theory (BST) and Crabtree & Newsholme's flux-oriented theory (Crabtree & Newsholme, 1987; 1995). Although initial attention focused on the differences among these three approaches, it was later realised that they indeed

converge on the same basic concepts despite differences in formalism. A more structured approach has been built from these theories and is known as metabolic control analysis (MCA) (Fell, 1992). The following sections are constructed considerably from the work of Professor Gregory Stephanopoulos (MIT) who has been architectural in unifying the approaches discussed in this Chapter (Stephanopoulos *et al*., 1998; Ehlde & Zacchi, 1997; Melendez-Hevia *et al*., 1996; Hatzimanikatis *et al*., 1996; Fell, 1997, 1998; Kell, 1987; Westerhoff *et al.,* 1991; Crabtree & Newsholme, 1985; Simpson *et al*., 1999; Van Dam, 1986; Kell & Westerhoff, 1986).

1.3.1 What is Metabolic Control Analysis?

MCA is a mathematical formalism, which provides a method to describe/model the control of metabolic systems. MCA attempts to describe the relative control that each component in a metabolic system (the independent variables or parameters) exerts on the pathway fluxes and metabolite concentrations (the dependent variables). The degree of control of any individual component of a metabolic system is determined by changing the level of that component and monitoring its effect on the system variable (flux or metabolite concentration) of concern. MCA relates the properties of the *in vivo* metabolic system to the properties of its component parts, in particular the concentrations of enzymes and allosteric effectors (Stephanopoulos *et al*., 1998; El Mansi & Stephanopoulos, 1999). MCA can simplify the complexities of metabolic (and other) systems. It gives a "snap-shot" of metabolism around a particular steady-state or *pseudo*-steady state (section 1.1). Moreover, the terms used (Control and Elasticity coefficients, the Summation and Connectivity theorems) are well defined (Stephanopoulos *et al*., 1998; El Mansi & Stephanopoulos, 1999).

1.3.2 Fundamentals of metabolic control analysis

The primary impetus behind the development of MCA was to quantify the level of contribution of each enzyme in a metabolic pathway to control of the overall flux. System parameters can, in principle, be changed at will, and as such they completely define the system. Properties that are determined by the values of the parameters, e.g., the flux through the pathway or intermediary metabolite concentrations, are considered to be system variables (Stephanopoulos *et al*., 1998; El Mansi & Stephanopoulos, 1999). To illustrate this definition of parameters and variables in the context of enzyme kinetics,

equation (14) is used as an example, when the two ends of a linear metabolic pathway are linked by an intermediate metabolite (X)[Stephanopoulos *et al*., 1998]:

$$\mathbf{(14)}\quad \mathbf{S} \overset{E_1}{\leftrightarrow} \mathbf{X} \overset{E_2}{\leftrightarrow} \mathbf{P}$$

The net rate, (or flux), of conversion of S to P at steady state is given by J. In MCA the aim is to study the influence of the parameters, i.e., enzyme activities, on the steady-state flux, and therefore, there is a need to distinguish between the rate of the individual reactions v and the overall steady-state flux, which is therefore termed J [Stephanopoulos *et al*., 1998].

A steady state is uniquely determined by the parameters of the system, i.e., the levels of the enzyme activities E_1 and E_2 and the concentrations of the substrate S and product P. The definition of the steady state entails determination of the intermediate metabolite concentration c_x, along with the pathway flux J and other derivative quantities. If the parameters are changed e.g., if E_1 is increased, a new steady state will emerge that is characterised by other values for variables, i.e., the concentration of the intermediate X and the net flux J through the pathway. Thus metabolite concentrations are considered to be unique variables, and it is assumed that they are distributed homogeneously over the enzymes that act on them (Stephanopoulos *et al*., 1998).

1.3.3 Control coefficients and the summation theorems

One objective of MCA is to relate the variables of a metabolic system to its parameters. Once this is done, the sensitivity of a system variable, such as the flux, with respect to the system parameters, namely, the enzyme activities, can be determined (El Mansi & Stephanopoulos, 1999). These sensitivities represent fundamental aspects of flux control as they summarise the extent of systematic flux control exercised by the activity of a single enzyme in the pathway (Stephanopoulos *et al*., 1998). Therefore, it is possible to solve for the concentrations of intracellular metabolites and also determine their sensitivity with respect to enzyme activities, effector concentrations, and other systems parameters. These sensitivities are summarily described by a set of coefficients, of which the most prominent are the control coefficients (CCs)[Stephanopoulos *et al*., 1998]. They describe how a parameter, e.g., the activity of an enzyme in the pathway, affects the variables of the system, e.g., the flux through the pathway (El Mansi & Stephanopoulos, 1999). The CCs only apply to the steady-state conditions studied, and this explains why the component

parts, e.g., enzyme activities, are described as parameters, whereas the properties of the system that may change as a result of a change in the parameters, e.g., fluxes and metabolite concentrations, are referred to as variables (El Mansi & Stephanopoulos, 1999).

The most important CCs are the so, called *flux control coefficients* (FCCs). The FCC is a parameter which describes in quantitative terms the relative contribution of a particular enzyme to flux control in a given pathway (El Mansi & Stephanopoulos, 1999). It is not an intrinsic property of the enzyme *per se* but rather a system property and so is subject to change as the environment changes (Stephanopoulos *et al*., 1998). It is calculated from the tangent to the curve of a log-log plot of flux (J) as a function of the enzymic activity or concentration (E) normalised by the corresponding steady-state flux and enzyme activity (equation 15 and Fig 1.4) [El Mansi & Stephanopoulos, 1999].

(15) $$C^j = \frac{EdJ}{JdE} = \frac{d\ln J}{d\ln E}$$

The definition in equation (15) is the original one proposed by Kacser and Burns (1973). The FCCs are defined in terms of *relative* flux and activity values, they are dimensionless and their magnitude is independent of flux and activity units used (Stephanopoulos *et al*., 1998). For a linear pathway they have values between 0 and 1 (El Mansi & Stephanopoulos, 1999). However, it is possible for an enzyme to have a flux CC with a negative value as is the case at branch points where one metabolite has to be partitioned between two enzymes (El Mansi & Stephanopoulos, 1999). In such a case the increase in flux through one branch is generally at the expense of the other.

Thus the enzyme with the largest FCCs exerts the largest control of flux at the particular steady state, as an increase in the activity of this enzyme results in the largest overall flux increase (Stephanopoulos *et al*., 1998). An important consequence of the normalisation of the FCCs is that, with respect to each flux, they all must sum to unity. This is known as the *flux-control summation theorem* (El Mansi & Stephanopoulos, 1999):

(16) $$\sum_{i=1}^{L} C_i^{jk} = 1 \qquad \mathbf{k \in \{1,\ 2,\ldots,\ L\}}$$

From equation (16), it is clear that FCCs are completely dependent upon the structure of the system and that nothing general can be said about their individual values. For very long

pathways, most FCCs may have small values; however, one step may still exist that exerts significant control over the flux if the magnitude of its FCC is significantly larger than that of the other FCCs (Stephanopoulos *et al*., 1998). For short pathways the FCCs may have much greater magnitudes, even for the case where flux control is distributed amongst more than one step (Stephanopoulos *et al*., 1998). FCCs therefore should only be compared with each other within the same pathway and never with FCCs of other pathways (Westerhoff & Van Dam, 1987; for the branching theorem). The small value of FCCs in long pathways explains why so many successive rounds of mutation and selection steps are needed usually in order to improve strains for the production of metabolites such as amino acids and antibiotics (Stephanopoulos *et al*., 1998). It should be noted that there have been objections both to the name and concept of FCCs. Some of the principal grounds for these objections have been reviewed by Fell (1992).

Originally, enzyme concentration was used as the parameter that was descriptive of enzymatic reaction rate. Enzyme concentration, however, is not particularly relevant to enzymatic activity and flux control, considering the fact that enzymatic activity principally is affected by the action of effectors binding to allosteric enzymes (Stephanopoulos *et al*., 1998). To account for this, *response coefficients* [RCs](17) were introduced (Kacser & Burns, 1973) that allow for the quantification of the flux sensitivities with respect to such effectors:

(17) $$R_{xi}^{jk} = \frac{e_i dJ_k}{J_k de_i} \qquad \mathbf{i, k \in \{1,\ 2, ..., L\}}$$

The RC reflects the effectiveness of a particular effector on the flux through a given pathway and is dependent on two factors, namely, the FCC of the target enzyme and the strength of the effector, given by its elasticity coefficient (EC)[El Mansi & Stephanopoulos, 1999].

Similarly to the FCCs, it is possible to define sensitivities for the response effect of system parameters on intracellular metabolite concentrations. Such sensitivities are termed *concentration control coefficients* (CCCs), where the variable affected by the enzyme activity E_i is a metabolite concentration c_j (El Mansi & Stephanopoulos, 1999):

(18) $$C_i^{xj} = \frac{E_i dc_j}{c_j dE_i} = \frac{d\ln c_j}{d\ln E_i} \qquad \mathbf{i, k \in \{1,\ 2, ..., L\},\ j \in \{1,\ 2, ...,\ K\}}$$

or more generally:

$$(19)\quad C_i^{xj} = \frac{v_i dc_j}{c_j dv_i} = \frac{d\ln c_j}{d\ln v_i} \quad \mathbf{i, k \in \{1,\ 2, ...,\ L\},\ j \in \{1,\ 2, ...,\ K\}}$$

These coefficients specify the relative change in the level of the jth intermediate, X_j (Stephanopoulos *et al*., 1998). Because the level of any intermediate remains unchanged when all enzyme activities are changed by the same factor, it follows that, for each of the K metabolites, the sum of all the CCCs must equal zero (Stephanopoulos *et al*., 1998):

$$(20)\quad \sum_{I=1}^{L} C^{xj}_i = 0 \qquad \mathbf{j \in \{1,\ 2, ...,\ K\}}$$

Equation (20) implies that for each metabolite at least one enzyme must exert negative control, i.e., when the level of that enzyme increases, the metabolite concentration decreases (El Mansi & Stephanopoulos, 1999). Thus, in the simple, two-step pathway of equation (14), the CCC C_2^x normally will be negative because the metabolite concentration c_x will decrease when the activity of the second enzyme is increased (Stephanopoulos *et al*., 1998).

Another important concept in MCA is the *elasticity coefficient* (EC). Which describes how flux is influenced by changes in the concentration of a given metabolite. The elasticity of an enzyme to a metabolite is defined by the log-log plot of the slope of the curve of enzyme units (reaction rate) plotted as a function of metabolite concentrations (substrate, product, effector [non-allosteric]) with the measurements taken at the metabolite concentration found *in vivo* (21) [El Mansi & Stephanopoulos, 1999]:

$$(21)\quad \varepsilon^i_{xj} = \frac{c_j \delta v_i}{v_i \delta x_j} = \frac{\delta \ln v_i}{\delta \ln c_j} \qquad \mathbf{i, \in \{1,\ 2, ...,\ L\},\ j \in \{1,\ 2, ...,\ K\}}$$

Elasticities have positive values for metabolites which stimulate enzymic activity (substrates, activators) and negative values for, those which decrease reaction rate (products and inhibitors)[El Mansi & Stephanopoulos, 1999]. Elasticity is, therefore, a parameter, which describes, in quantitative terms, the sensitivity and responsiveness of an enzyme to particular metabolite which could be a substrate, a product or an effector (Stephanopoulos *et al*., 1998).

The relationship between FCCs and elasticities is expressed in the following flux-control connectivity theorem (22) derived by Kacser & Burns (1973):

$$\textbf{(22)}\ \sum_{i=1}^{L} C_i^{jk}\varepsilon_{xj}^{i} = 0 \qquad \textbf{i} \in \textbf{\{1, 2, ..., L\}, j} \in \textbf{\{1, 2, …., K\}}$$

The connectivity theorem is considered to be the most important of the MCA theorems because it provides the means to understand how local enzyme kinetics affect control (El Mansi & Stephanopoulos, 1999). The connectivity value for any given enzyme can be calculated by multiplying its FCC by its EC with respect to the metabolite in question (El Mansi & Stephanopoulos, 1999). Naturally, enzymes, which are not affected by the metabolite in question will have an elasticity of zero and as such will make no contribution towards the final sum obtained (El Mansi & Stephanopoulos, 1999). Further analysis of connectivity values has revealed that large elasticities are associated with small FCCs, and vice versa (Stephanopoulos *et al*., 1998). The mathematical equations relating the connectivity theorem to linear pathways, branch points and cycles have been described and dealt with extensively (Fell, 1997).

As with FCCs, connectivity theorems have also been derived for CCCs, although they are slightly more complex (Stephanopoulos *et al*., 1998). When the CC and the elasticity refer to different metabolites, the connectivity theorem takes the form (23) [Stephanopoulos *et al*., 1998]:

$$\textbf{(23)}\ \sum_{i=1}^{L} C_i^{xi}\varepsilon_{xj}^{i} = 0 \qquad \textbf{j, ι} \in \textbf{\{1, 2, ..., L\}, j} \neq \textbf{ι}$$

Whereas if the metabolites are the same it takes the form:

$$\textbf{(24)}\ \sum_{i=1}^{L} C_i^{xi}\varepsilon_{xj}^{i} = -1 \qquad \textbf{j,} \in \textbf{\{1, 2, ..., L\}}$$

Generally less attention is paid to CCCs, but they provide important information when the results of MCA are to be used in the design of enzymatic amplifications. Furthermore, in the original derivation by Heinrich & Rapoport (1974), they were used to derive expressions for the FCCs (Stephanopoulos *et al*., 1998).

1.3.4 The determination of flux control coefficients

A number of experimental methods have been proposed to determine both the CCs and ECs. All of these methods involve, in one way or another, the determination of derivatives of non-linear functions, i.e., the slopes of tangents to non-linear functions at specific points (Fig 1.4). Various methods have been proposed in the literature for the determination of FCCs. These methods can be classified in three groups as follows:

- Direct methods, where the CCs are determined directly from flux and activity measurements following small but finite activity changes (by genetic alteration of expressed enzyme activity, titration with purified enzyme, titration with specific inhibitors); in general known as the "bottom" up approach, where every parameter in the system is measured (as well as pH and allosteric effector molecules). Although, in principle, elasticities can be measured on an isolated enzyme, such measurements are always open to doubts as to whether the artificial system actually reproduces the properties of the same enzyme *in situ*, because metabolites that interact with it *in situ* may be omitted or present but quantitatively different (Acerenza & Cornish-Bowden, 1997).

- Indirect methods, where the ECs are determined first and the FCCs subsequently are calculated from the theorems of MCA. It is noted that the latter produces a closed system whereby FCCs and elasticities can be determined from one another through the use of theorems. Such approaches are, the "top down" approach [Brown *et al*., 1990; Kholodenko, 1998; for a review of the "bottom up" approach Vs the "top down" approach, which allows for the coefficients based on relative flux alone]; co-response [Hofmeyr *et al*., 1993]; and the calculation of ECs from kinetic based models.

- Cascante *et al*. (1996) view MCA from another perspective, "production efficiency", where flux control cannot be considered independent of the control of metabolite concentrations. Delgado *et al*. (1993); derived an algorithm for evaluation of the CCs from measurements of the metabolite pools during transients. This approach seems attractive, but the estimated CCs are very sensitive to even small errors in measurement of the metabolite pool (Nielsen, 1994). For examples of the latter approaches see Stephanopoulos *et al*. (1998).

Vast numbers of theoretical examples of MCA litter the literature; experimentally this technique has only been applied successfully in a few cases. One, such case is for *Streptomyces clavuligerus* (Malmberg & Hu, 1991; Khetan, *et al*., 1999). The rate-limiting step in the biosynthesis of cephalosporin C was identified to be the supply of the precursor metabolite α-aminoadipic acid and thereafter the productivity was improved by cloning the gene for one of the key enzymes in the α-aminoadipic acid biosynthetic pathway (Malmberg *et al*., 1993; 1995).

Khetan *et al*. (1999) combined experimental and kinetic modelling approaches to examine the regulation of flux in the cephamycin biosynthetic pathway in *S. clavuligerus*. The kinetic parameters of lysine-6-aminotransferase (LAT), the first enzyme leading to cephamycin biosynthesis and one previously identified as being a rate-limiting enzyme, were characterised. LAT converts lysine to α-aminoadipic acid using α-ketoglutarate as a co-substrate. The Km values for lysine and α-ketoglutarate were substantially higher than their intracellular concentrations, suggesting that lysine and α-ketoglutarate may play a key role in regulating the flux of cephamycin biosynthesis. The important role of this precursor / co-substrate was supported by simulated results using a kinetic model (this analysis incorporated the collective data from a large number groups collected over a considerable amount of time). When the intracellular concentrations and high Km values were taken into account, the predicted intermediate concentration was similar to the experimental measurements. The results demonstrate the controlling roles that precursors and co-factors may play in the biosynthesis of secondary metabolites.

The fundamental principles of MCA require a basic knowledge of mathematics, which biologists either often lack or are reluctant to gain. The added disadvantage of large quantities of techno babble and the majority of papers in this field lacking any experimental evidence; have ultimately become MCA greatest disadvantage.

Appendices A to D offer a practical approach to the theories described in this Chapter. What should be ascertained from this Chapter and the appendices is that these approaches are unifying in nature i.e. compositional data and the draw of carbon to biosynthesis from flux-based strategies are needed to build on better matrix-algebra models, which in turn can only lead to a better understanding of kinetic-based strategies such as MCT, MCA, &

BST (Covert *et al*., 2001; Stephanopoulos *et al*., 1998; for more detailed discussions of the future goals and direction of the latter fields).

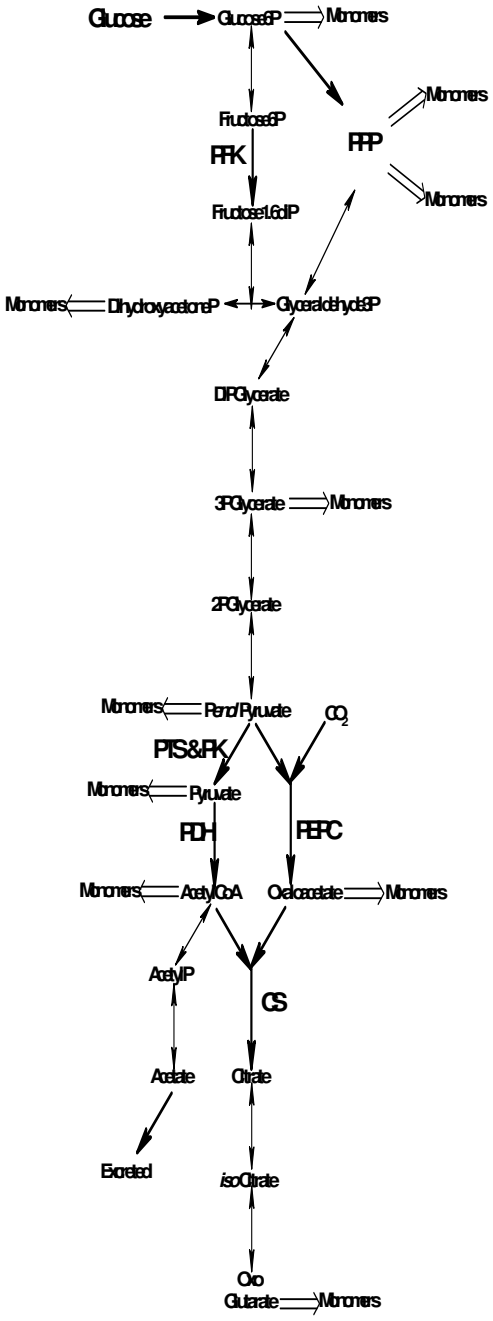

PEP: glucose transferase system

(1) Glc + = G6P + PYR

Storage compound: trehalose

(2) G6P + 0.5 ATP = 0.5 Trehal + 0.5 ADP

Embden-Meyerhof-Parnas pathway

(3) G6P = F6P

(4) F6P + ATP = 2 GAP + ATP

(5) GAP + ADP + NAD = NADH + G3P + ATP

(6) G3P = PEP + H_2O

(7) PEP + ADP = ATP + PYR

(8) PYR + NADH = LAC + NAD

Anaplerotic reaction: PEP carboxylase

(9) PEP + CO_2 = OAA

TCA cycle

(10) PYR + COA + NAD = ACCOA + CO_2 + NADH

(11) ACCOA + OAA + H_2O = ISOCIT + COA

(12) ISOCIT + NADP = AKG + NADPH + CO_2

(13) AKG + COA + NAD = SUCCOA + CO_2 + NADH

(14) SUCCOA + ADP = SUC + COA + ATP

(15) SUC + H_2O + FAD = MAL + FADH

(16) MAL + NAD = OAA + NADH

Acetate production or consumption

(17) ACCOA + ADP = AC + COA + ATP

Glutamate, glutamine, alanine, and valine production

(18) NH3 + AKG + NADPH = GLU + H_2O + NADP

(19) GLU + NH3 + ATP = GLN + ADP

(20) PYR + GLU = ALA + AKG

(21) 2 PYR + NADPH + GLU = VAL + CO_2 + H_2O + NADP + AKG

Pentosephosphate pathway

(22) G6P + H_2O + 2 NADP = RIBU5P + CO_2 + 2 NADPH

(23) RIBU5P = RIB5P

(24) RIBU5P = XYL5P

(25) XYL5P + RIB5P = SED7P + GAP

(26) SED7P + GAP = F6P + GAP

(27) XYL5P + E4P = F6P + GAP

Oxidative phosphorylation

(28) 2 NADH + O_2 + 4 ADP = 2 H_2O + 4 ATP + 2 NAD

(29) 2 FADH + O_2 + 2 ADP = 2 H_2O + 2 ATP + 2 FAD

Aspartate amino acid family

(30) OAA + GLU = ASP + AKG

(31) ASP + PYR + 2 NADPH + SUCCOA + GLU + ATP SUC + AKG + CO_2 + LYS + 2 NADP + COA + ADP

(32) LYS_{int} = LYS_{ext}

Biomass synthesis $C_{1.97}H_{6.46}O_{1.94}N_{0.345}$, 3.02 % ASH

(33) 0.021 G6P + 0.007 F6P + 0.09 RIB5P + 0.036 E4P + 0.013 GAP + 0.15 G3P + 0.052 PEP + 0.03 PYR + 0.332 ACCOA + 0.08 ASP + 0.033 LYS_{int} + 0.446 GLU + 0.025 GLN + 0.054 ALA + 0.04 VAL + 0.052 THR + 0.015 MET + 0.043 LEU + 3.82 ATP + 0.476 NADPH + 0.312 NAD = BIOMASS + 3.82 ADP + 0.364 AKG + 0.476 NADP + 0.312 NADH + 0.143 CO_2

(34) ATP = ADP + Pi

Fig 1.1 The above bioreaction network describes the biochemistry of glutamic acid bacteria. The PhD thesis of J.J Vallino and references therein can be consulted for evidence of the detected enzymatic activities that support the biochemistry depicted. This incorporates glucose-processing, ammonia uptake, and product forming pathways (Vallino, 1991).

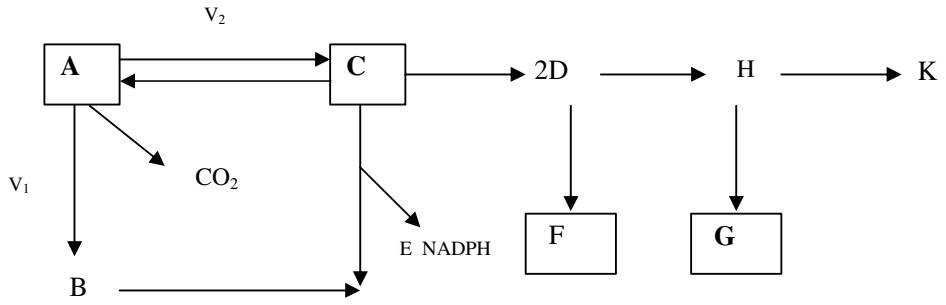

Fig 1.2 Schematic of flux split in a metabolic network that is only partially resolved by the extracellular metabolite (in boxes); Stephanopoulos *et al*. (1998).

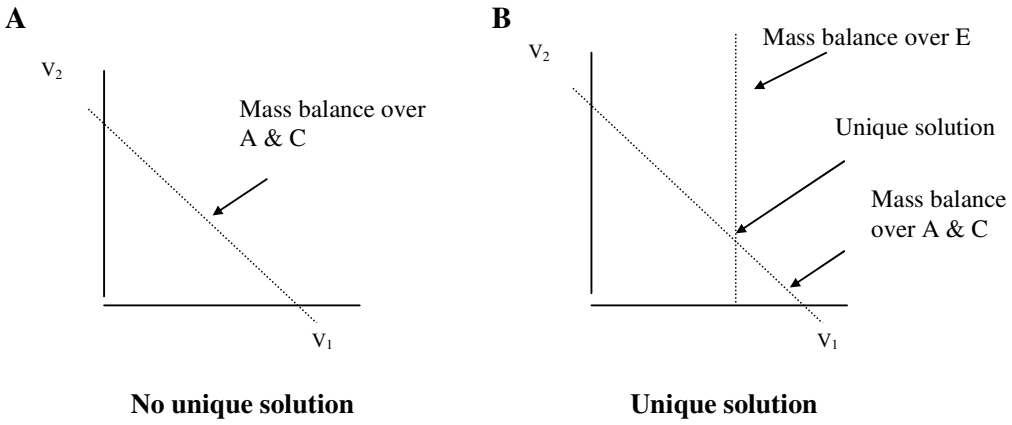

Fig 1.3 Fluxes in cyclic pathways without (A) and with (B) a co-metabolite (Based on Bonarius, 1998). (Numerical values are chosen arbitrary).

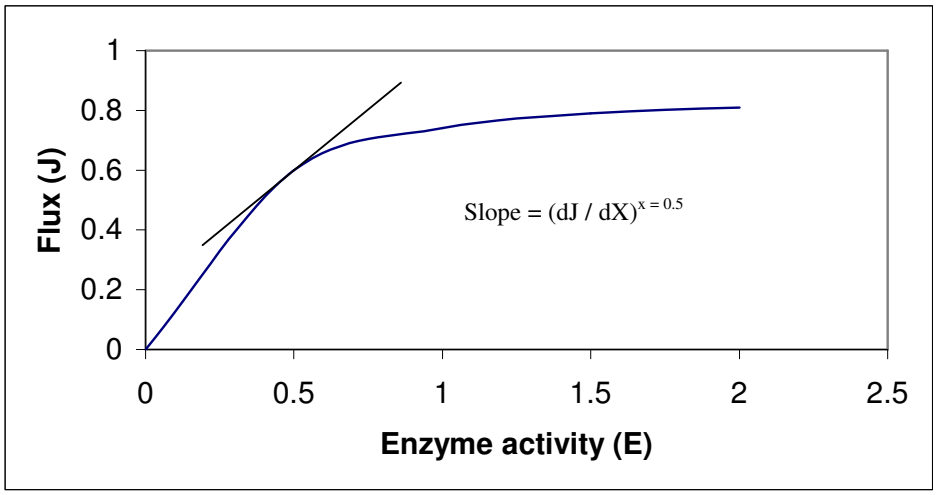

Fig 1.4 Scheme of the steady-state pathway flux J as a function of the activity of an intermediate enzyme in the pathway. The flux control coefficient for the enzyme at a particular enzyme activity is found by multiplying the slope of the tangent at that enzymatic activity by the enzyme activity and normalising with respect to the steady-state flux (taken from Stephanopoulos *et al*., 1998).

Chapter 2

A review of cellular metabolism: *Streptomyces*

2.0 Introduction

Streptomycetes are Gram-positive, spore-forming, saprophytic, soil bacteria. Furthermore streptomycetes are members of the same taxonomic order, *Actinomycetales* (Lechevalier & Lechevalier, 1981), as the causative agents of tuberculosis, diphtheria, & leprosy (*Mycobacterium tuberculosis*, *Corynebacterium diphtheriae*, & *Mycobacterium leprae*). The genomes of these pathogens have been sequenced (Cole *et al*., 1998; http: http://www.sanger.ac.uk/Projects/C_diphtheriae/; Cole *et al*., 2001). Streptomycetes do not cause disease, with the exceptions of the plant pathogen *Streptomyces* s*cabies,* and *S. ipomoea*, and *S. somaliensis,* which have been associated with actinomycetoma of animals, including man (Hodgson, 2000). In fact, the characteristic earthy odour of soil, is caused by the production of a series of streptomycete metabolites called geosmins (Broch, 2000). These are sesquiterpenoid compounds, a common geosmin is trans-1,-10-di-methyl-trans-9-decalol (Jachymova *et al*., 2002 for a diverse analytical analysis of the number and identity of these compounds in *Streptomyces*). The genus is defined by both chemotaxonomic and phenotypic characteristics. The major emphasis is on 16S rRNA homologies, in addition to cell wall analysis, fatty acid (FA) and lipid patterns (Williams *et al*., 1989; Wellington *et al*., 1992). One of the quickest methods for preliminary identification is the presence of the LL-isomer of diaminopimelic acid (LL-DAP) as the diamino acid in peptidoglycan. They secrete extracellular enzymes and absorb the soluble breakdown products from the interaction of these enzymes with insoluble polymers, such as protein, starch and cellulose (Hodgson, 2000). Their ecological niche is carbohydrate-rich but relatively nitrogen- and phosphate-poor (oligotrophic). Therefore streptomycetes have evolved novel methods to compete with bacteria, fungi and protozoa (Hodgson, 2000; Janecek *et al*., 1997; for reviews of the metabolic type of *Streptomyces*). Perhaps the most striking property of the streptomycetes is the extent to which they produce antibiotics (Watve *et al*., 2001 for a review of the number of known antibiotics, against the estimated occurrence of antibiotics in nature). They are unusual bacteria, which undergo complex morphological development.

Many aspects of their morphology and metabolism are analogous to fungi, which historically caused confusion over their classification (Hopwood, 1988).

2.1 Genomic era of *Streptomyces*

S. coelicolor (Hopwood, 1959; 1999) is genetically the most-studied strain of the streptomycetes. In July 2001, the genome of *S. coelicolor* was completely sequenced and annotated at the Sanger Centre (http://www.sanger.ac.uk/project/S_coelicolor) [Bentley *et al*., 2002]. Analysis has revealed a single linear chromosome (Volff & Altenbuchner, 2000; Chen *et al*., 1993) of more than 8.66 million base (Mb) pairs of DNA compared with just over 4 Mb for such organisms as *E. coli* & *Bacillus subtilis* (Bentley *et al*., 2002). They have a centrally-located origin, of replication, and a G+C content of 72.1 %. There are 7825 predicted genes, so the chromosome has an enormous coding potential. This compares with 4289 genes in *E. coli* 4099 in *B. subtilis* 6203 in the lower eukaryote *S. cerevisiae*; and a predicted 31780 in humans (http://www.ebi.ac.uk/genomes/)[Bentley *et al*., 2002]. The genome contains almost twice as many genes as that of *M. tuberculosis* (Cole *et al*., 1998). The genome shows a strong emphasis on regulation, with 965 proteins (12.3 %) predicted to have regulatory function and many duplicated gene sets that may re-present tissue-specific isoforms operating in different phases of colonial development a unique situation for any bacterium. There is a clear preference for carbon regulation. *S. coelicolor* codes for a remarkable 65 sigma factors, the next highest number so far found is 23 in *Mesorhizobium loti*, with a genome size of 7.6 Mb (Kaneko *et al*., 2000). Sigma factors act by binding to the RNA polymerase core enzyme, thus directing the selective transcription of gene sets. *S. coelicolor* also has an abundance of two-component regulatory systems. They typically act, in response to an extracellular stimulus via an integral membrane sensor protein that phosphorylates a response regulator, causing it to bind to specific promotor regions and then activate or repress transcription. Bentley *et al*. (2002) identified 85 sensor kinases and 79 response regulators, including 53 sensor-regulator pairs.

The *S. coelicolor* genome reveals much similarity at the level of individual gene sequences, and many similar gene clusters, near the centre of the chromosome compared to *M. tuberculosis*, *C. diphtheriae*, & *M. leprae*. The most strongly conserved is the gene cluster coding for the subunits of respiratory chain NADH dehydrogenase (systematic gene

numbers SCO4562-4575); the origin of replication (SCO3873-3892); urease activity (SCO1231-1236); pyrimidine biosynthesis (SCO1570-1580); pentose phosphate pathway / tricarboxylic acid cycle (SCO1921-1953); histidine and tryptophan biosynthesis (SCO2034-2054); cell division (SCO2077-2092); and ribosomal proteins (SCO4701-4724) (Bentley *et al*., 2002).

The genome sequence of *S. avermitilis* which is of industrial importance, has been completed (Omura *et al*., 2001; Ikeda, 2003). Initial comparative studies (Omura *et al*., 2001) have shown that, at least 8.7 Mb exist in the linear chromosome and twenty-five different gene clusters coding and regulating secondary metabolites have been identified in the genome. Virtually none of these clusters were located near the centre of the chromosome. The total length of these clusters occupies about 6.4 % of the genome. *S. coelicolor* appears to contain a different set of gene clusters for secondary metabolism from *S. avermitilis*. It may be that the chromosomal arm regions of different streptomycetes have been accumulated and evolved separately, and therefore contain a largely different complement of secondary metabolite genes representing a huge pool of metabolic diversity.

2.2 Development cycle of Streptomycete colony

Although they share a mycelial growth form, filamentous fungi and streptomycetes (as eukaryotes and prokaryotes, respectively) exhibit major differences at the cellular level. Fungi posses membrane-bound organelles and a cytoskeleton, providing sub cellular growth. These are absent in *Streptomyces*, which therefore must possess different growth mechanisms. Another major difference is the size of fungal hyphae. Fungal hyphae are typically an order of magnitude greater in diameter than those of streptomycetes. Despite these differences the two groups show remarkable similarities, providing an example of convergent evolution.

Streptomycetes exhibit a complex growth cycle with differing morphological states (Fig 2.1). Germination can be partially density-dependent, but the interaction does not cross species boundaries (Triger *et al*., 1991), suggesting that special signaling factors between spores of the same strain, cause inhibition of germination above a certain concentration. The advantage would be to limit the number of germinating spores in accordance with available nutrients.

One of the problems of a saprophytic life cycle, in which insoluble polymers are digested and the resulting monomers and oligomers are imported and used for biomass accumulation, is that this process takes time and relies on a high concentration of the digestive enzymes. A number of microbes have utilised substrate mycelium to solve this problem.

The cycle begins with the spore, which may lie dormant in the soil for many years. When nutrients and water become available, the spore germinates and outgrowth takes place (Fig 2.1). These organisms are said to be mycelial in nature, as they colonise soil particles by extending outwards in all directions (radial growth) in a fixed branched pattern. This is often called vegetative mycelium. They are immobile, other than having movement by growth, and burrow into the insoluble food matrix, digesting it as they grow. This immobility, thus increases the local concentration of the digestive enzymes, in turn the local concentration of digestive product is also kept high.

Inevitably, at some point, nutrients or water become in short supply and it is at this point that they differentiate, ultimately to form spores again. Initially, the differentiation process involves the formation of aerial mycelium in which the biomass no longer extends out radially, but rises up away from the plane of the radial growth and forms elaborate coiled structures which then septate after awhile and the spores are formed again. This spore-bearing mycelium gives the colony a white hairy appearance. There is direct evidence that the substrate hyphae lyse and the products of lysis are cannibalised by the growing aerial hyphae. Antibiotics are made at the time of differentiation between the vegetative mycelial and the aerial mycelial stages. Once a colony is washed with water the hydrophobic spores are released into the environment, owing to the surface tension. Streptomycete spores are not very resistant to environmental extremes e.g. temperature & pH. They are more resistant to desiccation than hyphal fragments. However, this probably reflects the biological role of *Streptomyces* spores i.e. as dispersal agents rather than resting stages (Hodgson 2000). Chater (1998) and Kelemen & Buttner (1998) have written reviews on the involvement of gene control in streptomycete differentiation, and Hodgson (1982; 2000) has reviewed physiological aspects.

In liquid culture, mycelia of such microorganisms are generally considered to be in either pellet (spherical agglomerates of one or more hyphal elements) or filamentous form

(dispersed as individual elements). In the latter case, hyphal entanglement can cause the suspension to be highly viscous and non-Newtonian. Liquid cultures do not follow the same morphological cycle as cultures grown on solid surfaces (soil or agar). Ideally, they go through a series of comparable physiological changes, starting with vegetative growth and switching to secondary metabolite synthesis when growth slows (Hopwood *et al*., 1992; Hopwood, 2000)[there is not enough space in this thesis to discuss the intricacies of mycelial differentiation and metabolic regulation but the following offer good reviews: Chater, 1989; Nielsen, 1996]. Two metabolically-distinct phases of culture development result: the trophophase when resources are committed to rapid growth, and the subsequent idiophase in which secondary metabolites are made (Bu'Lock, 1961). However, association with the idiophase is not a mandatory feature of secondary metabolism (Demain *et al*., 1983; Doull & Vining, 1990).

Both morphological and physiological differentiation, require different genes to be switched on at different times. Exactly which signals in the environment are recognised, and how such messages are communicated to the level of the gene, is not fully understood. However, different aspects of this intricate network have been elucidated in certain species of *Streptomyces*. Han *et al*. (1999) investigated the activity and distribution of the rate limiting enzyme lysine-6-aminotransferase (LAT)[the first rate limiting enzyme in the biosynthetic pathway of cephamycin C] by constructing green fluorescent protein (GFP) and LAT fusion protein (LAT-GFP) in *S. clavuligerus* and observing mycelia during various stages of cultivation. Using confocal microscopy it was demonstrated that the expression of LAT quickly diminished after inoculation from seed culture into the main culture. It reappeared only in some mycelia in early exponential phase. All mycelia became fluorescent in late exponential phase and green fluorescence diminished again in stationary phase. In solid phase analysis, abundant LAT expression was evident in the substrate mycelia but was completely absent in aerial hyphae (Han *et al*., 1999).

Studies have hinted at possible mechanisms involved in the regulation of secondary metabolism in streptomycetes. These involve rare codons (a good example is *bld*A gene of *S. coelicolor* which encodes a tRNA gene, Leu-tRNA, that reads a rare codon UUA) that are required for translation of a number of pathway-specific regulators of metabolite production; i.e. *act*II ORF4 and *red*Z for actinorhodin (ACT) and undecylprodigiosin (RED)

respectively [Guthrie *et al*., 1998; Szeszak *et al*., 1991; Leskiw *et al*., 1991a, b]). Pheromones (Horinouchi & Beppu, 1988), and possibly guanosine 5' diphosphate 3' diphosphate (ppGpp) or other mediators of the stringent response (Kelly *et al*., 1991; Strauch *et al*., 1991; Holt *et al*., 1992; Jones *et al*., 1996; Chakraburtty *et al*., 1996; Chakraburtty & Bill, 1997; An & Vining, 1978), and two-component sensory receptor/transcriptional activation function probably also play roles in secondary metabolite production.

2.3 Problems of studying primary metabolism

As has already been discussed, the streptomycete colony consists of a number of different cell types. Within any one of these cell types new metabolic pathways may be activated, and it may be difficult to distinguish between metabolites that are involved in differentiation and secondary metabolites. Claims have been made that in liquid culture the cells are exclusively of substrate mycelium. However, there have been reports that some streptomycetes can produce spores in liquid culture and that others can go through a microsporulation cycle (Hodgson, 1982; 2000). Metabolic differentiation is unlikely to be a synchronous event especially in liquid culture, which is a problem when studying streptomycete metabolism. It is exacerbated by the tendency of *Streptomyces* to form pellets and for growth to occur on the walls of the container above the liquid air/interface during liquid culture, especially in minimal & defined media. Pellet formation may hinder analysis and the exterior of the pellet will be in a different physiological state from those on the inside.

Liquid culture is the easiest way to obtain biomass for physiological studies and a number of methods have been used to minimise pellet growth. These include the use of baffles, springs & glass beads in the vessel and the incorporation of polymeric molecules (e.g. junlon & polyethylene glycol)[Hodgson, 1982]. Such actions, however circumvent one problem and cause others, as it is hard to remove these polymers from the sampled biomass (Hobbs *et al.*, 1989; Davidson, 1992).

Another problem of studying primary metabolism in *Streptomyces* is the nature of the strains used. If a comparison of primary metabolism is to be made, it is essential that the production of the secondary metabolite is consistently inducible and is produced at such a

level that it is easily assayable. This represents a problem, in that any strain isolated directly from the environment may not produce large quantities of the secondary metabolite. Therefore, there is the temptation to use strains that have been improved for metabolite production and compare them with still more highly producing strains. The potential problem with this approach is that the improvement of secondary metabolite yield may have come about by the specific deregulation of the metabolic events that one is hoping to study. This should be considered carefully, as random mutation may lead to increased yield in the short term, by inactivating pathways that may need to be reintroduced to achieve even higher yields in subsequent stages of a strain improvement program.

An additional problem arises when analysing metabolism, with the term biomass, which would initially appear to be a simple issue; but what is actually meant by this term is subject to conjecture and the answer to the question 'what is biomass?' (Mousdale, 1997) will be dependent on the objective of the researcher involved. Biomass, for example could be the number of cells visible under a microscope. However, this is also difficult to determine if filamentous cells are to be considered. It could also mean the number of cells possessing an intact membrane, but then again other issues are raised such as viability. Does a cell with an intact membrane have the necessary cellular machinery for carrying out the desired task? Or could it very simply mean the mass of the cells present. The arguments are endless, but it is clear that, before establishing which method to quantify biomass, the criteria necessary for any particular application should be assessed.

2.4 Carbohydrate uptake systems

Hexoses appear to be taken up in streptomycetes by an active transport system (Hodgson, 2000). In *S. clavuligerus*, glucose kinase activity was found to be a soluble intracellular activity and therefore not involved with transport. This was not surprising, as the strain could not use glucose as sole energy or carbon source. The strain could however use starch and maltose, which implied that there was a lesion in glucose transport, i.e. maltose and other starch degradation products could get into the cell where they were broken down to glucose and then phosphorylated. Garcia-Dominguez *et al*. (1989) confirmed this hypothesis when using respiratory inhibitors and proton-conducting ionophores, they found transport to be energised by the proton motive force. Glucose transport systems have been found in *S. violaceoruber* (Sabater & Asensio, 1973a) and in *S. antibioticus* (Salas & Hardisson, 1981)

spores. A number of carbohydrate (CHO) uptake systems have been identified and studied in streptomycetes. They are classified into two types; inducible and constitutive (a good review of inducible anabolic and catabolic enzymes can be found in Hodgson [2000]). The inducible CHO transport systems are generally induced by the substrate.

The mechanism of sugar uptake has been described for only a few CHOs (Parche *et al.*, 1999). It has been demonstrated five component biochemical ATP-binding cassette (ABC) permeases are important for transport of maltose in *S. coelicolor* (Von Wezel *et al.*, 1997a, b); cellobiose / cellotriose in *S. reticuli* (Schloesser & Schrempf, 1996; Schloesser *et al.*, 1997; 1999); and cellobiose, xylobiose and maltose in *S. lividans* (Hurtubise *et al*., 1995; Schloesser *et al*., 1997). The *S. coelicolor* genome sequence has 614 proteins (7.8 %) with predicted transport function. A large proportion of these are of the ABC transporter type, including 81 typical ABC permeases and 141 ATP-binding proteins (24 of which are fused to membrane-spanning domains)[Bentley *et al*., 2002]. A specific cellobiose-binding lipid anchored protein has been identified in *S. reticuli* (Hodgson, 2000). This protein is found in the periplasm of Gram-negative bacteria. Streptomycetes do not have a periplasm and therefore periplasmic proteins have to be anchored by a FA adduct, in this case palmitate (Schloesser & Schrempf, 1996). In some cases, oligo and disaccharides may be present inside and outside the cells, and it would be an competitive advantage to be able to transport a complex carbon and energy source into the cell (Hodgson, 2000).

In the Gram-negative and low G+C Gram-positive bacteria, the glucose- phosphotransferase system (PTS) plays a central role in carbon catabolite repression (CCR). The effect is exerted through exclusion and by precluding the expression of genes that require the adenosine 3'-5' cyclic monophosphate (cAMP) catabolite control protein complex for transcriptional activation. cAMP involvement in CCR in streptomycetes is still open to question (Tata & Menawat, 1994; Chatterjee & Vining, 1982a, b; Colombo *et al*., 1982). The PEP-PTS is fundamental in the control of catabolite repression (CR) in low G+C Gram-positive bacteria. Attempts to find a PEP-coupled phosphotransferase system (PEP-PTS) for glucose transport & phosphorylation in streptomycetes have proved unsuccessful. The PTS is a glucose uptake system found in *E. coli* and many other facultative anaerobic bacteria (Postma & Lengeler, 1985) in which free glucose outside the cell is phosphorylated and released into the cytoplasm as glucose-6-phosphate (G6P); phosphoenolpyruvate (PEP) acts

as the ultimate donor of the phosphate group. Titgemeyer *et al.* (1995) presented evidence for the presence of a PEP-PTS for fructose transport in *S. lividans*, *S. coelicolor* and *S. griseofuscus*. The presence of PTS components, resembling EI, HPr and a fructose-specific enzyme II; have been reported (Titgemeyer *et al*., 1994, 1995; Parche *et al*., 1999). The system was inducible by fructose in the first two strains and constitutive in the third. Specific fructose transport was not assayed, but membrane-bound PEP-dependent phosphorylation of fructose was observed, in addition to a soluble ATP-dependent fructose phosphorylation in *S. lividans* & *S. coelicolor* (Hodgson, 2000). There was already evidence of an ATP-dependent fructose kinase in the closely-related *S. violaceoruber* (Sabater *et al.*, 1972b). The constitutive PEP-dependent and ATP-dependent fructose phosphorylation activities found in *S. griseofuscus* were lower than the other two streptomycetes, and there was only poor evidence for a membrane-bound PEP-dependent phosphorylation of fructose in this streptomycetes (Hodgson, 2000). No PEP-dependent phosphorylation activity was found in any of the streptomycetes, nor were the HPr (Ser) kinase or HPr (Ser-P) phosphatase activities found (Hodgson, 2000). This implied *S. coelicolor* had fewer *pts* genes than *E. coli* which has several dozen and *B. subtilis* with 27 *pts* genes (Saier *et al*., 1994; Reizer *et al*., 1999). Nevertheless, more *pts* genes are present in *S. coelicolor* (obtained from a comparative analysis of the *S. coelicolor* genome sequence, Parche *et al*., 2000) than in the genomes of *Mycoplasma genitalium* or *Haemophilus influenzae*. That have five and seven *pts* genes, respectively and fully functional PTSs (Macfadyen *et al*., 1996; Reizer *et al*., 1996a, b, c).

2.4.1 Glucose repression

The apparent lack of a PTS system for glucose uptake in streptomycetes (Titgemeyer *et al.,* 1995) also suggests that the mechanism of glucose repression in these organisms may be very different from that in *E. coli* (Paulsen, 1996; Angell *et al.,* 1992). In *S. coelicolor*, glucose represses the expression of many genes involved in the utilisation of alternative carbon sources (e.g. arabinose, glycerol) (Hodgson, 1982; Smith & Chater, 1988; Delic *et al.,* 1992; Angell *et al.,* 1994; Hindle & Smith, 1994). The ATP-dependent glucose kinase (*glk*A) of *S. coelicolor* plays a crucial role in CCR. Although glucose transport is not affected in *glk*A mutants, they cannot utilise glucose, and glucose repression of a wide variety of genes involved in the utilisation of alternative carbon sources is relieved (Angell

et al., 1994). The ability of alternative GlkAs to restore glucose repression in *glk*A mutants suggests a direct regulation role of glycolytic flux (Angell *et al*., 1994). Furthermore, the role of GlkA appears to extend beyond glucose repression: *glk*A mutants are deficient in CCR when the repressing carbon source is not metabolised via GlkA (Kwakman & Postma, 1994). In this case GlkA may mediate glucose repression via the synthesis of a metabolite that acts as a repressing signal, with G6P being the best candidate. Alternatively, GlkA may function more directly in mediating glucose repression through interaction or modification of a regulatory protein that interacts with the promoter regions of glucose repressible genes (Angell *et al*., 1992). It is also conceivable that the glycolytic flux increases when glucose is phosphorylated and that this is an important signal in the glucose repression pathway (Angell *et al.,* 1992). Ingram *et al*. (1995) report the identification and characterisation of a mutation in *S. coelicolor*, that has a pleiotropic effect on several catabolite controlled promoters and they also suggest that glucose repression of *chi63* (chitinase gene) is independent of glucose kinase and there may be more than one mechanism of glucose repression in *Streptomyces* spp.

2.4.2 Catabolite repression

Carbon catabolite repression (CCR) is a wide-spread phenomenon which can be defined as the repression of enzyme synthesis by the presence of a catabolite in the growth medium, or a hierarchical use of carbon sources. Although this can be any catabolite, most interest has focused on the mechanism of repression by glucose. Catabolite repression (CR) is best understood in enteric bacteria where the PEP-dependent saccharide-PTS [see section 2.4 for a discussion of the involvement of the PTS in streptomycete metabolism] fulfills a dual role: it regulates the uptake of substrates (or the generation of cytoplasmic inducers) for CR sensitive pathways and also modulates the synthesis of cyclic 3,5-AMP (cAMP). The intracellular concentration of cAMP is controlled by, synthesis from ATP by adenyl cyclase, and destruction by cAMP phosphodiesterase and export out of the cell. The DNA binding cAMP receptor protein (CRP) is the key regulatory protein of the regulon (Kolb *et al*., 1993; Hindle and Smith 1994). A number of catabolite operons (e.g. lactose, galactose, arabinose and histidine) are dependent on the presence of the cAMP-CRP complex for expression of genes at levels required for catabolism of their substrate. If intracellular concentration of cAMP is high, the cAMP-CRP complex forms and binds to DNA, leading to the binding of

RNA polymerase holoenzyme by specific protein-protein interactions; provided, of course, there are no repressors to interfere in this interaction. The RNA polymerase can now initiate transcription of the operon, provided the appropriate inducers or anti-repressors are present.

In contrast to the enteric bacteria where the PTS and cAMP appear to play major roles, several studies on Gram-positive bacteria including *Bacillus* and *Streptomyces* species indicate that cAMP does not play a role in CR in these genera. In *Bacillus subtilis*, which has a functioning PTS, the inability to detect cAMP (Setlow 1973) except in conditions of oxygen stress (Mach *et al*., 1988) suggests that it is unlikely to be involved in CCR. Attempts to implicate cAMP as the regulatory molecule of CCR of both primary and secondary metabolism have failed to provide unambiguous results in all the streptomycetes examined. In a number of cases (Gersch & Strunk, 1980; Surowitz and Pfister, 1985b; Lishnevskaya *et al*., 1986) it was found that, in contrast to what is seen in *E. coli*, intracellular cAMP concentration was greatest in media containing glucose where growth rate was highest and lowest in media containing either no carbon and energy source or one that could not be catabolised. In contrast, Dobrova *et al*. (1984) reported that total and intracellular concentration of cAMP in *S. granaticolor* was lowest during active growth and increased only after growth had ceased. However, they reported that cAMP synthesis was possible only in the presence of a carbon and energy source, and confirmed that adenyl cyclase was most active in cells with a utilisable carbon and energy source. In this case it appeared that cAMP had the kinetics of a secondary metabolite. Additional correlations of growth events with cyclic nucleotide metabolism in streptomycetes have been reported. Gersch & Strunk (1980) and Amini (1994) reported that cAMP synthesis in *S. hygroscopicus* and *S. coelicolor*, respectively, was correlated with spore germination, although addition of exogenous cAMP inhibited germination of the former streptomycete.

Catabolite repression of the production of secondary metabolites by carbon and nitrogen sources has been discussed in a number of review articles e.g., Doull and Vining 1990; Vanek *et al*., 1988, 1990; Janecek *et al.*, 1997; Paulsen, 1996; Aharonowitz, 1980; Drew, 1977; Demain, 1979, 1980, 1986, 1992. Where CCR of carbon sources in the growth medium can be considered as hierarchical, CR of secondary metabolism leads to the repression or total inactivation of a pathway. A lower sensitivity to CR is a frequent phenomenon in high production strains (Wittler and Schugerl 1985).

Ikeda *et al*. (1988) showed that the addition of glucose in the early stage of fermentation suppressed not only avermectin production but also the activity of 6-phosphogluconate dehydrogenase (6PGDH) in the pentose phosphate pathway. On the other hand, when glucose was added at a late stage of fermentation, suppression of avermectin formation and 6PGDH activity was not observed but avermectin formation was increased. Glucose repression of uptake and/or metabolism of several other sugars was observed in *S. coelicolor* (Hodgson, 1982; Hodgson, 2000). Although *S. fradiae* is not reported to show CCR arising from glucose (Choi *et al*, 1998a, b), high transient glucose uptake rates have been shown to suppress tylosin production (Gray & Vu-Trong, 1987a, b; Sprinkmeyer & Pape, 1978; Gray & Bhuwapathanapun, 1980a, b). When glucose is added to a culture that is already in the idiophase, tylosin production halts (Gray & Bhuwapathanapun, 1980a, b; Tata & Menawat, 1994), production resumes at rates similar to those of the control, once the added glucose is metabolised, suggesting that glucose addition caused a repression effect on carboxylating enzymes, which showed reduced enzyme activities (Vu-Trong *et al*., 1980). However, these results do not explain the severe repression of tylosin synthesis. There is evidence that polyketide synthases (PKS) are repressed by glucose. Gallo & Katz (1972) showed that phenoxazinone synthase, a component of actinomycin chromophore, was repressed by glucose in this manner.

The synthesis of tylosin by *S. fradiae* is also inhibited by high phosphate concentrations (Madry *et al*, 1979; Vu-Trong *et al*., 1981; Gray & Bhuwapathanapun, 1980). Phosphate control of tylosin formation may be explained in part by the inhibition of FA degradation (Madry *et al*., 1979); the catabolism of long chain FAs leads to an enhanced precursor supply for the biosynthesis of tylactone (Sprinkmeyer & Pape, 1978; Vu-Trong *et al.*, 1980). Early addition of elevated levels of inorganic phosphate to *S. fradiae* cultures represses/reduces the activities of methyl-malonyl-CoA carboxyltransferase (MMCT) and propionyl-CoA carboxylase (see section 2.10.1). Observations suggest that the level of the adenylate pool rather than the adenylate energy charge probably play a more significant role in mediating phosphate control (Vu-Trong & Gray, 1982; Vu-Trong *et al*., 1980; 1981). The tylosin enzymes were not shown to be inhibited by physiological concentrations of ATP, G6P, phosphate or tylosin (Madry & Pape, 1982). There is also no indication of end product inhibition of hexokinase (HK), dTDP-D-glucose-4,6-dehydratase & macrocin-O-

methyltransferase influence on the tylosin biosynthetic pathway [see section 2.10.3] (Martin & Demain, 1980).

Data indicating that biosynthesis of secondary metabolites is repressed by excess NH_4 ions or by unsuitable amino acids (aas) are relatively frequent in the literature (Aharonowitz, 1980; Martin and Demain, 1980; Brana and Demain, 1988; Cimburkova *et al*., 1988; Bascaran *et al*. 1989a, b). The significance of the carbon-nitrogen ratio has often been stressed and a ratio of 10 : 1 has been considered as optimum (4 : 1 has been routinely used throughout the literature for *S. fradiae* [Sprinkmeyer & Pape, 1978; Gray & Bhuwapathanapun, 1980]). The common usage of soya meal in cultivation's of actinomycetes is apparently due to its slower utilisation during which NH_4 ions and repressive aas do not accumulate. In chemically defined media a slowly utilisable aa is commonly used as a nitrogen source (Demain, 1986).

In *S. fradiae* there is a strong correlation between nitrogen metabolism and biosynthesis of tylosin; tylosin production is stimulated by valine catabolism, by two valine dehydrogenase (VDH) isoenzymes (Nguyen *et al*., 1995; Vancura *et al*., 1987a; Vancura *et al.*, 1988a,b; for kinetics of repression of VDH see Lee & Lee, 1994; Lee, 1997) a key enzyme involved in propionate formation [see section 2.10.3] (Omura and Tanaka, 1986; Omura *et al*., 1983a, b). Ammonium ions also regulate the biosynthesis of FA units and aas (Vancura *et al*., 1987a, b; 1988a, b). The enzymes involved are NADP dependent glutamate dehydrogenase (Vancurova *et al*., 1989), alanine dehydrogenase (Vancura *et al.,* 1989) and threonine dehydratase (TDT)[Vancura *et al*., 1988a; Lee & Lee, 1991; 1993]. Ammonium has also been shown to be a strong repressing agent for other streptomycetes e.g., *S. noursei* (glutamate dehydrogenase; Grafe *et al*., 1979); *S. venezuelae* (proline transport; Shapiro & Vining, 1984); *S. niveus* (proline transport; Kominek, 1972); *S. michiganensis* (tyrosinase; Held & Kutzner, 1990). Natural zeolite and magnesium ion trapping agents have been shown to reduce NH_4 ion repression in a number of streptomycetes (Lee & Rho, 1999).

When investigating the control of spiramycin production by nitrogen CR in *S. ambofaciens* interesting results were obtained concerning the adaptability of streptomycete cells to environmental conditions during the first hours of cultivation (Untrau *et al*., 1994). Addition of NH_4 (25 $mmol.l^{-1}$ NH_4C1) at the beginning of cultivation stimulated spiramycin

production by about 23 %. Addition of NH_4 after 1 day of cultivation had no effect on the total yield of spiramycin. Under these conditions, spiramycin production was delayed for approximately 1 day. There was a critical phase (between 2 and 3 day) in the growth phase, during which excess of NH_4 ions had a maximum inhibitory effect on spiramycin biosynthesis.

2.5 The Central Metabolic Pathways

2.5.1 The Embden-Meyerhof-Parnas pathway

The Embden-Meyerhof-Parnas pathway (EMP) or glycolysis (Table 2.1 & Fig 2.2) is the central pathway of CHO metabolism present in almost all cells (Fothergill-Gilmore & Michels, 1993). It is evolutionary one of the earliest pathways for sugar degradation. Since enzymes belonging to this route (or modified ones) were also shown to be present in Archaea such as *Thermoproteus tenax* (Siebers & Hensel, 1993) and in the hyperthermophilic anaerobic bacterium *Thermotoga maritima* (Schröder *et al.,* 1994). The lower part of the EMP (trioses) is the most, conserved section, which also serves anabolic and catabolic processes (Dandekar *et al*., 1999; for a comparative analysis of various genomes). It has more stringent requirements for being maintained. It seems to be the older part of this metabolic pathway. A modified pathway with ADP-linked kinases was found in the hyperthermophilic archaeon *Pyrococcus furiosus* (Kengen *et al.,* 1994, 1996). The EMP serves various functions in cellular metabolism. During the breakdown of sugar molecules the favourable free energy of some reactions is harnessed to drive other cellular processes. Reducing equivalents are made available to the cell and building blocks are provided for the synthesis of for instance aas, FAs and sterols. The glycolytic pathway also shares branch points with other metabolic systems such as gluconeogenesis, the pentose phosphate pathway (PP pathway) and the TCA cycle (i.e., fructose 1,6-bisphosphate aldolase, phosphofructokinase, phosphoglycerate kinase, glyceraldehyde-3-phosphate dehydrogenase, & triose phosphate isomerase). In order to control these reactions and to adjust the glycolytic flux to the cellular needs for energy and for precursors of biosynthetic pathways, a number of control mechanisms have evolved. Two major control points have been identified, involving enzymes that catalyse irreversible steps: phosphofructokinase and pyruvate kinase [PK] (Hofmann, 1976; Uyeda, 1979; Fraenkel, 1996). The activity of these enzymes can be controlled allosterically by different glycolytic intermediates and also by

other metabolites. However, there is growing evidence that the regulation of glycolysis in streptomycetes differs in some steps from the conventional pathway present in many other organisms.

The existence of the EMP pathway has been reported for *S. coelicolor, S. antibioticus, S. scabies, & S. reticuli* (Salas *et al.,* 1984){probable identification of EMP enzymes in the *S. coelicolor* genome sequence; SCO1942, [*pgi2*]; SCO6659, [*pgi*]; SCO3197, [*pfkB*]; SCO2119, [*pfkA*]; SCO5426, [*pfkA2*]; SCO1214, [*pfkA3*]; SCO3649, [*fba*]; SCO0578, [*tpiA*]; SCO1945, [*tpiA*]; SCO1947, [*gap1*]; SCO7040, [*gap2*]; SCO7511, [*gap2*]; SCO1946, [*pgk*]; SCO2576, [*pgm2*]; SCO4209, [*pgm*]; SCO4470, [*gpmB*]; SCO6818, [pgm]; SCO7219, [pgm]; SCO3096, [*eno*]; SCO7638, [*eno2*]; SCO2119, [*pfkA*]; SCO5423 [*pfk2*]}. Isotope studies indicate glucose metabolism proceeds in the main via the Pentose Phosphate Pathway in the mycelium, whilst the EMP pathway was most active in germinating spores (Salas *et al*., 1984). Penzikova & Levtov (1966); established the existence of the EMP in *S. fradiae*, a producer of neomycin.

HK catalyses the first step in sugar utilisation (in the absence of a PTS system) by transfer of a phosphor group from ATP or other phosphor donors (GTP, polyphosphates (PolyPn)) to sugars, e.g. a glucose unit. Under physiological conditions, the reaction is essentially irreversible. In general, mammals and yeast HKs exist as different isoenzymes [ISEs](Fothergill-Gilmore & Michels, 1993). In *Actinomyces naeslundii* a PolyPn/ATP/GTP GlkA has been detected (Takahashi *et al.,* 1995). Also in organisms such as *M. tuberculosis* (Hsieh *et al.,* 1993) and *Propionibacterium shermanii* (Wood & Goss, 1985), PolyPn/ATP GlkAs have been characterised. It has been speculated that glucose phosphorylation was originally mediated by PolyPn's and when ATP became available in the environment a transition took place. This "bifunctional" GlkA thus could represent an intermediate in the evolution of these enzymes (Hsieh *et al.,* 1996a, b). Recently, a new ADP-dependent glucose kinase has been detected in the archaeon *P. furiosus* (Kengen *et al.,* 1995). In *S. coelicolor*, the gene coding for GlkA enzyme (*glk*) is ATP-dependent. Sabater *et al*. (1972) reported an ATP-dependent GlkA in *S. violaceoruber*. An ATP-dependent GlkA activity was also identified in *S. clavuligerus*. The presence of a PolyPn-dependent GlkA was reported by Hostalek *et al*. (1976) for *S. aureofaciens*. The enzyme was present only after

logarithmic growth, unlike the ATP dependent kinase, which was present only during logarithmic growth.

Phosphofructokinase (PFK) is postulated to be one of the main sites of regulation of the EMP pathway. The enzyme and its gene have been studied in *S. coelicolor* (Alves *et al*., 1997). Although PFK activity could not be detected in *S. antibioticus* (Torbochkina & Dormidoshina, 1964; Torbochkina *et al*., 1964). Evans & Ratledge (1984b) reported that PFK activity is susceptible to the intracellular NH^+_4 concentration. The enzyme that catalyses this irreversible step is usually an ATP-dependent phosphofructokinase (ATP-PFK) (Hofmann, 1976; Fothergill-Gilmore & Michels, 1993), of which there are two types (Evans *et al.,* 1981). The most commonly encountered bacterial ATP-PFK is subject to allosteric inhibition by PEP and activation by ADP and GDP. The enzyme is evolutionarily well-conserved (Scrimer & Evans, 1990; Wu *et al.,* 1991; Fothergill-Gilmore and Michels, 1993), with ATP-PFKs from Eukarya, Eubacteria, and archae show significant aa sequence similarity (Hellinga & Evans, 1985; Lee *et al.,* 1987; Heinisch *et al.,* 1989; Fothergill-Gilmore & Michels, 1993; Llanos *et al.,* 1993; Alves *et al.,* 1996a). The second type of ATP-PFK enzyme, is found only in *E. coli,* and is not sensitive to allosteric effectors (Kotzlar & Buc, 1977; Uyeda, 1979).

The actinomycete *Amycolatopsis methanolica* was found to employ the normal bacterial set of glycolytic and PP pathway enzymes, except for the presence of a Pyrophosphate-dependent phosphofructokinase (PPi-PFK) and a 3-phosphoglycerate mutase that is stimulated by 2,3-bisphosphoglycerate. It catalyses a readily reversible reaction; it can replace both ATP-PFK and fructose-1,6-bisphosphatase. Interestingly, studies with *A. methanolica* (Alves *et al.,* 1996b; 1994) raised questions about the regulation of glucose metabolism in actinomycetes in general due to its non-allosteric properties. This PPi-PFK enzyme is also present in other actinomycetes, in members of the *Pseudonocardiaceae* (Alves *et al.,* 1994), *Actinoplanaceae* (Seiler *et al.,* 1996) and in *A. naeslundii* (Takahashi *et al.,* 1995). *S. coelicolor* has been reported to have an ATP-PFK (Alves *et al.,* 1994). Interestingly, information on the primary sequence of the ATP-PFK enzyme from *S. coelicolor* showed that this enzyme has the same differences in the aa residues involved in ATP binding as the PPi-PFK from *A. methanolica* (Alves *et al*., 1997). It thus remains unclear what determines ATP/PPi specificity of PFK in these actinomycetes.

The use of PPi-PFK permits utilisation of PPi that is formed in many metabolic reactions like the biosynthesis and degradation of nucleic acids (DNA & RNA metabolism), proteins (Dawes & Senior, 1973; Kulaev & Vagabov, 1983) and polysaccharides (glycogen biosynthesis)[Takahashi *et al.,* 1995], rather than a loss through wasteful removal by hydrolysis (Kulaev & Vagabov, 1983; Mertens, 1991). On this basis, replacement of ATP-PFK by PPi-PFK could theoretically improve the net ATP yield of glucose degradation. This energetic advantage would be important in the case of fermentative metabolism. This rests on the assumption that the PPi used is a by-product of the biosynthesis of macromolecules. To allow such biosynthetic reactions to occur the concentration of PPi must be kept at a low level. This can be achieved by hydrolysis of PPi by the pyrophosphatase enzymes (Chen *et al.,* 1994). Interestingly, organisms possessing a PPi-PFK activity contain a very low level of pyrophosphatase activity e.g., *E. histolytica* (Reeves *et al.,* 1974), *G. lamblia* (Li & Philips, 1995), *T. vaginalis* (Mertens *et al.,* 1989), *A. naeslundii* (Takahashi *et al.,* 1995), *P. freudenreichii* (O'Brien *et al.,* 1975). In addition to the PPi-PFK activity, organisms such as *P. freudenreichii* and *E. histolytica*, possess other unusual PPi-dependent enzymes (Mertens, 1993). These are PEP carboxytransphosphorylase (PEC) and pyruvate orthophosphate dikinase (PPDK). In these examples the first reaction would provide PPi and the second reaction, towards the formation of pyruvate, would require PPi. These findings suggest that PolyPn can be utilised in these organisms as an intracellular reservoir of energy (Takahashi *et al.,* 1995). *S. coelicolor* has also been reported to contain PolyPn as an intracellular storage compound (Gray *et al*., 1990).

Recently, a third alternative form of PFK has been detected. The hyperthermophilic archaeon, *P. furiosus* employs a ADP-PFK enzyme in its modified EMP pathway involving ADP-dependent kinases (Kengen *et al.,* 1994, 1996). To explain the use of ADP instead of ATP in the PFK reaction it has been suggested that as ADP is more thermostable than ATP, then, when the ATP level is low (after a starvation period), the organism is still able to phosphorylate glucose using ADP.

Fructose-1,6-bisphosphate aldolase (FBA) catalyses the reversible cleavage of fructose-1,6-bisphosphate (F-1,6-P2) to glyceraldehydes 3-phosphate (G3P) and dihydroxyacetone

phosphate [DHAP] (von der Osten *et al.,* 1989; Fothergill-Gilmore & Michels, 1993). Two different classes of FBA can be distinguished based, on the reaction mechanisms (Alefounder *et al.,* 1989). Class 1 FBA, but not class 2, form an intermediate with their substrate through a Schiff base. Class 2 FBA, instead require a divalent cation like Ca^{2+}, Fe^{2+} or Zn^{2+} to stabilize the enzyme-substrate complex. Bacterial enzymes have been characterised revealing examples of both class 1 and 2 proteins (Fothergill-Gilmore & Michels, 1993). Eubacterial representatives of class 1 enzymes have been found in *E. coli* (Stribling and Perham, 1973), *Lactobacillus casei* (London, 1974) and Staphylococcal species (Rudolph *et al.,* 1992; Witke & Gotz, 1993). Examples of class 2 FBA have been found in yeast, *E. coli* (Alefounder *et al.,* 1989) and *C. glutamicum* (von der Osten *et al.,* 1989). *Streptomyces galbus* FBA has been cloned and sequenced and found to be a member of the class 2 family (Wehmeier, 2001).

The phosphorylation of glyceraldehyde 3-phosphate (G3P) to 1,3-bisphosphoglycerate, is catalysed by the enzyme glyceraldehyde-phosphate dehydrogenase (GAPDH). The primary sequences of different GAPDH enzymes have been determined (Fothergill-Gilmore & Michels, 1993). This enzyme is the most highly conserved enzyme from glycolysis and the best characterised one at the structural level (Fothergill-Gilmore & Michels, 1993). The enzymes from Eukarya and Eubacteria are clearly homologous whereas the enzymes from Archae have been shown to be very different from those of the other organisms (Fabry & Hensel, 1988; Fabry *et al.,* 1989; Zwickl *et al.,* 1990; Prub *et al.,* 1993). Doolittle *et al*. (1990) proposed a different evolutionary origin for Archaebacteria GAPDH when they found a slightly higher degree of similarity with a part of the sequence of bovine NAD / NADPH transhydrogenase. It was suggested that an Archaebacterial ancestor had pirated another enzyme for use as the equivalent of a GAPDH. Nevertheless, a common origin of GAPDH of Archaebacteria, Eubacteria and eukaryotes is supported by the occurrence of common sequence motifs, both in the NAD-binding domain and in the catalytic domain (Hensel *et al*., 1989). In the *S. aureofaciens*, the gene encoding GAPDH (*gap*) has been cloned and sequenced, showing 52 % aa identity with bacterial and eukaryotic *gap* genes (Kormanec *et al.,* 1995).

It is important to consider the problems associated with the rapidly growing list of the number of streptomycetes in which isoforms of particular enzymes have been discovered. In

the majority of cases the difference between the two isoenzymes was the direction to feed the NADPH/NADH ratio for furnishing NADH for cellular energetics and NADPH for reductive biosynthesis. These ISEs have distinct properties and are expressed during different physiological states of the cell and most interestingly are often regulated differently. ISEs that are important in primary metabolism have been shown to fall into two types: those that result in antibiotic autoimmunity; and those that are involved in primary or secondary metabolism. The GAPDH enzyme has been studied in *S. arenae* (Maurer *et al*., 1983) because there are two forms: one expressed during primary metabolism and one expressed as a resistance mechanism during the production of pentalenolactone (PL), an inhibition of the first ISE. The sesquiterpene antibiotic PL produced by *S. arenae* selectively and irreversibly inactivates the NAD-dependent GAPDH of prokaryotic and eukaryotic organisms. It therefore is a potent inhibitor of growth when glucose is the obligate carbon source. *S. arenae* is resistant to growth inhibition during antibiotic production only by forming an ISE of GAPDH which is insensitive to PL. The PL sensitive and insensitive forms have been sequenced and show the two ISEs exhibit little immunological cross reactivity and differ in size, aa composition, and several aa residues of their amino termini (Froehlich *et al*., 1989; 1996). The development of a complicated regulatory system involving two enzymes for the same function and degradation of the antibiotic-sensitive form with antibiotic production, instead of simply the use of the resistant protein throughout, should be of some advantage for the cell. In the case of *S. arenae*, the PL-insensitive GAPDH has a 3 – 4 times-lower maximal activity than the PL-sensitive enzyme (550 nKat/mg compared with 1870 nKat/mg of pure enzyme (Maurer *et al*., 1983)). This reduction of enzyme efficiency may be a side effect of the higher resistance. It may be economically advantageous to produce four times less of this major protein during most of the growth cycle (Froehlich *et al*., 1989). The gene of *S. aureofaciens* PL-sensitive GAPDH was identified as linked to an RNA polymerase sigma factor (Kormanec *et al*., 1997). The gene was shown to be induced by glucose and, in the absence of glucose, at the time of aerial mycelium formation (Kormanec *et al*., 1997).

Phosphoglycerate mutase (PGM) catalyses the interconversion of 3-phosphoglycerate (3PG) and 2-phosphoglycerate (2PG). It is a member of a family of enzymes, which catalyse reactions involving the transfer of phosphor groups among the three carbon atoms of phosphoglycerates. There are three major groups of PGM enzymes with different kinetic

properties (Fothergill-Gilmore & Michels, 1993). Group 1 type of PGMs are dependent upon 2,3-diphosphoglycerate (2,3-DPG) for activity. This form has been found in vertebrates, yeast (Fothergill-Gilmore & Watson, 1989) and also recently in *S. coelicolor* (White *et al.,* 1992) and, *A. methanolica* (Alves *et al.,* 1994). The second type is independent of 2,3-DPG, but requires manganese. This type occurs in *Bacillus* spp. A third type of mutase is independent of any cofactors, and is found in organisms such as higher plants and invertebrates. The cofactor-dependent PGM from *S. cerevisiae* is the best, studied PGM enzyme to date.

Enolase catalyses the dehydration of 2PG to PEP (Fothergill-Gilmore & Michels, 1993; Green *et al.,* 1993). Enolase has been more extensively studied in eukaryotes. Enolase appears to have a variety of functions in addition to its role in glycolysis. In the obligatively fermentative Gram-negative bacterium *Z. mobilis*, enolase is the most abundant glycolytic enzyme and it has been suggested to play a role in metabolic flux control in this organism (Pawluk *et al.,* 1986). Until now, no studies of this enzyme in actinomycetes have been carried out.

Pyruvate kinase (PK) is one of the major regulatory enzymes of the glycolytic pathway. It catalyses the last step of the glycolysis, the irreversible reaction from PEP to pyruvate [PYR] (Kayne, 1973). PKs are often regulated by a number of allosteric effectors like G6P, ribulose 5-phosphate (Ru5P), AMP and F-1,6-P2 (le Bras & Garel, 1993). Two different mechanisms of regulation at the activity level can be found in Eubacteria. *E. coli* and *Salmonella typhimurium* each have two differently regulated ISEs (Fothergill-Gilmore & Michels, 1993; Ponce *et al.,* 1995) with different kinetic properties. In *E. coli* the type 1 PK ISE is constitutive and allosterically activated by F-1,6-P2. This enzyme is also susceptible to a synergistic cooperative feedback inhibition by succinyl-CoA and ATP, and to inhibition by phosphate. The type 2 PK ISE is inducible and stimulated by AMP and by some sugar monophosphates, such as Ru5P and G6P (Ponce *et al.,* 1995). The physiological roles of the two PKs and their regulation may be as follows. When cells are grown on a glycolytic substrate, the intracellular concentration of F-1,6-P2 is high, thus stimulating the activity of ISE 1. Under conditions where gluconeogenesis is predominant, the F-1,6-P2 concentration is at such a low level that the enzyme is virtually inactive, whatever the concentration of PEP. However, the PEP level is such that the type 2 ISE can catalyse the reaction at 30 - 40

% of the maximum rate. A decrease of the cellular energy charge would then, via the effector AMP, activate the enzyme and increase the ATP concentration (Fothergill-Gilmore & Michels, 1993; Ponce *et al.,* 1995). In some protists and bacteria (*E. histolytica*, *Bacteroides symbiosus*, *G. lamblia* and *P. freudenreichii*) PK activity is absent and substituted by pyruvate orthophosphate dikinase (PPDK) (Wood *et al.,* 1977; Wood & Goss, 1985; Mertens, 1991). This enzyme differs in the use of the substrate PPi instead of ADP, and the fact that it catalyses both the forward and the reverse reactions. Like the PK enzyme, it also requires the ions K^+, $NH4^+$ and Mg^{2+} for its activity. This type of activity PPDK is associated with other pyrophosphate-linked reactions such as the PPi-PFK, PEC and PPi-acetate kinase (Mertens, 1993). PEP-driven transport system for glucose import and phosphorylation also allows PEP to be turned into PYR without requiring PK (Neidhardt, 1987)[see section 2.4 for discussion of the presence of the PTS in streptomycete metabolism].

PK has also been characterised from different Gram-positive bacteria such as *C. glutamicum* (Jetten *et al.,* 1994), *Brevibacterium flavum* (Ozaki & Shiio, 1969), *A. methanolica* (Alves, 1997), and from *S. coelicolor* (Bystrykh, 1993). In these organisms (except in *S. coelicolor*) the PK enzyme is regulated at the activity level being activated by AMP and inhibited by ATP. The *C. glutamicum* enzyme differs in that it does not require Mg^{2+} ions for activity but Mn^{2+} or Co^{2+} ions (Jetten *et al.,* 994). The *A. methanolica* PK was purified and characterised as an allosteric enzyme, sensitive to inhibition by Pi and ATP but stimulated by AMP.

Pyruvate dehydrogenase (lipoamide) complex [PDC] is usually used in Eubacteria (probable PDC identification in *S. coelicolor* genome sequence; positions SCO2180, [*pdhl*; pyruvate dihydrolipoamide dehydrogenase]; SCO2183, [*aceE1*; pyruvate decarboxylase]; SCO2371, [*aceE2*; pyruvate dihydrolipoyltransacetylase]; SCO3815, & SCO7124, [*aceE3*; pyruvate dihydrolipoyldehydrogenase]). The cluster of genes encoding the PDC of *S. seoulensis*, was cloned and sequenced (Youn *et al*., 2002). The genes of *S. seoulensis* consist of four open reading frames. The first gene, *lpd*, which encodes a lipoamide dehydrogenase, is followed by *pdhB* encoding a dihydrolipoamide acetyltransferase (E2p), *pdhR*, a regulatory gene, and *pdhA* encoding a PDC component (E1p). E1p had an unusual homodimeric subunit, which has been known only in Gram-negative bacteria. *S. seoulensis* E2p contains two lipoyl domains, like those of humans and *Streptococcus faecalis*. The over expressed *pdhR* gene

appears to show growth retardation and a decrease of E1p, indicating that *pdhR* regulates the function of the PDC by repressing the expression of E1p. A strain of *S. lividans* over expressing *S. seoulensis pdhR* showed a significant decrease in the level of ACT, implying a regulatory role for *Streptomyces* PDC in antibiotic biosynthesis (Youn *et al*., 2002). PDC (lipoamide) subunits are missing from *T. palladium*, *Helicobacter pylori*, *Aquifex aeolicus*, and Archae (anaerobes). Instead, these species harbour pyruvate synthase for this reaction (Hughes *et al*., 1998). Pyruvate formate-lyase which converts pyruvate to acetyl-CoA under strict anaerobic conditions, is also often present in Archaea. It is composed of the pyruvate formate lyse-activation enzyme and formate acetyltransferase (possible pyruvate formate lyase activating protein in *M. tuberculosis* genome sequence; position *Rv*3138; 42.2 % identity to *Methanobacterium thermoautotropicum*). Subsequent to this step alcohol dehydrogenase & acetaldehyde dehydrogenase are used. A third alternative is the use of PPDK (as previously discussed section 2.5.1; present in *M. tuberculosis* and *T. palladium*; O'Brien *et al*., 1975)[possible identification of PPDK in *S. coelicolor* genome sequence; positions SCO0208, SCO2494, & SCO2014; 67.5 %, 51.7 %, & 59.6 % respectively identity to *Microlispora rosea, Clostridium symbiosus, C. glutamicum*). *E. coli*, an adaptation generalist, harbors all three alternatives.

The majority of bacteria that use the EMP pathway can grow anaerobically on glucose and related sugars (Stryer, 1981; Hodgson, 2000). They harvest energy through substrate phosphorylation and generate reduced NAD by reduction of pyruvate to ethanol or lactate (Zubay, 1998). Hockenhull *et al.* (1954) reported that *S. griseus* produced low levels of lactate during growth on glucose under a restricted aeration regime; which would imply that lactate dehydrogenase was present. The generation of NAD in the reduction of pyruvate to lactate or ethanol sustains the continued operation of glycolysis under anaerobic conditions. This leads to a conundrum; why can streptomycetes not grow anaerobically on glucose? Perhaps this could be due to lactate dehydrogenase, and/or pyruvate decarboxylase plus ethanol dehydrogenase, are sensitive to these waste products (Hodgson, 2000). Alternatively there could be a requirement for oxygen in some other essential process (Hodgson, 2000).

2.5.2 Gluconeogenesis

The pathway of gluconeogenesis effectively reverses the flow of carbon occurring during glycolysis; the intermediary metabolites of gluconeogenesis are identical to those of the

glycolytic pathway (Table 2.1 & Fig 2.2). While the intermediates are the same, the pathways are actually different. In each direction there is at least one critical enzymatic step that is irreversible so that a particular enzyme catalyses the unidirectional flow of carbon. These enzymes have different allosteric inhibitors that regulate the direction of carbon flow. Biosynthesis of CHOs is favoured in *E. coli* when the cell has an adequate supply of ATP, whereas the catabolism of CHOs is favoured when ATP, carbon, nitrogen, or phosphate, etc. concentrations are relatively low. Gluconeogenesis requires the input of carbon atoms, such as occurs in a pyruvate molecule, FAs cannot be converted directly into CHOs via this pathway, unless they are fed through the glyoxylate bypass (see section 2.5.11).

Redman & Hornemann (1980) investigated the ability of *S. murayamaensis* & *S. verticillatus* to grow on PYR or alanine as the sole carbon source; and the activity of PPDK, that is responsible for the interconversion of PYR and PEP. The enzyme in the latter streptomycete was induced by growth on media containing alanine or pyruvate which implied that the enzyme was involved in gluconeogenesis. *S. achromogenes var streptozoticus* did not contain this enzyme (Hodgson, 2000). In an NMR study on *S. parvulus* by Inbar & Lapidot (1991) the main gluconeogenic step was identified as being a reaction converting oxaloacetate (OAA) to PEP. The enzyme responsible for this conversion was probably not PEP carboxylase (PEPC) as this enzyme is irreversible, but most likely PEP carboxykinase [PEPCK] (Zubay, 1998). Obanye (1994)[Obanye *et al*., 1996] detected the activity of the malic enzyme [MDH(dc)] (malate dehydrogenase decarboxylating); but could not detect PEPCK in *S. coelicolor* grown on minimal media (Hobbs *et al.,* 1989)[probable putative PEPCK in *S. coelicolor* genome sequence; position SCO4979; 58.36 % identity to *Chlorobium limicola*).

2.5.3 Entner-Doudoroff pathway

The Entner-Doudoroff pathway; although generally believed to be a more ancient catabolic route for glucose than EMP (Romano & Conway, 1996; Melendez-Hevia *et al*., 1997), is not as well conserved. Dandekar *et al*. (1999) reported it present only in Gram-negative bacteria. It has been reported as being non-functional, in *S. lividans, Streptomyces C5*, and *S. aureofaciens* (Dekleva & Strohl. 1988a). The absence of this pathway was also reported in *A. methanolica* (Alves *et al.*, 1994).

(2.5.4) The Tricarboxylic acid cycle (TCA)

Under aerobic conditions, the generation of energy by the decarboxylation of PYR with the concomitant formation of acetyl-CoA takes place. This activated acetyl unit is subsequently oxidised to CO_2 via the TCA cycle (Table 2.2 & Fig 2.3). Compounds that are degraded to acetyl-CoA, or to an intermediate of the TCA cycle, can be oxidised via this cycle. For example, FAs are degraded stepwise to acetyl-CoA, and various aas are converted to their ketoacids and then enter the cycle in this way.

Garner & Koffler (1951) came to the conclusion that *S. griseus* did not contain a functional TCA cycle, observing that this organism was unable to metabolise organic acids of the cycle without prior adaptation. However, the possibility that the acids were unable to traverse the cell membrane or wall was not considered. Moreover, in other *Streptomyces*, the presence of the TCA has been demonstrated conclusively. The existence of a complete TCA cycle in both *S. lividans* and *Streptomyces* C5; was proved in a study by Dekleva and Strohl (1988a). Functional TCA cycle enzymes have been found in *S. alboniger* (Surowitz & Pfister, 1985), *S. venezuelae* (Ahmed *et al* 1984), *S. rimosus* (Bormann & Hermann, 1968), *S. hygroscopicus* (Grafe *et al*, 1975) and *Streptomyces* C5 (Dekleva, 1987).

A number of enzymes that may be important in shuffling TCA cycle and EMP pathway intermediates have been reported in streptomycetes. Hostalek *et al.* (1969) devoted a lot of time to studying the enzymes of the TCA cycle in *S. aureofaciens*. Reporting the presence of all the expected enzymes of the complete cycle. It must be taken into account they used improved strains in the studies. Characterisation of citrate synthase (CS), showed similarities to *E. coli* CS, with ATP inhibition and AMP stimulation. However unlike *E. coli*, reduced NAD had no effect.

There are two forms of isocitrate dehydrogenase (ICDH) based on their subunit organisation. Type I ICDHs are homodimers with a subunit size of around 45 kDa. Although this group of enzymes are not controlled allosterically by effectors such as AMP, ADP, ATP, NADP, or NADPH, they are inhibited by glyoxylate (GLYOX) and OAA (Nimmo, 1986). Alternatively, Type II ICDHs have been shown to be monomeric and have the molecular weight of around 80 kDa and can have both NAD and NADP-linked activities; ATP inhibits the NAD-linked activity (Leyland and Kelly, 1991). However, the

specificity (defined as k_{cat}/k_m) of the enzyme for NAD is 400 times lower than that of NADP, indicating that this activity and the metabolic effect of ATP is probably insignificant. Significantly, the cloned and sequenced ICDH of *S. coelicolor* (Taylor, 1992) has a molecular weight of 80 kDa and is 69 % identical to the ICDH II from *Vibrio* spp., and 63 % identical to that of *Rhodomicrobium vannielii*. Further assays were performed to determine whether the *S. coelicolor* ICDH enzyme shares similar characteristic to that of *E. coli*. 1 mM ATP was found to inhibit activity by 61 %. However, ATP is known to chelate $MnCl_2$, perhaps explaining this reduction in activity. Addition of a further 1 mM of Mn^{2+}, which should negate any chelation, still produced an inhibition of 44 %, perhaps indicating that this effect was authentic. OAA also inhibited the *S. coelicolor* ICDH enzyme by 60 %. This inhibition was increased further with the addition of OAA and GLYOX. The ICDH enzyme was also inhibited by 1 mM NADH. This result has not been reported for any other NADP-dependent ICDH. Some ICDH are controlled by phosphorylation of the enzyme. Initial attempts to phosphorylate the enzyme using the *E. coli* kinase/phosphatase have proven to be unsuccessful. This does not however exclude the possibility of control by some sort of covalent modification catalysed by an enzyme with a different specificity.

Tinterova *et al*. (1969) reported the discovery of ISEs of malate dehydrogenase (MDH) showing different responses to OAA and requirements of Mg^{2+}. The purification and characterisation of MDH from *S. aureofaciens* (Mikulasova *et al.,* 1998) revealed a single enzyme with a strong preference for NADH and a more efficient back reaction, reduction of OAA. Surprisingly there was no evidence of product inhibition of malate oxidation i.e. excess OAA did not inhibit it.

2.5.5 Pentose phosphate pathway

The pentose phosphate pathway (PP pathway) consists of a complicated series of reactions that can be carried out by a large number of glucose-catabolising microorganisms (Table 2.3 & Fig 2.4). Its primary function is the generation of reducing power, in the form of NADPH via its oxidative branch, and of pentoses and tetroses for biosynthetic reaction (nucleoside and aa synthesis) in variable ratios. The balance between activity of the oxidative segments of the PP pathway is generally governed by one of these intracellular requirements:

(A) Much more ribose-5-phosphate (R5P) than NADPH is required.

(B) Requirements for NADPH and R5P are balanced.

(C) Much more NADPH than R5P is required G6P is completely oxidised to CO_2.

(D) Much more NADPH than R5P is required G6P is converted to pyruvate.

This involves transketolase (TK) and transaldolase (TA), which are employed by many microorganisms to degrade pentoses (Zubay, 1998). Thus, the pentose cycle can meet different requirements of metabolism. If there is excessive demand for pentoses, the TK and TA reactions of the pentose cycle can run in the reverse direction. Cochrane and Peck (1953) reported that in *S. reticuli* and *S. coelicolor* the PP pathway activity determined by radiorespirometry was the primary glucose catabolic route. However, Cochrane (1961) also acknowledged the results of Wang *et al.* (1958a, b) suggested only a minor role for this pathway in *S. griseus*. The enzymes oxidising G6P, 6-phosphogluconate (6PG), and R5P are constitutive in *S. coelicolor* (Cochrane *et al.*, 1953). Further, Salas *et al.* (1984) described a shift in the relative participation of the EMP and PP pathways during germination of *S. antibioticus* spores. During spore germination, the PP pathway continued to increase its participation in glucose catabolism relative to the EMP pathway, until it was the primary route during exponential growth.

The presence of a full PP pathway was reported by Salas *et al.* (1984) for *S. coelicolor, S. antibioticus, S. scabies & S. reticuli,* and this was confirmed by Dekleva & Strohl (1988a) for *Streptomyces* C5*, S. aureofaciens & S. lividans.* In most bacteria, the enzymes glucose-6-phosphate dehydrogenase (G6PDH) and 6-phosphogluconate dehydrogenase (6PGDH) are NADP dependent and hence, every G6P entering the PP pathway would generate two NADPH. In *S. lividans, Streptomyces* C5 *& S. aureofaciens*; and some other actinomycetes, the G6PDH is NADP-dependent, but the 6PGDH has been found to be NAD-dependent (Dekleva & Strohl, 1988a; Alves *et al.,* 1994). This means that only one NADPH is generated for every G6P entering the PP pathway. G6PDH has been purified from *S. aureofaciens* (Neuzil *et al*., 1986; 1988). They reported the discovery of two activities: an NAD-dependent one, which was sensitive to ATP, ADP, AMP, phosphate and feedback inhibition from PEP, and an NADPH-dependent one, which was sensitive to neither adenylate compounds nor phosphate. Both activities were sensitive to reduced NAD and NADP (Behal, 1987; Vining & Stuttard, 1988). *S. lincolensis*, *S. rimosus*, *S. lividans*, & *S. aureofaciens* have been reported to contain both NAD-G6PDH and NADP-G6PDH activity

(Purwantini *et al*., 1997), although only NADP-G6PDH activity was reported for *S. achromogenes* & *S. avermitilis*. These results could be interpreted as evidence for the existence of two ISEs of the enzyme. 6PGDH, also purified by Neuzil (1988), showed dual cofactor activity. Presumably, as the biosynthetic demand for NADPH is similar or greater to that of *E. coli*, this means that the PP pathway probably needs to be more active in streptomycetes to meet the biosynthetic demand for NADPH, or that another major pathway generating NADPH exists (Daae & Ison, 1999). An F_{420} –dependent glucose-6-phosphate dehydrogenase (FGD) was found in *Mycobacterium* (*M. tuberculosis*, *M. smegmatis M. avium*, *M. fortuitum*, *M. gordonae*, *M. kansasii*, & *M. leprae*) and *Nocardia.* spp (*N. asteroids*, *N. brasiliensis*, *N. otitidiscaviarum*, & *N. tartaricans*) but not in *Streptomyces.* spp (Purwantini *et al*, 1997). FGD catalyses the following reaction: F_{420} (5-deazaflavin) + G6P → H_2F_{420} + 6-phosphogluconolactone (possible identification of FGD in *S. coelicolor*; position SCO6495; 33.2 % identity to *M. smegmitis*). The possibility that G6PDH & 6PGDH exist as isoforms, or one enzyme with dual cofactor specificity; has received little attention in the literature, since Ragland *et al*. (1966).

2.5.6 Nucleotide transhydrogenase

Some organisms have a pyridine dinucleotide transhydrogenase (TH) which catalyses the following reaction:

NADP + NADH ⇔ NADPH + NAD

Two basic types of this enzyme exist. One is water-soluble and does not participate in energy production while the other is membrane-associated and can translocate protons across the membrane to produce ATP (Hoek & Rydström, 1988; Michal, 1999]. Although both energy and non-energy linked THs have been studied extensively, these studies have focused on relatively few organisms. Consequently, information regarding the existence of either TH is lacking in *Streptomyces* (probable identification of NADP-TH α & β subunits in *S. coelicolor* genome sequence, positions SCO7623 & SCO7622; 58.4 % & 68.8 % identities to *E. coli*; also contains possible hydrophobic membrane spanning regions as expected). Ragland *et al*. (1966) carried out extensive TH activity analysis on a number of bacteria. *S. coelicolor* showed no activity grown on glucose minimal media and extremely low activity when grown citrate. No NADP-dependent TH activity was detected in *S.*

noursei, which produces the nystatin variant polifungin against other macrolide synthesising bacteria (Roszkowski *et al*., 1971). These results could be susceptible to considerably large errors due to the use of a sonicator or appropriate buffer.

2.5.7 Anaplerotic pathways

Anaplerotic reactions are required for the sustained operation of the TCA cycle since metabolites cannot be removed from the cycle without replenishment (thoroughly reviewed by Stryer, 1981; Zubay, 1998; Michal, 1999). A number of anaplerotic reactions have been detected in *Streptomyces*, (Table 2.4 & Fig 2.5 & 2.6). PEP carboxykinase is detailed under the section on gluconeogenesis (Section 2.5.1). The degree of activity or expression of the enzymes listed in Table 2.4 appears to vary from species to species, as explained in the following sections.

2.5.8 Phosphoenolpyruvate carboxylase

In streptomycetes the enzyme involved in OAA formation has proved to be PEP carboxylase (PEPC) [Dekleva & Strohl, 1988a, b; Bramwell *et al.*, 1993; Coggins *et al.*, 1995]. The enzyme condenses PEP and CO_2 to form the acid and release orthophosphate (the previously sequenced PEPC in *S. coelicolor* [position SCO3127]; has good similarity to others, e.g. 38.4 % with *Rhodopseudomonas palustris*). In *E. coli*, positive effectors of PEPC activity typically include acetyl-CoA & F-1,6-P2 (Varisek *et al*., 1970). Negative effectors include nucleoside triphosphates, citrate, succinate and aspartate (Dekleva & Strohl, 1988a). PEPC was detected & purified in *Streptomyces* C5 (Dekleva & Strohl, 1988b). AMP and F-1,6-P2 were found to stimulate its activity slightly; OAA, malate, succinate, and aspartate strongly inhibited the enzyme, as did citrate and ATP, although to a lesser extent. Increased PEPC activity during polyketide biosynthesis in *S. aureofaciens* (Behal *et al*., 1977) and *Streptomyces* C5 (Dekleva & Strohl, 1988b) suggests that the activity of PEPC is closely-linked with differentiation and secondary metabolism, with a possible involvement in precursor supply. The same enzyme was also purified from *S. coelicolor* (Bramwell *et al*., 1993) although little on the properties of the enzyme and the regulation of the enzyme was reported. Another point of interest is a study of *S. griseus* where PEPC expression has been shown to require the presence of A-factor; and that A-factor-deficient mutants have low, but detectable levels of PEPC activity (Rickets, 2000).

There is some evidence in the case of *Streptomyces* that PEPC activity may be enhanced by the presence of ppGpp like in *E. coli* (Rickets, 2002) which is linked to the stringent response. This could possibly further link PEPC with secondary metabolism, and may not be surprising as anaplerotic reactions are most likely to occur once primary metabolisms is unable to continue to supply metabolic intermediates.

2.5.9 Pyruvate carboxylase

Pyruvate carboxylase (PC) catalyses a similar reaction to PEPC, but utilises PYR as a substrate and requires ATP and biotin as cofactors (probable pyruvate carboxylase enzyme in *S. coelicolor* genome sequence; position SCO0546; 76.36 % identity to *C. glutamicum*). PC activity has not been reported in *Streptomyces*. *S. coelicolor* autotrophic mutants of PEPC still required the addition of glutamate to compensate for the anaplerotic loss of carbon (personal communication I. Hunter). Therefore PC was not switched on. PC is considered to be the major anaplerotic route in *S. erythreus* (personal communication I. Hunter), as the gene for PEPC is not present in the genome sequence.

2.5.10 Malic enzyme (Malate dehydrogenase decarboxylating)

The malic enzyme (MDH[dc]) which catalyses the carboxylation reaction from malate to PYR. Original studies on *B. flavum* (Shiio *et al*., 1959; 1960) detected the presence of the MDH[dc] and demonstrated that it is specific for NADP (probable NADP-dependent enzyme in *S. coelicolor* genome sequence; position SCO2951; 58.8 % identity to *E. coli*; plus a probable NAD-dependent MDH[dc]; position SCO5261; 55.0 % identity to *Bacillus stearothermophilus*). The enzyme activities in *S. coelicolor* from glucose culture extracts of *S. coelicolor* were always much smaller than the activity observed for PEPC (Obanye, 1994; Obanye *et al*., 1996). Therefore, MDH[dc] is not believed to act in carboxylating mode to any great extent during growth on glucose but this may not be the case for other carbon sources. In *B. flavum* it has been reported that glutamate induces MDH[dc] (Mori & Shiio, 1987). Jechova *et al*. (1975) studied MDH[dc] from *S. aureofaciens*. The enzyme was repressed by about 50 % when acetate was present in the medium. The activity of the enzyme directly paralled the activity of FA synthesis pathways in this strain, which was active only during the growth phase (Behal *et al*., 1969).

2.5.11 Glyoxylate Bypass pathway

If the TCA cycle was to operate by catabolising acetyl-CoA, both of the carbons of the acetyl unit would be lost as CO_2 and alone would not allow net accumulation of carbon for biosynthesis and growth. Therefore growth on FAs or acetate, which are catabolised to acetyl-CoA, requires the operation of a separate anaplerotic pathway. The Glyoxylate Bypass pathway (GBP) is an inducible metabolic bypass of the TCA cycle (Zubay, 1998), and is wholly inclusive of two enzymes, isocitrate lyase (ICL) and malate synthase (MS) [Table 2.4]. The overall reaction (Table 2.4) gives a net gain of one C_4-dicarboxylic acid, which can be used by the TCA cycle to produce malate and OAA. Malate and OAA can also then be used to supply precursors required for biosynthesis. Malate can be converted to pyruvate by MDH[dc] and OAA can be converted to PEP using PEPCK. The PEP can then be used to generate the phosphorylated biosynthetic precursors. If other biosynthetic precursors are, required to be generated from oxo-glutarate (OGA) and succinyl-CoA, the carbon must be channelled through ICDH and ICL. This creates a branch point where ICDH and ICL compete for the same substrate, isocitrate. This is tightly regulated in *E. coli* to ensure efficient use of the available acetyl-CoA (Holms, 1986; Walsh & Koshland, 1984).

In addition to the GBP, preparatory sequences are needed, to convert the substrate into acetyl-CoA. If the substrate is acetate, activation requires only formation of a CoA derivative, which is catalysed by acetate thiokinase, with ATP hydrolysis as the driving force. If ethanol is the substrate it requires oxidation to acetate first, other two carbon substrates are possible; each requires specific processing to convert it to the acetyl-CoA with which the GBP itself begins. It is worth mentioning that the only bacterium in which FA transport and degradation have been studied in detail so far is *E. coli* (Nunn, 1986; Black & Dirusso, 1994; Clark & Cronan, 1996). Banchio & Gramajo (1997) reported one of first characterisation of FA uptake in a Gram-positive bacterium for *S. coelicolor*. Uptake of the medium chain FA octanoate showed the characteristics of simple diffusion, whereas the uptake of palmitate, a long-chain FA, occurred by both simple diffusion and active transport. Once inside the cell, FAs are degraded in a similar manner to the β-oxidative pathways of eukaryotic organisms. The first step is the activation to a fatty acyl-CoA, catalysed by the membrane bound acyl-CoA synthetase. Two oxidation steps then follow which yield one molecule each of $FADH_2$ and NADH. This is then followed by thiolytic

cleavage to give a fatty-acyl-CoA, which is two carbons shorter than the original fatty-acyl-CoA. The shortened FA then re-enters the cycle and repeats the sequence (Zubay, 1998).

It has been indicated that while strains such as *S. coelicolor* and *S. hygroscopicus* have fully functional GBP enzymes (Coggins *et al*., 1995; Takebe *et al*., 1991), strains such as *Streptomyces* C5, *S. lividans* and *S. aureofaciens* do not, and grow poorly on acetate as their sole carbon source (Dekleva and Strohl, 1988a). Although *S. lividans* and *S. coelicolor* grow poorly on acetate alone, they grow well on Tween, a source of FAs, which, following FA catabolism is equivalent to growth on C2 compounds (personal communication I Hunter; also see Hodgson, 2000). In general it is hard to find any literature reports of both ICL & MS enzymes being active in streptomycetes. In *S. aureofaciens*, MS was found but not ICL (Hostalek *et al*., 1969). MS has been identified in *S. arenae* grown on acetate or ethanol (Huettner *et al*., 1997) and *S. clavuligerus* grown on acetate solely (Chan & Sim, 1998); there was no evidence of ICL activity in the latter two strains. This may indicate that the GBP does not exist. Sprinkmeyer & Pape (1978) demonstrated through the use of a tylosin producing *S. fradiae* strain that CS was inhibited by acetyl-CoA, suggesting that in the presence of acetyl-CoA, less acetyl-CoA would be metabolised to citrate by condensation with OAA. Then if the pool of succinyl-CoA (see section 2.10.4) is important in the synthesis of tylactone precursors as stated in the literature (see section 2.10), it is therefore plausible to assume the possible involvement of the GBP in the catabolism of β–oxidation of FAs in *S. fradiae*.

Chapman (1994) purified, cloned and sequenced the ICL gene (*icl*) from *S. coelicolor*. Until the completion of the *S. coelicolor* Genome Project by the Sanger Centre, the existence of this gene was questioned (ICL identification in *S. coelicolor* genome sequence; position SCO0982; 74.82 % identity to *M. tuberculosis*). ICL has also been cloned expressed and purified for *S. clavuligerus* (Soh *et al*., 2001). Although gene sequencing reveals that *S. coelicolor* does not have a flanking ICL gene in the genomic organisation of the *ace*B genes, it does suggest that the GBP genes in streptomycetes are not clustered and may be under different or novel regulatory controls. This is in comparison to *E. coli*, where the genes encoding the metabolic and regulatory enzymes for the GBP are clustered in a single *ace*BAK operon (Chung *et al*., 1988). In *C. glutamicum*, the *ace*B and *ace*A genes are clustered together but are transcribed divergently by their own promoter, thus

suggesting the possibility of either a similar regulatory mechanism or an independent differential mechanism for the adaptation of growth (Reinscheid *et al*., 1994). It is important to note that ICL also has a regulatory role in carbon flux control. ICL is encoded for by the *ace*A gene on the *ace* operon, and is controlled by the phosphorylation of ICDH, as well as control over the isocitrate concentration. However, it has been suggested that ICL may itself be controlled by direct phosphorylation at a histidine residue (Brice & Kornberg, 1968). The removal of the C-terminal histidine from *Linum usitatissimum* ICL results in its complete inactivation (Khan & McFadden, 1982).

E. coli has two forms of MS enzymes: form A, which is encoded by *ace*B and is involved in the GBP and form G, which is encoded by *glc*B and is involved in the metabolism of glycolate (Molina *et al*., 1994). Malate synthase A has been identified in *S. coelicolor, S. clavuligerus & S. arenae*; no other forms of MS have been identified in streptomycetes (Loke & Sim, 2000). MS from *S. coelicolor & S. clavuligerus* have been successfully cloned, purified and characterised (Chan & Sim, 1998; Loke & Sim, 2000; Loke *et al*., 2002). Chapman (1994) found a second identifiable open reading frame downstream of the *icl* gene that codes for a second *ms* gene, and suggests that they may be part of an operon. Comparison studies of this gene with *ace*B gene of *S. arenae* have indicated an identity of 88.6 %, which is found on SCO6243 of the completed genome sequence. It is also over 60 % identical to *Ace*B – one of the two forms of malate synthase in *E. coli*.

In most bacteria, ICL activity is dependent on carbon source in the growth medium. Previous studies on carbon requirements of *S. clavuligerus* were based only on growth monitored up to 96 h of cultivation. However Soh *et al*. (2001) extended these studies to 16 days and it was observed that acetate indeed supported growth, but after a long lag period of about 4 days. This observation is similar to the study by Chan & Sim (1998), who detected MS activity in 10 - day plus fermentations of *S. clavuligerus*. In both cases, the increase in ICL & MS activity was not associated with the accumulation of biomass. Rather, the activities increased sharply after cessation of growth (Soh *et al*., 2001; Chan & Sim, 1998). It was noted by Chan & Sim (1998) and Dekleva & Strohl (1988a) that the late utilisation of acetate could be due to weak acid poisoning. It is possible to reduce this effect through the use of esterified FAs. Methylated FAs were chosen as the carbon source for tylosin

production by a number of workers with *S. fradiae.* Which was shown by Stark *et al*. (1961) to decrease week acid poisoning and increase tylosin yields.

The consistent absence of ICL activity in *Streptomyces* growing on C2 compounds has led to the suggestion of an alternative route to GLYOX. The alternative proposed pathway of GLYOX synthesis arose from the discovery of two genes that were essential for acetate utilisation: *ccr*, which encodes crotonyl-coenzyme A reductase and *mea*A, which encodes a novel vitamin B_{12}–dependent mutase (Hans & Reynolds, 1997). The authors proposed two pathways by which GLYOX could be generated from acetyl-CoA. Both pathways would require propionyl-CoA carboxylase, which has been identified in *S. coelicolor* (Bramwell *et al*., 1996). It is known that streptomycetes are capable of degrading valine to propionate, via 2-oxoisovalerate, isobutyrate, methacrylate, 3-hydroxymethylisobutyrate, 2-methylmalonate, and propionyl-CoA (Janecek *et al*., 1997). *S. collinus* has a similar gene product to that present in *Methylbacterium extorquens*, an ICL-negative methylotroph that can still grow with acetate as their sole carbon source. Although the biochemical pathway involved in the transformation of acetyl-CoA to GLYOX is unknown at present, it is proposed to involve 3-hydroxypropionate (Strauss & Fuchs, 1993). This entails the conversion of acetyl-CoA to propionyl-CoA via 3-hydroxypropionate, then to succinyl-CoA, followed by malonyl-CoA. The cycle concludes with the formation of acetyl-CoA and GLYOX. It may also involve the formation of OGA by another pathway. After the condensation of acetyl-CoA and OAA there is a series of steps, that produce β-methylmalyl-CoA, which cleaves to generate GLYOX and propionyl-CoA. In *M. extorquens* and therefore *S. collinus*, the *mea*A, *adh*A and *pcc*A genes, the last of which produces propionyl-CoA carboxylase, regulate both of these acetyl-CoA oxidative pathways (Chistoserdova & Lidstrom, 1996; Smith *et al.*, 1996). Mutants of *S. avermitilis* defective in the conversion of isobutyryl-CoA to methacryl-CoA were also affected in growth on acetate and butyrate, further supporting the hypothesis that *Streptomyces* employ the same or a similar pathway for acyl-CoA oxidation (Korotkova *et al*., 2002). If either or both the proposed GLYOX-generating pathways exist in *S. collinus* and are common to streptomycetes, it would explain why MS was present during acetate growth but not ICL. The implication would be that growth on aliphatic compounds, such as FAs involves the more common GBP with MS and ICL.

2.6 Organisation of genes encoding glycolytic enzymes

Gene fusion encoding enzymes involved in EMP have been identified in several bacteria. In some cases these genes code for enzymes catalysing irreversible steps in glycolysis such as ATP-PFK and PK. Alternatively genes encoding enzymes catalysing consecutive steps, such as GAPDH and phosphoglycerate kinase (PGK), may be fused. However, the genes encoding for the EMP in streptomycetes although are semi-clustered do not show any fused genes as found in other organisms, these findings show that considerable diversity exists among bacteria with respect to the transcriptional organisation of their glycolytic genes.

In all the reports of gene sequences and enzyme characterisation of primary metabolism in streptomycetes, an interesting common feature has been noted. In the enteric bacteria, some of the enzymes in the shikimate, tryptophan, tyrosine, phenylalanine and histidine biosynthesis pathways, and proline catabolism pathways are produced from fused genes (section 2.6). All the equivalent enzymes from streptomycetes are carried on separate genes. With the exception of *trp*EG gene fusion, which is very common in genes in secondary metabolism (Hodgson, 2000). Another occurring feature of streptomycetes aa biosynthetic genes is the occurrence of small open reading frames scattered amongst them. Examples occur in the *S. coelicolor* histidine (Limauro *et al*., 1990), tryptophan and proline (Hood *et al*., 1992) genes. This has also been observed in the *Saccharopolyspora erythraea* cysteine genes (Donadio *et al*., 1990). It is tempting to speculate that these may have some role in regulation.

2.7 Amino acid catabolism

Most amino acid (aa) catabolism in streptomycetes seems to be via pathways previously described in other bacteria. An exception is arginine, which is catabolised via γ-guanidinobutyramide and γ–guanidinobutyrate (Thoai *et al*., 1966). The enzymes involved were induced more than 15-fold by arginine. The histidine and proline catabolic pathways are induced by the cognate aa, but for histidine the true inducer is an intermediate of the pathway (Kendrick & Wheelis, 1982; Smith *et al*., 1995). About half the pathways studied seem to be constitutive, but the levels of the enzymes are very low and difficult to assay (Hodgson, 2000). Global CR of aa catabolism has been reported in streptomycetes, but CCR

of aa catabolism, common in enteric bacteria, does not seem to occur (Hood *et al*., 1992; Kendrick & Wheelis, 1982; Kroening & Kendrick, 1987; Hodgson, 2000)

2.7.1 Amino acid biosynthesis

The pathways of aa biosynthesis have been examined in numerous streptomycetes. The aas are apparently synthesised in the same way as they are in most bacteria, with a couple of minor differences (Table 2.5). Tyrosine is synthesised via arogenate as in Pseudomonads, rather than via hydroxyphenylpyruvate as in enteric bacteria (Keller *et al*., 1985). A more important difference is the presence of a trans-sulphuration pathway in streptomycetes. The pathway is characteristic of fungi (Kern & Inamine, 1981), allowing sulphur to be transferred either way between methionine and cysteine via cystathionine γ-lyase and cystathionine β-synthase (Hodgson, 2000). Lysine can be synthesised via OGA (normally associated with bacteria) or oxaloacetate (normally associated with fungi) genome analysis would indicate lysine biosynthesis is via OGA in streptomycetes (probable dihydrodipicolinate synthase [53.3 % identity to many bacterial dihydrodipicolinate synthase], dihydrodipicolinate reductase [56.1 % identity to many bacterial dihydrodipicolinate reductase], succinyl-diaminopimelate desuccinylase [52.1 % identity to *Corynebacterium glutamicum* succinyl-diaminopimelate desuccinylase], diaminopimelate epimerase [34.1 % identity to many bacterial diaminopimelate epimerase], and diaminopimelate decarboxylase [51.0 % identity to *C. glutamicum* diaminopimelate decarboxylase] identification in *S. coelicolor* genome sequence; positions SCO5744, SCO5739, SCO5139, SCO5793, and SCO5353).

A major difference between aa biosynthesis in streptomycetes and the enteric bacteria is its apparent lack of regulation. In the unicellular bacteria, most regulation is at the transcriptional level, with the aa product negatively-controlling expression of the genes encoding biosynthetic enzymes. The method of inhibition includes attenuation and aa binding to repressor proteins. There is very little evidence of such feedback inhibition of gene expression in streptomycetes. The only feedback regulation to date reported for *S. fradiae* is for threonine dehydratase repressed by isoleucine, valine, leucine, and threonine (Vancura *et al*., 1989) and acetohydroxy acid synthase (*ilv*BN) which is repressed by isoleucine, threonine, leucine; and stimulated by valine (Vancura *et al*., 1989). There are

reports that biosynthesis of arginine and the common aromatic & branched chain aas may be subject to feedback repression (Potter & Baumberg, 1996; Rodriguez-Garcia *et al*., 1997). Recently an attenuator was found upstream of the *trp*EG gene in *S. coelicolor*, which encodes the first enzyme of the tryptophan-specific pathway. Genes encoding the enzymes for the final part of the pathway (*trp*D, *trp*C, and *trp*BA) appeared to be regulated by growth phase (active in growth phase, non-active in stationary phase) and growth rate (the faster the growth, the more enzyme)[Hu *et al*., 1999].

It could be speculated that the scarcely regulated biosynthetic pathways reflect the growth of the streptomycetes under typically nutrient-limited conditions, compared with the enteric bacteria. In the gut, a plentiful supply of nutrients washes through at regular intervals, so the enteric bacteria have developed the ability to react quickly to feast and famine. For the streptomycetes, starvation is the rule and so they seem not to have evolved, or have lost, the ability to regulate aa biosynthesis at the gene level. How streptomycetes manage to avoid the apparent futile cycle of constitutive synthesis of an aa followed by degradation by constitutive catabolic enzymes is a mystery (Hodgson, 2000).

2.8 Fatty acid biosynthesis

It is known that the composition of fatty acids (FAs) in microorganisms is highly influenced by cultivation conditions under which the cell population is grown. However, the physiological changes caused by differences in FA composition are less understood (Vancura *et al*., 1987; Arima *et al*., 1973; Okazaki *et al*., 1973, 1974). Lipids produced by streptomycetes contain branched iso and anteiso FAs, whose amount and actual ratio are important with respect to membrane function and are regulated both at the genetic and physiological level (Batrakov & Bergelson, 1978).

The relationship between nitrogen metabolism and the biosynthesis of lipids and antibiotics has only been studied in a limited number of species. In regulatory mutants of *S. cinnamonensis* resistant to aa analogues, the effect of change in biosynthesis of endogenous precursors on the composition of FAs was described (Pospisil *et al*., 1985). The overproduction of valine is supposed to be the reason for both increased yield of monensin A and higher content of iso-even FAs, where valine serves as a precursor for isobutyrate (after isomerization) or butyrate units. The effect of exogenous substance on FA

composition and tylosin biosynthesis has been studied (Omura *et al*., 1984; Vancura *et al*., 1987a, b; 1988a). High NH_4 concentration decreases the quantity of branched chain FAs, while total lipids remain constant. The mechanism of NH_4 repression is at the enzyme level, by repression and inhibition of VDH, the first enzyme in valine catabolism. In *S. avermitilis* the yield of lipids and avermectins was influenced by NH_4 while the composition of FAs remained constant. The total synthesis of oligoketides in *S. avermitilis* seemed to be regulated at the level of global metabolic network (Novak *et al*., 1992). Grafe *et al*., (1982a, b) isolated and characterised mutants of *S. hygroscopicus* and *S. griseus* that cannot form aerial mycelium and have a different ratio of iso and anteiso acids, viz 16:0 and 15:0, respectively. The authors assumed that this fact is caused by a genetically-determined change of the biosynthesis of corresponding branched aas, i.e. valine and isoleucine, and that a mechanism regulating the composition of FAs exists in streptomycetes and that the function of such a regulator mechanism is necessary for differentiation. Analysis of the relative proportion of FAs in *S. lasaliensis* led to the conclusion that it was possible to deduce the relationship of biosynthetic precursors of even- and odd-number iso-acids (i.e., valine or leucine) to the metabolism of FAs, and also to infer the production of a certain type of antibiotic.

2.9 Ammonium assimilation

The potential pathways of assimilation of NH_3 in streptomycetes are shown in Table 2.6 & Fig 2.7. The central pathway of NH_3 incorporation in bacteria involves the enzymes glutamine synthetase (GS) and glutamate synthase (GOGAT)[Zubay, 1998]. A large number of bacteria have an additional enzyme that can lead to assimilation of NH_3. This enzyme, glutamate dehydrogenase (GDH), has low affinity for NH_3; but at high NH_3 concentration it can catalyse the formation of glutamate directly from NH_3 and OGA without the cleavage of ATP. Therefore, the cell can generate both glutamate and glutamine with the GDH-GOGAT couple in high – NH_3 conditions, or with the GS-GOGAT couple in low NH_3 conditions. Not all streptomycetes have GDH. The alternative to this is alanine dehydrogenase (ADH), with the presence of alanine transaminase (AOAT) to allow transfer of the amino group to Glu and hence to Gln via GOGAT (Hodgson, 2000). Another alternative mechanism of NH_3 assimilation might be via aspartate. Amination of an organic acid to form aspartate which must be followed by transamination of glutamate via oxaloacetate transaminase (GOAT),

alternatively called aspartate 2-oxoglutarate amino transferase or aspartate transaminase (Hodgson, 2000).

2.9.1 Glutamine synthetase (GS)

Streptomycetes contain two forms of GS (GS I & GS II; GS II has proved to be thermolabile and is thought to have a role in nitrogen catabolism) (Grafe *et al*., 1977). *S. glaucescens*, *S. fradiae*, *S. coelicolor*, *S. lividans*, *S. viridochromogenes* & *S. hygroscopicus* contained both ISEs (Hodgson, 2000). Amino acids and nucleotides inhibited both GS I and GS II enzyme activities (Hillemann *et al*., 1993). It is not known how GS II activity is regulated or coordinated with GS I activity in streptomycetes (Hodgson, 2000).

2.9.2 Glutamate synthase (GOGAT)

GOGAT has been identified in all streptomycetes so far analysed (Hodgson, 2000). The enzyme has a specific requirement for NADH in *S. noursei* and *S. clavuligerus* (Brana *et al* 1986). The activity of NADH-dependent GOGAT in *S. coelicolor*; was found to be modulated by the nitrogen source of the cell. When alanine was the nitrogen source GOGAT activity was almost seven-fold lower than when the cell was growing on a complex nitrogen source (Fisher, 1989).

2.9.3 Glutamate dehydrogenase (GDH)

GDH has been reported in a number of streptomycetes: *S. fradiae* (Romano & Nickerson, 1958; Vancura *et al*., 1989), *S. noursei* (Grafe *et al*., 1974b; 1977), *S. venezuelae* (Shapiro & Vining, 1983), *S. hygroscopicus* (Xia & Jiao, 1986), *S. cyanogenus* (Watanabe *et al*., 1976a, b), and *S. coelicolor* (Fischer, 1989). However, no activity could be found in *S. aureofaciens* (Vancura *et al*., 1988b). Minanbres *et al*. (2000) reported evidence for an AMP-requiring GDH of *S. clavuligerus*. In *S. noursei* the enzyme was NADP-dependent and the activity was increased in cells where GS was low, and vice versa. Excess NH_3 in the culture medium repressed GDH activity in *S. venezuelae*, *S. hygroscopicus* and *S. coelicolor*. The *S. venezuelae* and *S. coelicolor* enzymes were NAD-dependent. *S. fradiae* is a special case; containing two GDH activities, one was NADP-dependent whilst the other was NAD-dependent (Vancura *et al*., 1989). However, both ISEs were most active in cells

grown on 25 mM NH_4. AMP, ADP & ATP were shown to inhibit both the forward and reverse reactions, with ATP showing the most profound effect (Vancura *et al*., 1989). The NAD-dependent GDH was also purified and the deamination reaction found to be partially sensitive to adenyl nucleotides, but the reverse reaction was not (Nguyen *et al*., 1997).

2.9.4 Transaminases

Alanine dehydrogenase (ADH) if this enzyme has a role in NH_3 assimilation a transaminase, such as AOAT or perhaps alanine: 2-isovalerate transaminase (ATS) needs to be present (Hodgson, 2000). Neither of these transaminases was found in *S. coelicolor* (Fisher, 1989). No AOAT activity could be found in *S. clavuligerus* (Brana *et al*., 1986). However AOAT was reported to be present in *S. hygroscopicus,* as was alanine dehydrogenase (ADH) (Grafe *et al*., 1974a). AOAT was also present in *S. noursei* (Grafe *et al*., 1974b), *S. cyanogenus* (Watanabe *et al*., 1976a), and *S. avermitilis* (Novak *et al*., 1992). Romano & Nickerson (1958) reported the presence of glutamate synthase (GOAT) in *S. fradiae*. However they also reported, that they could find neither aspartase or aspartate dehydrogenase activities. These observations were taken to explain why aspartate could act as a sole nitrogen source but not as a sole carbon source. GOAT was also reported to be present in *S. noursei* (Grafe *et al.*, 1974b).

2.10 Secondary metabolism

Although primary biosynthetic pathways are common to the vast majority of micro-organisms, secondary metabolic routes are unique to a few microbial species. Secondary metabolism, is common amongst the filamentous bacteria, fungi and the spore forming Eubacteria (e.g. bacilli, pseudomonads and actinomycetes) but is not found for example, in the Enterobacteriaceae (Zähner & Maas, 1972). Not only do *Streptomyces* possess the mechanisms to synthesise these compounds but they also possess means of resistance in order not to cause self-death. During the normal life cycle of these organisms, sporulation occurs when their growth is impaired by the supply of oxygen (Clark *et al*., 1995), or nutrients (Section 2.4.2), or by other environmental factors. It is at this point of the life cycle that primary metabolites and signalling molecules accumulate (Horinouchi & Beppu, 1984; 1990; Onaka *et al*., 1998; for reviews of autoregulatory factors that effect secondary metabolism and morphology) induce secondary metabolism (Malik, 1980; Martin &

Demain, 1980). A characteristic feature of secondary metabolism is that any given organism usually produces a group of compounds belonging to the same class (Kurylowicz *et al.,* 1976). Normally these are relatively low molecular weight compounds (Maplestone *et al.,* 1992; Bevan *et al.,* 1995). Another feature of this type of metabolism is that a large number of products arise from relatively few intermediates in primary metabolism. Also, combinations of different primary metabolites are often used, e.g. in case of erythromycin where parts of the molecule are derived from propionate, glucose, and from methyl groups (Zähner & Maas, 1972; Zähner & Anke, 1983). In contrast to primary metabolites, secondary metabolites are not essential for growth (Vining, 1992). Primary metabolites are either building blocks for macromolecules, intermediates in reactions generating energy-rich compounds (ATP), coenzymes and vitamins. Secondary metabolites have no such vital roles in metabolism, but still may play an important role in the life cycle of the organism (Beppu, 1992). When the organism stops growing and enters a resting phase, accumulation of primary metabolites could occur. This is potentially harmful and it has been speculated that the cells avoid this by starting to produce secondary metabolites (Malik, 1980; Vining, 1992).

2.10.1 The Biosynthesis of Tylosin from *S. fradiae*

Tylosin is a macrolide antibiotic (Fig 2.8) that was first described in 1961 by McGuire *et al*. Tylosin is produced by *S. hygroscopicus* (Jensen *et al*., 1964), *S. rimosus* (Pape & Brillinger, 1973), and commercially produced by *S. fradiae*. It comprises of a central 16-membered polyketide lactone ring which is known as tylactone or prototylonolide, to which are attached three 6-deoxyhexose sugars, known as mycarose, mycaminose and mycinose (Jones *et al*., 1982). Its use, as with many other macrolides, is to treat Gram-positive bacterial infections in animals, where its activity acts by inhibiting protein synthesis by binding to the large ribosomal subunit. However, its use as a feed additive to promote growth in swine and poultry has promoted the emergence of its resistance in some Gram-positive organisms. Tylosin acts on microorganisms by inhibiting protein synthesis by a mechanism that involves the binding of tylosin to the ribosomes, preventing the formation of the mRNA-aminoacyl-tRNA-ribosome complex (Graham & Weisblum, 1979). The site of the binding of tylosin is on the 50S subunit of the ribosome (Graham & Weisblum, 1979). Graham & Weisblum (1979) have shown that tylosin producing *S. fradiae* contain N^6-

methyl adenine in their 23S ribosomal nucleic acid. Specific methylation of 23S RNA mediates co-resistance to the macrolide antibiotics (Zalacain & Cundliffe, 1989), linosanide, and streptogranin in clinical isolates of *S. aureus*. The presence of methylated RNA in *S. fradiae* could explain the mechanism by which the organism is resistant to its own antibiotic. Therefore, tylosin can now only be administered solely to treat infection rather than to prevent infection in Europe.

Tylosin biosynthesis occurs in three main parts: the synthesis of tylactone, the synthesis of the sugars, and the conversion of tylactone into tylosin. This biosynthesis has many interesting features including the involvement of metabolites derived from primary metabolism, in addition to the similarities between secondary metabolite formation and FA biosynthesis (i.e., polyketide synthesis) [Gray & Bhuwapathanapun, 1980b; Baltz & Seno 1988; Masamune *et al*., 1977].

2.10.2 The tylosin biosynthesis cluster

The *tyl* genes for tylosin biosynthesis are clustered within a defined region (85 Kb) of the *S. fradiae* genome and are flanked by resistance determinants *tlr*B and *tlr*C (Baltz *et al.*, 1988; Bate, 1999; Beckman *et al.*, 1989; Fouces *et al*., 1999; Cundliffe *et al*., 2001). This collection of 43 genes also includes a small number of open reading frames (ORFs) that are assigned and/or may not be essential to tylosin production. Extensive genetic and phenotypic complementation studies have led to several classes of blocked mutants, revealing the genetic organisation of the tylosin biosynthetic gene (*tyl*) cluster (Baltz & Seno, 1981; Fisherman *et al.*, 1987; Baltz & Seno, 1988). The *tyl*G region harbours the polyketide synthases (PKS) genes, while the *tyl*LM, *tylI*BA, and *tyl*CK regions contain genes for mycaminose and mycarose formation (Baltz & Seno, 1981; Fisherman, 1987; Baltz & Seno, 1988) [Baltz, 2000 for an interesting discussion of direction of the latter research undertaken by industry & academe over past 25 years].

2.10.3 The biosynthesis of tylactone precursors

It has been proposed (Masamune *et al.*, 1977) that the formation of macrolide lactone rings, are similar to the synthesis of saturated long chain FAs. Studies on the incorporation of ^{13}C precursors into tylosin indicated that the carbon skeleton of tylactone (Fig 2.9) is derived

from five propionates, two acetates, and one butyrate (Omura *et al.*, 1975, 1977; Dotzlaf *et al.*, 1984). They also reported that these metabolites not only serve the formation of the tylactone ring but also play a role in FA synthesis. Omura (1974) confirmed this through the addition of cerulenin (an inhibitor of FA synthesis) to a culture, which caused inhibition of tylosin and FA biosynthesis. Rezanka *et al.* (1991) further supported this idea, through the addition of labelled isobutyrate to cultures of *S. fradiae*. They determined that isobutyrate was transformed into butyrate and to an extent propionate, that was then incorporated into tylactone. The data of Omura *et al.* (1978, 1974, 1977) suggested that the precursors for tylactone biosynthesis were incorporated in the following manner. Propionate as one propionyl-CoA (primer); and four methylmalonyl-CoA molecules (interconversion of propionyl-CoA and methylmalonyl-CoA has been demonstrated in *S. fradiae* [Vu-Trong *et al.*, 1980]) acetate as two malonyl-CoA molecules, and butyrate as one ethylmalonyl-CoA molecule.

Malonyl-CoA is synthesised through the carboxylation of acetyl-CoA by an acetyl-CoA carboxylase, or another route involving PEPC and oxaloacetate dehydrogenase. (Harwood, 1988; Laakel *et al*., 1994). In other polyketide producing *Streptomyces.* spp, methyl-malonyl-CoA can be synthesised either from succinyl-CoA by methyl-malonyl-CoA mutase (Birch *et al*., 1993), or by propionyl-CoA carboxylase, (Bramwell *et al*., 1996), or from *n*-butyryl-CoA through isobutyryl-CoA mutase (Zerbe-Burkhardt *et al*., 1998).

A *tyl*A mutant of *S. fradiae* that is blocked in the production of tylosin sugars and therefore can only produce tylactone (Baltz & Seno, 1981), allowed Dotzlaf *et al.* (1983) to investigate the role of aas as sources for the tylactone precursors. By using radiolabelled tracer studies, Dotzlaf *et al.* (1983) reported that the tylactone precursors propionyl-CoA and methylmalonyl-CoA were derived from aas either directly (see compounds labelled with Roman Numeral I in Fig 2.9), or indirectly via the TCA cycle (see compounds labelled II).

Figure 2.9 indicates the involvement of the aas arginine, proline, leucine and phenylalanine in tylactone biosynthesis. Dotzlaf *et al.* (1983) have also shown the possible roles of CHO and lipid in tylactone biosynthesis by means of the TCA cycle, and that the CHO that enters the TCA cycle also seems to be the source for methylmalonyl-CoA and propionyl-CoA generation. The data suggest the possible source for ethylmalonyl-CoA is acetoacetyl-CoA,

which is derived from the interrupted β-oxidation of lipid.

The aa valine has been shown to be a starting primer in the synthesis of branched-chain FAs and tylactone biosynthesis. Recent studies by Zhang *et al.* (1999) have also shown the importance of valine, leucine and isoleucine catabolism in supplying FA precursors for macrolide biosynthesis in other *Streptomyces* species (Tang *et al*., 1994). Valine and isoleucine can be catabolised via 2-methyl-branched-chain acyl-CoA dehydrogenase to form propionyl-CoA and acetyl-CoA, propionyl-CoA and methylmalonyl-CoA, respectively. Leucine can be metabolised into acetyl-CoA and acetoacetate via isovaleryl-CoA dehydrogenase.

2.10.4 Biosynthesis of the polyketide backbone of tylactone

The polyketide backbone of tylactone is synthesised by a mechanism similar to those involved in the formation of FAs. The growth of polyketide carbon chain is initiated by the condensation of a starter unit with an extender unit. The starter and extender units are present in the host as Co-enzyme A (CoA) based thioesters. PKSs mainly use acetyl-CoA or propionyl-CoA as starter units with malonyl-CoA and methylmalonyl-CoA as the common extender units (this is not a set rule). Condensation is driven by decarboxylation of the extender unit. Polyketides synthesis differs from that of FAs in that one or more of the reactions may be carried out at different steps resulting in molecules containing keto, hydroxyl, enoyl or alkyl-functionality at specific points (Fig 2.10). Determination of functionality has been shown to occur at each specific stage, not on completion of the chain (Hutchinson *et al*., 1998; Hranueli *et al*., 2001). In their absence, a diketide will immediately undergo another round of condensation employing a new extender to become an unreduced triketide, and so on. The extension of the polyketide chain occurs by successive additions of CoA derivatives of carboxylic acids (see Fig 2.10 for the hypothetical biosynthesis of tylactone). The final step involves one final elongation step, termed *Tyl*GV through a mechanism similar to other PKS, this involves an enzyme that possesses an integral thioesterase allowing chain termination and ring closure (Butler *et al*., 1999). Yue *et al.* (1987) reported the first direct evidence for a mechanism of chain elongation and stepwise synthesis of FAs that ultimately cyclise to form tylactone. This was supported by Huber *et al.* (1990) who isolated three branched chain FAs from the culture broth of S. *fradiae* mutants blocked in tylactone synthesis and found they were precursors of

tylactone.

The enzymes that make these polyketide backbones can be categorised into Type I or Type II PKS complexes (PKSs). The Type I PKS gene clusters, such as those responsible for the biosynthesis of complex polyketides like the macrolide erythromycin, are multi-functional enzymes with a modular organisation. Each module is responsible for a single cycle of polyketide carbon chain extension and contains domains for necessary reduction activities (Hranueli *et al*., 2001). Where Type II PKSs, such as those responsible for the biosynthesis of aromatic polyketides like ACT, consist of up to six separate mono-bi-functional proteins (Hranueli *et al*., 2001). In contrast to the one to one correspondence between active sites and product structure of Type I PKSs, the Type II PKSs are structurally all very similar so it is not possible to predict the nature of the polyketide structure made from the structure and architecture of the genes.

2.10.5 The Synthesis of Mycinose, Mycaminose and Mycarose

Genes encoding biosynthesis of the three, tylosin sugars (Fig 2.11; adapted from Cundliffe, 1999) are arranged in three specific blocks [there are numerous reviews of the biosynthesis of amino sugars, Johnson & Liu, 1998; Hallis & Liu, 1999]. The mycinose biosynthetic genes (orfs 19*-25*) form a complete functional cassette (Bate & Cundliffe, 1999). Besides the methylation step the following reactions are necessary for the synthesis of dTDP-L-mycarose from dTDP-D-glucose: reduction at C2, inversion of configuration at C5 and (possibly the last step) stereo-specific reduction of the carbonyl group C4 leading to the L-configuration (Chen *et al.,* 1999a). *tyl*N the sugar bind covalently to tylactone to form tylosin (Chen *et al.,* 1999a). Three genes in the *tylI*BA region are believed to be involved in mycaminose biosynthesis (Merson-Davies & Cundliffe, 1994; Chen *et al.*, 1998b). *Tyl*A1 encodes α-D-glucose 1 phosphate thymidyltransferase, *tyl*A2 encodes TDP-D-glucose 4,6-dehydratase and *tyl*B is likely the gene for a pyridoxal 5' phosphate-dependent aminotransferase (Thorson *et al.*, 1993; Chen *et al.*, 1998a). Fig (2.11) shows how the biosynthesis of mycaminose is similar to mycarose (Bate *et al*., 2000). *tyl*MII encodes for the glycosyltransferase; and *tyl*MIII may encode a tautomerase which displays sequence similarity to some P450 enzymes but lacks the conserved cysteine residue that co-ordinates the heme iron (Gandecha *et al.*, 1997; Wallace *et al.*, 1995). The study by Pape & Brillinger

(1973) on the *S. rimosus* strain that produces tylosin has indicated that mycarose is derived from TDP-D-glucose and S-adenosyl-1-methionine and requires NADPH. It also has TDP-4-keto-6-deoxy-D-glucose and a second methylated TDP-sugar as intermediates with TDP-4-keto-6-deoxy-D-glucose then catalysed by the enzyme TDP-D-glucose oxidoreductase. While all of these assignments are based solely on sequence analysis, the identification of these genes has allowed initial speculation of their roles leading to a possible route for mycaminose biosynthesis (Chen *et al.,* 1998a). Chen *et al*. (1998b) and workers expressed several of these genes and examined the catalytic properties of the purified enzymes. The initial work clearly demonstrated that *tylM*I encodes the required methyltransferase and *Tyl*B (Chen *et al.,* 1998a) as the aminotransferase required for the C-3 transamination (Chen *et al.*, 1999) step in the biosynthesis of mycaminose.

2.10.6 The Conversion of Tylactone to Tylosin

Through analysing compounds accumulated by blocked mutants of *S. fradiae* in co-synthesis and bioconversion studies, it has been possible to determine the biosynthetic route to tylosin (Fig 2.12) [Seno *et al.,* 1977; Baltz & Seno, 1981; Omura *et al.*, 1982b; Baltz *et al.*, 1983]. The sequence involves the initial glycosylation at the 5' hydroxyl position with mycaminose, and is followed by the oxidation of C-20 to -CH_2OH, which is subsequently oxidised again to –CHO. The next part of the sequence involves the glycosylation at the C-23 hydroxyl position with 6-deoxy-D-allose. This is achieved bye *tylH*I, which encodes a cytochrome P450 that hydroxylates the polyketide ring at C-23, thus allowing the binding of the deoxyallose (Baltz & Seno, 1981; Omura *et al*., 1984). The 6-deoxy-D-allose is then added to produce demethyllactenocin, which is then glycosylated with the amino sugar mycarose to form demethylmacrocin. Demethylmacrocin is methylated to macrocin, which is subsequently methylated to tylosin (Fish & Cundliffe, 1997). Tylosin reductase has been purified from *S. fradiae,* which was speculated to catalyse the reduction of tylosin to relomycin, an industrial undesirable product. The activity of tylosin reductase is closely related to bacterial growth, suggesting involvement of the enzyme in primary metabolism (Huang *et al*., 1993).

Within this cluster there are four open reading frames which utilise the rare TTA codon and five regulatory genes. The first, *tylP*, encodes for γ-butyrolactone signal receptor

(Horinouchi & Beppu, 1986 for related γ-butyrolactone structures such as A-factor) which targets *tyl*Q (Stratigopoulos & Cundliffe, 2002). The genes *tyl*S and *tyl*T encode pathway-specific regulatory proteins of the *Streptomyces* antibiotic regulatory protein (SARP) family (Bate *et al*., 2002). Through mutational analysis, the last gene, *tyl*R, has been shown to control various aspects of tylosin production. Together these genes could be manipulated to affect yields in tylosin fermentation (Bate *et al*., 1999).

Developmental cycle of *Streptomyces coelicolor*.

(a) Below is a schematic representation of the *Streptomyces* life-cycle.

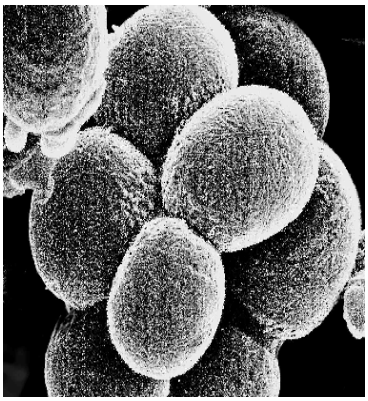

Close up of *Streptomyces coelicolor* spores (c. 1µm wide) showing surface structures (Scanning electron micrograph, Mark Buttner, Kim Findlay, John Innes Centre).

Young vegetative mycelium (c. 1 µm wide) of *Streptomyces* grown in liquid broth (light microscope ; Gabriella Kelemen John Innes Centre).

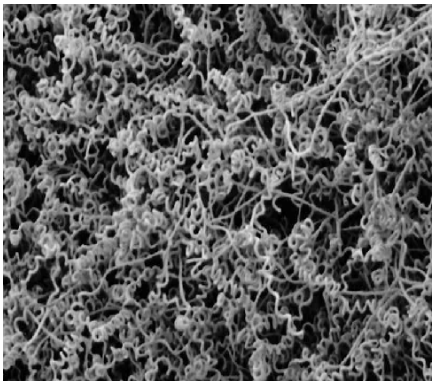

Mass of curled aerial mycelium (c. 1 µm wide) of *Streptomyces coelicolor* (Scanning electron micrograph, Mark Buttner, Kim Findlay, John Innes Centre).

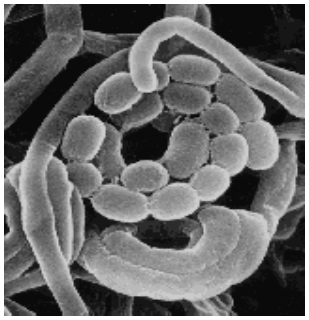

Aerial mycelium and spore of *Streptomyces coelicolor*. The mycelium and the oval spores are about 1µm wide, typical for bacteria and much smaller than fungal hyphae and spores. (Scanning electron micrograph, Mark Buttner, Kim Findlay, John Innes Centre).

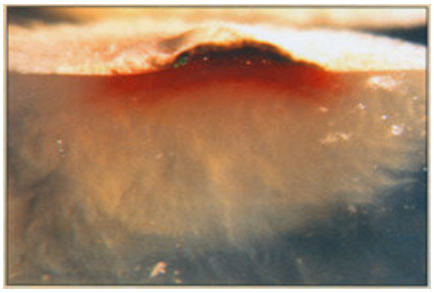

(b)

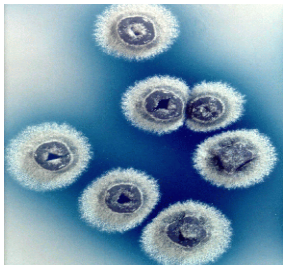

(c)

Fig 2.1. (a) Influenced by external factors such as starvation or drying out, an aerial mycelium develops with curled hyphae from the tips of which spores are secluded. This results in a complex life-cycle consisting of roughly three phases: vegetative mycelium, aerial mycelium and spores. The pictures (b) & (c) cross-section of a *Streptomyces coelicolor* colony (left) and a single streptomyces colony.

Table 2.1: Reactions of the Embden-Meyerhof-Parnas pathway

Hexokinase	**Glucose + ATP ↔ G6P + ADP**
G6P isomerase	**G6P ↔F6P**
Phosphofructokinase	**F6P + ATP → F-1,6-P2 + ADP**
Fru16dP aldolase	**F-1,6-P2 ↔DHAP + GAP**
Triose phosphate isomerase	**DHAP ↔ G3P**
G3P dehydrogenase	**G3P + NAD + P_i ↔ PG + NADH**
PG kinase	**PG + ADP ↔ 3PG + ATP**
Phosphoglycerate mutase	**3PG ↔2PG**
Enolase	**2PG ↔ PEP + H_2O**
PYR kinase	**PEP + ADP → PYR + ATP**
Pyruvate dehydrogenase complex (PDH)	**PYR + NAD + CoA → AcCoA + NADH + CO_2**

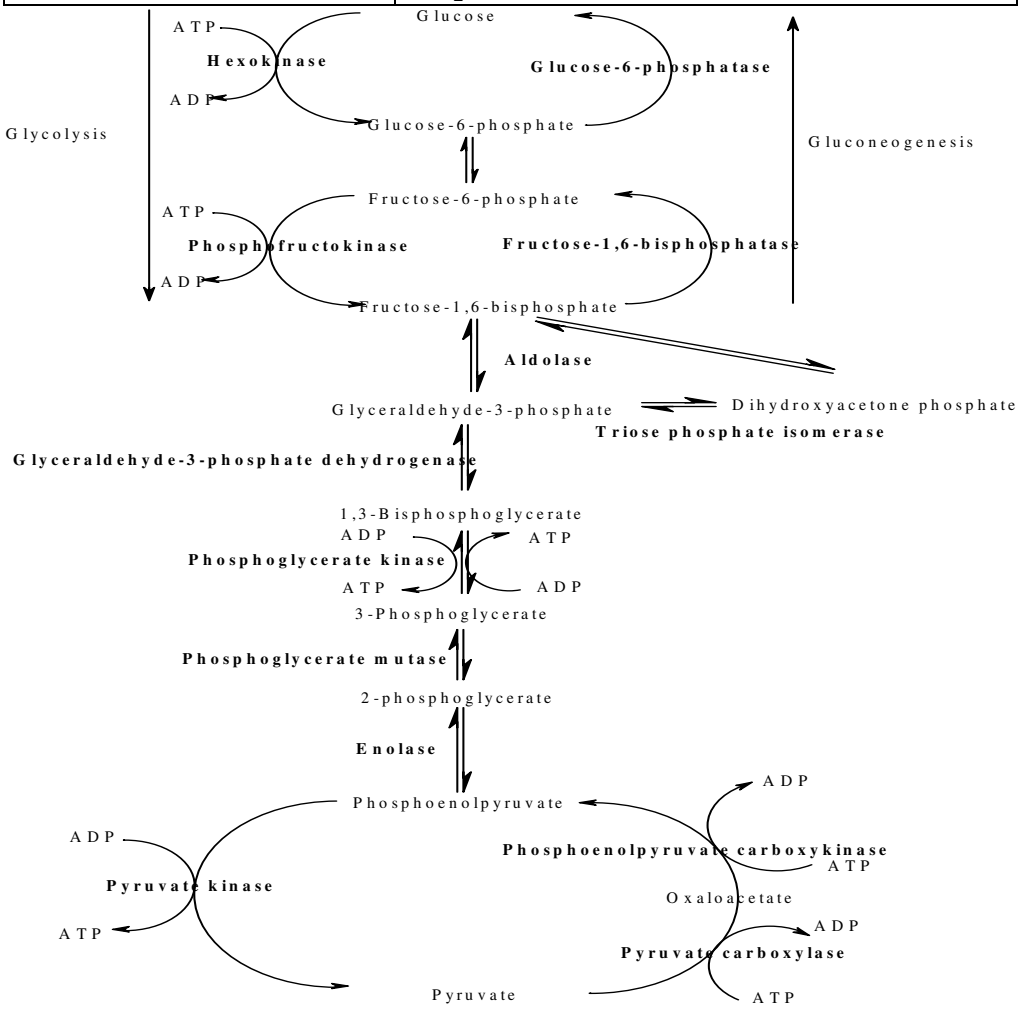

Fig 2.2 Tables and diagrams present enzymes and pathways present in the gluconeogenic and glycolytic pathways. Gluconeonesis and EMP pathway have the same intermediates but represent two distinct pathways because of irreversible reactions in each that are catalysed by different enzymes.

Table 2.2: The reactions of the TCA cycle

Pyruvate dehydrogenase complex (PDH)	**PYR + NAD +CoA → AcCoA + NADH + CO_2**
(1) Citrate synthase	**AcCoA + OAA + H_2O ↔ Cit + CoA**
(2) Aconitase	**Cit ↔ IsoCit**
(3) IsoCit dehydrogenase	**IsoCit + NADP →OGA + CO_2 + NADPH**
(4) Oxoglutarate dehydrogenase	**OGA + NAD + CoA → SucCoA + CO_2 +NADH**
(5) Succinate thiokinase	**SucCoA + GDP → Suc + GTP + CoA**
(6) Succinate dehydrogenase	**Suc + FAD → Fum + FADH**
(7) Fumarate hydratase	**Fum + H_2O ↔ Mal**
(8) Malate dehydrogenase	**Mal + NAD → OAA + NADH**

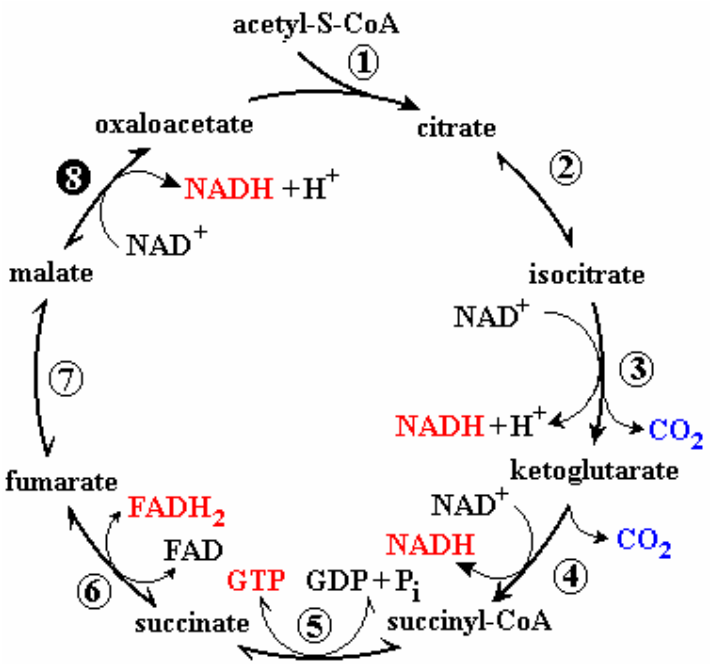

Fig 2.3 Tables and diagrams present enzymes and pathways present in the TCA cycle (Diagram adapted from Michal (1999).

Table 2.3: **Primary enzymes of the Pentose Phosphate Pathway.**

G6P dehydrogenase	**G6P + NADP → NADPH + 6PGL**
6-phosphogluconalactonase	**6PGL + H_2O → 6PG**
Glcn6P dehydrogenase	**6GP + NADP → Ru5P + NADPH + CO_2**
Ribu5P isomerase	**Ru5P ↔ R5P**
Ribu5P 3-epimerase	**Ru5P ↔ X5P**
Transketolase	**X5P + R5P ↔ S7P + G3P**
Transaldolase	**S7P + G3P ↔ F6P + E4P**
Transketolase	**X5P + E4P ↔ F6P + G3P**

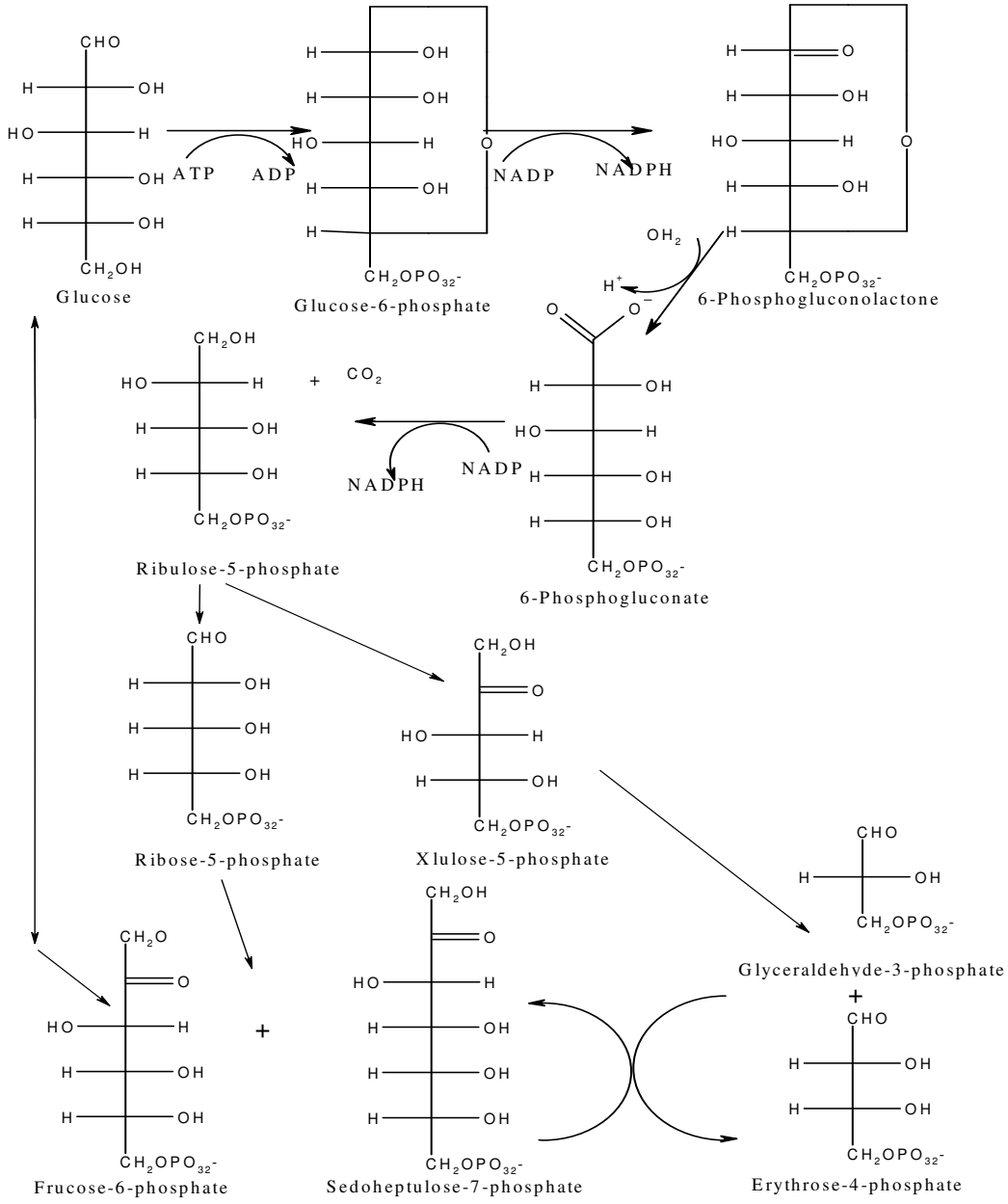

Fig 2.4 Tables and diagrams present enzymes and pathways involved in the pentose phosphate pathway (taken from Michal, 1999).

Table 2.4: Anaplerotic reactions detected in Streptomyces.

PEP carboxylase	**$PEP + CO_2 \rightarrow OAA$**
Pyruvate carboxylase	**$PYR + CO_2 + ATP \leftrightarrow OAA + ADP$**
PEP carboxykinase	**$OAA + ATP \rightarrow PEP + ADP + CO_2$**
Malate dehydrogenase decarboxylating	**$Mal + NADP \rightarrow PYR + NADPH + CO_2$**
Glyoxylate bypass:	
IsoCit lyase	**$IsoCit \leftrightarrow Suc + Glyox$**
Malate synthase	**$Glyox + AcCoA + H_2O \rightarrow Mal + CoA$**

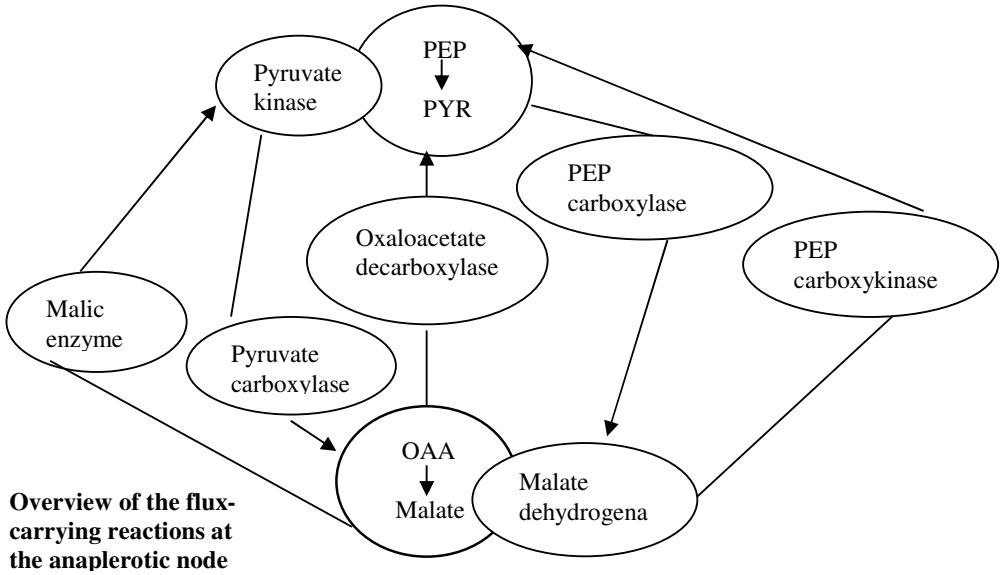

Overview of the flux-carrying reactions at the anaplerotic node

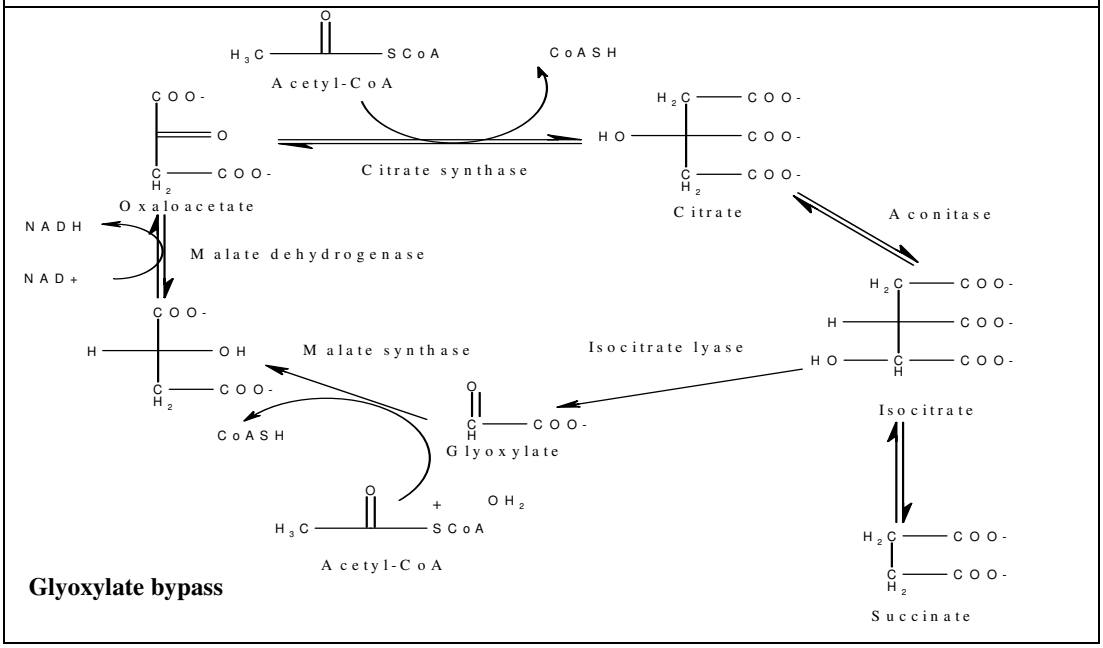

Glyoxylate bypass

Fig 2.5 & 2.6 Tables and diagrams present enzymes and pathways involved in pyruvate and phosphoenolpyruvate metabolism and the glyoxylate bypass (diagrams adapted from Michal, 1999).

Table 2.5: Biosynthetic pathways of amino acids

Amino acid	**Biosynthetic pathway**
Glutamate family (5)	Oxo-glutarate → Glu (Gln) → ornithine; Oxo-glutarate → Arg; Glu → α-aaa → Lys; Glu → Pro
Aspartate family (5)	Oxaloacetate → Asp → homoserine (Met) → Thr → Ile; Asp → Asn
Aromatic family (3)	PEP + erythrose-4-P → chorismate → prephenate → Phe / Tyr / Trp
Pyruvate family (3)	Pyruvate → α-ketoisovalerate → Val / Leu; Pyruvate → Ala
Serine family (3)	3-phosphoglycerate → Ser → Gly / Cys
Histidine (1)	Ribose-5-phosphate → His

Overview of amino acid biosynthesis in bacteria. The amino acids are classified into five families according to the specific precursor metabolite or amino acid that serves as the starting point for their synthesis. Histidine, which has a complex biosynthetic pathway, does not group with any of the other amino acids. The numbers indicate the reaction steps in the pathway. AKG, oxo-glutarate; ALA, Alanine; ARG, Arginine; ASN, Asparagine;

CHOR, Chorismate; CYS, Cysteine; E4P, Erythrose-4-phosphate; GLN, Glutamine; GLU, Glutamate; HIS, Histidine; ILE, Isoleucine; LEU, Leucine; LYS, Lysine; MET, Methionine; OAA, Oxaloacetate; PEP, Phosphoenolpyruvate; PG, Phosphoglycerate; PHE, Phenylalanine; PRO, Proline; PYR, Pyruvate; R5P, Ribose-5-phosphate; SER, Serine; THR, Threonine; TRP, Tryptophan; TYR, Tyrosine; VAL, Valine. Taken and adapted from Stephanopoulos *et al*. (1998).

Table 2.6: ammonium assimilation reactions

Glutamine synthetase (GS)	**Glu + NH_3 + ATP ↔ Gln + ADP**
Glutamate synthase (GOGAT)	**Gln + OGA + NADPH ↔ 2 Glu + NADP**
Glutamate dehydrogenase (GDH)	**NH_3 + OGA + NADPH ↔ Glu + NADP**
Oxaloacetate transaminase (GOAT)	**OGA + NH_3 + ATP ↔ Glu + ADP**
Alanine dehydrogenase (ADH)	**Pyr + NADH + NH_3 ↔ Ala + NAD**
Alanine: 2-oxo-glutarate transaminase (AOAT)	**Ala + OGA ↔ Pyr + Glu**

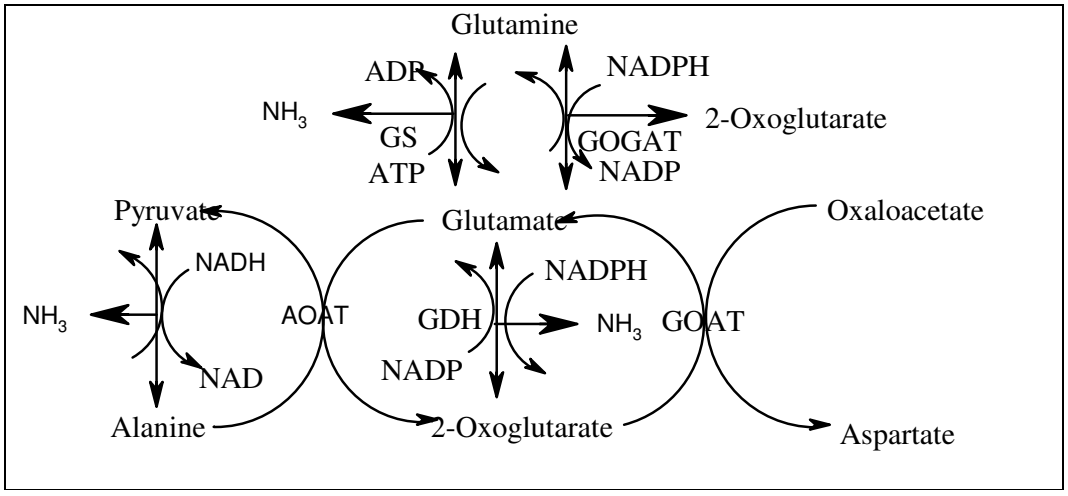

Fig 2.7 Potential pathways of ammonium assimilation in streptomycetes. GS, glutamine synthetase; GOGAT, glutamate synthase; GDH, glutamate dehydrogenase; ADH, alanine dehydrogenase; AOAT, alanine: 2-oxo-glutarate transaminase; GOAT, glutamate: oxaloacetate transaminase.

The structure of tylosin

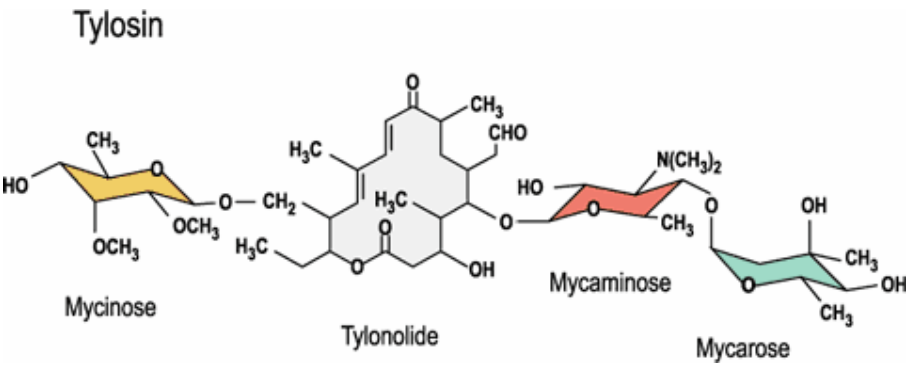

Fig 2.8 Tylosin, a macrolide antibiotic produced by *Streptomyces fradiae*, consists of a polyketide lactone substituted with three deoxyhexose sugars.

The proposed pathway for the biosynthesis of tylactone.

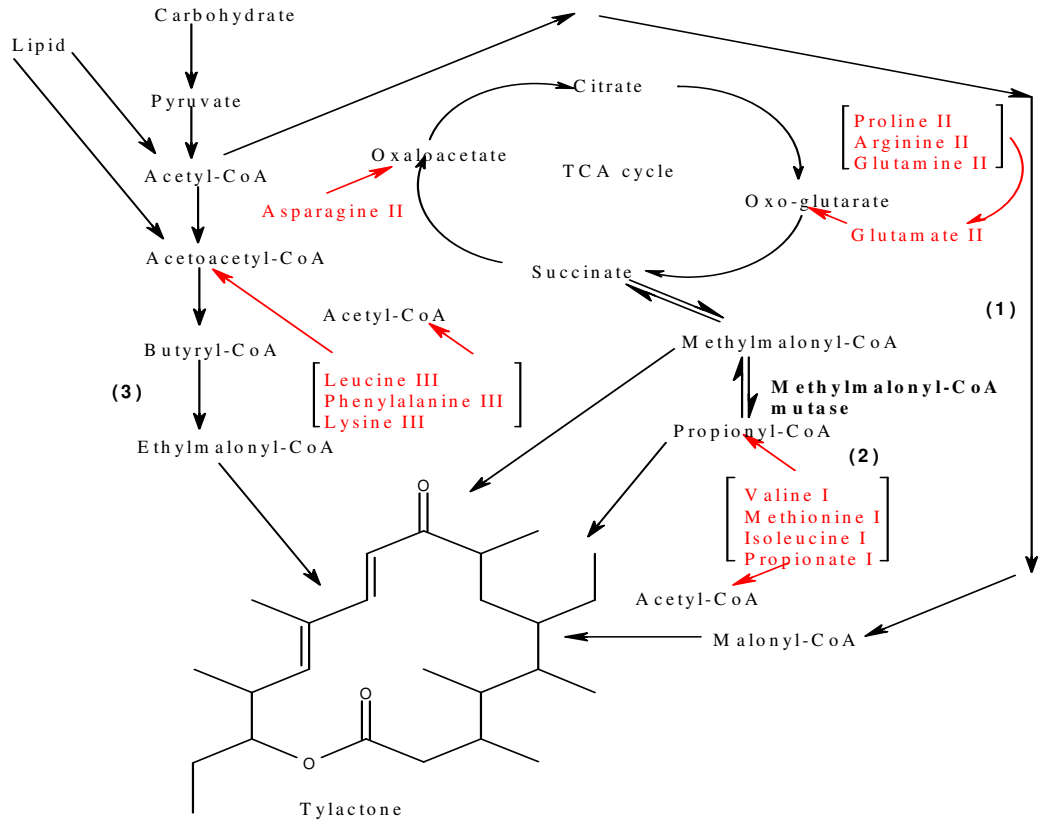

Acetyl-CoA carboxylase

(1) Acetyl-CoA + HCO_3^--carboxybiotin → Malonyl-CoA + biotinate

Methylmalonyl-CoA mutase **Methylmalonyl-CoA racemase**

(2) Succinyl-CoA ↔ L-Methylmalonyl-CoA ↔ D-Methylmalonyl-CoA

Propionyl-CoA de / carboxylase

↔ Propionyl-CoA + ATP + CO_2 + H_2O

Acetyl-CoA-ACP transacylase

(3) Acetyl-CoA + ACT-SH → Acetyl-ACP + CoASH

Malonyl-CoA-ACP transacylase

Malonyl-CoA + ACT-SH → Malonyl-ACP + CoASH

3-ketoacyl-ACP synthase **β-ketoacyl-ACP reductase**

Acetyl-ACP + Malonyl-ACP → Acetoacetyl-ACP + CO_2 + NADPH → D-β- hydroxybutyryl-ACP

β-hydroxybutyryl-ACP dehydratase **2,3-trans-enoyl-ACP reductase**

+ NADP → Crotonyl-ACP + H_2O + NADPH → Butyryl-

Butyryl-ACP carboxylase

ACP + NADP + HCO_3^--carboxybiotin → Ethylmalonyl-CoA + biotinate

Fig 2.9 The pathway of tylactone synthesis from acetyl-CoA and malonyl-CoA. Tylactone precursors propionyl-CoA and methylmalonyl-CoA are derived from amino acids either directly (see compounds labelled with Roman Numeral I), or indirectly via the TCA cycle (see compounds labelled II)[adapted from Dotzlaf *et al.* (1983)]. Acetyl and malonyl building blocks are introduced as acyl carrier protein (ACP) conjugates. Decarboxylation drives the β-ketoacyl-ACP synthase and results in the addition of two carbon units to the growing chain. Numbers in brackets indicate the corresponding reaction in the diagrammatic presentation.

Hypothetical representation of tylosin biosynthesis

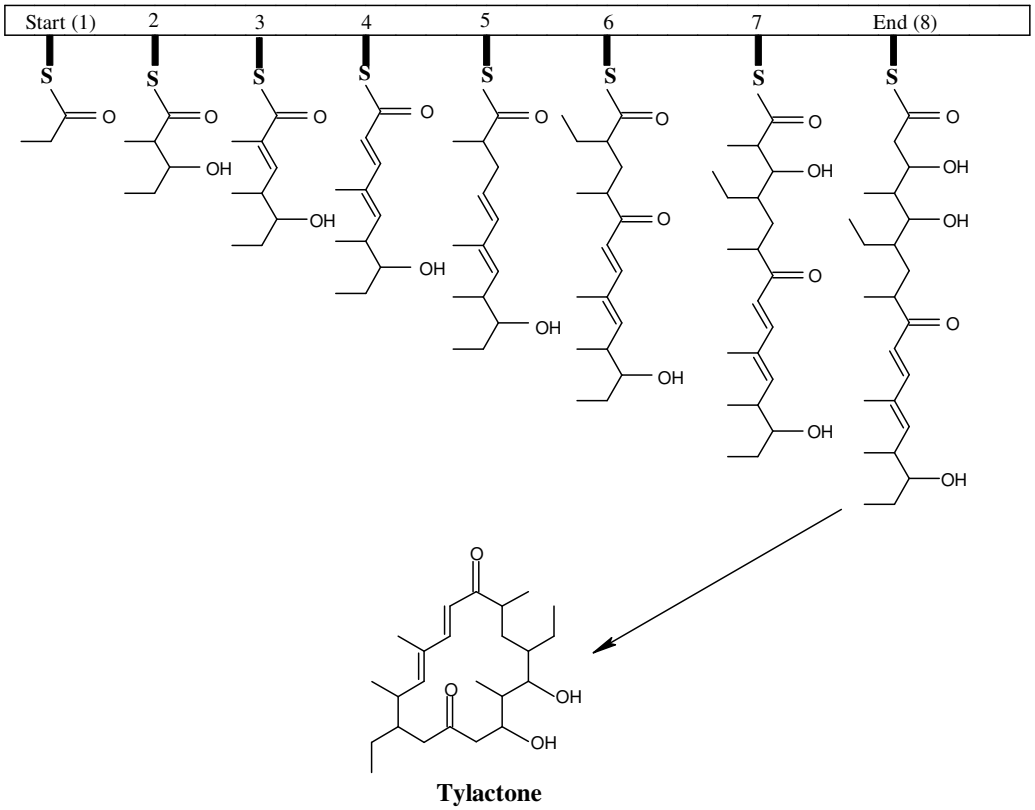

Fig 2.10 Hypothetical representation of the type I polyketide synthase complex responsible for the production of tylosin (linear arrangement of genes *tyl*GI, *tyl*GII, *tyl*GIII, *tyl*GIV, & *tyl*GV going from step 1 - 8). KS represents the polyketide synthase, carrying two thiol groups, one on the ketosynthase (condensing enzyme; KS) and other on the acyl carrier protein (ACP). The reaction steps are labeled: AT, acyl transferase; KS, ketosynthase, KR, ketoreductase; DH, dehydrase; ER, enoylreductase. Step (2) AT, ACP, KS, KR; (3) AT, ACP, KS, KR, DH; (4) AT,

ACP, KS, KR, DH; (5) AT, ACP, KS (6) AT, ACP, KS, KR, DH, ER; (7) AT, ACP, KS, KR; (8) AT, ACP, KS, KR.

Synthesis of the tylosin sugars.

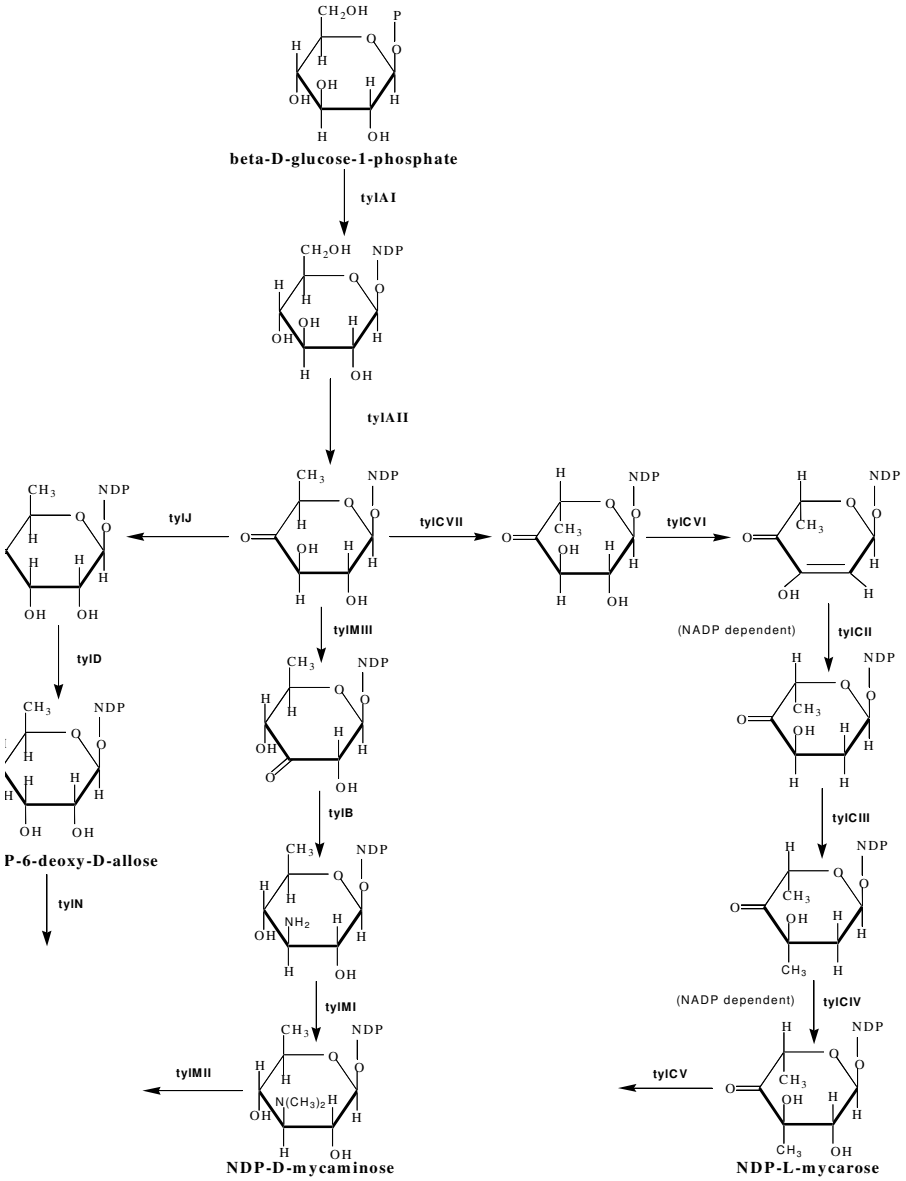

Fig 2.11 Synthesis of tylosin sugars. *Tyl*AI, NDP-glucose synthase; *tyl*AII, NDP-glucose 4,6-dehydratase; *tyl*J, 3-epimerase; *tyl*D, 4-ketoreductase; *tyl*N, deoxyallosyltransferase; *tyl*MIII, 3,4-isomerase; *tylB*, 3-aminotransferase; *tyl*MI, 3-N-methyltransferase; *tyl*MII, mycaminosyltransferase; *tyl*CVII, 5- (or 3,5-) epimerase; *tylCVI*, 2,3-dehydratase; *tyl*CII, 2,3-enoylreductase; *tyl*CIII 3-C-methyltransferase; *tyl*CIV, 4-ketoruductase; *tyl*CV, mycarosyltransferase (adapted from Cundliffe, 1999).

The proposed biosynthetic pathway for mycinose, mycaminose, & mycarose synthesis and the conversion to tylosin.

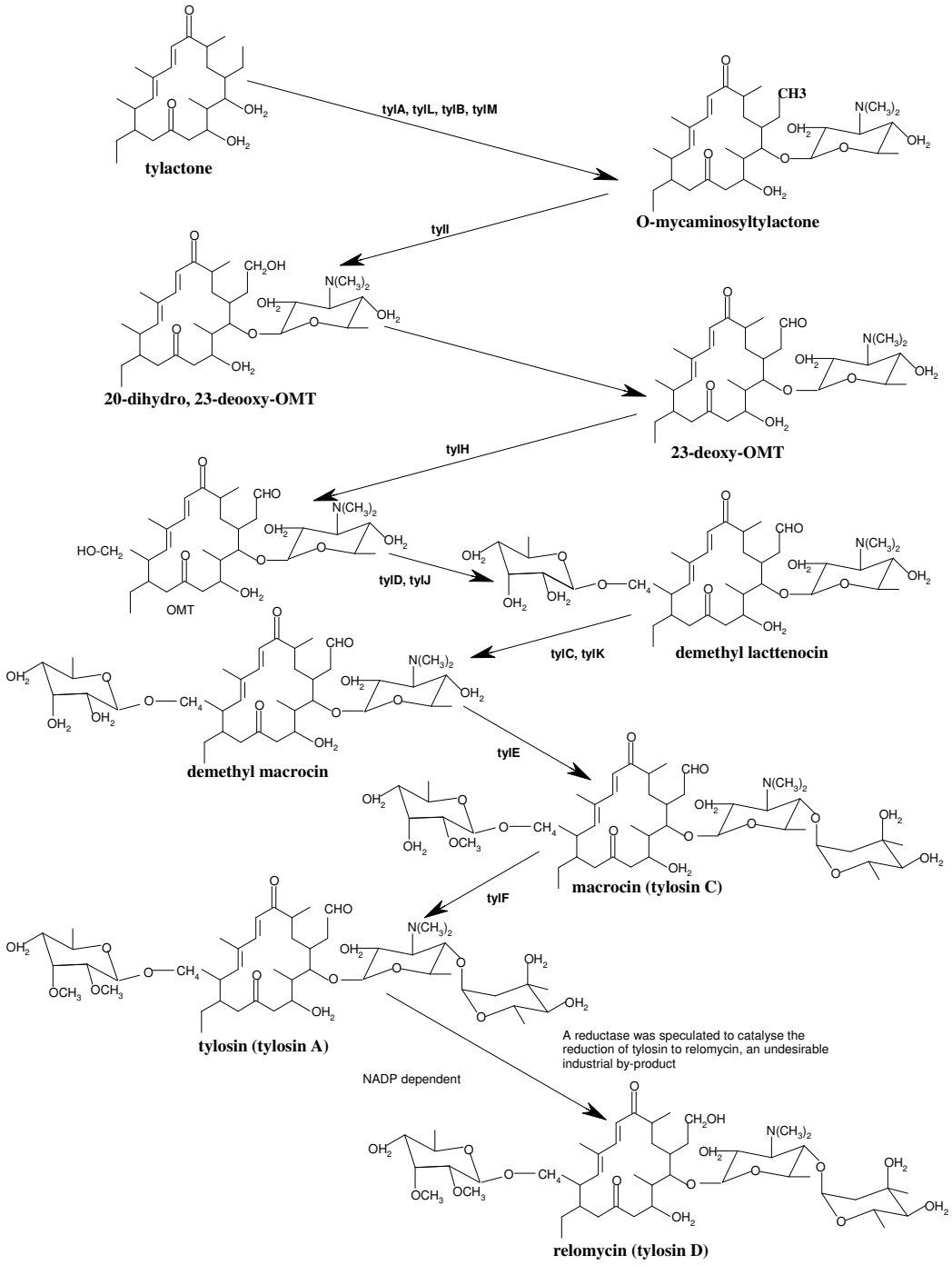

Fig 2.12 The biosynthetic route to tylosin and the attachment of the sugar residues under the influence of the genes *tyl*AI*, tyl*AII*, tyl*J*, tyl*D*, tyl*N*, tyl*E and *tyl*F in the different steps (adapted from Cundliffe, 1999 & Huang *et al*., 1993). *tyl*B, 3-aminotransferase; *tyII*, cytochrome P-450; *tyl*HI, cytochrome P450; *tyl*HII, tylodoxin (ferredoxin); tylD, 4-ketoructase; *tyl*J, 3-`epimerase; *tyl*E, 2"-O-methyltransferase; *tyl*F, 3"-O-methyltransferase.

Chapter 3

Microbiological techniques and standard media

3.1 Introduction

The following section has been constructed to complement Davidson (1992), Mousdale (1997), & Mousdale *et al.* (1999), which are theoretical in approach (and heavily constructed from the works of Sutherland & Wilkinson, 1971; Dawes *et al.,* 1971; Herbert *et al.,* 1971), whereas this section has been written from an applied application approach.

3.2 Strains

S. fradiae C373-5, C373-10, & C373-18 were used throughout this project (Supplied by Eli Lilly Ltd. Speke, UK.). Other strains used were *S. coelicolor* 1147, & *E. coli* ML308.

3.3 Sources and Preparation of materials

Unless otherwise stated, chemicals were purchased from either Sigma Chemical Company Ltd, BDH, British Oxygen Company (gases), Aminex, Phenomenex (HPLC columns), and Boehringer Mannheim. Bacterial culture media was purchased from Difco Laboratories, Oxoid Ltd, as well as Sigma Chemical Company Ltd.

3.3.1 Preparation of solutions and media

Solutions were prepared using glass distilled deionised water (dH_2O), further purified by passage through a SuperQ water purification system (Millipore). The pH of solutions was measured using an Orion digital pH meter (Model 420A). Where appropriate, sterilisation was achieved by either filtration through a 0.22 μm filter or by autoclaving for 15 min at 121^0 C.

3.4 Standard media for the proporgation of *Streptomyces*

3.4.1 Tryptone soya broth agar (TSA) or broth (TSB): Compromised the following components (gl^{-1}): 30.0 g of Oxoid tryptone soya broth powder, 15.0 g agar, made up to 1 L in distilled water (dH_2O). When used to culture *S. fradiae* tap water (tH_2O) was used.

3.4.2 SM-agar: Compromised the following components (gl^{-1}): 20.0 g soybean flour, 20.0 g mannitol, 16.0 g agar, 55.0 mg $CaCl_2$. Containing $CaCl_2$ for a faster and more intensive sporulation.

3.4.3 Yeast extract malt extract (YEME) agar: Compromised the following components (gl^{-1}): 3.0 g yeast extract, 5.0 g Difco bacta peptone, 3.0 g Oxoid malt extract, 10.0 g glucose, 340.0 g sucrose, 16.0 g agar, made up to 1 L in dH_2O.

3.4.4 AS1: Compromised the following components (gl^{-1}): 1.0 g yeast extract, 5.0 g soluble starch, 2.5 g NaCl, 10.0 g Na_2SO_4, 200.0 mg L-alanine, 200.0 mg L-arginine, 200.0 mg L-asparagine, 20.0 g agar. Adjust pH to 8.0 (with conc. KOH) before autoclaving. When generating spores for fermentation or conjugation usually nalidixic acid was added (addition after autoclaving), at a final concentration of 60.0 $\mu g.ml^{-1}$ to minimise contamination by other bacteria. The plates were incubated at 37^0 C or 30^0 C before use $MgCl_2$ (addition after autoclaving) was added to give a final concentration of 10 mM. Spores were washed off the slants with 8 ml sterile 0.85 % saline (Tata, 1994).

The addition of $MgSO_4.7H_2O$ (addition prior to autoclaving) for the cultivation of *S. fradiae* seems to enhance growth in all the above mediums (3.0 gl^{-1}).

3.5 Media for vegetative growth

3.5.1 Media for vegetative growth: Compromised the following components (gl^{-1}): 5.0 g tryptone, 3.0 g yeast extract, 3.0 g $MgSO_4$, 5.0 g glucose (addition of glucose was optional), made up to 1 L in dH_2O and the pH adjusted to 7.0 and autoclaved. This starting inoculation was found to be a good seed medium (personal communication; Arnold *et al.,* 2000).

3.5.2 Tippe Tylosin Vegetative media (in house Media for vegetative growth Eli Lilly Ltd: Compromised the following components (gl^{-1}): 10.0 g Primatone, 6.0 g beef extract, 2.5 g yeast extract, 15.0 g corn dextrin, 0.44 g soybean oil, and the pH adjusted to 7.0 and made up to 1 L and autoclaved.

3.6 Defined and minimal media for the proporgation of streptomycetes

3.6.1 *S. coelicolor* minimal medium for production of actinorhodin; the glucose salts minimal media for growth of *S. coelicolor* was based on the medium used by Hobbs *et al.* (1989) but did not contain the polyacrylate junlon. Davidson (1992) reported that the use of junlon interfered with colorimetric assays and was difficult to remove from the cells. The medium compromised the following components (gl^{-1}): 4.0 g glucose*, 1.5 g K_2HPO_4*, 4.5 g $NaNO_3$, 5.0 g NaCl, 5.0 g Na_2SO_4, 1.0 g $MgSO_4.7H_2O$, 0.83 g $CaCl_2.6H_2O$, 0.01 g $ZnSO_4$, 1.2 g Tris, 1 ml trace salt solution*. Trace salt solution* (per L); 2.00 g $ZnCl_2$, 1.00 g $MnCl_2.4H_2O$, 0.30 g H_3BO_3, 0.43 g $CuC1_2.2H_2O$, 0.25 g $Na_2MoO_4.2H_2O$, 8.70 g $FeCl_3$, 0.42 g NaI (*autoclaved separately). The medium was adjusted to pH 7.0 with HCl and autoclaved.

3.6.2 *S. coelicolor* defined medium for production of actinorhodin (Orduna & Theobald, 2000); the medium compromised the following components (gl^{-1}): 10 g maltose*, 8.9 g glutamate, 4.0 g K_2HPO_4*, 2.5 g NaCl, 2.5 g Na_2SO_4, 0.48 g $MgSO_4$, 10 mg $ZnSO_4$, 7.5 mg $CaCl_2$, mineral solution*, 1 ml (*autoclaved separately). Trace salt solution (per litre); 2.00 g $ZnCl_2$, 1.00 g $MnCl_2.4H_2O$, 0.30 g H_3BO_3, 0.43 g $CuC1_2.2H_2O$, 0.25 g $Na_2MoO_4.2H_2O$, 8.70 g $FeCl_3$, 0.42 g NaI. The medium was adjusted to pH 7.0 with HCl and autoclaved.

3.6.3 *E. coli* M9; Compromised the following components (gl^{-1}): to 750 ml sterile dH_2O (cooled to 50^0 C or less), 200 ml of 5 x M9 salts solution, 20 ml of 20 % solution of the appropriate carbon source (e.g., 20 % glucose), was added and made up to 1 L. 5 x M9 salts solution was made by dissolving the following salts in dH_2O to a final volume of 1 L: 64 g $Na_2HPO_4.7H_2O$, 15 g KH_2PO_4, 2.5 g NaCl, 5.0 g NH_4Cl. The salts solution was divided into 200 ml aliquots and sterilised by autoclaving.

3.6.4 ***S. fradiae***; a defined medium has been developed in house by Eli Lilly Ltd (adapted from Zhang *et al.,* 1996). and comprised the following components (gl^{-1}): 20.0 g glucose* or appropriate carbon source (40.0 g, glycerol^{+}; 20.0 g, fructose^{+}; 10.0 g, Sucrose^{+}, 20.0 g; galactose^{+}; 30.0 g, oxo-glutarate^{+}; 40.0 g, pyruvate^{+}; 40.0 g, phosphoglycerate^{+}; 40.0 g, glucose-6-phosphate^{+}; 24.0 g, glutamate^{+}; 60.0, acetic acid^{+}; 24.0 g, mannose^{+}; 24.0 g, xylose^{+}); 5.0 g glutamate or oxo-glutarate as appropriate; 20.0 g 3-[N-morpholino] propanesulfonic acid^{+} (MOPS), 0.4 g K_2HPO_4*, 0.4 g KH_2PO_4*, 1.0 g $MgSO_4.7H_2O$, 0.2 g NaCl, 0.5 g betaine, 0.1 g $CaCl_2$, 1.4 g $(NH_4)_2SO_4$*. Trace element solution 0.04 g (1.0 ml of 4 % soln; acidified) $FeSO_4.7H_2O$, 0.01 g (0.10 ml of 1 % soln) $CoCl_2.H_2O$, 2.0 ml Trace element solution$^{\wedge}$. Vitamin solution$^{\wedge}$ 1.2 mg Biotin, 1.2 mg Ca panthothenate, 1.2 mg niacin, 1.2 mg thiamine, 1.2 mg vitamin B_{12}, 1.2 mg Riboflavin ($^{\wedge}$filtered solutions 0.2 μm)[*autoclaved separately]{$^{+}$changes made to medium for this project}. Adjust pH to 7.0 and autoclave must be stored at 4^0 C. Incubate 24 - 36 hrs at 29.5^0 C at 250 rpm. L-glutamate was optional 5.0 gl^{-1} (on removal of glutamate^{+} or oxo-glutarate^{+}, $(NH_4)_2SO_4{}^{+}$ was increased to 4.0 gl^{-1}).

3.6.5 ***S. griseofuscus*** **defined medium for production of physostigmine:** a defined medium that was developed by Zhang *et al.* (1996) and compromised the following components (gl^{-1}): 15.0 g glucose*, 5 g NH_4Cl*, 1.0 g K_2HPO_4*, 5.0 g monosodium glutamate, 5.0 g $CaCO_3$, 21.0 g MOPS, trace element solution 1, 2 % (v/v); pre-sterilisation pH 7.0 (*autoclaved separately). Trace element solution 1$^{\wedge}$ had the following composition (gl^{-1}): 28.9 g $MgSO_4.7H_2O$, 0.5 g $FeSO_4$. $7H_2O$, 0.5 g $ZnSO_4.7H_2O$, 0.1 g $MnSO_4.H_2O$, 0.05 g $CuSO_4.5H_2O$, 0.04 g $CoCl_2.6H_2O$ ($^{\wedge}$filtered solutions 0.2 μm).

3.6.6 TSM 6 ***S. rimosus*** **Tetracycline synthesis minimal media:** a defined medium that was developed in house by Pfizer Ltd (personal communication I. Hunter) and comprised the following components (gl^{-1}): 10.0 g glucose* or 10.0 g mineral oil, MOPS 7.0 g, 0.5 g K_2HPO_4*, 0.28 g KH_2PO_4*, 2 g $Ca(NO_3)_2.4H_2O$, 2 g $NaNO_3$, 0.5 g NH_4NO_3, 0.5 g KCl, 0.4 g $MgSO_4.7H_2O$, 0.2 g $ZnSO_4$, 0.1 g $NH_4Fe(SO_4).12H_2O$, 0.05 g $MnSO_4.4H_2O$, 0.005 g $CuSO_4.5H_2O$, 0.005 g $NaMoO_4.2H_2O$, 0.031 g $CoCl_2.6H_2O$ (*autoclaved separately). The pH was adjusted to 7.00 with NaOH and autoclaved.

3.7 Production fermentation media

3.7.1 Semi defined media Omura *et al.* (1983) and Lee (1997): described a synthetic medium which compromised the following components (gl^{-1}): 10.0 g soluble starch, 2.5 g glucose, 1.3 g sodium lactate, 0.25 g $MgSO_4.H_2O$, 0.85 g (12.5 mmoles.1^{-1}) $(NH_4)_2SO_4$, 1.5 g $CaCl_2$, 0.0015 g $CuSO_4.5H_2O$, 0.0015 g $ZnSO_4.7H_2O$, 0.0015 g $FeSO_4.7H_2O$, 0.0015 g $CoCl_2.6H_2O$, 0.0015 g $MnCl_2.4H_2O$. The pH was adjusted to 7 and autoclaved. A solution of $(NH_4)_2SO_4$ and glucose was sterilised separately and added before inoculation.

3.7.2 Semi defined media Madry and Pape (1982): described a synthetic medium which compromised the following components (gl^{-1}): 2.0 g NaCl, 3.0 g $CaC1_2.2H_2O$, 1.0 mg (5.0 $mg.ml^{-1}$ stock solution, add 200 µl) $CoCl_2.6H_2O$, 2.3 g K_2HPO_4*, 5.0 g $MgSO_4.7H_2O$, 10.0 mg (50.0 $mg.ml^{-1}$ stock solution add 200 µl) $ZnSO_4.7H_2O$, 5.0 g betaine-HCl*, 5.0 g glucose*, 17.5 g L-glutamate, 3.0 g ferric ammonium citrate*, 25.0 g methyl oleate (*autoclaved separately). The medium was thoroughly mixed for approximately 10 min in a homogeniser, the pH was adjusted to 7.00 using 1 M KOH and the medium autoclaved.

3.7.3 Industrial complex medium: (in house complex media, Eli Lilly), which compromised the following components (gl^{-1}): 0.54 g betaine, 16.0 g yellow cream meal, 8.88 g fish meal, 1.05 g KCl, 0.40 ammonium phosphate dibasic, 4.10 g cotton seed flour, 8.88 g corn gluten meal, 60.0 g crude soybean oil, 2.03 g calcium carbonate, 0.00369 gl^{-1} nickel sulphate (0.46 g / 250 ml add 2 ml a L), 0.00304 gl^{-1} $CoCl_2.6H_2O$ (0.375g / 250 ml add 2 ml a L). The medium was thoroughly mixed for approximately 10 min in a homogeniser, the pH was adjusted to 7.35 using 1 M NaOH and the medium autoclaved.

3.8 Storage of organisms

Streptomycetes grow at a very slow rate (on average a doubling time of 2 hrs or more) and any manipulation is highly sensitive to microbial contamination. Therefore, all manipulations were carried out in a Class 2, microbiological safety cabinet. Mycelial suspensions were prepared as Chang & Elander (1986), with minor changes. 45 ml of

vegetative medium in a 250 ml Erlenmeyer flask was inoculated, and grown for 3 - 4 days at 29.5^0 C. 45 ml of 10 % glycerol was the added to give a final concentration of 5 %. 2 ml aliquots of the cell suspension were dispensed into cryotubes, the temperature reduced slowly, and stored at -70^0 C.

Spores of each strain were also stored on slopes, AS1 & TSA for *S. fradiae* and SM-agar for *S. coelicolor.* To acquire spores for pre-germination, the spore suspension was made after growth on AS1, TSA, or SM. After incubation at 30^0 C and formation of a homogenous greyish spore layer, the spores were harvested carefully after addition of 5 ml of sterile dH_2O; 100 µl of Triton X-100 was added and the suspension was sonicated for 1 min (Soniprep 150, MSE, UK). It was filtered through sterile glass wool, washed twice with 5 ml dH_2O centrifugation 10 min, 9000 g and finally re-suspended in 5 ml dH_2O. For conservation, the spores were re-suspended in 5 ml 20 % (v/v) glycerol and stored at -20^0 C. Spore suspensions prepared for *S. coelicolor* 1147 and *S. fradiae* C373-10 were prepared in this manner and had a titer of 1 - 3 x 10^9 and 1 - 4 x 10^4 respectively) spores ml^{-1}. For inoculation, the spore titer was adjusted to 1 x 10^6 spores ml^{-1}.

3.9 Growth apparatus

3.9.1 Shake flasks: For the preparation of the inoculum for a fermentation a 2000 ml Erlenmeyer flask with 500 ml of medium (section 3.5); was inoculated with a 2 ml mycelium suspension (see section 3.8), and grown for 5 days at 30^0 C at 250 rpm (Orbital shaker Gallenkamp). For shake flask experiments two sizes of shake flask were used; 50 ml Erlenmeyer flasks with cotton wool bungs containing 12 ml of medium, inoculated with 1.2 ml of inoculum (standard operating procedure, Eli Lilly Ltd.) and 1000 ml Erlenmeyer flasks with 90 ml of medium inoculated with 10 ml of culture.

3.9.2 Fermenters: For the majority of batch cultivations, 2.5 & 5.0 L Bioflow 3000 bench (New Brunswick Scientific) top fermenters were used. Applikon 7.0 & 20.0 L bioreactors (steam temperature control), were used on site at Eli Lilly Ltd. In the case of Bioflow bioreactors the temperature was regulated by a hot plate and mains cold water, and sensed by an RTD (resistance temperature detector). The air was supplied via a separate compressor (KNF pump model VP4) through a rotameter (1 $vol.vol^{-1}$, 10 $L.min^{-1}$ maximum). The pH was sensed by a glass electrode (Mettler Toledo 363-S7/120). The

dissolved oxygen (DO) probe was a Mettler Toledo inpro 6000 series O_2 sensor. At Eli Lilly Ltd, O_2 uptake and CO_2 production was measured by mass spectrometry VG (AET 206A)[see Appendix E for calculations]. Sterilisation of the fermenters and the medium was *in situ* (121^0 C, 30 min). Connections were sterilised by disinfectant containing 100 % ethanol spray. Inoculation of the fermenter was from a 2 L Erlenmeyer flask or 4 L Fernback flask, which could be attached to an outlet port via silicon tubing. Sampling was via an outlet port the sample removed was kept on ice at all times.

The industrial bioreactor for culturing *S. fradiae* C373-18 was a 3000 dm^3 pressurised baffled vessel (2.5 bars above the upper liquid level) was agitated by three 8-blade Rushton turbines attached to a central shaft. The impeller speed was 180 rpm. Air was fed axi-symmetrically at a typical rate for a fermentation of 1 $vol.vol.min^{-1}$ (v/v/m) through a ring sparger mounted just below the lowest impeller. A 10 % ammonium nitrate solution was fed at 0.83 dm^3hr^{-1} onto the free surface between the 60 th and the 144 th hour of production as a source of nitrogen for the microorganism (Vlaev *et al*., 2000).

3.9.3 Fermentation conditions: Batch culture was conducted in 2.5, 5.0, 7.0, & 20.0, L fermenters. Culture pH was maintained at 7.0 by automatic addition of 2 M NaOH and 2 M HCl . Temperature was maintained at 29.5^0 C and DO tension was maintained above 30 % saturation by aeration (0.5 - 1.2 v/v/m) and agitation (500 - 800 rpm), in the 20.0 L vessels; the 2.5, 5.0, & 7.0 L was set at 400 rpm and 1.0 v/v/m aeration.

3.10 Viability & contamination detection

Three methods were utilised to test for viability & detection of contamination.

3.10.1 Gram stain

The Gram-staining method differentiates bacteria into two groups based on the amount of (an amino sugar polymer) peptidoglycan in the cell walls (see Chapter 5, section 5.7.1). The cell walls of Gram-positive organisms contain this polymer, and the purple crystal violet dye forms an insoluble complex with the polymer in the presence of the iodine solution. There is little wash out during the decolourisation with alcohol acetone

solution. The cells do not counter stain with the red safranin dye, so Gram-positive cells appear purple when examined microscopically. Gram-negative cell walls contain low levels of peptidoglycan so very little complex is formed and the cells decolourise easily and stain red when the safranin dye is added. Cells from young cultures, less than 24 hours or less, give the most accurate results. The Gram stain reaction is one of the most common characteristics used to identify bacteria. Suspensions of colonies or liquid samples are placed onto glass microscope slides and allowed to dry. The slides are briefly heated to fix the organisms to the slide and alternatively stained and rinsed with water in the following sequence:

(1) Crystal violet for about 1 min, rinse with dH_2O.
(2) Iodine solution for about 1 min, rinse with dH_2O.
(3) Decolourise with acetone briefly, rinse well.
(4) Counter stain with safranin for about 30 seconds, rinse, dry and examine under 1000 x magnification.

3.10.2 Vital stain

The vital stain allows for the differentiation between cells that are alive and dead (method as Eli Lilly Ltd. standard operating protocol). To a heat fixed sample on a microscope slide:

(1) Apply methylene blue reagent (1 / 10 pre-diluted) for 30 seconds.
(3) Apply diluted Carbal Fuschin (1 / 10 pre-diluted) for 12 seconds.
(4) Wash with dH_2O.
(5) Allow slide to dry.
(6) View under microscope.

When viewed in the blue / red microscope vision zone live mycelia show as blue and dead contaminants show up as red (e.g. yeast cells). If any rods / cocci stain blue in this zone then contamination was present.

3.10.3 Viable spore counts

The viable spore count was determined by counting the number of colonies which grew (colony forming units, CFU), when an aliquot of a serially diluted spore suspension was plated on TSA plates and evenly spread using a turn-table style movement and a sterile glass spreader. Counts were made after incubation at 30^0 C for 5 days. The concentration of spores was calculated by multiplying the number of colonies by the appropriate dilution factor.

The degree of dispersion (ϕ) in shake flask cultures was calculated in the following way; the value is determined as the number of CFU per ml in liquid culture divided by the number of spores per ml initially inoculated (Hobbs *et al.,* 1989; de Orduna & Theobald, 2000).

3.11 Measurement of growth

Fermentation broths are notoriously variable in composition and properties, both between different processes and within any particular fermentation. To this end a number of analytical techniques were used (Clarke *et al.,* 1986; Sonnleitner *et al.,* 1992; Ison & Matthew, 1997; Lange & Heijnen, 2001) to reduce these inconsistencies.

3.11. 1 Wet weight

Samples taken from the fermenter or pooled cultures from 2 to 3 flasks were harvested in 250 ml centrifuge tubes (12400 g, 20 min, 4^0 C). The pellets were washed (12400 g, 10 min, 4^0 C) with ice-cold dH_2O, transferred with a small volume of chilled dH_2O to a pre-weighed 30 ml Beckman centrifuge tube, centrifuged (12100 g, 10 min, 4^0 C) and the tubes inverted and left to drain. Each, pellet was weighed and the mass expressed as gl^{-1}.

3.11.2 Dry weight filtration

10 ml samples of cultures were pipetted onto pre-dried, pre-weighed filters (Whatman No 1 paper), placed on a Buchner funnel connected to a vacuum pump, and washed three times with dH_2O. Filters were dried in a microwave oven (20 min at defrost and left to

cool for 20 min and desiccated for 24 hrs with silica gel to ensure no re-hydration of the filters). Each filter was weighed and the mass expressed as gl^{-1}.

3.11.3 Determination of specific growth rate (μ)

The specific growth rate (μ) for bacterial growth under batch culture conditions was calculated from the plot of ln biomass dry weight against time or ln DNA concentration against time. A straight line was fitted through the linear part of the curve using the graphics package, Origin. μ was given by the slope of the best-fit line during the growth phase (exponential / cubic phase).

3.12 Enzyme activities

3.12.1 Preparation of crude extracts for enzyme assays (Obanye, 1994)

The crude extract was prepared as follows (Obanye, 1994). Cells were collected by centrifugation for 15 min at 39500 g. The pellet was washed with 0.05 M Tris-HCl buffer pH 7.5, containing 5 mM $MgSO_4$, $(NH_4)_2SO_4$, 10 mM (to prevent precipitation of proteins), and passed 3 times through a French pressure cell [11000 psi] (SLM Aminco; speciconic instruments). The lysate was centrifuged for 15 min at 39500 g and the supernatant was used for the assay. Protein concentration was determined by the Reverse biuret method combined with the copper bathocuproine chelate reaction (section 3.20.5) [Matsushita *et al.,* 1993]; protein to protein variability was very low and individual proteins or protein mixtures can be measured accurately with this assay (see Chapter 5, section 5.4.3). In most cases, ammonium sulphate, to a final concentration of 10 mM, was added to the assay mixture to keep the proteins of the crude extract in a soluble state. In the case of the assays of glucose-6-phosphate and 6-phosphogluconate dehydrogenases, the crude extract was prepared in 0.01 M Tris-HCl, pH 8.0.

3.13 The enzyme assay procedure

0.8 ml of buffer was pipetted into a 1 ml quartz cuvette and 10 - 100 μl of crude extract was added. The cuvette contents were mixed using the pipette as an agitator. 5 - 10 μl of each of the remaining constituents of the assay cocktail constituents (with the exception of the substrate) were then added, with mixing in between additions. The basal

absorbance was determined in minutes before the substrate was added. The specific activity of the relevant enzyme, IU, was determined using the formula:

[(ΔA in minutes) / ε] / p

ε = the number of absorbance units that are equivalent to 1 μmole NADH in a 1 ml cuvette with a 1 cm path length or to 1 μmole of an equivalent metabolite.
p = cuvette protein concentration in mg protein.ml^{-1}.

3.13.1 6-phosphogluconate dehydrogenase and glucose-6-phosphate dehydrogenase (Francesco *et al.,* 1982).

Principle: The assay is based upon the rate of reduction of NAD or NADP (measured at 340 nm) in the presence of 6-phosphogluconate or glucose-6-phosphate respectively.

(a) NAD 6-phosphogluconate dehydrogenase (Obanye, 1994)

Reaction: **6-phosphogluconate + NAD → ribulose-5-phosphate + CO_2 + NADH**

Stock Solutions
Buffer: Tris-HCl 0.1 M, pH 7.5;

$MgC1_2$, 5 mM;

NAD, 5 mM;

Substrate: 6-phosphogluconate, 5 mM.

(b) NADP 6-phosphogluconate dehydrogenase

Reaction: **6-phosphogluconate + NADP → ribulose-5-phosphate + CO_2 + NADPH**

Stock Solutions
Buffer: Tris-HCl 0.1 M, pH 7.5;

$MgC1_2$, 5 mM;

NADP, 5 mM;

Substrate: 6-phosphogluconate 5 mM.

(c) NAD Glucose-6-phosphate dehydrogenase (Ujita & kimura, 1982b)

Reaction: **D-glucose-6-phosphate + NAD → 6-phosphoglucono-δ-lactone + NADH**

Stock Solutions
Buffer: 0. 1 M MES-KOH (4-morphollineeththanesulfonic), pH 6.6;

NAD, 20 mM;

$MgC1_2$, 5 mM;

Substrate: Glucose-6-phosphate, 15 mM.

(d) NADP Glucose-6-phosphate dehydrogenase (Ling *et al.,* 1966)

Reaction: **D-glucose-6-phosphate + NADP → 6-phosphoglucono-&-Iactone + NADPH**

Stock Solutions
Buffer: 0.1 M Tris-HCl, pH 7.5;

NADP, 5 mM;

$MgCl_2$, 5 mM;

Substrate: Glucose-6-phosphate, 5 mM.

3.13.2 PEP-carboxylase (Ozaki & Shiio, 1969)

Principle: The reaction is coupled with the activity of malate dehydrogenase and the assay depends upon the oxidation of NADH (measured at 340 nm) in the presence of oxaloacetate generated by the reaction.

AcCoA

Reaction: **Phosphoenolpyruvate + CO_2 → oxaloacetate + NADH => malate + NAD**

Stock Solutions
Buffer: Tris-HCl, pH 7.5;

NADH, 0.2 mM

Acetyl-CoA, 0.15 mM;

$MgC1_2$, 5 mM;

Malate dehydrogenase, 3 U;

PEP, 3 mM;

Starting reagent: $KHCO_3$, 10 mM.

3.13.3 Malate dehydrogenase decarboxylating

Principle: The assay is based upon the change in optical density at 340 nm during the reduction of NADP.

Reaction: **L-malate + NADP → pyruvate + CO_2 + NADPH**

Stock Solutions
Buffer: Tris-HCl, 0.1 M, pH 8.0;

$MgC1_2$, 10 mM;

$(NH_4)_2SO_4$, 10 mM;

NADP, 5 mM;

Substrate: L-malate, 15 mM.

3.13.4 Pyruvate kinase (Obanye, 1994)

Principle: The reaction is coupled with the activity of lactate dehydrogenase and the assay is based upon the oxidation of NADH (measured at 340 nm) in the presence of the pyruvate generated by the reaction.

Reaction: **PEP + ADP → PYR + ATP → PYR + NADH → lactate + NAD**

Stock Solutions
Buffer: 0.1 M Tris-HCl buffer, pH 7.5 (containing 20 % glycerol);

NADH, 0.2 mM;

$MgC1_2$, 5 mM;

KCl, 5 mM;

Lactate dehydrogenase, 3U;

PEP, 3 mM;

Starting reagent: ADP, 2 mM.

3.13.5 Hexokinase (Obanye, 1994)

The reaction is coupled with glucose-6-phosphate dehydrogenase, and the assay depends on the reduction of NADP (measured at 340 nm) in the presence of the glucose-6-phosphate generated by the action of hexokinase.

Reaction: **Hexose + ATP → hexose-6-phosphate + AMP + NADP → 6-phosphogluconate + NADPH**

Stock Solutions
Buffer: Tris-HCl 0.1 M, pH 8.5,

MgSO4, 5mM,

ATP, 5mM,

NADP, 5mM,

Glucose-6-phosphate dehydrogenase, 1 U;

Substrate: Glucose, 5mM.

3.14 Extraction techniques of biomass and lipids from complex and semi-complex fermentation broth

A number of solvent extraction methods were researched into in order to separate biomass, lipids, and other cellular components from complex medium samples. For biomass estimation they only give a rough estimation as all were based on a polarity gradient and do not take into account the density of cellular material. Realistically, to separate biomass from complex media both density and polarity would need to be taken into account.

3.14.1 Extraction method 1 (personal communication J. McIntyre)

5.0 g of broth was approximately weighed out into a 50 ml polypropylene tube. Then 10 ml of a 1 : 1 solution of methoxy-ethanol and chloroform was added to the broth and shaken vigorously for 1 min. The resultant solution was centrifuged at 1088 g for 10 min. The top layer of solvent was carefully removed using a Pasteur pipette and the solvent waste disposed off. This left a layer of cells and, beneath that of media. Dry weight was determined in the same way as section 3.11.2.

3.14.2 Extraction method 2 (Dole & Meinertz, 1960)

The ternary mixture, of heptane-isopropyl alcohol-water (Preparation of Doles two-phase extraction solution; 28 % 0.03 N H_2SO_4, 26 % iso-propanol, 36 % heptane. was mixed together), provides a convenient two-phase system for extraction of long chain fatty acids (Dole, 1956). When the solvent components are taken in suitable proportions, the phases separate rapidly without centrifugation. The long-chain fatty acids distribute

predominantly into the upper, non-polar phase, whereas the more polar acids remain below (Dole & Meinertz, 1960).

Procedure

10 ml of culture was added to a 50 ml falcon tube. Then 10 ml of the top layer and 10 ml of the bottom layer was added sealed and shaken well for 5 min. 15 ml hexane and 10 ml dH_2O was then added, and sealed and shaken well for 5 min. The resultant solution was allowed to stand until the layers separated (top layer [non-polar] will contain lipids, middle layer [neutral] will contain debris from the media, bottom layer [polar] will contain biomass). Dry weight and wet weight were determined as section 3.11.1 & 3.11.2 respectively.

3.14.3 Extraction method 3 / lipid extraction (in-house method; Eli Lilly Ltd.)

Procedure

5.0 ml of a well-mixed broth sample was transferred into a 125 ml flask or equivalent. 25 ml of the Doles solution (Preparation of Doles solution; 780 ml of isopropyl alcohol (propan-2-ol), 200 ml of heptane and 20 ml of phosphoric acid (66 %; v/v) was mixed together) was added, the flask was sealed and shaken vigorously for 1 min and left to stand for 5 min. Then 15 ml of dH_2O and 15 ml of heptane AR was added, the flask was sealed and shaken vigorously for 1 min and left to stand for 5 min. The layers were allowed to separate then the heptane upper layer was pipetted into pre-weighed tarred aluminum pan or equivalent. The heptane was allowed to evaporate in a fume hood and the pan reweighed to calculate the difference. The lipid mass was expressed as gl^{-1}.

3.15 Elemental analysis

All mycelial samples for elemental analysis were freeze-dried and ground to a finely divided powder which was then dried overnight in vacuo over P_2O_5.

3.15.1 Method for sulphur using sulphanazo III

The sample was combusted in an O_2 flask containing H_2O_2 as absorbant. After 30 min, the flask was washed down with dH_2O and the solution boiled to destroy the excess H_2O_2. The flask was then cooled to room temperature. Acetone and sulphanazo III

indicator was then added and the solution titrated with barium perchlorate solution. Calculation was titrant concentration × dilution factor / biomass weight, converted to percentage format.

3.15.2 Method for determination of phosphorus

The sample was digested in a mixture of conc. H_2SO_4, $HClO_4$ and Aqua Regia for 30 min. The flask was cooled to room temperature and the contents transferred with several washings of dH_2O into a conical flask. This solution was treated with conc. HCl, sodium molybdate and quinoline HCl. The resultant precipitate was weighed as a phospho-molybdate complex.

3.15.3 Simultaneous determination of C, H, and N in Perkin Elmer 2400 analyser

Approximately 1 - 2 mg of sample, was wrapped in an aluminium foil capsule and dropped into the combustion zone, where it was combusted at approximately 1800^0 C in pure oxygen. The gaseous products were carried by helium into a catalytic zone (~1000^0 C) containing chromium oxides, silver oxide on magnesium oxide, and silver vanadate - these provide oxidative properties and scrubbing efficiency ensuring the complete combustion of volatile substances and removal of common interferences. The combustion product was then passed through a tube of copper wire (650^0 C) to remove excess oxygen and to reduce any oxides of nitrogen formed during combustion of the sample. The mixture of CO_2, N_2 and H_2O and He were mixed thoroughly and passed into the detector system which retains each gas and elutes them at the characteristic retention time. Signals were converted to present the results as percentage of carbon, hydrogen, and nitrogen.

3.15.4 Ash content

As a number of protocols have been used to calculate the ash content of biomass by other workers, the following procedure was constructed to fit with the equipment at are disposal. Two methods were used one where the biomass was hydrolysed first (steps 1 - 6) and the other where no hydrolysis was undertaken and the biomass was just ashed in a furnace (steps 5 & 6).

(1) 1.0 g of freeze-dried biomass was added to thunberg tubes (heated for 1 hour at 100^0 C over silica gel before analysis).

(2) 10 ml dH_2O and 10 ml conc. HCl was then added.

(3) The tubes were flushed with oxygen-free nitrogen and quick frozen, in a dry ice-methanol mixture and sealed under vacuum.

(4) The tubes were then placed in a heated oven at 105^0 C for 25 hrs.

(5) The tubes were then opened and lyophilised to dryness.

(6) Then 20 ml of dH_2O was added and the mixture transferred to a pre-weighed silica crucible and lyophilised to dryness (heated for 1 hour at 100^0 C over silica gel before further analysis).

(7) The sample was heated gently in a muffle furnace until all organic matter was destroyed (continual step ups over an 8 hour period until 650^0 C was achieved, temperature held for 3 hrs) and then was left over night at 420^0 C.

(8) Each crucible was weighed and the ash content expressed as a percentage of the initial biomass weight.

3.15.5 Total Organic Carbon Analysis (TOCA)

Fractionated samples, extracellular medium or culture samples (1.0 ml to 1.5 ml); in the case biomass, were centrifuged (20000 g, 5 min), washed twice in 1.0 ml of buffer (10 mM KH_2PO_4, pH 7.0) and re-suspended in a final volume of 200 µl dH_2O. Total organic carbon was measured using a Shimadzu carbon analyser (model TOC-500, Shimaduzu Corporation, Japan).

Samples were carried on high purity air at a 150 $ml.min^{-1}$ either through the total carbon (TC) or inorganic carbon (IC) reaction tubes. The TC combustion tube was filled with a platinum oxidation catalyst and was maintained at 680^0 C. Samples (10 µl) passing through the tube were oxidised or combusted into CO_2, which was detected by a non-dispersive infra-red gas analyser (NDIR). The NDIR emitted a peak shaped detection signal and the peak area was directly proportional to the TC concentration in the sample. The area was compared to that of previously injected standard solution (potassium hydrogen phthalate, 400 ppm of carbon) [for example of calibration see Fig 3.1a).

The IC reaction tube was filled with a strong acid liquid with a halogen absorbing silver salt, maintained at 150^0 C, and only inorganic carbon compounds were combusted to CO_2. The CO_2 was detected as for TC, but using the IC standard that was a mixture of sodium hydrogen carbonate and sodium carbonate (400 ppm of carbon) [for example of calibration see Fig 3.1b] Three replicate samples were injected into the TOCA and the mean was calculated. Total organic carbon (TOC) was calculated by:

$$TOC = TC - IC$$

Dry weight measurements were calculated by multiplying TOC figures by the appropriate dilution factor and expressed as gl^{-1}.

3.15.6 Determination of total organic nitrogen (Mousdale, 1997)

For nitrogen estimation the Kjeldahl method is widely used. The nitrogen in organic material is converted to ammonium sulphate by digestion with H_2SO_4 in the presence of a catalyst. The ammonia can then be estimated.

A. Preparation of Kjeldahl digestion catalyst

50 ml dH_2O was placed in a glass beaker in an ice water mixture. Cautiously 50 ml of conc. H_2SO_4 was added with constant stirring with the beaker in the ice-water mixture. When the acid solvent was cool, 0.1 g selenium dioxide was added and stirred until it dissolved (the solution was stable indefinitely).

B. Preparation of Nessler reagent and Nitrogen standard

4 g Potassium iodide and mercuric iodide was dissolved in 25 ml of dH_2O. 3.5 g gum acacia was dissolved in 750 ml dH_2O. Then the solution of iodide was added slowly to the gum acacia solution with constant stirring (this was the Nessler reagent). The volume of the Nessler reagent was made up to 1000 ml and stored in a dark-brown glass container (stable for several weeks at room temperature). The nitrogen standard was prepared by dissolving 4.73 g ammonium sulphate in 100 ml dH_2O, when completely dissolved it was made up to 1000 ml (this gives l g nitrogen.l^{-1}).

C. Assay

0.1 ml (If the nitrogen content is < 0.1 gl^{-1}, add up to 1 ml and lyophilise the samples in the tubes before adding the catalyst) of each sample was added in triplicate to Pyrex tubes. A blank was prepared with 0.1 ml dH_2O. 0.25 ml of the Kjeldahl digestion catalyst was then added. The tubes were immediately placed in a heating block at 350^0 C. After exactly 15 min each tube was removed and left to cool to room temperature. 1.875 ml dH_2O, 3 ml 2 M NaOH and 2 ml Nessler reagent was then added to each tube sequentially. The resultant solution was vortexed and the absorbance read at 490 nm against the prepared dH_2O blank. The nitrogen content was determined by reference to a calibration line prepared from 0 - 0.1 ml ammonium sulphate standard (for example of calibration see Fig 3.1c).

3.16 Fractionation of biomass

A number of methods were used to obtain pure fractions of the macromolecular components:

(1) A modification of the method originally described by Schneider *et al.* (1950) incorporating the initial procedure of Ogur and Rosen (1950)[Hutchison and Munro, 1961; Fleck & Munro, 1962; Mousdale, 1997].
(2) A modification of the method described by Schmidt and Thannhauser. (1945) [Hutchison and Munro, 1961; Fleck & Munro, 1962].
(3) A three stage method for the determination of DNA, RNA & protein (Chomczynski, 1987).
(4) A multistage fractionation procedure adapted from Lange & Heijnen (2001).

3.16.1 Method 1 (Mousdale, 1997)

Method 1 was used for the majority of analysis throughout this project. This method extracts the macromolecular components depending on their solubility in differing acid and alkaline conditions in a four-step fractionation (see Chapter 3 section 3.16.1). An initial weak acid step [fraction 1] (0.2 M perchloric acid at 4^0 C for 24 hrs) was required to remove sugars (including polysaccharides) and low molecular weight molecules. These molecules included phosphorus (P) compounds, both inorganic and low molecular weight organic metabolites, and nucleotide co-enzymes (Hutchinson & Munro, 1961).

Interference by such small molecules was therefore eliminated in subsequent fractions. Early published methods used trichloroacetic acid (TrCA), although if total organic carbon (TOC) estimations of the macromolecular fraction is required, this acid is not appropriate as the acid would increase experimental error (because TrCA is a carbon containing compound). Weibel *et al*. (1974), Theobald *et al*. (1997) and Pfefferle *et al*. (1995) worked with yeast cells and evaluated two further acids. Formic acid was found to be less potent for lysis and interfered and inactivated enzyme assays. Where perchloric acid (PCA) does not interfere with TOCA analysis and will precipitate upon neutralisation, thus not interfering with enzyme assays (de Orduna & Theobald, 2000).

Fermentation samples were placed immediately on ice (Chapter 3, section 3.9.2) at harvesting, which ensured maximal velocity of sample cooling and hence effective inhibition of cell metabolism to minimise perturbation of intracellular metabolites.

The second step (fraction 2) in the fractionation involved a higher concentration of PCA suitable for extraction of nucleic acids (NAs). The carbohydrate-free pellet was incubated with 0.5 M PCA (3 % v/v) at 70^0 C for 2 hrs (Mousdale, 1997), which allows extraction of RNA and > 96 % of the DNA. This method is based on Burton (1956), where two consecutive 30 minute incubations with 0.5 M PCA were undertaken. Alternative methods using lower acid concentrations (Chiba & Sugahara, 1957) did not result in complete removal of DNA although RNA was fully extracted. Higher temperatures and strong acid were also reported to destroy the deoxyribose groups of DNA (Hutchinson & Munro, 1961).

Step three (fraction 3) was used to extract protein and lipids, as described by Lowry *et al*. (1951) using 1 M NaOH for 90 minutes at room temperature, or 30 minutes at 100^0 C (see Table 5.3). However, a much slower process of extraction was obtained, by incubating the residual pellet in 0.5 M NaOH at 37^0 C overnight (Davidson, 1992). The remaining material, both acid and alkali resolved, was re-suspended in dH_2O (fraction 4) and represented the fourth and final fraction. This material was assumed to be cell-wall associated i.e. peptidoglycan and protein.

(1) Fermentation broth samples were centrifuged at 10000 g for 30 min at 4^0 C.

(2) The resultant biomass was washed with dH_2O.

(3) Approximately 1 g of biomass (wet weight) was suspended in ice-cold 0.2 M PCA (high-purity PCA is necessary such as for spectroscopy grades) to a final concentration of 100 mg wet weight.ml^{-1}, and left overnight at 4^0 C.

(4) The sample was then centrifuged (12100 g, 20 min, 4^0 C) to separate the cold PCA fraction [fraction l, the cold PCA extract] from the pellet.

(5) The pellet was re-suspended in the same volume of 0.5 M PCA and digested at 70^0 C for 2 hrs.

(6) The resulting suspension was centrifuged (12100 g, 20 min, 20^0 C) and the hot PCA fraction was decanted (fraction 2).

(7) The pellet was re-suspended in the same volume of 0.5 M NaOH and incubated (37^0 C, overnight).

(8) The sample was centrifuged (12100 g, 20 min, 20^0 C), resulting in the alkali fraction (fraction 3).

(9) The pellet was re-suspended in the same volume of dH_2O giving the residue fraction (fraction 4), which, depending on particle size, was subjected to sonication (Dawe soniprobe, type 7532B).

The procedure produces four fractions, defined by their solubility in PCA or alkali conditions:

- **Cold PCA fraction**: Intracellular metabolites in addition to carbohydrates.
- **Hot PCA fraction**: Nucleic acids (DNA & RNA).
- **Alkali fraction**: Protein and lipid.
- **Residue fraction**: cell wall polymers.

3.16.2 Method 2 (Davidson, 1992)

Method 2 Baillie (1968) developed a method for extraction and separation of teichoic acid (TA) from the Gram-positive bacterium, *Bacillus subtilis*. The method was based on the NA extraction protocol of Schmidt and Thannhauser (1945) [Method 2, Chapter 3, section 3.16.2]. It involved an initial extraction of small molecules using weak acid (fraction 1), followed by alkaline extraction of NAs & TA (fraction 2). For the studies presented here, each step of Baillie's method (Baillie, 1968) was used, but DNA & RNA

was further extracted into 0.5 M PCA at 70^0 C for 2 hrs (fraction 3) and protein was extracted into 0.5 M NaOH at 37^0 C overnight (fraction 4). The remaining material, both acid and alkali resolved, was re-suspended in dH_2O (fraction 5) and represented the fifth and final fraction. This material was assumed to be cell-wall associated i.e. peptidoglycan and protein.

This method was undertaken to quantify teichoic acids (TAs), in conjunction with carbohydrate, DNA, RNA, Protein and cell wall material. Due to the fact that TAs can not be directly quantified, phosphate analysis has been readily been used by other workers for TA quantification studies (see section 3.21). This opens up a number of areas of concern from an experimental perspective. Phosphate analysis is notoriously difficult with the majority of detergents containing high levels of phosphate. This problem was dealt with in the following manner.

All glassware (pipettes, flasks, digestion tubes, etc.) were washed with chromic acid-sulphuric acid mixture before use. Then rinsed with dH_2O followed by methanol and chloroform, and used immediately. Digestion tubes, particularly, were not stored before use. Failure to follow these instructions resulted in development of an anomalous deep blue colour or a red colour, giving erroneously high P-values (section 3.22.4).

Procedure

(1) A washed (dH_2O) biomass pellet of known wet weight was re-suspended in ice cold, dH_2O to a concentration of 50 $mg.ml^{-1}$. 5 ml of suspended biomass (i.e., 250 mg) was transferred to 15 ml corex tubes and 1.25 ml 30 % ice-cold PCA (v/v) was added and then left on ice for 10 min.

(2) The sample was centrifuged (9800 g, 15 min, 4^0 C) and the supernatant (fraction 1) decanted into a falcon tube. The pellet was re-suspended in 5 ml 0.3 M KOH and incubated at 37^0 C for 90 min, after which it was chilled on ice for 10 min. 1.25 ml chilled 2 M PCA was then added to the solution which was left for a further 10 min on ice.

(3) Centrifugation (10000 g, 15 min 4^0 C) resulted in fraction 2, and the residual pellet was digested in 5 ml 0.5 M PCA at 70^0 C for 2 hrs, chilled on ice for 10 min and re-centrifuged (10000 g, 15 min 4^0 C) to give fraction 3.

(4) Re-suspension of the pellet in 5 ml 0.5 M NaOH with incubation at 37^0 C overnight and re-centrifugation (10000 g, 15 min 4^0 C) resulted in fraction 4.

(5) Fraction 5 was the outcome of addition of 5 ml dH_2O to the final pellet, followed by sonication.

- **Fraction 1**: Intracellular metabolites in addition to carbohydrates
- **Fraction 2**: Teichoic acids, DNA and RNA.
- **Fraction 3**: Nucleic acids (DNA and RNA).
- **Fraction 4**: Protein and lipid.
- **Fraction 5**: Cell wall polymers

3.16.3 Method 3

Chomczynski (1987, 1989, 1993, 1994, 1995) formulated a reagent for the single step simultaneous isolation of RNA, DNA and proteins from cell and tissue samples. The reagent is a mono-phase solution of phenol, guanidine thiocyanate, acetate buffer and solubilising agents. A biological sample is homogenised in the reagent and subjected to liquid phase separation. This results in a highly selective allocation of RNA, DNA and proteins to the aqueous phase, interface and organic phase, respectively.

RNA is precipitated from the aqueous phase with iso-propanol, and DNA & proteins are sequentially precipitated from the interface and organic phase with cesium chloride / sodium citrate solution and ethanol. Using this single step procedure, RNA can be isolated in about 1 hr and DNA and protein in about 3 hrs. The method for simultaneous isolation of RNA, DNA and protein is a newer version of the acid guanidine thiocyanate phenol chloroform extraction developed initially for isolating total RNA (Chomczynski, 1987).

Preparation of reagent

(1) 0.1 $mol.l^{-1}$ solution of sodium acetate-acetic acid buffer pH 5.0 was prepared as follows; sodium acetate trihydrate (13.61 gl^{-1}) and 0.1 M acetic acid. 700 ml of 0.1 M sodium acetate trihydrate and 300 ml of 0.1 M acetic acid were combined to make 0.1 $mol.l^{-1}$ solution of sodium acetate-acetic acid buffer pH 5.0 (Dawson *et al.,* 1987).

(2) Guanidinium thiocyanate 0.8 M (94.56 gl^{-1}), ammonium thiocyanate 0.4 M (30.45 gl^{-1}), 5 % glycerol & 38 % of phenol; was made up to 1 L with solution 1 (step 1).

Protocol

(1) 100 mg of biomass was homogenised in 2 ml of solution 2 (1 ml per 50 mg of biomass). Thereafter 0.2 ml (0.2 ml per 2 ml) of chloroform was added to the homogenate and the mixture was shaken and centrifuged at 12000 g for 10 min.

(2) The mixture formed an aqueous phase containing substantially pure RNA and an organic phase containing proteins and an interphase containing substantially pure, undegraded DNA. The aqueous phase was collected and combined with 2 ml of iso-propanol and centrifuged at 12000 g for 10 min.

(3) The sediment contained the total RNA. This was washed with 2 ml ethanol (75 %), centrifuged at 8000 g for 6 minutes, and dissolved in dH_2O (Fraction 1).

(4) The DNA was isolated using 1 ml of dH_2O added to the organic phase, and the interphase, then the DNA was precipitated from the interphase by the addition of 100 µl of 4.5 M $CsC1_2$, 0.5 M sodium citrate solution and 2 ml ethanol (75 %).

(5) The resulting mixture was centrifuged (10000 g, 15 min) and the sedimented DNA was washed with dH_2O.

(6) Proteins were precipitated from the organic phase by the addition of 6 ml iso-propanol. The suspension was centrifuged at 3000 g for 3 min, the protein precipitate was washed two times with 3 ml ethanol and dissolved in a solution containing 0.05 M EDTA & 0.2 M Tris-HCl pH 8.0.

3.16.4 Method 4 (Lange & Heijnen, 2001)

(1) The sampled biomass pellet was stored at -20^0 C until freeze-drying for 48 hrs at 10 Pa. The biomass was then further dried at 70^0 C for 48 hrs and stored at room temperature in a desiccator above silica gel.

(2) Macromolecular components were determined as follows; the carbohydrates were measured according to the phenol sulphuric assay (Chapter 3, section 3.18.2) on a mixture of 1 ml of sample solution (0.2 mg dry biomass.ml^{-1}). The results were then corrected for the presence of nucleic pentoses by using a relative absorbance of total nucleic acids (section 3.19.1).

(3) Total protein was determined by using the ninhydrin method (Chapter 3, section 3.20.6), 2 ml of re-suspended biomass (3 gl^{-1}).

(4) The cellular lipid components of 500 mg biomass were dissolved in 100 µl dH_2O and was extracted twice with 3.75 ml of a 2 : 1 mixture of methanol and chloroform washed and measured by gravimetric analysis (Chapter 3, section 3.23.3).

(5) RNA & DNA was extracted with 0.5 M PCA at 70^0 C for 2 hrs and measured with the orcinol and Burton assay (Chapter 3 sections, 3.19.4 & 3.19.2 respectively).

3.17 Estimation of macromolecular composition

The macromolecular composition of the biomass pellets was determined by means of spectrophotometric (Shimadzu UV-Vis 2401PC) & fluorometric (Shimadzu RF-5301 PC) analysis on the extracts and samples.

3.17.1 Standardisation of macromolecular compositional data

As different strains grow with different specific growth rates and show different substrate uptake rates, a comparison can only be done, by eliminating the individual time scales (calculated as King, 1997; King and Budenbender, 1997; who compared macromolecular compositional data for 25 streptomycetes). This was done in three steps:

The time was determined at which the substrate limitation, phosphate or ammonium, occurred. The first part of the cultivation was then linearly stretched or compressed so that the limitation occurred at a specified normalised time t_n, e.g. $t_n = 50$ (thus $t_n / t_{limitation} - \mu = t_{normalised}$). Normalising the next transition phase was characterised by DNA replication. Therefore, the time scale between the onset of substrate limitation ($t_{limitation}$) and the end of significant DNA replication was normalised by another factor to a fixed length, e.g., $\Delta t, = 30$ (set by King, 1997). King (1997) reported that the scatter in DNA measurements makes the determination of the end of DNA replication somewhat arbitrary. The end of significant DNA replication was set at t_{actual} so that the time scale between the onset of substrate limitation and the end of DNA replication had to be compressed by $30 / (t_{actual} - t_{limitation})$ = compression factor (h^{-1}). The time scale of the remaining data was normalised with a factor of 1 h^{-1}, that means the true time is replaced by its dimensionless equivalent. When this normalising procedure was done for all cultivations with all strains, the substrate limitation occurred at $t_n = 50$ and the end of

replication occurred at t_n = 50 + 30 = 80. When antibiotic yields and limitation times were considered to difficult to accurately determine. The culture was normalised to 80 (h^{-1}) up until the end of DNA replication and each time scale of the remaining data was normalised with a factor of 5 h^{-1} (i.e., 24 hrs = 5 places on the graph).

3.18 Total carbohydrate estimation

Two methods were used for the analysis of carbohydrates. In the first the anthrone assay which was applied to the cold PCA extract from the fractionation methods 1 & 2 (section 3.16.1 & 3.16.2). In the second the phenol-sulphuric acid assay was applied to a freeze-dried biomass (0.2 mg dry biomass ml^{-1}). The results were then corrected for the presence of nucleic pentoses by using a relative absorbance of total nucleic acids (as section 3.19.1).

3.18.1 Anthrone assay (Shields and Burnett, 1960)

This method measures many hexoses other than glucose, oligo- and polysaccharides (and some pentoses) and results are frequently referred to as total carbohydrate (expressed as glucose equivalents). The anthrone assay was originally described by Shields and Burnett (1960) but many variations have been devised (Mousdale, 1997). It typifies many well, established assays in that the structure of the chromophore is complex and the mechanism of the reaction is not understood.

Preparation of reagent

The reagent was prepared by adding 250 ml conc. H_2SO_4 to 100 ml of chilled dH_2O in a vessel on ice. 0.5 g of anthrone was then dissolved in the solution and stored in a brown bottle. The reagent was stable for one week at room temperature.

Assay procedure

100 µl of each sample, standard (Standard glucose solution of 0 - 1 $mg.ml^{-1}$ glucose in appropriate solute) and blank was added in triplicate to Pyrex tubes. 5 ml of anthrone reagent was then added. The tubes were placed immediately in a boiling water (tubes capped with glass pear drops or marbles to reduce evaporation) bath for 10 min, and then cooled for 10 min in cold water. The absorbance was measured at 620 nm, and the

carbohydrate concentration was determined by reference to a calibration line (for example of calibration see Fig 3.2a).

3.18.2 Phenol-sulphuric acid assay (Dubois *et al.,* 1956; Herbert, 1971)

Assay procedure

1.0 ml of the sample containing the equivalent of 10 - 100 µg glucose was pipetted into Pyrex tubes. A reagent blank containing 1 ml of dH_2O, and a set of glucose standards (e.g. 0, 25, 50, 75 & 100 µg glucose, in a volume of 1 ml) was prepared. 1 ml of 5 % phenol was then added to each tube and mixed thoroughly. 5 ml of conc. H_2SO_4 was then added, directing the stream of acid to the surface of the liquid and shaking the tube simultaneously, to effect fast and complete mixing. The tubes were then allowed to stand for 10 min, shaken vigorously and then placed in a water bath at 25^0 C for 20 min. The absorbance was measured at 490 nm (the colour was stable for several hours) and the carbohydrate concentration was determined by reference to a calibration line (for example of calibration see Fig 3.2b).

The characteristic yellow colour and intensity of the colour developed was a function of the phenol concentration. As the amount of phenol was increased, the absorbance rose to a maximum and then fell off. The optimum amount of phenol varies considerably with different sugars; the amount used above was a compromise. It was this value that gave the maximum colour with most other sugars. When the method was applied to known amount of sugars (e.g., after elution from paper chromatography) the optimum amount of phenol can be selected from the data of Dubois *et al.* (1956). Results obtained by the phenol reagent are always higher than those given by the anthrone reagent, presumably because the former reacts strongly with many different sugars. The anthrone assay was relatively insensitive e.g. cell wall components, such as heptoses, methylpentoses and uronic acids, and intracellular components, such as the ribose and deoxyribose components of RNA & DNA. The nucleic acids are particularly important, since they react so much more strongly with the phenol reagent than with the anthrone reagent.

3.19 Nucleic acids

A number of different techniques were undertaken to determine the nucleic acid composition of microbial biomass [Herbert *et al.,* 1971; Davidson, 1992; Mousdale, 1997). Out of these methods only the total nucleic acids, diphenylamine and the orcinol assay worked on the PCA fraction (Method 1 & 2, section 3.16.1 and 3.16.2 respectively) the diphenylamine assay and orcinol assay also worked on methods 3 & 4 (section 3.16.3 and 3.16.4 respectively).

3.19.1 Total nucleic acids UV absorbance

DNA concentration is usually measured by UV absorbance at 260 nm (1 A_{260} = 50 μg.ml^{-1}) in a 1 cm path length cuvette. The average extinction coefficient for double-stranded DNA (1 A_{260} = 50 μg.ml^{-1}), single stranded DNA (1 A_{260} = 33 μg.ml^{-1}), or RNA (1 A_{260} = 40 μg.ml^{-1}) is used to quantitate the nucleic acid directly from the absorbance at this wavelength. For accurate results, absorbance should be in the range of 0.05 - 0.10, which for a 1.0 ml assay, requires 2.5 - 5.0 μg of dsDNA. For dilute nucleic acid samples, the solution to be measured should also be relatively free of other components that would add significantly to the absorbance at 260 nm. Because of these limitations, alternative techniques have been sought that provide more sensitivity and are less influenced by background absorbance.

3.19.2 DNA estimation / Burton assay /diphenylamine assay (Richards, 1974)

The method used was a modification of that described by Burton (1956). The diphenylamine in the reagent is thought to combine with deoxypentoses formed from hydrolysis of purine residues. Inorganic phosphate is liberated in the early stages of the reaction, presumably from the phosphate-phosphate bridges between adjacent residues.

Reagent preparation

(1) The reagent was prepared by dissolving, 2.0 g diphenylamine in 50 ml glacial acetic acid and then adding 5 μl paraldehyde.

(2) A standard DNA gravimetric reference, was made by digesting macromolecular DNA (Calf Thymus DNA can often serve as a reference for most plant and animal

DNA because it is double-stranded, highly polymerised, and is approximately 58 % AT (42 % G+C). For bacterial DNA, a different standard may be needed because the A+T % varies widely depending on species. 200 $mg.l^{-1}$ in 0.5M PCA, at 70^0 C for 2 hrs, until fully dissolved and the actual concentration checked by A_{260} nm (50 $\mu g.ml^{-1}$ = 1.0).

Procedure

0.90 ml reagent was added to 0.45 ml of sample (hot PCA extract), or standard in triplicate in Eppendorf micro-centrifuge tubes. For each sample, a blank was prepared by incubating 0.45 ml sample with 0.90 ml of reagent blank; the blank was incubated and processed in parallel with the full assay mixture. After incubation at 37^0 C for 20 hrs, the assay mixtures were centrifuged for 3 min at 20000 g. The absorbance of the supernatant phase was measured at 600 nm against the reagent blank. The absorbance of the sample (0.45 ml 0.5 M PCA incubated with the full diphenylamine reagent) was subtracted from the absorbance of the reagent blank (for example of calibration see Fig 3.3a).

3.19.3 Fluorometric Hoechst assay (Paul & Myers, 1982)

In crude samples, higher salts concentration appear to cause the dissociation of protein from DNA, allowing the Hoechst 33258 dye to bind to DNA. For peak fluorescence, at least 200 mM NaCl is required for purified DNA and 2.0 to 3.0 M for crude samples. RNA does not interfere significantly with the DNA assay because Hoechst 33258 does not normally bind to RNA. Under high salt concentrations, fluorescence from RNA is usually less than 1 % of the signal produced from the same concentration of DNA.

Solution preparation

(1) Preparation of Hoechst 33258 stock dye solution (1 $mg.ml^{-1}$): 1 ml Hoechst 33258 (10 $mg.ml^{-1}$ solution) was diluted with 9 ml dH_2O (0.45 µm filtered dH_2O) and stored in an amber bottle at 4^0 C for up to 6 months.

(2) Preparation of 10 × TNE buffer stock solution: 12.11 g Tris base [Tris (hydroxymethyl) aminomethane], 3.72 g EDTA, disodium salt, dihydrate, 116.89 g NaCl, was dissolved in 800 ml dH_2O. The pH was adjusted to 7.4 with conc. HCl and made up to 1000 ml and filtered (0.45 µm) before use (stored at 4^0 C for up to 3 months).

(3) Preparation of 1 × TNE: 10 ml 10 × TNE was diluted with 90 ml 0.45 µm filtered dH_2O.

(4) Preparation calf Thymus DNA Standard: 12.5 $\mu g.ml^{-1}$ calf thymus DNA was diluted with 1 × TNE to desired concentration (0.2 A_{260} = 10 $\mu g.ml^{-1}$).

(5) Preparation of low range assay solution (for 10 - 500 $ng.ml^{-1}$ final DNA concentration): 10 µl Hoechst 33258 stock solution (1 $mg.ml^{-1}$) was diluted with 10 ml 10 × TNE and 90 ml 0.45 µm filtered dH_2O. The assay solution was kept at room temperature and Prepared fresh daily (do not filter once dye has been added).

(6) Preparation of high range assay solution (for 100 - 5000 $ng.ml^{-1}$ final DNA concentration): 100 µl Hoechst 33258 stock solution was diluted (1 $mg.ml^{-1}$) with 10 ml 10 × TNE and 90 ml 0.45 µm filtered dH_2O.

Procedure

The appropriate assay range most suitable for the samples was chosen. The experimental DNA solution was diluted in TE to a final volume of 1.0 ml and l.0 ml of the Hoechst working solution was added to achieve a final volume of 2.0 ml. Fluorescence was measured at 360 nm excitation and 460 nm emission. DNA concentration was then calculated from a calibration of calf thymus DNA standards stained with Hoechst (for example of calibration see Fig 3.3b & c).

3.19.4 RNA estimation / Orcinol assay Herbert *et al.* (1971)

Brown (1946) described a method using orcinol to detect the pentoses formed from the hydrolysis of RNA. Strong acid converts the pentoses to furfural; which produces a green colour on reacting with orcinol in a condensation reaction with ferric chloride ($FeCl_3$) as the catalyst. Hexoses interfere with this assay, this was eliminated with the fractionation method because the hot PCA (Method 1 & 2, section 3.16.1 & 3.16.2) fraction should be devoid of carbohydrates.

Reagents

(1) 0.03 % (w/v) $FeCl_3$ in conc. HCl.

(2) 20 % (w/v) orcinol (3,5-dihydroxytoluene) in 100 ml (95 %; v/v) ethanol (prepared daily).

(3) RNA stock solution (1 $mg.ml^{-1}$), yeast RNA.

(4) 0.5 M PCA.

Procedure

100 µl of sample (hot PCA extract), standard (RNA standards 0-150 $\mu g.ml^{-1}$) and a blank (100 µl of 0.5M PCA), in triplicate was added to glass test tubes and then 2.7 ml of 0.5 M PCA was added. 200 µl orcinol reagent was added to a final volume of 3.0 ml. 3.0 ml 0.03 % $FeCl_3$ solution was then added and the mixture placed in a boiling water bath for 20 min. Cooled to room temperature and the absorbance was measured at 665 nm against the blank. The assay was linear up to 100 $\mu g.ml^{-1}$ RNA (for example of calibration see Fig 3.3d).

3.19.5 Simple UV-spectrophotometric determination of RNA (Benthin *et al.,* 1991)

Procedure

Fermentation broth volumes equivalent to approximately 0.4 g RNA (2.5 g bacteria); were centrifuged (10000 g, 30 min, 4^0 C) in chilled test tubes, and the supernatant was discarded. The cells were washed three times with 3.0 ml cold 0.7 M PCA and digested with 3 ml 0.3 M KOH for 60 min at 37^0 C with occasional mixing. The extracts were then cooled and neutralised with 1.0 ml 3 M PCA. The supernatant was collected and the precipitate was washed twice with 4 ml cold 0.5 M PCA. Finally the extracts were made up to 15 ml with 0.5 M PCA and the solutions then centrifuged (10000 g, 30 min, 4^0 C) to remove any non-visible precipitate of $KClO_4$ that might be in the extracts. The RNA concentration was determined by measuring the absorbance at 260 nm using average nucleotide data (see section 3.19.1).

3.20 Protein estimation

A number of methods were used to determine the protein & amino acid content of the biomass (Walker, 1996).

3.20.1 Bradford assay (Bradford, 1976)

An assay described by Bradford (1976) has become the preferred method for quantifying protein in many laboratories. Coomassie brilliant blue combines with protein to give a

dye-protein complex with an absorption maximum of 595 nm. However, the formation of dye-protein complex is affected by the number of basic amino acids within a protein (the dye appears to bind most readily to arginyl and lysyl residues of proteins but does not bind to free amino acids). This specifically can lead to variation in the response of the assay with different proteins.

Preparation of Bradford solution

(1) 100 mg Coomassie blue G-250 dye (Biorad) was added, to 50 ml lab-grade ethanol (95 %; v/v) and stirred until dissolved (overnight). 100 ml orthophosphoric acid was then added (85 %; v/v) and mixed. This mixture was then added to 850 ml dH_2O and mixed and filtered (Whatman No 1 paper). The Bradford's reagent was stored in a dark bottle at room temperature (stock solution was made on a weekly basis).

(2) Preparation of standard solution of bovine serum albumin (BSA); a 10 $mg.ml^{-1}$ stock solution in the appropriate solute was prepared. 1 ml of solute was added drop wise to the standard stock solution while reading the absorbance (A) at A_{280} until a concentration of 1 $mg.ml^{-1}$ was achieved. When the A was 0.66 the solution was exactly 1 $mg.ml^{-1}$.

Bradford assay

100 µl of the sample (or appropriate dilution), standard (10 to 100 µg of BSA), or reagent blank were pipetted into test tubes. All analysis was carried out in triplicate. 3 ml of Bradford's reagent was added and mixed by inversion (avoid foaming, which will lead to poor reproducibility), and allowed to stand at room temperature for 5 min. The absorbance was measured at 595 nm and the protein concentration was then calculated from a calibration of the BSA standard (for example of calibration see Fig 3.4a).

3.20.2 Lowry assay (Lowry *et al.,* 1951)

The method is based on both the Biuret reaction in which the peptide bonds of proteins react with copper under alkaline conditions producing Cu^{+}, which reacts with the Folin reagent in the Folin-Ciocalteau reaction, which is poorly understood. In essence phosphomolybdotunsgate acid are reduced to heteropolymolybdenum blue by the copper-

catalysed oxidation of aromatic amino acids. The reaction results in a strong blue colour, which depends partly on the tyrosine and tryptophan content.

Preparation of reagents

(1) Solutions A, B, & C were prepared as followed: solution A: 2 % (w/v) Na_2CO_3 in dH_2O. Solution B: 1 % (w/v) $CuSO_4.5H_2O$ in dH_2O and Solution C: 2 % (w/v) sodium potassium tartrate in dH_2O.

(2) Complex-forming reagent was prepared as followed: prepare immediately before use by mixing the following three solutions A, B & C in the following proportions 100:1:1 (v / v / v - respectively).

(3) Folin reagent (commercially available).

Lowry assay

1 ml of the complex-forming reagent was added to 100 µl of sample, standard, or blank and left for 10 min at room temperature. (standards of 25 µg to 500 µg of BSA were used to obtain a standard curve, standard solution prepared as section 3.20.1). The tubes were left at room temperature for 30 min. The absorbance was measured at 750 nm and the protein concentration was then calculated from a calibration of the BSA standard (for example of calibration see Fig 3.4b).

3.20.3 Peterson precipitation method (Peterson, 1983)

Peterson (1983) described a precipitation step that allows the separation of proteins from biological matrixes and interfering substances and also consequently concentrates the protein sample. This allowed the quantification of proteins in dilute solution. This protocol can be applied to the alkali fraction methods 1 & 2 (section 3.16.1 & 3.16.2 respectively).

To a 1.0 ml protein sample 0.1 ml of 0.15 % deoxycholic acid (DOC) was added and mixed and allowed to stand at room temperature for 10 min, then 0.1 ml of 72 % trichloroacetic acid was added. The samples were then centrifuged for 30 min at 3000 g 20^0 C. After centrifugation the tubes were decanted and retained in an inverted position with a paper towel. Any remaining supernatant was removed by aspiration using a

Pasteur pipette. The samples were re-diluted in 0.3 % NaCl to an appropriate concentration (5 - 100 µg of protein to 1.0 ml with dH_2O).

3.20.4 Bicinchoninic acid assay (Smith *et al.,* 1985)

The principle is similar to the Lowry assay, since it also depends on the conversion of Cu^{2+} to Cu^{+} under alkaline conditions. The Cu^{+} is then detected by reaction with bicinchoninic acid (BCA). The two assays are of similar sensitivity, but since BCA is stable under alkali conditions, this assay has the advantage that it can be carried out as a one-step process compared to the two steps needed in the Lowry assay. The reaction results in the development of an intense purple colour with an absorbance maximum at 562 nm.

Preparation of reagents

(1) Reagent A was prepared as followed: 0.8 g $Na_2CO_3.H_2O$, 1.6 g NaOH, 1.6 g Sodium tartrate (dihydrate) was dissolved and made up to 100 ml with dH_20, and adjusted to pH 11.25 with 10 M NaOH.

(2) Reagent B was prepared as followed: 4.0 g BCA, in 100 ml dH_2O. Reagent C: 0.4 g $CuSO_4.5H_2O$, was made up to 10 ml with dH_2O.

(3) Standard working reagent (SWR) was prepared as followed: mix 1 volume of reagent C with 25 volumes of reagent B, and 26 vol of reagent A.

Assay procedure

To a 100 µl sample, blank and standards (1 $mg.ml^{-1}$; prepared as Bradford assay, in appropriate solute). 2 ml of SWR was added and mixed. Then incubated at 60^0 C for 30 min. The samples were cooled, and the absorbance read at 562 nm and the protein concentration was then calculated from a calibration of the BSA standard (for example of calibration see Fig 3.4c).

3.20.5 Reverse biuret method combined with the copper bathocuproine chelate reaction (Matsushita *et al,* 1993)

The reverse biuret method combined with the copper bathocuproine chelate reaction utilises the biuret-like reaction, whereby Cu^{2+} initially complexes with protein in alkaline

medium. Protein content is then determined by measuring the absorbance of a Cu^{+} bathocuproine complex, which is formed with excess Cu^{2+} not chelated to protein. Excess Cu^{2+} is reduced to Cu^{+} with ascorbic acid, which can then form a coloured complex with bathocuproine. The signal is inversely related to the amount of peptide bonds, in contrast to other common protein assays which are influenced by the side chains of specific amino acids. Therefore, protein to protein variability is very low and individual proteins or protein mixtures can be measured accurately.

Tartrate-complexed-Cu^{2+} + protein → Cu^{2+}-protein-chelate-complex (biuret reaction)
Excess tartrate-complexed Cu^{2+} + ascorbic acid → Cu^{+}
Cu^{+} + bathocuproine → Cu^{+}-bathocuproine chelate complex (measure at 485 nm)

Preparation of reagents

(1) Reagent A was prepared as followed; $CuSO_4.5H_2O$ 0.60 mmoles (150.0 mg) and 1.60 mmoles (450.0 mg) of potassium sodium tartrate were dissolved in 800 ml of dH_2O; then 0.60 mol (24.0 g) of NaOH was added and the reagent was diluted to 1 L with dH_2O.
(2) Reagent B was prepared as followed; ascorbic acid 1.39 mmol (250 mg) and 0.65 mmol (370 mg) of bathocuproinedisulfonic acid disodium salt was dissolved in dH_2O and diluted to 1 L. Reagents A & B were stable for at least 1 month when stored at 4^0 C.

Procedure

Reagent A and reagent B were allowed to warm to room temperature or placed in a 37^0 C water bath. A series of standards covering an appropriate concentration range were prepared by diluting a protein standard (1 $mg.ml^{-1}$; prepared as for the Bradford assay, section 3.20.1) in the same dilutent as the unknown sample. 100 µl of reagent A was added to the appropriate number of disposable semi-micro (1.5 ml) cuvettes. 50 µl of standard or sample was added to the appropriate cuvette and mixed. The cuvette was incubated at room temperature for at least 5 min. Prolonged incubation with reagent A (up to 1 hr) did not affect the assay performance. 100 µl of reagent B was the added to the first cuvette, mixed briefly, and after 30 seconds the absorbance immediately measured at 485 nm against a dH_2O or dilutent reference cuvette. This was repeated

sequentially with the remaining samples and a calibration curve constructed by plotting absorbance of the standards against their concentration (for example of calibration see Fig 3.4d).

3.20.6 Ninhydrin assay (Moore & Stein, 1948)

The assay is based on the reaction between amino acids and ninhydrin; which results in a blue coloured product (known as diketo-hydrindylidine-diketo-hydrindamine), CO_2 and an aldehyde.

Alkaline hydrolysis

900 µl of 13.5 M NaOH was added to 100 µl of the sample in 10 ml polypropylene tubes. Autoclave at 121^0 C for 20 min. Once the hydrolysates were cooled to room temperature, 2.0 ml of glacial acetic acid was added and vortexed to neutralise the digested protein solution.

Preparation of reagents

(1) 4.3 g citric acid and 8.7 g sodium citrate were dissolved in 250 ml dH_2O and the pH adjusted to 5.0.
(2) 400 mg stannous chloride was dissolved in the citrate solution [step 1] (this required gentle heating), and was stored at 4^0 C prior to use.
(3) 1 g of ninhydrin was dissolved in 25 ml 2-methoxyethonol (prepared on day of use).
(4) The ninhydrin and stannous chloride solutions were mixed together in a ratio of 1 : 1 (v/v).
(5) In addition, 5 0 % (v/v) propan-1-ol was required.

Assay procedure

500 µl of each sample was added in triplicate to 15 ml Pyrex test tubes. A blank and triplicate standards were prepared; with up to 500 µl of 1 mM leucine with the appropriate solute (standard and blank were put through same hydrolysis procedure as the samples). 1.5 ml of the ninhydrin / stannous chloride solution (preparation of reagents, step 3) was added to the samples, blank, and standards. The tubes were placed in a boiling water bath for 5 minutes and then cooled. Subsequently, 8 ml of 50 % (v/v) propanol-1-ol was added and vortexed. After being left at room temperature for 30 min,

the absorbance was measured at 570 nm and a calibration curve constructed by plotting absorbance of the standards against their concentration (for example of calibration see Fig 3.4e).

3.21 Determination of teichoic acids and teichuronic acids (Hancock, 1994)

Teichoic acid (TA) in the cell wall is readily detected and measured as organic phosphorus. The only other sources of phosphorus in purified walls are the attachment points of polysaccharides and teichuronic acids linked to peptidoglycan by phosphate esters. These sources contribute very little to the weight of the wall, whereas TA phosphorus would be expected to constitute between 0.5 % and 5 % of the weight of the wall. The procedure involves the conversion of organic phosphorus to inorganic orthophosphate followed by the measurement of inorganic phosphate by the method of Nakamura (1950)[section 3.21.5]. Preparation of a cell wall fraction generally facilitates clean analysis of covalently-linked wall components (Hancock, 1994; for a general purpose protocol for Gram-positive bacteria).

Preparation of cell-wall extracts

Biomass was suspended in ice-cold dH_2O (100 mg wet weight.ml^{-1}) and gradually an equal volume of a boiling SDS solution 8 % (w/v) was added whilst maintaining the temperature for 30 min. After cooling to room temperature, the insoluble crude cell wall was recovered by centrifugation (30000 g, 15 min). The SDS treatment was repeated at least once on the insoluble material. The final insoluble pellet was washed by re-suspension and centrifugation 5 times with (80^0 C) hot dH_2O.

Removal of nucleic acids and protein

The cell wall material was re-suspended in 0.05 M Tris-HCl, pH 7.0 containing 1 mM $MgCl_2$, and 0.2 mM mercaptoethanol. RNase A (5 Kunitz units.ml^{-1}) and DNase 1 (50 Kunitz units.ml^{-1}) were added and the mixture was incubated at 37^0 C for 3 hrs. The walls were recovered by centrifugation at 48000 g for 15 min, washed three times in Tris buffer (0.05 M Tris-HCl, pH 7.0), and re-suspended in the same buffer. Pronase (protease type XIV, Sigma), previously heated as a 10 mg.ml^{-1} solution in Tris buffer for 2 hr at 60^0 C, was added to a final concentration of 100 μg.$ml^{-1}$and the mixture incubated at 60^0 C

for 1 hr. The pure cell wall material was recovered by centrifugation at 48000 g for 15 min, washed four times with dH_2O, and lyophilised. TAs was quantified as inorganic phosphate (see phosphate analysis, section 3.22.4).

3.22 Estimation of extracellular components

3.22.1 Glucose estimation (Werner *et al.,* 1970)

Two approaches were used to estimate glucose utilisation throughout fermentations. A manual approach of the glucose oxidase (GOD) and peroxidase reactions (PERID) [Boehringer Mannheim; 124 036] and an automated biochemistry analyser (YSI 2700 select; Biochemistry analyser), using the same reaction chemistry was also used. In the assay, the two enzymes act sequentially to form a green coloured complex, which was quantified at 610 nm.

Principle

GOD

Glucose + O_2 + H_2O → Gluconate + H_2O_2

PERID

H_2O_2 + ABTS* (pale yellow) → Coloured complex + H_2O

*(di-ammonium 2,2'-azino-bis[3-ethylbenzothiazoline-6-sulphonate])

Procedure

The reagent solution was prepared according to the manufacturers directions and stored at 4^0 C. 900 µl of the reagent was added to 100 µl of appropriately diluted samples (1 in 40 dilution of samples up to 50 hrs of growth, 1 in 20 dilution thereafter), vortexed and incubated at 25^0 C for 25 min. The absorbance was measured at 610 nm.

3.22.2 Glycerol (Kreutz, 1962; Boehringer Mannheim, Cat. No. E 148 270)

Principle: Glycerol is phosphorylated by ATP to L-glycerol-3-phosphate in the reaction catalysed by glycerokinase (GK) [1].

GK

(1) Glycerol + ATP → L-glycerol-3-phosphate + ADP

The ADP formed in reaction 1 is reconverted to ATP by pyruvate kinase, in the presence of PEP (2). The pyruvate formed in reaction 2 is therefore stoichiometric with the ADP formed in reaction 1.

PK

(2) ADP + PEP → ATP + pyruvate

In the presence of the enzyme L-lactate dehydrogenase (L-LDH), pyruvate is reduced to L-lactate by NADH (3).

L-LDH

(3) Pyruvate + NADH → L-lactate + NAD

The amount of NADH oxidised in the above reaction is stoichiometric to the amount of glycerol converted to glycerophosphate in (1). The absorbance was measured at 340 nm. The assay was based upon the change in optical density at 340 nm during the oxidation of NADH.

Procedure

The reagent solutions, analytical procedure, and calculations were carried out according to the manufacturers directions. 1000 µl of solution (1)[co-enzyme buffer solution], 1900 µl of dH_2O, 10 µl solution (2) [PK & L-LDH] was added to 100 µl of appropriately diluted samples & blank (1 in 1000 dilution of samples up to 50 hrs of growth, 1 in 100, to 1 in 10 dilution thereafter). Wait for 10 min, then the reaction was initiated by adding 10 µl of solution (3) [GK] and inverted and incubated at 25^0 C for 15 minutes. NADH was quantified by means of its absorbance at 340 nm.

3.22.3 Colorimetric method for L-Glutamate (Beutler & Michal, 1974; Boehringer Mannheim; Cat. No. 139 092)

Principle: L-Glutamate is deaminated oxidatively by NAD to 2-oxoglutarate in the presence of the enzyme glutamate dehydrogenase (GDH) [1].

GDH

(1) L-glutamate + NAD + H_2O → 2-oxoglutarate + NADH + NH^+_4

In the reaction catalysed by diaphorase the NADH formed converts iodonitrotetrazolium chloride (INT) to formazan which is measured in the visible range 492 nm.

(2) NADH + INT* → NAD + INT-formazan

The equilibrium of the reaction lies far on the side of L-glutamate. Trapping of the NADH by the means of the indicator reaction; displaces the equilibrium in favour of 2-oxoglutarate.

Procedure

The reagent solutions, analytical procedure, and calculations were carried out according to the manufacturers directions. 600 µl of solution (1) [buffer solution], 2000 µl of dH_2O, 200 µl of solution 2 [diaphorase & NAD], 200 µl solution (3) [INT], were added to 200 µl of appropriately diluted samples & blank (1 in 1000 dilution of samples up to 50 hrs of growth, 1 in 100, to 1 in 10 dilution thereafter) wait for 10 min, the reaction was initiated by adding 10 µl of solution (4) [GDH] the resultant solution was then inverted and incubated at 25^0 C for 15 mins. The absorbance was measured at 492 nm.

3.22.4 Phosphate estimation (Mousdale, 1997)

Phosphate determinations were carried out to verify the nucleic acid values estimated by the Burton and orcinol methods, and for teichoic acid analysis. Utilisation of phosphate from the growth media was also determined by this assay. This procedure measures inorganic and organic phosphate esters.

Acid hydrolysis of organic phosphate esters

100 µl of conc. H_2SO_4 was added to 100 µl of the sample or standard followed by heating at 180^0 C in a dry block for 60 min. Once cooled to room temperature, 500 µl of H_2O_2 was added and the digestion was continued for 30 min. The H_2O_2 step was repeated if the solution did not go clear.

Preparation of ammonium molybdate and amidol reagents

(1) 8.3 g (w/v), ammonium molybdate was dissolved, in 100 ml dH_2O with gentle heating.
(2) 1 g (w/v) amidol (2,4-diaminophenol hydrochloride) was stirred vigorously into 100 ml 20 % (w/v) sodium metabisulphite and filtered (Whatman number 1 paper).
(3) 30 % (v/v) hydrogen peroxide.

Assay procedure

4.2 ml of dH_2O and 0.2 ml of ammonium molybdate solution was added to each sample digestion tube and triplicate standards (standards were put through same hydrolysis step as samples) with up to 100 µl 10 mM phosphate (with the appropriate solute). A stock solution of 1.36 $g.l^{-1}$ KH_2PO_4 (10 mM) was used for standards. The resultant solution was mixed by vortexing. A blank with 4.3 ml dH_2O was prepared. 0.4 ml of amidol reagent was then added, vortexed, and left to stand at room temperature for 60 min. The absorbance was measured at 620 nm and a calibration curve constructed by plotting absorbance of the standards against their concentration (for example of calibration see Fig 3.5a).

3.22.5 Ammonia / Phenate-indophenol assay (Weatherburn, 1971)

An intensely blue compound, indophenol, is formed by the reaction of ammonia, hypochlorite, phenol and nitroprusside.

Reagent preparation

(1) All solutions were prepared in ammonia free dH_2O.

(2) 5.0 g phenol, 10.0 g sodium nitroprusside was dissolved in 1000 ml dH_2O (SWR).

(3) 15 % sodium hypochlorite.

(4) A ammonium chloride standard was prepared (1 $mg.ml^{-1}$) in the appropriate solute.

Assay method

10 and 80 µg of ammonium standard was pipetted in 100 µl total volume into test tubes; and 100 µl of sample (or appropriate dilution), all analysis was undertaken in triplicate. 100 µl of the appropriate solute was pipetted into an additional tube to provide the reagent blank. 100 µl 15 % sodium hypochlorite, 1000 µl of SWR, and 5000 µl of dH_2O was added to each tube and, allowed to stand at room temperature for 10 min. The absorbance was read at 630 nm (read 5 - 60 min after mixing) and a calibration curve constructed by plotting absorbance of the, standards against their concentration (for example of calibration see Fig 3.5b).

3.23 Determination of total soluble lipid

The utilisation of the lipid is readily monitored by the sulfophosphovanillin assay or gravimetric analysis. The sulfophosphovanillin assay is based on that described by Zollner & Kirsch (1962) and was until recently available as a kit; for total lipid content. The assay is based on the reaction of lipids with sulphuric and phosphoric acids and vanillin to form a pinkish-coloured complex. It is important to establish that the correct chromophore is produced; carbohydrates can, for example, be charred by sulphuric acid to generate a dark coloured solution, which will contribute to the absorbance of the test wavelength (530 nm).

3.23.1 Vanillin assay (Zollner & Kirsch, 1962)

Preparation of reagents
The vanillin reagent was prepared as followed; 200.0 mg vanillin was dissolved in 5 ml ethanol, and 4 ml dH_2O, and made up to 100 ml with phosphoric acid.

Assay
0.05 ml of each sample was added in triplicate to 15 ml glass test tubes. Due the lack of sensitivity of the method, the alkali extract needed to be concentrated by extraction with hexane (or appropriate solvent) and evaporation and re-dilution at an appropriate concentration in hexane (by rotary evaporation). A blank was prepared with 0.05 ml hexane and triplicate standards [10 $mg.ml^{-1}$ oleic acid prepared in hexane] with sufficient hexane to make up to 0.05 ml. 2.0 ml conc. H_2SO_4 was then added. The tubes were then placed in a boiling water-bath for 20 min, removed and placed in cold water-bath for 10 min. 0.1 ml from each tube was then transferred to a fresh tube. 2.5 ml of the vanillin reagent was added, vortexed, and incubated for 25 min at 25^0 C. The absorbance was read at 530 nm in glass cuvettes against the blank prepared in step 3 and a calibration curve was constructed by plotting absorbance of the standards against their concentration (for example of calibration see Fig 3.6)

3.23.2 Gravimetric assay (Folch *et al,* 1957; adapted from Henriksen *et al.,* 1996)

500.0 mg wet weight or freeze-dried biomass was dissolved in 500 µl dH_2O in corex tubes. 3.75 ml of a 2 : 1 mixture of methanol and chloroform was added. Extraction was

facilitated by placing samples in an ultrasonic bath. The extract was washed with 1.25 ml 0.9 % NaCl solution; the two phases were separated by centrifugation (6000 g, 20 min, 0^0 C) and decanting. The chloroform was evaporated off overnight in a fumehood. The remaining lipid was quantified gravimetrically and the mass of lipid expressed as mg.g dry weight biomass and converted to percentage format (all measurements were performed in triplicate).

3.24 Spectrophotometric analysis of actinorhodin

Actinorhodin (ACT) was determined on whole broths. 2 ml of whole broth was treated with 1 ml 3 M KOH, vortexed until the biomass appeared totally disrupted, and centrifuged (15 min, 3000 g 4^0 C). The absorption of the blue supernatant was determined at 640 nm. The concentration of ACT was calculated on the basis of a molar absorption coefficient of 25320 M^{-1} .cm^{-1} (Bystrykh *et al.,* 1996).

3.25 HPLC equipment

All HPLC analyses was carried out on a Gilson 305/306 liquid chromatogram with a Gilson autoinjector 234, Gilson 119 UV detector, & Thermo spectrasystem spectrofluorometer FL2000. Connected to the chromatogram was a Phillips P3202 microcomputer using Gilson 715 system controller software.

3.25.1 HPLC of tylosin (Kanfer *et al.,* 1998; Heyden *et al.,* 1999)

Preparation of mobile phase

600 g of sodium perchlorate (anhydrous) was dissolved in 2400 ml of dH_2O and the pH adjusted to 2.5 (accurate pH measurement was critical) using conc. HCl. This solution was filtered through a 0.45 µm filter then 1600 ml of HPLC grade acetonitrile was added. The solution was well mixed using a magnetic stirrer and degassed by bubbling helium gas through it.

Sample and standard preparation

4 g of raw broth was accurately weighed into a clean, dry 100 ml volumetric flask (if using minimal media or defined media just filter [Whatman 113V filter paper]). A few drops of aluminium sulphate solution (5 %; v/v) was added to keep turbidity to a

minimum and made up to the mark with dH_2O. The flask contents were mixed, and left, to stand for at least 15 min. Using Whatman 113V filter paper, 6 - 8 ml of solution was filtered into a disposable plastic test tube.

Standard preparation, approximately 200.0 mg of tylosin standard was weighed (previously stored in desiccator at 60^0 C overnight) into a 500 ml volumetric flask and diluted to volume with dH_2O.

Assay for tylosin

The UV detector was set to 285 nm (range 0.4 AUFS). The C18 5 micron, 25cm x 4.6 rim id column was equilibrated (Phenomenex ser # 274206) with tylosin mobile phase until a stable baseline was achieved (1.0 $ml.min^{-1}$, at room temperature). 0.02 ml of the sample was injected into the sample injection port (with any necessary dilution to contain macrolides at concentrations less than those in standard solutions). The macrolide concentration was determined by reference to calibration lines of concentration against peak area. Identification of related macrolides was carried out using authentic standards (for example of standard HPLC trace chromatogram see Fig 3.7 and calibration graph see Fig 3.8).

3.25.2 HPLC of total amino acids in acid hydrolysates (Mousdale, 1997)

Careful hydrolysis of protein or peptide samples is one of the crucial steps for successful amino acid analysis. This was demonstrated clearly by the results of Yüksel *et al.* (1995) in which a sample which was pre-hydrolysed was analysed with 6.5 ± 4.0 % error while a similar sample which was hydrolysed individually by other laboratories resulted in 10.9 ± 3.7 % error. While base and enzymatic hydrolysis have special utility, acid hydrolysis (6 M HCl) is overwhelmingly the most common technique. Liquid phase hydrolysis, based on the work of Stein and Moore (1963), is considered the standard benchmark. Acid must be of the highest purity. Samples are hydrolysed under vacuum (or inert atmosphere to prevent oxidation) at 110^0 C for 24 hours. Drawbacks to acid hydrolysis include complete conversion of Asn and Gln to Asp and Glu, respectively, complete loss of Trp, partial destruction of Ser and Thr, and incomplete hydrolysis between β-branched amino acids (Val-Val, Ile-Ile). Remedies for many of these have been described. For Asn and Gln, the sample may be treated with bis (1,1- trifluroacetoxy) iodobenzene, thereby

obtaining diaminopropionic and diaminobutyric acid, respectively (Soby & Johnson, 1981). Extending the hydrolysis time to 48 and 72 hours provides a means to extrapolate back to zero time to obtain the actual values for Ser, Val, Thr, and Ile. Additions of fresh preparations of 0.1 % (w/v) phenol and 1 % 2-mercaptoethanol to 6 M HCl prevents halogenation of tyrosine and oxidation of methionine to methionine sulfoxide. Additives to preserve tryptophan include dodecanethiol (West & Crabb, 1992) and thioglycolic acid (Yano *et al.,* 1990), among others (Strydom *et al.,* 1993).

3.25.3 Post-column derivatisation

Ion exchange chromatography for the analysis of amino acids was first automated by Stein & Moore (1963), at Rockefeller University some 40 years ago. There have been many improvements over the years, especially in the first 20 years following their contributions. There have been relatively few methodological advancements in the past five years, but the technique is still in wide-spread use. Early technology utilised stepwise gradients of buffers for elution of amino acids from the ion exchange columns, but newer instruments utilise continuous gradients, an important advance that leads to fewer baseline disturbances. The core of the technique is the ion exchange column, composed of a hydrophilic cation exchange resin made of sulfonated polystyrenedivinylbenzene copolymer. The preparation of this resin is seemingly complex and not completely controlled, so that batch-to-batch differences can usually be detected. Separation of amino acids is seldom the result of the resin's ion exchange properties alone. Rather, partition effects, adsorption effects, and even size exclusion effects can be noted, and while these may complicate the prediction of the "expected" elution positions of individual amino acids, the reproducibility of any batch is very good and no practical complications arise.

According to Jarrett *et al.* (1986), separation of amino acids by reversed-phase high pressure chromatography required the use of two solvents, an aqueous solvent and a non-polar solvent. This combination with the column allowed the acidic and polar amino acids to be eluted first (Asp with the lowest pI elutes early), followed by those with short alkyl side chains, and then the hydrophobic amino acids (Arg with the highest pI elutes late; Trp, however, doesn't elute based on its pI and is affected strongly by adsorption

properties). Decreasing the pH also led to longer retention times of the acidic amino acids because of the strengthening interactions with the stationary phase; fluorescence was decreased with a decrease in pH (Cooper *et al.,* 1984). Temperature effects lead to increased elution volume of amino acids.

Various detection systems have been developed, with the classical one being ninhydrin. Reaction of ninhydrin with amino acids results in the development of a coloured compound (Rhueman's Purple) and is responsible for the specificity of the technique. Ninhydrin does not react with all amines, and many contaminating compounds will not react with ninhydrin but would be detected by some other techniques. Recent developments include "Trione," a more stable but less sensitive derivative, and fluorescent detection reagents including fluorescamine and o-phthalaldehyde (OPA) derivatisation reagent [Rajendra, 1983](the detection of cysteine and cystine can also be detected with the OPA derivative with the addition of 3,3'-dithiodipropiononic acid; Barkholt & Jensen, 1989). Utilising OPA, it can be shown that the sensitivity of postcolumn techniques is approximately the same as that of the pre-column techniques, but most workers still utilise ninhydrin (Walker & Mills).

3.25.4 Pre-column derivatisation

There are several pre-column derivatisation options (Furst *et al.,* 1990); 6-aminoquinolyl-N-hydroxysuccinimidyl carbamate (AQC). In this procedure, amino acids react with the AQC reagent, yielding urea-type compounds (Strydom & Cohen, 1993), and phenylisothiocyanate (PITC). PITC is by far the most common. For an excellent review on PITC derivatisation (Molna'r-Perl, 1994). An advantage of the PITC approach compared to other pre-column methods is that PITC reacts with both primary and secondary amines, whereas some other methods will not react with proline. Other advantages include sensitivity, UV detection (as opposed to fluorescence), and stability. Data from collaborative trials over a three year period (Yüksel *et al.,* 1995; Yüksel *et al.,* 1994; Strydom *et al.,* 1993) indicate that there is no significant difference in average error between PITC pre-column users and ninhydrin post-column users. In comparing post-column and pre-column methodologies, some advantages of the post-column methods should be noted:

(1) Since ion exchange properties dominate when the sample is loaded, most contaminants move rapidly through the post-column system and are discarded before separation of amino acids begins, resulting in better performance.
(2) Sample preparation is minimal compared to pre-column methods.
(3) The accuracy and precision of the data can be maintained at a high level with a reasonable amount of effort.

Advantages of the latter methods include very simple derivatisation procedures, stable derivatives, excellent separation, detection by either absorbance or fluorescence, and commercial availability of reagents. Disadvantages seemingly are limited: relatively long chromatography time (57 min turn around time) and high solvent consumption (unless microbore columns are utilised).

3.25.5 Calibration curves

Calibration curves can be developed for external or internal standards. For external standards, 3 or more concentrations of standard mixtures, and 6 or more repeats of each concentration are recommended to generate a concentration curve. Usually, if the standard values are within 3 % of the calibration values, the results will be within acceptable limits. Samples are then run in parallel with standards and should, of course, be in the same concentration range as the standards. Many workers recommend hydrolysis of the standards, especially since fewer workers are extrapolating to obtain Ser and Thr values. Appropriate use of external standards depends on accuracy of sample loading and the volumes of samples (which can be altered by desiccation during storage or other difficulties). Internal standards are also common, and should be developed by using 6 or more repeats of standards containing an added amino acid such as norleucine, taurine, or ε-n-amino caproic acid (i.e., one of which will behave similarly to the analytes but which is found in none of the samples and is resolved from all analytes). Addition of the internal standard to the samples allows for direct reporting of amino acid concentrations in the sample and the total recovery of sample after hydrolysis (Chapter 5, section 5.8).

3.25.6 Amino acid analysis protocol

In order to obtain good analyses, it was essential to use very clean and the highest quality reagents available. All glassware was soaked at room temperature in conc. HNO_3, or conc. HCl/conc. HNO_3 (1 : 1 v/v), always followed by extensive washing with high purity dH_2O. Tubes were usually dried in an oven overnight and kept under cover until use.

Acid hydrolysis of proteins and peptides

(1) 0.05 ml of the sample containing < 2 mM of any one amino acid was added to a hydrolysis tube [thunberg tubes] (coefficient worked out from total nitrogen analysis to estimate appropriate dilution factor assuming a nitrogen content of 16 %; see section 3.15.6).

(2) 0.02 ml 10 mM internal standard (taurine), 0.01 ml of 10 % dH_2O saturated phenol solution, 0.42 ml dH_2O, and 0.5 ml conc. HCl was added sequentially.

(3) The thunberg tubes were flushed with oxygen-free nitrogen, and quick frozen in dry ice-methanol mixture and sealed under vacuum.

(4) The tubes were immediately placed in heated oven at 105^0 C for 25 hrs.

(5) The tubes were cooled, opened, and lyophilised to dryness.

(6) 1 ml of 250 ppm solution of EDTA (500 mg in 10 ml HPLC grade H_2O) was added and step 5 repeated. Including EDTA prevents the variable yields of aspartic and glutamic acid. Samples were stored over silica gel until required and re-dissolved as step 6.

Primary amino acids were determined by pre-column derivatisation with OPA. OPA reacted with the primary amino acids, in the presence of 2-mercaptoethanol, to give highly fluorescent, thio-substituted iso-indole derivatives (Simons & Johnson, 1976), which were detected at excitation and emission wavelengths of 230 and 455 nm respectively.

B. Preparation of o-phthalaldehyde and 9-fluorenylmethyl chloroformate derivatisation reagent

50 mg of OPA was dissolved in 1 ml HPLC grade methanol and 0.04 ml MESH (2-hydoxyethylmercaptan β -mercaptoethanol) was added. 10 ml 0.2 mM potassium tetraborate (pH 9.5) was then added. The reagent is fairly stable when stored in a dark glass bottle at 4^0 C.

Secondary amino acids were derivatised, (pre-column) using FMOC-Cl (9-fluorenylmethyl chloroformate)[155 mg of FMOC-Cl was dissolved in 40 ml acetone], which reacts with both primary and secondary amino acids (Moye & Boning, 1979). The fluorescent fluorenylmethyl products, were detected at excitation and emission wavelengths of 260 and 313 nm respectively (Einarsson *et al.,* 1983).

C. Protocol 1; Gradient HPLC (column Ultracarb C8 4.6 × 150 mm; Phenomenex ser # 354816)

(1) Solvent A was prepared as followed: 25 mM sodium acetate (pH 5.7), 4.5 % tetrahydrofuran [THF] (v/v), and 3 % propan-2-ol [IPA] (v/v).

(2) Solvent B was prepared as followed: HPLC-grade methanol, 1.5 % THF (v/v), and 1.5 % IPA (v/v).

(3) The column was conditioned as followed (C8 HPLC ultracarb 4.6 × 150 mm) run with > 20 volumes of solvent B then a gradient was run over 10 min to 90 % solvent A and washed with > 20 column volumes 90 % solvent A.

(4) The gradient programme profile was as followed: 0 - 1 min 90 - 85 % A, 1 - 25 min 85 - 65 % A, 25 - 26 min 65 - 40 % A, 26 - 40 min 40 - 30 % A (reset to initial conditions over 5 min and re-equilibrate column over 10 min); flow rate 1.6 $ml.min^{-1}$ (for example of standard HPLC trace chromatogram see Fig 3.9).

D. Protocol 2; Gradient HPLC (column Adsorbospere OPA-HR, 5 µm, 150 x 4.6mm cartridge)

(1) Solvent A was prepared as followed: 25 mM sodium acetate (pH 5.9), 4.5 % 1,4-dioxan (v/v), and 3 % IPA (v/v).

(2) Solvent B was prepared as followed: HPLC-grade methanol, 1.5 % 1,4 dioxan (v/v), and 1.5 % IPA (v/v).

(3) The column was conditioned as followed (C8 HPLC ultracarb 4.6 x 150 mm) run with > 20 volumes of solvent B then a gradient was run over 10 min to 90 % solvent A and washed with > 20 column volumes 90 % solvent A.

(4) The gradient programme profile was as followed: 0 - 8 min 100 - 90 % A, 90 % - 82 % A, 17 - 27 min 82 - 69 % A, 27 - 36 min 69 - 25 %, 36 - 49 min 25 - 10 % A (reset to initial conditions over 5 min and re-equilibrate column over 10 min); flow rate 1.5 $ml.min^{-1}$ (for example of standard HPLC trace chromatogram see Fig 3.10).

E. Primary amino acids assay

0.02 ml of the sample was added to 0.02 ml OPA reagent in an Eppendorf microcentrifuge tube; and left at room temperature for exactly 60 sec. 0.02 ml of the reaction mixture was injected into the HPLC column via the sample injection port and immediately the gradient was started. The elution of OPA derivatives was monitored with a fluorescence detector (excitation wavelength 230 nm, emission wavelength 455 nm) at a sensitivity setting giving 50 % full-scale deflection with 0.1 mM L-valine. The amino acid content of the sample was measured by reference to an internal standard mixture (0.02 mM amino acids; the mixture contains 18 amino acids and their sequence of integration was: ASP-GLU-ASN-SER-GLN-HIS-GLY-THR-ALA-ARG-TYR-TAU-MET-VAL-TRP-PHE-ILE-LEU-LYS). The sample concentration was corrected for with the internal standard (taurine concentration should be 0.2 mM in final injected sample). Amino acids concentrations in the samples were calculated using the following equation: peak area of sample / peak area of standard x standard concentration x dilution factor = concentration of unknown.

F. Secondary amino acids assay

0.02 ml of the sample was added to 0.02 ml OPA and 0.02 ml FMOC-Cl reagent in an Eppendorf microcentrifuge tube; and left at room temperature for exactly 60 sec. 0.02 ml of the reaction mixture was injected into the HPLC column via the sample injection port and the gradient immediately started. The elution of FMOC-Cl derivatives was monitored with a fluorescence detector (excitation wavelength 260 nm, emission wavelength 313 nm) at a sensitivity setting giving 50 % full-scale deflection with 0.1 mM L-valine. The

amino acid content of the sample was measured by reference to an internal standard mixture (0.1 mM amino acids; proline and hydroxyproline)[for example of standard HPLC trace chromatogram see Fig 3.11]. Amino acids concentrations in the samples were calculated using the following equation: peak area of sample / peak area of standard x standard concentration x dilution factor = concentration of unknown.

3.26 HPLC analysis of carboxylic acid (Based on Mousdale, 1997 adapted from Guerrant *et al.,* 1982; Krausse & Ullmann, 1985, 1987, 1991)

Two classes of acidic metabolites are frequently encountered: sugar acids and carboxylic acids related to glycolysis and the Krebs cycle. Many diagnostic kits are available commercially; but HPLC methods can analyses for many different metabolites in parallel.

Organic acid extraction and Sample clean up

The HPLC analysis of organic acids gave poor baseline stability for complex fermentation broths, two methods of sample clean up were used. 1) Direct extraction with diethyl ether (1 : 1). 2) Extraction as described by Krausse & Ullmann (1987).

Protocol (Krausse & Ullmann, 1987)

5 ml of the broth culture was pipetted into a glass screw-capped culture tube firmly sealed with a glass cap. The following reagents were added: 50 µl of 50 % H_2SO_4 and 1 ml ether and vortexed for 1 min to mix the ether and aqueous phases. The tube was then centrifuged at 2000 g for 5 min. 20 µl from the ether phase was injected into the HPLC for analysis.

Assay for common aliphatic acids

The UV detector was set to 210 nm (range 0.32 AUFS). The Aminex 87H column 300 mm x 7.8 mm; (catalogue # 125-0140; guard column 125-0586) was equilibrated with 0.065 M H_2SO_4 until a stable baseline was achieved (1.0 $ml.min^{-1}$, 65^0 C); pH limits are between 1.8 and 2.2. All fermentation supernatant samples were filtered through a 0.22 µm filter. 0.02 ml of the sample was injected (with any necessary dilution to contain organic acids at concentrations less than those in standard solutions. The acid

concentration was calculated by reference to calibration lines of concentration against peak area (for examples of calibration see Fig 3.12a,b, c, d, e, f, & g). Identification of organic acids was carried out using authentic standards (5 mM or 10 mM) of pyruvate, oxo-glutarate, citrate, malate, lactate, fumarate, acetate, butyrate, and propionate (for example of standard HPLC trace chromatogram see Fig 3.12.

Elemental analysis

(a)Total organic carbon analysis

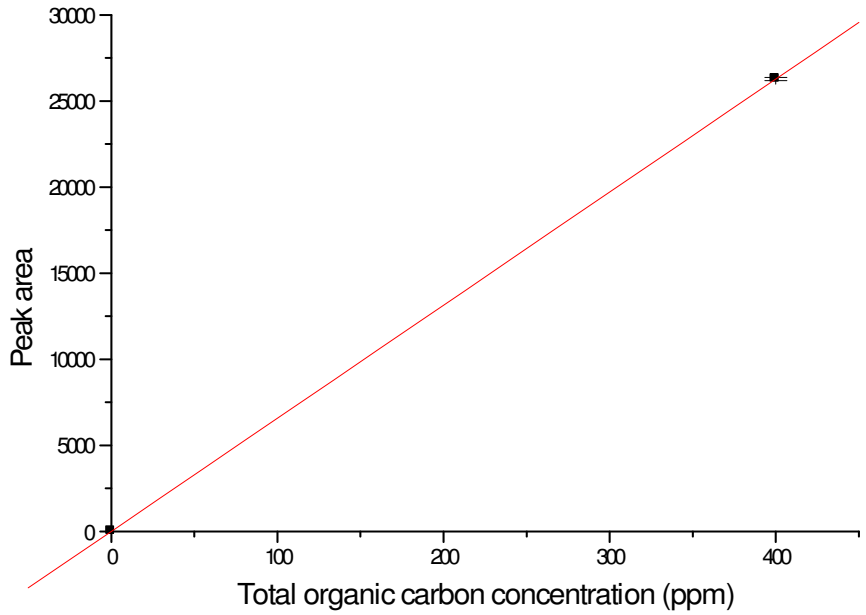

Fig 3.1a The standard curve was constructed using appropriate dilution of a known concentration 400 ppm potassium hydrogen phthalate. The graph shows the relationship between the optical density and the concentration of organic carbon. The assays were carried out in triplicate. The best-fit line was obtained using the linear regression function of the program Origin

Elemental analysis

(b)Total inorganic carbon analysis

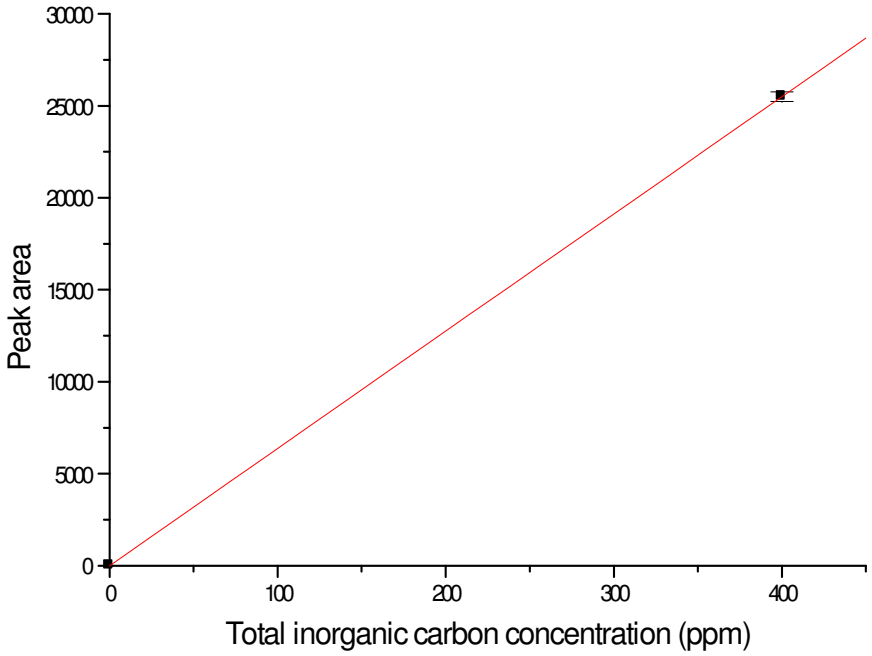

Fig 3.1b The standard curve was constructed using appropriate dilution of a known concentration 400 ppm sodium carbonate & potassium carbonate. The graph shows the relationship between the optical density and the concentration of inorganic carbon. The assays were carried out in triplicate. The best-fit line was obtained using the linear regression function of the program Origin V5.

Elemental analysis

(c) Total organic nitrogen analysis

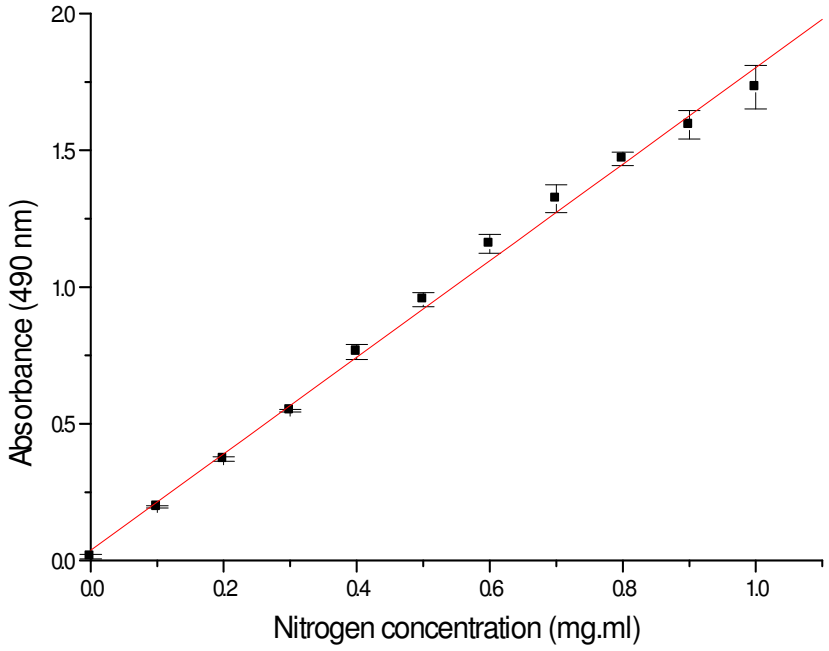

Fig 3.1c The standard curve was constructed using appropriate dilution of a known concentration of nitrogen 1 mg.ml^{-1}. The graph shows the relationship between the optical density and the concentration of nitrogen. The assays were carried out in triplicate. The best-fit line was obtained using the linear regression function of the program Origin V5.

Total carbohydrates calibration curves

(a) Anthrone assay

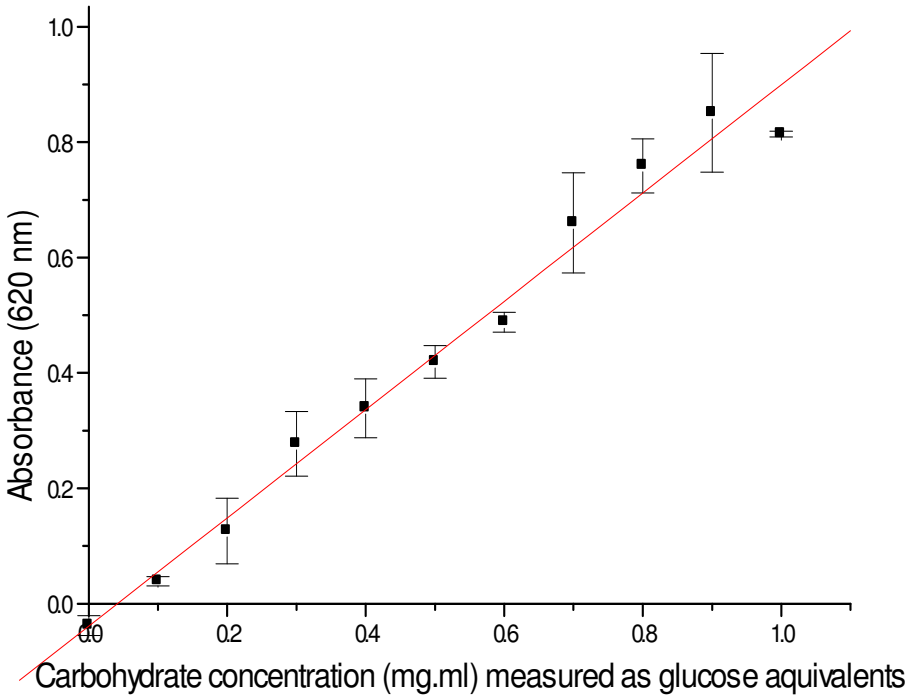

Fig 3.2a The standard curve was constructed using appropriate dilution of a known concentration 1 mg.ml^{-1} of glucose. The graph shows the relationship between the optical density and the concentration of glucose. The assays were carried out in triplicate. The best-fit line was obtained using the linear regression function of the program Origin V5.

Total carbohydrates calibration curves

(b) Phenol sulphuric assay

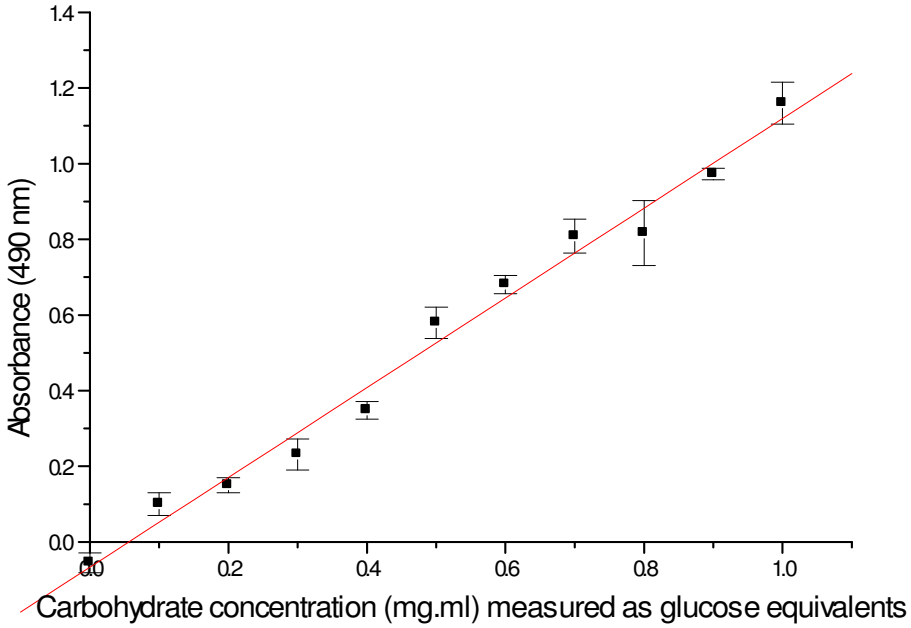

Fig 3.2b The standard curve was constructed using appropriate dilution of a known concentration 1 mg.ml^{-1} of glucose. The graph shows the relationship between the optical density and the concentration of glucose. The assays were carried out in triplicate. The best-fit line was obtained using the linear regression function of the program Origin V5.

Total Nucleic acids calibration curves

(a) Burton assay

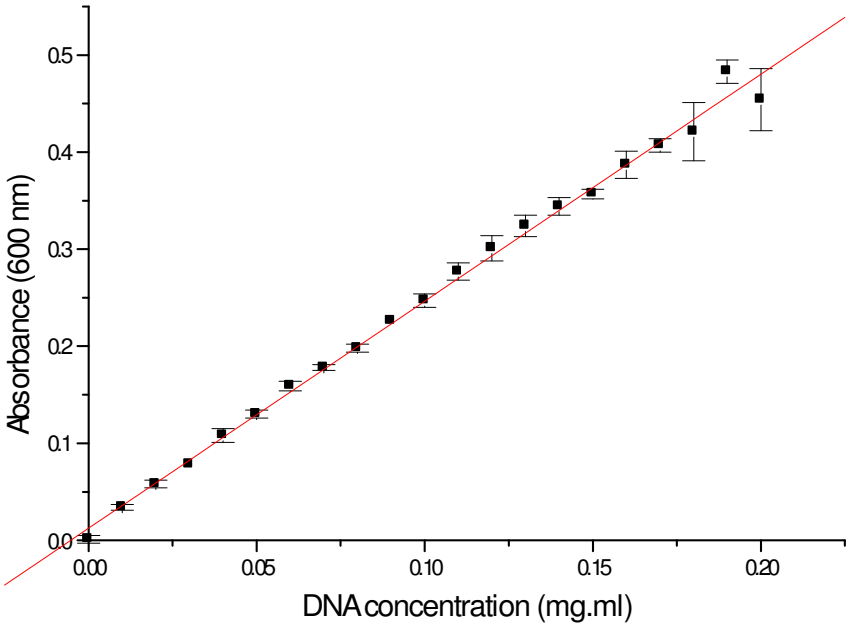

Fig 3.3a The standard curve was constructed using appropriate dilution of a known concentration 0.2 $mg.ml^{-1}$ of Calf Thymus DNA. The graph shows the relationship between the optical density and the concentration of DNA. The assays were carried out in triplicate. The best-fit line was obtained using the linear regression function of the program Origin V5.

Total Nucleic acids calibration curves

(b) Fluorescence Hoechst 33258 assay

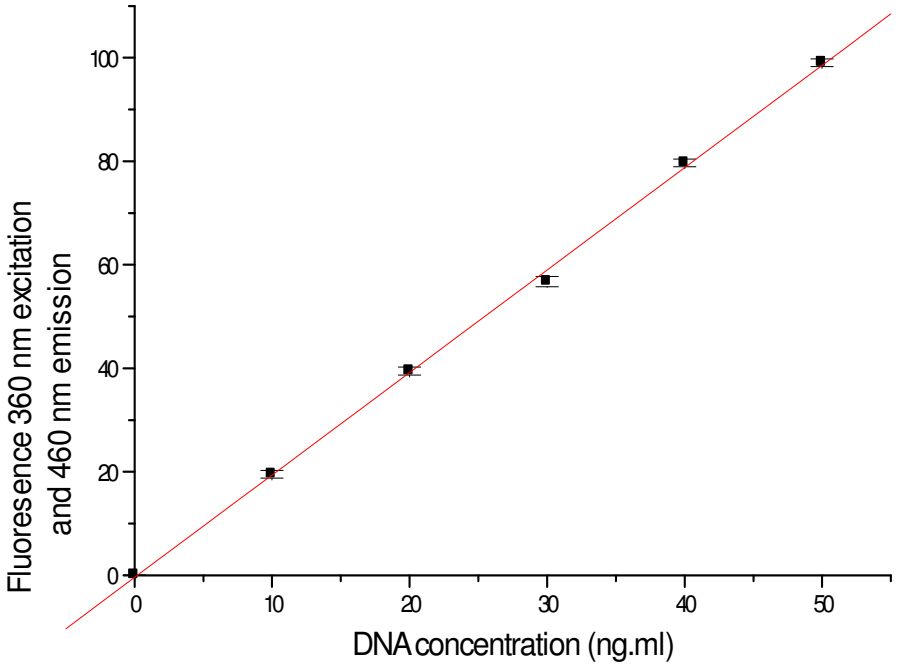

Fig 3.3b The low range close up calf thymus DNA stained with Hoechst 33258 dye and fluorescence measured. The graph shows the relationship between the optical density and the concentration of DNA. The assays were carried out in triplicate. The best-fit line was obtained using the linear regression function of the program Origin V5.

Total Nucleic acids calibration curves

(c) Fluorescence Hoechst 33258 assay

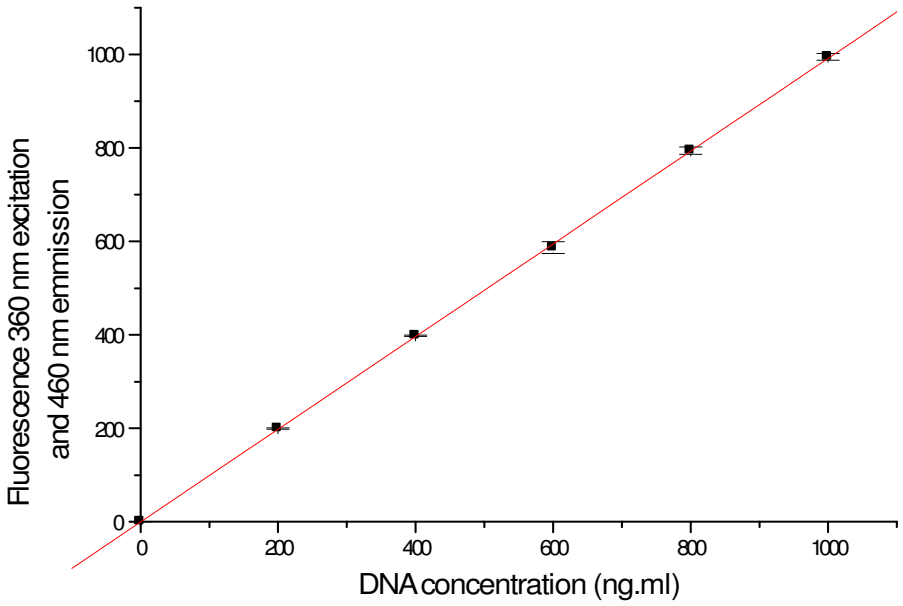

Fig 3.3c The complete range calf thymus DNA stained with Hoechst 33258 dye and fluorescence measured. The graph shows the relationship between the optical density and the concentration of DNA. The assays were carried out in triplicate. The best-fit line was obtained using the linear regression function of the program Origin V5.

Total Nucleic acids calibration curves

(d) Orcinol assay

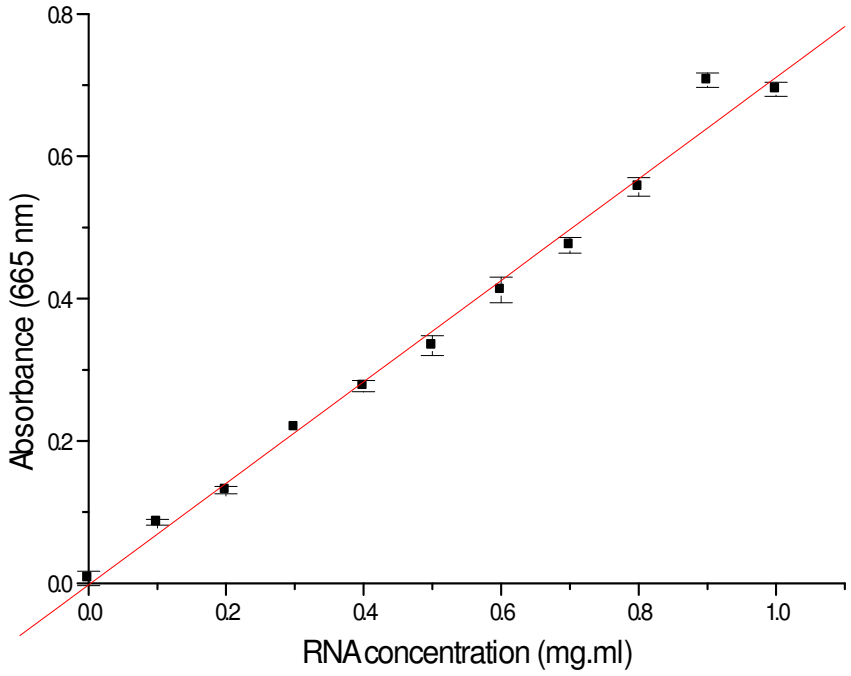

Fig 3.3d The standard curve was constructed using appropriate dilution of a known concentration 1.0 mg.ml^{-1} of bakers yeast RNA. The graph shows the relationship between the optical density and the concentration of RNA. The assays were carried out in triplicate. The best-fit line was obtained using the linear regression function of the program Origin V5.

Total Protein calibration Curves

(a) Bradford assay

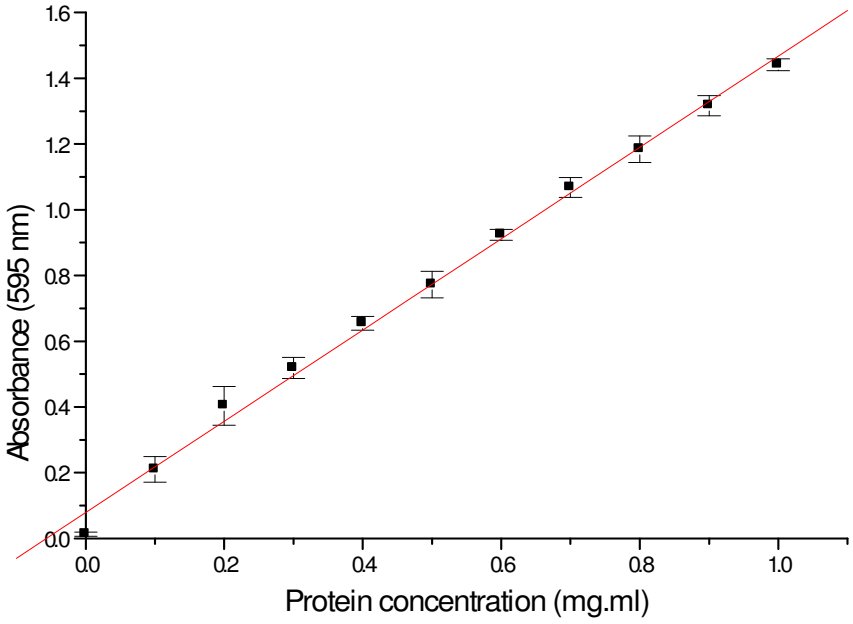

Fig 3.4a The standard curve was constructed using appropriate dilution of a known concentration 1 $mg.ml^{-1}$ of bovine serum albumin. The graph shows the relationship between the optical density and the concentration of protein. The assays were carried out in triplicate. The best-fit line was obtained using the linear regression function of the program Origin V5.

Total Protein calibration Curves

(b) Lowry assay

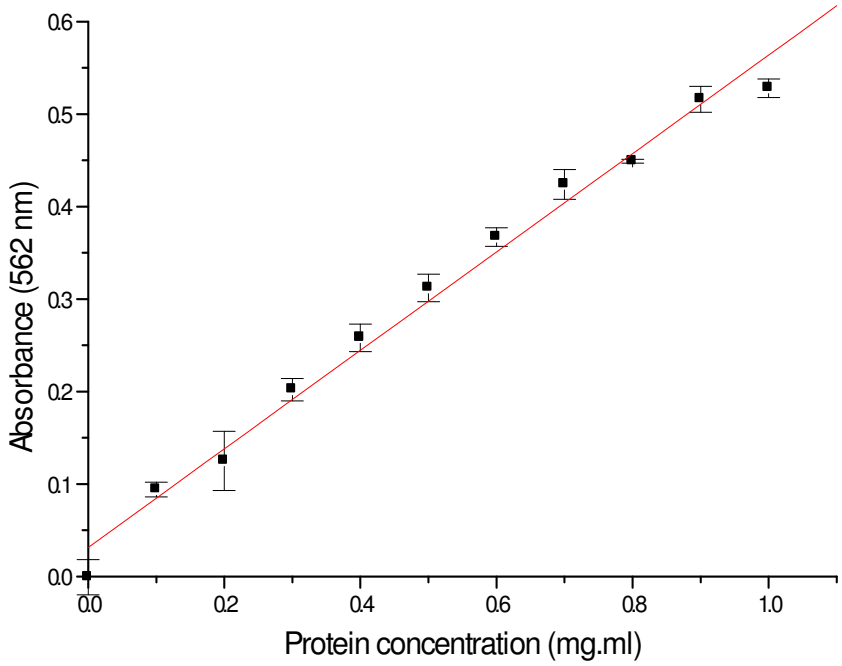

Fig 3.4b The standard curve was constructed using appropriate dilution of a known concentration 1 $mg.ml^{-1}$ of bovine serum albumin. The graph shows the relationship between the optical density and the concentration of protein. The assays were carried out in triplicate. The best-fit line was obtained using the linear regression function of the program Origin V5.

Total Protein calibration Curves

(c) Bicinchoninic acid assay

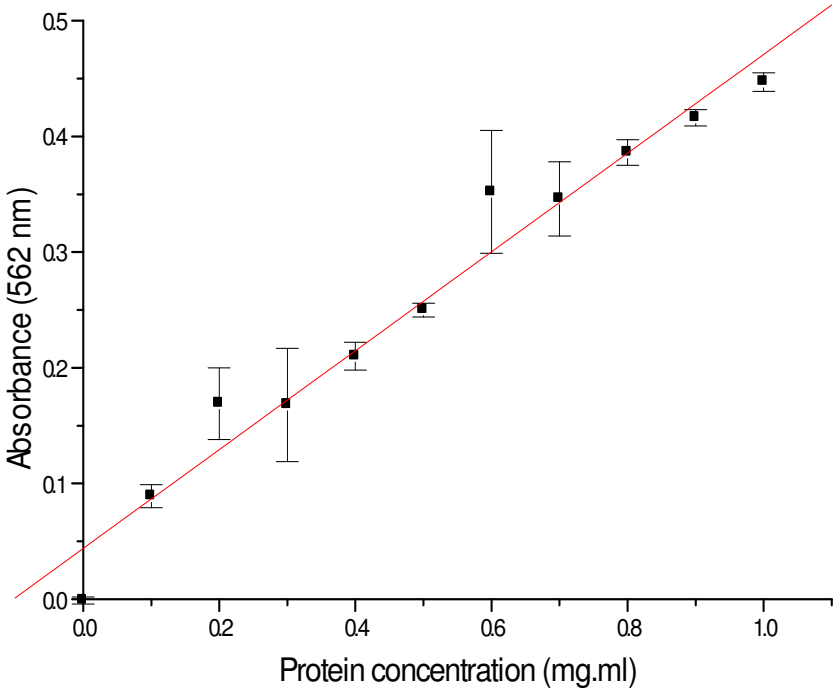

Fig 3.4c The standard curve was constructed using appropriate dilution of a known concentration 1 $mg.ml^{-1}$ of bovine serum albumin. The graph shows the relationship between the optical density and the concentration of protein. The assays were carried out in triplicate. The best-fit line was obtained using the linear regression function of the program Origin V5.

Total Protein calibration Curves

(d) Reverse biuret assay

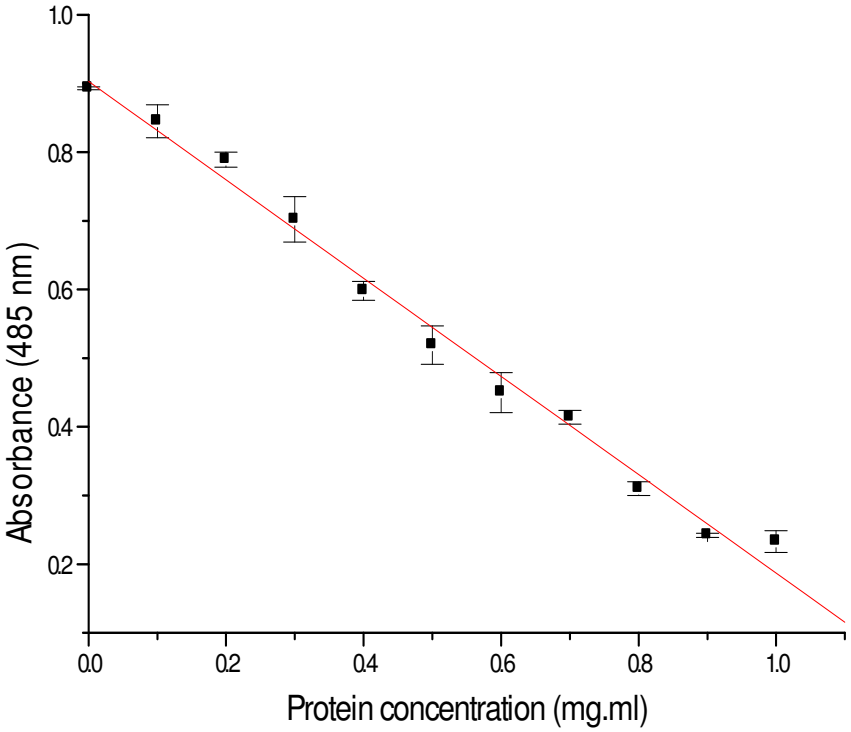

Fig 3.4d The standard curve was constructed using appropriate dilution of a known concentration 1 $mg.ml^{-1}$ of bovine serum albumin. The graph shows the relationship between the optical density and the concentration of protein. The assays were carried out in triplicate. The best-fit line was obtained using the linear regression function of the program Origin V5.

Total Protein calibration Curves

(e) Ninhydrin assay

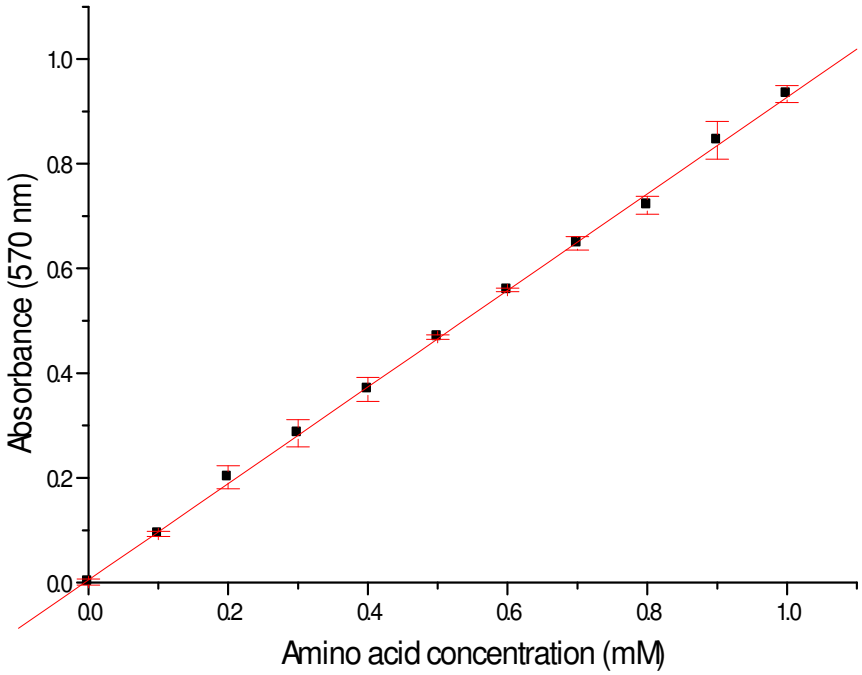

Fig 3.4e The standard curve was constructed using appropriate dilution of a known concentration 1 mM of leucine. The graph shows the relationship between the optical density and the concentration of total amino acids. The assays were carried out in triplicate. The best-fit line was obtained using the linear regression function of the program Origin V5.

Total phosphate & ammonia calibration Curves

(a) Phosphate assay

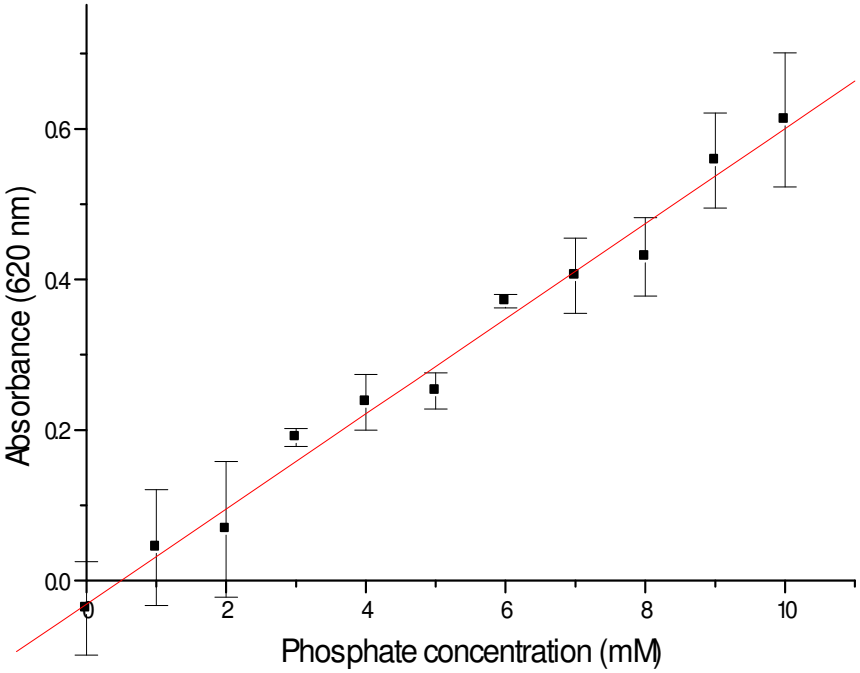

Fig 3.5a The standard curve was constructed using appropriate dilution of a known concentration 1 mM of phosphate. The graph shows the relationship between the optical density and the concentration of phosphate. The assays were carried out in triplicate. The best-fit line was obtained using the linear regression function of the program Origin V5.

Total phosphate & ammonia calibration Curves

(b) Ammonia assay

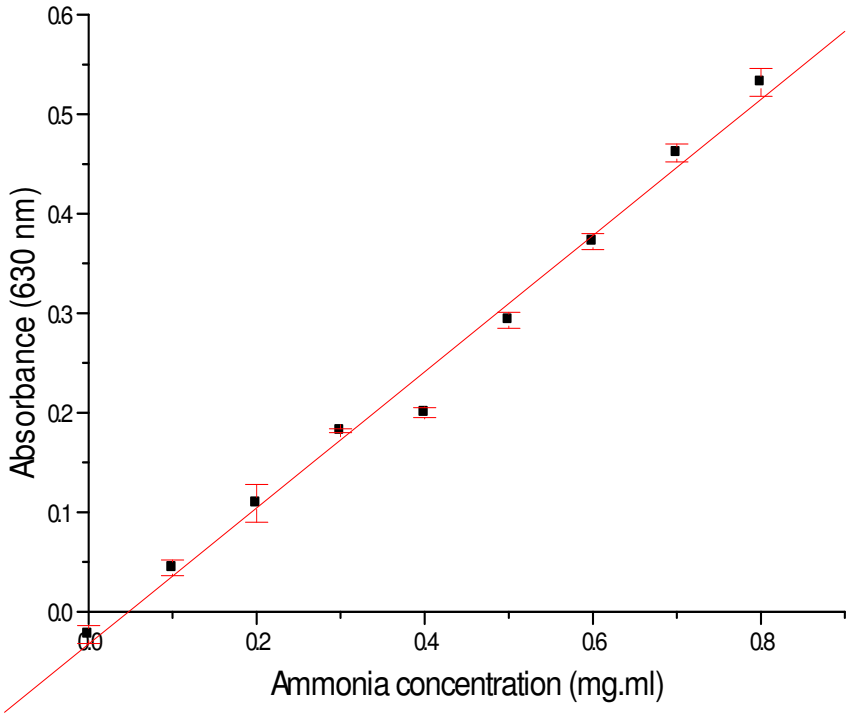

Fig 3.5b The standard curve was constructed using appropriate dilution of a known concentration 1 mg.ml^{-1} of ammonia. The graph shows the relationship between the optical density and the concentration of ammonia. The assays were carried out in triplicate. The best-fit line was obtained using the linear regression function of the program Origin V5.

Total lipids calibration Curves

Vanillin assay

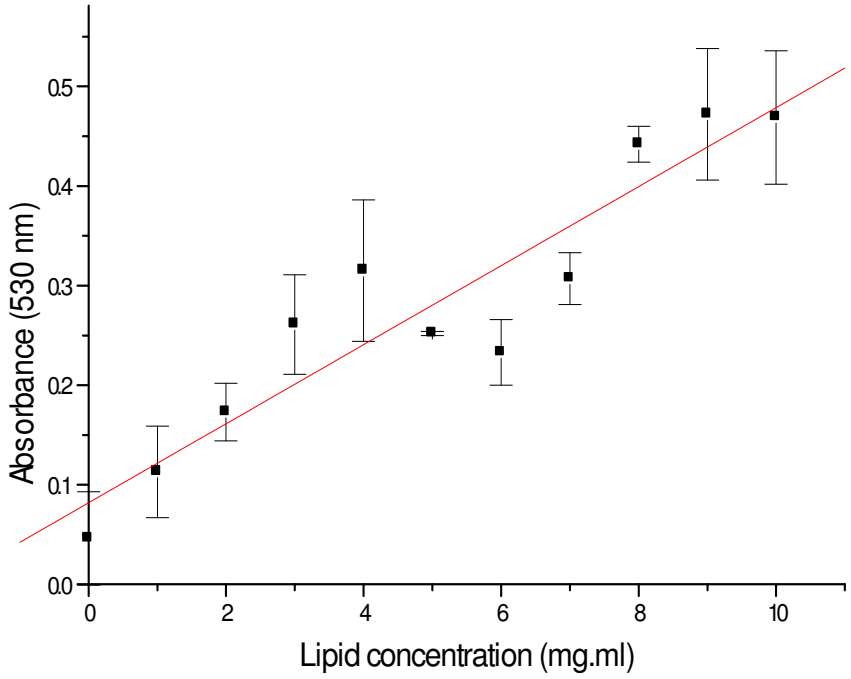

Fig 3.6 The standard curve was constructed using appropriate dilution of a known concentration 10 $mg.ml^{-1}$ of oleic acid. The graph shows the relationship between the optical density and the concentration of lipid. The assays were carried out in triplicate. The best-fit line was obtained using the linear regression function of the program Origin V5.

Chromatograms HPLC Macrolides

Trace 1

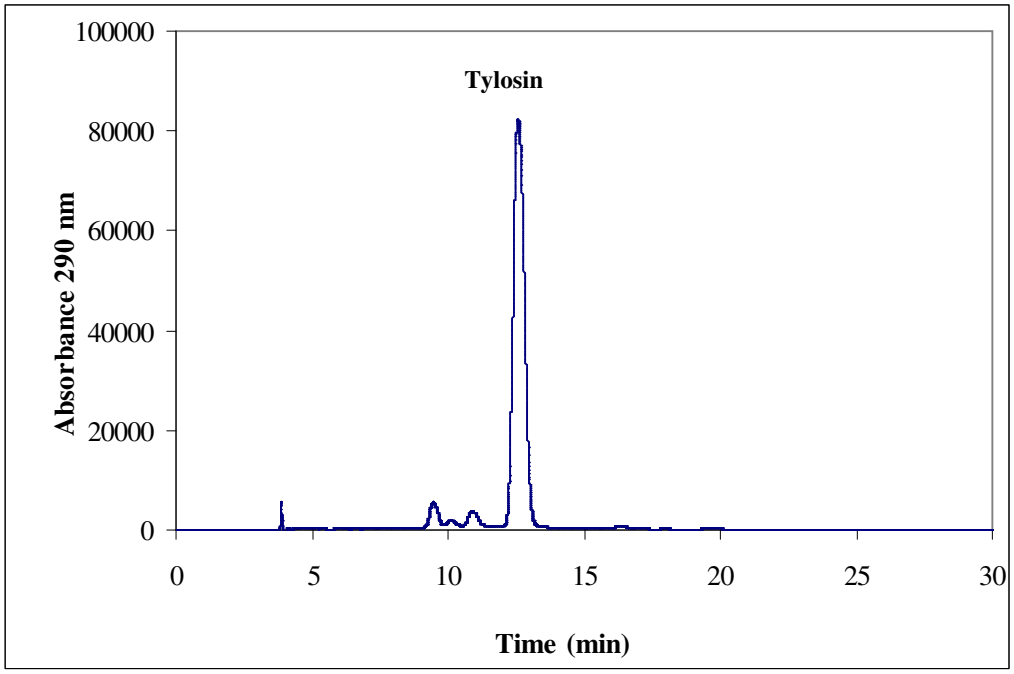

Trace 2

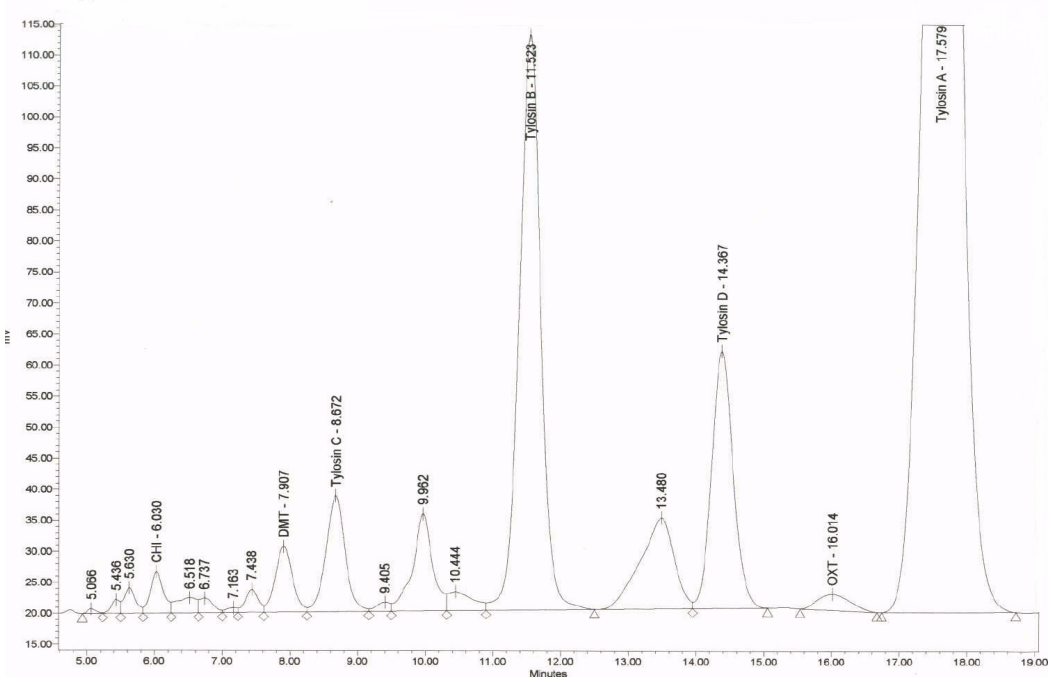

Fig 3.7 HPLC trace showing the separation of macrolides with the C18 5 micron, 25cm × 4.6 nm id Phenomenex column. Trace 1 work undertaken at the University of Strathclyde to quantify tylosin; trace 2 undertaken at Eli Lilly Ltd for speciation analysis.

Tylosin calibration

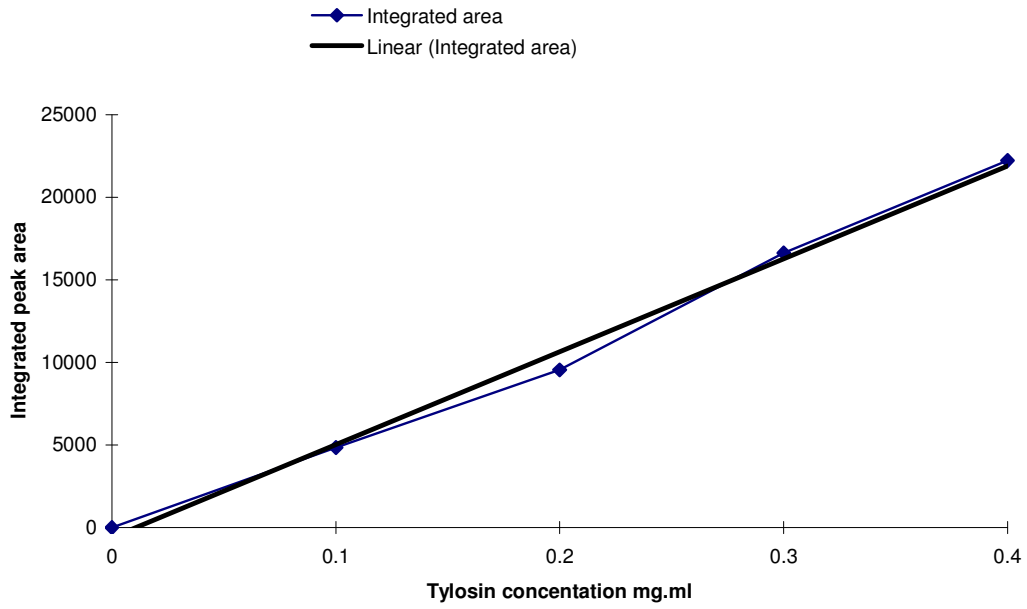

Fig 3.8 The standard curve was constructed using appropriate dilution of a known concentration 0.4 $mg.ml^{-1}$ of tylosin. The graph shows the relationship between the optical density and the concentration of tylosin. The assays were carried out in triplicate. The best-fit line was obtained using the linear regression function of the program Microsoft Excel.

Chromatograms HPLC amino acids protocol (1)

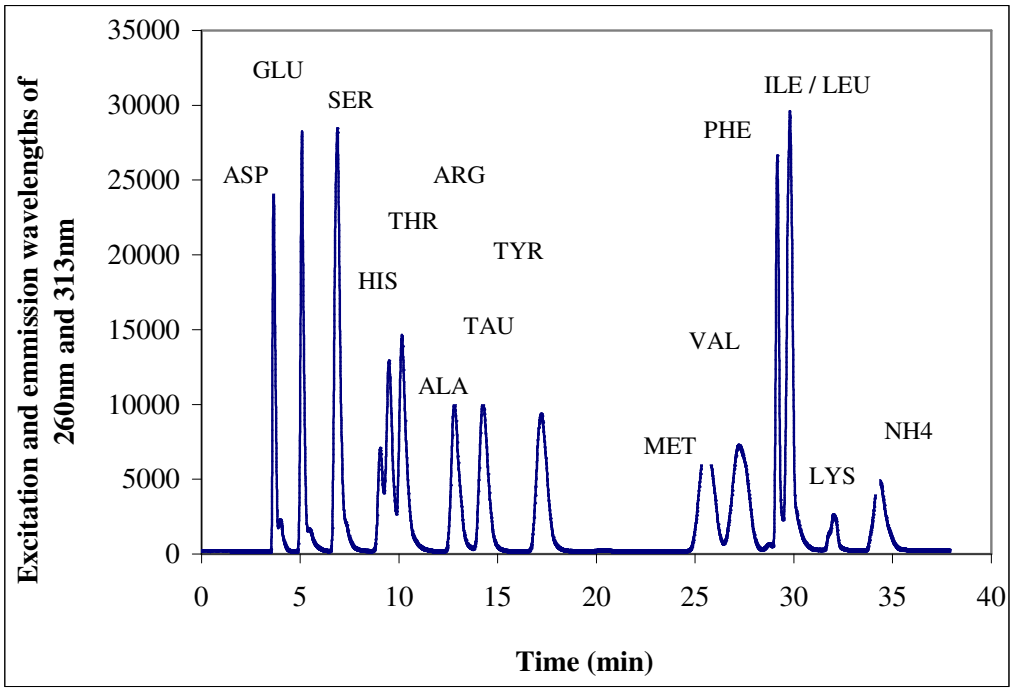

Fig 3.9. HPLC trace showing the separation of primary amino acids with the Ultracarb C8 5 micron, 15 cm × 4.6 Phenomenex column.

Chromatograms HPLC amino acids protocol (2)

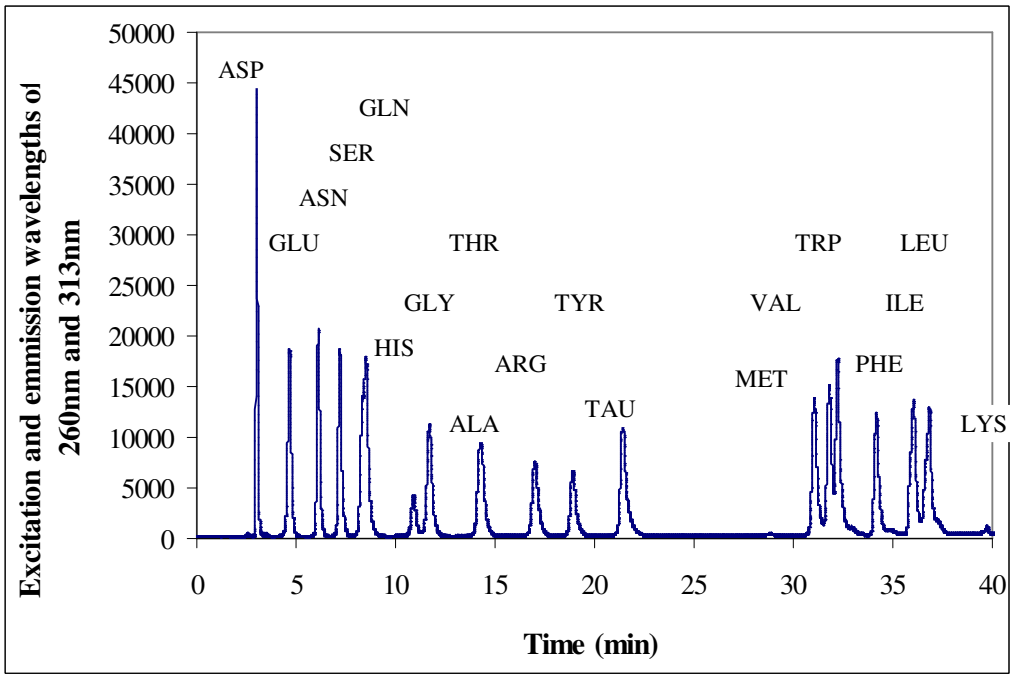

Figure 3.10 HPLC trace showing the separation of primary amino acids with the Adsorbospere OPA – HR, 5 micron, 15 cm × 4.6 column.

Chromatogram HPLC secondary amino acids protocol

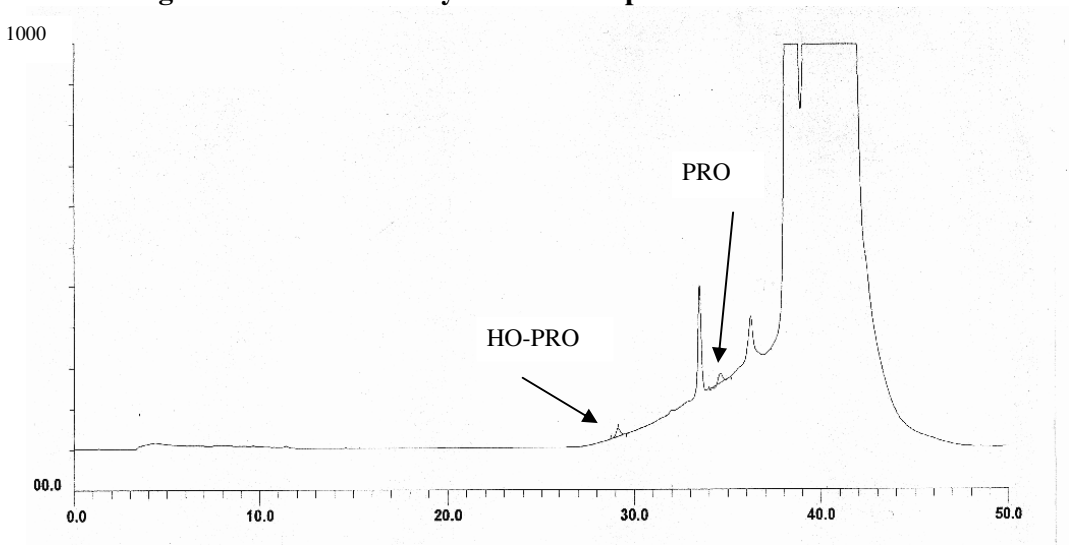

Fig 3.11 HPLC trace showing the separation of secondary amino acids with the Adsorbospere OPA – HR, 5 micron, 15 cm × 4.6 column.

Chromatograms HPLC Organic Acids

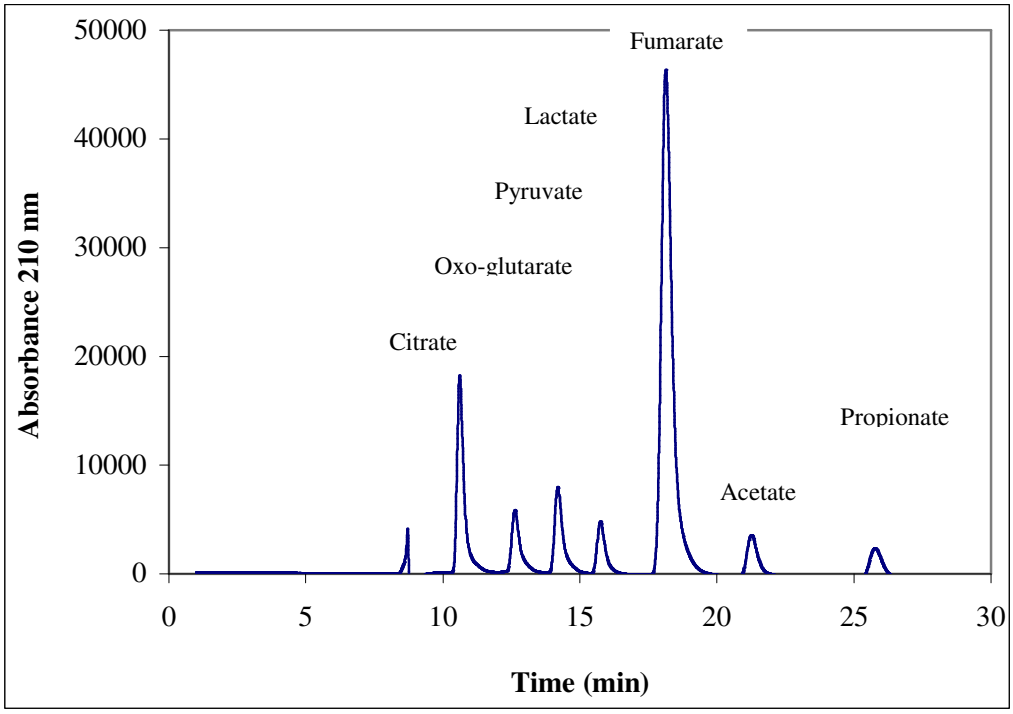

Fig 3.12 HPLC trace showing the separation of various organic acids with the Aminex 87H column 300 mm × 7.8 mm column.

Organic acid calibration Curves

(a) Citrate calibration

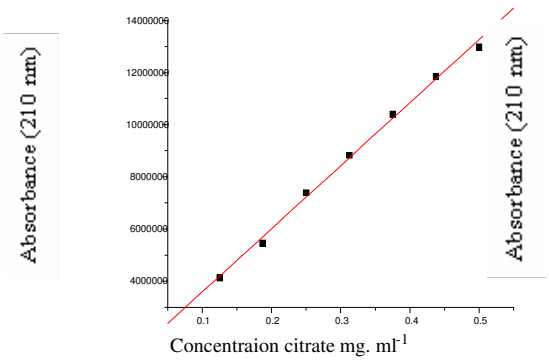

(b) Oxo-glutarate Calibration

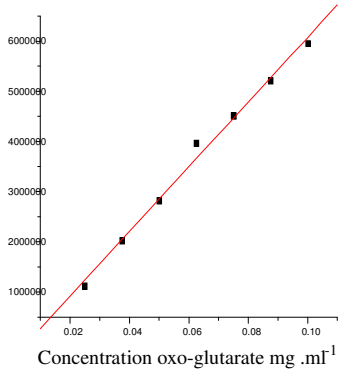

(c) Pyruvate calibration

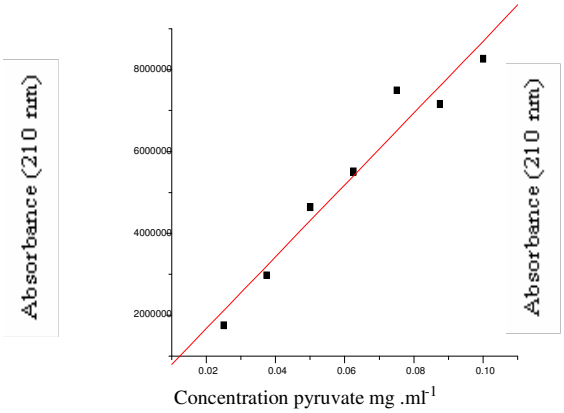

(d) Lactate calibration

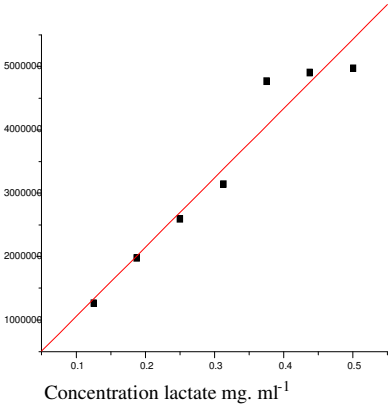

Fig 3.13a - g The standard curve was constructed using appropriate dilution of a known concentration of organic acids Vs peak area. The graph shows the relationship between the optical density and the concentration of organic acid. The assays were carried out in triplicate. The best-fit line was obtained using the linear regression function of the program Origin V5.

Organic acid calibration Curves

(e) Fumarate calibration

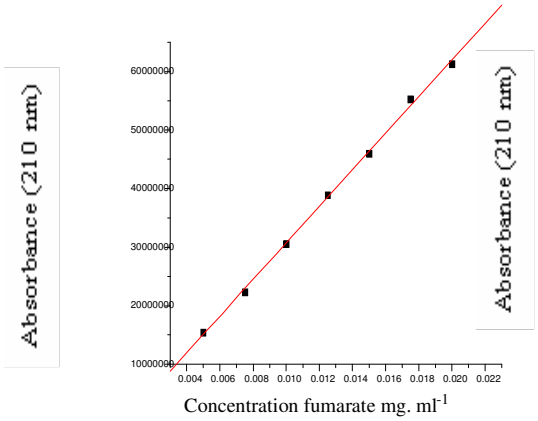

(f) Acetate calibration

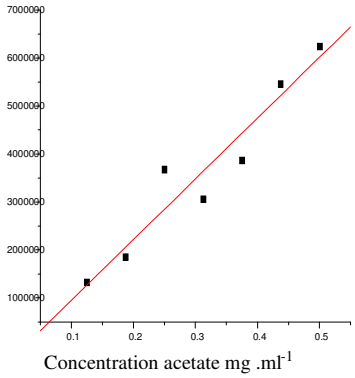

(g) Propionate calibration

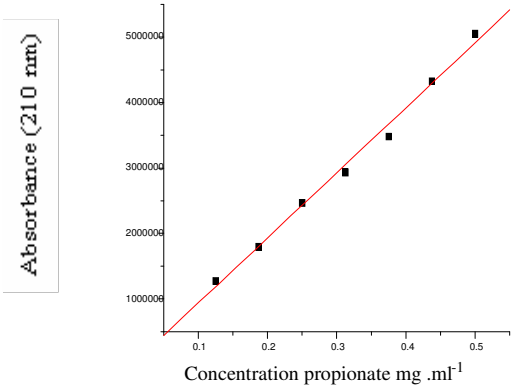

Fig 3.13a - g The standard curve was constructed using appropriate dilution of a known concentration of organic acids Vs peak area. The graph shows the relationship between the optical density and the concentration of organic acid. The assays were carried out in triplicate. The best-fit line was obtained using the linear regression function of the program Origin V5.

Chapter 4

Medium optimisation and growth behaviour of *Streptomyces fradiae* C373-10, C373-18 & *Streptomyces coelicolor* 1147

4.1 Introduction

The medium composition used depends largely on the purpose of the experiment. Herbert (1961) argued strongly for the general use of a defined medium, but it must be recognised that such media have many disadvantages. The organisms usually differ phenotypically from those grown in complex medium, for example in cell composition and division rate; their growth is more easily inhibited by over aeration or toxic cations or by imbalances between some of the constituents, notably amino acids; some bacteria need a large number of growth factors and, indeed, for some no minimal medium, is as yet known. All these disadvantages could probably be overcome with time, but meanwhile, complex media are still in general use although they introduce an uncontrolled metabolite balancing factor into any experiment.

The quantitative analysis published for many undefined media represent a step towards standardisation (Migo *et al*., 1995). Although the quantitative analysis has to be treated with caution, independent analysis shows that batches of the same medium differ considerably in composition. Furthermore many essential constituents are usually ignored, despite the evidence that even those required in trace amounts, like trace metals or vitamins, may have considerable effects on overall growth, product yield, and reproducibility. Chemically-defined media are usually preferred in laboratory research since they allow determination of the specific requirements for growth and product formation by systematically adding or eliminating chemical species from the formulation, with minimal complicated medium interactions and reproducible culture conditions. The advantages of chemically-defined media in laboratory research have been well documented in the literature (Zhang & Greasham, 1999 for review). It is without doubt that the success of such laboratory studies have assisted or could help greatly in the success of prospective commercial fermentation processes, a topic itself that deserves an extensive review.

A thorough research of flux-based analytical protocols, points to the need for a minimal or defined medium, with good kinetic and physiological studies already undertaken; in order

to simplify the flux analysis (Holms, 1996). In the case of many industrial *Streptomyces* spp. little research has been undertaking in developing such simplistic media. Generally it has been viewed by industry that increased antibiotic yield can be obtained at a faster process development rate through the large scale trials and optimisation of complex medium.

Both complex and semi-defined media have been described in the literature for *S. fradiae*. Initial reports on tylosin production described a complex medium consisting of molasses, nutrisoy flour, distillers solubles and calcium carbonate (McGuire *et al*., 1961). Baltz & Seno (1981) describe a complex medium consisting of (gl^{-1}): beet molasses (20.0), corn meal (15.0), fish meal (9.0), corn gluten (9.0), NaCl (1.0), $(NH_4)_2HPO_4$ (0.4), calcium carbonate (2.0), crude soybean oil (30.0). Despite the lack of any detailed reports on the optimisation of *S. fradiae* complex media; it would seem from the limited information available, that the following ingredients need to be present: a source of readily assimilable carbohydrate and a source of carbohydrate in the form of a starch, an insoluble protein source, and a source of lipids (see Chapter 3 section 3.7.3 for the industrial complex medium composition used throughout this work).

The production of tylosin on semi-complex media has also been reported. Omura *et al*. (1983) and Lee (1997) described a synthetic medium which comprised soluble, starch, glucose, sodium lactate, $MgSO_4.7H_2O$, $ZnSO_4.7H_2O$, $FeSO_47H_2O$, $CoCl_2.6H_2O$, $MnCl_2.4H_2O$, & $(NH_4)_2SO_4$ (see Chapter 3, section 3.7.1 for composition). Stark *et al*. (1961) published a detailed study on the effects of carbon source, amino acids, methylated fatty acids and inorganic components on mycelial growth and tylosin biosynthesis. The optimum medium developed contained the following (gl^{-1} except where stated); NaCl (2.0), $MgSO_4$ (5.0), $CoCl_2.6H_2O$ (0.001), iron (III) ammonium citrate (1.0), $ZnSO_4.7H_2O$ (0.01), $CaCO_3$ (3.0), glycine (7.0), L-alanine (2.0), L-valine (1.0), betaine (5.0), glucose (35.0), methyl oleate (25.0), K_2HPO_4 (2.3). Gray & Bhuwapathanapun (1980a, b) & Lee and Rho (1998) modified the above medium by the substitution of calcium chloride for calcium carbonate and sodium glutamate for glycine, valine, and alanine, resulting in a soluble medium suitable for use in continuous culture if the methyl oleate was fed separately. The cultures were incubated at 28 – 30^0 C under aerobic conditions for 7 – 10 days in batch culture. Initial pH was usually in the range 7.0 – 7.8 with final pH values when quoted in a similar range (Gray, 1981).

As a simple defined medium (i.e., one carbon source & one nitrogen source) had not been reported in the literature, it was therefore necessary to develop a medium capable of dispersed growth & tylosin production of *S. fradiae* cultured with a mono-saccharide or single component carbon source in batch process (equipment availability and the industrial process also being carried out in batch process led to a batch process being the most appropriate choice). A number of known secondary metabolite producing minimal medium compositions for other streptomycetes were tested to determine if reasonable biomass and tylosin production, could be achieved under these conditions. Further combinations of components and conditions were tested to verify if the chosen media compositions could be further enhanced (section 4.3.2). The best suited medium composition for the research to be undertaken was then stepped up to bench top scale bioreactors (section 4.5.3).

An alternative optimisation strategy, which has become popular especially in industry, is the use of statistically designed experiments that allow the investigator to evaluate more than one independent variable at a time (Greasham & Inamine, 1986; Greasham & Herber, 1997). The approach generally starts with screening to distinguish those variables (three to five) that have a significant effect on the desired response from a larger number of potential variables (more than five) with a minimum of testing, these employ fractional factorial designs such as the Plackett-Burman method (Plackett and Burman, 1946; Roseiro *et al*., 1992). A full factorial strategy is generally impractical for medium optimisation because of the huge number of trials involved, unless only a few variables (between two and four) are examined, as performed by Garcia-Ochoa *et al*. (1992). The next step is usually to find the combination of these variables that supports the best acceptable response in a timely manner, using a response-surface type of design, such as a central composite (Diamond, 1981) or Box-Behnken (Box and Behnken, 1960; Dupont de Nemours, 1975) design. Examples of the successful use of surface-response designs have been reported (Zhang *et al*., 1996). It was the ultimate aim of this work to use such a strategy to determine the best suited minimal medium combination to produce significant tylosin yields that fits with parameters set for the project.

4.2 Storage of organism, viability, & inoculum preparation

Early attempts at the cultivation of *S. fradiae* C373-10 at the University of Strathclyde showed poor reproducibility of mycelia cultured from the same generation mycelial stocks.

This may have been due to a number of factors, e.g. fast freezing, which reduced the viability of the vegetative mycelium. This made the length of the inoculation stage inconsistencies between batches; the literature accepts variability of 3 - 5 days, for vegetative growth in general anything from 3 - 12 days was achieved, this was considered to be unacceptable. Initially low viability was suspected to be the main cause of this variability. A number of attempts were made to store mycelial stocks solutions under different glycerol & DMSO concentrations on site at Eli Lilly Ltd. These mycelial stock solutions were all split into two batches, one batch was stored at Eli Lilly Ltd. and the other was stored at the University of Strathclyde. The stocks did not show any significant improvement at the university of Strathclyde, but they did grow well on site at Eli Lilly Ltd. (Speke). The high variability at the University of Strathclyde was then considered to be a nutrient associated problem. Therefore fresh seed medium components (Chapter 3, section 3.5.2) were obtained from Eli Lilly Ltd., these were then used with tap water, dH_2O (control), and with the addition of differing concentrations of $MgSO_4$ (personal communication J McIntyre, indicated that to culture *S. fradiae* C373-18 on TSB there was a need for the addition of $MgSO_4$). The addition of $MgSO_4$ (3.0 gl^{-1}) and the source of primatone was found to be important factors in seed variability. This was found to be only the case for *S. fradiae* C373-10 and not the C373-5 strain. Although the addition of $MgSO_4$ was not needed on site at Eli Lilly Ltd., therefore the process water was considered to be an important parameter in later strains of *S. fradiae* greater than the C373-5.

Initial culture handling training in house at Eli Lilly Ltd. recommended the use of 1 ml mycelial stock suspensions to inoculate 500 ml of vegetative medium (see Chapter 3, section 3.8) in a 2 L Erlenmeyer flask. Further an attempt was made to reduce differences observed between batch fermentations (Fig 4.1 – 4.20) for *S. coelicolor* 1147 and *S. fradiae* C373-10 where mycelial stock solutions were used. Spores were used from a single stock spore suspension stored in 20 % (V/V) glycerol at -20^0 C. For *S. coelicolor* 1147 Erlenmeyer flasks with cotton wool bungs containing 500 ml of medium were inoculated with spores to give a spore concentration of approximately 1×10^6 spores per ml^{-1} medium (i.e., 5×10^8 spores per flask). In the case of *S. fradiae* low viability counts hindered this method (i.e., $1 - 4 \times 10^3$) and long lag phases were indicative at shake flask and bench top fermenter level. Mycelial stock solutions were then used throughout the rest of the project.

This may have led to problems in comparing the cultures in the latter stages of the project i.e., an increase in batch to batch variability.

It was not possible to undertake a detailed analysis of the effects of the seed medium composition for this work. In order to eliminate carry over of any unknown components from the complex vegetative medium (Chapter 3, section 3.5.2). The initial inoculum was cultured for three days with vegetative medium (Chapter 3, section 3.5.2) and 10 % of this was used to inoculate the appropriate defined medium (training culture) for 2 days of which 10 % was then used to inoculate the production fermentation.

4.3 Formulation and initial development of a chemically defined medium

Medium formulation strategies reported in the literature fall into one of the following categories: cell composition requirements, pulse and medium shift experiments using continuous culture, statistically designed experiments, & genetic algorithms (Zhang & Greasham, 1999). Sometimes several of them are employed together during the course of medium development. A classical & statistical approach of medium optimisation was undertaken to improve the tylosin titer with a glucose minimal medium, and a glucose glutamate defined medium obtained from Eli Lilly Ltd. [originally designed for use in continuous culture experiments] (Chapter 3, section 3.6.4).

4.3.1 Classical approach

Generally glucose, NH_4, Mg, Na, K, Cl, SO_4, PO_4 ions are the basic requirements for the maximum growth of some representative heterotrophs in defined medium (Moat, 1979). While complex raw materials contain minerals and growth factors in abundance, these ingredients will have to be supplied specifically in a chemically-defined medium.

The initial formulation of a chemically-defined medium may be rationally developed on the basis of chemical composition of the microbe (White *et al*., 1991; Greasham and Herber, 1997). In this approach, the medium is composed of the elements found in the “typical” cell in the ratios in which they are present in the cell. The elemental compositions of most microorganisms are quite similar (Weishank & Garver 1967; Greasham and Herbert 1997). Although cellular composition is dependent on the cell type, i.e., bacterium, yeast, or fungus, it usually falls within the following percentage ranges on a dry weight basis):

carbon 45 % - 55 %; nitrogen 6 % - 14 %; potassium 0.5 % - 3 %; phosphorus 1 % - 3 %; magnesium 0.1 % - 1 %; sulphur 0.02 % - 1 %; and traces of calcium up to 1 %. Minor minerals are also present at (dry weight per 100 g): copper 0.1 – 1 mg, iron 1- 10 mg, zinc approximately 1 mg, and manganese 0 - 5 mg (Miller and Churchill, 1986). Such medium typically comprises a simple carbon source such as glucose, inorganic salts, or trace elements. Individual forms of amino acids and/or vitamins may also be included, depending on the nature of the microbe. Either carbon, nitrogen or phosphate are usually selected as the limiting nutrients. Carbon usually limits growth, whereas depletion of other nutrients sometimes results in abnormal growth, e.g., lipid production under conditions of nitrogen limitation, an increase in cell wall permeability under biotin limitation (Stanbury *et al*. 2000).

In most cases, an arbitrary selection of trace elements, their forms and concentrations is usually sufficient to provide satisfactory growth in traditional shake-flask and batch cultivations of many microorganisms. A general purpose trace element solution developed for *S. griseofuscus* for the production of physotigmine (Zhang *et al.,* 1996) was used with the in house minimal medium developed by Eli Lilly Ltd. All the other medium compositions and trace element solutions, used throughout this work were as stated in the literature (see Chapter 3, section 3.6). The importance of various minerals such as K, Na, Mg, Mn, Zn, Fe, Co, Mo, and Cu is illustrated in the production of glucoamylase by *Penicillium italicum* (Nandi and Mukherjee, 1991), with the optimised defined medium giving two-fold higher production. The presence of Mn as a metabolic ion significantly stimulated the production of polyene antibiotics PA-5 and PA-7 by *Streptoverticillium* spp. in chemically defined media (Soliveri *et al*., 1998). On the other hand, heavy metals such as Pb, Cu, Zn, Fe, and Mn were found to be very toxic to bacterial methanogenesis in synthetic medium (Nandan *et al*., 1990).

A mixture of nutrients/minerals/growth factors sometimes serves well as a starting medium (Zhang *et al*., 1996, Chapter 3, section 3.6.5; Petkovic, 1998, Chapter 3, section 3.6.6). Although the optimal medium composition for a fermentation process is generally strain-specific, starting with a reported medium for a related species can be of great help (Oliver *et al*., 1990; Bourque *et al*., 1995). Bacon (1985) found that one defined medium formulation supported growth and ergot alkaloid synthesis by five species of *Balansia* (*Clavivipitaceae*). Fu (1996) studied the commercially available Catlin defined medium

used to culture *Neisseria meningitidis* for production of the outer-membrane protein complex, which is useful as a protein carrier for conjugate vaccines, and was able to reduce the 50 or more components originally present to only 13. Compared to Catlin medium, this simple defined medium supported a two-fold higher cell density.

A number of different medium formulations were then tested for their ability to produce tylosin [see Table 4.1; for medium compositions and results; All Tables can be found in the companion CD; Appendix O Chapter 4] that have been previously used to produce tylosin, tetracycline, actinorhodin and physostigmine. Table 4.1 indicates the only media that significantly produced tylosin were the ones that were cultured with rich fatty acid sources or complex polysaccharides e.g., starch, methyl oleate, and mineral oil. The complex medium on average at shake flask trial level achieved 3.12 gl^{-1} (average 15 individual shake flasks). Other workers have reported in excess of 4.0 gl^{-1} (in house at Eli Lilly Ltd.). For the methyl oleate defined medium (Chapter 3, section 3.7.2) 0.373 gl^{-1} tylosin titer was achieved, where other workers have reported higher yields of 0.8 – 1.0 gl^{-1} (Arnold, 2000) with the *S. fradiae* C373-5 strain. These differences were considered to be due to different culturing conditions and medium source/preparation (Table 4.1).

Why starch, methyl oleate, and mineral oil were the only carbon sources to produce tylosin to any significant level was unclear. Two main hypothesis can be made, one where glucose has been linked to the repression of polyketide synthases in a number of organisms (see Chapter 2, section 2.9.2) and the second where the activation of secondary metabolism is linked with the activation of a particular pathway. The biosynthesis of bialaphos [a herbicide, 2-amino-4-(hydroxy)(methyl)-phosphinoylbutyryl-alanyl-alanine] produced by *S. hygroscopicus* has been linked to the activation of the glyoxylate bypass (Chapter 2, section 2.5.10)[Takebe *et al*., 1991]. The synthesis of bialaphos proceeds through the degradation of glucose to phosphoenolpyruvate, where it forms a C-P linkage, with the further addition of a methyl group from methionine. Followed by the addition of acetyl-CoA and the addition of two alanines forms bialaphos. Therefore bialaphos formation is considered to be closely related to glucose metabolism. Based on this hypothesis, sugar consumption and the activities of the TCA cycle enzymes were examined by Takebe *et al*. (1991) using a high producing strain and a strain of lower productivity cultured on a glucose or glycerol defined medium. The high producing strain had lower rate of sugar consumption and lower yield of cells, compared with the lower productivity strain. The

activities of the TCA cycle enzymes of the high producing strain were lower than those of the lower producing strain, while activities of the glyoxylate bypass enzymes of the high producing strain were higher. From these findings, it was suggested that the high producing strain suppress the flow from acetyl-CoA and pyruvate (as substrates of bialaphos) to the TCA cycle, and directs these substrates efficiently to secondary metabolism by activation of the glyoxylate bypass.

A starch based medium offers considerable difficulties for experimental analysis. Straightforward test-tube chemical and enzymatic assays can measure the overall utilisation of the carbohydrate. This type of carbohydrate input is, however, a population of molecular species with different molecular weights: in starch hydrolysates, for example, the average glucan oligomer may be maltoheptose, but different methods of manufacture can give variable mixtures of oligosaccharides. This is important because microorganisms utilise the different oligomers at different rates. The complex and methyl oleate based media were also too rich in carbon and nitrogen containing compounds to realistically apply a flux based strategy. Although a systematic strategy of analysing the media from minimal to the complex could offer a number of benefits to the complete understanding of a fermentation process (see Chapter 6, section 6.10 and discussion). The minimal medium and defined medium composition studied so far showed good biomass production levels but poor tylosin yields (Table 4.1). Therefore further analysis was undertaken to improve the tylosin yield by altering the carbon source, PO_4, $MgSO_4$, NH_4, and betaine levels. Stark *et al*. (1961) considered these factors extremely important to tylosin yield when developing the literature based methyl oleate defined medium (Chapter 3, section 3.7.2).

4.3.2 Statistically designed experiments

The glucose minimal medium and glucose glutamate defined medium (Chapter 3, section 3.6.4) had already been used for tylosin production in continuous culture and were considered the most suited to the needs of this project although tylosin yields obtained were considered too low to model secondary metabolism with a flux-based strategy (Table 4.1). Further shake flask trials were undertaken with a number of single component carbon sources to determine if the tylosin yield could be increased significantly in batch culture (see Table 4.2). The degree of dispersion ϕ was implemented throughout this investigation as a value for the characteristics of dispersed cell growth (Chapter 3, section 3.10.3). The value was defined as the number of colony forming units per ml in the liquid culture

divided by the number of spores per ml initially inoculated (Hobbs *et al.,* 1989; de Orduna & Theobald, 2000)[Chapter 3, section 3.10.3].

The best biomass yields and dispersion were obtained when glutamate or oxo-glutarate was an addition to the medium. No significant increase in tylosin titer was observed with any of the carbon sources tested (Table 4.2). It was found that *S. coelicolor* 1147 and *S. fradiae* C373-10 both were able to grow in a modified medium, containing glutamate or oxo-glutarate as the sole carbon and nitrogen source. The resulting biomass formation was summarised in Table 4.2. Pyruvate and oxo-glutarate showed good growth in shake flask trials but when stepped up to bench top fermenter, the pyruvate fermentation (seed training medium did not show the same trend) failed and the oxo-glutarate showed extremely poor growth (seed training medium did not show the same trend). The low pH at the time of sampling (Table 4.2) with a single carbon source minimal medium led to the decision to increase the initial MOPS concentration from 10 gl^{-1} to 25 gl^{-1} for all the seed medium and production medium formulations, increasing buffering capacity.

As expected increases to the nitrogen to carbon ratio increased biomass yield, but possibly at the expense of antibiotic production (Table 4.3). Although the obtained tylosin yields were considered too close to the detection limits of the system to accept any trend in the results (Table 4.3). This corresponded with Choi *et al*. (2000) who showed for *S. fradiae* that when a concentration of high ammonium ions was added to a culture medium, cell concentration increased. The pellet area of 1.2 - 9.0 ($\times 10^4$ μm^2) was about 8 - fold larger than those obtained from an amino acid mixture, which resulted in a decrease of apparent viscosity. Since nitrogen is essential for protein biosynthesis, nitrogen was the limiting factor as expected, the excess carbon cannot be consumed for protein formation and hence it does not lead to the production of biomass. Therefore the excess carbon could be excreted as organic acids, if not oxidised to CO_2 for energy production.

Altering the phosphate concentrations showed no significant tylosin titer increases (see Tables 4.4). Phosphate levels did show an increase in biomass production, but no significant increase in tylosin production was observed. While phosphate starvation can initiate actinorhodin (ACT) production in *S. coelicolor* with carbon and nitrogen abundant (Liao *et al*., 1995), excess phosphate fails to repress ACT biosynthesis, that occurs as the growth rate declines under nitrogen starvation. Likewise, in *S. venezuelae*, excess phosphate fails to repress chloramphenicol biosynthesis. In this aspect of regulation, these

two streptomycetes are distinctly different from *Streptomyces griseus* strains producing candicidin or streptomycin, where excess phosphate is severely repressive (Liras *et al*., 1990). Without this strong negative control, it is difficult in *S. coelicolor* and *S. venezuelae* to provoke an idiophase by adjusting initial phosphate levels. This may indicate that without evidence that the tylosin synthetic pathways were active with the minimal and defined medium formulations, little improvement can be achieved by changing phosphate concentrations.

When betaine was an addition to the medium (range 1.2 - 2.0 gl^{-1}) there was an considerable increase in biomass yield (range 7.99 - 9.49 gl^{-1}) and the ϕ dispersion (range 2.74 - 3.11) against the control (see Table 4.5). Betaine is an important component of the industrial complex medium, although the reason for this requirement has not been reported by other workers (Stark *et al*., 1961). It is used by a number of bacteria as a nitrogen and carbon source (Hodgson, 2000). Betaine has also been linked to osmoprotection in a number of bacteria. Why the addition of betaine led to such an effect with the minimal and defined medium formulations used for this work was not clear. Stark *et al*. (1961) reported betaine being an important component of methyl oleate defined medium (Chapter 3, section 3.7) but there was no inhibitory concentration point. This did not fit with the results for the glucose minimal and glucose glutamate defined medium (Table 4.5) where concentrations above 2.0 gl^{-1} showed an inhibitory effect on biomass production and the ϕ of dispersion.

Streptomycetes are unusual in their resistance to osmotic stress (Hodgson, 2000). The ability of cells to resist high osmotic pressure comes from the accumulation of compatible solutes within the cell. In enteric bacteria, the compatible solutes are betaine, aas and trehalose (Booth & Higgins, 1990). Streptomycetes have been found to accumulate aas proportionately to the size of the salt challenge. For *S. griseus* and *S. californicus* beyond 0.75 M NaCl there was little or no increase in concentration of intracellular aas. In *S. californicus* the aa pool increased 9.33 fold from no salt to 0.75 M NaCl. The composition of the aa pool also altered as it increased. At maximum stimulation, proline accounted for about 50 % of the free aa pool in *S. californicus*. Glutamine was the next most significant aa, and alanine the next. In cells not subject to osmotic challenge, glutamate predominates in the free aa pool (Killham & Firestone, 1984a). Addition of proline to salt stressed *S. griseus* (Killham & Firestone, 1984b), increased the growth yield of the streptomycete 55 % of the aa was imported in 0.75 M NaCl challenged cells; this rose to 71 % in 1 M NaCl. Import however, was tightly

regulated in the relative proportion of proline in the intracellular pool was not altered by the presence of exogenous proline. This implied that import of proline decreased the amount of *de novo* proline synthesis (Killham & Firestone, 1984a, b). The decrease in requirement for proline biosynthesis accounted for the increase in growth yield. The importance of osmoprotection (i.e., osmotic challenge) from some aas therefore needs to be considered when thinking about the regulation of aa biosynthesis. Osmotic challenge has not been characterised as yet in streptomycetes. It has been proposed that trehalose might act as an osmoprotectant in streptomycetes, but it has not been demonstrated that trehalose synthesis was activated by changes in osmotic pressure (Hodgson, 2000).

Table 4.6 would indicate that $MgSO_4$ was a minor limiting factor in the production of biomass in an *S. fradiae* fermentation cultured on the glucose minimal and glucose glutamate defined medium. As the concentrations below 1 gl^{-1} had a significant effect on the biomass yield.

Table 4.7 indicates when the ratio of glutamate to glucose, favours glutamate in the case of the methyl oleate medium (Chapter 3, section 3.7.2) considerably improved tylosin and biomass yields were obtained. Gray and Bhuwapathanapun (1980) have also shown under steady-state chemostat conditions that increasing the specific uptake rate of glutamate stimulated the specific production rate of tylosin. In the study of Gray and Bhuwapathanapun (1980) nitrogen repression was not analogous to carbon source repression as the increased uptake of glutamate increased rather than decreased the tylosin synthesis. In the case of the glucose glutamate defined medium the ratio favoured glucose for biomass production (Table 4.7) although there was no observable tylosin yield improvement.

With the achievement of such low antibiotic yields, any statistical surface response analysis (see section 4.1) was considered impractical and would lead to little enhancement to a medium optimisation strategy. Therefore the analysis undertaken was used to optimise biomass yield where the optimum concentration was highlighted in red (Table 4.1 – 4.7; highlighted figures in red indicate the optimum concentration for biomass formation and possibly tylosin production) and the data accumulated into one medium composition that was further tested at shake flask level. The accumulated data were as follows: for a glucose minimal medium (gl^{-1}) glucose 20.0, NH_4SO_4 (4.0), betaine (2.0), $MgSO_4$ (2.25), and

phosphate (1.2 – 2.4) and the rest of components were as Chapter 3, section 3.6.4, and for growth of glucose glutamate defined medium (gl^{-1}) glucose 20.0, glutamate (5.0), NH_4SO_4 (3.0 – 3.5), betaine (2.0), $MgSO_4$ (2.25), and phosphate (2.0 – 2.4) and the rest of components were as Chapter 3, section 3.6.4. The latter optimised media were assessed at shake flask level and showed biomass yields 6.0 - 7.0 gl^{-1} and 7.0 – 8.0 gl^{-1} and tylosin titer of 0.004 – 0.009 $mg.ml^{-1}$ respectively for the latter formulations.

No significant improvement in tylosin yields was obtained, with the medium optimisation strategy used in this work. Due to time constraints any further development of a defined medium was not a feasible undertaking (see Chapter 8, section 8.2). The decision was taken to use the medium developed by Eli Lilly Ltd. (Chapter 3, section 3.6.4) for the remainder of this project.

One of the objectives of this work was to incorporate a secondary metabolite producing pathway into a flux-based strategy to direct changes in the culture conditions. This was not a feasible objective, with such low antibiotic yields using minimal and defined medium. It was considered that changes in the phosphate and nitrogen concentrations would deliver limited data with such low antibiotic yields i.e., little impact on the flux of the primary metabolic pathway flux in relation to secondary metabolic pathways would be expected. The best-fit approach was then a strategy of incorporating a systematic approach to the analyses of *S. fradiae* C373-10 growth from a minimal medium with low antibiotic yields to the literature based methyl oleate defined medium with the goal of further incorporating a material balance of the industrial complex medium. In essence de-piecing the literature based defined medium and complex industrial medium to their basic carbon components and measuring how the individual components distribute to biosynthesis. It must be remembered that problems of low antibiotic yield are not only associated with *S. fradiae* C373-10 and *S. coelicolor* 1147 when cultured on minimal media but with the streptomycetes in general (see Chapter 8 for further discussion).

4.4 Primary objectives set for thesis

The initial objective of the thesis was to undertake a systematic strategy of building up knowledge of the elemental and macromolecular composition of *S. fradiae* C373-10 when cultivated with a single component carbon source, and link this to the literature based defined and the industrial complex media (see Chapter 5). The secondary objective was to

carry out flux analysis on minimal and defined media with a number of different carbon sources (i.e., glucose, fructose, glycerol, oxo-glutarate, pyruvate, glucose + glutamate, and glucose + oxo-glutarate), and carry out a rudimentary material balance with the industrial complex medium.

4.5 Batch cultivation of *S. fradiae* C373-10 & *S. coelicolor* 1147.

To eliminate carry-over of any unknown components from the complex vegetative medium (Chapter 3, section 3.5.1). The appropriate seed (defined) medium was inoculated with 10 % of the vegetative culture, which in turn was used to inoculate the production medium [10 % incolum](Fig 4.1 – 4.20). The resulting medium in the bioreactors achieved rapid growth only after a long lag phase (seen in the fructose [Fig 4.3]; glycerol [Fig 4.4 & 4.5]; oxo-glutarate [Fig 4.6]). This was not indicative of the shake flask trials that were undertaken in a similar manner. The reason for this was considered to be associated with a number of issues (1) there was not enough adequate research undertaken with the development of the minimal and defined medium compositions. (2) the vast array of different fermentation equipment increased the complexity of solving problems associated with the development of a defined medium (Fig 4.1 – 4.20). (3) trace metals in the water supply between the two sites of fermentation analysis (i.e., University of Strathclyde and Eli Lilly Ltd.) contributed to this problem. (4) the nitrogen source i.e., glutamate or oxo-glutarate had a considerable effect on the overall growth. Long lag phases were not observed with the glucose minimal medium [Fig 4.2 & 4.3], glucose glutamate [Fig 4.7 - 4.10], glucose oxo-glutarate defined medium [Fig 4.11 - 4.12]. Glutamate has been shown to be an excellent source of nitrogen for the growth of *Streptomyces* (Williams & Katz, 1977) and is even preferred to ammonium in *Streptomyces griseofuscus* (Zhang *et al.*, 1996). In *Streptomyces*, ammonium has been reported to be an inhibitory substrate for growth, especially when supplied in high concentrations (Ives & Bushell, 1997). This could explain the lag phase observed in the medium with ammonium.

The long lag phases would indicate that there might be certain nutrient limitations on the substrate utilisation apparatus at the start of the cultures. It would be of interest to determine if this nutrient limitation / repression were due the nitrogen source (i.e., glutamate or oxo-glutarate).

4.5.1 The bioengineering fermenter

Fermentations were run at 30^0 C (Chapter 3, section 3.9.3). Depending on the time of year, this temperature ranged from 5^0 C to 12^0 C above room temperature. As differences in the extent of the saturation of the air with water were inevitable, evaporation was possible. To determine the necessity for cold water to run through the condenser and the differences from fermenter to fermenter with the condenser port running. Measurements of a spiked Tris (tris (hydroxymethyl) amino ethane) content of glucose-MOPS-free medium were taken over a time period estimated to be equivalent to that of an *S. coelicolor* 1147 and *S. fradiae* C373-10 fermentation (0 - 100 hrs). Tris (121.1 MW) was used at a concentration of 10 mM, measured as 480 ppm of carbon (as determined by total organic carbon analysis [TOCA]; Chapter 3, section 3.15.5)[Table 4.8]. An increase in carbon concentration of the medium indicated an increase in Tris concentration, resulting from evaporation with no condenser port running, when the condenser was running there was still evaporation present, and fermenter to fermenter variability was considerably high (Table 4.8). Table 4.8 shows the increase in concentration of Tris in the medium. By 100 hours this had increased on average by 17.93 – 34.29 % (on average depending on bioreactor) without a condenser and 7.20 – 12.73 % (on average depending on bioreactor) with a condenser (Table 4.8). This indicates that different bioreactors will have a considerable effect on the batch to batch reproducibility of the analytical data to be undertaken in the following Chapters (Chapter 5 & 6).

Up to 20 batch fermentation were carried out with *S. fradiae* C373-10 and *S. coelicolor* 1147. Biomass samples were harvested from these fermentations at set time points, and samples were analysed for elemental and macromolecular compositional analysis (Chapter 5). Large sample volumes were necessary to obtain sufficient biomass to undertake this analysis. These volumes were of 500 ml up to 50 hrs after inoculation and 250 ml thereafter. For cultures to be maintained at a constant temperature, the temperature probe in the fermenter had to be submerged (also taken into account were the pH, antifoam, and dissolved oxygen probes). This required a minimum volume in the fermenter (for 5 L vessel, a minimum of 2 L was required), allowing only 3 L of culture to be removed prior to the final sample. Therefore, only a small number of samples could be taken at 24 hr periods and it was not feasible to sample in triplicate. It was decided that appropriate addition of sterile dH_2O would replace the sample and the evaporation during that time period (taken into account by gravimetric analysis). A dH_2O container on a digital balance

was connected to the fermenter by a peristaltic pump and the weight of the required dH_2O addition to the appropriate volume mark on the fermenter corrected for and recorded (all calculations & results from this point take this addition into account).

4.5.2 Definition and measurement of dry biomass

The basis for standardisation of all measurements/data (see Chapter 5 & 6) was dried biomass. Therefore, it was essential to establish a clear, workable, and reproducible procedure to obtain "dry" biomass. Even drying at 105^0 C might not remove all water from the biomass (Guarakan *et al*., 1990), whereas changes to the extracted lipid were reported at this temperature; therefore, evaporation of other volatile compounds cannot be excluded.

Analysis of the different methods of pretreatment (drying at 105^0 C for 24 h, drying at 70^0 C for 48 h and drying in a microwave oven) indicated a varying degree of water removal (Table 4.9). Nevertheless, this difference was nearly compensated for by the different weight loss during subsequent storage above silica gel (Table 4.9). Hence, the water content in the so-called dry biomass was nearly independent of the preceding drying method, if followed by sufficiently long subsequent storage in a desiccator. Storage in a desiccator conveniently provided an independent reference state for the biomass for further analysis and the rate of water absorption was greatly reduced compared with samples taken directly from a drying oven (Table 4.9).

The measurements were hampered by the rapid weight increase after the drying, resulting in high STDEVs (results not included). Additional dry weight estimations were calculated using TOCA of the wet weight biomass (assuming 1 g dry weight biomass was composed of 50 % carbon, Chapter 3, section 3.15.5) and gravimetric analysis of freeze dried broth to further verify and reconcile (mean between the methods) the growth data. These estimations were found to be similar to the measured values, within 10 % error (Table 4.10), with a slightly lower average STDEV. Freeze dried (heated at 100^0 C for 1 h and stored over silica) samples showed a similar trend in results and a high STDEV (Table 4.10). Due to the labour intensity and equipment availability of the latter methods it was not feasible to extend this reconciliation of the data throughout the fermentation analysis. Although this does warrant further research, strategies to reduce inconsistency in dry weight measurements must ultimately be employed to reduce accumulating error in the compositional analysis and flux estimation (Table 4.12).

A decision was made to undertake all analysis with use of a microwave due to this equipment being available at all locations of work (University of Strathclyde and Eli Lilly Ltd. Speke). Cultivation of *S. fradiae* C373-10 and *S. coelicolor* 1147 in the bioengineering bioreactors resulted in variable results for dry weight (gl^{-1}) and wet weight (gl^{-1}) determinations. The average reconciled data are shown in Table 4.10. High STDEVs were observable for the glucose [Fig 4.1 - 4.2], glucose glutamate [Fig 4.7 - 4.10], glucose oxo-glutarate [Fig 4.11 - 4.12] and methyl oleate defined medium [Fig 4.13 - 4.15], this analysis was undertaken at Eli Lilly. This was reduced in the fructose [Fig 4.3], glycerol [Fig 4.4 - 4.5], and oxo-glutarate [Fig 4.6], this analysis was undertaken at the University of Strathclyde. The high STDEVs were considered to be increased by the unreliability of the microwave equipment (where one microwave run could take anything from 30 mins to 1 hr)[Table 4.11]. Comparison of wet weight and dry weight values (as measured by filtration, Chapter 3, section 3.11) showed that as a fermentation progressed, there was a possible trend where the proportion of dry mycelial weight per gram of wet weight decreased for *S. fradiae* fermentations [expressed as a percentage](Table 4.11) this revealed that as a fermentation progressed, the proportion of dry mycelial weight per gram of wet weight increased (Table 4.11). This was the opposite for *S. coelicolor* fermentation (Table 4.11).

Standard errors were within acceptable limits for all samples, especially those harvested early in a fermentation (Table 4.12). Measurements of some samples gave negative values (only in case of *S. coelicolor*). Alternative methods of dry weight determination, such as the use of foil cups, corex tubes or freeze drying whole broth samples, resulted in similarly high STDEV (results not shown). It was possible that due to the morphology of streptomycetes in general, an homogenous distribution of cells at sampling was not achieved. This has been noted by other workers for which *Streptomyces* species tend to form cell pellets in the culture fluids and biofilms on surfaces during growth (Melzoch *et al*., 1997). Because cell distribution in the culture medium is not uniform, calculation of culture parameters is difficult, and a reliable estimate of the metabolically active biomass is not feasible.

4.5.3 Bench top scale fermentation profiles

Profiles of the measured extracellular on-line and off-line variables of the fermentations undertaken with *S. fradiae* C373-10, C373-18 and *S. coelicolor* 1147 cultured on a number

of medium compositions are illustrated in Figures 4.1 - 4.20. Fig 4.1 and 4.2, represents *S. fradiae* C373-10 cultured on a glucose minimal medium (fermentation 1 & 2 respectively); Fig 4.3, fructose minimal medium; Fig 4.4 and 4.5, glycerol minimal medium (fermentation 1 & 2 respectively); Fig 4.6, oxo-glutarate minimal medium; Fig 4.7 – 4.10, glucose glutamate defined medium (fermentations 1, 2, 3 & 4 respectively); Fig 4.11 – 4.12, glucose oxo-glutarate defined medium (fermentations 1 & 2 respectively); Fig 4.13 – 4.15, methyl oleate defined medium (Chapter 3, section 3.7)[fermentations 1, 2, & 3 respectively); Fig 4.16 – 4.18, *S. fradiae* C373-18 cultured on a industrial complex medium (fermentation 1, 2, & 3 respectively) and *S. coelicolor* 1147 (fermentation 1 & 2 respectively) cultured on a glucose minimal medium (Fig 4.19 - 4.20). A & B, depicts the profiles of biomass (dry weight)[gl^{-1}], carbon source utilisation (gl^{-1}), phosphate (gl^{-1}) and nitrogen uptake (gl^{-1}), B depicts tylosin (gl^{-1}) production and wet weight (gl^{-1}). The fermenter load was maintained constant, by correcting the fermenter liquid volume back to the initial volume, after sample removal; and this was used for the on-line calculation of the volumetric OUR ($mmoles.min^{-1}$), CER ($mmoles.min^{-1}$) and RQ (see Appendix E for calculation), the dissolved oxygen [DO] (%) profile was also included values as depicted in Figure 4.1 (C). D, depicts the excretion of organic acids ($mg.ml^{-1}$) into the medium over the course of the fermentations.

The fermentation profiles of *Streptomyces* cultures can be designated as four separate phases, as portrayed in Figures 4.13 – 4.15 (methyl oleate defined medium, was chosen as the main example which produced the highest antibiotic yield). Phase I of the fermentation was marked by complete utilisation of phosphate and ammonium (or first carbon source) and the production of organic byproducts, such as pyruvate, acetate, and oxo-glutarate. Phase II of the culture was marked by the termination of growth, decreasing respiration and RQ. This was indicated by a plateau in respiration, and a decrease in biomass concentration. Phase III marks the initiation of antibiotic synthesis which can take place any where between phase I – II. Phase IV marked the initiation of the death phase as all the nutrients were depleted (cultures were not usually taken this far). Phase I, II & III were the main sampling points for the methyl oleate defined medium [SP I, II, and III] (SP denotes, sampling point) and phase I & II were the main sampling points (SP I & II) for the minimal and defined medium formulations used to undertake the material balances. 1 g of biomass was sampled for a every 24 hr point of the culture, stored and further analysed for macromolecular content (see Chapter 4, section 4.5.1, Chapters 5 & 6). In the majority of

S. fradiae C373-10 cultures, phase III and IV were not used as a SP for the flux analysis (Chapter 6) due to antibiotic synthesis being very low, only SP III (representing phase III) was used for the methyl oleate defined medium for which antibiotic synthesis was considerable compared with the minimal and defined media (Fig 4.1 – 4.20).

4.5.4 Growth behaviour of *S. fradiae* C373-10, C373-18 and *S. coelicolor* 1147 cultures

The maximal specific growth rate (μ) was calculated from biomass yield measurements ($\mu_{biomass}$), DNA content (μ_{DNA}), and an average ($\mu_{average}$)[reconciled data] between them (Table 4.12). For the glucose minimal medium (fermentations 1 & 2 respectively) the μ was $\mu_{biomass}$ = 0.018, and 0.018 μ_{DNA} = 0.034, and 0.038, and $\mu_{average}$ = 0.025, and 0.028 respectively (see Table 4.12 for the μ for fructose glycerol, and oxo-glutarate minimal mediums). The calculated percentage difference between the μ_{DNA} 89.12 % and $\mu_{average}$ 77.80 % (on average calculated from the $\mu_{biomass}$) and the STDEV (40.30 %) was considered to be a consequence of the infrequent sampling time points i.e., 24 hr periods (see section 4.5.1) although percentage STDEV between the same sample and method were relatively low.

The glycerol minimal medium fermentation (Fig 4.5, Ferm 2) [All fermentation numbers relate to the same cultures throughout Chapter 4, 5, 6 & 7; *S. fradiae* C373-10 cultures for glucose (Ferm 1 & 2); fructose (Ferm 1); glycerol (Ferm 1 & 2); oxo-glutarate (Ferm 1); glucose glutamate (Ferm 1 - 4); glucose oxo-glutarate (Ferm 1 & 2); methyl oleate medium (Ferm 1 - 3); Industrial complex (Ferm 1 & 2); *S. coelicolor* cultures for glucose (Ferm 1 & 2)] was the only one undertaken with a full gas analysis profile (1 days data missing). The volumetric oxygen uptake rate, $q_{O2}x$, increased with biomass concentration and reached its maximum when the biomass concentration was at its maximum. When glycerol was depleted, it dropped sharply. The volumetric uptake rate for *S. fradiae* C373-10 cultured on glycerol was 1.78 mmoles O_2 g $cell^{-1}$ h^{-1}, for the methyl oleate defined media (Fig 4.13 & 4.14, Ferm 1 & 2) it was 0.781 and 1.16 mmoles O_2 g $cell^{-1}$ h^{-1} respectively and for the complex industrial medium (Fig 4.16 - 4.18, Ferm 1, 2 & 3) 0.059 mmoles O_2 g $cell^{-1}$ h^{-1}, 0.023 mmoles O_2 g $cell^{-1}$ h^{-1}, and 0.120 mmoles O_2 g $cell^{-1}$ h^{-1} respectively (using dry weights calculated from Table 4.11). There is scant information in the literature concerning the oxygen uptake rate of other *Streptomyces* cultures despite the industrial significance of these cultures. The specific oxygen uptake rate of *S. aureofaciens* was 2 - 3 mmoles O_2 g

cell^{-1} h^{-1}, that of *S. clavuligerus* was 10 mmoles O_2 g cell^{-1} h^{-1}, that of *S. lividans* was 0.09 mmoles O_2 g cell^{-1} h^{-1}, and that of *S. coelicolor* 0.034 mmoles O_2 g cell^{-1} h^{-1} (Ozergin-Ulgen and Mavituna, 1998).

Careful analysis of growth of *S. fradiae* C373-10 on the glucose glutamate defined and glucose oxo-glutarate defined media did not reveal a diauxic lag phase (Fig 4.7 - 4.12). Diauxic growth is a phenomenon characteristic of glucose repression and inducer exclusion in the enteric bacteria. When a cell is presented with growth-limiting glucose and excess glucose-repressible catabolite, the cell metabolises the glucose alone first. Once glucose is exhausted, the cell ceases growing until the enzymes necessary for the catabolism of the second catabolite have been induced. This period of growth cessation is referred to as the diauxic lag. Hodgson (1982) and Hanel *et al*. (1987) could not find a diauxic lag phase when *S. coelicolor* was grown in medium containing glucose and excess alternative repressible carbon source and *S. chrysomallus* on glucose and xylose were co-metabolised. Since glucose transport systems in streptomycetes have low affinity for their substrate –K_m values of 0.12 mM to 6.1 mM. Taking this into consideration with the observations that comparative growth rates of streptomycetes are slower than those of enteric bacteria, whilst the time taken to activate, transcribe and translate genes are about the same, it is perhaps not surprising that diauxic lags are rarely seen in streptomycetes. It should also be noted that the PEP-coupled phosphotransferase system (PEP-PTS) mechanism of inducer exclusion makes a significant contribution to delay induction of the catabolism genes and thus to the creation of diauxic lag (see Chapter 2, section 2.4).

Figure 4.7A - 4.11A also illustrated that glutamate degradation was followed by an increase of ammonia concentration in the extracellular medium, suggesting that glutamate was used as a carbon source before being used as a nitrogen source in the latter stages of the fermentation. The shift from glutamate to glucose degradation did not lead to a cessation in biomass formation. There was also an increase of the dissolved oxygen (DO) observed around 30 hrs of the process time. Limiting conditions led to a cessation of growth at 120 hrs (Fig 4.7 A, B - 4.11 A, B). The μ was calculated to be for growth on a glucose glutamate defined medium for fermentations 1, 2, 3, and 4 respectively $\mu_{biomass}$ = 0.018, 0.011, 0.014, and 0.019 μ_{DNA} = 0.072, 0.066, 0.067, and 0.081 $\mu_{average}$ = 0.045, 0.039, 0.041, and 0.050 respectively (Table 4.12). The observed difference in STDEV (48.29 % on average) between the calculation of the μ from biomass, DNA and the average

composition was considered a consequence of the unreliability of the microwave equipment on site at Eli Lilly Ltd (see section 4.5.2). The microwave time cycle was inconsistent from run to run (see section 4.5.2 for further discussion). The μ's for the methyl oleate defined medium were as follows for fermentations 1 - 3 respectively, $\mu_{biomass}$ = 0.048, 0.048, and 0.056, μ_{DNA} = 0.025, 0.019, and 0.029, and $\mu_{average}$ = 0.036, 0.034, and 0.040 respectively.

Fig. 4.13 – 4.15 A shows the time course for the literature based methyl oleate defined medium (Chapter 3, section 3.7) for the *S. fradiae* C373-10 bioprocess and how the concentrations of the analytes of interest (methyl oleate, glucose, glutamate, phosphate, dry wt, and ammonium) change with time. For the literature-based methyl oleate defined medium (Chapter 3 section 3.7.2) the corresponding seed medium was considered to be too complex for a flux analysis strategy to be undertaken (seed medium 3, Chapter 3, section 3.5.3) therefore further seed medium compositions were analysed for suitability. Arnold *et al*. (2000) [personal communication] used two seed medium compositions based on tryptone & yeast extract with the addition of glucose being optional (Chapter 3, section 3.5.1, seed medium 1, with glucose; seed medium 2 without glucose). Three fermentations were undertaken to determine the effects that seed medium 1 & 2 had on overall antibiotic yield of the methyl oleate defined medium (Fig 4.13, seed medium 1; Fig 4.14, seed medium 2; Fig 4.15, seed medium 3) in addition the literature based vegetative medium i.e., seed medium 3. A number of observations can be made which are useful for model building. Three of these analytes; glucose, glutamate and ammonium were fully utilised within the first third of the process. This process phase [phase I], shows greatest change in concentration of these analytes, and therefore this period was crucial for any model building strategy. It was difficult to recognise the preferential carbon source being utilised by the organism (possibly glutamate). The culturing of *S. fradiae* C373-10 on a glucose and glutamate medium indicate *S. fradiae* showed preference for glutamate (Fig 4.7 – 4.10). Although this was likely consequence of the choice of the seed medium. When the literature based methyl oleate defined medium was inoculated with culture from different media (Fig 4.13, seed medium 1, Chapter 3, section 3.5.1 minus glucose; Fig 4.14, seed medium 2, Chapter 3, section 3.5.1; Fig 4.15, seed medium 3, Chapter 3, section 3.5.2). There were different specific uptake rates for glutamate, glucose, with considerable differences also observed in the tylosin titer. This was possibly due to the late utilisation of NH_4 which may have had a repressive effect on tylosin synthesis (see Chapter 2, section

2.4.2). It has been stated that antibiotic-producing activity of actinomycetes tends to be decreased by the use of metal deficient media, nitrogen source, prolonged seed incubation time and higher temperatures (Higashida, 1984).

Glutamate has been reported to have a stimulatory effect on tylosin synthesis (Gray & Bhuwapathanapun, 1980) and like glucose is used up within the first third of the fermentation. It has been suggested the rapid uptake of these analytes allows the maintenance of high levels of enzymes in the tylosin biosynthetic pathway (Gray, 1980). Glutamate, as a nitrogen source, supports rapid growth of both *S. coelicolor* and *S. venezuelae*. The evidence that *S. coelicolor* supplied with glutamate and a growth-limiting carbon source can produce ACT demonstrates that glutamate *per se* is not severely repressive. In *S. venezuelae*, glutamate in combination with growth-limiting carbon sources supports only low yields of chloramphenicol (Liao *et al*., 1995), and thus the absence of repression is less certain. The quality of the inoculum is often stated as an important factor in determining the performance of the final stages of a fermentation (Warr *et al*., 1996). The composition of the seed and training media used throughout this work, do need further research. Although further improvements to the seed mediums used for the minimal and defined media were unlikely to be the sole factor hindering tylosin synthesis. Therefore further medium optimisation of the defined media was considered necessary.

The rapid utilisation of glucose coincides with the exponential growth phase, which took place over 30 hours (Fig 4.13A); it was clear that this exponential growth phase carried on right up to the cessation of growth at around the 90 hour. This was another important time frame for model building, where the concentration was changing most significantly [phase II]. There was also a decrease in OUR and CER and lower respiration at 24 hrs, which was likely a consequence of glucose depletion (Table 4.12). The DO decreased from 30 % to 70 % before falling again to 30 % as the cells moved from glucose to glutamate and on to methyl oleate consumption. Glucose was depleted after about 45 hours at which point the organism switched to use the other carbon source, methyl oleate, which was then used up gradually during the entire time course of the fermentation. The onset of methyl oleate usage corresponded to the start of tylosin production as recognised by other workers (Vu-Trong & Gray, 1987). Tylosin production was most rapid between 80 & 120 hrs (phase III). Therefore the fermentation could be considered as having three phases [phase I, II, & III] (see Fig 4.13 – 4.15). Which were of importance to any flux-based strategy. Another

analyte modelled in this process was ammonium (Fig 4.13A – 4.15A). High levels of ammonium ion are not desirable and studies have shown that tylosin production decreases with increasing ammonium ion concentration (see Chapter 2, section 2.4.2).

Additional analysis of the industrial complex medium was also undertaken (Fig 4.16 - 4.18). This necessitated research into a number of biomass (medium component separation techniques) separation techniques to undertake an estimation of the true dry weight and wet weight biomass composition, which in turn was used to undertake further compositional analysis. Separation of biomass was considered important to verify that biomass compositional contents of the various defined medium composition were similar to the methyl oleate defined medium and industrial complex medium (analysis presented in Chapter 5). Three solvent extraction techniques were tested that have been used by a number of other workers (extraction technique 1, Chapter 3, section 3.14.1; extraction technique 2, Chapter 3, section 3.14.2; extraction technique 3, Chapter 3, section 3.14.3). Initial analysis indicated that the two phase extraction technique (extraction technique 2, Chapter 3, section 3.14.2)[Dole & Meinertz, 1960] was most suited to this work (results not shown). It separates medium components on the basis of a polarity gradient, although high density contaminates can be seen at the beginning of the process (lower phase of the extraction protocol). The fraction could have been further cleaned up through the incorporation of a density gradient to the method although time constraints restricted further research. Dry weight was estimated to be on average 24.0 gl^{-1} at 150 hrs (Table 4.12) this was consistent with capacitance estimation of the biomass content undertaken on-site at Eli Lilly Ltd. [26.0 gl^{-1} on average]. RQ was 0.9 from 0 - 50 hrs of the fermentation and decreased to 0.7 at the onset of fatty acid utilisation (Fig 4.16C – 4.18C). The tylosin production rate showed a linear relationship to the biomass production rate and spin solids (%), although viscosity unexpectedly did not show this trend (Fig 4.16B - 4.18B). It has been reported that both tylosin biosynthesis and apparent viscosity were influenced by amino acids produced from the natural nitrogen source (Choi *et al*., 2000). The *S. fradiae* cells decomposed the natural nitrogen source by protease and consumed the resulting amino acids, which dramatically increased the apparent viscosity. The increase in apparent viscosity was considered to be due to changes in mycelial morphology and not to cell concentration. The μ's for the industrial complex medium were as follows for fermentations 1 - 3 respectively, $\mu_{biomass}$ = 0.017, 0.019, and 0.028. Considerable

differences from the acquired DNA data made interpretation of μ from these results impractical (see Table 5.9J).

Two fermentations were used to examine the pattern of growth of *S. coelicolor* 1147 in batch culture. Collection and analysis of *S. coelicolor* biomass was considered important for verification of the analytical protocols to be used in Chapter 5. Fermentations 1 & 2 were cultured on Hobbs (1989) glucose minimal medium under the same conditions (Chapter 3, section 3.6.1). Growth followed a similar pattern as observed by other workers (Hobbs *et al*., 1989; Davidson, 1992). The maximum biomass concentration was attained after 115 hrs of the cultivation at which time glucose was exhausted. Other workers indicated that this time also coincided with nitrate exhaustion (Ates *et al*., 1997). As can be seen from Fig 4.19 and 4.20 phosphate was not fully consumed by the cells and 28 % (on average) of the initial phosphate remained unused. The end of growth phase was indicated by the production of undecylprodigiosin (as determined visually) and stationary phase (as measured by the cessation of increase in wet weight, approximately 40 to 60 hours after cultivation) and was reached prior to the complete utilisation of glucose. Production of actinorhodin (ACT) was observed to be produced at phosphate concentration of approximately 1.0 - 1.3 gl^{-1} prior to a reduction in the rate of biomass formation. This corresponds with other workers (Davidson, 1992). In general, as described below, the pattern of biomass production and ACT synthesis was variable.

Comparison of the pattern of growth in fermentations 1 & 2 (Fig 4.19 and 4.20), showed considerable differences. No lysis was indicated by dry weight measurements and the time of onset of stationary phase in fermentation 2 was possibly later. The growth pattern in fermentation 2 (Fig 4.20) was irregular, suggesting that dry weight measurements may have been inaccurate (although STDEVs were very small). The maximum concentrations of biomass and ACT were 40.0 mgl^{-1} and 45.0 mgl^{-1}, respectively. During the growth phases of a fermentations 1 & 2, the DO level had fallen to below 40 % and 69 % respectively (Fig 4.19 and 4.20), although ACT was produced in both cultures. The differences were considered to be due to inadequate calibration of the DO probe. However, a similar pattern in both DO was reported by Davidson (1992). Davidson (1992) reported the DO and pH showed synchronous increase in fermentations, which was hypothesised to indicate the time of the switching of *S. coelicolor* 1147 into secondary metabolism. The defined medium of Hobbs *et al.* (1989) was glucose-limited, containing only 2.0 gl^{-1} of

glucose. However other researchers have used a higher glucose concentration, which was used to enhance biomass formation (Ozergin-Ulgen and Mavituna 1993). Increasing the initial glucose concentration from 9.5 to 13.1 gl^{-1} resulted in a 59.0 % increase in the maximum biomass concentration and a ACT titer of 5.0 - 16.0 mgl^{-1}. A further increase, however, in initial glucose concentration from 13.1 gl^{-1} to 15.6 gl^{-1} resulted in a decrease of 21.0 % in maximum biomass concentration and a ACT titer of 17.5 - 12.0 mgl^{-1}. The initial $NaNO_3$ concentration was kept constant at 4.5 gl^{-1} while the initial glucose concentration has been increased eight fold, indicating a shift to nitrogen-limitation growth conditions. Therefore the glucose limited culture used by Hobbs *et al*. (1989) may not have been the best medium suited to pursue this work to culture *S. coelicolor*. Hobbs *et al*. (1989) carbon-limited medium was originally chosen because it had been used in previous compositional work carried out in this laboratory (Davidson, 1992).

4.6 Organic acid excretion

Hockenhull *et al.* (1954) noted that during exponential growth of *S. griseus*, pyruvate was excreted into the medium. Kannan & Rehacek (1970), reported the excretion of TCA intermediates into the medium by *S. antibioticus*. Since these initial reports, quite a number of papers have been published on this phenomenon. Ahmed *et al.* (1984) reported acid secretion by older mycelium during nitrogen-limited growth in *S. venezuelae*; during the transition to acid excretion the rate of glycolysis remained constant but there was loss of oxo-glutarate dehydrogenase activity. Unlike the case of *S. aureofaciens* (Doskocil *et al.*, 1959), the acids were not reabsorbed into the cell and used later, presumably because the activity remained low.

Surowitz & Pfister (1985) examined acid secretion in *S. alboniger* cells growing on glucose and pyruvate, this strain had been shown by Redshaw *et al.* (1976) to secrete organic acids during growth on glucose. These acids were found to inhibit aerial mycelium formation, but this inhibition could be reversed by the addition of adenine. They also concluded contrary to the observation in *S. venezuelae*, that the enzymes of the TCA cycle were not affected by growth on glucose, however the rate of glycolysis increased. A lack of balance between glycolysis and the TCA cycle was considered responsible for the acid excretion. This imbalance was corrected by the addition of adenine, although re-absorption and use of the acid at a later stage was not ruled out. Dekleva & Strohl (1987) reported the acidogenesis of

S. peuceticus; in contradiction to all previous reports, this strain produced large amounts of acid only in the stationary phase, and then only in some cases. All cultures produced oxo-glutarate. However, again, the excess acid was reabsorbed for reuse. These authors also reported that *S. lividans* and *S. coelicolor* did not produce acid under their conditions.

It is clear that acid secretion is a result of imbalance between glycolysis and the TCA cycle. Some strains appear to shut down the TCA cycle that may be a consequence of ageing, possibly a step in the shift from primary to secondary metabolism. The inability of some strains to stimulate the TCA cycle whilst stimulating glycolysis might be a consequence of the mode of gene regulation in that organism (Hodgson, 2000). Acidogenesis also might be a stopgap method of dealing with excess glucose. Energy could be gained by substrate phosphorylation, and the product of glycolysis, in this case pyruvate, could be secreted into the medium for use later when the glucose supply is exhausted. Storage of high molecular weight compounds may also occur at this time. Therefore, pyruvate assimilation could occur for biosynthesis of such compounds. For example, trehalose biosynthesis is known to occur very late during cultivation of *S. parvulus* and *S. coelicolor* possibly during stationary phase (Inbar & Lapidot, 1991) (Hodgson, 2000). From radioactive labeling patterns, Inbar and Lapidot (1991) proposed that PEP was an intermediate for trehalose biosynthesis from exogenous aspartate. It is possible that pyruvate may be used in a similar fashion to aspartate. Although it is difficult to compare the metabolism of mycelia grown in submerged culture with mycelia grown on solid medium, trehalose is the major carbon source for spore germination. It is predominantly the aerial hyphae that synthesis trehalose on solid media. Therefore the aerial hyphae could utilise such an excreted molecule for biosynthesis of trehalose.

It was not known to what extent, excretion of organic acid occurred during growth of *S. fradiae* C373-10 and C373-18 cultured on a number of different carbon sources. Total organic carbon analysis (TOCA)[Chapter 3, section 3.15.5] of the cultured extracellular medium (minimal and defined medium; see Table 4.13 Part 1 & 2 TOCA was not undertaken with medium containing oil). Sampling at inoculation and SP II (as section 4.5.4) had revealed the presence of a significant proportion of unaccountable carbon not derived from a previously measured medium components. This carbon was therefore likely to have been produced by *S. fradiae* and, based on accounts of keto-acid excretion by other streptomycetes, may have been derived from pyruvate and oxo-glutarate. Although organic

excretion is widespread in streptomycetes (see Chapter 8 for further discussion); the type and extent to which organic acids were excreted by *S. fradiae* C373-10 and C373-18 have not been previously quoted in the literature. In house observations, Eli Lilly Ltd. have detected pyruvate, oxo-glutarate, acetate, malate, lactate, fumarate, butyrate and propionate. Therefore HPLC analysis (Chapter 3, section 3.25.3) was undertaken to determine if and to what extent organic acids were produced in the minimal, defined and industrial complex media (Fig 4.1 D – 4.17 D). Table 4.13 Part 1 & 2 indicates that when organic acids were taken into account, there still was a considerable proportion of carbon unaccounted for. It was possible that the estimation of the carbon was an over estimate (calculation incorporated carbon dioxide evolution [CER] data, and the elemental composition of the biomass as calculated by Chapters 5 & 6 where appropriate). TOCA of the medium was hindered by accounting for the carbon content of MOPS of the medium (MOPS at a concentration of 25.0 gl^{-1} [FW = 209.3] accounts for 1.43 C.moles.l^{-1} or 17.16 gl^{-1} of carbon). The addition of MOPS was to increase buffering capacity of the medium (see section 4.3.2) so bench top and shake flask trials could be undertaken in unison. This may have been a misjudgment that led to further inaccuracies in a carbon balance with TOCA of the extracellular medium.

The HPLC chromatogram base line for organic acid analysis was adjusted manually in the majority of cases, due to high interference from the medium components (which intensified with the methyl oleate and industrial complex medium) as the fermentation developed. As the samples were only run singularly this increased the experimental error (as can be seen from the graphs Fig 4.1D - 4.17D).

Sample clean up techniques were further investigated using the organic acid extraction and quantification sample clean up protocol of Krausse & Ullmann (1985, 1987, 1991; the procedure was as Chapter 3, section 3.25) and further extraction of any neutral or acidic exipients into a low polarity solvent such as diethyl ether (Watson, 1999). No improved sample clean up was achieved with these methods and it was more likely they were at the expense of quantitative reproducibility (results not shown). Further work could have been carried out in this area with de-proteinisation of the broth to try and further enhance sample clean up (i.e., de-proteinisation with acetone for example).

A number of organic acids were produced by *S. fradiae* C373-10 cultured on a number of different carbon sources (see section 4.6, Fig 4.1 – 4.20 & section 6.6.4). The organic acids

detected were acetate, malate, pyruvate, oxo-glutarate, propionate, butyrate, and fumarate. The reason why they were produced is as yet unknown. They were mainly produced throughout the growth phase and possibly re-assimilated during production or stationary phases (see Fig 4.1 – 4.19). Acetate, propionate, and butyrate were detected under a number of fermentation conditions where high and low levels of tylosin were detected. This may indicate the secretion of these organic acids was not a consequence of imbalances in precursor supply. An acidogenic phase initiated at the start of exponential / cubic growth and finished at the cessation of growth. The cultures became acidostatic and re-assimilation of some of the organic acids may possibly have occurred.

It was possible that O_2 limitation may have had some influence on organic acid excretion. For example, at a dissolved oxygen (DO) concentration of 1 %, the obligate aerobe *Bacillus stearothermophilus* has been shown to excrete oxo-glutarate in glucose-sufficient cultures, in addition to acetate and lactate (Martins & Tempest, 1991). The extent of accumulation was higher in K^+-limited cultures than in NH_3-limited cultures. Measurement of glycolytic and TCA cycle enzyme activities was carried out during this study. Whereas activities of the glycolytic enzymes increased as the O_2 concentration decreased, activities of some of the TCA cycle enzymes decreased. Oxygen limitation affects the kinetics of dehydrogenases in the TCA cycle because the NADH produced by them cannot be re-oxidised rapidly. However, in the *B. stearothermophilus* cultures, oxo-glutarate dehydrogenase activity increased with decreasing, O_2 concentration although the activity did not match those of the other TCA cycle enzymes. Thus oxo-glutarate was excreted. It is possible, therefore, that O_2 limitation, which presumably occurred in the pellets of *S. fradiae* mycelia in various medium composition, may have also accounted for a decrease in flux through the TCA cycle and an increase in organic acid production. A large intracellular pool of OGA is also often maintained by many organisms as a way of scavenging NH_3 under nitrogen limiting conditions (Neijssel & Tempest, 1976). This hypothesis has routinely been used to explain the excretion of this metabolite by microorganisms under these conditions.

4.6.1 Comparison of the acetate, butyrate, and propionate concentration: required to continue tylosin production at a linear rate of synthesis compared to the typical tylosin synthesis profile.

Observations in the late stages of *S. fradiae* fermentation indicated increased levels of acetate, propionate and butyrate (Fig 4.1D – 4.17D). But there was significant irreproducibility of estimation of these acids by HPLC for the industrial complex medium. Organic acid analysis incorporating anion analysis was repeated on site at Eli Lilly Ltd. using ion chromatography [IC](for a *S. fradiae* C373-18 fermentation on the industrial complex medium).

A significant portion of the inorganic anions measured and reported in Table 4.14A was from the process water used in the fermentation medium. Table 4.14B indicates the concentration of selected anions measured in fermentation process water. It was the intention to analyse further the ion content of water at the University of Strathclyde and Eli Lilly Ltd. Speke, but this was not feasible due to time constraints.

However, the retention times for acetate, butyrate, and propionate altered considerably from HPLC run to run, on average 5 – 7 % difference, where as for the other organic acids they were in the range of < 2 % (acceptable limit). Further analysis with other analytical methods would be desirable to assess further the fermentation profile of propionate, acetate, and butyrate (see section 4.5 – 4.6).

The ion chromatic analysis of short chain fatty acids over the course of the fermentation detected the presence of acetate and butyrate (Fig 4.21). Propionate was not detected in the fermentation broth at a level of 5 ppm or greater which was the detection limit of the ion chromatogram. This did not correlate with the HPLC work already undertaken in section 4.5 which indicated the production of acetate and propionate, the difference in the results could be due to fermentation lots, medium composition (the majority analysis for section 4.5 was undertaken with minimal and defined medium compositions), a different strain (*S. fradiae* C373-10 was used throughout section 4.5, where the analysis with some of the complex medium processes were undertaken with the *S. fradiae* C373-10 and C373-18), or experimental error between the analytical techniques. The exact cause for acetate accumulation is not currently understood. Therefore further experimentation was required to elucidate the significance and extent of secretion of butyrate and propionate.

Comparing tylosin synthesis in the industrial complex medium with acetate, butyrate, and propionate concentration required the following calculation. The biosynthesis of one mole of tylosin requires the incorporation of 2 moles of acetate, 1 mole of butyrate and 5 moles of propionate (see Chapter 2, section 2.10.2). One hypothesis for the accumulation of tylosin precursors in fermentation broth is that the rate of precursor incorporation into tylosin is reduced in the later hours of the fermentation, but the synthesis rate is not reduced at the same rate. The theoretical level of tylosin that could be produced from the precursors measured at 150 hours was then calculated for acetate and butyrate. The maximum concentration of tylosin that could be produced was assumed to be the concentration if the synthesis rate had remained linear through 150 hrs (Fig 4.22a - d). The maximum concentration of tylosin at 150 hrs was 13.6 gl^{-1}. The difference between the average measured titer (best-fit line) and the maximum titer was 3.0 gl^{-1} or 0.0033 gram moles of tylosin. To produce 0.0033 moles of tylosin, 0.0066 moles (0.39 gl^{-1}) acetate and 0.0033 moles of butyrate (0.29 gl^{-1}) were required. From the residual (150 hrs) concentration of acetate compared to the steady state concentrations during the 40 – 100 fermentation hours time frame, 60 % of the acetate necessary was available. Averaging the butyrate values from 60 to 105 hours and subtracting this value from the measured butyrate concentration at 150 hours, 0.0159 gl^{-1} butyrate was available (0.00018 g.moles). If 0.29 gl^{-1} butyrate was required to produce maximum additional tylosin, only 5.5 % of the necessary butyrate and propionate was present in the medium.

If antibiotic precursor supply was considered as a rate limiting issue, from this work (section 4.5 – 4.6). The complex industrial medium with *S. fradiae* C373-10 would indicate low levels of butyrate compared to acetate and propionate then increasing enzymes involved in butyryl-CoA synthesis may offer a return i.e., via ethylmalonyl-CoA. Alternatively, organic acid analysis of the minimal and defined medium formulations showed low levels of propionate compared with acetate and butyrate then increasing enzymes involved in propionyl-CoA and methyl-malonyl-CoA formation i.e., propionyl-CoA carboxylase (see section 4.6) could also be considered as sites for intervention.

Choi *et al*. (1998b) reported that the activity of methylmalonyl-CoA carboxyltransferase was highest in oil-based cultures of *S. fradiae* compared with cultures grown on glucose or starch. Tylosin levels paralleled the transferase activity. Interestingly, intracellular levels of acetate, propionic, and butyric acid also paralleled enzyme activity and tylosin results with

the oil based medium gave the highest levels of about 1 $g.g^{-1}$ dry wt of each acid. Addition of propionic acid to the various media was reported to increase tylosin titers significantly. This effect was more pronounced in glucose and starch based media. If carbon is utilised for tylactone synthesis from a number of branch points e.g., acetyl-CoA, propionyl-CoA, and butyryl-CoA it may make more sense to remove the competition between these pathways i.e., the glyoxylate branch point (removing competition between IDH and ICL). It was also possible that the CoA pool/flux and the kinetic 'pull' of the antibiotic precursors may be a limiting step in the tylosin biosynthetic pathway (see Chapter 8, for discussion).

The latter results indicate the need for more robust analytical techniques in the analysis of acetate, butyrate, and propionate or the necessity to carry out a more efficient sample clean up. Although the data do indicate that at least two precursors for tylosin synthesis accumulate to some degree toward the later stages of the fermentation. Organic acid analysis deserves further investigation to determine when this increase begins and if it can be related to the increase in broth viscosity or limitation in supply of tylosin precursors.

4.7 Summary, future work and directions

It was necessary to develop an adequate defined medium, to acquire all of the required compositional data to undertake a flux-based analysis. A number of different medium formulations were tested for their ability to produce tylosin. That have been previously used to produce tylosin, tetracycline, actinorhodin and physostigmine. The only media that significantly produced tylosin were ones that were cultured with a rich fatty acid source or complex polysaccharides. This was in good agreement with other studies (Gray and Bhuwapathanapun, 1980; Stark, 1961). The latter studies also indicate with the literature based defined medium that tylosin production starts as glucose concentration declines to zero. It was most unexpected that the mono- or di- saccharides researched in this Chapter did not yield any further enhancements to tylosin yields. When betaine was an addition to the medium there was a considerable increase in biomass yield and the degree of dispersion. No significant improvement in tylosin yields was obtained, with the medium optimisation strategy used in this work. For further research it is more likely that a fed batch or continuous culture system would have produced tylosin to greater extent where the culture could have been kept constantly nutrient limited.

A number of organic acids were produced by *S. fradiae* C373-10 cultured on a number of different carbon sources. The organic acids detected were acetate, malate, pyruvate, oxo-glutarate, propionate, butyrate, and fumarate. The reason why they were produced is as yet unknown. Comparing tylosin synthesis in the industrial complex medium with acetate, butyrate, and propionate production. Indicated that 60 % of the available carbon as tylactone precursors, was contained in acetate and 5.5 % in propionate and butyrate. If antibiotic precursor supply was considered as a rate limiting issue. Then increasing enzymes involved in butyryl-CoA synthesis may offer a return i.e., via ethylmalonyl-CoA or increasing enzymes involved in propionyl-CoA and methyl-malonyl-CoA formation i.e., propionyl-CoA carboxylase could also be considered as sites for intervention.

One of the objectives of this work was to incorporate a secondary metabolite producing pathway into a flux-based strategy. With the achievement of such low antibiotic yields, this was unlikely to be a rewarding strategy. The approach chosen was then a strategy of incorporating a systematic approach to the analyses of *S. fradiae* growth from a minimal medium with low antibiotic yields to the literature based methyl oleate defined medium with the goal of further incorporating a material balance of the industrial complex medium. In essence de-piecing the medium to its basic carbon components and measuring how the individual components distribute to biosynthesis.

Growth curves of *S. fradiae* C373-10 and metabolite profiles during growth on a glucose minimal medium (Ferm 1) [Applikon 7 L vessel]{rpm 400}.

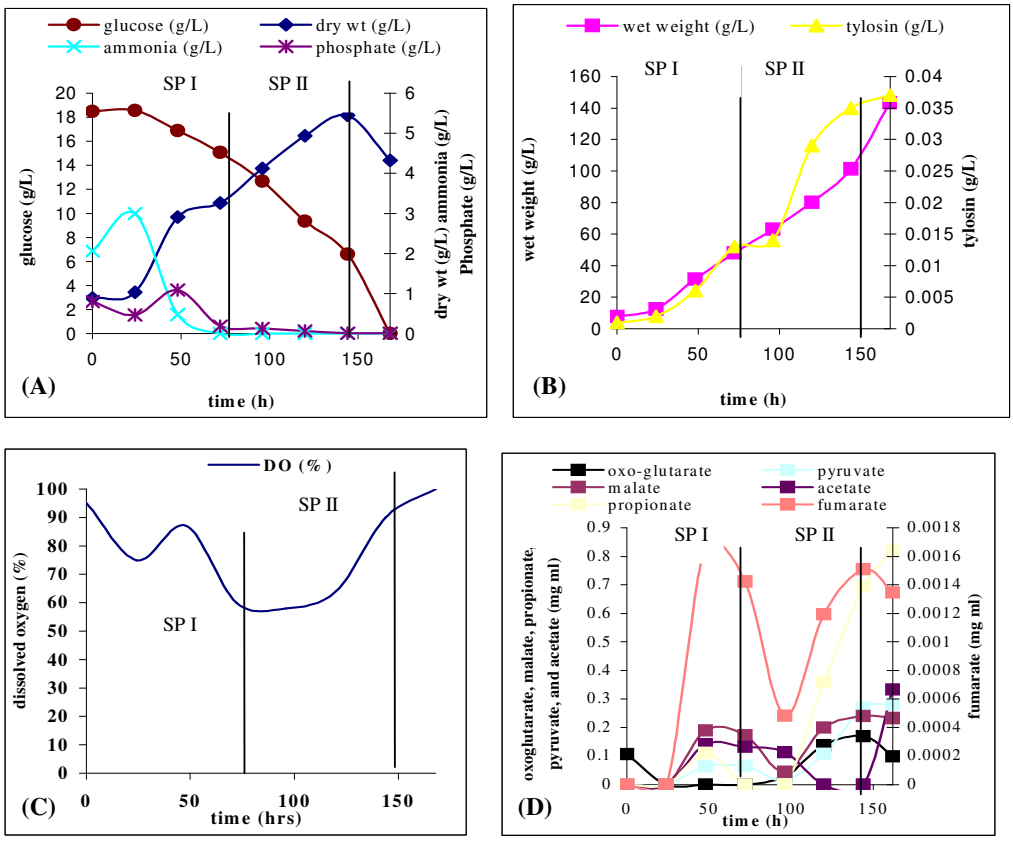

Fig 4.1. Profile of the measured extracellular on-line and off-line variables of a *S. fradiae* C373-10 fermentation cultured on a glucose minimal medium (Ferm 1). The fermenter load was maintained constant, by correcting the fermenter liquid volume back to the initial volume, after sample removal; and this was used for the on-line calculation of the volumetric OUR, CER and RQ (dissolved oxygen [DO] profile is also included) values as depicted in (C), (see Appendix E for discussion of calculations). A, depicts the profiles of biomass (dry weight), carbon source utilisation, phosphate and nitrogen uptake, B depicts tylosin production and wet weight. D, depicts the excretion of organic acids into the media over the course of the fermentation. 1 g of biomass for was collected at every 24 hr point of the culture and analysed (see Chapter 3 for analytical methods; Chapter 5 for macromolecular composition; Chapter 6 for flux analysis). Main samples points were as section 4.5.3 (Ferm 1 & 2) Day 4, phase 1, Day 7 & 6, phase II.

Growth curves of *S. fradiae* C373-10 and metabolite profiles during growth on a glucose minimal media (Ferm 2)[Applikon 7 L vessel]{rpm 400}.

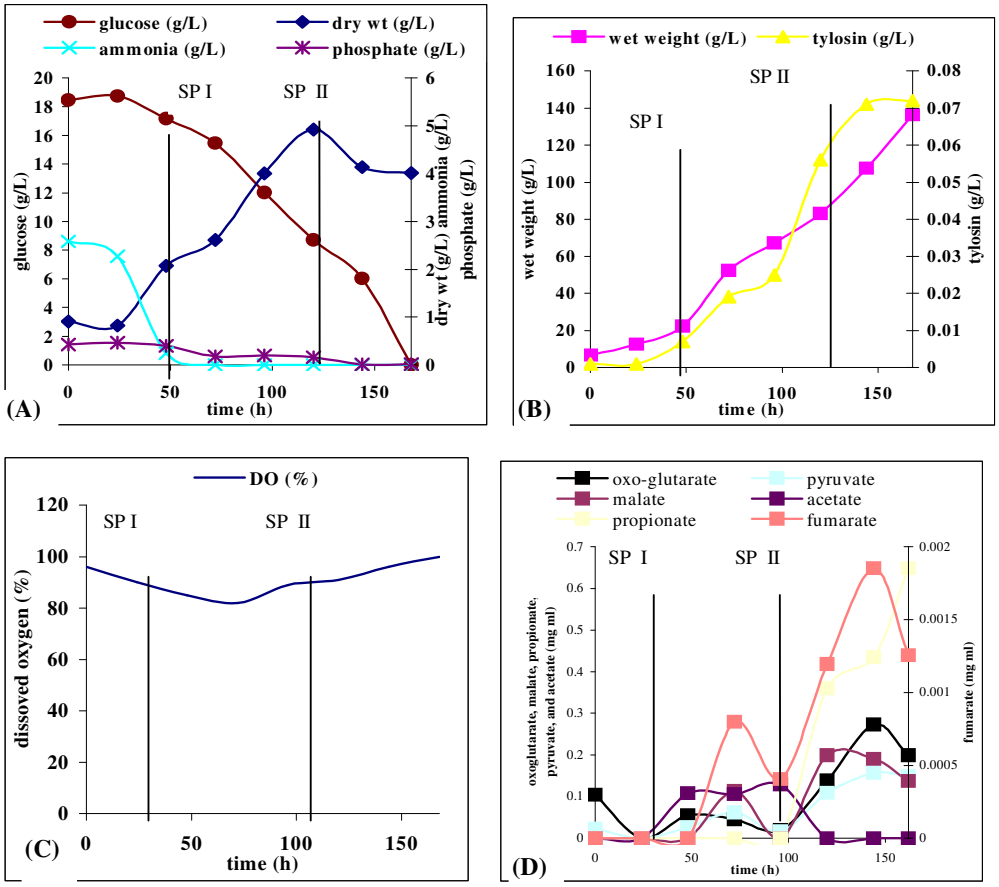

Fig 4.2. Profile of the measured extracellular on-line and off-line variables of a *S. fradiae* C373-10 fermentations cultured on a glucose minimal medium (Ferm 2). The fermenter load was maintained constant, by correcting the fermenter liquid volume back to the initial volume, after sample removal; and this was used for the on-line calculation of the volumetric OUR, CER and RQ (dissolved oxygen [DO] profile is also included) values as depicted in (C), (see Appendix E for discussion of calculations). A, depicts the profiles of biomass (dry weight), carbon source utilisation, phosphate and nitrogen uptake, B depicts tylosin production and wet weight. D, depicts the excretion of organic acids into the media over the course of the fermentations. 1 g of biomass for was collected at every 24 hr point of the culture and analysed (see Chapter 3 for analytical methods; Chapter 5 for macromolecular composition; Chapter 6 for flux analysis). Main samples points were as section 4.5.3 (Ferm 1 & 2) Day 4, phase 1, Day 7 & 6, phase II.

Growth curves of *S. fradiae* C373-10 and metabolite profiles during growth on a fructose minimal medium [New Brunswick 5 L vessel]{rpm 400}.

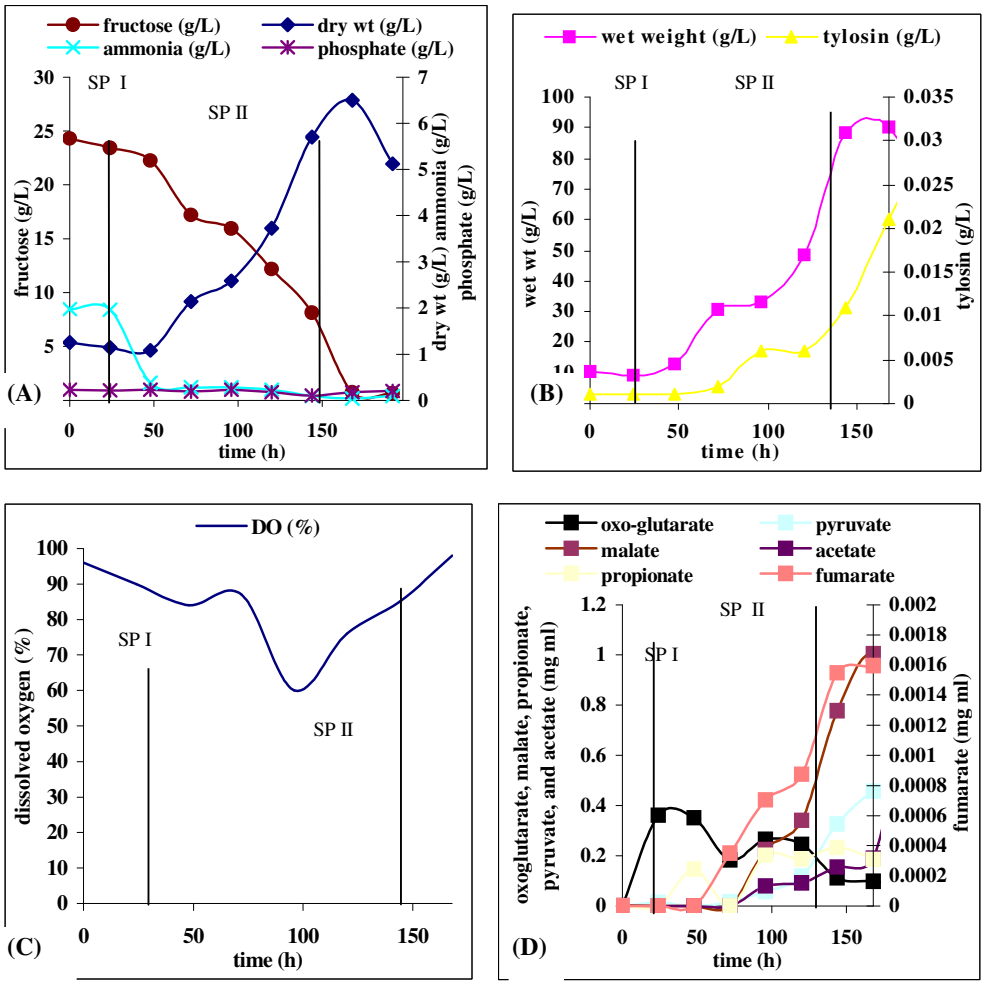

Fig 4.3. Profile of the measured extracellular on-line and off-line variables of a *S. fradiae* C373-10 fermentations cultured on a fructose minimal medium (Ferm 1). The fermenter load was maintained constant, by correcting the fermenter liquid volume back to the initial volume, after sample removal; and this was used for the on-line calculation of the volumetric OUR, CER and RQ (dissolved oxygen [DO] profile is also included) values as depicted in (C), (see Appendix E for discussion of calculations). A, depicts the profiles of biomass (dry weight), carbon source utilisation, phosphate and nitrogen uptake, B depicts tylosin production and wet weight. D, depicts the excretion of organic acids into the media over the course of the fermentations. 1 g of biomass for was collected at every 24 hr point of the culture and analysed (see Chapter 3 for analytical methods; Chapter 5 for macromolecular composition; Chapter 6 for flux analysis). Main samples points were as section 4.5.3 Day 4, phase I, Day 8, phase II.

Growth curves of *S. fradiae* C373-10 and metabolite profiles during growth on a glycerol minimal medium (Ferm 1)[New Brunswick 5 L vessel]{rpm 400}.

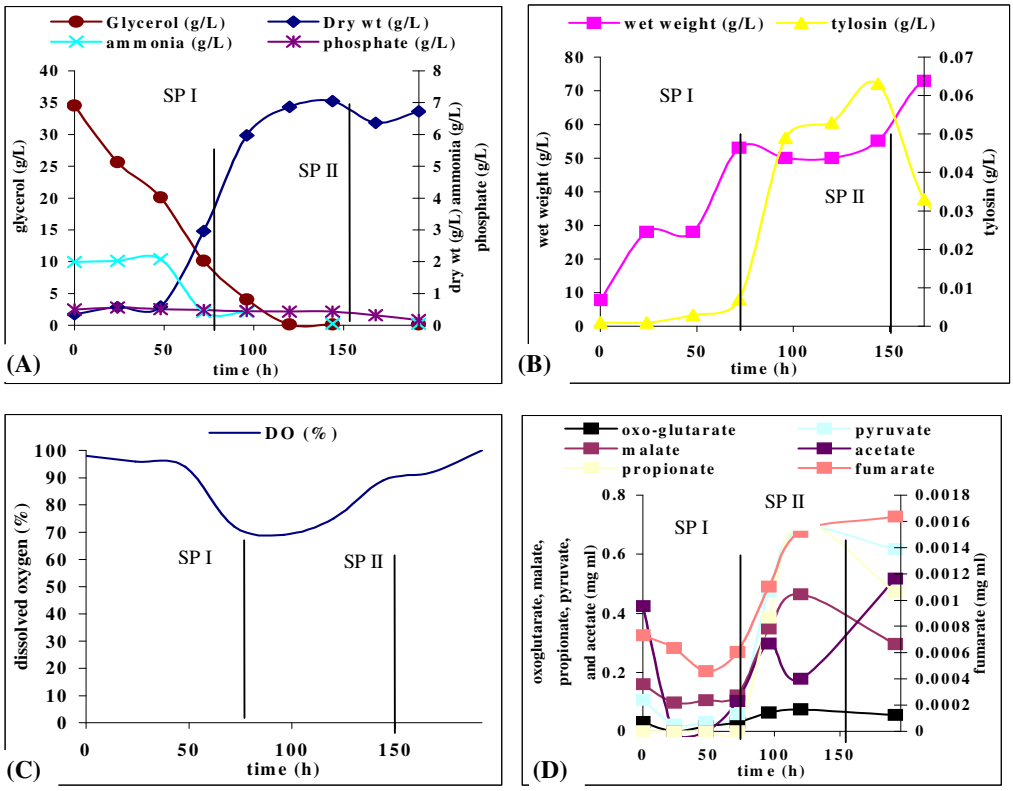

Fig 4.4. Profile of the measured extracellular on-line and off-line variables of a *S. fradiae* C373-10 fermentation cultured on a glycerol minimal medium (Ferm 1). The fermenter load was maintained constant, by correcting the fermenter liquid volume back to the initial volume, after sample removal; and this was used for the on-line calculation of the volumetric OUR, CER and RQ (dissolved oxygen [DO] profile is also included) values as depicted in (C), (see Appendix E for discussion of calculations). A, depicts the profiles of biomass (dry weight), carbon source utilisation, phosphate and nitrogen uptake, B depicts tylosin production and wet weight. D, depicts the excretion of organic acids into the media over the course of the fermentations. 1 g of biomass for was collected at every 24 hr point of the culture and analysed (see Chapter 3 for analytical methods; Chapter 5 for macromolecular composition; Chapter 6 for flux analysis). Main samples points were as section 4.5.3 (Ferm 1 & 2) Day 6 & 4, phase I, Day 7 & 9, phase II.

Growth curves of *S. fradiae* C373-10 and metabolite profiles during growth on a glycerol minimal medium (Ferm 2)[Applikon 20 L vessel]{rpm set between 300-700 and DO set point controlled at 30 %}.

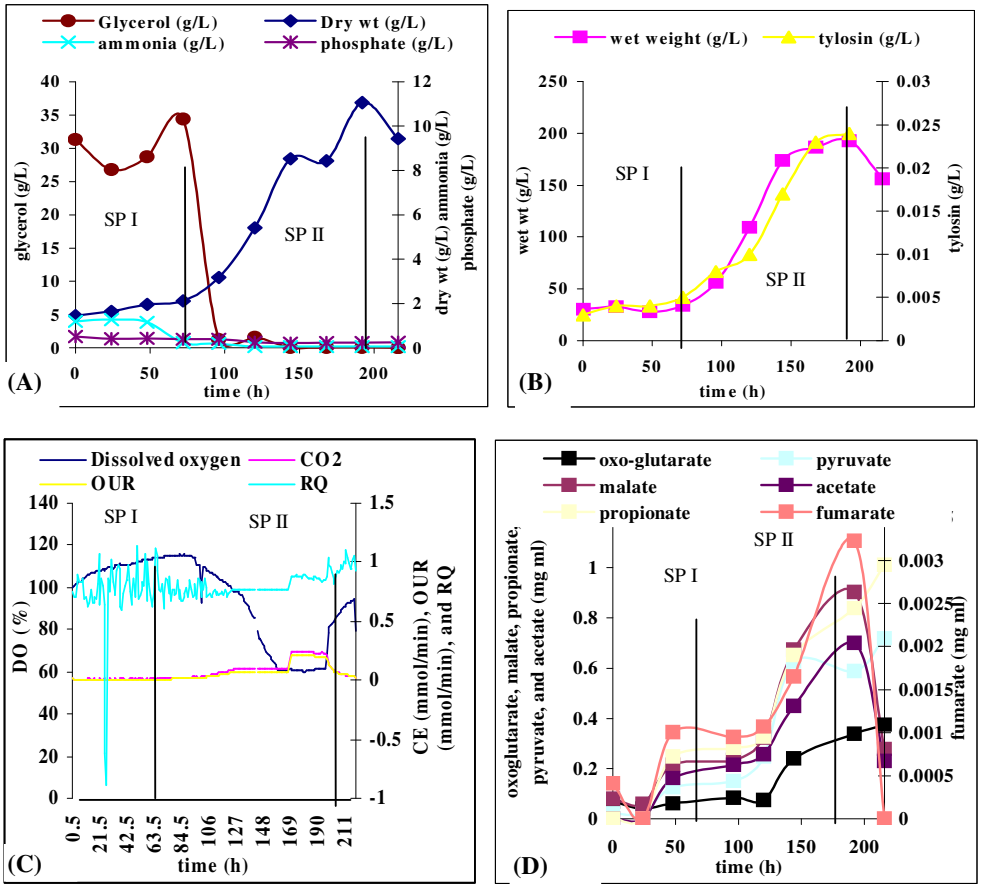

Fig 4.5. Profile of the measured extracellular on-line and off-line variables of a *S. fradiae* C373-10 fermentation cultured on a glycerol minimal medium (Ferm 2). The fermenter load was maintained constant, by correcting the fermenter liquid volume back to the initial volume, after sample removal; and this was used for the on-line calculation of the volumetric OUR, CER and RQ (dissolved oxygen [DO] profile is also included) values as depicted in (C), (see Appendix E for discussion of calculations). A, depicts the profiles of biomass (dry weight), carbon source utilisation, phosphate and nitrogen uptake, B depicts tylosin production and wet weight. D, depicts the excretion of organic acids into the media over the course of the fermentations. 1 g of biomass for was collected at every 24 hr point of the culture and analysed (see Chapter 3 for analytical methods; Chapter 5 for macromolecular composition; Chapter 6 for flux analysis). Main samples points were as section 4.5.3 (Ferm 1 & 2) Day 6 & 4, phase I, Day 7 & 9, phase II.

Growth curves of *S. fradiae* C373-10 and metabolite profiles during growth on a oxo-glutarate minimal medium (Ferm 1)[New Brunswick 5 L vessel]{rpm 400}.

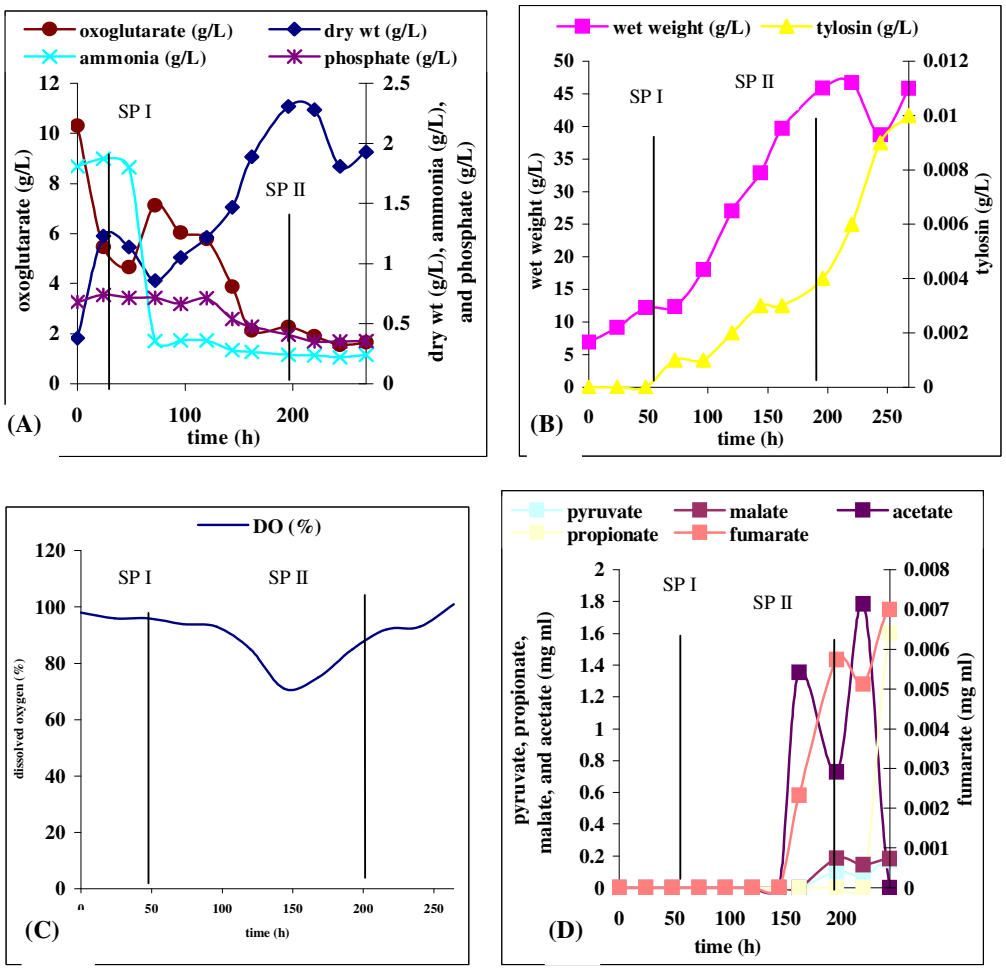

Fig 4.6. Profile of the measured extracellular on-line and off-line variables of a *S. fradiae* C373-10 fermentation cultured on a oxo-glutarate minimal medium (Ferm 1). The fermenter load was maintained constant, by correcting the fermenter liquid volume back to the initial volume, after sample removal; and this was used for the on-line calculation of the volumetric OUR, CER and RQ (dissolved oxygen [DO] profile is also included) values as depicted in (C), (see Appendix E for discussion of calculations). A, depicts the profiles of biomass (dry weight), carbon source utilisation, phosphate and nitrogen uptake, B depicts tylosin production and wet weight. D, depicts the excretion of organic acids into the media over the course of the fermentations. 1 g of biomass for was collected at every 24 hr point of the culture and analysed (see Chapter 3 for analytical methods; Chapter 5 for macromolecular composition; Chapter 6 for flux analysis). Main samples points were as section 4.5.3 (Ferm 1) Day 4, phase I, Day 10, phase II.

Growth curves of *S. fradiae* C373-10 and metabolite profiles during growth on a glucose glutamate defined media (Ferm 1) [Applikon 7 L vessel]{rpm 400}.

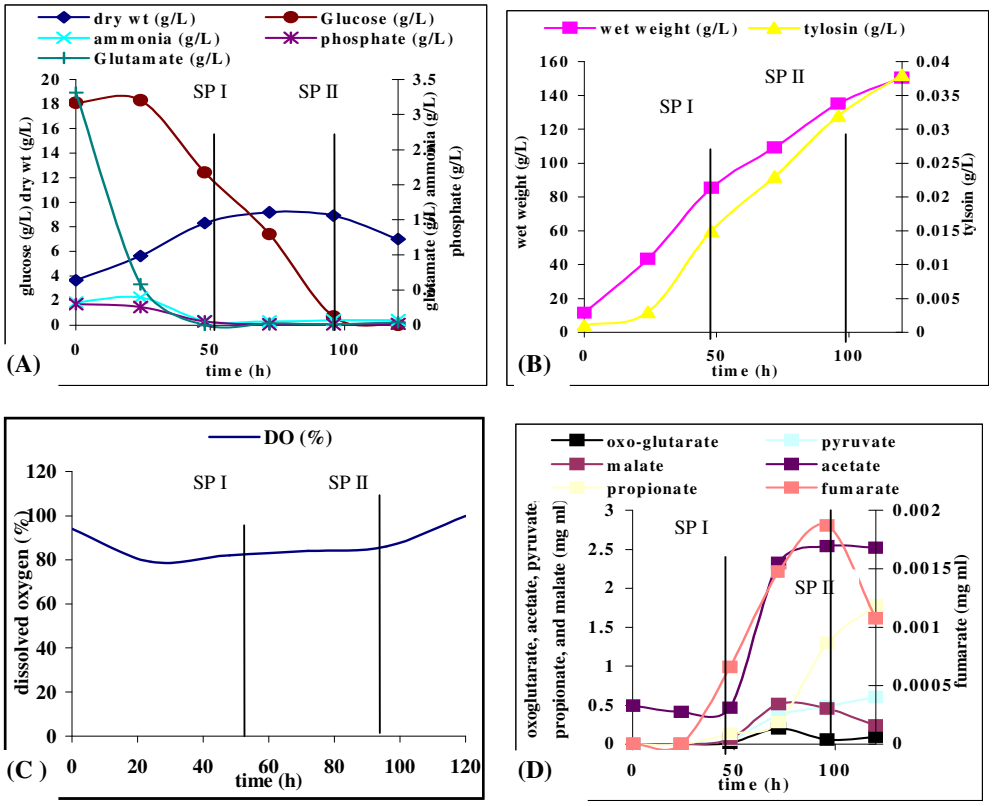

Fig 4.7. Profile of the measured extracellular on-line and off-line variables of a *S. fradiae* C373-10 fermentation cultured on a glucose glutamate defined medium (Ferm 1). The fermenter load was maintained constant, by correcting the fermenter liquid volume back to the initial volume, after sample removal; and this was used for the on-line calculation of the volumetric OUR, CER and RQ (dissolved oxygen [DO] profile is also included) values as depicted in (C), (see Appendix E for discussion of calculations). A, depicts the profiles of biomass (dry weight), carbon source utilisation, phosphate and nitrogen uptake, B depicts tylosin production and wet weight. D, depicts the excretion of organic acids into the media over the course of the fermentations. 1 g of biomass for was collected at every 24 hr point of the culture and analysed (see Chapter 3 for analytical methods; Chapter 5 for macromolecular composition; Chapter 6 for flux analysis). Main samples points were as section 4.5.3 (Ferm 1 - 4) Day 2, phase I, Day 5, phase II.

Growth curves of *S. fradiae* C373-10 and metabolite profiles during growth on a glucose glutamate defined medium (Ferm 2)[Applikon 7 L vessel]{rpm 400}.

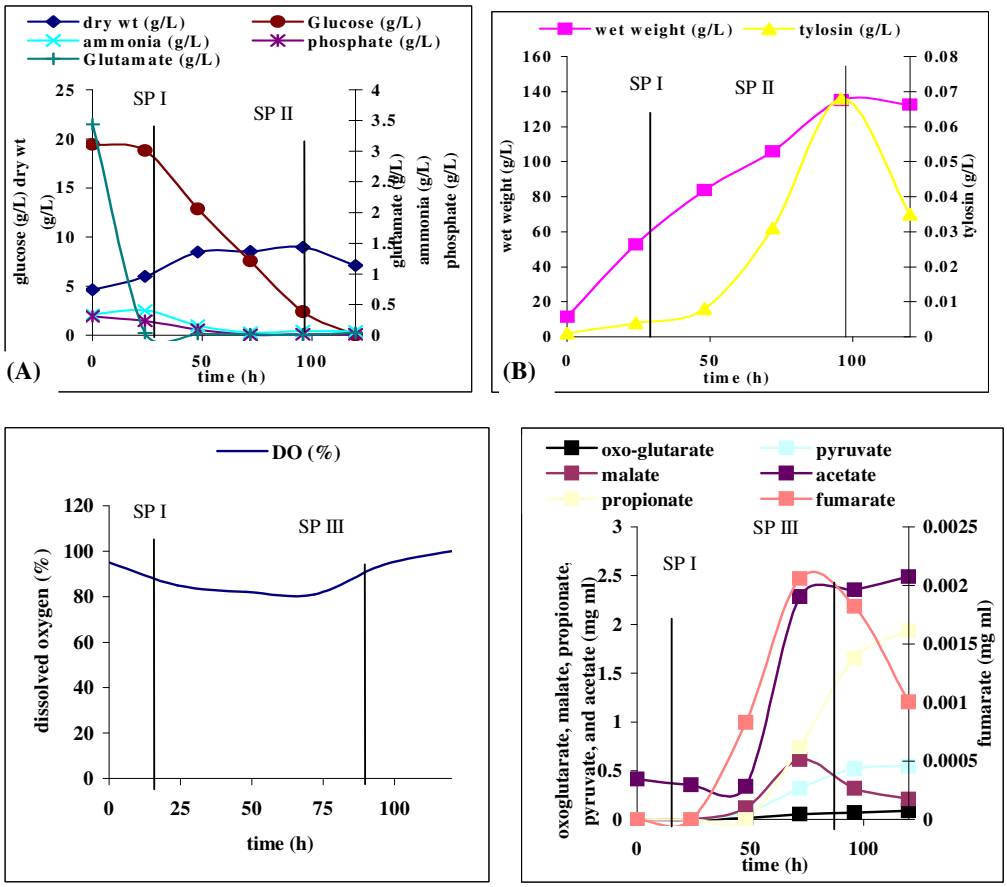

Fig 4.8. Profile of the measured extracellular on-line and off-line variables of a *S. fradiae* C373-10 fermentation cultured on a glucose glutamate defined medium (Ferm 2) The fermenter load was maintained constant, by correcting the fermenter liquid volume back to the initial volume, after sample removal; and this was used for the on-line calculation of the volumetric OUR, CER and RQ (dissolved oxygen [DO] profile is also included) values as depicted in (C), (see Appendix E for discussion of calculations). A, depicts the profiles of biomass (dry weight), carbon source utilisation, phosphate and nitrogen uptake, B depicts tylosin production and wet weight. D, depicts the excretion of organic acids into the media over the course of the fermentations. 1 g of biomass for was collected at every 24 hr point of the culture and analysed (see Chapter 3 for analytical methods; Chapter 5 for macromolecular composition; Chapter 6 for flux analysis). Main samples points were as section 4.5.3 (Ferm 1 - 4) Day 2, phase I, Day 5, phase II.

Growth curves of *S. fradiae* C373-10 and metabolite profiles during growth on a glucose glutamate defined medium (Ferm 3)[Applikon 7 L vessel]{rpm 400}.

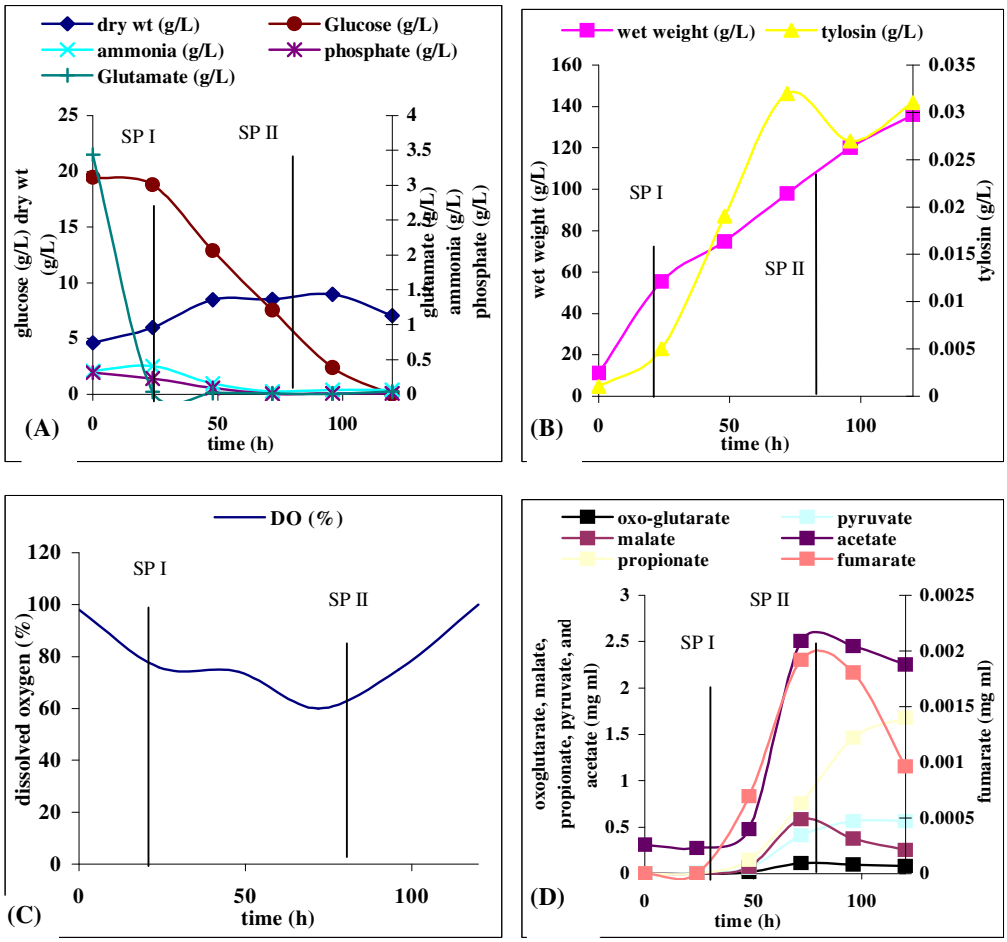

Fig 4.9. Profile of the measured extracellular on-line and off-line variables of a *S. fradiae* C373-10 fermentation cultured on a glucose glutamate defined medium (Ferm 3). The fermenter load was maintained constant, by correcting the fermenter liquid volume back to the initial volume, after sample removal; and this was used for the on-line calculation of the volumetric OUR, CER and RQ (dissolved oxygen [DO] profile is also included) values as depicted in (C), (see Appendix E for discussion of calculations). A, depicts the profiles of biomass (dry weight), carbon source utilisation, phosphate and nitrogen uptake, B depicts tylosin production and wet weight. D, depicts the excretion of organic acids into the media over the course of the fermentations. 1 g of biomass for was collected at every 24 hr point of the culture and analysed (see Chapter 3 for analytical methods; Chapter 5 for macromolecular composition; Chapter 6 for flux analysis). Main samples points were as section 4.5.3 (Ferm 1 - 4) Day 2, phase I, Day 5, phase II.

Growth curves of *S. fradiae* C373-10 and metabolite profiles during growth on a glucose glutamate defined medium (Ferm 4)[Applikon 7 L vessel]{rpm 400}.

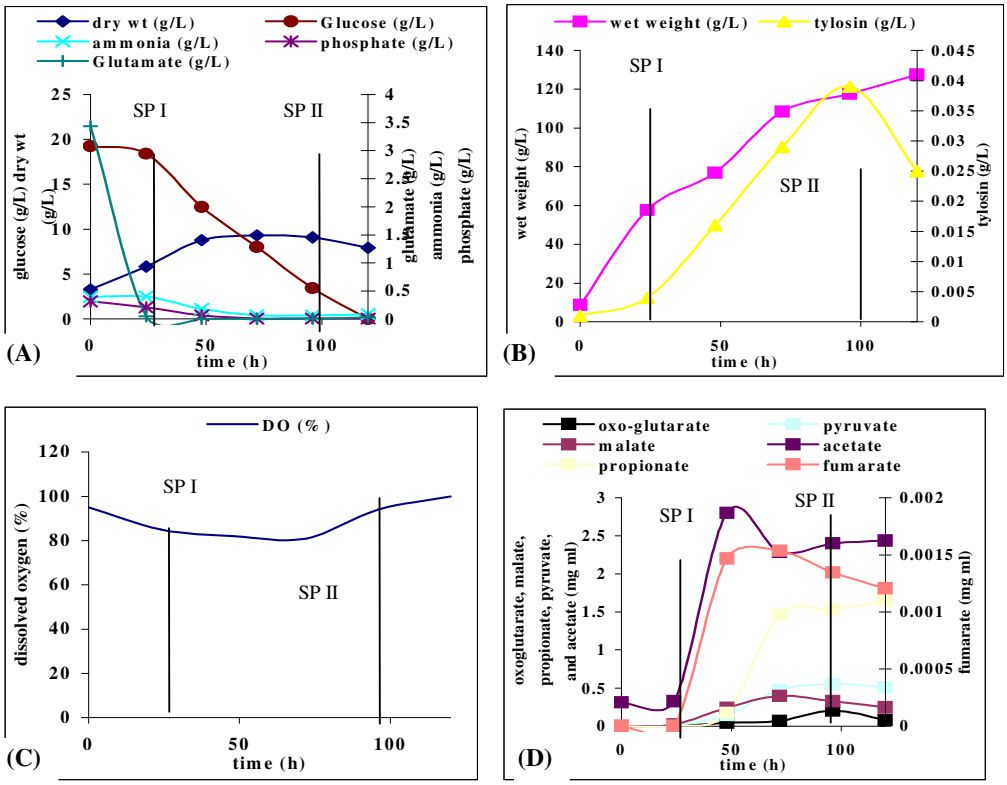

Fig 4.10. Profile of the measured extracellular on-line and off-line variables of a *S. fradiae* C373-10 fermentation cultured on a glucose glutamate defined medium (Ferm 4). The fermenter load was maintained constant, by correcting the fermenter liquid volume back to the initial volume, after sample removal; and this was used for the on-line calculation of the volumetric OUR, CER and RQ (dissolved oxygen [DO] profile is also included) values as depicted in (C), (see Appendix E for discussion of calculations). A, depicts the profiles of biomass (dry weight), carbon source utilisation, phosphate and nitrogen uptake, B depicts tylosin production and wet weight. D, depicts the excretion of organic acids into the media over the course of the fermentations. 1 g of biomass for was collected at every 24 hr point of the culture and analysed (see Chapter 3 for analytical methods; Chapter 5 for macromolecular composition; Chapter 6 for flux analysis). Main samples points were as section 4.5.3 (Ferm 1 - 4) Day 2, phase I, Day 5, phase II.

Growth curves of *S. fradiae* C373-10 and metabolite profiles during growth on a glucose oxo-glutarate defined medium (Ferm 1)[Applikon 7 L vessel]{rpm 400}.

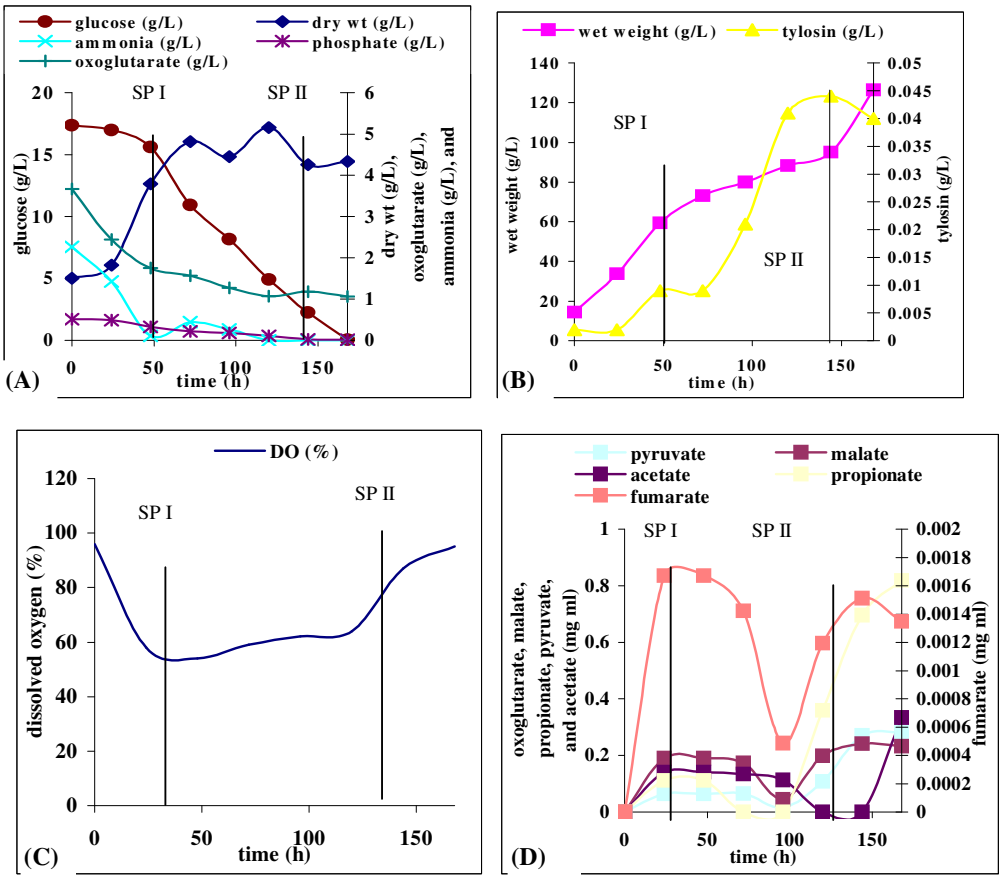

Fig 4.11. Profile of the measured extracellular on-line and off-line variables of a *S. fradiae* C373-10 fermentation cultured on a glucose oxo-glutarate defined medium (Ferm 1). The fermenter load was maintained constant, by correcting the fermenter liquid volume back to the initial volume, after sample removal; and this was used for the on-line calculation of the volumetric OUR, CER and RQ (dissolved oxygen [DO] profile is also included) values as depicted in (C), (see Appendix E for discussion of calculations). A, depicts the profiles of biomass (dry weight), carbon source utilisation, phosphate and nitrogen uptake, B depicts tylosin production and wet weight. D, depicts the excretion of organic acids into the media over the course of the fermentations. 1 g of biomass for was collected at every 24 hr point of the culture and analysed (see Chapter 3 for analytical methods; Chapter 5 for macromolecular composition; Chapter 6 for flux analysis). Main samples points were as section 4.5.3 (Ferm 1) Day 4, phase I, Day 10, phase II.

Growth curves of *S. fradiae* C373-10 and metabolite profiles during growth on a glucose oxo-glutarate defined medium (Ferm 2)[Applikon 7 L vessel]{rpm 400}.

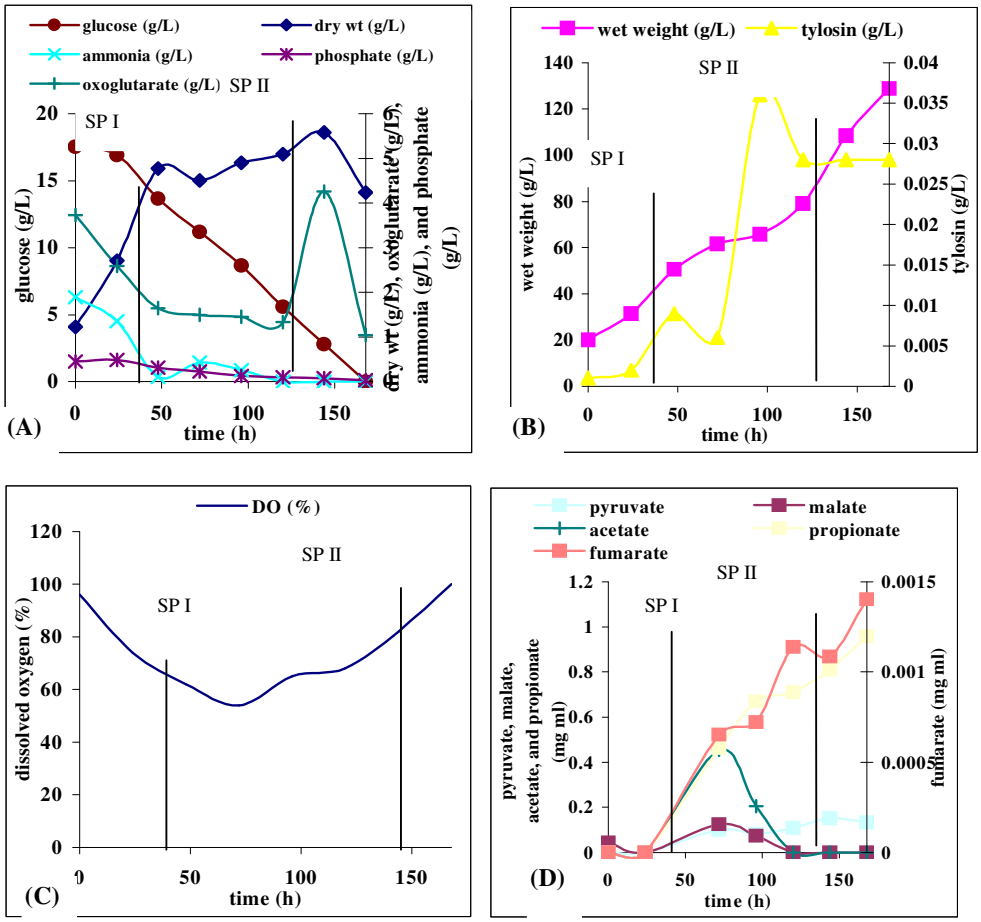

Fig 4.12. Profile of the measured extracellular on-line and off-line variables of a *S. fradiae* C373-10 fermentation cultured on a glucose oxo-glutarate defined medium (Ferm 2). The fermenter load was maintained constant, by correcting the fermenter liquid volume back to the initial volume, after sample removal; and this was used for the on-line calculation of the volumetric OUR, CER and RQ (dissolved oxygen [DO] profile is also included) values as depicted in (C), (see Appendix E for discussion of calculations). A, depicts the profiles of biomass (dry weight), carbon source utilisation, phosphate and nitrogen uptake, B depicts tylosin production and wet weight. D, depicts the excretion of organic acids into the media over the course of the fermentations. 1 g of biomass for was collected at every 24 hr point of the culture and analysed (see Chapter 3 for analytical methods; Chapter 5 for macromolecular composition; Chapter 6 for flux analysis). Main samples points were as section 4.5.3 (Ferm 1 & 2) Day 3, phase I, Day 7, phase II.

Growth curves of *S. fradiae* C373-10 and metabolite profiles during growth on methyl oleate defined medium (Ferm 1; seed medium 1, Chapter 3, section 3.5.1 with glucose)[Applikon 20 L vessel]{rpm set between 300 – 700 and DO set point controlled at 30 %}.

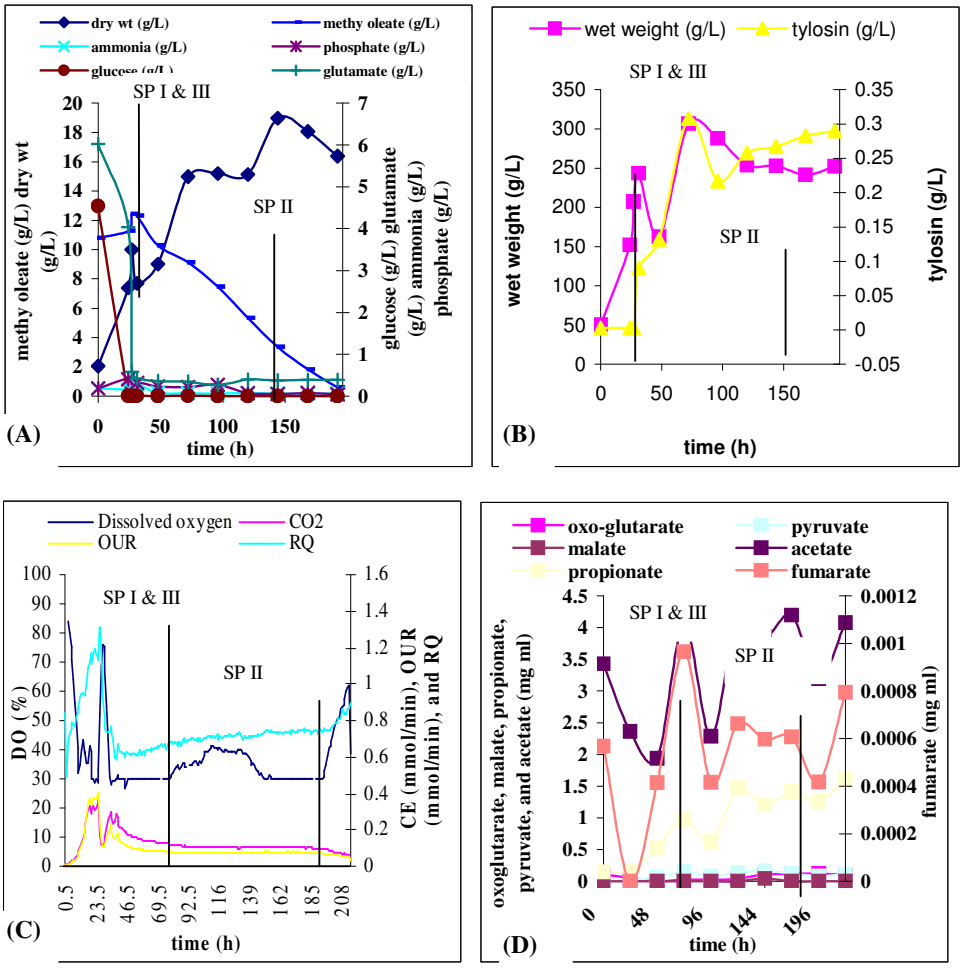

Fig 4.13. Profile of the measured extracellular on-line and off-line variables of a *S. fradiae* C373-10 fermentation cultured on a methyl oleate defined medium (Chapter 3, section 3.7)[Ferm 1). The fermenter load was maintained constant, by correcting the fermenter liquid volume back to the initial volume, after sample removal; and this was used for the on-line calculation of the volumetric OUR, CER and RQ (dissolved oxygen [DO] profile is also included) values as depicted in (C), (see Appendix E for discussion of calculations). A, depicts the profiles of biomass (dry weight), carbon source utilisation, phosphate and nitrogen uptake, B depicts tylosin production and wet weight. D, depicts the excretion of organic acids into the media over the course of the fermentations. 1 g of biomass for was collected at every 24 hr point of the culture and analysed (see Chapter 3 for analytical methods; Chapter 5 for macromolecular composition; Chapter 6 for flux analysis). Main samples points were as section 4.5.3 (Ferm 1 - 3) Day 2, Day 3, & Day 3, phase I, Day 3, Day 4, & Day 4, phase III, Day 9, Day 9, & Day 7, phase II.

Growth curves of *S. fradiae* C373-10 and metabolite profiles during growth on methyl oleate defined medium (Ferm 2; seed medium 2, Chapter 3, section 3.5.2 minus glucose) [Applikon 20 L vessel]{rpm set between 300 – 700 and DO set point controlled at 30 %}.

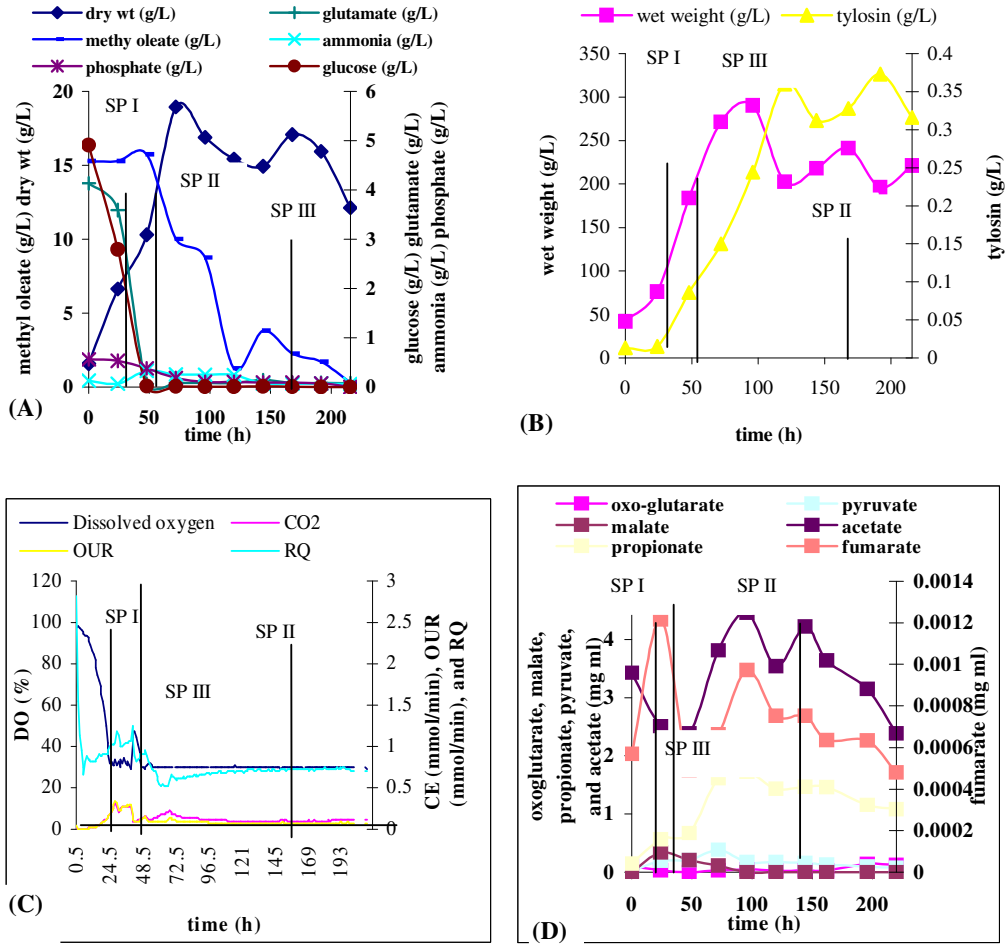

Fig 4.14. Profile of the measured extracellular on-line and off-line variables of a *S. fradiae* C373-10 fermentation cultured on a methyl oleate defined medium (Chapter 3, section 3.7)[Ferm 2). The fermenter load was maintained constant, by correcting the fermenter liquid volume back to the initial volume, after sample removal; and this was used for the on-line calculation of the volumetric OUR, CER and RQ (dissolved oxygen [DO] profile is also included) values as depicted in (C), (see Appendix E for discussion of calculations). A, depicts the profiles of biomass (dry weight), carbon source utilisation, phosphate and nitrogen uptake, B depicts tylosin production and wet weight. D, depicts the excretion of organic acids into the media over the course of the fermentations. 1 g of biomass for was collected at every 24 hr point of the culture and analysed (see Chapter 3 for analytical methods; Chapter 5 for macromolecular composition; Chapter 6 for flux analysis). Main samples points were as section 4.5.3 (Ferm 1 - 3) Day 2, Day 3, & Day 3, phase I, Day 3, Day 4, & Day 4, phase III, Day 9, Day 9, & Day 7, phase II.

Growth curves of *S. fradiae* C373-10 and metabolite profiles during growth on Grays defined medium (Ferm 3) [Applikon 20 L vessel]{rpm set between 300 – 700 and DO set point controlled at 30 %}.

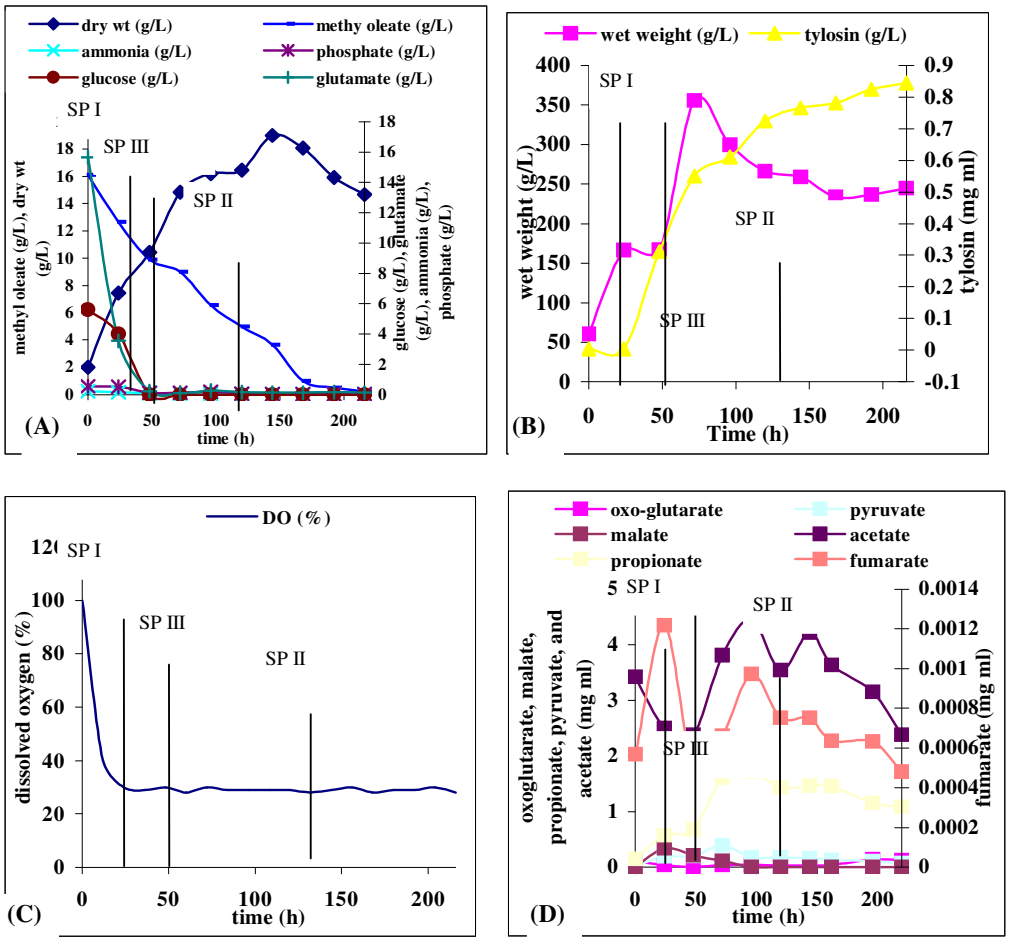

Fig 4.15. Profile of the measured extracellular on-line and ıe variables of a *S. fradiae* C373-10 fermentation cultured on a methyl oleate defined medium (Chapter 3, section 3.7)[Ferm 3). The fermenter load was maintained constant, by correcting the fermenter liquid volume back to the initial volume, after sample removal; and this was used for the on-line calculation of the volumetric OUR, CER and RQ (dissolved oxygen [DO] profile is also included) values as depicted in (C), (see Appendix E for discussion of calculations). A, depicts the profiles of biomass (dry weight), carbon source utilisation, phosphate and nitrogen uptake, B depicts tylosin production and wet weight. D, depicts the excretion of organic acids into the media over the course of the fermentations. 1 g of biomass for was collected at every 24 hr point of the culture and analysed (see Chapter 3 for analytical methods; Chapter 5 for macromolecular composition; Chapter 6 for flux analysis). Main samples points were as section 4.5.3 (Ferm 1 - 3) Day 2, Day 3, & Day 3, phase I, Day 3, Day 4, & Day 4, phase III, Day 9, Day 9, & Day 7, phase II.

Growth curves of *S. fradiae* C373-10 and metabolite profiles during growth on an industrial complex medium (Ferm 1) [Applikon 20 L vessel]{rpm set between 300 – 700 and DO set point controlled at 30 %}.

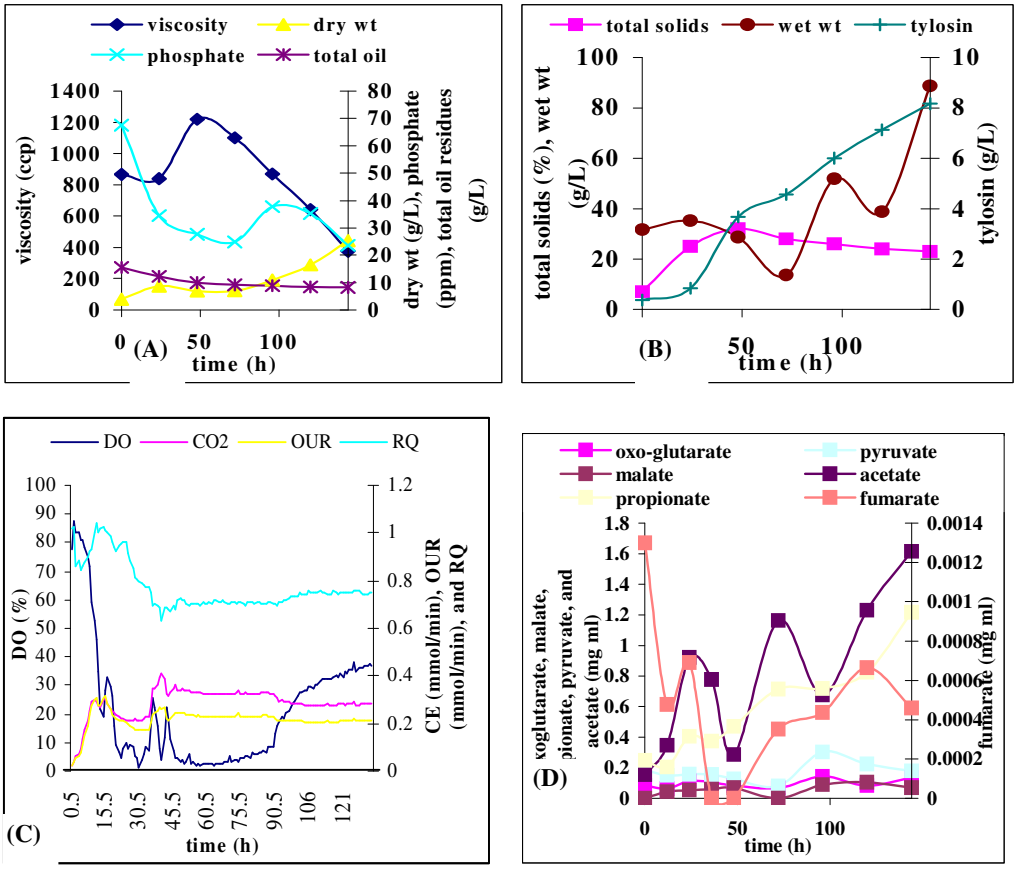

Fig 4.16. Profile of the measured extracellular on-line and off-line variables of a *S. fradiae* C373-10 fermentation cultured on a industrial complex medium (Ferm 1). The fermenter load was maintained constant, by correcting the fermenter liquid volume back to the initial volume, after sample removal; and this was used for the on-line calculation of the volumetric OUR, CER and RQ (dissolved oxygen [DO] profile is also included) values as depicted in (C), (see Appendix E for discussion of calculations). A, depicts the profiles of biomass (dry weight), carbon source utilisation, phosphate and nitrogen uptake, B depicts tylosin production and wet weight. D, depicts the excretion of organic acids into the media over the course of the fermentations. 1 g of biomass for was collected at every 24 hr point of the culture and analysed (see Chapter 3 for analytical methods; Chapter 5 for macromolecular composition; Chapter 6 for flux analysis).

Growth curves of *S. fradiae* C373-10 and metabolite profiles during growth on an industrial complex medium (Ferm 2) [Applikon 20 L vessel]{rpm set between 300 – 700 and DO set point controlled at 30 %}.

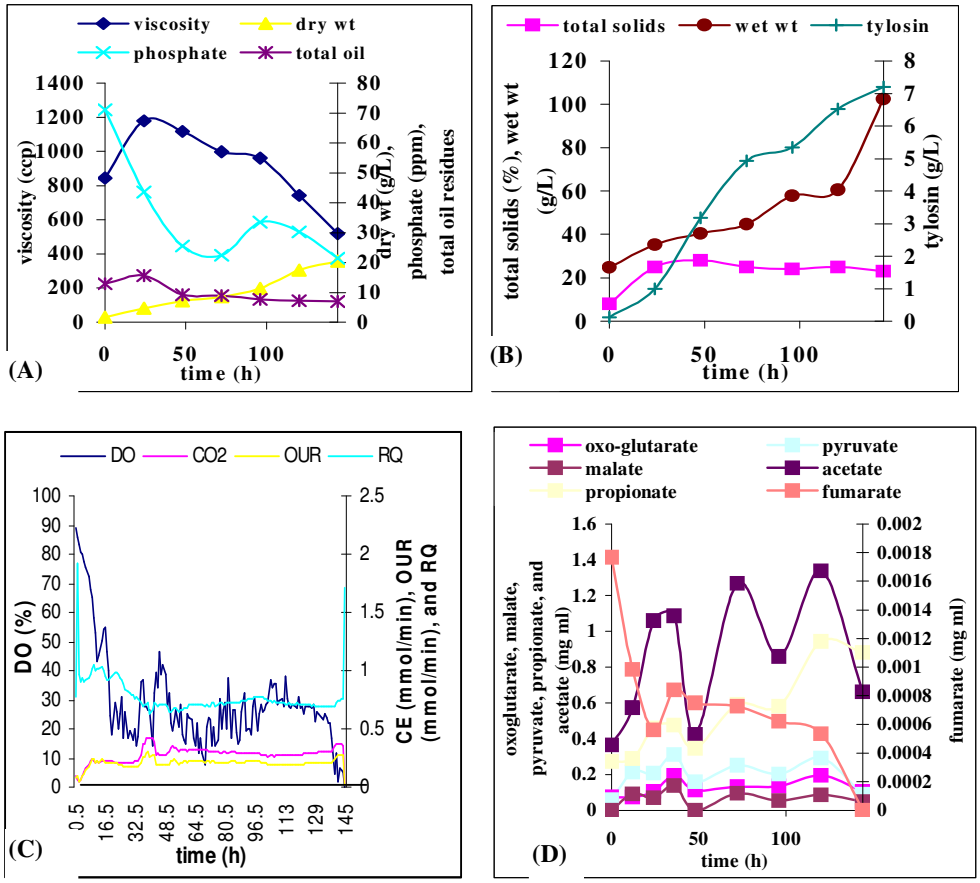

Fig 4.17. Profile of the measured extracellular on-line and off-line variables of a *S. fradiae* C373-10 fermentation cultured on a industrial complex medium (Ferm 2). The fermenter load was maintained constant, by correcting the fermenter liquid volume back to the initial volume, after sample removal; and this was used for the on-line calculation of the volumetric OUR, CER and RQ (dissolved oxygen [DO] profile is also included) values as depicted in (C), (see Appendix E for discussion of calculations). A, depicts the profiles of biomass (dry weight), carbon source utilisation, phosphate and nitrogen uptake, B depicts tylosin production and wet weight. D, depicts the excretion of organic acids into the media over the course of the fermentations. 1 g of biomass for was collected at every 24 hr point of the culture and analysed (see Chapter 3 for analytical methods; Chapter 5 for macromolecular composition; Chapter 6 for flux analysis).

Growth curves of *S. fradiae* C373-10 and metabolite profiles during growth on an industrial complex medium (Ferm 3) [Applikon 20 L vessel]{rpm set between 300 – 700 and DO set point controlled at 30 %}.

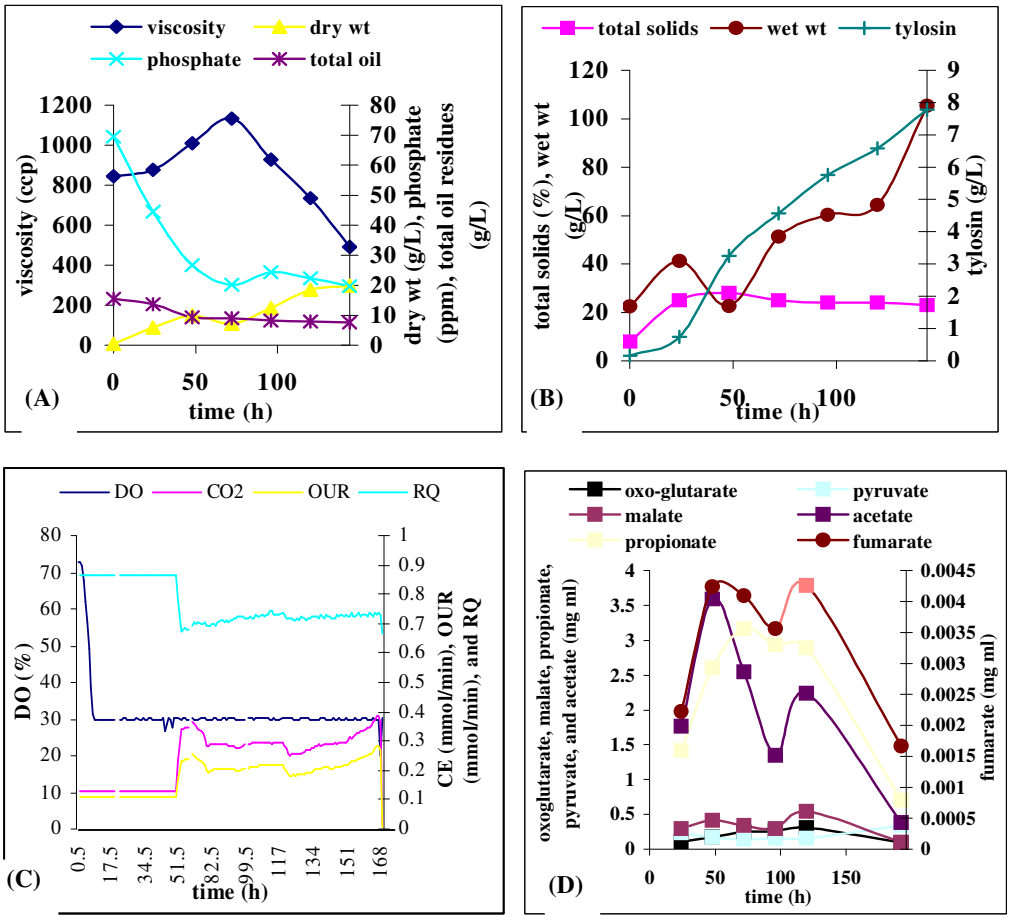

Fig 4.18. Profile of the measured extracellular on-line and off-line variables of a *S. fradiae* C373-10 fermentation cultured on a industrial complex medium (Ferm 3). The fermenter load was maintained constant, by correcting the fermenter liquid volume back to the initial volume, after sample removal; and this was used for the on-line calculation of the volumetric OUR, CER and RQ (dissolved oxygen [DO] profile is also included) values as depicted in (C), (see Appendix E for discussion of calculations). A, depicts the profiles of biomass (dry weight), carbon source utilisation, phosphate and nitrogen uptake, B depicts tylosin production and wet weight. D, depicts the excretion of organic acids into the media over the course of the fermentations. 1 g of biomass for was collected at every 24 hr point of the culture and analysed (see Chapter 3 for analytical methods; Chapter 5 for macromolecular composition; Chapter 6 for flux analysis).

Fig 4.19 & 4.20. Growth curves of *S. coelicolor* 1147 cultured on glucose (Ferm 1 & 2 respectively)[New Brunswick 2.5 L vessel] {rpm 400}.

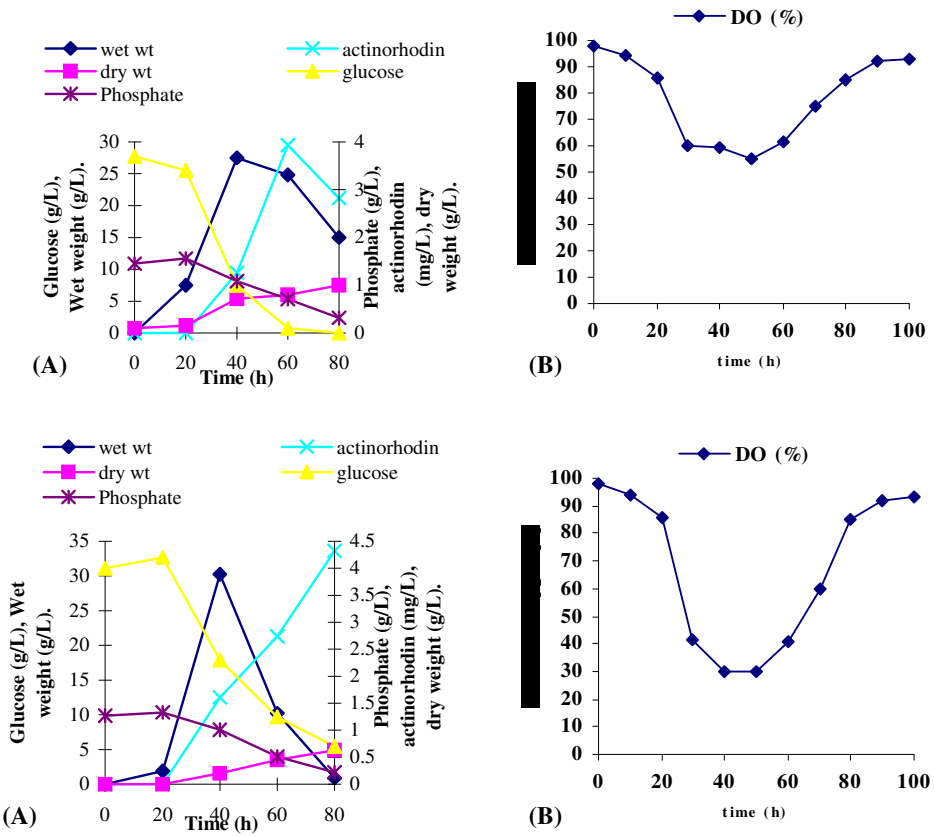

Fig 4.19. Profile of the measured extracellular on-line and off-line variables of a *S. coelicolor* fermentation cultured on a glucose minimal medium (Ferm 1 & 2). A, depicts the profiles of biomass (dry weight & wet weight), carbon source utilisation, phosphate and nitrogen uptake, actinorhodin production B depicts DO. 1 g of biomass for was collected at every 24 hr point of the culture and analysed (see Chapter 3 for analytical methods; Chapter 5 for macromolecular composition; Chapter 6 for flux analysis).

Organic acid profile of the industrial complex medium *S. fradiae* C373-18

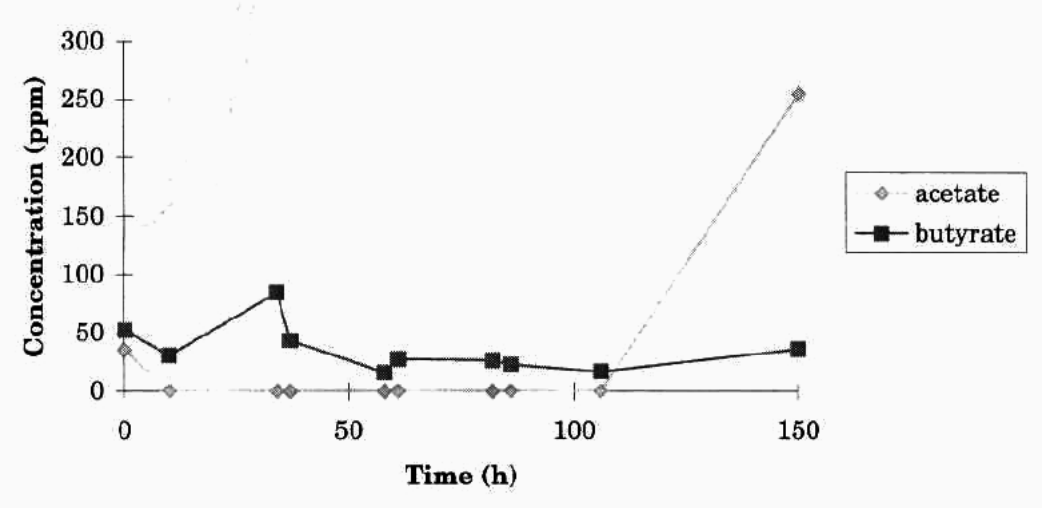

Fig 4.21 Acetate and butyrate concentration in tylosin broth samples cultured with *S. fradiae* C373-18. The analysis was undertaken onsite at Eli Lilly Ltd. (Schreiweis, 1999) utilizing ion chromatography.

Tylosin synthesis rate compared to a theoretical linear rate

(a) Tylosin synthesis rate (strain C373-18) analysis undertaken onsite at Eli Lilly Ltd. (Schreiweis, 1999)

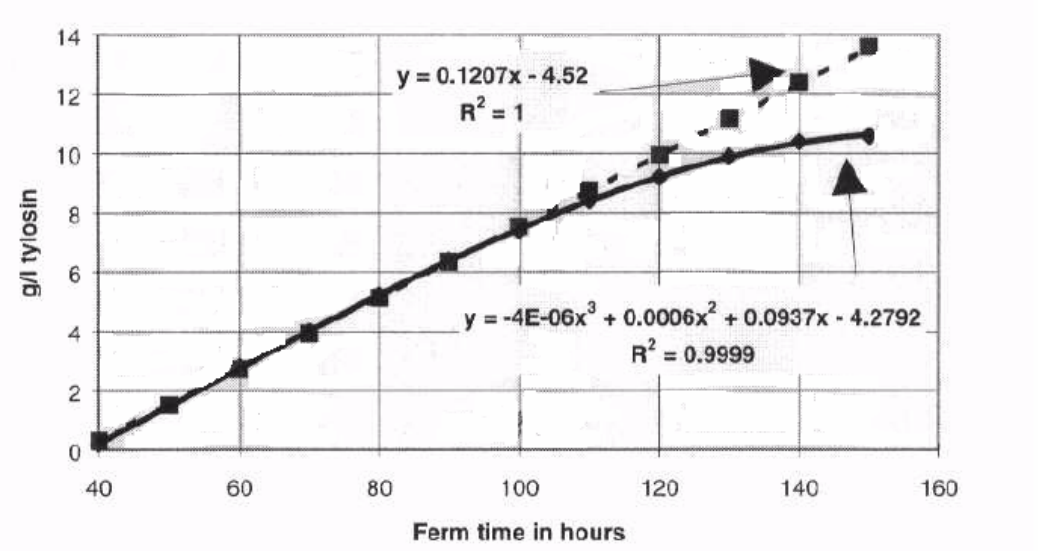

(b) Tylosin synthesis rate (strain C373-10)[corresponds to Fig 4.16]

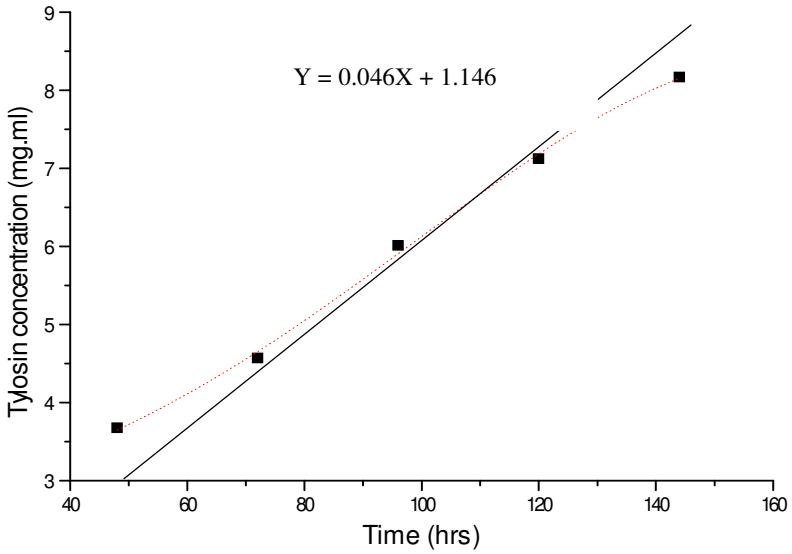

Fig 4.22 Graphical representation of the average tylosin synthesis rate for strain (Fig 4.16 - 4.18) C373-18 compared to the extrapolation of a linear synthetic rate based

on the production rate experienced in the 40 to 100 hour fermentation period of the industrial complex fermentation.

Tylosin synthesis rate compared to a theoretical linear rate

(c) Tylosin synthesis rate (strain C373-10) [corresponds to Fig 4.17]

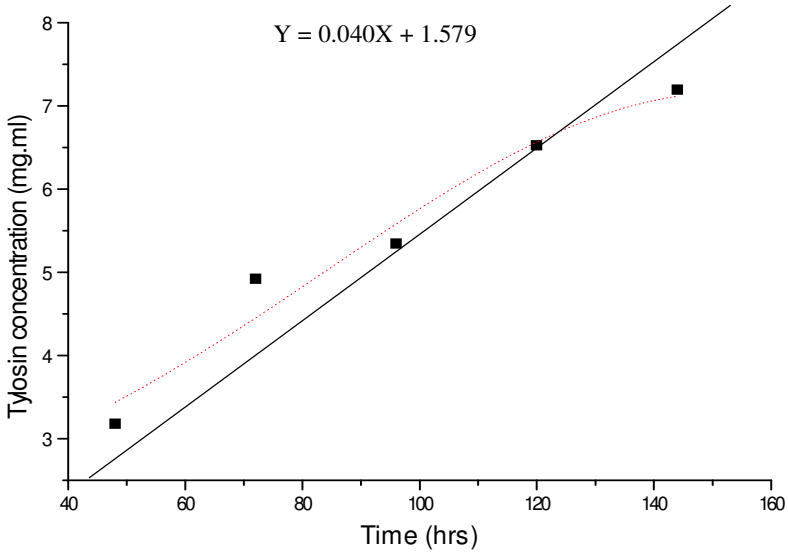

(d) Tylosin synthesis rate (strain C373-10) [corresponds to Fig 4.18]

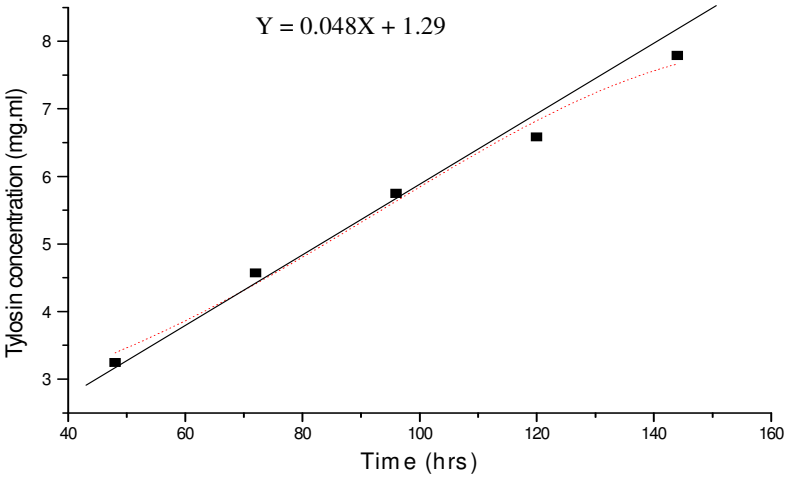

Fig 4.22 Graphical representation of the average tylosin synthesis rate for strain (Fig 4.16 - 4.18) C373-18 compared to the extrapolation of a linear synthetic rate based

on the production rate experienced in the 40 to 100 hour fermentation period of the industrial complex fermentation.

Chapter 5

Elemental and molecular biomass composition of *S. coelicolor* 1147 & *S. fradiae* C373-10

5.0 Introduction

Cells consist of a large variety of different biopolymers and macromolecules. Knowledge of their composition and quantity is essential for a metabolic and energetic analysis of the biomass growth and product yield. However, analysis is laborious and prone to errors, due to the complexity of the biomass.

Two types of analysis are performed i.e., elemental or molecular. The elemental composition is required for the "black box" description of the biomass [see Chapter 1, section 1.2 and Appendix A; Duboc *et al*., 1995; Heijnen & Roels, 1981; Verduyn *et al*., 1991], whereas analysis of the monomeric and macromolecular composition must be considered for flux calculations in metabolic models (see Appendix B; Holms, 1986; Parrau *et al*., 1991). However, Vallino & Stephanopoulos (1993) based their flux analysis on the measured elemental composition, and the molecular biomass composition was fitted accordingly (see Chapter 1, section 1.2.3, Fig 1.1). Precise knowledge of the biomass composition is required for parameters derived from flux analysis, such as the P/O ratio (The ratio of the number of ATP's produced to the number of atmospheric oxygen atoms converted to water) and the growth-dependent maintenance requirement. Exact data are further needed in dynamic models to, for example, quantify the depletion of intracellular metabolite pools during pulses due to anabolic fluxes (see Chapter 1, section 1.2.3).

Considerable time and effort has been spent on the exact determination of the elemental composition of microbial biomass and the required analytical procedure (Battley, 1995; Duboc *et al*., 1995; Guarakan *et al*., 1990; Vriezen, 1998). Although carbon (C), hydrogen (H), and nitrogen (N) determination is commonly done with good precision, the oxygen (O) content is rarely measured but is derived by subtraction from the content of the measured elements and ash content (Nielsen & Villadsen, 1994). Battley (1995) indicated that the quantification of elements through ash content measurements can lead to significant errors. The quantity of oxygen bound is the major unknown in the ash and the

unclear fate of sulphur (S) during the process cause a large uncertainty in the ash determination and subsequently, in the amount of oxygen calculated for the biomass (Battley, 1995; Duboc *et al*., 1995). Dried biomass can readily and rapidly re-absorb humidity, changing weight and composition of the sample, which can further distort the hydrogen and oxygen measurements (Gurakan *et al*., 1990). Nonetheless, the material and energetic balancing of biological processes requires the exact quantity of the molecular composition of the organism.

The quantification of the cellular components such as lipids or carbohydrates (CHOs) has also received increasing attention (Herbert *et al*., 1971; Oura, 1972; Schulze, 1995; Stewart, 1975; Vriezen, 1998). For simplicity, the biomass is commonly described as consisting of five groups of macromolecules: proteins, CHOs, lipids, RNA, and DNA. Together with water and metals, these components give the molecular composition of the biomass. The required analytical methods for these macromolecules are laborious and prone to interference due to the wide range of different molecules collectively measured as, for example, CHOs (measured as glucose equivalents) and the varying degree of polymerisation in different proteins. In addition, inaccuracies accrue from the measurement of the macromolecules from individual monomeric components i.e., usually one or two amino acids (aas) of a standard protein are used to account for the total protein (section 5.4.3). Therefore if the aa composition alters from species to species, this will have a considerable effect on a compositional study. Again, the hygroscopic nature of dried biomass complicates these measurements. Precise quantification of the water content is also problematic. Hence, complete analysis of a microorganism cultivated under well defined growth conditions is rarely reported in terms of both elemental and molecular composition.

It is obvious that the elemental composition of biomass as well as its molecular composition should be consistent, since a known molecular composition directly defines the elemental composition. Comparison of both values frequently shows discrepancies (Duboc *et al*., 1995; Vriezen, 1998). Duboc *et al*. (1995) stated that this mismatch was mainly due to large errors in the quantification of the polymer content. Schulze (1995) reported the measured carbon : nitrogen ratio based on the molecular biomass composition and found that the carbon : nitrogen ratio as measured by elemental analysis lies on

average 20 % above the value derived from the molecular components (see section 5.10.3). However, a systematic matching of the information from both elemental and molecular analysis; has only been attempted by Lange & Heijnen (2001) for *Saccharomyces cerevisiae*.

The precise knowledge of these values is essential for energetic and metabolic calculations. Vriezen (1998) noted that fluxes in a metabolic network of hybridoma cultures may vary by up to 50 %, depending on the measured polymer composition. Nissen *et al*. (1997) reported that a small error in the protein measurements leads to large errors in the calculated metabolic fluxes, for example, errors in protein content are magnified by a factor of two for NADH generation by mitochondria.

The objective of this chapter (results tables can be found in Appendix O) was to obtain a consistent description of the dry biomass composition of *S. fradiae* C373-10, when cultured on a number of different carbon sources with respect to the elemental and polymeric composition. A number of different analytical methods for carbon, nitrogen, phosphate, sulphur, DNA, RNA, CHOs, lipids, teichoic acids, peptidoglycan, protein, and aa determination were applied to improve the quantitative description of the biomass and a reconciled description of the acquired data was presented (average between assays). The macromolecular and elemental analysis of *S. coelicolor* 1147 and *E .coli* ML308 was also undertaken to verify the analytical protocols used by other workers [All fermentation numbers relate to the same cultures throughout Chapter 4, 5, 6 & 7; *S. fradiae* C373-10 cultures for glucose (Ferm 1 & 2); fructose (Ferm 1); glycerol (Ferm 1 & 2); oxo-glutarate (Ferm 1); glucose glutamate (Ferm 1 - 4); glucose oxo-glutarate (Ferm 1 & 2); methyl oleate medium (Ferm 1 - 3); Industrial complex (Ferm 1 & 2); *S. coelicolor* cultures for glucose (Ferm 1 & 2)].

5.1 Methodology for separation and determination of macromolecules

This section describes, in detail, the methods used to extract the different macromolecules from *S. coelicolor* 1147, *S. fradiae* C373-10, and *E. coli* ML308 biomass. To ensure an effective extraction and inactivation procedure, some conditions were taken into account; complete and immediate inactivation of the enzyme activity to prevent any metabolite conversion; total membrane permeabilization or cell lysis for a quantitative metabolite

release, and finally, the stability of the metabolites during extraction and until determination.

It was desirable to use a quick quantitatively accurate biomass fractionation protocol that allows complete characterisation of the biomass. Little research has been carried out in this area, the use of techniques such as Schneider *et al*. (1950) (Herbert, 1971; Davidson, 1992; Mousdale, 1997; protocols as Chapter 3 section 3.16). The descriptions of these protocols in the literature are confusing in what they can achieve, due to the complexity of the medium and their accuracy.

5.2 Fractionated of biomass

An initial experiment, using method 1 was undertaken to assess the effects of delayed time of cooling of the sample on the macromolecular concentrations (CHO, DNA, RNA, protein, & lipid)[Table 5.1; All Tables can be found in the companion CD; Appendix O Chapter 5]. Ineffective sample cooling (sample temperature > 5^0 C) or delayed cooling (> 10^0 C) resulted in decreased RNA concentration in comparison to cooled control samples, although there was little effect on CHO, DNA, protein, and lipid concentrations (Table 5.1). de Orduna & Theobald (2000) reported increases in intracellular metabolite concentrations such as glucose-6-phosphate (G6P) if sample cooling was delayed.

de Orduna & Theobald (2000) undertook further research of the effects of different extraction conditions on CHO and intracellular metabolite yields G6P and fructose-6-phosphate) of fraction 1 (Method 1, Chapter 3, section 3.16.1) with *S. coelicolor*. In order to ensure a quantitative extraction, a number of different PCA (0.1 – 2 M) concentration, and several incubation periods (1 – 24 hrs) were assessed. PCA at 0.2 M for 24 hrs was sufficient for complete release of G6P and CHO. The incubation time with the acid was found to be unimportant at a concentration of 1 M. Freeze-thaw-cycles or sonication in addition to the acid extraction procedure did not increase G6P or CHO extraction efficiency. A concentration of 0.2 M PCA at 4^0 C for 24 hrs was therefore considered to be sufficient to extract all small intracellular metabolites and CHOs. G6P was found to be stable in acid and neutral extracts for at least 11 weeks at 4^0 C and -18^0 C.

Difficulty arose when analysing streptomycete samples due to the sample being flaky after centrifugation (12400 g, 4^0 C, 30 min), which made separation of the supernatant and biomass difficult; this in turn decreased the quantitative reliability. This was alleviated by centrifuging the biomass, as before and filtering the sample through a 0.45 μm filter in a syringe holder. Then the residue biomass was collected on the filter paper and was then washed back into the next fractionation solute (for quantitative differences between non-filtered and filtered samples see Table 5.4 & 5.5). Table 5.4 and 5.5 possibly indicate a reduction in average STDEV between non-filtered and filtered extraction procedure. The high STDEV for CHO was reduced, this was considered likely due to a reduction in contamination from proteins and biomass which can cause charring with the anthrone assay (Chapter 3, section 3.18.1).

5.3 Efficiency of macromolecular extraction methods

The methods used for determining macromolecular content were those readily used by other workers (Davidson, 1992; Mousdale, 1997); the anthrone assay for CHOs, the orcinol assay for RNA, the Burton assay for DNA, the Bradford assay for protein, and the vanillin assay for lipids (all run in triplicate per sample and in triplicate per extract procedure). The macromolecular composition of each sample was calculated in terms of dry weight ($mg.g^{-1}$ dry weight) and contents from samples harvested at similar times were expressed as means (Table 5.4 – 5.9). Standard deviations (STDEVs), which are distribution parameters, were also calculated to give an indication of the extent of distribution of the values about the means (Green & Margerison, 1978), these were expressed in the same units as the means or the mean percentage STDEV.

Prior to determining the composition of *S. fradiae* C373-10, *S. coelicolor* 1147 and *E. coli* ML308 biomass, it was necessary to establish the reproducibility of the fractionation methods 1, 2, 3, and 4 (Chapter 3, sections 3.16.1, 3.16.2, 3.16.3, and 3.16.4 respectively)[sections 5.1.2 - 5.1.5] and that of the appropriate spectrophotometric macromolecular estimation methods.

An initial analysis was undertaken to assess the efficiency of fractionation methods 1, 2, & 3. Five individual *S. fradiae* C373-10 cultures were cultured in a 2.5 L bioreactor on a glucose glutamate defined medium (Chapter 3, section 3.6.4) for each time frame (24, 48,

72, 96, & 120 hrs). The total biomass for each time frame was separated into 12 lots of 1 g wet weight biomass and then split into triplicate sample lots and fractionation methods 1, 2, & 3 was applied. The efficiency of DNA extraction was evaluated by determination of the DNA content using the diphenylamine reaction (Chapter 3, section 3.19.2, Burton, 1956). The concentration of DNA extracted from *S. fradiae* biomass was close for methods 1, 2 & 3 (see Table 5.2 Parts 1, 2, and 3 companion tables). RNA was evaluated in a similar way using the orcinol reagent (Chapter 3, section 3.19.4, Herbert *et al*., 1971). When the orcinol assay was applied to method 3 the yield of RNA exceeded method 1 & 2 (see Table 5.2 Parts 1, 2, and 3 companion tables). This was likely due to the use of guanidine thiocyanate, which would act as an RNA stabilising agent. Protein was evaluated by the Bradford assay (Chapter 3, section 3.20.1) for methods 1, 2, & 3 and the ninhydrin assay (Chapter 3, section 3.20.6) for method 4 (Table 5.7 & 5.10). However a quantitative analysis of proteins extracted by method 3 was found to be problematic (see Table 5.2 Parts 1, 2, and 3 companion tables). The protein content using method 3 was significantly lower compared to fractionation method 1 and 2 (see Table 5.2 Parts 1, 2, and 3 companion tables). The ninhydrin assay gave significantly the highest protein content for method 4 (Table 5.7 & 5.10) against methods 1, 2, and 3. When re-applying the ninhydrin assay to methods 1, 2, 3 & Table 5.10 similar protein concentrations were achieved indicating that the Bradford assay for polymeric analysis does not compare well with the ninhydrin assay for total aa analysis (see Table 5.2 Parts 1, 2, and 3 companion tables)[see section 5.3.4 for further analysis of the protein fraction]. STDEVs were consistently high for all the fractionation methods. The mean STDEV for method 1 & 2 showed the highest average (Table 5.2 Parts 1, 2, and 3 companion tables). This was likely because the biomass was not extracted efficiently between the protocol steps, where as method 3 disruption of the biomass was used throughout the procedure (in which sample loss between fractions was probably reduced).

The correspondence between the individual samples run in triplicate indicated reproducibility of the standard assays (see Table 5.43 for STDEVs of individual assays), but the same samples fractionated in triplicate and then analysed showed high STDEVs (Table 5.4 – 5.9). This indicated that sample preparation or the fractionation protocol was the main factor that increased error and the reproducibility of the compositional data. The

size of the average STDEV from the means for method 1 were (Table 5.9) in the range of 14 % to 121 % indicating the large differences between similarly-grown biomass samples.

Further work was therefore undertaken to remove these discrepancies with the use of extraction method 2 (Table 5.8) [the average STDEV mean values were in the range of 4.64 % to 62.74 %], and freeze dried samples stored over silica [Table 5.6]{the average STDEV mean values were in the range of 15.68 % to 84.87 %} and freeze dried samples analysed with method 1 (Table 5.6) and 4 (Table 5.7)[the average STDEV mean values were in the range of 27.57 % to 131.51 %] fractionation method 4 would have been expected to remove any discrepancy caused by using wet weight and dry weight weighting factors. Although there were improvements between Tables 5.4 - 5.6 and Table 5.7 & 5.8 mean STDEV it was not considered significant. The STDEVs achieved in this work compared with other workers in this area (Davidson, 1992; Lange & Heijnen, 2001), and do seem to be typical and readily accepted as the norm.

The initial analysis undertaken indicated that methods 1 & 2 offered the most user semi-friendly protocols with the additional advantage of offering a 1 - 5 step protocol for the complete analysis of CHO, DNA, RNA, protein, lipid and cell wall components. Therefore any further analysis undertaken in the following sections used method 1 (Table 5.9A – I; corresponding to Chapter 4, Fig 4.1 – 4.20) & 2 (Table 5.8; corresponding to Chapter 4, Fig 4.7 – 4.10).

5.4 Spectrophotometric determination of macromolecular composition

Because each macromolecule was extracted under a number of different conditions e.g., for methods 1 & 2, acid or alkali conditions, standard solutions were prepared using the appropriate extraction solution. An attempt was made to cross-check the fractions for every macromolecule using standard solutions dissolved in dH_2O. However, using standards thus prepared, a non-linear curve was obtained for DNA standards assayed by the Burton assay (which reflected the requirement for PCA in the assay). A lower level of absorbance was obtained for RNA standards as compared to those dissolved in 0.5 M PCA. In addition, interference from CHO groups in the cold PCA fraction invalidated NA estimation, while NAs interfered in CHO analysis in the hot PCA fraction. In the case of protein analysis it was possible to cross-check the fractions through the use of the Peterson

precipitation [Chapter 3, section 3.20.3](Peterson, 1983) method. The proteins in all the fractions were precipitated and re-dissolved in dH_2O. Initial attempts at this protocol showed high STDEV for fraction methods 1 & 2 (Chapter 3, section 3.16.1 & 3.16.2 respectively) although fractions 3 & 4 (alkali fractions) showed reasonable comparison to non-precipitated samples. Between 10.55 - 29.16 % more protein was further accounted for with the addition of all the fractions (see Table 5.15 Part B) using the Peterson precipitation method and the Bradford assay. For further analysis, the ninhydrin assay, and HPLC analysis were undertaken (see section 5.3.3 and 5.14 Part 1 & 2). The anthrone assay (Chapter 3, section 3.18.1) was not sensitive enough to detect the presence of CHOs in the alkali fraction (proteins & lipids). Protein and lipid were likely to have residues of CHO. Therefore a less sensitive technique was used namely the phenol-sulphuric acid assay (Chapter 3, section 3.18.2). Unfortunately the proteins could char and give falsely high readings. The total soluble lipids could be extracted with solvents and concentrated and measured by gravimetric analysis or by the vanillin assay (Chapter 3, section 3.23) applied successfully to methods 1, 2, and 4 and whole biomass (see section 5.3.4).

All assay standards [i.e., for protein (bovine serum albumin {BSA}), RNA (yeast RNA), and DNA (calf thymus)] were corrected to there average extinction coefficient (OD) for the appropriate stock solution concentration (as Chapter 3). Initial analysis indicated a 2 - 5 % difference between corrected and non-corrected OD assay determinations for RNA and 10 % for DNA and protein standards (results not incorporated).

5.4.1 Total carbohydrate analysis

The intracellular accumulation of polysaccharides has been described in a wide variety of microorganisms (Dawes and Senior, 1973), e.g., yeast, fungi, and different bacterial species. Endogenous storage compounds have received very little attention in streptomycetes. Thus, although the occurrence of reserve polysaccharides in *S. viridochromogenes*, *S. antibioticus*, *S. fluorescens*, *S. griseus* (Brana *et al.*, 1980, 1982) & *S. coelicolor* (Davidson, 1992) have been detected, no detailed studies have been made on their molecular structure. In Brana *et al*. (1980, 1982) investigation significant amounts of polysaccharide were detected (e.g., 15 – 20 % of the cell dry weight, depending on the species). From this work *S. coelicolor* 1147 and *S. fradiae* C373-10 show intracellular polysaccharide content of 5 – 20 % (cell dry weight) depending on the carbon source

(Table 5.10). The highest polysaccharide content for *S. coelicolor* was observed whilst grown on glucose and for *S. fradiae* grown on glucose and glycerol (see Table 5.4 - 5.10 and Fig 5.1a-f [expressed as gl^{-1} for the time course of intracellular polysaccharide accumulation profile normalised to 90 to make easier comparison of cultures [see Chapter 3, section 3.17.1, for approach]).

S. fradiae C373-10 grown on an methyl oleate defined medium (Chapter 3, section 3.7) showed significantly lower content of lipid. Solvent extraction was necessary to determine accurate dry weights (Chapter 3, section 3.15.2) of the methyl oleate defined medium and the complex medium (the need to remove the methyl oleate component). Therefore an experiment was designed to evaluate the effects of the solvent extraction on the reproducibility of CHO, DNA, RNA, protein, and lipid composition. *S. fradiae* C373-10 was grown on a glucose minimal medium (shake flasks) and separated into six 1 g wet weight biomass lots. The three pure biomass samples were analysed with no solvent extraction and three were extracted with solvent [Chapter 3, section 3.15.2] (Table 5.11). Only the lipid content as expected showed a drastic decline. Further analysis with the complex medium showed drastically poor CHO, RNA, DNA, & protein recovery. This was considered to be due to poor recovery of the biomass (Table 5.9I).

Brana *et al*. (1982) used electron microscopy to investigate the cellular localization of polysaccharides in *S. viridochromogenes*, *S. antibioticus*, *S. fluorescens*, and *S. griseus*. In thin sections stained specifically for CHOs, electron dense granules were observed in the cytoplasmic regions of the hyphae. These polysaccharide granules, like those in the other bacteria, appeared to be arranged in clusters of different diameters with no surrounding membranes. The structures of the intracellular polysaccharides were comparable to glycogen isolated from other bacteria and animal tissues but were clearly different from plant amylopectin.

In many bacteria the presence of an intracellular glycogen store enables the bacteria to exist in starvation conditions more efficiently than bacteria that do not possess such a store. It is also known that there is a close correlation between maintenance energy requirement and the glycogen degradation rate, which enables the bacteria to survive for longer time periods in these conditions. This survival is thought to be in part due to the

reduction in protein and RNA degradation by degradation of glycogen providing carbon and energy (Zubay, 1998; Michal, 1999). In *S. coelicolor* this survival role for glycogen, would seem to be replaced by a different role based on the complex developmental regulation and osmotic gradients necessary for the redistribution of water (Hodgson, 2000). Trehalose has been reported to increase throughout the vegetative and aerial mycelium growth on solid medium and glycogen synthesis initiates in two stage early rapid growth phase and again following aerial mycelium formation (Hoskisson *et al*, 2001). It was not possible to differentiate between trehalose and glycogen growth patterns with this work, but there was an observable increase in CHO concentration throughout the growth phase (Fig 5.1a – t).

5.4.2 Total nucleic acid analysis

Two methods for extraction and quantification of DNA were compared (1) a spectrophotometric method using diphenylamine assay for DNA (Chapter 3, section 3.19.2)[applied to Method 1, Chapter 3, section 3.16.1]. (2) A fluorometric method utilizing selective fluorochromes (Hoechst 33258 for DNA)[applied to a buffered disrupted cells as Chapter 3, section 3.19.3].

The fluorometric method was found to be inactive in the PCA fraction, even after neutralisation of the solute (results not included). Hoechst is a groove-binding DNA ligand that becomes brightly fluorescent when it binds to the double-stranded β- form of DNA (Loontiens *et al*., 1991) which is the biologically-active form. Paul & Myers (1982) reported that denatured DNA gives a low contribution to Hoechst-DNA fluorescence. This means that Hoechst did not bind to the hydrolysed DNA. It was therefore likely that when the DNA molecular structure was altered by hydrolysis in PCA, formation of the Hoechst DNA complex was compromised and thus the fluorescence was greatly reduced (these results were similar to Dell Anno *et al*., 1998; for marine sample analysis).

Table 5.12 indicates that DNA concentrations measured spectrophotometrically, differed with fluorometric yields (cell disruption and buffer as Chapter 3, section 3.19.3), which were significantly lower. A possible explanation for the significant DNA yield discrepancies was that while the diphenylamine were relatively unaffected by DNA base composition and DNA molecular structure. By contrast Hoechst fluorescence binds to AT

sites on DNA and the difference between an AT / GC balanced standard has a great effect on the results from a high GC rich DNA sample (as shown by Mordy & Carlson, 1991). Therefore, when DNA was quantified with Hoechst, sample concentrations appear to be affected [Table 5.12](calf thymus 60 % A+T; Comings, 1975).

Estimations of total RNA content of biomass was determined by the orcinol assay (Chapter 3, section 3.19.4), a simple UV method (Chapter 3, section 3.19.5) [extraction procedure incorporated into assay], and total NAs (Chapter 3, section 3.19), and back calculated by difference from the determined DNA content by the diphenylamine assay (Chapter 3, section 3.19.2). Calculation by difference can be biased by interferences from protein in the extracts, in contrast, to the independent assessments of RNA by spectrophotometric determination (i.e., the diphenylamine assay and the orcinol assay). The method for RNA quantification described by Benthin (1991)[simple UV method] compared well with the orcinol and total NAs assays, although the UV method showed greatly reduced STDEV. The orcinol assay gave the highest RNA cellular content on average (see Table 5.12).

Table 5.13 uses fractionation method 1 & 2 (Chapter 3, section 3.16.1 & 3.16.2) to further assess the efficiency of extraction of KOH & PCA on DNA and RNA content. Method 1 extracts DNA & RNA with one step with 0.5 M PCA, where method 2 extracts DNA, RNA and teichoic acids (TAs) in a two step protocol with 0.3 M KOH & 0.5 M PCA (fraction 2; TAs, DNA and RNA and fraction 3; DNA and RNA). RNA and DNA was detected in both fraction 2 and 3 of method 2. On average 50 - 60 % of the RNA was extracted by the KOH extraction step. Both methods compared well for total NA recovery although method 2 showed the highest recovery factor. *E. coli* ML308 showed a 80 - 90 % recovery of RNA for the KOH extraction method 2. This could indicate that the streptomycete cell wall was refractory to the KOH extraction step.

5.4.3 Protein determination

Since a standard protein assay (the Bradford assay; Chapter 3 section 3.20.1) could only account for up to 8 - 12 % dry weight of the protein content of biomass (Table 5.14, Part 1) and TOCA of the alkali fraction (Chapter 3, section 3.16.1, Method 1, fraction 3) indicated their was considerably more carbon than estimated by the Bradford assay [Table 5.18, part 1, section 5.5] and the alkali fraction was assumed to contain only lipid and protein. This

would indicate that the protein or lipid concentration of *S. fradiae* C373-10 was higher than had been determined by this work (section 5.4). To determine if an error occurred in the measurement of protein, *E. coli* ML308 (three samples grown in shake flasks) was grown on a minimal glucose medium (Chapter 3, section 3.6.3); fractionated (Chapter 3, section 3.16.1, Method 1) and assayed in the same way as that for *S. fradiae* C373-10 and *S. coelicolor* 1147 (three samples grown in shake flasks). These results (Table 5.10) compare well for *S. coelicolor* and *E. coli* to that obtained by other workers (Bremer & Dennis, 1987; Davidson, 1992; King, 1997; King & Budenbender, 1997). This would then indicate that the Bradford assay is the source of error for protein determination with *S. fradiae*. Further analysis was therefore undertaken to determine if the Bradford assay results were correct. This included determination of the TOC content of each biomass fraction compared with the amount of carbon derived from the macromolecular composition in each fraction (section 5.4), verification against alternative methods of protein estimation and fractionation (see following section), and elemental & molecular elemental comparative analysis (section 5.10).

Initially, the Lowry method for protein determination (Chapter 3, section 3.20.2) was used to cross check against the Bradford assay. However, this assay is sensitive to interference from a large number of chemicals including NaOH (Smith *et al*., 1985). Protein from *S. coelicolor* 1147, *S. fradiae* C373-10, and *E. coli* ML308 were extracted as method 1 (Chapter 3, section 3.16.1) with 0.5 M NaOH (Table 5.14, Part 1). Consequently, BSA standards were dissolved in the same solvent but were shown to have lower absorbance equivalents than standards dissolved in dH_2O. Although all protein determinations carried out using the Lowry assay included BSA standards dissolved in 0.5 M NaOH, measurements of protein from batch culture fermentations of *S. coelicolor* 1147, *S. fradiae* C373-10, and *E. coli* ML308 showed significantly different protein concentrations; in the case of *S. coelicolor* accounting for up to 25.63 - 29.54 % of the dry weight (Table 5.14, Part 1), and up to 9.56 - 23.91 % in the case of *S. fradiae*, and 38.59 - 48.95 % for *E. coli* (the results for *E. coli* fit with the expected cellular composition obtained by other workers [Bremer & Dennis, 1987]).

The bicinchoninic acid assay (BCA) requires a very high pH (pH 11.25) and the assay is resistant to interference from a variety of chemicals including 0.1 M NaOH. Therefore,

standards dissolved in 0.5 M NaOH were used to determine the amount of protein in the alkali fractions of *S. coelicolor* 1147, *S. fradiae* C373-10, and *E. coli* ML308 biomass (Table 5.14). The level of protein detection by the BCA assay was comparable to, but slightly higher than, that by the Bradford assay (Table 5.14, Part 1) for *S. fradiae*, *S. coelicolor*, and *E. coli*. Therefore, the BCA method also seemed unsuitable for protein estimation in 0.5 M NaOH. The use of standards dissolved in 0.5 M NaOH resulted in a purple colour which was darker than that observed using standards in dH_2O. Interference by 0.5 M NaOH was therefore visible.

The reverse biuret method (Chapter 3, section 3.20.5) the signal is inversely related to the amount of peptide bonds, in contrast to other common protein assays which are influenced by specific aas side chains (i.e., Bradford assay, Lowry assay, and BCA assay). Therefore, protein to protein variability is very low and individual proteins or protein mixtures can be measured accurately. The level of protein detected by the reverse biuret assay against the Lowry, Bradford, and BCA assays on the whole was four fold higher for *S. fradiae* C373-10, 1.5 fold higher for *S. coelicolor* 1147. Protein content of *E. coli* showed little difference between the different protein assays. This would indicate that the protein standard chosen, in this case BSA, has had an effect on the amount of protein detected between the species. Similar results were observed by King (1997) and King & Budenbender (1997) for *S. tendae, S. collinus, S. lusitanus, S. olivaceus, S. cinnamoomeus, S. diastatachromogenes* and *S. noursei*. *S. noursei* showed the most profound effects between different protein assay techniques. These results indicate that the differences between aa composition of different bacterial species will have a considerable effect on the accuracy of protein assays i.e., the Bradford assay.

The dye in the Bradford assay works by binding to basic aas i.e., arginine and lysine residues (to view the biomass composition of *S. coelicolor* 1147 and *S. fradiae* C373-10 & C373-18 aas, see Chapter 6, Tables 6.1 – 6.27 for aa composition on a mM g dry weight of biomass basis; see section 5.7). The lysine and arginine, particularly lysine on average were 4 fold lower in *S. fradiae* C373-10 compared with *E. coli* ML308, and *S. coelicolor* 1147 on average was 1.5 fold lower compared with *E. coli*. The Lowry (Folin-Ciocalteau) method [Chapter 3, section 3.20.2], which is based on the oxidation of tyrosine and tryptophan residues with Folin and Ciocalteau's reagent. Tyrosine and tryptophan were 5.2

fold less in *S. fradiae* C373-10 compared with *E. coli* ML308, and *S. coelicolor* 1147 on average was 1.2 fold less compared with *E. coli* calculated from the total aa analysis (section 5.8). If BSA was therefore considered to have a similar aa composition to *E. coli* biomass; the aa composition of streptomycetes will have a considerable effect on the chosen protein assay.

The choice of an appropriate standard was considered important for any further analysis, as the intensity of colour produced for a particular protein is dependent on the amount of an individual amino acid/acids present. The choice of standard is difficult and therefore it would be more beneficial in compositional studies to use a standard method of protein measurement with the added benefit that the choice of the protein standard will have no effect on the assay reliability. The ninhydrin assay and total aa analysis by HPLC probably offer the most accurate methods of protein determination but were not user-friendly and were time consuming. Therefore the reverse biuret method (Chapter 3, section 3.20.5) should be considered as a standard method of protein determination in bacterial compositional research.

Further analysis of the aa composition of *S. coelicolor* 1147 and *S. fradiae* C373-10 was undertaken with HPLC analysis of the alkali and residue fractions (using HPLC, see Chapter 3, section 3.24.2), and biomass hydrosylates [Table 5.14 all measurements given in percentage grams dry weight protein]. Total aa composition of whole biomass hydrosylates obtained from HPLC analysis was not comparable with that of the sum of the alkali and residue fraction of method 1. Table 5.14 indicates that pre-treatment of biomass with extraction method 1 (fraction 3 & 4 added together) achieves the highest recovery of aas against whole biomass hydrosylates. Further analysis of the alkali and residue fractions indicated that aas accounted for 35.05 – 38.96 % on average of the biomass on a dry weight basis and 7.96 - 9.68 % of the aas accounted for in the residue fraction (Method 1).

The considerable differences in protein composition between similar cultures and the differences between the Bradford, Lowry, BCA, and the reverse biuret assays (Table 5.14, Part 1), also suggests, that protein degradation may also have occurred during the alkali extraction and could possibly account for the high STDEV and discrepancies between samples and assays. This would have resulted in the presence of aas or peptide chains too

small to be measured. An attempt was therefore made to establish the presence of free aas in all the fractions of method 1. This involved the use of the ninhydrin assay (Chapter 3, section 3.20.6) during which a reaction occurs between the reagent and free or hydrolysed aas. To undertake total aa analysis of methods 1 and 2, the samples described in Table 5.8 and 5.9A were subjected to further alkali hydrolysis with 13.5 M NaOH to liberate free aas (as Chapter 3, section 3.20.6). The resulting amino groups were then quantified using the ninhydrin assay (Table 5.15). The collective protein composition was comparable to the results obtained from the reverse biuret method (Chapter 3, section 3.20.5)[Table 5.14, Part 1]. Further assessment of the distribution of aas of fraction 1 - 4 (Method 1) and fractions 1 - 5 (Method 2)[Table 5.15], indicate that inefficiency in protein extraction recovery between fractions was also a considerable factor effecting reproducibility of the protein determination.

To further investigate the possibility that the higher percentage of carbon accounted for by the ninhydrin assay and HPLC analysis was due to the ability to detect free aas rather than proteins, the alkali fractions were again assayed by the ninhydrin assay method but the digestion step using 13.5 M NaOH was eliminated. Because the assay detects free amino groups, only those of single aas and aas at the N-terminal of proteins would be measured. Subtraction of this measurement from the previous one involving liberated aas would give an indication of the amount of protein or peptide chains present within the fractions (Table 5.16) this gives the concentration of undetected proteins in addition to a measure of the experimental error. These results indicated considerable differences with the determination of the amount of proteins and peptides (Table 5.16). This would then indicate the further need to increase the reproducibility of the extraction procedure or the need to collect samples under steady-state conditions to increase the reproducibility of the compositional data obtained.

5.4.4 Determination of the total lipid content and estimation of lipid components

The literature on the effect of environmental factors on microbial lipid composition is enormous. Moreover it is, a fairly old literature, since methods for analysing lipids began to be developed long before techniques were devised for separating cell constituents. Many of these reports are more or less casual in nature - systematic and detailed studies are decidedly in the minority. Moreover, the more detailed reports deal very largely with yeasts and

moulds, with prokaryotic microorganisms being much less favoured. Eukaryotic microorganisms can contain a large content of lipids and can be induced to grow under conditions that lead to high lipid production. Lipids have also been shown to accumulate in streptomycetes particularly in response to nitrogen starvation (Hoskisson *et al*, 2001).

There are two further generalisations that must be stressed concerning the effect of environmental factors on microbial lipid composition. The first of these concerns methodology. Total lipids are extracted from populations of microorganisms using various mixtures of organic solvents. Before extraction the organisms may be freshly harvested or freeze-dried. Whatever solvent regime is used, it is important to verify these results with other techniques. Very few workers undertake this. The second generalisation concerns the experimental design adopted when assessing the effect of environmental factors on microbial lipid composition. With very few exceptions, batch-grown microorganisms were used and this has severe limitations (Evans & Ratledge, 1984a, b) on experimental reproducibility. Therefore the results achieved for this work and others work need to be considered carefully, and further work undertaken to assess their reproducibility.

Davidson (1992) accounted for the total cellular lipid composition with a theoretical calculation, using data from *S. lividans* (see Appendix G for calculation), and considered the lipid content of streptomycetes in general, to be insignificant for a flux analysis. This assumption was assessed further in the following section and gave a further evaluation of the reproducibility of the protein extraction and determination methods.

Gravimetric analysis is usually the preferred method of quantifying the total lipid content of bacteria (Lange & Heijnen, 2001). However, it requires considerable quantities of biomass. An alternative method is the vanillin assay, which has been routinely used to quantify total soluble lipids (Chapter 3, section 3.23), which was applied to the alkali fraction of extraction method 1 & 2 (Chapter 3, section 3.16.1 & 3.16.2 respectively). Initially, it was found not to be sensitive enough to detect lipids in the alkali fraction. Therefore, extraction and concentration of the sample was considered necessary for further analysis.

There are no publications on extraction of lipids from the alkali fraction (Chapter 3, section 3.16.1, Method 1), but Mousdale (1997) indicated that thin layer chromatography

can be undertaken to assess the composition of the lipids of the alkali fraction of method 1. Different solvents were evaluated to extract and concentrate the sample: namely dichloro-methane, hexane, & chloroform-methanol mixture. The vanillin assay was then applied to quantify the lipids in the alkali fraction. Dichloro-methane was found to be the most efficient at extraction (results not shown). Initial experiments gave a lipid content of 2 - 3 % dry wt of biomass for *S. fradiae* C373-10 cultured on a glucose minimal medium [Chapter 3, section 3.6.4] (see Tables 5.4 - 5.10 for the lipid composition of biomass on various carbon sources). Davidson (1992) quotes *S. lividans* as having a lipid content of 5.5 % dry wt for growth on glucose minimal medium. When glutamate was included in the medium the lipid content of 5 - 11 % dry wt of biomass was detected for *S. fradiae* (Table 5.17).

This high lipid content when the glucose minimal medium (Chapter 3, section 3.6.4) was supplemented with glutamate was investigated further to determine if this result was reproducible or due to experimental error of the vanillin assay. Traditional gravimetric analysis (Chapter 3, section 3.23.3) was undertaken. *S. fradiae* C373-10 was cultured in shake flasks on glucose, fructose, glycerol minimal media, glucose + glutamate, fructose + glutamate, & glycerol + glutamate defined media (Chapter 3, section 3.6.4). Pooled samples for each growth condition were separated into six 1 g wet weight biomass lots. Three were subjected to fraction method 1, extracted with solvent, concentrated and analysed with the vanillin assay (Chapter 3, section 3.23.2), in unison with CHO analysis by the anthrone assay of the cold PCA fraction [Method 1, fraction 1](Chapter 3, section 3.18.1). In addition gravimetric analysis of the alkali fraction (Chapter 3, section 3.23.3) was undertaken. Three biomass samples were also analysed by whole biomass gravimetric analysis (Chapter 3, section 3.23.3). The average STDEV for both methods was below 1 % and there was a general trend between the two assays where the lipid content was consistently higher when glutamate was present in media (Table 5.17) and when cultured on a single carbon source the CHO content of cells was slightly higher.

Changes in the total cellular lipid composition of yeast has been reported by a number of workers. Evans & Ratledge (1984b) using *Rhodosporidium toruloides* examined how the nitrogen in medium affected lipid accumulation, as it had been reported previously that certain yeasts could accumulate substantially more lipid when various organic nitrogen

sources, rather the NH_4, were used for growth (Blinc & Hocevar, 1953; Witter *et al*., 1974). Changes in cell composition of *R. toruloides* were monitored during growth of batch cultures with NH_4Cl and glutamate as nitrogen sources. CHO was synthesised at the expense of lipid in NH_4-grown cells, whereas in glutamate-grown cells lipid accumulation was predominated. Total biomass and protein concentration were similar in both cultures. Glucose labeling studies [U-^{14}C], [1-^{14}C] and [6-^{14}C] showed that glucose assimilation of cells cultured with glutamate as the nitrogen source, was principally via the EMP pathway (72 %), with 28 % being metabolised by the PP pathway. When urea or glutamate, were added to the cell suspensions, glucose catabolism was significantly stimulated, with the flux of carbon via the PP pathway increasing to about 89 % of the total. The intracellular NH_4 concentration was also high during the first 40 hrs of growth when cultured with urea or glutamate (Evans and Ratledge, 1984a). Phosphofructokinase (PFK) was fully active and lipid accumulation commenced. PFK was then implicated as the likely controlling enzyme to explain these events. However, although there observations explain how lipid accumulation took place during the first 40 hrs of the fermentation they do not provide an explanation for continued synthesis after this time when it would have been expected that the negative effect of NH_4 on citrate inhibition of PFK would disappear after exhaustion of the nitrogen source. The observation for *S. fradiae* C373-10 cultured on a glucose glutamate defined medium where glutamate was completely consumed within the first 24 – 48 hr period (see Chapter 4, Fig 4.1 - 4.20) but lipid accumulation still persisted (Fig 5.1a - t; Table 5.17) this was consistent with the findings of Evans and Ratledge (1984). Table 5.10 & 5.17 both indicate that when lipid accumulation was high CHO accumulation was low and vice versa. Although *S. fradiae* does not accumulate lipid to the extent of *R. toruloides,* it does represent a considerable carbon sink, although whether this was at levels to interact with antibiotic synthesis could not be concluded from this work.

The major properties of the *R. toruloides* PFK enzyme were examined to determine its regulatory role during lipid biosynthesis (Evans and Ratledge 1984b). Unlike the enzyme from *S. cerevisiae*, no inhibition was found with 10 mM-ATP. ADP was not inhibitory either. NH_4 ions increased activity 11-fold by increasing the affinity of the enzyme for both F6P and ATP. K^+ ions also stimulated activity but to a lesser extent. Activity was severely inhibited by citrate, isocitrate and *cis*-aconitate but this inhibition was alleviated dramatically by NH_4. It was concluded that the interplay between the prevailing

intracellular concentrations of NH_4 and citrate was the major determent of the activity of PFK *in vivo,* which thus governed the extent to which glucose was converted either to lipid or CHO (Evans and Ratledge, 1984b).

An ATP-dependent PFK has been identified and purified from *S. coelicolor* (Alves *et al*., 1994, 1997)[see Chapter 2 section 2.5.1, for a detailed discussion of PFK], although little research was carried out by these workers on the properties of the enzyme. PEP was found to inhibit the enzyme strongly (Alves *et al*., 1997). It may be the case that streptomycete PFK's may have similar properties to yeast PFK's. If lipid accumulation was the preferred route for antibiotic synthesis expressing a PFK that has a preference for this route, there would be a parallel with high lipid-producing strains such as *Rhodosporidium toruloides*. Over expression of an enzyme may not be enough in itself, as streptomycete molecular biology and protein purification often lack the detailed kinetic studies (Alves 1994, 1997 study of PFK in *S. coelicolor* and *A, methanolica*) that have been undertaken by other disciplines e.g., yeast researchers (Evans and Ratledge, 1984; study of PFK in yeast against Alves, 1994, 1997). The latter analysis does indicate the need for an increase in the characterisation of the kinetic properties of these enzymes in streptomycete research.

5.5 Total carbon analysis of biomass fractions

Determination of the total organic carbon (TOC) concentration [Chapter 3, section 3.15.5] in biomass fractions (Method 1 & 2, Chapter 3, section 3.16.1 & 3.16.2 respectively) allowed the relative amount of biomass carbon in each fraction to be calculated (Tables 5.18 – 5.20A Part 1 & 2 & B). A comparison of the carbon content of the fractions with the amount of carbon derived from macromolecules assayed by each extraction method (Method 1 and 2) aids in determining the presence of previously undetected molecules. Such a comparison of fractionation methods 1 and 2 (Method 1 & 2; Chapter 3, section 3.16.1 & 3.16.2 respectively), was undertaken.

S. fradiae C373-10 biomass samples cultured on a glucose glutamate defined medium (Chapter 3, section 3.6.4)[corresponds to Table 5.9A], *S. coelicolor* 1147 and *E. coli* ML308 both cultured on glucose minimal media (Chapter 3, section 3.6.1 and 3.6.3 respectively) [corresponds to Table 5.9H & 5.9G] were subjected to each fractionation method (Method 1 & 2), and the appropriate macromolecular assay and TOCA analyses

was applied. To determine the proportion of biomass carbon extracted into each fraction, the values were then expressed as the molecular content of each fraction (C.μg), and the carbon content of each fraction (C.μg)[to express these macromolecules in terms of carbon the equations in Appendix F were used], and expressed in percentage format of the unaccounted for TOC of each fraction. In addition the percentage distribution of carbon between the fractions was also tabulated. The calculated carbon values from the macromolecular content of each fraction and the TOC concentration in the fractions were then tabulated to allow comparison (Tables 5.18A & B, *S. fradiae* C373-10; Method 1, 5.19A & B, *S. fradiae* C373-10, Method 2; *S. coelicolor* 1147 & *E. coli* ML308 Method 1 and 2, 5.20A & B).

Generally, the alkali fraction contained the largest portion of the biomass carbon with values of greater than 50 %. The hot PCA fraction contained 11 % - 25 % on average of the TOC, which agreed reasonably with combined NA content determined by macromolecular analyses. The cold PCA fraction extracted the least amount of carbon, but a significant proportion of the carbon was unaccounted for. It was expected that the cold PCA fraction would comprise a minor fraction as only small molecules such as nucleotides and aas would be solubilised by the weak acid. The final fraction of *S. fradiae* biomass (the residue fraction) contained approximately 12 - 30 % of the TOC of the biomass. Cell wall associated material was present within this fraction. Because *Streptomyces* are Gram-positive bacteria and therefore have extensive cell walls, it seemed feasible that a large proportion of the biomass carbon was present in the residue fraction. Therefore, the proportion of biomass carbon extracted into each fraction was consistent with expectations. The only difference with method 2 was that KOH fraction contains DNA, RNA & TAs, and the hot PCA fraction contains RNA & DNA. Previous analysis indicated that RNA & DNA were not extracted efficiently by method 2 (section 5.2; Table 5.13) and therefore macromolecular RNA and DNA analysis was applied to fraction 2 & 3 (the KOH & the HOT fraction, Method 2; assays diphenylamine & orcinol assay Chapter 3, section 3.19.2 and 3.19.4 respectively).

The combined carbon content (fraction 2 & 3, KOH & hot PCA fractions, Method 2) of these two fractions was comparable to the carbon content of the hot PCA fraction (Method 1)[Table 5.18A Part 1 & 2 & 5.19A Part 1 & 2]. Similarly, the amount of carbon in

fraction 4 (Method 2) and the alkali fraction (Method 1; fraction 3) were in agreement. Fraction 1 and 5 (Method 2), which correspond to the cold fraction and the residue fraction (Method 1) respectively, were also in reasonable agreement. Fraction 1 (Method 1) contained a higher relative percentage proportion of carbon. This may be indicative of more efficient extraction of the small molecules by 0.2 M PCA overnight (Method 1) while the extraction time for method 2 was only 10 minutes. de Orduna & Theobald (2000) reported that the duration of weak acid extraction had little effect on the extraction of intracellular metabolites. However, this shorter extraction period may have had a considerable effect on extraction of intracellular CHO.

The combined concentrations of carbon derived from the NAs (RNA and DNA) did not correspond to the TOC present in the hot PCA fraction (HOT, fraction 2, Method 1). Up to 70 % of the carbon in the hot PCA fraction of most samples was accounted for (Table 5.18A Part 1 & 2, 5.19A Part 1 & 2, and 5.20 Part 1 & 2). However in a number of cases, the combined monomeric NA values exceeded those of the TOC in the hot PCA fraction. Method 2 fraction 3 (KOH) showed the highest proportion of unaccountable carbon (90 - 97 % on average). The remaining carbon contained in fraction 2 (Method 1) and fractions 2 & 3 (Method 2) suggested that either incomplete estimation of the NA content of the hot PCA fractions had occurred or that an additional acid soluble compound had been extracted into the fractions. Because the values of NAs expressed as per gram of biomass (dry weight) were consistent with other workers (Shahab *et al*., 1996; Davidson, 1992) for streptomycetes, it would appear unlikely that the excess carbon was due to undetermined NA. Degradation of NAs and protein, resulting in extraction of the smaller products into fraction 1 (Method 2), was probably unlikely as the carbon contents of their respective fractions in both methods 1 and 2 were in reasonable agreement (Table 5.18B, 5.19B, and 5.20 Part 1 & 2). A possible suggestion was that the cell-wall associated polymer, teichoic acid (see section 5.6) had been extracted. Subsequent determination of phosphate in this fraction (see section 5.6) showed that this was probably the case (section 5.6).

The protein and lipid content of the alkali fraction accounted for a considerable proportion of the carbon but the carbon content of the residue fraction was only partially accounted for. The residue fraction was assumed to contain only cell-wall associated material. Therefore, carbon derived from protein was not expected to be equal to the TOC present in

the fraction. There was a possibility that insoluble pigments (e.g. melanoid) might account for further carbon in the alkali fraction. If present they can usually be estimated by absorbance (420 nm or 500 nm for melanoid). An absorbance scan carried out from 180 - 700 nm for fraction 3 & 4 (Method 1) and fraction 4 & 5 (Method 2) indicated know unknown peaks that could have been attributed to pigments.

Table 5.20 Part 1 & 2 shows a comparison of the cumulative unaccountable carbon recovery for *E. coli* ML308, *S. coelicolor* 1147 and *S. fradiae* C373-10. Unaccountable carbon recovery was between 30 - 65 % on average (Tables 5.18A Part 1 & 2, and 5.19A Part 1 & 2) for the *S. coelicolor* and *S. fradiae* where *E. coli* it was in the range of 20 - 66 % (Table 5.20 Part 1 & 2). These results are in good agreement with Davidson (1992) for *S. coelicolor* 1147 and 209.

A good comparative analysis was difficult to undertake. Which showed considerable in coincidences. Also the loss of one assay data point had considerable repurcussions on the overall calculation. Which can be seen for Method 2 Table 5.19 (A part 1 & 2 B) *S. fradiae* C373-10 where the carbon data was to sparse to be statistically acceptable. Further analysis with other elemental strategies was undertaken in section 5.10 to further assess the acceptability of the carbon balance undertaken in this section.

5.6 Preliminary analysis for estimation of macromolecular content

The overall picture of macromolecular composition for *S. fradiae* C373-10 *& S. coelicolor* 1147 data accumulated from Tables (Tables 5.4 – 5.10) was one of great variation. Nevertheless, use of all the mean values given in Tables 5.4 - 5.10 allowed a tentative composition of *S. fradiae* C373-10 to be given as 3 – 8 % RNA, 3 – 6 % DNA, 14 – 38 % protein, 4 – 20 % CHO, and 2 – 10 % lipid on average this represented 54.58 % of the mycelial mass (see Tables 5.4 - 5.9 for the total cellular percentage composition throughout the fermentation profile). A similar rough estimation for *S. coelicolor* 1147 was obtained (10 % - 15 % RNA, 4 – 6 % DNA, 21 – 36 % protein, 12 – 25 % CHO, and 3 – 5 % lipid); other than the protein content this corresponded with Davidson (1992), for the macromolecular content of *S. coelicolor* 1147 & 209 grown in batch culture; using the same analytical protocols (fractionation Method 1, Chapter 3, section 3.16.1) and medium (10 % - 15 % RNA, 4 – 6 % DNA, 10 – 21 % protein, 12 – 25 % CHO, and 3 – 5 % lipid).

On reanalysing Davidson's (1992) data using the protein composition calculated from the aa analysis undertaken by this worker but not used by Davidson (1992). The protein content was closer to 21 – 31 %.

Shahab *et al*. (1996) reported a protein content of 31 – 45 %, DNA 3.5 – 4.5 %, and RNA 10 – 22 % (w/w) of the biomass for *S. coelicolor* grown in continuous culture; this represented 56 – 63 % of the mycelial mass (with a 10 % STDEV error rate). Reisenberg & Bergter (1979), examined the macromolecular composition of *S. hygroscopicus* grown in both batch and continuous culture. It appears similar qualitatively to that of *S. coelicolor* 1147 and *S. fradiae* C373-10. The macromolecular composition of *E. coli* B/r grown in a glucose minimal medium was 55 % protein, 20.5 % RNA and 3.1 % DNA (Dennis & Bremer, 1974). In this medium, *E. coli* has a doubling time of 40 minutes whereas streptomycetes grow in a glucose minimal medium with a approximate doubling time of 2 - 8 hrs. It was therefore more feasible to compare the composition of *S. fradiae* with the composition of *E. coli* growing at a slower growth rate. At a doubling time of 100 minutes, *E. coli* has the composition: 72 % protein, 14 % RNA and 5 % DNA. The NA contents of both species at these slow growth rates were therefore similar, although, in absolute terms, the *Streptomyces* chromosome (at 8.67 Mb) for *S. coelicolor*; Bentley *et al*., 2002) is 58.25 % larger than that of *E. coli* (5.0 to 5.1 Mb; http://www.sanger.ac.uk/Projects/Microbes/).

E. coli possesses regulatory mechanisms that coordinate cell growth with the synthesis of essential macromolecules. While fundamental differences have been identified in the growth habit and chromosome structure of *E. coli* and *Streptomyces*, little is known about their regulatory mechanisms. Shahab *et al*. (1996) reported a relationship between the macromolecular composition of *S. coelicolor* and its specific growth rate (μ)[Table 5.21]. Changes in the macromolecular content of *S. coelicolor* and *E. coli* with μ appear to be essentially similar. However the data indicated that RNA content of *S. coelicolor*, grown under the same μ, exceeds that of *E. coli* grown at the same μ. The data also suggest that overlapping rounds of replication were not a feature of DNA synthesis in *S. coelicolor*. This may be a function of the organisms low maximum μ. Alternatively, it may be a consequence of regulatory mechanisms which act to inhibit the initiation of DNA synthesis in a linear chromosome which was already undergoing replication.

Table (5.22) accounts for differences between the size and GC content of *S. coelicolor* and *E. coli* genomes. The differences were removed by recalculating the data into the protein content per genome, and the number genomes per cell mass (taken from Shahab *et al*. 1996). The linear relationship between RNA content per genome and μ observed for *S. coelicolor* (Shahab *et al*. 1996) suggests that, as with *E. coli*, the demands of growth for protein synthesis in this microorganism are met by changes in the number of ribosomes. However the maximum μ of *S. coelicolor* is five times less that that of *E. coli*. Therefore it could be argued that the demand for protein synthesis is considerably less in *S. coelicolor*. Assuming that the observed RNA content was mostly rRNA (see Appendix H), and that ribosome structure is similar in the two organisms, the apparently higher RNA content of *S. coelicolor* hyphae might be due to a low maximum specific ribosome activity, ribosomes operating submaximally, and / or a higher proportion of ribosomes being present in an inactive form. A relatively high ribosomal content may have evolved in *Streptomyces* to support the high proportion of extracellular protein synthesised by these organisms as adaptation to growth on solid substrata (Shahab *et al*., 1996)

The main apparent difference in macromolecular composition of *S. fradiae* C373-10, *S. coelicolor* 1147 and *E. coli* ML308, however, was the protein content. *E. coli* contains 55 % protein on average (or 72 %, at low growth rates). According to the above results, *S. fradiae* was measured to have up to 21 – 50 % protein depending on the growth conditions (SP II, time points were given in Table 5.10, and Chapter 4, section 4.5.3).

5.6.1 The pattern of macromolecular change throughout growth of *S. coelicolor* 1147, *S. fradiae* C373-10 and *E. coli* ML308

During exponential growth of a micro-organism, biosynthesis of macromolecules occurs at a rate similar to the biomass production rate. Therefore, increases in protein, RNA or DNA concentration per unit volume of a culture may be parallel to that of biomass concentration and could thus be used to measure growth rate (Mandelstam *et al*., 1982). As the exponential phase draws to an end, the organism enters the stationary phase and then the death phase. When cells enter stationary phase, however, the macromolecules undergo separate processes: DNA replication ceases while RNA and protein degradation occurs to provide precursors for newly synthesised RNA or proteins.

To determine the pattern of macromolecular change during growth of *S. coelicolor* 1147, *S. fradiae* C373-10, and C373-18 the fermentations described in Chapter 4 (Fig 4.1 - 4.20) were analysed for macromolecular content using fractionation method 1 & 2 (Chapter 3, section 3.16.1) and the diphenylamine and orcinol assay methods for NA determination (Chapter 3, section 3.19). The reverse biuret assay was used for protein determination (Chapter 3, section 3.20.5); the anthrone assay for CHO determination (Chapter 3, section 3.18.1), and the vanillin assay for lipid determination (Chapter 3, section 3.23.1)[accumulated data Tables 5.4 - 5.10]. The resulting mean macromolecular contents in the biomass fractions were then expressed as concentrations of the appropriate fermentation cultures and the values for each fermentation were plotted against time of harvesting (Fig 5.1a - r). Long time intervals were present between points on the graph because of the large sample volumes (up to 250 ml)[see Chapter 4, section 4.5 for discussion] required to allow harvesting of sufficient biomass.

The patterns of macromolecular changes in the fermentations (Chapter 4, Fig 4.1 - 4.20)[Fig 5.1a - r] follow those expected from the general description of batch growth (Davidson, 1992). Due to differences in the specific growth rate, and substrate uptake rates between different strains and strains cultivated under different conditions. A comparison can only be undertaken, by eliminating the individual time points (calculated as King, 1997; King and Budenbender, 1997; who compared macromolecular compositional data for 25 streptomycetes). The cultures were normalised to 80 h^{-1} up until the end of DNA replication and each time point of the remaining data was normalised with a factor of 5 h^{-1} (i.e., 24 hrs = 5 places on the graph). The time could have been normalised further but antibiotic yields in the case of *S. fradiae* C373-10 were too low to distinguish the initiation antibiotic synthesis and nutrient limitation (see Chapter 3 section 3.17.1 standard normalisation procedure). It was not clear from growth patterns of *S. fradiae* C373-10 whether growth was exponential. Examples of exponential growth of streptomycetes have been reported by several workers. Riesenberg & Bergter (1984) reported exponential growth of *S. hygroscopicus* using various levels of Tris and MOPS buffer in the medium to prevent clumping. Hobbs *et al*. (1989) obtained exponential growth of *S. coelicolor* using the polyanionic compound, junlon, as a dispersant. In the majority of cases exponential growth has not been reported for streptomycetes. This is most likely due to the growth characteristics of the mycelial organism, which may grow as dispersed hyphal fragments or

as pellets. The growth of pellets will be exponential until the density of the pellet results in limitation by diffusion. Under such limitation the internal biomass of the pellet will not receive a supply of nutrients, nor will potentially toxic products diffuse out. Thus, the growth of the pellet proceeds from the outer shell of the biomass, which is the actively-growing zone (Pirt, 1975). It is possible for new pellets to generated by fragmentation of old pellets and thus, the behaviour of a pelleted culture may be intermediate between an exponential and cubic growth rate (Stanbury *et al*., 2000).

The concentration patterns exhibited by RNA and protein in general were observed to follow the pattern of the biomass concentration throughout the cultivation. The initiation of stationary phase was followed by degradation of RNA and protein. This was in agreement with labelling experiments (^{14}C uracil) by Vu-Trong and Gray (1986) for *S. fradiae* cultured on methyl oleate defined medium. During stationary phase, DNA concentrations in bacterial cultures reach a plateau. This was also observed for *S. coelicolor* and *S. fradiae* fermentations (Fig 5.1a - r).

5.6.2 Hyphal protein to RNA ratio

The ribosomal efficiency quantity proposed by Alroy & Tannenbaum (1973), was not undertaken, the data was graphed as the DNA / RNA ratio (Bushell & Fryday, 1983) to make comparison of different growth conditions an easier task. The ratio of hyphal RNA content peaked as the carbon source became limiting (Fig 5.2a - i). It was possible that the ratio increased after each q value ($q_{glucose}$ q_{NH4} and q_{PO4})[indicated by sampling point I & II on Fig 5.2a - i] approached zero but further analysis would be needed to verify this. A maximum was observed during each different nutrient limitation phase. This was not observed for *S. coelicolor* 1147 (Fig 5.2a & b). These results were consistent with findings of Pitt & Bull (1982), and Bushell & Fryday (1983). Pitt & Bull (1982), suggested that ribosomal efficiency in *Trichoderma auroviridie* was controlled by the nature and availability of the growth-limiting concentrations of ammonia and glucose.

Considerable differences were observed in the DNA / RNA ratio between similar cultures, indicating poor reproducibility of the acquired compositional data. The low number of sampling points may have also had a considerable effect. The most reproducible results were observed when the same fermentation equipment was used (Fig 5.2a, Fig 5.2b, &

5.2f)[see Chapter 4, Fig 4.1 - 4.20 for equipment parameters]. This would indicate that to decrease compositional error dedicated fermentation equipment was desirable.

5.7 Teichoic acids

The surface of Gram-positive bacteria consists of teichoic acid (TA), which is a polymer of glycerol (or another sugar such as ribitol linked by phosphodiester bridges (Fig 5.3). Teichoic acid is attached to the N-acetylglucosamine-N-acetylmuramic acid (NAG-NAM) backbone of peptidoglycan (section 5.6.1, Fig 5.4) by a phosphodiester bond. The presence of TAs in *S. albus*[*], *S. albocyaneus*, *S. antibioticus*[*], *S. azureus*, *S. chrysomallus*, *S. coelicolor*, *S. cyanoalbus*, *S. diastaticus*[*], *S. flavofungini*[*], *S. griseus*, *S. hawaiiensis*, *S. kanamyceticus*[*], *S. kursanovii*, *S. levoris*[*], *S. ostreogriseus*, *S. rimosus*[*], *S. rutersensis*[*], *S. thermovulgaris*[*], *S. tumemacerans*[*], & *S. violaceus* (Naumova *et al*., 1980) led to the conclusion that these biopolymers were widely spread in the genus *Streptomyces*. Most streptomycetes examined in the survey contained glycerol([*]) or ribitol TA, but in some cases the residue was unknown (Naumova *et al*., 1980). Structurally, TAs closely resemble those of other genera of Gram-positive bacteria and in many cases represent poly (glycerol phosphate) and poly (ribitol phosphate) chains. The proportion of sugar residues substituants varied widely for streptomycetes (Naumova *et al*., 1980; Naumova, 1988).

Initial TOCA indicated that a considerable proportion of carbon in fraction 2, (KOH) method 2, was unaccounted for (as section 5.3.6)[87.29 % on average, KOH fraction 2, Method 2]. It was thus considered that TAs could account for this discrepancy. Two methods were used to quantify TAs in *S. coelicolor* 1147 and *S. fradiae* C373-10: 1) Baillie (1968) protocol (Method 2, Chapter 3, section 3.16.2) based on the nucleic acid extraction protocol of Schmidt and Thannhauser (1945) and 2) Hancock's 1994 method of separating complete bacterial cell wall (Chapter 3, section 3.21). Both measure the TA content as organic phosphorus (Chapter 3, section 3.22.4 for method).

The fractionated biomass samples that had been already analysed for TOCA (Tables 5.18A Part 1 & 2 & B and 5.19A Part 1 & 2 & B) were further analysed for TAs (Table 5.24 & 5.25 Part 1 & 2). These fractions were also subjected to phosphate determination (in triplicate). In addition, the phosphate contents of the cold PCA fraction (Method 1) and the hot PCA fraction were measured. The combined RNA & DNA contents of the fractions

were then expressed in terms off phosphate (total NA-P). An estimation of the TA content of the fractions was obtained from the TA phosphate (TA-P). This was calculated by subtracting the NA phosphate from the total phosphate measured in the fractions. Exact quantification of carbon derived from TA was therefore not possible but estimates were calculated using the assumptions that TA in *S. coelicolor* 1147 (Table 5.23) and *S. fradiae* C373-10 (Table 5.24 and 5.25) was composed of either a glycerol backbone or a ribitol backbone. The number of carbons in one unit of TA would therefore be either 9 or 11 (TA also contains an additional group which in this case was assumed to be a sugar group). Expressing both NA and TA in terms of μg of carbon and subtracting the values from the TOC (Tables 5.24 Part 3 & 5.25 Part 2). Assuming a glycerol backbone and ribitol backbone, 18.1 % and 10.7 % of the carbon remained unidentified in each method (1 & 2). The TA composition for *S. coelicolor* 1147 was in the range of 14 - 21 % and 15 - 18 % for *S. fradiae*. Teichoic acid estimation by phosphate analysis for *S. coelicolor* 1147 and *S. fradiae* C373-10 for this work was comparable to Davidson (1992) i.e., 20.04 % - 13.73 % for *S. coelicolor* 1147.

On comparison with the cold PCA fraction [fraction 1] and the hot PCA fraction [fraction 2] (Method 1), the remaining phosphate content of fractions 1, 2, and 3 combined (Method 2) was observed to be higher. This would indicate incomplete extraction of phosphate-containing metabolites. The distribution of phosphate between methods 1 and 2 would indicate TA was distributed between the cold PCA and hot PCA fraction of method 1 and further work was needed to assess if it was efficiently extracted into fraction 2, method 2. Both the method of Baillie and Hancock show reasonable correlation e.g., for example 11 - 34 % for *S. fradiae* C373-10 but further verification was needed (Table 5.23 - 5.25). Baillie's method was the more user friendly of the two techniques.

The wide distribution of TAs highlights them as having important functions in the life style of actinomycete cells. A property of these polymers, which may be a major determinant of their function, is their anionic nature. The physiological role of TAs has been associated with ion exchange in the cell (Naumova, 1989). Possibly, the presence of the particular acyl groups either enhances the anionic properties of the polymer (e.g., the presence of succinic acid half-ester and lactylphosphoryl groups) or, diminishes them (e.g., O-L-lysyl residues). It may well be that this is one of the functions of these structural

components of the TAs. Recent research in various laboratories has made it clear that the cell wall has a very dynamic structure that responds promptly to environmental alterations and varies with the developmental cycle and morphological modification of the bacterial cell. The variations mainly occur in the anionic carbohydrate-containing polymers. Morphological modifications are known to be mediated by autolytic enzymes whose ligands are TAs in certain instances (Naumova, 1988). The role of O-acetyl residues does not contribute to the anionic properties of the TA, since these residues, which have been shown to occur in varying amounts in TAs of many streptomycetes, are neutral when bound to the polymer. For example, whereas the *S. thermovulgaris* polymer contains 1 or 2 residues per 13 monomers of the chain (Naumova & Dmitrieva, 1974), this ratio is 1 : 4 in *S. rimosus* (Dmitrieva, 1976). Interestingly, the cell wall of the latter organism contains many more O-acetyl groups than its TA may accommodate, which may indicate that this residue is also carried by other polymers. The involvement of ATP in the formation ester bonds between acetyl residues and polyols has been demonstrated (Baddiley & Neuhaus, 1960), and the reactivity of this bond is close to that of an acetyl bond. Retaining the acetic acid residues in their active forms, the cell probably utilises them in certain biosynthetic processes a possibility that may be discussed in the light of the acetate theory of tetracycline production (Hutchinson, 1981). There may be a possibility that tetracycline could be synthesised without a CoA intermediate

Teichoic acid levels in actinomycete walls vary greatly. Rarely do actinomycete cell walls contain TA and peptidoglycan solely; most often, another carbohydrate-containing polymer, occasionally even a phosphorylated one, is also found in the cell wall. The quantitative ratio of these polymers varies during the growth of a submerged culture. Generally, TA is found in highest amounts in actinomycetes during the logarithmic growth phase and is replaced progressively by polysaccharide as the organism enters stationary phase (Streshinskaya, 1979). In some streptomycetes, the ratio of peptidoglycan to TA has been established during an early growth stage. For example, the *S. thermovulgaris* wall contains one TA for every 6 to 7 disaccharide units (Naumova, 1988), while that of *S. rimosus* has ratio of 1 : 20 (Dmitrieva, 1976).

5.7.1 Cell wall compositional analysis

Most bacterial cells are surrounded by rigid walls, which protect the cytoplasm and the fragile plasma membrane from influences of the outer environment. These walls also maintain the shape of the cells and give protection against osmotic lysis. As a result of extensive studies between 1950 and 1980, detailed knowledge is available about the function and chemical composition of bacterial cell walls. Peptidoglycan is a polymer generally comprised of N-acetylglucosamine (NAG), N-acetylmuramic acid (NAM), L(D)-alanine and *meso*-diaminopimelic acid (*meso*-DAP). *Streptomyces* peptidoglycan, however, contains LL-diaminopimelic acid (LL-DAP) in the structure. Peptidoglycan of *S. coelicolor* is of the A3γ type (Bergeys, 2000) with a single glycine interaction bridge with LL-DAP (LL-A_2pm) as the diamino acid (Fig 5.4). Streptomycete cell walls have been reported to contain a high quantity of glycine (Minnikin & Cross, 1984, Pridham & Tresner, 1974).

Therefore, to verify the content of the residue fractions and to quantify peptidoglycan from *S. coelicolor* 1147 and *S. fradiae* C373-10, aa analysis was performed on the residue fractions of method 1 (Chapter 3, section 3.16.1). Determination of the aa composition was carried out using whole biomass samples processed through fraction method 1 (Chapter 3, section 3.16.1), this resulted in the residue fraction (fraction 4) presumed to contain cell wall associated components (Method 1, Chapter 3, section 3.16.1), e.g., peptidoglycan.

Several of the aas present in whole biomass samples of *S. fradiae* were detected in the residue fractions (Table 5.26). The results of aa analysis of the fractionated biomass of *S. coelicolor* 1147 and *S. fradiae* C373-10, indicate alanine, arginine, glycine & glutamate were present in the highest amounts. Several other aas were also found (Table 5.26), but at lower proportions, indicating the presence of low amounts of proteins in the isolated cell wall residue fraction (Method 1, Chapter 3, section 3.16.1). The contribution of the proteins to cell wall dry weight for *S. coelicolor* 1147 and *S. fradiae* C373-10 were in the range of 20 – 30 %. In Coryneform bacteria, this ranges from 7 to 15 %, and in *B. brevis* about 56 % (Van der Wal *et al*., 1997). However, it was possible that some of the aas detected in the residual fraction of *S. coelicolor* 1147, *S. fradiae* C373-10, and *E. coli* ML308 were components of the cross-link polyglycine (UDP-N-Acetylmuramyl-

pentapeptide) bridge in the peptidoglycan molecule (Table 5.26). According to Neidhardt (1987), *E. coli* peptidoglycan consists of NAG, alanine and glutamate in the ratio 1:2:1. The ratios of these aas in residue fractions were calculated with respect to NAG (for *E. coli*; Neidhardt, 1990). The average amount of NAG present in *S. coelicolor* 1147 (measured by HPLC; Davidson, 1992) was calculated to be 51.4 μmoles.g^{-1} dry weight. The peptidoglycan, repeating unit has a MW of 904 which gives a weight of 46.5 mg.g^{-1} and, therefore, 4.6 % of *S. coelicolor* on a dry weight basis (Davidson, 1992). NAG was not measured in this work but a rough ratio was calculated from the known alanine and glutamate concentrations of the residue fraction (Table 5.27). This gave on average 5.42 % peptidoglycan for *S. coelicolor* 1147 and 7.74 % for *S. fradiae* C373-10 dry weight and 4.29 % peptidoglycan for *E. coli* ML308 (Table 5.27) using alanine to calculate the ratio and 7.23 % peptidoglycan for *S. coelicolor* 1147 and 12.17 % for *S. fradiae* C373-10 dry and 3.16 % peptidoglycan for *E. coli* ML308 using glutamate to calculate the ratio. *E. coli* has been reported to contain 2.5 % peptidoglycan (Neidhardt, 1987) which would indicate in the case of *E. coli* the method of peptidoglycan determination used here compared reasonably well. The peptidoglycan content of coryneform bacteria accounts for 23 – 31 % of the cell dry weight (e.g. *Corynebacterium* spp. DSM440, 16 - 23 %; *Rhodococcus erthropolis*, 24 %; *Rhodococcus opacus*, 31 %). The peptidoglycan in the cell walls of the *B. brevis* strain accounts for about 5 % of the cell wall dry weight. This may suggest that there maybe more dominant compounds present in the *B. brevis* cell wall (Hanson & Phillips, 1981) and possibly in streptomycetes. This would indicate further assessment is needed to assess the contribution the cell-wall has on biosynthetic demand.

Classical studies of cell wall composition usually require disruption of the cells by mechanical forces and the subsequent isolation and purification of the cell wall fragments. Although the isolation procedure may lead to undesired losses of cell wall constituents, these studies generally give precise information on the cell wall composition. More rapid and also less risky methods involve the analysis of whole cells (Keddie and Cure, 1977). However, the information obtained in this way has generally a more qualitative character. In Gram-positive bacteria the wall accounts for a considerable proportion of the cell dry weight.

A more sophisticated method for the determination of the fraction of cell weight represented by cell wall material was given by Marquis (1968). According to his method, whole cells were suspended in protoplast-stabilising medium and were treated with lysozyme, which digests the cell envelope. The wall weight can then be determined after centrifugation and drying of the solution. Although this method can give reliable results, its applicability is limited because not all bacterial strains have cell envelopes which can be completely hydrolysed by lysozyme. In 1968 Tipper (Tipper, 1968; Hanson and Phillips, 1981) proposed an analytical method for the quantitative determination of muramic acid in isolated cell walls. In this procedure D-lactate is eliminated from muramic acid by alkaline hydrolysis of cell wall material followed by an enzymatic determination of the D-lactate concentration. A few years later, Hadzija (Hadzija, 1974; Van der Wal *et al*., 1997) reported a simple colorimetric method for the quantitative determination of D-lactate in cell wall hydrolysates. The analysis undertaken in the present work of the cell wall composition was qualitative at best, further research with Hadzija (1974) analytical technique (Hadzija, 1974; Van der Wal *et al*., 1997) may prove interesting with the particular interest of applying this technique to extraction method 1, fraction 4, residue fraction (Chapter 3 section 3.16.1) in conjunction with whole cell wall material. Little research has been carried out using fractionation method 1 for cell wall analysis. Initial results although interesting, show the need to further assess the capability of this fractionation method towards cell wall analysis.

5.8 Identification and quantification of the amino acid composition of *S. coelicolor* 1147, *S. fradiae* C373-10, C373-18 and *E. coli* ML308 biomass

The aa composition of *S. fradiae* C373-10 & *S. coelicolor* 1147 was determined by HPLC (Chapter 3, section 3.24.2). However, it is important to note that glutamate and aspartate determinates are the sum of glutamine + glutamate and asparagine + aspartate during acid hydrolysis. Cysteine and tryptophan were not determined by HPLC since acid hydrolysis results in oxidation of cysteine to cystine (a disulphide) and tryptophan is very unstable (Inglis, 1983)[Chapter 3, section 3.25.2]. Initial analyses to investigate the variability and the effects of increasing hydrolysis time on the aa composition (Table 5.28) gave STDEVs that were on average in the range of 5 – 20 %. This was considered to be within acceptable experimental error limits. The tryptophan content of hydrolysates deteriorated with

increasing hydrolysis time. It therefore may be possible to analyses the tryptophan composition at the 6 hr hydrolysis time [as indicated in Chapter 3, section 3.24.2](Table 5.28) further work would need to be undertaken to test this hypothesis. No other aa showed any major observable increase and reduction during the 6 - 24 hr time period.

Carbon recovery was in the range of 80 – 90 % on average for Table 5.28. The sample carbon recovery for all aa analyses undertaken was in the range of 50 – 60 % on average. This loss was corrected using the internal standard (taurine). The reason for such low carbon recovery was unclear. The use of thunberg tubes was considered to contribute to this source of error. Thunberg tubes seem to be the standard method of aa hydrolysis. An alternative would have been to use fast seal disposable glass tubing or lypholisation vials under vacuum. Another method would have been to research in to microwave digestion vessels that have pressure control. Whether an inert gas could be incorporated in to the equipment would be an engineering problem. Although this equipment is expensive at present. The poor carbon recovery and loss of samples through thunberg tube seals braking, leads to the need to further assess this hydrolysis method to improve the reproducibility of the compositional data.

For all the fermentations a sample was removed daily (as Chapter 4, Fig 4.1 - 4.19) for aa analysis. These were stored in three formats (1) The total broth (10 ml of broth was combined with 10 ml of 0.4 M PCA) (2) The additive alkali and residue fraction of method 1 (Chapter 3, section 3.16.1). Table 5.14 (section 5.3.3) indicated that pretreatment of the biomass with method 1 (Chapter 3, section 3.16.1) had the most significant aa recovery. Therefore fractionation method 1 was used for the majority of the aa analysis work throughout this project.

A general pattern of aa composition was evident for all samples analysed (Table 5.30 – 5.33). The relative proportions of aas in each sample were compared by expressing their amounts as percentages of the total aa content (Tables 5.30 – 5.33). Alanine was the most abundant aa for *S. coelicolor* 1147, *S. fradiae* C373-10 and *E. coli* ML308, (Table 5.29 & 5.32; Fig 5.5A - E) closely followed by glycine. Streptomycetes have been reported to contain a high proportion of glycine in their cell walls (Pridham & Tresner, 1974; Davidson, 1992). Glycine has also been reported to be an important component of

streptomycete ion transport proteins (Doyle *et al*., 1998), and this may account for the high glycine proportion in addition to a possible glycine peptidoglycan bridge. Methionine was the least abundant. Table 5.30 & Fig 5.5A compares results obtained from this work for *S. coelicolor* and *E. coli* with other workers cultured on a glucose minimal medium (taken from Davidson, 1992; Holms, 1986). In both cases, aa analysis compares well with this work. arginine shows small changes at the beginning, middle, and end points of the fermentations. At first this was considered to be due to experimental error (inconsistencies from hydrolysis) but this phenomenon showed in all the fermentations (Table 5.29 - 5.32) analysed. These inconsistencies can be seen in Table 5.29 - 5.32, where arginine in a number of cases was considerably high and changed throughout a culture. This may have been a consequence of arginine being available as a free intracellular aa. Vinning and Stuttard (1983) reported the free aa composition of *S. aureofaciens* to be Ala 8.1 %, Asp 2.3 %, Glx 82.3 % (glutamate + glutamine), Gly 1.8 %, Leu, 0.9 % Pro 1.0 %, Ser 1.0 % Val 0.7 % an average for growth under a number of nitrogen sources. Further work with accounting for the free intracellular content of *S. fradiae* would have been desirable to test this hypothesis.

The percentage aa composition for *S. coelicolor* 1147 and *S. fradiae* C373-10 was determined to be very similar in all the samples analysed, within 1 % to 5 % on average of each other (Table 5.29 - 5.32) when run in triplicate. However the majority of the analyses was not undertaken in triplicate due to time constraints of the project. The least abundant aas were tyrosine, histidine and methionine (Table 5.29 - 5.32). Tyrosine and histidine were also the least abundant aas in *E. coli* (Holms, 1986)[Table 5.27]. However, tryptophan was the least abundant aa in *E. coli*, whereas methionine was placed fourteenth among the twenty aas. Although alanine and glycine were also present in the highest amounts in the enterobacterium, their percentages were lower than those in *S. coelicolor* 1147 and *S. fradiae* C373-10 (this was in agreement with Davidson, 1992) and *S. fradiae* C373-10 by 3 to 5 % (Tables 5.29 - 5.32). *S. fradiae* shows similar patterns of aa percentage composition to *S. coelicolor* [Table 5.29 – 5.32]. Although the average order of requirement indicates glycine as the most abundant aa and showed an average aa decreasing order of requirement of GLY > ALA > ASP > GLU > ARG > LEU > VAL > PRO > THR > ILE > TYR > PHE > LYS > HIS > SER > MET > TRP.

Further analysis of the streptomycete aa composition showed considerable inconsistencies between cultures. Increasing the number of triplicates, may have lowered this difference, but it was unlikely that the undetermined cysteine & tryptophan (usually comprise 2 % and 1 %) would account for the overall difference. Cysteine was calculated as 1 % of the total measured aas. Although it would not be possible to account accurately for all the aas (see Chapter 3 section 3.25.2 for discussion) with the protocol used in this work. Other differences were considered a consequence of the hydrolysis protocol and HPLC method i.e., using area calculations instead of a calibration line, poor carbon recovery, and chromatogram peaks (near the end of the chromatogram) becoming irreproducible with increasing age of the column. Another source of error may have been the residue fraction not being accounted for adequately in a number of cases. These inconsistencies can be seen in Table 5.29 - 5.32, where glycine in a number of cases was considerably high and changed throughout a glucose glutamate defined medium (Table 5.31). The protocols used were standard methods used throughout bacterial research. Proportions of the majority of aas agree between *S. fradiae* C373-10*, S. coelicolor* 1147, and compare to *E. coli* ML308. Combining the *E. coli* percentage contents of glutamate and aspartate with their aminated forms (glutamine and asparagine) resulted in higher values than those obtained from *S. fradiae* or *S. coelicolor*. It may be that the samples had lower amounts of these aas or that complete detection of both types of aa had not occurred.

The changes in amounts of aas during the complex industrial medium fermentation was also undertaken (Table 5.33) by removing broth samples at the start of the fermentation and the end of the fermentation. The amounts of aas such as phenylalanine, leucine, methionine and isoleucine decreased (Fig 5.6A & B from inoculum to harvest). These aas have been shown to be sources of carbon for the precursors of tylactone, so a decrease in their amount may indicate that they were a limiting factor in tylosin production and that a protein source high in these aas would benefit the fermentation (see Chapter 2 section 2.9). Conversely, cysteine, tryptophan and alanine levels increased during the fermentation. They have been shown not to be significantly involved in tylosin synthesis (see Chapter 2, section 2.9). This could indicate that they were a inhibiting factor in tylosin formation by diverting carbon into cellular biosynthesis. Table 5.33 shows similarities between the aa composition of whole broth, gluten and fish meal and the aa composition of *S. fradiae* C373-10 biomass cultured on minimal medium (Table 5.29 - 5.32).

Whilst undertaking this work, the ammonia feed blocked on one bioreactor at 75 hrs. This showed interesting aa results compared to controls (Fig 5.6B). While the aa composition was similar at inoculation, it showed significant differences at harvest. Further research in this area would be beneficial to increase the understanding of aa metabolism and oil metabolism towards tylosin production in a complex industrial medium (this could be undertaken using tracer studies and atom mapping matrixes [see Chapter 1 section 1.2.3, Chapter 6, section 6.9, & Chapter 8, discussion]). To undertake this analysis further research with a semi complex medium (the addition of 20 aas) with a single carbon source was considered desirable (see Chapter for discussion).

To understand better the interaction of aas in the industrial complex medium, it was considered to attempt to differentiate between the aa composition of biomass and the medium. Biomass was extracted from the industrial complex medium as chapter 4 (section 4.5.4). The extracted biomass from the complex medium gave poorly reproducible results. This was considered to be due to the recovery of biomass (dry weight and wet weight) due to initial studies indicating that carbon loss through solvent extraction was not that severe (Chapter 4, section 4.5.4)[Table 5.11]. The compositional information was incorporated into average compositional table for biomass growth in a complex medium (see Chapter 6, Tables 6.1 - 6.27).

5.8.1 The relative abundance of amino acids Vs codon usage

The codon usage of 64 streptomycete genes has been determined (Wright & Bibb, 1992)[Bentley *et al*., 2002 quotes a G+C content of 72.1 %]. It was shown that there was preferential use in these genes of aa codons with G or C in the third position. The amounts of each aa required for translation of 63 of the genes were compared with the aa composition of *S. coelicolor* 1147 obtained from Davidson (1992) and *S. coelicolor* 1147 & *S. fradiae* C373-10 from this work. The codon usage tables determined by Wright and Bibb (1992) were converted to a percentage format (Table 5.34 Part 1) of course this assumes expression, it maybe possible now or in the future to improve on this analysis by transcriptome analysis. The measured aa composition was of whole *E. coli*, *S. coelicolor* and *S. fradiae* cells, therefore aas present in the cell wall, were included (additive alkali and residue fraction of Method 1, Chapter 3, section 3.16.1).

The average relative amounts and order of requirement of several of the aas for *S. coelicolor* 1147 and *S. fradiae* C373-10 were very similar (within 10 % error) compared to the expected order of requirement calculated from genomic codon usage tables. *S. coelicolor* showed little difference between the amino acids, methionine, lysine, isoleucine, phenylalanine, threonine, tryptophan, proline, serine, tyrosine and glutamate and small differences were observed for alanine, valine, glycine, leucine, arginine, and aspartate (Table 5.34 Part 1). This suggests that the relative amounts of these aas present within the 63 genes analysed by Wright and Bibb (1992) were possibly typical for the majority of the proteins present within a streptomycete cell. Methionine, phenylalanine and tyrosine were minor components of the composition of *S. coelicolor* and this may be reflective of their restrictive codon sequences. For example, methionine has only one codon (ATG) whereas phenylalanine and tyrosine have two each but they were AT rich (Phe: TTT, TTC; Tyr: TAT, TAC). Another reason why methionine is present in very low amounts in *S. coelicolor* & *S. fradiae* (as compared to *E. coli*) may be that the ATG initiation codon (formyl-methionine) was not always used in streptomycete genes to the same extent as in *E. coli* genes.

Some Streptomycete ORF's have the valine codon GTG as their initiation codon, for example *idh* (encoding isocitrate dehydrogenase) of *S. coelicolor* (Taylor, 1992). Since analysis of the amino-terminal of isocitrate dehydrogenase did not reveal the identity of the initial residue N-terminal sequence analysis of phosphoglycerate mutase from *S. coelicolor* also did not identify the initial residue (White *et al*., 1992). It was proposed that the residue was methionine and that it had been cleaved during post-translational processing. However, it has been reported that *Streptomyces* sometimes miss read the valine codon for formyl-methionine (personal communication Professor I Hunter).

The most abundant aas in the 63 genes of *S. coelicolor* 1147 & *S. fradiae* C373-10 were, alanine, arginine, glycine, leucine and valine. All have G or C in the first position of their codons and A or T in their third position. Alanine codons have GC in the first and second position that may explain the presence of the higher proportion of the aa content of *S. coelicolor* 1147 & *S. fradiae* C373-10 as compared to the composition of *E. coli* ML308.

Observed differences in the use and measured abundance of the streptomycete aas was originally believed to be a consequence of the limited number of genes available from *Streptomyces* for determination of their codon usage. Genome sequence analysis has revealed the codon usage table constructed by Wright & Bibb (1992) to be near perfect. It is possible that, in other proteins, aas with similar properties, perhaps not solely structural, may be interchanged. For example, AT rich positively charged may be replaced by similarly charged arginine (White *et al*., 1992), which has some GC rich codons. In addition, differences may be due to the measurement of *S. coelicolor* aa from different cellular compartments (i.e., cell walls).

Table 5.34 Part 2 also shows the sequence of the order of requirement for the aa families for *S. coelicolor* 1147 and *S. fradiae* C373-10 was PYR > oxo-glutarate > 3-phosphoglycerate > G6P > oxaloacetate and for *E. coli* ML308 was PYR > oxo-glutarate > 3-phosphoglycerate > G6P > oxaloacetate (results adapted from Holms, 1986)[see Chapter 6, section 6.4; for the order of requirement of the precursor metabolites on a carbon atom basis]. Glutamate and aspartate families are all produced from the TCA cycle intermediate metabolites, whereas phenylalanine, valine and leucine are produced from the glycolysis intermediates, pyruvate, and PEP. Oxygen excess in aa producing organisms gives rise to abundant TCA cycle intermediates, whereas O_2 limitation should result in less glucose being oxidised via the TCA cycle, allowing more intermediates to be available for phenylalanine, valine and leucine biosynthesis. Thus, some degree of metabolic disruption results in greater production of amino acid demand from pyruvate. The investigation Hirose and Shibai (1980) investigation of aa biosynthesis by *Brevibacterium flavum* provide an excellent example of the effects of dissolved O_2 concentration on the production of a range of closely-related metabolites. These workers demonstrated the critical dissolved O_2 concentration for *B. flavum* to be 0.01 mgl^{-1} and considered the extent of O_2 supply to the culture in terms of the degree of 'oxygen satisfaction', defined as respiratory rate of the culture expressed as a function of the maximum respiratory rate. Thus, a value of O_2 satisfaction below unity implied that the dissolved O_2 concentration was below the critical level. The oxygen requirements of *E. coli* (substrate glucose), *Pseudomonas* C (substrate methanol), and *Pseudomonas* spp. (substrate octane) were 0.4, 1.2, and 1.7 g $O_2.g^{-1}$dry wt respectively. The production of members of the glutamate and aspartate families of aas was affected detrimentally by levels of O_2 satisfaction below 1.0,

whereas optimum production of phenylalanine, valine, and leucine occurred at O_2 satisfaction levels of 0.55, 0.60 and 0.85, respectively. It would be of further interest to determine the effect of codon bias on the order of requirement of aa families, under different conditions i.e., the critical dissolved O_2 concentration range for a number of secondary metabolite producing bacterial species in conjunction with bacteria with diverse codon differences. It may be the case that to reduce metabolic disruption, codon bias does not necessitate a change in the order of requirement of aa families.

5.8.2 Metabolic costs of amino acid biosynthesis

The synthesis of aas (see Appendix B, Table 1.1b) has a large metabolic cost. Therefore protein synthesis from central metabolic intermediates requires large amounts of ATP, NADPH, NADH, NH_4, and sulphur as well the cost of polymerisation of aas. The fraction of carbon that is allocated to aa production must be closely balanced with the fraction that leads to energy production via the TCA cycle.

The importance of the metabolic costs to the biosynthesis of aas to *E. coli* ML308 (results adapted from Holms, 1986), *S. coelicolor* 1147, & *S. fradiae* C373-10 was assessed. The molecular weight (MW) of amino acids for a protein has been shown to correlate positively with the proteins expression level and with its size (i.e., increasing MW equals increasing metabolic cost)[Seligmann, 2003]. This was considered an acceptable strategy for measuring the effects of metabolic costs on codon usage. *S. coelicolor* and *S. fradiae* C373-10 cultured on a glucose minimal medium (Fig 5.7a calculated from the aa composition and genomic codon usage tables) showed preferences for low cost aas. With the exception of arginine which was a metabolic expensive aa (7 ATP, 1 NADH, 4 NADPH, 4 NH_4; Chapter 8, Tables 8.1 - 8.4). This was reflected for *S. coelicolor* 1147 and *S. fradiae* C373-10 Fig (5.7a) where arginine was shown as the 3 rd – 6 th most abundant aa on average. *E. coli* ML308 cultured on a glucose minimal medium showed a considerable difference in the spread of aa metabolic costs (Fig 5.7a)[results adapted from Holms, 1986]. Figures 5.4b and c were included to assess the differences in codon bias calculated from experimental aa results and bioinformatics. These results indicate a tight control over expression of a number of co-factor expensive aas (e.g., ILE, PRO, THR). Although there has been reported to be an absence of product feedback regulation of aa catabolism and anabolism (Hodgson, 2000) in

streptomycetes. End product control has been recognised in *S. coelicolor* and *S. fradiae* (Potter & Baumberg, 1996; Vancura *et al*., 1989) for isoleucine, valine, leucine, and Threonine (see Chapter 8 for discussion).

In a oligotrophic environment it would be expected that an organism would have evolved to use this limitation to control its growth, and therefore it would be expected that streptomycetes codon usage (aa composition) versus the metabolic cost would reflect the most abundant aas having low metabolic costs (i.e., NADPH, NADH, ATP, NH_4, 1-C, & S) and little regulation, and the least abundant with high metabolic costs would be tightly regulated. Thus it could be postulated that codon bias could be a first step of regulating the cellular economy of supply and demand (see Chapter 8 for discussion).

This approach was further applied to whole broth samples of *S. fradiae* C373-18 cultured on complex industrial medium (Chapter 3, section 3.7.3). Where the inoculation point was sampled (0 point)[Fig 5.7b] and the harvest point (Fig 5.7b) both showed similar aa distribution of codon usage vs. metabolic costs to the aa composition of the biomass of *S. fradiae* C373-10 cultured on a minimal medium (Fig 5.7b). The only observable difference being the down turn in the order of requirement for arginine from the 0 point to the harvest.

Further analysis was undertaken to separate the biomass from the complex medium with the extraction procedure already used in Chapter 4 (section 4.5.4) (for method see Chapter 3, section 3.14.2). The complex biomass samples showed a considerably different spread of codon usage vs. the metabolic costs and the order of aa requirement (Fig 5.7b) against previous tables for *S. fradiae* C373-10 (Fig 5.7b). This could further fit with the hypothesis already made in section 5.7 that arginine was a free intracellular aa and the extraction protocol extracted small carbon containing molecules, or the extraction procedure did not give an accurate representation of biomass.

M. tuberculosis show a similar profile of aa codon usage (Fig 5.7c) [codon usage tables were used as know amino acid data was available] to *S. coelicolor* 1147 and *S. fradiae* C373-10. Other bacteria e.g., *Tetrahymena pyriformis* (25 % GC), *Bacillus cereus* (35 % GC), *Bacillus megatherium* (38 % GC), *Bacillus subtilis* (42 % GC), *Salmonella typhimurium* (50 % GC), *Aerobacter aerogenes* (57 % GC), *Serratia marcescens* (58 % GC), *Sarcina lutea* (64 % GC), *Pseudomonas aeruginosa* (65 % GC), *Alcaligenes faecalis*

(67 % GC), *Micrococcus lysodeikticus* (72 % GC)[Fig 5.7c] which show increasing GC codon bias (results adapted from Sueoka, 1961 and codon usage tables) also show a preference for low cost aas. There were three main aa groups (1) five aas whose frequencies decrease with G+C content Ile, Phe, Lys, Tyr, Leu. (2) Nine aas whose frequencies increase and then decrease (Asp, Glu, Ser, Val, His, Cys, Met, and Trp). (3) Four aas (Gly, Pro, Ala, Arg) whose frequencies increase with G+C content (Fig 5.7c). Lobry (1997) used factorial mapping to analyse aa data of streptomycetes which indicated similar results to this work.

It would be of benefit to continue this work in conjunction with assessing the metabolic costs of free intracellular aa, and compartmentation to streptomycete metabolism.

5.9 Compiled macromolecular and monomeric compositions of *S. fradiae* C373-10 and *S. coelicolor* 1147.

The analysis carried out using *S. fradiae* C373-10 & *S. coelicolor* 1147 sampled biomass and presented in the previous sections (5.1 - 5.8) was used to compile a macromolecular composition. An approximate macromolecular composition for *S. coelicolor* 1147 was considered to be CHO 6.3 – 11.74 %, RNA 5.06 – 8.62 %, DNA 3.79 – 11.16 %, protein 26.32 – 50.45 %, lipid, 11.57 – 15.00 % teichoic acid (TA) 8.46 – 17.85 %, & peptidoglycan 5.42 % for growth on a glucose minimal medium (Chapter 3, section 3.6.4) and an approximate macromolecular composition for *S. fradiae* C373-10 was considered to be CHO 15.0 – 20.0 %, RNA 10.0 - 13.0 %, DNA 3.0 – 5.0 %, protein 36.0 –51.0 %, lipid, 2.5 – 3.6 TA 10.0 – 13.0 %, & peptidoglycan 7.74 % for growth on a glucose glutamate defined medium (Chapter 3, section 3.6.4). This demonstrated that for *S. fradiae* C373-10 84.24 – 113.34 % and for *S. coelicolor* 1147 66.92 – 120.24 % of the composition had been accounted for (see Tables 5.4 - 5.9). Studies on the macromolecular content of *E. coli* (strain B) were initiated by Taylor (1946). The currently used composition of *E. coli* B/r, which was established by Dennis & Bremer (1974), was 55.0 % protein, 20.5 % RNA (total) and 3.1 % DNA. Shahab *et al*. (1996) reported 31.0 – 45.0 % protein, 10.0 – 22.0 % RNA and 3.5 - 4.5 % DNA content of *S. coelicolor* and accounted for 56.0 - 63.0 % of mycelial carbon. Davidson (1992) approximated the macromolecular content of *S. coelicolor* 1147 to be 53.0 % protein, 14.0 % RNA, 6.0 % DNA, 5.5 % lipid and 4.6 % peptidoglycan, and accounted for 83.1 % of mycelial carbon (protein was accounted for

with TOCA) and 12.0 - 21.0 % protein, 14.0 % RNA, 6.0 % DNA, 5.5 % lipid and 4.6 % peptidoglycan, and accounted for 46.60 % of mycelial carbon (protein was accounted for with macromolecular analysis). Reisenberg & Bergter (1979) examined the macromolecular composition of *S. hygroscopicus* grown in both batch and continuous culture. The macromolecular composition reported for *S. hygroscopicus* appears qualitatively similar to *S. coelicolor* 1147 & *S. fradiae* C373-10, its protein content is significantly less than that observed in *E. coli.*

The protein content of *E. coli* B/r per cell increases with μ (Bremer & Dennis, 1987). This reflects the increase in the cell's demands for these components at high μ's and results in an increase in the average mass of a cell. Also, at high μ's, the DNA content per cell increases with μ as a result of overlapping rounds of DNA replication. However, the DNA content per cell mass decreases because the average mass of a cell increases faster than the mass of DNA in the cell. The proportion of the cell's mass represented by protein remains approximately constant since the mass of protein per cell increases in direct proportion with the average mass of the cell. In contrast, the RNA content per cell mass increases with μ, because the RNA portion increases faster than the average cell mass.

Trends in the proportions of protein, RNA and DNA per cell mass in streptomycetes appear to be similar to those observed in *E. coli*. However, Shahab *et al*. (1996) reported that the *S. coelicolor* hyphal growth unit (HGU), [i.e., hyphal compartment] size appears approximately constant up to a relative μ of about 0.7. Therefore it would appear that changes in the proportions of each macromolecule in *S. coelicolor* probably do not arise from an overall increase in cell size.

5.9.1 Determination of the monomeric composition from the macromolecular composition of *S. fradiae* C373-10 and *S. coelicolor* 1147

Determination of the monomeric composition of *E. coli* given by Neidhardt (1987) was carried out both by analytical measurements and by expression of the macromolecular content in terms of monomers and converted to compositional tables as Holms (1986, 1996, 1997, 2001)[see Appendix B]. The construction of compositional tables for *S. coelicolor* 1147, *S. fradiae* C373-10 and C373-18 was as followed: the aa, & CHO

composition were calculated from the results of this Chapter (section 5.1 - 5.8). The nucleotide composition of the biomass was calculated from the DNA and RNA estimation based on the findings that *Streptomyces* DNA was, on average 73 % G+C rich (Pridham & Tresner, 1974)[Chapter 2, section 2.1] and the rRNA and tRNA sequences, which make up 96 % of the total RNA was approximately 60 % rich (see Appendix H). The fatty acid composition of streptomycete composition was calculated as Appendix G. The constructed monomeric tables were expressed in the units of mmoles.g^{-1} dry weight biomass and C.mmoles.g^{-1} dry weight biomass. These results are presented in Chapter 6 (Tables 6.1 – 6.27).

5.10 Elemental composition of *S. fradiae* C373-10 and *S. coelicolor* 1147 biomass

The macromolecular and monomeric compositions of biomass samples of *S. coelicolor* 1147, *S. fradiae* C373-10 and C373-18 were presented in the preceding sections (section 5.1 - 5.8). Further compositional analysis involves the elements that allow mass balance equations to be formulated. These equations represent the stoichiometry of thousands of chemical reactions required to produce bacterial biomass (see Chapter 1, section 1.2.1). Elemental analysis was carried out on all fermentations prior to the end of growth phase (Table 5.37; all sampling points were as Chapter 4, i.e., sampling point II, except for the methyl oleate defined medium where sample points I, and III were analysed in addition).

Although lysis may have occurred in these samples, it was still possible to carry out analysis for the elements C, H, N, S & P. All analyses was carried out in triplicate. The oxygen content was calculated by subtraction from 100 % as Fig 5.8 (including the subtraction of the theoretical ash content where appropriate). The empirical formula of the biomass was computed by expressing each element as the number of gram atoms (by dividing the percentage value of the elements by their specific atomic masses). The values were then normalised with respect to a carbon unit of 1.0 (Fig 5.8). Following lyophilisation of 21 *S. coelicolor* 1147, *S. fradiae* C373-10 and *E. coli* ML308 samples (see Table 5.38 - 5.40) cultured on a number of different carbon sources, each sample was further subdivided again, to give a total of 63 samples (all samples were run in triplicate)[Table 5.35 Part 1 & 2].

In comparison to the elemental composition of *E. coli* (Ingraham *et al*., 1983), the carbon and hydrogen content were very similar [Table 5.35 Part 1 &2]. *E. coli* contains 20 - 30 % oxygen & 14 % N, with an empirical formula of $CH_{1.9}O_{0.3}N_{0.24}$ (Table 5.34 & 5.37). According to Roels (1980), "most micro-organisms" have an empirical formula of $CH_{1.65}O_{0.52}N_{0.2}$ (Table 5.36). The higher oxygen content observed in other *Streptomyces* spp. (*S. coelicolor*, Davidson, 1992; *S. thermonitrificans*, Burke, 1991; *S. cattleya*, Burke & Fryday, 1983)[see Table 5.36] was also observed when *S. fradiae* C373-10 and *S. coelicolor* 1147 was cultured on a minimal glucose medium compared to *E. coli* ML308 and with no ash content accounted for (Table 5.37 Part 1)[$CH_{2.04}O_{0.62}N_{0.19}P_{0.023}S_{0.022}$ for *S. fradiae* C373-10; $CH_{1.90}O_{0.56}N_{0.15}$ for *S. coelicolor* 1147; $CH_{1.94}O_{0.38}N_{0.26}S_{0.007}P_{0.015}$ for *E. coli* ML308]. The MW of one C.mole biomass was calculated to be 28.12 for *S. fradiae* C373-10, 26.02 *S. coelicolor* 1147, and 24.39 for *E. coli* ML308 (Table 5.37 Part 2).

The electron balance expressed as the degree of reduction (γ) can be calculated as a further indicator for inconsistencies within the data sets (see Appendix D for theory). The γ of a mass balance component was defined by Erickson *et al*. (1979). The γ was calculated to be 4.22 for *S. fradiae* C373-10, 4.41 *S. coelicolor* 1147, and 4.39 for *E. coli* ML308 (Table 5.37 Part 2).

Biomass from a glucose minimal medium and methyl oleate defined medium on average showed a higher elemental oxygen composition for *S. fradiae* C373-10 (Table 5.37 Part 1). The high oxygen content of streptomycetes has been, reported by other workers. The ash content (oxidised mineral components) was further taken into account to determine the effect of ash content on the elemental oxygen composition as, there were no reports in the literature for streptomycete research that this had been previously accounted for. The percentage ash composition was analysed by three methods [see Table 5.37] (1) biomass was ashed in a kiln at 600^0 C (see Chapter 3, section 3.15.4 for method), (2) Biomass was ashed after acid treatment (see Chapter 3, section 3.15.4 for method), (3) The theoretical ash content was calculated in the following way; phosphorous typically comprises 50 % of the total ash (Burke, 1991). An approximation for the residue can be made (proportion for phosphorus minus that of sulphur). Theoretical ash content for *S. fradiae* C373-10 was calculated to be 0.31 % on average and 1.15 % on average for *S. coelicolor* 1147 (Fig 5.8).

An average theoretical ash content was calculated from four shake flask cultures for *S. fradiae* C373-10 and *S. coelicolor* 1147 and the elemental C, H, N, S, & P was analysed in triplicate (Table 5.38). The experimentally determined non-hydrolysed ash content showed an average ash content of 9.8 % of the biomass, against 5.5 % for the hydrolysed ash content (see Table 5.38). The percentage ash content has been reported for *C. utilis* (7.0 %), *Klebsiella aerogenes* (3.6 %), *S. cerevisiae* (5.5 - 9.7 %), *E .coli* (5.5 %), *Pseudomonas fluorescens* (7.9 %), *Aspergillus niger* (7.5 %), and an average ash composition of 6.0 % (Christensen *et al*., 1995; Roels, 1983)[Table 5.36]. There seems be no standard bench mark method to account for bacterial ash content. Table 5.34 would indicate large discrepancies in the measurement of the ash content of streptomycete biomass between experimentally determined (non-hydrolysed samples and hydrolysed samples) and the theoretical determination (with an mean percentage STDEV between the methods of 4.44 for *S. fradiae*, 4.46 for *S. coelicolor* and 0.68 for *E. coli*; Table 5.36). The methods used to calculate the ash content gave consistently different results (Chapter 3, section 3.15.4) complete acid hydrolysis and non acid hydrolysis before ashing gave similar results in case of *E. coli* ML308, but inconsistencies were seen in the case of *S. fradiae* & *S. coelicolor* (Table 5.37). Further elemental analysis using a technique such as inductively coupled plasma (ICP) may be advisable where the elements such as P, K, Na, Mg, Ca, Fe, Mn, Cu, and Zn can be analysed. If high enough temperatures can be reached, any element can be excited to a level where it will produce emission of radiation. In this method all the elements are pooled as one *pseudo*-element "M" and subtracted from 100 % with C, H, and N and the empirical formulae calculated. Lange & Heijnen (2001) accounted for the total metal content for *S. cerevisiae* in this way the total metal content was estimated to be 2.51 % of the biomass lower than the traditionally expected ash measurement (i.e., *S. cerevisiae* 5.5 - 9.7 %).

The average theoretical ash content and the experimentally determined hydrolysed ash content were used to calculate the empirical formula, the molecular mass, and the degree of reduction for *S. coelicolor* 1147, *S. fradiae* and *E. coli* ML308 biomass cultured on a number of different carbon sources (where the ash content was presented in the following way: E, no ash content taken into account, E1 theoretical ash content taken into account, E2 non-hydrolysed ash content taken into account, and E3 hydrolysed ash content taken into account)[Table 5.37 Part 1 & 2]. Table 5.37 Part 1 & 2 would indicate that the ash

content had a considerable effect on the elemental oxygen composition. Although the calculated oxygen composition was considerably lower than the expected empirical formula (Table 5.36).

5.10.1 Measurement of elemental biomass composition calculated from the molecular composition

The empirical elemental composition formula of *S. fradiae* C373-10*, S. coelicolor* 1147, and *E. coli* ML308 (results calculated from Holms, 1986 for *E. coli* data) biomass based on the measured macromolecular composition [Table 5.35 Part 1 & 2, and 5.38](Tables 6.1 to 6.29, Chapter 6, were converted to the compositional atomic requirements and then number of grams of each atom were calculated and thus converted to a percentage format and the empirical formula calculated as section 5.9). The molecular elemental empirical formula and the molecular mass for *S. fradiae* C373-10 cultured on a glucose minimal medium was $CH_{2.07}O_{0.64}N_{0.31}P_{0.003}S_{0.002}$ and 29.37 and average formula of $CH_{1.99}O_{0.57}N_{0.25}P_{0.003}S_{0.020}$ and 27.34 for *S. coelicolor* 1147 cultured on a glucose minimal medium was $CH_{1.98}O_{0.62}N_{0.24}P_{0.004}S_{0.040}$ and 28.63; and *E. coli* ML308 cultured on a glucose minimal medium was $CH_{2.03}O_{0.62}N_{0.22}P_{0.009}S_{0.023}$ and 28.05.

The MW of one C.moles *S. fradiae* C373-10 biomass cultured on glucose calculates to 29.37, almost 1.86 g.moles less than determined by elemental analysis with a theoretical ash content and 3.38 g.moles less when determined by the experimentally determined hydrolysed ash content. The considerable difference with the calculation for the molecular mass, between the elemental and the molecular elemental analysis was likely a consequence of differences between the oxygen, phosphate, and sulphur accountability. The C : N ratio differed for both the elemental and molecular empirical formula; 4.37 versus 4.35 $g.g^{-1}$ on average (Table 5.42)[medium average C / N elemental ratio of 13.13]{Table 5.42}. The percentage difference between the elemental and the molecular elemental C / N ratio was from ± 1.43 - 71.94 % (± 28.12 % on average)[Table 5.42].

The higher elemental oxygen content seen in *S. coelicolor* 1147 and *S. fradiae* C373-10 seemed to correlate with biomass samples that were high in CHO content and low in lipid content. This high oxygen state was only observed for growth on glucose minimal medium and the methyl oleate defined medium for *S. fradiae* C373-10. This fits with the results of

section 5.3.4 for the total soluble lipid composition of biomass in which carbon was 'pushed' to CHO storage when NH_4 was the nitrogen source and to lipid storage accumulation when glutamate was the nitrogen source. The differences observed for the methyl oleate defined medium biomass were considered a consequence of the solvent extraction procedures used to extract clean biomass (as observed in section 5.4.3) affecting the lipid balance. This led to the hypothesis that these macromolecules may have a considerable effect on the elemental composition. A sensitivity analysis revealed that if the CHO and lipid were removed systematically from molecular elemental calculation, then this would lead to an elemental composition of $CH_{1.81}O_{0.49}N_{0.11}P_{0.001}S_{0.04}$ minus CHO and $CH_{1.81}O_{0.76}N_{0.13}P_{0.002}S_{0.05}$ minus the lipid. Further analysis using the average compositional data (Chapter 6, Table 6.1 - 6.27) in which the lipid and CHO data (Chapter 5, Table 5.17) for growth on glucose, fructose, glycerol minimal medium, glucose glutamate, fructose glutamate, and glycerol glutamate defined medium were interchanged and then converted to a molecular elemental composition. This led to a molecular elemental empirical formula for the glucose, fructose, and glycerol incorporating average compositional data, of $CH_{2.00}O_{0.68}N_{0.24}P_{0.003}S_{0.019}$, $CH_{2.00}O_{0.68}N_{0.24}P_{0.003}S_{0.020}$, and $CH_{1.99}O_{0.62}N_{0.28}P_{0.003}S_{0.023}$ (average between Table 6.3 - 6.4, Chapter 6), and a composition of $CH_{2.01}O_{0.61}N_{0.23}P_{0.003}S_{0.019}$, $CH_{2.00}O_{0.68}N_{0.24}P_{0.003}S_{0.020}$, and $CH_{2.01}O_{0.59}N_{0.25}P_{0.003}S_{0.020}$ (average between Table 6.9 - 6.12, Chapter 6) for the average glucose glutamate, fructose glutamate, and glycerol glutamate composition (average between Table 6.26 Chapter 6). All showed little deviation with changes in the CHO lipid ratio for all six lipid and CHO compositions (corresponding to Table 5.17). Therefore the balance between the CHO and lipid content of streptomycete biomass may not be the only factor leading to the higher elemental oxygen level.

The γ of *S. fradiae* C373-10 biomass cultured on a number of different carbon sources can be seen in Tables 5.37 Part 1 & 2, 5.38, and 5.40. The γ was calculated with respect to the molecular elemental and elemental techniques. Despite the inconsistencies between both sets of measurements, both compare well with values reported in the literature for streptomycetes (Burke, 1991; Davidson, 1992; Bushell & Fryday, 1983), with the largest discrepancies between the oxygen, sulphur, and phosphorus content (Tables, 5.39, and 5.40). Values in the range of 4 to 4.25 for biomass analysis have been reported for other microorganisms (Table 5.35 Part 1 & 2, 5.37 Part 1 & 2, 5.38, and 5.40).

The equations 1 – 3 (Appendix D) were used to further verify and calculate the maximum possible biomass yield for the glycerol fermentations using the γ calculated from Tables 5.37 Part 1 & 2, 5.38, and 5.40. When *S. fradiae* C373-10 was cultured on a glycerol minimal medium (fermentations 1 & 2 respectively). The biomass yield was 0.29 and 0.31 $g.g^{-1}$ for the elemental, and 0.35 & 0.33 $g.g^{-1}$ for the molecular elemental (with no ash content taken into account), 0.29 & 0.31 $g.g^{-1}$ (with the theoretical ash content taken into account), 0.28 & 0.29 $g.g^{-1}$ (with the hydrolysed ash content taken into account), 0.26 & 0.28 $g.g^{-1}$(with non-hydrolysed ash content taken into account) 0.32 & 0.21 $g.g^{-1}$ calculated experimentally was achieved (Table 5.39 Part 1 & 2, & 5.40). This would indicate that -8.48 - 30.70 % of the carbon in the culture was accounted for with the present method and further assessment of the elemental balance was needed.

Equation 4 (Appendix D) allows a rapid evaluation of the oxygen demand of a culture and does not require that the quantities of NH_3, CO_2 and H_2O involved in the stoichiometric equation (Chapter 2, section 1.2). The O_2 demand for the *S. fradiae* C373-10 glycerol minimal medium fermentations (fermentations 1 & 2 respectively) using equation 5 were calculated to be 2.71 and 2.72 O_2 g mmoles O_2 per g moles glycerol consumed for the elemental, and 2.80 & 2.83 $g.g^{-1}$ for the molecular elemental (with no ash content taken into account), 2.71 & 2.72 O_2 g mmoles O_2 per g moles (with the theoretical ash content taken into account), 2.68 & 2.69 O_2 g mmoles O_2 per g moles (with the hydrolysed ash content taken into account), 2.66 & 2.67 O_2 g mmoles O_2 per g moles (with non-hydrolysed ash content taken into account) 1.78 O_2 g mmoles O_2 per g moles (gas analysis only undertaking on fermentation 2; as Chapter 4, section 4.5.4) calculated experimentally (Table 5.37 Part 1 & 2, & 5.40). The considerable difference between the theoretical and experimental O_2 consumption rate (51 - 55 % on average) may possibly be a consequence of limitation on nutrient diffusion from the pelted nature of streptomycete growth or experimental error.

Further assessment of the O_2 demand using equations (5 & 6; Appendix D)[taken from Stanbury *et al*., 2000] that incorporate biomass production and substrate utilisation was undertaken to further test the validity of the on-line gas-analysis. The O_2 demand for the *S. fradiae* C373-10 glycerol minimal medium fermentations (fermentations 1 & 2 respectively) using equation 6 were calculated to be 0.31 and 2.43 O_2 g mmoles O_2 per g

moles glycerol consumed for the elemental, and 1.22 & 3.20 O_2 g mmoles O_2 per g moles for the molecular elemental (with no ash content taken into account), 0.32 & 2.39 O_2 g mmoles O_2 per g moles (with the theoretical ash content taken into account), -0.0008 & 2.10 $g.g^{-1}$ (with the hydrolysed ash content taken into account), and -0.28 & 1.83 O_2 g mmoles O_2 per g moles (with non-hydrolysed ash content taken into account) using equation 5. The O_2 demand for the *S. fradiae* C373-10 glycerol minimal medium fermentations (fermentations 1 & 2 respectively) using equation 6 (Appendix D) was calculated to be 1.54 and 3.07 O_2 g moles O_2 per g moles glycerol. These results would indicate that one glycerol fermentation with gas analysis was not enough to assess the reliability of the elemental balances undertaking with this work.

The calculation of the elemental composition from the molecular monomer composition showed good reproducibilitys between experimentally-determined elemental methods. This would indicate this was a satisfactory way of checking the consistency of elemental analysis

5.10.2 Reconciled elemental biomass composition

Table 5.40 presents the reconciled elemental data (mean values) with the calculated percentage error between the elemental and molecular elemental composition (Table 5.37 Part 1 & 2; Table 5.38]. The reconciled *S. coelicolor* 1147 biomass showed a slightly lower oxygen content than reported by other workers ($CH_{1.86}O_{0.61}N_{0.15}$, reported by Davidson, 1992) and the results for *E. coli* fit with other workers (Table 5.36). The mean percentage difference between the elemental and monomeric oxygen content was ± 7.71 % when no ash content was taken into account, ± 7.06 % when the theoretical ash was taken into account, ± 35.52 % when hydrolysed ash content was accounted for, and ± 69.73 % when the non-hydrolysed. Hypothetically, the most likely empirical formula was the one incorporating the theoretical ash content as this showed the lowest mean percentage difference between the elemental data and the molecular elemental composition.

The experimentally determined elemental composition conflicted in several ways with that based on the molecular elemental composition of the biomass. The measured carbon and nitrogen fractions were lower than the molecular elemental content [Table 5.35 Part 1 & 2]. Repeated measurements and critical analysis of the sample handling and analysis did

not provide a satisfactory explanation for the difference. TOCA & total organic nitrogen analysis (TONA) [Chapter 3, section 3.15.6] measurements were undertaken to underpin the results of the elemental analysis (Table 5.35 Part 1 & 2). The discrepancies between these measurements have never been addressed before. The main problem with the elemental analysis was the effect that water contamination has on the analysis. Dry biomass rapidly absorbs water; even in environments considered to be under desiccation.

Comparison of the TOCA measurements with the elemental analysis showed a good agreement (Table 5.35 Part 1 & 2) despite large variations with individual cultures. A comparison of the STDEVs (Table 5.43) shows that the accuracy of this method must be improved before it can be considered as a full substitute for the elemental analysis of carbon. Determination of nitrogen content failed expectations; the difference between the molecular elemental, elemental and TONA techniques showed considerable differences, which in turn had a detrimental effect on the γ calculation.

The error values (Table 5.35 Part 1 & 2) between different experimental techniques were rather large compared with values commonly reported for these methods (Duboc *et al*., 1995). However the differences between the STDEVs of measurements on a single sample and between samples of repeated cultures indicated that these values were subject to errors outside the chemical analysis. Sampling and sample handling were probable sources, but small variations in culture conditions were also likely to have an influence.

The percentage difference in carbon and nitrogen would indicate a considerable proportion of the biomass was not accounted for, possibly cell wall components. The high experimental difference for sulphur (± 43.25 % on average) and phosphorus (± 47.90 %) indicated that a considerable proportion of sulphur and phosphorus-containing molecules were unaccounted for in the monomeric and macromolecular analysis. Phosphorus was likely to be accounted for in the cell wall fraction as TAs (section 5.7). The percentage difference in sulphur was unexpected. *S. fradiae* C373-10 has been shown in this work to require $MgSO_4$ for growth. It could be feasible there is a need for high levels of sulphur for a byproduct (see Chapter 8 discussion).

5.10.3 The black box model (mass balance equation)

Fermentation mass balance equation for biomass based on the stoichiometry may be calculated (see Appendix A, for example of calculation), based on the molecular formula for biomass (formulated in previous section 5.9 - 5.9.2). Such analysis has already been undertaking for *S. thermonitrificans* (Burke, 1991) and *S. cattleya* (Bushell & Fryday, 1983)[see Table 5.27 & 5.28 for results].

(Equation 1) 0.39 $C_3H_8O_3$ + 0.05 O_2 + 0.20NH_3 → $CH_{2.00}O_{0.53}N_{0.20}$ + 0.18 CO_2 + 0.27 H_2O

The fermentation mass balance (equation 1) was calculated for the period 0 – 192 hrs, adopting the rationale of Herbert (1976) & Doran (1997). The multi-phasic nature of this period (see Chapter 4 for fermentation profiles) suggests that resolution of the mass balance over shorter time intervals could have been more revealing, but the lack of on-line gas analysis data and the accuracy of the assays for the components concerned precluded this approach. Extracellular products from carbon analysis were considered too low to have an effect on the balance. Microscopical analysis of the media did not point to lysis having occurred. An accurate Monod yield factor per unit weight substrate consumed (see Appendix A for calculation) may be obtained from the balance, although without gas analysis from the other fermentations this data must be viewed with care. The value (0.70) was high but consistent with that achieved for *S. cattleya* and *S. thermonitrificans* (although both of these were cultured on glucose).

5.11 Summary, future work and directions

Initial analysis indicated that macromolecular extraction methods 1 & 2 (Chapter 3, 3.16) offered the most user semi-friendly protocols with the additional advantage of offering a 1 - 5 step protocol for the complete analysis of CHO, DNA, RNA, protein, lipid and cell wall components. An approximate macromolecular composition for *S. fradiae* C373-10 was considered to be CHO 15.0 – 20.0 %, RNA 10.0 - 13.0 %, DNA 3.0 – 5.0 %, protein 36.0 – 51.0 %, lipid, 2.5 – 3.6 teichoic acid 10.0 – 13.0 %, & peptidoglycan 7.74 % for growth on a glucose + glutamate defined medium. When minimal media was supplemented with glutamate there was an increase in the cellular lipid content and when cultured on a single

carbon source the CHO content of cells was increased. Both methods 1 & 2 compared well for total NA recovery although only 50 – 60 % of the RNA was extracted by method 2. *E. coli* ML308 showed an 80 - 90 % recovery of RNA for the KOH extraction method 2. This could indicate that the streptomycete cell wall was refractory to the KOH extraction step.

Initial analysis would indicate that the Bradford assay was a source of error for protein determination with *S. fradiae*. Further analysis was therefore undertaken to determine if the Bradford assay results were correct. The Reverse biuret method combined with the copper bathocuproine chelate reaction (section 3.20.5) [Matsushita *et al.,* 1993] was used to verify this analysis. The protein to protein variability was very low and individual proteins or protein mixtures can be measured accurately with this assay. The level of protein detected by the reverse biuret assay against the Lowry, Bradford, and BCA assays on the whole was four fold higher for *S. fradiae* C373-10, 1.5 fold higher for *S. coelicolor* 1147. The protein content of *E. coli* showed little difference between the different protein assays. This would indicate that the amino acid composition of the organism and the protein standard chosen, in this case BSA, had an effect on the amount of protein detected between the species. These results indicate that the differences between aa composition of different bacterial species will have a considerable effect on the accuracy of protein assays. Therefore the reverse biuret method should be considered as a standard method of protein determination in bacterial compositional research.

Total carbon analysis was used to verify the accuracy of the macromolecular analysis undertaken with methods 1 & 2. This indicated up to 90 – 97 % of the carbon in the KOH (method 2) fraction of most samples was unaccounted for. A possible suggestion was that the cell-wall associated polymer, teichoic acid had been extracted. Taking teichoic acid into account and assuming a glycerol backbone or ribitol backbone, 18.1 % and 10.7 % of the carbon remained unidentified in method 2.

The average relative amounts and order of requirement of several of the aas for *S. fradiae* was very similar compared to the expected order of requirement calculated from genomic codon usage tables. The average order of requirement for *S. fradiae* indicates glycine as the most abundant aa and showed an average aa decreasing order of requirement of GLY >

ALA > ASP > GLU > ARG > LEU > VAL > PRO > THR > ILE > TYR > PHE > LYS > HIS > SER > MET > TRP. By contrast the costs of amino acid biosynthesis vs. codon usage showed a preference for low cost amino acids with the exception of arginine. The sequence of the order of requirement for the amino acid families for *S. fradiae* and *E. coli* showed no deviation. It may be the case to reduce metabolic disruption codon bias does not necessitate a change in the order of requirement of amino acid families. The amino acid composition of the industrial complex medium and whole biomass also showed a similar composition.

The biomass composition of *S. fradiae* grown in batch culture under nitrogen limitation was analysed for its elemental and for its molecular composition. Both descriptions initially resulted in conflicting results concerning the elemental composition, MW, and degrees of reduction. Repeated measurements and critical analysis of the sample handling and analysis did not provide a satisfactory explanation for the difference. The difference in carbon and nitrogen would indicate a considerable proportion of the biomass was not accounted for, possibly cell wall components. The high experimental difference for sulphur and phosphorus indicated that a considerable proportion of sulphur and phosphorus-containing molecules were unaccounted for. Phosphorus was likely to be accounted for in the cell wall fraction as teichoic acids.

In conclusion, analysis of *S. fradiae* C373-10 biomass resulted in compositional data at the macromolecular, monomeric and elemental level. Balancing of the elemental and molecular elemental measurement values ensured that the reconciled values of the biomass were inherently consistent. The resulting data represent the best estimate of elemental and molecular biomass composition based on all available data. The values obtained, however, are not definitive and further work is required to obtain information comparable to that reported for *E. coli*. Nevertheless, the monomeric compositions of biomass samples were considered sufficient to calculate throughputs and therefore, fluxes to biomass through the central metabolic pathways of *S. fradiae* C373-10 (see Chapter 6) the data from this Chapter were then converted to compositional tables (as Holms, 1986, 1996, 1997, 2001) [section 5.8.1; Tables 6.1 - 6.27; Figures 6.1 – 6.29; All Tables can be found in the companion CD; Appendix O Chapter 6 & P)].

Macromolecular change during fermentations of *S. coelicolor* 1147and *S. fradiae* C373-10 in bioengineering fermenters.

***S. coelicolor* 1147**

(a) glucose (Ferm 1)

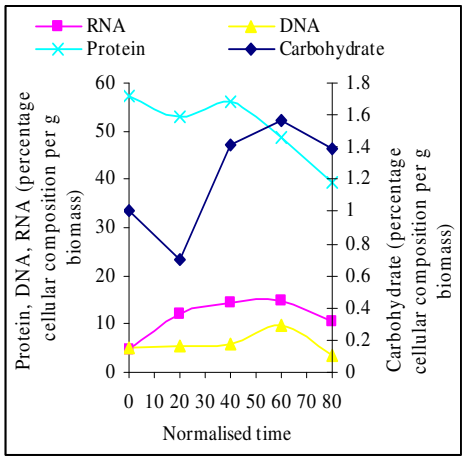

(b) glucose (Ferm 2)

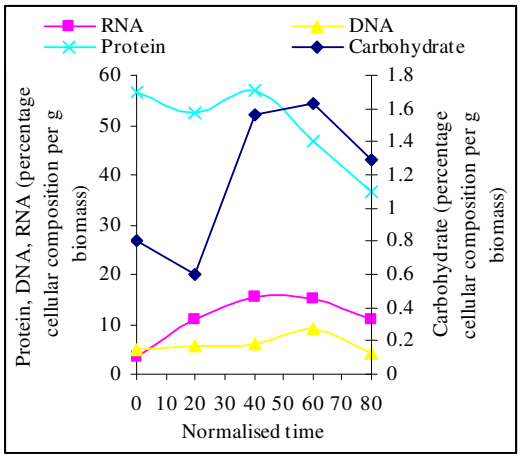

***S. fradiae* C373-10**

(c) glucose (Ferm 1)

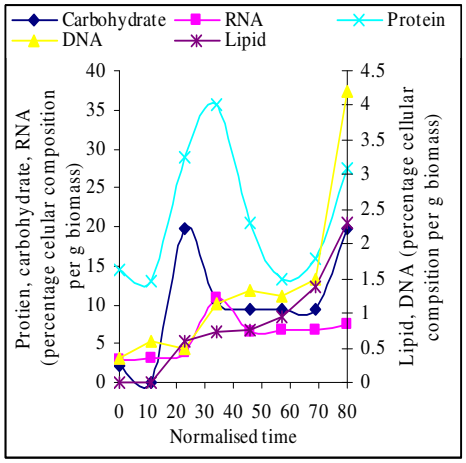

(d) glucose (Ferm 2)

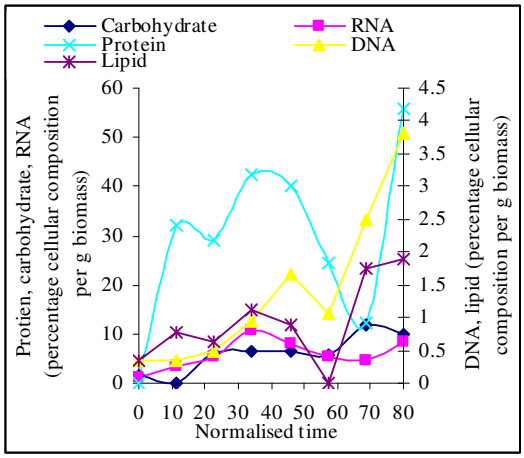

Fig 5.1 Samples taken during fermentations were subjected to fractionation method 1 (Chapter 3, section 3.16.1). The resulting fractions were assayed for the total RNA, DNA, carbohydrate, protein, & lipid biomass content expressed as the percentage cellular composition per g of biomass. Due to differences in the specific growth rate, and substrate uptake rates between different strains and strains cultivated under different conditions. A comparison can only be done, by eliminating the individual time scales (calculated as King, 1997; King and Budenbender, 1997; who compared macromolecular compositional data for 25 streptomycetes). Therefore graphs show the change in macromolecular concentration in the cultures with respect to normalised time. This protocol would usually be undertaken as Chapter 3, section 3.17.1. From this work antibiotic yields and limitation times were considered in sufficient to distinguish between. Therefore the cultures were normalised to 80 h^{-1} up until the end of DNA replication and each time scale of the remaining data was normalised with a factor of 5 h^{-1} (i.e., 24 hrs = 5 places on the graph).

Macromolecular change during fermentations of *S. coelicolor* 1147and *S. fradiae* C373-10 in bioengineering fermenters.

(e) fructose (Ferm 1)

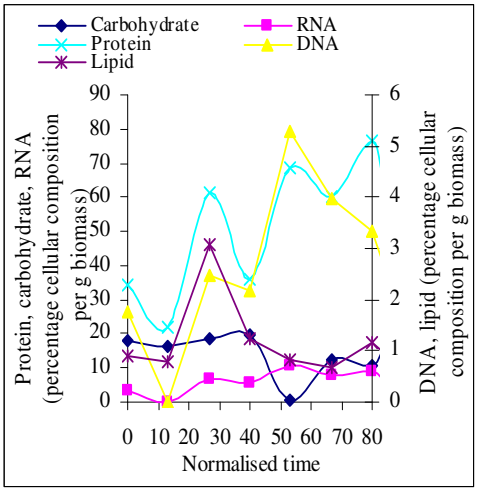

(f) glycerol (Ferm 1)

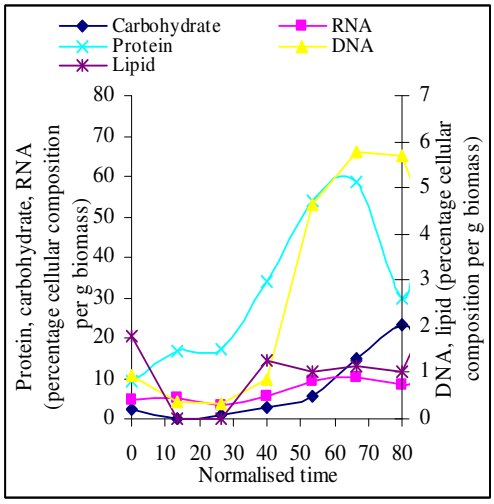

(g) glycerol (Ferm 2)

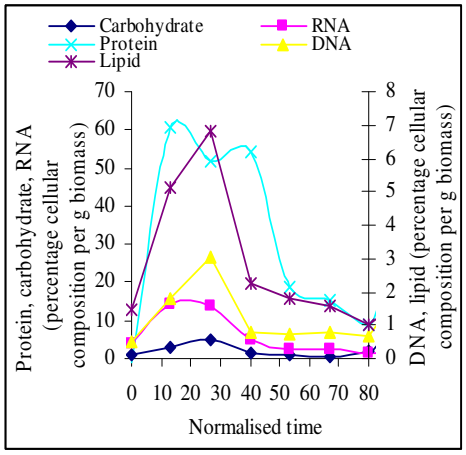

(h) oxo-glutarate (Ferm 1)

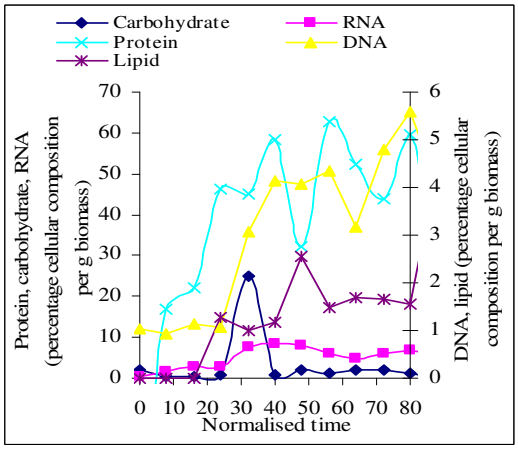

Fig 5.1 Samples taken during fermentations were subjected to fractionation method 1 (Chapter 3, section 3.16.1). The resulting fractions were assayed for the total RNA, DNA, carbohydrate, protein, & lipid biomass content expressed as the percentage cellular composition per g of biomass. Due to differences in the specific growth rate, and substrate uptake rates between different strains and strains cultivated under different conditions. A comparison can only be done, by eliminating the individual time scales (calculated as King, 1997; King and Budenbender, 1997; who compared macromolecular compositional data for 25 streptomycetes). Therefore graphs show the change in macromolecular concentration in the cultures with respect to normalised time. This protocol would usually be undertaken as Chapter 3, section 3.17.1. From this work antibiotic yields and limitation times were considered in sufficient to distinguish between. Therefore the cultures were normalised to 80 h^{-1} up until the end of DNA replication and each time scale of the remaining data was normalised with a factor of 5 h^{-1} (i.e., 24 hrs = 5 places on the graph).

Macromolecular change during fermentations of *S. coelicolor* 1147and *S. fradiae* C373-10 in bioengineering fermenters.

(i) glucose glutamate (Ferm 1)

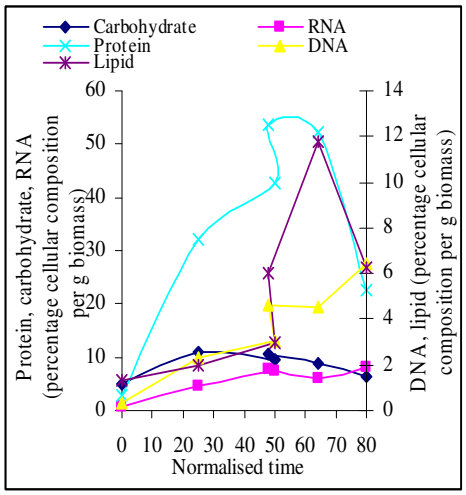

(j) glucose glutamate (Ferm 2)

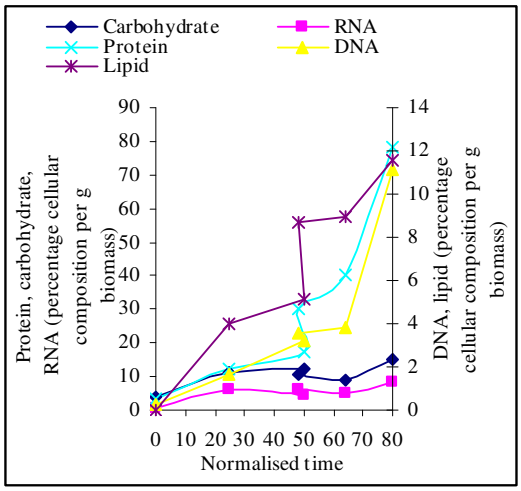

(k)glucose glutamate (Ferm 3)

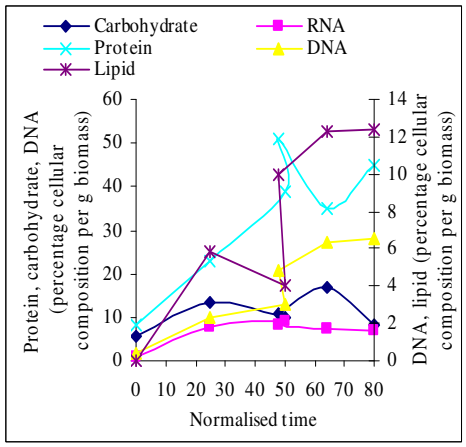

(l) glucose glutamate (Ferm 4)

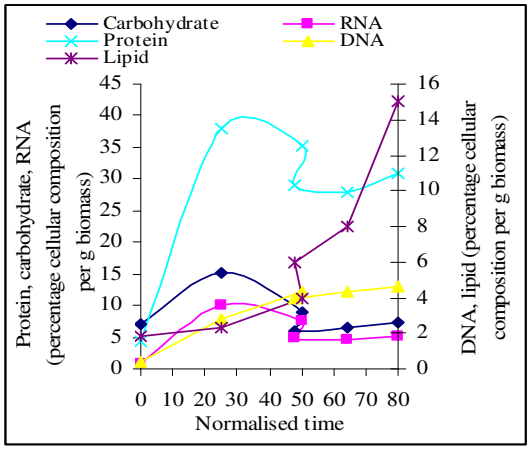

Fig 5.1 Samples taken during fermentations were subjected to fractionation method 1 (Chapter 3, section 3.16.1). The resulting fractions were assayed for the total RNA, DNA, carbohydrate, protein, & lipid biomass content expressed as the percentage cellular composition per g of biomass. Due to differences in the specific growth rate, and substrate uptake rates between different strains and strains cultivated under different conditions. A comparison can only be done, by eliminating the individual time scales (calculated as King, 1997; King and Budenbender, 1997; who compared macromolecular compositional data for 25 streptomycetes). Therefore graphs show the change in macromolecular concentration in the cultures with respect to normalised time. This protocol would usually be undertaken as Chapter 3, section 3.17.1. From this work antibiotic yields and limitation times were considered in sufficient to distinguish between. Therefore the cultures were normalised to 80 h^{-1} up until the end of DNA replication and each time scale of the remaining data was normalised with a factor of 5 h^{-1} (i.e., 24 hrs = 5 places on the graph).

Macromolecular change during fermentations of *S. coelicolor* 1147and *S. fradiae* C373-10 in bioengineering fermenters.

(m) glucose oxo-glutarate (Ferm 1)

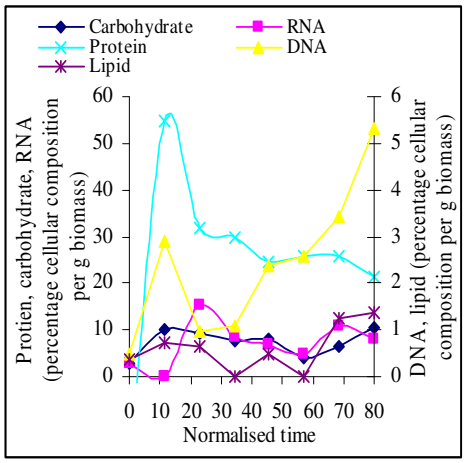

(n) glucose oxo-glutarate (Ferm 2)

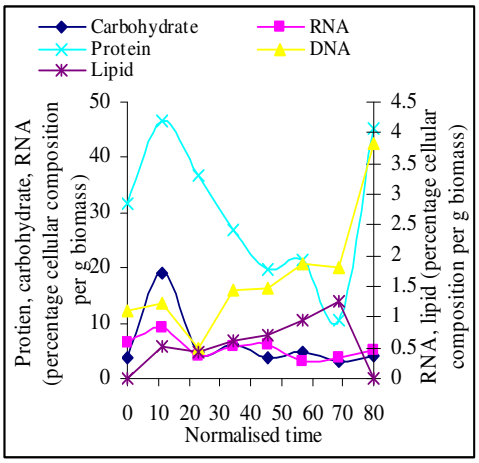

(o) methy-oleate medium (Ferm 1)

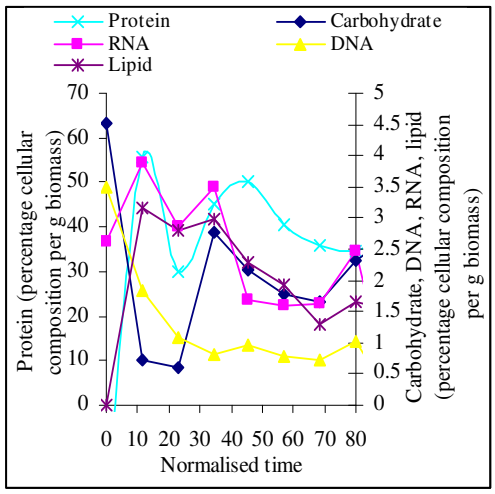

(p) methy-oleate medium (Ferm 2)

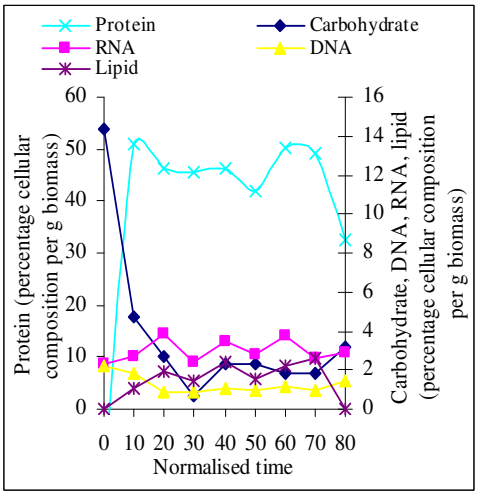

Fig 5.1 Samples taken during fermentations were subjected to fractionation method 1 (Chapter 3, section 3.16.1). The resulting fractions were assayed for the total RNA, DNA, carbohydrate, protein, & lipid biomass content expressed as the percentage cellular composition per g of biomass. Due to differences in the specific growth rate, and substrate uptake rates between different strains and strains cultivated under different conditions. A comparison can only be done, by eliminating the individual time scales (calculated as King, 1997; King and Budenbender, 1997; who compared macromolecular compositional data for 25 streptomycetes). Therefore graphs show the change in macromolecular concentration in the cultures with respect to normalised time. This protocol would usually be undertaken as Chapter 3, section 3.17.1. From this work antibiotic yields and limitation times were considered in sufficient to distinguish between. Therefore the cultures were normalised to 80 h^{-1} up until the end of DNA replication and each time scale of the remaining data was normalised with a factor of 5 h^{-1} (i.e., 24 hrs = 5 places on the graph).

Macromolecular change during fermentations of *S. coelicolor* 1147and *S. fradiae* C373-10 in bioengineering fermenters.

(q) methy-oleate medium (Ferm 3)

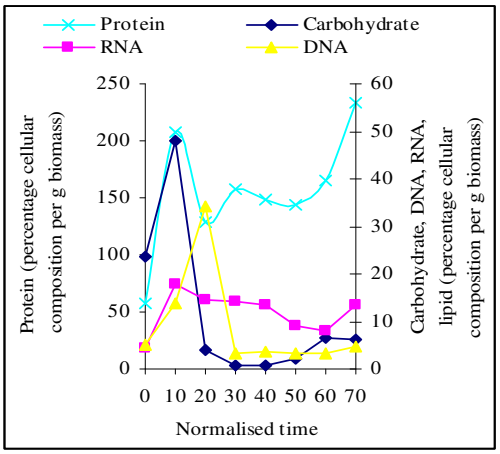

(r) complex medium (Ferm 1)

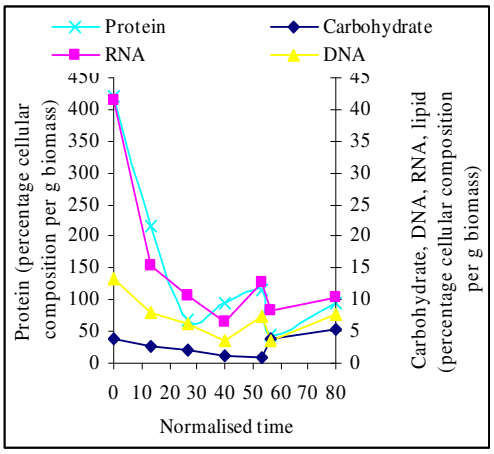

(s) complex medium (Ferm 2)

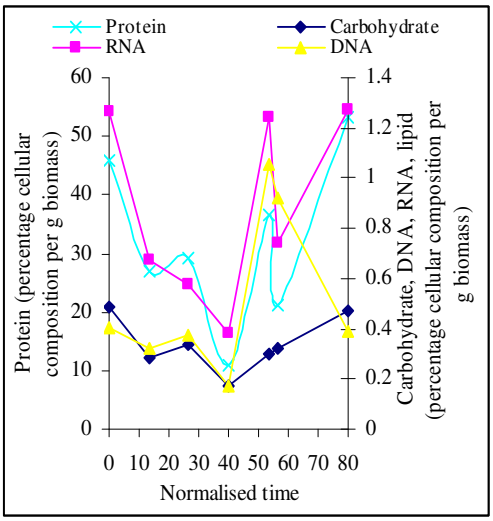

(t) complex medium (Ferm 3)

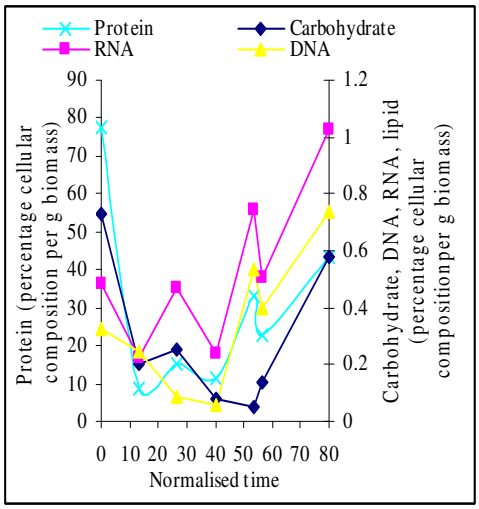

Fig 5.1 Samples taken during fermentations were subjected to fractionation method 1 (Chapter 3, section 3.16.1). The resulting fractions were assayed for the total RNA, DNA, carbohydrate, protein, & lipid biomass content expressed as the percentage cellular composition per g of biomass. Due to differences in the specific growth rate, and substrate uptake rates between different strains and strains cultivated under different conditions. A comparison can only be done, by eliminating the individual time scales (calculated as King, 1997; King and Budenbender, 1997; who compared macromolecular compositional data for 25 streptomycetes). Therefore graphs show the change in macromolecular concentration in the cultures with respect to normalised time. This protocol would usually be undertaken as Chapter 3, section 3.17.1. From this work antibiotic yields and limitation times were considered in sufficient to distinguish between. Therefore the cultures were normalised to 80 h^{-1} up until the end of DNA replication and each time scale of the remaining data was normalised with a factor of 5 h^{-1} (i.e., 24 hrs = 5 places on the graph).

RNA protein ratio in batch cultures of *S. coelicolor* 1147 & *S. fradiae* C373-10

(a) *S. coelicolor* 1147
(glucose Ferm 1 & 2)

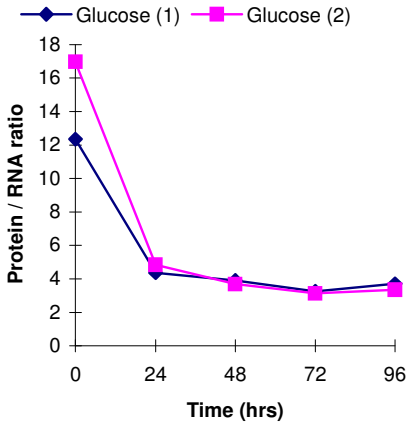

(b) *S. fradiae* C373-10
(glucose Ferm 1 & 2)

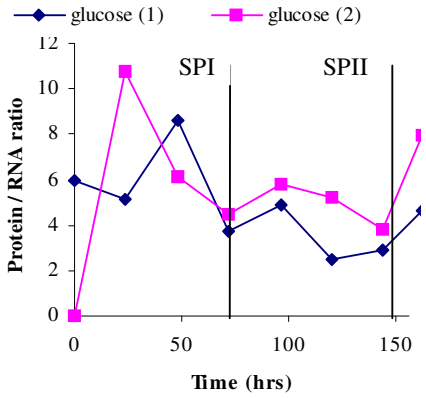

***S. fradiae* C373-10**
(c) glycerol Ferm 1 & 2

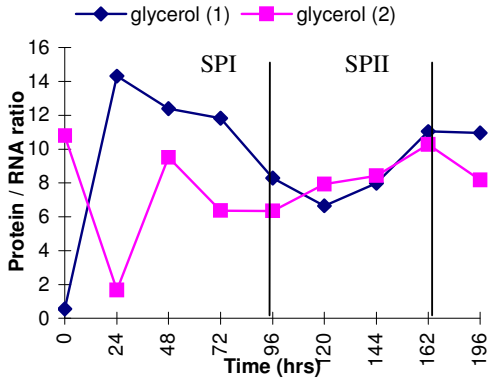

(d) fructose

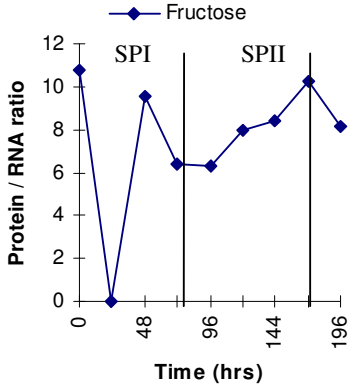

Fig 5.2 Samples taken during fermentations of *S. coelicolor* 1147 and *S. fradiae* C373-10 cultured on a number of different carbon sources. Fermentations were as Chapter 4 and subjected to fractionation method 1 (Chapter 3, section 3.16.1). The resulting fractions were assayed for total RNA (Chapter 3, section 3.19.4, the orcinol assay)[gl^{-1}] and protein (Chapter 3, section 3.20.5, reverse biuret method combined with the copper bathocuproine chelate reaction) (gl^{-1}) and expressed as the RNA/protein ratio. The graphs show the changes in the RNA/protein ratio in batch cultures with respect to time (h^{-1}). [Glucose (Ferm 1 & 2) Day 4, phase 1, Day 7 & 6, phase II; fructose (Ferm 1) Day 4, phase I, Day 8, phase II; glycerol (Ferm 1 & 2) Day 6 & 4, phase I, Day 7 & 9, phase II; oxo-glutarate (Ferm 1) Day 4, phase I, Day 10, phase II; glucose glutamate (Ferm 1 - 4) Day 2, phase I, Day 5, phase II; glucose oxo-glutarate (Ferm 1 & 2) Day 3, phase I, Day 7, phase II; methyl oleate medium (Ferm 1 - 3) Day 2, Day 3, & Day 3, phase I, Day 3, Day 4, & Day 4, phase III, Day 9, Day 9, & Day 7, phase II].

RNA protein ratio in batch cultures of *S. coelicolor* 1147 & *S. fradiae* C373-10

(e) oxo-glutarate

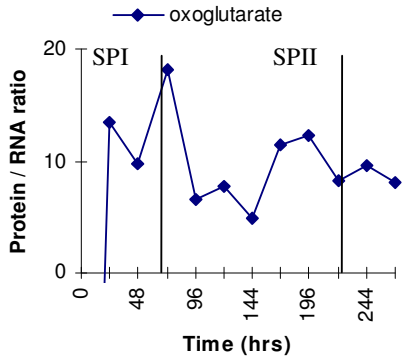

(f) glucose glutamate (Ferm 1 - 4)

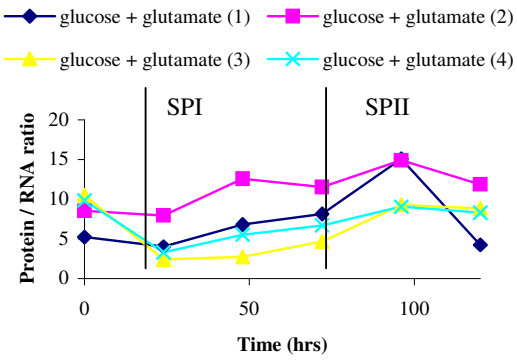

(g) glucose oxo-glutarate (Ferm 1 & 2)

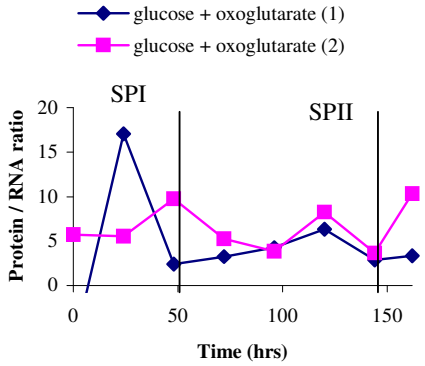

(h) methyl oleate medium

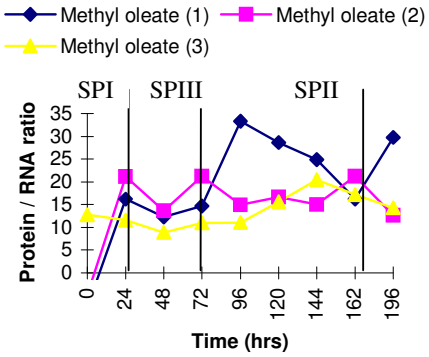

Fig 5.2 Samples taken during fermentations of *S. coelicolor* 1147 and *S. fradiae* C373-10 cultured on a number of different carbon sources. Fermentations were as Chapter 4 and subjected to fractionation method 1 (Chapter 3, section 3.16.1). The resulting fractions were assayed for total RNA (Chapter 3, section 3.19.4, the orcinol assay)[gl^{-1}] and protein (Chapter 3, section 3.20.5, reverse biuret method combined with the copper bathocuproine chelate reaction) (gl^{-1}) and expressed as the RNA/protein ratio. The graphs show the changes in the RNA/protein ratio in batch cultures with respect to time (h^{-1}). [Glucose (Ferm 1 & 2) Day 4, phase 1, Day 7 & 6, phase II; fructose (Ferm 1) Day 4, phase I, Day 8, phase II; glycerol (Ferm 1 & 2) Day 6 & 4, phase I, Day 7 & 9, phase II; oxo-glutarate (Ferm 1) Day 4, phase I, Day 10, phase II; glucose glutamate (Ferm 1 - 4) Day 2, phase I, Day 5, phase II; glucose oxo-glutarate (Ferm 1 & 2) Day 3, phase I, Day 7, phase II; methyl oleate medium (Ferm 1 - 3) Day 2, Day 3, & Day 3, phase I, Day 3, Day 4, & Day 4, phase III, Day 9, Day 9, & Day 7, phase II].

RNA protein ratio in batch cultures of *S. coelicolor* 1147 & *S. fradiae* C373-10

(i) industrial complex medium

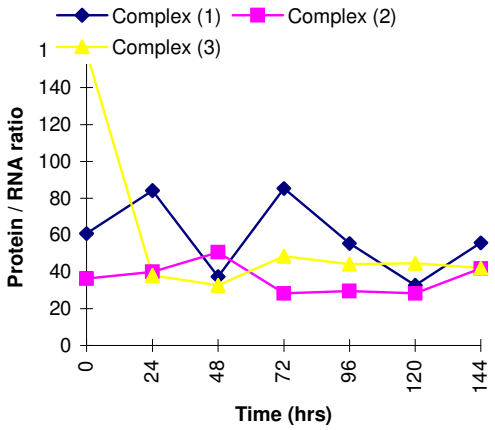

Fig 5.2 Samples taken during fermentations of *S. coelicolor* 1147 and *S. fradiae* C373-10 cultured on a number of different carbon sources. Fermentations were as Chapter 4 and subjected to fractionation method 1 (Chapter 3, section 3.16.1). The resulting fractions were assayed for total RNA (Chapter 3, section 3.19.4, the orcinol assay)[gl^{-1}] and protein (Chapter 3, section 3.20.5, reverse biuret method combined with the copper bathocuproine chelate reaction) (gl^{-1}) and expressed as the RNA/protein ratio. The graphs show the changes in the RNA/protein ratio in batch cultures with respect to time (h^{-1}). [Glucose (Ferm 1 & 2) Day 4, phase 1, Day 7 & 6, phase II; fructose (Ferm 1) Day 4, phase I, Day 8, phase II; glycerol (Ferm 1 & 2) Day 6 & 4, phase I, Day 7 & 9, phase II; oxo-glutarate (Ferm 1) Day 4, phase I, Day 10, phase II; glucose glutamate (Ferm 1 - 4) Day 2, phase I, Day 5, phase II; glucose oxo-glutarate (Ferm 1 & 2) Day 3, phase I, Day 7, phase II; methyl oleate medium (Ferm 1 - 3) Day 2, Day 3, & Day 3, phase I, Day 3, Day 4, & Day 4, phase III, Day 9, Day 9, & Day 7, phase II].

Structure of teichoic acid

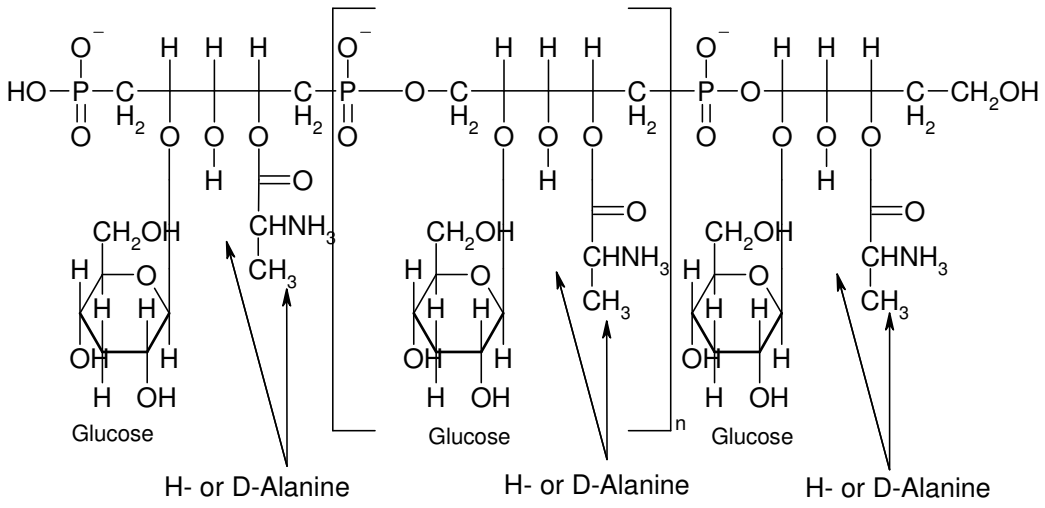

Ribitol teichoic acid from *Bacillus subtilis*

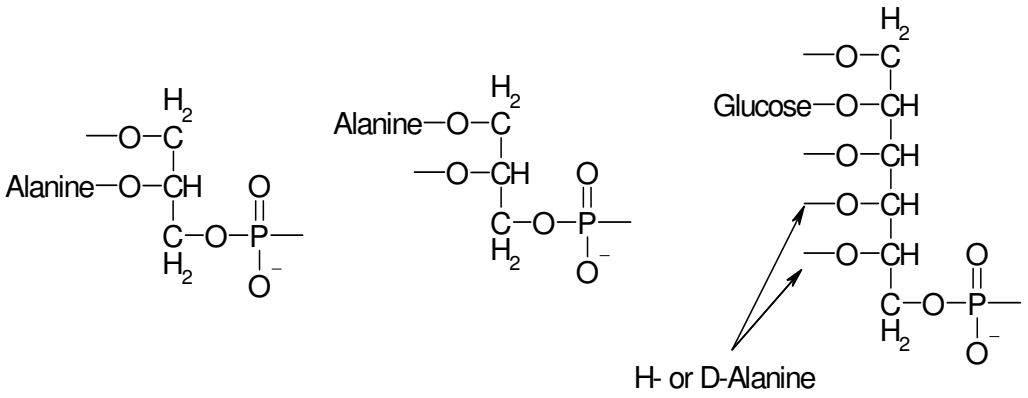

Fig 5.3 Structure of teichoic acid. Teichoic acids are covalently linked to the peptidoglycan of Gram-positive bacteria. T hese polymers of (a, b) glycerol phosphate or (c) ribitol phosphate are linked by phosphodiester bonds. Substituted groups found in streptomycetes were L-lysyl, acetyl groups & β-D-O-gluco-pyranosyl groups. Further available hydroxyl groups can be ester linked to alanine or to sugars such as glucose.

Structure of peptidoglycan

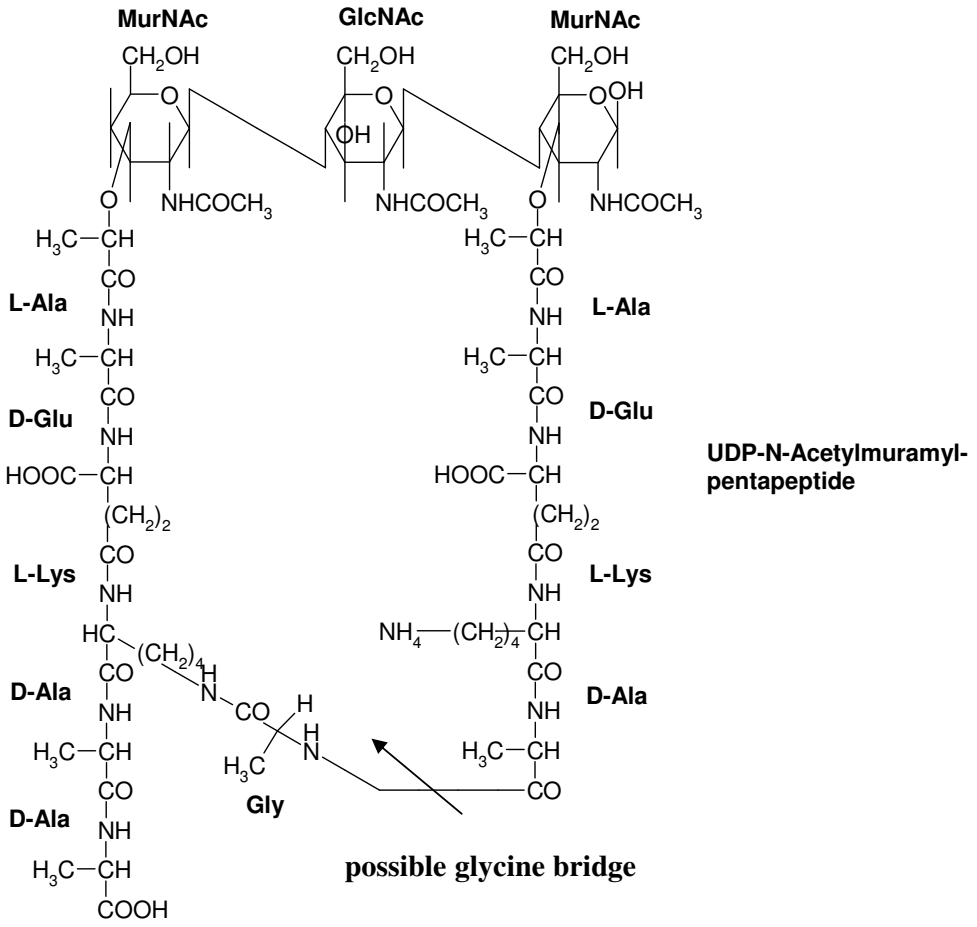

Fig 5.4 Adapted from Goodfellow & Cross, 1984; Minnikin & O'Donnell, 1984 (the residue position numbers are given in brackets), and an interpeptide bridge of 1 to 6 amino acids long exists between positions lysine and alanine (Minnikin & O'Donnell, 1984; Stanier *et al*., 1981). N-acetylglucosamine, GlcNAc; N-acetylmuramic acid, MurNAc.

The amino acid compositions of *S. fradiae* C373-10, *S. coelicolor* 1147 and *E. coli* ML308 expressed as the order of requirement vs. the alphabetical order of amino acids cultured on glucose minimal medium compositions.

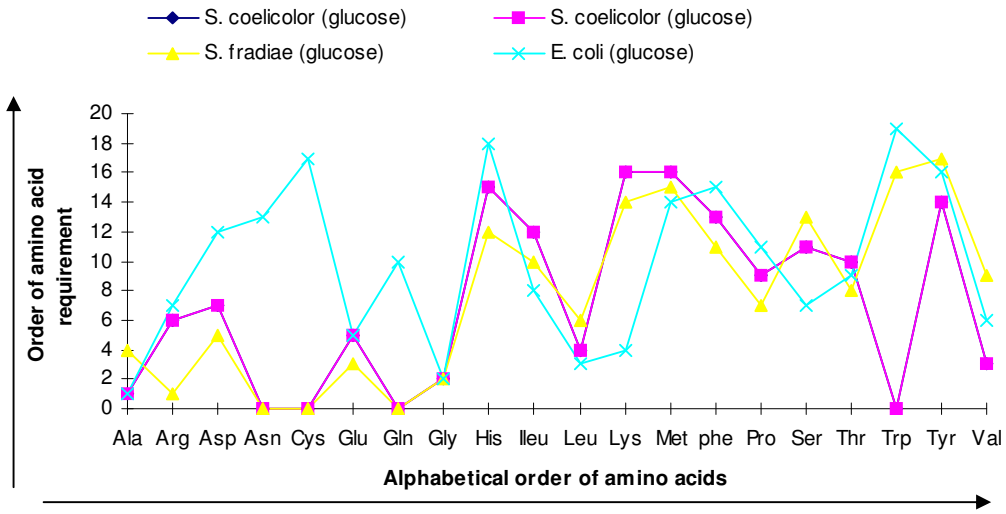

Fig 5.5A The graph corresponds to the amino acid compositions of *S. fradiae* C373-10, *S. coelicolor* 1147 and *E. coli* ML308 expressed as the order of decreasing amino acid requirement (→) vs. the alphabetical order of amino acids (→). Amino acid analysis was undertaken by HPLC (Chapter 3, section 3.25) and expressed as the percentage (%) composition of 1 g dry weight of *S. fradiae*, *S. coelicolor* and *E. coli* biomass and converted to the order of amino acid requirement corresponding to Tables 5.29 & 5.30. Samples were obtained from this project for *S. coelicolor* & *S. fradiae* cultured on a glucose minimal medium (Chapter 3, section 3.6.1 & 3.6.4). The results for *E. coli* ML308 cultured on a glucose minimal medium were adapted from Holms (1986).

The amino acid compositions of *S. fradiae* C373-10 expressed as the order of requirement vs. the alphabetical order of amino acids cultured on different minimal medium compositions.

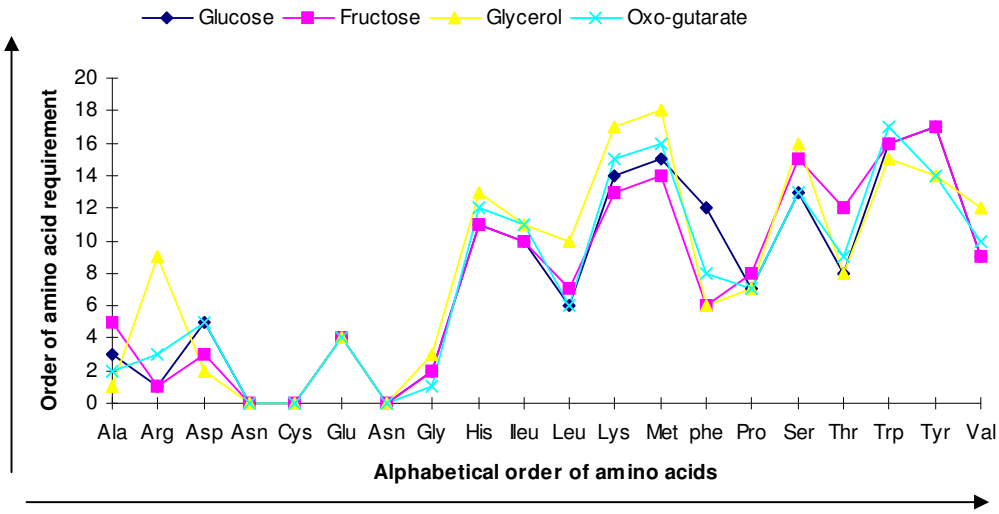

Fig 5.5B The graph corresponds to the amino acid compositions of *S. fradiae* C373-10 expressed as the order of decreasing amino acid requirement (→) vs. the alphabetical order of amino acids (→). Amino acid analysis was undertaken by HPLC (Chapter 3, section 3.25) and expressed as the percentage (%) composition of 1 g dry weight of *S. fradiae* biomass and converted to the order of amino acid requirement corresponding to Table 5.30. Samples were obtained from this project for *S. fradiae* cultured on a glucose, glycerol, fructose, and oxo-glutarate minimal medium (Chapter 3, section 3.6.4).

The amino acid compositions of *S. fradiae* C373-10 expressed as the order of requirement vs. the alphabetical order of amino acids cultured on a methyl oleate defined medium.

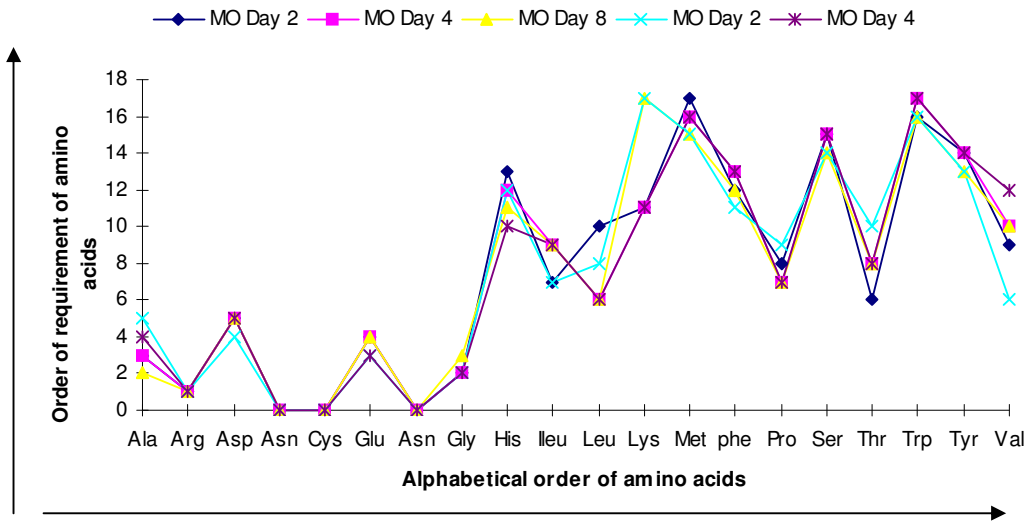

Fig 5.5C The graph corresponds to the amino acid compositions of *S. fradiae* C373-10 expressed as the order of decreasing amino acid requirement (→) vs. the alphabetical order of amino acids (→). Amino acid analysis was undertaken by HPLC (Chapter 3, section 3.25) and expressed as the percentage (%) composition of 1 g dry weight of *S. fradiae* biomass and converted to the order of amino acid requirement corresponding to Table 5.30. Samples were obtained from this project for *S. fradiae* cultured on a methyl oleate defined medium (Chapter 3, section 3.7.2). MO, methyl oleate defined medium.

The amino acid compositions of *S. fradiae* C373-10 expressed as the order of requirement vs. the alphabetical order of amino acids cultured on a glucose glutamate defined medium.

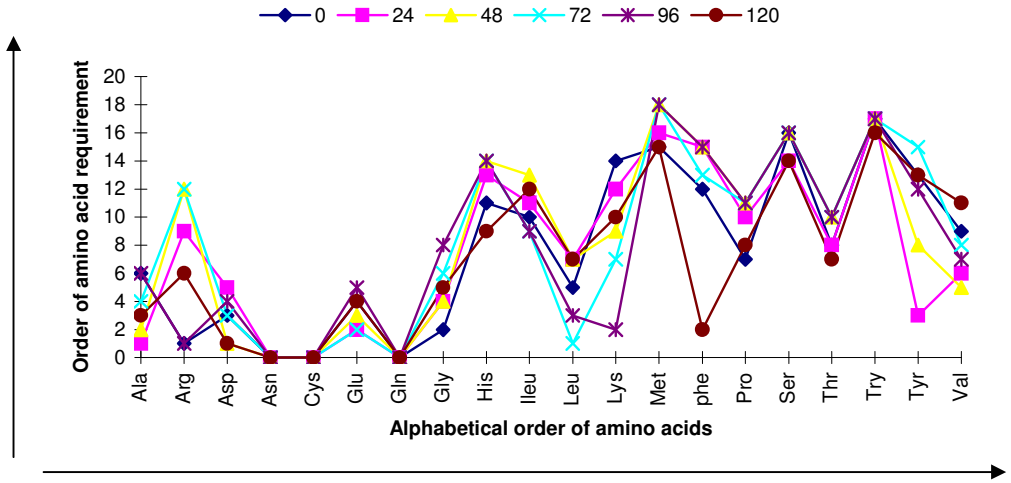

Fig 5.5D The graph corresponds to the amino acid compositions of *S. fradiae* C373-10 expressed as the order of decreasing amino acid requirement (→) vs. the alphabetical order of amino acids (→). Amino acid analysis was undertaken by HPLC (Chapter 3, section 3.25) and expressed as the percentage (%) composition of 1 g dry weight of *S. fradiae* biomass and converted to the order of amino acid requirement corresponding to Table 5.31. Samples were obtained from this project for *S. fradiae* biomass cultured and detected throughout a glucose glutamate defined medium (Chapter 3, section 3.6.4).

The amino acid compositions of *S. fradiae* C373-10 expressed as the order of requirement vs. the alphabetical order of amino acids cultured on a glucose oxo-glutarate defined medium.

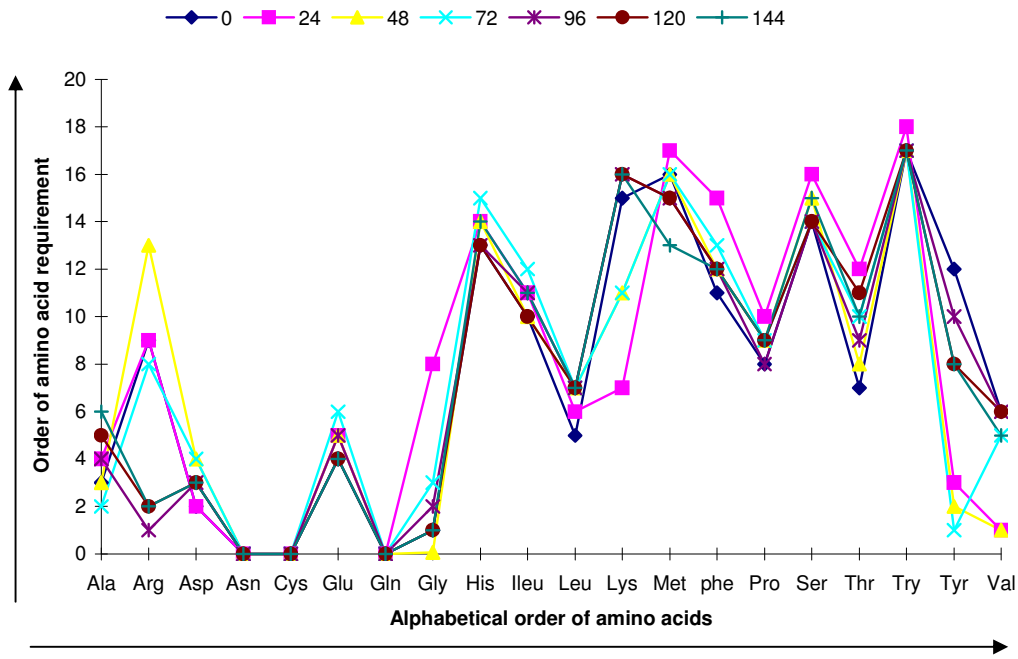

Fig 5.5E The graph corresponds to the amino acid compositions of *S. fradiae* C373-10 expressed as the order of decreasing amino acid requirement (→) vs. the alphabetical order of amino acids (→). Amino acid analysis was undertaken by HPLC (Chapter 3, section 3.25) and expressed as the percentage (%) composition of 1 g dry weight of *S. fradiae* biomass and converted to the order of amino acid requirement corresponding to Table 5.32. Samples were obtained from this project for *S. fradiae* biomass cultured and detected throughout a glucose oxo-glutarate defined medium fermentation (Chapter 3, section 3.6.4).

The amino acid compositions of *S. fradiae* C373-10 expressed as the order of requirement vs. the alphabetical order of amino acids cultured on a industrial complex process.

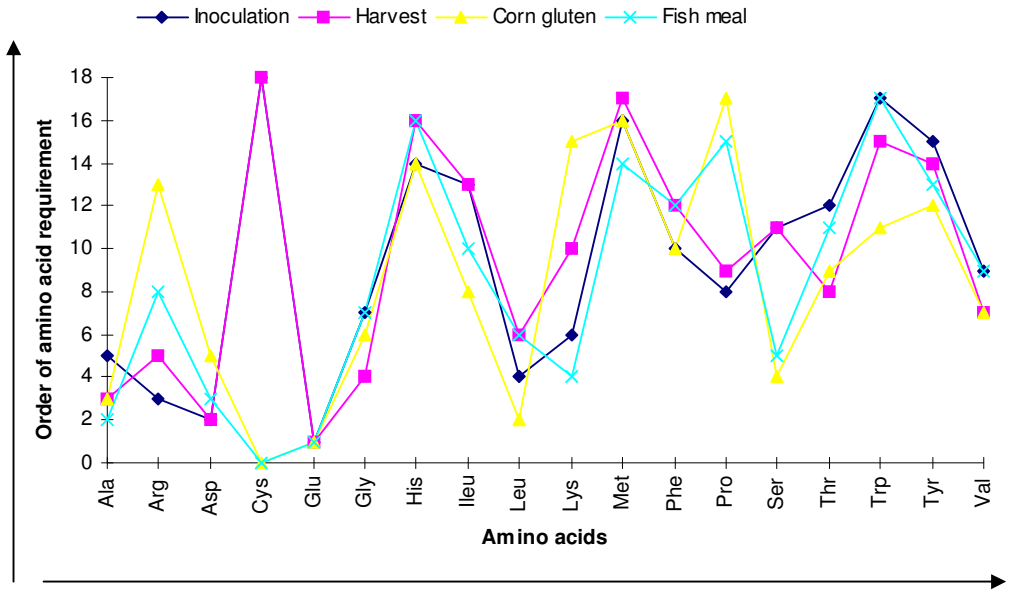

Fig 5.5F The graph corresponds to the amino acid compositions of *S. fradiae* C373-10 expressed as the order of decreasing amino acid requirement (→) vs. the alphabetical order of amino acids (→). Amino acid analysis was undertaken by HPLC (Chapter 3, section 3.25) and expressed as the percentage (%) composition of 1 g dry weight of *S. fradiae* biomass and converted to the order of amino acid requirement. Samples were obtained from this project for *S. fradiae* fermentation liquor composition at inoculation and harvest cultured on a industrial complex medium (Chapter 3, section 3.7.3) and the composition of individual medium components corn gluten and fish meal was presented in the same format corresponds to Table 5.33.

Change in amino acid composition in an industrial complex medium

(A) Mean percentage changes of amino acids between 0 hours and harvest

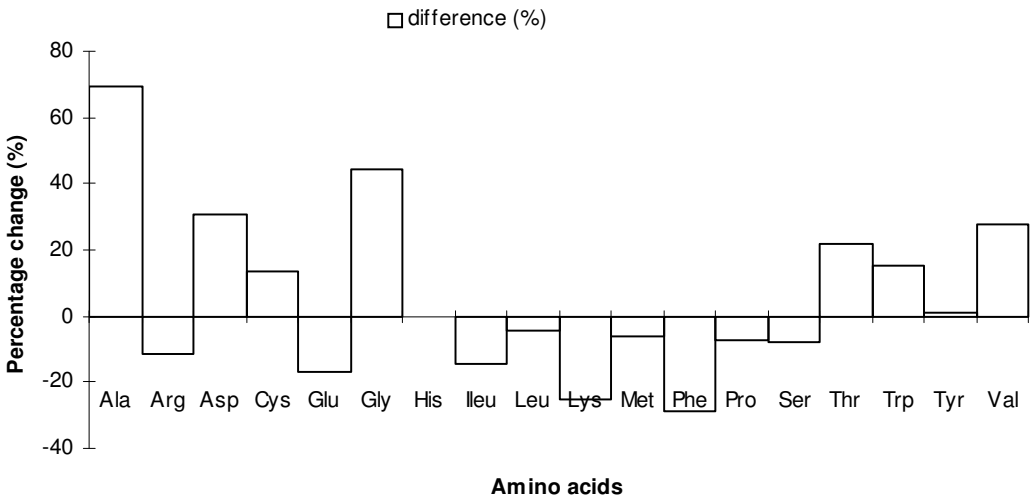

Fig 5.6 A Samples were collected from an industrial scale *S. fradiae* C373-18 culture grown on the industrial complex medium (Chapter 3, section 3.7.3). Sampling points were taken at 0 hours and at harvest. Amino acid analysis was undertaken with HPLC analysis (Chapter 3, section 3.25.2). The results were expressed as the percentage (%) total change in amino composition of the medium composition.

(B) Mean percentage changes of amino acids between alpha and beta lots

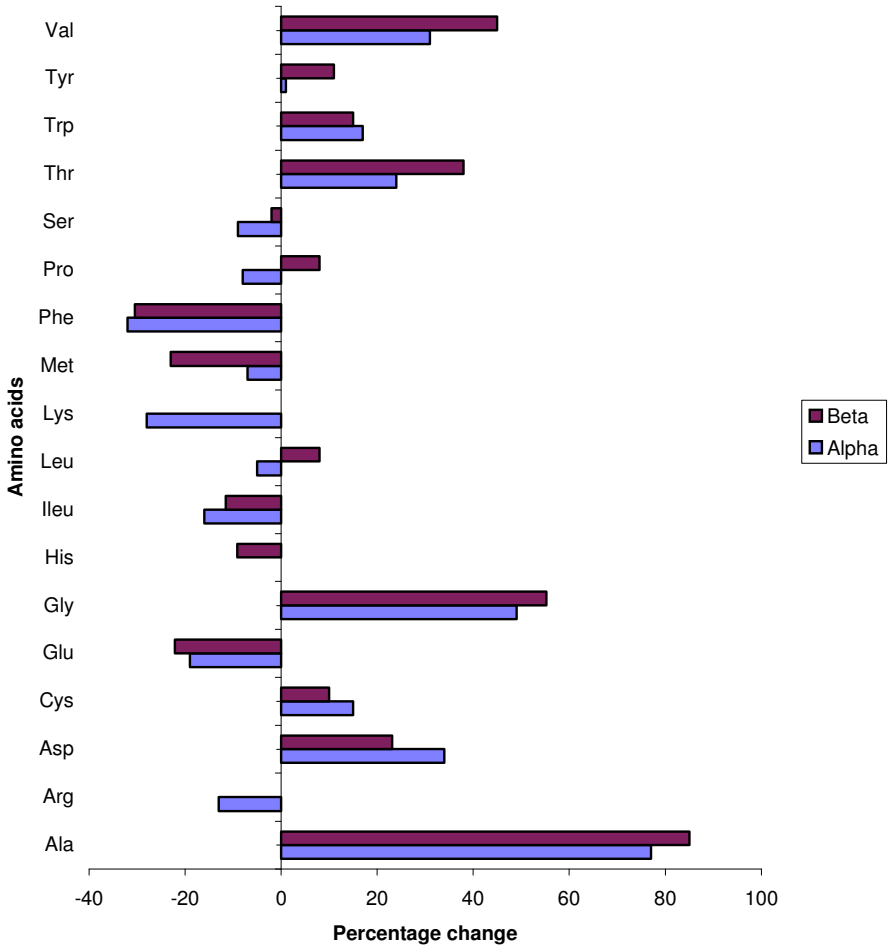

Fig 5.6 B Samples were collected from two 20 L bench top scale *S. fradiae* C373-18 culture grown on the industrial complex medium (Chapter 3, section 3.7.3). Alpha lot was the control and the beta lot was where one fermentations NH_4OH feed jammed through the period. Sampling points were taken at 0 hours and at harvest. Amino acid analysis was undertaken with HPLC analysis (Chapter 3, section 3.25.2). The results were expressed as the percentage (%) total change in amino composition of the medium composition.

Order of codon requirement against metabolic costs

(a) The effects of amino acid metabolic costs on *E. coli*, *S. coelicolor* and *S. fradiae* biomass.

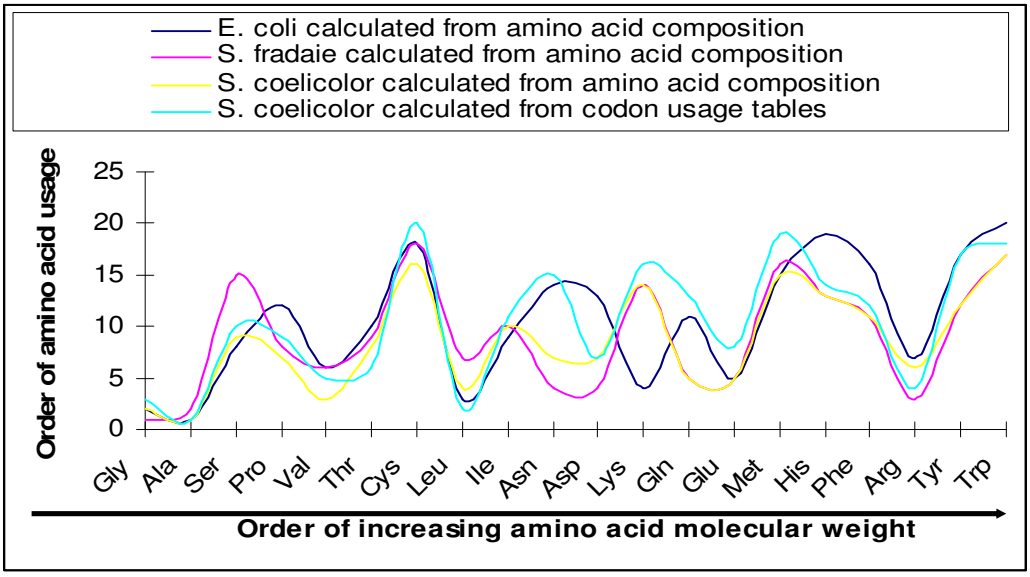

(b) The effects of amino acid metabolic costs on a *S. fradiae* industrial process.

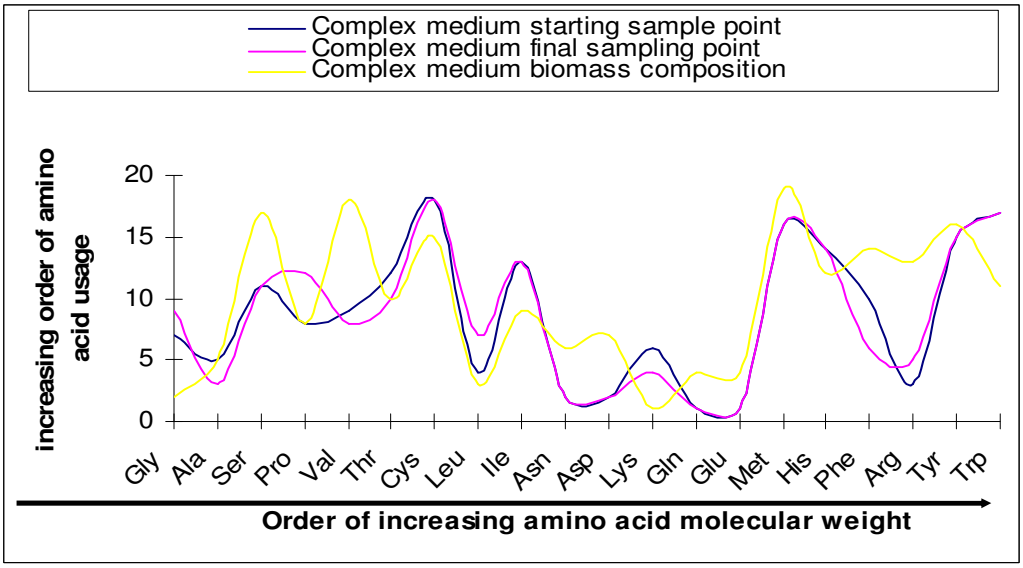

Fig 5.7a & b The negative correlation between the frequencies of usage of amino acids and their biosynthetic cost suggests that organisms minimise costs of protein biosynthesis. Amino acid molecular weight (MW) for a protein has been shown to correlate positively with the proteins expression level and with its size. This was considered an acceptable strategy of measuring the effects of metabolic costs on codon usage (i.e., increasing molecular weight increasing metabolic cost). Results where indicated are taken from codon usage tables and

experimental amino acid analysis (i.e., increasing order of requirement). Results taken from other workers were indicated as appropriate.

Order of codon requirement against metabolic costs

(c) The effects of metabolic cost on a number of eubacteria increasing in G+C content

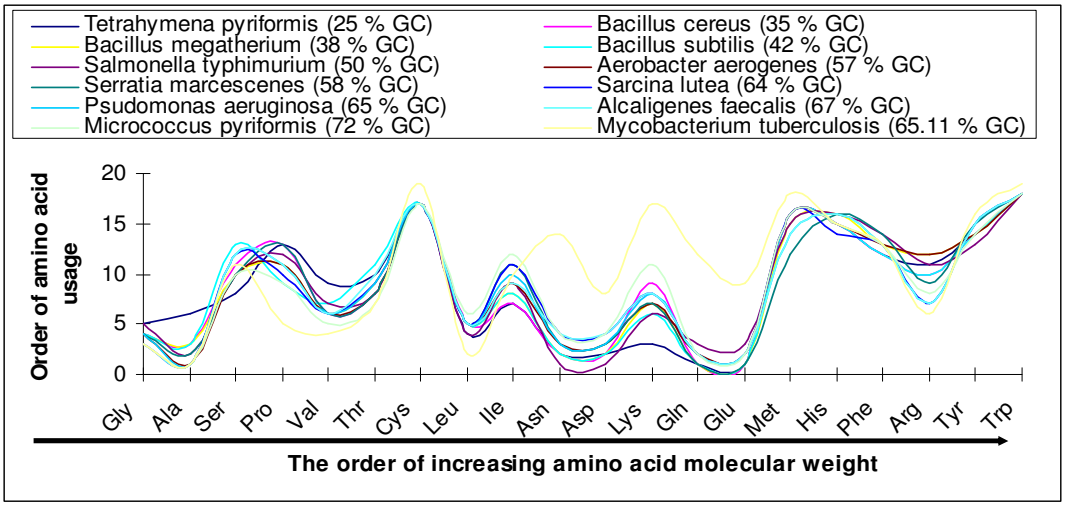

Fig 5.7c The negative correlation between the frequencies of usage of amino acids and their biosynthetic cost suggests that organisms minimise costs of protein biosynthesis. Amino acid molecular weight (MW) for a protein has been shown to correlate positively with the proteins expression level and with its size. This was considered an acceptable strategy for measuring the effects of metabolic costs on codon usage (i.e., increasing molecular weight equals increasing metabolic cost). Results where indicated are taken from codon usage tables and experimental amino acid analysis (i.e., increasing order of requirement). Results taken from other workers were indicated as appropriate.

Theoretical elemental analysis for *S. fradiae* C373-10 cultured on glucose

Analysis	**C: 43.62 %, H: 7.12 %, N: 8.45 %, P: 2.93 %, S: 2.68 % (0.31 %; minus ash estimate)**
Difference	**O: 33.15 %**
Number of gram atoms	**C: 3.63, H: 7.12, N: 0.60, O: 2.07, P: 0.10, S: 0.08**
Empirical formula	$\mathbf{CH_{1.96}\ O_{0.62}\ N_{0.17}\ P_{0.022}\ S_{0.021}}$
Molecular mass	**27.51 g ([12 × 1] + [1 × 1.96] + [16 × 0.62] + [14 × 0.17] + [30 × 0.022] + [32 × 0.021])**
Degree of reduction	**4.23 (see Appendix G for calculation)**

Fig 5.8 Proportion for phosphorus on average for *S. fradiae* C373-10 cultured on glucose 2.63 % minus the sulphur content on average 2.93 %, total ash content for *S. fradiae* C373-10 was calculated to be 0.31 % on average and 1.15 % on average for *S. coelicolor* 1147)[see Table 5.38].

Chapter 6

Determination of throughputs and fluxes through the central metabolic pathways of *S. fradiae* to biomass and antibiotic production

6.1 Introduction

Fermentation processes produce/use biomass to synthesis a desirable product. Growth of the biomass and synthesis of product are usually sequential. A production strain is usually selected for its biosynthetic capabilities, when grown in a batch, fed-batch or a continuous process. In continuous culture feedstocks (inputs) are added continuously to sustain the metabolic fluxes through the biomass to products (outputs). One important feature of fed-batch growth is a low production rate of biomass can be achieved. A batch process is far simpler, due to it being a partially closed system. Conditions inside a vessel are transient since fluxes to biomass increases as nutrients are continually utilised and products are secreted.

Fluxes are channeled through specific metabolic pathways and provided these pathways are known, careful measurement of all inputs and outputs of the fermentation provides the data from which fluxes through all the pathways can be computed (see Appendix B; for example of method). A full diagram for the central metabolic pathways (CMPs) can then be constructed which relates the utilisation of inputs to the provision of the precursors required to maintain the anabolic fluxes to product (see Appendix B and Figures 6.1 - 6.25 Appendix U; All summary Tables can be found in the companion CD; Appendix O Chapter 6).

This Chapter applies, expands upon, and discusses the problems associated with the strategy for metabolic flux analysis (MFA) developed by Harry Holms (Holms, 1986, 1996, 1997, 2001; see Appendix B for a worked example of technique) and originally applied to *E. coli* fermentation data. The strategy will be applied to *S. fradiae* C373-10 and *S. coelicolor* 1147 fermentation data throughout the following section. Davidson (1992) was one of the first to apply this strategy to a streptomycete fermentation (*S. coelicolor* 1147 & 209) and reported a number of difficulties in obtaining consistent calculated data from a flux analysis that fits the experimentally determined CO_2 evolution rate [CER]. From this work it was proposed that this was due to the units of measurement used in the initial calculation (calculations were as Holms, 1986, 1996, 1997, 2001[Appendix B]). Therefore *S. coelicolor* 1147 was used as a

test organism to correlate the work undertaken in this laboratory with Davidson (1992) and *S. fradiae* C373-10 was used satisfy the initial aims set out for the project.

To construct compositional tables (as Holms, 1986, 1996, 1997, 2001) it was important to obtain accurate information on the specific precursor requirements for the subsequent flux analysis, and to determine the monomeric biomass composition, which is known to change with environmental conditions and growth rate (see Chapter 5). For this purpose the relative fractions of the major biomass components (protein, amino acids [aas], RNA, DNA, carbohydrate, lipids, etc.) of *S. coelicolor* 1147 and *S. fradiae* C373-10 were determined in the previous Chapter (Chapter 5). Previous workers (Holms, 1986, 1996, 1997, 2001; Davidson, 1992) used one average compositional table (e.g., Table 6.26 & 6.27; Appendix P see the worked example in Appendix B) in the construction of all their flux diagrams (e.g., Figures 6.1 – 6.25). For this work both average and individual compositional tables were investigated (Tables 6.1 – 6.27; Appendices P & Q).

Metabolic fluxes are dynamic and dependent on the growth-rate of the organism (see Appendix B), the higher the growth-rate, the higher the flux (velocity). Fluxes were, therefore, calculated by multiplying throughputs (mmoles.g^{-1}) by the specific growth rate (μ) to give units of mmoles.g^{-1}. dry wt biomass h^{-1} normalised to 100. In the case of this work C.mmoles.g^{-1}. dry wt biomass h^{-1} normalised to 100 were used due to these units being more compatible with *Streptomyces* metabolism [see Table 6.31; section 6.3.1]. This was achieved by multiplying the fluxes from each precursor by the number of carbon atoms in the molecule. The normalisation factor was calculated by dividing the normalised carbon source input (100) by the carbon source input C.mmoles.g^{-1}. dry wt biomass h^{-1} (normalisation factor denoted by N, on Figures 6.1 – 6.25). Multiplying each of the fluxes (C.mmoles.g^{-1} dry wt biomass h^{-1}) by the N factor presents the data in percentage format. The overall application of the method is most easily described by the example presented in Appendix B [All fermentation numbers relate to the same cultures throughout Chapter 4, 5, 6 & 7; *S. fradiae* C373-10 cultures for glucose (Ferm 1 & 2); fructose (Ferm 1); glycerol (Ferm 1 & 2); oxo-glutarate (Ferm 1); glucose glutamate (Ferm 1 - 4); glucose oxo-glutarate (Ferm 1 & 2); methyl oleate medium (Ferm 1 - 3); Industrial complex (Ferm 1 & 2); *S. coelicolor* cultures for glucose (Ferm 1 & 2)].

6.2 Metabolic flux analysis: a multidisciplinary field

The growth of the organism on different substrates is likely to lead to differences in fluxes since metabolic adjustment occurs to allow for provision of all precursors for biosynthesis. For example, the flux through isocitrate dehydrogenase (ICDH) of *E. coli* grown on glucose was calculated to be equivalent to the flux through aconitase (a preceding enzyme in the TCA cycle). However, growth on acetate resulted in a flux through ICDH of two thirds that of aconitase (Holms, 1986). Growth of *E. coli* on acetate requires the enzymes of the glyoxylate bypass (GBP) to provide precursors for biosynthesis by the gluconeogenic route. This reduction in flux was indicative of the effects of regulation of the activity of ICDH (Holms, 1986). The flux ratios (see Tables 6.29 & 6.30 for example) often show that the feedstock programme is not optimal and the resulting imbalance is redressed by excretion or accumulation of additional carbon compounds as waste or storage products. Identification of these waste products and the fluxes to them can establish a list of priorities for intervention.

Flux analysis in essence is the organisation of data. Therefore this thesis should only be viewed as a preliminary investigation, that as more information becomes increasingly readily available, this work can be improved on. The following points should be taken into account when considering this work:

(1) The central and biosynthetic pathways utilised by streptomycetes are, as yet, not completely clear, although the genome of *S. coelicolor* has been sequenced (Chapter 2, section 2.1). Initial comparative analysis with a number of closely-related organisms (see Chapter 2, section 2.5 - 2.9.4) would indicate there are general similarities between the CMPs of *E. coli* and *S. coelicolor*. The differences from *Streptomyces* to *Streptomyces*, are as yet unknown. Therefore an extensive literature search was undertaken in Chapter 2. From this, it was deduced that the CMPs and the metabolic intermediates used as precursors for monomer biosynthesis in streptomycetes are similar to those in *E. coli*. Therefore the CMPs presented in the following sections were constructed from the work of Holms (1986, 1996, 1997, 2001) for *E. coli* metabolism.

(2) The approximate compositions of *S. fradiae* C373-10 & *S. coelicolor* 1147 biomass were not determined as comprehensively as that of *E. coli*, but the data for the enterobacterium had been gathered from analyses carried out by several groups over a period of 50 years. Even so, the inventory for *E. coli* is not yet complete and will become more accurate in

time. This also applies to the determination of fluxes through the CMPs. For example, in the 1950's not all of the components and metabolic pathways of *E. coli* had been elucidated. However, Roberts *et al*. (1955) described how the available knowledge of the metabolism of *E. coli* could be used to calculate the flow of metabolites from the glucose substrate to synthesis of biomass (using glutamate, aspartate, pyruvate, serine and the TCA cycle intermediates as precursors). At that time, the proportion of the flow to biomass was reported to be 30 % (with 45 % to CO_2 and 25 % excreted). 30 years later, the measured proportion of flow to biomass has been reported to be more than double that value, i.e. 63 % (Holms, 1986, 1996, 1997, 2001) with 21 % to CER.

(3) The application of flux analysis is realistically a group exercise that is undertaken by a multidisciplinary team (Beocarta Ltd.; formerly Bioflux Ltd., have used this technique to great success in the industrial community). The down side of this is the time needed to undertake such analyses, and test the theorised improvements.

The procedure of flux analysis can therefore be considered as three phases.

6.2.1 Phase I- fine tuning

The calculated flux diagrams (see Appendix B; & Figures 6.1 – 6.25) present a precise description of a current process and allows 'fine tuning' to be carried out:

(1) It is not uncommon to find that a fraction of input is excreted or accumulated after very few metabolic steps. These disadvantages or wasteful fluxes can be avoided by redefining the programme of nutrient addition to match the requirements of the biomass for precursors as defined by analysis. Conversely supply or mobilisation of inputs which restrict flux to precursors can be increased.

(2) Analysis of flux to excreted or accumulated waste products identifies the fluxes at divergent or convergent junctions that should be increased or decreased to balance fluxes to give the desired product.

(3) Frequently the balance of inputs (e.g. carbon / nitrogen ratio) cannot provide the optimal mix of precursors required to maintain maximal fluxes to monomers and adjustments to the ratio can usually improve productivity.

The results from phase I defines the parameters for process engineers to optimise the process.

6.2.2 Phase II – Changes to the process

Phase I of a flux analysis often highlights junctions at which flux distribution is particularly unbalanced. Radical methods may be required to redress these:

(1) Usually it is beneficial to replace or reduce supply of complex inputs. The aim of this is to achieve the simplest possible feedstock programme that will supply the fluxes required for product syntheses.
(2) Expression of some desirable enzymes may be repressed. Synthesis of these enzymes can be achieved by manipulation of the nutrient generating the repression signal or by selection to give constitutive expression.
(3) Conversely, some enzymes may divert flux away from product and these must be eliminated by genetic intervention.
(4) Genomic DNA for some desirable enzymes may have been lost during the strain selection process and must be reintroduced by molecular biology techniques.

Phase II will lead to improved biomass capable of higher productivity. It does this by directing the attention of the microbial physiologist and the genetic engineer to those junctions where intervention will be beneficial. It compliments the standard approach of strain improvements using screening for increased product formation. Phase II generates a new strain and therefore a new process which must be analysed as in phase I to produce a new flux diagram. Strain and process improvement is therefore a continuous process.

6.2.3 Phase III – Maximisation of productivity

Flux through the biomass generates trends that show how far inputs are off the target set by the biosynthetic capability. In phase III, strategies should be designed to identify these trends, devise means to measure them and then use them to continuously regulate these inputs by appropriate means. By these means sub-optimal biomass is self-driven to achieve its maximum potential (Holms, 1991).

6.3 Construction of compositional tables

In general, the conversion of precursors to monomers follows well-conserved known biosynthetic routes. These are independent of the carbon source - or, in other words, pyruvate is used to make alanine whether the cells are growing on glucose, glucuronate, glycerol or acetate. Furthermore, the provision of precursors must match exactly their utilisation for biosynthesis (although this is an assumption that there is no futile cycling). An important function of the CMPs is to accept the flux of carbon input and divide and distribute it into the fluxes to precursors and hence monomers. Monomer biosynthesis requires both enzymatic reactions and input of energy, as does polymerisation, cell assembly, and cell division. In short, the CMPs fulfill a dual function - provision of the correct spectrum of precursors and the energy required to convert these into new biomass. The genome precisely defines the spectrum of precursors required and the biosynthetic routes by which these are processed define the energy requirements. There is little scope for any variation. The bacterial composition is generally maintained at a narrow, physiologically viable level e.g., a shortfall in pyruvate for alanine biosynthesis cannot be compensated by a surplus of another precursor to make a different aa. Whatever the carbon input, the CMPs of any bacteria are able to channel it into the correct spectrum of precursors and at least the amount of energy required for their further processing.

The monomeric composition of *S. coelicolor* 1147 & *S. fradiae* C373-10 & C373-18 biomass samples (Chapter 5) determined during this work were considered to be sufficient for computation of approximate monomeric compositional tables (Tables 6.1 – 6.27). The average monomeric composition of 1 g dry weight of biomass was converted to compositional tables as Holms (1986, 1996, 1997, 2001) and Davidson (1992)[for *E. coli* average composition from Neidhardt (1987) & Ingraham *et al*. (1983) was used] to determine the total amounts of intermediates in the CMPs, required for monomer biosynthesis (e.g., aas, nucleotides, carbohydrates, lipids, etc.). As described in Appendix B, there are eight of these intermediates which act as precursors: glucose-6-phosphate (G6P), triose-phosphate (TP), phosphoglycerate (PG), phosphoenolpyruvate (PEP), pyruvate (PYR), acetyl-CoA (AcCoA), oxaloacetate (OAA) and oxo-glutarate (OGA). Erythrose-4-phosphate (E4P) and ribose-5-phosphate (R5P) were included as precursors but, for the purpose of this flux analysis G6P was used as their starting precursor (see Appendix B; Table 1.2b)[Holms, 1986]. Individual compositional Tables (Tables 6.1 to 6.27) summarise the macromolecular

composition for *S. coelicolor* 1147 (Table 6.1 - 6.2) & *S. fradiae* C373-10 (Tables 6.3 - 6.25) cultured on a number of different carbon sources and the industrial strain C373-18 cultured on the industrial complex medium (Table 6.27). Also included was an average compositional table (Table 6.26; calculated from Tables 6.3 – 6.25). All tables were calculated in units of mmoles.g^{-1} dry wt and then converted to C.mmoles.g^{-1}dry wt (see section 6.1).

6.4 Total amount of precursors required for biosynthesis

The total amounts of precursors required for the biosynthesis of 1 g dry weight of *S. coelicolor* 1147 and *S. fradiae* C373-10 & C373-18 biomass are given in Tables 6.1 to 6.27 (constructed for sampling point II Chapter 4, section 4.5.3, Fig 4.1 - 4.20). The left hand column contains the monomeric composition of the biomass sample (see Appendix B for worked example). The right hand column contains the amounts of precursors needed to produce each monomer. For example, one mole of PYR and one mole OAA are required for the biosynthesis of one mole of isoleucine, whereas leucine is formed from two moles of PYR and one mole of acetyl-CoA. The total requirement of carbon for biosynthesis of each precursor is given in the bottom row (mmoles.g^{-1}dry wt and converted to C.mmoles.g^{-1}dry wt).

From the precursor tables for *S. coelicolor* (Tables 6.1 & 6.2); the demand for PYR was the highest (Tables 6.1 to 6.2); this corresponds with the work of Davidson (1992). This was feasible because PYR was the precursor of several abundant aas in *S. coelicolor* including alanine (see Chapter 5, section 5.7). The second most required precursor was AcCoA, used mainly for the synthesis of fatty acids (FAs). However, in both bacteria, TP was only used for FA formation and was therefore required in the least amount.

The total amount of TP was calculated from the lipid composition of *S. lividans,* for *S. coelicolor* and *S. fradiae* were assumed to have the same composition (see Appendix G, calculation as Davidson, 1992) and so remained constant in Tables 6.1, 6.2, 6.21, 6.23 & 6.25 regardless of sample content. This method was also used to calculate the amount of AcCoA required for FA biosynthesis. This was calculated in this way to correlate with the work of Davidson (1992) for *S. coelicolor* & *S. fradiae* cultures when lipid analysis was not analytically feasible i.e., solvent extraction had been undertaken on the samples (see Chapter 5, section 5.3.4). In the case of *S. fradiae* the lipid content was a measured variable (see

Appendix G, calculated as Davidson, 1992, where the total content of cellular lipid was known (section 5.3.4) and the TP and AcCoA content corrected) due to the fact that a calculated lipid content could give misleading results.

The average order of the remaining precursors were required in the order OAA > PG > OGA > PEP > TP. Apart from PYR and AcCoA, this order was the same to the order of requirement of *E. coli* biomass. In the case of *S. fradiae* the average most required precursor was AcCoA and PYR second. For the glucose oxo-glutarate defined medium PYR was the first and PG second (see Table 6.28). For the glucose glutamate defined medium AcCoA was the first order of requirement with G6P second (see Table 6.28). The average order for all (Tables 6.3 – 6.25) the remaining precursors was AcCoA > PYR > G6P > OAA > OGA > PG > PEP > TP (Table 6.28).

6.5 Metabolic throughput estimations

Tabulating the amount of each monomer present in 1 g dry weight biomass with the amount of required precursors, allows calculation of the total amount of precursors needed for biosynthesis of whole biomass (Tables 6.1 – 6.27). These values represent the outputs from the CMPs and are connected to the input (glucose, or appropriate carbon source) via throughputs (Holms, 1986, 1996, 1997, 2001). Throughputs were calculated by subtracting from the input (see Appendix B for example). Throughputs can be back calculated from Figures 6.1 – 6.25 by dividing all the figures by the normalisation factor (N) and then dividing again by the μ thus units of C.mmoles.g^{-1}dry wt were obtained (throughput diagrams and all workings can be found in the Compendium if required).

6.6 Computation of metabolic fluxes to biomass

Metabolic fluxes (expressed as C.mmoles.g^{-1}. dry wt biomass h^{-1}) were functions of throughputs of the CMPs and of the μ of the organism (the reconciled μ data was used, as Chapter 4, Table 4.12). Computation of the fluxes was obtained by multiplying throughputs by the μ through glycolysis and the TCA cycle and normalising to 100 (see Figures 6.1 – 6.25). The results of fluxes through the pathways and to biosynthesis and organic acid excretion are presented in Figures 6.1 to 6.25 as black boxes. The large throughputs to CO_2

were reflected in each flux diagram by the large fluxes through the TCA cycle (CER given in the red boxes).

All flux diagrams were worked out using three methods 1) in mmoles. g^{-1} dry wt biomass h^{-1} as Holms (1986, 1996, 1997, 2001). 2) In mmoles. g^{-1} dry wt and converted to C.mmoles.g^{-1} dry wt biomass h^{-1} after construction of initial diagram [1] (as Holms 1986; Davidson 1992). 3) Conversion from C.mmoles.g^{-1} to C.mmoles.g^{-1} dry wt biomass h^{-1} from the outset (method adapted for this thesis, see Appendix B). All the latter methods were worked out with individual and average compositional tables. Only diagrams using the units C.mmoles.g^{-1} dry wt biomass h^{-1} from the outset (3) were included in this work (see section 6.3.3 for discussion & sensitivity analysis behind this decision).

An initial, comparison of the fluxes to biomass of *S. coelicolor* 1147 & *S. fradiae* C373-10 compared with *E. coli* ML308 showed an approximate 2 to 3 fold difference in magnitude through glycolysis and the TCA cycle, even though *E. coli* also excreted acetate during growth (see Appendix B; Holms, 1986, 1996, 1997, 2001).

6.6.1 Comparison of fluxes to biomass

The main differences in fluxes were those through phosphoenolpyruvate carboxylase (PEPC), pyruvate dehydrogenase (PDH), citrate synthase (CS), and from oxo-glutarate dehydrogenase (OGDH) with subsequent reactions in TCA cycle. Although it was not possible to compare these ratios in *S. fradiae* fermentations with subsequent reactions in TCA cycle and antibiotic synthesis due to low antibiotic yields (see section 6.6.4). If antibiotic synthesis was included in any of the flux based models, there was no significant observable differences of the requirement of carbon for biosynthesis for *S. coelicolor* 1147 or *S. fradiae* C373-10.

S. coelicolor was used as an example in the following discussion because it had the highest antibiotic titer. The fluxes through most of the central metabolic enzymes were decreased during secondary metabolism but there was an increase through PEPC by two-fold (Fig 6.27; the increase in the flux through PEPC at the different sampling points [see Chapter 4, section 4.5.3, Fig 4.1 - 4.20 for sampling points] I & II for *S. coelicolor* 1147 cultured on glucose [Ferm 1], sampling point (SP) I, 4.1 %, SP II 7.70 %; [Ferm 2] SP I, 5.66 %, SP II, 9.03 %; for *S. fradiae* cultured on glucose [Ferm 1] SP I, 10.99, SP II, 20.76; [Ferm 2] SP I, 4.64 %,

SP II 7.64 %; cultured on fructose SP I, 1.24 %, SP II 2.41 %; and cultured on glycerol [Ferm 1] SP I, 1.33 %, SP II 2.29 %; [Ferm 2] SP I, 1.51 %, SP II, 2.67 %). The lower fluxes through PDH and OGDH reflected the assumed accumulation of PYR and OGA (Ahmed *et al*., 1984; Surowitz & Pfister, 1985; Hostalek *et al*., 1969). Due to the synthesis of ACT, less AcCoA would have been available for production of citrate via CS. Finally, the drop in flux through the TCA cycle from OGDH (due to the excretion of excess carbon represented as oxo-glutarate) would have caused a reduction in the amount of OAA produced via MDH. Therefore, increased flux through PEPC would have occurred to maintain the higher flux through the initial TCA enzymes.

Flux diagrams for *S. fradiae* C373-10 cultured on fructose were prepared (Figures 6.5 & 6.6). Titgemeyer *et al.* (1995) presented evidence for the presence of a PEP-PTS for fructose transport in *S. lividans*, *S. coelicolor* and *S. griseofuscus* (Chapter 2, section 2.4). Therefore the diagrams (Fig 6.5 & 6.6) were prepared on the basis that fructose entered by an active transport and via a PEP-PTS. There was no observable differences between the diagrams to identify which was more plausible (see Chapter 2 section 2.4 for discussion of the PTS in streptomycete metabolism).

Figures 6.24 & 6.25 represent the demand of carbon for biosynthesis for growth on a methyl oleate defined medium (Chapter 3, section 3.7), and constructed for the second phase of the fermentation (see Chapter 4, section 4.5.3, Fig 4.13 - 4.15) days 3 – 9. It was initially considered possible to apply flux analysis by segmenting the fermentation up, into a number of phases, but this turned out to be cumbersome. However, this does illustrate one of the problems inherent in flux analysis. It was known by measurement, that a flux of 9.82 and 5.72 (Ferm 1 & 2, day 3 - day 9; Figures 6.24 and 6.25 respectively) [C.mmoles.g^{-1} normalised to 100] was drawn from PYR and 11.45 and 6.63 from PEP for biosynthesis of monomers. The allocation of fluxes was assumed to be directed through the most direct route. In this case malate dehydrogenase decarboxylating (MDH[dc]) enzyme would convert malate to PYR and by PEPCK would convert OAA to PEP. However, there is a route from PEP to PYR by PK (see Chapter 2, section 2.5). It follows for example, that the flux from malate to PYR and the PEP could go extensively to PEP and then from PEP to PYR.

The requirement of carbon for biosynthesis by *S. fradiae* C373-10 growing on a single carbon source was an order of magnitude lower compared with *S. coelicolor* 1147 (Figures

6.1 – 6.25). When glutamate was an addition to the medium the requirement of carbon to biosynthesis achieves similar levels to that of *S. coelicolor*. The AcCoA branch point between biosynthesis and acetate excretion, also shows significant increases in the carbon flux when glutamate was an addition to the medium with an equal flux to the extracellular environment through acetate secretion (see Figures 6.14 – 6.17).

6.6.2 Estimated percentage (%) carbon balance

The fluxes to biomass and CO_2 production were used to compare inputs and outputs of the system, for *S. fradiae* C373-10*, S. coelicolor* 1147*,* and *E. coli* ML308 (calculated from Holms, 1986) by expressing all values in terms of percentage carbon flux in relation to the carbon source input (see Tables 6.31 [sensitivity analysis between mmoles.g^{-1} dry wt biomass h^{-1} and C.mmoles.g^{-1} dry wt biomass h^{-1} as units of measurement for *S. fradiae* and *E. coli*], 6.32 [mmoles.g^{-1} dry wt biomass h^{-1}], & 6.33 [C.mmoles.g^{-1} dry wt biomass h^{-1}]. Due to considerable differences between the use of the units of measurement and the lack of on-line gas analysis both units of measurement were used to further assess fermentation data (Table 6.32 [mmoles.g^{-1} dry wt biomass h^{-1}], & 6.33 [C.mmoles.g^{-1} dry wt biomass h^{-1}]).

Jonsbu *et al*. (2001) reported 54.1 % demand of carbon to biosynthesis for *S. noursei* this compared to 34.44 % for *S. coelicolor* 1147 and 27.35 % for *S. fradiae* C373-10 on average for this work. Table 6.31 (mmoles.g^{-1}dry wt as starting units) would indicate a considerable percentage of the carbon source was evolved as CO_2 (see section 6.6.3 for in depth discussion). The percentage carbon recovered also corresponds with that of Melzoch *et al*. (1997) [Table 6.30 & 6.31] i.e., 99 – 103 % for *S. noursei*. For *S. coelicolor* and *S. fradiae,* this was in the range of 74 – 111 % using the units mmoles.g^{-1} dry wt biomass h^{-1}.

The considerable amount of unaccountable carbon on average 20 % - 30 % for C.mmoles.g^{-1} dry wt biomass h^{-1} as the units of measurement from the outset was possibly due to a number of issues: 1) experimental error as implied by the high standard deviations seen from the compositional analysis undertaken in Chapter 5 (Chapter 5, Table 5.43). 2) Excretion of unaccounted for metabolites in the extracellular environment, TOCA undertaken in Chapter 4 (section 4.6, Tables 4.13 Part 1 & 2) indicated 10 - 60 % of the carbon in the extracellular medium was unaccounted for. Initial total organic carbon analysis (TOCA) of *S. coelicolor* 1147 and *S. fradiae* C373-10 biomass indicated on average 40 - 60 % of the carbon was unaccounted for compared with 20 - 40 % of the carbon for *E. coli* (Chapter 5, section 5.5).

Previous work in Chapter 5 (section 5.4) would indicate that the intracellular metabolites (e.g. G6P, fructose-6-phosphate, PYR, malate, etc.) were unusually high against *E. coli.* For instance, the intracellular fraction contained a considerable proportion of unaccounted for carbon (i.e. the cold PCA fraction [Chapter 5, section 5.4] or the cell wall material accounted for a greater proportion of carbon than estimated [Chapter 5, section 5.4]).

This opens up one question, why when using the units of C.mmoles.g^{-1} dry wt h^{-1} was there a large proportion of the carbon unaccounted for (Table 6.31, 6.32, & 6.33)? It was also possible due to the high level of flux through glycolysis and the TCA cycle that using the units of mmoles.g^{-1}dry wt distorted the results. The most probable site of this distortion was at aldolase, where 1 mole of fructose-1,6-diphosphate was converted to 1 mole of glyceraldehydes-3-phosphate and 1 mole of dihydroxyacetone phosphate. The use of C.mmoles.g^{-1}dry wt negates the need to take this into account, as 6 atoms of carbon flow through this step of the pathway before and after the aldol cleavage. This distortion was not observed with the glutamate and oxo-glutarate flux diagrams where aldolase was calculated in reverse direction from biosynthesis and not directly from the carbon source input as the glucose, fructose and glycerol flux diagrams. The considerably high unaccountable carbon (Table 6.31, 6.32, & 6.33) was probably a contributory factor that further increased this distortion (Tables 6.31 – 6.33). In the case of *E. coli* this was not recognised (Holms 1986, 1996, 1997, 2001). This was likely due to the high efficiency of the conversion of carbon source to biomass by *E. coli,* given by (Holms, 1986)[section 6.6.6].

6.6.3 Carbon dioxide evolution

Additional information obtained from the flux diagrams (Figures 6.1 – 6.25) was the amount of CO_2 produced per gram dry weight biomass per hour. CO_2 was evolved by the reactions of PDH, ICDH, MDH[dc], PEPCK, and OGDH. A small amount of CO_2 was also produced during flux from G6P to pentose phosphate in the pentose phosphate pathway (PP pathway) when ribose groups for nucleotides were formed. However, CO_2 was required for carboxylation of PEP in the formation of OAA via PEPC.

Table 6.31, 6.32, & 6.33 was an initial sensitivity analysis undertaken to determine the effect that different units of measurement have on the estimated CER between *S. coelicolor, S. fradiae,* and *E. coli* (*E. coli* calculated from Holms, 1986). When the units of mmoles.g^{-1} dry

wt biomass h^{-1} were used in the construction of flux diagrams, the highest proportion of carbon flux in the streptomycete fermentations was to CO_2 (for *S. coelicolor* 69.6 % & 66.7 %; and for *S. fradiae* it ranged from 50 % - 70 % depending on the carbon source. These results correspond with the work of Davidson (1992); which would indicate continuous cycling of the TCA cycle with very little drainage to biosynthesis. This cycling was more clearly shown in the flux diagrams (Figures 6.7 – 6.10; for *S. fradiae* C373-10 cultures grown on glycerol [Ferm 1 & 2] calculated in both mmoles.g^{-1} dry wt h^{-1} and C.mmoles.g^{-1} dry wt h^{-1} normalised to 100). In a glucose minimal medium (Table 6.30), *E. coli* was shown to evolve only 23.1 % of the input carbon as CO_2 (Holms, 1986).

When using the units C.mmoles.g^{-1} dry wt biomass h^{-1} from the outset in the construction of a flux diagram the proportion of carbon flux to CO_2 was 33.32 % to 38.80 % for *S. coelicolor*; and for *S. fradiae* it ranged on average between 35.35 % and 49.77 % (Table 6.32)[depending on the carbon source]. When the units of mmoles.g dry wt and C.mmoles.g.dry wt were used to calculate the respiratory quotient (RQ) with the experimentally determined oxygen uptake rate. The RQ was considerably higher than expected (2.60 mmoles.g dry wt and 1.48 C.mmoles.g dry wt respectively for the glycerol fermentation). Indicating considerable inconsistencies between the modelled variables and experimental results

For *E. coli* CER was between 24.82 % to 37.14 % the high carbon recovery of 112 % was considered to be due to rounding up of figures and inaccuracies in accounting for the PTS (Table 6.31). Delgado and Liao (1997) calculated the CER for *E. coli* to be 36.67 %. Emmerling *et al*. (2002) calculated the CER for *E. coli* JM101 under different medium limited conditions and dilution rates to be 32.67 %, for carbon limited (0.09 h^{-1}); 70.22 % for carbon limitation (0.40 h^{-1}); 20.19 % for nitrogen limitation (0.09 h^{-1}) & calculated the CER for *E. coli* PB25 (pyruvate kinase [PK] deficient mutant) under different medium limited conditions and dilution rates to be 33.26 %, for carbon limited (0.09 h^{-1}); 71.23 % for carbon limitation (0.40 h^{-1}); 19.28 % for nitrogen limitation (0.09 h^{-1}). The medium used by Holms (1986, 1996, 1997, 2001) was nitrogen limited. Therefore it was likely the units C.mmoles.g^{-1} dry wt biomass h^{-1} produce the best-fit flux diagram to the experimental results for *E. coli*.

Hobbs *et al*. (1990) reported maximum CO_2 production by *S. coelicolor* grown on a glucose minimal medium of 0.8 % (flow rate 2 L per h^{-1}) in the effluent gas, the maximum dry

weight of the biomass was 3 gl^{-1}. In the fermentation described by Davidson (1992), the maximum biomass produced by *S. coelicolor* in the same medium was 0.44 gl^{-1} a 6.8 fold difference, and the maximum CO_2 evolved 0.15 %, a 5.3 fold difference to that measured by Hobbs *et al*. (1990). A maximum of 2 gl^{-1} dry wt was achieved with the same medium for this work (Hobbs *et al*., 1990). However, additional measurements were required to verify this. Bushell and Fryday (1983) reported a carbon conversion of 52 % from glucose to biomass for *S. cattleya* (*S. cattleya* biomass contains 47.5 % carbon; Bushell and Fryday, 1983) and 48 % to CO_2. Davidson (1992) converted the data from Bushell and Fryday (1983) into the rate of evolution of CO_2 into relation of carbon source input. This resulted in 122.89 mmoles CO_2 evolved from the culture during the 25 hr period. This was equivalent to 1.48 g of carbon from 7.2 g of glucose, i.e., a conversion to CO_2 of 51.2 %.

Melzoch *et al*. (1997), studied the effect of the growth environment on ACT production by *S. coelicolor* in an aerobic chemostat culture at a constant dilution rate under different nutrient limitations. From this work specific production rates were calculated for ACT (q_{act}), glucose (q_{glu}), oxygen (q_{O2}), carbon dioxide (q_{CO2}), and growth yields (Y_s) [the CER was converted to the percentage CER in relation to the carbon source input to facilitate comparison of this data with the data obtained in this project]. The CER were as follows: 42.90 % for carbon limitation, 19.08 % for nitrogen limitation, 57.13 % for phosphorus limitation, 51.81 % for sulphur limitation, 50.54 % for potassium limitation, 73.91 % for magnesium limitation, and with an average CER of 49.23 %. The CER under different limitation conditions for *S. clavuligerus* were as follows 55.49 % for carbon, 31.77 % for phosphate, 23.03 % for nitrogen, and with an average CER of 36.76 % (results recalculated from Kirk *et al*., 2000). For the *S. coelicolor* cultures (Melzoch *et al*., 1997) the specific rates of O_2 consumption and CO_2 evolution were lowest when the organisms were grown under carbon limitation and highest under potassium limitation. In relation of carbon source input to CER, there was good correlation with *E. coli, S. coelicolor*, and *S. clavuligerus* that the efficiency of CER follows the same trend (nitrogen > carbon > etc.). The data of the other limitations (phosphorus, and sulphur) were between these two extremes, the data for magnesium limitation were puzzling in that they were almost identical to those for carbon limitation. It was noted by Melzoch *et al*. (1997) that the steady state dry weight might have been incorrectly estimated due to pelleting of the biomass increasing errors in the calculations. Further research was carried out by Melzoch *et al*. (1997) to study the effect of

dilution rate on the specific production rates of CER under carbon-limited conditions. Four different dilution rates for *S. coelicolor* were investigated and the percentage CER's were as followed 19.59 % at 0.04 h^{-1}, 45.15 % at 0.06 h^{-1}, 58.92 % at 0.09 h^{-1} and 76.91 % at 0.16 $h^{-1,}$ and with an average CER of 47.22 %. The specific rates of glucose consumption, oxygen consumption, and CO_2 production followed the usual trend in that they increased with growth rate. There was however, a deviation from the classical linear relationship between the these growth parameters and the dilution rate: above 0.09 h^{-1} there was a sharp increase in the q_{O2} and q_{CO2} values, which was also noticeable in the percentage CER correlated to the carbon source input. The specific rate of ACT production, on the other hand, followed a completely different pattern. It was low at dilution rates lower than 0.05 h^{-1}, peaked at D = 0.06 h^{-1}, and declined to almost 0 at the highest dilution rate tested (0.128 h^{-1}). This would correspond with ACT production belonging to late growth events, such as the development of competence, sporulation, cell differentiation, etc.

However experimental data was further required to verify which of the latter calculated CERs were accurate for the latter *Streptomyces* cultures. An attempt was therefore made to measure experimentally the flux to CO_2 produced during one glycerol fermentation (glycerol; Fermentation 2, Table 6.7 and 6.31, Figure 6.10), two methyl oleate defined medium fermentations (Fermentation 1 & 2, Tables 6.21 - 6.25, Fig 6.24 & 6.25), and three industrial complex fermentations for *S. fradiae* C373-10 and C373-18. Due to complications and limitations with equipment the measurement of CO_2 in the effluent gas was performed only with the last fermentation, and the determination of the amount of CO_2 produced serves as an example of the information and calculations required (see Appendix E, for required calculations). Using different curve fitting algorithms (Gaussian & Lorentz curve fitting algorithms; Origin 5.0) the CER for the glycerol fermentation was calculated to be between 33 % and 46 % depending on algorithm (a number of algorithms were needed to compensate for 24 hrs of missing data). The calculated proportion of carbon to CO_2 evolution for *S. fradiae* C373-10 cultured on a methyl oleate medium (Chapter 3, section 3.7) was calculated to be in the range of 64.14 % & 46.48 % for fermentations 1 & 2 respectively.

A carbon balance was used to determine (Chapter 5) the allocation of carbon over the course of an industrial fermentation (Chapter 4, Fig 4.16, Fermentation 1). This results in 36 % of the carbon being converted to CO_2, 11 % was converted to tylosin, 8 % remained as oil residues and 44 % remained as biomass (dry weights calculated by extraction with solvents

Chapter 3, section 3.13) or left the fermenter as sampling or foam out. These results were similar to internal studies by Eli Lilly Ltd. (Schreiweis *et al*., 1999). These results were open to error due to the number of different mass spectrometers being used, and infrequent calibration of the equipment on site at Eli Lilly Ltd.

It was therefore not possible from this work to verify which of the models from this Chapter was correct. It was assumed that all the cultures had a low μ and were carbon limited for *S. coelicolor* 1147 and nitrogen limited *S. fradiae* C373-10. The measurements made during this fermentation project support the diagrams designed and constructed with units of C.mmoles.g^{-1} dry wt h^{-1} (Figures 6.1 – 6.25). This was only an assumption at best as further on-line gas analysis (namely CER), which would support the flux analysis and therefore the competence of the MFA to streptomycete cultures, could not be undertaken.

6.6.4 Flux to excreted products

Calculation of the flux to actinorhodin (ACT) after cessation of biomass production by *S. coelicolor* 1147 showed that the flux to the antibiotic synthesis was only 1.4 % to 1.7 % of the total input (similar results to Davidson, 1992). In the case of *S. fradiae* flux to tylosin was in the range (0.05 % for minimal medium and 0.5 % for defined medium). Although these fluxes were very small, they were greater than the primary fluxes from PEP and TP in a number of cases. Small fluxes in the comparison to biomass synthesis introduce errors. The sensitivity analysis undertaken by Naeimpoor & Mavituna (2000) for *S. coelicolor* indicated that the fluxes to antibiotic synthesis have to be in excess of 2 % or there was no observable effect on overall flux. Therefore fluxes to antibiotic synthesis were not included in the models or considered any further (Figures 6.1 – 6.25).

Studies undertaken by Naeimpoor & Mavituna (2000) for *S. coelicolor* indicate the highest specific acetate excretion rate and the highest total specific metabolite excretion rates occurred during in nitrogen limitation. This is consistent with the observation of many researchers that high C : N ratios lead to the excretion of organic metabolites. Since nitrogen is essential for protein synthesis, when nitrogen is limited, the excess carbon cannot be consumed for protein formation and hence it does not lead to the production of biomass. Therefore, excess carbon could be excreted as organic acids if not oxidised to CO_2 for energy production. Naeimpoor & Mavituna (2000) calculated the carbon losses for *S.*

coelicolor as formate and acetate and were in the range of 26.1 %, 10.5 %, 6.9 %, and 6.0 % (additive value) of the utilised carbon for N, P, S, and K limitations, respectively, confirming that N and P were the two most important elements in biomass formation.

Experiments with alternative carbon sources for *S. fradiae* C373-10 (see Chapter 4, Fig 4.1d - 4.18d for fermentation acid production profiles) show that glucose (1.21 %, PYR; 0.81 % OGA; 1.10 % malate; average between Figures 6.3 & 6.4; presented as a percentage of the carbon source input), glycerol (2.12 %, PYR; 1.96 %, acetyl-CoA; 0.52 % OGA; 1.18 % malate; average between Figures 6.7 & 6.8), oxo-glutarate (0.27 %, PYR; 1.47 %, acetyl-CoA; 1.12 % malate) support acid production. Glucose supports acid production to higher levels when combined with an organic nitrogen source such as glutamate (0.38 %, PYR; 3.53 %, acetyl-CoA; 0.53 % malate; average between Figures 6.12 & 6.15 [day 2]; 3.01 %, PYR; 10.97 %, acetyl-CoA; 0.46 % OGA; 1.10 % malate; average between Figures 6.16 & 6.19 [day 5]) and oxo-glutarate (1.15 %, PYR; 1.64 %, acetyl-CoA; 2.22 % malate average between Diagrams 6.20 & 6.21 [day 3]; 6.74 %, PYR; 4.78 %, acetyl-CoA; 3.40 % malate; average between Figures 6.22 & 6.23 [day 8]) in addition to ammonia. Fructose showed lowest acid production (0.37 %, PYR; 0.69 %, acetyl-CoA; -0.06 % OGA; 0.92 % malate; average between Figures 6.5 & 6.6). In most media, acids were possibly re-assimilated towards the end of rapid growth and during the stationary phase. Conversion of the consumed carbon to undesirable acid by-products was greater in defined medium (around 12 %; collective value) than complex medium (around 4 %; collective value).

6.6.5 Ratios of fluxes

On careful analysis of Tables 6.1 – 6.27, there were significant differences between similar fermentations (e.g., between Tables 6.1 & 6.2 [growth of *S. coelicolor* 1147 cultured on a glucose minimal medium]; 6.1, G6P, 0.995; TP, 0.064; PG, 0.908; PEP, 0.294; PYR, 1.94; OAA, 0.967; OGA, 0.583; AcCoA, 1.949; Table 6.2, G6P, 1.427; TP, 0.064; PG, 1.054; PEP, 0.520; PYR, 2.519; OAA, 1.224; OGA, 0.923; AcCoA, 2.059). Analogous with the monomeric compositional tables for biomass to production, the throughput diagrams also show significant differences (Figures 6.1 – 6.25). However, the ratios of fluxes to products (antibiotics and organic acid ratios divided by PFK × 1000)[results not included] and biosynthesis with respect to PFK or appropriate enzyme designated by # in Tables 6.29 (units of measurement mmoles.g^{-1}dry wt) & 6.30 (units of measurement C.mmoles.g^{-1}dry

wt), were calculated to be very similar. These ratios of the fluxes show clear similarities between environmentally-similar cultures (Tables 6.29 & 6.30). It was not possible to identify any rigid or flexible nodes (branch points) [see Chapter 1, section 1.2] in the CMPs from Tables 6.29 & 6.30. There were no identifiable deviations (perturbations) with either units of measurement of mmoles.g^{-1}dry wt or C.moles.g^{-1}dry wt, at any of the branch points analysed (Tables 6.29 & 6.30). This could be due to a number of reasons 1) inaccuracies accrued from the compositional analysis undertaken in Chapter 5. 2) The analytical work undertaken in Chapter 5 did not account adequately for the carbon content of biomass (a carbon accountability of within 10 % is readily accepted by other workers), which could have distorted the results. 3) Up to 4 different designs of bioreactor were used throughout this work (Chapter 3, section 3.8), which was likely to increase the batch-to-batch differences and discrepancies (see Chapter 1, section 1.1). 4) The μ has been reported to have a considerable effect on the fluxes. Daae & Ison (1999) reported the μ and changes in the μ have the greatest effect on a flux analysis (see Chapter 7, section 7.3.1). Hence reducing the μ sensitivities will result in reduced accumulated sensitivities & errors (see Chapter 1 & 7).

6.6.6 Outputs and Efficiency

Flux determinations also provide information on the efficiency of conversion of input carbon to output carbon by the organism. According to Holms (1986), an indicator of efficiency of utilisation of glucose to provide biomass is given by the ratio of biosynthetic flux to the flux too CO_2. Table 6.35 presents the results of Tables 6.31, 6.32 & 6.33 in mmoles.g^{-1} dry wt h^{-1} and C.mmoles.g^{-1} dry wt h^{-1} units for the demand of carbon for biosynthesis and CER. These are then converted to the efficiency of the CMPs (Dividing the demand of carbon to biosynthesis by the CER)[as Holms, 1986; Davidson, 1992]. The efficiency of conversion for *E. coli* grown on a glucose minimal medium was calculated to be 2.7 [initial units used mmoles.g^{-1} converted to C.mmoles.g^{-1} (as Holms, 1986)]. For *S. coelicolor* grown in minimal medium corresponding to this work and Davidson (1992) the efficiency of the CMPs was calculated to be in the order of 0.4 - 0.5 [initial units used mmoles.g^{-1} converted to C.mmoles.g^{-1} (see Table 6.34). Therefore, in addition to providing an indication of areas of regulation of fluxes, the Holms strategy (Holms, 1986) of flux determination can give a measure of efficiency of growth of the organism concerned with the conditions used. The

flux to CO_2 (23.1 %) during growth of *E. coli* was less than that of *S. coelicolor* and *S. fradiae* fermentation; which suggested greater efficiency of *E. coli* biosynthetic pathways. The efficiency of the conversion of carbon in *S. fradiae* fermentation with the addition of glutamate or OGA was greatly improved when the units mmoles.g^{-1}dry wt and C.mmoles.g^{-1}dry wt (were used from the outset). The glucose + glutamate and glucose + oxo-glutarate defined media showed reasonable correlation between a molar and carbon molar (Table 6.34) basis which may indicate that the proportion of carbon flowing through the PP pathway was lower. A correlation between these units possibly implies decreased activity of the PP pathway, as the distortion of the results decreases, as more carbon passes through the aldolase reaction sequence (see section 6.6.2). This does not correlate with the enzyme assays undertaken in section 6.8, which implied a significant activity for the PP pathway. To allow any further comparison between the results presented in Table 6.34 further on-line gas analysis will be needed to verify this work (namely CER)[see section 6.6.2].

6.6.7 Maintenance energy

Many cellular reactions require the consumption of ATP without contributing to a net synthesis of biomass, and these reactions are usually referred to as maintenance reactions. Some of these are associated with growth, e.g., to maintain the electrochemical gradients across the plasma membrane, whereas others are independent of the μ of the cells e.g., futile cycling and organic acid excretion. Holms (2001) termed maintenance energy as thermodynamic inefficiency (Th.In) for example *E. coli* generates more energy (ATP and NADPH) within the CMPs than is required to convert precursors to biomass, the excess is presumably dissipated as heat (i.e., Th.In). In the case of acetate excretion in *E. coli*, acetate diminishes the Th.In, if acetate was not excreted, and all was oxidised to CO_2 in the TCA cycle, the culture might kill itself by overheating.

In glucose minimal medium, the growth rate of *E. coli* in substrate-sufficient cultures is 0.94 h^{-1} (Holms, 1986). The maximum growth rate reached by *S. coelicolor* was 0.12 h^{-1}, and *S. fradiae* 0.045 h^{-1}. It was possible therefore, that the central metabolic activity of *S. coelicolor* and *S. fradiae* was mainly directed towards production of energy for maintenance.

Initial attempts by Naeimpoor & Mavituna (2000) to calculate the maintenance energy requirements of *S. coelicolor*, were hindered by the maximum μ's used from experimental

data for different nutrient limitations, causing considerable differences in the calculated maintenance energy. To account for the effect of different μ's they were fixed at the experimental dilution rate of 0.06 h^{-1}. It should be realised that even by considering the experimental measurements as constraints, the calculated maximum theoretical μ was not far from the experimental dilution rate of 0.06 h^{-1}. This would indicate that growth-associated maintenance accounted for a considerable proportion of the overall maintenance requirement. The highest values of maintenance energy were related to K limitations. This emphasises the fact that potassium ions in the medium play an important role in cell survival and also explains why the experimental specific glucose uptake and CERs are highest under K limitation compared with other nutrient limitations (e.g. carbon, nitrogen, sulphate, phosphate; see section 6.6.6)[Naeimpoor & Mavituna, 2000]. Naeimpoor & Mavituna (2000) flux analysis would indicate most of the excess glucose consumed was oxidised to produce ATP. Nitrogen limitation on the other hand gives the lowest value of the maintenance energy requirement this can be explained by the highest maximum theoretical μ obtained for nitrogen limitation. In the case of nitrogen limitation when setting the μ to 0.06 h^{-1} this increases the calculated maximum maintenance energy requirement by 62 % to compensate for the high theoretical μ (0.093 h^{-1}). This confirms that with nitrogen limitation, excess carbon cannot be directed into the biomass because nitrogen is lacking for the biosynthesis of proteins, which constitute nearly 50 % of the biomass. P and S limitations fit between the two limitations discussed above (Naeimpoor & Mavituna, 2000).

6.6.8 Metabolite pool sizes and control of the CMPs

Many of the intermediate pools in the CMPs are so small that they have never been measured and the enzyme activities available to process them are, relatively large. What regulates or limits flux through such enzymes is the pool size of the substrate. There is at least one example for *E. coli* where isocitrate lyase (ICL) of the GBP is in direct competition with the TCA cycle enzyme isocitrate dehydrogenase (ICDH). Although ICDH has a much higher affinity for isocitrate (ISOCIT), flux through ICL and thence the anaplerotic enzyme malate synthase (MS) is assured by virtue of high intracellular levels of ISOCIT and the partial inactivation of ICDH (El-Mansi *et al*., 1985). Although the *in vivo* signal which triggers the expression of the GBP enzymes is yet to be determined.

de Orduna and Theobald (2000) showed fast changes of the G6P intracellular content precisely signaled transitions in the flow of carbon through the EMP pathway and PP pathway of *S. coelicolor*. There is therefore some evidence that, in some small segments of the CMPs, pool sizes are extremely important. Unfortunately, information on pool sizes is fragmentary and much of it was gathered some time ago for *E. coli* using what are now considered to be inadequate methodologies. Pool sizes, preferably of all the intermediates of the CMPs, must be measured accurately in a variety organisms before it is possible to relate flux distribution to regulation of the CMPs.

6.7 NADPH requirements for growth

Obanye (1994)[Obanye *et al*., 1996] reported that batch growth of *S. coelicolor* was accompanied by major changes in central metabolism. Particularly important was the change from the domination of the EMP pathway during a fast, acidogenic growth phase to a slow "acidostatic" phase of growth during which flux through the PP pathway becomes significant. Methylenomycin production was initiated at the beginning of this second phase of growth (Obanye, 1994; Obanye *et al*., 1996). It was envisaged that the uptake of glucose was deregulated. As the glucose concentrations used during this work were at similar levels, it was feasible that a high affinity glucose (carbon source) uptake system would be saturated during the initial stages of growth (and during most of the exponential / cubic growth phase). Such an uptake mechanism, however, might be amply suited to natural environments in which some carbon sources are a scarce commodity (e.g. glucose).

The result of deregulated uptake of carbohydrate uptake could be a lack of co-ordination between carbon catabolism on the one hand and anabolic reactions on the other. The result would be inappropriately high NADH/NAD ratio throughout most of the rapid exponential growth phase. This, in turn, would give rise to a partial inhibition of major NADH-generating steps, e.g. OGDH and pyruvate dehydrogenase, leading to the accumulation of the corresponding ketoacids, OGA and PYR (in the case of *S. fradiae* this could account for malate in the extracellular environment as malate dehydrogenase is another major NADH-generating enzyme), which were excreted into the medium. While OGA is being produced, it was envisaged that enough NADPH was being generated by the NADPH-generating isocitrate dehydrogenase step to complement any production of this coenzyme by the PP pathway.

As the pH of the external medium continues to fall due to acid production, the ΔpH-driven ATP synthase becomes increasingly active. As a result of this superfluous synthesis of ATP, it was envisaged that flux through the TCA cycle becomes insufficient to generate enough NADPH to complement that produced by the PP pathway, during a time of increased reductive biosynthesis. A number of events at this point might redress the situation:

(I) a ΔpH-driven transhydrogenase could begin to convert cellular NADH to NADPH (see Chapter 2, section 2.5.5).

(II) an increase in the flux through the pentose phosphate pathway could occur.

(III) futile cycling of C4 intermediates for example could account for a considerable proportion of the NADPH requirement (ATP spillage).

It has been speculated that methylenomycin biosynthesis for *S. coelicolor* is one of the avenues by which the streptomycete cell counteracts an increase in the energy charge. However, it is envisaged that, to a large extent, methylenomycin biosynthesis is also regulated by the availability of NADPH. With regard to the effect of pH on the NADH/NAD ratio. It has been reported that low culture pH gives rise to reduced NADH/NAD ratio in *Enterococcus faecalis* growing anaerobically (Neijssel & Teixeira de Mattos, 1994; Snoep *et al*., 1991). This in turn gives rise to unexpected activity of the PDH complex (PDH is reputed to be inactive under anaerobic growth conditions).

The NADPH requirements for cell growth and tylosin production were therefore evaluated. The previous evaluations were based on an assumption of similar NADPH requirements for cell growth of *P. chrysogenum* & *S. noursei*, where the *P. chrysogenum* NADPH requirement was taken to be 8.5 mmoles NADPH g^{-1} dry weight in a defined medium (Nielsen, 1997). The synthesis of aas was considered to constitute more than 95 % of the total NADPH requirement for cell growth. The theoretical NADPH requirement for *E. coli* biomass synthesis was calculated to be 18.22 mmoles NADPH g^{-1} dry wt biomass h^{-1} (Ingraham *et al*., 1983). A balance for NADPH cell growth requirement was given in Table 6.35 part 1 during the growth phase.

NADPH was also necessary as reductive power for the biosynthesis of tylosin through the keto-reduction and enoyl-reduction of acetate, propionate, and butyrate groups of the carbon units being assembled into the polyketide chain (see Chapter 2 section 2.10.4). The NADPH requirement for nystatin, was calculated to be 41 mmoles NADPH g^{-1}.nystatin (Jonsbu *et al*.,

2001). The NADPH requirement was calculated to be 12.01 mmoles NADPH g^{-1} for tylosin (theoretical calculation from Tables 2.3, 2.4, 2.5 & 2.6). Calculation of the NADPH requirement for antibiotic production was only possible for the methyl oleate defined medium (Chapter 3, section 3.7) due to the achievement of low antibiotic yields in the majority of fermentations [see Chapter 4, Fig 4.1 - 4.20](section 6.6.4). This was calculated to be 3.40 & 3.79 mmoles.g^{-1}dry wt and 0.085 & 0.072 mmoles.g^{-1} dry wt biomass h^{-1} for fermentations 1 & 2 respectively (Figures 6.24 & 6.25).

The theoretical NADPH requirement for cell growth was calculated from Tables 6.1 – 6.27 (mmoles.g^{-1} dry wt biomass h^{-1}) and converted to theoretical fluxes (multiplied by the μ) presented in Table 6.35 Part 1. Unfortunately there are several errors in the these theoretical calculations: (1) no account was made for the NADPH requirement for transport processes i.e., NH_3. (2) No data was included for polymerisation reactions and the formation of biomass. (3) The NADPH requirement for precursor formation was not included. (4) No account was made for NADPH requirement for ATP (NADH) formation from the activity of a nucleotide transhydrogenase (TH). (5) It was assumed that ammonia and sulphate were non-limiting (the energetic cost of the reduction of sulphate to H_2S was included in the costs of Met and Cys). (6) Energetic costs for aa and nucleotide biosynthesis from precursor metabolites were calculated for *E. coli* (Zubay, 1998; Stanier *et al*., 1986). For an assessment of the NADPH cost of precursor supply see Chapter 8 (see Chapter 8, Tables 8.1 - 8.5; Akashi & Gojobori, 2002).

The NADPH produced from the flux diagrams (Figs 6.1 – 6.25) was designated in mmoles.g^{-1}dry wt biomass and mmoles.g^{-1} dry wt biomass h^{-1} (Table 6.35 Part 1). Y_{TCA} represents the maximum production of NADPH from ICDH (Figures 6.1 – 6.25) if NADP-ICDH was operational, Y_{PPP} represents the maximum production of NADPH from (Figures 6.1 – 6.25) the PP pathway when G6PDH & 6PGDH were both considered to be, NADP-dependent. Y_X represents the maximum production of NADPH ($Y_{TCA} + Y_{PPP}$). The latter data was used to estimate if the flux of carbon through NADPH producing pathways of the flux diagrams (Figs 6.1 – 6.25) was likely a correct assumption. Table 6.35 Part 2 further assesses the contribution of altering the NADPH requirements to resolve the flow of carbon passing through the PP pathway by co-factor balancing strategy (see Chapter 1, section 1.2.3). PPP (1) gives the percentage flux passing through the PP pathway from Tables (6.1 – 6.25) with no alterations to the data (Table 6.35, Part 2); PPP (2) gives the percentage flux passing

through the PP pathway when the carbon flow through PP pathway is corrected to the theoretical requirement with an operational NADP-ICDH (Table 6.35, Part 2); PPP (3) gives the percentage flow of flux through the PP pathway when corrected to the theoretical NADPH requirement if the PP pathway was the only NADPH generating pathway (Table 6.35, Part 2).

In the glucose (Fermentation 1 & 2 respectively), fructose & glycerol (Ferm 1 & Ferm 2) fermentations Y_{TCA} NADPH producing capacity was higher than the theoretical NADPH capacity. This could indicate that the NADP-ICDH in these cultures was not operational, a TH was active or that there were other expensive NADPH-consuming enzyme/enzymes operational. One other theoretical possibility is a NAD-dependent isocitrate dehydrogenase might be used to modulate NADPH concentration, e.g., induced to avoid NADPH accumulation and the PP pathway flux is simultaneously reduced. A NADPH oxidase may also be operative to prevent excessive accumulation of NADPH. Bruheim *et al.* (2002) determined experimentally that this was not the case in *S. lividans*.

It can be seen from Table 6.35, Parts 1 & 2 that the constructed models (Figures 6.1 – 6.25) were not likely to account for the true carbon flux through the PP pathway. The considerable number of isoenzymes present in streptomycetes further hinders the reliability of any co-factor balancing strategy. At best this was an estimation. It should be noted that the latter calculations assume that there was no operational TH. When glutamate was added to the glucose minimal medium, there was a considerable increase in the theoretical NADPH requirement therefore, glutamate could possibly have a stimulatory role on a NADPH producing pathway (Table 6.35, Part 1). The increased NADPH requirement is mainly due to an increase in the FA content of the cell. This was considered to be a possible sight of experimental error and further researched in Chapter 5, section 5.3.4.

The ratio of flux through the PP pathway compared with the EMP pathway for *E. coli* grown on a glucose minimal medium was 1:018 for Holms (1986, 1996, 1997, 2001; see Appendix B) which corresponds with the conclusion of other workers (Delgado & Liao, 1997) 1:013. Table 6.35 Part 1 & 2 indicates that for *E. coli* the theoretical requirement was higher than that produced from the PP pathway, which would indicate a TH or futile cycling was present, although nitrogen uptake was not included in this calculation and may have caused some error in the interpretation of the results.

Jonsbu *et al*. (2001) reported the NADPH requirement for *S. noursei* to be more than two-fold higher in the growth phase compared to the production phase. This was mainly considered to be due to a lower μ in the latter. However, the formation of NADPH was found to be in excess in both phases (Jonsbu *et al*., 2001). These calculations were based on the formation of 2 moles of NADPH per mole of G6P entering the PP pathway and 1 mole NADPH per isocitrate being converted to OGA (via ICDH). No NADP dependent transhydrogenase activity was detected. The decrease in the integrated PP pathway flux in the growth and production phase lowered the formation of NADPH. It seemed that the PP pathway flux was adjusted according to the reduced requirement for NADPH in the production phase. In the growth phase, the formation of NADPH through the TCA cycle contributed relatively little to the formation of NADPH in the production phase. There was an increase in the relative integrated TCA flux in the production phase, even though the total NADPH requirement for the cell growth and nystatin production dropped. The TCA cycle has been reported to be an important source of generation of NADPH. Roszkowski *et al*. (1971) found ICDH to be the most active NADP-dependent dehydrogenase system in *S. noursei* and *S. erythreus*.

6.8 Enzyme activity studies

An investigation into the variation in the enzyme activity in extracts from shake flask trials of *S. coelicolor* 1147 and *S. fradiae* C373-10 cell samples (see Table 6.36 for enzyme activity ratios & Figure 6.27, G6P branch point, Figure 6.28 PEP branch point), taken over the growth cycle. This was carried out to test whether assumed pathways were active as suggested in the previous sections (6.1 - 6.7). The variation of enzyme activity over the growth cycle of antibiotic producing microorganisms has been investigated extensively (Ahmed *et al*., 1984; Surowitz & Pfister, 1985; Hostalek *et al*., 1969). An important point to note in the analysis of these results is that the experimental values for enzyme activities themselves are meaning less. Such activity levels are dependent upon the particular assay conditions and the sensitivity of particular enzymes to those conditions, as well as upon the inherent stability of the enzyme. Variation in enzyme activity is important, as well as the way in which such variation relates to the growth cycle. Two branch points were considered important to the further investigation of metabolic fluxes in streptomycete cultures: the

G6PDH branch point (hexokinase [HK], G6PDH, & 6PGDH) and the PEP branch point {MDH[dc], PK, PEPCK, PEPC}.

Initial studies with *S. coelicolor* 1147 and *S. fradiae* C373-10 were carried out on HK, 6PGDH, and G6PDH to attempt to determine the ratio of the split between the PP pathway and the EMP pathway and whether it corresponded with that predicted by Figures 6.1 – 6.25 and to identify which isoforms were active through the growth cycle. Using the *S. coelicolor* fermentation as an example (Fig 6.27) there was a significant increase in the activities of NAD-G6PDH, and to a lesser extent, the NADP-G6PDH during the production phase of growth. There were considerable similarities between enzyme activities of *S. coelicolor* 1147 and *S. fradiae* C373-10 cultures, although the NAD-dependent isoforms showed a considerably lower activity in *S. fradiae* cultures (Fig 6.27). There was no significant variation in the 6PGDH activity over the growth cycle. The enzyme activity ratios between HK / G6PDH (additive co-factor activity dependencies NAD- & NADP-) & HK / 6PGDH (additive co-factor activity dependencies NAD- & NADP-) did not correlate to Table 6.36 Part 1 incorporating ratios from Fig 6.1 - 6.25 & Tables 6.35 Part 1 & 2. The G6PDH and 6PGDH ratio would indicate and reinforce the assumption that, in the majority of cases, the PP pathway was not producing enough NADPH, as calculated from the flux diagrams (Figs 6.1 – 6.25) to support biosynthesis. This would correspond with the calculated theoretical NADPH requirement (section 6.7), that actual flux through this pathway was considerably higher. Using the HK : 6PGDH enzyme ratio the results would indicate that the flux through the PP pathway was possibly close to the value for PPP (3) calculated in Table 6.35 Part 1 & 2 (see section 6.7). These results were susceptible to error and open to question for a number of reasons 1) the flux-based analysis was undertaken in bioreactors where as the analysis of enzyme activities was undertaken in shake flasks. From Chapter 4 (Fig 4.1 - 4.20) it can be seen that long lag phases were indicative of the bench top cultures this was not seen at the shake flask level (results not shown). 2) All the latter calculations assume that there was no TH activity present, and all NADPH producing enzymes and consuming pathways were known.

The enzymes around the PEP branch point show particularly interesting variation of PK activity. In *S. coelicolor* 1147 (Fig 6.28a), it rose quickly to a maximum value during the 0.0 – 96 hr period, when the medium glucose concentration was high (see Chapter 4 for

fermentation profiles). Below a certain minimum level of medium glucose concentration (0.8 gl^{-1}; fermentation profiles not included for shake flask experiments), the activity of this enzyme fell quickly. MDH[dc] exhibited high activity while high external glucose concentrations were extant, but activity decreased with falling glucose concentration (probably in response to falling availability of glucose-derived metabolic intermediates). PEPC activity rose steadily throughout the growth cycle, attaining a maximal activity throughout the production phase coincident with the high activities of the relevant PP pathway enzyme activities. Figures 6.28 b (*S. fradiae*, glucose minimal medium), c (*S. fradiae*, glucose glutamate defined medium), d (*S. fradiae*, glucose oxo-glutarate defined medium) show similar enzyme activity around PEP branch point for *S. fradiae*. MDH[dc] activity increases at least two fold when glutamate was added to the *S. fradiae* glucose minimal medium. This may indicate that glutamate may have a stimulatory role on MDH[dc] a major NADPH generating pathway. At 96 hrs into the cultivation the activities of PEPC, PK, & MDH[dc], indicate a considerable proportion of cyclic activity. This could be due to the process being a batch culture. Hypothetically, with the high level of flux through the TCA cycle, it could be assumed that PEPC activity would increase to compensate for this and account for the excretion of metabolites.

The enzyme activity ratios (Table 6.36 Part 1) were on average 1 : 1 for PK/PEPC nearing the end of the culture or at the sampling point. This was not consistent with the flux based diagrams (Figures 6.1 – 6.25)[Table 6.36 Part 2]. It was most likely a consequence of differing isoenzyme activities throughout the growth cycle would invalidate the use of co-factor balancing (Chapter 1; section 1.2.3) in *Streptomyces.* spp. It would be therefore beneficial to complement this work through ^{13}C-labelling strategies in conjunction with atom mapping matrixes (Chapter 1; section 1.2.3 & 1.2.4). This would offer the additional benefit of identifying and quantifying futile cycles. Therefore the split between PK / PEPC was unlikely a true representation of the flux through these two competing pathways. The activity of PEPC has been shown to increase throughout cultivation of *S. coelicolor* (Chapter 2; section 2.5.7)[Bramwell *et al*., 1993] and *S. fradiae* [Kang *et al*., 1987; Kang and Lee, 1987]. In addition, increased activity of PEPC was three fold greater than that during the growth phase. in cultures of *Streptomyces* spp. C5 was only detected during the stationary phase (Dekleva & Strohl, 1988b). The flux diagrams (Figures 6.1 – 6.25) obtained do not show this fact as only the demand of carbon to biosynthesis was accounted for (OGA & OAA additive carbon requirement see Appendix B); and futile cycling of C4 intermediates

(i.e. PEPC > MDH > MDH[dc] >) for example was not taken into account. It may be the case that to understand *Streptomyces* spp. metabolism a finer biochemical resolution of the depicted steps was desirable. Therefore different analytical methods may need to be applied (see section 6.9).

B. subtilis producing riboflavin was investigated using the methodology of biosynthetic directed fractional ^{13}C-labelling (Sauer *et al*., 1997). The metabolic fluxes in the central metabolism, including the PP pathway, the EMP pathway, and the TCA cycle, were estimated, in addition to two futile cycles involving MDH[dc] and PEPCK were identified and quantified. Futile cycles around the PYR branch point have been reported for several organism when ^{13}C-labelled substrates were used (Marx *et al*, 1996; Sauer *et al*., 1997; Schmidt *et al*., 1999; Christiansen *et al*., 2002). Since no net fluxes are associated with futile cycles, the activity of futile cycles cannot be assessed by traditional approaches of metabolite balancing (see Chapter 1)[Holms, 1986, 1996, 1997, 2001; Aiba & Matsuoka, 1979; Vallino, 1991; Stephanopoulos *et al*., 1998]. Christiansen *et al*. (2002) reported that there was a futile cycle with a substantial flux present in PYR metabolism in *B. clausii* the ATP expended in the futile cycle was between 12 – 16 % of the ATP needed for biomass formation and the activity of the futile cycle therefore results in a significant drain in ATP from the CMPs. This may limit the capacity for protein production since ATP lost in the futile cycle cannot be used for protein or biomass production. Jonsbu *et al*. (2001) used ^{13}C – labeling to undertake a flux analysis with *S. noursei* (see Chapter 1, section 1.2.3). The flux distribution pattern obtained in chemostat cultures (material balance) of *P. chrysogenum* showed an anaplerotic pathway flux from PYR to OAA equal to the integrated flux calculated for *S. noursei* (Jonsbu *et al*., 2001). In contrast, the reverse flux (glucogenic) was of the same order as the anaplerotic flux (Christensen & Nielsen, 2000).

It was most likely the case that the latter enzyme activities were a response to the adaptation by streptomycetes to their natural environment of carbon-rich, -nitrogen and phosphate-poor conditions. Obtaining power from the same pathway with the ability to quickly responded to feast and famine conditions (i.e., for PP pathway NADP-G6PDH, NAD-G6PDH, NADP-6PGDH, & NAD-6PGDH and ICDH for the TCA cycle) would be a strong evolutionary response. However, protein engineering indicates that the evolutionary favour of a NADP-

ICDH was probably a result of niche expansion during growth on acetate, where ICDH provides 90 % of the NADPH necessary for biosynthesis (Dean & Golding, 1997).

6.9 Correlation of metabolic flux analysis with tracer studies of other workers

The contribution of each of the two major glucose catabolic pathways (PP pathway and EMP pathways) to carbon flux during batch growth of *S. coelicolor* producing methylenomycin was investigated by Obanye (1994) [Obanye *et al*., 1996] using glucose labeled at the C1 (PP pathway), C6 (TCA cycle), and C3, 4 (EMP pathway) positions. In batch culture, during the growth phase, there was a fall in the C1 - C6 / C3, 4 ratio (i.e., [flux through the PP pathway] / [flux through the EMP pathway]) to a minimum value at the mid-exponential phase. The value of this ratio at its minimum varied from 0.14 to 0.3. After this point, this ratio rose again to achieve a maximum at or around the point at which growth slowed and methylenomycin production was initiated. During this slow growth phase, the PP/EMP ratio remained elevated. The value of the maximum during the latter stages of growth varied from between about 0.6 and 1.74. The calculated PP/EMP ratio for *S. coelicolor* cultured on glucose from Figures 6.1 & 6.2 (taken into account the differences in fluxes for NADPH requirement Table 6.35 part 1 & 2; section 6.9) was 0.05 (PPP (1)), 0.20 (PPP(2)), and 0.40 (PPP(3)) [average data] ratio for *S. fradiae* cultured on glucose from Figures 6.3 & 6.4 was 0.03 (PPP (1)), and 0.20 (PPP(3)) samples taken before the end of the exponential growth phase. This would correlate with the enzyme studies undertaken (section 6.8) that the PP pathway was more active than the flux diagrams would indicate (see section 6.8).

From the latter results, it was assumed that the carbon flux through the PP pathway was less than that passing through the EMP pathway during the exponential growth phase for *S. coelicolor*. Tracer studies undertaken by Obanye (1994)[Obanye *et al*., 1996] indicated when the μ had slowed, and methylenomycin was being produced, relative flux through the PP pathway increased and, in some experiments, exceeded that through the EMP pathway. However, the variation observed between replicate samples suggested that the data only provided a qualitative picture. The specific rates of production of C1 - C6 CO_2 (PP flux) and C6 CO_2 (TCA flux), increased the PP/EMP ratio during the production of methylenomycin appeared to be associated predominantly with a real increase in the PP/EMP flux rather than in the TCA flux. The other important metabolic parameter was

the EMP/TCA ratio, which was also seen to fall during the exponential phase, reaching a minimum value at or around the time that the PP/EMP ratio attained its maximum. The value of the EMP/TCA ratio, at its minimum, varied between 2.12 and 2.97. Thereafter, the ratio rose again during the production phase, attaining a maximum of between 3.64 and 5.62. Thus not only was there a real increase in the specific rate of C1 - C6 CO_2 production, representing a real increase in PP flux, but also there was also increase in the specific rate of C3, 4 CO_2 production (flux through pyruvate dehydrogenase). The highest values of the PP/EMP ratio were found during the periods of slowest growth. However experiments using continuous-flow cultures established that the μ itself was not responsible for the variations in both ratios (Obanye, 1994; Obanye *et al*., 1996). The calculated EMP/TCA ratio for *S. coelicolor* cultured on glucose from Figures 6.1 & 6.2 was 1.57 [average data] and for *S. fradiae* cultured on glucose from Figures 6.3 & 6.4 was 1.64 samples taken before the end of the exponential growth phase.

6.10 The application of flux analysis to an industrial complex medium

In the production of industrially important antibiotics, a complex medium containing various carbon sources, aas, & FAs is normally used, and the metabolic fluxes prevailing with industrial medium therefore are different from metabolic fluxes during growth on minimal medium. Initial attempts were made to quantify and construct compositional tables for *S. fradiae* C373-18 (Table 6.27) whilst growing on the industrial complex medium (Chapter 5, section 5.7). The analytical techniques used to undertake this analysis need further verification. It was also not feasible to use this data any further, due to the complexity of the medium other than to make a comparison. It was never a realistic belief that this would link up with the minimal medium used, but was a prerequisite of the project.

Amino acid uptake, synthesis and regulation in streptomycetes (section 2.7) can only be partly understood by material balancing methods (section 1.2) and the methods employed in this work were of limited use to have any realistic chance of correlating flux through biosynthetic pathways for a step up strategy from minimal medium to a semi-complex medium. It may be more advisable to undertake this analysis with tracer-based studies incorporating atom mapping matrices in conjunction with a material balance (sections 1.2.3 & 1.2.4). Techniques such as applying ^{13}C-labelled substrates to a complex medium

are not straightforward, since uptake of naturally labeled substrates from the medium influences both the metabolite balance and the labeling patterns in the biomass components. Metabolic network analysis for growth on a rich medium therefore requires a precise assessment of aa uptake (Christensen & Nielsen, 1999a, b; Marx *et al*., 1996; Szyperski, 1995). The amounts of the aas taken into account from the medium can be taken into account, using fully labeled substrates, since the uptake of naturally labeled aas from the medium will be reflected in the labeling of the aas in the biomass (Christiansen *et al*., 2002).

Christiansen *et al*. (2002) used the latter method to analyse the metabolic fluxes of *B. clausii* in batch culture with a semi-rich medium containing 15 of the 20 aas and glucose [U-^{13}C] and [1-^{13}C] systematically, while correcting for the aa uptake. It was found that there was no general trend in which aas were synthesised *de novo* with a semi-rich medium. Threonine and serine were completely synthesised from other metabolites and not taken up from the medium. Phenylalanine, leucine, and isoleucine were solely taken up and not synthesised from glucose whereas a group of aas including proline, lysine, glycine, and valine was partly synthesised *de novo* and partly taken up from the medium. The presence of the aas in the medium in batch cultivation elevated the μ from 0.33 to 0.55 h^{-1}, and the flux through the PP pathway decreased from 40 % – 34 % and resulted in an increase in the flux through the TCA cycle from 60 % to 83 %.

The work of Christiansen *et al*. (2002) was the first example of an aa atom mapping matrix. The industrial complex production medium for *S. fradiae* was too complex for this analysis. Therefore it would be desirable to carry out further research for the further construction and optimisation of the defined medium for *S. fradiae* (see Chapters 4 & 8, sections 4.3 & 8.1) or find another streptomycete that fits the experimental parameters. Culturing *S. fradiae* in a semi-complex medium with all 20 aas may lead to a better understanding of the preference of aas. It would be of interest to establish the order of their anabolic and catabolic preference for high metabolic biosynthetic cost aas against low metabolic biosynthetic cost aas and how this affects secondary metabolism. Early aa studies with *S. fradiae* (Metzger *et al*., 1984) reported that glutamate and lysine each stimulated growth, whereas aspartate and tyrosine had an adverse effect on growth. Isoleucine, valine and alanine stimulated tylosin production. In addition, aa interactions were quoted as having affects on tylosin production. The missing piece of information in

the *S. fradiae* fermentation seems to be the role that aa metabolism plays in a complex industrial medium as the majority of research to date has only considered the process as oil-based.

6.11 Summary, future work and directions

Metabolic flux analysis (MFA) was developed by Harry Holms (Holms, 1986, 1996, 1997, 2001) and originally applied to *E. coli* fermentation data. A number of difficulties were met when applying this technique to a streptomycete culture i.e., obtaining consistent calculated data from a flux analysis that fits the experimentally determined CER and closure of the carbon balance/index. From this work it was proposed that this was due to the units of measurement used in the initial calculation. When the units of mmoles.g^{-1} dry wt biomass h^{-1} were used in the construction of flux diagrams, the highest proportion of carbon flux in the streptomycete fermentations was to CO_2 on average 64.07 %. When using the units C.mmoles.g^{-1} dry wt biomass h^{-1} from the outset in the construction of a flux diagram the proportion of carbon flux to CO_2 on average was 39.31 %.

However experimental data was further required to verify which of the latter calculated CERs were accurate for the latter *Streptomyces* cultures. It was therefore not possible from this work to verify which of the models from this Chapter was correct. It was assumed that all the cultures had a low μ and were carbon limited for *S. coelicolor* 1147 and nitrogen limited *S. fradiae* C373-10. Carbon dioxide evolution in relation of carbon source input, it would be expected that the efficiency of CER would follow the same trend (nitrogen > carbon > etc.). Therefore it was conceivable that CER was high for carbon limitation and low for nitrogen limitation. It was therefore not possible from this work to verify which of the models from this Chapter was correct. The measurements made during this fermentation project support the diagrams designed and constructed with units of C.mmoles.g^{-1} dry wt h^{-1} to the best of are knowledge. This was only an assumption at best as further on-line gas analysis was needed to support the flux analysis.

This opens up the question, why when using the units of C.mmoles.g^{-1} dry wt h^{-1} was there a large proportion of the carbon unaccounted for? This was possiblely due to the high level of flux through glycolysis and the TCA cycle that using the units of mmoles.g^{-1}dry wt

distorted the results. The most probable site of this distortion was at aldolase. This distortion was not observed with the glutamate and oxo-glutarate flux diagrams where aldolase was calculated in reverse direction from biosynthesis and not directly from the carbon source input as the glucose, fructose and glycerol flux diagrams. The considerably high unaccountable carbon found when the units of C.mmoles.g^{-1} dry wt h^{-1} was used. Was probably a contributory factor that further increased this distortion (20 – 30 % on average).

The theoretical NADPH requirement for cell growth calculated from the flux diagrams and converted to theoretical fluxes. Showed for the glucose, fructose & glycerol fermentations the maximum production of NADPH when the NADP-ICDH was operational (with no alteration to the PP pathway flux) was higher than the theoretical NADPH capacity (calculated from the biomass composition). This could indicate that the NADP-ICDH in these cultures was not operational, a TH was active or that there were other expensive NADPH-consuming enzyme/enzymes operational. When glutamate was added to the glucose minimal medium, there was a considerable increase in the theoretical NADPH requirement therefore, glutamate could possibly have a stimulatory role on a NADPH producing pathway. The increased NADPH requirement is mainly due to an increase in the FA content of the cell. It was then likely that the constructed flux diagrams were not likely to account for the true carbon flux but the net flux to biosynthesis.

Further enzyme assays were undertaken to test whether assumed pathways were active as suggested by the flux diagrams. The enzyme activity ratios between HK / G6PDH & HK / 6PGDH did not correlate to the flux diagrams. The G6PDH and 6PGDH ratio would indicate and reinforce the assumption that, in the majority of cases, the PP pathway was not producing enough NADPH, as calculated from the flux diagrams to support biosynthesis. This would correspond with the calculated theoretical NADPH requirement, that actual flux through this pathway was considerably higher than calculated for. It was most likely that differing isoenzyme activities throughout the growth cycle would invalidate the use of co-factor balancing in *Streptomyces.* spp. It was then likely the case that the constructed flux diagrams using the Holms (Holms, 1986) strategy in Chapter 6 were not likely to account for the true carbon flux but the net flux to biosynthesis. It would be therefore beneficial to complement this work through ^{13}C-labelling strategies in conjunction with atom mapping matrixes. This would offer the additional benefit of

identifying and quantifying futile cycles.

The flux diagrams would indicate that the fluxes through most of the central metabolic enzymes were decreased during secondary metabolism but there was an increase through PEPC at least by two-fold. The enzyme activity ratios were on average 1 : 1 for PK/PEPC. This was not consistent with the flux based diagrams. Therefore the split between PK / PEPC was unlikely a true representation of the flux through these two competing pathways. The flux diagrams only account for the anaplerotic flux and do not account for futile cycling. Since no net fluxes are associated with futile cycles, the activity cannot be assessed by material flux-based strategies.

The main aim of this thesis was to test whether Holms (1986) approach to flux analysis could be successfully applied to a streptomycete fermentation. Unfortunately the approach has many limitations, although this study should be considered as a preliminary investigation bringing information together. It would be of benefit to assess further this approach with a continuous culture strategy which would increase the reliability of the compositional data, reduce the multi-phasic nature of the culture and increase the ability to reliably predict the isoenzymatic nature of the culture.

Variation of the Glucose-6-phosphate dehydrogenase branch point enzyme levels (mU/mg) during batch culture.

S. coelicolor grown on glucose

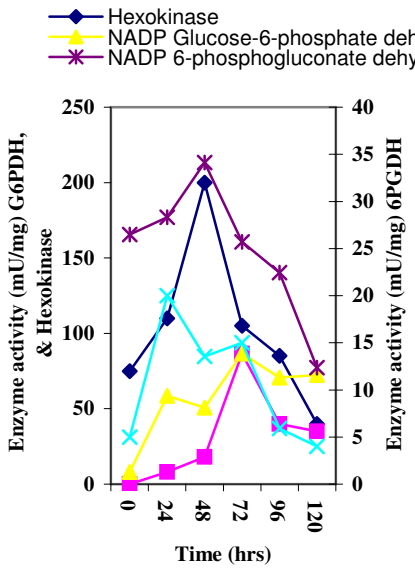

S. fradiae grown on glucose

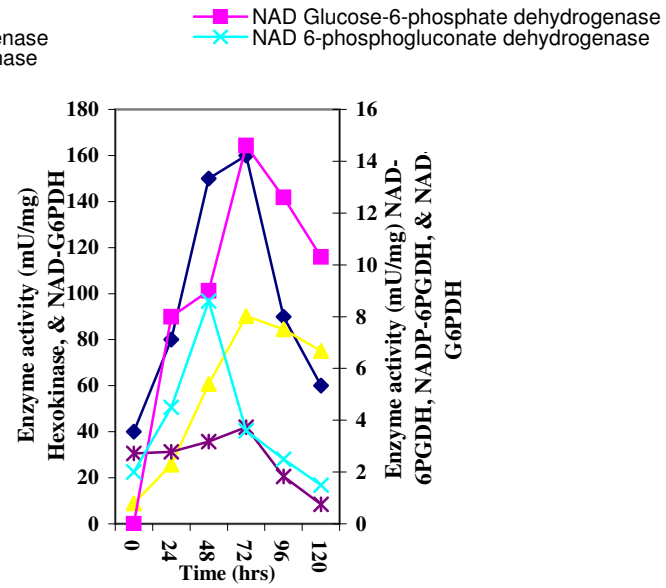

S. fradiae grown on glucose glutamate

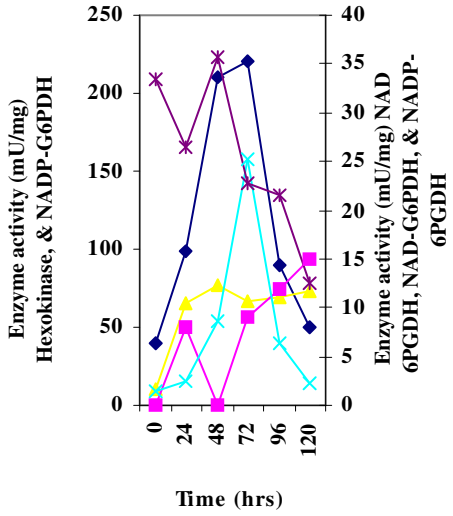

S. fradiae grown glucose oxo-glutarate

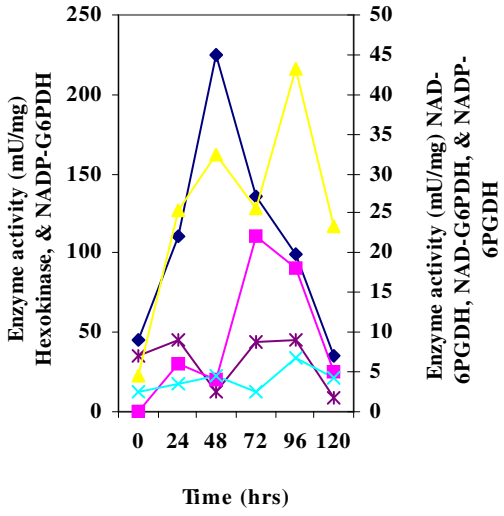

Fig 6.27 Each curve represents the combination of points from three independent shake flask experiments and plotted against time (hrs). *S. fradiae* C373-10 and *S. coelicolor* 1147 were cultured on a number of different medium compositions *S. fradiae* C373-10 was cultured on glucose minimal medium, glucose glutamate, glucose oxo-glutarate defined media (Chapter 3, section 3.6.4), *S. coelicolor* 1147 was cultured on a glucose minimal medium (Chapter 3, section 3.6.1).Each curve was drawn with a line connector function. HK assay (Chapter 3, section 3.13.1); NAD-glucose-6-phosphate dehydrogenase (Chapter 3, section 3.13.2); NADP-glucose-6-phosphate dehydrogenase (Chapter 3, section 3.13.2); NAD-6-phosphogluconate dehydrogenase (Chapter 3, section 3.13.2); NADP-6-phosphogluconate dehydrogenase (Chapter 3, section 3.13.2).

Variation of the phosphoenolpyruvate branch point enzyme levels (mU/mg) during batch culture of *S. coelicolor* 1147 & *S. fradiae* C373-10 under number of different carbon sources.

S. coelicolor grown on glucose

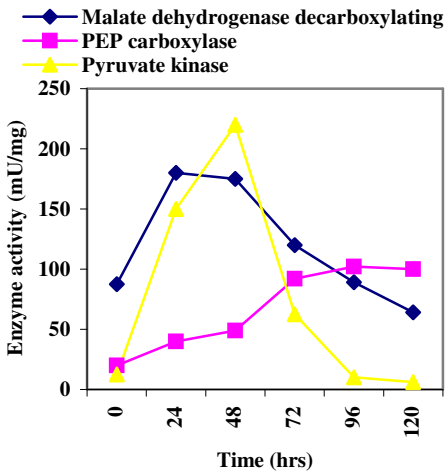

S. fradiae grown on glucose

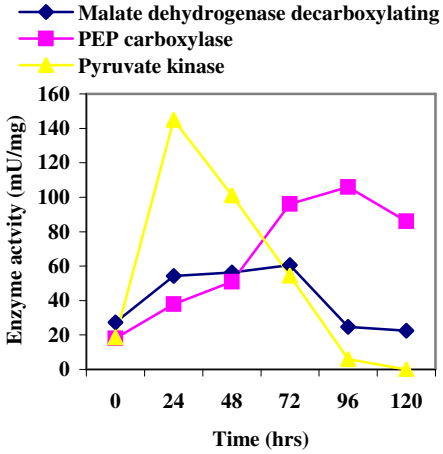

S. fradiae grown on glucose glutamate

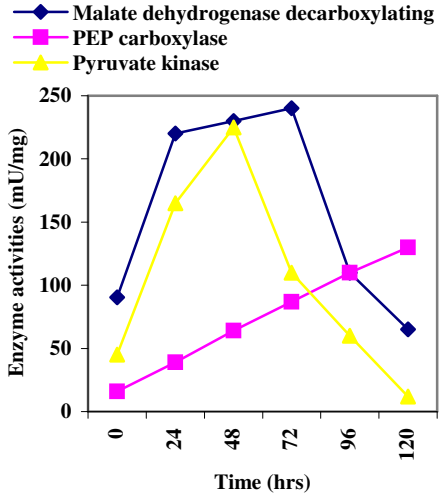

S. fradiae grown glucose oxo-glutarate

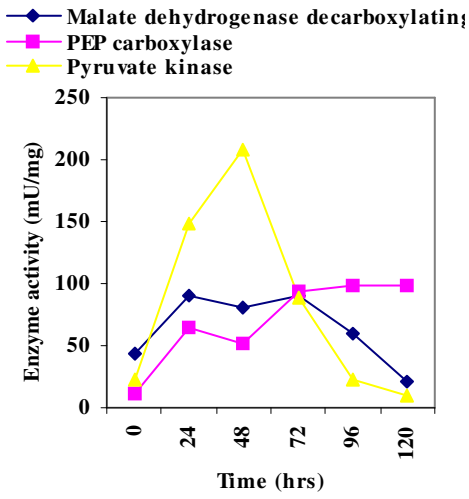

Fig 6.28 Each curve represents the combination of points from three independent shake flask experiments and plotted against time (hr). *S. fradiae* C373-10 and *S. coelicolor* 1147 were cultured on a number of different medium compositions *S. fradiae* C373-10 was cultured on glucose minimal medium, glucose glutamate, glucose oxo-glutarate defined media (Chapter 3, section 3.6.4), *S. coelicolor* 1147 was cultured on a glucose minimal medium (Chapter 3, section 3.6.1). Each curve was drawn with a line connector function. PEP carboxylase assay (Chapter 3, section 3.13.3); MDH(dc) assay (Chapter 3, section 3.13.4); PK(Chapter 3, section 3.13.4).

Chapter 7

Matrix algebra & sensitivity issues: Formulation of the bioreaction network

7.0 Introduction

The construction of a metabolic flux analysis (MFA) model is in principle a straightforward task, (Holms, 1986, 1996, 1997, 2001) requiring knowledge only of the stoichiometric relationships of the biochemical network and the biochemical demands on this network. Application of mathematical structure to the model can be a difficult task. Ensuring consistency within the chosen set of balanced equations and calculability of the chosen rates is not always so straightforward, as illustrated by a number of authors (Noorman *et al*., 1991; 1996; Van der Heijden *et al*., 1994a, b; Bonarius *et al*., 1997). To undertake a flux-based strategy, after undertaking an extensive literature search and classification of the desired stoichiometry (see Chapter 2), the normal route of action is usually to proceed with a flux analysis of the experimental data. However, the BRNE skeleton and the stoichiometric relationships it self can also provide considerable information, of course no quantitative data can be obtained, but a number of sensitivity issues can be addressed.

The main aim of this Chapter was to apply matrix algebra flux analytical techniques exemplified by Stephanopolous & Vallino (1990)[Chapter 1, section 1.2] to the fermentation experiments described in Chapter 4 (Fig 4.1 – 4.20) and the compositional data collected in Chapter 5. This would allow comparison of Holms (1986) flux-based strategy with matrix algebra approaches, and test which method was better suited to the study of streptomycete metabolism. The lack of detailed on-line gas analysis limited the number, type, and quality of the flux models that could be constructed. Two stoichiometric models 1 & 2 (Appendices L & M, respectively) were constructed for the central metabolic pathways (CMPs) of *S. fradiae* C373-10 for this work. Model 1 was constructed to simulate a strategy of flux estimation similar to the approach used in Chapter 6 (Holms, 1986) using matrix algebra. Model 2 was constructed using a standard matrix algebra approach readily accepted in the literature.

The matrix algebra approach (Stephanopolous & Vallino, 1991) requires that a bioreaction network (BRNE) be constructed. Model 2 was based on the stoichiometric bioreaction

networks proposed by Daae & Ison (1999; for *S. lividans*)[Appendix J], Kirk *et al*. (2000; for *S. clavuligerus*)[Appendix I], and Avignone Rossa *et al*. (2002; for *S. lividans*)[Appendix K]. Only metabolites at branch points in the CMPs were included. For example the entire EMP pathway contains 9 enzymatic steps between glucose-6-phosphate and pyruvate. These steps were combined into only seven fluxes in both BRNEs (Flux no 2 - 8; see Appendix L & M, models 1 & 2) this could be further reduced as glyceraldehyde-3-phosphate, 3-phosphoglycerate and phosphoenolpyruvate only appear at branch points in the BRNE. Further reduction of the BRNE was not undertaken, this left open the possibility of the incorporating other secondary metabolites into a universal model for streptomycetes [All fermentation numbers relate to the same cultures throughout Chapter 4, 5, 6 & 7; *S. fradiae* C373-10 cultures for glucose (Ferm 1 & 2); fructose (Ferm 1); glycerol (Ferm 1 & 2); oxo-glutarate (Ferm 1); glucose glutamate (Ferm 1 - 4); glucose oxo-glutarate (Ferm 1 & 2); methyl oleate medium (Ferm 1 - 3); Industrial complex (Ferm 1 & 2); *S. coelicolor* cultures for glucose (Ferm 1 & 2)].

7.1 Matrix algebra and flux analysis previous work

Although MFA incorporating matrix algebra has been applied to an extensive number of genera (Chapter 1, section 1.2.9), thus far there have been only a few reports applying matrix algebra techniques to *Streptomyces* spp. Daae & Ison (1999) presented a theoretical sensitivity assessment of a biochemical network for *S. lividans*, analysing how the estimation of intracellular fluxes were affected by perturbations in the measured fluxes. Their analysis showed that changes of up to 20 % in the level of biomass precursors did not affect the estimation of intracellular fluxes significantly and that the specific growth rate (μ) and oxygen consumption had the greatest impact on the flux calculations. Employing experimental data from the literature (taken from Melzoch *et al*., 1997), Naeimpoor and Mavituna (2000) applied MFA to cultures of *S. coelicolor* under a number of different nutrient limitations. There was no description of the biochemical network developed and several stoichiometric and assumed experimental constraints were used to solve the underdetermined system obtained. Using this approach, nitrogen limitation appeared to give the highest specific production rate of the antibiotic actinorhodin (ACT) and the lowest maintenance energy, although it was accompanied by the highest specific production rate of other excretory metabolites. Avignone-Rossa *et al*. (2002) applied MFA to a stoichiometric model for *S. lividans*. The relationships between antibiotic production, biomass accumulation, and carbon flux through the major carbon

metabolic pathways were analysed. Distribution of carbon flux through the catabolic pathways was shown to be dependent on growth rate, as well as on the carbon and energy source (glucose or gluconate) used. Increasing growth rates promoted an increase in the flux of carbon through glycolysis and the PP pathway. The synthesis of both ACT and the antibiotic undecylprodigisin (RED) were found to be inversely related to flux through the pentose phosphate pathway (PP pathway).

7.2 Suggestions and assumptions for the construction of a bioreaction network

Without relying on two many ambiguous assumptions, the construction of a BRNE from our present knowledge of streptomycete metabolism was feasible (see Chapter 2). Incorporated unsolvable reaction sequences within the BRNE are commonly known as singularities (e.g., futile cycling). A number of decisions were taken to remove singularities from the constructed BRNE.

(1) One of two pathways at a branch point can sometimes be removed by examining the kinetics of the branch enzymes. If the lead enzyme of a branch has a poor affinity for the branch metabolite, or exhibit similar activities, then it may be acceptable to delete the branch from the network (e.g., glutamate dehydrogenase, glutamate synthase, and glutamine synthetase). Likewise, if two competing branches exhibit similar activities and metabolite affinities, then it may be acceptable to apply mathematical constraints to set a percentage branch point split (i.e., setting a percentage branch point split) i.e., the PP pathway against glycolysis (Vallino & Stephanopoulos, 1990). For example Vallino and Stephanopoulos (1990) used radiolabeling experiments to calculate the percentage of glucose entering the PP pathway from the flux estimate, and assumed partial recycling of fructose-6-phosphate (F6P). This assumes that the fraction of F6P that is recycled back into the PP pathway is the same as the fraction of glucose that enters the PP pathway. An example of the calculation that can be interchanged to account for the proportion of glucose entering the PP pathway and EMP, based on partial recycling, is given by (brackets [ ] represent the flux in each reaction)

$$\text{PP pathway } (\%) = \frac{100\,[(\text{Glc} + \text{ATP} \rightarrow \text{G6P} + \text{ADP}) - (\text{G6P} \leftrightarrow \text{F6P})]}{[(\text{Glc} + \text{ATP} \rightarrow \text{G6P} + \text{ADP}) + (\text{S7P} + \text{GAP} \leftrightarrow \text{F6P} + \text{E4P}) + (\text{X5P} + \text{E4P} \leftrightarrow \text{F6P} + \text{GAP})]}$$

Models 1 & 2 both calculate the branch point split between the EMP & PP pathway and the EMP and the TCA cycle through co-factor balancing (as Chapter 1, section 1.2.3). The NAD- and NADP-dependencies for the enzymes G6PDH, 6PGDH, & ICDH were set to the co-factor dependencies stated (see Chapter 6, section 6.7). This was considered a best-fit assumption for the multi-phasic nature of batch cultures.

(2) The network would be unsolvable if the glyoxylate bypass (GBP) and TCA cycle were both operational. The reality was probably that whilst one was operational the other could be semi operational. Accepting a major flux pathway over another has been reported by other workers to have little impact on the overall flux analysis (Vallino & Stephanopolous, 1990).

(3) The presence of a nucleotide transhydrogenase [TH](Kirk *et al*., 2000; reaction 46, Appendix I), renders NADH and NADPH indistinguishable from the stand point of metabolite balances if other NADPH producing pathways are present (i.e., G6PDH, 6PGDH, ICDH, and MDH[dc]). Little evidence has been presented in the literature that a TH is active in streptomycete metabolism (see Chapter 2, section 2.5.6). Therefore this reaction sequence was not included in models 1 & 2 (Appendices L & M).

(4) If necessary the Entner-Doudoroff pathway can be incorporated by deleting G6P isomerase. This pathway is not believed to be active in streptomycetes (see Chapter 2, section 2.5.3).

(5) The carboxylase-decarboxylase reactions between PEP or PYR and OAA or MAL can usually be considered as one reaction with minimal alteration in network flux (Vallino & Stephanopolous, 1990)[reaction 24 & 27, model 1 & 2 Appendices L & M respectively]{see Chapter 2, section 2.5.7 – 2.5.10}.

(6) If the reactions of a pathway depend on flux directionality (i.e., glycolysis versus gluconeogensis), then the appropriate reactions can be set as reversible with the direction in the BRNE depending on the appropriate flux parameters.

(7) Alternative pathways can be incorporated in to BRNE (see Appendix L & M for the reactions that could be removed or added to build alternative BRNE e.g., for carbon sources: glucose (BRNE), glycerol (A), and fructose (B)[Appendix L], products: ACT (A), and undecylprodigiosin (A)[Appendix N], nitrogen sources: nitrate (B), glutamate (C), NH_4 (D), and oxo-glutarate (E)[Appendix N].

All calculations for this work were carried out through the use of Bionet (Vallino, 1991) and Fluxmap V1.0 programs which has been used by other workers in the field. Bionet was found difficult to use and would not accept a number of reactions, which limited its capabilities. Fluxmap was more user friendly, incorporating diagrammatic conversion tools. However when BRNE described previously by others were entered into this program, it gave greater condition numbers (CN)[for discussion of the concept and theory be find conditional analysis see Appendix N) than had already determined (personal results, not shown). This was considered a consequence of a number of workers using different units of measurement. When the units used were C.moles instead of moles, this greatly reduced the CN (personal communication, Avignone-Rosso). This would fit with results obtained for Chapter 6 where the units of C.mmoles.g dry wt biomass h^{-1} were considered to give the best-fit flux estimation to the experimental results (Chapter 6, section 6.6.3).

7.2.1 Construction of a bioreaction network for *Streptomyces fradiae* C373-10

The BRNE for model 1 was constructed for cultures of *S. fradiae* C373-10 grown on glucose (Chapter 4, Fig 4.1 & 4.2), glycerol (Chapter 4, Fig 4.4 & 4.5) and fructose (Chapter 4, Fig 4.3) as the sole carbon sources, and with NH_3 as nitrogen source (see Appendix L). The BRNE for model 2 was constructed for cultures of *S. fradiae* C373-10 cultured with glycerol and NH_3 as the carbon and nitrogen source respectively (the lack of gas analysis led to model 2 only being used for one glycerol fermentation (Chapter 4, Fig 4.5, Ferm 2)[Appendix M].

The stoichiometric matrices (models 1 & 2) were constructed as follows. Glycolysis, the TCA, and PP pathway were constructed, from literature based research (see Chapter 2) and three stoichiometric matrices already constructed (Kirk *et al*., 2000, Appendix I; Daae & Ison, 1999, Appendix J; Appendix K, Avignone Rossa *et al*., 2002). The reaction of glycolysis were considered to be reversible where appropriate, to facilitate the change of parameters for other carbon and nitrogen sources (see Appendices L & M). The GBP was not added to the model, as an unsolvable reaction arises if the GBP and the TCA cycle were operational at the same time (see Chapter 1). However, the GBP will be active only during growth on either acetate or lipids. Because glucose, fructose, and glycerol were used as the carbon source throughout this part of the study, the GBP was not included in any of the stoichiometric matrices (see Appendices L & M). The aa and nucleic acid biosynthesis pathways were constructed from standard biochemistry texts (see Chapter 2) and Hodgson (2000), where appropriate Zubay (1998),

Michal (1999) were used to fill in the gaps. Biochemistry texts indicate only small differences in aa metabolism between streptomycetes and other bacteria (Hodgson, 2000)[see Chapter 2, section 2.7].

A number of enzymes are associated with NH_3 assimilation in *Streptomyces* (see Chapter 2, section 2.9): glutamate dehydrogenase (GDH), glutamine synthetase (GS), and glutamate synthase (GOGAT). If all these enzymes were included in the stoichiometric model (see Appendices L & M), unsolvable pathways would arise. However GOGAT has been reported to only be active during nitrogen starvation (see Chapter 2, section 2.9). Since the batch cultivation initially has a high NH_3 concentration, this reaction was not included. *Streptomyces* have two glutamate dehyogenases: an NADH-dependent dehydrogenase as well as an NADPH-dependent dehydrogenase (Chapter 2, section 2.9). The NADPH-dependent GDH was reported to be involved in the anabolism whereas NADH-dependent dehydrogenase was reported to be involved in catabolic metabolism. The activity of the NADH-specific dehydrogenase has been found to be low compared with the NADPH-specific GDH (see Chapter 2, section 2.9). Therefore the NADPH-dependent glutamate dehydogenase was used in the construction of the BRNE (see Appendices L & M)[see Chapter 8 for further discussion].

The addition of nitrogen metabolism and uptake reactions to the stoichiometric models 2 (see Appendices M) opens up a number of good discussion points. It would be easier to carry out flux analysis in continuous culture, where the prediction and behaviour of the organism would make the construction of the BRNE an easier undertaking. The opposite was true for batch culture where the nature of the system was multi-phasic. For example, in batch culture GDH would be active in the early stages of the fermentation when NH_4 concentration was high and GOGAT would be active in the later stages (see Chapter 2, section 2.9) of the fermentation when NH_3 concentrations were low. Therefore a steady-state cannot be met realistically in batch culture, and the multi-phasic nature of a batch culture has to be a major concern in achieving any accurate flux estimation.

The presence of the enzyme nicotinamide TH, which catalyses the reversible transfer of reduction equivalents from NADPH to NADH (see Chapter 2, section 2.5.5), was crucial to solve a matrix algebra MFA model, since a unsolvable reaction arises if this reaction was included in the stoichiometric models (see Appendices L & M). Its physiological role is not

completely understood as yet, but it could act as a protective buffer against the dissipation of either the cellular redox power or the energy supply, and therefore it was considered not likely to play an important role in the overall cellular metabolism under normal growth conditions (see Chapter 2, section 2.5.5). A TH was added to the network of Kirk *et al*. (2000) because the PP pathway was not believed to be active (see Appendix I) in *S. clavuligerus*. The only data for existence of a TH activity in *Streptomyces,* appears to be from Ragland *et al*. (1966). *S. coelicolor* was found to have no TH activity when grown on a glucose minimal medium, but low TH activity, when grown on a citrate minimal medium. A putative TH has been identified in the *S. coelicolor* genome sequence, ORFs SCO7623 & SCO7622, are 58.4 % & 68.8 % identical to *E. coli*. This sequence also contains a possible hydrophobic membrane spanning regions as would be expected (see Chapter 2, section 2.5.8). In *E. coli* an energy-dependent transhydrogenase is formed only during growth with glucose in minimal medium (Stouthamer, 1973) and is repressed by the presence of aas. A mixture of 2 aas gives partial, and a mixture of 4 aas complete repression. Therefore an assumption was made, where the TH reaction was considered not to be operational and was not incorporated into the stoichiometric models (see models 1 & 2; Appendices L & M). Therefore a TH reaction sequence can only be incorporated if more evidence of its activity becomes available.

Ragland *et al*. (1966) undertook studies on a number of bacterial hydrogenases. A number of organisms were reported to have NADP-G6PDH, NAD-G6PDH, NADP-6PGDH, and NAD-6PGDH dependent activities (the role of the NADP- and NAD- dependency has not as yet been linked to dual factor specificity or the existence of isoenzymes). There is also no evidence that organisms that lack TH activity have dehydrogenase dual co-factor specificity or organisms that have TH activity favour NADP dehydrogenase dependency (Ragland *et al*., 1966). It was concluded that this could be a further way of regulating reducing power and energy production, or an adapted response to feast or famine conditions that *Streptomyces* have adapted to, due to oligotrophic conditions in their natural environment. The enzyme studies undertaken in Chapter 6 (section 6.8) corroborate with the studies with *S. coelicolor* undertaken by Obanye (1994; Obanye *et al*., 1996) indicated that NADP-dependent G6PDH was favoured during the growth phase of *S. coelicolor*. Increase in activity of NAD-dependent G6PDH was observed during the production phase. There were no significant variations in the NAD- or NADP- dependent 6PGDH activities over the growth cycle.

Dual enzyme specificity also opens up additional problems in solving any matrix algebra flux analysis. Daae & Ison (1999) took account of the difference in the dual co-enzyme specifically or isoenzymes (ISEs) for G6PDH and 6PGDH (NAD and NADP-dependent)[see Chapter 2, section 2.5.4], by assigning G6PDH as NADPH-dependent and 6PGDH as NAD-dependent. Their literature search indicated that this was an acceptable assumption. Enzyme studies undertaken in Chapter 6 (section 5.8) indicate that this may not be an acceptable assumption for *S. coelicolor* 1147 as the NADPH and NADH dependent activities change throughout the fermentation. *S. fradiae* C373-10 showed similar results (Chapter 6, section 6.8), although the NAD-dependent enzyme activity was not active to the same extent as in *S. coelicolor* 1147. Only the NADPH-dependent reactions were added to the stoichiometric matrix (Appendices L & M) at this time.

The introduction of the ATP/NADPH balance could be misleading, from the present literature research (see Chapter 2). This work must then be viewed with care, but it does offer a basis on which to build better models. There is a lack of detailed kinetic studies on TH activity and the number of ISEs present within streptomycete metabolism. Any future detailed flux-based analysis for a streptomycete would need to quantify accurately the flux through the PP pathway and remove the distortion of other pathways i.e., GC-MS incorporating atom mapping matrices (see Chapter 1, section 1.2.3) or the analysis should be undertaken in continuous culture to avoid the multi-phasic nature of batch culture.

Enzyme studies were also initiated to determine if *S. coelicolor* 1147 and *S. fradiae* C373-10 contained the enzymes PEPCK, MDH[dc] enzyme and PEPC and which pathway was active through the growth phase under different carbon sources (Chapter 6, section 5.8). Chapter 6 clearly indicates growth on glucose, fructose, and glycerol. MDH[dc] and PEPC were both active, with PEPC carrying the majority of the flux. Although PEPCK activity was not detected it may have been the case that the inappropriate assay procedure was undertaken. Project time constraints led to the inability of further assessment of other assays for PEPCK. When *S. fradiae* was grown on a glucose glutamate defined medium a similar trend was seen, with an increase in the MDH[dc] activity. With the glucose oxo-glutarate defined medium, there was an overall lower PEPC activity (Chapter 6, section 6.8). It was difficult to determine the relative contributions of MDH[dc] enzyme and PEPC but the MDH[dc] was active in the early phases of the fermentation and reduced as the fermentation progressed. It was feasible that at some

points of the fermentation futile cycling around the PYR and PEP branch points accounted for a considerable proportion of the flux (Chapter 6). To allow for this anaplerotic reactions PEPCK and PEPC were calculated as one reversible reaction, although the largest proportion of the flux would flow towards OAA (see Appendices L & M). The MDH[dc] reaction sequence was not added to the BRNE (see Appendices L & M) as the flow of carbon could not be assessed by the flux methods used during this work (Holms, 1986; Vallino & Stephanopolous, 1990)[see Chapter 1, 6, & 8 for a further discussion of the current methods that could be undertaken to determine the contribution of futile cycling to a metabolic network].

For model 1 the biosynthesis of the nucleotides (fluxes 16 - 17) and macromolecules, amino acids [aas](fluxes 25 – 45) and the ATP requirement of polymerisation was included [the energy requirements to polymerise 1 g of biomass were calculated as Ingraham, *et al*., 1983]: (1) Lipids (flux 50), (2) RNA/DNA (flux 49), protein (flux 51), and carbohydrates (flux 52). To account for maintenance and futile cycles, a reaction sequence was also included to dissipate excess ATP (flux 48). For model 2 the biosynthesis of the nucleotides (fluxes 48 - 51), aas (fluxes 28 – 47) was incorporated. The macromolecular, precursor, ATP and NADPH requirements of polymerisation were incorporated into one stoichiometric reaction sequence for the formation of biomass (flux 56)[the energy requirements to polymerise 1 g of biomass was calculated as Daae and Ison, 1999] and also incorporated the biosynthetic pathway to tylactone synthesis (constructed sequence adapted from Chapter 2, Tables 2.24, 2.25, and 2.26). To account for maintenance and futile cycles, a reaction was also included to dissipate excess ATP (flux 55).

Reactions 46 & 47 (model 1; Appendix L) and reactions 53 & 54 (model 2; Appendix M) represent the oxidative phosphorylation reactions of the cell. For eukaryotes, the theoretical stoichiometry of oxidative phosphorylation (the P/O ratio) is 3 moles of ATP synthesised for each mole of NADH oxidised or 2 moles of ATP synthesised for each mole of succinate (or FADH) oxidised. For prokaryotes, protons are transported at only two locations (two protons at each location) against 3 locations for eukaryotes, and because the stoichiometry of the prokaryotic F_1F_0-ATPase (or ATP synthase) is 1 ATP / $2H^+$, the theoretical stoichiometry of oxidative phosphorylation yields 2 moles of ATP synthesised for each mole of NADH oxidised. Therefore a P/O ratio of 2 was assumed (as seen in Appendices I - M). Hence, the number of ATP molecules produced per molecule of NADH was assumed to be 2. It was further assumed

that compared to NADH, FADH produced 2/3 the amount of ATP or set to 1 FADH converted to 1 ATP (see Appendcies I - M). The above assumptions are all fairly standard relationships in a number of eubacteria (Stephanopoulos *et al*., 1998). The P/O ratio value for *B. subtilis* was reported as 1.3 (Goel *et al*., 1993).

The stoichiometric model 1 (see Appendix L) constructed for glucose as sole carbon source consists of 64 intracellular metabolites and 56 reactions, the degree of freedom is 8 (the minimum number of metabolites that have to be measured), with a CN of 97.56; which can be considered a well conditioned system, where the flux estimation should be acceptable (see Table 7.1 for parameters of other stoichiometric matrixes; All Tables can be found in the companion CD; Appendix O Chapter 7). The stoichiometric model 2 (Appendix M) constructed for glycerol as sole carbon source consists of 73 intracellular metabolites and 62 reactions the degree of freedom of 11 (the minimum number of metabolites that have to be measured), with a CN of 167.73 (see Appendix N for theory); which can be considered a well conditioned system, in which the flux estimation should be acceptable (see Table 7.1 for parameters of other stoichiometric parameters when the carbon source and NADPH balance were altered for models 1 & 2).

7.3 Calculated flux sensitivities with respect to changes in measured fluxes

The sensitivities of the calculated fluxes to changes in the measured fluxes were determined using the equations in Appendix N (calculated with use of Fluxmap computer software) for matrix algebra model 1 (Table 7.2). Although sensitivities were reported as positive and negative values this was ignored (as Daae and Ison, 1999). The sensitivities were analysed for all measured metabolites (for method 1, CO_2 and O_2 was also included; although they were measured variables). Further analysis of other metabolites and reaction sequences was cumbersome with the Fluxmap package, as it does not allow conversion of the data to other computer packages such as Microsoft Excel. The two or three highest sensitivities are highlighted in bold for each measured flux and the total sensitivity was presented as an accumulated absolute value of all the sensitivities. The sensitivities presented in Table 7.2 were calculated on the basis that only the specified measured flux changes and that all the other measured fluxes stay the same. The perturbation was therefore required to be very small, as in a real system, large variations in, for example, carbon uptake rates, would clearly affect the specific growth rate, etc. Hence, the sensitivity analysis will not give the answer as

to which new "steady-state" or metabolic pattern the system will adapt to after a significant disturbance, but will examine the initial dynamics of the system response. It was clear from the work of Daae and Ison (1999) that changes in the μ had the greatest impact on the calculated fluxes with an accumulated sensitivity (Table 7.3; taken from Daae & Ison, 1999) of 46.09 for glucose as sole carbon source matrix (for matrix see Appendix J). Changes in the oxygen utilisation rate and oxo-glutarate (OGA) secretion rate only had one third of the effect on the system but were the next most influential measurements. The least important measurement was surprisingly the CO_2 evolution rate, at an accumulated sensitivity of 6.33. The relatively high accumulated sensitivity calculated for the μ, was not entirely unexpected. In the stoichiometric matrix, this reaction affects the highest number of intermediates. These intermediates, however, were mostly metabolic monomer building blocks and not metabolic precursors. Nevertheless, the greater part of the accumulated sensitivity was due to the CMPs and not pathways involved in synthesis of monomers for biomass. This was also true for the sensitivities of the other measured fluxes. The μ, and changes in the μ, of fermentations of *S. lividans* were usually an order of magnitude lower than for the other measured reaction fluxes. Hence reducing the μ sensitivities results, in reduced accumulated sensitivities. Daae & Ison (1999) reported that reducing the μ sensitivities by an order of magnitude results in considerably lower accumulated sensitivities, and oxygen utilisation rate becomes the next predominating parameter. This may not be entirely unexpected as oxygen utilisation is closely related to energy production, which again is related to the majority of the metabolic reactions.

Table 7.4 shows the results from a similar sensitivity analysis for the constructed stoichiometric models 1 & 2 (see Appendix L & M) with alterations to the matrix. Model 1 showed poor reproducibility to the sensitivity to accumulated error between matrices using different carbon sources, to the sensitivity analysis undertaken by Daae and Ison (1999) [although μ was not a variable in the sensitivity analysis undertaken]. Model 2 shows good reproducibility, to the sensitivity analysis undertaken by Daae and Ison (1999). Oxygen uptake showed the highest sensitivity to the accumulation of error in the matrix and nitrogen the next highest. The contribution of CO_2 was not significantly high, this was not surprising as CO_2 was taken up and released from a number of pathways, so from a material balance point of view the effects would cancel. This would result in no significant effect on

understanding flux partitioning, unless a finer tuned analysis was undertaken i.e., GC-MS ^{13}C labeling (see Chapter 1). The Fluxmap program did not allow further assessment of the influence of specific growth on accumulated error towards flux estimates using stoichiometric models 1 & 2. The low calculated CNs for stoichiometric models 1 & 2 (Table 7.1) indicate a well-defined matrix that could be used for flux-based analysis. It was therefore considered that the data analysis protocol previously described by Daae and Ison (1999) was good system to test further the acceptability of the stoichiometric matrices and the flux estimates obtained. Further comparison with other algebraic flux programs would also have been desirable.

7.3.1 Estimated fluxes through the CMPs of *S. fradiae* C373-10 using matrix algebra models 1 & 2

The flux analysis for model 1 (carried out for glucose [Ferm 1 & 2]{Fig 7.1 - 7.2}, fructose [Ferm 1]{Fig 7.3}, glycerol [Ferm 1 & 2]{Fig 7.4 - 7.5}) & model 2 (glycerol [Ferm 2]{Fig 7.6}) data obtained for measurements from Chapters 4 & 5 respectively (compositional data for model 1 was corrected to the compositional data obtained from Chapter 5 for *S. fradiae* C373-10; compositional data for model 2 was taken from average *E. coli* data which was used to fit with other workers [see Chapter 1, section 1.2.6).

Unexpectedly all the constructed models and previous workings for model 1 (results for workings not shown) indicate negative values around the TCA cycle (Fig 7.1 – 7.5). This would indicate that the cycle was running in the reverse direction or the metabolic costs of co-factor supply could not be met by the bioreaction network as presented. It is not impossible for the TCA cycle to operate in the reverse direction, but most of the TCA cycle reactions are favoured thermodynamically in the forward direction. For example the ΔG^0 for the conversion of isocitrate to OGA is -20.9 kJ $(mol)^{-1}$ [Zubay, 2000] and a large concentration ratio of OGA to isocitrate would be required to allow this reaction to run in the opposite direction. It was therefore hypothesised that the multi-phasic nature of the batch culture experiments makes any solution of the biosynthetic demand of flux cumbersome at best with method 1 (Vallino & Stephanopoulos, 1990 [Chapter 7]), which was similar to the strategy used in Chapter 6 (Holms, 1986). Model 2 offers the best-fit model to the experimental data for a number of reasons. Calculated sensitivities fit with that measured by

other workers (Daae and Ison, 1999)[Table 7.3 & 7.4]. There were no negative values for fluxes around the TCA cycle. Furthermore, there is better agreement between the measured enzyme activities (Chapter 6, section 6.8) and flux predictions using the flux-based strategy used in Chapter 6. The estimated fluxes observed for tylosin were unrealistic against the yields of tylosin determined experimentally. This was considered a consequence of the rigidity of reaction sequence 62 (Appendix M)[where propionyl-CoA, ethylmalonyl-CoA, methylmalonyl-CoA, and malonyl-CoA were incorporated into tylactone], with the preceding reactions accounting for the excretion of propionate and butyrate.

Whilst constructing the BRNE for method 2 it was noticed that oxygen and nitrogen sensitivities were considerably high compared with the other measured metabolites and that to reduce the conditional number NH_4 had to be included in the model. This would indicate that the balances between nitrogen, oxygen, and carbon were the most important factors to consider in estimating fluxes accurately. By contrast Holms (1986) strategy has carbon input as the most important factor affecting fluxes. Unfortunately with the lack of detailed gas analysis undertaken the estimated fluxes and sensitivity issues could not be assessed any further during this work.

To further assess models 1 & 2 the branch-point flux ratios were compared to previous enzyme activity studies and the flux analysis using Holms strategy (Chapter 6). The EMP/PP pathway ratio for model 1 glucose Ferm 1, 1:0.29; glucose Ferm 2, 1:0.27; fructose Ferm 1, 1:0.31; glycerol Ferm 1, 1:0.34; glycerol Ferm 2, 1:0.35; for model 2, glycerol Ferm 2, 1:1.30 and for the PK/PEPC for model 1 glucose Ferm 1, 1:1.12; glucose Ferm 2, 1:1.37; fructose Ferm 1, 1:0.77; glycerol Ferm 1, 1:0.84; glycerol Ferm 2, 1:0.86; for model 2, glycerol Ferm 2, 1:0.26. Using the enzyme activity ratio calculated in Chapter 6, section (6.8) for HK : 6PGDH indicate that the flux through the PP pathway was possibly close to the value PPP (3) calculated in Table 6.35 Part 1 & 2 (see Chapter 6, section 6.7) for the Holms (Chapter 6) strategy when incorporating co-factor balancing. The HK / G6PDH enzyme ratio showed good comparison to model 2, indicating a high proportion of flux through the PP pathway, although further experimental work would need to be undertaken to verify this. The enzyme activity ratios (Table 6.33 Part 1) were on average 1 : 1 for PK/PEPC nearing the end of the fermentation. This was not consistent with the flux-based diagrams (Diagrams 6.1 – 6.25)[Table 6.33 Part 2] for the Holms strategy (Chapter 6) or the matrix algebra approach.

This would indicate that to solve the distribution of flux through the PYR & PEP branch points a finer tuned flux analysis strategy would be needed.

7.3.2 The effects of compositional data on estimated fluxes

From the work undertaken in Chapter 5, determination of the monomeric composition was found to be laborious, time consuming, and expensive, and without previous work to corroborate with, prone to error. Hence the implications of committing oneself to such a study must be considered. Although monomeric composition of a specific strain may change slightly with varying growth conditions and/or different phases of a fermentation, the monomeric composition of bacterial species or strains in general might not be significantly different (see Chapter 5, section 5.7). The RNA, DNA, protein, lipid, teichoic acids, peptidoglycan, etc., could have been assembled differently, but the overall composition would be similar. Considerable differences in amino acid composition were observed for *S. fradiae* and *S. coelicolor* against other bacteria. Therefore it was considered a variation of more than 20 % in each of the monomeric components was not likely. A study was initiated to test the significance of bacterial composition on a flux-based analysis (strategy similar to Daae and Ison, 1999). A number of bacterial compositions were incorporated into model 1 & 2 (Appendices L & M) reaction 51 & 56 respectively. Standard *E. coli* composition data was used for setting 1 (Ingraham *et al*., 1983), the upper limit was increased by 20 % (setting 2), the lower limit was decreased by 20 % (setting 3). *S. fradiae* C373-10 biomass composition (setting 4) was set at settings 4 (average or appropriate composition table adapted from Chapter 6, Tables 6.1 – 6.29).

In this assessment throughput diagrams were used (all figures were normalized to 100). Calculated fluxes were presented in Table 7.5 & 7.6 (models 1 & 2). Little change was observed for flux estimations at the various settings (setting 1 – 4) for model 1. This was likely due to the compositional setting being set rigidly for model 1 (see Appendix L). This was done by setting the individual reactions for RNA, DNA, carbohydrate, lipid, and protein to the percentage macromolecular composition of *S. coelicolor* 1147 and *S. fradiae* C373-10 calculated from Chapter 5 (Table 5.10). The same trend was also observed for model 2 (Appendix M), which was considered not to be such a rigid bioreaction network. Another hypothesis could be that different bacterial aas profiles do not alter the branch point distribution of aas, which in turn shows little overall impact on estimated fluxes. This was

further considered in Chapter 5 (section 5.8.1) where codon bias was shown to affect the order of requirement of aas but did not show significant impact on the order of requirement of the branch point aa families (see Chapter 5, section 5.7.1). As can be seen from Table 7.6 (model 2), setting 1, 2, 3, & 4 generally showed little observable deviation between the estimated fluxes (0 – 1.5 % on average). It may therefore be concluded that the changes in the biomass composition will have little or no impact on the primary metabolic fluxes. Further work will need to be undertaken to assess further the importance of biomass composition of *S. fradiae* C373-10*, S. coelicolor* 1147 & *E. coli* ML308. Given the latter results it will be of great interest to see if the Holms method (Holms, 1986, 1996, 1997, 1998), which puts great emphasis on knowing the monomeric composition and the matrix algebra flux analysis (Vallino & Stephanopoulos, 1990) method correlate for a system under steady state (i.e., continuous culture).

7.3.3 Co-factor and isoenzyme effects on estimated fluxes

To assess further the effects of NADP and NAD-dependent ISEs on flux estimations for models 1 and 2 (Table 7.5 & 7.6) i.e., G6PDH and 6PGDH were set to two different parameters for models 1 & 2. This was considered a useful way to assess the effects of flux through the PP pathway on the stoichiometric model (Appendices L & M) settings 1, 2, 3, & 4 (as section 7.4.2) were NADP-G6PDH, NADP-6PGDH and setting 5 was NADP-G6PDH, NAD-6PGDH. Greater than 1 - 88 % differences can be observed in estimated fluxes between setting 1, 2, 3, 4, & 5 (CNs for BRNE can be found in Table 7.1) due to changes in ISE settings. The highest differences were observed for the reaction sequences for oxidative phosphorylation and ATP dissipation. Conditional number analysis (Table 7.1) would indicate the most acceptable BRNE produced to be totally NADPH dependent (model 1, NADPH/NADPH, CN = 57.96 average; NADPH/NADH, CN = 97.77 average; model 2, NADPH/NADPH, CN = 168.81 average; NADPH/NADH, CN = 408.14 average). This would indicate that altering ISE activities on the metabolic state/phase will have the greatest impact on measured fluxes for both flux strategies (Holms, 1986 [Chapter 6]; Vallino, 1991 [Chapter 7]) used throughout this work. The latter work is in good agreement with Chapter 6 in which discrepancies in accounting for the NADPH balance caused 10 – 40 % differences in estimated fluxes (Chapter 6, section 6.7) through the PP pathway against 19.0 - 25.0 % for

the matrix algebra analysis. In most organisms, the production of NADPH during glucose breakdown easily can be calculated.

7.4 Summary, future work and directions

The main aim of this Chapter was to apply a matrix algebra flux-based approach to a streptomycete fermentation. The power of matrix algebra is that it offers the opportunity of testing sensitivity issues on a BRNE before any fluxes are measured. The sensitivities of the calculated fluxes to changes in the measured fluxes were determined for two constructed BRNEs for this work (Models 1 & 2).

Model 1 showed poor reproducibility to the sensitivity to accumulated error between matrices to the sensitivity analysis undertaken by Daae and Ison (1999). Model 2 shows good reproducibility, to the sensitivity analysis undertaken by Daae and Ison (1999). Oxygen uptake showed the highest sensitivity to the accumulation of error in the matrix and nitrogen the next highest. The contribution of CO_2 was not significantly high, this was not surprising as CO_2 was taken up and released from a number of pathways, so from a balancing point of view it would bring closures to a material balance but may not have a significant effect on understanding flux partitioning.

A sensitivity analysis of the effect of theoretical compositional changes to the BRNE showed little effect on the estimated fluxes. A hypothesis was then made using data collected in Chapter 5, that the synthesis of aas of a number of pathways does not alter the redistribution of aas families, which in turn shows little overall impact on estimated fluxes. It may therefore be concluded that the changes in the biomass composition of an organism for example by codon bias will have little or no impact on the primary metabolic fluxes. Theoretical changes to the NAD/NADPH dependencies on the BRNE showed the greatest effect on the calculated fluxes. The highest differences were observed for the reaction sequences for oxidative phosphorylation and ATP dissipitation. This would indicate that altering ISE activities will have the greatest impact on measured fluxes for both flux-based strategies used throughout this work. The latter work is in good agreement with Chapter 6 where discrepancies in accounting for the NADPH balance caused 10 – 40 % differences in estimated fluxes through the PP pathway against 19.0 - 25.0 % for the matrix algebra analysis.

The estimated fluxes through the CMPs of *S. fradiae* C373-10 using matrix algebra for model 1 unexpectedly indicated negative values around the TCA cycle. This would indicate the cycle was running in the reverse direction or the metabolic costs of co-factor supply could not be met by the present bioreaction network. Model 2 offers the best-fit model to the experimental data for a number of reasons, calculated sensitivities fit with that measured by other workers. There were no negative values for fluxes around the TCA cycle. It was therefore hypothesised that the multi-phasic nature & the number and use of isoenzymes throughout a streptomycete batch culture makes any solution of the biosynthetic demand of flux cumbersome at best with the flux-based strategies used in this work.

Further assessment of the EMP/PP pathway and PK/PEPC branch points with enzyme assays. Indicate that the flux through the PP pathway was possibly close to the percentage flux through the PP pathway when corrected to the theoretical NADPH requirement [PPP (3) as Chapter 6]. The enzyme activity ratios were on average 1 : 1 for PK/PEPC nearing the end of the culture this was not consistent with the flux based diagrams for the Holms strategy or the matrix algebra approach, this would indicate the flux through the PYR & PEP branch points would need a finer tuned flux analysis strategy.

It was believed that the incorporation of Holms strategy (Holms, 1986) for flux analysis or matrix algebra strategies (Vallino & Stephanopolous, 1990) could offer a good system of analysing metabolic networks and the biosynthetic demand for streptomycetes. Although the use of the latter methods (Holms, 1986; Vallino & Stephanopolous, 1990) with batch culture were cumbersome to apply. The use of tracer studies such as undertaken by Christiansen *et al*. (2002) may offer a more robust method of analysing metabolic networks in batch and continuous culture in addition to the possibility of quantify futile cycling around the PEP and PYR branch points or the strategies undertaken in this work should have been further assessed in continuous culture.

Flux analysis *S. fradiae* C373-10 with glucose (Ferm 1) as sole carbon source (Model 1)

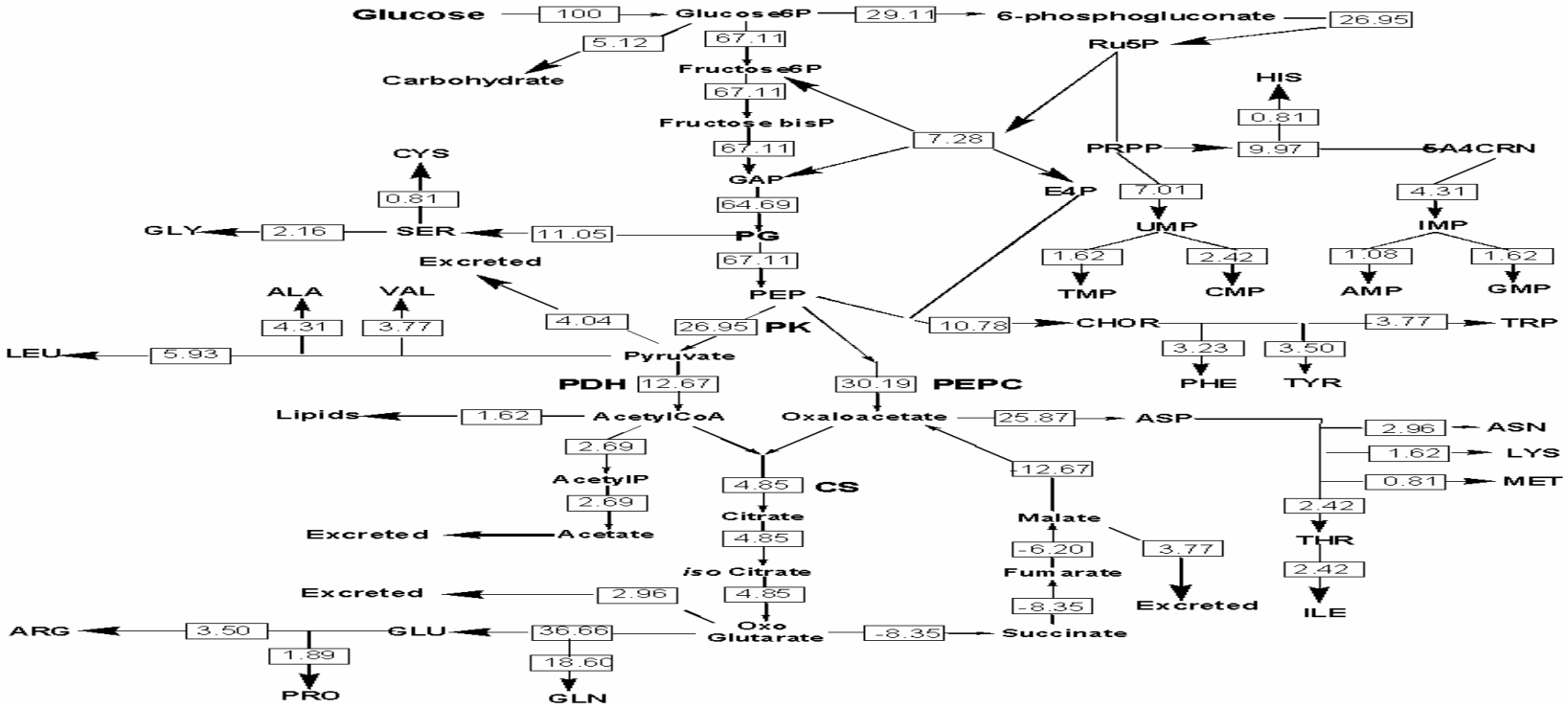

Fig 7.1 represents the fluxes through central metabolism of *S. fradiae* C373-10 (fermentation model 1, Chapter 4, Fig 4.1, Ferm 1) cultured on glucose. The fluxes were calculated using the Fluxmap computer program and bioreaction model 1 (Appendix L). The measured parameters were the uptake rates of glucose (data taken from Chapter 4), and the production rates of malate, pyruvate, oxo-glutarate, acetate (data taken from Chapter 4), and rate of synthesis of the key macromolecular pools, i.e., DNA, RNA, protein, lipid, and carbohydrate (data taken from Chapter 5 & 6).

Flux analysis *S. fradiae* C373-10 with glucose (Ferm 2) as sole carbon source (Model 1)

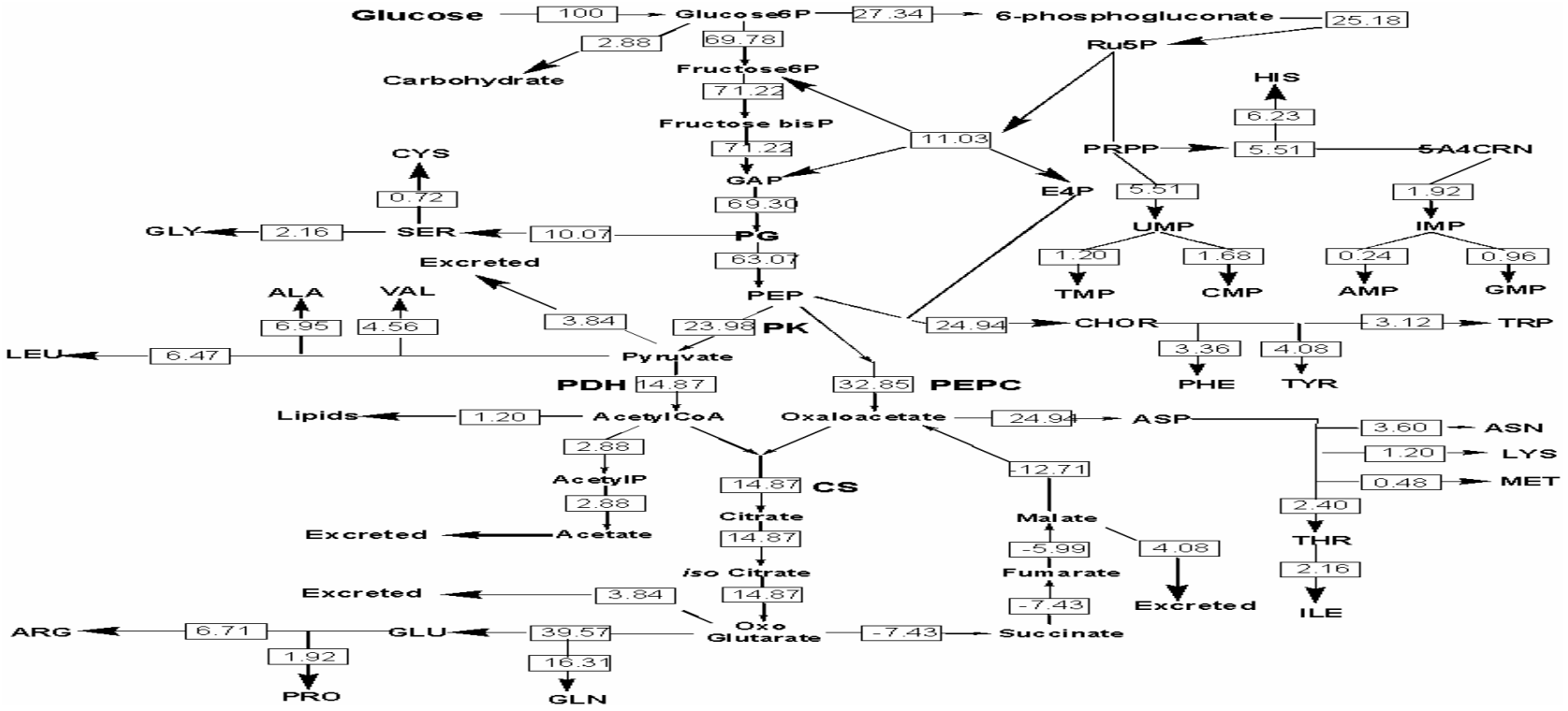

Fig 7.2 represents the fluxes through central metabolism of *S. fradiae* C373-10 (fermentation model 2, Chapter 4, Fig 4.2, Ferrm 2) cultured on glucose. The fluxes were calculated using the Fluxmap computer program and bioreaction model 1 (Appendix L). The measured parameters were the uptake rates of glucose (data taken from Chapter 4), and the production rates of malate, pyruvate, oxo-glutarate, acetate (data taken from Chapter 4), and rate of synthesis of the key macromolecular pools, i.e., DNA, RNA, protein, lipid, and carbohydrate (data taken from Chapter 5 & 6).

Flux analysis *S. fradiae* C373-10 with fructose as sole carbon source (Model 1)

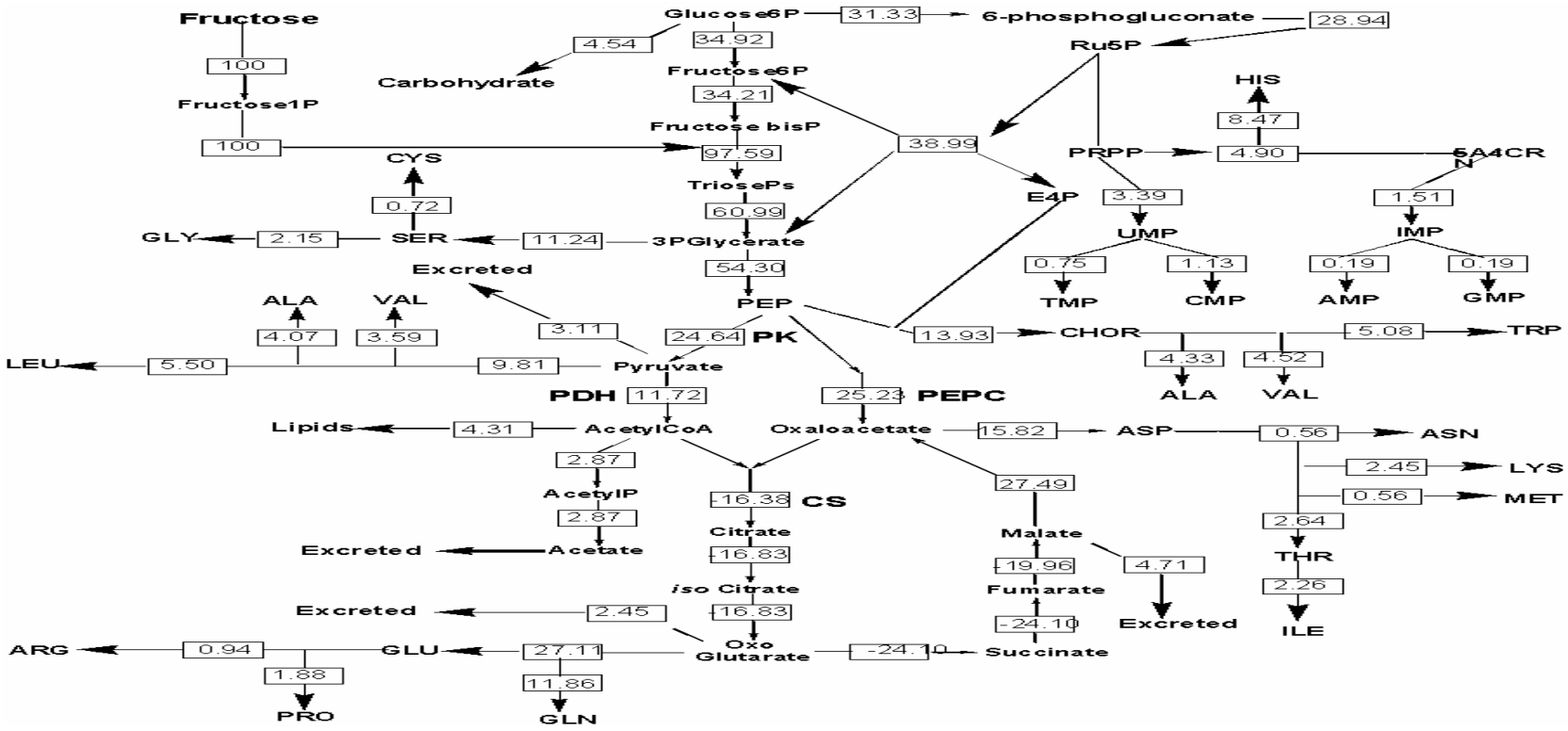

Fig 7.3 represents the fluxes through central metabolism of *S. fradiae* C373-10 (fermentation model 1, Chapter 4, Fig 4.3, Ferm 1) cultured on fructose. The fluxes were calculated using the Fluxmap computer program and bioreaction model 1 (Appendix L). The measured parameters were the uptake rates of fructose (data taken from Chapter 4), and the production rates of malate, pyruvate, oxo-glutarate, acetate (data taken from Chapter 4), and rate of synthesis of the key macromolecular pools, i.e., DNA, RNA, protein, lipid, and carbohydrate (data taken from Chapter 5 & 6).

Flux analysis *S. fradiae* C373-10 with glycerol (Ferm 1) as sole carbon source (Model 1)

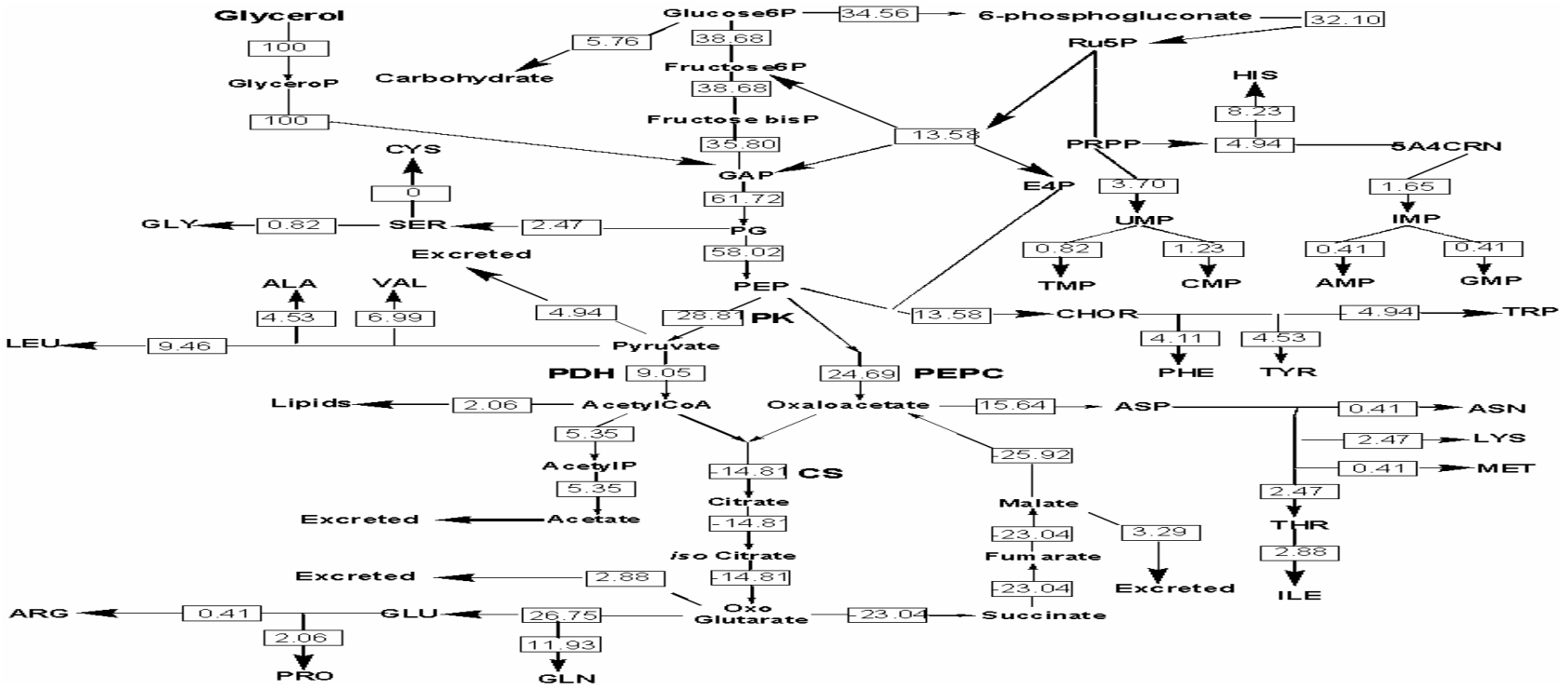

Fig 7.4 represents the fluxes through central metabolism of *S. fradiae* C373-10 (fermentation model 1, Chapter 4, Fig 4.4, Ferm 1) cultured on glycerol. The fluxes were calculated using the Fluxmap computer program and bioreaction model 1(Appendix L). The measured parameters were the uptake rates of glycerol (data taken from Chapter 4), and the production rates of malate, pyruvate, oxo-glutarate, acetate (data taken from Chapter 4), and rate of synthesis of the key macromolecular pools, i.e., DNA, RNA, protein, lipid, and carbohydrate (data taken from Chapter 5 & 6).

Flux analysis *S. fradiae* C373-10 with glycerol (Ferm 2) as sole carbon source (Model 1)

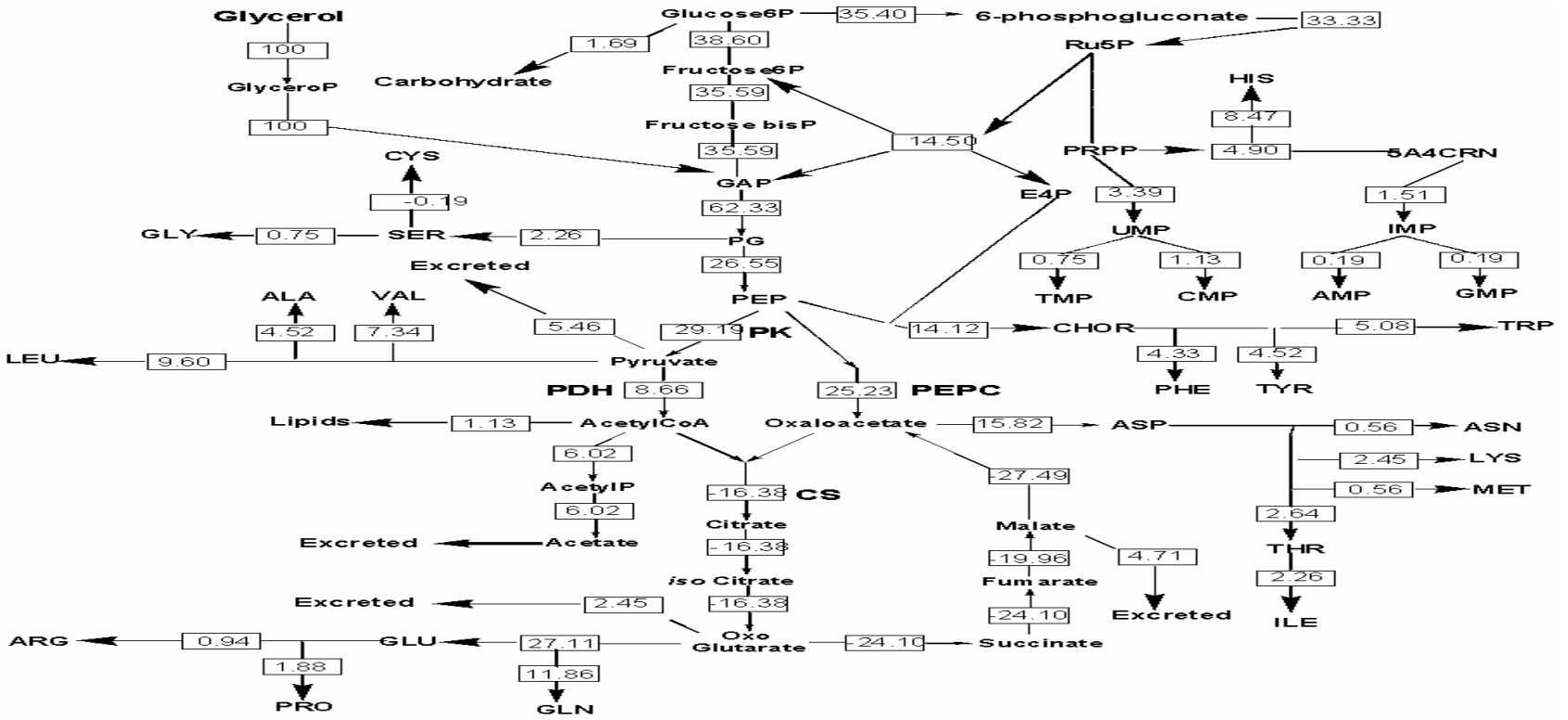

Fig 7.5 represents the fluxes through central metabolism of *S. fradiae* C373-10 (fermentation model 1, Chapter 4, Fig 4.5, Ferm 2) cultured on glycerol. The fluxes were calculated using the Fluxmap computer program and bioreaction model 1 (Appendix L). The measured parameters were the uptake rates of glycerol (data taken from Chapter 4), and the production rates of malate, pyruvate, oxo-glutarate, acetate (data taken from Chapter 4), and rate of synthesis of the key macromolecular pools, i.e., DNA, RNA, protein, lipid, and carbohydrate (data taken from Chapter 5 & 6).

Flux analysis *S. fradiae* C373-10 with glycerol (Ferm 2) as sole carbon source (Model 2)

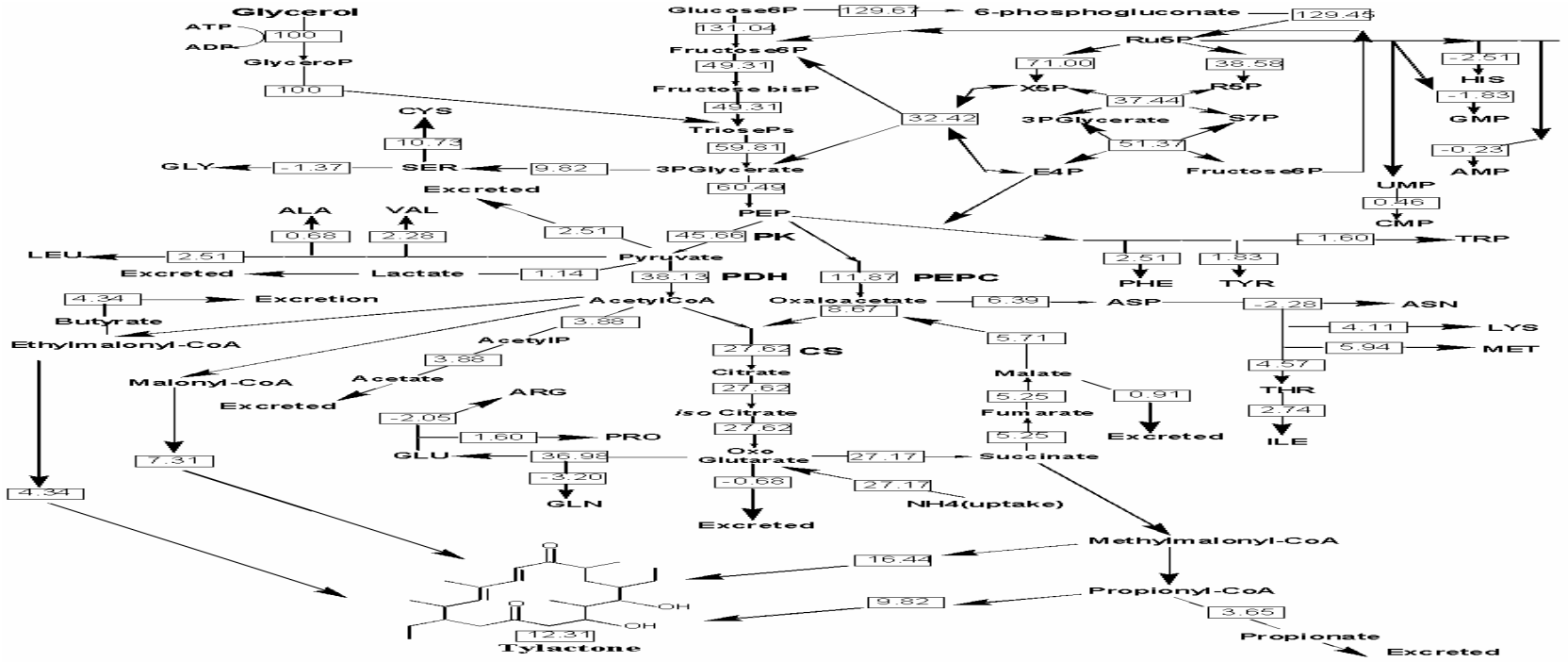

Fig 7.6 represents the fluxes through central metabolism of *S. fradiae* C373-10 (fermentation model 2, Chapter 4, Fig 4.1, Ferm 2) cultured on glycerol. The fluxes were calculated using the Fluxmap computer program and bioreaction model 2 (Appendix M). The measured parameters were the uptake rates of glycerol, and oxygen (data taken from Chapter 4), and the production rates of carbon dioxide, malate, pyruvate, oxo-glutarate, acetate, lactate, fumarate butyrate, propionate, tylosin (data taken from Chapter 4), and rate of synthesis of the key macromolecular pools, i.e., DNA, RNA, protein, lipid, and carbohydrate (data taken from Chapter 5 & 6) measured as one reaction sequence.

Chapter 8

Discussion & conclusions

8.0 Introduction

This thesis deals with the quantitative measurement of fluxes during primary and secondary metabolism of *S. fradiae* C373-10. Two requirements were necessary for this, 1) growth of *S. fradiae* C373-10 on a defined minimal medium with a simple carbon source such as glucose, fructose, glycerol etc., without the use of carbon-based dispersion agents, 2) the determination of the extracellular medium, elemental, molecular elemental, molecular monomeric, and the macromolecular composition of the bacterium and further verification of the analytical reproducibility. Several discussion points arose from the direction taken to achieve these requirements and they will be elaborated upon in the following sections (section 8.1 - 8.11).

8.1 Medium optimisation

Difficulties in obtaining the *S. fradiae* C373-10 strain until one year into the project, and access to fermentation equipment 1.5 years into the project put severe time constraints on what could actually be achieved with this study.

Initially a number of different media that had been previously been used to produce tylosin, tetracycline, actinorhodin and physostigmine were tested for their ability to produce tylosin. The only media that significantly produced tylosin were ones that were cultured with a rich fatty acid source e.g., mineral oil or complex polysaccharides e.g., starch. This was in good agreement with other studies (Gray and Bhuwapathanapun, 1980; Stark, 1961).

For further medium optimisation a minimal medium that had been formulated for continuous culture in house at Eli Lilly Ltd. (adapted from a medium developed for the production of physostigmine by *S. griseofuscus,* Zhang *et al*., 1996) was adapted for batch processes. Medium optimisation trials were undertaken (section 4.3), with various carbon & nitrogen sources in addition to differing betaine, phosphate and $MgSO_4$ concentrations. Unfortunately antibiotic production was not at a level sufficient, to identify any of the components tested had any great impact on tylosin production. It has been proposed by a number of workers that some single component carbohydrates (CHOs) or polyols (e.g. glucose, fructose, glycerol,

etc.) may have repressive effects on polyketide synthases (section 2.4) and a sustained carbon-limited environment may be the only way of achieving the reasonable antibiotic yields with these carbon sources.

When betaine was an addition to the medium there was an considerable increase in biomass yield and the ϕ dispersion against the control (see Table 4.5). Betaine is an important component of the industrial complex medium, although the reason for this requirement has not been reported by other workers (Stark *et al*., 1961). It is used by a number of bacteria as a nitrogen and carbon source (Hodgson, 2000). Betaine has also been linked to osmoprotection in a number of bacteria (see section 4.3 for a discussion). Why the addition of betaine led to such an effect with the minimal and defined medium formulations used for this work was not clear. Stark *et al*. (1961) reported betaine being an important component of methyl oleate defined medium (section 3.7) but there was no inhibitory concentration point. This did not fit with the results for the glucose minimal and glucose glutamate defined medium (Table 4.5) where concentrations above 2.0 gl^{-1} showed an inhibitory effect on biomass production and the ϕ of dispersion.

Thus to achieve reasonable antibiotic yields on a defined medium further variables would need to be taken into account such as the addition of various amino acids [aas]. Lee & Rho (1999) indicated that valine, had a great effect on tylosin production. When valine [1.0 gl^{-1}] was added at 5 days, tylosin productivity was 250 mg g $biomass^{-1}$; increasing the valine concentration to 1.5 gl^{-1} led to a decrease in tylosin production). Therefore it was believed that further analysis of other components would need to be taken into account. Due to complexity of the optimisation strategy for tylosin production in defined medium, shake flask trials were likely to be to labour intensive to develop a defined medium capable of producing tylosin with the parameters set for by this project (section 4.3 - 4.3.2). It is then more likely that a fed batch to continuous culture strategy would have produced tylosin to a greater extent as the culture could have been kept nutrient limited.

Alternative optimisation strategies such as the Plackett-Burman and Box-Behnken (Box and Behnken, 1960; Dupont de Nemours, 1975) design, was considered in Chapter 4. Applying this analyses to a *S. fradiae* optimisation strategy was considered pointless. With the

achievement of such low antibiotic yields, any statistical surface response analysis used in this work, would deliver little enhancement to a medium optimisation strategy (see Chapter 4).

A better approach to these problems would have been to adopt a continuous culture strategy for medium optimisation. This would have improved the speed at which medium optimisation could have been undertaken. In addition the dilution rate and growth conditions could have been assessed further for the best strategy to enhance tylosin yield. This technique has been used to optimise defined media for various microorganisms, including *Bacillus caldotenax* (Kuhn *et al*., 1979), *Cellulomonas* spp. and *Bacillus cereus* (Summers *et al*., 1979), *E. coli* B/r (Reiling *et al*., 1985) and *B. stearothermophilus* (Amartey *et al*., 1991). A more soundly based approach to medium formulation would have been to use the pulse and medium-shift technique described by Kuhn *et al*. (1979) and Goldberg and Er-Al (1981). This approach is a modification of the pulse technique, which permits the establishment of a constant culture environment, thus allowing the identification and optimisation of growth-limiting nutrients. San Martin *et al*. (1992) used this technique to develop a synthetic medium for the continuous cultivation of a *Bacillus stearothermophilus* strain under anaerobic conditions. The procedure required the establishment of a carbon-limited continuous culture in a defined medium containing 18 aas and 5 vitamins. Once steady state was attained, the aa concentration in the incoming medium was reduced by 50 %. If the cell density decreased substantially as a result of dilution of an essential aa to a level where it had become the growth-limiting nutrient, aas were injected sequentially into the bioreactor. When a significant response in biomass and residual carbon source concentration were detected, a new medium was prepared with increased concentration of the corresponding aa/s and a new two-fold dilution of the remaining aas. The procedure was repeated until all non-essential aas had been removed from the medium. The final medium contained 4 aas and 5 vitamins, and showed similar growth characteristics to a medium containing yeast extract and tryptone. By using the pulse and shift technique, Reiling *et al*. (1985) developed a highly concentrated minimal medium for *E. coli* B/r, achieving high cell densities in batch cultivations at the 50 L bioreactor scale. Schuster *et al*. (1995) employed this technique to develop a synthetic medium to produce cell wall fragments for *B. stearothermophilus* PV72 by varying the growth conditions in continuous culture.

At the beginning of this work, emphasis was placed on achieving significant antibiotic yields, following previous research undertaking in this laboratory (Davidson, 1992; for *S. coelicolor* 1147 & 209). In both cases the projects failed to optimise a minimal medium capable of producing adequate antibiotic yields. Naeimpoor & Mavituna (2000) indicated that unless antibiotic yields are in excess of 2 % of the carbon source there was little effect on calculated observable fluxes. Results from section 6.6.4 show that the flux to ACT after cessation of biomass production by *S. coelicolor* 1147 was only 1.4 % to 1.7 % of the total carbon input (similar results to Davidson, 1992). In the case of *S. fradiae* flux to tylosin was in the range (0.05 % to 0.5 % for minimal and defined medium respectively).

A *S. lividans* strain carrying the ACT-pathway-specific activator gene (actII-ORF4) from *S. coelicolor* on a multi-copy plasmid (pIJ68), might have been a better choice of test organism for this work, which has been shown to produce large amounts of ACT (Bruheim *et al*., 2002). Over 5 g $ACT.l^{-1}$ was produced over 7 days of the fermentation and 17 % of the carbon substrate was converted to ACT in the stationary phase. This constitutes 20 – 30 % of the maximum theoretical yield. It must also be noted that flux analysis is at full potential only whilst growth is at a *pseudo*-steady state (section 1.1). It was most unlikely that a steady state was achieved during antibiotic production for streptomycete batch cultures undertaken in this work, due to the antibiotic production being in most cases non-growth associated and multi-phasic. A better way of utilising flux analysis towards *Streptomyces* research would have been to carry the research out in continuous culture under a number of different dilution rates or use different historical strains of the organism thus being able to map how the primary metabolic pathways have changed through yield enhancing strategies. A further problem was the semi-complex defined medium needed to achieve adequate tylosin yields (section 4.5.3). The development of a multistage chemostat, may offer a system that could remove a number of the problems associated with flux analysis strategies e.g., quantifying fluxes through individual stages of the culture, removing the necessity to use organisms that can produce the desired product on a minimal or defined medium, and the ability to achieve reasonable antibiotic yields without mass medium optimisation strategies. The advantage of a multi-stage chemostat is that different conditions prevail in the separate stages. Although the adoption of multistage systems in research and industry has been extremely limited, due to the complexity of the system.

Another problem was that the flux-based strategy was set at the beginning of the project. This was flawed in approach. One needs to balance antibiotic yield with medium simplicity for any flux-based strategy. Antibiotic yield must not be less than a statistically-acceptable level (section 6.9 – 6.10). It is better advised to design, the flux-based strategy i.e., metabolic flux analysis (MFA), material balancing, or ^{13}C analysis utilising atom mapping matrices (see Chapter 1 & sections 6.9 & 6.10) to fit the medium and growth conditions and not the medium and the growth condition forced to fit the flux analysis. MFA has been successfully applied to a number of bacteria, the most extensively analysed has been *E. coli* ML308 (section 1.2.6), with extensive medium design strategies, kinetic based analysis and compositional data already accumulated over a number of years (40 - 50 years). Therefore if the medium developed does not realistically mimic the required growth pattern i.e., antibiotic production with balanced biomass yields, the ultimate aim of the work must be viewed with care. However if the medium does support the required growth pattern and will be used for further research, any information gained stands a good chance of enhancing modelling techniques in the future. It must be remembered when viewing this work that any medium development strategy is realistically a project in its own right.

One of the objectives of this work was to incorporate a secondary metabolite producing pathway into a flux-based strategy. This was not a realistic objective with the level of antibiotic produced with the developed minimal media. The framework chosen was a strategy of incorporating a systematic approach to the analysis of *S. fradiae* growth from a minimal medium with low antibiotic yields to the literature based methyl oleate defined medium with the goal of further incorporating a material balance of the industrial complex medium. In essence de-piecing the medium to its basic carbon components and measuring how the individual components distribute to biosynthesis.

8.2 Analytical protocols and the assessment and verification of compositional analysis data

Waksman *et al*. (1946) published a paper on the metabolism and the chemical nature of *S. griseus*. It was noted by the authors then *"that considerable information has accumulated concerning the distribution of streptomycetes in nature and their cultural characteristics, comparatively little is known of the chemical composition of the mycelium, their physiology and their nutrient requirements"*. Despite this recognition over 60 years ago very little is still

known about primary metabolism in streptomycetes, though their has been a great surge in genetic information & knowledge of secondary metabolic pathways.

The direction of this work was to carry out a systematic, elemental, molecular elemental, molecular monomeric, and macromolecular analysis with a large number of diverse analytical procedures, with the intention of carrying out a reconciliation procedure of the acquired compositional data. This strategy was used to great success (as undertaken in section 5.13.1 - 5.13.3) for observing differences between the elemental and macromolecular analysis.

Initial analysis indicated that macromolecular extraction methods 1 & 2 (section 3.16) offered the most user semi-friendly protocols with the additional advantage of offering a 1 - 5 step protocol for the complete analysis of CHO, DNA, RNA, protein, lipid and cell wall components. An approximate macromolecular composition for *S. fradiae* C373-10 was considered to be CHO 15.0 – 20.0 %, RNA 10.0 - 13.0 %, DNA 3.0 – 5.0 %, protein 36.0 – 51.0 %, lipid, 2.5 – 3.6 teichoic acid 10.0 – 13.0 %, & peptidoglycan 7.74 % for growth on a glucose + glutamate defined medium.

When media was supplemented with glutamate there was an increase in the cellular lipid composition and when cultured with a single carbon source the CHO content of cells was slightly higher. Changes in the total cellular lipid composition of yeast has been reported by a number of workers. Evans & Ratledge (1984b) using *Rhodosporidium toruloides* examined how the nitrogen in medium affected lipid accumulation, as it had been reported previously that certain yeasts could accumulate substantially more lipid when various organic nitrogen sources, rather the NH_4, were used for growth (Blinc & Hocevar, 1953; Witter *et al*., 1974). PFK was implicated as the likely controlling enzyme to explain these events. Unlike the enzyme from *S. cerevisiae*, no inhibition was found with 10 mM-ATP. ADP was not inhibitory either. NH_4 ions increased activity 11-fold by increasing the affinity of the enzyme for both F6P and ATP. K^+ ions also stimulated activity but to a lesser extent. Activity was severely inhibited by citrate, isocitrate and *cis*-aconitate but this inhibition was alleviated dramatically by NH_4. It was concluded that the interplay between the prevailing intracellular concentrations of NH_4 and citrate was the major determent of the activity of PFK *in vivo,* which thus governed the extent to which glucose was converted either to lipid or CHO (Evans and Ratledge, 1984b).

An ATP-dependent PFK has been identified and purified from *S. coelicolor* (Alves *et al*., 1994, 1997)[see Chapter 2 section 2.5.1, for a detailed discussion of PFK], although little research was carried out by these workers on the properties of the enzyme. PEP was found to inhibit the enzyme strongly (Alves *et al*., 1997). It may be the case that streptomycete PFK's may have similar properties to yeast PFK's. If lipid accumulation was the preferred route for antibiotic synthesis expressing a PFK that has a preference for this route, there would be a parallel with high lipid-producing strains such as *Rhodosporidium toruloides*. Over expression of an enzyme may not be enough in itself, as streptomycete molecular biology and protein purification often lack the detailed kinetic studies (Alves 1994, 1997 study of PFK in *S. coelicolor* and *A, methanolica*) that have been undertaken by other disciplines e.g., yeast researchers (Evans and Ratledge, 1984; study of PFK in yeast against Alves, 1994, 1997). The latter analysis does indicate the need for an increase in the characterisation of the kinetic properties of these enzymes in streptomycete research.

Both macromolecular extraction/fractionation methods 1 & 2 compared well for total nucleic acids recovery although only 50 – 60 % of the RNA was extracted by the KOH fraction (method 2). *E. coli* ML308 showed an 80 - 90 % recovery of RNA for the KOH extraction (method 2). This could indicate that the streptomycete cell wall was refractory to the KOH extraction step (section 5.5 & 5.7). Total carbon analysis was used to verify the reliability of the macromolecular analysis carried out on methods 1 & 2. This indicated up to 90 – 97 % of the carbon in the KOH fraction of most samples was unaccounted for. A possible suggestion was that the cell-wall associated polymer, teichoic acid had been extracted. Taking teichoic acid into account and assuming a glycerol backbone and ribitol backbone, 18.1 % or 10.7 % of the carbon remained unidentified in the KOH fraction of method 2 (section 5.7).

Initial analysis would indicate that the Bradford assay was a source of error for protein determination with *S. fradiae* (section 5.4.3). Further analysis was therefore undertaken to determine if the Bradford assay results were correct. The level of protein detected by the reverse biuret assay against the Lowry, Bradford, and BCA assays on the whole was four fold higher for *S. fradiae* C373-10, 1.5 fold higher for *S. coelicolor* 1147. The protein content of *E. coli* showed little difference between the different protein assays. This would indicate that the

amino acid composition of the organism and the protein standard chosen, in this case BSA, had a considerable effect on the amount of protein detected between bacterial species.

The dye in the Bradford assay works by binding to basic aas i.e., arginine and lysine residues (to view the biomass composition of *S. coelicolor* 1147 and *S. fradiae* C373-10 & C373-18 aas, see Chapter 6, Tables 6.1 – 6.27 for aa composition on a mM g dry weight of biomass basis; see section 5.7). The lysine and arginine, particularly lysine on average were 4 fold lower in *S. fradiae* C373-10 compared with *E. coli* ML308, and *S. coelicolor* 1147 on average was 1.5 fold lower compared with *E. coli*. The Lowry (Folin-Ciocalteau) method [section 3.20.2], which is based on the oxidation of tyrosine and tryptophan residues with Folin and Ciocalteau's reagent. Tyrosine and tryptophan were 5.2 fold less in *S. fradiae* C373-10 compared with *E. coli* ML308, and *S. coelicolor* 1147 on average was 1.2 fold less compared with *E. coli* calculated from the total aa analysis (section 5.8). If BSA was therefore considered to have a similar aa composition to *E. coli* biomass; the aa composition of streptomycetes will have a considerable effect on the chosen protein assay.

The choice of an appropriate standard was considered important for any further analysis, as the intensity of colour produced for a particular protein is dependent on the amount of an individual amino acid/acids present. The choice of standard is difficult and therefore it would be more beneficial in compositional studies to use a standard method of protein measurement with the added benefit that the choice of the protein standard will have no effect on the assay reliability. The ninhydrin assay and total aa analysis by HPLC probably offer the most accurate methods of protein determination but were not user-friendly and were time consuming. Therefore the reverse biuret method (section 3.20.5) should be considered as a standard method of protein determination in bacterial compositional research.

The elemental analysis as well as molecular composition were consistent with values reported by, for example, Duboc *et al*. (1995; 1996), Dekkers *et al*. (1981), and Schulze (1995) for *S. cerevisiae*. The percentage difference in unaccountable carbon (2.36 % on average), and nitrogen (16.04 % on average)[Table 5.41] between the elemental analysis and the molecular elemental analysis would indicate a considerable proportion of the biomass was unaccounted for possibly cell wall components (section 5.10). The high experimental difference for sulphur

(43.25 % on average) and phosphorus (47.90 %) indicated that a considerable proportion of sulphur and phosphorus containing molecules were unaccounted for in the molecular monomeric and macromolecular analysis (section 5.13.3). Phosphorus was likely to be accounted for in the cell wall fraction as teichoic acids (section 5.6). The percentage difference in sulphur was unexpected. *S. fradiae* C373-10 was shown in this work to require high levels of $MgSO_4$ for growth, which corresponds with work at Eli Lilly Ltd. and Stark (1961). It could therefore be the case there was a need for high levels of sulphur for a byproduct.

Sulphur-containing shunt metabolites have been reported in *S. fradiae* metabolism, collectively known as bound tylosin. The chemical composition and nature of bound tylosin is unknown. Bound tylosin has been theorised to be a non butyl-acetate extractable complex formed between the aldehyde group on the tylactone ring and another chemical entity and there seems to be an equilibrium between free tylosin and bound tylosin in the region of 90 : 10 (personal communication J. McIntyre, Eli Lilly Ltd). Bound tylosin was reported to have a lower bio-activity (personal communication J. McIntyre). The chemical reactivity of tylosin centres around two main reactive points. The first is the aldehyde group and the second is the unsaturated ketone group (Figure 8.1 – 8.2). Aldehydes and ketones may be thought of as being derived from alcohols by removal of two hydrogen atoms, one from the hydroxy function and one from the neighbouring carbon. The oxygen within the carbonyl group bears two-lobe pairs of electrons, and therefore carbonyl groups are slightly basic. In addition the C-O bond was polarised making the carbonyl carbon electrophilic (the carbon - oxygen double bond was then prone to addition). Both of these two properties shape the behaviour of aldehydes and ketones. Therefore aldehydes and ketones will react with a wide range of chemical compounds such as NH_3, thiols, amines, alcohols, aas and bisulphites. All these compounds will react with the aldehyde group -with no detrimental effect on the UV absorbance of tylosin i.e. the tylosin chromophore remains intact (see Figure 8.1 and 8.2). However this will not be the case if the same compounds reacted with the unsaturated ketone group i.e. the chromophores properties would alter.

A number of experiments were undertaken in house at Eli Lilly Ltd. to test if the properties of the chromophore would change with the addition of a number of metabolites. There was evidence that free tylosin could be released from fermentation broths by the addition of an

aldehyde, the added aldehyde would be more reactive than the aldehyde group attached to the tylactone ring. This would change the equilibrium between tylosin and bound tylosin due to the chemical entity that would normally react with the tylactone aldehyde. When tylosin broth was treated with 2 % sulphuric acid and 2 % paraldehyde at 60^0 C for 20 minutes there was an increase in the amount assayed compared with the same broth that has been assayed untreated. Sodium metabisulphite reacts readily with both aldehydes and ketones to form a polar compound. A quantity of tylosin standard was dissolved in 4 % sodium metabisulphite solution and then run on the tylosin HPLC system. The chromatogram for tylosin + sodium metabisulphite showed no trace of tylosin A but there was a peak at the retention time for relomycin (tylosin D). This was expected as tylosin D does not have an aldehyde functional group (section 2.10). The addition of 2 % NH_3 to a tylosin standard solution reduced the mean integrated area by 14.04 %. The retention time also slightly increased with the addition of NH_3 solution. This fact will cause a molecular shift that will in turn change the λ_{max} for tylosin and hence the reduced area.

It is the recommendation of this work, in conjunction with work carried out by Eli Lilly Ltd. and with the added inability to balance the sulphur content of a defined medium, that further diode array work should be carried out, firstly on a standard dissolved in 2 % Ammonia solution and 2 % sulphate solution, and then on a fermenter broth for the further analysis of antibiotic shunt metabolites with altered chromophores. This will determine if tylosin can be detected when a compound has reacted with the unsaturated ketone group and if there are other rich carbon pools in a tylosin fermentation broth.

Biomass from a glucose minimal medium and methyl oleate defined medium on average showed a higher elemental oxygen composition for *S. fradiae* C373-10 (Table 5.39 Part 1)[$CH_{2.04}O_{0.62}N_{0.19}P_{0.023}S_{0.022}$ for *S. fradiae* C373-10; $CH_{1.90}O_{0.56}N_{0.15}$ for *S. coelicolor* 1147; $CH_{1.94}O_{0.38}N_{0.26}S_{0.007}P_{0.015}$ for *E. coli* ML308]. The high oxygen content of streptomycetes has been, reported by other workers. The ash content (oxidised mineral components) was further taken into account to determine the effect of ash content on the elemental oxygen composition as, there were no reports in the literature for streptomycete research that this had been previously accounted for. When the ash content was taken into account, there was a considerable effect on the elemental oxygen composition. Although the oxygen content was still considerably higher than the bacterial average empirical formula. For statistical

acceptance of compositional data sets for *S. cerevisiae* also required the inclusion of water in the list of biomass components (Lange & Heijnen, 2001) the elemental and molecular biomass composition of data thus exhibited a reduced oxygen and the protein content. No clear trend was obvious for the other constituents.

The error margins for all the analytical methods used throughout this work (Table 5.43) were rather large compared with values commonly reported for the applied methods (Duboc *et al*., 1995). However the difference between the standard deviations of measurements on a single sample and between samples of repeated cultures indicated that these values were subject to errors outside the chemical analysis. Sampling and sample handling were probable sources, in addition to the use of a dry / wet weight weighting factor used to calculate the compositional data. Small variations in culture conditions were also likely to have an influence. There is a need to assess further the analytical assays undertaken with this work with appropriate standards so that strategies for statistical analysis can be incorporated to reduce the error margins further. The application of statistical reconciliation methods (Wang & Stephanopoulos, 1983) could prove of benefit for the further analysis of streptomycete composition. Reconciliation is a systematic method that is capable of both detecting the presence of grossly-biased measurement errors in a bioreactor through statistical hypothesis testing. The different measurements are placed in a network, based on elemental balances relating all measurements with each other. The most likely set of consistent values for the biomass composition was calculated with this network based on the measured data and the error margin of each measurement (see Figure 8.3 for the elemental and molecular relational network used for reconciliation of *S. cerevisiae* Lange & Heijnen, 2001). The use of such a network enables simple comparison of different analytical methods. For example reconciliation and averaging data were used to great effect for a systematic comparison between the elemental and molecular elemental composition for *S. coelicolor* and *S. fradiae* (section 5.13.3), although this reconciliation strategy was somewhat simplistic compared to other workers (Wang & Stephanopoulos, 1983; Lange & Heijnen, 2001). It would have been advantageous to have expanded the scope to the analysis of the molecular monomeric and macromolecular compositions. The choice of appropriate standards between the analytical protocols caused considerable error between a number of techniques (e.g., RNA, DNA, & protein)[Table 5.14, Part 1 & 2 where differences of 50 – 60 % on average was observed between protein assays, Table 5.12 where differences of 87 % on average was observed

between DNA assays and 13 % on average for RNA techniques] and made any reconciliation strategy infeasible.

The resulting data from this work represent the best estimate of elemental and molecular biomass composition based on all available measurements. Further statistical reconciliation methods need to be undertaken in the future to minimise errors for example, from carbon recovery or calculation of the cell's energetic requirements to increase the accuracy of black box balancing or metabolic model calculations.

In conclusion, analysis of *S. fradiae* C373-10 biomass resulted in compositional data at the macromolecular, monomeric and elemental level. Balancing of the elemental and molecular elemental measurement values ensured that the reconciled values of the biomass were inherently consistent. The resulting data represent the best estimate of elemental and molecular biomass composition based on all available data. The values obtained, however, are not definitive and further work is required to obtain information comparable to that reported for *E. coli*. Nevertheless, the monomeric compositions of biomass samples were considered sufficient to calculate throughputs and therefore, fluxes to biomass through the central metabolic pathways of *S. fradiae* C373-10 (see Chapter 6) the data from this Chapter were then converted to compositional tables (as Holms, 1986, 1996, 1997, 2001) [section 5.8.1; Tables 6.1 - 6.27; Figures 6.1 – 6.29; All Tables can be found in the companion CD; Appendix O Chapter 6 & P)].

8.3 The metabolite costs of amino acid biosynthesis

The average relative amounts and order of requirement of several of the aas for *S. fradiae* was very similar compared to the expected order of requirement calculated from genomic codon usage tables (section 6.4). Although the average order of requirement indicates glycine as the most abundant aa and showed an average aa decreasing order of requirement of GLY > ALA > ASP > GLU > ARG > LEU > VAL > PRO > THR > ILE > TYR > PHE > LYS > HIS > SER > MET > TRP. By contrast the costs of amino acid biosynthesis vs. codon usage showed a preference for low cost amino acids with the exception of arginine.

Biosynthesis of a bacterial cell, with organic compounds as sources of energy and carbon, requires approximately 20 to 60 billion high-energy phosphate bonds (~P) [Stouthamer,

1973]. Energy, in the form of high-energy phosphate bonds (~P) and reducing power (~H), is lost through diversion of intermediates from fueling reactions and further energy is required to convert starting metabolites to aas. The energetic requirement for aa biosynthesis for a given codon in the genome is the product of the cost per encoded aa and the number of times the codon is translated. Abundant *E. coli* proteins are found in concentrations of 50,000 - 100,000 molecules per cell (Neidhardt, 1990; VanBogellen, 1996); the energetic savings for a single aa replacement in a highly expressed gene can therefore be millions of ~P or greater than 0.025 % of the total energy budget for biosynthesis of macromolecules. Less abundant proteins, however, may be in concentrations as low as a few molecules per cell. This 105 - fold difference in the metabolic costs of aa usage should translate, in protein codon sequences to the fitness benefit of encoding less energetically costly aas. Additional metabolic constraints on protein structure could include the energetic costs of aa biosynthesis (Richmond, 1970; Karlin & Buchner, 1992; Lobry & Gautier, 1994; Dufton, 1997; Craig & Weber, 1998; Jansen & Gerstein, 2000), the biochemical complexity of synthetic pathways (Karlin & Buchner, 1992, Craig & Weber, 1998; Jansen & Gerstein, 2000), availability of nutrients (Mazel & Marlière, 1989; Baudouin-Cornu *et al*., 2001; Craig *et al*., 1999), and the speed and accuracy of protein synthesis (Lobry & Gautier, 1994, Percudani *et al*., 1997; Eigen & Schuster, 1979; Gutierrez *et al*., 1996).

Mutational processes and relationships between primary structure and function are considered to be the major determinants of both aa composition and rates of protein evolution (King & Jukes, 1969; Doolittle, 1979; Li, 1997). Natural selection preserves or enhances protein specificity, activity, or stability by favouring codons that encode particular aas in gene regions corresponding to critical locations in the primary structure of proteins. At less constrained locations, a combination of mutation pressure and genetic drift account for encoded aas. A number of studies have established that differences in mutational biases explain some of the variation in aa composition among bacterial species (Sueoka, 1961; Lobry, 1997; Gu *et al*., 1998; Karlin & Buchner, 1992). However, the relationship between the efficiency and energetics of protein synthesis and the primary structure of proteins has received less attention. If a substantial fraction of aas are synthesised in bacterial cells and energy is limiting survival or reproduction, then the aa composition of proteins encoded in the genome should be biased toward less energetically costly aas. The extent to which aa composition is biased to reduce metabolic costs should be a positive function of the numbers of proteins

synthesised, per generation, from each gene (Akashi & Gojobori, 2002). If survival or reproduction is, at least at times, energy-limited in bacteria, natural selection should act more strongly, and produce a greater skew toward metabolically-efficient aas, as a positive function of gene expression levels.

The metabolic costs of synthesising the precursors and 20 aas used in proteins are shown in Table 8.1 & 8.2 (All Tables can be found in the companion CD; Appendix O Chapter 8). The cost of using a particular precursor metabolite is the number of high-energy phosphate bonds, ~P, carried in ATP and GTP, plus the number of available hydrogen atoms, H, carried in NADH, NADPH, and FADH2, that would have been gained if the metabolite had remained in energy-producing pathways minus the numbers of these molecules gained before diversion. For each aa, the energetic requirements of its biosynthetic pathway were added to the costs of its starting metabolite(s) [Table 8.3] to obtain a total metabolic cost per molecule synthesised for *E. coli* metabolism. Amino acids that require chemical intermediates early in fueling reaction pathways (the aromatic aas and His) are more costly than those derived from intermediates downstream in glycolysis (the serine family) and the tricarboxylic acid cycle (the aspartate and glutamate families). Therefore energetic costs were converted to a common currency of ~P based on a proportion of two ~P per H for *E. coli* ML308, *S. fradiae* C373-10 and *S. coelicolor* 1147 (Neidhardt, 1990)[Table 8.4 - 8.5]. Although precursor costs depend on the particular source of carbon, costs of aa biosynthesis seem to be highly correlated for growth on different substrates (glucose vs. acetate, r2 = 0.968; glucose vs. malate, r2 = 0.998)[Table 8.3]. In the latter analysis the average cost of biosynthesis for each aa for growth on a number of substrates was employed (Table 8.3). All results were similar for *S. coelicolor* 1147 and *S. fradiae* C373-10 showing an average standard deviation of 22.02 (Table 8.5; Table 8.4 shows how the calculation was undertaken for *E. coli*). Table 8.6 would indicate that the energetic costs were an important factor in streptomycete metabolism, as the difference in energetic costs between *E. coli* ML308 (119.31), *S. coelicolor* 1147 (79.45 on average) and *S. fradiae* C373-10 (71.26 on average) were quite significant. Further analysis would need to be undertaken to assess the complex medium but initial studies would indicate energy was still well conserved in an complex industrial medium (*S. fradiae* C373-18; Table 8.5; 57.56). Several factors might further confound the interpretation of these results. First, in the analyses above, energetic costs were converted to numbers of ~P based on a proportion of

two ~P per H (through oxidative phosphorylation). However, in *E. coli*, this ratio may depend on growth conditions i.e., availability of O_2 (Neidhardt, 1990), which may in turn cause slippage in membrane energy transduction.

Organisms such as *E. coli* and *B. subtilis* may often grow in nutrient-rich and nutrient-poor conditions (in the mammalian lower intestine and soil, respectively) where growth may not be energy-limited and where they may obtain a substantial fraction of their aas from their environments rather than through biosynthesis. However, periodic selection in nutrient-depleted conditions may be sufficient to skew aa composition. The Akashi & Gojobori (2002) analysis addressed the duration or severity of energy limitation required to generate associations between aa composition and gene expression levels in *E. coli* and *B. subtilis*. However the latter two organism may not offer the best model system to assess the severity of energy limitation required to generate associations between aa composition and gene expression levels. *S. coelicolor* and *M. tuberculosis* may offer improved model systems, both have evolved in an nutrient limited environmental niche with an observable gene expression bias towards low cost aas (Chapter 5, section 5.7.2, Figure 5.7a, b, & c).

The predicted association between aa composition and gene expression requires tight regulation of aa biosynthetic pathways according to the chemical requirements of the cell. In bacteria, both end-product inhibition of biosynthetic enzymes and transcriptional control of biosynthesis operons contribute to fine-tuned control of aa concentrations (Zubay, 1998). DNA microarray analyses of mRNA levels show strong induction of aa biosynthesis genes in *E. coli* growing in glucose minimal medium (with NH_3 as the sole nitrogen source) relative to cells in rich medium (containing aas) [Tao *et al*., 1999]. This induction is pronounced for genes encoding enzymes that function in the initial steps of biosynthetic pathways. Thus, a mutation in a protein-coding gene that reduces the demand for a particular aa should reduce flux through its biosynthetic pathway and alter the metabolic budget.

The identification of negative associations between expression levels and usage of energetically costly aas depends critically on the relationship between codon bias of synonymous codons and the translation rates of genes. tRNA abundances have been quantified in *E. coli* (Ikemura, 1985) and *B. subtilis* (Kanaya *et al*., 1999). In both species, codon usage is biased toward "major" codon(s) that are generally recognised by abundant

tRNAs. Such patterns are consistent with major codon preference, or discrimination by natural selection among synonymous codons to enhance translational elongation rates and/or to reduce the frequency of aa miss-incorporation's during protein synthesis (Ikemura, 1985; Andersson & Kurland, 1990; Sharp & Matass, 1994). Variation in usage of synonymous codons by two dimensional gel electrophoresis is correlated with quantification of protein abundance in both *E. coli* (Eyre-Walker, 1996; Kanaya *et al*., 1996; Karlin *et al*., 2001) and *B. subtilis* (Karlin *et al*., 2001) and supports that the fitness benefit to encoding a major codon is a function of its translation rate.

The analysis of Akashi & Gojobori (2002) showed strong statistical support for increasing usage of less energetically costly aas in abundant proteins in both *B. subtilis* and *E. coli*. These patterns do not appear to result from relationships between functional and expression classes of proteins, mutational biases, or biases in estimates of translation rates. In highly expressed genes, the average cost of aa biosynthesis was reduced by 2.5 and 2.0 ~P per aa per protein synthesised in *B. subtilis* and *E. coli*, respectively. Although selection to enhance metabolic efficiency was likely to be weak for a given codon, the energetic savings for biosynthesis of the proteome may be in the hundreds of millions of ~P per generation (therefore a precise estimate will require knowledge of the whole-genome distribution of rates of protein synthesis). Examination of relationships between aa usage and gene expression may provide a broadly applicable strategy to identify energetic constraints on protein structure. Analysis to date (Akashi & Gojobori, 2002) depends on positive relationships between bias in usage of synonymous codons and the translation rates of proteins and is thus restricted to organisms undergoing major codon preference. This entails calculated energetic costs of aa biosynthesis and tests for associations between estimated gene expression levels and selection for metabolic efficiency in the proteomes encoded in *E. coli* and *B. subtilis* genomes. This entails the use of the method adapted from Kanaya *et al*. (1999). Identifying major codons through correspondence analysis, within each synonymous family, codons that contribute positively to the major trend in codon usage, MGU, = (number of major codons)/(number of major codons + number of minor codons) in each gene. Recently developed methods that quantify abundances for thousands of different proteins (Washburn *et al*., 2001) will allow tests of energetic selection in the proteomes of a larger number of species. Gene expression can be highly condition dependent, however, and such estimates will need to be obtained for a number of different environments.

Amino acids differ in physiochemical properties and evolutionary substitutability. Zubay (1998) divides aas into three broad categories. "Internal" aas (Phe, Leu, Ile, Met, Val) that have hydrophobic R groups and are generally found in the interior of protein three-dimensional structures. "External" aas (His, Arg, Lys, Gln, Glu, Asn, Asp) have hydrophilic R groups and are most often found in solvent-exposed regions of proteins. Finally, aas that function in either category are classified as "ambivalent" (Trp, Tyr, Cys, Ala, Ser, Gly, Pro, Thr). Akashi & Gojobori (2002) tested correlations for the costs of biosynthesis calculated within exterior, interior, and the ambivalent classes of aas in *E. coli* and *B. subtilis*. G+C pressure was different for integral membrane proteins and non-integral membrane proteins, in which Ile, Ala, Phe, Ser, and Val were affected in integral membrane proteins and Lys, Asn, and Arg in non-integral membrane proteins (Lobry, 1997). The most absolute variations of aa frequencies in the biological range (from 25 % to 75 % range for G+C) for the complete genome were for Ala (± 6.80 %), Gly (± 5.43 %), Leu (± 6.58), Lys (± 20.69), Glu (± 12.04 %), Val (± 6.55 %), Arg (± 13.22 %), Ser (± 8.89 %), Ile (± 7.52 %), Thr (± 6.40 %), Gln (± 5.77 %), Pro, (± 11.62 %), Asp (± 15.0 %), Asn (± 5.0 %), Met (± 7.52 %), Phe (± 7.72 %), Tyr (± 9.40 %), Cys (± 7.72 %), His (6.88 %), and Trp (± 5.48 %). Therefore the study of the influence of G+C content on average amino-acid composition of proteins may not be that informative. Further hydropathy analysis of the aas of *S. fradiae* and *S. coelicolor* showed no common trend (results not included).

The ratio of aas falling into different physiochemical categories may differ among proteins expressed at different levels [e.g., in *S. cerevisiae*, mRNA abundances are lower for integral membrane protein genes than for cytosolic protein genes (Drawid *et al*., 2000)]. However, such differences do not appear to explain reduced energetic costs of highly expressed proteins. Correlations in the abundances of different aas (Karlin & Buchner, 1992) and relationships between aa composition and gene expression (Lobry & Gautier, 1994; Jansen & Gerstein, 2000; Gutierrez *et al*., 1996) have been noted previously in unicellular microorganisms. The analysis of Akashi & Gojobori (2002) indicated that the abundances of many aas also change within broad functional categories of proteins as a function of estimates of translation rates. In both *B. subtilis* and *E. coli*, Trp, Phe, His, Cys, and Leu decrease in frequency in highly expressed genes, and less costly aas such as Glu, Asp, and Gly increase in abundance. These patterns also suggest that simple mutational differences related to

transcription rates do not account for the relationship between costs and codon bias. Amino acids encoded by AT-rich codons (Phe, Tyr, Met, Ile, Asn, Lys) and those encoded by GC-rich codons (Gly, Ala, Arg, Pro) do not show common trends related to gene expression. Figure 5.7a - c would indicate that mutational pressure towards A/T or G/C codon bias may not be the only factor that affects metabolic efficiency. The spectrum of aas from a number of organisms forming a linear scale from A+T-rich to G+C-rich genomes (Figure 5.7 a - c). Although they do seem to show changes in metabolic efficiency they are not as extreme as would be expected. On average, A/T-rich codons tend to encode more costly aas, and G/C-rich less costly aas. Their was an observable trend in G+C-rich organisms i.e., *M. tuberculosis, S. coelicolor, S. fradiae*, and *Micrococcus lysodeikticus* to use low cost aas.

Further assessment of the order of requirement of aa biosynthesis for *S. coelicolor* 1147, *S. fradiae* C373-10, and *E. coli* ML308 shows interesting results for aspartate and tryptophan (positions for *S. coelicolor* 1147 ASP, 7, TRP 17; *S. fradiae* C373-10, *E. coli* ML308, ASP, 12, TRP 19; on average). Aspartate and tryptophan are branch points that have both been implicated in co-factor generation in streptomycetes. The precursor NAD and NADP is synthesised via tryptophan degradation in *S. antibioticus* (Hodgson, 2000). This role was not universal in streptomycetes, as aspartate oxidation (a match for L-aspartate oxidase has been detected in the *S. coelicolor* genome sequence, position SC03382, with 42.9 % identity to *E. coli*) was used by *S. venezuelae* and *S. parvulus* (Lingens and Vollprecht, 1964).

Further analysis is advisable to determine which pathway for NAD and NADP synthesis in streptomycetes is switched on. Why streptomycetes may have evolved to use tryptophan degradation as an alternative to aspartate oxidase is bewildering. Tryptophan show considerable codon bias for the low end of the order of requirement of aas compared to aspartate (see section 5.7). This infers tight regulation of this pathway (see section 8.6). It may then be the case that tryptophan degradation is incorporated when a precursor from the pathway in addition to energy and reducing power are all components of the secondary metabolites, such as actinomycin D (Hitchcock and Katz, 1988) and streptonigrin (Hartley and Speedie, 1984). This would indicate there is a need to take into account precursor supply as well as energy and reducing power production in any strategy to increase antibiotic yields in streptomycetes.

8.4 Metabolic modelling and metabolic fluxes

Estimation of metabolic fluxes based on stoichiometric models is without doubt a valuable and easy-to-use tool. Nevertheless, the uncertainties arising from the assumptions made about imprecisely understood biological functions clearly illustrate the problems associated with a purely stoichiometric flux analysis. Such an analysis is predetermined by the number of assumptions made and the knowledge of the reactions involved. Many reactions in the central metabolism (such as coupling of NADPH formation to biosynthetic requirements, operation of futile cycles, and slippage in membrane energy transduction) are not as yet fully understood in streptomycetes. Therefore the intention of MFA was not to include the cell metabolism in fine, but rather to focus on the most important fluxes present in the cell. As already illustrated, cellular metabolism contains many enzyme systems which are only activated during growth on certain substrates (see section 2.4.2). These pathways were therefore omitted i.e., when cultured on glucose, the glyoxylate bypass (GBP) was considered inactive. However, they are often found to be present in the cell extract, albeit, with a very low activity.

MFA has been reasonably applied to *S. lividans*. The percentage conversion of carbon into product for *S. lividans* (i.e., ACT; tripyrrole undecylprodigiosin RED) appeared to be different under different growth conditions (0, 0.05, 0.10, 0.15 h^{-1}) and carbon sources tested i.e., glucose and gluconate (Avignone-Rossa *et al*., 2002), for example at zero growth rate with glucose as carbon source, 14 % of the glucose was consumed and converted into ACT. This yield decreased to 0.6 % at the highest dilution rate (0.15 h^{-1}), whereas yields of RED ranged from 2.4 % to 0.01 % with gluconate and yield values followed the same trend. However, the values were much lower than those observed with glucose. Average carbon conversion to ACT ranged from 1.6 % to 0.02 % whereas for RED they ranged from 3.3 % to 0.01 %. Avignone-Rossa *et al*. (2002) used the latter data to apply a MFA to a stoichiometric model, to analyse the relationship between primary & secondary metabolism. The distribution of carbon flux through the catabolic pathways was shown to be dependent on growth rate, as well as on the carbon and energy source. Increasing growth rates promoted an increase in the flux of carbon through the EMP and the PP pathway. The synthesis of both ACT and RED was found to be inversely related to the flux through the PP pathway.

Daae and Ison (1999) presented a primary metabolic network for *S. lividans*, but they assumed in their stoichiometric model that isocitrate dehydrogenase was NAD-dependent, which may not be the case. Naeimpoor and Mavituna (2000) carried out MFA on the *S. coelicolor* data of Melzoch *et al*. (1997). The reactions in the network were not given, and only the carbon precursor consumption was mentioned for ACT biosynthesis. Their flux estimates would be different if NADPH consumption for ACT biosynthesis was included. Their results also strongly depend (as for Daae and Ison, 1999) upon the use of the NAD-NADH / NADP-NADPH balance/constraint, which may not be a valid constraint (see section 1.2.3) shown in Chapter 6 & 7 (section 6.7) and Bruheim *et al*. (2002).

Harry Holms (Holms, 1986, 1996, 1997, 2001) strategy of MFA was originally applied to *E. coli* fermentation data. A number of difficulties were met when applying this technique to a streptomycete culture i.e., obtaining consistent calculated data from a flux analysis that fits the experimentally determined CER and closure of the carbon balance/index. From this work it was proposed that this was due to the units of measurement used in the initial calculation. When the units of mmoles.g^{-1} dry wt biomass h^{-1} were used in the construction of flux diagrams, the highest proportion of carbon flux in the streptomycete fermentations was to CO_2 on average 64.07 %. When using the units C.mmoles.g^{-1} dry wt biomass h^{-1} from the outset in the construction of a flux diagram the proportion of carbon flux to CO_2 on average was 39.31 %. The units of measurement showed little effect on the construction of *E. coli* flux diagrams

Further experimental data was required to verify which of the latter calculated CERs were accurate for the latter *Streptomyces* cultures. It was assumed that all the cultures had a low μ and were carbon limited for *S. coelicolor* 1147 and nitrogen limited *S. fradiae* C373-10. Carbon dioxide evolution in relation of carbon source input, it would be expected that the efficiency of CER would follow the same trend as maintenance energy requirements (i.e., nitrogen > carbon > etc.)[see section 6.6.1 – 6.6.7]. Therefore it was conceivable that CER was high for carbon limitation and low for nitrogen limitation. It was therefore not possible from this work to verify which of the models from this Chapter was correct. The measurements made during this fermentation project possibly support the diagrams designed and constructed with units of C.mmoles.g^{-1} dry wt h^{-1} to the best of are knowledge. This was only an assumption at best as further on-line gas analysis was needed to support the flux analysis.

When using the units of C.mmoles.g^{-1} dry wt h^{-1} there was a large proportion of the carbon unaccounted for and when using the units of mmoles.g^{-1}dry wt there was a distortion in calculated fluxes affecting CER. This was possiblely due to the high level of flux through PP pathway bypassing glycolysis. The most probable site of this distortion was at aldolase. This distortion was not observed with the glutamate and oxo-glutarate flux diagrams where aldolase was calculated in reverse direction from biosynthesis and not directly from the carbon source input as the glucose, fructose and glycerol flux diagrams. The considerably high unaccountable carbon was probably a contributory factor that further increased this distortion on average 20 – 30 % (Chapter 5).

To calculate correct fluxes it was necessary to obtain precise measurements of the specific consumption rates and specific production. In this work the physiological studies were carried out in batch culture. In general, fed batch or batch culture are used for industrial production systems. To this end, batch culture was used throughout this work to match the industrial process. The use of batch culture conditions led to large differences in the μ's between similar cultures, large errors in analytical compositional data and an increase in the labour intensity, since it requires more information on the time derivatives of the measured metabolites to be accounted for (section 1.1). Continuous culture would have been more desirable due to the rates being determined from a single but well-established measurement of the substrates and the products at any given μ.

For batch flux-based strategies it was difficult to correlate whether the calculated fluxes were in good agreement (Holms, 1986; Stephanopoulos *et al*., 1998) with the actual realistic fluxes and it would be interesting to measure one or more fluxes from the network (possibly use, tracer studies, and further enzyme assays or possibly intracellular metabolites) to get an impression of the validity of the flux calculations. It is especially important to validate the metabolite balance used for the calculation of the split ratio between fluxes through the EMP pathway and the TCA cycle and PP pathway mainly (i.e., the G6P branch point (G6PDH & 6PGDH) and the PEP & PYR ranch points [PEPC, PEPCK, MDH(dc), PK & PDH]), because NADPH was produced & consumed by a number of reactions that were difficult to quantify. The application of MFA to streptomycetes was further confounded by the number of isoenzymes / or dual co-factor enzymes, for example glucose-6-phosphate dehydrogenase (G6PDH) & phosphogluconate-6-phosphate dehydrogenase (6PGDH). This made any

accurate analysis of the EMP pathway with the PP pathway precarious at best (section 1.2.2) with a co-factor balancing strategy.

The theoretical NADPH requirement for cell growth was calculated from the flux diagrams developed in Chapter 6 and converted to theoretical fluxes. In the glucose, fructose & glycerol fermentations the maximum production of NADPH when the NADP-ICDH was operational (with no alteration to the PP pathway flux) was higher than the theoretical NADPH capacity (section 6.7). This could indicate that the NADP-ICDH in these cultures was not operational, a TH was active or that there were other expensive NADPH-consuming enzyme/enzymes operational. When glutamate was added to the glucose minimal medium, there was a considerable increase in the theoretical NADPH requirement therefore, glutamate could possibly have a stimulatory role on a NADPH producing pathway. The increased NADPH requirement is mainly due to an increase in the FA content of the cell. It was then likely the case that the constructed flux diagrams using the Holms (Holms, 1986) strategy in Chapter 6 were not likely to account for the true carbon flux but the net flux to biosynthesis.

The NADPH requirement of polyketides is known to be of considerable expense to the bacterial cell e.g., 41 mmoles.g^{-1}.nystatin, 12.01 mmoles.g^{-1}.tylosin, 9.48 mmoles.g^{-1}.ACT, 4.34 mmoles.g^{-1}.oxytetracycline, and 7.13 mmoles.g^{-1}.tetracycline (see Chapter 6, section 6.7 for a discussion). In balanced growth equations, the number of available electrons is conserved by virtue of the fact that the amounts of each chemical element are conserved, indicating the degree of reduction could a useful parameter to further assess a material balance (see Chapter 5, section 5.10.3). The degree of reduction (γ) for ACT is 3.94 [calculation based on the definition of Roels (1983), see Appendix D for calculation]. This implies that ACT is slightly more oxidised than, for example glucose ($\gamma = 4.0$) and acetyl-CoA ($\gamma = 4.00$) the precursor for ACT. However, reducing power in the form of NADPH is required for the synthesis of ACT according to an evaluation of the biosynthetic pathway (Bruheim *et al*., 2002). The γ for tylosin ($C_{46}H_{77}NO_{17}$) is 4.87 which indicates that tylosin is more reduced than the majority of carbon sources used for its cultivation in this project (e.g., γ = for glucose, 4.00; glutamate, 3.60; oxo-glutarate 3.60; pyruvate, 3.33; fructose, 4.00; glycerol, 4.67; oleic acid, 5.67; palmitic acid, 5.75 and methyl oleate, 5.68). Therefore NADPH requirements may play a more significant role than for ACT synthesis. It is interesting that a highly reduced carbon source was needed to produce a highly reduced

product such as tylosin, although considering that the γ of the precursors propionate (4.67) and butyrate (5.00) were similar this may be understandable. Other antibiotics show similar trends, where tetracycline and oxytetracycline ($C_{22}H_{24}N_2O_8$) have a γ of 4.09 and 4.00 respectively (Davidson, 1992, quotes an oxytetracycline producing strain of *S. rimosus* when cultured on a complex glucose containing medium had a relative flux of 22.6 % to oxytetracycline). It would be of interest to see if this was a universal phenomenon. If this was the case, the old hypothesis that antibiotic synthesis was an overflow mechanism should be reconsidered. If this was not the case the γ of the carbon source and the product would have been expected to show a measurable deviation between product and interfering carbon substrates. Although further assessment may indicate this is not the case e.g., neomycin ($C_{12}H_{26}N_4O_6$) of 4.17 [interfering carbon source glucose], cycloserine ($C_3H_6N_2O_2$) of 2.67 [interfering carbon source glycerol], streptomycin ($C_{21}H_{39}N_7O_{12}$) of 3.71 [interfering carbon source glucose], cephamycin C ($C_{19}H_{23}N_4O_9S$) of 3.52 [interfering carbon source glycerol], kanamycin ($C_{18}H_{36}N_9O_{11}$) of 4.11 [interfering carbon source glucose], novobiocin ($C_{31}H_{36}N_2O_{11}$) of 4.26 [interfering carbon source citrate{γ = 3.00}], physostigmine ($C_{15}H_{21}N_3O_2$) of 4.53, and chloramphenicol ($C_{11}H_{12}Cl_2N_2O_5$) of 3.27. Which may indicate that further expansion of this technique was needed incorporating preferred carbon sources, excretion products, compositional monomers and products (see Chapter 5, section 5.10.3). Further more this type of analysis shows interesting results for its use as a first step in medium optimisation strategies.

The flux distribution calculated from the present work should therefore be considered as a qualitative approximation that is consistent with the data and our understanding of the organism to date. Although the absolute flux distribution might still be uncertain, the relative differences between the environmental differences were probably realistic estimates.

For matrix algebra approaches, the use of average *E. coli* compositional data has been advocated (Daae & Ison, 1999) as standard for a flux analysis of other organisms (Calik & Ozdamar, 1999 & Calik *et al*., 1999, for *Bacillus licheniformis*; Vallino and Stephanopoulos 1990, *Corynebacterium glutamicum*; Kirk *et al*., 2000, where average *Streptomyces* compositional data was used from *S. coelicolor*, and *S. hygroscopicus* for *S. clavuligerus*; Hua *et al*., 2001, for *Torulopsis glabrata*; Avignone-Rossa *et al*., 2002 for *S. coelicolor*) or the elemental composition of the test organism was used to correct for this from known *E. coli*

compositional data (Hua & Shimizu, 1999 for worked example). This was a dangerous assumption, yes it was/is the case that a comparison of compositional data for *E. coli* with other compositional data shows little impact on estimated fluxes (in particular the aa content)[see section 7.3.1]{Daae and Ison, 1999}. Then balancing carbon input to carbon distribution is then overlooked, which is the most important factor in any material balance. Without undertaking adequate compositional verification a major carbon sink may be therefore overlooked. Although Holms (1986, 1996, 1997, 2001) strategy never undertook such a detailed compositional analysis, it had previously been undertaken to a very high standard by a number of the workers over the past 50 years (Neidhardt, 1990). Using average compositional data may be a flawed approach, if the metabolic system is not well defined, such as in the case of streptomycetes. If average *E. coli* data is used and a similar bioreaction network/model is applied there is little effect on the fluxes. But if a component has not been taken into account compositionally then the acquired data can only be misleading. Both this project & previous research (Davidson, 1992) undertook a comparative analysis strategy to balance inconsistencies between the macromolecular, molecular, & elemental cellular composition (see Chapter 5). The results obtained from both projects did not achieve the desired reproducibility required for such an analysis, this necessitates the need for further work in this area.

The effect of theoretical compositional changes to the constructed matrix algebra BRNE for *S. fradiae* showed little effect on the estimated fluxes (section 7.3.2). A hypothesis was then made using data collected in Chapter 5, that the synthesis of aas of a number of pathways does not alter the redistribution of aas families, which in turn shows little overall impact on estimated fluxes. It may therefore be concluded that the changes in the biomass composition of an organism for example by codon bias will have little or no impact on the primary metabolic fluxes.

Theoretical changes to the NAD/NADPH dependencies on the BRNE showed the greatest effect on the calculated fluxes (section 7.3.3). The highest differences were observed for the reaction sequences for oxidative phosphorylation and ATP dissipitation. This would indicate that altering ISE activities will have the greatest impact on measured fluxes for both flux-based strategies used throughout this work. The latter work indicate that fluxes alter between

15 - 40 % with changes to the NADPH producing enzymes (i.e., NADP-G6PDH, NADP-6PGDH, NADP-ICDH, MDH[dc]). This would indicate that co-factor balancing would lead (section 1.2.3) to grave inaccuracies in any MFA strategy for the analysis of streptomycete metabolism.

The estimated fluxes through the CMPs of *S. fradiae* C373-10 using matrix algebra for model 1 unexpectedly indicated negative values around the TCA cycle. This would indicate the cycle was running in the reverse direction or the metabolic costs of co-factor supply could not be met by the present bioreaction network. Model 2 offers the best-fit model to the experimental data for a number of reasons, calculated sensitivities fit with that measured by other workers. There were no negative values for fluxes around the TCA cycle. It was therefore hypothesised that the multi-phasic nature & the number and use of isoenzymes throughout a streptomycete batch culture makes any solution of the biosynthetic demand of flux cumbersome at best with the flux-based strategies used in this work.

Further assessment of the EMP/PP pathway and PK/PEPC branch points with enzyme assays. Indicate that the flux through the PP pathway was possibly close to the percentage flux through the PP pathway when corrected to the theoretical NADPH requirement [PPP (3) as Chapter 6]. The enzyme activity ratios were on average 1 : 1 for PK/PEPC nearing the end of the culture this was not consistent with the flux based diagrams for the Holms strategy or the matrix algebra approach, this would indicate the flux through the PYR & PEP branch points would need a finer tuned flux analysis strategy.

It was believed at the start of this work that the incorporation of Holms strategy (Holms, 1986 [Chapter 6]) for flux analysis or matrix algebra strategies (Vallino, 1991 [Chapter 7]) could offer a good system of analysing metabolic networks and the biosynthetic demand for streptomycetes. Although the use of the latter methods / strategies (Holms, 1986 [Chapter 6]; Vallino, 1991 [Chapter 7]) with batch culture were cumbersome to apply. The use of tracer studies such as undertaken by Christiansen *et al*. (2002) may offer a more robust method of analysing metabolic networks in batch and continuous culture in addition to the possibility of quantifying futile cycling around the PEP and PYR branch points (section 6.10). Then the use of ^{13}C quantification studies for flux-based analysis may be a more appropriate. Tracer study approaches with ^{13}C utilising atom mapping matrices (section 1.2) could account for the split

between the PP pathway, the EMP pathway, and the TCA cycle, plus they also offer the capability to account for futile cycling involving MDH[dc], PEPCK, PEPC and PK. Since no net fluxes are associated with futile cycles, the activity cannot be assessed by traditional approaches of metabolite balancing (see section 1.2)[Holms, 1986, 1996, 1997, 2001; Aiba & Matsuoka, 1979; Vallino, 1991; Stephanopoulos *et al*., 1998]. Enzyme studies undertaken in Chapter 6 (section 6.8) in conjunction with co-factor balancing work (section 6.7 & 6.8) indicated that futile cycling was a factor that should be considered when studying streptomycete metabolism in the future.

The use of continuous culture has been recommended throughout this project as a better system to apply a flux analysis strategy to. The main reasons for this are as follows:

(1) The multi-phase nature of batch culture with the addition of not being able to account for isoenzyme activity (i.e., not being able to set an accurate percentage branch point split) throughout the culture make any flux analysis strategy cumbersome to apply (see Chapter 4 - 7).

(2) Continuous culture needs to be used to obtain a better statistical verification, measure of and reproducibility of the compositional data obtained (see Chapter 5 & 8, section 8.3).

(3) Although batch culture generally produces higher antibiotic titers against continuous culture. In the case of *S. fradiae* continuous would have achieved higher antibiotic yields for glucose minimal media as this medium was originally developed in house at Eli Lilly Ltd. for continuous culture (section 8.1).

(4) The high accumulated sensitivity for the μ, uptake and secretion of measured metabolites could be reduced through the use of continuous culture and in turn reducing the accumulated sensitivity of the system (see section 7.3.1).

Flux analysis has been much promoted in the literature as an important tool in the optimisation of fermentation processes. The basic idea is to establish a quantitative picture of all of the major metabolic fluxes in the cell by analysing the uptake and secretion of metabolites during the course of a fermentation (Holms, 1986; Gram, 1997). Experience from this work indicates that a flux analysis as such, is of little value because it relates too specifically to the one process being scrutinised. Even more importantly, the results that make the large difference are found in the initial phases of the flux analysis, from the construction of a bioreaction network.

Despite the tenor of the preceding discussion, it was not the intention to advocate the avoidance of material balancing based analysis but, rather the wish to enhance the awareness of its limitations and to avoid assumptions about metabolic function whenever possible.

8.5 Recommendations & possible sites for inter-convention

It was difficult to identify possible areas of regulation of flux to ACT or tylosin production because the estimated flux to antibiotic synthesis was considered too small to be significant (section 6.4). However, an attempt was made to highlight sites of inter-convention to increase flux to ACT (via acetyl-CoA) or tylosin [via acetyl-CoA, propionyl-CoA, ethylmalonyl-CoA, and methylmalonyl-CoA](and therefore increasing the volumetric productivity). The use of fermentation profiles, compositional data and the constructed flux diagrams (Chapters 4, 5, & 6, Tables 6.1 – 6.29, Figures 6.1 – 6.25) with an in depth literature search (Chapter 2) of the streptomycete central metabolic pathways (CMPs). The flux diagrams constructed in Chapter 6 and enzyme assays, would indicate that the fluxes through most of the central metabolic enzymes were decreased during secondary metabolism but there was an increase through PEPC at least by two-fold. This would indicate PEPC as a possible candidate enzyme involved in secondary metabolism. It has been suggested that PEPC may have a role in the provision of metabolic precursors or energy for production of secondary metabolites (Dekleva & Strohl, 1988b).

Overexpression of PEPC in *E. coli*, Millard *et al*. (1996) enhanced the production of succinic acid. The average amount of succinic acid increased from 3.27 to 4.44 gl^{-1} when the carboxylase was induced. Additionally, the enzyme activity has been amplified in *Brevibacterium glutamicum* and in *C. glutamicum* (Sano *et al*., 1987; O'Regan *et al*., 1989; Delaunay & Uy, 1999). Through increasing the activity of PEPC by 50 % in *B. glutamicum*, Sano *et al*. (1987) increased the production of proline and threonine by 71 % and 12 %, respectively. O'Regan *et al*. (1989) increased lysine production by 10 - 15 %. Furthermore, PEPC activity appears to be essential for glutamate synthesis in *C. glutamicum* (Delaunay & Uy, 1999)[producing glutamate under biotin limitation, incorporating a strategy to increase cell glutamate permeability using penicillin or Tween 80]. It is most active at the beginning of the glutamate excretion phase and the interruption of the gene coding for PEPC significantly disrupts glutamate production. However, amplifying and enhancement of PEPC by at least 45

%, results in no significant recovery of glutamate production. The over expression of PEPC enzyme of *S. coelicolor* did not enhance ACT production (Bramwell *et al*., 1993). The role of PEPC activity during secondary metabolite biosynthesis thus remains unclear. Rickets (2000) reported enhancement of PEPC has increased the production of oxytetracycline in *S. rimosus*, although the overexpression strategy used proved to be unstable.

The question then has to be asked, can an increase in activity of one enzyme during the idiophase, solely mean that PEPC is directly involved in the supply of precursors to antibiotic synthesis? The case could be argued that the organism is redirecting carbon storage compounds in a low nutrient environment to maintain a dynamic equilibrium balancing energy and reducing power. Where in the case of primary metabolite producing organism i.e., the production of aas, increasing PEPC activity shows direct returns, up to a point until there is feedback in the regulation. Although feedback regulation is often removed through the use of auxotrophic mutants (i.e., homoserine dehydrogenase for *C. glutamicum* for lysine over production). Then viewing over expression of PEPC and increased productivity as the phenomenon of one enzyme on metabolism maybe is a misnomer.

It must be remembered that metabolic control is shared between enzymes: "*enzymes are democratic, not aristocratic"* (Stephanopoulos *et al*., 1998; Kacser & Burns, 1973). In most cases, the over expression of a single enzyme will exert a minimal effect upon flux. Instead, significant increases in flux are more likely to be achieved by coordinated increases in the levels of groups of enzymes, or bottlenecks close to the end of secondary metabolic pathways. The consequences of this democratic architecture is that the groups of enzymes will significantly increase in complexity as one differentiates between increasing primary metabolite yields to secondary metabolites. This principle has been elegantly demonstrated for aromatic aa biosynthesis in Yeast (Niederberger *et al*., 1992), and penicillin biosynthesis in filamentous fungi. The small value of flux control coefficients (section 1.3) in long pathways explains why so many successive rounds of mutation and selection steps usually are needed in order to improve strains for the production of metabolites such as aas and antibiotics.

In most organisms i.e. *E. coli* & *C. glutamicum* the PEP branch point is rigid or tightly regulated. Under nominal conditions, PEP preferentially enters the PK branch due to its

higher affinity for PEP. With PEPC being inhibited by aspartate (see section 2.5.6) in many bacteria, brought about by the low affinity of aspartate kinase (AK) for its substrate. Then any attempt to redirect the flow of carbon into the PEPC branches will cause an increase in aspartate concentration. Consequently affecting carbon flux through AK, results in PEPC inhibition and a drop in the PEPC branch split ratio. Vallino (1991), undertook a flux analysis of *C. glutamicum*, using kinetic modelling and nodal simulation of the PEPC branch point. It was reported that under normal conditions, PEP preferentially enters the PK branch due to its higher affinity for PEP. Any attempt to redirect the flow of carbon into the PEPC branch caused an increase in aspartate concentration due to the low affinity of AK for its substrate, and a drop in AcCoA concentration due to the high activity of CS. The combination of high aspartate and low AcCoA concentrations resulted in synergistic inhibition of PEPC activity and a precipitous drop in the PEPC flux. The net result of attempting to increase the PEPC split ratio by blocking or reducing activity of the PK branch, was the attenuation of both branches, hence, the PEP node was strongly rigid. Furthermore, even if the ASP inhibition of PEPC was removed, the kinetics of PK and AK still rendered the PEP node weakly rigid. It was postulated that the rigidity of the PEP node could be circumvented by transforming *C. glutamicum* with a PEPC enzyme that is not inhibited by ASP or requires AcCoA activation. The simulations indicated that *C. glutamicum* transformed in this manner might also excrete aspartate due to the low activity of AK (consequently, amplification of AK might also be necessary).

Kang *et al*. (1987) & Kang and Lee (1987) reported similar rigidity of the *S. fradiae* PEP branch point. It was found that cell growth and tylactone formation was controlled by the metabolic flux of oxaloacetate. It was clear that cell growth was favoured by the activities of PEPC, CS and aspartate aminotransferase (ASAT), while tylactone synthesis was stimulated by the activity of methylmalonyl-CoA carboxyltransferase (MMCT)[section 2.10]. Further assessment of the role of glutamate and oxo-glutarate (OGA) on the activity of these enzymes indicated that if glutamate concentration was increased, biomass yield increased, ASAT activity increased, PEPC activity decreased, MMCT activity decreased, and tylosin productivity decreased. If OGA concentrations were increased, biomass yield decreased, had little effect on ASAT activity, PEPC activity decreased, had little effect on MMCT activity, and possible increased tylosin productivity. It was clear that the activity of ASAT was not regulated by OGA, while the enzyme level was very closely regulated by glutamate

concentration. These results must be interpreted carefully. The medium used contained glucose, glutamate, and methyl oleate and of all the activities were determined three days into a culture. Methyl oleate consumption initiated only after two days. This would indicate that PEPCK and MDH(dc) should have been active as well. Therefore to determine the rigidity of the PEP branch point in streptomycete metabolism further enzyme analysis needs to undertaken. Although it could be concluded that the negative effect of glutamate (the final concentration of tylosin was reduced with addition of more than 20 gl^{-1} of glutamate) on the tylosin titer resulted from the over-activity of ASAT, by which more oxaloacetate, an essential intermediate, was converted to aspartate rather than to MMCT and tylosin precursors. Therefore any increase in PEPC activity may deliver little return in tylosin productivity without an increase in the rigidity of the ASAT branch point. This could be brought about by over expressing a PEPC enzyme that lacks regulation by AcCoA and/or aspartate and increasing the rigidity of the ASAT branch point. Gene silencing strategies using antisense RNA could be a strategy to test this hypothesis. Silencing of gene expression by transcription of an artificial antisense construct has been employed successfully with fungi (Kitamoto *et al*., 1999; Zhang *et al*., 1998). This approach is particularly useful when the target gene is represented by multiple copies of the genome or when complete disruption of the gene function is lethal or gives an undesirable phenotype. Antisense expression of a portion of the gene encoding the major carbon catabolite repressor CREA in *Aspergillus nidulans* resulted in a substantial increase in the levels of glucose-repressible enzymes, both endogenous and heterologous, in the presence of glucose (Bautista *et al*., 2000). The depression effect was approximately one-half of that achieved in a null *cre*A mutant. However, growth parameters and colony morphology in the antisense transformants were not affected. A project is being undertaking in this laboratory entailing increasing the activity of PEPC in *S. coelicolor* 1147 & *S. fradiae* C373-10. Further purification and kinetic analysis of this enzyme needs to be undertaken to assess how rigid the regulation of the PEP branch point is in streptomycete metabolism. It also would be of interest to carry out further enzyme activity analysis and intracellular metabolite analysis under a number of different growth conditions to assess further the potential regulation points of the PEP branch point, i.e., with a pulsed continuous culture strategy.

Effectorless PEPC enzymes can be found in organisms that utilise radically different metabolic control architectures, such as those using photosynthesis. In particular, the

C*yanobacterium* s*ynechococcus* spp. was reported to harbour such an enzyme (Vallino, 1991). Further simulation strategies should be undertaken to indicate by how much the enzyme should be amplified by, so that it can compete effectively with PK for PEP. A slightly different approach to circumventing this feedback inhibition would be to transform *S. coelicolor* or *S. fradiae* with a gene that encodes pyruvate carboxylase [section 2.5.8] that is similarly resistant to the effects of aspartate and AcCoA. This approach is quite promising since it effectively removes the PEP principle node and localises the flux partitioning control at the pyruvate node. Furthermore if transient flux-based experiments were, undertaken with a inhibitor such as arsenate, the extent pyruvate accumulation could be determined. If the affinity of pyruvate dehydrogenase complex for pyruvate is relatively weak, semi-de-regulation of this branch point could be achieved. Pyruvate carboxylase enzymes with the desired properties have been reported in strains of *Pseudomonas* (i.e., methylotroph *Hyphomicrobium methylovorum*)[Yoshida *et al*., 1995], as well as in *Brevibacterium lactofermentum* (Tosaka *et al*., 1979).

Enzyme studies undertaken in Chapter 6 show the enzymes around the PEP branch point show particularly interesting variation. In *S. coelicolor* 1147 (Fig 6.28a), pyruvate kinase activity rose quickly to a maximum value during the 0.0 – 96 hr period, when the medium glucose concentration was high (see Chapter 4 for fermentation profiles). Below a certain minimum level of medium glucose concentration (0.8 gl^{-1}; fermentation profiles not included for shake flask experiments), the activity of this enzyme fell quickly. MDH[dc] exhibited high activity while high external glucose concentrations were extant, but activity decreased with falling glucose concentration (probably in response to falling availability of glucose-derived metabolic intermediates). PEPC activity rose steadily throughout the growth cycle, attaining a maximal activity throughout the production phase coincident with the high activities of the relevant PP pathway enzyme activities. At 96 hrs into the cultivation the activities of PEPC, PK, & MDH[dc], indicate a considerable proportion of cyclic activity. This could be due to the process being a batch culture.

A strategy to redirect futile cycles towards the formation of NADPH could be a worthwhile investigation as the NADPH requirement for polyketide biosynthesis is of considerable expense to the bacterial cell. Enzyme activity studies undertaken in Chapter 6 (section 6.8) indicated that futile cycling of four carbon unit containing metabolites (PEPC and MDH[dc])

increased two to three days after the beginning of the culture period (Figure 6.26). The extent of flux through these pathways could not be determined with the work undertaken here i.e., enzyme studies or MFA (Chapter 6 & 7). An approach to increase futile cycling, could be induced by the simultaneous overexpression of PEPCK and PEPC or MDH[dc] and PEPC. Generally these enzymes are maintained at a low level (Chambost & Fraenkel, 1980; Chao & Liao, 1994; Daldal & Fraenkel, 1983) in *E. coli*. In *E. coli* and *B. subtilis*, relative PEPCK fluxes are usually well below 30 % of the glucose uptake (Dauner *et al*., 2001a,b; Daldal & Fraenkel, 1983; Sauer *et al*., 1997, 1999). The sole exception is for *C. glutamicum*, for which the PEPCK flux of about 70 % of the specific glucose uptake rate reported for carbon-limited chemostat culture at D = 0.1 h^{-1} (Peterson *et al*., 2000).

Another possible site of intervention highlighted by this work was glucose-6-phosphate dehydrogenase (G6PDH) and 6-phosphogluconate dehydrogenase (6PGDH)[see section 2.5.4]. Enzyme assays undertaken in Chapter 6 (section 6.8) show evidence for dual co-factor specificity (i.e., NAD & NADP) or two isoenzymes for G6PDH & 6PGDH (Figure 6.27). *S. coelicolor* 1147 and *S. fradiae* C373-10 both show similar trends in co-factor specificity, although the NAD specificity was reduced in *S. fradiae* cultures. Enzyme activity studies with *S. coelicolor* producing methylenomycin (Obanye, 1994; Obanye *et al*., 1996) have reported similar evidence for two 6PGDH isoenzymes. Obanye (1994) reported for *S. coelicolor* that NADP-G6PDH was favoured during the growth phase, and increased activities of transketolase and NAD-G6PDH was favoured during the antibiotic production phase. There were no significant variations in the NAD- or NADP- 6PGDH activities over the growth cycle (1 : 1 ratio). It was proposed that increased activity of these enzymes was a response to the fall in carbon flux through the EMP pathway which, itself, was signified by the fall in pyruvate (Obanye, 1994; Obanye *et al*., 1996).

Knocking out the isoenzymes that generate NADH in favour of NADPH production would lead to an excess of NADPH that could be pushed to antibiotic production (if a TH was not active). If G6PDH and 6PGDH were single species with dual co-enzyme specificity, then a foreign gene could be introduced that favours NADPH production. This would increase the levels of NADPH for antibiotic production; which is believed to be high for polyketide biosynthesis (see section 8.2), and the reduction in NADH synthesis may in turn push more carbon from organic acid excretion to antibiotic synthesis. Oxygen limitation is considered to

affect the kinetics of dehydrogenases in the TCA cycle, where an increase in favour of NADPH production may alleviate this. Claudio Avignone-Rossa postulated that knocking out NAD-G6PDH & NAD-6PGDH activities would increase the NADPH supply to antibiotic production for *S. coelicolor* (unpublished results; personal communication Claudio Avignone-Rossa).

An alternative approach could be to use benzothiocyanate (BT), which was used effectively in *S. aureofaciens* fermentations to stimulate chlorotetracycline and tetracycline synthesis (Behal *et al*., 1983). BT influences low-producing strains more than high producing strains. The action of BT has been hypothesised to influence the synthesis of G6PDH and other dehydrogenases in the tetracycline biosynthesis pathway. Enzyme synthesis was apparently inhibited as the enzyme activity in vitro was not influenced; it was concluded that it affected the NAD dependent G6PDH (Behal, 1987). Hence if this effect was universal in streptomycetes, it could offer a quick method of observing the effect of increased NADPH production on secondary metabolism. However, the analysis would need to be carried out on a number of strains from the parent to the production strain.

Enzyme studies undertaken in Chapter 6 (section 6.8) indicated that glutamate may have a possible stimulatory role on NADPH-producing pathways. This correlates with the calculation of an increased demand of carbon to biosynthesis, and with an increase in the theoretical NADPH requirement, and an increase in the flux to lipid biosynthsis and acetate excretion calculated from flux diagrams in Chapter 6. The most probable candidate was MDH[dc]. It was difficult to judge how carbon and nitrogen sources affected the CMPs without further analysis. In *B. flavum* it has been reported that glutamate induces MDH[dc] (Mori & Shiio, 1987)[see section 2.5.9). The activity of the enzyme directly paralled the activity of FA synthesis pathways in *S. aureofaciens* which was active only during the growth phase (Behal *et al*., 1969). Glutamate was a major component of the industrial complex medium for tylosin production (section 3.7.3), therefore it could be postulated that the positive effect of glutamate on MDH(dc) and the NADPH requirements were important for tylosin production. Kang & Lee (1987) reported evidence that the biomass concentration of *S. fradiae* fermentation increased with increasing glutamate : glucose ratio. It would be beneficial to extend this work with further enzyme assays (i.e., MDH[dc], PEPC, PEPCK, & PK) to determine the effects of glutamate and other aas on the PEP branch point. This could be undertaken with changes of

the glutamate concentration of the industrial production medium (section 3.7.3) and the glucose to glutamate (or appropriate aa) ratio for the literature based methyl oleate defined medium (section 3.7.2).

If the formulated defined media used in this work had yielded adequate antibiotic yields, the relative contribution of NADP-dependent enzymes to antibiotic synthesis could have been researched further. The strategy would have been to measure the effects of NADPH requirements between primary metabolism & secondary metabolism. For example this could have been tested in a stepwise fashion by using a combination of carbon sources, e.g., glucose and xylose, and two nitrogen sources, NH_3 and nitrate. The metabolism of xylose and nitrate requires additional consumption of NADPH (Zubay, 1998; Michal 1999; standard texts for metabolic pathways). Xylose, is reduced to xylitol, using NADPH as the electron donor. Xylitol is subsequently oxidised to xylulose using NAD as electron acceptor. Finally, xylulose is phosphorylated to xylulose-5-phosphate, which is catabolised further via the PP pathway. This implies that, when the cells are grown on xylose as the sole carbon source for each mole of xylose consumed, 1 mole of NADPH is oxidised and 1 mole of NADH is reduced. When nitrate is used as the nitrogen source, it has to be reduced to NH_3 through the action of nitrate and nitrite reductase. The co-factor can be either NAD or NADPH (section 2.8). Therefore, the impact of nitrate reduction on NADPH demand is not known exactly. In the worst-case scenario 4 moles of NADPH are required for the reduction of 1 mole of nitrate; in the best-case scenario, only 1 mole of NADPH and 3 moles of NADH are required. This analysis could be carried out in batch or continuous culture with differing combinations of the two C & N sources (glucose & NH_3 [1; co-factor cost or best average]; xylose & NH_3 [2]; glucose and NO_2 [2.8]; xylose and NH_3 [3.8]). With the systematic measurement of biomass & antibiotic yield it would therefore be possible to test if NADPH has a deleterious effect on biomass composition, production and antibiotic yield. Hypothetically a diminishing response to the differing medium compositions would be expected. If the latter media were rerun with the addition of glutamate and there was a significant stimulatory effect on NADP-producing pathways, then there would be measurable positive effects on biomass production, composition & antibiotic yield. Hence the role of co-factor supply/regeneration could be evaluated.

Although no significant tylosin yield was achieved in this work with minimal and defined medium formulations, there was a significant increase in the demand of carbon for biosynthesis when glutamate was used as an additive to the glucose minimal medium for *S. fradiae* C373-10 (section 3.6.4). Where excess NADPH was probably converted or pushed towards preparatory pathways (carbon storage), as overflow metabolism. If antibiotic synthesis had been initiated, the excess NADPH might have been pushed to antibiotic synthesis, which would have indicated that antibiotic synthesis was possibly an overflow mechanism for when co-factor levels were too high. Therefore the accumulation kinetics of other metabolites, the production of which might involve the utilisation of NADPH, should be studied in *S. coelicolor* 1147 and *S. fradiae* C373-10. An investigation would be particularly important of FA biosynthesis. If such biosynthesis was most significant towards the end of growth, simultaneously with that of idiolite synthesis, it would suggest that the metabolic changes observed using flux-based analysis and enzyme studies correlated with radio respiratory studies undertaken by Obanye (1994)[Obanye *et al*., 1996 and this work] for *S. coelicolor* (section 6.8). These did not result specifically in idiolite production, but displayed the necessity to synthesise a large battery of NADPH-dependent metabolites. This could be confirmed using mutants that are null for antibiotic production (such as SCP1$^-$ that would encode methylenomycin for *S. coelicolor*). If null mutants gave rise to a failure to observe increase in the flux through the NADP producing pathways during the latter part of the growth cycle, this would suggest that this flux increase observed in the antibiotic producing strains was specifically associated with antibiotic production. If the NADP producing pathways were still active and the NADPH expensive secondary metabolites were produced, this may indicate that antibiotic synthesis was the result of overflow mechanism due to high NADPH levels. It is my personal belief that the elimination of antibiotic producing capability will have little effect on the metabolic kinetics. Rather antibiotic production is probably representative of a more global phenomenon.

Further enzymatic studies of the nitrogen uptake pathways would have complemented this work i.e., NAD-GDH, NADP-GDH, and GS and GOGAT. *S. fradiae* contains both a NAD and NADP-GDH activity (Hodgson, 2000)[section 2.9.3]. The NADP-dependent GDH is believed to be active in anabolism and the NAD-GDH active in catabolism. This information might be used to modulate NADPH concentration, e.g., induced at high NADPH

accumulation if the PP pathway flux is simultaneously reduced. Without this data, it can only be speculated that an NADP-dependent GDH was active.

If the rationale holds that shifting the cellular metabolic economy to increase NADPH producing pathways increases antibiotic synthesis. Marx *et al*. (1999) researched the shift in metabolic demand through an over expression of the NADH-GDH gene of *Peptostreptococcus asaccharolyticus* incorporating ^{13}C atom mapping matrices. Although this enzyme normally serves to degrade glutamate, it is able to substitute for the missing biosynthetic route in *E. coli* mutants, replacing the normal NADPH-coupled synthesis step with one coupled to NADH pool (Snedecor *et al*., 1991). This offers a number of problems in streptomycete research where an isogenic strain needs to be constructed, which in the case of *S. fradiae* will be hampered with two forms of GDH already being present. Codon usage bias between the organisms is an inherent problem of expressing foreign genes in streptomycetes. The *P. asaccharolyticus* NADH-GDH gene, has a G+C content of 36 % which is typical of the DNA composition of the organism (32 % GC). The codon usage is therefore very biased. Nearly 77 % of the third-position choices are A's or T's. Many of the codons are rarely used in strongly expressed *E. coli* and *Streptomyces* genes, yet a high level of expression was reported in *E. coli* (Snedecor *et al*., 1991). Marx *et al*. (1999) applied this concept, in which NADPH fluxes were quantified in an L-lysine producer of *C. glutamicum* grown into metabolic and isotopic steady state with [1-^{13}C] glucose. In this case, where the organisms NADPH-dependent GDH consumes reducing power, the NADPH flux generated was 210 % (molar flux relative to glucose uptake rate) with its major part (72 % of the total) generated via the PP pathway activity. An isogenic strain in which the GDH of *C. glutamicum* was replaced by the NADH-GDH of *P. asaccharolyticus* was made and the metabolite fluxes were again estimated. The major response to this local perturbation was a drastically reduced NADPH generation of only 139 %. Most of the NADPH (62 % of the total) was now generated via the TCA cycle activity. This indicates the extraordinary flexibility of CMPs and provides a picture of the global regulatory properties of the CMP of *C. glutamicum.* It would of interest to determine if this flexibility of the CMPs has evolved in the same manner in *Streptomyces*.

A number of organic acids were produced by *S. fradiae* C373-10 cultured on a number of different carbon sources. The organic acids detected were acetate, malate, pyruvate, oxo-

glutarate, propionate, butyrate, and fumarate. The reason why they were produced is as yet unknown (see section 4.6 for discussion). Comparing increased tylosin production with the availability of tylactone precursors in the industrial complex medium indicated 60 % of the available carbon was contained in acetate and 5.5 % in propionate and butyrate. If antibiotic precursor supply was considered as a rate limiting issue (section 4.6.1). Then increasing enzymes involved in butyryl-CoA synthesis may offer a return i.e., via ethylmalonyl-CoA or increasing enzymes involved in propionyl-CoA and methyl-malonyl-CoA formation i.e., propionyl-CoA carboxylase could also be considered as sites for intervention.

For any yield enhancing strategy there must be a balance between precursor supply and co-factor availability (i.e., energy production and reducing power). How this balance is controlled in *Streptomyces* is open to conjecture (see Chapter 2, 6, 7 & section 8.4). Most current metabolic engineering studies have focused on enzyme levels and on the effect of the amplification, addition, or deletion of a particular pathway supplying the desired precursor. Although it is generally known that cofactors play a major role in the production of different fermentation products, their role has not been studied thoroughly and systematically. It is conceivable that in cofactor-dependent production systems, cofactor availability and the proportion of cofactor in the active form may play an important role in dictating the overall process yield. Hence, the manipulation of these cofactor levels may be crucial in order to further increase antibiotic production.

San *et al*. (2002) demonstrated the manipulation of cofactors with *E. coli,* could be achieved by external and genetic means. The NADH/NAD ratio can be altered experimentally by using carbon sources with different oxidation states. Furthermore the metabolite distribution can be influenced by a change in the NADH/NAD ratio as mediated by the oxidation state of the carbon source used. It was also demonstrated that the total level of NADH levels can be increased by over expression of the *pnc*B gene (pyridine nucleotide cycle; nicotinate phosphoribosyltransferase). The increase in the total NADH levels can be achieved even in a complex media. Anderlund *et al*. (1999) & Nissen *et al*. (2001) studied the physiological effect of the conversion between the NADH and NADPH coenzyme systems in *S. cerevisiae* expressing the membrane-bound TH from *E. coli* (*pnt*A and *pnt*B) and *Azotobacter vinelandii* (soluble TH predominant equilibrium in the direction of NADH). The objective was to determine if the membrane-bound TH could work in reoxidation of NADH to NAD in *S.*

cerevisiae and thereby reduce glycerol formation during anaerobic fermentation. Membranes isolated from the recombinant strains exhibited reduction of 3-acetylpyridine-NAD by NADPH and by NADH in the presence of NADP, which demonstrated that an active enzyme was present. However, unlike *E. coli* most of the TH activity was not present in the yeast plasma membrane, rather, the enzyme appeared to remain localised in the membrane of the endoplasmic reticulum. During an anaerobic glucose fermentation it was observed that the formation of oxo-glutarate, glycerol, and acetic acid in a strain expressing a high level of TH was inceased, which indicated that increased NADPH consumption and NADH production had occurred. The intracellular concentrations of NADH, NAD, NADPH, and NADP were measured in cells expressing TH. The reduction of the NADPH pool indicated that the TH transferred reducing equivalents from NADPH to NAD.

Depending on the intracellular concentrations of NADH, NAD, NADPH, and NADP, NADH can be consumed and NADPH can be produced by the TH (studied by NMR and fluorescence spectroscopy incorporating measurement of the redox potential). Therefore if TH activity was expressed in a streptomycete, it might result in a decrease in organic acid production and a decrease in carbon flux through the PP pathway, where there is a loss of carbon in the form of carbon dioxide. The reduction in organic acid formation and the reduction in carbon dioxide could then be directed towards product formation. This is only likely to increase secondary metabolite synthesis if the PP pathway is not the major route of flux of carbon to secondary metabolism. The biosynthesis of bialaphos produced by *S. hygroscopicus* has been linked to flux through the EMP and TCA cycle and activation of the GBP (section 2.5.10)[Takebe *et al*., 1991]. The major role of organic acid excretion has been postulated to assist in maintaining the redox balance of the cell, whereby surplus NADH formed in cellular anabolic reactions is reoxidised to NAD. It could therefore be of benefit to overexpress TH in *Streptomyces* metabolism converting excess NADH to NADPH. The problem with this approach is NADH will be in short supply in the production phase, when the TH will favour the reverse of the formation of NADH. This may be detrimental to antibiotic production of NADPH-rich secondary metabolites. It would be of particular benefit in future streptomycete research to determine the effects of co-factor supply on antibiotic production

8.6 Streptomycete primary metabolism: some interesting conclusions on supply and demand

Streptomycetes appear to be facultative oligotrophs. The control of primary metabolism may be taken as a reflection of the ecological niche of these bacteria. Streptomycetes normally live in soil, which is a competitive environment. Soil is dependent on plant productivity for input of nutrients, and plants tend to be carbon-rich (due to the ready availability of CO_2 fixation, but nitrogen-limited). The saprophytic streptomycetes will have evolved to adapt for survival in this nitrogen limited environment. Thus enteric bacteria might be expected to have more coordination control mechanisms than soil bacteria.

Examination of the control of CHO catabolism reveals a plethora of inducible CHO catabolite systems, including extracellular enzymes for degradation of insoluble polymers, some to gain access to utilisable compounds, some to release such compounds, and transport systems for soluble products of digestion and intracellular catabolite pathways. The wide range of catabolic pathways observed and studied reflects the wide-range of utilisable CHO substrates available in soil. The multitude of catabolite systems in the streptomycetes, and the CHOs resources available in soil, implies a strong need for coordinated control of CHO catabolism. This appears to be reflected in the carbon catabolite repression system in streptomycetes (section 2.4.2). This system, while not yet well understood and different from what is found in other bacteria, is clearly widespread and wide ranging in this control. An interesting observation was made when examining CHO transport. Constitutive permeases have low affinity but high capacity (Hodgson, 2000). The low-affinity permeases probably reflect again the relatively CHO abundant conditions. If CHO polymers are being degraded *in situ* then it would be expected relatively high local concentrations of mono-saccharides. Amino acid transport, on the other hand, appears to utilise mainly high-affinity transport systems (Hodgson, 2000), which can be rationalised by the relatively deficient aa environment.

The most unusual characteristic of aa biosynthesis in streptomycetes is there rarity of feedback gene repression by the product of the pathways (Hodgson, 2000). It should be noted that in a number of cases stimulation of gene expression rather than repression was seen when the cognitive aa was added to the medium. End product control has been recognised in *S. coelicolor* and *S. fradiae* (Potter & Baumberg, 1996; Vancura *et al*., 1989) for Ile, Val, Leu,

and Thr. A similar absence of repression of aa biosynthesis has been seen in *Caulobacter crescentus* (Ross and Winkler, 1988). This Gram-negative bacterium also lives in a low nutrient environment i.e., ponds and rivers. There was evidence that cysteine biosynthesis was tightly regulated (Bellofatto *et al*., 1984) which might not be surprising as this aa was involved in carbon, sulphur and nitrogen metabolism and is one of the most expensive aas synthesised. The isolation of methionine overproducing mutants of *S. fradiae* using the analogue ethionine would imply that methionine metabolism is regulated and the system can be altered by mutation, but it need not mean there is gene regulation; i.e., feedback repression or attenuation (Hodgson, 2000).

There is evidence that the regulation of the late genes of tryptophan biosynthesis for *S. coelicolor* was not via feedback repression, but as a response to the growth rate and growth phase of the culture (Hu *et al*., 1999). Maximal expression of the *trp*D, *trp*C, & *trp*BA genes occurred in the early exponential phase. Therefore, tryptophan biosynthesis was subjected to a global regulatory system, whereby maximal production was correlated with maximum need, i.e., when the cell was growing at its fastest. Proline biosynthesis was not subject to similar regulation in *S. coelicolor* (Hodgson, 2000).

It appears that half of the pathways for aa and nucleotide catabolism are inducible and around half the others are expressed at low levels and constitutive. This raises the interesting question: how do streptomycetes avoid futile cycling of aas? Unfortunately because the enteric bacteria and other copiotrophs have been studied so well, there is tendency to think that the absence of such systems is a problem for streptomycetes, rather than appreciate that the physiology of enteric bacteria and streptomycetes is bound to be different. In other words, the streptomycetes can pick and choose their carbon and energy source because they are available in excess, whilst the nitrogen sources are limited and they must sequester what they can. If aas are often not available, streptomycetes will have to synthesis the required aa. It could therefore be postulated that shutdown mechanism did not evolve or have been lost.

Hood *et al*. (1992) reported the loss of proline catabolism in a cell that constitutively produces proline leads to activation of a secondary metabolic pathway that utilises proline. This reveals another important aspect of streptomycetes physiology is the presence of tightly regulated secondary metabolism. If nitrogen catabolism and biosynthesis are less tightly regulated than

in other bacteria, the old idea of secondary metabolism as a form of overflow metabolism may be due for revival (Hodgson, 2000). The change in the concept is that primary metabolism is relatively poorly controlled. A biological role for secondary metabolism may be to deal with unbalanced production of primary metabolism when streptomycetes are supplied with unusual "feast" conditions that are not the norm for their biological niche. The normal status for streptomycetes in soil will be for famine of nitrogenous compounds and feast of CHO.

8.7 Tangents and future research interests

During the course of this research, several interesting questions arose predominately related to the biochemistry of *S. fradiae* C373-10 and streptomycetes in general and could not be investigated any further due to time constraints. They are all Ph.D. research based projects in their own right which should be undertaken in time:

(1) A systematic mathematical procedure capable of detecting the presence of gross errors in the measurements and of reconciling the connection between data sets by using the maximum likely hood principle should be applied to the biomass of a streptomycete (Lange and Heijnen, 2001). The biomass composition of a streptomycete should be further analysed in a chemostat under a number of limitation conditions and analysed for its elemental composition, molecular elemental, molecular monomeric and for its macromolecular composition. The proposed method would increase the accuracy of biomass composition data of its elements and its molecules by providing a best estimate based on all available data and thus provide an improved and consistent basis for MFA as well as black box modelling.

(2) Amino acid analysis has been undertaken routinely for 30 - 40 years with increasing genome sequences and bioinformatic techniques becoming available. It would be my recommendation that further analysis in this area be undertaken. It would be of interest to see how codon bias has effected internal, external and ambivalent aa compositional alignment of the streptomycetes.

(3) An in depth analysis of the change in enzyme activity levels of the TCA cycle, PP pathway, and glycolysis would be desirable under a number of growth conditions, with emphasis on the detection of the number of isoenzymes and their time profiles would be desirable.

(4) A systematic flux-based analysis of a streptomycete fermentation undertaken in continuous culture, using the two metabolic flux based strategies used in this work (Chapter 6 & 7) in conjunction with tracer based flux-based strategies incorporating atom mapping matrixes (Chapter 1, section 1.2). To assess the best technique of analysing a streptomycete fermentation with the least number of metabolites measured. An alternative strategy would have been to undertake a similar analysis as Yang *et al*. (2002). Where *Synechocystis* gene expression patterns at mRNA and protein levels were measured by using semi-quantitative reverse transcriptional PCR and two-dimensional electrophoresis, and intracellular metabolite flux distribution in *Synechocystis* using carbon isotope labeling techniques. There findings demonstrated that the information obtained from the analysis of mRNA expression, protein expression, and metabolic flux distribution is necessary to understand the regulatory events in complex networks. However, the detection of mRNA may need a more powerful technique than PCR, to enable high throughput analysis of gene expression at the transcriptional level.

(5) Most current metabolic engineering studies have focused on enzyme levels and on the effect of the amplification, addition, or deletion of a particular pathway. Although it is generally known that cofactors play a mayor role in the production of different fermentation products, their role has not been thoroughly and systematically studied in streptomycete research. It is conceivable that in cofactor-dependent production systems, cofactor availability and the proportion of cofactor in the active form may play an important role in dictating the overall process yield. Hence, the manipulation of these cofactors levels may be crucial in order to further increase antibiotic production. This could be undertaken with a number of strategies increasing the NADH, NADPH, & CoA levels (see section 8.5). Another interesting strategy would be to increase the effects of futile cycling i.e., PEPC & MDH[dc] pushing ATP spillage in the direction of reducing power. The latter strategies can only increase our understanding of the balance between precursor availability and cofactor supply.

(8.8) Concluding remarks

One point of interest that can be concluded from this study is the way that molecular biologists, microbial physiologists biochemists, enzymologist and biochemical engineers research interests are coordinated. A molecular biology paper written by Ruijter *et al.* (2000)

will be used as an example; this paper was challenged by Ratledge (2000) on the grounds that the results were predictable from the published physiology ignored by the authors. This was robustly contested by one of the authors (Ruijter, 2000). The merits of this particular case are of little consequence, because it is one among many, but there is little doubt that the authors did not give a full review of the available literature. As Holms (2001) said *"What is important is the underlying principle that science is indivisible and that research initiated in ignorance of what is already known is unlikely to give the best return for the investment put into it"*. Molecular biologists are by no means the only researchers who fall into this trap but the beauty of their ever-improving technology can sometimes be adopted as a justification in itself. Pallen (1999) used the accumulation of genome sequencing data as an example of this fact where " *…genome sequencing risks becoming expensive molecular stamp-collecting, without the tools to determine the data and fuel the hypothesis-driven laboratory-based research".*

Communication is the only way forward between academic disciplines, and to the industrial community. To this end metabolic engineering was born (Stephanopoulos *et al*., 1998) to bridge this gap. The ultimate goal was to approach molecular biology with a systematic approach but not in turn make molecular biology mathematically unapproachable, but to open a future to molecular biology that has an ordered logical approach. With the advent of micro-array technology and proteomics, approaches that organise and enhance existing data such as MFA have to be the tools of the future. Molecular biology is moving faster than any scientific field in the history of the sciences, but what is already done must not be forgotten. Improvements of metabolic modelling technology must be involved, with the aim of making them more user friendly.

The concluding remarks of this work should only be considered, as a discussion of an intense experience in a small amount of time. Although the concluding remarks mirror what others have implied with vastly more experience.

The unsaturated ketone group on the tylactone ring when reacted with ammonia

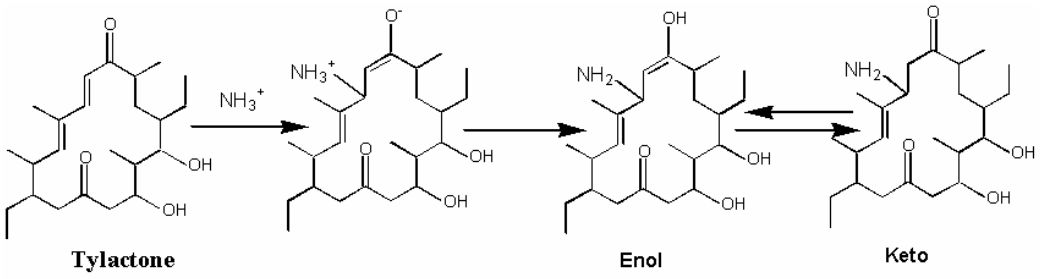

Fig 8.1 Aldehydes and ketones will react with a wide range of chemical compounds such as ammonia, thiols, amines, alcohols, amino acids and bisulphites. All these compounds will react with the aldehyde group. Hypothetical example of such reactions with the tylactone ring.

The unsaturated ketone group on the tylactone ring when reacted with sodium bisulphite

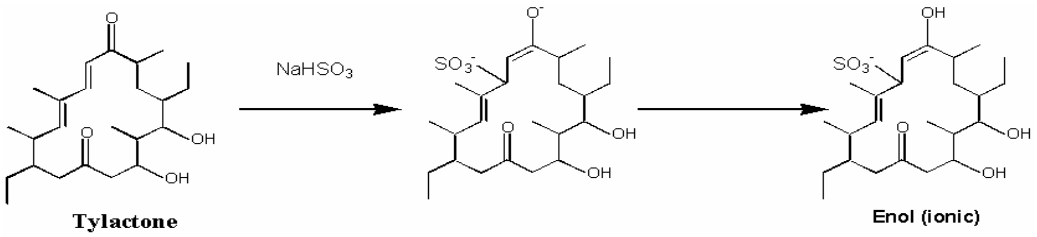

Fig 8.2 Aldehydes and ketones will react with a wide range of chemical compounds such as ammonia, thiols, amines, alcohols, amino acids and bisulphites. All these compounds will react with the aldehyde group. Hypothetical example of such reactions with the tylactone ring.

An example of a constructed relational network of compounds

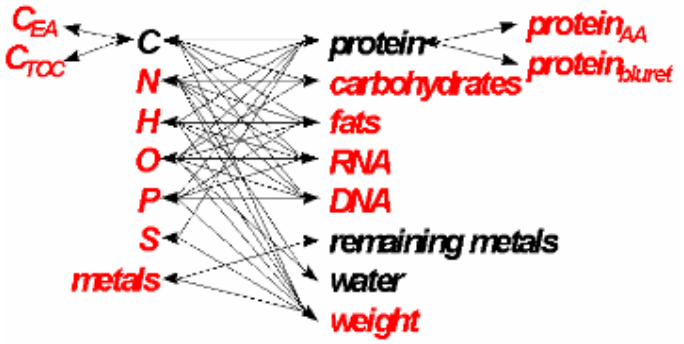

Fig 8.3 An example of a constructed relational network of compounds, measured and unmeasured, subscripts indicate method: Elemental Analysis, Total Organic Carbon, total Amino Acid, Protein analysis [biuret method](adapted from Lange & Heijnen, 2001).

REFERRENCES

Abel, C.B.L., Lindon, J.C., Noble, D., Rudd, B.A.M., Sidebottom, P.J., and Nicholson, J.K. (1999). **Characterization of metabolites in intact *Streptomyces citricolor* culture supernatants using high-resolution nuclear magnetic resonance and directly coupled high-pressure liquid chromatography-nuclear magnetic resonance spectroscopy.** Analytical Biochemistry. 270: 220-230.

Acerenza, L., and Cornish-Bowden, A. (1997). **Generalization of the double-modulation method for *in situ* determination of elasticities**. Biochemical journal. 327: 217-223.

Aharonowitz, Y. (1980a). **Nitrogen metabolite regulation of antibiotic biosynthesis**. Annual Review of Microbiology. 34: 209-233.

Aharonowitz, Y., & Friedrich, C.G. (1980b). **Alanine dehydrogenase of the β-lactams antibiotic producer *Streptomyces clavuligerus***. Archives Microbiology. 125: 137-142.

Ahmed, Z.U., Shapiro, S., & Vining, L.C. (1984). **Excretion of α-keto acids by strains of *Streptomyces venezuelae*.** Canadian Journal Microbiology. 30: 1014-1021.

Aiba, S. & Matsuoka, M. (1979). **Identification of metabolic model: citrate production from glucose by *Candida lipolytica***. Biotechnology and Bioengineering. 21: 1373-1386.

Akashi, H., and Gojobori, T. (2002). **Metabolic efficiency and amino acid composition in the proteomes of *Escherichia coli* and *Bacillus subtilis***. PNAS. 99 (6): 3695-3700.

Alefounder, P. R., Baldwin, S. A., Perham, R. N., and. Shorts, N. J (1989). **Cloning, sequence analysis and overexpression of the gene for the class II fructose 1,6-bisphosphate aldolase of *Escherichia coli***. Biochemical journal. 257: 529-534.

Alroy, Y., and Tannenbaum, S.R. (1973). **The influence of environmental conditions on the macromolecular composition of *Candida utilis*.** Biotechnology and Bioengineering. 15: 239-256.

Alves, A. M. C. R., Meijer, W.G., Vrijbloed, J.W., and Dijkhuizen, L. (1996). **Characterization and phylogeny of the *pfp* gene of *Amycolatopsis methanolica* encoding PPi-dependent phosphofructokinase**. Journal of Bacteriology. 178: 149-155.

Alves, A.M.C.R., Euverink, G.J.W., Bibb, M.J., & Dijkhuizen, L. (1997). **Identification of ATP-dependent phosphofructokinase as a regulatory step in the glycolytic pathway of the actinomycete *Streptomyces coelicolor* A3(2)**. Applied Environmental Microbiology. 63: 956-961.

Alves, A.M.C.R., Euverink, G.J.W., Hektor, H.J., Hessels, G.I., Vlag, V., Vrijbloed, J.W., Hondmann, J., Visser, J., & Dijkhuizen, L. (1994). **Enzymes of glucose and methanol metabolism in the *Actinomycete Amycolatopsis methanolica***. Journal of Bacteriology. 176: 22: 6827-6835.

Amartey, S.A., Leak, D.J., and Hartley, B.S. (1991). **Development and optimization of a defined medium for aerobic growth of *Bacillus stearothermophilus* LLD-15.** Biotechnology Letters. 13: 621-626.

Amini, F. (1994). **The role of 3'5'-cyclic adenosine monophosphate (cAMP) in *Streptomyces coelicolor* A3(2).** PhD thesis, University of Warwick, Coventry, UK.

An, G., & Vining, L.C. (1978). **Intracellular levels of guanosine 5'-diphosphate 3'-diphosphate (ppGpp) and guanosine 5'-triphosphate 3'-diphosphate (pppGpp) in cultures of *Streptomyces griseus* producing streptomycin.** Canadian Journal of Microbiology. 24: 502-511.

Anderlund, M., Nissen, T.L., Nielsen, J., Villadsen, J., Rydström, J., Hahn-Hägerdal, B., Kielland-Brandt, M.C. (1999). **Expression of the *E. coli pnt*A and *pnt*B genes encoding nicotinamide nucleotide transhydrogenase in *Saccharomyces cerevisiae* and its effect on product formation during anaerobic glucose fermentation.** Applied and Environmental Microbiology 65: 2333-2340.

Andersson, S.G.E., and Kurland, C.G. (1990). **Codon preferences in free living microorganisms.** Microbiol Rev. 54: 198-210.

Angell, S., Lewis, C. G., Buttner, M. J., and Bibb, M. J. (1994). **Glucose repression in *Streptomyces coelicolor* A3(2): A likely regulatory role for glucose kinase**. Mol. Gen. Genet. **244**:135-143.

Angell, S., Schwarz, E., and Bibb, M. J. (1992). **The glucose kinase gene of *Streptomyces coelicolor* A3(2): its nucleotide sequence, transcriptional analysis and role in glucose repression.** Molecular Microbiology. **6**:2833-2844.

Arima, K., Okazaki, H., Ono, H., Yamada, K., and Beppu, T. (1973). **Effect of exogenous fatty acids on the cellular fatty acid composition and neomycin formation in a mutant strain of *Streptomyces fradiae*.** Agr Biol Chem. 37: 2313-2317.

Aristidou, A.A., San, K., and Bennet, G.N. (1999). **Metabolic flux analysis of *Escherichia coli* expressing the *Bacillus subtilis* acetolactate synthase in batch and continuous cultures.** Biotechnology and Bioengineering. 63 (6): 735-749.

Arnold, S.A., Crowley, J., Vaidyanathan, S., Matheson, L., Mohan, P., Hall, J.W., Harvey, L.M., and McNeil, B. (2000). **At-line monitoring of a submerged filamentous bacterial cultivation using near-infrared spectroscopy**. Enzyme and Microbial Technology. 27: 691-697.

Ates, S., Elibol, M., and Mavituna, F. (1997). **Production of actinorhodin by *Streptomyces coelicolor* in batch and fed-batch cultures.** Process Biochemistry. 32 (4): 273-278.

Avignone-Rossa, C., White, J., Kuiper, A., Postma, P.W., Bibb, M., and Teixeira de Mattos, M.J. (2002). **Carbon flux distribution in antibiotic-producing chemostat cultures of *Streptomyces lividans*.** Metabolic Engineering. 4: 138-150.

Bacon, C.W. (1985). **A chemically defined medium for the growth and synthesis of ergot alkaloids by species of *Balansia*.** Mycologia. 77: 418-423.

Baddiley, J., and Neuhaus, F.C. (1960). **The enzyme activation of D-alanine.** Biochemical journal. 75: 579-587.

Bailey, J.E. (1991). **Toward a Science of Metabolic Engineering**. Science. 252: 1668-1674.

Baillie, R.D. (1968). **Teichoic acids of *Bacillus subtilis***. Ph.D. thesis. University of Glasgow.

Baltz R.H, & Seno, E,T. (1988). **Genetics of *Streptomyces fradiae* and tylosin biosynthesis**. Annual Review Microbiology. 42: 547-74.

Baltz, R. (2000). **Sweet home actinomycetes: The 1999 MDS panlabs lecture.** Journal of Industrial Microbiology and Biotechnology. 24 (2): 79-88.

Baltz, R.H & Seno, E, T. (1981). **Properties of *Streptomyces fradiae* mutants blocked in biosynthesis of the macrolide antibiotic tylosin.** Antimicrobial Agents and Chemotherapy. 20: 2: 214-225.

Baltz, R.H., Seno, E.T., Stonesifer, J., & Wild, G.M. (1983) **Biosynthesis of the macrolide antibiotic tylosin a preferred pathway from tylactone to tylosin.** The Journal of Antibiotics. 36: 2: 131-141.

Banchio, C., & Gramajo, H.C. (1997). **Medium and long chain fatty acid uptake and utilization by *Streptomyces coelicolor* A3(2): first characterization of a gram-positive bacterial system**. Microbiology. 143: 2439-2447.

Barkholt, V., and Jensen, A.L. (1989). **Amino acid analysis: determination of cysteine plus half-cystine in proteins after hydrochloric acid hydrolysis with a disulfide compound as additive.** Analytical Biochemistry. 177 (2): 318-322.

Bascaran, V., Hardisson, C. & Brana, A.F. (1989a). **Regulation of nitrogen catabolic enzymes in *Streptomyces clavuligerus***. Journal of General Microbiology. 135: 2465-2474.

Bascaran, V., Hardisson, C. & Brana, A.F. (1989b). **Isolation and characterization of nitrogen-deregulated mutants of *Streptomyces clavuligerus***. Journal of General Microbiology. 135: 2475-2482.

Bate, N., & Cundliffe, E. (1999). **The mycinose biosynthetic genes of *Streptomyces fradiae*, producer of tylosin**. Journal of Industrial Microbiology & Biotechnology. 23: 118-122.

Bate, N., Butler, A.R., Gandecha, A.R., and Cundliffe, E. (1999). **Multiple regulatory genes in the tylosin biosynthetic cluster of *Streptomyces fradiae*.** Chem Biol. 6: 617-624.

Bate, N., Butler, A.R., Gandecha, A.R., and Cundliffe, E. (1999). **The mycinose biosynthetic genes of *Streptomyces fradiae*, producer of tylosin.** J Ind Microbiol Biotech. 23: 118-122.

Bate, N., Butler, A.R., Smith, I.P., and Cundliffe, E. (2000). **The mycarose biosynthetic genes of *Streptomyces fradiae*, producer of tylosin.** Microbiology UK. 146: 139-146.

Bate, N., Stratigopoulos, G. and Cundliffe, E. (2002) **Differential roles of two SARP-encoding regulatory genes during tylosin biosynthesis.** Molecular Microbiology. 43, 449-458.

Batrakov, S.G., and Bergelson, L.D. (1978). **Lipids of streptomycetes. Structural investigation and biological interrelation.** Chem Phys Lipids. 21: 1-29.

Battley, E.H. (1995). **An apparent anomaly in the calculation of ash-free dry weight for the determination of cellular yields**. Applied and Environmental Microbiology. 61: 1655-1657.

Baudouin-Cornu, P., Surdin-Kerjan, Y., Marlière, P., and Thomas, D. (2001). **Molecular evolution of protein biast composition.** Science. 293: 297-300.

Bautista, L.F., Aleksenko, A., Hentzer, M., Santerre-Henriksen, A., and Nielsen, J. (2000). **Antisense silencing of the *cre*A gene in *Aspergillus nidulans***. Applied and Environmental Microbiology. 66 (10): 4579-4581.

Baylis, H.A., and Bibb, M.J. (1987). **The nucleotide sequence of 16S ribosomal-RNA gene from *Streptomyces coelicolor* A3(2).** Nucleic Acids Research. 15: 7176.

Beckmann, R.J., Cox, K., and Seno, E.T. (1989). **A cluster of tylosin biosynthetic genes is interrupted by a structurally unstable segment containing four repeated sequences.** In Genetics and Molecular Biology of Industrial Microorganisms (ed. C.L. Hershberger, S.W. Queener and G. Hegemen), American Society for Microbiology, Washington, DC. 176-186.

Behal, V. (1987). **The tetracycline fermentation and its regulation.** CRC. Critical Reviews in Biotechnology. 5 (4): 275-318.

Behal, V., Cudlin, J., and Vanek, Z. (1969). **Regulation of biosynthesis of secondary metabolites. III: Incorporation of 1-^{14}C-acetic acid into fatty acids and chlortetracycline in *Streptomyces aureofaciens*.** Folia Microbiol. 14: 117-120.

Behal, V., Hostalek, Z., and Vanek, Z (1983). **Anhydrotetracycline oxygenase activity and biosynthesis of tetracyclines in *Streptomyces aureofaciens*.** Biotechnology Letters. 1:275-318.

Behal, V., Jechova, V., Vanek, Z., and Hostalek, Z. (1977). **Alternative pathways of malonyl CoA formation in *Streptomyces aureofaciens*.** Phytochemistry. 16: 347.

Bellofatto, V., Shapiro, L., and Hodgson, D.A. (1984). **Generation of Tn5 promotor probe and its use in the study of gene expression in *Caulobacter crescentus.*** Proc Natl Acad Sci USA. 81: 1035-1039.

Benthin, S., Nielsen, J., and Villadsen, J. (1991). **A simple and reliable method for the determination of cellular RNA content**. Biotechnology Techniques. 5 (1): 39-42.

Bentley, S.D., Chater, K.F., Cerdeno-Tarraga, A.M., Challis, G.L., Thomson, N.R., James, K.D., Harris, D.E., Quail, M.A., Kieser, H., Harper, D., Bateman, A., Brown, S., Chandra, G., Chen, C.W., Collins, M., Cronin, A., Fraser, A., Goble, A., Hidalgo, J., Hornsby, T., Howarth, S., Huang, C.H., Kieser, T., Larke, L., Murphy, L., Oliver, K., O'Neil, S., Rabbinowitsch, E., Rajandream, M.A., Rutherford, K., Rutter, S., Seeger, K., Saunders, D., Sharp, S., Squares, R., Squares, S., Taylor, K., Warren, T., Wietzorrek, A., Woodward, J., Barrell, B.G., Parkhill, J., and Hopwood, D.A. (2002). **Complete genome sequence of the model actinomycete *Streptomyces coelicolor* A3(2).** Nature. 417: 141-147.

Beppu, T. (1992). **Secondary metabolites as chemical signals for cellular differentiation.** Gene 115:159-165.

Bergeys Manual of Systematic Bacteriology. (2000)[4 Vol. Set]. Editor: Williams, S. T. Publisher**:** Lippincott, Williams & Wilkins. Baltimore, USA.

Beutler, H.O., and Michal, G. (1974). *In* **methodender enzymatischen analyse** (Bergmeyer H.U., Hrsg). 3 Aufl, bd. 2, S 1753-1759, Verlag Chemie, Weinheim, and (1974) in methods of enzymatic analysis (Bergmeyer, H. U., ed) 2nd ed., vol 4, pp 1708-1713, verlag chemie, Weinheim/Academic Press, Inc, New York and London.

Bevan, P., Ryder, H., and Shaw. I. (1995). **Identifying small-molecule lead compounds: the screening approach to drug discovery.** TIBTECH. 13:115-121.

Birch, A., Eeiser, A., Robinson, J. (1993) **Cloning, sequencing, and expression of the gene encoding methylmalonyl-CoA mutase from *S. cinnamonensis*.** Journal of Bacteriology. 175: 3511-3519.

Black, P.N., & Dirusso, C. (1994)**. Molecular and biochemical analyses of fatty acid transport, metabolism and gene regulation by *E. coli***. Biochim. Biophys. Acta. 1210: 123-145.

Blinc, M., and Hocevar, B. (1953). **Fettanreicherung on *Rhodotorula gracilis***. Monatshefte fur chemie und verwandte teile wissenschaften. 84: 1127-1131.

Blum, J.J., and Stein, R.B. (1982). **On the analysis of metabolic networks**. In Biological Regulation and Development. Edited by R.F. Goldenberger & K.R. Yamamoto. New York: Plenum Press. 99-125.

Bonarius, H.P.J., Schmid, G., and Tramper, J. (1997). **Flux analysis of underdetermined metabolic networks: the quest for the missing constraints.** TIBTECH. 15: 308-314.

Bonarius, H.P.J., Timmerarends, B., de Gooijer, C.D., and Tramper, J. (1998). **Metabolite-balancing techniques Vs. ^{13}C tracer experiments to determine metabolic fluxes in hybridoma cells.** Biotechnology and Bioengineering. 58 (2 & 3): 258-262.

Booth, I.R., and Higgins, C.F. (1990). **Osmoregulation. Enteric bacteria and osmotic stress: intracellular potassium glutamate as a secondary signal of osmotic stress?** FEMS Microbiol Rev. 75: 239-246.

Bormann, E.J., & Herrmann, R. (1968). **Zur pyruvat- und α-ketoglutaratausscheidung durch *Streptomyces rimosus***. Archiv Fur Mikrobiologie. 63: 41-52.

Bourque, D, Pomerleau, Y., Groleau, D. (1995). **High-cell-density production of poly-β-hydroxybutyrate (PHB) from methanol by *Methylbacterium extorquens*: production of high-molecular-mass PHB.** Applied Microbiology and Biotechnology. 44: 367-376.

Box, G.E.P., and Behnken, D.W. (1960). **Some new three level designs for the study of quantitative variables.** Technometrics. 2: 367-376.

Bradford, M.M. (1976). **A rapid and sensitive method for the quantitation of microgram quantities of protein utilizing the principle of protein dye binding**. Analytical Biochemistry. 72: 248-254.

Bramwell, H., Hunter, I.S., Coggins, J.R., Nimmo, H.G. (1996) **Propionyl-CoA carboxylase from *S. coelicolor* A3(2): cloning of the gene encoding the biotin- containing subunit**. Microbiology. 142: 649-655.

Bramwell, H., Nimmo, H.G., Hunter, I.S., & Coggins, J.R. (1993). **Phosphoenolpyruvate carboxylase from *Streptomyces coelicolor* A3(2): purification of the enzyme, cloning of the ppc gene and over-expression of the protein in a streptomycete**. Biochemical Journal. 293: 131-136.

Brana, A.F., Manzanal, M.B., and Hardisson, C. (1982). **Characterization of intracellular polysaccharides of *Streptomyces*.** Canadian Journal of Microbiology. 28: 1320-1323.

Brana, A.F., Manzanal, M.B., and Hardisson. (1980). **Occurrence of polysaccharide granules in sporulating hyphae of *Streptomyces viridochromogenes*.** Journal of Bacteriology. 144: 1139-1142.

Brana, A.F., Paiva, N., & Demain, A.L. (1986). **Pathways and regulation of ammonium assimilation in *Streptomyces clavuligerus***. Journal of General Microbiology. 132: 1305-1317.

Brand, M.D. (1996). **Top down metabolic analysis**. Journal of Theoretical Biology. 182: 351-360.

Bremer, H., and Dennis, P.P. (1987). **Modulation of chemical composition and other parameters of the cell by growth rate**. In: *Escherichia coli and Salmonella typhimurium: Cellular and Molecular Biology*. Edited by F.C Neidhardt., J.L, Ingraham., K. Brooks Low., B, Magasanik., M. Schaechter & H.E. Umbarger. Washington, D.C: American Society for Microbiology. 1527-1542.

Broch Biology of Microorganisms. (2000). Ninth edition. Editors: Madigan., Martinko., Parker. Prentice Hall. Upper Saddle River, New Jersey, USA.

Brown, A.H. (1946). **Determination of pentose in the presence of large quantities of glucose**. Archives of Biochemistry. 118: 269-278.

Brown, C., Hafner, R.P., & Brand, M.D. (1990). **The top-down approach to the determination of control coefficients for metabolic control theory**. European Journal of Biochemistry. 188: 321-325.

Brown, D., Hitchcock, M.J.M., and Katz, E. (1986). **Purification and characterization of kynurenine formamidase activities from *Streptomyces parvulus*.** Canadian Journal of Microbiology. 32: 465-472.

Bruheim, P., Butler, M., Ellingsen, T.E. (2002). **A theoretical analysis of the biosynthesis of actinorhodin in a hyper-producing *Streptomyces lividans* strain cultivated on various carbon sources**. Applied Microbiology and Biotechnology. 58: 735-742.

Bu'Lock, J.D. (1961). **Intermediary metabolism and antibiotic synthesis.** Advances in Applied Microbiology. 3: 293-342.

Buckland, B. (1985). **Fermentation exhaust gas analysis using mass spectrometry.** Bio/Technology. 3: 982-988.

Burke, F.M. (1991). **Fermentation development of *Streptomyces thermonitrificans*** ISP5579. PhD Thesis, University of Glasgow.

Burton, K. (1956). **A study of the conditions and mechanism of the diphenylamine reaction for the colorimetric determination of deoxyribonucleic acid**. Biochemical Journal. 62: 315-323.

Bushell, M.E and Fryday, A. (1983). **The application of materials balancing to the characterization of sequential secondary metabolite formation in *Streptomyces cattleya* NRRL 8057**. Journal of General Microbiology. 129: 1733-1741.

Butler, A.R., Bate N., Cundliffe, E. (1999) **Impact of thioesterase activity on tylosin biosynthesis in *Streptomyces fradiae*.** Chemistry & Biology. 6: 287-292.

Bystrykh, L.V., Vonck, J., Van Bruggen, E.F.J., Van Beeumen, J., Samyn, B., Govorukhina, N.I., Arfman, N., Duine, J.A., and Dijkhuizen, L. (1993). **Electron microscopic analysis and structural characterization of novel NADP(H)-containing methanol-N,N'-dimethyl-4-nitrosoaniline oxidoreductases from the Gram-positive methylotrophic bacteria *Amycolatopsis methanolica* and *Mycobacterium gastri* MB19**. Journal of Bacteriology. 175:1814-1822.

Calik, P., and Ozdamar, T.H. (1999). **Mass flux balance-based model and metabolic pathway engineering analysis for serine alkaline protease synthesis by *Bacillus licheniformis***. Enzyme Microb. Technology. 24: 621-635.

Calik, P., Calik, G., Takac, S., and Ozdamar, T.H. (1999). **Metabolic flux analysis for serine alkaline protease fermentation by *Bacillus licheniformis* in a defined medium: Effects of the oxygen transfer rate.** Biotechnology and Bioengineering. 64 (2): 151-159.

Cascante, M., Llorens, M., Melendez-Hevia, E., Puigjaner, J., Montero, F., and Marti, E. (1996). **The metabolic productivity of the cell factory**. Journal Theoretical Biology. 182: 317-325.

Chakraburtty, R., and Bibb, M. (1997). **The ppGpp synthetase gene (relA) of *Streptomyces coelicolor* A3(2) plays a conditional role in antibiotic production and morphological differentiation.** Journal of Bacteriology. 179 (8): 5854-5861.

Chakraburtty, R., White, J., Takano, E., and Bibb, M. (1996). **Cloning characterization and disruption of a (p)ppGpp synthetase gene (relA) of *Streptomyces coelicolor* A3 (2).** Molecular Microbiology. 19 (2): 357-368.

Chambost, J.P., and Fraenkel, D.G. (1980). **The use of 6-labeled glucose to assess futile cycling in *Escherichia coli*.** J Biol Chem. 255: 2867-2869.

Chan, M., and Sim, T.S. (1998). **Malate synthase from *Streptomyces clavuligerus* NRRL3585: cloning, molecular characterization and its control by acetate.** Microbiology. 144: 3229-3237.

Chang, L.T., & Elander, R.P. (1986). **Long term preservation of industrially important microorganisms.** In Manual of Industrial Microbiology and Biotechnology. Ed . Demain & Solomon, N,A. ASM Press. Washington D. C., USA.

Chao, Y.P., and Liao, J.C. (1994). **Metabolic responses to substrate futile cycling in *Escherichia coli.*** J Biol Chem. 269: 5122-5126.

Chapman, P.G. (1994). **Studies of the glyoxylate bypass of *S. coelicolor* A3(2): Purification of the isocitrate lyase and cloning of the id gene. PhD Thesis. Dept. of Genetics.** Glasgow University.

Chater, K.E. (1989). **Multilevel regulation of *Streptomyces* differentiation**. TIG. 5: (11) 372-377.

Chater, K.F. (1998). **Taking a genetic scalpel to the to the *Streptomyces* colony**. Microbiology 144: 1465-1478.

Chatterjee, S., and Vining, L.C. (1982a). **Catabolite repression in *Streptomyces venezuelae* induction of β-galactosidase, chloramphenicol production and intracellular cyclic 3',5'-monophosphate concentrations.** Canadian Journal of Microbiology. 28: 311-317.

Chatterjee, S., and Vining, L.C. (1982b). **Glucose suppression of β-galactosidase activity in a chloramphenicol-producing strain of *Streptomyces venezuelae.*** Canadian Journal of Microbiology. 28: 593-599.

Chen, C.W., Lin, Y.S., Kieser, H.M., Hopwood, D.A. (1993). **The chromosomal DNA of *Streptomyces lividans* 66 appears to be linear.** Journal of Cellular Biochemistry. 17: 291-291.

Chen, H., Agnihotri, G., Guo, Z., Que, N. L. S., Chen, X.H., & Liu, H. (1999a). **Biosynthesis of mycarose: isolation and characterization of enzymes involved in the C-2 deoxygenation**. Journal of the American Chemical Society. 121: 8124-8125.

Chen, H., Guo, Z., & Liu, H. (1998). **Expression, purification, and characterization of *Tyl*M1, an N, N-Dimethyltransferase involved in the biosynthesis of mycaminose**. Journal of the American Chemical Society. 120: 9951-9952.

Chen, H., Yeung, S., Que, N.L.S., Muller, T., Schmidt, R.R., & Liu, H. (1999b). **Expression, purification, and characterization of *Tyl*B, an aminotransferase involved in the biosynthesis of mycaminose**. Journal of the American Chemical Society. 121: 7166-7167.

Chen, H.C., and Wilde, F. (1991). **The effect of dissolved oxygen and aeration rate on antibiotic production of *Streptomyces fradiae*.** Biotechnology and Bioengineering. 37: 591-595.

Chen, J., Brevet, A., Fromant, M., Lévêque, F., Schmitter, J.M., Blanquet, S., and Plateau, P. (1994). **Pyrophosphatase is essential for growth of *Escherichia coli*.** Journal of Bacteriology. 172:5686-5689.

Chesbro, W. (1988). **The domains of slow bacterial growth**. Canadian Journal of Microbiology. 34: 427-435.

Chiba, Y. and Sugahara, K. (1957). **The nucleic acid content of chloroplasts isolated from spinach and tobacco leaves.** Archives of Biochemistry and Biophysics. 71: 367-376.

Chistoserdova, L.V., Lidstrom, M.E. (1996) **Molecular characterisation of a chromosomal region involved in the oxidation of acetyl-CoA into glyoxylate in the ICL neg. methylotroph, *Methylobacterium extorquens* AMI.** Microbiology 142: 1459-1468.

Choi, D.B., Park, E.Y., and Okabe, M. (2000). **Dependence of apparent viscosity on mycelial morphology of *Streptomyces fradiae* culture in various nitrogen sources.** Biotechnology Progress. 16: 525-532.

Choi, D.B., Park, Y., & Okabe, M. (1998b). **Effects of rapeseed oil on activity of methylmalonyl-CoA carboxyltransferase in culture of *Streptomyces fradiae***. Biosci. Biotechnol. Biochem. 62: 5: 902-906.

Choi, Du Bok., Park, E.Y., & Okabe, M. (1998a). **Improvement of tylosin production from *Streptomyces fradiae* culture by decreasing the apparent viscosity in an air-lift bioreactor.** Journal of fermentation and bioengineering. 86: 4: 413-417.

Chomczynski, P. (1989). **Product and process for isolating RNA**. United States Patent 4 843 155.

Chomczynski, P. (1993). **A reagent for the single-step simultaneous isolation of RNA, DNA and proteins from cell and tissue samples**. Biotechniques. 15: 3: 532-537.

Chomczynski, P., & Sacchi, N. (1987). **Single step method of RNA isolation by acid guanidinium thiocyanate phenol chloroform extraction**. Analytical Biochemistry. 162: 156-159.

Chomczynski, P. (1994). **Shelf stable product and process for isolating RNA, DNA and Proteins**. United States Patent 5 346 994.

Chomczynski, P., & Mackey, K. (1995). **Substitution of chloroform by bromochloropropane in the single-step method of RNA isolation.** Analytical Biochemistry. 225: 163-164.

Christensen, B., and Nielsen, J. (1999a). **Isotopomer analysis using GC-MS**. Metabolic Engineering. 1: 8-16.

Christensen, B., and Nielsen, J. (1999b). **Metabolic network analysis. A powerful tool in metabolic engineering**. Adv. Biochem. Eng. Biotechnol. 66: 209-231.

Christensen, B., and Nielsen, J. (2000). **Metabolic network analysis of *Penicillium chrysogenum* using ^{13}C-labeled glucose.** Biotechnology and Bioengineering. 68: 652-659.

Christensen, B., and Nielsen, J. (2000). **Metabolic network analysis of *Penicillium chrysogenum* using ^{13}C-labelled glucose.** Biotechnology and Bioengineering. 68: 252-259.

Christensen, L.H., Henriksen, C.M., Nielsen, J., Villadsen, J., and Egel-Mitani, M. (1995). **Continuous cultivation of *P. chrysogenum*. Growth on glucose and penicillin production**. Journal of Biotechnology. 42: 95-107.

Christiansen, T., Christensen, B., and Nielsen, J. (2002). **Metabolic network analysis of *Bacillus clausii* on minimal and semirich medium using 13C-labeled glucose.** Metabolic Engineering. 159-169.

Chung, T., Klumpp, D.J., and LaPorte, D.C. (1988) **Glyoxylate bypass operon *of E. coli*: Cloning and determination of the functional map.** Journal of Bacteriology. 170: 386-392.

Cimburkova, E., Zima, J., and Novak, J. (1988). **Nitrogen regulation of avermectin biosynthesis in *Streptomyces avermitilis* in a chemically defined medium.** Journal of Basic Microbiology. 28: 491-499.

Clark, G.J., Langley, D., and Bushell, M.E. (1995). **Oxygen limitation can induce microbial secondary metabolite formation: investigations with miniature electrodes in shaker and bioreactor culture.** Microbiology. 141: 663-669.

Clarke, D., & Cronan, J.E., Jr. (1996). **Two-carbon compounds and fatty acids as carbon sources. In *E. coli* and *Salmonella*: Cellular and molecular Biology**. PP 343-357. Edited by F.C. Neidhardt and others. American Society for Microbiology. Washington DC, USA.

Clarke, D.J., Blake-Coleman, B.C., Carr, R.J.G., Calder, M.R., and Atkinson, T. (1986). **Monitoring reactor biomass**. Trends in Biotechnology. 4: 173-178.

Cochrane, V.W. (1961**). Physiology of *Actinomycetes***. Annual Reviews in Microbiology. 1-26.

Cochrane, V.W., Peck, H.D., & Harrison, A. (1953). **The metabolism of species of Streptomyces: 7. The hexosemonophosphate shunt and associated reactions**. Biochemistry. 66: 17-23.

Coggins, J.R., Hunter, I.S. Nimmo, H.G., Bramwell, H., Taylor, R.D., Walker, G.E., White, P.J., and Wylie, A. (1995). **Deregulation of fluxes to precursors of secondary metabolites in *S. coelicolor***. Internal Report. Dept. Biochem. And Genetics, Glasgow University.

Cole, S.T., Eiglmeier, K., Parkhill, J., James, K.D., Thomson, N.R., Wheeler, P.R., Honore, N., Ganier, T., Churcher, C., Harris, D., Mungall, K., Basham, D., Brown, D., Chillingworth, T., Connor, R., Davies, R.M., Devlin, K., Duthoy, S., Feltwell, T., Fraser, A., Hamlin, N., Holroyd, S., Hornsby, T., Jagels, K., Lacroix, C., Maclean, J., Moule, S., Murphy, L., Oliver, K., Quail, M.A., Rajandream, M-A., Rutherford, K.M., Rutter, S., Seeger, K., Simon, S., Simmonds, M., Skelton, J., Squares, R., Squares, S., Stevens, K., Taylor, K., Whitehead, S., Woodward, J.R., and Barrell, B.G. (2001). **Massive gene decay in the *leprosy bacillus*.** Nature. 409: 1007-1011.

Cole, S.T., Brosch, R., Parkhill, J., Garnier, T., Churcher, C., Harris, D., Gordon, S.V., Eiglmeier, K., Gas, S., Barry, C.E., Tekaia, F., Badcock, K., Basham, D., Brown, D., Chillingworth, T., Connor, R., Davies, R., Devlin, K., Feltwell, T., Gentles, S., Hamlin, N., Holroyd, S., Hornsby, T., Jagels, K., Barrell, B.G., *et al*. (1998). **Deciphering the biology of *Mycobacterium tuberculosis* from the complete genome sequence.** Nature. 393: 537-44.

Colombo, A.L., Crespi-Perellino, N., & Micalizio, S. (1982). **Relationships between growth, cyclic AMP and tylosin production in two mutants of *Streptomyces fradiae***. Journal of Biosciences 4: 11: 747-752.

Comings, D.E. (1975). **Mechanism of chromosome binding.** VIII. Hoechst 33258-DNA interaction. Chromosoma. 52: 229-243.

Cooney, C.L. (1979). **Conversion yields in penicillin production: theory versus practice.** Process Biochemistry. 14 (5): 31-33.

Cooney, C.L., and Acevedo, F. (1977). **Theoretical conversion yields for penicillin synthesis.** Biotechnology and bioengineering. 19: 1449.

Cooper, J.D.H., Ogden, G., McIntosh, J.M.C., and Turnell, D.C. (1984). **The stability of the o-phthalaldehyde/2-mercaptoethanol derivatives of amino acids: An investigation using high pressure liquid chromatography with a pre-column derivatization technique.** Analytical Biochemistry. 142: 98-102.

Cornish-Bowden, A. (1989). **Metabolic control theory and biochemical systems theory: different objectives, different assumptions, different results**. Journal of Theoretical Biology. 136: 365-377.

Cornish-Bowden, A. (1998). **Two centuries of catalysis**. Journal of Biosciences. 23: 87-92.

Cornish-Bowden, A. (1999). **Enzyme kinetics from a metabolic perspective**. Biochem. Soc. Trans.

Covert, M, W., Schilling, C, H., Famili, I., Edwards, J.S., Goryanin, I.I., Selkov, E., and Palsson, B,O. (2001). **Metabolic modeling of microbial strains *in silico***. Trends in Biochemical Sciences. 26 (3): 179-186.

Crabtree, B. & Newsholme, E.A. (1985). **A quantitative approach to metabolic control.** Current Topics in Cellular Regulation. 25: 21-76.

Crabtree, B. & Newsholme, E.A. (1987). **A systematic approach to describing and analysing metabolic control systems**. TIBS. 12: 4-12.

Craig, C.L., and Weber, R.S. (1998). **Selection costs of amino acid substitutions in *Col*E1 and *Col*Ia gene clusters harbored by *Escherichia coli*.** Molecular and Biological evolution. 15: 774-776.

Craig, C.L., Hsu, M., Kaplan, D., and Pierce, N.E. (1999). **A comparison of the composition of silk proteins produced by spiders and insects.** Int J Biol Macromol. 24: 109-118.

Crameri, A., Raillard, S.A., Bermudez, E., and Stemmer, W.P (1998). **DNA shuffling of a family of genes from diverse species accelerates directed evolution.** Nature. 391: 288-297.

Cundliffe, E. (1999) **Organization and control of the tylosin-biosynthetic genes of *Streptomyces fradiae*.** Actinomycetologica. 13: 68-75.

Cundliffe, E., Bate, N., Butler, A., Fish, S., Gandecha, A., and Merson-Davies, L. (2001). **The tylosin-biosynthetic genes of *Streptomyces fradiae*.** Antonie Van Leewenhoek International Journal of General and Molecular Microbiology. 79 (3-4): 229-234.

Daae, E.B., & Ison, A.P. (1999). **Classification and sensitivity analysis of a proposed primary metabolic reaction network for *Streptomyces lividans***. Metabolic Engineering. 1: 153-165.

Daae, E.B., and Ison, A.P. (1989). **A simple structured model describing the growth of *Streptomyces lividans*.** Biotechnology and Bioengineering. 58 (2 & 3): 263-266.

Daldal, F., and Fraenkel, D.G. (1983). **Assessment of futile cycling involving reconversion of fructose-6-phosphate to fructose-1,6-bisphoshate during gluconeogenic growth of *Escherichia coli*.** Journal of Bacteriology. 153: 390-394.

Dandekar, T., Schuster, S., Snel, B., Huynen, M., and Bork, P. (1999). **Pathway alignment: application to the comparative analysis of glycolytic enzymes.** Biochemical Journal. 343: 115-124.

Darlington, W.A. (1964). **Aerobic hydrocarbon fermentation - practical evaluation.** Biotechnology and Bioengineering. 6 (2): 241 - 242.

Dauner, M., Storni, T., Sauer, U. (2001a). ***Bacillus subtilis* metabolism and energetics in carbon limited and excess-carbon chemostat culture.** Journal of Bacteriology. 183 (24): 7308-7317.

Dauner, M.J., Bailey, E., and Sauer, U. (2001b). **Metabolic flux analysis with a comprehensive isotopomer model in *Bacillus subtilis*.** Biotechnology and Bioengineering. 76: 144-156.

Davidson, A.O. (1992). **Quantitative microbial physiology of *Streptomyces coelicolor* A3(2).** PhD thesis. University of Glasgow.

Dawes, E. A. and Senior, P.E. (1973). **The role and regulation of energy reserve polymers in microorganisms.** Adv. Microb. Physiol. 10:135-266.

Dawes, E.A., McGill, D.J., and Midgley, M. (1971). **Analysis of fermentation products.** In Methods in Microbiology. Academic Press (Norris J.R and Ribbon D. W; Eds). 6A, 3, 53-215.

Dawson, R.M.C., Elliot, D.C., Elliot, W.H., and Jones, K.M. (1987). **Data for biochemical research.** Oxford Science Publication. Third edition.

de Orduna, R.M., and Theobald, U. (2000). **Intracellular glucose-6-phosphate content in *Streptomyces coelicolor* upon environmental changes in a defined medium.** Journal of Biotechnology. 77: 209-218.

Dean, A.M., and Golding, G.B. (1997). **Protein engineering reveals ancient adaptive replacements in isocitrate dehydrogenase.** Proc Natl Acad Sci U S A. 1:94 (7): 3104-3109.

Dekkers, J.G.J., de Kok, H.E., and Roels, J.A. (1981). **Energetics of *Saccharomyces cerevisiae* CBS 426: comparison of anaerobic and aerobic glucose limitation.** Biotechnology and Bioengineering. 23: 1023-1035.

Dekleva, M.L., & Strohl, W.R. (1988a). **Biosynthesis of ε-rhodomycinone from glucose by *Streptomyces* C5 and comparison with intermediary metabolism of other polyketide producing streptomycetes.** Canadian Journal of Microbiology. 34: 1235-1240.

Dekleva, M.L., & Strohl, W.R. (1988b). **Activity of phosphoenolpyruvate carboxylase of an anthracycline-producing streptomycete**. Canadian Journal of microbiology. 34:1241-1246.

Dekleva, M.L., and Strohl, W.R. (1987). **Glucose stimulated acidogenesis by *Streptomyces peuceticus*.** Canadian Journal of Microbiology. 33: 1129-1132.

Delaunay, S., Uy, D. (1999) **Importance of phosphoenolpyruvate carboxylase of *C. glutamicum* during the temperature triggered glutamic acid fermentation.** Metabolic Engineering. 1, 334-343.

Delgado, J., and Liao, J.C. (1997). **Inverse flux analysis for reduction of acetate excretion in *Escherichia coli***. Biotechnology Progress. 13: 361-367.

Delgado, J., Meruane, J., and Liao, J.C. (1993). **Experimental determination of flux control distributions in biochemical systems: *In vitro* model to analyze transient metabolite concentrations.** Biotechnology and Bioengineering. 41: 1121-1128.

Delic, I., Robbins, P., and Westpheling, J. (1992). **Direct repeat sequences are implicated in the regulation of two *Streptomyces* chitinase promoters that are subject to carbon catabolite control.** Proc. Natl. Acad. Sci. USA **89**:1885-1889.

Dell'Anno, A., Fabiano, M., Duineveld, G.C.A., Kok, A., & Danovaro, R. (1998). **Nucleic acid (DNA, RNA) quantification and RNA/DNA ratio determination in marine sediments: Comparison of spectrophotometric, fluorometric, and high performance liquid chromatography methods and estimation of detrital DNA**. Applied and Environmental Microbiology. 64: 9: 3238-3245.

Demain, A.L (1979). **Carbon source regulation of idiolite biosynthesis in Actinomycetes.** In. Regulation of secondary metabolism in *Actinomycetes*. 4: 127-133.

Demain, A.L. (1980). **Do antibiotics function in nature**. Search. 11: 5: 148-151.

Demain, A.L. (1986). **Control of secondary metabolism in *actinomycetes***. Pp. 215-225 in G. Szabo *et al*. (Eds): Biological, Biochemical and Biomedical Aspects of *Actinomycetes*. Akademiai Kiado, Budapest.

Demain, A.L. (1992). **Microbial secondary metabolism: A new theoretical frontier for academia, a new opportunity for industry**. pp. 3-16 in D.J. Chadwick, J. Whelan (Eds): Secondary Metabolites: their function and evolution. Ciba Foundation Symp. 171. Wiley, Chichester.

Dennis, P.P., and Bremer, H. (1974). **Macromolecular composition during steady-state growth of *Escherichia coli* B/r.** Journal of Bacteriology. 119 (1): 270-281.

Desai, R.P., and Harris, L.M. (1999). **Metabolic flux analysis elucidates the importance of the acid-formation pathways in regulating solvent production by *Clostridium acetobutylicum*.** Metabolic Engineering. 1: 206-213.

Desai, R.P., Nielsen, L.K., & Papoutsakis, E.T. (1999). **Stoichiometric modeling of *Clostridium acetobutylicum* fermentations with non-linear constraints**. Journal of Biotechnology. 71: 191-205.

Diamond, J.D. (1981). **Practical experimental design for engineers and scientists.** Van Norstrand Reinhold, New York, USA.

Dmitrieva, N.F., *et al*. (1976). **The variations occurring in the anionic carbohydrate-containing polymers in *Streptomyces rimosus* cell walls.** Khimiya. 102: 477-481.

Dobrova, Z., Naprstek, J., Jiresova, M., and Janecek, J. (1984). **cAMP and adenylate cyclase activity in *Streptomyces granaticolor*.** FEMS Microbiology Letters. 22 (3): 197-200.

Dole, V.P., and Meinertz, H. (1960). **Microdetermination of long-chain fatty acids in plasma and tissues.** The Journal of Biological Chemistry. 235 (9): 2595-2599.

Donadio, S., Shafiee, A., and Hutchinson, C.R. (1990). **Disruption of a rhodanese-like gene results in a cysteine auxotrophy in *Saccharopolyspora erythraea*.** Journal of Bacteriology. 172: 350-360.

Doolittle, R.F. (1979). In: **The Proteins.** Eds. Neurath, H and Hill, R.L (Academic, New York), 3rd Ed. 4: 1-118.

Doran, P.M. (1997). **Bioprocess Engineering Principles**. Academic Press. 24 – 28 Oval Road, London NW1 7DX, UK.

Doskocil, J., Hostalek, Z., Kasparova, J., Zajicek, J., & Herald, M. (1959). **Development of *Streptomyces* Aureofaciens in submerged culture.** Journal of Biochemical and Microbiological Technology and Engineering. 1: 3: 261-271.

Dotzlaf, J.E., Metzger, L.S., & Foglesong, M.A. (1984). **Incorporation of amino acid derived carbon into tylactone by *Streptomyces fradiae* GS14**. Antimicrobial Agents and Chemotherapy. 25: 2: 216-220.

Doull, J.L., & Vining, L.C. (1990). **Physiology of antibiotic production in actinomycetes and some underlying control mechanisms**. Biotech. Adv. 8: 141-158.

Doyle, D.A., Cabral, J.M., Pfeutzner, R.A., Kuo, A., Gulbis, J.M., Cohen, S.L., Chait, B.T., and MacKinnon, R. (1998). **The Structure of the Potassium Channel: Molecular Basis of K+ Conduction and Selectivity.** Science. 280: 69-76.

Drawid, A., Jansen, R., and Gerstein, M. (2000). **Genome-wide analysis relating expression level with protein subcellular localization.** Trends Genet. 16: 426-430.

Drew, S.W. (1977). **Effect of primary metabolites on secondary metabolism**. Annual Review of Microbiology. 31: 343-356.

Duboc, P., Marison, I., von Stockar, U. (1996). **Physiology of *Saccharomyces cerevisiae* during cell cycle oscillations.** Journal of Biotechnology. 51: 57-72.

Duboc, P., Schill, N., Menoud, L., van Gulik, WM, von Stockar, U. (1995). **Measurements of sulphur, phosphorus and other ions in microbial biomass: influence on correct determination of elemental composition and degree of reduction.** Journal of Biotechnology. 43: 145-158.

Dubois, M., Gilles, K.A., Hamilton, J.K., Rebers, P.A., & Smith, F. (1956). **Colorimetric method for determination of sugars and related substances.** Analytical Chemistry. 28: 3: 350-356.

Dufton, M.J. (1997). **Genetic code synonym quotas and amino acid complexity: cutting the cost of proteins?** Journal Theoretical Biology. 187: 165-173.

Dupont de Nemours, E.I. (1975). **Strategy of experimentation, revised edition.** Dupont de Nemours, Wilmington, D.E.

Edwards, J.S., and Palsson, B.O. (2000a). **The *Escherichia coli* MG1655 *in silico* metabolic genotype: Its definition, characteristics, and capabilities**. Proc. Natl. Acad. Sci. U.S.A. 97: 5528-5533.

Edwards, J.S., and Palsson, B.O. (2000b) **Metabolic flux balance analysis and the *in silico* analysis of *Escherichia coli* K-12 gene deletions**. BMC Bioinformatics 1: 1-10.

Edwards, J.S., Ramakrishna, R., Schilling, C.H., Palsson, B.O. (1999). **Metabolic Flux Balance Analysis.** Metabolic Engineering. pp. 13-57. Edited by Lee SY, Papoutsakis, E. T.

Ehlde, M., & Zacchi, G. (1997). **A general formalism for metabolic control analysis**. Chemical Engineering Science. 52: 15: 2599-2606.

Eigen, M., and Schuster, P. (1979). **The Hypercycle, a Principle of Natural Self-Organization** (Springer, Berlin). 64.

Einarsson, S., Josefson, B., and Lagerkvist, S. (1983). **Determination of amino acids with 9-fluorenylmethyl chloroformate and reversed phase high-performance chromatography**. Journal of Chromatography. 282: 609-618.

El-Mansi, E.M.T., and Stephanopoulos, G. (1999). **Flux control analysis: basic principles and industrial applications.** Fermentation Microbiology and Biotechnology. Edited E.M.T El-Mansi and C.F.A Bryce. Taylor and Francis. 9.

El-Mansi, E.M.T., Nimmo, H.G., and Holms, W.H. (1985). **The role of isocitrate in control of the phosphorylation of isocitrate dehydrogenase in *Escherichia coli*.** FEBBS Lett. 183: 251-255.

Elson, S.W., Baggaley, K.H., Fulston, M., Nicholson, N.H., Tyler, J.W., and Edwards, J. et al. (1993). **2 Novel arginine derivatives from a mutant of *Streptomyces clavuligerus*.** J Chem Soc Chem Commun. 1993: 1211.

Emmerling, M., Dauner, M., Ponti, A., Fiaux, J., Hochuli, M., Szyperski, T., Wuthrich, K., Bailey, J.E., and Sauer, U. (2002). **Metabolic flux response to pyruvate kinase knockout in *Escherichia coli*.** Journal of Bacteriology. 184 (1): 152-164.

Erickson, L.E., Minkenich, I.G., and Eroshin, V.K. (1979). **Utilization of mass-energy balance regularities in the analysis of continuous culture data.** Biotechnology and Bioengineering. 21: 575-591.

Evans, C.T., and Ratledge, C. (1984a). **Effect of nitrogen source on lipid accumulation in oleaginous yeasts.** Journal of General Microbiology. 130: 1693-1704.

Evans, C.T., and Ratledge, C. (1984b). **Phosphofructokinase and the regulation of the flux of carbon from glucose to lipid in the oleaginous yeast *Rhodosporidium toruloides***. Journal of General Microbiology. 130: 3251-3264.

Evans, P.R., Farrants, G.W., and Hudson. P.J. (1981). **Phosphofructokinase: Structure and control.** Phil. Trans. R. Society 293:53-62.

Eyre-Walker, A. (1996). **Synonymous codon bias is related to gene length in *Escherichia coli*: selection for translational accuracy.** Mol Biol Evol. 13: 864-872.

Fabry, S., and Hensel, R. (1988). **Primary structure of glyceraldehyde-3-phosphate dehydrogenase deduced from the nucleotide sequence of the thermophilic archaebacterium *Methanothermus fervidus***. Gene 64:189-197.

Fabry, S., Lang, J., Niermann, T., Vingron, M., and Hensel. R. (1989). **Nucleotide sequence of the glyceraldehyde-3-phosphate dehydrogenase gene from the mesophilic methanogenic archaebacteria *Methanobacterium bryantii* and *Methanobacterium formicicum***. European Journal of Biochemistry. 179:405-413.

Fell, D. & Thomas, A. (1995). **Physiological control of metabolic flux: the requirement for multisite modulation**. Biochemical Journal. 311: 35-39.

Fell, D. (1992). **Metabolic control analysis: a survey of its theoretical and experimental development**. Biochemical Journal. 286:313-330.

Fell, D. (1997). **Understanding the control of metabolism**. Frontiers in Metabolism 2. Portland Press. London, UK.

Fell, D. (1998). **Increasing the flux in metabolic pathways a metabolic control analysis perspective**. Biotechnology & Bioengineering. 58: (5) 121-124.

Fell, D.A., and Small, J.R. (1986). **Fat synthesis in adipose tissue. An examination of stoichiometric constraints.** Biochemical journal. 238 (3): 781-786.

Fish, S.A & Cundliffe, E. (1997). **Stimulation of polyketide metabolism in *Streptomyces fradiae* by tylosin and its glycosylated precursors**. Microbiology. 143: 3871-3876.

Fisher, S.H. (1989). **Glutamate synthesis in *Streptomyces coelicolor***. Journal of Bacteriology. 171: 2372-2377.

Fishman, S.E., Cox, K., Larson, J.L., Larson, P.A., Reynolds, E.T., Seno, W.K., Yeh, R., Van Frank, and Hershberger, C.L. (1987). **Cloning genes for the biosynthesis of a macrolide antibiotic.** Proc Natl Acad. Sci USA. 84: 8248-8252.

Fleck, A., and Munro, H.N. (1962). **The precision of ultraviolet absorption measurements in the Schmidt-Thannhauser procedure for nucleic acid estimation.** Biochimica ET Biophysica Acta. 55: 571-583.

Folch, J., Lees, M., and Stanley, G.H.S. (1957). **A simple method for the isolation and purification of total lipides from animal tissues.** J Biol Chem. 226: 497-509.

Foster, J.W., and Katz, E. (1981). **Control of actinomycin D biosynthesis in *Streptomyces parvulus*: Regulation of tryptophan oxygenase activity.** Journal of Bacteriology. 148: 670-677.

Fothergill-Gilmore, L. A. and P. A. M. Michels. (1993). **Evolution of glycolysis.** Prog. Biophys. Mol. Biol 59:105-235.

Fouces, R., Mellado, E., Diez, B, Barredo, J.L. (1999) **The tylosin biosynthetic cluster from *Streptomyces fradiae*: genetic organization of the left region**. Microbiology. 145: 855-868.

Fraenkel, D.G. (1996). In ***E. coli* and *Salmonella*: Cellular and molecular biology** (Neidhardt, F.C., ed). 189-198. FC American Society for Microbiology (ASM). Press, Washington, DC, USA.

Francesco, M.W., Boccu, E., and Fontana, A. (1982). **6-phosphogluconate dehydrogenase from *Bacillus stearothermophilus***. In Methods in Enzymology: Carbohydrate Metabolism Part D. 89: 282-291. Edited by W.A, Wood. Academic Press, Inc. London, UK.

Froehlich, K.U., Kannwischer, R., Rudiger, M. and Mecke, D. (1996) **Pentalenolactone-insensitive glyceraldehydes-3-phosphate dehydrogenase from *S. arenae* is closely related to GAPDH from thermostable eubacteria and plant chloroplasts.** Archives of Microbiology. 165, 179-186.

Furst, P., Pollack, L., Graser, T.A., Godel, H., and Stehle, P. (1990). **Appraisal of four pre-column derivatization method for high performance liquid chromatography determination of free amino acids in biological materials.** Journal of. Chromatography. 499, 557- 569.

Fu, J. (1996). **Defined medium OMPC fermentation process.** US patent 5494808.

Gallo, M., and Katz, E. (1972). **Regulation of secondary metabolite biosynthesis: catabolite repression of phenoxazinone synthase and actinomycin formation by glucose.** Journal of Bacteriology. 109: 659-667.

Gandecha, A.R., Large, S.L., and Cundliffe, E. (1997). **Analysis of four tylosin biosynthetic genes from the *tyl*LM region of the *Streptomyces fradiae* genome.** Gene. 184: 197-203.

Garcia-Dominguez, M., Martin, J.F., & Liras, P. (1989). **Characterization of sugar uptake in wild-type *Streptomyces clavuligerus*, which is impaired in glucose uptake and in a glucose-utilizing mutant.** Journal of Bacteriology. 171: 6808-6814.

Garcia-Ochoa, F., Santos, V.E., and Fritsch, A.P. (1992). **Nutritional study of *Xanthomonas campestris* in xanthan gum production by factorial design of experiments.** Enzyme Microb Technol. 14: 991-996.

Garner, H.R., and Koffler, H. (1951). **Preliminay evidence against the existence of a krebs cycle in *Streptomyces griseus*.** Bact Proc. 139.

Gersch, D., and Strunk, C. (1980). **Cyclic adenosine-3',5'-monophosphate as 'first messenger' in *Streptomyces hygroscopicus* - bimodal regulation of germination and growth.** Current Microbiology. 4 (5): 271-275.

Gill, J.A., Liras, P., and Martin, J.F. (1984). **The polyenes: Properties, biosynthesis and fermentation.** 513-529. In E.J. Vandame (ed). Biotechnology of Industrial Antibiotics. Marcel Dekker, London, UK.

Goel, A., Ferrance, J., Jeong, J. & Ataai, M.M. (1993). **Analysis of metabolic fluxes in batch and continuous cultures of *Bacillus subtilis***. Biotechnology and Bioengineering. 42: 686-696.

Goldberg, I., and Er-Al, Z. (1981). **The chemostat - an efficient technique for medium optimization.** Proc Biochem. 16: 2-8.

Goodfellow, M., and Cross, T. (1984). Classification. In M. Goodfellow, S. T. Williams, and M. Mordarski. (Eds). **The Biology of the actinomycetes.** Academic Press. New York, USA. 7-164.

Grafe, U., Bocker, H., and Thrum, H. (1979). **Regulative influence of o-aminobenzoic acid on the biosynthesis of nourseothricin in cultures of *Streptomyces noursei* JA 3890b: IV. Bistability of metabolism of the mechanism and the mechanism of action of aminobenzoic acids.** Z Allg Mikrobiol. 19: 235-246.

Grafe, U., Bocker, H., Reinhardt, G., & Thrum, H. (1974a). **Alanine-dehydrogenasektivitat und antibioticumbildung in kulturen des *Streptomyces hygroscopicus* JA 6599**. Z. Allg. Mikrobiol. 14: 181-192.

Grafe, U., Bocker, H., Reinhardt, G., & Thrum, H. (1974b). **Regulatative beeinflussung der nourseothricinbiosynthese durch o-aminobenzoesaure in kulturen des *Streptomyces noursei* JA 3890b**. Z. Allg. Mikrobiol. 14: 659-673.

Grafe, U., Bocker, H., & Thrum, H. (1977). **Regulative influence of o-aminobenzoic acid on the biosynthesis of nourseothricin in cultures of *Streptomyces noursei* JA 3890b. II. Regulation of glutamine synthetase and the role of glutamine synthetase/glutamate synthase pathway**. Z. Allg. Mikrobiol. 17: 201-209.

Grafe, U., Reinhardt, G., and Thrum, H. (1975). **Indzierbare Akkumulation von α-ketoglutarsaure in kulturen eines makrolidantibioticum-bildenden stammes von *Streptomyces hygroscopicus*.** Z Allg Mikrobiol. 15: 575-583.

Graham, M.Y., and Weisblum, B. (1979). **23S ribosomal ribonucleic acid of macrolide producing streptomycetes contains methylated adenine.** Journal of Bacteriology. 137: 1464-1467.

Gram, A. (1997). **Biochemical engineering and industry.** Journal of Biotechnology. 59: 19-23.

Gray, D.I., Gooday, G.W., and Prosser, J.I. (1990). **Histological staining of nuclear material in hyphae of *Streptomyces coelicolor* A3(2).** Journal of Microbiological Methods. 12: 163-172.

Gray, P.P & Bhuwapathanapun, S. (1980b). **Tylosin: properties, biosynthesis, and fermentation**. Biotechnology Letters. 10: 743-757.

Gray, P.P & Vu-Trong. K. (1987a). **Extended cyclic fed-batch tylosin fermentations**. Biotechnology Letters. 9: 9: 617-620.

Gray, P.P. (1980). **Tylosin.** Journal of Fermentation Biotechnology. Healthcare Products. 83-93.

Gray, P.P., & Bhuwapathanapun. S. (1980a). **Production of the macrolide antibiotic tylosin in batch and chemostat cultures**. Biotechnology and Bioengineering. 22: 1785-1804.

Gray, P.P., & Vu-Trong. (1987b). **Production of the macrolide antibiotic tylosin in cyclic fed-batch culture**. Biotechnology & Bioengineering. 29: 33-40.

Greasham, R.L., and Herber, WK. (1997). **Design and optimization of growth media.** In: Rhodes, P.M, Standury, P.F (Eds). Applied microbial physiology: a practical approach. Oxford University Press, Oxford. 53-74, UK.

Greasham, R.L., and Inamine, E. (1986). **Nutritional improvement of processes**. In: Demain A.L, Solomon, NA (Eds) Manual for industrial microbiology and biotechnology. ASM, Washington. 41-48.

Green, G.A., Girardot, R., Baldacini, O., and Ledig, M. (1993). **Characterization of enolase from *Clostridium difficile*.** Curr. Microbiology. 26:53-56.

Green, J.R., and Margerison, D. (1978). "**Statistical treatment of experimental data. Physical sciences Data 2".** Elsevier Scientific Publishing Company. Amsterdam.

Grund. A.D., Ensign, J.C. (1978) **Role of carbon dioxide in germination of spores of *S. viridochromogenes*.** Archives of Microbiology. Sept; 118(3): 279-288.

Gu, X., Hewett-Emmett, D., and Li, W.H. (1998). **Directional mutational pressure affects the amino acid composition and hydrophobicity of proteins in bacteria.** Genetica. 102/103: 383-391.

Guarakan, T., Marison, I.W., von Stockar, U., Gustafsson, L., Gnaiger, E. (1990). **Proposal for a standardized sample handling procedure for the determination of elemental composition and enthalpy of combustion of biological material.** Thermochim Acta. 172: 251-266.

Guebel, D.V., and Torres Darias, N.V. (2001). **Optimization of the citric acid production by *Aspergillus niger* through a metabolic flux balance model.** Journal of Biotechnology. 4 (1).

Guerrant, G.O., Lambert, M.A., and Moss, C.W. (1982). **Analysis of short-chain acids from anaerobic bacteria by high-performance liquid chromatography**. Journal of Clinical Microbiology. 16 (2): 355-360.

Guthrie, E.P., Flaxman, C.S., White, J. *et al*. (1998). **A response-regulator-like activator of antibiotic synthesis from *Streptomyces coelicolor* A3(2) with an amino-terminal domain that lacks a phosphorylation pocket**. Microbiology. 144: 727-738.

Gutierrez, G., Marquez, L., and Martin, A. (1996). **Preference for guanosine at first codon position in highly expressed *Escherichia coli* genes: a relationship with translational efficiency.** Nucleic Acids Res. 24: 2525-2527.

Hadzija, O. (1974). **A simple method for the quantitative determination of muramic acid.** Analytical Biochemistry. 60: 512-517.

Hallis, T.M., and Liu, H.W. (1999). **Learning nature's strategies for making deoxy sugars: pathways, mechanisms, and combinatorial applications.** Accounts of Chemical Research. 32 (7): 579-588.

Han, L., Khetan, A., Hu, W.S., and Sherman, D.H. (1999). **Time-lapsed confocal microscopy reveals temporal and spatial expression of the lysine ε-aminotransferase gene in *Streptomyces clavuligerus*.** Molecular Microbiology. 34 (5): 878-886.

Hancock, I.C. (1994). **Analysis of cell wall constituents of Gram-positive bacteria.** Chemical Methods in Prokaryotic Systematics. Edited by Goodfellow, M., and O'Donnell. 3. 63-84.

Hans, L., Reynolds, K.A. (1997) **A novel alternate anaplerotic pathway to the glyoxylate cycle in streptomycetes**. Journal of Bacteriology. Aug; 179(16): 5157-64.

Hanson, R.S., and Phillips, J.A. (1981). **Chemical composition.** In: Manual of Methods for General Bacteriology (Eds. P. Gerhardt., R.G.E, Murray., and G.B, Phillips). American Society for Microbiology, Washington, DC, USA. 328-364.

Hartley, D.L., and Speedie, M.K. (1984). **A tryptophan C-methyltransferase involved in streptonigrin biosynthesis in *Streptomyces flocculus*.** Biochemical Journal. 220: 309-313.

Harwood, J.L. (1988) **Fatty acid metabolism**. Annu. Rev. Plant Physiol. 39, 101-138.

Hatzimanikatis, V., Floudas, C.A., and Bailey, J.E. (1996). **Analysis and design of metabolic reaction networks via mixed-integer linear optimization**. AIChE J. 42: 1277-1292.

Heijnen, J.J., and Roels, J.A. (1981). **A macroscopic model describing yield and maintenance relationships in aerobic fermentation processes.** Biotechnology and Bioengineering. 23: 739-763.

Heinisch, J., Ritzel, R.G., Von, B.R.C., Aguilera, A., Rodicio, R., and Zimmermann, F.K. (1989). **The phosphofructokinase genes of yeast evolved from two duplication events.** Gene. 78: 309-322.

Heinrich, R., and Rapoport, T.A. (1974). **A linear steady state treatment of enzymatic chains. General properties, control and effector strength.** European Journal of Biochemistry. 42: 89-95.

Held, T., and Kutzner, H.J. (1990). **Transcription of the tyrosinase gene in *Streptomyces michiganensis* DSM 40015 is induced by copper and repressed by ammonium.** J Gen Microbiol. 136: 2413-2419.

Hellinga, H.W., and Evans, P.R. (1985). **Nucleotide sequence and high level expression of the major *Escherichia coli* phosphofructokinase**. European Journal of Biochemistry. 149: 363-373.

Herbert, D. (1976). **Stoichiometric aspects of microbial growth**. In A.C.R. Dean., D.C. Ellwood., C.G.T. Evans and J. Melling (Eds). Continuous culture 6: Applications and New Fields. Ellis Horwood, Chichester. 1-39.

Herbert, D., Phipps, P.J., & Strange, R.E. (1971). **Chemical analysis of microbial cells**. Microbial Physiology. 3: 209-344.

Heyden, Y.V., Saevels, J., Roets, E., Hoogmartens. J., Decolin, D., Quaglia, M.G., Bossche, W.V., Leemans, R., Smeets, O., Van de Vaart, F., Mason, B., Taylor, G.C., Undeberg, W., Bult, A., Chiap, P., Crommen, J., De Beer, J., Hansen, S.H., and Maasart, D.L. (1999). **Interlaboratory studies on two high-performance liquid chromatographic assays for tylosin (tartrate).** Journal of Chromatography A. 830: 3-28.

Higashide, E. (1984). **The macrolides: properties, biosynthesis and fermentation.** In: Biotechnology of Industrial Antibiotics (Drugs and the pharmaceutical Sciences Vol 22). Edited by Vandamme E.J. 451-509. Marcel Dekker, New York, USA.

Higgins, H. (1965). **Dynamics and control in cellular reactions**." Control of Energy Metabolism," pp. 13-36. Edited by Chance, B., Estabrook, R.W., and Williamson, J.R.. Academic Press. New York, USA.

Higgins, J. (1963). **Analysis of sequential reactions**. Annuals of the New York Academy of Science. 108: 305-321.

Hindle, Z., and Smith. C.P. (1994). **Substrate induction and catabolite repression of the *Streptomyces coelicolor* A3(2) *g*lycerol operon are mediated through the GylR protein**. Molecular Microbiology. 12:737-745.

Hirose, Y., and Shibai, H. (1980). **Effect of oxygen on amino acids fermentation.** Advances in Biotechnology. 1: 329-333 (Editors Moo-Young, M., Robinson, C.W., and Vezina, C). Pergamon Press, Toronto.

Hitchcock, M.JM and Katz, E. (1988). **Purification and characterization of tryptophan dioxygenase from *Streptomyces parvulus*.** Arch Biochem Biophys. 261: 148-160.

Hobbs, G., Frazer, C. M., Gardner, D.C.J., Cullum, J.A., Oliver, S.G (1989). **Dispersed growth of *Streptomyces* in liquid culture**. Applied Microbiology and Biotechnology. 31: 272-277.

Hobbs, G., Obanye, A.I.C., Petty, J., Mason, J.C., Barratt, E., Gardner, D.C.J., Flett, F., Smith, C.P., Broda, P., and Oliver, S.G. (1990). **An investigation approach to studying regulation of production of the antibiotic methylenomycin by *Streptomyces coelicolor* A3(2).** Journal of Bacteriology. 174: 1487-1494.

Hockenhull, D.J.D., Fantes, K.H., Herbert, M., and Whitehead, B. (1954). **Glucose utilization by *Streptomyces griseus*.** Journal of General Microbiology. 10: 353-370.

Hodgson, D.A. (1982) **Glucose repression of carbon source uptake and metabolism in *Streptomyces coelicolor* A3(2) and its perturbation in mutants resistant to 2-deoxyglucose.** J. Gen. Microbiol. 128: 2417-2430.

Hodgson, D.A. (2000). **Primary metabolism and its control in streptomycetes: A most unusual group of bacteria.** Advances in Microbial Physiology. 42: 47-235.

Hoek, J.B., and Rydström, J. (1988). **Physiological roles of nicotinamide nucleotide transhydrogenase.** Biochemical Journal. 254: 1-10.

Hofmann, E. (1976). **The significance of phosphofructokinase to the regulation of carbohydrate metabolism.** Rev Physiol Biochem Pharmacol. 75: 1-67.

Hofmeyr, J.H., Cornish-Bowden, A., and Rohwer, J.M. (1993). **Taking enzyme kinetics out of control; putting control into regulation.** European Journal of Biochemistry. 212: 833-837.

Hofmeyr, J.H.S., and Cornish-Bowden, A. (2000). **Regulating the cellular economy of supply and demand**. FEBS Letters. 476: 47-51.

Hoggarth, J.H., Cushing, K.E., Mitchell, J.J., and Ritchie, D.A. (1994). **Induction of resistance to novobiocin in the novobiocin-producing organism *Streptomyces niveus.*** FEMS Microbiol Lett. 116: 131-136.

Holms, W.H. (1986). **The central metabolic pathways of *E. coli* relationship between flux and control at a branch point, of conversion to biomass, and excretion of acetate**. Current topics in Cellular Biotechnology. 28: 69-105.

Holms, W.H. (1991). **Improvements to microbial productivity by analysis of metabolic fluxes.** Journal of Chemical Technology and Biotechnology. 50: 139-141.

Holms, W.H. (1996). **Flux analysis and control of the central metabolic pathways in *E. coli.*** FEMS microbiology reviews. 19: 85-116.

Holms, W.H. (1997). **Metabolic flux analysis**. In A practical approach: to microbial physiology. Edited by P.M. Rhodes and P.F. Stanbury. IRL Press at Oxford University Press. 9: 213-247.

Holms, WH. (2001). **Flux analysis: a basic tool of microbial physiology**. Adv. Microb. Physiol. 45: 271-340.

Holt, T.G., Chang, C., Laurent-Winter, C., Murakami, T., Garrels, J.I., Davies, J.E., and Thompson, C.J. (1992). **Global changes in gene expression related to antibiotic synthesis in *Streptomyces hygroscopicus*.** Molecular Microbiology. 6 (8): 969-980.

Hood, D.W., Heidstra, R., Swoboda, U.K., and Hodgson, D.A. (1992). **Molecular genetic analysis of proline and tryptophan biosynthesis in *Streptomyces coelicolor* A3(2): interaction between primary and secondary metabolism: a review.** Gene. 115: 5-12.

Hopwood, D.A. (1959). **Linkage and the mechanism of recombination in *Streptomyces coelicolor*.** Ann NY Acad Sci. 81: 887-898.

Hopwood, D.A. (1992). **Understanding the genetic control of antibiotic biosynthesis and sporulation in *Streptomyces***. Microbiology. 20: 3-10.

Hopwood, D.A. (1999) **Forty years of genetics with *Streptomyces*: from in vivo through in vitro to *in silico*.** Microbiology. 145, 2183-2202.

Horinouchi, S. and T. Beppu. (1984). **Production in large quantities of actinorhodin and undecylprodigiosin induced by *afs*B in *Streptomyces lividans*.** Agric. Biol. Chem. 48: 2131-2133.

Horinouchi, S. and T. Beppu. (1990). **Autoregulatory factors of secondary metabolism and morphogenesis in actinomycetes.** Crit Rev Biotechnol 10 (3): 191-204.

Hoskisson, P.A., Hobbs, G. and Sharples, G.P. (2001). **Antibiotic production, accumulation of intracellular carbon reserves and sporulation in *Micromonospora echinospora*** (ATCC 15837). *Canadian Journal of Microbiology* 47, 148-152.

Hostalek, Z., Tinterova, M., Jechova, V. *et al*. (1969). **Regulation of biosynthesis of secondary metabolites. I. Biosynthesis of chlortetracycline and tricarboxylic acid cycle activity**. Biotechnology and Bioengineering. 11: 539-548.

Hostalek, Z., Tobek, I., Bobyk, M.A., and Kulayev, I.S. (1976). **Role of ATP-glucokinase and polyphosphate glucokinase in *Streptomyces aureofaciens*.** Folia Microbiol. 21: 131-138.

Hranueli, D., Peric, N., Borovicka, B., Bogdan, S., Cullum, J., Waterman, P.G., and Hunter, I.S. (2001). **Molecular Biology of Polyketide Biosynthesis.** Food Technol Biotechnol. 39 (3): 203-213.

Hsieh, P.C., Shenoy, B.C., Haase, C.F., Jentoft, J.E., and Phillips, N.F.B. (1993). **Involvement of tryptophan(s) at the active site of polyphosphate/ATP glucokinase from *Mycobacterium tuberculosis***. Biochemistry **32**:6243-6249.

Hsieh, P.C., Shenoy, B.C., Samols, D., and Phillips, N.F.B. (1996b). **Cloning, expression, and characterization of polyphosphate glucokinase from *Mycobacterium tuberculosis***. J. Biol. Chem. 271:4909-4915.

Hsieh, P.C., Kowalczyk, T.H., and Philips. N.F.B. (1996a). **Kinetic mechanisms of polyphosphate glucokinase from *Mycobacterium tuberculosis***. Biochemistry 35:9772-9781.

Hu, D.S.J., Hood, D.W., Heidstra, R., and Hodgson, D.A. (1999). **The expression of the *trp*D, *trp*C, and *trp*BA genes of *Streptomyces coelicolor* A3(2) is regulated by growth rate and growth phase but not by feedback repression.** Molecular Microbiology. 32: 869-880.

Hua, Q., and Shimizu, K. (1999). **Effect of dissolved oxygen concentration on the intracellular flux distribution for pyruvate fermentation**. Journal of Biotechnology. 68: 135-147.

Hua, Q., Araki, M., Koide, Y., and Shimizu, K. (2001). **Effects of glucose, vitamins, and DO concentrations on pyruvate fermentations using *Torulopsis glabrata* IFO 0005 with metabolic flux analysis.** Biotechnology progress. 17: 62-68.

Hua, Q., Fu, P.C., Yang, C., and Shimizu, K. (1998). **Microaerobic lysine fermentations and metabolic flux analysis**. Biochem. Eng. J., 2, 89-100.

Huang, S.L., T. C. Hassell., and W. K. Yeh. (1993). **Purification and properties of NADPH-dependent tylosin reductase from *Streptomyces fradiae*.** J. Biol. Chem. 268: 18987-18993.

Huber, M.L.B., Paschal, J.W., Leeds, J.P., Kirst, H.A., and Wind, J.A. (1990). **Branched chain fatty acids produced by mutants of *Streptomyces fradiae*, putative precursors of the lactone ring of tylosin.** Antimicrobial Agents and Chemotherapy. 34: 1535-41.

Huettner, S., Mecke, D., & Froehlich, K.U. (1997) **gene cloning and sequencing and enzyme purification of the malate synthase of *Streptomyces arenae***. Gene. 188: 239-246.

Hughes, N.J., Clayton, C.L., Chalk, P.A., and Kelly, D.J. (1998). ***Helicobacter pylori par*CDAB and *oor*DADC genes distinct pyruvate: florodoxin and 2-oxo-glutarate: acceptor oxidoreductases also redirect electron transport to NADP**. Journal of Bacteriology. 180: 1119-1128.

Hunter, I. (1992). **Function and evolution of secondary metabolites-no easy answer**. TIBTECH. 10: 144-146.

Hurtubise, Y., Shareck, F., Kluepfel, D., and Morosoli, R.A. (1995). **Cellulase / xylanase-negative mutant of *Streptomyces lividans* 1326 defective in cellobiose and xylobiose uptake is mutated in a gene encoding a protein homologous to ATP-binding proteins.** Molecular Microbiology. 17: 367-377.

Hutchison, C.R. (1998). **Combinatorial biosynthesis for new drug discovery.** Curr Opin Microbiol. 1: 319-329.

Hutchison, W.C., & Munro, H.N. (1961). **The determination of nucleic acids in biological materials: a review**. The Analyst. 86: 768-813.

Ikeda H., Ishikawa J., Hanamoto A., Shinose M., Kikuchi H., Shiba T., Sakaki Y., Hattori M., Omura S. (2003). **Complete genome sequence and comparative analysis of the industrial microorganism *Streptomyces avermitilis*.** Nat. Biotechnol. 21: 526-531.

Ikemura, T. (1985). **Codon usage and transfer-RNA content in unicellular and multicellular organisms.** Mol Biol Evol. 2 (1): 13-34.

Inbar, L., & Lapidot, A. (1991). **^{13}C-nuclear magnetic resonance and gas chromatography-mass spectrometry studies of carbon metabolism in the actinomycin D Producer *Streptomyces parvulus* by use of ^{13}C-labeled precursors**. Journal of Bacteriology. 173: 7790-7801.

Inglis, A.S. (1983). **Single hydrolysis method for all amino acids, including cysteine and tryptophan.** Methods in Enzymology. 91: 26-36.

Ingraham, J.L., Maaloe, O., and Neidhardt, F.C. (1983). "**Growth of the bacterial cell".** Sinauer associates, Publishers Sunderland, Massachusetts, USA.

Ingram, C., Delic, I., and Westpheling, J. (1995). ***ccr*AI: A mutation in *Streptomyces coelicolor* that a affects the control of catabolite repression.** Journal of Bacteriology. 177: 3579-3586.

Ison, A. P., and Mathew, G. B. (1997). **Measurement of biomass**. Applied Microbial Physiology. A Practical Approach Edited by P. M. Rhodes, Bioscot Ltd, Edinburgh, and P. F., University of Hertfordshire. Press at Oxford University Press.

Ives, P. R., & Bushell, M. E. (1997). **Manipulation of the physiology of clavulanic acid production in *Streptomyces clavuligerus*.** Microbiology 143, 3573-3579.

Jachymova, J., Votruba, J., Viden, I., and Rezanka, T. (2002). **Identification of *Streptomyces* Odor Spectrum.** Folia Microbiologica. 47 (1) 37-41.

Janecek, J., Tichy, P., Spizek, J., & Vanek, Z. (1997). **Constitution of the metabolic type of streptomycetes during the first hours of cultivation**. Folia Microbiology. 42: 2: 75-96.

Jansen, R., and Gerstein, M. (2000). **Analysis of the yeast transcriptome with structural and functional categories: characterizing highly expressed proteins.** Nucleic Acids Res. 28: 1481-1488.

Jarret, H.W., Cooksy, K.D., Ellis, B., and Anderson, J.M. (1986). **The separation of o-phthalaldehyde derivatives of amino acids by reversed-phase chromatography on acetyl-silica columns.** Analytical Biochemistry. 153: 189-198.

Jechova, V., Hostalek, Z., & Vanek, Z. (1975). **Regulation of biosynthesis of secondary metabolites. XVII: Purification and properties of malate dehydrogenase (decarboxylating) in *Streptomyces aureofaciens***. Folia Microbiology. 20: 137-141.

Jensen, A.L., Darken, M.A., Shultz, J.S., Shay, A.J. (1964). **Relomycin: Flask and tank fermentation studies.** Antimicrobial Agents and Chemotherapy. 49-53.

Jetten, M.S.M., Gubler, M.E., Lee, S.H., and Sinskey, A.J. (1994). **Structural and functional analysis of pyruvate kinase from *Corynebacterium glutamicum*.** Applied Environmental Microbiology. 60:2501-2507.

Johnson, D.A., and Liu, H.W. (1998). **Mechanisms and pathways from recent deoxysugar biosynthesis research.** Current Opinion in Chemical Biology. 2 (5): 642-649

Johnson, M.J. (1964). **Utilisation of hydrocarbons by microorganisms**. Chem Ind. 36: 1532 - 1537.

Jones, C., Thompson, A., and England, R. (1996). **Guanosine 5'-diphosphate 3'-diphosphate (ppGpp), guanosine 5'-diphosphate 3'-monophosphate (ppGp) and antibiotic production in *Streptomyces clavuligerus*.** Microbiology UK. 142: 1789-1795.

Jones, N.D., Chaney, M.O., Kirst, H.A., Wild, G.M., Baltz, R.H., Hamill, R.L., and Paschal, J.W. (1982). **Novel fermentation products from *Streptomyces fradiae* X-ray crystal structure of 5-O-mycarosyltylactone and proof of the absolute configuration of tylosin.** Journal of Antibiotics. 35 (4): 420-425.

Jonsbu, E., Christensen, B., and Nielsen, J. (2001). **Changes of *in vivo* fluxes through central metabolic pathways during the production of nystatin by *Streptomyces noursei* in batch culture.** Applied Microbial Biotechnology. 56: 93-100.

Jorgensen, H., Nielson, J. & Villadsen, J. (1995a). **Metabolic flux distributions in *Penicillium chrysogenum* during fed batch cultivations**. Biotechnology and Bioengineering. 46: 117-131.

Jorgensen, H., Nielson, J. & Villadsen, J., & Mollgaard, H. (1995b). **Analysis of penicillin biosynthesis during fed-batch cultivations with a high yielding strain of *Penicillium chrysogenum***. Applied Microbiology Biotechnology. 43: 123-130.

Kacser, H & Burns, J.A. (1973b). **In rate control of biological processes**. Davies, D.D. ed. Pp65-104. Cambridge University Press.

Kacser, H & Burns, J.A. (1979). **Molecular democracy: Who shares the controls?** Biochemical Society Transactions. 7: 1149-1160.

Kacser, H. & Burns, J.A. (1973a). **The control of flux**. Symp. Soc. Exp. Biol. 27: 65-104.

Kacser, H. (1991). **The control of enzyme systems in vivo: Elasticity analysis of the steady state.** Biochemical Society Transactions 11: 35-43.

Kanaya, S., Kudo, Y., Kamura, Y., & Ikemura, T. (1996). **Detection of genes in *Escherichia coli* sequences determined by genome projects and prediction of protein production levels, based on multivariate diversity in codon usage.** Comput Appl Biosci. 12: 213-225.

Kanaya, S., Yamada, Y., Kudo, Y., and Ikemura, T. (1999). **Studies of codon usage and tRNA genes of 18 unicellular organisms and quantification of *Bacillus subtilis* tRNAs: gene expression level and species-specific diversity of codon usage based on multivariate analysis.** Gene. 238: 143-155.

Kaneda, T. (1991). **Iso- and anteiso-fatty acids in bacteria: biosynthesis, function and taxonomic significance.** Microbiological Reviews. 55: 288-302.

Kaneko, T., *et al*. (2000). **Complete genome structure of the nitrogen-fixing symbiotic bacterium *Mesorhizobium loti*.** DNA Res. 7: 331-338.

Kanfer, I., Skinner, M. F., and Walker, R.B. (1998). **Analysis of macrolide antibiotics.** Journal of chromatography A. 812: 255-286.

Kang, H.A., and Lee, K.J. (1987). **Regulation of cell growth and tylosin biosynthesis through flux control of metabolic intermediate in *Streptomyces fradiae*.** Korean Journal of Microbiology. 25 (3): 189-197.

Kang, H.A., Lee, J. H., and Lee, K.J. (1987). **Regulation of tylosin biosynthesis by cell growth rate in *Streptomyces fradiae***. Korean Journal of Microbiology. 25 (4): 353-359.

Kannan, L.V., & Rehacek, Z (1970). **Metabolism of *Streptomyces antibioticus*: variation of organic and amino acids**. Indian Journal Biochemistry. 7: 137-138.

Karlin, S., and Bucher, P. (1992). **Correlation-analysis of amino-acid usage in protein classes.** Proc Natl Acad Sci USA. 89: 12165-12169.

Karlin, S., Mrázek, J., Campbell, A., and Kaiser, D. (2001). **Characterizations of highly expressed genes of four fast-growing bacteria.** Journal of Bacteriology. 183: 5025-5040.

Katz, E., Brown, D., Hitch, M. J. M., ***et al***. (1984). **Regulation of tryptophan metabolism and its relationship to actinomycin D synthesis**. In: Biological, Biochemical ad Biomedical Aspects of Actinomycetes (L. Ortiz-Ortiz, L.F., Bojalil and V. Yakolef, Eds). 325-342. Academic press, New York.

Kayne, F. J. (1973). **Pyruvate kinase**. The enzymes. Vol 8. p. 353-382. Academic Press, New York.

Keddie, R.M., and Cure, G.L. (1977). **The cell wall composition and distribution of free mycolic acids in named strains of coryneform bacteria and in isolates from various natural sources.** J Appl Bacterial. 42: 229-252.

Kelemen, G.H., & Buttner. (1998). **Initiation of aerial mycelium formation in *Streptomyces***. Current Opinion in Microbiology. 2: 106.

Kell, D.B. (1987). **Forces, fluxes and the control of microbial growth and metabolism.** Journal of general Microbiology. 133: 1651-1665.

Kell, D.B., and Westerhoff, H.V. (1986). **Towards a rational approach to the optimization of flux in microbial biotransformations.** TIBTECH. 137-142.

Keller, B., Keller, E., and Lingens, F. (1985). **Arogenate dehydrogenase from *Streptomyces phaeochromogenes*: purification and properties.** Biol Chem. Hoppe-Seyler. 366: 1063-1066.

Kelly, K.S., Ochi, K., and Jones, G.H. (1991). **Pleiotropic effects of a relc mutation in *Streptomyces antibioticus*.** Journal of Bacteriology. 173 (7): 2297-2300.

Kendrick, K.E., and Wheelis, M.L. (1982). **Histidine dissimilation in *Streptomyces coelicolor*.** J Gen Microbiol. 128: 2029-2040.

Kengen, S.W.M., Stams, A.J.M., and de Vos, W.M. (1996). **Sugar metabolism of hyperthermophiles.** FEMS Microbiol. Rev. **18**:119-137.

Kengen, S.W.M., de Bok, F.A.M., van Loo, N.D., Dijkema, C., Stams, A.J.M., and de Vos, W.M. (1994). **Evidence for the operation of a novel Embden-Meyerhof pathway that involves ADP-dependent kinases during sugar fermentation by *Pyrococcus furiosus***. J. Biol. Chem. **269**:17537-17541.

Kengen, S.W.M., Tuininga, J.E., de Bok, F.A.M., Stams, A.J.M., and de Vos, W.M. (1995). **Purification and characterization of a novel ADP-dependent glucokinase from the hyperthermophilic archaeon *Pyrococcus furiosus*.** J. Biol. Chem. 270:30453-30457.

Kern, B.A., and Inamine, E. (1981). **Cystathionine γ-lyase activity in the cephamycin C producer *Streptomyces lactamdurans*.** Journal of Antibiotics. 34: 583-589.

Khan, F.R., and McFadden, B.A. (1982). **Isocitrate lyase from - flax terminal residues, composition, active-site, and catalysis.** Plant Physiology. 70 (4): 943-948.

Khetan, A., Malmberg, L.H., Kyung, Y.S., Sherman, D.H and Hu, W.S. (1999). **Precursor and cofactor as a check valve for cephamycin biosynthesis in *Streptomyces clavuligerus***. Biotechnol. Prog. 15:1020-1027.

Kholodenko, B.N., Cascante, M., Hoek, J.B., Westerhoff, H.V., and Schwaber, J. (1998). **Metabolic design: How to engineer a living cell to desired metabolite concentrations and fluxes**. Biotechnology and Bioengineering. 59 (2): 239-247.

Killham, K & Firestone, M.K (1984a). **Salt stress control of intracellular solutes in streptomycetes indigenous to saline soils**. Applied Environmental Microbiology. 47: 301-306.

Killham, K., & Firestone, M.K. (1984b). **Proline transport increases growth efficiency in salt-stressed *Streptomyces griseus***. Applied Environmental Microbiology. 48: 239-241.

King, J.L., and Jukes, T.H. (1969). **Non-Darwinian evolution.** Science. 164: 788-797.

King, R. (1997). **A structured mathematical model for a class of organisms: I. Development of a model for *Streptomyces tendae* and application of model-based control.** Journal of biotechnology. 52: 219-234.

King, R., and Budenbender, C. (1997). **A structured mathematical model for a class of organisms: II. Application of the model to other strains.** Journal of biotechnology. 52: 235-244.

Kirk, S., Avignone-Rossa, C. A., and Bushell, M. E. (2000). **Growth limiting substrate affects antibiotic production and associated metabolic fluxes in *Streptomyces clavuligerus*.** Biotechnology Letters. 22: 1803-1809.

Kisaalita, W.S., Slininger, P.J., and Bothast, R.J. (1993). **Defined media for optimal pyoverdine production by *Pseudomonas fluorescens* 2-79**. Applied Microbiology and Biotechnology. 39: 750-755.

Kitamoto, N., Yoshino, S., Ohmiya, K., and Tsukagoshi, N. (1999). **Sequence analysis overexpression and antisense inhibition of a β-xylosidase gene *xyl*A from *Aspergillus oryzae***. KBN616. Applied Environmental Biotechnology. 65: 20-24.

Kolb, A., Busby, S., Buc, H., Garges, S., and Adhya, S. (1993). **Transcriptional regulation by cAMP and its receptor protein.** Ann Rev Biochem. 62: 749-795.

Kominek, L.A. (1972). **Biosynthesis of novobiocin by *Streptomyces niveus*.** Antimicrobial Agents and Chemotherapy. 1: 123-134.

Kormanec, J., Lempelová, A., Farkasovšky, M., and Homerová, D. (1995). **Cloning, sequencing and expression in *Escherichia coli* of a *Streptomyces aureofaciens* gene encoding glyceraldehyde-3-phosphate dehydrogenase**. Gene 165:77-80.

Kormanec, J., Lempelová, A., Novakova, R., et al. (1997) **Expression of the *Streptomyces aureofaciens* glyceraldehyde-3-phosphate dehydrogenase gene (*gap*) is developmentally regulated and induced by glucose**. Microbiology. 143, 3555-3561.

Korotkova, N., Chistoserdova, L., Kuksa, V., and Lidstrom, M.E. (2002). **Glyoxylate regeneration pathway in the methylotroph *Methylbacterium extorquens* AM1.** Journal of Bacteriology. 184: 1750-1758.

Kotzlar, D. and Buc, H. (1977). **Two *Escherichia coli* fructose-6-phosphate kinases. Preparative purification, oligomeric structure and immunological studies.** Biochim. Biomed. Acta 484:35-48.

Krausse, R., & Ullmann, U. (1985). **Studies on the identification of Campylobacter species using biochemical tests and high performance liquid chromatography**. Zbl. Bakt. Hyg. A. 260: 342-360.

Krausse, R., & Ullmann, U. (1987). **Identification of anaerobic bacteria using high performance liquid chromatography**. Zbl. Bakt. Hyg. A. 265: 340-352.

Krausse, R., & Ullmann, U. (1991). **A modified procedure for the identification of anaerobic bacteria by high performance liquid chromatography - quantitative analysis of short chain fatty acids.** Zbl. Bakt. 276: 1-8.

Kreutz, F.H (1962). **Enzymatische glycerinbestimmung.** Klin. Wochenschrift. 40: 362-363.

Kroening, T.A., and Kendrick, K.E. (1987). ***In vivo*** **regulation of histidine ammonia-lyase activity from *Streptomyces griseus*.** Journal of Bacteriology. 169: 823-824.

Kromberg, H.L. (1966) **The role and control of the glyoxylate cycle in *E. coli***. Biochemical journal. 99: 1-11.

Kroukamp, O., Rohwer, J.M., Hofmeyr, J.H.S., and Snoep, J.L. (2002). **Experimental supply-demand analysis of anaerobic yeast energy metabolism.** Kluwer Academic Publisher. 1-7.

Kuhn, H., Friederich, U., and Fiechter, A. (1979). **Defined minimal medium for a thermophilic *Bacillus sp*. Development by chemostat pulse and shift technique.** Eur J Appl Microbiol. 6: 341-349.

Kulaev, I.S. and Vagabov, V.M. (1983**). Polyphosphate metabolism in microorganisms**. Adv. Microb. Physiol. **24**:83-171.

Kurylowicz, W., Chojnowski, W., Raczynska-Bojanowska, K., and Kowszyk-Gindifer, Z. (1976). **Antibiotics in microbial metabolism**. *In* W. Kurylowicz (ed.), Antibiotics. A critical review. Polish Medical, Warsaw.

Kwakman, J.H.J.M. and Postma, P.W. (1994) **Glucose kinase has a regulatory role in carbon catabolite repression in *Streptomyces coelicolor***. Journal of Bacteriology. 176, 2694-2698.

Laakel, M., Lebrihi, A., Khaoua, S., Schneider, F., Lefebvre, G., and Germain, P. (1994). **A link between primary and secondary metabolism: Malonyl-CoA formation in *Streptomyces ambofaciens* growing on ammonium ions or valine**. Microbiology 140:1451-1456.

Lange, H.C., and Heijnen, J.C. (2001). **Statistical reconciliation of the elemental and molecular biomass composition of *Saccharomyces cerevisiae***. In: Biotechnology and Bioengineering. 75 (3): 334-344.

le Bras, G, and Garel, J-R. (1993). **Pyruvate kinase from *Lactobacillus bulgaricus*. Possible regulation by competition between strong and weak effectors.** Biochimie (Paris) 75:797-802.

Lechevalier, H.A., and Lechevalier, M.P. (1981). **Introduction to the order *Actinomycetales*.** *In* M.P. Starr, H. Stolp, H.G. Truper, A. Balows, and H.G. Schlegel (eds.), The Prokaryotes. pp. 1915-1922. Springer Verlag AG, Berlin.

Lee, C.P., Kao, M.C., B. French, B.A., Putney, S.D., and Chang, S.H. (1987). **The rabbit muscle phosphofructokinase gene. Implications for protein structure, function and tissue specificity**. J. Biol. Chem. 262:4195-4199.

Lee, P.C., Loh, P.C., & Ho, C.C. (1997). **Production of tylosin by *Streptomyces fradiae* in palm oil medium**. World Journal of Microbiology & Biotechnology. 13: 69-71.

Lee, S.H & Lee, K.J. (1993). **Aspartate aminotransferase and tylosin biosynthesis in *Streptomyces fradiae***. Applied and Environmental Microbiology. 59: 3: 822-827.

Lee, S.H., & Lee, K.J. (1991). **Relationship between threonine dehydratase and biosynthesis of tylosin in *Streptomyces fradiae***. Journal of General Microbiology. 137: 2547-2553.

Lee, S.H., & Lee, K.J. (1994). **Kinetics of the repression of tylosin biosynthesis by ammonium ion in *Streptomyces fradiae***. Journal of Biotechnology. 32: 149-156.

Lee, S.H., & Rho, Y.T. (1999). **Improvement of tylosin fermentation by mutation and medium optimization**. Letters in Applied Microbiology. 28: 142-144.

Leskiw, B.K., Bibb, M.J., and Chater, K.F. (1991a). **The use of a rare codon specifically during development.** Molecular Microbiology. 5 (12): 2861-2867.

Leskiw, B.K., Lawlor, E.J., Fernandez-Abalos, J. M., and Chater, K.F. (1991b). **TTA codons in some genes prevent their expression in a class of developmental, antibiotic-negative, *Streptomyces* mutants.** Proceedings of the National Academy of Sciences of the United States of America. 88 (6): 2461-2465.

Leyland, M.L Kelly, D.J. (1991) **Purification and characterization of a monomeric isocitrate dehydrogenase with dual coenzyme specificity from the photosynthetic bacterium *Rhodomicrobium vannielii*.** European Journal of Biochemistry. 202, 85-93.

Li, W.H. (1997). **Molecular Evolution.** (Sinauer, Sunderland, M.A). 185-190.

Li, Z. and Philips, N.F.B. (1995). **Pyrophosphate-dependent phosphofructokinase from *Giardia lamblia*: Purification and characterization.** Protein Express. Purif. **6**:319-328.

Liao, X., Vining, L.C., and Doull, J.L. (1995). **Physiological control of trophophase-idiophase separation in streptomycete cultures producing secondary metabolites.** Canadian Journal Microbiology. 41: 309-315.

Limauro, D., Avitabile, A., Cappellano, C., Puglia, A.M., and Bruni, C. B. (1990). **Cloning and characterization of the histidine biosynthetic gene cluster of *Streptomyces coelicolor* A3(2).** Gene. 90: 31-41.

Ling, K.H., Paetkau, V., Marcus, F., and Lardy, H.A. (1966). **Phosphofructokinase I. Skeletal muscle.** *In* Methods in Enzymology: Carbohydrate Metabolism. 9: 425-429. Edited by W.A. Wood. London: Academic Press, Inc.

Lingens, F., und Vollprecht, P. (1964). **Zur biosynthese der nicotinsaure in steptomyceten, algen, phycomyceten und hefe**. Z Physiol. Chem. 339: 64-74.

Lishnevskaya, E.B., Kuzina, Z.A., Asinovskaya, N.K., Belousova, II., Malkov, M.A., and Rovinskaya, A.Y. (1986). **Cyclic adenosine-3'5'-monophosphoric acid in *Streptomyces antibioticus* and its possible role in the regulation of oleandomycin biosynthesis and culture growth.** Mikrobiologiya. 55 (3): 455-460.

Llanos, R.M., Harris, C.J., Hillier, A.J., and Davidson, B.E. (1993). **Identification of a novel operon in *Lactococcus lactis* encoding three enzymes for lactic acid synthesis: phosphofructokinase, pyruvate kinase and lactate dehydrogenase.** Journal of Bacteriology. 175: 2541-2551.

Lobry, J.R. (1997). **Influence of genomic G+C content on average amino-acid composition of protein from 59 bacterial species.** Gene. 205: 309-316.

Lobry, J.R., and Gautier, C. (1994). Hydrophobicity, **expressivity and aromaticity are the major trends of amino-acid usage in 999 *Escherichia-coli* chromosome-encoded genes.** Nucleic acids Research. 33: 3174-3180.

Loke, P., and Sim, T.S. (2000). **Molecular cloning, heterologous expression and functional characterisation of a malate synthase gene from *Streptomyces coelicolor* A3(2).** Canadian Journal of Microbiology. 46: 764-769.

Loke, P., Goh L.L., Seng Soh, B., Yeow, P., and Sim, T.S. (2002). **Purification and characterization of recombinant malate synthase enzymes from *Streptomyces coelicolor* A3(2) and *S. clavuligerus* NRRL3585.** Journal of Industrial Microbiology & Biotechnology. 28 (4): 239-243.

Longacre, A., Reimers, J.M., Gannon, J.E., and Wright, B.E. (1997). **Flux analysis of glucose metabolism in *Rhizopus oryzae* for the purpose of increasing lactate yields.** Fungal Genetics and Biology. 21: 30-39.

Loontiens, F.G., McLaughlin, L.W., Diekmann, S., and Clegg, R.M. (1991). **Binding of hoechst 33258 and 4'6-diamidino-2-phenylindole to self-complementary decadeoxynucleotides with modified exocyclic base substitutents.** Biochemistry. 30: 182-189.

Lowry, O.H., Rosebrough, N.J., Farr, A.L., and Randall, R.J. (1951). **Protein measurement with the folin phenol reagent.** Journal of Biological Chemistry. 193: 265-275.

Macfadyen, L.P., Dorocicz, I.R., Reizer, J., Saier, M.H., and Redfield, R.J. (1996). **Regulation of competence development and sugar utilization in *Haemophilus influenzae* Rd by phosphoenolpyruvate: fructose phosphotransferase system.** Molecular Microbiology. 21: 941-952.

Mach, H., Hecker, M., and Mach, F. (1988). **Physiological studies on cAMP synthesis in *Bacillus subtilis*.** FEMS Microbiol Lett. 52: 189-192.

Madden, T., Ward, J.M., & Ison, A.P. (1996). **Organic acid excretion by *Streptomyces lividans* TK24 during growth on defined carbon and nitrogen sources**. Microbiology, 142: 3181-3185.

Madry, N., & Pape, H. (1981). **Regulation of tylosin biosynthesis by phosphate – possible involvement of transcriptional control**. In: Actinomycetes, Zbl. Bakt. Suppl 11 (KP Scall, G. Pulverer (Eds). Fischer, Stuttgart New York, pp 441-445.

Madry, N., & Pape, H. (1982). **Formation of secondary metabolism enzymes in the tylosin producer *Streptomyces* T59-235**. Archives of Microbiology. 131: 170-173.

Madry, N., Sprinkmeyer, R., & Pape, H. (1979). **Regulation of tylosin synthesis in *Streptomyces*: effects of glucose analogs and inorganic phosphate**. European journal of Applied Microbiology and Biotechnology. 7: 365-370.

Majewski, R.A., and Domach, M.M. (1990). **Simple constrained optimization view of acetate overflow in *E. coli*.** Biotechnology and Bioengineering. 35: 732-738.

Malik, V.S. (1980). **Microbial secondary metabolism**. TIBS. 68-72.

Malmberg, L.H., and Hu, W.S. (1991). **Kinetic analysis of cephalosporin biosynthesis in *Streptomyces clavuligerus*.** Biotechnology and Bioengineering. 38: 941-947.

Malmberg, L.-H., Hu, W.S., and D.H. Sherman. (1993). **Precursor flux control through targeted chromosomal insertion of the lysine e-aminotransferase (*lat*) gene in cephamycin C biosynthesis**. Journal of Bacteriology. 175.

Malmberg, L.-H., Hu, W.S., and D.H. Sherman. (1995). **Effects of enhanced lysine e-aminotransferase activity on cephamycin biosynthesis in *Streptomyces clavuligerus*.** Appl. Microbiol. Biotechnol. 44:198-205.

Mandelstam, J., McQuillen, K., and Dawes, I. Eds. (1982). **"Biochemistry of Bacterial Growth".** Blackwell Scientific Publications.

Maplestone, R.A., Stone, M.J., and Williams, D.H. (1992). **The evolutionary role of secondary metabolites - a review**. Gene 115:151-157.

Marquis, R.E. (1968). **Salt-induced contraction of bacterial cell walls.** Journal of Bacteriology. 95: 775-781.

Marr, A.G., Nilson, E.H., and Clarke, D.J. (1963)**. The maintenance requirement of *Escherichia coli*.** Annals of the New York Academy of Sciences. 102: 536-548.

Martin, J.F. (1983). **Biochemistry and genetic regulation of commercially important antibiotics.** In Polyenes. L.C. Vining (ed). Addison-Wesley, London.

Martin, J.F., & Demain, A.L. (1980). **Control of antibiotic biosynthesis**. Microbiological Reviews. 44: 230-251.

Martins, M.L.L., and Tempest, D.W. (1991). **Metabolic response of *Bacillus stearothermophilus* chemostat to a secondary oxygen limitation.** Journal of General Microbiology. 137: 1391-1396.

Marx, A., de Graaf, A.A., Wiechert, W., Eggeling, L., and Sahm, H. (1996). **Determination of fluxes in the central metabolism of *Corynebacterium glutamicum* by nuclear magnetic resonance spectroscopy combined with metabolite balancing.** Biotechnology and Bioengineering. 49: 111-129.

Marx, A., Eikmanns, B.J., Sahm, H., de Graaf, A.A., and Eggeling, L. (1999). **Response of the central metabolism in *Corynebacterium glutamicum* to the use of an NADH-dependent glutamate dehydrogenase**. Metabolic Engineering. 1: 35-48.

Masamune, S., Bates, G.S., & Corcoran, J.W. (1977). **Macrolides. Recent progress in chemistry and biochemistry**. Angew. Chem. Int. Ed. Engl. 16: 585-607.

Mateles, R.I. (1971). **Calculation of the oxygen required for cell production**. Biotechnology and Bioengineering. 13 (4): 581-582.

Matsushita, M., Irino, T., Komoda, T., & Sakagishi, Y. (1993). **Determination of proteins by a reverse biuret method combined with the copper bathocuproine chelate reaction**. Clinica Chimica Acta. 216: 103-111.

Maurer, K.H., Pfeiffer, F., Zehender, H., and Mecke, D. (1983)**. Characterization of 2 glyceraldehyde-3-phosphate dehydrogenase isoenzymes from the pentalenolactone producer *Streptomyces arenae*.** Journal of Bacteriology. 153: 930-936.

Mazel, D., and Marlière, P. (1989). **Adaptive eradication of methionine and cysteine from cyanobacterial light-harvesting proteins.** Nature. 341: 245-248.

McGuire, J.M., Boniece, W.S., Higgens, C.E., Hoehn, M.M., Stark, W.M., Westhead, J., Wolfe, N.R. (1961) **Tylosin, a new antibiotic. In Microbial studies.** Antibiot. Chemo. 11, 320-327.

McIntyre, J.J., Bull, A.T., and Bunch, A.W (1996). **Vancomycin production in batch culture and continuous culture - *Amycolatopsis orientalis* culture medium optimization.** Biotechnology and Bioengineering. 49: 412-420.

Melendez-Hevia, E., Sicilia, J., Ramos, M.T., Canela, E.I., and Cascante, M. (1996). **Molecular bureaucracy: Who controls the delays**? Journal of Theoretical Biology. 182: 333-339.

Melendez-Hevia, E., Waddell, T.G., Heinrich, R., and Montero, F. (1997). **Theoretical approaches to the evolutionary optimisation of glycolysis derived analysis.** European Journal of Biochemistry. 244: 527-543.

Melzoch, K., de Mattos, T.M.J., and Neijssel, O.M. (1997). **Production of actinorhodin by *Streptomyces coelicolor* A3(2) grown in chemostat culture.** Biotechnology and Bioengineering. 54 (6): 557-582.

Merson-Davies, L.A., and Cundliffe, E. (1994). **Analysis of five tylosin biosynthetic genes from the *tyll*BA region of *Streptomyces fradiae* genome.** Molecular Microbiology. 13: 349-355.

Mertens, E. (1991). **Pyrophosphate-dependent phosphofructokinase, an anaerobic glycolytic enzyme?** FEBS Lett. 285:1-5.

Mertens, E. (1993). **ATP versus pyrophosphate: Glycolysis revisited in parasitic protists**. Parasitol. Today 9:122-126.

Mertens, E., van Schaftingen, E., and Muller, M. (1989). **Presence of a fructose-2,6-bisphosphate-insensitive pyrophosphate: fructose-6-phosphate phosphotransferase in the anaerobic protozoa *Tritrichomonas foetus, Trichomonas vaginalis* and *Isotricha prostoma***. Mol. Biochem. Parasitol. 37:183-190.

Metzger, L.S., Dotzlaf, J.E., Foglesong, M.A. (1984). **Development of a defined medium for tylosin producing strains of *Streptomyces fradiae***. Abstr. Annu Meet Am Soc Microbial. 199.

Michal, G. (1999). **Biochemical Pathways: An atlas of biochemistry and molecular biology.** Wiley New York. Edited by Gerhard Michal.

Migo, V.P., So, R.S., Deseo, M, A., and Madamba, L.S.P. (1995). **Chemical composition of Philippine molasses.** The Philippine Agriculturist. 78: (1): 53-62.

Mikulasova, D., Kollarova, M., Miginiac-Maslow, M. (1998). **Purification and characterization of a malate dehydrogenase from *Streptomyces aureofaciens*.** FEMS Microbiology Letters. 159: 299-305.

Millard, C.S., Chao, Y-P, Liao, J.C., Donnelly, M.I. (1996) **Enhanced production of succinic acid by overexpression of phosphoenolpyruvate carboxylase in *E. coli*.** Applied Environmental Microbiology. 62: 1808-1810.

Miller, T.L., and Churchill, B.W. (1986). **Substrates for large-scale fermentations.** In: Demain A.L., Solomon, N.A. (Eds). Manual for industrial microbiology and biotechnology. American Society for Microbiology, Washington, D.C. 122-136.

Minkevich, I.G., & Eroshin, V.K. (1973). **Productivity and heat generation of fermentation under oxygen limitation.** Folia Microbiology. 18 : 376-385.

Minnikin, D.E., and O'Donnell, A.G. (1984). **Actinomycete envelope lipid and peptidoglycan composition.** *In* M. Goodfellow, M. Mordarski and S.T. Williams (Eds). The Biology of actinomycetes. Academic Press. 337-388.

Mira de Orduna, R., & Theobald, U. (2000). **Intracellular glucose-6-phosphate content in *Streptomyces coelicolor* upon environmental changes in a defined medium**. Journal of biotechnology. 77: 209-218.

Moat,, A.G. (1979). **Growth. In: Microbial physiology**. Wiley, New York. 444-544.

Molina, I., Pellicer, M.T., Aguilar, J., Baldoma, L. (1994) **Molecular characterization of *E. coli* malate synthase G with differentiation with the malate synthase A isoenzyme**. European Journal of Biochemistry. 221, 541-548.

Molna'r-Perl, I. (1994). **Advances in the high performance liquid chromatography determination of phenylthiocarbanyl amino acids.** J. Chromatogr. A 661, 43- 50.

Moore, S. and Stein, W.H. (1963). **Chromatographic determination of amino acids by the use of automatic equipment.** Methods in Enzymology 6, 819-831.

Moore, S., & Stein, W.H. (1948). **Photometric ninhydrin method for use in the chromatography of amino acids**. Journal of Biological Chemistry. 176: 367-389.

Mordy, C.W., and Carlson, D.J. (1991). **An evaluation of fluorescence techniques for measuring DNA and RNA in marine microorganisms.** Mar Ecol. Prog. Ser. 73: 283-293.

Mori, M., and Shiio, I. (1987). **Pyruvate formation and sugar metabolism in an amino-producing bacterium, *Brevibacterium flavum*.** Agricultural and Biological Chemistry. 51 (1): 129-138.

Mousdale, D.M. (1997) **The analytical chemistry of microbial cultures. In A practical approach: to microbial physiology**. Edited by P. M. Rhodes, Bioscot Ltd, Edinburgh, and P. F., University of Hertfordshire. Press at Oxford University Press. 7: 167-192.

Mousdale, M.N., Melville, J.C., and Fischer, M. (1999). **Optimization of fermentation processes by quantitative analysis: From analytical biochemistry to chemical engineering**. Fermentation Microbiology and Biotechnology. Edited by E.M.T El-Mansi and C.F.A Bryce. Taylor and Francis.

Moye, A.H., and Boning, A.J. (1979). **A versatile fluorogenic labelling reagent for primary and secondary amines: 9-fluorenylmethyl chloroformate**. Analytical Letters. 12 (B1): 25-35.

Naeimpoor, F., and Mavituna, F. (2000). **Metabolic Flux Analysis in *Streptomyces coelicolor* under Various Nutrient Limitations**. Metabolic Engineering. 2:(2) 140-148.

Nandan, R., Tondwalker, V., and Ray, P.K. (1990). **Biomethanation of spent wash: heavy metal inhibition of methanogenesis in synthetic medium.** J Ferment Bioeng. 69: 276-281.

Nandi, R., and Mukherjee, S.K (1991). **Studies on the mineral requirement of *Penicillium italicum* for the production of glucoamylase by submerged fermentation - effect of mineral, trace element concentration; culture medium optimization.** Zestralbl Mikrobiol. 146: 285-289.

Naumova, I. (1988). **The teichoic acids of actinomycetes.** Microbiological Sciences. 5 (9): 275-279.

Naumova, I.B., and Dmitrieva, N.F. (1974). Biokhimia. 39: 201-209 (in Russian).

Naumova, I.B., Kuznetsov, V.D., Kudrina, K.S., and Bezzubenkova, A.P. (1980). **The occurrence of teichoic acids in streptomycetes.** Archives of Microbiology. 126: 71-75.

Neidhardt, F.C. (1987). **Chemical composition of *Escherichia coli*.** In F.C. Neidhardt., J.L. Ingraham, K.B., Low., B. Magasanik., M. Schaechter and H.E. Umbarger (Eds). "*Escherichia coli* and *Salmonella typhimurium*": Cellular and Molecular Biology. Washington DC: ASM Press.

Neidhardt, F.C. (1990). **Chemical composition of *Escherichia coli*.** Part 1: Molecular architecture and assembly of cell parts.

Neijssel, O.M. and Tempest, D.W. (1976). **The role of energy-spilling reactions in the growth of *Klebsiella aerogenes* NCTC 418 in aerobic chemostat culture.** Archives of Microbiology. 110: 305-311.

Neijssel, O.M., and de Teixeira, M.J. (1994). **The energetics of bacterial growth: a reassessment.** Molecular Microbiology. 12: 179-182.

Neri, D., Szyperski, T., Otting, G., Senn, H., and Wuthrich, K. (1989). **Stereospecific nuclear magnetic resonance assignments of the methyl groups of valine and leucine in the DNA-binding domain of the 434-repressor by biosynthetically directed fractional ^{13}C labelling**. Biochemistry. 28: 7510-7516.

Neuzil, J., Novotna, J., Behal, V., and Hostalek, Z. (1986). **Inhibition studies of glucose-6-phosphate dehydrogenase from tetracycline-producing *Streptomyces aureofaciens*.** Biotechnol Appl Biochem. 8: 375-378.

Neuzil, J., Novotna, J., Erban, V., *et al*. (1988). **Glucose-6-phosphate dehydrogenase from tetracycline-producing *Streptomyces aureofaciens*: some properties and regulatory aspects of the enzyme.** Biochem Int. 17: 187-196.

Nguyen, K. T., Nguyen, L.T., Kopecky, J., & Behal, V. (1997). **Properties of NAD-dependent glutamate dehydrogenase from the tylosin producer *Streptomyces fradiae***. Canadian Journal of Microbiology. 43: 1005-1010.

Nguyen, L.T., Nguyen, K.T., Spizek, J., and Behal, V. (1995). **The tylosin producer, *Streptomyces fradiae*, contains a second valine dehydrogenase.** Microbiology. 141: 1139-1145.

Niederberger, P., Prasad, R., Miozzari, G., Kacser, H. (1992). **A strategy for increasing an *in vivo* flux by genetic manipulations. The tryptophan system of yeast.** Biochemical Journal. 287: 473-479.

Nielsen, J. & Villadsen. J. (1994). **Bioreaction principles**. Academic press. Phenom, New York.

Nielsen, J. (1994). **Physiological engineering-towards a new science.** pp. 30 -38. Proc. The IChemE research event, London.

Nielsen, J. (1996). **Modelling the morphology of filamentous microorganisms.** TIBTECH. 14: 438-443.

Nielsen, J. (1997). **Physiological Engineering Aspects of *Penicillium chrysogenum*.** Technical University of Denmark, Lyngby, Denmark.

Nielsen, J. (1998). **Metabolic engineering: techniques for analysis of targets for genetic manipulations.** Biotechnology and Bioengineering. 58: 125-132.

Nissen, T.L., M. Anderlund, J. Nielsen, J. Villadsen and M.C. Kielland-Brandt. (2001). **Expression of a cytoplasmic transhydrogenase in *Saccharomyces cerevisiae* results in formation of 2-oxoglutarate due to depletion of the NADPH pool.** Yeast 18: 19-32.

Nissen, T.L., Schulze, U., Nielsen, J., & Villadsen, J. (1997). **Flux distributions in anaerobic, glucose-limited continuous cultures of *Saccharomyces cerevisiae***. Microbiology. 143: 203-218.

Noorman, H.J., Heijnen, J.J., and Luyben, K, Ch. A.M. (1991). **Linear relations in microbial reaction systems: A general overview of their origin, form and use.** Biotechnology and Bioengineering. 38: 603-618.

Noorman, H.J., Romein, B., Luyben, K, Ch. A.M., and Heijnen, J.J. (1996). **Classification, error detection and reconciliation of process information in complex biochemical systems.** Biotechnology and Bioengineering. 49: 364-376.

Novak, J., Curdova, E., Jechova, V. *et al*. (1992). **Enzymes of ammonium assimilation in *Streptomyces avermitilis***. Folia Microbiology. 37: 261-266.

Nun, W.D. (1986). **A molecular view of fatty acid catabolism in *E. coli***. Microbiological Reviews. 50: 179-192.

Obanye, A.I.C (1994). **Carbon flux and the production and the production of the antibiotic methylenomycin by *Streptomyces coelicolor* A3(2).** Ph.D., Manchester, UMIST. 44-7273.

Obanye, A.I.C., Hobbs, G., Gardner, D.C.J. and Oliver, S.G. (1996) **Correlation between carbon flux through the pentose phosphate pathway and production of the antibiotic methylenomycin in *Streptomyces coelicolor* A3(2).** Microbiology. 142, 133-137.

O'Brien, W.E., Bowien, S., and Wood, H.G. (1975). **Isolation and characterization of a pyrophosphate-dependent phosphofructokinase from *Propionibacterium shermanii*.** J. Biol. Chem. 250:8690-8695.

Ogur, M., & Rosen, G. (1950). **The nucleic acids of plant tissues. 1. The extraction and estimation of deoxypentose nucleic acid and pentose nucleic acid.** Plant Nucleic Acids. 262-276.

Okazaki, H., Beppu, T., and Arima, K. (1974). **Induction of antibiotic formation in *Streptomyces* sp. No. 362 by the change of cellular fatty acid spectrum.** Agr Biol Chem. 38: 1455-1461.

Okazaki, H., Ono, H., Yamada, K., Beppu, T., and Arima, K. (1973). **Relationship among cellular fatty acid composition, amino acid uptake and neomycin formation in a mutant strain of *Streptomyces fradiae*.** Agr Biol Chem. 37: 2319-2325.

Oliver, S.G., Hobbs, G., Obanye, A., and Gardner, D.C.J. (1990). **Development of a synthetic medium for *Streptomyces* Fermentation - effect of charged polymer on antibiotic production from *Streptomyces coelicolor*.** Pract Adv Ferment Technol. 1: 1-9.

Omura, S., & Tanaka, Y. (1986). **Macrolide antibiotics**. Journal of Antibiotics. 12: 360-391.

Omura, S., Takeshima, H., Nakagawa, A., Miyazawa, J., Piriou, F., & Lukacs, G. (1977). **Studies on the biosynthesis of 16-membered macrolide antibiotics using carbon-13 nuclear magnetic resonance spectroscopy.** 16: 13: 2860-2866.

Omura, S., Ikeda, H., Ishikawa, J., Hanamoto, A., Takahashi, C., Shinose, M., Takahashi, Y., Horikawa, H., Nakazawa, H., Osonoe, T., Kikuchi, H., Shiba, T., Sakaki, Y., and Hattori, M. (2001). **Genome sequence of an industrial microorganism *Streptomyces avermitilis*: Deducing the ability of producing secondary metabolites.** PNAS. 98 (21): 12215-12220.

Omura, S., Kitao, C., Miyazawa, J., Imai, H., Takeshima, H. (1978) **Bioconversion and biosynthesis of 16-membered macrolide antibiotic, tylosin, using enzyme inhibitor cerulenin.** Journal of Antibiotics. 31: 254-256.

Omura, S., Nakagawa, A., Takeshima, H., Miyazawa, J., Kitao, C. (1975). **A ^{13}C nuclear magnetic resonance study of the biosynthesis of the 16-membered macrolide antibiotic tylosin.** Tetrahedr. Lett. 50: 4503-4506.

Omura, S., Takeshima, H. (1974) **Inhibition of the biosynthesis of leucomycin, a macrolide antibiotic, by cerulenin.** Journal of Biochemistry. 75: 193-195.

Omura, S., Takeshima, H., Nakagawa, A., Kanemoto, N., Lukacs, G. (1976) **Studies on carboxylic acid metabolism in a macrolide-producing microorganism using carbon-13 magnetic resonance.** Bioorg. Chem. 5: 451-454.

Omura, S., Tanaka, Y., Mamada, H., & Masuma, R. (1984b). **Effect of ammonium ion, inorganic phosphate and amino acids on the biosynthesis of prototylonolide, a precursor of tylosin aglycone**. Journal of Antibiotics. 37: 5: 494-502.

Omura, S., Tanaka, Y., Mamada, H., and Masuma, R. (1983b). **Ammonium ion suppresses the biosynthesis of tylosin aglycone by interference with valine catabolism in *Streptomyces fradiae*.** Journal of Antibiotics. 36: 1792-1794

Omura, S., Tomoda, H., Yamamoto, S., Tsukui, M., & Tanaka, H. (1984a). **Studies on two dioxygenases involved in the synthesis of tylosin in *Streptomyces fradiae***. Biochimica *et* Biophysica Acta. 802: 141-147.

Omura, S., Tsuzuki, K., Tanaka, Y., Sakakibarah, H., Aizawa, M., and Lukacs, G. (1983a). **Valine as a precursor of n-butyrate unit in the biosynthesis of macrolide aglycone.** Journal of Antibiotics. 36: 614-616.

Onaka, H., Nakagawa, T., and Horinouchi, S. (1998). **Involvement of two A-factor receptor homologues in *Streptomyces coelicolor* A3(2) in the regulation of secondary metabolism and morphogenesis.** Molecular Microbiology. 28 (4): 743-753.

O'Regan, M., Thierbach, G., Bachmann, B., Villeval, D., Lepage, P., Viret, J.F. and Lemoine, Y. (1989). **Cloning and nucleotide sequence of the phosphoenolpyruvate carboxylase-coding gene of *Corynebacterium glutamicum* ATCC13032.** Gene. 77 (2): 237-251.

Oura, E. (1972). **The effect of aeration on the growth energetics and biochemical composition of bakers yeasts**. Ph.D. thesis. University of Helsinki, Finland.

Ozaki, H., and Shiio, I. 1969. **Regulation of the TCA cycle and glyoxylate cycles in *Brevibacterium flavum*. II. Regulation of phosphoenolpyruvate carboxylase and pyruvate kinase**. Journal of Biochemistry. 66:297-311.

Ozergin-Ulgen, K., and Mavituna, F. (1993). **Actinorhodin production by *Streptomyces coelicolor* A3(2): kinetic parameters related to growth, substrate uptake and production.** Applied Microbiology and Biotechnology. 40: 457-462.

Ozergin-Ulgen, K., and Mavituna, F. (1998). **Oxygen transfer and uptake in *Streptomyces coelicolor* A3(2) culture in a batch bioreactor.** J. Chem. Technol. Biotechnol. 73: 243 - 250.

Pallen, M.J. (1999). **Microbial genomes.** Molecular Microbiology. 32: 907-912.

Pape, H., & Brillinger, G.U. (1973). **Metabolic products of microorganisms. 113. Biosynthesis of thymidine diphosphomycarose in a cell free system from *Streptomyces rimosus***. Archives Microbiology. 25-35.

Parche, S., Nothaft, H., Kamionka, A., and Titgemeyer, F. (2000). **Sugar uptake and utilisation in *Streptomyces coelicolor*: a PTS view to the genome.** Antonie van Leeuwenhoek. 78: 243-251.

Parche, S., Schmid, R., & & Titgemeyer, F. (1999). **The phosphotransferase system (PTS) of *Streptomyces coelicolor*: identification and biochemical analysis of a histidine phosphocarrier protein HPr encoded by the gene *pts*H.** European Journal of Biochemistry. 265: 308-317.

Parrau, J.L., Heijnen, J.J., and Luyben, K.Ch.A.M. (1991). **Linear relations in microbial reaction systems: a general overview of their origin, form, and use.** Biotechnology and Bioengineering. 38: 603-618.

Paul, J.H., & Myers, B. (1982). **Fluorometric determination of DNA in aquatic microorganisms by use of hoechst 33258.** Applied and Environmental Microbiology. 43: 6: 1393-1399.

Paulsen, I. T. (1996). **Carbon metabolism and its regulation in *Streptomyces* and other high GC Gram positive bacteria.** Research in Microbiology 147: 535-541.

Paulsen, I.T. (1996). **Carbon metabolism and its regulation in *Streptomyces* and other high GC Gram-positive bacteria.** Research in Microbiology. 147 (6-7): 535-541.

Pawluk, A., Scopes, R.K., and Griffiths-Smith, K. (1986). **Isolation and properties of the glycolytic enzymes from *Zymomonas mobilis***. Biochemical journal. 238: 275-281.

Penzikova, G.A., and Levtov, M.M. (1966). **Patterns of carbohydrate metabolism of *Actinomycetes fradiae* grown on media containing starch or glucose.** Biokhimiya. 31: (6): 1073-1077. Translation.

Percudani, R., Pavesi, A., and Ottonello, S. (1997). **Transfer RNA gene redundancy and translational selection in *Saccharomyces cerevisiae*.** J Mol Biol. 268: 322-330.

Peterson, G.L. (1983). **Determination of total protein**. Methods in Enzymology. 91: 95-356.

Peterson, S., de Graaf, A.A., Eggeling, L., Mollney, M., Wiechert, W., and Sahm, H. (2000). ***In vivo* quantification of parallel and bi-directional fluxes in the anaplerosis of *Corynebacterium glutamicum*.** J Biol Chem. 275: 35932-35941.

Petkovic, (1998). **An Investigation of the Molecular Genetics of the Gene Cluster for Oxytetracycline Biosynthesis from *Streptomyces rimosus*.** PhD Thesis, University of Ljubljana, Slovenia.

Pfefferle, U., Ochi, K., and Fiedler, H.P. (1995). **The stringent response and the induction of nikkomycin production in *Streptomyces tendae*.** Actinomycetologica. 9: 118-123.

Pirt, S.J. (1965). **The maintenance energy of bacteria in growing cultures**. Proceedings of the Royal Society of London. 163: 224-231.

Pirt, S.J. (1975). **General nutrition. In: Principles of microbe and cell cultivation.** Blackwell, Oxford. 117-136.

Pitt, D.E., and Bull, A.T. (1982). **Influence of culture conditions on the physiology and composition of *Trichoderma aureoviride*.** Journal of General Microbiology. 128: 1517-1527.

Plackett, R.L., and Burman, J.P. (1946). **The design of optimum multifactorial experiments.** Biometrika. 33: 305-325.

Plohl, M., and Gamulin, V. (1990). **Five transfer RNA genes lacking CCA termini are clustered in the chromosome of *Streptomyces rimosus*.** Molecular and General Genetics. 222: 129-134.

Ponce, E., N. Flores, A. Martinez, F. Valle, and F. Bolivar. (1995). **Cloning of the two pyruvate kinase isoenzymes structural genes from *Escherichia coli*: the relative roles of these enzymes in pyruvate biosynthesis**. Journal of Bacteriology. 177: 5719-5722.

Pons, A., Dussap, C.G., Pequignot, C., and Gros, J.B. (1996). **Metabolic flux distribution in *Corynebacterium melassecola* ATCC 17965 for various carbon sources.** Biotechnology and Bioengineering. 51: 177-189.

Pospisil, S., Rezanka, T., Viden, I., Krumphanzl, V., and Vanek, Z. (1985). **Altered fatty acid composition in regulatory mutants of *Streptomyces cinnamonensis*.** FEMS Microbiol Lett. 27: 41-43.

Postma, P.W., and Lengeler, J.W. (1985). **Phosphoenolpyruvate: carbohydrate phosphotransferase system of bacteria.** Microbiological Reviews. 49 (3): 232-269.

Potter, C. A. and Baumberg, S. (1996). **End-product control of enzymes of branched-chain amino acid biosynthesis in *Streptomyces coelicolor*.** Microbiology- (UK). 142: 1945-1952.

Pramanik, J. & Keasling, J.D. (1997). **Stoichiometric model of *E. coli* metabolism: incorporation of growth-rate dependent biomass composition and mechanistic energy requirements**. Biotechnology & Bioengineering. 56: 4: 398-421.

Pramanik, J., & Keasling, J.D. (1998). **Effect of *Escherichia coli* biomass composition on central metabolic fluxes predicted by a stoichiometric model**. Biotechnology and Bioengineering. 60: 2: 230-238.

Pramanik, J., Trelstad, P.L. Schuler, A.J., Jenkins, D. & Keasling, J.D. (1999). **Development and validation of a flux–based stoichiometric model for enhanced biological phosphorus removal metabolism**. Water Research. 33: (2): 462-476.

Pridham, T.G., and Tresner, H.D. (1974). ***Streptomycetaceae.*** In R.E. Buchanan and N.E. Gibbons (Eds). "Bergey's Manual of Determinative Bacteriology". Baltimore: The Williams and Wilkins Company. 8th, ed. 748-845.

Prub, B., Meyer, H.E., and Holldorf, A.W. (1993). **Characterization of the glyceraldehyde 3-phosphate dehydrogenase from the extremely halophilic archaebacterium *Haloarcula vallismortis*.** Archives of Microbiology. 160:5-11.

Purwantini, E., Gillis, T.P., and Daniels, L. (1997). **Presence of F_{420}-dependent glucose-6-phosphate dehydrogenase in *Mycobacterium* and *Nocardia* species, but absence from *Streptomyces* and *Corynebacterium* species and methanogenic Archaea.** FEMS Microbiology Letters. 146: 129-134.

Ragland, T.E., Kawasaki, T., & Lowenstein, J.M. (1966) **Comparative aspects of some bacterial dehydrogenases and transhydrogenases.** Journal of Bacteriology. 91, 236-244.

Rajendra, W. (1987). **High performance liquid chromatography determination of amino acids in biological samples by precolumn derivatization with o-phthalaldehyde.** Journal of Liquid Chromatography. 10 (5): 941-955.

Ratledge, C. (2000). **Look before you clone.** FEMS Microbiol Lett. 189: 317-318.

Redman, K.L., & Hornemann, U. (1980) **Utilization of Cibacron Blue 3G-A Sepharose 6B in the isolation and enrichment of pyruvate, phosphate dikinase, alanine dehydrogenase and phosphoenolpyruvate carboxylase from mitomycin-producing *Streptomyces verticillatus***. Journal of Antibiotics. 33: 863-877.

Redshaw, P.A., McCann, P.A., Sankaran, L., and Pogell, B.M. (1976). **Control of differentiation in streptomycetes: involvement of extrachromosomal deoxyribonucleic acid and glucose repression in aerial mycelia development.** Journal of Bacteriology. 125: 698-705.

Reed, R., Holms, D., Weyers, J., and Jones, A. (1998). **Practical skills in biomolecular sciences.** Addison-Wesley. Publisher Prentice Hall.

Reeves, R. E., D. J. South, H. J. Blytt, and L. G. Warren. (1974). **Pyrophosphate: D-Fructose 6-phosphate 1-phosphotransferase. A new enzyme with the glycolytic function 6-phosphate 1-phosphotransferase**. J. Biol. Chem. 249: 7737-7741.

Reiling, H.E., Laurila, H., and Fiechter, A. (1985). **Mass culture *of Escherichia coli*: medium developed for low and high density cultivation of *Escherichia coli* B/r in minimal and complex media.** J Biotechnology. 2: 191-206.

Reinscheid, D.J. Eikmanns, B.J., and Sahm, H. (1994)**. Malate synthase from *Corynebacterium glutamicum*: sequence analysis of the gene and biochemical characterization of the enzyme.** Microbiology. 140: 3099-3108.

Reizer, J., Charbit, A., and Saier M.H. (1996a). **Novel phosphotransferase system genes revealed by bacterial genome analysis: operons encoding homologues of sugar-specific permease domains of the phosphotransferase system and pentose catabolic enzymes.** Genomic Sci Technol. 1: 53-75.

Reizer, J., Paulsen, I.T., Reizer, A., Titgemeyer, F., and Saier M.H. (1996b). **Novel phosphotransferase system revealed by bacterial analysis: the complete complement of pts genes in *Mycoplasma genitalium*.** Microb Comp Genomics. 1: 151-164.

Reizer, J., Reizer, A., and Saier M.H. (1996c). **Novel PTS proteins revealed by bacterial genome sequencing: a unique fructose-specific phosphoryl transfer protein with two HPr-like domains in *Haemophilus influenzae*.** Res Microbiol. 147: 209-215.

Rezanka, T., Reichelova, J., & Kopecky, J. (1991). **Isobutyrate as a precursor of n-butyrate in the biosynthesis of tylosin and fatty acids.** FEMS Microbiology Letters. 84: 33-36.

Richards, G.M. (1974). **Modifications of the diphenylamine reaction giving increased sensitivity and simplicity in the estimation of DNA**. Analytical Biochemistry. 57: 369-376.

Richmond, R.C. (1970). **Non-Darwinian evolution: a critique**. Nature. 225: 1025-1028.

Rickets, A. (2002). **Over expression of phosphoenolpyruvate carboxylase in *Streptomyces rimosus*.** Ph. D Strathclyde University.

Riesenberg, D., and Bergter, F. (1979). **Dependence of macromolecular composition and morphology of *Streptomyces hygroscopicus* on specific growth rate.** Z Allg Mikrobiol. 19: 415-430.

Righelato, R.C., Trinci, A.P.J., Pirt, S.J., and Peat, A. (1968)**. The Influence of maintenance energy and growth rate on the metabolic activity, morphology and conidiation of *Penicillium chrysogenum*.** J. Gen. Micro. 50 (1): 399-412.

Roberts, R.B., Abelson, P.H., Cowie, D.B., Bolton, E.T., and Britten, R.J. (1955). **Studies of biosynthesis in *Escherichia coli*.** Carnegie Institute of Washington Publication 607. Washington DC. 184-206.

Rock, C.O., Calder, R.B., Karim, M. A., and Jackowski, S. (2000). **Pantothenate kinase regulation of the intracellular concentration of coenzyme A**. J. Biol. Chem. 275: 1377-384.

Roels, J. A. (1980). **Simple model for the energetics of growth on substrates with different degrees of reduction.** Biotechnology and Bioengineering. 22: 33-53.

Roels, J. A. (1983). **Energetics and Kinetics in Biotechnology.** Amsterdam: Elsevier Biomedical Press.

Rokem, J.S., Schon, A., and Soll, D. (1990). **Sequence of a $tRNA^{gly}$ from *Streptomyces coelicolor*.** Nucleic Acid Research. 18: 3988.

Romano, A.H., & Nickerson, W.J. (1958). **Utilisation of amino acids as carbon sources by *Streptomyces fradiae***. Journal of Bacteriology. 75: 161-166.

Romano, A.H., and Conway, T. (1996). **Evolution of carbohydrate metabolic pathways.** Res Microbiol. 147: 448-455.

Roscher, A., Kruger, N. J., and Ratcliffe, R.G. (2000). **Strategies for metabolic flux analysis in plants using isotope labelling**. Journal of Biotechnology. 77: 81-102.

Roseiro, J.C., Esgalhado, M.E., Amaral Collaco, M. T., Emery, A.N. (1992). **Medium development of xanthan production**. Process Biochemistry. 27: 167-175.

Ross, C.M., and Winkler, M.E. (1988). **Regulation of tryptophan biosynthesis in *Caulobacter crescentus*.** Journal of Bacteriology. 170: 769-774.

Roszkowski, J., Ruczaj, Z., Sawnor-Korszynska, D., Kotiuszko, D., Morawska, H., Siejko, D., Raczynska,-Bojanoowska, K. (1971). **NADPH-regenerating systems in microorganisms producing macrolide antibiotics.** Acta Microbiol Pol Ser B. 15: 448-452.

Roubos, J.A., Krabben, P., Luiten, R.G.M., Babuska, R., and Heijnen, J.J. (2001). **A semi-stoichiometric model for a *Streptomyces* fed-batch cultivation with multiple feeds.** Computer Appl Biotech. 8: 299-304.

Rozario, C., Smith, M.W., and Muller, M. (1995). **Primary sequence of a putative pyrophosphate-linked phosphofructokinase gene of *Giardia lamblia***. Biochim. Biophys. Acta 1260: 218-222.

Rudolph, R., Siebendritt, R., and Kiefhaber, T. (1992). **Reversible unfolding and refolding behavior of a monomeric aldolase from *Staphylococcus aureus*.** Protein Sci. 1:654-666.

Ruijter, G.J.G. (2000). **Life is not that simple. Reply to 'look before you clone'.** FEMS Microbiol Lett. 189: 318-319.

Sabater, B., and Asensio, C. (1973). **Transport of hexoses in *Streptomyces violaceoruber*.** Eur J Biochem. 39: 201-205.

Sabater, B., Sebastian, J., & Asensio, C. (1972). **Identification and properties of an inducible mannokinase from *Streptomyces violaceoruber*.** Biochim Biopsy Acta. 284: 406-413.

Saier, M.H., and Reizer, J. (1994). **The bacterial phosphotransferase system: new frontiers 30 years later.** Molecular Microbiology. 13: 755-764.

Salas, J.A., & Hardisson, C. (1981) **Sugar uptake during germination of *Streptomyces antibioticus* spores**. Journal of General Microbiology. 125: 25-31.

Salas, J.A., Quiros, L.M., & Hardisson, C. (1984). **Pathways of glucose catabolism during germination of Streptomyces spores**. FEMS Microbiology Letters. 22: 229-233.

San Martin, R., Bushell, D, Leak, D. J., and Hartley, B. S. (1992). **Development of a synthetic medium for continuous anaerobic growth and ethanol production with a lactate dehydrogenase mutant of *Bacillus stearothermophilus*.** J Gen Microbiol. 138: 987-996.

San, K., Bennet, G.N., Berrios-Rivera, S.J., Vadali, R. V., Yang, Y., Horton, E., Rudolph, F.B., Sariyar, B., and Blackwood, K. (2002). **Metabolic engineering through cofactor manipulation and its effects on metabolic flux redistribution in *Escherichia coli*.** Metabolic Engineering. 4: 182-192.

Sano, K., Ito, K., Miwa, K., Nakamori, S. (1987) **Amplification of the phosphoenolpyruvate carboxylase gene of *Brevibacterium glutamicum* to improve amino-acid production.** Agric. Biol. Chem. 51, 597-599.

Santosh, K., Puneker, N.S., SatyaNarayan, V., and Venkatesh, K.V. (2000). **Metabolic fate of glutamate and evaluation of flux through the 4-aminobutyrate (GABA) shunt in *Aspergillus niger*.** Biotechnology and Bioengineering. 67 (5): 575-584.

Sauer, U., Cameron, D. C., & Bailey, J.E. (1998). **Metabolic capacity of *Bacillus subtilis* for the production of purine nucleosides, riboflavin, and folic acid**. Biotechnology & Bioengineering. 59: 2: 227-238.

Sauer, U., Hatzimanikatis, V. Hohmann, H.P., Manneberg, M., Loon, A.P.G.M., & Bailey, J.E. (1996). **Physiology and metabolic fluxes of wild type and riboflavin producing *Bacillus subtilis***. Applied and Environmental Microbiology. 62: 10: 3687-3696.

Sauer, U., Hatzimanikatis, V., Bailey, J.E., Hochull, M., Szyperski, T., & Wuthrich, K. (1997). **Metabolic fluxes in riboflavin producing *Bacillus subtilis***. Nature Biotechnology. 15: 448-452.

Sauer, U., Lasko, D. R., Fiaux, J., Hochuli, Glaser, R., Szyperski, Wuthrich, K., and Bailey, J.E. (1999). **Metabolic flux ratio analysis of genetic and environmental modulations of *Escherichia coli* central carbon metabolism.** Journal of Bacteriology. 181: 6679-6688.

Savageau, M. A. (1969a). **Biochemical systems analysis. I. Some mathematical properties of the rate law for the component enzymatic reactions.** Journal Theoretical Biology. 25: 365-369.

Savageau, M. A. (1969b). **Biochemical systems analysis. II. The steady state solutions for an n-pool system using a power-law approximation.** Journal Theoretical Biology. 25: 370-379.

Savageau, M. A. (1970). **Biochemical systems analysis. III. Dynamic solutions using a power-law approximation.** Journal Theoretical Biology. 26: 215-226.

Savageau, M. A., Voit, E.O., and Irvine, D. H. (1987a). **Biochemical systems theory and metabolic control theory: 1. Fundamental similarities and differences.** Mathematical Biosciences. 86: 127-145.

Savageau, M. A., Voit, E.O., and Irvine, D. H. (1987b). **Biochemical systems theory and metabolic control theory: 2. The role of summation and connectivity relationships.** Mathematical Biosciences. 86: 147-169.

Savinell, J.M. & Palsson, B. O. (1992a). **Network analysis of intermeditary metabolism using linear optimization, 1 development of mathematical formalism**. Journal Theoretical Biology. 154: 421-454.

Savinell, J.M. & Palsson, B. O. (1992b). **Network analysis of intermeditary metabolism using linear optimization 2. Interpretation of hybridoma cell metabolism**. Journal Theoretical Biology. 154: 455-473.

Savinell, J.M., Lee, G. M. & Palsson, B. O. (1989). **On the orders of magnitude of epigenic dynamics and monoclonal antibody production**. Bioprocess Engineering. 4: 231-234.

Schilling, C.H., Edwards, J.S., & Palsson, B. O. (1999b). **Toward metabolic phenomics: analysis of genomic data using flux balance**. Biotechnology Progress. 15: 288-295.

Schilling, C.H., Edwards, J.S., Letscher, D., & Palsson, B. O. (2001). **Combining pathway analysis with flux balance analysis for the comprehensive study of metabolic systems.** Biotechnology and Bioengineering. 71 (4): 286-302.

Schilling, C.H., Schuster, S., Palsson, B. O., & Heinrich, R. (1999a). **Metabolic pathway analysis: basic concepts and scientific applications in the post-genomic era**. Biotechnology Progress. 15: 296-303.

Schloesser, A., & Schrempf, H. (1996). **A lipid-anchored binding protein is a component of an ATP-dependent cellobiose/cellotriose-transport system from cellulose degrader *Streptomyces reticuli***. European journal of biochemistry. 242: 332-338.

Schloesser, A., Jantos, J., Hackmann, K, & Schrempf, H. (1999). **Characterization of the binding protein-dependent cellotriose transport system of the cellulose degrader *Streptomyces reticuli***. Applied Environmental Microbiology. 65: 2636-2643.

Schloesser, A., Kampers, T., & Schrempf, H. (1997). **The *Streptomyces* ATP-binding component MsiK assists in cellobiose and maltose transport.** Journal of Bacteriology. 179: 2092-2095.

Schmidt, G., & Thannhauser, S.J. (1945). **A method for the determination of deoxyribonucleic acid, ribonucleic acid, and phosphoproteins in animal tissues**. 83-89.

Schmidt, G., and Thannhauser, S.J. (1945). **A method for the determination of deoxyribonucleic acid, ribonucleic acid, and phosphoproteins in animal tissue**. Journal Biol Chem. 161: 83-89.

Schmidt, K., & Norregaard, L.C. (1999). **Quantification of intracellular metabolic fluxes from fractional enrichment and ^{13}C-^{13}C coupling constraints on isotopomer distribution in labeled biomass components**. Metabolic Engineering. 1: 166-179.

Schmidt, K., Marx, A., de-Graaf, A. A., Wiechert, W., Sahm, H., Nielsen, J & Villadsen, J. (1998). **^{13}C tracer experiments and metabolite balancing for metabolic flux analysis: Comparing two approaches**. Biotechnology and Bioengineering. 58: (2&3): 254-257.

Schmidt, K., Nielsen, J., and Villadsen, J. (1999). **Quantitative analysis of metabolic fluxes in *Escherichia coli*, using two-dimensional NMR spectroscopy and complete isotopomer models.** Journal of Biotechnology. 71: 175-189.

Schneider, W.C., Hogeboom, G.H., and Ross, H.E. (1950). **Intracellular distribution of enzymes. VII. The distribution of nucleic acids and adenosinetriphosphatase normal mouse liver and mouse hepatoma**. Journal of the National Cancer Institute. 977-983.

Schreiweis, A. L., McAfoos, L. S., and Kemmerling, M.K. (1999). **Tylosin fermentation material balance**. *Internal publication* Eli Lilly Ltd.

Schröder, C., Selig, M., and Schönheit, P. (1994). **Glucose fermentation to acetate, CO_2 and H_2 in the anaerobic hyperthermophilic eubacterium *Thermotoga maritima* involvement of the Embden-Meyerhof pathway**. Archives of Microbiology. 161:460-470.

Schulze, U. (1995). **Anaerobic physiology of *Saccharomyces cerevisiae*.** Ph.D. thesis. Technical University of Denmark, Copenhagen, Denmark.

Schuster, K.C., Mayer, H.F., Kieweg, R., Hampel, W. A., and Sara, M. (1995). **A synthetic medium for continuous culture of the S-layer *carrying Bacillus stearothermophilus* PV72 and studies on the influence of growth conditions on cell wall properties.** Biotechnology and Bioengineering. 48: 66-77.

Schuster, S., Dandekar, T., and Fell, D. A. (1999). **Detection of elementary flux modes in biochemical networks: a promising tool for pathway analysis and metabolic engineering.** Trends in Biotechnology. 17: 53-60.

Scrimer, T. and Evans, P. (1990). **Structural basis of the allosteric behaviour of phosphofructokinase.** Nature 343:140-145.

Seligmann, H. (2003). **Cost-minimization of amino acid usage.** J Mol Evol. 56 (2): 151-61.

Seiler, U., Pape, H., and Schröder, W. (1996**). A pyrophosphate-dependent phosphofructokinase (PFK) from *Actinoplanes* spec**. Abstracts of the VAAM meeting, Bayreuth, Germany 119(Abstract).

Senn, H., Werner, B., Messerie, B.A., Weber, C., Traber, R., and Wuthrich, K. (1989). **Stereospecific assignment of the methyl H-NMR lines of valine and isoleucine in polypeptides by nonrandom ^{13}C labelling**. FEBS Letter. 249: 113-118.

Seno, E. T., Pieper, R.L., & Huber, F. M. (1977). **Terminal stages in the biosynthesis of tylosin**. Antimicrobial agents and Chemotherapy. 11: 3: 455-461.

Setlow, P. (1973). **Inability to detect cyclic AMP in vegetative or sporulating cells or dormant spores of *Bacillus megaterium*.** Biochem Biophys Res Commun. 52: 365-372.

Shahab, N., Flett, F., Oliver, S.G., and Butler, P. R. (1996). **Growth rate control of protein and nucleic acid content in *Streptomyces coelicolor* A3(2) and *Escherichia coli* B/r.** Microbiology. 142: 1927-1935.

Shapiro, S., & Vining, L.C. (1983). **Nitrogen metabolism and chloramphenicol production in *Streptomyces venezuelae***. Canadian Journal of Microbiology. 29: 1706-1714.

Shapiro, S., & Vining, L.C. (1984). **Suppression of nitrate utilization by ammonium and its relationship to chloramphenicol production in *Streptomyces venezuelae*.** Canadian Journal of Microbiology. 30: 798-804.

Sharp, P.M., and Matass, G. (1994). **Codon usage and genome evolution.** Curr Opin Genet Dev. 4: 851-860.

Shi, H., Shiraishi, M., and Shimizu, K. (1997). **Metabolic flux analysis for biosynthesis of poly(β-hydroxybutyric acid) in *Alcaligenes eutrophus* from various carbon sources.** Journal of Fermentation and Bioengineering. 84 (6): 579-587.

Shields, R., and Burnett, W. (1960). **Determination of protein-bound carbohydrate in serum by a modified anthrone method.** Analytical Chemistry. 32: 885-886.

Shiio, I., Otsuka, S.I., Takahashi, M. (1959). **Glutamic acid formation from glucose by bacteria. I. Enzymes of the Embden-Meyerhof-Parnas pathway, the Krebs cycle, and the glyoxylate bypass in cell extracts of *Brevibacterium flavum*.** J Bioch 46: 1303-1311.

Shiio, I., Otsuka, S.I., Tsunoda, T. (1960). **Glutamic acid formation from glucose by bacteria. IV. Carbon dioxide fixation and glutamate formation in *Brevibacterium flavum*.** Journal of Biochemistry. 48: 110-120.

Shimizu, H., Takiguchi, N., Tanaka, H., and Shioya, S. (1999). **A maximum production strategy of lysine based on a simplified model derived from a metabolic reaction network.** Metabolic Engineering. 1: 25-34.

Siebers, B, and Hensel, R. (1993). **Glucose catabolism of the hyperthermophilic archaeum *Thermoproteus tenax***. FEMS Microbiol. Lett. 111:1-8.

Simons, J.S.S., and Johnson, D.F. (1976). **The structure of the fluorescent adduct formed in the reaction of o-phthalaldehyde and thiols with amines**. Journal of the American Chemical Society. 7098-7099.

Simpson, T.W., Follstad, B. D., and Stephanopoulos, G. (1999). **Analysis of the pathway structure of metabolic networks.** Journal of Biotechnology. 71: 207-223.

Smith, C.P., and Chater, K.F. (1988) **Cloning and transcription analysis of the entire glycerol utilization (glyabx) operon of *S. coelicolor* A3 (2) and identification of a closely associated transcription unit.** Molecular and General Genetics. 211: 129-137.

Smith, D. D. S., Wood, N. J., and Hodgson, D. A. (1995). **Interaction between primary and secondary metabolism in *Streptomyces coelicolor* A3(2): role of pyrroline-5-carboxylate dehydrogenase.** Microbiology. 141: 1739-1744. (Addendum in Microbiology 141, 2351).

Smith, L.M., Meijer, W.G., Dijkhuizen, L., Goodwin, P. (1996) **A protein having similarity with methylmalonyl-CoA mutase is required for the assimilation of methanol and ethanol by *Methylobacterium extorquens* AMI**. Microbiology. 142, 657-684.

Smith, P.K., Krohn, R.I., Hermanson, G.T., Mallia, A. K., Gartner, F.H, Provenzano, M. D., Fujimoto, E.K., Goeke, N. M., Olson, B.J., & Klenk, D. C. (1985). **Measurement of protein using bicinchoninic acid**. Analytical Biochemistry. 150: 76-85.

Snedecor, B., Chu, H., and Chen, E. (1991). **Selection, expression, and nucleotide sequencing of the glutamate dehydrogenase gene of *Peptostreptococcus asaccharolyticus*.** Journal of Bacteriology. 173 (19): 6162-6167.

Snoep, J.L., Joost, M., de Teixeira, M., and Neijssel, O.M. (1991). **Effect of the energy source on the NADH/NAD ratio and on pyruvate catabolism in anaerobic chemostat cultures of *Enterococcus faecalis* NCTC 775.** FEMS Microbiology Letters. 81: 63-66.

Soby, L.M. and Johnson, P. (1981). **Determination of asparagine and glutamine in polypeptides using bis (1,1-trifluoroacetoxy)iodobenzene.** Analytical Biochemistry. 113, 149-153.

Soh B. S., Loke P., and Sim T.S. (2001). **Cloning, heterologous expression and purification of an isocitrate lyase from *Streptomyces clavuligerus* NRRL 3585. (2001).** Biochimica et Biophysica Acta (BBA) / Gene Structure and Expression. 3 (2): 112-117.

Soliveri, J., Mendoza, A., and Arias, M.E. (1988). **Effect of different nutrients on the production of polyene antibiotics PA-5 and PA-7 by *Streptoverticillium sp*. 43/16 in chemically defined media.** Applied Microbiology and Biotechnology. 28: 254-257.

Sonnleitner, B., Locher, G., and Fiechter, A. (1992). **Minireview: Biomass determination**. Journal of Biotechnology. 25: 5-22.

Sprinkmeyer, R., & Pape, H. (1978)**. Effects of glucose and fatty acids on the formation of the macrolide antibiotic tylosin by *Streptomyces***. Genetics of *Actinomycetes*. 51-58.

Stanbury, P.F., Whitaker, A., and Hall, S.J. (2000). **Principles of Fermentation Technology.** Second edition. Butterworth Heinemann.

Stanier, R.Y., Adelberg, E.A., and Ingraham, J.L. (1981). "**General Microbiology".** The Macmillan Press Ltd.

Stanier, R.Y., Ingraham, J.L., Wheelis, M. L., and Painter, P. R. (1986). **The Microbial World.** Prentice Hall, Englewood Cliffs, N.J. 5th Edition.

Stark, W.M., Daily, W. A., & McGuire, J.M. (1961). **A fermentation study of the biosynthesis of tylosin in synthetic media**. Sci. Repts. 1st. Super. Sanita. 1: 340-354.

Stephanopoulos, G. & Sinskey, A.J. (1993). **Metabolic engineering – methodologies and future prospects.** TIBTECH. 11: 392-396.

Stephanopoulos, G. & Vallino. J.J., (1991). **Network rigidity and metabolic engineering in metabolite overproduction**. Science. 252:1675-1681.

Stephanopoulos, G. (1999). **Metabolic fluxes and metabolic engineering**. Metabolic Engineering. 1: 1-11.

Stephanopoulos, G.N., Aristidou, A. A. & Nielsen, J. (1998). **Metabolic engineering: principles and methodologies**. Academic Press. 24 – 28 Oval Road, London , NW1 7DX, UK.

Stewart, P. R. (1975). **Analytical methods for yeast**. In: Prescott D.M, editor. Methods in cell biology: yeast cells. New York, Academic Press.

Stouthamer, A.H. (1973). **A theoretical study on the amount of ATP required for synthesis of microbial cell material.** Antonie van Leeuwenhoek. 39: 545-565.

Stratigopoulos, G. and Cundliffe, E. (2002) **Expression analysis of the tylosin-biosynthetic gene cluster: pivotal regulatory role of the *tylQ* product.** Chem. Biol. 9, 71-78.

Strauch, E., Takano, E., Baylis, H.A & Bibb, M.J. (1991). **The stringent response in *Streptomyces coelicolor* A3(2)**. Molecular Microbiology. 5: 289-298.

Strauss, G., and Fuchs, G. (1993). **Enzymes of a novel autotrophic CO_2 fixation pathway in the phototrophic bacterium *Chloroflexus aurantiacus*, the 3-hydroxypropionate cycle.** European Journal of Biochemistry. 215: 633-643.

Streshinskaya, G. M., Naumova, I. B., and Panina, L. I. (1979). **Anionic carbohydrate containing polymers of the bacterial cell wall.** Mikrobiologiya. 48: 814-819.

Stribling, D, and Perham, R. N. (1973). **Purification and characterization of two fructose diphosphate aldolases from *Escherichia coli* (Crooke's strain).** Biochemical journal. 131:833-841.

Strydom, D. J. and Cohen, S.A. (1993) in **Techniques in Protein** Chemistry IV (Angeletti, R.H., Ed.) Academic Press, San Diego, CA, 299-307.

Stryer, L. (1981). **Biochemistry**. Second edition. W.H Freeman and company. San Francisco.

Sueoka, N. (1961). **Correlation between base composition of deoxyribonucleic acid and amino acid composition of protein.** Biochemistry. 47: 1141-1149.

Summers, R.J., Boudreaux, D. P., and Srinivasan, V.R. (1979). **Continuous cultivation for apparent optimization of defined media for *Cellulomonas sp*. And *Bacillus cereus*.** Applied and Environmental Microbiology. 38: 66-71.

Surowitz, K.G., & Pfister, R.M. (1985). **Glucose metabolism and pyruvate excretion by *Streptomyces alboniger***. Canadian Journal of Microbiology. 31: 702-706.

Sutherland, I.W., and Wilkinson, J.F. (1971), **Chemical extraction methods of microbial cells.** Methods in Microbiology. Academic Press (Norris J.R and Ribbon D. W; Eds). 6A, 4, 347-383.

Suzuki, Y., and Yamada, T. (1988). **The nucleotide sequence of 16S rRNA gene from *Streptomyces lividans* TK21.** Nucleic Acids Research. 16: 370.

Szeszak, F., Vitalis, S., Bekesi, I., Szabo, G. (1991) **Presence of Factor C in streptomycetes and other bacteria. Genetics and Product** Formation in Streptomyces: 11-18. Plenum Press.

Szyperski, T. (1995). **Biosynthetically directed fractional ^{13}C-labelling in proteinogenic amino acids. An efficient analytical tool to investigate intermediary metabolism.** European Journal of Biochemistry. 242: 433-448.

Takahashi, N., Kalfas, S., and Yamada, T. (1995). **Phosphorylating enzymes involved in glucose fermentation of *Actinomyces naeslundii***. Journal of Bacteriology. 177:5806-5811.

Takebe, H., Matsunaga, M., Hiruta, O., Satoh, A., Tanaka, H. (1991). **Relationship between sugar consumption and tricarboxylic acid cycle enzyme activity in a high bialaphos-producing strain.** Journal of Fermentation and Bioengineering. 71: 110-113.

Tang, L., Zhang, Y.X., Hutchinson, C.R. (1994) **Amino acid catabolism and antibiotic synthesis: Valine is a source of precursors for macrolide biosynthesis in *Streptomyces ambofaciens* and *Streptomyces fradiae***. Journal of Bacteriology. 176:6107-6119.

Tanida, S., Hasegawa, T., and Higashida, E. (1980). **Macbecins I and II, new antitumor antibiotics. I. Producing organism, fermentation and antimicrobial activities.** Journal of Antibiotics. 33: 199-204.

Tao, H., Bausch, C., Richmond, C., Blattner, F.R., and Conway, T. (1999). **Functional genomics: Expression analysis of *Escherichia coli* growing on minimal and rich media.** Journal of Bacteriology. 181: 6425-6440.

Tata, M., & Menawat, A.S. (1994). **Cyclic AMP regulation of tylosin biosynthesis and secondary metabolism in *Streptomyces fradiae***. Biotechnology & Bioengineering. 44: 283-290.

Taylor, A. R. (1946). **Chemical analysis of the T_2 bacteriophage and its host, *Escherichia coli* (strain B)*.** Journal of Biological Chemistry. 165: 271-284.

Taylor, R. D. (1992) **Purification and characterisation of the isocitrate dehydrogenase from *S. coelicolor* and cloning of its gene**. Ph.D. Thesis. Dept. Biochem. And Mol. Biol. Glasgow University.

Teushcer, G. (1967). **Metabolic pathway of L-tryptophan in *Streptomyces* species.** Phytochemistry. 6: 141-144.

Theobald, U., Mailinger, W., Baltes, M., Rizzi, M., and Reuss, M. (1997). ***In vivo* analysis of metabolic dynamics in Saccharomyces cerevisiae: I. Experimental observations.** Biotechnology and Bioengineering. 55: 305-316.

Thoai, N.V., Thome-Beau, F., and Olomucki, A. (1966). **Induction et specificite des enzymes de la nouvelle voie catabolique de l'arginine.** Biochim Biophys Acta. 115: 73-80.

Thorson, J.S., Lo, S.F., Liu, H.W., and Hutchinson, C.R. (1993). **Biosynthesis of 3,6-dideoxyhexose: new mechanistic reflection upon 2,6-deooxy, 4,6-dideoxy, and amino sugar construction.** Journal American Chemical Society. 115: 6993-6994.

Tinterova, M., Hostalek, Z., and Vanek, Z. (1969). **Regulation of biosynthesis of secondary metabolites. VI: Characteristics of isoenzymes of malate dehydrogenase in *Streptomyces aureofaciens*.** Foli Microbiol. 14: 135-140.

Tipper, D. J. (1968). **Alkali-catalyzed elimination of D-lactic acid from muramic acid and it derivatives and the determination of muramic acid.** Biochemistry. 7: 1441-1449.

Titgemeyer, F., Walkenhorst, J., Cui, X., Reizer, J., & Saier, M.H. (1994). **Proteins of the phosphoenolpyruvate: sugar phosphotransferase systems in *Streptomyces*: possible involvement in the regulation of antibiotic production**. Research in Microbiology. 145: 89-92.

Titgemeyer, F., Walkenhorst, J., Reizer, J., Stuiver, M.H., Cui, X., & Saier, M.H. (1995). **Identification and characterization of phosphoenolpyruvate: fructose phosphotransferase systems in three *Streptomyces* species.** Microbiology. 141: 51-58.

Torbochkina, L.I., & Dormidoshina, T. A. (1964). **Mechanism of glucose dissimilation in oleandomycin-producing *Actinomyces antibioticus***. Mikrobiologiya. 33: 325-331.

Tosaka, O., Morioka, H., Takinami, K. (1979). **The role of biotin-dependent pyruvate carboxylase in L-lysine production.** Agric Biol Chem. 43: 1513-1519.

Triger, E.G., Polyanskaya, L.M., Kozhevin, P.A., and Zvyagintsev, D.G. (1991). **Autoregulation of spore germination in *Streptomyces* grown on rich and poor media.** Microbiology. 60 (3): 322-325.

Troost, T., Hitchcock, M.J.M., and Katz, E. (1980). **Distinct kynureninase and hydroxykynureninase enzymes in an actinomycin-producing strain of *Streptomyces parvulus*.** Biochim Biopsy Acta. 612: 97-106.

Ujita, S and Kimura, K. (1982). **Glucose-6-phosphate dehydrogenase, vegetative and spore *Bacillus* subtilis.** In Methods in Enzymology: Carbohydrate Metabolism. Part D 89: 258-261.

Umbarger, H.E. (1977). **A one-semester project for the immersion of graduate students in metabolic pathways.** Biochemical Education. 5: 67-71.

Untrau, S., Lebrihi, A., Lefebore, G., and Germain, P. (1994). **Nitrogen catabolite regulation of spiramycin production in *Streptomyces ambofaciens*.** Current Microbiol. 28: 111-118.

Uyeda, K. (1979). **Phosphofructokinase**. Adv. Enzymol. 48:193-244.

Valentine, B. P., and Bailey, C.R. (1993). The late Andrew Doherty, Morris, J., Elson, S.W., Baggaley, K.H. *et al*. **Evidence that arginine is a later metabolic intermediate than ornithine in the biosynthesis of clavulanic acid by *Streptomyces clavuligerus*.** J Chem Soc Chem Commun. 1993: 1210.

Vallino, J.J. & Stephanopoulos, G. (1990). **Flux determination in cellular bioreaction networks: Applications to lysine fermentations**. 205-219. Eds Frontiers in Bioprocessing CRC press Boca Raton.

Vallino, J.J. & Stephanopoulos, G. (1993). **Metabolic flux distributions in *Corynebacterium glutamicum* during growth and lysine overproduction**. Biotechnology & Bioengineering. 41 (6): 633-646.

Vallino, J.J. & Stephanopoulos, G. (1994b). **Carbon flux distributions at the glucose-6-phosphate branch point in *Corynebacterium glutamicum* during lysine overproduction.** Biotechnology Progress. 10: 327-334.

Vallino, J.J. (1991). **Identification of branch-point restrictions in microbial metabolism through metabolic flux analysis and local network perturbations**. Ph.D. Thesis, Massachusetts Institute of Technology, Cambridge, MA.

Vallino, J.J. and Stephanopoulos, G. (1994a). **Carbon flux distributions at the pyruvate branch point in *Corynebacterium glutamicum* during lysine overproduction**. Biotechnology Progress. 10 (3): 320-326.

Van Dam, K. (1986). **Biochemistry is a quantitative science**. TIBS. 11: 13-14.

Van der Heijden, R.T.J.M., Heijnen, J.J., Hellinga, C., Romein, B., and Luyben, K.Ch.A.M. (1994a). **Linear constraint relations in biochemical reaction systems: I. Classification of the calculability and the balance ability of conversion rates.** Biotechnology and Bioengineering. 43: 3-10.

Van der Heijden, R.T.J.M., Heijnen, J.J., Hellinga, C., Romein, B., and Luyben, K.Ch.A.M. (1994b). **Linear constraint relations in biochemical reaction systems: I. Classification of the calculability and the balanceability of conversion rates.** Biotechnology and Bioengineering. 43: 11-20.

Van der Rest, M.E., Frank., C. and Molenaar, D. (2000). **Functions of the membrane-associated and cytoplasmic malate dehydrogenases in the citric acid cycle of *E. coli***. Journal of Bacteriology., 182, 6892-6899.

Van der Wal, A., Norde, W., Bendinger, B., Zehnder, A.J.B., and Lyklema, J. (1997). **Chemical analysis of isolated cell walls of Gram-positive bacteria and determination of the cell wall to cell mass ratio.** Journal of Microbiological Methods. 28: 147-157.

Van Gulik, W.M., & Heijnen, J.J. (1995). **A metabolic network stoichiometry analysis of microbial growth and product formation**. Biotechnology & Bioengineering. 48: 681-698.

van Gulik, W.M., de Laat, W.T.A.M., and Vinke, J.L., et al. (2000). **Application of metabolic flux analysis for the identification of metabolic bottlenecks in the biosynthesis of penicillin-G.** Biotechnology and Bioengineering. 68 (6): 602-618.

van Wezel, G. P., White, J., Bibb, M. L., and Postma, P.W. (1997b). **The *mal*EFG gene cluster of *Streptomyces coelicolor* A3(2): characterization, disruption and transcriptional analysis.** Mol Gen Genet. 254: 604-608.

van Wezel, G. P., White, J., Young, P., Postma, P.W., & Bibb, M.J. (1997a). **Substrate induction and glucose repression of maltose utilization by *Streptomyces coelicolor* A3(2) is controlled by *mal*R, a member of the *lac*I-*gal*R family of regulatory genes.** Molecular Microbiology. 23: 537-549.

VanBogellen, R.A., Abshire, K.Z., Pertsemlidis, A., Clark, R., and Neidhardt, F.C. (1996). In ***Escherichia coli* and *Salmonella*: Cellular and Molecular Biology.** Magasanik, B., Reznikoff, W.S., Riley, M., Schaecter, A and Umbarger, H.E (Am Soc Microbiol, Washington, DC) 2 nd Ed. 2067-2117.

Vancura, A., Rezanka, T., Marsalek, J., Kristan, V., & Basarova, G. (1987a). **Fatty acids and production of tylosin-like compounds in *Streptomyces fradiae***. Journal of Basic Microbiology. 27: 3: 167-171.

Vancura, A., Rezanka, T., Marsalek, J., Vancurova, I., Kristan, V., & Basarova, G. (1987b). **Effect of ammonium ions on the composition of fatty acids in *Streptomyces fradiae*, producer of tylosin.** FEMS Microbiology Letters. 48: 357-360.

Vancura, A., Rezanka, T., Marsalek. J., Melzoch, K., Basarova, G., & Kristan, V. (1988a). **Metabolism of L-threonine and fatty acids and tylosin biosynthesis in *Streptomyces fradiae***. FEMS Microbiology Letters. 49: 411-415.

Vancura, A., Vancurova, I., Kopecky, J., Marsalek, J., Cikanek, D., Basarova, G., & Kristan, V. (1989a). **Regulation of branched-chain amino acid biosynthesis in *Streptomyces fradiae*, a producer of tylosin**. Archives of Microbiology. 151: 537-540.

Vancura, A., Vancurova, I., Volc, J., Fussey, S.P.M., Flieger, M., Neuzil, J., Marsalek, J., & Behal, V. (1988b). **Valine dehydrogenase from *Streptomyces fradiae*: purification and properties**. Journal of General Microbiology. 134: 3213-3219.

Vancurova, I., Vancura, A., Volc, J., Kopecky, J., Neuzil, J., Basarova, G., & Behal, V. (1989b). **Purification and properties of NADP-dependent glutamate dehydrogenase from *Streptomyces fradiae*.** Journal of General Microbiology. 135: 3311-3318.

Vanek, Z., Hostalek, Z., and Spizek, J. (1990). **Overproduction of microbial products - facts and ideas.** Biotechnology Advances. 8 (1): 1-27.

Vanek, Z., Novak, J., & Jechova, V. (1988). **Primary and secondary metabolism.** Pp. 389-394 in Y. Okami., T. Beppu., H. Ogawara (Eds): *Biology of Actinomycetes 88*. Japan Scientific Societies Press, Tokyo.

Varma, A. & Palsson, B.O. (1994a). **Metabolic flux balancing: basic concepts, scientific and practical use**. Bio/Technology. 12: 994-998.

Varma, A. & Palsson, B.O. (1994b). **Stoichiometric flux balance models quantitatively predict growth and metabolic by-product secretion in wild-type *E. coli* w31110**. Applied Environmental Microbiology. 60: 3724-3731.

Varma, A. & Palsson, B.O. (1995). **Parametric sensitivity of stoichiometric flux balance models applied to wild type *E. coli* metabolism**. Biotechnology & Bioengineering. 45: 69-79.

Varma, A., Boesch, B.W. & Palsson, B.O. (1993b). **Biochemical production capabilities of *E. coli***. Biotechnology & Bioengineering. 42: 59-73.

Varma, A., Boesch, B.W. & Palsson, B.O. (1993a). **Stoichiometric interpretation of *E. coli* glucose catabolism under various oxygenation rates**. Applied and Environmental Microbiology. P2465-2473.

Varner, J., and Ramkrishna, D. (1999). **Mathematical models of metabolic pathways.** Current Opinion in Biotechnology. 10: 146-150.

Verduyn, C., Postma, E., Scheffers, W. A., and van Dijken, J. P. (1991). **A theoretical evaluation of growth yields of yeasts**. Ant van Leeuwenhoek. 59: 49-63.

Verhoff, F.H., and Spradlin, J.E. (1976). **Mass and energy balance analysis of metabolic pathways applied to citric acid production by *Aspergillus niger*.** Biotechnology and Bioengineering XVIII:425-432.

Vining, L.C. (1992). **Secondary metabolism, inventive evolution and biochemical diversity-a review**. Gene. 115: 135-140.

Vinning, L.C., and Stuttard, C. (1988). **Genetics and biochemistry of antibiotic production.** 13. Tetracyclines. Behal, V., and Hunter, I.S. Butterworth-Heinemann. 359-384.

Vlaev, D., Mann, R., Lossev, V., Vlaev, S. D., Zahradnik, J., and Seichter, P. (2000). **Macro-mixing and *Streptomyces fradiae*: modelling oxygen and nutrient segregation in an industrial bioreactor.** Trans IChemE. 78 Part A: 354-362.

Voit, E.O., & Savageau, M. A.. (1985). **S-system analysis of biological systems.** In V. Capasso, E. Grosso, & S. L. Paveri-Fontana (Eds.), Mathematics in biology and medicine (pp. 517-524). Berlin: Springer-Verlag.

von der Osten, C.H., Barbas, C.F., and Wong, C.H. (1989). **Molecular cloning, nucleotide sequence and fine-structural analysis of the *Corynebacterium glutamicum fda* gene: structural comparison of *C. glutamicum* fructose-1,6-bisphosphate aldolase to class I and class II aldolases**. Molecular Microbiology. 3:1625-1637.

Vriezen, N. (1998). **Physiology of mammalian cells in suspension culture**. Ph.D. thesis. Technical University Delft. The Netherlands.

Vu-Trong, K., & Gray, P.P. (1982). **Continuous culture studies on the regulation of tylosin biosynthesis**. Biotechnology & Bioengineering. 24: 1093-1103.

Vu-Trong, K., and Gray, P.P. (1986). **Patterns of RNA synthesis in batch and cyclic fed-batch cultures of tylosin-producing *Streptomyces fradiae*.** Biotechnology Letters. 8 (12): 849-852.

Vu-Trong, K., and Gray, P.P. (1987). **Influence of ammonium on the biosynthesis of the macrolide antibiotic tylosin.** Enzyme Microb Tech. 9: 1785-1804.

Vu-Trong, K., Bhuwapathanapun, S., & Gray, P.P. (1980). **Metabolic regulation in tylosin producing *Streptomyces fradiae*: regulatory role of adenylate nucleotide pool and enzymes involved in biosynthesis of tylonolide precursors.** Antimicrobial Agents and Chemotherapy. 17: 4: 519-525.

Vu-Trong, K., Bhuwapathanapun, S., & Gray, P.P. (1981). **Metabolic regulation in tylosin producing *Streptomyces fradiae*: phosphate control of tylosin biosynthesis**. Antimicrobial Agents and Chemotherapy. 19: 2: 209-212.

Waksman, S.A., Schatz, A., and Reilly, C.H. (1946). **Metabolism and the chemical nature of *Streptomyces griseus*.** Biochemistry. 16: 753-759.

Walker, J (1996). The **protein protocols** handbook / edited by John M. Walker. Publication Details: Towota, N. J. : Humana Press.

Walker, V., and Mills, G. A. (1995). **Quantitative methods for amino acid analysis in biological fluids.** Ann Clin Biochem. 32: 28-57.

Wallace, K.K., Bao, Z.Y., Hong, D., Digate, R., Schuler, G., Speedie, M.K., and Reynolds, K.A. (1995). **Purification of crontyl-CoA reductase from *Streptomyces collinus* and cloning sequencing and expression of the corresponding gene in *Escherichia coli*.** European Journal of Biochemistry. 233: 954-962.

Walsh, K., and Koshland, jr. D. E. (1984). **Determination of flux through the branch-point of two metabolic cycles: The tricarboxylic acid cycle and the glyoxylate shunt.** J. Biol. Chem. 259: 9646-9654.

Wang, C.H., Bialy, J.J., Klungsoyr, and Gilmour, C.M. (1958b). **Studies on the biosynthesis of *Streptomyces*. III. Glucose catabolism in *Streptomyces griseus*.** Journal of Bacteriology. 75: 31-37.

Wang, C.H., Stern, I., Gilmour, C.M., Klungsoyr, S., Reed, D. J., Bialy, J.J., and Cheldelin, V.H. (1958a). **Comparative study of glucose metabolism and the radiorespirometric method.** Journal of Bacteriology. 76: 207-216.

Wang, H.Y., C. L. Cooney and D.I.C. Wang. (1979). **On-Line Gas Analyses for Material Balances and Control.** Biotechnology and Bioengineering. Symp. 8.

Wang, N.S., and Stephanopoulos, G. (1983). **Application of macroscopic balances to the identification of gross measurement errors**. Biotechnology and Bioengineering. 25: 2177-2208.

Warr, S.R.C., Gershater, C.J.L., and Box, S.J. (1996). **Seed stage development for improved fermentation performance: increased milbemycin production by *Streptomyces hygroscopicus*.** Journal of Industrial Microbiology. 16: 295-300.

Washburn, M.P., Wolters, D., and Yates, R. (2001). **Large-scale analysis of the yeast proteome by multidimensional protein identification technology.** Nat Biotech. 19: 242-247.

Watanabe, Y., Ohe, T., & Morita, M. (1976a). **Control of the formation of uricase in *Streptomyces* spp. By nitrogen and carbon sources**. Agric. Biol. Chem. 40: 131-139.

Watanabe, Y., Ohe, T., & Tsujisaka, Y. (1976b). **Changes in the metabolic pathways of hypoxanthine in *Streptomyces***. Journal of General Microbiology. 22: 13-23.

Watson, D.G. (1999). **Pharmaceutical Analysis. A textbook for pharmacy students and pharmaceutical chemists.** Churchill Livingston.

Watve, M.G., Tickoo, R., Jog, M.M., and Bhole, B. D. (2001). **How many antibiotics are produced by the genus *Streptomyces*?** Archives of Microbiology. 176 (5): 386-390.

Weatherburn, M.W. (1971). **Phenol-hypochlorite reaction for determination of ammonia.** Analytical Chemistry. 39 (8): 971-979.

Wehmeier, U. F. (2001). **Molecular cloning, nucleotide sequence and structural analysis of the *Streptomyces galbus* DSM40480 *fda* gene: the *S. galbus* fructose-1,6-bisphosphate aldolase is a member of the class II aldolases.** FEMS Microbiol. Lett. 197: 53-58.

Weibel, E.K., Mor, J.R., and Fiechter, A. (1974). **Rapid sampling of yeast cells and automated assays of adenylate, citrate, pyruvate and G6P pools.** Analytical Biochemistry. 58: 208-216.

Weishank, D.J. and Garver, J.C. (1967). **Theory and design of aerobic fermentations.** In: Peppler, H.J (ed). Microbial Technology. Re-inhold. New York. 417-449.

Wellington, E.M., Stackebrandt, E., Sanders, D., Wolstrup, J., and Jorgensen, N.O. (1992). **Taxonomic status of *Kitastatosporia*, and proposed unification with *Streptomyces* on the basis of phenotypic and 16S rRNA analysis and emendation of *Streptomyces*.** Waksman and Henrici 1943, 339^{AL}. Int J Syst Bacteriol. 42: 156-160.

Werner, W.H., Rey, H.G., and Wielinger, Z. (1970). **Glucose oxidase and peroxidase reactions for the quantitative determination of glucose.** Analyst Chem. 252: 224.

West, K. and Crabb, J.W. (1992) in **Techniques in Protein.** Chemistry III (Angeletti, R.H., Ed.) Academic Press, San Diego, CA, 233-242.

Westerhoff, H. V. and Van Dam, K. (1987) **Thermodynamics and Control of Free-energy Transduction.** Elsevier, Amsterdam.

Westerhoff, H.V., Heeswijk, W.V., Kahn, D., and Kell, D.B. (1991). **Quantitative approaches to the analysis of the control and regulation of microbial metabolism**. Antonie van Leeuwenhoek. 60: 193-207.

White, P.J., Nairn, J., Price, N. C. et al. (1992) **Phosphoglycerate mutase from *Streptomyces coelicolor* A3(2): purification and characterisation of the enzyme and cloning and sequencing analysis of the gene.** Journal of Bacteriology. 174, 434-440.

Williams, S.T., Goodfellow, M., Alderson, G. (1989) **Genus Streptomyces** Watkman and Hendrici 1943. In Bergey's Manual of Determinative Bacteriology, vol 4, 2453- 2492. Edited by Williams, S.T., Sharpe, M.E., Holt, J.G. Baltimore: Williams & Willkins.

Williams, W. K., & Katz, E. (1977). **Development of a chemically defined medium for the synthesis of actinomycin D by *Streptomyces parvulus*.** Antimicrobial Agents and Chemotherapy 11, 281-290.

Witke, C. and Gotz, F. (1993). **Cloning, sequencing, and characterization of the gene encoding the class I fructose-1,6-bisphosphate aldolase of *Staphylococcus carnosus*.** Journal of Bacteriology. 175:7495-7499.

Witter, B., Debuch, H., and Steiner, M. (1974). **Die lipide von *endomycopsis vernalis* bei verschiedener steckstoff-ernahrung.** Archives of Microbiology. 101: 321-335.

Wittler, R., & Schugerl, K. (1985**). Interrelation between penicillin productivity and growth.** rate. Applied Microbiology Letters. 110: 239-242.

Wood, H.G. (1985). **Inorganic phosphate and polyphosphates as sources of energy.** Curr. Top. Cell. Metab. 26:355-369.

Wood, H.G. and Goss, N. H. (1985). **Phosphorylation enzymes of the propionic bacteria and the roles of ATP, inorganic phosphate, and polyphosphates**. Proc. Natl. Acad. Sci. USA 82:312-315.

Wood, H.G., O'Brien, W.E., and Michaelis G. (1977). **Properties of carboxytransphosphorylase, pyruvate phosphate dikinase, pyrophosphate-phosphofructokinase and PPi-acetate kinase and their roles in the metabolism of inorganic pyrophosphate**. Applied Environmental Microbiology. 45:85-155.

Wright, F. and Bibb, M.J. (1992). **Codon usage in the G+C rich *Streptomyces* genome.** Gene 113:55-65.

Wu, L.F., Reizer, A., Reizer, J., Cai, B., Tomich, J.M., and Saier, M.H.J. (1991). **Nucleotide sequence of the *Rhodobacter capsulatus fru*K gene, which encodes fructose-1-phosphate kinase: Evidence for a kinase superfamily including both phosphofructokinases of *Escherichia coli*.** Journal of Bacteriology. 173: 3117-3127.

Wuthrich, K., Szyperski, T., Leiting, B., and Otting, G. (1992). **Biosynthetic pathways of the common proteinogenic amino acids investigated by fractional 13C-labelling and NMR spectroscopy.** pp 41-48. In Frontiers and New Horizons in Amino Acid Research. Takai, K. (ed). Elsevier, Amsterdam.

Xia, T., & Jiao, R. (1986) **Studies on glutamine synthetase from *Streptomyces hygroscopicus ver*.** Jinggangensis. Scientia Sin. (Ser.B). 29: 379-388.

Xie, L. & Wang, D.I.C. (1994a). **Stoichiometric analysis of animal cell growth and its application in medium design**. Biotechnology and Bioengineering. 43: 1164-1174.

Xie, L. & Wang, D.I.C. (1994b). **Fed-batch cultivation of animal cells using different medium design concepts and feeding strategies**. Biotechnology and Bioengineering. 43: 1175-1189.

Xie, L. & Wang, D.I.C. (1994c). **Stoichiometric analysis of animal cell growth and its application in medium design**. Biotechnology and Bioengineering. 43: 1164-1174.

Xie, L. & Wang, D.I.C. (1996a). **Material balance studies on animal cell, metabolism using a stoichiometrically based reaction network**. Biotechnology and Bioengineering. 52: 579-590.

Xie, L. & Wang, D.I.C. (1996b). **Energy metabolism and ATP balance in animal cell cultivation using a stoichiometrically based reaction network**. Biotechnology and Bioengineering. 52: 591-601.

Yamane, Y.I., Higashida, K., Nakashimada, Y., Kakiizono, T. & Nishio, N. (1997). **Influence of oxygen and glucose on primary metabolism and astaxanthin production by *Phaffia rhodozyma* in batch and fed batch cultures: kinetic and stoichiometric analysis**. Applied and Environmental Microbiology. 63: 4471-4478.

Yang, C., Hua, Q., and Shimizu, K. (2002). **Integration of the information from gene expression and metabolic fluxes for the analysis of the regulatory mechanisms in *Synechocystis*.** Applied Microbiology and Biotechnology. 58: 813-822.

Yang, Y., San, K., & Bennet, G.N. (1999b). **Redistribution of metabolic fluxes in *Escherichia coli* with fermentative lactate dehydrogenase overexpression and deletion**. Metabolic Engineering. 1: 141-152.

Yang, Y., Bennet, G.N., & San, K. (1998). **Genetic and Metabolic Engineering**. Process Biotechnology. 1: 3: 1-9.

Yang, Y., Bennet, G.N., & San, K. (1999c). **Effect of inactivation of nuo and ackA-pta on redistribution of metabolic fluxes in *Escherichia coli***. Biotechnology & Bioengineering. 65: 3: 291-297.

Yang, Y. T., Aristidou, A. A., San. K., & Bennett, G.N. (1999a). **Metabolic flux analysis of *E. coli*, deficient in the acetate production pathway and expressing the *Bacillus subtilis* acetolactate synthase**. Metabolic Engineering. 1: 26-34.

Yoshida, T., Tanaka, Y., Mitsunaga, T., and Izumi, Y. (1995). **COASAC-independent phosphoenolpyruvate carboxylase from an obligate methylotroph *Hyphomicrobium methylovorum* GM2 - Purification and characterization.** Bioscience Biotechnology and Biochemistry. 59 (1): 140-142.

Youn, H. (2002). **Sequence analysis functional expression of the structural and regulatory genes for pyruvate dehydrogenase complex from *Streptomyces seoulensis.*** The Journal of Microbiology. 40 (1): 43-50.

Yu"ksel, K.U"., et al. (1994) in **Techniques in Protein** Chemistry V (Crabb, J.W., Ed.) Academic Press, San Diego, CA, 231-240.

Yue, S., Duncan, J.S., Yamamoto, Y., Hutchinson, C.R. (1987) **Macrolide biosynthesis. Tylactone formation involves the possessive addition of three carbon units.** J. Am. Chem. Soc. 109: 1253-1255.

Yüksel, K.Ü., et al. (1995). in **Techniques in Protein** Chemistry VI (Crabb, J.W., Ed.) Academic Press, San Diego, CA, in press.

Zähner, D. and Maas, W.K. (1972). Biosynthesis. *In* H. Zähner and T. Anke (eds.), **Biology of antibiotics**. pp. 34-62. Springer Verlag, New York.

Zähner, H. and Anke, T. (1983). **Evolution of secondary pathways**. *In* J. W. Bennet and E. Ciegler (eds.), Differentiation and secondary metabolism in fungi. pp. 153-171. Marcel Dekker, New York.

Zalacain, M., and Cundliffe, E. (1989). **Methylation of 23S rRNA caused by *tyr*A (*erm*SF), a tylosin resistance determinant from *Streptomyces fradiae*.** Journal of Bacteriology. 171: 4254-4260.

Zalacain, M., and Cundliffe, E. (1991). **Cloning of *tlr*D, a fourth resistance gene, from the tylosin producer, *Streptomyces fradiae*.** Gene. 97: 137-142.

Zeng, A.P., Menzel, K. & Deckwer, W.D. (1996a). **Kinetic, dynamic and pathway studies of glycerol metabolism by *Klebsiella pneumonia* in anaerobic continuous culture: 1 the phenomena and characterization of oscillitation and hysteresis**. Biotechnology and Bioengineering. 52: 549-560.

Zeng, A.P., Menzel, K. & Deckwer, W.D. (1996b). **Kinetic, dynamic and pathway studies of glycerol metabolism by *Klebsiella pneumonia* in anaerobic continuous culture: 2 Analysis of metabolic rates and pathways under oscillation and steady state conditions**. Biotechnology and Engineering. 52: 561-571.

Zerbe-Burkhardt, K., Ratnatilleke, A., Phillipon, N., Birch, A., Leiser, A., Crijbloed, J., Hess, D., Hunziker, P., Robinson, J. (1998) **Cloning, sequencing, expression, and insertional inactivation of the gene for the large subunit of the coenzyme B12-dependent isobutyryl-CoA mutase from *S. cinnamonensis*.** J. Biol. Chem. 273: 6508-6517.

Zhang, J., and Greasham, R. (1999). **Chemically defined media for commercial fermentations.** Applied Microbiology and Biotechnology. 51: 407-421.

Zhang, J., Marcin, C., Shifflet, M.A., Salmon, P., Brix, T., Greasham, R., Buckland, B., and Chartrain, M. (1996). **Development of a defined medium fermentation process for physotigmine production by *Streptomyces griseofuscus***. Applied Microbiology and Biotechnology. 44: 568-575.

Zhang, J., Reddy, J., Salmon, P., Buckland, Gresham, R. (1998). **Process characterization studies to facilitate validation of a recombinant protein fermentation**. In Kelly B, Ramelmeier A (Eds) ACS Symp Ser. 698: 12-27.

Zhang, Y-X, Denoya, C.D., Skinner, D.D., Fedechko, R.W., McArthur, H.A.I., Morgenstern, M.R., Davies, R.A., Lobo, S., Reynolds, K.A., Hutchinson, C.R. (1999) **Gene encoding acyl-CoA dehydrogenase (AcdH) homologues *from S. coelicolor* and *S. avermitilis* provide insights into the metabolism of small branched-chain fatty acids and macrolide antibiotic production.** Microbiology. 145: 2323-2334.

Zhu, Y., Rinzema, A., Tramper, J., & Bol, J. (1996). **Medium design based on stoichiometric analysis of microbial transglutaminase production by *Streptoverticillium mobaraense***. Biotechnology and Bioengineering. 50: 291-298.

Zollner, N., and Kirsch, K. (1962). **Total soluble lipid analysis undertaken by the vanillin assay.** Z. ges. Exp. Med. 135: 545.

Zubay, G.L. (1998). **Biochemistry**. Fourth Edition. McGraw Hill.

Zupke, C., Sinskey, A.J., & Stephanopoulos, G. (1995). **Intracellular flux analysis applied to the effect of dissolved oxygen on hybridomas**. Applied Microbiology and Biotechnology. 44: 27-36.

Zupke, G., and Stephanopoulos, G. (1994). **Modeling of isotope distributions and intracellular fluxes in metabolic networks using atom mapping matrices.** Biotechnology progress. 10: 489-498.

Zwickl, P., Fabry, S., Bogedain, C., Haas, A., and Hensel, R. (1990). **Glyceraldehyde-3-phosphate dehydrogenase from the hyperthermophilic Archaebacterium *Pyrococcus woesei*: characterization of the enzyme, cloning and sequencing of the gene, and expression in *Escherichia coli*.** Journal of Bacteriology. 172:4329-4338.

Appendix A

Case study 1

Elemental balances for cell growth (based on Doran, 1997)

Production of single-cell from hexadecane is described by the following reaction equations:

$$\underset{\text{Carbon source}}{\mathbf{C_wH_xO_yN_z}} + \mathbf{\mathit{a}O_2} + \mathbf{\mathit{b}NH_3} \rightarrow \underset{\text{Biomass}}{\mathbf{\mathit{c}CH_\alpha O_\beta N_\delta}} + \mathbf{\mathit{d}CO_2} + \mathbf{\mathit{e}H_2O} + \underset{\text{Product}}{\mathbf{\mathit{f}C_jH_kO_lN_m}}$$

$$C_{16}H_{34} + aO_2 + bNH_3 \rightarrow cCH_{1.66}O_{0.27}N_{0.20} + dCO_2 + eH_2O$$

If the elemental formula and RQ (see Appendix E for experimental definition) are known then it is possible to solve the stoichiometric coefficients.

Solution

C balance:	$16 = c + d$	**(1)**
H balance:	$34 + 3b = 1.66c + 2e$	**(2)**
O balance:	$2a = 0.27c + 2d + e$	**(3)**
N balance:	$b = 0.20c$	**(4)**
RQ:	$0.43 = d / a$	**(5)**

The solution can be achieved in many different ways; usually it is a good idea to express each variable as a function of only one other variable. b is already written simply as a function of c in (4); then expressing the other variables solely in terms of c. From (1):

$d = 16 - c$ **(6)**

From (5):

$a = d / 0.43 = 2.326d$ **(7)**

Combining (6) and (7) gives an expression for a in terms of c only:

$a = 2.326\ (16 - c)$

$a = 37.22 - 2.326c$ **(8)**

Substituting (4) into (2) gives:

$34 + 3(0.20c) = 1.66c + 2e$

$34 = 1.06c + 2e$
$e = 17 - 0.53c$ **(9)**

substituting (8), (6) and (9) into (3) gives:
$2(37.22 - 2.326c) = 0.27c + 2(16 - c) + (17 - 0.53c)$
$25.44 = 2.39c$
$c = 10.64$

Using this result for c in (8), (4), (6) and (9) gives:
$a = 12.48$
$b = 2.13$
$d = 5.37$
$e = 11.36$

Checking that these coefficient values satisfy equations (1) – (5), the complete reaction equation is:

$C_{16}H_{34} + 12.5\ O_2 + 2.13\ NH_3 \rightarrow 10.6\ CH_{1.66}O_{0.27}N_{0.20} + 5.37\ CO_2 + 11.4\ H_2O$ **(10)**

To normalise to carbon content and biomass to one mole, each element of the equation is divided by the biomass coefficient value:

$0.1\ C_{16}H_{34} + 1.18\ O_2 + 0.20\ NH_3 \rightarrow cCH_{1.66}O_{0.27}N_{0.20} + 0.50\ CO_2 + 1.07\ H_2O$ **(11)**

From this, a stoichiometric yield value (g cells/g substrate) may be calculated;

$$\text{Yield} = 20.70 / (0.1 \times 226) \text{ cells g hexadecane}^{-1}$$
$$= 0.916 \text{ g biomass g hexadecane}^{-1}$$
$$= 207.02 \text{ g biomass mole hexadecane}^{-1}$$

Although elemental balances are useful, the presence of water in, equation (10) causes some problems in practical application. Because water is usually present in great excess and changes in water concentration are inconvenient to measure or experimentally verify, H and O balances can present difficulties. Instead, a useful principle is conversion of reducing power or available electrons, which can be applied to determine quantitative relationships between substrates and products (see Appendix D).

Appendix B

Case Study 2

Metabolic flux analysis of *E. coli* ML 308 growing on glucose as sole carbon source (Holms, 1986, 1996, 1997, 2001)

Holms (1986), probably carried out some of the earliest work with flux analysis, which initially was not readily accepted, by the academic community, but has become fundamental to the construction of a new scientific field (metabolic engineering; Stephanopolous *et al.,* 1998). Which follows a simple logical arithmetic approach. The basis of flux analysis is the organisation of data. In general these are the uptake of feedstock(s) [mmoles.g^{-1} dry wt biomass], biomass growth rate, μ, (per hour), the monomeric composition of biomass (mmoles.g^{-1} dry wt biomass), and other outputs (mmoles.g^{-1} dry wt biomass) such as organic acid excretion, CO_2 evolution, and product excretion (mmoles.g^{-1} dry wt biomass).

The first task is to calculate the outputs to biosynthesis of the monomers in 1 g dry weight biomass (Table 1.1b constructed from data obtained from Neidhardt, 1987 *et al*., 1987 [Table 1.2b]; & Ingraham *et al*., 1983). Biomass uses only a few precursors to maintain flux to many monomers, and it follows that any one precursor is the output from the central metabolic pathways (CMPs) for the biosynthesis of several monomers or, in other words, biosynthetic routes diverge from CMPs. Oxo-glutarate (OGA) is a good example of this (Chapter 2; Section 2.6; Table 2.7) in that it is the precursor not only for glutamate but glutamine, proline, and arginine (Arg) as well. While glutamate is amidated to glutamine in one step, there are four reactions required to convert glutamate to proline and eight to make it into Arg. The flux through each of the eight enzymes on the route to Arg is the same and is defined by the amount of Arg required to make biomass. It then follows that, if you know the amount of Arg that produces 1 g of biomass (which for *E. coli*, is 0.252 mmoles Arg g^{-1} dry wt)[Neidhardt, 1987], therefore 0.252 mmoles of glutamate must be made to supply the Arg for 1 g dry wt biomass. In the

same way, it happens that the proline content of biomass is also 0.252 mmoles and for glutamine is 0.201 mmoles and for glutamate itself is 0.353 mmoles. Thus in order to supply this family of amino acids for 1 g dry wt biomass, a total of 1.058 moles glutamate must be made and, to do this, 1.058 mmoles of OGA must be taken from the CMPs and this number is important to flux analysis.

A second example is pyruvate [PYR] (Chapter 2; Section 2.6; Table 2.7); which is the precursor of alanine, valine, and leucine. Each of these monomers is ultimately made by amination of a keto-acid, and involves amino donors being regenerated by oxidative catabolism, and further reduction, oxidation and dehydration reactions. In this approach these latter reactions can be ignored. What is fundamental is that the monomeric content of the biomass is equivalent to the number of moles of precursor required to produce one mole of monomer (see Table 1.1b & 1.2b; column 2 respectively, metabolic cost). e.g., One mole of alanine requires one mole of PYR; one mole of valine requires two moles of PYR; one mole of leucine requires two moles of PYR, and one mole of AcCoA.

This data can now be collected into Table. 1.2b. Lipid is taken to be phospholipid of C_{16} fatty acids and all the carbohydrates (e.g. sugars and amino sugars of the cell wall) are presumed to be derived from glucose-6-phosphate (G6P) while pentose and tetroses are also taken from this precursor via the Pentose phosphate pathway (PP pathway). Table. 1.2b gives the amount of moles of each precursor required to make the measured amount in mmoles of each monomer ($mmoles.g^{-1}$) and the calculated summation gives the draw of carbon to biosynthesis. Multiplying each calculated summation by the number of carbon atoms contained in the initiating precursor results in the total draw of carbon atoms from the resulting pathway ($C.mmoles.g^{-1}$).

Fig 1.1b & 1.2b represent the pathways to precursors active in *E. coli*, for growth on glucose & OGA (adapted from Holms, 2001). These are then converted to flow chart diagrams (Fig 1.3b & 1.4b). Each conversion of substrate to product is

indicated by an arrow with a box in the middle which will eventually contain the flux of this particular enzymatic conversion. Every output of precursors to biosynthesis is similarly accommodated.

The overall application of the method is most easily described by an example (Fig 1.5b & 1.6b) of the analysis of flux through the CMPs in *E. coli* ML308 growing aerobically on a glucose/salts minimal medium. Only carbon will be considered but it is quite possible to do MFA for nitrogen, phosphate, sulphur, etc. It takes 11.244 mmoles glucose to make 1 g dry weight *E. coli* ML308 at a growth rate of $\mu = 0.94$, under these growth conditions, so the flux of glucose uptake is 10.569 mmoles glucose.g^{-1}.h^{-1}. This is rounded up to 10.57 and the flux to acetate excretion measured as 4.89 mmoles. g^{-1}.h^{-1}. The rest is simple arithmetic (Fig 1.5b). As 1.86 mmoles glucose.g^{-1}.h^{-1} (Table 1.3b; column 4 [G6P]) is used for biosynthesis, 8.71 is left over to go into glycolysis where it is then split in two by aldolase to give triosephosphates (17.42) of which 0.13 is donated to biosynthesis (Table 1.2b; column 3 [TP]) and so on. Of the flux (16.01) arriving at PEP, 0.52 is used directly for biosynthesis (Table 1.2b; column 5 [PEP]), 2.58 ultimately for biosynthesis via PEPC (PEPC is an anaplerotic replenishing route; it then calculated by the addition of the draw to biosynthesis of OAA & OGA; Table 1.2b; column 7 [OAA] & 8 [OGA]) and 10.57 to bring in glucose by PTS with the same flux to PYR. The balance (2.34) phosphorylates ADP to ATP generating another flux to PYR. All that remains are straightforward fluxes to biosynthesis and excretion of acetate while the surplus acetyl CoA, or more properly its equivalent, is oxidised in the Krebs cycle regenerating the oxaloacetate (OAA) used to first make citrate. The final result (Fig 1.6b) is a complete description of the net fluxes through all the metabolic routes of the CMPs from glucose to all the precursors for biosynthesis at μ_{max} (0.94). There is a clear division into two parts with PEP at the crossroads.

It is considered to be more revealing to compare fluxes on the basis of moles of carbon; two approaches can be used to calculate on this basis 1) conversion to

moles of carbon after the construction of Fig 1.6b. 2) Conversion of all the data to moles of carbon from the outset, and then the model is formulated in exactly the same manner (this removes the sequence of aldolase splitting F-1,6-P2 to 2 moles of G3P). CO_2 is calculated by dividing the total number of moles of carbon flowing through a CO_2 evolving or consuming pathway (i.e., PDH, PEPC), by the number of carbon atoms from the proceeding precursor this equals the CO_2 evolved. The CO_2 evolved minus the original value, equals the remaining carbon flowing through the pathway. The flux through PTS equals 50 % of the substrate carbon source (glucose). Such a treatment is shown in Fig 1.7b for *E. coli* ML308 growing on glucose. The differences between both strategies were researched in Chapter 6.

Additional information obtained from the flux diagrams was the amount of CO_2 produced per gram dry weight biomass per hour. CO_2 is evolved by the reactions of PDH, ICDH, MDH(dc), PEPCK, and OGDH. A small amount of CO_2 is also produced during flux from G6P to pentose phosphate in the PP pathway when ribose groups for nucleotides are formed. However, CO_2 is required for carboxylation of PEP in the formation of OAA via PEPC. The effluxes to biomass and CO_2 production were used to compare inputs and outputs of the system, for *E. coli* metabolism by expressing all values in terms of percentage carbon flux in relation to the carbon source input (see Tables 1.3b [sensitivity analysis between mmoles.g^{-1} dry wt biomass h^{-1} and C.mmoles.g^{-1} dry wt biomass h^{-1} as units of measurement], and Chapter 6, Table 6.31 [mmoles.g^{-1} dry wt biomass h^{-1}], & Table 6.32 [C.mmoles.g^{-1} dry wt biomass h^{-1}]. In a glucose minimal medium (Table 6.30), *E. coli* was shown to evolve only 23.1 % of the input carbon as CO_2 (Holms, 1986). When using the units C.mmoles.g^{-1} dry wt biomass h^{-1} in the construction of a flux diagram the proportion of carbon flux to CO_2 was between 24.82 % to 37.14 % the high carbon recovery of 112 % was considered to be due to rounding up of figures and inaccuracies in accounting for the PTS (Table 1.4b).

Flux through the CMPs generates a surplus of 2[H] and ATP and these are used to power biosynthesis of monomers and their subsequent polymerisation. At the same

time, nitrogen, phosphate and sulphur must be taken from the inorganic salts in the medium and processed into forms suitable for incorporation. The intracellular pools of the various cofactors involved in these events remain constant in the steady state of growth maintained in these experiments. How is this achieved? What of the non-carbon fluxes? NH_4 is a good example to illustrate the quite different problems which these entail. The principal routes for NH_4 incorporation are via glutamate and glutamine which are, of course, themselves monomers used in biosynthesis. They both utilise a reductive ammination for NH_4 incorporation (Fig 1.8b taken from Holms, 2001). The amount of OGA and glutamate aminated exceeds the flux from OGA to monomers by approximately 5.5 - fold. More than 80 % of the glutamate and glutamine made are used as amino-donors for the biosynthesis of other monomers (Holms, 1986) and thus regenerate the molecules from which they were made. These are carbon cycles which allow NH_4 incorporation so that, although 5.49 mmoles OGA are aminated, 4.50 mmoles are used as amino donor thus regenerating OGA leaving a net flux of 0.99 mmoles to biosynthesis of monomers which is the net flux of carbon, which appears in the computation of a flux analysis.

How flux analysis was applied to *E. coli* ML308 fermentations is a long but interesting story (see Holms, 2001; for an in depth discussion). One good example of the success of flux analysis is the production of clavulanic acid (made by *S. clavuligerus*) which is a potent inhibitor of penicillinase (Holms, 1986). Originally, this was thought to be made from ornithine but, when flux analysis showed that the fermentation also generated urea, it was realised that the precursor was Arg and this was subsequently proved experimentally (Elson, *et al*., 1993; Valentine & Bailey, 1993).

Table 1.1b Monomeric composition of *Escherichia coli* (From Neidhardt, 1987).

Optimal production of the twelve biosynthetic precursors and the metabolic cofactors.			
Compound	**μmol/g dry wt**	**Compound**	**μmol/g dry wt**
Amino Acids		**Phospholipids**	
Alanine	488	Phosphatidyl serine	2.58
Arginine	281	Phosphatidyl ethanolamine	96.75
Asparagine	229	Phosphatidyl glycerol	23.22
Aspartate	229	Cardiolypin	6.45
Cysteine	87	Fatty acid composition (% of total fatty acid)	
Glutamate	250	Myristic acid (2.68)	
Glutamine	250	Myristoleic acid (7.70)	
Glycine	582	Palmitic acid (38.23)	
Histidine	90	Palmitoleic acid (10.74)	
Isoleucine	276	Heptadecenoic acid (16.11)	
Leucine	428	cis-Vaccenic acid (0.90)	
Lysine	326	Oleic acid (17.91)	
Methionine	146	Nonadecenoic acid (5.73)	
Phenylalanine	176	Cell Wall Structures	
Proline	210	Lipopolysaccharide	8.4
Serine	205	Peptidoglycan	27
Threonine	241	Cofactors and other molecules	
Tryptophan	54	5-Methyl-THF	50
Tyrosine	131	Putrescine	35
Valine	402	Spermidine	7
Protein synthesis/processing (ATP/ Amino Acid)	4.306	NAD	2.15
Ribonucleotides		NADH	0.05
ATP	165	NADP	0.13
GTP	203	NADPH	0.4
CTP	126	UDP-Glucose	3
UTP	136	ATP	4
RNA synthesis/processing (ATP/Nucleotide)	0.4	ADP	2
Deoxyribonucleotides		AMP	1
dATP	24.7	CoA	0.03
dTTP	24.7	Acetyl-CoA	0.04
dGTP	25.4	Succinyl-CoA	0.01
dCTP	25.4	Glycogen	154
DNA synthesis/processing (ATP/Nucleotide)	1.372		

Data for other carbon sources is available online. G6P, glucose-6-phosphate; F6P, fructose-6-phosphate; R5P, ribose-5-phosphate; E4P,erythrose 4-phosphate; T3P1, glyceraldehyde 3-phosphate; 3PG, 3-phosphoglycerate; PEP, phosphoenolpyruvate; PYR, pyruvate; ACCOA, acetyl-CoA; AKG, α-ketoglutarate; SUCCOA, succinyl-CoA; OA, oxaloacetate.

Table 1.2b Amounts of precursors required for the biosynthesis of monomers in *E. coli* ML 308 (from Holms, 1986).

Monomer	Metabolic cost	Monomer content	G6P	TP	PG	PEP	PYR	OAA	OGA	AcCoA
Alanine	**1 PYR**	0.454					0.454			
Arginine	**1 OGA**	0.252							0.252	
Aspartate	**1 OAA**	0.201						0.201		
Asparagine	**1 OAA**	0.101						0.101		
Cysteine	**1 PG**	0.101			0.303					
Glutamate	**1 OGA**	0.353							0.353	
Glutamine	**1 OGA**	0.201							0.201	
Glycine	**1 PG**	0.403			0.403					
Histidine	**1 PEP**	0.05	0.05							
Isoleucine	**1 OAA, 1 PYR**	0.252					0.252	0.252		
Leucine	**2 PYR, 1 ACCOA**	0.403					0.806			0.403
Lysine	**1 PYR, 1 OAA**	0.403					0.403	0.403		
Methionine	**1 OAA**	0.201					-0.201	0.201		
phenyalanine	**2 PEP, 1G6P**	0.151	0.151			0.302				
Proline	**1 OGA**	0.252							0.252	
Serine	**1 PG**	0.302			0.302					
Threonine	**1 OAA**	0.252						0.252		
Trytophan	**1 PEP, 1 G6P, 1 PEP**	0.05	0.1		0.05	0.05				
Tyrosine	**2 PEP, 1 G6P,**	0.101	0.101			0.202				
Valine	**2 PYR**	0.302					0.604			
A	**1 PG, 1 PEP**	0.115	0.115		0.115					
DA	**1 PG, 1 PEP**	0.024	0.024		0.024					
G	**1 PG, 1 PEP**	0.115	0.115		0.115					
DG	**1 PG, 1 PEP**	0.024	0.024		0.024					
C	**1 OAA, 1 PEP**	0.115	0.115					0.115		
DC	**1 OAA, 1 PEP**	0.024	0.024					0.024		
U	**1 OAA, 1 PEP**	0.115	0.115					0.115		
DT	**1 OAA, 1 PEP**	0.024	0.024					0.024		
C16 FA	**8 ACCOA**	0.28								2.24
Glucero-phosphate	**1 G6P**	0.14		0.14						
Carbohydrate	**1 G6P**	1.026	1.026							
Total mmoles.g^{-1}			**1.984**	**0.14**	**1.336**	**0.554**	**2.318**	**1.688**	**1.058**	**2.643**
Total C-mmoles.g^{-1}			**11.90**	**0.42**	**4.008**	**1.662**	**6.954**	**6.752**	**5.290**	**5.286**

All numbers are mol/kg dry weight biomass. G6P, glucose-6-phosphate; TP, triose-phosphate; PG, phosphoglycerate; PEP, phosphoenolpyruvate; PYR, pyruvate; OAA, oxaloacetate; OGA, oxo-glutarate; ACCOA, acetyl-coenzyme A.

Table 1.3b Flux of carbon from the central pathways to biosynthesis, acetate, and CO_2 during growth of *E. coli* ML 308 on glucose in batch culture.

***E. coli* ML308**				
Glucose minimal medium				
	mM g dry wt biomass[a]	**%**	**C.mM g dry wt biomass[b]**	**%**
Input	**63.42**		**63.42**	
Output				
G6P	9.3	14.66	9.3	14.66
TP	0.39	0.61	0.39	0.61
PG	3.84	6.05	3.84	6.05
PEP	1.56	2.46	1.56	2.46
PYR	6.95	10.96	6.95	10.96
AcCoA	4.96	7.82	4.96	7.82
OAA	4.95	7.80	4.95	7.80
OGA	6.36	10.03	6.36	10.03
Net CO2	15.74	24.82	23.56	37.14
AcCoA	9.78	15.42	9.78	15.42
Carbon to biosynthesis		**60.41**		**60.41**
Carbon recovered[a]		**100.65**		**112.98**

The recovery of carbon exceeds 100 % from rounding up of figures and because the flux from G6P includes that to pentose phosphate (which involves a loss of CO_2) which is also included in the net CO_2 evolved. [a]Calculated by Holms (1986). [b]The method designed for this work.

Pathways to precursors of monomers during growth on glucose

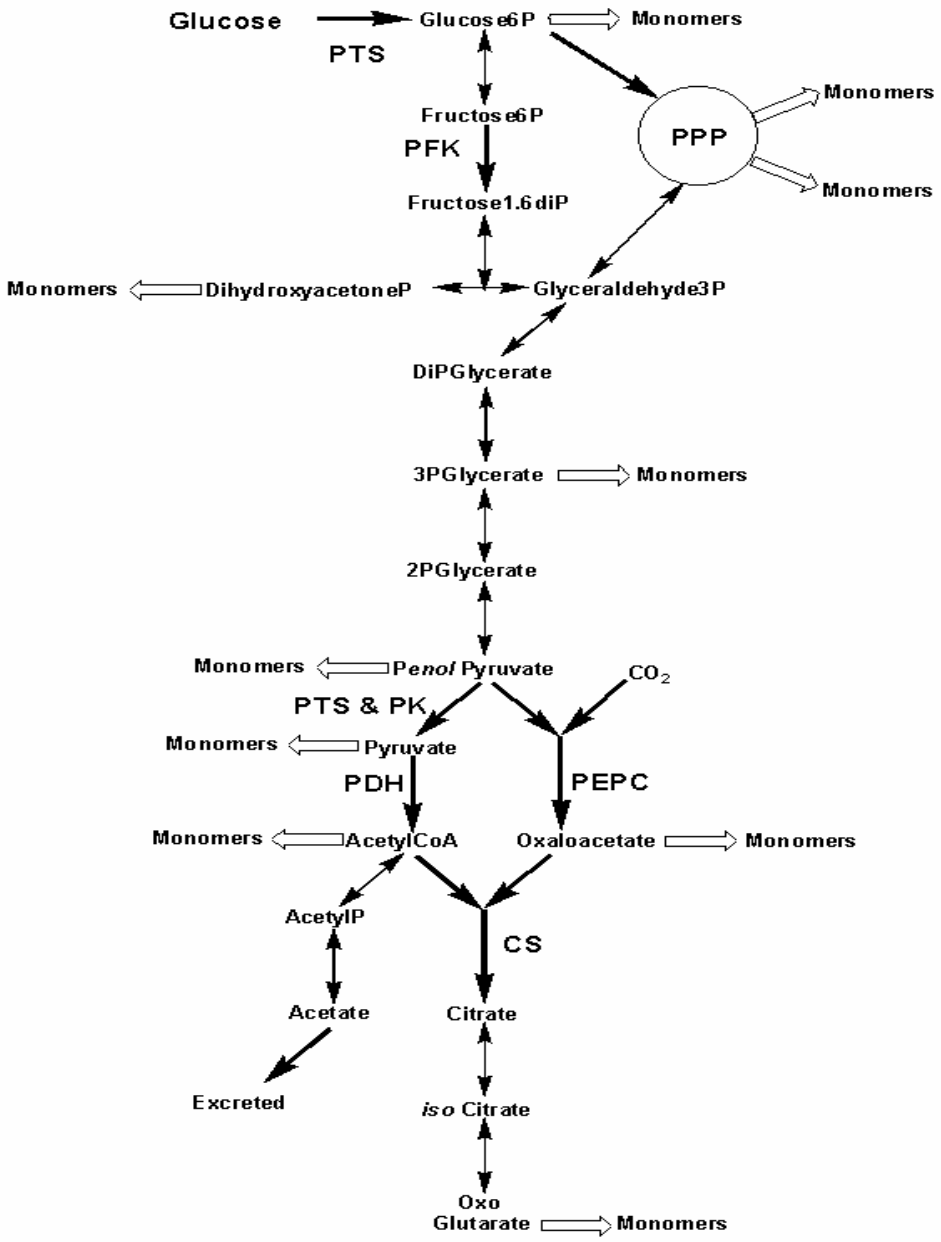

Fig 1.1b Routes to monomers from glucose (adapted from Holms, 2001).

Pathways to precursors of monomers during growth on oxo-glutarate

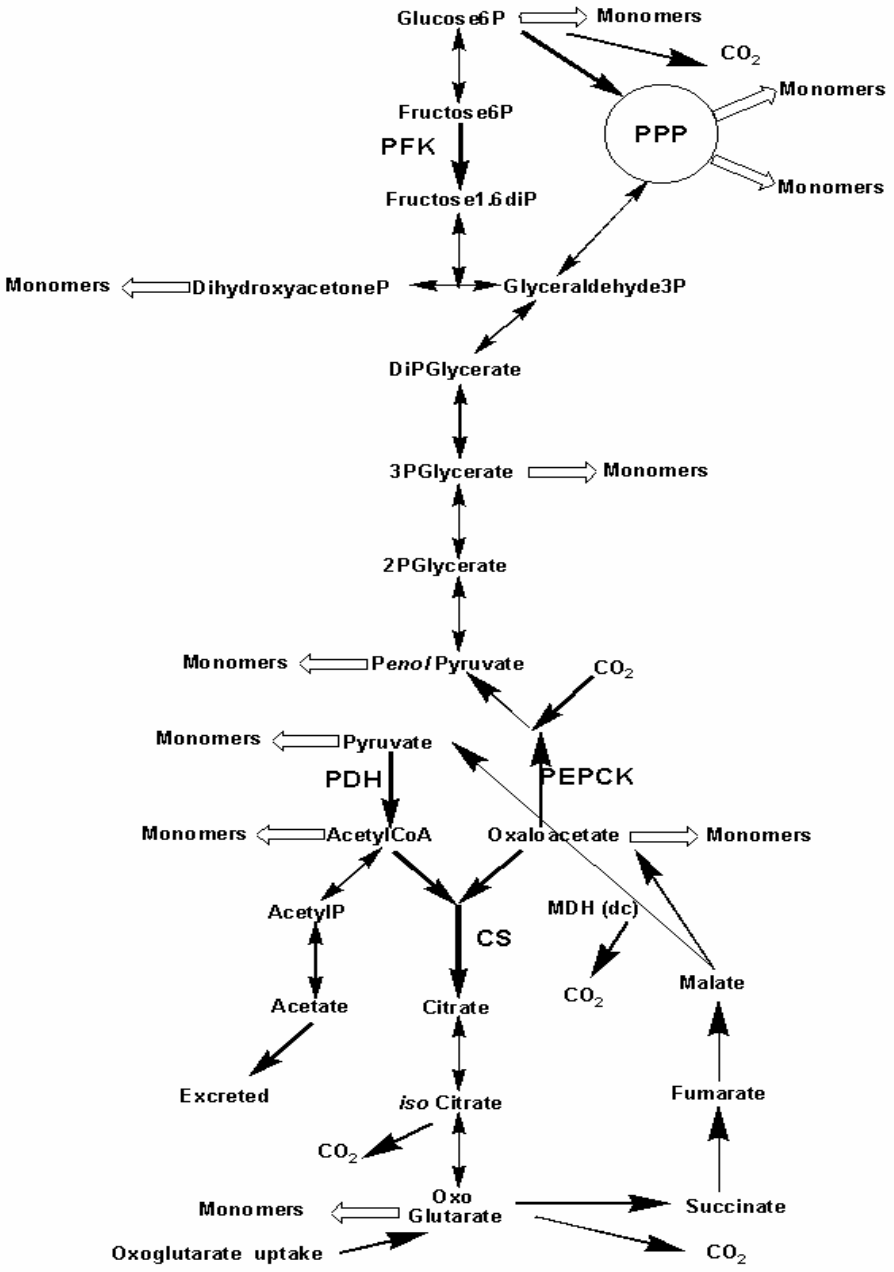

Fig 1.2b Routes to monomers from oxo-glutarate (adapted from Holms, 2001).

Flux diagram for growth on glucose

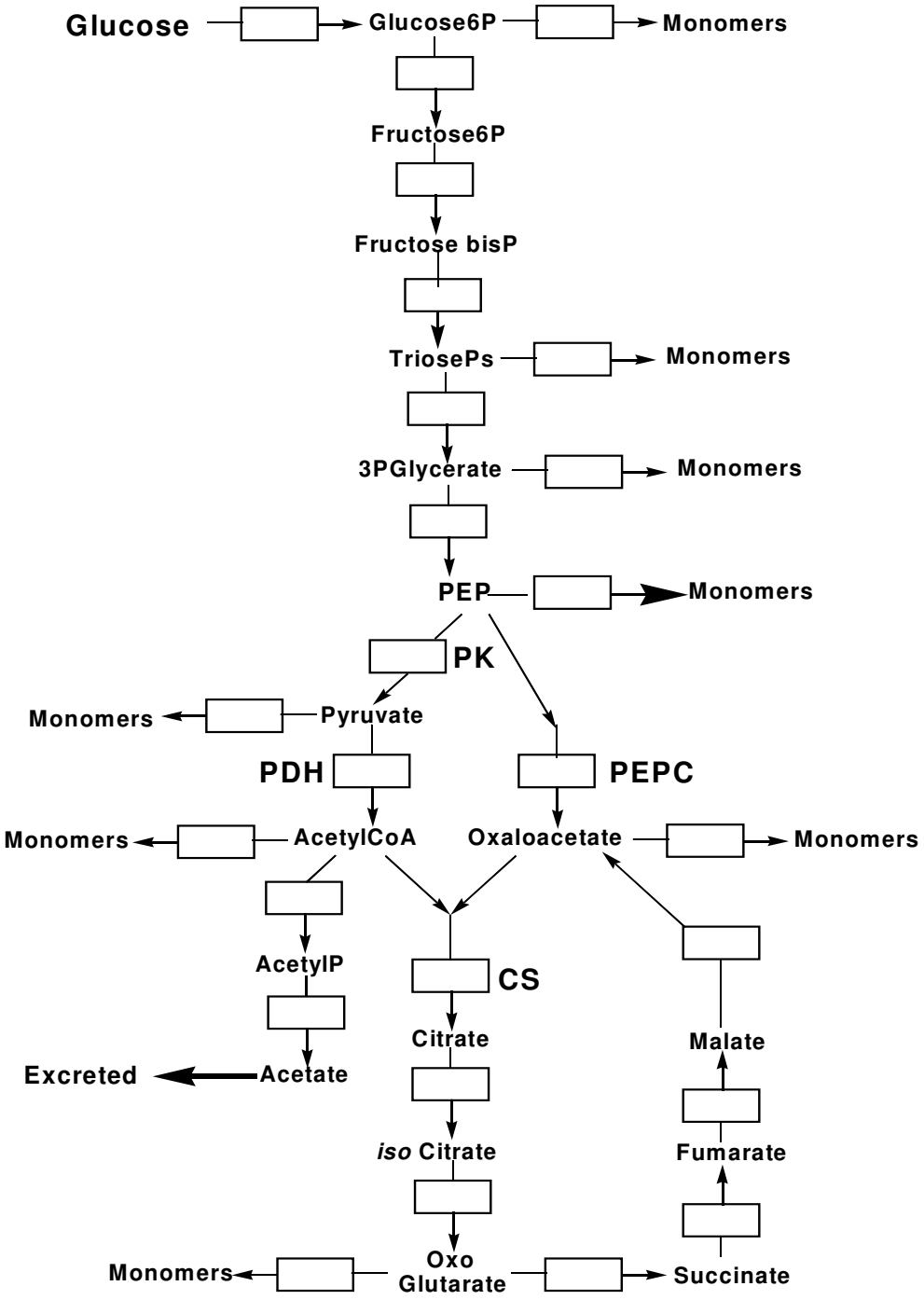

Fig 1.3b Routes to monomers from glucose (adapted from Holms, 2001).

Flux diagram for growth on Oxo-glutarate

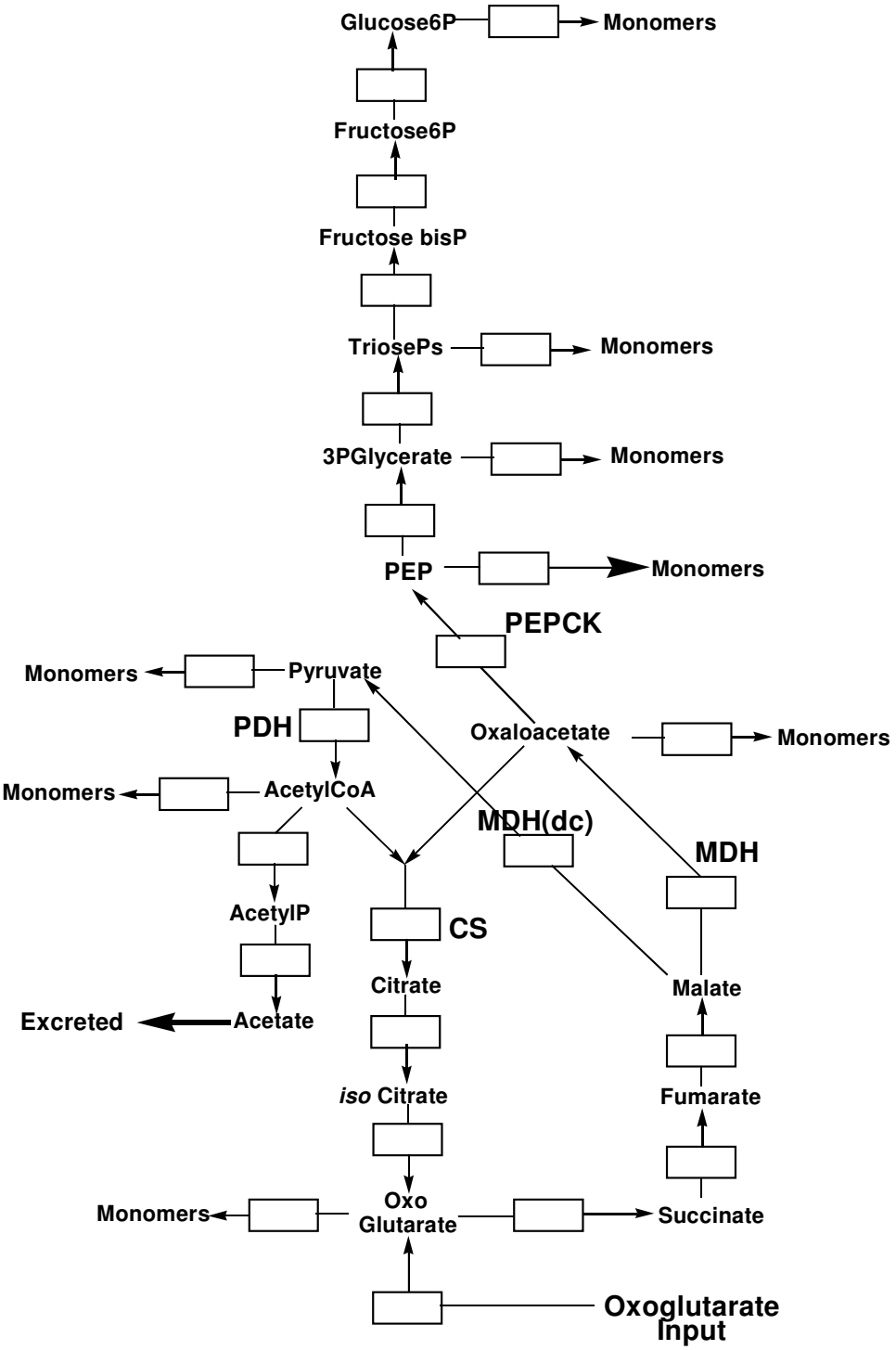

Fig 1.4b Routes to monomers from oxo-glutarate (adapted from Holms, 2001).

Flux diagram for growth on glucose of *E.coli* ML308 showing those fluxes directly derived from measured data (mmoles.g^{-1} dry wt.h^{-1}).

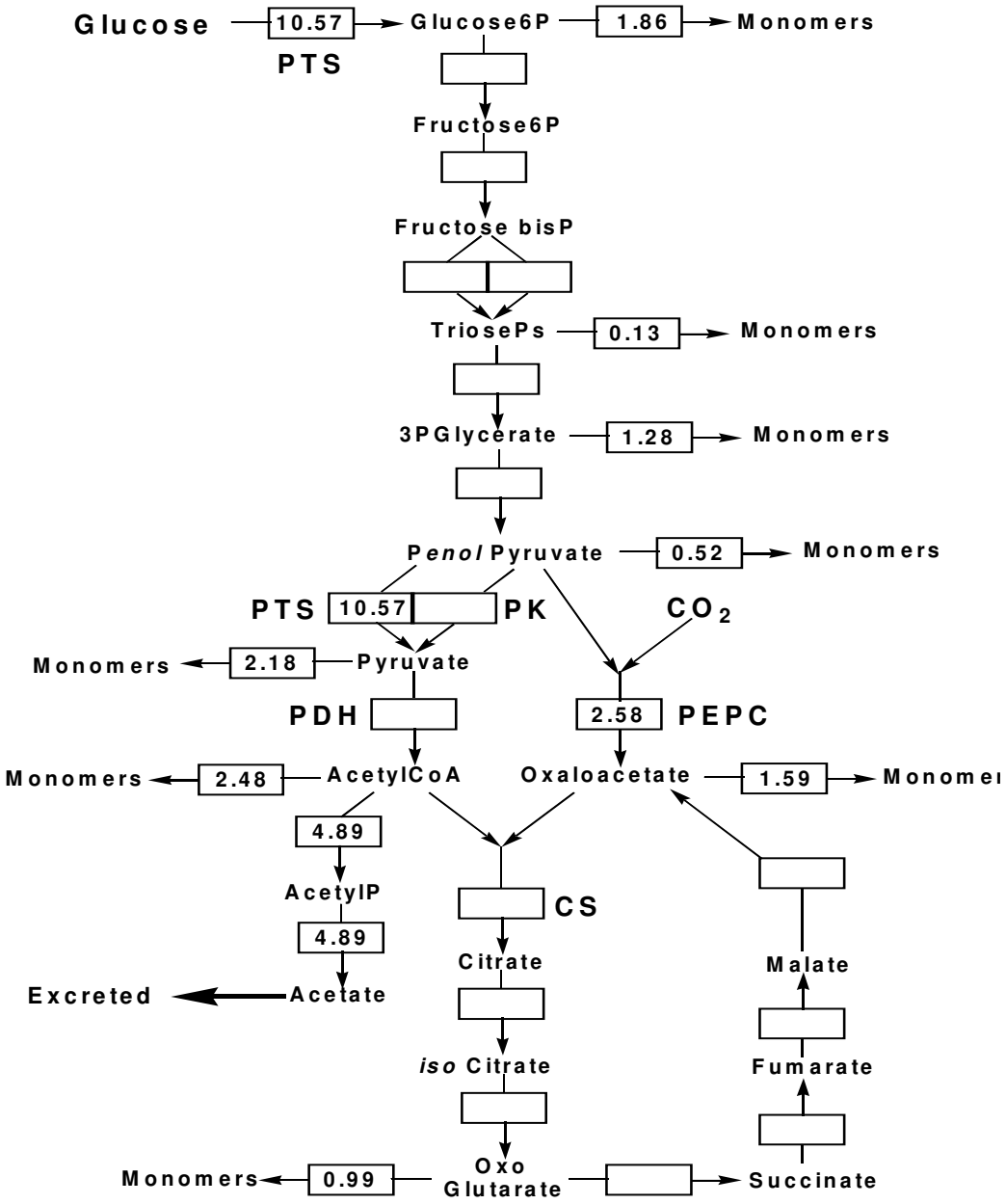

Fig 1.5b Input and outputs of the CMPs during growth on glucose (taken from Holms, 2001).

Flux diagram for growth on oxo-glutarate complete flux analysis of growth of *E. coli* ML308 (mmoles.g^{-1} dry wt.h^{-1}).

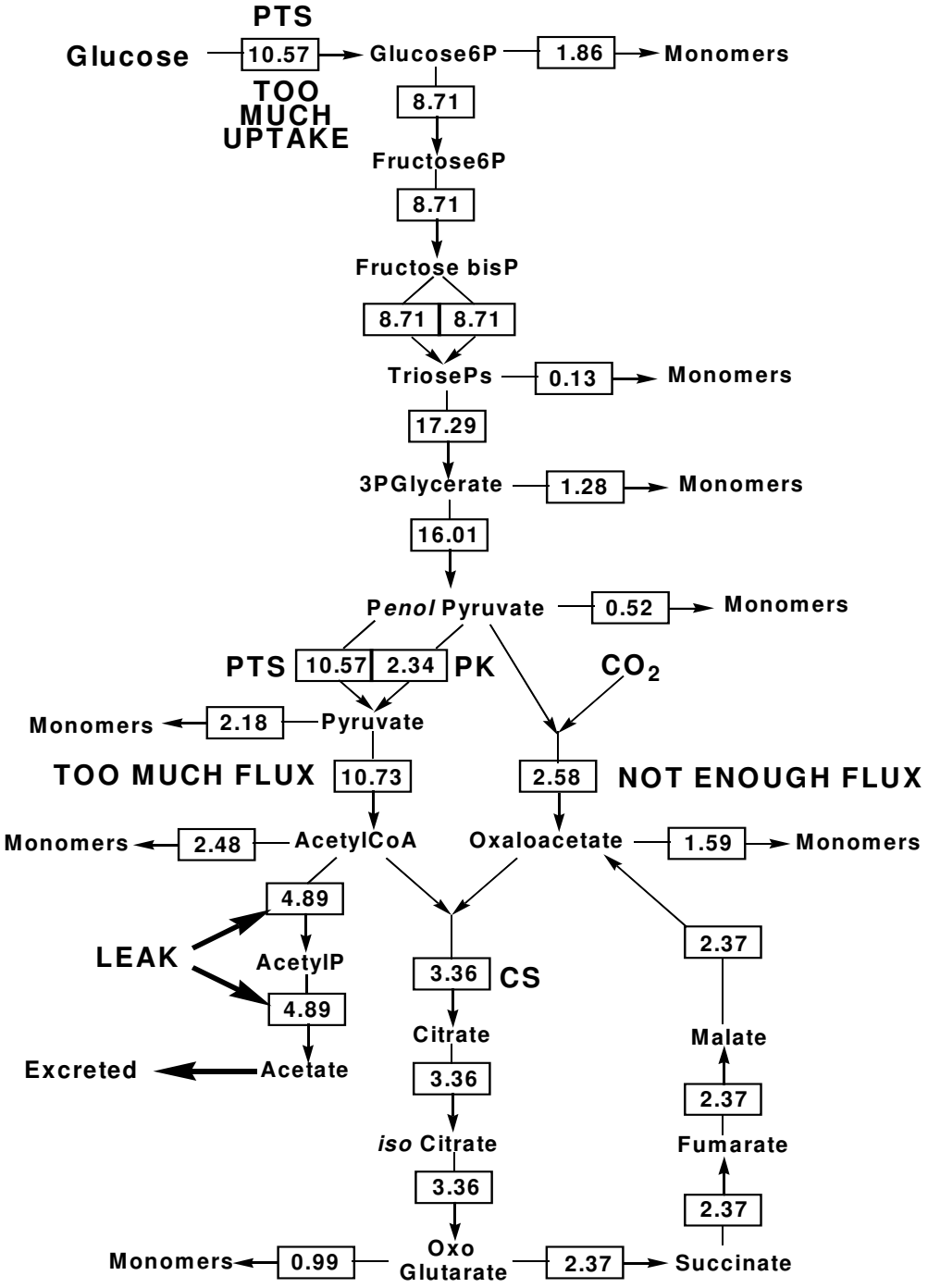

Fig 1.6b Flux diagram of growth on glucose (taken from Holms, 2001).

Complete flux analysis of growth of *E. coli* ML308 on glucose. Fluxes are C.mmoles.g^{-1} dry wt / h.

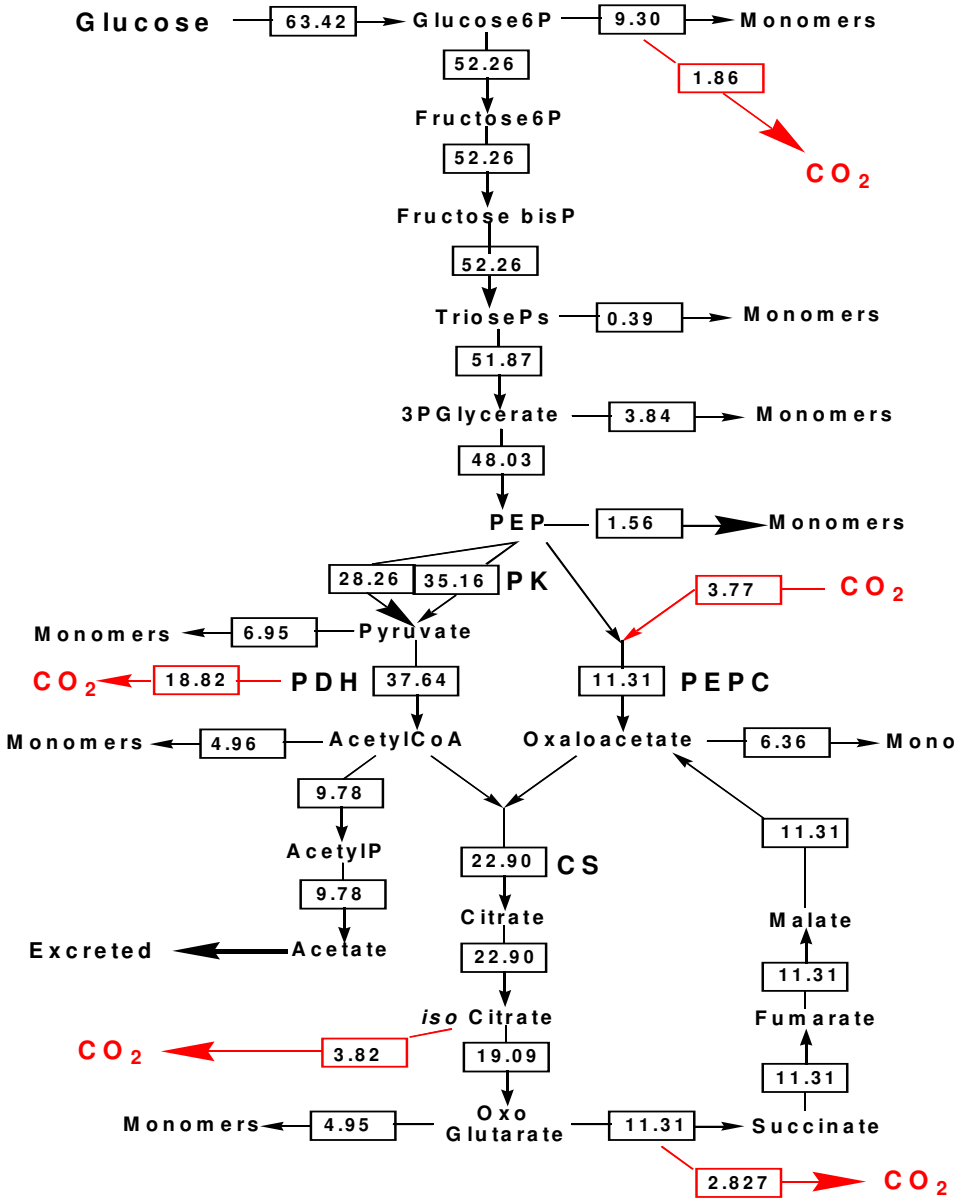

Fig 1.7b All figures are converted to moles of carbon before the construction of the flux diagram and then formulated in exactly the same manner as Holms (1986)[this removes the sequence of aldolase splitting FDP to 2 moles of G3P]. CO_2 is calculated by dividing the total moles of carbon flowing through a CO_2 evolving or consuming pathway (PDH, PEPC) by the number of carbons from the metabolite of interest this equals the CO_2 evolved. The CO_2 evolved minus the original value, equals the remaining carbon flowing through the pathway etc. The summation of equals the flow of carbon to CO_2. The flux through PTS is equals 50 % of the substrate carbon source (glucose).

Throughputs for monomers derived from oxo-glutarate and provision of amino donors to other reactions (moles / g dry wt biomass) in *E. coli* ML308.

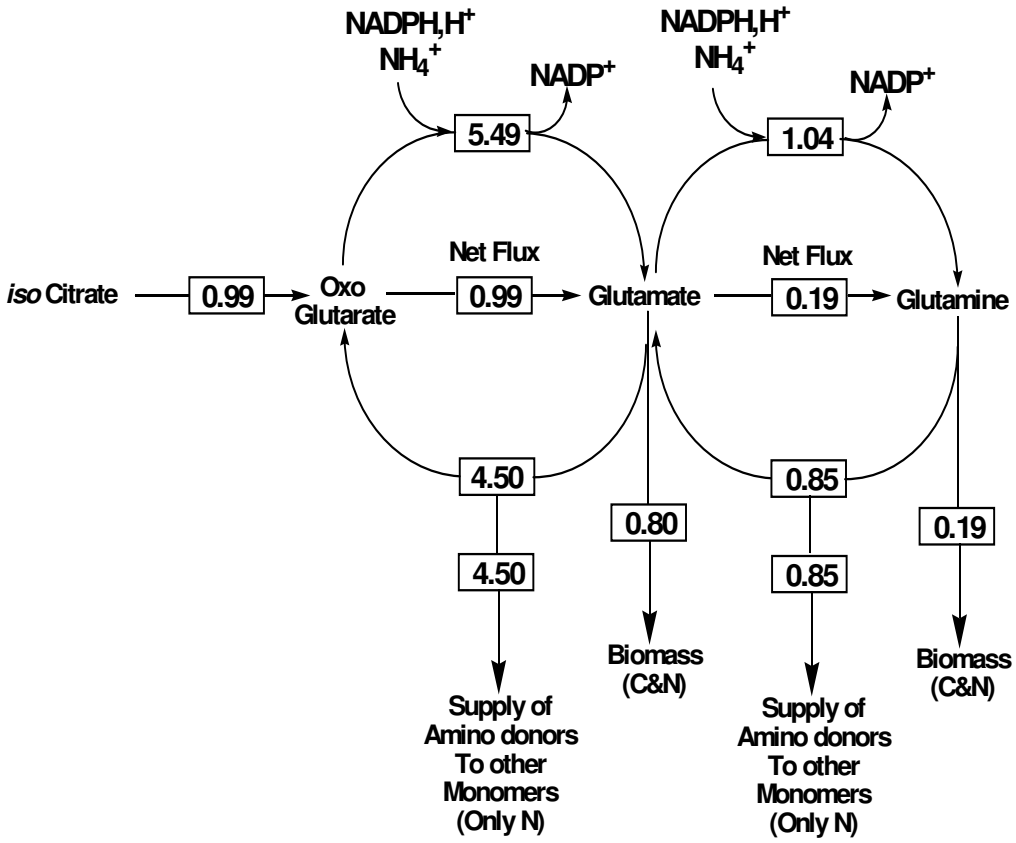

Fig 1.8b Flux of nitrogen to monomers during growth on glucose (taken from Holms, 20001).

Appendix C

Case Study 3

Metabolic flux analysis of citric acid fermentation by *Candida lipolytica* (Aiba & Matsuoka, 1979; Stephanopoulos *et al*., 1998)

To illustrate the concept of metabolic flux analysis utilising matrix algebra, one of the first examples in this area was the study of *C. lipolytica* producing citric acid carried out by Aiba and Matsuoka (1979) (see Stephanopoulos *et al*., 1998; for a good review of this work). Aiba & Matsuoka employed the simplified metabolic network shown in Fig 1.1c, which includes the EMP pathway, the TCA cycle, the glyoxylate shunt, PYR carboxylation, and the formation of the major macromolecular pools, i.e., proteins, carbohydrates, and lipids. The anaplerotic routes are necessary to replenish TCA cycle intermediates when citrate and isocitrate are secreted to the extracellular medium. The introduction of secretion reactions (indicated by the dotted lines Fig 1.1c) allows the application of the *pseudo*-steady state (PSS) assumption for all pathway intermediates. Carbon dioxide participates in several reactions, and it is therefore included as an extra-cellular compound that is secreted with a rate v_{16}. A balance therefore may also be introduced around this compound. With this structured model, some of the fluxes can be measured directly.

The stoichiometry of the individual reactions is quite simple because, except for the conversion of glucose to PYR, all stoichiometric coefficients are 1 or –1. By applying the PSS assumption to all branch points in the network (Fig 1.1c), it is possible to derive equations (1) - (11) for the individual reaction rates eq (1). All rates are given in moles per gram dry weight per hour of the compound formed in the reaction.

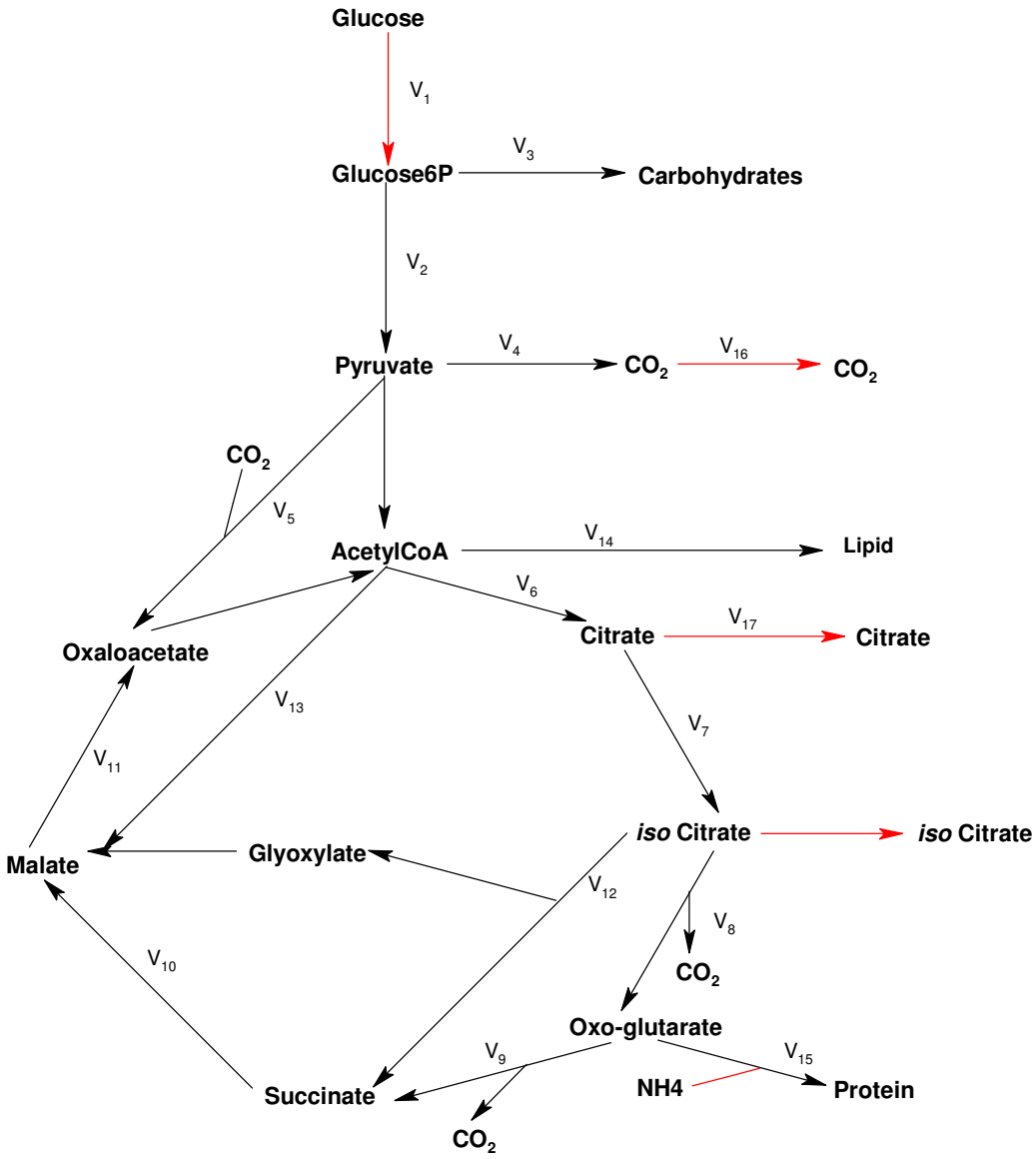

Fig 1.1c Simplified metabolic network for *C. lipolytica*. Abbreviations: G6P, glucose-6-phosphate; PYR, pyruvate; ACCOA, acetyl-CoA; OAA, oxaloacetate; CIT, citrate; ICT, Isocitrate; OGT, oxo-glutarate; SUC, succinate; MAL, malate; GOX, glyoxylate. Broken lines represent transport reactions, whereas solid lines represent intracellular reactions.

With 18 reaction rates and 11 balance equations, there are 7 degrees of freedom. Thus, if 7 reaction rates are measured, the other rates can be calculated. In their analysis, Aiba & Matsuoka (1979) measured six reaction rates in the network: the

glucose uptake rate (r_{glc} = V1); the carbon dioxide production rate (r_c = V16); the citric acid production rate (r_{cit} = V17); the extracellular isocitrate production rate (r_{ISCIT} = V18); the protein synthesis rate (r_{prot} = V15); and the carbohydrate synthesis rate (r_{car} = V3). The rates r_{prot} and r_{car} were found from measurements of the protein and carbohydrate contents, respectively, of the biomass (in a steady state chemostat). In addition to the six measurements, Aiba & Matsuoka (1979) imposed a constraint by setting one of the rates in the network equal to zero. Three different cases were examined, reflecting three different models of citric acid biochemistry:

Model 1: The glyoxylate shunt is inactive, i.e., V12 = 0

Model 2: Pyruvate carboxylase is inactive, i.e., V5 = 0

Model 3: The TCA cycle is incomplete, i.e., V9 = 0

With the proceeding six measured rates (r), the system of equations is determined exactly for each of these models and can be solved to determine the unknown reaction rates. This can be done by sequential elimination of the unknown rates, e.g.,

(1) $\mathbf{V2 = 2(r_{glc} - r_{car})}$

A more general approach is to use matrix algebra calculations. The following material illustrates how the unknown fluxes are calculated in the case of model 1. For this purpose, we first rewrite equations (1) - (11) in matrix notation using the stoichiometric matrix G (Chapter 1; Section 1.2.2; Fig 1.2c):

Fig 1.2c

$$\begin{bmatrix} V1 - 0.5V2 - V3 \\ V2 - V4 - V5 \\ V4 - V6 - V13 - V14 \\ V6 - V7 - V17 \\ V7 - V8 - V12 - V18 \\ V8 - V9 - V15 \\ V9 - V10 + V12 \\ V10 - V11 + V13 \\ V12 - V13 \\ V5 + V11 - V6 \\ V4 - V5 + V8 + V9 - V16 \end{bmatrix} =$$

Reaction rates

Balance equations	V1	V2	V3	V4	V5	V6	V7	V8	V9	V10	V11	V12	V13	V14	V15	V16	V17	V18
(1) G6P	1	-0.5	-1	0	0	0	0	0	0	0	0	0	0	0	0	0	0	0
(2) PYR	0	1	0	-1	-1	0	0	0	0	0	0	0	0	0	0	0	0	0
(3) AcCoA	0	0	0	1	0	-1	0	0	0	0	0	0	-1	-1	0	0	0	0
(4) CIT	0	0	0	0	0	1	-1	0	0	0	0	0	0	0	0	0	-1	0
(5) ISOCIT	0	0	0	0	0	0	1	-1	0	0	0	-1	0	0	0	0	0	-1
(6) OGA	0	0	0	0	0	0	0	1	-1	0	0	0	0	0	-1	0	0	0
(7) SUC	0	0	0	0	0	0	0	0	1	-1	0	1	0	0	0	0	0	0
(8) MAL	0	0	0	0	0	0	0	0	0	1	-1	0	1	0	0	0	0	0
(9) GOX	0	0	0	0	0	0	0	0	0	0	1	-1	0	0	0	0	0	0
(10) OAA	0	0	0	0	1	-1	0	0	0	0	1	0	0	0	0	0	0	0
(11) CO2	0	0	0	1	-1	0	0	1	1	0	0	0	0	0	0	-1	0	0

v

Note that reaction 13 could have been eliminated as the pseudo-steady state assumption for glyoxylate implies that the rate of this reaction is equal to V12.

When rates V1, V2, V3, V16, and V17 are measured (indicated by the corresponding subscribed r variables) and there was no isocitrate secretion (V18 = 0), for the case of model 1 V12 was set to zero and columns 1, 3, 12, 15, 16, 17 and 18 were collected in the matrix G_m (measured), whereas the remaining columns were collected in matrix G_c (non-measured) i.e., as equation $v_c = -(G^T_c)^{-1} G^T_m v_m$ (Chapter 1; Section 1.2.2; Fig 1.3c):

Fig 1.3c

Non-measured

	V2	V4	V5	V6	V7	V8	V9	V10	V11	V13	V14
G6P	0.5	0	0	0	0	0	0	0	0	0	0
PYR	1	-1	-1	0	0	0	0	0	0	0	0
AcCoA	0	1	0	-1	0	0	0	0	0	-1	-1
CIT	0	0	0	1	-1	0	0	0	0	0	0
ISOCIT	0	0	0	0	1	-1	0	0	0	0	0
OGA	0	0	0	0	0	1	-1	0	0	0	0
SUC	0	0	0	0	0	0	1	-1	0	0	0
MAL	0	0	0	0	0	0	0	1	-1	1	0
GOX	0	0	0	0	0	0	0	0	1	0	0
OAA	0	0	1	-1	0	0	0	0	1	0	0
CO2	0	1	-1	0	0	1	1	0	0	0	0

$^{-1}$ ×

Measured

	V1 (r_{glc})	V3 (r_{car})	V12 (0)	V15 (r_{prot})	V16 (r_c)	V17 (r_{cit})	V18 (r_{ict})
G6P	1	-1	0	0	0	0	0
PYR	0	0	0	0	0	0	0
AcCoA	0	0	0	0	0	0	0
CIT	0	0	0	0	0	-1	0
ISOCIT	0	0	-1	0	0	0	-1
OGA	0	0	0	-1	0	0	0
SUC	0	0	1	0	0	0	0
MAL	0	0	0	0	0	0	0
GOX	0	0	-1	0	0	0	0
OAA	0	0	0	0	0	0	0
CO2	0	0	0	0	-1	0	0

The complexity of the solution, i.e., the intracellular fluxes are functions of almost all the measured rates. In such cases, solution of the algebraic equations by Gaussian elimination may be quite cumbersome, whereas the matrix equation is easily solved using computer programs like Mathematica, Mable, or Matlab. By calculating the unknown rates (or fluxes) at different dilution rates in a steady state chemostat, i.e., for different sets of measured rates, Aiba & Matsuoka (1979), concluded that model 1 describes reasonable values for the fluxes. Furthermore, *in vitro* measurements of the activity of four different enzymes (pyruvate carboxylase, citrate synthase, isocitrate dehydrogenase, and isocitrate lyase) correlated fairly well with the calculated fluxes. When the two other models were tested, it was found that some of the fluxes were negative, e.g., model 2 predicts that OGA is converted to isocitrate. This is not impossible, but most, unlikely, most reactions are favoured thermodymically in the direction specified by the arrows in (Fig 1.1b). Thus, the ΔG^0 for the conversion of isocitrate to OGA is –20.9 KJ $(mol)^{-1}$, and a large concentration of OGA to isocitrate would be required to allow this reaction to run in the opposite direction. Furthermore, there is better agreement between the measured enzyme activities and flux predictions by using model 1 than with the two other models. Aiba and Matsuoka (1979), therefore concluded that glyoxylate is inactive or operates at a very low rate in *C. lipolytica* under citric acid production conditions.

Appendix D

Electron balances (Roels, 1983)

Available electrons

Refers to the number of electrons available for transfer to oxygen on combustion of a substrate to CO_2, H_2O and nitrogen (N) containing compounds. The number of available electrons found in organic material is calculated from the valence of various elements: 4 for C, 1 for H, -2 for O, 5 for P, and 6 for S. The number of available electrons for N depends on the reference state: -3 if ammonia is the reference, 0 for molecular nitrogen N_2, and 5 for nitrate. The reference state for cell growth is usually chosen to be the same as the nitrogen source; this can easily be changed if other nitrogen sources are employed (Roels, 1983).

Degree of reduction (γ)

γ is defined as the number of equivalents of available electrons in that quantity of material containing 1 g atom of carbon. Therefore, for substrate $C_wH_xO_yN_z$, the number of available electrons is $(4w + x - 2y - 3z)$. The degree of reduction for the substrate, γ, is therefore $(4w + x - 2y - 3z)/w$. Degrees of reduction relative to NH_3 and nitrate for various substrates is given in Doran (1997).

The maximum possible yield can be calculated from the γ of the product (γ_p), organism (γ_B), the substrate (γ_s) and the elemental balance, and the fractional allocation of available electrons in the substrate can be written as:

(1) $1 = 4a/w\gamma_s + c\gamma_B/ w\gamma_s + fj\gamma_p/ w\gamma_s$ (equations relates to Chapter 1, section 1.2 & Appendix A) [Doran, 1997]

The first term on the right-hand side is the fraction of available electrons transferred from the substrate to oxygen, the second term is the fraction of available electrons transferred to biomass, and the third term is the fraction of available electrons transferred to product. This relationship can be used to obtain upper bounds for the yields of biomass and product

from substrate (2). ζ_B is used to define the available electrons in the substrate transferred to biomass:

(2) $\zeta_B = c\gamma_B / w\gamma_s$ [Doran, 1997]

In the absence of product formation, if all available electrons were used for biomass synthesis, ζ_B would equal zero. Under these conditions, the maximum value of the stoichiometric coefficient *c* (equation relates to Chapter 1, section 1.2) is:

(3) $c_{max} = w\gamma_s/\gamma_B$(molecular biomass /molecular weight of substrate) [Doran, 1997]

Oxygen demand is another important parameter that is related directly to the electrons available for transfer to O_2; the O_2 demand can therefore be derived from an appropriate electron balance (4).

(4) a = ¼ ($w\gamma_s + c\gamma_B - fj\gamma_p$) [equations relates to Chapter 1, section 1.2 & Appendix A] {Doran, 1997}

The equations 5 & 6 can also be used to calculate the O_2 demand of an organism:

(5) (A/Y) - B = C [taken from Stanbury *et al*., 2000]

Where A = the amount of O_2 for combustion of 1 g of substrate to CO_2, H_2O And NH_3, if N is present in the substrate; B = the amount of O_2 required for the combustion of 1 g cells to CO_2, H_2O And NH_3; Y = the cell yield (g cells g^{-1} substrate); and C = g O_2 consumed for the production of 1 g of cells.

(6) Y_0 = {(C + H - O)/YM} - 1.58 [taken from Stanbury *et al*., 2000]

Where Y_0 = the g O_2 consumed g^{-1} cell produced; Y = the cell yield (g cells g^{-1} substrate); M = the molecular weight of the carbon source; and C, H, and O = the number of atoms of C, H and O per molecule of C substrate.

Appendix E

On-line data analysis (calculations taken from Barry Buckland [1985]).

Calculation 1 Carbon dioxide concentration (CDC) [% CO_2]

$$CDC = \frac{\text{Ea (\%CO2)} \times \text{Ia (\%N2)} - \text{Ia (\% CO2)}}{\text{Ea (\%N2)}}$$

Where Ia is incoming air and Ea is exhaust air. Nitrogen is assumed to be inert. Because the water vapour concentration changes between inlet and outlet, and because the mass spectrometer automatically sum all measured parameters to 100 %, it is necessary to correct for these changes using an inert gas (argon can also be used). The % CO_2 in the inlet air is consistently low. The computer occasionally receives a signal of less than zero; because this causes it to abort the calculation, the subtraction of % CO_2 in the inlet can be omitted.

Calculation 2 Oxygen concentration (XC) [% O_2]

$$XC = \frac{\text{Ia (\% O2)} - \text{Ea (\% O2)} \times \text{Ia (\% N2)}}{\text{Ea (\% N2)}}$$

Calculation 3 Respiratory Quotient (RQ)

$$RQ = \frac{\text{CDC}}{\text{XC}} = \frac{\text{CO2 evolved}}{\text{O2 consumed}}$$

Interpreting RQs – the complete oxidation of carbohydrates should give values close to 1.0 in agreement with calculation 3, while the oxidation of fats will give values close to 0.7 and protein oxidation will produce values of about 0.8 (Reed *et al*., 1998).

Calculation 4 Carbon dioxide evolution rate (CER)

$$CER = \frac{\text{CDC} \times \text{air flow rate*} \times \text{constant}}{\text{Liquid volume**}}$$

*Measured on-line using a mass flow meter (incoming air) [$L.min^{-1}$]

**Measured on-line using a DP (differential pressure) cell (L)

Calculation 5 Oxygen uptake rate (OUR)

$$OUR = \frac{\text{XC} \times \text{air flow rate} \times \text{constant}}{\text{Liquid volume}} \qquad (mmoles.L.h^{-1})$$

Appendix F

The expression of macromolecules in terms of carbon content (adapted from Davidson, 1992)

CHO carbon

(1) μg CHO.ml^{-1} × 0.4 (No of carbon atoms × the atomic mass / the molecular weight) = ppmC (μg.ml^{-1})

Assuming CHO (measured as glucose equivalents) has a molecular weight of 180 with an average of 6 carbon atoms per molecule.

Protein carbon

(2) μg protein.ml^{-1} × 0.5 = ppmC (μg.ml^{-1})

Assuming each amino acid has an average molecular weight of 120 with 5 carbon atoms per molecule.

RNA carbon

(3) μg RNA.ml^{-1} / 340 = μmoleRNA.ml^{-1}

μmoleRNA.ml^{-1} × 0.218 = μmole AMP.ml^{-1}
× 0.192 = μmole UMP.ml^{-1}
× 0.329 = μmole GMP.ml^{-1}
× 0.263 = μmole CMP.ml^{-1}

Assuming RNA is composed of 21.8 % A, 19.2 % U, 32.9 % G and 26.3 % C (see appendix H).

+ μmole AMP.ml^{-1} × 10
+ μmole UMP.ml^{-1} × 9
+ μmole GMP.ml^{-1} × 10

$+ \mu mole\ CMP.ml^{-1} \times 9 = total\ \mu mole.ml^{-1}$

$total\ \mu mole.ml^{-1}C \times 12 = \mu gC.ml^{-1}$ (ppm).

DNA carbon

(4) $\mu g\ DNA.ml^{-1} / 324 = \mu moleDNA.ml^{-1}$

$\mu moleDNA.ml^{-1} \times 0.15 = \mu mole\ AMP.ml^{-1}$

$\times 0.15 = \mu mole\ TMP.ml^{-1}$

$\times 0.35 = \mu mole\ GMP.ml^{-1}$

$\times 0.35 = \mu mole\ CMP.ml^{-1}$

Assuming *Streptomyces* DNA contains 70 % GC mol.

$+ \mu mole\ AMP.ml^{-1} \times 10$

$+ \mu mole\ TMP.ml^{-1} \times 9$

$+ \mu mole\ GMP.ml^{-1} \times 10$

$+ \mu mole\ CMP.ml^{-1} \times 9 = total\ \mu mole.ml^{-1}$

$total\ \mu mole.ml^{-1}C \times 12 = \mu gC.ml^{-1}$ (ppm).

Lipid carbon

(5) $\mu g\ Lipid.ml^{-1} \times 0.75 = \mu gC.ml^{-1}$ (ppm)

Assuming lipid (measured as oleic acid equivalents) has an average molecular weight of 255 with an average of 16 carbon atoms per molecule.

Appendix G

Fatty acid composition of *S. lividans* for use in precursor tables of *S. coelicolor* 1147& *S. fradiae* C373-10

Calculation taken from Davidson (1992)

The lipid composition of *E. coli* (Neidhardt, 1987) was calculated on the basis of an average C_{16} fatty acid (Table 1.1g & 1.2g). This calculation was also used to determine the fatty acid composition of *S. coelicolor* 1147 & *S. fradiae* C373-10. According to Grafe *et al.* (1986), *S. lividans* biomass (as dry weight) is composed of 5.5 % lipid. For the purposes of this flux calculation, the lipid composition of *S. coelicolor* 1147 & *S. fradiae* C373-10 was assumed to be equivalent to that of *S. lividans*. Experimental results were used to further enhance and verify the compositional analysis undertaken in Chapter 5. The following calculations were taken from Davidson (1992).

Table 1.1g Lipid composition of 1g dry weight *S. lividans* biomass (55 mg total lipid)

	Lipid		Fatty acids		
	%	**mg**	**μmole[a]**	**Chains**	**mmole**
Neutral lipid	60.4	33.22	38.9	3	0.117
Glycolipid	12.1	6.66	8.5	2	0.017
Phospholipid	20.9	11.5	16.3	2	0.033
Glycerol			**63.7**		
Total C16 fatty acids					**0.167**

[a] assuming an average fatty acid chain of C_{16} has a molecular weight of 255.

Table 1.2g Composition of lipid species:

	Branched chain fatty acids		**Amino acid precursor (mmoles)**	
	Iso[b] (%)	**anteiso[c] (%)**	**leucine**	**isoleucine**
Neutral lipid	86.2	9.7	0.1	0.011
Glycolipid	83.3	11.2	0.014	0.002
Phospholipid	82.9	13.1	0.027	0.004
			0.141	**0.017**

[b], iso-branched chain fatty acids have leucine as a precursor; [c], anteiso-branched chain fatty acids have isoleucine as a precursor. Grafe *et al.* (1986) measured an average of 95.4 % branched fatty acids. This is higher than that cited for *S. coelicolor* (84 %; Kaneda, 1991).

Appendix H

Determination of nucleotide contents of *Streptomyces* RNA (calculation taken from Davidson [1992])

E. coli RNA contains 81.5 % rRNA, 14.5 % tRNA and 4.0 % mRNA. The nucleotide content of RNA has been calculated as 26.2 % AMP, 32.2 % GMP, 20 % CMP and 21.6 % UMP (Neidhardt, 1987, based on data from Roberts *et al*., 1955). This is different to the DNA content of 24.6 % dAMP, 25.4 % dGMP, 25.4 % dCMP and 24.6 % dTMP (Neidhardt, 1987) because rRNA is the major species in total RNA and has a composition different from that of total RNA. To determine the nucleotide content of *Streptomyces* RNA, it was therefore necessary to examine the published sequences of a number of *Streptomyces* RNA species.

Table 1.1H GC mol % of rRNA and tRNA

rRNA[a]	tRNA[b]
58.5 % (Suzuki & Yamada, 1988) for *S. lividans* 58.9 % (Baylis & Bibb, 1987) for *S. coelicolor*	$tRNA^{gly}$ 64 % (Rokem *et al*., 1990) for *S. coelicolor* $tRNA^{gln\ 1,2}$ 51 % (Plohl & Gamulin, 1990) for *S. rimosus* $tRNA^{glu\ 1,2,3}$ 70.3 % (Plohl & Gamulin, 1990) for *S. rimosus*

[a]Average 58.7 % GC rich. [b]Average 61.8 % GC rich.

Streptomyces DNA is approximately 70 % GC rich and this would be reflected in GC mol % of mRNA. However, the sequences of other RNA species showed lower GC contents (Table 1.1H). To determine the amount of each individual nucleotide in *Streptomyces* RNA each base was counted in all the above mentioned sequences. The values were then expressed as a percentage of the total bases in the sequence:

	A (%)	G (%)	C (%)	U (%)	
rRNA	22.75	32.9	25.8	18.55	(mean of 2)
tRNA	16.0	33.2	29.5	23.2	(mean of 5)

rRNA is present in *E. coli* in approximately 6 fold greater quantities than tRNA. Therefore, allowing for this, an average composition of *Streptomyces* RNA is:

A (%)	**G (%)**	**C (%)**	**U (%)**
21.8	32.9	26.3	19.2

with limits of 58 % to 63 % GC mol %.

Appendix I

Bioreaction network for *Streptomyces clavuligerus* (Kirk *et al*., 2000)[units of measurement C.moles]

! **Biochemistry of *Streptomyces Clavuligerus***
!
! **Carbon source uptake reactions** -
!
1: Glycerol + 1/3 ATP + 1/3 FAD => G3P + 1/3 ADP + 1/3 FADH
!
! **Embden-Meyerhof-Parnas pathway** -
!
2: G3P + 1/6 ADP <=> F6P + 1/6 ATP
3: F6P <=> G6P
4: G3P <=> 1/3 ADP + 1/3 NAD => PG + 1/3 ATP + 1/3 NADH
5: PEP + 1/3 ADP => PYR + 1/3 ATP
!
! **Pentose-phosphate pathway** -
!
6: X5P + R5P <=> 1/4 S7P + 3/5 G3P
7: S7P + 3/7 G3P <=> 6/7 F6P + 4/7 E4P
8: 6/5 F6P + 3/5 G3P <=> X5P + 4/5 E4P
9: Ru5P <=> R5P
10: Ru5P <=> X5P
!
! **TCA cycle** -
!
11: PYR + 1/3 NAD => ACCOA + 1/3 NADH + 1/3 CO2
12: ACCOA + 2 OAA => 3 ISOCIT
13: ISOCIT + 1/6 NADP <=> 5/6 AKG + 1/6 NADPH + 1/6 CO2
14: AKG + 1/5 NAD + 1/5 ADP <=> 4/5 SUCCOA + 1/5 NADH + 1/5 CO2 + 1/5 ATP
15: SUCCOA + 1/4 FAD => MAL + 1/4 FADH2
16: MAL + 1/4 NAD <=> OAA + 1/4 NADH
!
! **Anaplerotic reactions** - (PEPC and PEPCK incorporated as one reversible reaction)
!
17: PEP + 1/3 CO2 <=> 4/3 OAA
!
! **Nucleotide biosynthesis**
!
18: 1/2 R5P + 4/5 ATP + 3/10 GLY + 2/5 ASP + GLN + 1/10 NADH + 1/5 CO2 + 2/5 ASP => AMP + 2/5 FUM + 4/5 ADP + GLU + 1/10 NAD + 2/5 FUM
19: 1/2 R5P + 9/10 ATP + 3/10 GLY + 2/5 ASP + GLN + 1/10 NADH + 1/5 CO2 + 1/10 NAD + 1/2 GLN => GMP + 1/2 GLU + 1/10 NADH + 9/10 ADP + GLU + 1/10 NAD + 2/5 FUM
20: 5/9 GLU + 5/9 R5P + 2/3 ATP + 4/9 ASP + 1/9 NAD <=> UTP + 2/3 ADP + 5/9 GLU + 1/9 NADH
21: UTP + 5/9 GLU + 1/9 ADP => CMP + 1/9 ATP + 5/9 GLU
!
! **Amino acid biosynthesis**
!

22: AKG + 1/5 NH4 + 1/5 NADPH <=> GLU + 1/5 NADP
23: GLU + 1/5 NH4 + 1/5 ATP => GLN + 1/5 ADP
24: GLU + 1/5 ATP + 2/5 NADPH => PRO + 1/5 ADP + 2/5 NADP
25: GLU + 1/2 ATP + 1/10 NAPPH + 1/10 NH4 + 1/10 CO2 + 2/5 ASP => 3/5 ARG + 1/2 AKG + 1/2 ADP + 2/5 FUM + 1/10 NADP
26: ASP + GLU + 1/5 ACCOA + 3/10 ATP + 1/5 NADPH + 1/5 NAD => 3/5 LYS + 1/2 AKG + 1/10 CO2 + 3/10 ADP + 1/5 NADP + 1/5 NADH
27: G3P + 5/3 GLU + 1/3 NAD => SER + 5/3 AKG + 1/3 NADH
28: SER + 2/3 NAD => 2/3 GLY + 1/3 CO2 + 2/3 NADH
29: SER + 4/3 NADPH + 1/3 ATP => CYS + 4/3 NADP + 1/3 ADP
30: OAA + 5/4 GLU => ASP + 5/4 AKG
31: ASP + 1/4 NH4 + 1/2 ATP => ASG + 1/4 ADP
32: ASP + 1/2 ATP + 1/2 NADPH => THR + 1/2 ADP + 1/2 NADP
33: ASP + 1/2 ATP + 1/2 NADPH + 3/4 CYS + 1/4 CO2 + 3/4 NADH => 5/4 MET + 3/4 PYR + 1/4 NH4 + 1/2 ADP + 1/2 NADP + 3/4 NAD
34: THR + 3/4 PYR + 1/4 NADPH + 5/4 GLU => 1.5 ILEU + 1/4 NH4 + ¼ NADP + 1/4 CO2 + 5/4 AKG
35: PYR + 5/3 GLU => ALA + 5/3 AKG
36: 6/5 PYR + 1/5 NADPH + GLU => VAL + AKG + 1/5 CO2 + 1/5 NADP
37: 6/5 PYR + 1/5 NADPH + 2/5 ACCOA + GLU + 1/5 NAD + 1/5 ATP => 6/5 LEU + AKG + 2/5 CO2 + 1/5 NADH + 1/5 ADP + 1/5 NADP
38: 3/5 PEP + 2/5 E4P + 1/10 NADPH + 1/10 ATP + 1/2 GLU => 9/10 PHE + 1/2 AKG + 1/10 CO2 + 1/10 ADP + 1/10 NADP
39: 3/5 PEP + 2/5 E4P + 1/10 NADPH + 1/10 ATP + 1/2 GLU + 1/10 NAD => 9/10 TYR + 1/2 AKG + 1/10 CO2 + 1/10 ADP + 1/10 NADP
40: 3/5 PEP + 2/5 E4P + 1/10 NADPH + 1/10 ATP + 1/2 GLU + 1/2 R5P + 1/5 ATP + 3/10 SER => 11/10 TRP + 1/10 CO2 + 3/10 G3P + 1/2 GLU + 3/10 PYR + 1/5 ADP + 1/10 ADP + 1/10 NADP
41: R5P + ATP + 1/5 NH4 + GLU + 2/5 NAD + 1/5 NADPH + 1/5 CO2 => 6/5 HIS + 1/5 NADH + 1/5 NADP + ADP + AKG
42: GLU + 1/5 ATP + 1/5 NADPH + GLU => ORN + 1/5 ADP + 1/5 NADP + AKG
!
! **Oxidative phosphorylation and ATP dissipitation**
!
43: O2 + 2 NADH + 4 ADP => 4 ATP + 2 NAD
44: O2 + 2 FADH + 2 ADP => 2 ATP + 2 FAD
45: ATP => ADP
46: NADPH <=> NADH
!
! **Biosynthesis of RNA & DNA**
!
47: 0.0246 AMP + 0.0246 GMP + 0.0323 UMP + 0.00295 CMP + 0.34 ATP => RNA/DNA + 0.34 ADP
!
! **Biosynthesis of lipid (palmitate)**
!
48: 8 ACCOA + 15 ATP + 15 NADPH + O2 => Lipid + 15 ADP + 15 NADP
!
! **Biosynthesis of protein**
!
49: 0.085 GLU + 0.029 GLN + 0.0496 PRO + 0.054 ARG + 0.096 LYS + 0.0312 SER + 0.032 GLY + 0.0012 CYS + 0.0666 ASP + 0.0229 ASN + 0.0428 THR + 0.0143 MET + 0.065 ISO + 0.077 ALA + 0.0743 VAL + 0.0995 LEU + 0.0677 PHE + 0.0515 TYR + 0.0173 TRY + 0.022 HIS + 0.826 ATP => Protein + 0.826 ADP

!
! **Biosynthesis of polycaccharides**
!
50: 1/6 G6P + 1/6 ATP => Polysaccharide + 1/6 ADP
51: Polysaccharide => $Polyaccharide_{Extracellular}$
!
! **Urea cycle**
!
52: ARG => 1/5 UREA + 4/5 Ornithine
53: Ornithine + 4/5 ASP + 1/5 ATP => 9/5 Arginosuccinate
54: Arginosuccinate => 2/5 FUM + 3/5 ARG
55: UREA => CO2 + 2 NH4
!
! **Clavulanic acid biosynthesis**
!
56: 3/8 PYR + 3/4 ARG + 1/4 NADPH + 1/8 FAD + 15/8 AKG + 3/8 O2 => Clavulanic acid + 1/4 NADP + 1/8 FADH + 3/2 Succinate + 3/8 CO2 + 1/8 UREA + NH4

The bioreaction network constructed by Kirk *et al*. (2000) for the analysis of *S. clavuligerus* primary metabolic pathways. The units of measurement were the fraction represented by the transfer of carbon atoms. Intermeditate metabolite nomemclature: AcCoA, acetyl-CoA; ADP, adenosine-5'-monophosphate AKG, oxo-glutarate; ALA, alanine; AMP, adenosine monophosphate; ARG, arginine; ASN, aspargine; ASP, aspartate; ATP, adenosine triphosphate; CHOR, chorismate; CMP, cytidine monophosphate; CO2, carbon dioxide; CYS, cysteine; E4P, erythrose-4-phosphate; FAD, Flavin adenine nucleotide (oxidised form); F6P, fructose-6-phosphate; FADH, $FADH_2$, flavin adenine nucleotide (reduced form); FUM, fumarate; G6P, glucose-6-phosphate; GAP, glyceraldehyde-3-phosphate; GLN, glutamine; glutamate, GLU; GLY, glycine; GMP, guanosine monophosphate; HIS, histidine; ILE, isoleucine; ISOCIT, isocitrate; IMP, inosine monophosphate; LEU, leucine; LYS, lysine; MAL, malate; MET, methionine; NAD, nicotinamide adenine dinucleotide (oxidised form) NADH, nicotinamide adenine dinucleotide (reduced form); NADPH, nicotinamide adenine dinucleotide phosphate; NH4, ammonia; O2, oxygen; OAA, oxaloacetate; PEP, phosphoenolpyruvate; PG, phosphoglycerate; PHE, phenylalanine; PRO, proline; PRPP, 5-phosphoribosyl-1-pyrophosphate; PYR, pyruvate; R5P, ribose-5-phosphate; Ru5P, ribulose-5-phosphate; S7P, seduheptulose-7-phosphate; SER, serine; SUCCOA, succinyl-CoA; THR, threonine; TMP, thymidine monophosphate; TRP, tryptophan; TYR, tyrosine; UTP, uridine monophosphate; VAL, valine; X5P, xylulose-5-phosphate; PEPCK, phosphoenolpyruvate carboxykinase; PEPC, phosphoenolpyruvate carboxylase.

Appendix J

Bioreaction network *Streptomyces lividans* (Daae & Isson, 1999)[units of measurement moles]

!
! ***Streptomyces lividans*** **Proposed primary metabolic biochemistry**
!
! **Carbon source uptake reactions** -
!
1: Glucose + ATP => G6P + ADP
!
! **Embden-Meyerhof-Parnas pathway** -
!
2: G6P <=> F6P
3: F6P + ATP => 2.0 GAP
4: 2.0 GAP + ADP + NAD <=> F6P + PG + ATP
5: PG <=> PEP
6: PEP + ADP => ATP + PYR
7: PYR + NAD + ADP => AcCoA + ATP + NADH
!
! **Pentose-phosphate pathway** -
!
8: G6P + NAD + NADP => Ru5P + NADH + NADPH + CO2
9: Ru5P <=> X5P
10: Ru5P ⇔ R5P
11: R5P + X5P <=> GAP + S7P
12: S7P + GAP <=>F6P + E4P
13: E4P + X5P <=> F6P + GAP
!
! **TCA cycle** -
!
14: ACCOA + OAA + NAD => AKG + CO2 + NADH
15: AKG + ADP + NAD + FAD => FUM + ATP + NADH + CO2 + FADH
16: FUM + NAD <=> NADH + OAA
!
! **Anaplerotic reactions** - (PEPC and PEPCK incorporated as one reversible reaction)
!
17: PEP + CO2 + ADP<=> OAA + ATP
!
! **Nucleotide biosynthesis**
!
18: R5P + ATP => PRPP + ADP
19: PRPP + GLN + ASP + 2.0 ATP + NAD => UMP + GLU + NADH + 2.0 ADP
20: UMP + GLN + ATP => GLU + CMP + ADP
21: MTHF + UMP => TMP
22: PRPP + GLY + FTHF + 2.0 GLN + CO2 + 2.0 ATP => 5A4CRN + 2.0 GLU + 2.0 ADP
23: 5A4CRN + FTHF + ASP + ATP => FUM + IMP + ADP
24: IMP + ASP + ATP => FUM + AMP
25: IMP + GLN + ATP + NAD => GMP + NADH + GLU + ADP
!

! **Amino acid biosynthesis**
!
26: E4P + NADPH + 2.0 PEP => CHOR + NADP
27: CHOR + NH4 => PHE + CO2
28: CHOR + NH4 => TYR + CO2
29: CHOR + SER + GLN + PRPP + ATP => G3P + PEP + CO2 + GLU + TRP + ADP
30: PYR + GLU => AKG + ALA
31: 2.0 PYR + NADPH + GLU => VAL + CO2 + AKG + NAD
32: 2.0 PYR + AcCoA + GLU => LEU + 2.0 CO2 + AKG
33: AKG + NH4 + NADH + ATP => GLU + NADH + ADP
34: GLU + NH4 + ATP => GLN + ADP
35: GLU + 2.0 NADPH + ATP => PRO + 2.0 NADP + ADP
36: GLU + GLN + ASP + NADPH + CO2 + 4.0 ATP => ARG + AKG + FUM + NADP + ADP
37: GLU + OAA => AKG + ASP
38: ASP + NH4 + ATP => ASN + ADP
39: GLU + ASP + 2.0 NADPH + PYR + ATP => LYS + AKG + CO2 + 2.0 NADP + ADP
40: MTHF + ASP + 2.0 NADPH + 2.0 ATP => MET + 2.0 NADP + 2.0 ADP
41: ASP + 2.0 NADPH + 2.0 ATP => THR + 2.0 NADP + 2.0 ADP
42: THR + PYR + NADPH => ILE + CO2 + NADP
43: GLU + PG + NAD => SER + NADH + AKG
44: SER => CYS
45: SER => MTHF + GLY
46: GLN + PRPP + ATP => HIS + GLU + 5A4CRN + ADP
!
! **Oxidative phosphorylation and ATP dissipitation**
!
47: 0.5 O2 + NADH + 2.0 ADP => 2.0 ATP + NAD
48: 0.5 O2 + FADH + 1.33 ADP => 1.33 ATP + FAD
49: ATP => ADP
50: NADPH + AcCoA + ATP => NADH + CO2 + FADH + FTHF + ADP
51: FTHF + NADH => MTHF + NAD
!
! **Biosynthesis of protein**
!
52: 0.09 HIS + 0.087 CYS + 0.276 ILE + 0.241 THR + 0.146 MET + 0.326 LYS + 0.229 ASN + 0.281 ARG + 0.21 PRO + 0.428 LEU + 0.402 VAL + 0.5432 ALA + 0.054 TRP + 0.334 SER + 0.131 TYR + 0.176 PHE + 0.2284 GMP + 0.1897 AMP + 0.585 GLY + 0.0247 TMP + 0.0485 MTHF + 0.1514 CMP + 0.136 UMP + 0.5478 GLU + 0.25 GLN + 0.229 ASP + 0.0276 OAA + 0.0235 S7P + 0.0235 R5P + 5.1875 NADPH + 2.4998 AcCoA + 0.0276 PYR + 0.0511 PEP + 0.0235 PG + 0.129 G3P + 4.2856 ATP + 0.0709 F6P + 0.154 G6P => 0.0235 NADH + 0.2109 AKG
!
! **Other reactions**
!
53: PYR => PYR_{ext}
54: AKG => AKG_{ext}
55: ALA_{ext} => ALA
56: $O2_{ext}$ => O2
57: $CO2_{ext}$ => CO2
!

The bioreaction network construction by Daae & Isson (1999) for the analysis of S. lividans primary metabolic pathways. Units of measurement moles. Intermeditate

metabolite nomemclature: 5A4CRN, 5-aminoimidazole-4-carboxamide ribonucleotide; AcCoA, acetyl-CoA; ADP, adenosine-5'-monophosphate AKG, oxo-glutarate; ALA, alanine; AMP, adenosine monophosphate; ARG, arginine; ASN, aspargine; ASP, aspartate; ATP, adenosine triphosphate; CHOR, chorismate; CMP, cytidine monophosphate; CO2, carbon dioxide; CYS, cysteine; E4P, erythrose-4-phosphate; F6P, fructose-6-phosphate; FAD, Nicotinamide adenine dinucleotide (oxidised); FADH, flavin adenine nucleotide (reduced); FTHF, formyl tetrahydrofolate; FUM, fumarate; G6P, glucose-6-phosphate; GAP, glyceraldehyde phosphate; GLN, glutamine; GLY, glycine; GMP, guanosine monophosphate; HIS, histidine; ILE, isoleucine; IMP, inosine monophosphate; LEU, leucine; LYS, lysine; MET, methionine; MTHF, methylene tetrahydrofolate; NAD, nicotinamide adenine dinucleotide (oxidised) NADH, nicotinamide adenine dinucleotide (reduced); NADP, nicotinamide adenine dinucleotide phosphate (oxidised); NADPH, nicotinamide adenine dinucleotide phosphate (reduced); NH4, ammonia; O2, oxygen; OAA, oxaloacetate; PEP, phosphoenolpyruvate; PG, phosphoglycerate; PHE, phenylalanine; PRO, proline; PRPP, 5-phosphoribosyl-1-pyrophosphate; PYR, pyruvate; R5P, ribose-5-phosphate; Ru5P, ribulose-5-phosphate; S7P, seduheptulose-7-phosphate; SER, serine; THR, threonine; TMP, thymidine monophosphate; TRP, tryptophan; TYR, tyrosine; UMP, uridine monophosphate; VAL, valine; X5P, xylulose-5-phosphate; PEPCK, phosphoenolpyruvate carboxykinase; PEPC, phosphoenolpyruvate carboxylase; ext, extracellular.

Appendix K

Bioreaction network *Streptomyces lividans* (Avignone Rossa *et al*., 2002)[units of measurement C.moles]

!
! **Glycolysis**
!
(1) Glucose + 0.167 ATP => G6P + 0.167 ADP
(2) G6P => F6P
(3) F6P + 0.167 ATP => G3P + 0.167 ADP
(4) G3P + 0.333 ADP + 0.333 NAD => PG + 0.333 ATP + 0.333 NADH
(5) PG => PEP
(6) PEP + 0.333 ADP => PYR + 0.333 ATP
(7) PYR + 0.333 NAD => 0.667 AcCoA + 0.333 CO2 + 0.333 NADH
!
! **TCA cycle**
!
(8) PYR + 0.333 NADH => Lactate + 0.333 NAD
(9) AcCoA + 2 OAA <=> 3 ISOCIT
(10) ISOCIT + 0.167 NADP <=> 0.833 OKG + 0.167 NADPH + 0.167 CO2
(11) OKG + 0.2 NAD + 0.2 ADP <=> 0.8 SUCC + 0.2 CO2 + 0.2 ADH + 0.2 ATP
(12) SUCC + 0.25 FAD <=> MAL + 0.25 FADH
(13) MAL + 0.25 NAD + <=> OAA + 0.25 NADH
!
! **Organic acid excretion**
!
(14) OKG => OKG_{ext}
(15) ISCIT => $Citrate_{ext}$
(16) PYR => PYR_{ext}
!
! **Pentose Phosphate Pathway**
!
(17) G6P + 0.333 NADP => 0.833 Ru5P + 0.667 CO2 + 0.333 NADPH
(18) Ru5P <=> R5P
(19) Ru5P <=> X5P
(20) X5P +R5P <=> 1.4 S7P + 0.6 G3P
(21) S7P + 0.429 G3P <=> 0.857 F6P + 0.571 E4P
(22) X5P + 0.8 E4P <=> 1.2 F6P + 0.6 G3P
!
! **Amino acid biosynthesis**
!
(23) PG + 1.667 GLU + 0.333 NAD => SER + 0.333 NADH + 1.667 OKG
(24) SER => 0.667 GLY
(25) PYR + 0.833 GLU + 0.333 AcCoA => 0.833 OKG + 0.333 CO2 + LEU
(26) OAA + 1.25 GLN <=> ASP + 1.25 OKG
(27) ASP + 0.416 ATP + 0.50 NADPH + 0.25 PYR + 0.417 GLU => 0.5 LYS + 0.333 THR + 0.417 MET + 0.417 ADP + 0.5 NADP + 0.083 CO2
(28) OKG + 0.2 NH4 + 0.2 NADPH <=> GLU + 0.2 NADP
(29) GLU + 0.2 ATP + 0.2 NH4 => GLN + 0.2 ADP

(30) GLU + 0.2 ATP + 0.4 NADPH => PRO + 0.2 ADP + 0.4 NADP
!
! **Anaplerotic reactions-**(PEPC and PEPCK incorporated as one reversible reaction)
!
(31) PEP + 0.333 CO2 => 1.333 OAA
!
! **Oxidative phosphorylation and ATP dissipitation**
!
(32) 2 NADH + O2 + 4 ADP => 4 ATP + 2 NAD
(33) ATP => ADP
!
! **Biomass composition**
!
(34) 0.03 Glucose-6-P + 0.011 F6P + 0.113 R5P + 0.036 E4P + 0.01 + G3P + 0.113 PG + 0.039 PEP + 0.094 PYR + 0.165 AcCoA + 0.075 OKG + 0.11 OAA + 0.05 LYS + 0.2 NH4 + 0.031 GLU + 0.031 GLN + 0.973 ATP + 0.343 NADPH + 0.078 NAD + 0.065 LEU + 0.019 MET + 0.024 THR => Biomass + 0.973 ADP + 0.343 NADP + 0.078 NADH + 0.036 CO2
!
! **Nitrogen source uptake**
!
(35) Nitrate + 8 NADH => NH4 + 8 NAD
!
! **Secondary metabolic pathways**
!
(36) AcCoA + 0.437 ATP + 0.875 NADPH => ACT + 0.437 ADP + 0.875 NADP

The bioreaction network construction by Avignone Ross *et al*. (2002) for the analysis of *S. lividans* primary metabolic pathways. Units of measurement moles. Intermeditate metabolite nomemclature: ACT, actinorhodin; AcCoA, acetyl-CoA; ADP, adenosine-5'-monophosphate AKG, oxo-glutarate; ALA, alanine; AMP, adenosine monophosphate; ARG, arginine; ASN, aspargine; ASP, aspartate; ATP, adenosine triphosphate; CHOR, chorismate; CMP, cytidine monophosphate; CO2, carbon dioxide; CYS, cysteine; E4P, erythrose-4-phosphate; F6P, fructose-6-phosphate; FAD, Nicotinamide adenine dinucleotide (oxidised); FADH, flavin adenine nucleotide (reduced); FUM, fumarate; G6P, glucose-6-phosphate; GAP, glyceraldehyde phosphate; GLN, glutamine; GLY, glycine; GMP, guanosine monophosphate; HIS, histidine; ILE, isoleucine; IMP, inosine monophosphate; ISOCIT, isocitrate; LEU, leucine; LYS, lysine; MET, methionine; NAD, nicotinamide adenine dinucleotide (oxidised) NADH, nicotinamide adenine dinucleotide (reduced); NADP, nicotinamide adenine dinucleotide phosphate (oxidised); NADPH, nicotinamide adenine dinucleotide phosphate (reduced); NH4, ammonia; O2, oxygen; OAA, oxaloacetate; PEP, phosphoenolpyruvate; PG, phosphoglycerate; PHE, phenylalanine; PRO, proline; PRPP, 5-phosphoribosyl-1-pyrophosphate; PYR, pyruvate; R5P, ribose-5-phosphate; Ru5P, ribulose-5-phosphate; S7P, seduheptulose-7-phosphate; SER, serine; THR, threonine; TMP, thymidine monophosphate; TRP, tryptophan; TYR, tyrosine; UMP, uridine monophosphate; VAL, valine; X5P, xylulose-5-phosphate; PEPCK, phosphoenolpyruvate carboxykinase; PEPC, phosphoenolpyruvate carboxylase; ext, extracellular.

Appendix L

Bioreaction network model 1 *Streptomyces fradiae* (designed for this project)[units of measurement C.moles]

! Carbon source uptake reactions - Glucose
!
1: Glucose + 0.167 ATP => G6P + 0.167 ADP
!
! Embden-Meyerhof-Parnas pathway -
!
2: G6P <=> F6P
3: F6P + 0.167 ATP => GAP + 0.167 ADP
4: GAP + 0.333 ADP <=> PG + 0.333 ATP
5: PG <=> PEP
6: PEP + 0.333 ADP => PYR + 0.333 ATP
7: PYR + 0.333 NAD + 0.333 ADP => 0.666 ACCOA + 0.333 ATP + 0.333 NADH + 0.333 CO2
!
! TCA cycle -
!
8: 0.333 ACCOA + 0.666 OAA + 0.167 NAD <=> 0.167 NADH + 0.833 AKG + 0.167 CO2
9: AKG + 0.2 ADP + 0.2 NAD + 0.2 FAD <=> 0.8 FUM + 0.2 ATP + 0.2 NADH + 0.2 CO2 + 0.2 FADH
10: FUM + 0.25 FAD <=> MAL + 0.25 FADH2
11: MAL + 0.25 NAD <=> OAA + 0.25 NADH
!
! Pentose-phosphate pathway -
!
12: G6P + 0.167 NAD => 6PG + 0.167 NADH
13: 6PG + 0.167 NADP => 0.833 Ru5P + 0.167 NADPH + 0.167 CO2
14: Ru5P <=> 0.4 F6P + 0.6 E4P
15: 0.555 Ru5P + 0.444 E4P <=> 0.667 F6P + 0.333 GAP
!
! Nucleotide biosynthesis
!
16: Ru5P + 0.2 ATP => PRPP + 0.2 ADP
17: 0.357 PRPP + 0.357 GLN + 0.286 ASP + 0.25 ATP + 0.125 NAD => 0.643 UMP + 0.357 GLU + 0.125 NADH + 0.25 ADP
18: 0.643 UMP + 0.357 GLN + 0.07 ATP => 0.643 CMP + 0.357 GLU + 0.07 ADP
19: UMP => TMP
20: 0.278 PRPP + 0.111 GLY + 0.555 GLN + 0.055 CO2 + 0.111 ATP => 0.444 5A4CRN + 0.555 GLU + 0.111 ADP
21: 0.667 5A4CRN + 0.333 ASP + 0.08 ATP => 0.667 IMP + 0.333 FUM + 0.08 ADP
22: 0.692 IMP + 0.308 ASP + 0.08 ATP => 0.692 AMP + 0.308 FUM + 0.08 ADP
23: 0.643 IMP + 0.357 GLN + 0.07 ATP + 0.07 NAD => 0.643 GMP + 0.07 NADH + 0.357 GLU + 0.07 ADP
!
! Anaplerotic reactions - (PEPC and PEPCK incorporated as one reversible reaction)
!
24: 0.75 PEP + 0.25 CO2 + 0.25 ADP <=> OAA + 0.25 ATP
!
! Amino acid biosynthesis

!
25: 0.4 E4P + 0.1 NADPH + 0.6 PEP => CHOR + 0.1 NADP
26: CHOR => 0.9 PHE + 0.1 CO2
27: CHOR => 0.9 TYR + 0.1 CO2
28: 0.435 CHOR + 0.130 SER + 0.217 GLN + 0.217 PRPP + 0.04 ATP => 0.130 GAP + 0.130 PEP + 0.04 CO2 + 0.217 GLU + 0.478 TRP + 0.04 ADP
29: 0.375 PYR + 0.625 GLU => 0.625 AKG + 0.375 ALA
30: 0.545 PYR + 0.09 NADPH + 0.454 GLU => 0.454 VAL + 0.09 CO2 + 0.454 AKG + 0.09 NAD
31: 0.461 PYR + 0.154 ACCOA + 0.385 GLU => 0.461 LEU + 0.154 CO2 + 0.385 AKG
32: AKG + 0.2 NADH + 0.2 ATP => GLU + 0.2 NADH + 0.2 ADP
33: GLU + 0.2 ATP => GLN + 0.2 ADP
34: GLU + 0.4 NADPH + 0.2 ATP => PRO + 0.4 NADP + 0.2 ADP
35: 0.333 GLU + 0.333 GLN + 0.267 ASP + 0.07 NADPH + 0.07 CO2 + 0.07 ATP => 0.4 ARG + 0.333 AKG + 0.267 FUM + 0.07 NADP + 0.07 ADP
36: 0.444 OAA + 0.555 GLU => 0.444 ASP + 0.555 AKG
37: 0.444 ASP + 0.555 GLN + 0.111 ATP => 0.444 ASN + 0.555 GLU + 0.111 ADP
38: 0.333 ASP + 0.417 GLU + 0.167 NADPH + 0.2 PYR + 0.08 ATP => 0.5 LYS + 0.417 AKG + 0.08 CO2 + 0.167 NADP + 0.08 ADP
39: ASP + 0.5 NADPH + 0.5 ATP => MET + 0.5 NADP + 0.5 ADP
40: ASP + 0.5 NADPH + 0.5 ATP => THR + 0.5 NADP + 0.5 ADP
41: 0.571 THR + 0.429 PYR + 0.143 NADPH => 0.857 ILE + 0.143 CO2 + 0.143 NADP
42: 0.375 PG + 0.625 GLU + 0.125 NAD => 0.375 SER + 0.125 NADH + 0.625 AKG
43: SER => CYS
44: SER => GLY
45: 0.5 PRPP + 0.5 GLN + 0.1 ATP => 0.4 HIS + 0.5 GLU
!
! Oxidative phosphorylation and ATP dissipitation
!
46: O2 + 2 NADH + 4 ADP => 4 ATP + 2 NAD
47: O2 + 2 FADH + 2 ADP => 2 ATP + 2 FAD
48: ATP => Maintenance
!
! Biosynthesis of RNA & DNA (setting 1, average *E. coli* compositional data; taken from Avignone-Rossa *et al*., 2002)
!
49: 0.0246 AMP + 0.0246 GMP + 0.0323 TMP + 0.00295 CMP + 0.34 ATP => RNA/DNA + 0.34 ADP
!
! Biosynthesis of lipid (palmitate)
!
50: 0.14 ACCOA + 0.131 ATP + 0.131 NADPH + 0.008 O2 => Lipid + 0.131 ADP + 0.131 NADP
!
! Biosynthesis of protein (setting 1, average *E. coli* compositional data; taken from Avignone-Rossa *et al*., 2002)
!
51: 0.059 ALA + 0.065 ARG + 0.035 ASP 0.017 ASN + 0.013 CYS + 0.076 GLU + 0.0434 GLN + 0.035 GLY + 0.013 HIS + 0.065 ILE + 0.104 LEU + 0.104 LYS + 0.043 MET + 0.059 PHE + 0.054 PRO + 0.039 SER + 0.044 THR + 0.024 TRP + 0.039 TYR +0.065 VAL + 0.950 ATP => Protein + 0.950 ADP
!
! Biosynthesis of polycaccharides
!

52: 0.24 G6P + 0.04 ATP => Polysaccharide + 0.04 ADP
!
! Other reactions
!
53: ACCOA => ACCOAext
54: PYR => PYRext
55: AKG => AKGext
56: MAL => MALext
!

Alternative carbon source uptake pathways
(A)
1: Glycerol + 0.333 ATP + 0.333 FAD => GAP + 0.333 ADP + 0.333 FADH
2: GAP + 0.167 ADP => F6P + 0.167 ATP
3: F6P <=> G6P
(B)
3: Fructose + 0.167 ATP => F1P + 0.167 ADP
4: F1P + 0.167 ATP ⇔ 2.0 G3P + 0.167 ADP

Alternative bacterial biomass compositional data

Setting 2: Average biomass composition increased by 20 % (setting 2, average *E. coli* compositional data; taken from Avignone-Rossa *et al*., 2002)
51: 0.074 ALA + 0.082 ARG + 0.043 ASP + 0.022 ASN+ 0.016 CYS + 0.095 GLU + 0.054 GLN + 0.043 GLY + 0.016 HIS + 0.081 ILE + 0.131 LEU + 0.131 LYS + 0.054 MET + 0.073 PHE + 0.068 PRO + 0.049 SER + 0.054 THR + 0.030 TRP + 0.049 TYR + 0.082 VAL + 1.250 ATP => Protein + 1.250 ADP
49: 0.063 AMP + 0.063 GMP + 0.057 TMP + 0.057 CMP + 0.41 ATP => RNA/DNA + 0.41 ADP
Setting 3: Average biomass composition decreased by 20 % (setting 2, average *E. coli* compositional data; taken from Avignone-Rossa *et al*., 2002)
51: 0.049 ALA + 0.054 ARG + 0.029 ASP + 0.015 ASN + 0.011 CYS + 0.064 GLU + 0.036 GLN + 0.028 GLY + 0.011 HIS + 0.054 ILE + 0.087 LEU + 0.087 LYS + 0.036 MET + 0.049 PHE + 0.045
PRO + 0.033 SER + 0.036 THR + 0.020 TRP + 0.033 TYR + 0.054 VAL + 0.833 ATP => Protein + 0.833 ADP
49: 0.095 AMP + 0.095 GMP + 0.086 TMP + 0.086 CMP + 0.27 ATP => RNA/DNA + 0.27 ADP
Setting 3: Average biomass composition for S. fradiae (setting 4, adapted from Chapter 5)
51: 0.073 ALA + 0.164 ARG + 0.079 ASP + 0.011 CYS + 0.048 GLU + 0.048 GLN + 0.062 GLY + 0.026 HIS + 0.052 ILE + 0.073 LEU + 0.023 LYS + 0.002 MET + 0.06 PHE + 0.052 PRO + 0.006 SER + 0.0395 THR + 0.005 TRP + 0.089 TYR + 0.081 VAL + 0.974 ATP => Protein + 0.974 ADP

The bioreaction network construction model 1 for this project for the analysis of *S. fradiae* C373-10 and *S. coelicolor* 1147 primary metabolic pathway. Alternative carbon and nitrogen uptake pathways are also presented for alternative models. Alternative biomass compositional data are alos given that were incorporated into the constructed models to calculate the effect that biomass composition has on metabolic fluxes. Units of measurement moles. Intermeditate metabolite nomemclature: 5A4CRN, 5-aminoimidazole-4-carboxamide ribonucleotide;

AcCoA, acetyl-CoA; ADP, adenosine-5'-monophosphate AKG, oxo-glutarate; ALA, alanine; AMP, adenosine monophosphate; ARG, arginine; ASN, aspargine; ASP, aspartate; ATP, adenosine triphosphate; CHOR, chorismate; CMP, cytidine monophosphate; CO2, carbon dioxide; CYS, cysteine; E4P, erythrose-4-phosphate; F6P, fructose-6-phosphate; FAD, Nicotinamide adenine dinucleotide (oxidised); FADH, flavin adenine nucleotide (reduced); FTHF, formyl tetrahydrofolate; FUM, fumarate; G6P, glucose-6-phosphate; GAP, glyceraldehyde phosphate; GLN, glutamine; GLY, glycine; GMP, guanosine monophosphate; HIS, histidine; ILE, isoleucine; IMP, inosine monophosphate; LEU, leucine; LYS, lysine; MET, methionine; MTHF, methylene tetrahydrofolate; NAD, nicotinamide adenine dinucleotide (oxidised) NADH, nicotinamide adenine dinucleotide (reduced); NADP, nicotinamide adenine dinucleotide phosphate (oxidised); NADPH, nicotinamide adenine dinucleotide phosphate (reduced); NH4, ammonia; O2, oxygen; OAA, oxaloacetate; PEP, phosphoenolpyruvate; PG, phosphoglycerate; PHE, phenylalanine; PRO, proline; PRPP, 5-phosphoribosyl-1-pyrophosphate; PYR, pyruvate; R5P, ribose-5-phosphate; Ru5P, ribulose-5-phosphate; S7P, seduheptulose-7-phosphate; SER, serine; THR, threonine; TMP, thymidine monophosphate; TRP, tryptophan; TYR, tyrosine; UMP, uridine monophosphate; VAL, valine; X5P, xylulose-5-phosphate; PEPCK, phosphoenolpyruvate carboxykinase; PEPC, phosphoenolpyruvate carboxylase; ext, extracellular.

Appendix M

Bioreaction network (model 2) *Streptomyces fradiae* (designed for this project)[units of measurement C.moles]

!
! Glycolysis
!
1: Glycerol + 0.333 ATP + FAD => Glyceraldehyde-3-P + 0.333 ADP + 0.333 FADH
2: Glyceraldehyde-3-P + 0.167 ADP => Fructose-6-P + 0.167 ATP
3: Fructose-6-P => Glucose-6-P
4: Glyceraldehyde-3-P + 0.333 ADP + 0.333 NAD => 3-P-Glycerate + 0.333 ATP + 0.333 NADH
5: 3-P-Glycerate => Phosphoenolpyruvate
6: Phosphoenolpyruvate + 0.333 ADP => Pyruvate + 0.333 ATP
7: Pyruvate + 0.333 NAD => 0.667 Acetyl-CoA + 0.333 CO2 + 0.333 NADH
!
! TCA cycle
!
8: Pyruvate + 0.333 NADH => Lactate(ext) + 0.333 NAD
9: Acetyl-CoA + 2 Oxaloacetate <=> 3 Isocitrate
10: Isocitrate + 0.167 NADP <=> 0.833 Oxoglutarate + 0.167 NADPH + 0.167 CO2
11: Oxoglutarate + 0.2 NAD + 0.2 ADP <=> 0.8 Succinate + 0.2 CO2 + 0.2 NADH + 0.2 ATP
12: Succinate + 0.25 FAD <=> Malate + 0.25 FADH
13: Malate + 0.25 NAD <=> Oxaloacetate + 0.25 NADH
!
! Organic acid excretion
!
14: Oxoglutarate => Oxoglutarate(ext)
15: Pyruvate => Pyruvate(ext)
16: Malate => Malate(ext)
17: Acetyl-CoA => Acetate(ext)
18: Ethylmalonyl-CoA => 0.80 Butyrate(ext) + 0.20 CO2
19: Propionyl-CoA => Propionate(ext)
20: Fumarate => Fumarate(ext)
!
! Pentose Phosphate Pathway
!
21: Glucose-6-P + 0.167 NADP => 6-phosphogluconate + 0.167 NADPH
22: 6-phosphogluconate + 0.167 NADP => 0.833 Ribulose-5-P + 0.167 CO2 + 0.167 NADPH
23: Ribulose-5-P <=> Ribose-5-P
24: Ribulose-5-P <=> Xylulose-5-P
25: Xylulose-5-P + Ribose-5-P <=> 1.4 Sedoheptulose-7-P + 0.6 Glyceraldehyde-3-P
26: Sedoheptulose-7-P + 0.429 Glyceraldehyde-3-P <=> 0.857 Fructose-6-P + 0.571 Erythrose-4-P
27: Xylulose-5-P + 0.8 Erythrose-4-P <=> 1.2 Fructose-6-P + 0.6 Glyceraldehyde-3-P
!
! Amino acid biosynthesis
!
28: Oxoglutarate + 0.2 NH4 + 0.2 NADPH <=> Glutamate + 0.2 NADP
29: Glutamate + 0.2 NH4 + 0.2 ATP => Glutamine + 0.2 ADP
30: Glutamate + 0.2 ATP + 0.4 NADPH => Proline + 0.2 ADP + 0.4 NADP

31: Glutamate + 0.5 ATP + 0.1 NADPH + 0.1 NH4 + 0.1 CO2 + 0.4 Aspartate => 0.6 Arganine + 0.5 Oxoglutarate + 0.5 ADP + 0.4 Fumarate + 0.1 NADP
32: 0.333 Asparate + 0.417 Glutamate + 0.167 NADPH + 0.2 Pyruvate + 0.08 ATP => 0.5 Lysine + 0.417 Oxogutarate + 0.08 CO2 + 0.167 NADP + 0.08 ADP
33: Glyceraldehyde-3-P + 1.667 Glutamate + 0.333 NAD => Serine + 1.667 Oxoglutarate + 0.333 NADH
34: Serine + 0.666 NAD => 0.666 Glycine + 0.333 CO2 + 0.666 NADH
35: Serine + 1.333 NADPH + 0.333 ATP => Cysteine + 1.333 NADP + 0.333 ADP
36: Oxaloacetate + 6.25 Glutamate => Aspartate + 6.25 Oxoglutarate
37: Aspartate + 0.25 NH4 + 0.5 ATP => Asparganine + 0.25 ADP
38: Aspartate + 0.5 ATP + 0.5 NADPH => Threonine + 0.5 ADP + 0.5 NADP
39: Aspartate + 0.5 ATP + 0.5 NADPH + 0.75 Cysteine + 0.25 CO2 + 0.75 NADH => 1.25 Methionine + 0.75 Pyruvate + 0.25 NH4 + 0.5 ADP + 0.5 NADP + 0.75 NAD
40: Threonine + 0.75 Pyruvate + 0.25 NADPH + 1.25 Glutamate => 1.5 Isoleucine + 0.25 NH4 + 0.25 NADP + 0.25 CO2 + 1.25 Oxoglutarate
41: Pyruvate + 1.667 Glutamate => Alanine + 1.667 Oxoglutarate
42: 1.2 Pyruvate + 0.2 NADPH + Glutamate => Valine + Oxoglutarate + 0.2 CO2 + 0.2 NADP
43: 1.2 Pyruvate + 0.2 NADPH + 0.4 Acetyl-CoA + Glutamate + 0.2 NAD + 0.2 ATP => 1.2 Leucine + Oxoglutarate + 0.4 CO2 + 0.2 NADH + 0.2 ADP + 0.2 NADP
44: 0.6 Phosphoenolpyruvate + 0.4 Erythrose-4-P + 0.1 NADPH + 0.1 ATP + 0.5 Glutamate => 0.9 Phenylalanine + 0.5 Oxoglutarate + 0.1 CO2 + 0.1 ADP + 0.1 NADP
45: 0.6 Phosphoenolpyruvate + 0.4 Erythrose-4-P + 0.1 NADPH + 0.1 ATP + 0.5 Glutamate + 0.1 NAD => 0.9 Tyrosine + 0.5 Oxoglutarate + 0.1 CO2 + 0.1 ADP + 0.1 NADP
46: 0.6 Phosphoenolpyruvate + 0.4 Erythrose-4-P + 0.1 NADPH + 0.1 ATP + 0.5 Glutamate + 0.5 Ribulose-5-P + 0.2 ATP + 0.3 Serine => 1.1 Tryptophan + 0.1 CO2 + 0.3 Glyceraldehyde-3-P + 0.5 Glutamate + 0.3 Pyruvate + 0.2 ADP + 0.1 ADP + 0.1 NADP
47: Ribulose-5-P + ATP + 0.2 NH4 + Glutamate + 0.4 NAD + 0.2 NADPH + 0.2 CO2 => 1.2 Histidine + 0.2 NADH + 0.2 NADP + 0.2 ADP + Oxoglutarate
!
! Nucleotide biosynthesis
!
48: 0.5 Ribulose-5-P + 0.8 ATP + 0.3 Glycine + 0.4 Aspartate + Glutamate + 0.1 NADH + 0.2 CO2 + 0.4 Aspartate => AMP + 0.4 Fumarate + 0.8 ADP + Glutamate + 0.1 NAD + 0.45 Fumarate
49: 0.5 Ribulose-5-P + 0.9 ATP + 0.3 Glycine + 0.4 Aspartate + Glutamine + 0.1 NADH + 0.2 CO2 + 0.1 NAD + 0.5 Glutamate => GMP + 0.5 Glutamate + 0.1 NADH + 0.9 ADP + Glutamate + 0.1 NAD + 0.4 Fumarate
50: 0.555 Glutamate + 0.555 Ribulose-5-P + 0.666 ATP + 0.444 Aspartate + 0.111 NAD <=> UTP + 0.666 ADP + 0.555 Glutamate + 0.111 NADH
51: UTP + 0.555 Glutamate + 0.111 ADP => CMP + 0.111 ATP + 0.555 Glutamate
!
! Anaplerotic reactions
!
52: Phosphoenolpyruvate + 0.333 CO2 => 1.333 Oxaloacetate
!
! **Oxidative phosphorylation and ATP dissipitation**
!
53: 2 NADH + O2 + 4 ADP => 4 ATP + 2 NAD
54: 2 FADH + O2 + 2 ADP => 2 ATP + 2 FAD
55: ATP => ADP
!
! Biomass composition
!
56: 0.09 Histidine + 0.087 Cysteine + 0.276 Isoleucine + 0.241 Threonine + 0.146 Methionine + 0.326 Lysine + 0.229 Asparganine + 0.281 Arganine + 0.21 Proline + 0.428 Leucine + 0.402 Valine

+ 0.5432 Alanine + 0.054 Tryptophan + 0.334 Serine + 0.131 Tyrosine + 0.176 Phenylalanine + 0.2284 GMP + 0.1897 AMP + 0.585 Glycine + 0.0247 TMP + 0.1514 CMP + 0.136 UMP + 0.5478 Glutamate + 0.25 Glutamine + 0.229 Aspartate + 0.0276 Oxaloacetate + 0.0235 Sedoheptulose-7-P + 0.0235 Ribulose-5-P + 5.1875 NADPH + 2.4998 Acetyl-CoA + 0.0276 Pyruvate + 0.0511 Phosphoenolpyruvate + 0.0235 3-P-Glycerate + 0.129 Glyceraldehyde-3-P + 4.2856 ATP + 0.0709 Fructose-6-P + 0.154 Glucose-6-P => Biomass + 0.0235 NADH + 0.2109 Oxoglutarate
!
! Nitrogen source uptake
!
57: 0.2 NH4(uptake) + Oxoglutarate + 0.20 NADPH <=> Glutamate + 0.20 NADP
!
! Tylosin synthesis
!
58: 0.666 Acetyl-CoA + 0.333 CO2 + 0.333 ATP => Malonyl-CoA + 0.333 ADP
59: Succinate => Methylmalonyl-CoA
60: Methylmalonyl-CoA => 0.75 Propionyl-CoA + 0.25 CO2
61: 0.40 Acetyl-CoA + 0.60 Malonyl-CoA + 0.40 NADPH + 0.40 ATP => Ethylmalonyl-CoA + 0.40 NADP + 0.40 ADP
62: 0.086 Propionyl-CoA + 0.171 Malonyl-CoA + 0.571 Methylmalonyl-CoA + 0.171 Ethylmalonyl-CoA + 0.20 NADPH => 0.60 Tylactone + 0.20 NADP + 0.40 CO2
!

Alternative pathways
(A) Actinorhodin and undecylprodigiosin
58: Acetyl-CoA + 0.437 ATP + 0.875 NADPH => Actinorhodin + 0.437 ADP + 0.875 NADP
59: 0.60 Pyruvate + 0.16 ATP + 0.20 NAD + 0.24 Serine + 0.40 Proline + 0.16 Glycine => Undecylprodigisin + 0.40 CO2 + 0.16 ADP + 0.20 NADH
(B) Nitrate metabolism
57: Nitrate(uptake) + 8 NADH => NH4 + 8 NAD
(C) Glutamate uptake reaction
Glu_{ext} + AKG + 0.2 NADPH <=> 2 GLU + 0.2 NADP
(D) NH4 uptake reactions
$NH4_{ext}$ + AKG + 0.2 NADPH <=> GLU + 0.2 NADP
(E) Oxoglutarate plus NH4 uptake reaction
$NH4_{ext}$ + AKG_{ext} + 0.2 NADPH <=> GLU + 0.2 NADP

Setting 2; Average biomass composition increased by 20 % (setting 1, average *E. coli* compositional data; taken from Daae & Isson 1999)

56: 0.108 Histidine + 0.104 Cysteine + 0.331 Isoleucine + 0.289 Threonine + 0.175 Methionine + 0.391 Lysine + 0.275 Asparganine + 0.337 Arganine + 0.252 Proline + 0.514 Leucine + 0.482 Valine + 0.652 Alanine + 0.065 Tryptophan + 0.401 Serine + 0.157 Tyrosine + 0.211 Phenylalanine + 0.274 GMP + 0.228 AMP + 0.702 Glycine + 0.030 TMP + 0.182 CMP + 0.163 UMP + 0.657 Glutamate + 0.030 Glutamine + 0.275 Aspartate + 0.033 Oxaloacetate + 0.028 Sedoheptulose-7-P + 0.028 Ribulose-5-P + 6.225 NADPH + 2.999 Acetyl-CoA + 0.033 Pyruvate + 0.061 Phosphoenolpyruvate + 0.028 3-P-Glycerate + 0.155 Glyceraldehyde-3-P + 5.143 ATP + 0.085 Fructose-6-P + 0.185 Glucose-6-P => Biomass + 0.028 NADH + 0.253 Oxoglutarate

Setting 3; Average biomass composition decreased by 20 % (setting 1, average *E. coli* compositional data; taken from Daae & Isson 1999)

56: 0.072 Histidine + 0.070 Cysteine + 0.221 Isoleucine + 0.193 Threonine + 0.117 Methionine + 0.261 Lysine + 0.183 Asparganine + 0.225 Arganine + 0.168 Proline + 0.342 Leucine + 0.322 Valine + 0.435 Alanine + 0.043 Tryptophan + 0.267 Serine + 0.105 Tyrosine + 0.141 Phenylalanine

+ 0.183 GMP + 0.152 AMP + 0.468 Glycine + 0.020 TMP + 0.121 CMP + 0.109 UMP + 0.438 Glutamate + 0.20 Glutamine + 0.183 Aspartate + 0.022 Oxaloacetate + 0.019 Sedoheptulose-7-P + 0.019 Ribulose-5-P + 4.15 NADPH + 1.999 Acetyl-CoA + 0.022 Pyruvate + 0.041 Phosphoenolpyruvate + 0.019 3-P-Glycerate + 0.103 Glyceraldehyde-3-P + 3.428 ATP + 0.057 Fructose-6-P + 0.123 Glucose-6-P => Biomass + 0.019 NADH + 0.169 Oxoglutarate

Setting 4; Average biomass composition for S. fradiae C373-10 for growth on glycerol (adapted from Chapter 5; intracellular metabolites and co-factor were not changed)

0.028 Histidine + 0.033 Cysteine + 0.082 Isoleucine + 0.169 Threonine + 0.01 Methionine + 0.024 Lysine + 0.01 Asparganine + 0.09 Arganine + 0.107 Proline + 0.112 Leucine + 0.05 Valine + 0.355 Alanine + 0.01 Tryptophan + 0.035 Serine + 0.046 Tyrosine + 0.241 Phenylalanine + 0.048 GMP + 0.0267 AMP + 0.195 Glycine + 0.0246 TMP + 0.0493 CMP + 0.0246 UMP + 0.195 Glutamate + 0.01 Glutamine + 0.221 Aspartate + 0.0276 Oxaloacetate + 0.0235 Sedoheptulose-7-P + 0.0235 Ribulose-5-P + 5.1875 NADPH + 2.4998 Acetyl-CoA + 0.0276 Pyruvate + 0.0511 Phosphoenolpyruvate + 0.0235 3-P-Glycerate + 0.129 Glyceraldehyde-3-P + 4.2856 ATP + 0.0709 Fructose-6-P + 0.154 Glucose-6-P => Biomass + 0.0235 NADH + 0.2109 Oxoglutarate

The bioreaction network model 2 construction for this project for the analysis of *S. fradiae* C373-10 and *S. coelicolor* 1147 primary metabolic pathway. Alternative biomass compositional data are also given that were incorporated into the constructed models to calculate the effect that biomass composition has on metabolic fluxes. Units of measurement moles. Intermeditate metabolite nomemclature: AcCoA, acetyl-CoA; ADP, adenosine-5'-monophosphate AKG, oxo-glutarate; ALA, alanine; AMP, adenosine monophosphate; ARG, arginine; ASN, aspargine; ASP, aspartate; ATP, adenosine triphosphate; CHOR, chorismate; CMP, cytidine monophosphate; CO2, carbon dioxide; CYS, cysteine; E4P, erythrose-4-phosphate; F6P, fructose-6-phosphate; FAD, Nicotinamide adenine dinucleotide (oxidised); FADH, flavin adenine nucleotide (reduced); FUM, fumarate; G6P, glucose-6-phosphate; GAP, glyceraldehyde phosphate; GLN, glutamine; GLY, glycine; GMP, guanosine monophosphate; HIS, histidine; ILE, isoleucine; IMP, inosine monophosphate; LEU, leucine; LYS, lysine; MET, methionine; NAD, nicotinamide adenine dinucleotide (oxidised) NADH, nicotinamide adenine dinucleotide (reduced); NADP, nicotinamide adenine dinucleotide phosphate (oxidised); NADPH, nicotinamide adenine dinucleotide phosphate (reduced); NH4, ammonia; O2, oxygen; OAA, oxaloacetate; PEP, phosphoenolpyruvate; PG, phosphoglycerate; PHE, phenylalanine; PRO, proline; PRPP, 5-phosphoribosyl-1-pyrophosphate; PYR, pyruvate; R5P, ribose-5-phosphate; Ru5P, ribulose-5-phosphate; S7P, seduheptulose-7-phosphate; SER, serine; THR, threonine; TMP, thymidine monophosphate; TRP, tryptophan; TYR, tyrosine; UMP, uridine monophosphate; VAL, valine; X5P,xylulose-5-phosphate; PEPCK, phosphoenolpyruvate carboxykinase; PEPC, phosphoenolpyruvate carboxylase; ext, extracellular.

Appendix N

Sensitivity analysis (adapted from Stephanopoulos *et al*., 1998)

Condition number

The first step of a sensitivity analysis is to examine whether the system is well-posed, i.e., check whether the stoichiometric matrix is well-conditioned. A measure of the sensitivity of a matrix is the so-called condition number (CN).

The general definition of the CN is a measure of the sensitivity of a matrix, which is given by (eq. 1):

$$(1) \quad C(G^T) = \|G^T\| \; \left\| (G^T)^{\#} \right\|$$

Where $\| \; \|$ indicates any matrix norm and $(G^T)^{\#}$ is the *pseudo*-inverse of the stoichiometric matrix. Calculation of the CN is quite complex. In order to use this equation it is, however, necessary to calculate the norm of a matrix. The norm of a matrix measures the largest amount by which any vector x is amplified by matrix multiplications.

However, because it is generally time-consuming to use this equation, computer software packages like Matlab, Mathematica, Fluxmap, Bionet, or Maple are generally used.

The magnitude of the CN provides important information about requirements for the accuracy of the measured fluxes, as the measurements have to be carried out with a precision that carries the same number of digits as there are in the CN. Thus, if a CN has five digits, it is necessary to measure fluxes precisely to the fifth digit. This opens a problem; fermentation rates rarely can be quantified with precision greater than two digits (e.g., the specific growth rate of microorganisms can be specified to two decimal places with reasonable precision), a requirement for a well-conditioned stoichiometric matrix is that the CN lies between 1 and 100

(Stephanopolous *et al*., 1998) or between 1 and 1000 (Kirk *et al*., 2000). There are considerable differences in the literature of what is an acceptable CN, many of these workers use different mathematical packages which will also have an effect on the CN. The CN for the model of Vallino and Stephanopolous. (1993) is 62 and that of the model of Nissen *et al*. (1997) is 22. If the CN is greater than 1000 the stoichiometric matrix is ill-conditioned, and it may be necessary to modify the biochemistry used in the development of the model. It should be noted that no measurements are needed for the calculation of the CN, and the metabolic model therefore can be tested before any calculations are carried out.

Sensitivity analysis

The dynamic properties such as the sensitivity of the calculated fluxes to changes in the measured fluxes can also be investigated without experimental data. A method based on stoichiometry alone is presented in eq. (2). The accumulated impact of each of the measured fluxes may be found by taking the sum of the absolute values of the individual sensitivities (all negative values converted to positive).

$$\frac{\delta v_c}{\delta v_m} = -(G^T_c)^{-1} G^T_m \qquad (2)$$

In eq. (2) the element in the jth row and ith column specifies the sensitivity of the jth flux (which is calculated) with respect to variations in the measurements of the ith flux. Thus, the elements of the solution matrix provide information about the sensitivity of the system.

Comment:

Table 4.1. *S. fradiae* C373-10 tylosin yields cultured on a number of different literature based defined mediums.

Medium composition	No Days	Dry wt (gl^{-1})	ϕ	Tylosin yield ($mg.ml^{-1}$)
Glucose minimal	5	6.99 ± 1.56	0.3 ± 0.18	0.09
Glucose glutamate defined	5	5.33 ± 0.99	0.6 ± 0.21	0.06
***S. griseofuscus* defined medium**	5	7.19 ± 1.25	0.86 ± 0.10	0.07
New minimal medium (minus junlon)	5	2.16 ± 0.62	0.21 ± 0.12	0.03
Tetracycline minimal (glucose)	5	5.83 ± 0.12	0.24 ± 0.15	0.035
Tetracycline minimal (mineral oil)	7	5.89 ± 0.44	0.30 ± 0.16	0.111
Maltose glutamate defined medium for *S. coelicolor*	6	7.85 ± 0.97	0.99 ± 0.09	0.06
Starch based medium	8	6.10 ± 0.12	2.16 ± 0.61	0.169
methyl oleate defined medium	10	9.10 ± 0.56	3.89 ± 0.48	0.373
Complex medium	8	18.93 ± 0.64	2.66 ± 0.49	3.123

Shake flask trials were undertaken on a number of literature based mediums that were known to produce tylosin or other antibiotics. *S. fradiae* C373-10 was cultured in 100 ml Erlenmeyer flasks with 40 ml of medium inoculated with 4 ml of an appropriate seed training medium was used to reduce carry over of complex vegetative substrates (Chapter 3, section 3.5.2). New minimal medium for production of actinorhodin (Chapter 3, section 3.6.1), glucose minimal medium (Chapter 3, section 3.6.4), glucose glutamate defined medium (Chapter 3, section 3.6.4), tetracycline minimal medium (glucose) (Chapter 3, section 3.6.6), tetracycline minimal medium (plus 10 % mineral oil) (Chapter 3, section 3.6.6), methyl oleate defined medium (Chapter 3, section 3.7.2), starch based defined medium (Chapter 3, section 3.7.1), and industrial tylosin complex medium (Chapter 3, section 3.7.3). All analysis was undertaken in triplicate and the standard deviation was presented as plus or minus the unit of measurement. ϕ, degree of dispersion (Chapter 3, section 3.10.3). Dry weight were determined as Chapter 3, section 3.11.2; tylosin was determined by HPLC (Chapter 3, section 3.25.1).

Table 4.2. The effects of a number of carbon sources on biomass and tylosin yield.

Carbon source	Carbon source concentration (gl^{-1})	No Days grown	pH	Dry wt (gl^{-1})	ϕ	Tylosin yield ($mg.ml^{-1}$)
S. fradiae						
Glucose	20.0	5	4.44	5.66 ± 1.76	0.54 ± 3.89	0.07
Glycerol	40.0	5	4.63	3.54 ± 0.53	0.33 ± 4.55	0.04
Fructose	20.0	5	4.55	5.18 ± 1.66	0.6 ± 4.62	0.06
Sucrose	10.0	5	4.80	5.32 ± 1.67	0.8 ± 5.99	0.03
Galactose	20.0	5	4.70	4.82 ± 1.23	0.21 ± 4.89	0.04
Oxo-glutarate	30.0	7	6.10	4.56 ± 2.29	0.24 ± 1.12	0.035
Pyruvate	40.0	7	4.60	3.85 ± 3.33	0.3 ± 6.89	0.095
Phospho-glycerate	40.0	5	7.01	3.69 ± 4.53	0.58 ± 8.63	0.01
Glucose-6-phosphate	20.0	7	6.63	3.86 ± 1.28	0.44 ± 4.56	0.03
Glutamate	24.0	7	5.90	4.11 ± 1.45	0.14 ± 9.56	0.01
Acetic acid	60.0	10	NG	NG	NG	NG
Mannose	20.0	7	7.01	6.99 ± 2.66	0.89 ± 2.34	0.03
Arabinose	24.0	7	7.52	5.40 ±1.94	0.99 ± 5.44	0.04
Xylose	24.0	7	7.06	5.98 ± 2.40	1.01 ± 6.22	0.06
Glucose + glutamate	20.0 + 5.0	5	7.0	6.99 ± 2.66	0.89 ± 2.34	0.03
Glycerol + glutamate	40.0 + 5.0	5	7.53	5.4 ± 1.94	0.99 ± 5.44	0.04
Fructose + glutamate	20.0 + 5.0	5	7.01	5.98 ± 2.40	1.01 ± 6.22	0.05
Sucrose + glutamate	10.0 + 5.0	5	6.98	8.78 ± 2.07	1.22 ± 10.11	0.06
Glucose + oxo-glutarate	20.0 + 5.0	5	6.12	5.69 ± 3.24	0.86 ± 0.33	0.07
Glycerol + oxo-glutarate	40.0 + 5.0	5	5.93	6.58 ± 2.87	0.99 ± 0.21	0.09

Fructose + oxo-glutarate	20.0 + 5.0	5	6.35	7.14 ± 1.11	0.88 ± 0.36	0.08
Sucrose + oxo-glutarate	10.0 + 5.0	5	6.11	7.85 ± 0.63	1.04 ± 0.45	0.05
S. coelicolor						**Actinorhodin ($mg.ml^{-1}$)**
Glutamate	4.8	5	7.02	0.80 ± 0.46	0.66 ± 0.27	5.16
Glucose	4.0	5	5.24	1.23 ± 0.57	0.39 ± 0.14	40.1
Oxo-glutarate	6.0	5	4.89	0.64 ± 0.62	0.43 ± 0.22	2.19

Shake flask trials were undertaken on a number of medium formulations. *S. fradiae* C373-10 & *S. coelicolor* 1147 were cultured in 100 ml Erlenmeyer flasks with 40 ml of medium inoculated with 4 ml of an appropriate seed training medium was used to reduce carry over of complex vegetative substrates (Chapter 3, section 3.5.2). New minimal medium for production of actinorhodin (Chapter 3, section 3.6.1), glucose minimal medium (Chapter 3, section 3.6.4), glucose glutamate defined medium (Chapter 3, section 3.6.4). The latter three mediums carbon substrate were interchanged with a range of simple carbon sources to determine their effects on tylosin & actinorhodin production and biomass yield. Carbon source concentration was equivalent to the same concentration of carbon contained in glucose. All analysis was undertaken in triplicate and the standard deviation was presented as plus or minus the unit of measurement. ϕ, degree of dispersion (Chapter 3, section 3.10.3). Dry weight were determined as Chapter 3, section 3.11.2; tylosin was determined by HPLC (Chapter 3, section 3.25.1) actinorhodin assay as Chapter 3, section 3.24. NG, no growth.

Table 4.3. The effects of Nitrogen concentration on biomass and tylosin yield.

Nitrogen concentration $[NH_4(SO_4)_2]$ (gl^{-1})	No Days grown	Dry wt (gl^{-1})	ϕ	Tylosin yield ($mg.ml^{-1}$)
Glucose minimal media				
0.5	5	1.79 ± 0.67	0.21 ± 0.12	0.03
1	5	1.55 ± 0.23	0.12 ± 0.01	0.04
1.5	5	1.87 ± 0.49	0.24 ± 0.13	0.05
2	5	1.99 ± 0.95	0.36 ± 0.17	0.06
2.5	5	2.18 ± 0.56	0.38 ± 0.19	0.01
3.0	5	3.51 ± 0.96	0.40 ± 0.20	0.01
3.5	5	4.49 ± 1.11	0.60 ± 0.26	0.02
Control	5	5.66 ± 1.76	0.54 ± 3.89	0.07
4.5	5	6.48 ± 1.33	0.68 ± 0.33	0.01
5.0	5	6.66 ± 2.24	0.79 ± 0.37	0.01
5.5	5	6.04 ± 2.68	0.84 ± 0.24	0.01
6.0	5	7.51 ± 2.45	0.99 ± 0.38	0.01
Glucose glutamate defined medium				
0.5	5	3.16 ± 0.99	0.33 ± 0.11	0.03
1	5	4.55 ± 1.65	0.64 ± 0.17	0.05
Control	5	6.99 ± 2.66	0.89 ± 2.34	0.03
2	5	6.83 ± 0.97	0.95 ± 0.22	0.04
2.5	5	7.18 ± 1.87	1.14 ± 0.33	0.06
3.0	5	8.21 ± 1.99	0.92 ± 0.37	0.09
3.5	5	8.93 ± 2.16	0.96 ± 0.46	0.06
4.0	5	2.11 ± 5.66	0.30 ± 0.34	0.04
4.5	5	8.39 ± 2.64	0.64 ± 0.31	0.03
5.0	5	9.39 ± 2.67	0.79 ± 0.41	0.06
5.5	5	8.66 ± 2.99	0.80 ± 0.32	0.07
6.0	5	8.67 ± 3.16	1.06 ± 0.46	0.08

Shake flask trials were undertaken on a number of medium formulations. *S. fradiae* C373-10 was cultured in 100 ml Erlenmeyer flasks with 40 ml of medium inoculated with 4 ml of an appropriate seed training medium was used to reduce carry over of complex vegetative substrates (Chapter 3, section 3.5.2). The glucose minimal medium (Chapter 3, section

3.6.4), glucose glutamate defined medium (Chapter 3, section 3.6.4) ammonium sulphate levels were altered to determine the effects this had on tylosin production and biomass yield. All analysis was undertaken in triplicate and the standard deviation were presented as plus or minus the unit of measurement. ϕ, degree of dispersion (Chapter 3, section 3.10.3). Dry weight were determined as Chapter 3, section 3.11.2; tylosin was determined by HPLC (Chapter 3, section 3.25.1). Control same medium composition as Chapter 3, section 3.6.4 with no alterations. Highlighted figures in red indicate the optimum concentration for biomass formation and tylosin production.

Table 4.4. The effects of Phosphate on biomass and tylosin yield.

Phosphate concentration (gl^{-1})	No Days grown	Dry wt (gl^{-1})	ϕ	Tylosin yield ($mg.ml^{-1}$)
Glucose minimal medium				
0.4	5	3.79 ± 1.45	0.21 ± 0.11	0.03
Control	5	5.66 ± 1.76	0.54 ± 3.89	0.07
1.2	5	6.87 ± 0.96	0.64 ± 0.36	0.035
1.6	5	6.99 ± 2.16	0.55 ± 0.12	0.06
2.0	5	7.18 ± 1.33	0.30 ± 0.19	0.07
2.4	5	7.25 ± 1.47	0.65 ± 0.28	0.02
Glucose glutamate defined medium				
0.4	5	3.16 ± 2.47	0.89 ± 0.18	0.04
Control	5	6.99 ± 2.66	0.89 ± 2.34	0.03
1.2	5	7.93 ± 0.96	1.12 ± 0.63	0.05
1.6	5	7.54 ± 1.16	0.95 ± 0.19	0.06
2.0	5	7.80 ± 2.71	0.94 ± 0.23	0.03
2.4	5	8.24 ± 2.11	1.11 ± 0.17	0.02

Shake flask trials were undertaken on a number of medium formulations. *S. fradiae* C373-10 was cultured in 100 ml Erlenmeyer flasks with 40 ml of medium inoculated with 4 ml of an appropriate seed training medium was used to reduce carry over of complex vegetative substrates (Chapter 3, section 3.5.2). The glucose minimal medium (Chapter 3, section 3.6.4), glucose glutamate defined medium (Chapter 3, section 3.6.4) phosphate levels were altered to determine the effects this had on tylosin production and biomass yield. All analysis was undertaken in triplicate and the standard deviation were presented as plus or minus the unit of measurement. ϕ, degree of dispersion (Chapter 3, section 3.10.3). Dry weight were determined as Chapter 3, section 3.11.2; tylosin was determined by HPLC (Chapter 3, section 3.25.1). Control same medium composition as Chapter 3, section 3.6.4 with no alterations. Highlighted figures in red indicate the optimum concentration for biomass formation and tylosin production.

Table. 4.5. The effects of Betaine concentration on biomass and tylosin yield.

Glucose defined medium.

Betaine concentration (gl^{-1})	No Days grown	Dry wt (gl^{-1})	ϕ	Tylosin yield ($mg.ml^{-1}$)
Control	5	5.66 ± 0.35	0.54 ± 0.22	0.01
0.75	5	6.51 ± 0.97	1.86 ± 0.13	0.01
1	5	6.87 ± 0.88	2.66 ± 0.16	0.03
1.25	5	7.99 ± 0.23	2.74 ± 0.08	0.04
1.5	5	8.65 ± 0.27	2.81 ± 0.09	0.08
1.75	5	9.13 ± 0.34	2.97 ± 0.10	0.09
2.0	5	9.49 ± 0.39	3.11 ± 0.12	0.10
2.25	5	7.55 ± 1.12	1.53 ± 0.19	0.09
2.5	5	3.48 ± 1.16	0.99 ± 0.17	0.09
2.75	5	2.55 ± 0.09	0.41 ± 0.21	0.06
3.0	5	1.04 ± 0.52	0.37 ± 0.44	0.05
3.25	5	1.03 ± 0.41	0.23 ± 0.04	0.04
3.5	5	1.16 ± 0.44	0.48 ± 0.03	0.05
3.75	5	0.55 ± 0.03	0.33 ± 0.09	0.06
4.0	5	0.93 ± 0.12	0.12 ± 0.08	0.03
4.25	5	0.99 ± 0.13	0.10 ± 0.11	0.01
4.5	5	1.80 ± 0.18	0.14 ± 0.12	0.02
4.75	5	0.54 ± 0.09	0.15 ± 0.07	0.02
5.0	5	0.93 ± 0.02	0.16 ± 0.01	0.03

Glucose glutamate defined medium

Betaine concentration (gl^{-1})	No Days grown	Dry wt (gl^{-1})	ϕ	Tylosin yield ($mg.ml^{-1}$)
Control	5	6.89 ± 0.12	0.46 ± 0.09	0.01
0.75	5	7.11 ± 0.15	1.99 ± 0.14	0.01
1	5	7.89 ± 0.46	3.11 ± 0.79	0.02
1.25	5	8.14 ± 0.54	3.24 ± 0.34	0.03
1.5	5	9.95 ± 0.21	3.45 ± 0.47	0.06
1.75	5	10.11 ± 0.17	3.89 ± 0.03	0.09

2.0	5	10.55 ± 0.98	4.01 ± 0.29	0.11
2.25	5	10.01 ± 0.66	1.07 ± 0.32	0.10
2.5	5	9.99 ± 0.51	0.80 ± 0.37	0.08
2.75	5	8.13 ± 0.49	0.79 ± 0.42	0.03
3.0	5	7.14 ± 0.41	0.54 ± 0.15	0.06
3.25	5	6.22 ± 0.37	1.01 ± 0.10	0.09
3.5	5	6.01 ± 0.39	1.02 ± 0.07	0.01
3.75	5	6.10 ± 0.11	1.55 ± 0.34	0.02
4.0	5	5.89 ± 0.18	0.40 ± 0.08	0.01
4.25	5	4.00 ± 0.22	0.39 ± 0.11	0.01
4.5	5	1.09 ± 0.56	0.22 ± 0.03	0.01
4.75	5	1.80 ± 0.19	0.11 ± 0.03	0.03
5.0	5	1.20 ± 0.81	0.10 ± 0.10	0.01

Shake flask trials were undertaken on a number of medium formulations. *S. fradiae* C373-10 was cultured in 100 ml Erlenmeyer flasks with 40 ml of medium inoculated with 4 ml of an appropriate seed training medium was used to reduce carry over of complex vegetative substrates (Chapter 3, section 3.5.2). The glucose minimal medium (Chapter 3, section 3.6.4) betaine levels were altered to determine the effects this had on tylosin production and biomass yield. All analysis was undertaken in triplicate and the standard deviation were presented as plus or minus of the units of measurement. ϕ, degree of dispersion (Chapter 3, section 3.10.3). Dry weight were determined as Chapter 3, section 3.11.2; tylosin was determined by HPLC (Chapter 3, section 3.25.1). Control same medium composition as Chapter 3, section 3.6.4 with no alterations. Highlighted figures in red indicate the optimum concentration for biomass formation and tylosin production.

Table 4.6. The effects of $MgSO_4$ concentration on biomass and tylosin yield.

$MgSO_4$ concentration (gl^{-1})	No Days grown	Dry wt (gl^{-1})	ϕ	Tylosin yield ($mg.ml^{-1}$)
0.5	5	1.79 ± 0.96	0.54 ± 0.11	0.03
0.75	5	3.55 ± 1.38	0.65 ± 0.09	0.02
Control	5	5.66 ± 1.27	0.64 ± 0.12	0.04
1.25	5	6.65 ± 2.41	0.81 ± 0.18	0.05
1.5	5	6.18 ± 3.62	0.31 ± 0.17	0.02
1.75	5	6.55 ± 1.55	0.46 ± 0.22	0.03
2.0	5	6.49 ± 1.59	0.60 ± 0.14	0.03
2.25	5	7.89 ± 2.41	0.99 ± 0.32	0.03
2.5	5	6.48 ± 1.47	0.58 ± 0.29	0.04
2.75	5	6.53 ± 0.63	0.99 ± 0.19	0.05
3.0	5	6.04 ± 2.18	0.84 ± 0.07	0.06
3.25	5	6.06 ± 1.97	0.74 ± 0.62	0.04
3.5	5	6.16 ± 1.85	0.83 ± 0.02	0.03
3.75	5	6.24 ± 1.36	1.12 ± 0.66	0.02
4.0	5	6.93 ± 1.14	0.82 ± 0.25	0.03
4.25	5	6.57 ± 1.57	0.94 ± 0.33	0.04
4.5	5	6.80 ± 1.86	0.85 ± 0.04	0.03
4.75	5	6.77 ± 1.92	0.95 ± 0.37	0.01
5.0	5	6.93 ± 0.94	0.96 ± 0.42	0.06

Shake flask trials were undertaken on a number of medium formulations. *S. fradiae* C373-10 was cultured in 100 ml Erlenmeyer flasks with 40 ml of medium inoculated with 4 ml of an appropriate seed training medium was used to reduce carry over of complex vegetative substrates (Chapter 3, section 3.5.2). The glucose minimal medium (Chapter 3, section 3.6.4) magnesium sulphate levels were altered to determine the effects this had on tylosin production and biomass yield. All analysis was undertaken in triplicate and the standard deviation were presented as plus or minus the unit of measurement. ϕ, degree of dispersion (Chapter 3, section 3.10.3). Dry weight were determined as Chapter 3, section 3.11.2; tylosin was determined by HPLC (Chapter 3, section 3.25.1). Control same medium composition as Chapter 3, section 3.6.4 with no alterations. Highlighted figures in red indicate the optimum concentration for biomass formation and tylosin production.

Table 4.7. The effects of carbon / nitrogen ratio on biomass and tylosin yield.

Glucose concentration (gl^{-1})	Glutamate concentration (gl^{-1})	C/N ratio	No Days grown	Dry wt (gl^{-1})	ϕ	Tylosin yield ($mg.ml^{-1}$)
Glucose glutamate defined medium						
20	**5**	1 / 0.04	5	6.99 ± 0.21	0.89 ± 0.41	0.06
15	**10**	1 / 0.08	5	4.95 ± 0.63	0.61 ± 0.12	0.03
10	**15**	1 / 0.12	5	3.86 ± 0.89	0.60 ± 0.01	0.04
5	**20**	1 / 0.16	5	3.16 ± 0.74	0.58 ± 0.09	0.03
Methyl oleate defined medium						
20	**5**	1 / 0.04	7	8.93 ± 1.31	3.84 ± 0.20	0.426
15	**10**	1 / 0.08	7	7.80 ± 0.82	2.72 ± 0.16	0.353
10	**15**	1 / 0.12	7	5.95 ± 0.87	3.80 ± 0.13	0.467
5	**20**	1 / 0.16	7	7.95 ± 1.62	2.96 ± 0.08	0.552
Glucose oxo-glutarate defined medium						
20	**5**	1 / 0.04	5	5.69 ± 1.23	0.86 ± 0.10	0.07
15	**10**	1 / 0.08	5	2.18 ± 0.99	0.30 ± 0.18	0.05
10	**15**	1 / 0.12	5	4.49 ± 0.97	0.60 ± 0.26	0.04
5	**20**	1 / 0.16	5	3.48 ± 1.11	0.58 ± 0.24	0.01
Methyl oleate defined medium						
20	**5**	1 / 0.04	7	8.88 ± 1.47	3.33 ± 0.13	0.288
15	**10**	1 / 0.08	7	5.82 ± 1.74	2.12 ± 0.09	0.311
10	**15**	1 / 0.12	7	6.93 ± 0.98	2.14 ± 0.07	0.267
5	**20**	1 / 0.16	7	7.16 ± 1.26	2.16 ± 0.01	0.312

Shake flask trials were undertaken on a number of medium formulations. *S. fradiae* C373-10 was cultured in 100 ml Erlenmeyer flasks with 40 ml of medium inoculated with 4 ml of an appropriate seed training medium to reduce carry over of complex vegetative substrates (Chapter 3, section 3.5.2). The glucose glutamate defined medium (Chapter 3, section 3.6.4) and methyl oleate defined medium (Chapter 3, section 3.7.2). The latter two mediums glucose glutamate and glucose oxo-glutarate ratios were altered to determine the effects this had on tylosin production and biomass yield. All analysis was undertaken in triplicate and the standard deviations were presented as plus minus the units of measurement. ϕ, degree of dispersion (Chapter 3, section 3.10.3) and dry weight were determined as Chapter 3, section 3.11.2; tylosin was determined by HPLC (Chapter 3, section 3.25.1). Highlighted figures in red indicate the optimum concentration for biomass formation and tylosin production.

Table 4.8 Increase in concentration of Tris with time in a number of different bioreactors

New Brunswick bioreactor (2.5 L)					
minus condenser			**Plus condenser**		
Time (h)	**TOC (ppm)**	**Tris (gl^{-1})^x**	**Time (h)**	**TOC (ppm)**	**Tris (gl^{-1})^x**
0	478.90 ± 24.99	1.21	**0**	476.21 ± 39.97	1.20
20	464.22 ± 67.89	1.17	**20**	486.93 ± 24.77	1.23
40	480.96 ± 15.34	1.21	**40**	499.25 ± 74.98	1.26
60	524.16 ± 20.09	1.32	**60**	512.63 ± 43.56	1.29
80	544.89 ± 21.12	1.37	**80**	522.99 ± 30.11	1.32
100	564.78 ± 50.99	1.42	**100**	536.85 ± 23.45	1.35
Percentage difference (%)		**17.93**			**12.73**
New Brunswick bioreactor (5 L)					
minus condenser			**Plus condenser**		
Time (h)	**TOC (ppm)**	**Tris (gl^{-1})^x**	**Time (h)**	**TOC (ppm)**	**Tris (gl^{-1})^x**
0	480.12 ± 12.19	1.21	**0**	454.87 ± 13.99	1.15
20	499.32 ± 45.66	1.26	**20**	462.22 ± 36.58	1.16
40	587.23 ± 25.78	1.48	**40**	484.56 ± 44.74	1.22
60	622.54 ± 57.89	1.57	**60**	455.29 ± 52.22	1.15
80	625.89 ± 93.48	1.58	**80**	424.97 ± 87.91	1.07
100	644.77 ± 20.98	1.62	**100**	487.62 ± 15.14	1.23
Percentage difference (%)		**34.29**			**7.20**

Bioreactors containing 2.5 & 5.0 L (Chapter 3, section 3.9) of a minimal medium minus glucose and MOPS (Chapter 3, section 3.6.4) with addition of Tris (the only carbon containing compound in the medium was Tris) and run for 100 hrs. Samples were removed and analysed for total organic carbon (TOC) using total organic acid analysis (TOCA)[Chapter 3, section 3.15.5]. Results obtained as ppm of carbon were expressed as gl^{-1} of Tris. X, the concentration of Tris (MW 121.1) in the minimal medium was 1.2 gl^{-1} (10 mM) which was equivalent to 480 ppm of carbon. Standard deviations were presented as plus or minus the unit of measurement

Table 4.9 Comparison of drying temperature and storage method (over silica gel) for the determination of dry weights.

Sample	24 hrs at 70^0 C dried over silica	24 hrs at 70^0 C measured directly	24 hrs at 105^0 C dried over silica
1	7.56 ± 0.11	7.84 ± 0.32	7.44 ± 0.06
2	6.93 ± 0.18	8.41 ± 0.48	7.16 ± 0.07
3	7.14 ± 0.09	7.96 ± 0.56	6.84 ± 0.12
Mean STDEV	**Percentage ± 1.76**	**± 5.62**	**± 1.17**

Sample	24 hrs at 105^0 C measured directly	20 minutes in microwave dried over silica	20 minutes in microwave measured directly
1	7.57 ± 0.21	7.67 ± 0.09	7.81 ± 0.17
2	6.97 ± 0.14	7.01± 0.15	7.58 ± 0.16
3	8.93 ± 0.16	7.02 ± 0.18	7.19 ± 0.14
Mean STDEV	**Percentage ± 2.17**	**± 1.93**	**± 2.08**

Dry weight measurements of samples from three different shake flasks cultures grown on a glucose glutamate defined medium for 5 days (Chapter 3, section 3.6.4) were determined by three different drying methods to determine the dry weight (Chapter 3, section 3.11.2) and expressed as gl^{-1}. In addition the weights were determined immediately after drying and after storage over silica gel for 24 hrs. Standard deviations (STDEV) were given as plus or minus the unit of measurement. nd, not determined or undetermined. The average percentage STDEV was also presented.

Table 4.10 Comparison of dry weight determinations

Fermentation	Wet weight (gl^{-1})	Dry weight (gl^{-1}) microwave filtration method	Dry weight (gl^{-1}) determined by TOCA	Dry weight (gl^{-1}) freeze dried samples	Spin solids (%)
Ferm 1; Day 1	7.59 ± 0.16	0.89 ± 0.15	0.75 ± 0.09	0.85 ± 0.34	0.5 ± 0.01
Ferm 2; Day 1	6.67 ± 0.68	0.91 ± 0.50	0.79 ± 0.12	0.99 ± 0.13	0.5 ± 0.05
Mean	**7.13 ± 0.42**	**0.90 ± 0.32**	**0.77 ± 0.10**	**0.92 ± 0.23**	**0.5 ± 0.03**
Percentage STDEV	± 5.89	± 35.55	± 12.99	± 25.00	± 6.00
Ferm 1; Day 2	12.38 ± 0.52	1.03 ± 0.55	0.91 ± 0.10	0.90 ± 0.32	1.0 ± 0.22
Ferm 2; Day 2	12.48 ± 0.85	0.82 ± 0.08	0.96 ± 0.13	0.84 ± 0.24	0.5 ± 0.10
Mean	**12.43 ± 0.68**	**0.92 ± 0.31**	**0.93 ± 0.11**	**0.87 ± 0.28**	**0.75 ± 0.16**
Percentage STDEV	± 5.47	± 33.69	± 11.83	± 32.18	± 21.33
Ferm 1; Day 3	31.31 ± 2.26	2.91 ± 0.87	2.60 ± 0.07	2.51 ± 0.27	3.0 ± 0.31
Ferm 2; Day 3	22.19 ± 2.21	2.07 ± 0.75	2.47 ± 0.01	2.36 ± 0.13	2.0 ± 0.29
Mean	**26.75 ± 2.23**	**2.49 ± 0.81**	**2.53 ± 0.04**	**2.43 ± 0.20**	**2.5 ± 0.30**
Percentage STDEV	± 8.34	± 32.53	± 1.58	± 8.23	± 12.00
Ferm 1; Day 4	48.11 ± 0.71	3.26 ± 0.40	3.21 ± 0.15	3.25 ± 0.17	5.0 ± 0.25
Ferm 2; Day 4	52.39 ± 11.15	2.61 ± 0.36	2.99 ± 0.21	2.45 ± 0.14	5.5 ± 0.27
Mean	**50.25 ± 5.93**	**2.93 ± 0.38**	**3.10 ± 0.18**	**2.85 ± 0.15**	**5.25 ± 0.26**
Percentage STDEV	± 11.80	± 12.96	± 5.81	± 5.26	± 4.95
Ferm 1; Day 5	63.03 ± 0.05	4.13 ± 0.15	3.97 ± 0.10	3.99 ± 0.11	7.0 ± 0.02
Ferm 2; Day 5	67.19 ± 0.82	4.00 ± 0.23	3.85 ± 0.09	4.11 ± 0.10	7.0 ± 0.09
Mean	**65.11 ± 0.43**	**4.06 ± 0.19**	**3.91 ± 0.09**	**4.05 ± 0.10**	**7.0 ± 0.05**
Percentage STDEV	± 0.66	± 4.68	± 2.30	± 2.47	± 0.71
Ferm 1; Day 6	80.19 ± 3.09	4.94 ± 0.70	4.81 ± 0.14	5.12 ± 0.23	6.5 ± 0.05
Ferm 2; Day 6	83.12 ± 3.44	4.92 ± 0.51	4.85 ± 0.11	4.82 ± 0.28	6.0 ± 0.11
Mean	**81.65 ± 3.26**	**4.93 ± 0.60**	**4.83 ± 0.12**	**4.97 ± 0.25**	**6.25 ± 0.08**
Percentage STDEV	± 3.99	± 12.17	± 2.48	± 5.03	± 1.28
Ferm 1; Day 7	101.35 ± 5.76	5.45 ± 0.95	4.92 ± 0.06	4.99 ± 0.24	6.0 ± 0.08
Ferm 2; Day 7	107.56 ± 1.80	4.14 ± 0.48	4.80 ± 0.04	4.54 ± 0.26	6.5 ± 0.16
Mean	**104.45 ± 3.78**	**4.79 ± 0.71**	**4.85 ± 0.05**	**4.76 ± 0.25**	**6.25 ± 0.12**
Percentage STDEV	± 3.61	± 14.82	± 1.03	± 5.25	± 1.92
Ferm 1; Day 8	143.23 ± 8.84	4.32 ± 0.55	4.25 ± 0.33	4.11 ± 0.21	6.0 ± 0.04
Ferm 2; Day 8	136.24 ± 3.34	4.01 ± 0.61	4.10 ± 0.13	3.97 ± 0.25	5.0 ± 0.14
Mean	**139.73 ± 6.09**	**4.16 ± 0.58**	**4.17 ± 0.23**	**4.04 ± 0.23**	**5.5 ± 0.09**
Percentage STDEV	**± 4.35**	**± 13.94**	**± 5.51**	**± 5.69**	**± 1.64**

Dry weight measurements of samples from fermentation 1 & 2 cultured on glucose minimal medium (Chapter 4, figures 4.3 - 4.4) were determined by three different methods and expressed as gl^{-1}. Wet weight (Chapter 3, section 3.11.1); dry weight (Chapter 3, section 3.11.2) microwave filtration method (Chapter 3, section 3.11.2); dry weight determined by TOCA (Chapter 3, section 3.15.5); dry weight determined by drying an aliquot of fermentation broth and further heated for 3 hrs at 100^0 C and stored over silica gel freeze dried samples, and spin solids. Standard deviations (STDEV) were given as plus or minus the unit of measurement. nd, not determined or undetermined.

Table 4.11 Tabulated dry weight, wet weight, dry weight expressed as percentage of wet weight, Percentage content of biomass water content, and average standard deviation.

Fermentation	Dry wt (mg.ml^{-1})	Wet wt (mg.ml^{-1})	Dry weight expressed as percentage of wet weight (%)	Percentage water content of biomass (%)
***S. fradiae* C373-10 Glucose defined medium**				
Ferm 1; Day 1	0.89 ± 0.55	23.03 ± 2.9	3.88	96.12
Ferm 2; Day 1	0.91 ± 0.82	17.86 ± 1.13	5.09	94.90
Ferm 1; Day 2	1.03 ± 0.58	24.75 ± 0.73	4.07	95.93
Ferm 2; Day 2	0.82 ± 0.01	24.96 ± 1.2	3.20	96.79
Ferm 1; Day 3	2.91 ± 0.87	62.61 ± 3.19	4.64	95.36
Ferm 2; Day 3	2.07 ± 0.75	44.38 ± 3.12	4.66	95.34
Ferm 1; Day 4	3.26 ± 0.40	96.23 ± 1.15	3.39	96.61
Ferm 2; Day 4	2.61 ± 0.35	104.77 ± 3.09	2.49	97.51
Ferm 1; Day 5	4.13 ± 0.15	126.05 ± 0.07	3.31	96.69
Ferm 2; Day 5	4.00 ± 0.23	134.38 ± 1.16	2.98	97.02
Ferm 1; Day 6	4.94 ± 0.70	163.93 ± 3.55	3.01	96.99
Ferm 2; Day 6	4.92 ± 0.51	170.09 ± 3.85	2.89	97.11
Ferm 1; Day 7	5.45 ± 0.95	209.91 ± 7.21	2.60	97.40
Ferm 2; Day 7	4.14 ± 0.48	209.94 ± 5.18	1.97	98.03
Ferm 1; Day 8	4.32 ± 0.48	288.84 ± 2.38	1.52	98.47
Ferm 2; Day 8	4.01 ± 0.17	274.13 ± 1.65	1.47	98.53
Percentage STDEV	**± 23.72**	**± 3.48**		
Glucose oxo-glutarate defined medium				
Ferm 1; Day 1	1.50 ± 0.30	13.63 ± 0.8	11.00	88.99
Ferm 2; Day 1	1.23 ± 0.83	21.37 ± 1.26	4.80	95.20
Ferm 1; Day 2	1.81 ± 0.07	67.49 ± 0.15	3.28	96.72
Ferm 2; Day 2	2.71 ± 0.21	63.03 ± 2.43	4.29	95.71
Ferm 1; Day 3	3.79 ± 0.70	118.7 ± 8.0	3.19	96.81
Ferm 2; Day 3	4.77 ± 0.11	101.05 ± 1.31	4.72	95.28
Ferm 1; Day 4	4.81 ± 1.02	146.36 ± 7.34	3.29	96.71
Ferm 2; Day 4	4.51 ± 0.28	123.12 ± 1.52	3.66	96.34
Ferm 1; Day 5	4.45 ± 0.23	159.89 ± 10.49	2.78	97.22
Ferm 2; Day 5	4.90 ± 0.26	131.6 ± 3.76	3.72	96.28
Ferm 1; Day 6	5.16 ± 0.75	178.49 ± 2.03	2.89	97.11
Ferm 2; Day 6	5.10 ± 0.59	163.6 ± 5.64	3.11	96.88
Ferm 1; Day 7	4.25 ± 0.08	191.42 ± 1.06	2.22	97.78
Ferm 2; Day 7	5.58 ± 0.90	219.96 ± 3.34	2.46	97.54
Ferm 1; Day 8	4.33 ± 0.63	257.07 ± 4.17	1.68	98.32
Ferm 2; Day 8	4.24 ± 0.22	259.51 ± 1.77	1.63	98.36
Percentage STDEV	**± 13.85**	**± 3.03**		
Glucose Glutamate defined medium				
Ferm 1; Day 1	3.65 ± 0.07	12.95 ± 0.55	27.82	72.17
Ferm 2; Day 1	4.63 ± 1.12	10.815 ± 0.58	42.84	57.16
Ferm 3; Day 1	3.75 ± 0.49	11.665 ± 0.56	34.86	65.14

Ferm 4; Day 1	3.30 ± 0.85	9.425 ± 0.82	36.78	63.22
Ferm 1; Day 2	5.62 ± 0.199	42.62 ± 0.64	13.19	86.81
Ferm 2; Day 2	5.99 ± 0.02	53.95 ± 1.31	11.11	88.89
Ferm 3; Day 2	5.88 ± 0.40	61.38 ± 5.92	9.58	90.42
Ferm 4; Day 2	5.85 ± 0.66	59.47 ± 1.87	9.84	90.16
Ferm 1; Day 3	8.31 ± 0.98	85.19 ± 1.93	9.76	90.24
Ferm 2; Day 3	8.47 ± 0.84	93.62 ± 10.9	9.05	90.94
Ferm 3; Day 3	7.08 ± 0.25	74.69 ± 0.21	9.48	90.52
Ferm 4; Day 3	8.78 ± 1.03	77.55 ± 0.19	11.33	88.67
Ferm 1; Day 4	9.17 ± 0.16	118.89 ± 9.57	7.98	92.02
Ferm 2; Day 4	8.54 ± 0.36	108.52 ± 2.74	11.52	88.48
Ferm 3; Day 4	8.80 ± 0.43	101.34 ± 3.5	8.68	91.32
Ferm 4; Day 4	9.33 ± 0.10	110.47 ± 2.07	8.45	91.55
Ferm 1; Day 5	8.90 ± 0.45	134.6 ± 5.46	6.61	93.39
Ferm 2; Day 5	8.96 ± 0.86	134.56 ± 1.0	6.66	93.34
Ferm 3; Day 5	7.96 ± 0.42	120.08 ± 0.06	6.63	93.37
Ferm 4; Day 5	9.08 ± 0.60	117.65 ± 6.63	5.47	94.53
Ferm 1; Day 6	7.00 ± 0.78	150.57 ± 18.33	4.65	95.35
Ferm 2; Day 6	7.08 ± 0.69	132.66 ± 1.54	3.77	96.23
Ferm 3; Day 6	7.48 ± 0.17	136.34 ± 0.54	5.53	94.47
Ferm 4; Day 6	7.94 ± 0.38	127.54 ± 5.06	5.83	94.17
Percentage STDEV	**± 7.93**	**± 7.67**		
Glycerol defined medium				
Ferm 1; Day 1	1.45 ± 0.73	30.28 ± 0.05	4.79	95.21
Ferm 2; Day 1	0.35 ± 0.11	7.80 ± 0.15	4.49	95.51
Ferm 1; Day 2	1.65 ± 0.41	32.60 ± 0.11	5.06	94.94
Ferm 2; Day 2	0.58 ± 0.15	28.00 ± 0.02	2.07	97.93
Ferm 1; Day 3	1.96 ± 0.37	27.65 ± 0.09	7.09	92.91
Ferm 2; Day 3	0.59 ± 0.06	28.00 ± 0.31	2.11	97.89
Ferm 1; Day 4	2.11 ± 0.25	34.02 ± 0.05	6.20	93.80
Ferm 2; Day 4	2.96 ± 0.11	53.00 ± 0.06	5.58	94.41
Ferm 1; Day 5	3.17 ± 0.06	56.27 ± 0.06	5.63	94.37
Ferm 2; Day 5	5.97 ± 0.61	50.00 ± 0.57	11.94	88.06
Ferm 1; Day 6	5.41 ± 0.11	109.12 ± 0.17	4.96	95.04
Ferm 2; Day 6	6.87 ± 0.08	50.00 ± 0.42	13.74	86.26
Ferm 1; Day 7	8.52 ± 0.53	173.96 ± 0.17	4.90	95.10
Ferm 2; Day 7	7.04 ± 0.81	55.13 ± 0.01	12.77	87.23
Ferm 1; Day 8	8.44 ± 0.33	186.62 ± 0.17	4.52	95.48
Ferm 2; Day 8	6.37 ± 1.58	72.91 ± 0.57	8.74	91.26
Ferm 1; Day 9	11.05 ± 0.90	193.01 ± 0.17	5.72	94.27
Ferm 2; Day 9	6.73 ± 1.30	67.24 ± 0.57	10.01	89.99
Ferm 1; Day 10	9.44 ± 0.99	156.06 ± 0.18	6.05	93.95
Ferm 2; Day 10	9.44 ± 1.06	150.6 ± 1.19	6.27	90.56
Percentage STDEV	**± 14.40**	**± 0.46**		
Fructose defined medium				
Ferm 1; Day 1	1.25 ± 0.16	10.55 ± 0.07	11.85	88.15
Ferm 1; Day 2	1.14 ± 0.23	9.128 ± 0.01	12.49	87.51
Ferm 1; Day 3	1.08 ± 0.14	13.03 ± 0.02	8.29	91.71
Ferm 1; Day 4	2.14 ± 0.14	30.43 ± 0.05	7.03	92.97
Ferm 1; Day 5	2.59 ± 0.30	33.20 ± 0.16	7.80	92.20

Ferm 1; Day 6	3.73 ± 0.21	48.19 ± 0.03	7.74	92.26
Ferm 1; Day 7	5.70 ± 0.13	88.08 ± 0.33	6.47	93.53
Ferm 1; Day 8	6.50 ± 0.24	90.39 ± 0.07	7.19	92.81
Ferm 1; Day 9	5.12 ± 0.41	61.00 ± 0.14	8.39	91.61
Percentage STDEV	**± 9.30**	**± 0.26**		
oxo-glutarate defined medium				
Ferm 1; Day 1	0.38 ± 0.08	6.93 ± 0.03	5.48	94.51
Ferm 1; Day 2	1.23 ± 0.21	9.16 ± 0.003	13.43	86.57
Ferm 1; Day 3	1.14 ± 0.11	12.20 ± 0.01	9.35	90.65
Ferm 1; Day 4	0.86 ± 0.08	12.36 ± 0.03	6.96	93.04
Ferm 1; Day 5	1.05 ± 0.37	18.02 ± 0.02	5.83	94.17
Ferm 1; Day 6	1.22 ± 0.01	27.02 ± 0.06	4.51	95.48
Ferm 1; Day 7	1.47 ± 0.04	32.86 ± 0.11	4.47	95.53
Ferm 1; Day 8	1.89 ± 0.06	39.71 ± 0.09	4.76	95.24
Ferm 1; Day 9	2.31 ± 0.21	45.88 ± 0.05	5.03	94.96
Ferm 1; Day 10	2.28 ± 0.10	46.74 ± 0.10	4.88	95.12
Ferm 1; Day 11	1.81 ± 0.31	38.75 ± 0.04	4.67	95.33
Ferm 1; Day 12	1.93 ± 0.38	45.86 ± 0.19	4.21	95.79
Percentage STDEV	**± 12.44**	**± 0.21**		
methyl oleate defined medium				
Ferm 1; Day 1	2.05 ± 0.38	50.77 ± 26.37	4.05	95.95
Ferm 2; Day 1	1.56 ± 0.77	42.06 ± 4.38	3.7	96.3
Ferm 3; Day 1	1.99 ± 0.45	60.23 ± 10.16	3.30	96.69
Ferm 1; Day 2	7.39 ± 1.12	152.36 ± 22.56	4.85	95.15
Ferm 2; Day 2	6.64 ± 0.38	76.27 ± 10.09	8.7	91.29
Ferm 3; Day 2	7.44 ± 0.37	166.23 ± 11.26	4.48	95.52
Ferm 1; Day 3	9.02 ± 0.40	162.41 ± 69.13	5.35	94.65
Ferm 2; Day 3	10.30 ± 0.79	183.84 ± 0.23	5.6	94.4
Ferm 3; Day 3	10.44 ± 0.12	166.99 ± 0.46	6.25	93.75
Ferm 1; Day 4	14.99 ± 0.06	306.87 ± 17.03	4.88	95.11
Ferm 2; Day 4	18.94 ± 2.52	271.3 ± 9.46	6.98	93.02
Ferm 3; Day 4	14.85 ± 0.16	355.66 ± 25.52	4.17	95.82
Ferm 1; Day 5	15.19 ± 1.42	287.73 ± 26.79	5.28	94.72
Ferm 2; Day 5	16.88 ± 2.02	290.39 ± 12.53	5.81	94.18
Ferm 3; Day 5	16.19 ± 0.11	299.38 ± 20.99	5.41	94.59
Ferm 1; Day 6	15.14 ± 2.70	253.91 ± 1.53	5.96	94.04
Ferm 2; Day 6	15.43 ± 1.20	202.45 ± 11.81	7.62	92.38
Ferm 3; Day 6	16.44 ± 0.92	258.99 ± 5.62	6.35	93.65
Ferm 1; Day 7	18.98 ± 0.69	252.84 ± 3.03	7.51	92.49
Ferm 2; Day 7	14.93 ± 1.62	217.95 ± 4.74	6.85	93.15
Ferm 3; Day 7	18.99 ± 0.74	233.37 ± 9.96	8.14	91.86
Ferm 1; Day 8	18.07 ± 2.73	241.405 ± 5.56	7.49	92.51
Ferm 2; Day 8	17.07 ± 1.48	241.3 ± 19.09	7.33	92.66
Ferm 3; Day 8	18.06 ± 0.99	236.94 ± 11.47	7.62	92.38
Ferm 1; Day 9	16.39 ± 0.11	252.49 ± 16.11	6.49	93.51
Ferm 2; Day 9	15.93 ± 1.59	196.4 ± 2.97	8.11	91.89
Ferm 3; Day 9	15.92 ± 0.09	244.99 ± 10.36	6.50	93.50
Ferm 1; Day 10	16.65 ± 0.18	22.23 ± 5.74	7.49	92.51
Ferm 2; Day 10	12.13 ± 0.81	221.3 ± 17.54	5.48	94.52
Ferm 3; Day 10	nd	nd	nd	Nd

Percentage STDEV	**± 9.11**	**± 9.34**		
***S. fradiae* C373-18 Industrial complex medium**				
Ferm 1; Day 1	3.92 ± 1.66	31.78 ± 1.66	27.86	12.33
Ferm 2; Day 1	1.73 ± 1.23	24.74 ± 2.58	23.01	6.99
Ferm 3; Day 1	0.53 ± 1.55	22.47 ± 3.12	21.94	2.36
Ferm 1; Day 2	8.73 ± 2.37	35.30 ± 1.97	26.57	24.73
Ferm 2; Day 2	4.72 ± 2.99	35.14 ± 1.55	30.42	13.43
Ferm 3; Day 2	5.93 ± 2.47	41.14 ± 1.84	35.21	14.41
Ferm 1; Day 3	6.86 ± 1.55	28.77 ± 2.94	21.91	23.84
Ferm 2; Day 3	7.14 ± 5.46	40.47 ± 4.19	33.33	17.64
Ferm 3; Day 3	9.99 ± 4.22	22.53 ± 1.95	12.54	44.34
Ferm 1; Day 4	7.06 ± 2.22	13.53 ± 0.70	6.47	52.18
Ferm 2; Day 4	8.51 ± 4.10	44.74 ± 2.46	36.23	19.02
Ferm 3; Day 4	7.07 ± 3.97	51.28 ± 1.44	44.21	13.78
Ferm 1; Day 5	10.86 ± 1.85	51.86 ± 1.40	41.00	20.94
Ferm 2; Day 5	11.39 ± 2.88	57.87 ± 1.62	46.48	19.68
Ferm 3; Day 5	12.47 ± 2.63	60.25 ± 2.89	47.78	20.70
Ferm 1; Day 6	16.53 ± 5.99	38.82 ± 50.17	22.29	42.58
Ferm 2; Day 6	17.51 ± 4.12	60.65 ± 3.19	43.14	28.87
Ferm 3; Day 6	18.47 ± 2.62	64.33 ± 4.48	45.86	28.71
Ferm 1; Day 7	25.39 ± 3.21	88.69 ± 3.47	63.30	28.63
Ferm 2; Day 7	20.47 ± 4.89	102.47 ± 2.33	82.00	19.98
Ferm 3; Day 7	19.91 ± 5.74	105.40 ± 10.28	85.49	18.89
Percentage STDEV	**± 48.47**	**± 12.11**		
***S. coelicolor* 1147 Glucose minimal medium**				
Ferm 1; Day 1	0.1 ± 0.1	0.1 ± 0.04	0	0
Ferm 2; Day 1	0.1 ± 0.01	0.1 ± 0.01	0	0
Ferm 1; Day 2	0.16 ± 0.11	7.5 ± 0.23	7.34	2.13
Ferm 2; Day 2	0.10 ± 0.09	1.9 ± 0.48	1.8	5.26
Ferm 1; Day 3	0.72 ± 0.04	27.5 ± 0.85	26.78	2.62
Ferm 2; Day 3	0.20 ± 0.02	30.23 ± 2.13	30.03	0.66
Ferm 1; Day 4	0.80 ± 0.09	24.8 ± 0.95	24.00	3.22
Ferm 2; Day 4	0.45 ± 0.10	10.23 ± 1.25	9.78	4.40
Ferm 1; Day 5	1.00 ± 0.04	15.00 ± 0.97	14.00	6.67
Ferm 2; Day 5	0.63 ± 0.03	9.01 ± 0.09	93.01	6.99
Percentage STDEV	**± 32.65**	**± 11.20**		

Dry weight measurements (Chapter 3, section 3.11.2) of samples taken from *S. fradiae* C373-10 and *S. coelicolor* 1147 cultured on a number of medium compositions (are illustrated in Figures 4.1 to 4.20). Fig 4.1 to 4.2, glucose minimal medium (fermentation 1 & 2 respectively); Fig 4.3, fructose; Fig 4.4 – 4.5, glycerol minimal medium (fermentation 1 & 2 respectively); Fig 4.5, oxo-glutarate minimal medium; Fig 4.6 – 4.10, glucose glutamate defined medium (fermentations 1, 2, 3 & 4 respectively); Fig 4.11 – 4.12, glucose oxo-glutarate defined medium (fermentations 1 & 2 respectively); Fig 4.13 –4.16, methyl oleate medium (Chapter 3, section 3.7)[fermentations 1, 2, & 3 respectively); Fig 4.17 – 4.20, complex medium (fermentation 1, 2, & 3 respectively) and *S. coelicolor* cultured on a glucose minimal medium. Dry weight and wet weight determinations were also expressed as percentage of wet weight (%) and the percentage water content of the biomass (%). Standard deviations (STDEV) were given as plus or minus the unit of measurement. All measurements are given in gl^{-1}, unless stated. nd, not determined or undetermined.

Table 4.12 Specific growth rate for bench top fermentations.

Fermentation / organism	Specific growth rate [calculated from biomass] (h^{-1})	Specific growth rate [calculated from DNA concentration] (h^{-1})	Reconciled specific growth rate [average] (h^{-1})	STDEV
***S. fradiae* C373-10**				
Glucose (Ferm 1)	0.018	0.033	0.025	± 0.007
Glucose (Ferm 2)	0.018	0.038	0.028	± 0.010
Mean percentage STDEV	**± 0**	**± 2.49**	**± 2.00**	
Glucose glutamate (Ferm 1)	0.018	0.072	0.045	± 0.027
Glucose glutamate (Ferm 2)	0.011	0.066	0.039	± 0.027
Glucose glutamate (Ferm 3)	0.014	0.067	0.041	± 0.026
Glucose glutamate (Ferm 4)	0.019	0.081	0.050	± 0.031
Mean percentage STDEV	**± 1.49**	**± 0.59**	**± 0.69**	
Glucose oxo-glutarate (Ferm 1)	0.018	0.029	0.023	± 0.005
Glucose oxo-glutarate (Ferm 2)	0.019	0.022	0.021	± 0.002
Mean percentage STDEV	**± 0.95**	**± 4.85**	**± 1.61**	
Glycerol (Ferm 1)	0.030	0.013	0.022	± 0.008
Glycerol (Ferm 2)	0.018	0.051	0.035	± 0.016
Mean percentage STDEV	**± 8.84**	**± 20.99**	**± 8.06**	
Fructose (Ferm 1)	0.019	0.030	0.024	± 0.005
Oxo-glutarate (Ferm 1)	0.008	0.024	0.016	± 0.008
Mean percentage STDEV	**± 14.40**	**± 3.92**	**± 7.07**	
MO (Ferm 1)	0.048	0.025	0.036	± 0.011
MO (Ferm 2)	0.048	0.019	0.034	± 0.014
MO (Ferm 3)	0.056	0.029	0.043	± 0.013
Mean percentage STDEV	**± 1.01**	**± 2.30**	**± 1.39**	
Industrial complex medium (Ferm 1)	0.017	nd	nd	Nd
Industrial complex medium (Ferm 2)	0.019	nd	nd	Nd
Industrial complex medium (Ferm 3)	0.028	nd	nd	Nd
Mean percentage STDEV	**± 3.05**	**nd**	**nd**	
***S. coelicolor* 1147**				
Glucose minimal medium (Ferm 1)	0.116	0.038	0.077	± 0.04
Glucose minimal medium (Ferm 2)	0.074	-1.07	-0.498	± 0.57
Mean percentage STDEV	**± 7.81**	**± -37.96**	**± 48.29**	

The specific growth rate (calculated as Chapter 3, section 3.11.3) for *S. coelicolor* 1147 and *S. fradiae* C373-10. dry weight and DNA concentration was determined as Chapter 3, section 3.11.2 & 3.19.2 respectively. Bench top fermentations were as Fig 4.1 - 4.20. Standard deviations (STDEV) were given as plus or minus the unit of measurement. The percentage was also presented for each method. All figures were given as h^{-1}. MO, methyl oleate defined medium (Chapter 3, section 3.7.2). nd, not determined.

Table 4.13 Part 1 (Part 1 & 2 companion tables) The change in total organic carbon analysis of t

Fermentation	Theoretical carbon source concentration converted to g of carbon (gl^{-1})	Dry weight biomass converted to g of carbon (gl^{-1})	Organic acids production converted to g of carbon (gl	
Glucose				
Ferm 1; Day 1	7.4	0.40	nd	
Ferm 2; Day 1	7.39	0.41	nd	
Ferm 1; Day 7	2.64	2.45	0.21	
Ferm 2; Day 7	2.43	1.86	0.25	
Glucose oxo-glutarate				
Ferm 1; Day 1	6.95	0.67	nd	
Ferm 2; Day 1	7.01	0.55	nd	
Ferm 1; Day 3	6.24	1.69	0.48	
Ferm 2; Day 3	5.47	2.12	0.22	
Ferm 1; Day 7	0.89	1.89	1.28	
Ferm 2; Day 7	1.12	2.49	0.79	
Glucose glutamate				
Ferm 1; Day 1	8.59	1.80	nd	
Ferm 2; Day 1	9.19	2.28	nd	
Ferm 3; Day 1	8.90	1.85	nd	
Ferm 4; Day 1	9.11	1.63	nd	
Ferm 1; Day 2	7.56	2.77	0.64	
Ferm 2; Day 2	7.53	2.95	0.39	
Ferm 3; Day 2	7.29	2.90	0.41	
Ferm 4; Day 2	7.38	2.88	0.13	
Ferm 1; Day 5	0.29	4.38	1.42	

Ferm 2; Day 5	0.97	4.41	1.46	
Ferm 3; Day 5	1.22	3.92	1.26	
Ferm 4; Day 5	1.38	4.47	1.41	
Glycerol				
Ferm 1; Day 1	13.50	0.70	nd	
Ferm 2; Day 1	12.25	0.17	nd	
Ferm 1; Day 7	0.059	4.11	0.89	
Ferm 2; Day 9	0.028	3.25	0.50	
Fructose				
Ferm 1; Day 1	9.72	0.58	nd	
Ferm 1; Day 8	0.304	3.01	0.14	
Oxo-glutarate				
Ferm 1; Day 1	65.45	0.16	nd	
Ferm 1; Day 10	2.91	0.99	1.89	

S. fradiae C373-10 was cultured on a number of different carbon sources and medium compositior *fradiae* were as followed (gl^{-1}) glucose (20.0), glucose (20.0) glutamate (5.0), glucose (20.0) oxo-glu Chapter 3, section 3.6.4]. The carbon concentration of the medium was converted to gl^{-1} of carbon c was termed the theoretical carbon content of the extracellular medium. Dry weight biomass was cc multiplying the dry weight determination for the time frame by the elemental carbon content determin 1). The total organic acids produced for the specific time frame were converted to g of carbon (gl recovery incorporating dry weights, organic acids and the appropriate carbon source were cc Measurements are the means of triplicate. nd, not determined or undetermined.

Table 4.13 Part 2 (Part 1 & 2 companion tables) The change in total carbon analysis of the extra

Fermentation	CER taken from chapter 6 and converted to gl^{-1}	The theoretical total carbon recovery incorporating dry weights, organic acids and appropriate carbon source (gl^{-1})	The theoretical total carbon recovery incorporating dry weights, organic acids and appropriate carbon source (gl^{-1}) plus the CER taken from chapter 6 and converted to gl^{-1}	TOCA of the extracellular medium (gl^{-1})	m t f a	
Glucose						
Ferm 1; Day 1	nd	nd	nd	9.63 ± 0.59*		
Ferm 2; Day 1	nd	nd	nd	8.62 ± 0.23*		
Ferm 1; Day 7	3.65	5.3	8.95	5.89 ± 0.66*		
Ferm 2; Day 7	2.98	4.54	7.52	4.11 ± 0.98*		
Glucose oxo-glutarate						
Ferm 1; Day 1	nd	nd	nd	8.75 ± 0.17*		
Ferm 2; Day 1	nd	nd	nd	7.96 ± 0.38*		
Ferm 1; Day 3	2.5	8.41	10.91	6.93 ± 0.51*		
Ferm 2; Day 3	2.85	7.81	10.66	7.28 ± 0.74*		
Ferm 1; Day 7	3.1	4.06	7.16	4.21 ± 0.63*		
Ferm 2; Day 7	3.11	4.4	7.51	3.52 ± 0.28*		
Glucose glutamate						
Ferm 1; Day 1	nd	nd	nd	10.01 ± 1.23*		
Ferm 2; Day 1	nd	nd	nd	11.45 ± 2.18*		
Ferm 3; Day 1	nd	nd	nd	9.97 ± 0.93*		
Ferm 4; Day 1	nd	nd	nd	10.08 ± 0.79*		
Ferm 1; Day 2	3.93	10.97	14.9	9.23 ± 1.45*		
Ferm 2; Day 2	3.93	10.87	14.8	9.99 ± 0.67*		
Ferm 3; Day 2	4.37	10.6	14.97	9.57 ± 0.82*		
Ferm 4; Day 2	3.97	10.39	14.36	9.74 ± 1.73*		

Ferm 1; Day 5	3.12	6.09	9.21	3.12 ± 0.13*		
Ferm 2; Day 5	3.66	6.84	10.5	2.97 ± 0.14*		
Ferm 3; Day 5	3.96	6.4	10.36	3.55 ±0.26*		
Ferm 4; Day 5	3.28	7.26	10.54	4.11 ± 0.99*		
Glycerol						
Ferm 1; Day 1	N/A	nd	nd	14.52 ± 1.11*		
Ferm 2; Day 1	N/A	nd	nd	13.69 ± 0.94*		
Ferm 1; Day 7	6.37	5.059	11.43	2.41 ± 0.15*		
Ferm 2; Day 9	6.08	3.778	9.86	3.97 ± 0.24*		
Fructose						
Ferm 1; Day 1	N/A	nd	nd	10.59 ± 1.55*		
Ferm 1; Day 8	4.5	3.454	7.95	2.16 ± 0.33*		
oxo-glutarate						
Ferm 1; Day 1	N/A	nd	nd	30.26 ± 1.09*		
Ferm 1; Day 10	23.45	5.79	29.24	6.85 ± 0.44*		

The carbon dioxide evolution rate (CER) was calculated in Chapter 6 and was presented as g of carbon (g
(TOCA) [as Chapter 3, section 3.15.5] was undertaken on the extracellular medium and expressed as g of ca
MOPS concentration (MOPS at a concentration of 25.0 gl^{-1} [FW = 209.3] accounts for 1.43 C.moles.l^{-1} or 17
the total carbon theoretical recovery incorporating determined dry weights, organic acids and the appropriate
frame and the CER was expressed as gl^{-1}. This should equal the initial input (indicated by underlined figure
calculated as the percentage difference between the total carbon recovery incorporating determined dry weights
carbon source for the specific time frame and the CER compared the TOCA and CER. Measurements were t
not determined or undetermined.

Table 4.14A Organic acids produced during an industrial process

Fermentation time (hrs)	10	34	58	82	106
Propionate (ppm)	0.0	0.0	0.0	17.9	0.0
Butyrate (ppm)	30.3	84.5	15.9	26.5	16.9
Pyruvate (ppm)	0.0	0.0	0.0	0.0	0.0
Chloride (ppm)	567.0	496.9	469.3	469.4	473.7
Nitrate (ppm)	10.8	24.1	17.7	22.1	16.6
Sulphate (ppm)	109.6	95.9	89.1	86.3	63.0
Phosphate (ppm)	67.6	34.5	27.6	24.9	37.8

Table 4.14A. Summary of other anion concentrations monitored by ion chromatography. *S. fradiae* C373-18 cultured on an industrial complex medium. Analysis undertaken internally by Eli Lilly Ltd. (Schreiweis, 1999).

Table 4.14B The anion content of process water

Fluoride	Butyrate	Chloride	Caproate	Nitrate	Sulphate
41.3	33.6	1575	0	189.7	6426

Table 4.14B. composition of process water used for fermentation media make up. Values are reported in parts per million. Analysis undertaken internally by Eli Lilly Ltd. (Schreiweis, 1999).

Table 4.15 Standard deviation of measurements in the average percentage (%) of values of all the analysis undertaken in the proceeding Chapter.

Standard Deviation of measurements in % of values		
Measurement	**Single sample**	**Between cultures**
Mass calculations		
Dry weights	1 - 20	1 - 20
Wet weights	0.1 - 1.2	0.1 - 1.1
Spin solids	0.02 - 0.22	0.09 - 0.26
Specific growth rate		
$\mu_{biomass}$	nd	7.81
μ_{DNA}	nd	37.96
Organic acids (HPLC)		
Acetate	1 - 10	1 - 10
Pyruvate	2 - 10	2 - 10
Oxo-glutarate	2 - 10	2 - 10
Malate	2 - 10	2 - 10
Lactate	2 - 10	2 - 10
Propionate	1 - 10	1 - 10
Butyrate	2 - 16	2 - 16
Fumarate	1 - 8	1 - 8
Carbon sources		
Glucose	2 - 8	1 -15
Glycerol	3 - 5	10 - 40
Fructose	2 - 6	nd
glutamate	4 - 5	0.8 - 20
Other extracellular medium components		
NH_4	2 - 7	6
PO_4	1.3 - 5	3 - 25
Oil	1 - 7	10 - 30
Antibiotic analysis		
Tylosin (HPLC)	3 - 4	3 - 5
Actinorhodin	2 - 3	2 - 4

Tabulated total standard deviation of single and between different cultures. All figures given in percentage (%) format. Analytical techniques used throughout out this work were as follows: dry weight (Chapter 3, section 3.11.2), wet weight (Chapter 3, section 3.11.1), spin solids, ammonia analysis (Chapter 3, section 3.22.5), phosphate (Chapter 3, section 3.22.4), oil residue (Chapter 3, section 3.14.1, 3.14.2, & 3.14.3), tylosin assay (Chapter 3, section 3.25.1), actinorhodin (Chapter 3, section 3.24), glucose assay (Chapter 3, section 3.22.2), glycerol assay (Chapter 3, section 3.19.4), glutamate assay (Chapter 3, section 3.22.3), organic acid analysis (Chapter 3, section 3.26) and the specific growth rate calculated by dry weight estimation ($\mu_{biomass}$) and DNA analysis (μ_{DNA}). nd; not undertaken.

Table 5.1 The effects of sample storage on the reproducibility of the macromolecular composition of *S. fradiae* biomass.

Fractionated immediately					
	CHO	**RNA**	**DNA**	**Protein**	**Lipid**
1	130.6	93.57	23.78	340.55	6.99
2	139.94	109.4	18.06	440.74	8.56
3	145.71	93.7	24.43	461.89	4.34
Mean	138.75	98.89	22.09	414.39	6.63
STDEV	**± 7.62**	**± 9.10**	**± 3.50**	**± 64.82**	**± 2.13**
Delayed cooling (left to sit at room temperature for 1 hr)					
1	146.77	56.9	25.78	562.78	7.74
2	130.90	34.56	28.67	355.89	6.74
3	129.34	10.75	32.89	447.67	2.33
Mean	135.67	34.07	29.11	455.45	5.60
STDEV	**± 9.64**	**± 23.08**	**± 3.58**	**± 103.66**	**± 2.88**
1 weeks					
1	122.23	98.85	32.15	499.23	2.34
2	110.56	125.28	34.85	323.16	9.99
3	189.63	156.23	12.35	424.36	6.74
Mean	140.81	126.79	26.45	415.58	6.36
STDEV	**± 42.68**	**± 28.72**	**± 12.28**	**± 88.36**	**± 3.84**
2 weeks					
1	156.75	60.96	12.67	301.97	2.76
2	123.45	111.45	36.89	358.89	6.34
3	216.78	113.67	40.99	369.78	7.65
Mean	165.66	95.36	30.18	343.54	5.58
STDEV	**± 47.30**	**± 29.81**	**± 15.30**	**± 36.42**	**± 2.53**
6 weeks					
1	156.24	93.24	24.56	365.99	5.68

2	144.62	89.24	58.69	440.28	6.87
3	176.84	75.21	11.23	590.24	9.89
Mean	159.23	85.90	31.49	465.50	7.48
STDEV	**± 16.32**	**± 9.47**	**± 24.48**	**± 114.23**	**± 2.17**
12 weeks					
1	147.52	110.28	34.52	510.54	6.53
2	220.34	98.52	25.62	491.92	7.74
3	123.67	93.21	21.58	341.25	8.96
Mean	163.84	100.67	27.24	447.90	7.74
STDEV	**± 50.36**	**± 8.73**	**± 6.62**	**± 92.83**	**± 1.21**
Fractionated immediately and stored reanalysed at 12th week					
1	174.52	95.26	35.64	351.62	5.34
2	210.98	98.74	34.26	364.59	6.89
3	189.52	110.23	46.34	410.23	9.68
Mean	191.67	101.41	38.75	375.48	7.30
STDEV	**± 18.32**	**± 7.83**	**± 5.40**	**± 30.78**	**± 2.20**
Total percentage STDEV	**± 15.37**	**± 12.93**	**± 26.53**	**± 10.87**	**± 24.85**

Biomass was obtained from a 2.5 L fermentation cultured on a glucose glutamate defined medium (Chapter 3, section 3.6.4). In order to eliminate carry-over of any unknown components from the complex vegetative medium (Chapter 3, section 3.5.1). The appropriate a training medium was inoculated with 10 % of the vegetative culture and this was used to inoculate the production medium [10 % inoculum]. Biomass was harvested at 72 hrs after inoculation. Each washed sample pellet was divided into 18 samples of approximate equal weight samples (1 g wet weight) which were fractionated using extraction method 1 (Chapter 3, section 3.16.1; all solutions were filtered and the residue biomass washed back in to the following step) at a concentration of 100 $mg.ml^{-1}$ (wet weight) after storage at -70^{0} C for the quoted time period. The resulting fractions were analysed in triplicate for the macromolecular content by the appropriate assay. Carbohydrate, the anthrone assay (Chapter 3, section 3.18.1); DNA, the diphenylamine assay (Chapter 3, section 3.19.2); RNA, the orcinol assay (Chapter 3, section 3.19.4); protein, the ninhydrin assay (Chapter 3, section 3.20.6); lipid, the vanillin assay (Chapter 3, section 3.23.1). All figures were expressed as $mg.g^{-1}$ dry weight biomass (the macromolecular composition was calculated by working out a weighting coefficient between the wet weight [Chapter 3, section 3.11.1] and dry weight [Chapter 3, section 3.11.2] biomass determinations). nd, not determined; STDEV, standard deviation. Standard deviations were given as plus or minus the given unit.

Table 5.2 Part 1. (Table 5.3 Parts 1, 2 & 3 companion tables) Comparison of four different macromolecular extraction protocols (Methods 1, 2, & 3) on *S. fradiae* C373-10 biomass.

Extraction method	DNA Method 1 (Fraction 2)	RNA Method 1 (Fraction 2)	Bradford assay Method 1 (Fraction 3 & 4)	Ninhydrin assay for total amino acids Method 1 (fraction 3 & 4)
Fermentation time frame				
24	16.33 ± 61.23	30.45 ± 12.78	30.25 ± 111.63	141.23 ± 99.96
24	8.33 ± 47.22	47.58 ± 28.47	56.84 ± 121.47	157.86 ± 102.35
24	10.34 ± 54.32	64.52 ± 36.52	45.68 ± 104.36	211.75 ± 54.63
Mean STDEV	**11.67 ± 54.26**	**47.52 ± 25.92**	**44.26 ± 112.49**	**170.28 ± 85.65**
48	8.64 ± 41.17	48.79 ± 14.15	87.95 ± 98.75	258.97 ± 65.97
48	9.66 ± 35.68	54.62 ± 24.51	90.65 ± 47.56	296.53 ± 85.47
48	12.88 ± 26.69	66.58 ± 28.97	60.53 ± 85.26	286.45 ± 103.91
Mean STDEV	**10.39 ± 34.51**	**56.66 ± 22.54**	**79.71 ± 77.19**	**280.65 ± 85.12**
72	15.46 ± 27.79	106.58 ± 19.96	88.56 ± 25.98	312.65 ± 12.65
72	18.59 ± 25.52	112.65 ± 27.58	90.12 ± 36.45	356.98 ± 26.35
72	21.36 ± 62.28	130.78 ± 34.61	55.28 ± 42.78	368.41 ± 56.92
Mean STDEV	**18.47 ± 38.53**	**116.67 ± 27.38**	**77.99 ± 35.07**	**346.01 ± 27.76**
96	30.96 ± 29.97	156.89 ± 45.69	157.89 ± 147.52	412.89 ± 97.77
96	35.26 ± 14.48	136.87 ± 24.67	122.69 ± 136.92	457.62 ± 85.23
96	40.12 ± 45.56	126.52 ± 37.89	130.84 ± 55.85	488.97 ± 46.24
Mean STDEV	**35.45 ± 30.00**	**140.09 ± 36.08**	**137.14 ± 113.43**	**453.16 ± 76.41**
120	42.16 ± 27.87	60.52 ± 62.31	189.62 ± 95.26	499.51 ± 54.44
120	45.89 ± 21.21	47.89 ± 39.95	190.99 ± 54.98	512.36 ± 67.52
120	46.27 ± 34.63	23.64 ± 25.47	211.23 ± 47.89	487.26 ± 82.22

Mean STDEV	**44.77 ± 27.90**	**44.02 ± 42.58**	**197.28 ± 66.04**	**499.71 ± 68.06**
Total Mean % STDEV	**± 236.00**	**± 47.85**	**± 106.28**	**± 24.53**

Five individual *S. fradiae* C373-10 cultured to set time points (24, 48, 72, 96, & 120 hrs) were grown in a 2.5 L bioreactor vessel on a glucose glutamate defined medium (Chapter 3, section 3.6.4) for each time frame. In order to eliminate carry-over of unknown components from the complex vegetative medium (Chapter 3, section 3.5.1). The appropriate seed training medium was inoculated with 10 % of the vegetative culture and this was used to inoculate the production medium [10 % incolumn]. The pooled biomass was separated into 12 lots of 1 g wet weight biomass for each time frame and further separated into triplicate sample lots. Each triplicate of samples was fractionated with methods 1, 2 & 3 (as Chapter 3, section 3.16.1, 3.16.2 & 3.16.3 respectively). The macromolecular content of each fraction were determined as follows DNA, diphenylamine assay (Chapter 3, section 3.19.2); RNA, orcinol assay (Chapter 3, section 3.19.4); Protein, the Bradford assay and the ninhydrin assay (Chapter 3, section 3.20.1 and 3.20.6). All values were expressed as $mg.g^{-1}$ dry weight biomass (dry wt was calculated by working out a weighting coefficient between wet weight [Chapter 3, section 3.11.1] and dry weight [Chapter 3, section 3.11.2] biomass determinations) and were denoted by means of plus / minus their standard deviations. The means between triplicate fractionated samples were obtained from biomass harvested at the same time period. The total Mean percentage (%) standard deviation was also presented for each assay. nd, not determined; STDEV, standard deviation.

Table 5.2 Part 2. (Table 5.3 Parts 1, 2 & 3 companion tables) Comparison of four different macromolecular extraction protocols (Methods 1, 2 & 3) on *S. fradiae* C373-10 biomass.

Extraction method	DNA Method 2 (Fraction 2 & 3)	RNA Method 2 (Fraction 2 & 3)	Bradford assay Method 2 (Fraction 4 & 5)	Ninhydrin assay for total amino acids Method 2 (fraction 4 & 5)
Fermentation time frame				
24	18.39 ± 19.78	32.87 ± 14.79	21.26 ± 9.85	111.99 ± 122.17
24	15.56 ± 21.56	51.27 ± 20.62	41.79 ± 51.23	145.67 ± 58.88
24	21.52 ± 30.33	68.92 ± 37.97	13.96 ± 66.99	175.92 ± 89.97
Mean STDEV	**18.49 ± 23.89**	**51.02 ± 24.46**	**25.67 ± 176.02**	**144.53 ± 90.34**
48	17.77 ± 41.52	74.46 ± 41.11	75.82 ± 25.69	221.63 ± 126.98
48	19.63 ± 27.78	62.23 ± 51.13	60.21 ± 44.74	288.97 ± 174.62
48	15.52 ± 13.63	72.26 ± 37.97	36.95 ± 46.93	254.78 ± 55.29
Mean STDEV	**17.64 ± 27.64**	**69.65 ± 43.40**	**57.66 ± 39.12**	**255.13 ± 118.96**
72	22.63 ± 28.56	122.36 ± 65.67	80.45 ± 11.68	333.66 ± 101.78
72	24.96 ± 34.58	110.96 ± 39.99	50.16 ± 28.96	384.72 ± 97.98
72	25.53 ± 47.79	104.52 ± 43.33	66.24 ± 36.36	398.56 ± 65.23
Mean STDEV	**24.37 ± 36.98**	**112.61 ± 49.66**	**65.62 ± 25.67**	**372.31 ± 88.33**
96	35.69 ± 12.66	166.33 ± 102.67	144.45 ± 55.28	423.96 ± 150.64
96	41.23 ± 18.97	144.74 ± 65.32	110.33 ± 65.27	469.12 ± 106.36
96	42.26 ± 22.74	122.68 ± 87.79	103.67 ± 29.84	498.28 ± 99.99
Mean STDEV	**39.73 ± 18.12**	**144.58 ± 85.26**	**119.48 ± 50.13**	**463.79 ± 118.99**
120	51.12 ± 42.11	51.68 ± 24.21	199.64 ± 52.89	487.52 ± 59.98
120	55.66 ± 16.45	20.36 ± 18.67	155.43 ± 65.22	444.27 ± 61.12
120	59.97 ± 18.18	39.98 ± 19.93	204.16 ± 82.16	488.96 ± 57.78

Mean STDEV	**55.58 ± 25.58**	**37.34 ± 20.94**	**186.41 ± 66.76**	**473.58 ± 59.63**
Total Mean % STDEV	**± 105.44**	**± 54.88**	**± 105.82**	**± 34.98**

Five individual *S. fradiae* C373-10 cultured to set time points (24, 48, 72, 96, & 120 hrs) were grown in a 2.5 L bioreactor vessel on a glucose glutamate defined medium (Chapter 3, section 3.6.4) for each time frame. In order to eliminate carry-over of unknown components from the complex vegetative medium (Chapter 3, section 3.5.1). The appropriate seed training medium was inoculated with 10 % of the vegetative culture and this was used to inoculate the production medium [10 % incolumn]. The pooled biomass was separated into 12 lots of 1 g wet weight biomass for each time frame and further separated into triplicate sample lots. Each triplicate of samples was fractionated with methods 1, 2 & 3 (as Chapter 3, section 3.16.1, 3.16.2 & 3.16.3 respectively). The macromolecular content of each fraction were determined as follows DNA, diphenylamine assay (Chapter 3, section 3.19.2); RNA, orcinol assay (Chapter 3, section 3.19.4); Protein, the Bradford assay and the ninhydrin assay (Chapter 3, section 3.20.1 and 3.20.6). All values were expressed as $mg.g^{-1}$ dry weight biomass (dry wt was calculated by working out a weighting coefficient between wet weight [Chapter 3, section 3.11.1] and dry weight [Chapter 3, section 3.11.2] biomass determinations) and were denoted by means of plus / minus their standard deviations. The means between triplicate fractionated samples were obtained from biomass harvested at the same time period. The total Mean percentage (%) standard deviation was also presented for each assay. nd, not determined; STDEV, standard deviation.

Table 5.2 Part 3. (Table 5.3 Parts 1, 2 & 3 companion tables) Comparison of four different macromolecular extraction protocols (Methods 1, 2 & 3) on *S. fradiae* C373-10 biomass.

Extraction method	Method 3, DNA	Method 3, RNA	Method 3, Protein Lowry assay	Ninhydrin assay for total amino acids Method 3
Fermentation time frame				
24	14.79 ± 4.56	41.89 ± 20.19	30.68 ± 18.96	189.75 ± 95.52
24	8.46 ± 3.62	22.87 ± 14.43	40.19 ± 26.36	12.66 ± 84.75
24	6.92 ± 1.47	12.69 ± 2.36	92.26 ± 34.18	154.77 ± 52.32
Mean STDEV	**10.05 ± 3.22**	**25.82 ± 145.66**	**54.38 ± 26.50**	**119.06 ± 77.53**
48	9.95 ± 4.78	50.97 ± 20.98	101.46 ± 69.96	297.88 ± 150.42
48	10.16 ± 3.97	41.26 ± 27.79	115.68 ± 70.19	155.79 ± 97.73
48	4.69 ± 1.45	14.96 ± 36.86	87.77 ± 50.12	216.66 ± 52.26
Mean STDEV	**8.27 ± 3.40**	**35.73 ± 195.21**	**101.64 ± 63.42**	**223.44 ± 166.80**
72	20.16 ± 9.68	89.94 ± 62.24	84.43 ± 30.25	333.18 ± 187.96
72	18.97 ± 6.56	54.66 ± 36.98	97.77 ± 34.49	267.97 ± 147.52
72	25.64 ± 10.77	108.82 ± 44.17	107.93 ± 54.28	211.69 ± 42.26
Mean STDEV	**21.59 ± 9.00**	**84.47 ± 314.46**	**96.71 ± 39.67**	**270.95 ± 125.91**
96	35.62 ± 15.52	126.67 ± 39.65	114.79 ± 52.26	456.92 ± 54.63
96	27.89 ± 19.93	168.99 ± 41.17	157.93 ± 57.98	287.96 ± 94.85
96	12.99 ± 17.27	154.73 ± 54.89	211.39 ± 66.93	444.34 ± 79.58
Mean STDEV	**25.50 ± 17.54**	**150.13 ± 45.27**	**161.37 ± 59.06**	**396.41 ± 76.35**
120	41.79 ± 20.16	85.55 ± 65.28	198.98 ± 47.72	487.93 ± 52.24
120	34.44 ± 14.42	26.93 ± 31.47	256.65 ± 101.48	511.30 ± 24.79
120	41.19 ± 17.73	54.76 ± 28.69	277.64 ± 97.85	499.77 ± 87.78

Mean STDEV	**39.14 ± 17.44**	**55.75 ± 41.81**	**244.42 ± 82.35**	**499.67 ± 54.94**
Total Mean % STDEV	**± 47.34**	**± 129.34**	**± 45.49**	**± 66.74**

Five individual *S. fradiae* C373-10 cultured to set time points (24, 48, 72, 96, & 120 hrs) were grown in a 2.5 L bioreactor vessel on a glucose glutamate defined medium (Chapter 3, section 3.6.4) for each time frame. In order to eliminate carry-over of unknown components from the complex vegetative medium (Chapter 3, section 3.5.1). The appropriate seed training medium was inoculated with 10 % of the vegetative culture and this was used to inoculate the production medium [10 % incolumn]. The pooled biomass was separated into 12 lots of 1 g wet weight biomass for each time frame and further separated into triplicate sample lots. Each triplicate of samples was fractionated with methods 1, 2 & 3 (as Chapter 3, section 3.16.1, 3.16.2 & 3.16.3 respectively). The macromolecular content of each fraction were determined as follows DNA, diphenylamine assay (Chapter 3, section 3.19.2); RNA, orcinol assay (Chapter 3, section 3.19.4); Protein, the Lowry assay and the ninhydrin assay (Chapter 3, section 3.20.2 and 3.20.6). All values were expressed as $mg.g^{-1}$ dry weight biomass (dry wt was calculated by working out a weighting coefficient between wet weight [Chapter 3, section 3.11.1] and dry weight [Chapter 3, section 3.11.2] biomass determinations) and were denoted by means of plus / minus their standard deviations. The means between triplicate fractionated samples were obtained from biomass harvested at the same time period. The total Mean percentage (%) standard deviation was also presented for each assay. nd, not determined; STDEV, standard deviation.

Table 5.3 The effects of NaOH concentrations and incubation conditions on protein extraction efficiency.

Sample number	Bradford assay	(%)	Ninhydrin assay	(%)
1 M NaOH for 90 minutes at 30^0 C				
1	108.81	10.88	432.13	43.21
2	109.02	10.90	424.56	42.46
3	108.99	10.90	411.86	41.19
STDEV	**± 0.113**	**± 0.01**	**± 10.24**	**± 1.02**
1 M NaOH for 30 minutes at 100^0 C				
1	115.26	11.53	467.82	46.78
2	133.91	13.39	425.98	42.60
3	110.24	11.02	511.22	51.12
STDEV	**± 12.47**	**± 1.25**	**± 42.62**	**± 4.26**
0.5 M NaOH for 24 hrs at 37^0 C				
1	139.12	13.91	499.22	49.92
2	123.48	12.35	511.46	51.15
3	151.98	15.20	489.76	48.99
STDEV	**± 14.27**	**± 1.43**	**± 10.88**	**± 1.09**
0.5 M NaOH for 48 hrs at 37^0 C				
1	144.56	14.46	474.89	47.49
2	134.77	13.48	498.12	49.81
3	156.89	15.69	467.45	46.74
STDEV	**± 11.08**	**± 1.11**	**± 15.99**	**± 1.60**

Biomass obtained from three shake flask (2 L erlenmeyer flasks with 500 ml of medium) cultures of *S. fradiae* C373-10 grown on a glucose minimal medium (Chapter 3, section 3.6.4) and harvested at 72 hrs after inoculation. In order to eliminate carry-over of any unknown components from the complex vegetative medium (Chapter 3, section 3.5.1). The appropriate a training medium was inoculated with 10 % of the vegetative culture and this was used to inoculate the production medium [10 % inoculum]. Each washed sample pellet was divided into 18 samples of approximate equal wet weight (1 g wet weight) which were fractionated using macromolecular extraction method 1 (Chapter 3, section 3.16.1; all solutions were filtered and the residue biomass washed back in to the following step) at a concentration of 100 $mg.ml^{-1}$ (wet weight) and stored at -70^0 C. Changes were made to the alkali fractionation procedure i.e., one set of triplicates was extracted with 1 M NaOH for 90 mins at 30^0 C, the second set triplicates was extracted with 1 M NaOH for 30 min at 100^0 C, the third set of triplicates was extracted with 0.5 M NaOH for 24 hrs and the fourth set of triplicates was extracted with 0.5 M NaOH for 48 hrs. The resulting alkali fractions were then analysed in triplicate for their protein content with the Bradford assay (Chapter 3, section 3.20.1) and the ninhydrin assay (Chapter 3, section 3.20.6). All figures were expressed as $mg.g^{-1}$ dry weight biomass and converted to percentage format (the macromolecular composition was calculated by working out a weighting coefficient between the wet weight [Chapter 3, section 3.11.1] and dry weight [Chapter 3, section 3.11.2] biomass determinations). nd, not determined ; STDEV, standard deviation. STDEVs were given as plus the minus the unit of measurement.

Table 5.4 The extraction and quantification of macromolecular concentrations of *S. fradiae* C373-10 biomass cultured on a glucose minimal medium using macromolecular extraction method 1 (non-filtered extraction technique was used).

Fermentation / time (days)	CHO	RNA	DNA	Protein	Lipid	Total percentage cellular composition (%)
Ferm 1; Day 1	26.54 ± 40.12	27.88 ± 16.24	0.52 ± 0.55	99.57 ± 36.95	3.68 ± 1.16	15.82
Ferm 2; Day 1	37.66 ± 60.23	63.83 ± 19.85	0.68 ± 0.89	182.82 ± 74.52	4.66 ± 2.88	28.96
Mean STDEV	**32.1 ± 50.17**	**45.85 ± 18.04**	**0.60 ± 0.72**	**141.19 ± 55.73**	**4.17 ± 2.02**	**22.39**
Ferm 1; Day 2	90.12 ± 48.79	69.95± 45.26	0.74 ± 0.21	100.23 ± 12.38	7.20 ± 1.56	26.82
Ferm 2; Day 2	62.35 ± 69.69	74.52 ± 6.52	0.98 ± 0.36	95.62 ± 28.97	5.05 ± 8.99	23.85
Mean STDEV	**76.23 ± 59.24**	**72.23 ± 25.89**	**0.86 ± 0.28**	**97.92 ± 20.67**	**6.12 ± 5.27**	**25.34**
Ferm 1; Day 3	155.62 ± 102.36	106.23 ± 48.79	0.98 ± 0.29	194.52 ± 115.26	6.25 ± 9.99	46.36
Ferm 2; Day 3	124.98 ± 42.31	87.54 ± 27.58	1.06 ± 0.54	216.23 ± 66.58	4.16 ± 12.13	43.40
Mean STDEV	**140.3 ± 72.33**	**96.88 ± 38.18**	**1.02 ± 0.41**	**205.37 ± 90.92**	**5.20 ± 11.06**	**44.88**
Ferm 1; Day 4	187.34 ± 102.34	98.08 ± 40.12	0.93 ± 0.19	313.26 ± 44.51	15.62 ± 4.85	61.52
Ferm 2; Day 4	167.27 ± 110.17	81.37 ± 9.94	1.64 ± 0.07	274.59 ± 19.82	6.24 ± 6.88	53.11
Mean STDEV	**177.30 ± 106.25**	**89.72 ± 25.03**	**1.28 ± 0.13**	**293.92 ± 32.16**	**10.93 ± 5.86**	**57.32**
Ferm 1; Day 5	180.85 ± 81.70	99.04 ± 4.93	1.80 ± 0.28	253.80 ± 16.34	5.02 ± 7.89	54.05
Ferm 2; Day 5	96.49 ± 53.77	87.36 ± 5.01	1.82 ± 0.23	246.06 ± 33.33	7.08 ± 12.63	43.88
Mean STDEV	**138.67 ± 67.73**	**93.2 ± 4.97**	**1.81 ± 0.25**	**249.93 ± 24.83**	**6.05 ± 10.26**	**48.97**
Ferm 1; Day 6	111.67 ± 72.62	61.84 ± 14.79	1.88 ± 0.54	193.53 ± 16.58	9.89 ± 15.26	37.88
Ferm 2; Day 6	115.77 ± 64.27	66.78 ± 29.03	2.09 ± 0.41	240.69 ± 23.38	9.61 ± 1.45	43.49
Mean STDEV	**113.72 ± 68.44**	**64.31 ± 21.91**	**1.98 ± 0.47**	**217.11 ± 19.98**	**9.75 ± 8.35**	**40.69**
Ferm 1; Day 7	142.96 ± 64.72	147.62 ± 21.48	16.12 ± 9.53	306.24 ± 33.71	12.63 ± 30.21	62.56
Ferm 2; Day 7	104.24 ± 83.99	68.85 ± 15.43	1.67 ± 0.38	273.69 ± 78.92	12.51 ± 12.13	46.10

Mean STDEV	**123.6 ± 74.35**	**108.23 ± 18.45**	**8.89 ± 4.95**	**289.96 ± 56.31**	**12.57± 21.17**	**54.33**
Ferm 1; Day 8	104.71 ± 37.16	81.16 ± 8.13	1.83 ± 0.28	136.38 ± 10.96	13.59 ± 2.96	33.77
Ferm 2; Day 8	41.14 ± 78.24	51.49 ± 51.55	1.26 ± 0.29	266.07 ± 4.31	14.56 ± 12.86	37.45
Mean STDEV	**72.92 ± 57.70**	**66.32 ± 29.84**	**1.54 ± 0.28**	**201.22 ± 7.63**	**14.07 ± 7.91**	**35.61**
Total Mean percentage STDEV	**± 74.55**	**± 30.50**	**± 36.72**	**± 19.12**	**± 108.71**	

Biomass was obtained from a *S. fradiae* C373-10 fermentation cultured on a glucose minimal medium [7 L bioreactor vessel](Chapter 3, section 3.6.4). In order to eliminate carry-over of any unknown components from the complex vegetative medium (Chapter 3, section 3.5.1). The appropriate seed training medium (cultured in a 4 L fernbach shake flask with 700 ml of medium) was inoculated with 10 % of the vegetative culture and was used to inoculate the production medium [10 % incolumn]. All cultures were cultivated under the same conditions (30^0 C, 400 rpm). The biomass was harvested at 0, 24, 48, 72, 96, 120, 144, and 168 hrs after inoculation. Pooled samples were centrifuged down to a pellet and washed with dH_2O. Each washed sample pellet was divided into triplicate samples of approximate equal wet weight, which was fractionated with method 1 (Chapter 3, section 3.16.1) at a concentration of 100 $mg.ml^{-1}$ (wet weight) and stored at -70^0 C. The resulting fractions were analysed in triplicate for macromolecular content by the appropriate assay. Carbohydrate, the anthrone assay (Chapter 3, section 3.18.1); DNA, the diphenylamine assay (Chapter 3, section 3.19.2); RNA, the orcinol assay (Chapter 3, section 3.19.4); protein, the ninhydrin assay (Chapter 3, section 3.20.6); lipid, the vanillin assay (Chapter 3, section 3.23.1). The means were obtained from biomass samples harvested at the same time period. All figures were expressed as $mg.g^{-1}$ dry weight biomass (the macromolecular composition was calculated by working out a weighting coefficient between the wet weight [Chapter 3, section 3.11.1] and dry weight [Chapter 3, section 3.11.2] biomass determinations). CHO, carbohydrate, RNA, ribonucleic acid; DNA, deoxyribonucleic acid; nd, not determined; STDEV, standard deviation. Standard deviations were given as plus or minus the unit of measurement. The total cellular composition was calculated as followed ([DNA + RNA + CHO + protein + lipid]/10). The total Mean percentage STDEV was also presented for each assay.

Table 5.5 The extraction and quantification of macromolecular concentrations of *S. fradiae* C373-10 biomass cultured on a glucose glutamate defined medium using macromolecular extraction method 1 (all solutions were filtered and the residue biomass washed back into the following step).

Fermentation / time (days)	CHO	RNA	DNA	Protein	Lipid	Total cellular composition (%)
Ferm 1; Day 1	50.65 ± 9.96	8.69 ± 14.52	3.62 ± 18.32	18.89 ± 3.12	12.83 ± 1.44	9.47
Ferm 2; Day 1	36.75 ± 6.76	5.74 ± 28.61	2.96 ± 4.26	22.28 ± 6.25	6.59 ± 2.87	7.43
Ferm 3; Day 1	57.25 ± 45.12	10.63 ± 42.11	4.03 ± 9.94	56.31 ± 8.24	12.54 ± 15.64	14.08
Ferm 4; Day 1	69.3 ± 10.60	9.42 ± 57.18	3.58 ± 12.57	30.21 ± 9.69	18.02 ± 25.67	13.05
Mean STDEV	**53.49 ± 18.11**	**8.62 ± 35.60**	**3.55 ± 11.27**	**31.92 ± 6.82**	**12.49 ± 11.40**	**11.01**
Ferm 1; Day 2	107.85 ± 12.56	47.04 ± 17.89	22.74 ± 22.63	218.98 ± 58.12	39.84 ± 14.84	43.65
Ferm 2; Day 2	112.59 ± 14.69	59.95 ± 21.49	16.11 ± 21.54	82.98 ± 16.32	40.23 ± 28.95	31.19
Ferm 3; Day 2	133.04 ± 18.56	78.53 ± 26.39	23.00 ± 2.85	156.61 ± 20.13	58.84 ± 32.16	45.00
Ferm 4; Day 2	151.99 ± 21.36	99.82 ± 54.23	28.42 ± 1.13	259.91 ± 85.62	22.93 ± 87.96	56.31
Mean STDEV	**126.37 ± 16.79**	**71.33 ± 30.00**	**22.57 ± 12.04**	**179.62 ± 45.05**	**40.46 ± 40.98**	**44.04**
Ferm 1; Day 3	96.03 ± 2.86	75.41 ± 12.45	30.46 ± 16.32	292.89 ± 19.63	52.14 ± 21.57	40.97
Ferm 2; Day 3	124.00 ± 1.44	47.21 ± 23.67	32.34 ± 12.54	119.58 ± 15.26	50.94 ± 2.96	37.41
Ferm 3; Day 3	100.42 ± 8.95	90.47 ± 42.10	29.92 ± 18.97	266.15 ± 12.37	40.72 ± 3.62	52.77
Ferm 4; Day 3	89.23 ± 4.12	76.79 ± 28.79	43.07 ± 19.95	240.92 ± 18.95	21.59 ± 33.68	47.16
Mean STDEV	**102.42 ± 4.35**	**72.47 ± 26.75**	**33.95 ± 16.94**	**229.88 ± 16.55**	**41.35 ± 15.46**	**44.58**
Ferm 1; Day 4	107.41 ± 5.96	77.15 ± 10.24	45.96 ± 24.63	367.39 ± 72.11	90.23 ± 45.62	68.81
Ferm 2; Day 4	104.29 ± 6.83	62.98 ± 9.98	35.40 ± 22.54	205.40 ± 12.96	87.10 ± 23.58	49.52
Ferm 3; Day 4	106.07 ± 12.56	82.46 ±2.14	48.43 ± 21.36	349.34 ± 52.13	99.87 ± 11.37	68.62
Ferm 4; Day 4	nd	nd	nd	nd	nd	nd
Mean STDEV	**105.92 ± 8.45**	**74.20 ± 7.45**	**43.26 ± 22.84**	**307.38 ± 45.73**	**92.40 ± 26.86**	**62.32**
Ferm 1; Day 5	87.53 ± 24.57	59.91 ± 40.63	44.99 ± 7.58	358.10 ± 15.62	117.63 ± 47.85	66.82
Ferm 2; Day 5	91.75 ± 36.89	51.04 ± 39.65	37.91 ± 16.95	452.36 ± 33.89	152.36 ± 56.32	78.54
Ferm 3; Day 5	167.43 ± 47.52	74.35 ± 74.52	63.57 ± 12.35	240.31 ± 35.62	123.12 ± 11.25	66.88

Ferm 4; Day 5	64.24 ± 39.74	45.77 ± 12.48	43.28 ± 2.11	512.46 ± 10.51	196.87 ± 9.26	86.26
Mean STDEV	**102.74 ± 37.18**	**57.77 ± 41.82**	**47.44 ± 9.75**	**390.81 ± 23.91**	**147.49 ± 31.17**	**74.62**
Ferm 1; Day 6	63.02 ± 12.56	82.11 ± 25.64	63.96 ± 12.36	153.42 ± 12.36	62.78 ± 1.32	42.53
Ferm 2; Day 6	153.68 ± 18.97	86.20 ± 28.95	111.68 ± 14.52	534.77 ± 14.52	115.67 ± 6.58	100.20
Ferm 3; Day 6	80.28 ± 21.45	69.71 ± 34.13	65.66 ± 19.85	308.09 ± 19.85	124.115 ± 14.38	64.79
Ferm 4; Day 6	74.05 ± 58.79	52.47 ± 21.34	46.00 ± 20.54	211.93 ± 20.54	150.11 ± 17.59	53.46
Mean STDEV	**92.76 ± 52.94**	**72.62 ± 27.51**	**71.82 ± 16.82**	**302.05 ± 16.82**	**113.17 ± 9.97**	**65.24**
Total Mean percentage STDEV	**± 23.31**	**± 105.26**	**± 88.67**	**± 13.52**	**± 54.55**	

Biomass was obtained from a *S. fradiae* C373-10 fermentation cultured on a glucose minimal medium [7 L bioreactor vessel](Chapter 3, section 3.6.4). In order to eliminate carry-over of any unknown components from the complex vegetative medium (Chapter 3, section 3.5.1). The appropriate seed training medium (cultured in a 4 L fernbach shake flask with 700 ml of medium) was inoculated with 10 % of the vegetative culture and was used to inoculate the production medium [10 % incolumn]. All cultures were cultivated under the same conditions (30^0 C, 400 rpm). The biomass was harvested at 0, 24, 48, 72, 96, 120, 144, and 168 hrs after inoculation. Pooled samples were centrifuged down to a pellet and washed with dH_2O. Each washed sample pellet was divided into triplicate samples of approximate equal wet weight, which was fractionated with method 1 (Chapter 3, section 3.16.1; all solutions were filtered and the residue biomass washed back into following step) at a concentration of 100 $mg.ml^{-1}$ (wet weight) and stored at -70^0 C. The resulting fractions were analysed in triplicate for macromolecular content by the appropriate assay. Carbohydrate, the anthrone assay (Chapter 3, section 3.18.1); DNA, the diphenylamine assay (Chapter 3, section 3.19.2); RNA, the orcinol assay (Chapter 3, section 3.19.4); protein, the ninhydrin assay (Chapter 3, section 3.20.6); lipid, the vanillin assay (Chapter 3, section 3.23.1). The means were obtained from biomass samples harvested at the same time period. All figures were expressed as $mg.g^{-1}$ dry weight biomass (the macromolecular composition was calculated by working out a weighting coefficient between the wet weight [Chapter 3, section 3.11.1] and dry weight [Chapter 3, section 3.11.2] biomass determinations). CHO, carbohydrate, RNA, ribonucleic acid; DNA, deoxyribonucleic acid; nd, not determined; STDEV, standard deviation. Standard deviations were given as plus or minus the unit of measurement. The total cellular composition was calculated as followed ([DNA + RNA + CHO + protein + lipid]/10). The total Mean percentage STDEV was also presented for each assay.

Table 5.6 The extraction and quantification of macromolecular concentrations of *S. fradiae* C373-10 biomass cultured on a glucose defined medium using fractionation method 1 (all solutions were filtered and the residue biomass washed back into the following step) and the cell dry weight calculated from freeze dried biomass dry and wet weight calculations.

Fermentation	Carbohydrate	RNA	DNA	Protein	Lipid	Total percentage cellular composition (%)
Ferm 1; Day 1	nd	nd	nd	nd	nd	nd
Ferm 2; Day 1	nd	nd	nd	nd	nd	nd
Mean STDEV	**nd**	**nd**	**nd**	**nd**	**nd**	**nd**
Ferm 1; Day 2	86.55 ± 39.96	65.68 ± 12.23	1.23 ± 0.77	111.46 ± 44.79	3.99 ± 1.11	26.89
Ferm 2; Day 2	75.23 ± 45.27	77.77 ± 14.87	0.94 ± 0.58	125.47 ± 52.31	4.49 ± 1.69	28.39
Mean STDEV	**80.89 ± 42.61**	**71.72 ± 13.55**	**1.08 ± 0.67**	**118.46 ± 48.55**	**4.24 ± 1.40**	**27.64**
Ferm 1; Day 3	177.89 ± 48.87	90.86 ± 2.13	0.99 ± 1.45	195.78 ± 12.64	6.54 ± 2.14	47.21
Ferm 2; Day 3	150.42 ± 27.77	87.79 ± 4.79	1.16 ± 3.69	189.75 ± 14.85	5.99 ± 1.82	43.51
Mean STDEV	**164.15 ± 38.32**	**89.32 ± 3.46**	**1.07 ± 2.57**	**192.76 ± 13.74**	**6.26 ± 1.98**	**45.36**
Ferm 1; Day 4	199.99 ± 41.11	101.11 ± 11.22	2.11 ± 0.97	353.64 ± 98.23	6.29 ± 3.12	66.31
Ferm 2; Day 4	175.62 ± 23.39	84.45 ± 9.99	2.47 ± 0.99	299.87 ± 44.21	5.20 ± 2.47	56.76
Mean STDEV	**187.80 ± 32.25**	**92.78 ± 10.60**	**2.29 ± 0.98**	**326.75 ± 22.10**	**5.74 ± 2.79**	**61.54**
Ferm 1; Day 5	120.63 ± 25.57	102.36 ± 21.96	2.96 ± 1.46	313.66 ± 62.24	6.58 ± 2.17	54.62
Ferm 2; Day 5	150.66 ± 21.27	88.96 ± 39.65	4.56 ± 1.22	274.59 ± 54.43	7.97 ± 2.69	52.67
Mean STDEV	**135.64 ± 23.42**	**95.66 ± 30.80**	**3.76 ± 1.34**	**294.12 ± 58.33**	**7.27 ± 2.43**	**53.65**
Ferm 1; Day 6	110.10 ± 19.98	65.66 ± 10.78	2.17 ± 4.56	278.99 ± 25.69	9.87 ± 4.12	46.68
Ferm 2; Day 6	115.77 ± 12.24	59.98 ± 9.52	3.97 ± 2.87	244.44 ± 17.98	9.66 ±1.29	43.38
Mean STDEV	**112.93 ± 16.11**	**62.82 ± 10.15**	**3.07 ± 3.71**	**261.71 ± 21.83**	**9.76 ± 2.70**	**45.03**
Ferm 1; Day 7	99.99 ± 13.37	60.12 ± 3.53	9.54 ± 1.33	311.13 ± 30.84	12.35 ± 1.66	49.31
Ferm 2; Day 7	102.33 ± 41.77	50.42 ± 6.69	7.46 ± 1.87	277.97 ± 95.78	12.85 ± 2.79	45.10
Mean STDEV	**101.16 ± 27.57**	**55.27 ± 5.11**	**8.50 ± 1.60**	**294.55 ± 63.31**	**12.60 ± 2.22**	**47.21**
Ferm 1; Day 8	66.35 ± 28.89	44.23 ± 7.45	6.58 ± 1.96	200.22 ± 46.28	13.87 ± 9.64	33.12

Ferm 2; Day 8	95.55 ± 24.46	55.55 ± 9.71	4.75 ± 4.77	197.88 ± 30.31	14.48 ± 1.13	27.27
Mean STDEV	**33.17 ± 26.67**	**49.89 ± 8.58**	**5.67 ± 3.36**	**199.05 ± 38.29**	**14.17 ± 5.38**	**30.19**
Total Mean percentage STDEV	**± 28.85**	**± 15.68**	**± 84.87**	**± 19.12**	**± 32.85**	

Biomass was obtained from a *S. fradiae* C373-10 fermentation cultured on a glucose glutamate defined medium [7 L bioreactor vessel](Chapter 3, section 3.6.4 In order to eliminate carry-over of any unknown components from the complex vegetative medium (Chapter 3, section 3.5.1). The appropriate seed training medium (cultured in a 4 L fernbach shake flask with 700 ml of medium) was inoculated with 10 % of the vegetative culture and was used to inoculate the production medium [10 % incolumn]. All cultures were cultivated under the same conditions (30^0 C, 400 rpm). The biomass was harvested at 0, 24, 48, 72, 96, 120, 144, and 168 hrs after inoculation. Pooled samples were centrifuged down to a pellet and washed with dH_2O. Each washed sample pellet was divided into triplicate samples of approximate equal wet weight, which was fractionated with method 1 (Chapter 3, section 3.16.1; all solutions were filtered and the residue biomass washed back into following step) at a concentration of 100 $mg.ml^{-1}$ (wet weight) and stored at -70^0 C. The resulting fractions were analysed in triplicate for macromolecular content by the appropriate assay. Carbohydrate, the anthrone assay (Chapter 3, section 3.18.1); DNA, the diphenylamine assay (Chapter 3, section 3.19.2); RNA, the orcinol assay (Chapter 3, section 3.19.4); protein, the ninhydrin assay (Chapter 3, section 3.20.6); lipid, the vanillin assay (Chapter 3, section 3.23.1). The means were obtained from biomass samples harvested at the same time period. All figures were expressed as $mg.g^{-1}$ dry weight biomass (the macromolecular composition was calculated by working out a weighting coefficient between freeze dried broth samples and wet weight [Chapter 3, section 3.11.1] biomass determinations). CHO, carbohydrate, RNA, ribonucleic acid; DNA, deoxyribonucleic acid; nd, not determined; STDEV, standard deviation. The total cellular composition was calculated as followed ([DNA + RNA + CHO + protein + lipid]/10). The total Mean percentage STDEV was also presented for each assay.

Table 5.7 The extraction and quantification of macromolecular concentrations of *S. fradiae* C373-10 biomass cultured on a glucose glutamate defined medium with fractionation method 4 (as Lange & Heijnen, 2001).

Fermentation	CHO	RNA	DNA	Protein	Lipid	Total percentage cellular composition (%)
Ferm 1; Day 1	79.99 ± 10.71	10.85 ± 2.11	2.11 ± 0.89	85.63 ± 52.12	12.86 ± 1.12	19.14
Ferm 2; Day 1	82.36 ± 30.62	7.92 ± 1.63	4.85 ± 1.11	99.99 ± 26.12	9.85 ± 2.51	20.49
Mean STDEV	**81.17 ± 20.66**	**9.38 ± 1.87**	**3.48 ± 1.00**	**92.81 ± 39.12**	**11.35 ± 1.81**	**19.82**
Ferm 1; Day 3	69.99 ± 21.23	62.12 ± 32.10	36.92 ± 15.63	254.56 ± 100.01	46.62 ± 9.96	47.02
Ferm 2; Day 3	96.88 ± 52.33	78.45 ± 27.41	40.19± 6.22	289.36 ± 95.28	20.63 ± 5.63	52.551
Mean STDEV	**83.43 ± 36.78**	**70.28 ± 29.75**	**38.55 ± 10.92**	**271.96 ± 97.64**	**33.62 ± 7.79**	**49.79**
Ferm 1; Day 5	156.32 ± 50.62	48.22 ± 10.63	50.11 ± 10.52	411.63 ± 122.36	106.52 ± 25.54	77.28
Ferm 2; Day 5	131.52 ± 96.52	56.75 ± 9.98	45.62 ± 11.62	369.52 ± 97.75	156.32 ± 45.45	75.97
Mean STDEV	**143.9 ± 73.57**	**52.48 ± 10.30**	**47.86 ± 11.07**	**390.57 ± 110.05**	**131.42 ± 35.49**	**76.63**
Total Mean percentage STDEV	**± 40.15**	**± 27.57**	**± 27.73**	**± 35.73**	**± 131.51**	

Biomass was obtained from a *S. fradiae* C373-10 fermentation cultured on a glucose glutamate medium [2 L shake flasks](Chapter 3, section 3.6.4). In order to eliminate carry-over of any unknown components from the complex vegetative medium (Chapter 3, section 3.5.1). The appropriate seed training medium (cultured in a 4 L fernbach shake flask with 700 ml of medium) was inoculated with 10 % of the vegetative culture and was used to inoculate the production medium [10 % incolumn]. All cultures were cultivated under the same conditions (30^0 C, 250 rpm on a rotary shaker). The biomass was harvested at 0, 48 and 96 hrs. Each sample was then washed with dH_2O. The biomass pellet was stored at – 70^0 C until freeze drying for 48 hrs at 10 Pa. The biomass was then further dried at 70^0 C for 48 h and stored at room temperature in a desiccator above silica gel. Macromolecular components were determined as followed; the carbohydrates were measured according to the phenol sulphuric assay on a mixture of 1 ml of sample solution (0.2 mg dry biomass.ml^{-1}), the results were then corrected for the presence of nucleic pentoses by using a relative absorbance of total nucleic acids (section 3.19.1). Total protein was determined by using the ninhydrin assay, 2.0 ml of resuspended biomass (3 gl^{-1})[Chapter 3, section 3.20.6]. The cellular lipid components of 500 mg biomass were dissolved in 100 µl dH_2O were extracted twice with 3.75 ml of a 2:1 mixture of methanol and chloroform and measured by gravimetric analysis (Chapter 3, section 3.23.2). RNA & DNA were extracted with 0.5 M $HClO_4$ acid and measured with orcinol (Chapter 3, section 3.19.4) and Burton assay (Chapter 3, section 3.19.2). All figures were expressed as mg.g^{-1} dry weight biomass (the macromolecular composition was calculated by working out a weighting coefficient between the wet weight [Chapter 3, section 3.11.1] and dry weight [Chapter 3, section 3.11.2] biomass determinations). CHO, carbohydrate, RNA, ribonucleic acid; DNA, deoxyribonucleic acid; nd, not determined; STDEV, standard deviation. Standard deviations were given as plus or minus the unit of measurement. The means were obtained from biomass samples harvested from the same time period. The total cellular composition was calculated as followed ([DNA + RNA + CHO + protein + lipid]/10). The total Mean percentage STDEV was also presented for each assay.

Table 5.8 The extraction and quantification of macromolecular concentrations of *S. fradiae* C373-10 biomass cultured on a glucose glutamate defined medium using fractionation method 2 (all solutions were filtered and the residue biomass washed back into the following step).

Fermentation	CHO	RNA	DNA	Protein	Lipid	Total percentage cell composition (%)
Ferm 1; Day 2	124.34 ± 11.65	29.43 ± 12.45	14.97 ± 1.56	227.09 ± 3.61	20.42 ± 5.56	41.63
Ferm 2; Day 2	144.16 ± 22.32	19.80 ± 28.39	8.04 ± 4.74	313.29 ± 25.68	40.23 ± 4.89	52.55
Ferm 3; Day 2	159.37 ± 18.62	28.79 ± 35.17	11.63 ± 6.55	252.78 ± 2.28	58.84 ± 10.23	51.14
Ferm 4; Day 2	174.94 ± 16.23	34.39 ± 46.27	10.76 ± 13.21	387.34 ± 8.57	22.93 ± 18.97	63.04
Mean STDEV	**150.70 ± 17.21**	**28.10 ± 30.57**	**11.35 ± 6.51**	**295.13 ± 10.03**	**35.60 ± 9.91**	**52.09**
Ferm 1; Day 3	126.13 ± 21.28	128.53 ± 37.57	15.73 ± 8.21	376.80 ± 10.25	25.96 ± 14.23	67.31
Ferm 2; Day 3	126.76 ± 1.95	120.04 ± 51.50	11.70 ± 15.80	432.78 ± 12.62	50.94 ± 18.95	74.22
Ferm 3; Day 3	139.58 ± 27.69	80.61 ± 57.88	11.12 ± 14.19	420.77 ± 29.89	40.72 ± 21.26	62.08
Ferm 4; Day 3	95.26 ± 4.26	57.96 ± 13.31	28.34 ± 2.98	498.26 ± 11.97	24.56 ± 10.23	70.44
Mean STDEV	**121.93 ± 13.80**	**78.79 ± 40.06**	**16.72 ± 10.29**	**432.15 ± 16.18**	**35.54 ± 16.17**	**68.51**
Ferm 1; Day 4	130.60 ± 16.40	93.57 ± 11.61	22.77 ± 13.76	456.86 ± 13.43	99.56 ± 30.33	80.34
Ferm 2; Day 4	139.94 ± 25.20	109.40 ± 32.82	18.06 ± 9.86	461.72 ± 45.86	87.10 ± 27.58	81.62
Ferm 3; Day 4	144.71 ± 27.32	92.70 ± 7.24	26.43 ± 11.05	499.56 ± 2.83	106.23 ± 54.21	86.96
Ferm 4; Day 4	135.67 ± 12.34	117.84 ± 6.89	nd	nd	111.23 ± 102.36	nd
Mean STDEV	**137.73 ± 17.23**	**103.38 ± 12.91**	**22.42 ± 11.66**	**472.71± 15.52**	**101.03 ± 53.62**	**82.97**
Ferm 1; Day 5	155.86 ± 48.32	111.55 ± 36.52	25.76 ± 8.56	547.67 ± 69.34	117.63 ± 4.78	95.85
Ferm 2; Day 5	144.89 ± 37.58	93.53 ± 30.05	20.83 ± 8.45	nd	155.62 ± 20.36	nd
Ferm 3; Day 5	124.74 ± 30.19	84.05 ± 6.85	39.86 ± 7.20	404.53 ± 58.98	123.12 ± 36.98	77.63
Ferm 4; Day 5	156.69 ± 65.37	78.02 ± 22.81	21.64 ± 12.68	532.62 ± 1.24	145.68 ± 21.54	93.46
Mean STDEV	**145.54 ± 45.36**	**91.79 ± 24.06**	**27.02 ± 9.22**	**494.94 ± 32.39**	**135.51 ± 20.91**	**88.98**

Ferm 1; Day 6	155.56 ± 65.44	61.09 ± 14.86	20.73 ± 34.65	534.22 ± 24.70	62.78 ± 21.58	83.44
Ferm 2; Day 6	103.64 ± 35.38	74.52 ± 8.26	71.10 ± 11.13	594.03 ± 90.30	115.67 ± 2.15	95.90
Ferm 3; Day 6	102.77 ± 15.90	68.21 ± 1.06	28.32 ± 25.62	489.24 ± 5.96	124.11 ± 26.34	81.26
Ferm 4; Day 6	47.90 ± 18.49	60.02 ± 5.33	20.79 ± 16.60	484.56 ± 13.36	150.11 ± 21.87	76.34
Mean STDEV	**102.47 ± 33.80**	**65.96 ± 7.38**	**35.23 ± 22.00**	**525.51 ± 33.58**	**113.17 ± 17.98**	**84.23**
Total Mean percentage STDEV	**± 19.98**	**± 40.92**	**± 62.74**	**± 4.64**	**± 32.89**	

Biomass was obtained from a *S. fradiae* C373-10 fermentation cultured on a glucose glutamate defined medium [7 L bioreactor vessel](Chapter 3, section 3.6.4)[corresponds to Tables 5.9 A]. In order to eliminate carry-over of any unknown components from the complex vegetative medium (Chapter 3, section 3.5.1). The appropriate seed training medium (cultured in a 4 L fernbach shake flask with 700 ml of medium) was inoculated with 10 % of the vegetative culture and was used to inoculate the production medium [10 % incolumn]. All cultures were cultivated under the same conditions (30^0 C, 400 rpm). The biomass was harvested at 0, 24, 48, 72, 96, and 120 hrs after inoculation. Pooled samples were centrifuged down to a pellet and washed with dH_2O. Each washed sample pellet was divided into triplicate samples of approximate equal wet weight, which was fractionated with method 2 (as Chapter 3, section 3.16.2; all solutions were filtered and the residue biomass washed back into the following step) at a concentration of 50 $mg.ml^{-1}$ (wet weight) and stored at -70^0 C. The resulting fractions were analysed in triplicate for macromolecular content by the appropriate assay. Carbohydrate, the anthrone assay (Chapter 3, section 3.18.1); DNA, the diphenylamine assay (Chapter 3, section 3.19.2); RNA, the orcinol assay (Chapter 3, section 3.19.4); protein, the ninhydrin assay (Chapter 3, section 3.20.6); lipid, the vanillin assay (Chapter 3, section 3.23.1). The means were obtained from biomass samples harvested at the same time period. All figures were expressed as $mg.g^{-1}$ dry weight biomass (the macromolecular composition was calculated by working out a weighting coefficient between dry weight [Chapter 3, section 3.11.2] and wet weight [Chapter 3, section 3.11.1] biomass determinations). CHO, carbohydrate, RNA, ribonucleic acid; DNA, deoxyribonucleic acid; nd, not determined; STDEV, standard deviation. The total cellular composition was calculated as followed ([DNA + RNA + CHO + protein + lipid]/10). The total Mean percentage STDEV was also presented for each assay.

Table 5.9A - I The extraction and quantification of macromolecular concentrations of *S. fradiae* C373-10, *S. coelicolor* 1147, and *E. coli* ML308 biomass cultured on a number of different carbon sources using fractionation method 1 (all solutions were filtered and the residue biomass washed back into the following step).

Table 5.9 A Glucose glutamate defined medium fermentations 1 - 4 (fermentation profiles and time points as Chapter 4, Fig 4.7 - 4.10)

Fermentation / time (days)	Carbohydrate	RNA	DNA	Protein	Lipid	Total percentage cellular composition (%)
Ferm 1; Day 1	49.88 ± 12.44	8.44 ± 15.89	3.46 ± 2.19	35.58 ± 3.69	12.16 ± 2.67	10.95
Ferm 2; Day 1	51.36 ± 16.33	9.67 ± 25.63	3.89 ± 3.67	25.97 ± 4.58	13.68 ± 5.62	10.46
Ferm 3; Day 1	50.97 ± 9.65	9.88 ± 12.56	3.47 ± 1.87	40.89 ± 6.78	11.11 ±4.89	11.63
Ferm 4; Day 1	55.63 ± 8.67	10.99 ± 11.74	3.01 ± 2.13	30.11 ± 9.69	15.06 ± 3.77	11.48
Mean STDEV	**51.96 ± 11.77**	**9.74 ± 16.45**	**3.46 ± 2.46**	**33.14 ± 6.18**	**13.00 ± 4.24**	**11.13**
Ferm 1; Day 2	120.11 ± 21.24	70.44 ± 20.14	20.22 ± 5.67	220.36 ± 58.97	40.12 ± 16.85	47.12
Ferm 2; Day 2	116.27 ± 19.96	65.23 ± 18.88	19.93 ± 4.52	130.66 ± 60.58	36.54 ± 36.36	36.86
Ferm 3; Day 2	118.98 ± 12.44	69.88 ± 29.97	18.97 ±8.69	155.57 ± 30.12	38.97 ± 42.74	40.24
Ferm 4; Day 2	110.66 ± 13.36	68.93 ± 30.99	21.12 ± 1.23	211.89 ± 66.98	26.93 ± 30.52	43.95
Mean STDEV	**116.50 ± 16.75**	**68.62 ± 24.99**	**20.06 ± 5.03**	**179.62 ± 54.16**	**35.64 ± 31.62**	**42.04**
Ferm 1; Day 3	100.89 ± 5.99	75.89 ± 12.22	31.11 ± 4.28	249.96 ± 20.85	52.49 ± 23.89	51.03
Ferm 2; Day 3	97.85 ± 4.11	76.52 ± 8.68	35.63 ± 3.33	230.79 ± 45.21	51.36 ± 27.83	49.21
Ferm 3; Day 3	102.39 ± 4.33	86.92 ± 12.98	37.74 ± 3.87	201.45 ± 31.62	48.88 ± 30.66	47.74
Ferm 4; Day 3	105.87 ± 3.37	82.36 ± 14.75	32.27 ± 5.74	260.49 ± 57.89	36.97 ± 14.47	51.80
Mean STDEV	**101.75 ± 29.45**	**80.42 ± 12.16**	**34.19 ± 4.30**	**235.67 ± 38.89**	**47.42 ± 24.21**	**49.94**
Ferm 1; Day 4	106.33 ± 11.56	85.93 ± 16.67	40.15 ± 5.69	316.93 ± 60.58	95.64 ± 12.26	64.50
Ferm 2; Day 4	103.56 ± 12.63	86.97 ± 22.47	42.89 ± 11.14	255.69 ± 20.63	92.87 ± 25.87	58.20
Ferm 3; Day 4	104.78 ± 13.96	99.93 ± 25.69	44.78 ± 9.44	358.79 ± 60.27	99.99 ± 26.38	70.83

Ferm 4; Day 4	nd	nd	nd	nd	nd	nd
Mean STDEV	**104.89 ± 12.72**	**90.94 ± 21.61**	**42.61 ± 8.76**	**310.47 ± 47.16**	**96.17 ± 21.50**	**48.38**
Ferm 1; Day 5	104.89 ± 18.75	60.23 ± 30.27	49.99 ± 8.47	391.56 ± 15.66	118.97 ± 31.24	72.56
Ferm 2; Day 5	108.95 ± 9.67	59.95 ± 31.85	47.85 ± 6.23	420.68 ± 26.85	125.63 ± 13.56	76.31
Ferm 3; Day 5	106.32 ± 5.36	75.62 ± 42.22	48.82 ± 4.52	346.97 ± 27.27	134.89 ± 21.24	71.26
Ferm 4; Day 5	101.23 ± 4.89	69.87 ± 20.12	49.93 ± 1.96	499.62 ± 10.89	136.63 ± 52.36	85.73
Mean STDEV	**105.35± 9.67**	**66.42 ± 31.11**	**49.15 ± 5.29**	**414.71 ± 20.17**	**129.03 ± 29.60**	**76.46**
Ferm 1; Day 6	89.52 ± 12.89	70.11 ± 17.17	80.96 ± 6.36	214.52 ± 12.44	69.99 ± 2.45	52.51
Ferm 2; Day 6	90.86 ± 14.56	65.24 ± 12.32	75.62 ± 7.33	387.92 ± 14.59	112.36 ± 6.86	73.20
Ferm 3; Day 6	91.54 ± 16.96	67.82 ± 25.62	77.77 ± 8.74	311.14 ± 20.63	136.25 ± 19.85	68.45
Ferm 4; Day 6	90.45 ± 17.93	69.92 ± 30.74	65.52 ± 1.28	266.89 ± 22.68	149.87 ± 27.29	64.26
Mean STDEV	**90.59 ± 15.58**	**68.27 ± 21.46**	**74.97 ± 5.93**	**295.12 ± 17.58**	**117.12 ± 14.11**	**64.61**
Total Mean percentage STDEV	**± 14.22**	**± 55.15**	**± 24.42**	**± 15.42**	**± 38.91**	

Table 5.9 B Glucose oxo-glutarate defined medium fermentations 1 - 2 (fermentation profiles and time points as Chapter 4, Fig 4.11 - 4.12)

Fermentation / time (days)	Carbohydrate	RNA	DNA	Protein	Lipid	Total percentage cellular composition (%)
Ferm 1; Day 1	50.62 ± 86.95	65.66 ± 40.12	1.12 ± 0.74	110.23 ± 45.89	5.89 ± 1.68	23.35
Ferm 2; Day 1	86.93 ± 94.52	70.59 ± 24.78	2.46 ± 1.52	156.48 ± 69.96	7.44 ± 4.58	32.39
Mean STDEV	**68.77 ± 90.73**	**68.12 ± 32.45**	**1.79 ± 1.13**	**133.35 ± 57.92**	**6.66 ± 3.13**	27.87
Ferm 1; Day 2	111.26 ± 56.78	86.54 ± 51.11	1.89 ± 0.99	100.69 ± 78.96	7.88 ± 4.79	30.83
Ferm 2; Day 2	132.68 ± 62.22	45.68 ± 74.89	3.11 ± 1.79	147.89 ± 156.23	9.64 ± 3.96	33.90
Mean STDEV	**121.97 ± 59.50**	**66.11 ± 63.00**	**2.50 ± 1.39**	**124.29 ± 117.59**	**8.76 ± 4.37**	32.36
Ferm 1; Day 3	160.53 ± 111.24	111.22 ± 67.88	2.45 ± 1.89	214.58 ± 249.86	9.12 ± 2.14	49.79
Ferm 2; Day 3	198.67 ± 45.28	151.47 ± 46.67	3.89 ± 2.11	256.97 ± 211.63	7.48 ± 4.22	61.85
Mean STDEV	**179.60 ± 78.26**	**131.34 ± 57.27**	**3.17 ± 2.00**	**235.77 ± 230.74**	**8.30 ± 3.18**	**55.82**
Ferm 1; Day 4	196.58 ± 96.87	99.68 ± 78.44	4.89 ± 1.47	347.98 ± 189.23	11.78 ± 7.89	66.09
Ferm 2; Day 4	244.75 ± 115.76	110.27 ± 44.44	6.58 ± 1.96	389.79 ± 174.52	2.13 ± 7.46	75.35
Mean STDEV	**220.66 ± 106.31**	**104.97 ± 61.44**	**5.73 ± 1.71**	**368.88 ± 181.87**	**6.95 ± 7.67**	**70.72**
Ferm 1; Day 5	274.86 ± 56.88	157.84 ± 30.98	7.85 ± 4.63	456.99 ± 142.89	15.89 ± 10.16	91.34
Ferm 2; Day 5	133.69 ± 78.93	128.95 ± 65.56	9.64 ± 0.89	411.46 ± 155.28	12.46 ± 2.17	69.62
Mean STDEV	**204.27 ± 167.90**	**143.39 ± 98.27**	**8.74 ± 2.76**	**434.22 ± 149.08**	**14.17 ± 6.16**	**80.48**
Ferm 1; Day 6	186.42 ± 78.88	84.52 ± 45.85	8.44 ± 5.44	356.97 ± 222.21	12.17 ± 5.48	64.85
Ferm 2; Day 6	146.28 ± 89.90	96.32 ± 56.99	9.68 ± 5.96	416.92 ± 189.45	13.64 ± 7.74	68.28
Mean STDEV	**166.35 ± 84.39**	**90.42 ± 51.42**	**9.06 ± 5.70**	**386.94 ± 205.83**	**12.90 ± 6.61**	**66.57**
Ferm 1; Day 7	156.43 ± 90.11	65.27 ± 99.30	11.45 ± 7.49	317.17 ± 178.23	10.49 ± 4.92	56.08
Ferm 2; Day 7	111.78 ± 178.92	39.85 ± 47.70	10.11 ± 0.97	296.53 ± 154.87	9.78 ± 6.66	46.80
Mean STDEV	**134.10 ± 134.51**	**52.56 ± 73.50**	**10.78 ± 4.23**	**306.85 ± 166.55**	**10.13 ± 5.79**	51.44
Ferm 1; Day 8	104.52 ± 78.92	57.82 ± 70.52	9.54 ± 8.99	158.77 ± 99.96	13.87 ± 4.79	34.45

Ferm 2; Day 8	96.58 ± 68.52	64.87 ± 84.49	4.56 ± 4.75	246.58 ± 84.47	4.67 ± 5.62	41.73
Mean STDEV	**100.55 ± 73.72**	**61.34 ± 77.50**	**7.05 ± 6.87**	**202.67 ± 92.21**	**9.27 ± 5.20**	**38.09**
Total Mean percentage STDEV	**± 74.56**	**± 79.42**	**± 55.81**	**± 59.30**	**± 66.48**	

Table 5.9 C Glucose defined medium fermentations 1 - 2 (fermentation profiles and time points as Chapter 4, Fig 4.1 - 4.2)

Fermentation / time (days)	Carbohydrate	RNA	DNA	Protein	Lipid	Total percentage cellular composition (%)
Ferm 1; Day 1	22.07 ± 35.13	28.08 ± 18.95	3.40 ± 1.12	98.65 ± 56.98	nd	nd
Ferm 2; Day 1	16.47 ± 26.78	10.40 ± 9.66	3.51 ± 0.66	nd	3.56 ± 2.99	nd
Mean STDEV	**19.27 ± 30.95**	**19.24 ± 14.30**	**3.45 ± 0.89**	**98.65 ± 56.98**	**1.78 ± 2.99**	**9.31**
Ferm 1; Day 2	nd	31.02 ± 33.62	6.07 ± 3.65	88.87 ± 75.89	nd	nd
Ferm 2; Day 2	nd	34.18 ± 6.87	3.55 ± 1.44	218.19 ± 23.68	7.86 ± 5.48	nd
Mean STDEV	**nd**	**32.6 ± 20.24**	**4.81 ± 2.54**	**153.53 ± 49.78**	**7.86 ± 5.48**	**nd**
Ferm 1; Day 3	197.33 ± 51.11	38.06 ± 24.44	4.79 ± 1.56	197.32 ± 45.62	5.88 ± 9.53	44.34
Ferm 2; Day 3	61.11 ± 13.36	54.84 ± 19.97	4.97 ± 4.62	199.49 ± 89.78	6.21 ± 8.66	32.66
Mean STDEV	**129.22 ± 32.23**	**46.45 ± 22.20**	**4.88 ± 3.09**	**198.40 ± 67.70**	**6.04 ± 9.09**	**38.50**
Ferm 1; Day 4	104.54 ± 14.55	108.27 ± 41.15	11.30 ± 5.69	244.33 ± 111.11	7.26 ± 6.70	47.57
Ferm 2; Day 4	63.34 ± 39.87	108.84 ± 37.77	9.46 ± 1.29	288.98 ± 45.69	11.16 ± 2.39	48.18
Mean STDEV	**83.94 ± 27.21**	**108.55 ± 39.46**	**10.38 ± 3.49**	**266.65 ± 78.40**	**9.21 ± 4.54**	**47.87**
Ferm 1; Day 5	93.98 ± 45.61	64.99 ± 11.16	13.38 ± 2.63	140.08 ± 78.95	7.51 ± 16.45	31.99
Ferm 2; Day 5	65.13 ± 32.22	79.15 ± 9.99	16.53 ± 3.69	273.04 ± 86.26	8.99 ± 8.23	44.29
Mean STDEV	**79.55 ± 38.91**	**72.07 ± 10.57**	**14.95 ± 3.16**	**206.56 ± 82.60**	**8.25 ± 12.34**	**38.14**
Ferm 1; Day 6	94.47 ± 22.14	67.23 ± 33.39	12.44 ± 3.11	90.24 ± 85.46	9.53 ± 1.11	27.39
Ferm 2; Day 6	55.92 ± 11.78	55.28 ± 14.14	10.55 ± 8.54	168.08 ± 54.79	nd	nd
Mean STDEV	**75.19 ± 16.96**	**61.25 ± 23.76**	**11.49 ± 5.82**	**129.16 ± 70.12**	**9.53 ± 1.11**	**28.19**
Ferm 1; Day 7	94.90 ± 33.69	68.56 ± 17.78	14.81 ± 2.67	108.57 ± 46.23	13.75 ± 4.56	30.06

Ferm 2; Day 7	118.33 ± 34.56	44.56 ± 65.62	24.79 ± 5.22	82.49 ± 47.85	17.62 ± 7.68	28.78
Mean STDEV	**106.61 ± 34.12**	**56.56 ± 41.70**	**19.80 ± 3.94**	**95.53 ± 47.04**	**15.68 ± 6.12**	**29.42**
Ferm 1; Day 8	196.96 ± 56.24	75.05 ± 35.64	41.98 ± 1.67	188.37 ± 87.52	22.92 ± 9.87	52.53
Ferm 2; Day 8	100.59 ± 48.99	82.35 ± 41.15	38.13 ± 1.99	381.36 ± 35.94	18.89 ± 10.64	62.13
Mean STDEV	**148.77 ± 52.61**	**78.70 ± 38.39**	**40.05 ± 1.83**	**284.86 ± 61.73**	**20.90 ± 10.25**	**57.33**
Total Mean percentage STDEV	**± 51.79**	**± 58.78**	**± 38.59**	**± 48.70**	**± 97.45**	

Table 5.9 D Glycerol defined medium fermentations 1 - 4 (fermentation profiles and time points as Chapter 4, Fig 4.4 - 4.5)

Fermentation / time (days)	Carbohydrate	RNA	DNA	Protein	Lipid	Total percentage cellular composition (%)
Ferm 1; Day 1	21.49 ± 45.63	45.20 ± 20.31	9.52 ± 4.66	64.30 ± 22.79	17.97 ± 4.68	15.85
Ferm 2; Day 1	9.55 ± 12.65	38.22 ± 22.69	5.04 ± 2.63	-7.92 ± 11.34	14.76 ± 2.96	5.96
Mean STDEV	**15.52 ± 29.14**	**41.71 ± 21.50**	**7.28 ± 3.64**	**28.19 ± 17.06**	**16.36 ± 3.82**	**10.90**
Ferm 1; Day 2	nd	49.29 ± 51.23	3.48 ± 1.62	113.83 ± 89.92	nd	nd
Ferm 2; Day 2	29.70 ± 58.93	141.53 ± 100.46	18.30 ± 2.69	302.34 ± 35.67	51.10 ± 9.63	54.30
Mean STDEV	**29.70 ± 58.93**	**95.41 ± 75.84**	**10.89 ± 2.15**	**208.08 ± 62.79**	**51.10 ± 9.63**	**54.30**
Ferm 1; Day 3	10.28 ± 5.62	30.72 ± 15.96	3.30 ± 2.56	117.58 ± 90.45	nd	nd
Ferm 2; Day 3	46.91 ± 17.85	140.38 ± 25.63	30.17 ± 7.98	258.11 ± 98.63	68.43 ± 5.67	54.40
Mean STDEV	**28.59 ± 11.73**	**85.55 ± 20.79**	**16.73 ± 5.27**	**187.84 ± 94.54**	**68.43 ± 5.67**	**54.40**
Ferm 1; Day 4	26.41 ± 85.23	56.02 ± 32.15	8.58 ± 3.65	231.24 ± 115.79	12.81 ± 2.11	33.51
Ferm 2; Day 4	14.21 ± 42.13	51.54 ± 36.35	7.68 ± 5.75	369.70 ± 130.27	22.64 ± 3.59	46.58
Mean STDEV	**20.31 ± 63.68**	**53.78 ± 34.25**	**8.13 ± 4.70**	**300.47 ± 123.03**	**17.72 ± 2.85**	**40.04**
Ferm 1; Day 5	55.99 ± 65.82	91.20 ± 41.52	46.36 ± 9.86	739.05 ± 211.68	10.37 ± 2.65	94.30
Ferm 2; Day 5	8.35 ± 10.45	25.77 ± 56.24	7.51 ± 1.65	313.68 ± 157.94	17.88 ± 3.45	37.32
Mean STDEV	**32.17 ± 38.13**	**58.48 ± 48.88**	**26.93 ± 5.75**	**526.36 ± 184.81**	**14.12 ± 3.05**	**65.81**
Ferm 1; Day 6	147.44 ± 115.26	100.73 ± 35.85	57.70 ± 5.27	410.27 ± 101.26	11.45 ± 3.89	72.76
Ferm 2; Day 6	4.89 ± 1.23	26.25 ± 21.24	8.14 ± 5.69	255.43 ± 98.74	15.60 ± 4.58	31.03
Mean STDEV	**76.16 ± 58.24**	**63.49 ± 28.54**	**32.92 ± 5.48**	**332.85 ± 100.00**	**13.52 ± 4.23**	**51.89**
Ferm 1; Day 7	232.50 ± 89.52	84.99 ± 11.96	56.94 ± 9.77	nd	nd	nd

Ferm 2; Day 7	17.719 ± 20.16	13.53 ± 24.56	6.87 ± 2.68	150.28 ± 66.23	10.39 ± 6.28	19.88
Mean STDEV	**125.11 ± 54.84**	**49.26 ± 18.26**	**31.90 ± 6.22**	**150.28 ± 66.23**	**10.39 ± 6.28**	**36.69**
Ferm 1; Day 8	157.34 ± 131.23	88.80 ± 39.46	46.83 ± 3.67	654.50 ± 89.90	18.20 ± 2.78	96.57
Ferm 2; Day 8	45.78 ± 51.27	18.42 ± 27.89	13.24 ± 4.99	291.08 ± 99.67	13.72 ± 3.64	38.22
Mean STDEV	**101.56 ± 91.25**	**53.61 ± 33.67**	**30.03 ± 4.33**	**472.79 ± 94.78**	**15.96 ± 3.21**	**67.39**
Ferm 1; Day 9	30.41 ± 21.58	34.29 ± 11.11	27.32 ± 2.96	513.33 ± 46.52	11.27 ± 6.97	61.66
Ferm 2; Day 9	47.34 ± 45.62	15.15 ± 12.36	12.05 ± 4.27	236.08 ± 85.74	16.18 ± 5.29	32.68
Mean STDEV	**38.87 ± 33.60**	**24.72 ± 11.73**	**19.68 ± 3.61**	**374.70 ± 66.13**	**13.72 ± 6.13**	**47.17**
Total Mean percentage STDEV	**± 121.19**	**± 68.82**	**± 33.46**	**± 30.47**	**± 27.30**	

Table 5.9 E Fructose defined medium fermentation 1 (fermentation profiles and time points as Chapter 4, Fig 4.3)

Fermentation / time (days)	Carbohydrate	RNA	DNA	Protein	Lipid	Total percentage cellular composition (%)
Ferm 1; Day 1	178.02 ± 57.78	31.70 ± 11.62	17.69 ± 2.63	233.85 ± 72.29	8.96 ± 5.63	47.02
Ferm 1; Day 2	163.48 ± 61.11	nd	nd	149.09 ± 84.96	7.77 ± 4.36	nd
Ferm 1; Day 3	187.92 ± 30.25	64.72 ± 41.62	24.90 ± 5.69	420.40 ± 111.54	30.61 ± 1.68	72.85
Ferm 1; Day 4	195.90 ± 16.35	56.74 ± 37.96	21.84 ± 12.46	246.59 ± 156.24	12.23 ± 4.78	53.33
Ferm 1; Day 5	5.91 ± 68.89	108.46 ± 20.11	52.88 ± 37.85	470.16 ± 211.85	8.12 ± 9.62	64.55
Ferm 1; Day 6	123.82 ± 32.33	76.17 ± 19.96	39.69 ± 41.16	413.01 ± 20.22	6.64 ± 25.55	65.93
Ferm 1; Day 7	104.82 ± 69.98	90.89 ± 9.63	33.38 ± 29.97	522.95 ± 49.99	11.51 ± 54.89	76.35
Ferm 1; Day 8	163.74 ± 96.63	55.86 ± 6.68	24.34 ± 20.64	392.31 ± 54.36	9.16 ± 11.63	64.54
Ferm 1; Day 9	16.52 ± 29.62	51.33 ± 14.46	24.82 ± 11.11	286.93 ± 143.28	7.60 ± 5.84	38.72
Total Mean percentage STDEV	**± 176.79**	**± 32.92**	**± 61.17**	**± 33.45**	**± 149.72**	

Table 5.9 F Oxo-glutarate defined medium fermentation 1 (fermentation profiles and time points as Chapter 4, Fig 4.6)

Fermentation / time (days)	Carbohydrate	RNA	DNA	Protein	Lipid	Total percentage cellular composition (%)
Ferm 1; Day 1	20.39 ± 42.22	5.23 ± 5.55	10.26 ± 4.62	-244.65 ± 111.89	nd	nd
Ferm 1; Day 2	5.25 ± 36.65	14.54 ± 20.28	9.33 ± 5.89	116.58 ± 206.62	nd	nd
Ferm 1; Day 3	4.50 ± 2.11	26.27 ± 19.96	11.23 ± 6.11	152.24 ± 194.58	nd	nd
Ferm 1; Day 4	9.66 ± 5.69	28.64 ± 17.62	10.73 ± 9.97	315.36 ± 101.96	12.60 ± 6.69	37.70
Ferm 1; Day 5	250.65 ± 111.16	77.09 ± 30.62	30.63 ± 12.28	307.93 ± 95.84	10.09 ± 7.14	67.64
Ferm 1; Day 6	9.85 ± 10.23	86.03 ± 42.21	41.23 ± 2.63	398.31 ± 56.68	11.66 ± 15.52	54.71
Ferm 1; Day 7	20.32 ± 5.45	78.81 ± 55.89	40.82 ± 40.52	219.93 ± 86.54	25.47 ± 12.86	38.53
Ferm 1; Day 8	10.20 ± 6.66	61.88 ± 21.47	43.30 ± 20.23	429.51 ± 156.98	14.87 ± 7.86	55.98
Ferm 1; Day 9	18.99 ± 9.96	48.25 ± 30.28	31.80 ± 19.56	358.64 ± 198.47	17.01 ± 10.10	47.47
Ferm 1; Day 10	21.60 ± 30.30	61.19 ± 18.17	48.05 ± 15.52	300.54 ± 36.68	16.63 ± 20.56	44.80
Ferm 1; Day 11	12.30 ± 7.76	69.83 ± 45.56	55.92 ± 10.11	407.43 ± 42.26	15.42 ± 9.63	56.09
Ferm 1; Day 12	4.78 ± 3.65	54.89 ± 10.23	46.14 ± 14.46	255.58 ± 87.78	33.29 ± 15.58	39.47
Total mean percentage STDEV	**± 131.95**	**± 62.82**	**± 49.26**	**± 43.76**	**± 72.51**	

Table 5.9 G Methyl oleate defined medium fermentations 1 - 2 (fermentation profiles and time points as Chapter 4, Fig 4.13 - 4.14)

Fermentation / time (days)	Carbohydrate	RNA	DNA	Protein	Lipid	Total percentage cellular composition (%)
Ferm 1; Day 1	45.18 ± 39.92	26.10 ± 17.85	34.81 ± 10.66	-148.26 ± 86.53	nd	nd
Ferm 2; Day 1	47.53 ± 54.48	26.64 ± 12.56	18.65 ± 9.36	347.35 ± 196.23	10.74 ± 5.64	45.09
Mean STDEV	**46.35 ± 47.20**	**26.37 ± 15.20**	**26.73 ± 10.01**	**99.54 ± 141.38**	**10.74 ± 5.64**	20.44
Ferm 1; Day 2	7.33 ± 3.11	38.90 ± 19.87	18.32 ± 9.42	380.81 ± 114.28	31.52 ± 10.11	47.69
Ferm 2; Day 2	26.77 ± 15.63	38.44 ± 26.34	8.34 ± 9.47	315.93 ± 98.56	19.70 ± 9.65	40.92
Mean STDEV	**17.05 ± 9.37**	**38.67 ± 23.10**	**13.33 ± 9.44**	**348.37 ± 106.42**	**25.61 ± 9.88**	44.30
Ferm 1; Day 3	6.11 ± 6.62	28.50 ± 31.40	10.90 ± 5.23	204.81 ± 56.62	28.12 ± 6.45	27.84
Ferm 2; Day 3	6.36 ± 9.63	24.12 ± 16.75	8.39 ± 3.68	311.55 ± 97.78	14.45 ± 5.89	36.49
Mean STDEV	**6.23 ± 8.12**	**26.31 ± 24.07**	**9.64 ± 4.45**	**258.18 ± 77.20**	**21.28 ± 6.17**	32.16
Ferm 1; Day 4	27.64 ± 19.99	34.99 ± 15.52	8.12 ± 4.12	308.27 ± 110.45	29.81 ± 15.52	40.88
Ferm 2; Day 4	22.73 ± 18.54	35.11 ± 16.23	10.15 ± 5.55	317.10 ± 56.89	23.74 ± 10.12	40.88
Mean STDEV	**25.18 ± 19.26**	**35.05 ± 15.87**	**9.13 ± 4.83**	**312.68 ± 83.67**	**26.77 ± 12.82**	40.88
Ferm 1; Day 5	21.75 ± 52.56	17.01 ± 19.36	9.63 ± 5.68	343.44 ± 250.44	23.01 ± 11.56	41.48
Ferm 2; Day 5	22.76 ± 21.24	28.17 ± 21.53	9.65 ± 6.65	285.65 ± 146.11	15.56 ± 14.58	36.18

Mean STDEV	**22.25 ± 36.90**	**22.59 ± 20.44**	**9.64 ± 6.16**	**314.54 ± 198.27**	**19.28 ± 13.07**	38.83
Ferm 1; Day 6	17.81 ± 22.65	15.97 ± 25.68	7.81 ± 2.45	277.55 ± 121.62	19.21 ± 21.45	33.84
Ferm 2; Day 6	18.10 ± 25.61	37.52 ± 24.53	11.63 ± 4.68	342.82 ± 146.28	22.08 ± 14.86	43.21
Mean STDEV	**17.95 ± 24.13**	**26.74 ± 25.10**	**9.72 ± 3.56**	**310.18 ± 133.95**	**20.64 ± 18.15**	38.52
Ferm 1; Day 7	16.46 ± 12.23	16.37 ± 22.22	7.27 ± 7.85	245.49 ± 50.11	12.82 ± 8.99	29.84
Ferm 2; Day 7	18.45 ± 15.63	25.86 ± 89.93	9.64 ± 8.65	335.38 ± 86.45	25.98 ± 12.44	41.53
Mean STDEV	**17.45 ± 13.93**	**21.11 ± 56.07**	**8.45 ± 8.25**	**290.43 ± 68.28**	**19.40 ± 10.71**	35.68
Ferm 1; Day 8	23.20 ± 10.22	24.56 ± 12.78	10.37± 2.11	237.41 ± 162.58	16.67 ± 4.56	31.22
Ferm 2; Day 8	31.90 ± 15.63	29.32 ± 16.45	14.21 ± 7.77	222.85 ± 112.78	nd	nd
Mean STDEV	**27.55 ± 12.92**	**26.94 ± 14.61**	**12.29 ± 4.94**	**230.13 ± 56.39**	**16.67 ± 4.56**	30.52
Ferm 1; Day 9	24.94 ± 12.26	14.00 ± 14.96	6.08 ± 5.62	252.76 ± 78.98	16.02 ± 6.89	31.38
Ferm 2; Day 9	nd	nd	nd	nd	nd	nd
Mean STDEV	**24.94 ± 12.26**	**14.00 ± 14.96**	**6.08 ± 5.62**	**126.38 ± 78.98**	**16.02 ± 6.89**	15.69
Total mean percentage STDEV	**± 94.69**	**± 128.53**	**± 59.45**	**± 39.43**	**± 56.93**	

Table 5.9 H *S. coelicolor* 1147 cultured on a glucose minimal medium fermentations 1 - 2 (fermentation profiles and time points as Chapter 4, Fig 4.19 - 4.20).

Fermentation / time (h)	Carbohydrate	RNA	DNA	Protein	Total percentage cellular composition (%)
0	10.02 ± 2.86	46.20 ± 12.36	49.73 ± 18.32	570.86 ± 3.00	67.68
0	8.02 ± 5.11	33.35 ± 15.47	48.63 ± 9.16	566.21 ± 47.88	65.62
Mean STDEV	**9.02 ± 3.98**	**39.77 ± 13.91**	**49.18 ± 13.74**	**568.53 ± 25.44**	**66.65**
24	6.02 ± 2.36	108.08 ± 51.15	56.23 ± 21.10	523.69 ± 75.52	69.40
24	7.04 ± 3.33	121.09 ± 60.23	52.82 ± 18.41	528.06 ± 12.63	70.90
Mean STDEV	**6.53 ± 2.84**	**114.58 ± 55.69**	**54.52 ± 19.75**	**525.87 ± 44.07**	**70.15**
48	14.20 ± 8.52	144.28 ± 25.90	58.04 ± 3.26	562.60 ± 50.12	77.91
48	15.66 ± 6.45	154.23 ± 41.44	59.62 ± 11.52	568.90 ± 49.99	79.84
Mean STDEV	**14.93 ± 7.48**	**149.25 ± 33.67**	**58.83 ± 7.39**	**565.75 ± 50.05**	**78.88**
72	16.25 ± 9.98	149.23 ± 47.74	89.23 ± 2.63	466.39 ± 1.60	72.11
72	15.71 ± 7.41	149.42 ± 39.92	97.60 ± 10.92	485.86 ± 36.66	74.86
Mean STDEV	**15.98 ± 8.69**	**149.42 ± 43.83**	**93.41 ± 6.77**	**476.12 ± 19.13**	**73.48**
96	13.90 ± 6.11	105.84 ± 44.60	36.81 ± 5.49	392.00 ± 60.23	54.85
96	12.96 ± 4.62	109.36 ± 21.53	40.68 ± 11.11	366.00 ± 23.23	52.90
Mean STDEV	**13.43 ± 5.36**	**107.60 ± 33.06**	**38.74 ± 8.30**	**379.00 ± 41.73**	**53.88**
Total mean percentage STDEV	**± 46.68**	**± 33.45**	**± 20.98**	**± 7.32**	

Table 5.9 I *E. coli* ML308 cultured on a glucose minimal medium in shake flasks.

Fermentation / time (h)	CHO	RNA	DNA	PROT	LIPID	Total percentage cellular composition (%)
Ferm 1, 24 hrs	9.41 ± 4.86	33.47 ± 5.16	26.39 ± 11.62	488.38 ± 58.16	54.79 ± 20.13	61.24
Ferm 2, 24 hrs	9.69 ± 1.11	48.77 ± 12.14	23.95 ± 12.36	426.67 ± 31.24	54.14 ± 15.51	56.32
Total mean percentage STDEV	**± 31.55**	**± 20.15**	**± 47.82**	**± 9.61**	**± 32.69**	**58.78**

Table 5.9 J Industrial complex medium fermentations 1 - 2 (fermentation profiles and time points as Chapter 4, Fig 4.16)

Fermentation / time (days)	Carbohydrate	RNA	DNA	Protein	Total percentage cellular composition (%)
Ferm 1; Day 1	3.85 ± 2.11	41.48 ±10.15	13.39 ± 2.16	420.70 ± 24.56	47.94
Ferm 1; Day 2	2.73 ± 5.12	15.50 ± 9.98	7.98 ± 3.58	217.32 ± 51.23	24.35
Ferm 1; Day 3	2.17 ± 10.23	10.80 ± 10.56	6.16 ± 4.47	67.51 ± 49.85	8.66
Ferm 1; Day 4	1.29 ± 1.16	6.66 ± 5.87	3.59 ± 1.57	94.65 ± 39.99	10.62
Ferm 1; Day 5	0.98 ± 1.25	12.66 ± 10.14	7.32 ± 2.46	116.79 ± 100.12	13.77
Ferm 1; Day 6	3.84 ± 2.56	8.27 ± 5.41	3.65 ± 10.12	45.14 ± 40.13	6.09
Ferm 1; Day 7	5.30 ± 5.18	10.25 ± 9.78	7.57 ± 7.85	95.27 ± 100.85	11.84
Total mean percentage STDEV	**± 156.52**	**± 73.67**	**± 84.55**	**± 60.85**	

S. fradiae C373-10, *S. coelicolor* 1147, and *E. coli* ML308 were cultured on a number of different carbon sources and medium compositions. Medium compositions for *S. fradiae* were as followed (gl^{-1}) glucose (20.0), fructose (20.0), glycerol (40.0), oxo-glutarate (30.0), glucose (20.0) glutamate (5.0), glucose (20.0) oxo-glutarate (5.0)[other components as Chapter 3, section 3.6.4], and methyl oleate defined medium [as Chapter 3, section 3.7.2]; *S. coelicolor* and *E. coli* (cultured in 2 L erlenmeyer flask with 500 ml of medium) were both cultured on glucose minimal media (as Chapter 3, section 3.6.1 and 3.6.3 respectively). In order to eliminate carry-over of any unknown components from the complex vegetative medium (Chapter 3, section 3.5.1). The appropriate seed training medium was inoculated with 10 % of the vegetative culture and was used to inoculate the production medium [10 % incolumn]. A number of different bioreactors and fermentation equipment were used, information given to this in the title sequences in Chapter 4, Fig 4.1 - 4.20. All cultures were cultivated under the same conditions (30^0 C, 400 rpm). The biomass was harvested as stated after inoculation. Pooled samples were centrifuged down to a pellet and washed with dH_2O. Each washed sample pellet was divided into triplicate samples of approximate equal wet weight, which was fractionated with method 1 (Chapter 3, section 3.16.1; all solutions were filtered and the residue biomass washed back into following step) at a concentration of 100 $mg.ml^{-1}$ (wet weight) and stored at -70^0 C. The resulting fractions were analysed in triplicate for macromolecular content by the appropriate assay. Carbohydrate, the anthrone assay (Chapter 3, section 3.18.1); DNA, the diphenylamine assay (Chapter 3, section 3.19.2); RNA, the orcinol assay (Chapter 3, section 3.19.4); protein, the ninhydrin assay (Chapter 3, section 3.20.6); lipid, the vanillin assay (Chapter 3, section 3.23.1). The means were obtained from biomass samples harvested at the same time period. All figures were expressed as $mg.g^{-1}$ dry weight biomass (the macromolecular composition was calculated by working out a weighting coefficient between the wet weight [Chapter 3, section 3.11.1] and dry weight [Chapter 3, section 3.11.2] biomass determinations). CHO, carbohydrate, RNA, ribonucleic acid; DNA, deoxyribonucleic acid; nd, not determined; STDEV, standard deviation. Standard deviations were given as plus or minus the unit of measurement. The total cellular composition was calculated as followed ([DNA + RNA + CHO + protein + lipid]/10). The total mean percentage STDEV was also presented for each assay.

Table 5.10 The percentage macromolecular composition of *S. fradiae* C373-10, *S. coelicolor* 1147, and *E. coli* ML308 at the end of the growth phase.

Fermentation / organism	CHO (%)	RNA (%)	DNA (%)	Protein by Bradford assay (%)	Amino acids by the ninhydrin assay (%)	Lipid (%)	Total (%) composition
***S. fradiae* C373-10 glucose minimal medium**							
Ferm 1; Day 8	19.70	7.50	4.20	4.59	26.32	2.29	60.01
Ferm 2; Day 8	10.06	8.23	3.81	9.30	63.06	1.89	87.05
G/O							
Ferm 1; Day 7	6.48	10.85	3.41	4.32	44.01	1.26	66.02
Ferm 2; Day 7	4.11	5.15	3.82	7.53	38.69	nd	nd
G/G							
Ferm 1; Day 5	8.75	5.99	4.50	8.73	43.68	11.76	74.69
Ferm 1; Day 6	6.30	8.21	6.40	3.74	40.28	6.28	67.47
Ferm 2; Day 5	9.17	5.10	3.79	nd	41.15	nd	nd
Ferm 2; Day 6	15.37	8.62	11.17	13.04	41.24	11.57	87.96
Ferm 3; Day 5	16.74	7.43	6.36	5.86	26.32	12.31	69.16
Ferm 3; Day 6	8.03	6.97	6.57	7.51	33.73	12.41	67.70
Ferm 4; Day 5	6.42	4.58	4.33	nd	50.45	nd	nd
Ferm 4; Day 6	7.40	5.25	4.60	5.17	28.70	15.01	24.35
Glycerol							
Ferm 1; Day 9	3.04	3.43	2.73	12.52	14.02	1.127	32.88
Ferm 2; Day 9	4.73	1.51	1.20	2.34	23.80	1.62	40.96
Fructose							
Ferm 1; Day 8	16.37	5.59	2.43	9.57	15.65	0.91	21.44
Oxo-glutarate							
Ferm 1; Day 12	0.48	5.49	4.61	6.23	7.52	3.33	31.52

Methyl oleate defined medium							
Ferm 1; Day 9	2.32	2.46	1.04	5.79	37.79	1.67	42.53
Ferm 2; Day 9	1.84	2.59	0.96	8.18	38.22	2.60	57.42
***E. coli* ML308 glucose minimal medium**							
Ferm 1 Day 2	0.94	13.35	2.64	51.26	48.84	5.48	71.25
Ferm 2 Day 2	0.97	14.88	2.39	52.48	42.67	5.41	66.32
***S. coelicolor* 1147 glucose minimal medium**							
Ferm 1 Day 8	15.20	10.99	3.66	28.45	51.92	2.56	84.33
Ferm 2 Day 8	20.34	13.26	5.12	34.12	36.88	3.64	75.60

S. fradiae C373-10, *S. coelicolor* 1147, and *E. coli* ML308 were cultured on a number of different carbon sources and medium compositions. Medium compositions for *S. fradiae* were as followed (gl^{-1}) glucose (20.0), fructose (20.0), glycerol (40.0), oxo-glutarate (30.0), glucose (20.0) glutamate (5.0), glucose (20.0) oxo-glutarate (5.0)[other components as Chapter 3, section 3.6.4], and methyl oleate defined medium [as Chapter 3, section 3.7.2]; *S. coelicolor* and *E. coli* (cultured in 2 L erlenmeyer flask with 500 ml of medium) were both cultured on glucose minimal media (as Chapter 3, section 3.6.1 and 3.6.3 respectively). In order to eliminate carry-over of any unknown components from the complex vegetative medium (Chapter 3, section 3.5.1). The appropriate seed training medium was inoculated with 10 % of the vegetative culture and was used to inoculate the production medium [10 % incolumn]. A number of different bioreactors and fermentation equipment were used, information given to this in the title sequences in Chapter 4, Fig 4.1 - 4.20. All cultures were cultivated under the same conditions (30^0 C, 400 rpm). The biomass was harvested as stated after inoculation. Pooled samples were centrifuged down to a pellet and washed with dH_2O. Each washed sample pellet was divided into triplicate samples of approximate equal wet weight, which was fractionated with method 1 (Chapter 3, section 3.16.1; all solutions were filtered and the residue biomass washed back into following step) at a concentration of 100 $mg.ml^{-1}$ (wet weight) and stored at -70^0 C. The resulting fractions were analysed in triplicate for macromolecular content by the appropriate assay. Carbohydrate, the anthrone assay (Chapter 3, section 3.18.1); DNA, the diphenylamine assay (Chapter 3, section 3.19.2); RNA, the orcinol assay (Chapter 3, section 3.19.4); protein, the ninhydrin assay (Chapter 3, section 3.20.6); lipid, the vanillin assay (Chapter 3, section 3.23.1). The means were obtained from biomass samples harvested at the same time period. All figures were expressed as $mg.g^{-1}$ dry weight biomass (the macromolecular composition was calculated by working out a weighting coefficient between the wet weight [Chapter 3, section 3.11.1] and dry weight [Chapter 3, section 3.11.2] biomass determinations). CHO, carbohydrate, RNA, ribonucleic acid; DNA, deoxyribonucleic acid; G/G, glucose glutamate defined medium; G/O, glucose oxo-glutarate defined medium nd, not determined; STDEV, standard deviation. Standard deviations were given as plus or minus the unit of measurement. The total cellular composition was calculated as followed ([DNA + RNA + CHO + protein + lipid]/10). The total mean percentage STDEV was also presented for each assay. All sample points presented were considered to be at the end of the growth phase i.e., sampling point II, corresponding to Chapter 4, Fig 4.1 – 4.20.

Table 5.11 The effects of the solvent extraction procedure (Chapter 3, section 3.14.2) on the efficiency of macromolecular extraction of fractionation method 1.

No extraction used solvent extraction					
Sample	**Carbohydrate**	**DNA**	**RNA**	**Protein**	**Lipid**
1	168.71	26.79	184.20	465.21	2.29
2	205.78	28.81	179.11	368.91	1.89
3	174.39	32.93	164.93	487.61	3.11
Mean	182.96	29.51	176.08	440.58	2.43
STDEV	**± 19.97**	**± 3.13**	**± 9.99**	**± 63.07**	**± 0.62**
With solvent extraction					
Sample	**Carbohydrate**	**DNA**	**RNA**	**Protein**	**Lipid**
1	199.12	31.98	166.92	474.56	0.01
2	206.71	29.87	182.11	455.71	0.11
3	187.56	26.74	165.34	425.61	0.06
Mean	197.80	29.53	171.46	451.96	0.06
STDEV	**± 9.64**	**± 2.64**	**± 9.26**	**± 24.69**	**± 0.05**

Biomass was obtained from three shake flask cultures of *S. fradiae* C373-10 cultured on a glucose minimal medium (Chapter 3, section 3.6.4) and harvested at 72 hrs after inoculation. In order to eliminate carry-over of any unknown components from the complex vegetative medium (Chapter 3, section 3.5.1). The appropriate seed training medium was inoculated with 10 % of the vegetative culture and was used to inoculate the production medium [10 % incolumn]. The washed pellet was divided into 6 samples of approximate equal wet weight. One set triplicates were put through the doles biomass extraction procedure and separated and the second set had no extraction procedure undertaken. The samples were then fractionated with method 1 (Chapter 3, section 3.16.1; all solutions were filtered and the residue biomass washed back into following step) at a concentration of 100 $mg.ml^{-1}$ (wet weight) and stored at -70^{0} C. The resulting fractions were analysed in triplicate for macromolecular content by the appropriate assay. Carbohydrate, the anthrone assay (Chapter 3, section 3.18.1); DNA, the diphenylamine assay (Chapter 3, section 3.19.2); RNA, the orcinol assay (Chapter 3, section 3.19.4); protein, the ninhydrin assay (Chapter 3, section 3.20.6); lipid, the vanillin assay (Chapter 3, section 3.23.1). The means were obtained from biomass samples harvested at the same time period. All figures were expressed as $mg.g^{-1}$ dry weight biomass (the macromolecular composition was calculated by working out a weighting coefficient between freeze dried broth samples and wet weight [Chapter 3, section 3.11.1] biomass determinations). CHO, carbohydrate, RNA, ribonucleic acid; DNA, deoxyribonucleic acid; nd, not determined; STDEV, standard deviation. The total cellular composition was calculated as followed ([DNA + RNA + CHO + protein + lipid]/10).

Table 5.12 Determination of the efficiency of extraction and quantification of macromolecular RNA & DNA.

Fermentation period / Fractionation Method	M 1, orcinol assay for RNA	M 1, diphenylamine assay for DNA	M 1 Total nucleic acids minus the orcinol assay, for DNA	Cell disruption and Fluorometric analysis, for DNA	Extraction with KOH, simple UV method, for RNA	Reconciled data for RNA	Reconciled data for DNA
0	28.08 ± 5.12	3.40 ± 0.86	4.66 ± 1.25	1.22 ± 0.25	24.66 ± 0.46	26.37 ± 2.79	3.09 ± 0.79
0	10.40 ± 6.52	3.51 ± 1.12	4.55± 1.86	1.12 ± 0.36	8.99 ± 1.13	9.69 ± 3.82	3.06 ± 1.11
0	31.02 ± 4.12	6.07 ± 1.56	6.88 ± 1.78	1.90 ± 0.11	27.55 ± 0.72	29.28 ± 2.42	4.95 ± 1.15
STDEV between lots	**23.17 ± 5.25**	**4.33 ± 1.18**	**5.36 ± 1.63**	**1.41 ± 0.24**	**20.40 ± 0.77**	**21.78 ± 3.01**	**3.70 ± 1.01**
24	34.18 ± 3.25	3.55 ± 2.22	9.98 ± 2.89	2.13 ± 0.15	26.23 ± 0.31	30.20 ± 1.78	5.22 ± 1.75
24	38.06 ± 1.23	4.79 ± 2.54	10.99 ± 3.33	2.45 ± 0.56	22.24 ± 0.21	30.15 ± 0.72	6.08 ± 2.14
24	54.84 ± 1.89	4.96 ± 0.95	12.99 ± 6.89	2.64 ± 0.89	45.64 ± 0.11	50.24 ± 1.00	6.86 ± 2.91
STDEV between lots	**42.36 ± 2.12**	**4.43 ± 1.90**	**11.32 ± 4.37**	**2.41 ± 0.53**	**31.37 ± 0.21**	**36.86 ± 1.16**	**6.05 ± 2.27**
48	108.27 ± 10.26	11.30 ± 0.98	20.95 ± 10.12	4.54 ± 0.94	99.23 ± 0.15	103.75 ± 5.20	12.26 ± 4.01
48	108.84 ± 12.36	9.45 ± 0.32	22.34 ± 2.36	4.78 ± 0.54	99.62 ± 0.16	104.23 ± 6.26	12.19 ± 1.07
48	64.99 ± 5.58	13.38 ± 1.85	30.41 ± 5.89	6.76 ± 0.45	62.48 ± 1.23	63.73 ± 3.40	16.85 ± 2.73
STDEV between lots	**94.03 ± 9.40**	**11.38 ± 1.05**	**24.57 ± 6.12**	**5.36 ± 0.64**	**87.11 ± 0.51**	**90.57 ± 4.96**	**13.76 ± 2.60**
72	79.15 ± 7.89	16.53 ± 0.23	44.44 ± 6.11	6.89 ± 0.98	77.12 ± 0.99	78.13 ± 4.44	22.62 ± 2.44
72	67.23 ± 6.52	12.44 ± 4.56	89.65 ± 25.69	6.74 ± 0.56	62.35 ± 0.33	64.79 ± 3.42	36.28 ± 10.27
72	55.28 ± 1.23	10.55 ± 0.68	50.49 ± 12.65	7.65 ± 0.41	52.33 ± 0.43	53.80 ± 0.83	22.90 ± 4.58
STDEV between lots	**67.22 ± 5.21**	**13.17 ± 1.82**	**61.53 ± 14.81**	**7.09 ± 0.65**	**63.93 ± 0.58**	**65.58 ± 2.90**	**27.26 ± 5.76**

96	68.56 ± 6.89	14.81 ± 2.89	33.89 ± 10.47	15.67 ± 0.44	66.23 ± 2.51	67.39 ± 4.70	21.46 ± 4.60
96	44.56 ± 1.85	24.79 ± 1.74	26.74 ± 8.59	18.90 ± 0.56	42.56 ± 3.51	43.56 ± 2.68	23.48 ± 3.63
96	75.05 ± 2.13	41.98 ± 1.26	30.26 ± 9.99	17.65 ± 0.61	41.47 ± 7.67	58.26 ± 4.90	29.96 ± 3.95
STDEV between lots	**62.72 ± 3.62**	**27.19 ± 1.96**	**30.30 ± 9.68**	**17.41 ± 0.54**	**50.09 ± 4.56**	**56.40 ± 4.09**	**24.97 ± 4.06**
Total mean percentage STDEV	**± 11.50**	**± 20.90**	**± 29.88**	**± 13.05**	**± 3.49**	**± 7.65**	**± 24.21**

Biomass was obtained from three shake flask cultures for each time frame for *S. fradiae* C373-10 cultured on a glucose glutamate defined medium (Chapter 3, section 3.6.4). In order to eliminate carry-over of any unknown components from the complex vegetative medium (Chapter 3, section 3.5.1). The appropriate seed training medium was inoculated with 10 % of the vegetative culture and was used to inoculate the production medium [10 % incolumn]. The washed pellet was divided into 9 samples (three sets of triplicates for each fractionation protocol) of approximate equal wet weight. One set of triplicates was fractionated with method 1 (Chapter 3, section 3.16.1; all solutions were filtered and the residue biomass washed back in to following step) at concentration of 100 $mg.ml^{-1}$ (wet weight) and stored at -70^{0} C. The resulting fractions were analysed in triplicate for nucleic acid content by the diphenylamine assay (as Chapter 3, section 3.19.2), orcinol assay (as Chapter 3, section 3.19.4), total nucleic acids (as Chapter 3, section 3.19.1). The second set of triplicates were disrupted with a French press (cell disruption) and the fractions were analysed in triplicate for DNA content using the fluorometric Hoechst assay (as Chapter 3, section 3.19.3). The final set of triplicates used the simple UV spectrophotometric extraction and assay procedure for RNA content was undertaken as Chapter 3, section 3.19.5. All figures were expressed as $mg.g^{-1}$ dry weight biomass (the macromolecular composition was calculated by working out a weighting coefficient between the wet weight [Chapter 3, section 3.11.1] and dry weight [Chapter 3, section 3.11.2] biomass determinations). RNA, ribonucleic acid; DNA, deoxyribonucleic acid; nd, not determined; STDEV, standard deviation; M, method. The reconciled data was the mean between the different assays. The total mean percentage STDEV was also presented for each assay.

Table 5.13 The determination of the efficiency of extraction and quantification of DNA and RNA with extraction methods 1 and 2

	M 1/ F 2		M 2 / F 2		M 2 / F 3		percentage difference between M 1 & 2	percentage difference between M 1 & 2	M 2 / F 2 percentage content total	M 2 / F 2 percentage content total	M 2 / F 3 percentage content total	M 2 / F 3 percentage content total
Fermentation	**RNA**	**DNA**	**RNA**	**DNA**	**RNA**	**DNA**	**RNA**	**DNA**	**RNA**	**RNA**	**DNA**	**DNA**
***S. fradiae* C373-10**												
Ferm 1; Day 2	61.76	23.52	67.42	8.37	16.80	41.86	± 5.66	± 26.71	80.05	19.95	16.66	83.34
Ferm 2; Day 2	69.85	18.48	42.98	2.36	22.14	29.60	± 26.87	± 13.49	65.99	34.00	7.40	92.60
Ferm 3; Day 2	92.93	26.28	27.08	4.57	27.13	42.27	± 65.85	± 20.56	49.95	50.04	9.75	90.25
Ferm 4; Day 2	117.01	35.02	62.57	6.54	37.01	52.39	± 54.45	± 23.91	62.83	37.17	11.09	88.90
Ferm 1; Day 3	139.67	34.56	130.26	9.74	37.47	56.07	± 9.41	± 31.26	77.66	22.34	14.81	85.19
Ferm 2; Day 3	107.23	40.24	nd	8.11	52.72	54.05	nd	± 21.92	nd	nd	13.05	86.95
Ferm 3; Day 3	94.77	37.02	70.24	7.57	69.89	54.96	± 24.53	± 25.51	50.13	49.87	12.10	87.90
Ferm 4; Day 3	105.77	44.56	60.24	4.56	15.11	79.36	± 45.52	± 39.37	79.95	20.05	5.44	94.56
Ferm 1; Day 4	123.94	52.84	85.52	3.57	42.46	84.21	± 38.42	± 34.93	66.82	33.18	4.06	95.93
Ferm 2; Day 4	117.68	40.33	nd	4.12	40.25	64.92	nd	± 28.72	nd	nd	5.97	94.03
Ferm 3; Day 4	128.82	53.95	nd	5.65	37.76	88.96	nd	± 40.65	nd	nd	5.97	94.03
Ferm 4; Day 4	nd	nd	nd	5.61	50.96	nd	nd	nd	nd	nd	nd	nd
Ferm 1; Day 5	115.68	49.27	48.61	8.74	30.49	82.47	± 67.78	± 41.95	61.45	38.55	9.59	90.41
Ferm 2; Day 5	97.80	42.14	53.35	8.54	20.13	69.59	± 44.45	± 35.99	72.61	27.39	10.93	89.07
Ferm 3; Day 5	116.38	67.17	37.96	7.45	3.02	117.09	± 78.42	± 57.37	92.62	7.38	5.98	94.02
Ferm 4; Day 5	84.78	49.62	39.08	6.99	25.06	79.42	± 45.90	± 36.80	60.93	39.07	8.10	91.90
Ferm 1; Day 6	112.66	81.29	50.68	4.57	30.46	117.17	± 61.97	± 40.45	62.46	37.54	3.75	96.25

Ferm 2; Day 6	123.46	117.25	62.40	4.23	13.12	205.06	± 61.06	± 92.05	82.63	17.37	2.02	97.98
Ferm 3; Day 6	103.81	78.469	49.34	8.37	46.72	120.80	± 54.47	± 50.69	51.36	48.63	6.48	93.52
Ferm 4; Day 6	82.48	54.30	42.33	7.90	12.32	84.20	± 40.15	± 37.79	77.45	22.54	8.58	91.42
Percentage STDEV									**68.43**	**31.57**	**8.51**	**91.49**
***S. coelicolor* 1147**												
Sample 1	22.65	8.36	17.45	2.04	2.49	5.64	± 5.2	± 0.68	87.51	12.49	26.56	73.44
Sample 2	25.12	9.99	15.11	3.06	2.69	5.14	± 10.01	± 1.79	84.89	15.11	37.32	62.68
Sample 3	23.33	7.01	14.52	4.12	2.99	5.87	± 8.81	± 2.98	82.92	17.08	41.24	58.76
Percentage STDEV									**85.11**	**14.89**	**35.04**	**64.96**
***E. coli* ML308**												
Sample 1	33.47	26.39	30.67	2.01	4.41	25.63	-2.8	-1.25	87.43	12.57	7.27	92.73
Sample 2	48.77	23.95	33.69	1.02	5.22	21.48	-15.08	1.45	86.58	13.42	4.53	95.47
Percentage STDEV									**87.01**	**12.99**	**5.90**	**94.10**

S. fradiae C373-10, *S. coelicolor* 1147, and *E. coli* ML308 cultured on a number of different carbon sources and medium compositions. Medium compositions were as followed, *S. fradiae* was cultured on a glucose glutamate defined medium (Chapter 3, section 3.6.4), *S. coelicolor* and *E. coli* were both cultured on glucose minimal media (Chapter 3, section 3.6.1 and 3.6.3 respectively). Biomass was harvested at the stated times. The collected biomass was washed with dH_2O and divided into two sets of triplicates of approximate equal wet weight. The triplicates were then fractionated with method 1 and 2 (Chapter 3, section 3.16.1 & 3.16.2 respectively; all solutions were filtered and the residue biomass washed back into the following step) at a concentration of 100 $mg.ml^{-1}$ and 50 $mg.ml^{-1}$ respectively (wet weight) and stored at -70^0 C. The resulting fractions were analysed in triplicate for macromolecular content by the appropriate assay, DNA, the diphenylamine assay (Chapter 3, section 3.19.2); RNA, the orcinol assay (Chapter 3, section 3.19.4). All figures were expressed as $mg.g^{-1}$ dry weight biomass (the macromolecular composition was calculated by working out a coefficient between the wet weight [Chapter 3, section 3.11.1] and dry weight [Chapter 3, section 3.11.2] biomass determinations) and converted to percentage format. The percentage difference between methods 1 and 2 (fractions 2 & 3) was also presented. This gave an estimation of the efficiency of nucleic acid extraction. The total mean percentage STDEV was also presented for each assay. nd, not determined; F, fraction; M, method; STDEV, standard deviation.

Table 5.14 Part 1 (Part 1 & 2 are companion tables) The determination of the efficiency of extraction and quantification of protein by the Lowry, Bradford, reverse Biuret, Ninhydrin assay, BCA, and HPLC assays (data corresponds to Tables 5.9 A - J).

Fermentation / organism	Bradford (%)	Lowry (%)	Reverse biuret (%)	BCA (%)
***S. fradiae* C373-10**				
Ferm 1; Day 1	0.46	1.08	9.86	6.89
Ferm 2; Day 1	0.54	1.45	7.41	12.85
Ferm 3; Day 1	1.37	6.62	7.53	8.67
Ferm 4; Day 1	0.74	1.77	7.00	7.14
Mean STDEV	**0.78 ± 0.41**	**2.73 ± 2.60**	**7.95 ± 1.29**	**8.89 ± 2.76**
Ferm 1; Day 2	5.34	3.26	21.95	10.13
Ferm 2; Day 2	2.02	4.35	24.33	14.52
Ferm 3; Day 2	3.82	8.11	22.45	15.16
Ferm 4; Day 2	6.34	11.17	19.79	9.58
Mean STDEV	**4.38 ± 1.88**	**6.72 ± 3.62**	**22.13 ± 1.87**	**12.34 ± 2.89**
Ferm 1; Day 3	7.14	3.88	28.88	11.12
Ferm 2; Day 3	2.92	6.62	27.98	14.65
Ferm 3; Day 3	6.49	10.31	22.28	8.23
Ferm 4; Day 3	5.88	10.88	17.06	9.11
Mean STDEV	**5.60 ± 1.86**	**7.92 ± 3.29**	**24.05 ± 5.50**	**10.78 ± 2.85**
Ferm 1; Day 4	8.96	4.23	32.70	15.23
Ferm 2; Day 4	5.01	9.87	31.01	16.17
Ferm 3; Day 4	8.52	5.78	28.83	12.36
Ferm 4; Day 4	nd	nd	nd	nd
Mean STDEV	**5.62 ± 2.16**	**4.97 ± 2.91**	**23.13 ± 1.94**	**10.94 ± 1.98**
Ferm 1; Day 5	8.73	2.26	44.60	15.89
Ferm 2; Day 5	nd	nd	nd	nd
Ferm 3; Day 5	5.86	15.72	35.16	12.36

Ferm 4; Day 5	nd	nd	nd	nd
Mean STDEV	**3.65 ± 2.03**	**4.49 ± 9.52**	**19.94 ± 6.68**	**7.06 ± 2.50**
Ferm 1; Day 6	3.74	9.56	60.45	16.89
Ferm 2; Day 6	13.04	23.91	38.87	15.14
Ferm 3; Day 6	7.51	13.20	44.97	18.52
Ferm 4; Day 6	5.17	10.86	39.14	20.14
Mean STDEV	**7.36 ± 4.09**	**14.38 ± 6.53**	**45.86 ± 10.13**	**17.67 ± 2.15**
***E. coli* ML308**				
Ferm 1 Day 2	45.62	48.95	49.85	47.52
Ferm 2 Day 2	42.36	38.59	48.52	51.23
Ferm 3 Day 2	36.58	42.15	48.97	50.82
Mean STDEV	**41.52 ± 4.58**	**43.23 ± 5.26**	**49.11 ± 0.68**	**49.86 ± 2.03**
***S. coelicolor* 1147**				
Ferm 1 Day 4	21.56	25.63	44.52	24.63
Ferm 2 Day 4	19.88	29.54	36.98	26.35
Ferm 3 Day 4	24.52	26.34	46.87	28.54
Mean STDEV	**21.99 ± 2.35**	**27.17 ± 2.08**	**42.79 ± 5.17**	**26.51 ± 1.96**
Total Mean percentage STDEV	**± 2.42**	**± 4.48**	**± 4.16**	**± 2.39**

S. fradiae C373-10 was cultured on a glucose glutamate medium [Chapter 3, section 3.6.4](corresponds to Table 5.9 A), *S. coelicolor* 1147 and *E. coli* ML308 were both cultured on a glucose minimal media (Chapter 3, section 3.6.3 and 3.6.1 respectively)[corresponds to Table 5.9 H and I]. The alkali fractions method 1 (Chapter 3, section 3.16.1) were assayed in triplicate for soluble protein by the Lowry assay (Chapter 3, section 3.20.2), the Bradford assay (Chapter 3, section 3.19.5), the ninhydrin assay (Chapter 3, section 3.20.6), reverse biuret assay combined with the copper bathocuproine chelate reaction (Chapter 3, section 3.20.5), bicinchoninic acid assay (Chapter 3, section 3.20.4), and total amino acid analysis by HPLC (Chapter 3, section 3.25.2). HPLC and ninhydrin analysis was also undertaken on whole biomass hydrosylates. The standards were prepared in the appropriate solute. All figures were expressed as $mg.g^{-1}$ dry weight biomass and converted to percentage format. The reconciled data was the mean between all the assays. All analysis was undertaken in triplicate and presented as a mean. The total mean percentage STDEV was also presented for each assay. nd, not determined; STDEV, standard deviation.

Table 5.14 Part 2 (Part 1 & 2 are companion tables) The determination of the efficiency of extraction and quantification of protein by the Lowry, Bradford, reverse Biuret, Ninhydrin assay, BCA, and HPLC assays (data corresponds to Tables 5.9 A - J).

Fermentation / organism	HPLC Alkaline (%)	HPLC Alkaline + residue (%)	HPLC Biomass (%)	Ninhydrin (%)	Ninhydrin whole biomass (%)	Reconciled data (%)
***S. fradiae* C373-10**						
Ferm 1; Day 1	2.45	3.38	3.37	3.25	4.89	3.96
Ferm 2; Day 1	2.71	3.74	3.02	2.89	5.68	4.48
Ferm 3; Day 1	6.70	9.26	7.09	6.14	7.14	6.72
Ferm 4; Day 1	1.56	2.15	3.14	4.95	8.97	4.16
Mean STDEV	**3.35 ± 2.28**	**4.63 ± 3.16**	**4.15 ± 1.96**	**4.31 ± 1.52**	**6.67 ± 1.79**	**4.83 ± 1.28**
Ferm 1; Day 2	14.47	19.18	20.22	27.45	27.65	16.63
Ferm 2; Day 2	12.77	13.19	12.30	8.35	26.48	13.15
Ferm 3; Day 2	14.59	nd	nd	22.13	25.36	15.95
Ferm 4; Day 2	30.89	42.69	40.06	31.99	21.47	23.78
Mean STDEV	**18.18 ± 8.51**	**18.76 ± 15.59**	**18.14 ± 14.30**	**22.48 ± 10.24**	**25.24 ± 2.68**	**17.38 ± 4.53**
Ferm 1; Day 3	27.70	38.28	38.07	38.11	41.23	26.05
Ferm 2; Day 3	26.39	36.47	32.14	22.14	45.89	23.91
Ferm 3; Day 3	22.52	31.13	40.12	55.04	47.95	27.12
Ferm 4; Day 3	11.16	15.42	18.64	19.37	36.25	15.97
Mean STDEV	**21.94 ± 7.52**	**30.32 ± 10.39**	**32.24 ± 9.68**	**33.66 ± 16.47**	**42.83 ± 5.21**	**23.26 ± 5.04**
Ferm 1; Day 4	38.86	53.70	51.10	50.94	47.52	33.69
Ferm 2; Day 4	20.77	28.70	25.45	26.69	36.23	22.21
Ferm 3; Day 4	17.09	35.79	32.16	29.12	39.85	23.28
Ferm 4; Day 4	nd	nd	nd	nd	37.46	37.46
Mean STDEV	**19.18 ± 11.65**	**29.55 ± 11.65**	**27.18 ± 12.88**	**26.69 ± 13.30**	**40.26 ± 13.35**	**29.16 ± 7.58**
Ferm 1; Day 5	23.30	43.68	39.45	32.29	45.63	28.43
Ferm 2; Day 5	25.25	41.15	nd	nd	42.35	36.25

Ferm 3; Day 5	18.66	26.32	20.12	12.30	35.21	20.19
Ferm 4; Day 5	31.05	50.45	nd	nd	25.62	35.71
Mean STDEV	**24.56 ± 5.13**	**40.40 ± 10.17**	**14.89 ± 13.67**	**11.15 ± 14.13**	**37.20 ± 8.86**	**30.14 ± 7.53**
Ferm 1; Day 6	40.28	55.68	53.42	52.76	44.52	37.48
Ferm 2; Day 6	41.24	56.99	57.13	69.93	51.23	40.83
Ferm 3; Day 6	33.73	46.61	50.12	28.53	49.52	32.52
Ferm 4; Day 6	28.70	39.66	42.29	21.53	36.46	27.11
Mean STDEV	**35.99 ± 5.89**	**49.73 ± 8.15**	**50.74 ± 6.32**	**43.19 ± 6.32**	**45.43 ± 22.29**	**34.48 ± 5.99**
***E. coli* ML308**						
Ferm 1 Day 2	42.36	50.23	nd	nd	50.27	47.83
Ferm 2 Day 2	45.96	51.24	nd	nd	45.63	46.22
Ferm 3 Day 2	46.99	50.78	nd	nd	36.98	44.75
Mean STDEV	**45.10 ± 2.43**	**50.75 ± 0.51**	nd	nd	**44.29 ± 6.74**	**46.27 ± 4.54**
***S. coelicolor* 1147**						
Ferm 1 Day 4	nd	24.63	nd	45.62	46.99	33.37
Ferm 2 Day 4	nd	38.72	nd	42.61	43.21	33.90
Ferm 3 Day 4	nd	54.59	nd	38.87	40.12	37.12
Mean STDEV	nd	**39.31 ± 14.99**	nd	**42.37 ± 3.38**	**43.44 ± 3.44**	**34.80 ± 2.03**
Total mean percentage STDEV	**± 6.20**	**± 9.48**	**± 9.87**	**± 13.00**	**± 5.05**	**± 4.44**

S. fradiae C373-10 was cultured on a glucose glutamate medium [Chapter 3, section 3.6.4](corresponds to Table 5.9 A), *S. coelicolor* 1147 and *E. coli* ML308 were both cultured on a glucose minimal media (Chapter 3, section 3.6.3 and 3.6.1 respectively)[corresponds to Table 5.9 H and I]. The alkali fractions method 1 (Chapter 3, section 3.16.1) were assayed in triplicate for soluble protein by the Lowry assay (Chapter 3, section 3.20.2), the Bradford assay (Chapter 3, section 3.19.5), the ninhydrin assay (Chapter 3, section 3.20.6), reverse biuret assay combined with the copper bathocuproine chelate reaction (Chapter 3, section 3.20.5), bicinchoninic acid assay (Chapter 3, section 3.20.4), and total amino acid analysis by HPLC (Chapter 3, section 3.25.2). HPLC and ninhydrin analysis was also undertaken on whole biomass hydrosylates. The standards were prepared in the appropriate solute. All figures were expressed as $mg.g^{-1}$ dry weight biomass and converted to percentage format. The reconciled data was the mean between all the assays. All analysis was undertaken in triplicate and presented as a mean. The total mean percentage STDEV was also presented for each assay. nd, not determined; STDEV, standard deviation.

Table 5.15 Determination of the total amino acid and protein content of each fraction of method 1 & 2 measured by the Bradford assay and the ninhydrin assay.

Ninhydrin assay **Petersons precipitate incorporating the Bradford assay**

Biomass Fractionation / M 1	M 1 (mg.g^{-1} dry wt)	M 1 (%)	Biomass fractionation Method 2	M 2 (mg.g^{-1} dry wt)	M 2 (%)	Biomass fractionation Method 1	M 1 (mg.g^{-1} dry wt)	M 1 (%)	Biomass fractionation Method 2	M 2 (mg.g^{-1} dry wt)	M 2 (%)
COLD			**COLD**			**COLD**			**COLD**		
Ferm 1; Day 6	8.81	0.88	Ferm 1; Day 6	9.99	0.99	Ferm 1; Day 6	2.13	0.21	Ferm 1; Day 6	nd	nd
Ferm 2; Day 6	6.57	0.66	Ferm 2; Day 6	7.52	0.75	Ferm 2; Day 6	1.23	0.12	Ferm 2; Day 6	nd	nd
Ferm 3; Day 6	13.64	1.36	Ferm 3; Day 6	8.87	0.88	Ferm 3; Day 6	3.64	0.36	Ferm 3; Day 6	nd	nd
Ferm 4; Day 6	8.52	0.85	Ferm 4; Day 6	6.54	0.65	Ferm 4; Day 6	2.52	0.25	Ferm 4; Day 6	nd	nd
HOT			**KOH**			**HOT**			**KOH**		
Ferm 1; Day 6	48.89	4.89	Ferm 1; Day 6	1.25	0.12	Ferm 1; Day 6	5.12	0.51	Ferm 1; Day 6	nd	nd
Ferm 2; Day 6	28.79	2.88	Ferm 2; Day 6	2.34	0.23	Ferm 2; Day 6	4.66	0.47	Ferm 2; Day 6	nd	nd
Ferm 3; Day 6	41.53	4.15	Ferm 3; Day 6	4.96	0.50	Ferm 3; Day 6	4.89	0.49	Ferm 3; Day 6	nd	nd
Ferm 4; Day 6	59.45	5.94	Ferm 4; Day 6	4.87	0.49	Ferm 4; Day 6	5.78	0.58	Ferm 4; Day 6	nd	nd
ALKALI			**HOT**			**ALKALI**			**HOT**		
Ferm 1; Day 6	360.28	36.03	Ferm 1; Day 6	38.95	3.89	Ferm 1; Day 6	37.4	3.74	Ferm 1; Day 6	nd	nd
Ferm 2; Day 6	380.59	38.06	Ferm 2; Day 6	26.35	2.63	Ferm 2; Day 6	130.4	13.04	Ferm 2; Day 6	nd	nd
Ferm 3; Day 6	389.65	38.96	Ferm 3; Day 6	14.56	1.46	Ferm 3; Day 6	75.1	7.51	Ferm 3; Day 6	nd	nd
Ferm 4; Day 6	350.53	35.05	Ferm 4; Day 6	47.52	4.75	Ferm 4; Day 6	51.72	5.172	Ferm 4; Day 6	nd	nd
RESIDUE			**ALKALI**			**RESIDUE**			**ALKALI**		
Ferm 1; Day 6	89.93	8.99	Ferm 1; Day 6	269.39	26.94	Ferm 1; Day 6	9.18	0.92	Ferm 1; Day 6	55.63	5.56
Ferm 2; Day 6	96.82	9.68	Ferm 2; Day 6	347.52	34.75	Ferm 2; Day 6	10.12	1.01	Ferm 2; Day 6	89.96	8.99
Ferm 3; Day 6	79.62	7.96	Ferm 3; Day 6	359.89	35.99	Ferm 3; Day 6	8.47	0.85	Ferm 3; Day 6	90.53	9.05
Ferm 4; Day 6	96.63	9.66	Ferm 4; Day 6	423.69	42.37	Ferm 4; Day 6	10.45	1.04	Ferm 4; Day 6	101.23	10.12
Total protein			**RESIDUE**			**Total protein**			**RESIDUE**		
Ferm 1; Day 6	**507.91**	**50.79**	Ferm 1; Day 6	141.52	14.15	Ferm 1; Day 6	53.83	5.38	Ferm 1; Day 6	nd	nd
Ferm 2; Day 6	**512.77**	**51.28**	Ferm 2; Day 6	121.89	12.19	Ferm 2; Day 6	146.41	14.64	Ferm 2; Day 6	nd	nd

Ferm 3; Day 6	**524.44**	**52.44**	Ferm 3; Day 6	201.63	20.16	Ferm 3; Day 6	92.1	9.21	Ferm 3; Day 6	nd	nd
Ferm 4; Day 6	**525.13**	**52.51**	Ferm 4; Day 6	89.63	8.96	Ferm 4; Day 6	70.47	7.05	Ferm 4; Day 6	nd	nd
Unaccountable carbon			**Total protein**			**Unaccountable carbon**			**Total protein**		
Ferm 1 Day 6	**147.63**	**14.76**	**Ferm 1; Day 6**	**461.10**	**46.11**	**Ferm 1 Day 6**	**37.4**	**10.55**	**Ferm 1; Day 6**	nd	nd
Ferm 2 Day 6	**132.18**	**13.22**	**Ferm 2; Day 6**	**505.62**	**50.56**	**Ferm 2 Day 6**	**130.4**	**29.16**	**Ferm 2; Day 6**	nd	nd
Ferm 3 Day 6	**134.18**	**13.47**	**Ferm 3; Day 6**	**589.25**	**58.98**	**Ferm 3 Day 6**	**75.1**	**18.06**	**Ferm 3; Day 6**	nd	nd
Ferm 4 Day 6	**164.60**	**16.45**	**Ferm 4; Day 6**	**572.25**	**57.22**	**Ferm 4 Day 6**	**51.72**	**13.84**	**Ferm 4; Day 6**	nd	nd
			Unaccountable carbon						**Unaccountable carbon**		
			Ferm 1 Day 6	**191.71**	**19.15**				**Ferm 1 Day 6**	nd	nd
			Ferm 2 Day 6	**158.10**	**15.80**				**Ferm 2 Day 6**	nd	nd
			Ferm 3 Day 6	**230.02**	**23.00**				**Ferm 3 Day 6**	nd	nd
			Ferm 4 Day 6	**143.56**	**14.85**				**Ferm 4 Day 6**	nd	nd

Previously obtained fractions for method 1 & 2 (Chapter 3, section 3.16.1 & 3.16.2) for *S. fradiae* C373-10 cultured on a glucose glutamate defined medium (Chapter 3, section 3.6.4)[corresponding to Table 5.9 A] were further analysed to determine the distribution of amino acids and protein between the fractions of method 1 & 2 (Method 1, fractions 1 - 4, COLD, HOT, Alkali, and Residue; Method 2, fractions 1 - 5, COLD, KOH, HOT, Alkali, and Residue) and to what extent this affects the overall protein recovery. The fractions were analysed in triplicate with the ninhydrin assay (Chapter 3, section 3.20.6) and the Bradford assay (Chapter, section 3.20.1). All figures were expressed in $mg.g^{-1}$ dry weight biomass (the macromolecular composition was calculated by working out a weighting coefficient between the wet weight [Chapter 3, section 3.11.1] and dry weight [Chapter 3, section 3.11.2] biomass determinations) and converted to the percentage format. Total protein represents the total protein content of all the fractions for method 1 and 2. The unaccounted for carbon (in red) represents the proportion of protein that would not be accounted for if only the alkali fraction was analysed. nd, not determined; M, method.

Table 5.16 The measurement of the amount of protein or peptide chains contained in the alkali fraction

Fermentation / sample	Total amino acids (ninhydrin assay) with alkaline hydrolysis	Total amino acids (ninhydrin assay) without alkaline hydrolysis	Amount of proteins and peptides
Ferm 1; Day 1	48.9 ± 10.93	98.6 ± 21.14	-49.7
Ferm 2; Day 1	56.8 ± 15.24	74.1 ± 18.89	-17.3
Ferm 3; Day 1	71.4 ± 9.52	75.3 ± 25.62	-3.9
Ferm 4; Day 1	89.7 ± 7.45	70.0 ± 9.86	19.7
Mean STDEV	**66.7 ± 10.78**	**79.5 ± 18.88**	**-12.8**
Ferm 1; Day 2	276.5 ± 20.56	219.5 ± 40.52	57.0
Ferm 2; Day 2	264.8 ± 25.63	243.3 ± 30.03	21.5
Ferm 3; Day 2	253.6 ± 15.32	224.5 ± 42.21	29.1
Ferm 4; Day 2	214.7 ± 12.22	197.9 ± 39.12	16.8
Mean STDEV	**252.4 ± 18.43**	**221.3 ± 37.97**	**31.1**
Ferm 1; Day 3	412.3 ± 60.28	288.8 ± 50.12	123.5
Ferm 2; Day 3	458.9 ± 45.62	279.8 ± 49.85	179.1
Ferm 3; Day 3	479.5 ± 32.60	222.8 ± 60.24	256.7
Ferm 4; Day 3	362.5 ± 50.12	170.6 ± 55.55	191.9
Mean STDEV	**428.3 ± 47.15**	**240.5 ± 53.94**	**187.8**
Ferm 1; Day 4	475.2 ± 60.21	327.0 ± 54.87	148.2
Ferm 2; Day 4	362.3 ± 40.12	310.1 ± 60.38	52.2
Ferm 3; Day 4	398.5 ± 51.11	288.3 ± 80.97	110.2
Ferm 4; Day 4	374.6 ± 23.35	nd	nd
Mean STDEV	**402.6 ± 43.70**	**231.3 ± 49.05**	**171.3**
Ferm 1; Day 5	456.3 ± 20.24	446.0 ± 90.09	10.3
Ferm 2; Day 5	423.5 ± 40.36	nd	nd
Ferm 3; Day 5	352.1 ± 27.27	351.6 ± 100.11	0.5
Ferm 4; Day 5	256.2 ± 15.56	nd	nd
Mean STDEV	**372.0 ± 25.86**	**199.4 ± 47.55**	**171.3**
Ferm 1; Day 6	445.2 ± 40.12	604.5 ± 150.32	-159.3
Ferm 2; Day 6	512.3 ± 15.26	388.7 ± 90.52	123.6

Ferm 3; Day 6	495.2 ± 25.52	449.7 ± 80.96	45.5
Ferm 4; Day 6	364.6 ± 20.69	391.4 ± 60.23	-26.8
Mean STDEV	**454.3 ± 25.40**	**458.6± 95.51**	**-4.25**
Total mean STDEV	**± 28.56**	**± 50.48**	

Previously was obtained fractions for method 1 & 2 (Chapter 3, section 3.16.1 & 3.16.2) for *S. fradiae* C373-10 cultured on a glucose glutamate defined medium (Chapter 3, section 3.6.4) and in addition to biomass obtained from five shake flask cultures grown for *S. coelicolor* 1147 mycelium and *E. coli* ML308 cultured on a glucose minimal medium (Chapter 3, section 3.6.1 and 3.6.3). The appropriate seed defined medium designated a training medium was inoculated with 10 % of the vegetative culture which in turn was used to inoculate the production medium [10 % inoculum]. Further analysis was undertaken to estimate the proportion of protein and peptide chains within the alkali fraction of method 1 (method 1, Chapter 3, section 3.16.1)[samples corresponding to Table 5.9A]. The resulting alkali fraction was further analysed in triplicate for total amino acids, with the ninhydrin assay (Chapter 3, section 3.20.6) with and without alkali hydrolysis. All figures were expressed as $mg.g^{-1}$ dry weight (the macromolecular composition was calculated by working out a weighting coefficient between the wet weight [Chapter 3, section 3.11.1] and dry weight [Chapter 3, section 3.11.2] determinations) and converted to the amount of protein or peptided molecules. nd, not determined. STDEV, standard deviation. Standard deviations were given as plus or minus the given unit. All samples were analysed in triplicate.

Table 5.17 The comparison and verification of three lipid analysis protocols for the estimation the total lipid composition of *S. fradiae* C373-10 biomass cultured on a number of minimal medium compositions with and without the addition of glutamate.

Fermentation profile	Gravimetric analysis of whole biomass (%)	Gravimetric analysis of the alkali fraction (%)	Vanillin assay of the alkali fraction (%)	Anthrone assay of the cold PCA fraction Method 1 (%)
Glucose minimal medium				
48	0.59 ± 0.04	0.44 ± 0.01	0.56 ± 0.03	5.14 ± 3.21
96	0.76 ± 0.05	0.81 ± 0.03	1.11 ± 0.12	7.49 ± 2.13
120	2.39 ± 0.09	3.12 ± 0.05	2.56 ± 0.11	16.99 ± 1.56
Glucose glutamate defined medium				
48	5.89 ± 0.04	4.89 ± 0.01	4.67 ± 0.14	5.41 ± 1.11
96	6.89 ± 0.06	7.11 ± 0.11	7.03 ± 0.36	6.59 ± 2.14
120	12.41 ± 0.08	11.32 ± 0.23	13.56 ± 0.57	9.87 ± 3.17
Fructose minimal medium				
48	3.06 ± 0.11	0.49 ± 0.09	1.56 ± 0.21	8.74 ± 2.61
96	0.89 ± 0.91	1.12 ± 0.08	1.44 ± 0.36	12.45 ± 2.89
120	0.91 ± 0.12	1.56 ± 0.01	1.12 ± 0.47	15.87 ± 1.59
Fructose glutamate defined medium				
48	7.11 ± 0.18	6.25 ± 0.02	6.31 ± 0.23	4.17 ± 2.74
96	8.14 ± 0.08	7.89 ± 0.03	7.84 ± 0.45	6.58 ± 2.61
120	15.54 ± 0.09	12.46 ± 0.16	12.87 ± 0.91	10.17 ± 3.62
Glycerol minimal medium				
48	6.89 ± 0.14	4.23 ± 0.16	3.05 ± 0.58	3.46 ± 0.89

96	1.79 ± 0.69	1.12 ± 0.19	1.01 ± 0.64	5.11 ± 1.52
120	1.39 ± 0.05	1.44 ± 0.08	1.23 ± 0.78	5.17 ± 1.69
Glycerol glutamate defined medium				
48	4.65 ± 0.09	5.68 ± 0.48	5.17 ± 0.41	2.15 ± 0.66
96	5.69 ± 0.12	5.44 ± 0.16	5.78 ± 0.37	6.23 ± 1.69
120	11.35 ± 0.97	10.23 ± 0.68	9.55 ± 0.84	5.99 ± 2.87

S. fradiae C373-10 was cultured on a number of different carbon sources. Medium compositions for *S. fradiae* were as followed (gl^{-1}) glucose (20.0), fructose (20.0), glycerol (40.0), glucose (20.0) glutamate (5.0), fructose (20.0) glutamate (5.0), glycerol (20.0) glutamate (5.0)[other components as Chapter 3, section 3.6.4]. The biomass was harvested at 48, 96, and 120 hrs after inoculation. The biomass was washed with dH_2O and divided into six lots of approximate equal wet weight. One set of triplicates were subjected to fractionation method 1 (Chapter 3, section 3.16.1) and the cold PCA fraction was analysed for carbohydrates with the anthrone assay (Chapter 3, section 3.18.1) and the alkaline fraction was analysed for lipids with the gravimetric analysis (as Chapter 3, section 3.23.3) and the vanillin assay (Chapter 3, section 3.23.1). The second set of triplicates were analysed with solvent extraction and gravimetric analysis was applied (Chapter 3, section 3.23.3). All samples were analysed in triplicate. All figures were expressed as $mg.g^{-1}$ dry weight biomass (the macromolecular composition was calculated by working out a weighting coefficient between the wet weight [Chapter 3, section 3.11.1] and dry weight [Chapter 3, section 3.11.2] biomass determination) and converted to the percentage composition. nd, not determined. Standard deviations were given as plus or minus the unit of measurement.

Table 5.18A Part 1 (Part 1 & 2 companion tables) Comparison of the total carbon content of *S. fradiae* C373-10 biomass cultured on a glucose glutamate defined medium, fractions (Method 1) were determined for their macromolecular estimation and direct carbon measurement (corresponds to Table 5.9 A).

Fermentation	CHO (ppm)	Cold (ppm)	CHO total unaccountable carbon (%)	RNA (ppm)	RNA/DNA total unaccountable carbon (%)	PROT (ppm)	LIPID (ppm)	ALK (ppm)	PROT/LIPID total unaccountable carbon (%)	PROT (ppm)	RES (ppm)	PROT total unaccountable carbon (%)
Ferm 1; Day 1	305.08	544.6	**43.98**	13.70	**85.15**	34.70	166.01	555.6	**63.88**	45.6	411.2	**11.09**
Ferm 2; Day 1	283.88	566.3	**49.87**	16.49	**87.60**	52.47	165.2	1123.2	**80.62**	34.1	343.5	**9.93**
Ferm 3; Day 1	373.6	456.3	**18.12**	17.75	**64.22**	109.51	2118	2531.9	**12.02**	45.8	456.7	**10.03**
Ferm 4; Day 1	531.84	999.4	**46.78**	18.91	**81.66**	70.71	287.59	330.65	**-8.36**	67.9	321.9	**21.09**
Ferm 1; Day 2	277.32	356	**22.10**	15.83	**54.22**	171.66	230.6	311.56	**-29.11**	112.3	213.4	**52.62**
Ferm 2; Day 2	254.2	389.2	**34.69**	17.72	**74.79**	57.12	200.44	500.7	**48.56**	118.9	255.9	**46.46**
Ferm 3; Day 2	280.52	659.23	**57.45**	21.67	**69.93**	100.68	270.84	600.6	**38.14**	105.1	256.8	**40.93**
Ferm 4; Day 2	305.88	700.53	**56.34**	26.29	**81.50**	159.46	132.30	211.6	**-37.89**	97.7	244.7	**39.93**
Ferm 1; Day 3	187.36	445.6	**57.95**	19.26	**82.61**	174.22	330.25	400.9	**-25.83**	99	600.1	**16.50**
Ferm 2; Day 3	249.64	521.3	**52.11**	12.44	**79.20**	66.99	208.19	321.4	**14.38**	98.1	454.2	**21.60**
Ferm 3; Day 3	189.16	660.23	**71.35**	22.30	**59.04**	152.84	185.32	245.6	**-37.69**	92.12	321.7	**28.63**
Ferm 4; Day 3	203.04	712.3	**71.49**	22.87	**36.02**	167.13	264.8	399.1	**-8.23**	67.9	890.1	**7.63**
Ferm 1; Day 4	179.76	289.6	**37.93**	16.90	**33.08**	187.46	311.58	567.8	**12.11**	118.9	567.8	**20.94**
Ferm 2; Day 4	168.12	312.5	**46.20**	13.29	**58.62**	100.94	2956.0	589.1	**32.62**	112.4	412.9	**27.22**
Ferm 3; Day 4	190.16	366.2	**48.07**	19.35	**93.25**	190.95	456.8	656.7	**1.36**	123.6	321.5	**38.44**
Ferm 4; Day 4	nd	nd	**nd**	nd	**nd**	nd	nd	nd	**nd**	nd	nd	**nd**

Ferm 1; Day 5	115.36	330.6	**65.11**	20.67	**62.90**	143.90	331.57	400.2	**-18.81**	145.8	397.5	**36.68**
Ferm 2; Day 5	121.24	350.8	**65.44**	17.65	**84.17**	nd	335.6	340.4	**nd**	154.6	354.2	**43.65**
Ferm 3; Day 5	222.12	451.29	**50.78**	25.82	**62.07**	97.196	667.03	700.8	**-9.05**	110.2	345.1	**31.93**
Ferm 4; Day 5	99.2	660.58	**84.98**	18.50	**63.94**	nd	754.2	901.2	**nd**	97.5	315.8	**30.87**
Ferm 1; Day 6	58.48	253.85	**76.96**	19.95	**61.45**	43.41	149.40	1226.98	**84.29**	56.3	356.88	**15.77**
Ferm 2; Day 6	163.68	410.03	**60.08**	24.03	**58.84**	173.64	526.49	295.10	**-137.25**	23.1	260.47	**8.87**
Ferm 3; Day 6	88.04	548.85	**83.96**	20.01	**79.62**	103.00	299.74	332.22	**-21.23**	14.1	785.31	**1.79**
Ferm 4; Day 6	91.96	338.56	**72.84**	17.06	**94.62**	80.23	386.03	375.79	**-24.07**	27.8	243.01	**11.44**
Mean			**52.25**		**65.82**				**2.60**			**24.46**

S. fradiae C373-10 biomass samples cultured on a glucose glutamate defined medium (Chapter 3, section 3.6.4) and grown in a 7 L bioreactor (see Chapter 4 for fermentation description and profiles)[corresponding to Table 5.9 A]. Each biomass sample was washed and subjected to extraction procedure method 1 (Chapter 3, section 3.16.1 all solutions were filtered and the residue biomass washed back in to the following step) at concentration of 100 $mg.ml^{-1}$ (wet weight) and stored at -70^{0} C. The resulting fractions were analysed in triplicate for macromolecular content by the appropriate assay. Carbohydrate, the anthrone assay (Chapter 3, section 3.18.1); DNA, the diphenylamine assay (Chapter 3, section 3.19.2); RNA, the orcinol assay (Chapter 3, section 3.19.4); protein, the ninhydrin assay (Chapter 3, section 3.20.6); lipid, the vanillin assay (Chapter 3, section 3.23.1). The macromolecule concentrations in each resulting fraction were determined and expressed as parts per million (ppm = $\mu g.ml^{-1}$) of carbon in the columns headed CHO (carbohydrate [ppm]), RNA, DNA, LIPID and PROT (protein)[Table 5.18A Part 1]{see Appendix F for calculation}. These values were then calculated as the percentage (%) of the total unaccountable carbon (Table 5.18A Part 2) in each fraction and the total unaccountable carbon of all fractions. Fractions as method 1, COLD (fraction 1), HOT (fraction 2), ALKALI (fraction 3) and RESIDUE (fraction 4) fraction were measured by total organic carbon analysis (Chapter 3, section 3.15.5). Table 5.18B presents his data in the format of percentage (%) proportion of carbon in each fraction. nd, not determined.

Table 5.18A Part 2 (Part 1 & 2 companion tables) Comparison of the total carbon content of *S. fradiae* C373-10 biomass cultured on a glucose glutamate defined medium, fractions (Method 1) were determined for their macromolecular estimation and direct carbon measurement (corresponds to Table 5.9 A).

Fermentation	Total macromolecular carbon content (ppm)	Total organic elemental carbon content (ppm)	The amount of total unaccountable carbon (%)
Ferm 1; Day 1	385.50	1245.34	**69.04**
Ferm 2; Day 1	358.76	1845.47	**80.56**
Ferm 3; Day 1	463.65	3130.41	**85.19**
Ferm 4; Day 1	646.93	956.63	**32.37**
Ferm 1; Day 2	441.20	659.73	**33.12**
Ferm 2; Day 2	420.92	980.98	**57.09**
Ferm 3; Day 2	445.49	1113.96	**60.01**
Ferm 4; Day 2	475.65	902.19	**47.28**
Ferm 1; Day 3	345.12	1396.75	**75.29**
Ferm 2; Day 3	392.86	1044.70	**62.39**
Ferm 3; Day 3	345.09	794.43	**56.56**
Ferm 4; Day 3	350.06	1484.36	**76.42**
Ferm 1; Day 4	358.66	1263.20	**71.61**
Ferm 2; Day 4	326.53	1159.40	**71.86**
Ferm 3; Day 4	382.04	2038.37	**81.26**
Ferm 4; Day 4	Nd	nd	**nd**
Ferm 1; Day 5	322.70	1028.71	**68.63**
Ferm 2; Day 5	328.22	1090.82	**69.91**

Ferm 3; Day 5	412.69	1308.57	**68.46**
Ferm 4; Day 5	256.47	1467.75	**82.53**
Ferm 1; Day 6	174.90	1816.78	**90.37**
Ferm 2; Day 6	275.36	830.86	**66.86**
Ferm 3; Day 6	166.69	1518.30	**89.02**
Ferm 4; Day 6	173.33	1687.55	**89.73**
The mean amount of total unaccountable carbon (%)			**65.03**

S. fradiae C373-10 biomass samples cultured on a glucose glutamate defined medium (Chapter 3, section 3.6.4) and grown in a 7 L bioreactor (see Chapter 4 for fermentation description and profiles)[corresponding to Table 5.9 A]. Each biomass sample was washed and subjected to extraction procedure method 1 (Chapter 3, section 3.16.1 all solutions were filtered and the residue biomass washed back in to the following step) at concentration of 100 $mg.ml^{-1}$ (wet weight) and stored at -70^{0} C. The resulting fractions were analysed in triplicate for macromolecular content by the appropriate assay. Carbohydrate, the anthrone assay (Chapter 3, section 3.18.1); DNA, the diphenylamine assay (Chapter 3, section 3.19.2); RNA, the orcinol assay (Chapter 3, section 3.19.4); protein, the ninhydrin assay (Chapter 3, section 3.20.6); lipid, the vanillin assay (Chapter 3, section 3.23.1). The macromolecule concentrations in each resulting fraction were determined and expressed as parts per million (ppm = $\mu g.ml^{-1}$) of carbon in the columns headed CHO (carbohydrate [ppm]), RNA, DNA, LIPID and PROT (protein)[Table 5.18A Part 1]{see Appendix F for calculation}. These values were then calculated as the percentage (%) of the total unaccountable carbon (Table 5.18A Part 2) in each fraction and the total unaccountable carbon of all fractions. Fractions as method 1, COLD (fraction 1), HOT (fraction 2), ALKALI (fraction 3) and RESIDUE (fraction 4) fraction were measured by total organic carbon analysis (Chapter 3, section 3.15.5). Table 5.18B presents his data in the format of percentage (%) proportion of carbon in each fraction. nd, not determined.

Table 5.18B Comparison of carbon distribution of method 1 fractions determined from direct carbon measurement and presented as the percentage of the total carbon in each fraction (corresponds to Table 5.9A).

Fermentation	Cold (%)	Hot (%)	Alkali (%)	Residue (%)	Fermentation	Cold (%)	Hot (%)	Alkali (%)	Residue (%)
Ferm 1; Day 1	31.19	13.43	31.82	23.55	**Ferm 1; Day 4**	19.12	5.919	37.48	37.48
Ferm 2; Day 1	23.98	13.92	47.55	14.54	**Ferm 2; Day 4**	21.92	7.80	41.32	28.96
Ferm 3; Day 1	12.79	3.466	70.95	12.80	**Ferm 3; Day 4**	15.54	42.95	27.87	13.64
Ferm 4; Day 1	52.34	13.48	17.32	16.86	**Ferm 4; Day 4**	nd	nd	nd	nd
Ferm 1; Day 2	35.83	11.34	31.35	21.48	**Ferm 1; Day 5**	25.54	12.82	30.92	30.71
Ferm 2; Day 2	29.14	14.20	37.49	19.16	**Ferm 2; Day 5**	25.49	24.04	24.73	25.74
Ferm 3; Day 2	38.42	11.60	35.00	14.97	**Ferm 3; Day 5**	26.40	12.40	41.00	20.19
Ferm 4; Day 2	45.30	25.19	13.68	15.82	**Ferm 4; Day 5**	32.33	8.11	44.10	15.45
Ferm 1; Day 3	24.97	18.93	22.47	33.63	**Ferm 1; Day 6**	12.73	7.82	61.54	17.90
Ferm 2; Day 3	34.43	14.33	21.23	30.00	**Ferm 2; Day 6**	34.72	18.22	24.99	22.06
Ferm 3; Day 3	47.73	11.26	17.75	23.26	**Ferm 3; Day 6**	27.67	15.97	16.75	39.60
Ferm 4; Day 3	33.52	5.82	18.78	41.88	**Ferm 4; Day 6**	17.33	50.99	19.24	12.44
Ferm 1; Day 4	19.12	5.919	37.48	37.48					
Ferm 2; Day 4	21.92	7.80	41.32	28.96					
Ferm 3; Day 4	15.54	42.95	27.87	13.64					
Ferm 4; Day 4	nd	nd	Nd	nd					

S. fradiae C373-10 biomass samples cultured on a glucose glutamate defined medium (Chapter 3, section 3.6.4) and grown in a 7 L bioreactor (see Chapter 4 for fermentation description and profiles)[corresponding to Table 5.9 A]. Each biomass sample was washed and subjected to extraction procedure method 1 (Chapter 3, section 3.16.1 all solutions were filtered and the residue biomass washed back in to the following step) at concentration of 100 $mg.ml^{-1}$ (wet weight) and stored at -70^{0} C. The resulting fractions were analysed in triplicate for macromolecular content by the appropriate assay. Carbohydrate, the anthrone assay (Chapter 3, section 3.18.1); DNA, the diphenylamine assay (Chapter 3, section 3.19.2); RNA, the orcinol assay (Chapter 3, section 3.19.4); protein, the ninhydrin assay (Chapter 3, section 3.20.6); lipid, the vanillin assay (Chapter 3, section 3.23.1). The macromolecule concentrations in each resulting fraction were determined and expressed as parts per million (ppm = $\mu g.ml^{-1}$) of carbon in the columns headed CHO (carbohydrate [ppm]), RNA, DNA, LIPID and PROT (protein)[Table 5.18A Part 1]{see Appendix F for calculation}. These values were then calculated as the percentage (%) of the total unaccountable carbon (Table 5.18A Part 2) in each fraction and the total unaccountable carbon of all fractions. Fractions as method 1, COLD (fraction 1), HOT (fraction 2), ALKALI (fraction 3) and RESIDUE (fraction 4) fraction were measured by total organic carbon analysis (Chapter 3, section 3.15.5). Table 5.18B presents his data in the format of percentage (%) proportion of carbon in each fraction. nd, not determined.

Table 5.19A Part 1 (Part 1 & 2 companion tables) Comparison of the total carbon content of *S. fradiae* C373-10 biomass cultured on a glucose glutamate defined medium, fractions (Method 2) were determined for their macromolecular estimation and direct carbon measurement (corresponds to Table 5.8)

Fermentation	CHO (ppm)	Cold (ppm)	CHO total unaccountable carbon (%)	RNA (ppm)	KOH (ppm)	KOH total unaccountable carbon (%)	RNA (ppm)	DNA (ppm)	HOT (ppm)	RNA/DNA total unaccountable carbon (%)	PROT (ppm)	LIPID (ppm)	ALK (ppm)	PROT/LIPID total unaccountable carbon (%)
Ferm 1; Day 2	272.8	523.8	**47.92**	29.13	250.2	**88.36**	116.88	120.42	600.23	**60.46**	171.86	nd	511.69	**nd**
Ferm 2; Day 2	231.6	499.5	**53.63**	33.76	244.8	**86.21**	65.53	74.95	555.4	**74.71**	87.66	170.33	658.32	**60.81**
Ferm 3; Day 2	204.4	427.1	**52.14**	38.63	268.5	**85.61**	38.57	50.72	512.3	**82.57**	137.99	232.65	489.75	**24.32**
Ferm 4; Day 2	247.56	980.4	**74.75**	50.15	311.8	**83.92**	84.77	108.18	200.36	**3.70**	127.42	86.53	546.23	**60.83**
Ferm 1; Day 3	140	330.4	**57.63**	49.28	455.8	**89.19**	171.33	185.41	411.2	**13.24**	275.48	nd	689.27	**nd**
Ferm 2; Day 3	158.26	310.7	**49.06**	71.93	505.2	**85.76**	nd	nd	482.3	**nd**	93.95	175.51	nd	**nd**
Ferm 3; Day 3	175.6	299.12	**41.29**	88.95	611.2	**85.45**	89.40	112.92	999.1	**79.75**	185.25	143.82	711.56	**53.75**
Ferm 4; Day 3	198.8	550.2	**63.87**	23.15	752.1	**96.92**	92.32	98.29	564.66	**66.24**	189.67	nd	564.28	**nd**
Ferm 1; Day 4	114.8	323.6	**64.52**	48.14	289.6	**83.37**	96.96	117.23	426.35	**49.76**	191.68	nd	600.28	**nd**
Ferm 2; Day 4	177.6	299.5	**40.70**	43.91	245.7	**82.13**	nd	nd	nd	**nd**	184.71	263.27	nd	**nd**
Ferm 3; Day 4	139.48	255.4	**45.39**	45.74	264.3	**82.69**	nd	nd	nd	**nd**	100.51	nd	654.87	**nd**
Ferm 4; Day 4	94.44	500.1	**81.11**	59.35	202.4	**70.67**	nd	nd	nd	**nd**	112.02	nd	789.24	**nd**
Ferm 1; Day 5	63.56	155.2	**59.05**	27.21	152.3	**82.13**	43.37	53.30	364.89	**73.50**	111.49	290.69	587.46	**31.54**
Ferm 2; Day 5	100.4	154.3	**34.93**	17.98	149.5	**87.97**	47.67	57.49	546.28	**80.75**	74.68	nd	890.24	**nd**

Ferm 3; Day 5	80.4	165.8	**51.51**	2.70	234.9	**98.85**	33.93	42.33	402.56	**81.05**	122.19	612.48	990.57	**25.83**
Ferm 4; Day 5	67.44	211.4	**68.10**	26.16	175.2	**85.07**	40.80	58.03	386.54	**74.43**	92.08	nd	1234.6	**nd**
Ferm 1; Day 6	15.12	112.70	**86.58**	19.15	272.53	**92.97**	31.87	60.15	356.96	**74.22**	83.11	109.23	325.97	**40.99**
Ferm 2; Day 6	27.84	179.91	**84.52**	9.44	233.26	**95.95**	44.92	55.35	263.87	**61.99**	101.45	461.94	510.52	**-10.36**
Ferm 3; Day 6	23.96	143.17	**83.26**	34.57	248.80	**86.11**	36.50	61.24	207.29	**52.85**	114.03	255.20	328.46	**-12.41**
Ferm 4; Day 6	41.04	145.88	**71.87**	10.38	286.71	**96.38**	35.65	53.79	658.08	**86.41**	89.27	349.51	293.17	**-49.67**
Mean			**51.25**			**87.28**				**36.52**				**87.43**

S. fradiae C373-10 was cultured on a glucose glutamate defined medium (Chapter 3, section 3.6.4) and grown in a 7 L bioreactor (see Chapter 4 for fermentation description and profiles)[corresponding to Table 5.8]. Each biomass sample was washed and subjected to extraction procedure method 2 (Chapter 3, section 3.16.2 all solutions were filtered and the residue biomass washed back in to the following step) at concentration of 50 $mg.ml^{-1}$ (wet weight) and stored at -70^0 C. The resulting fractions were analysed in triplicate for macromolecular content by the appropriate assay. Carbohydrate, the anthrone assay (Chapter 3, section 3.18.1); DNA, the diphenylamine assay (Chapter 3, section 3.19.2); RNA, the orcinol assay (Chapter 3, section 3.19.4); protein, the ninhydrin assay (Chapter 3, section 3.20.6); lipid, the vanillin assay (Chapter 3, section 3.23.1). The macromolecule concentrations in each resulting fraction were determined and expressed as parts per million (ppm = $\mu g.ml^{-1}$) of carbon in the columns headed CHO (carbohydrate [ppm]), RNA, DNA, LIPID and PROT (protein)[Table 5.19A Part 1]{see Appendix F for calculation}. These values were then calculated as the percentage (%) of the total unaccountable carbon (Table 5.18A Part 2) in each fraction and the total unaccountable carbon of all fractions. COLD (fraction 1), KOH (fraction 2), HOT (fraction 3), ALKALI (fraction 4) and RESIDUE (fraction 5) fraction as measured by total organic carbon analysis (Chapter 3, section 3.15.5). Table 5.19B presents his data in the format of percentage (%) proportion of carbon in each fraction. nd, not determined.

Table 5.19A Part 2 (Part 1 & 2 companion tables) Comparison of the total carbon content of *S. fradiae* C373-10 biomass cultured on a glucose glutamate defined medium, fractions (Method 2) were determined for their macromolecular estimation and direct carbon measurement (corresponds to Table 5.8)

Fermentation	PROT (ppm)	RES (ppm)	PROT total unaccountable carbon (%)	Total macromolecular carbon content (ppm)	Total organic elemental carbon content (ppm)	The amount of total unaccountable carbon (%)
Ferm 1; Day 2	112.3	212.87	**47.24**	nd	2098.79	**nd**
Ferm 2; Day 2	118.9	247.56	**51.97**	782.73	2205.58	**64.51**
Ferm 3; Day 2	105.1	236.45	**55.55**	808.07	1934.1	**58.22**
Ferm 4; Day 2	97.7	211.32	**53.77**	802.30	2250.11	**64.34**
Ferm 1; Day 3	99	200.33	**50.58**	nd	2087	**nd**
Ferm 2; Day 3	98.1	211.34	**53.58**	nd	nd	**nd**
Ferm 3; Day 3	92.12	236.48	**61.04**	888.06	2857.46	**68.92**
Ferm 4; Day 3	67.9	256.86	**73.56**	nd	2688.1	**nd**
Ferm 1; Day 4	118.9	880.24	**86.49**	nd	2520.07	**nd**
Ferm 2; Day 4	112.4	256.84	**56.24**	nd	nd	**nd**
Ferm 3; Day 4	123.6	330.21	**62.57**	nd	nd	**nd**
Ferm 4; Day 4	134.8	321.48	**58.07**	nd	nd	**nd**
Ferm 1; Day 5	145.8	299.56	**51.33**	735.43	1559.41	**52.84**
Ferm 2; Day 5	154.6	246.57	**37.30**	nd	1986.89	**nd**
Ferm 3; Day 5	110.2	387.2	**71.54**	1004.2	2181.03	**53.95**
Ferm 4; Day 5	97.5	269.32	**63.80**	nd	2277.02	**nd**

Ferm 1; Day 6	56.3	127.06	**55.69**	374.93	1195.23	**68.63**
Ferm 2; Day 6	23.1	103.53	**77.69**	724.05	1291.08	**43.92**
Ferm 3; Day 6	14.1	567.52	**97.51**	539.60	1495.23	**63.91**
Ferm 4; Day 6	27.8	156.55	**82.24**	607.42	1540.39	**60.57**
The amount of total unaccountable carbon (%)			**48.16**			**33.35**

S. fradiae C373-10 was cultured on a glucose glutamate defined medium (Chapter 3, section 3.6.4) and grown in a 7 L bioreactor (see Chapter 4 for fermentation description and profiles)[corresponding to Table 5.8]. Each biomass sample was washed and subjected to extraction procedure method 2 (Chapter 3, section 3.16.2 all solutions were filtered and the residue biomass washed back in to the following step) at concentration of 50 $mg.ml^{-1}$ (wet weight) and stored at -70^0 C. The resulting fractions were analysed in triplicate for macromolecular content by the appropriate assay. Carbohydrate, the anthrone assay (Chapter 3, section 3.18.1); DNA, the diphenylamine assay (Chapter 3, section 3.19.2); RNA, the orcinol assay (Chapter 3, section 3.19.4); protein, the ninhydrin assay (Chapter 3, section 3.20.6); lipid, the vanillin assay (Chapter 3, section 3.23.1). The macromolecule concentrations in each resulting fraction were determined and expressed as parts per million (ppm = $\mu g.ml^{-1}$) of carbon in the columns headed CHO (carbohydrate [ppm]), RNA, DNA, LIPID and PROT (protein)[Table 5.19A Part 1]{see Appendix F for calculation}. These values were then calculated as the percentage (%) of the total unaccountable carbon (Table 5.18A Part 2) in each fraction and the total unaccountable carbon of all fractions. COLD (fraction 1), KOH (fraction 2), HOT (fraction 3), ALKALI (fraction 4) and RESIDUE (fraction 5) fraction as measured by total organic carbon analysis (Chapter 3, section 3.15.5). Table 5.19B presents his data in the format of percentage (%) proportion of carbon in each fraction. nd, not determined.

Table 5.19B Comparison of carbon distribution of method 2 fractions determined from direct carbon measurement and presented as the percentage of the total carbon in each fraction (corresponds to Table 5.9A).

Fermentation	CHO (%)	KOH (%)	HOT (%)	AKALI (%)	RESIDUE (%)	Fermentation	CHO (%)	KOH (%)	HOT (%)	AKALI (%)	RESIDUE (%)
Ferm 1; Day 2	24.96	11.92	28.60	24.38	10.14	**Ferm 1; Day 5**	9.95	9.77	23.40	37.67	19.21
Ferm 2; Day 2	22.65	11.10	25.18	29.85	11.22	**Ferm 2; Day 5**	7.76	7.52	27.49	44.81	12.41
Ferm 3; Day 2	22.08	13.88	26.49	25.32	12.22	**Ferm 3; Day 5**	7.60	10.77	18.46	45.42	17.75
Ferm 4; Day 2	43.57	13.86	8.90	24.28	9.39	**Ferm 4; Day 5**	9.28	7.69	16.97	54.22	11.83
Ferm 1; Day 3	15.83	21.84	19.70	33.03	9.60	**Ferm 1; Day 6**	9.43	22.80	29.86	27.27	10.63
Ferm 2; Day 3	nd	nd	nd	Nd	nd	**Ferm 2; Day 6**	13.93	18.07	20.44	39.54	8.02
Ferm 3; Day 3	10.47	21.39	34.96	24.90	8.28	**Ferm 3; Day 6**	9.57	16.64	13.86	21.97	37.95
Ferm 4; Day 3	20.47	27.98	21.01	20.99	9.55	**Ferm 4; Day 6**	9.47	18.61	42.72	19.03	10.16
Ferm 1; Day 4	12.84	11.49	16.92	23.82	34.93						
Ferm 2; Day 4	nd	nd	nd	Nd	nd						
Ferm 3; Day 4	nd	nd	nd	Nd	nd						
Ferm 4; Day 4	nd	nd	nd	Nd	nd						

S. fradiae C373-10 was cultured on a glucose glutamate defined medium (Chapter 3, section 3.6.4) and grown in a 7 L bioreactor (see Chapter 4 for fermentation description and profiles)[corresponding to Table 5.8]. Each biomass sample was washed and subjected to extraction procedure method 2 (Chapter 3, section 3.16.2 all solutions were filtered and the residue biomass washed back in to the following step) at concentration of 50 $mg.ml^{-1}$ (wet weight) and stored at -70^{0} C. The resulting fractions were analysed in triplicate for macromolecular content by the appropriate assay. Carbohydrate, the anthrone assay (Chapter 3, section 3.18.1); DNA, the diphenylamine assay (Chapter 3, section 3.19.2); RNA, the orcinol assay (Chapter 3, section 3.19.4); protein, the ninhydrin assay (Chapter 3, section 3.20.6); lipid, the vanillin assay (Chapter 3, section 3.23.1). The macromolecule concentrations in each resulting fraction were determined and expressed as parts per million (ppm = $\mu g.ml^{-1}$) of carbon in the columns headed CHO (carbohydrate [ppm]), RNA, DNA, LIPID and PROT (protein)[Table 5.19A Part 1]{see Appendix F for calculation}. These values were then calculated as the percentage (%) of the total unaccountable carbon (Table 5.18A Part 2) in each fraction and the total unaccountable carbon of all fractions. COLD (fraction 1), KOH (fraction 2), HOT (fraction 3), ALKALI (fraction 4) and RESIDUE (fraction 5) fraction as measured by total organic carbon analysis (Chapter 3, section 3.15.5). Table 5.19B presents his data in the format of percentage (%) proportion of carbon in each fraction. nd, not determined.

Table 5.20A Part 1 (Part 1 & 2 companion tables) Comparison of the total carbon content of *S. coelicolor* 1147 and *E. coli* ML308 biomass in relation to the macromolecular determination by method 1 (corresponds to Tables 5.9 H & I).

Fermentation	CHO	Cold	CHO (%)	RNA	DNA	RNA/DNA total	HOT	RNA/DNA total (%)	PROT	LIPID	PROT/LIPID total	ALK	PROT/LIPID total %
***S. coelicolor* 1147**													
Ferm 1, Day 5	5.2	96.8	94.63	162.4	86.4	248.8	428.4	41.92	322.5	nd	322.5	1014	68.19
Ferm 2, Day 5	29.7	118.7	74.98	149.8	97	246.8	203.4	-21.34	428.3	nd	428.3	1253.3	65.83
Ferm 3, Day 5	41.7	262	84.08	114.7	55.6	170.3	331.7	48.66	405	nd	405	1265.6	67.99
Ferm 4, Day 5	63.8	207.2	69.21	169.5	78.8	248.3	428.4	42.04	183.8	nd	183.8	1067.1	82.77
Ferm 5, Day 5	60	201	70.15	253.8	89.3	343.1	527	34.90	211.2	nd	211.2	1171.8	81.98
Ferm 6, Day 5	28.6	132.2	78.37	184	60.4	244.4	391	37.49	505	nd	505	1182.9	57.31
Ferm 7, Day 5	28.6	162.4	82.39	246.7	127.4	374.1	558	32.96	800	nd	800	1596.4	49.89
Mean			**79.11**					**30.95**					**67.71**
E. coli ML308													
Ferm 1; 24 hrs	31.546	294.01	89.27	112.17	88.43	200.60	280.90	28.59	1636.65	183.61	1820.27	2295.17	20.69
Ferm 2; 24 hrs	30.488	312.69	90.25	153.43	75.35	228.78	266.93	14.29	1342.30	170.33	1512.63	2132.69	29.07
Mean			**89.76**					**21.44**					**24.88**

Fermentation	PROT	RES	PROT %	Total macromolecular carbon content (ppm)	Total organic elemental carbon content (ppm)	The amount of total unaccountable carbon (%)
***S. coelicolor* 1147**						
Ferm 1, Day 5	52.5	260.2	79.82	629	1799.4	65.04
Ferm 2, Day 5	93.8	796.2	88.22	798.6	2371.6	66.33
Ferm 3, Day 5	29.6	406.6	92.72	646.6	2265.9	71.46
Ferm 4, Day 5	74.4	522.5	85.76	570.3	2225.2	74.37
Ferm 5, Day 5	92.5	496.4	81.36	706.8	2396.2	70.50
Ferm 6, Day 5	106	485.5	78.18	884	2191.6	59.66
Ferm 7, Day 5	117.5	597.9	80.35	1320.2	2914.7	54.70

Mean			**83.77**			**66.01**
***E. coli* ML308**						
Ferm 1; 24 hrs	212.87	481.08	55.75	2265.28	3351.16	32.40
Ferm 2; 24 hrs	247.56	433.67	42.91	2019.46	3145.98	35.81
Mean			**49.33**			**34.11**

S. coelicolor 1147 (cultured in a 5 L bioreactor) and *E. coli* ML308 (cultured in shake flasks) were both cultured on a glucose minimal medium (Chapter 3, section 3.6.1 and 3.6.3 respectively) [see Chapter 4 for fermentation description and profiles]{corresponds to Tables 5.9H & I}. Each biomass sample was washed and subjected to fractionation procedure method 1 (Chapter 3, section 3.16.1 all solutions were filtered and the residue biomass washed back in to the following step) at concentration of 100 $mg.ml^{-1}$ (wet weight) and stored at -70^{0} C. The resulting fractions were analysed in triplicate for the macromolecular content by the appropriate assay. Carbohydrate, the anthrone assay (Chapter 3, section 3.18.1); DNA, the diphenylamine assay (Chapter 3, section 3.19.2); RNA, the orcinol assay (Chapter 3, section 3.19.4); protein, the ninhydrin assay (Chapter 3, section 3.20.6); lipid, the vanillin assay (Chapter 3, section 3.23.1). The macromolecular concentrations in each resulting fraction were determined and expressed as parts per million (ppm = $\mu g.ml^{-1}$) of carbon in the columns headed CHO (carbohydrate [ppm]), RNA, DNA, LIPID and PROT (protein)[Table 5.20A Part 1]. These values were then calculated as the percentage (%) of the total unaccountable carbon (Table 5.20A Part 1) in each appropriate fraction COLD (fraction 1), HOT (fraction 2), ALKALI (fraction 3) and RESIDUE (fraction 4) were measured by total organic carbon analysis (Chapter 3, section 3.15.5). Table 5.20B presents his data in the format of percentage (%) proportion of carbon in each fraction. nd, not determined.

Table 5.20A Part 2 (Part 1 & 2 companion tables) Comparison of the total carbon content of *S. coelicolor* 1147 and *E. coli* ML308 biomass in relation to the macromolecular determination by method 2.

Fermentation	CHO	Cold	CHO (%)	RNA	DNA	RNA/DNA total	KOH	KOH (%)	RNA	DNA	RNA / DNA total	HOT	RNA / DNA total (%)	PROT	ALK	PROT (%)
***S. coelicolor* 1147**																
Ferm 1, Day 5	45.63	316.9	85.60	205.63	8.63	214.26	1315	83.71	52.13	86.23	138.36	785	82.37	325.69	3418	90.47
Ferm 2, Day 5	54.69	360	84.81	256.21	10.13	266.34	1348	80.24	47.77	101.74	149.51	1440	89.62	421.59	2438	82.71
Ferm 3, Day 5	100.01	348.8	71.33	169.96	24.47	194.43	1538	87.36	23.33	99.97	123.3	1297	90.49	548.7	2438	77.49
Mean			**80.58**					**83.77**					**87.49**			83.56
***E. coli* ML308**																
Ferm 1; 24 hrs	39.97	250.13	84.02	249.85	10.52	260.37	900.42	71.08	25.86	99.63	125.49	811.24	84.53	1500.12	2163.11	30.65
Ferm 2; 24 hrs	42.22	269.87	84.35	311.2	11.69	322.89	899.11	64.09	31.11	85.41	116.52	799.52	85.43	1861.23	2115.89	12.04
Mean			**84.19**					**67.58**					**84.98**			21.34

Fermentation	PROT	RES	PROT %	Total macromolecular carbon content (ppm)	Total organic elemental carbon content (ppm)	The amount of total unaccountable carbon (%)
***S. coelicolor* 1147**						
Ferm 1, Day 5	205.23	1065	80.73	929.17	6899.9	86.53
Ferm 2, Day 5	145.63	1272	88.55	1037.76	6858	84.87
Ferm 3, Day 5	101.36	987	89.73	1067.8	6608.8	83.84
Mean			**86.34**			85.08
***E. coli* ML308**						
Ferm 1; 24 hrs	289.66	589.97	50.90	2215.61	4714.87	53.01
Ferm 2; 24 hrs	352.74	611.53	42.32	2695.6	4695.92	42.60

Mean	**46.61**	**47.80**

S. coelicolor 1147 (cultured in shake flasks) and *E. coli* ML308 (cultured in shake flasks) were both cultured on a glucose minimal medium (Chapter 3, section 3.6.1 and 3.6.3 respectively). Each biomass sample was washed and subjected to fractionation procedure method 2 (Chapter 3, section 3.16.2 all solutions were filtered and the residue biomass washed back in to the following step) at concentration of 50 $mg.ml^{-1}$ (wet weight) and stored at -70^{0} C. The resulting fractions were analysed in triplicate for the macromolecular content by the appropriate assay. Carbohydrate, the anthrone assay (Chapter 3, section 3.18.1); DNA, the diphenylamine assay (Chapter 3, section 3.19.2); RNA, the orcinol assay (Chapter 3, section 3.19.4); protein, the ninhydrin assay (Chapter 3, section 3.20.6); lipid, the vanillin assay (Chapter 3, section 3.23.1). The macromolecular concentrations in each resulting fraction were determined and expressed as parts per million (ppm = $\mu g.ml^{-1}$) of carbon in the columns headed CHO (carbohydrate [ppm]), RNA, DNA, LIPID and PROT (protein)[Table 5.20A Part 2]. These values were then calculated as the percentage (%) of the total unaccountable carbon (Table 5.20A Part 2) in each appropriate fraction COLD (fraction 1), KOH (fraction 2), HOT (fraction 3), ALKALI (fraction 4) and RESIDUE (fraction 5) were measured by total organic carbon analysis (Chapter 3, section 3.15.5). Table 5.20B Part 2 presents his data in the format of percentage (%) proportion of carbon in each fraction. nd, not determined.

Table 5.20B Comparison of carbon distribution of *S. coelicolor* 1147 and *E. coli* ML308 method 1 & 2 fractions determined from direct carbon measurement and presented as the percentage of the total carbon in each fraction (corresponds to Table 5.9 H & I).

Method 1

Fermentation	Cold (%)	Hot (%)	Alkali (%)	Residue (%)
***S. coelicolor* 1147**				
Ferm 1, Day 5	5.38	23.81	56.35	14.46
Ferm 2, Day 5	5.00	8.58	52.85	33.57
Ferm 3, Day 5	11.56	14.64	55.85	17.94
Ferm 4, Day 5	9.31	19.25	47.95	23.48
Ferm 5, Day 5	8.39	21.99	48.90	20.73
Ferm 6, Day 5	6.03	17.84	53.97	22.15
Ferm 7, Day 5	5.57	19.14	54.77	20.51
***E. coli* ML308**				
Ferm 1; 24 hrs	8.77	8.38	68.49	14.35
Ferm 2; 24 hrs	9.94	8.48	67.79	13.78

Method 2

Fermentation	Cold (%)	KOH (%)	Hot (%)	Alkali (%)	Residue (%)
***S. coelicolor* 1147**					
Ferm 1, Day 5	4.59	19.06	11.388	49.54	15.43
Ferm 2, Day 5	5.25	19.66	20.99	35.55	18.55
Ferm 3, Day 5	5.28	23.27	19.62	36.89	14.93
***E. coli* ML308**					
Ferm 1; 24 hrs	5.30	19.09	17.21	45.88	12.51
Ferm 2; 24 hrs	5.75	19.15	17.03	45.06	13.02

S. coelicolor 1147 (cultured in a 5 L bioreactor) and *E. coli* ML308 (cultured in shake flasks) were both cultured on a glucose minimal medium (Chapter 3, section 3.6.1 and 3.6.3 respectively) [see Chapter 4 for fermentation description and profiles]. Each biomass sample was washed and objected to fractionation procedure methods 1 & 2 (Chapter 3, section 3.16.1 & 3.16.2 respectively; all solutions were filtered and the residue biomass washed back in to the following step) at concentration of 100 $mg.ml^{-1}$ and 50 $mg.ml^{-1}$ respectively (wet weight) and stored at -70^{0} C. The resulting fractions were analysed in triplicate for the macromolecular content by the appropriate assay. Carbohydrate, the anthrone assay (Chapter 3, section 3.18.1); DNA, the diphenylamine assay (Chapter 3, section 3.19.2); RNA, the orcinol assay (Chapter 3, section 3.19.4); protein, the ninhydrin assay (Chapter 3, section 3.20.6); lipid, the vanillin assay (Chapter 3, section 3.23.1). The macromolecular concentrations in each resulting fraction were determined and expressed as parts per million (ppm = $\mu g.ml^{-1}$) of carbon in the columns headed CHO (carbohydrate [ppm]), RNA, DNA, LIPID and PROT (protein)[Table 5.20A Part 1 & 2]. These values were then calculated as the percentage (%) of the total unaccountable carbon (Table 5.20 Part 1) in each appropriate fraction COLD (fraction 1), KOH (fraction 2), HOT (fraction 3), ALKALI (fraction 4) and RESIDUE (fraction 5) were measured by total organic carbon analysis (Chapter 3, section 3.15.5). Table 5.20B Part 2 presents his data in the format of percentage (%) proportion of carbon in each fraction. nd, not determined.

Table 5.21 The protein, RNA and DNA for *E. coli* and *S. coelicolor* grown in steady-state continuous culture.

Units		*E. coli* B/r						
	μ (h^{-1})	**0.42**	**0.69**	**1.04**	**1.39**	**1.73**		
Protein content	**$g.g^{-1}$**	0.670	0.601	0.531	0.529	0.529		
RNA content	**$g.g^{-1}$**	0.133	0.152	0.174	0.205	0.248		
DNA Content	**$g.g^{-1}$**	0.042	0.029	0.022	0.019	0.017		
Units		***S. coelicolor 1147***						
	μ (h^{-1})	**0.024**	**0.048**	**0.109**	**0.148**	**0.195**	**0.24**	**0.3**
Protein content	**$g.g^{-1}$**	0.456	0.432	0.412	0.429	0.416	0.347	0.313
RNA content	**$g.g^{-1}$**	0.098	0.100	0.167	0.171	0.175	0.200	0.216
DNA Content	**$g.g^{-1}$**	0.044	0.042	0.036	0.033	0.033	0.036	0.035

The protein, RNA and DNA contents g per 100 g biomass for *E. coli* and *S. coelicolor* grown in steady-state continuous culture over a range of μ's (0.024 – 1.73 h^{-1}) with a modified YEME medium. Results taken from Shahab *et al*. (1996).

Table 5.22 The protein, RNA and DNA contents g per 100 genome for *E. coli* and *S. coelicolor* grown in steady-state continuous culture.

Units		*E. coli* B/r						
	μ (h^{-1})	**0.42**	**0.69**	**1.04**	**1.39**	**1.73**		
DNA content	**10^{12} genomes g^{-1}**	9.11	6.21	4.68	4.01	3.78		
Protein per genome	**10^{-13} genomes g^{-1}**	0.74	0.97	1.13	1.32	1.40		
RNA per genome	**10^{-14} genomes g^{-1}**	1.46	2.45	3.73	5.12	6.55		
Units		***S. coelicolor 1147***						
	μ (h^{-1})	**0.024**	**0.048**	**0.109**	**0.148**	**0.195**	**0.24**	**0.3**
DNA content	**10^{12} genomes g^{-1}**	5.06	4.83	4.14	3.80	3.80	4.14	4.03
Protein per genome	**10^{-13} genomes g^{-1}**	0.90	0.89	0.99	1.13	1.10	0.84	0.78
RNA per genome	**10^{-14} genomes g^{-1}**	1.94	2.07	4.03	4.50	4.61	4.83	5.36

The protein, RNA and DNA contents g per 100 genome for *E. coli* and *S. coelicolor* grown in steady-state continuous culture over a range of μ's (0.024 – 1.73 h^{-1}) with a modified YEME medium. Results taken from Shahab *et al*. (1996).

Table 5.23 The extraction and quantification of teichoic acid by direct phosphate analysis using three alternative teichoic acid quantitative protocols on *S. coelicolor* 1147 biomass samples cultured on a glucose minimal medium (corresponds to Tables 5.9 A - J).

Teichoic acid estimation by phosphate analysis											
Methods / Fractions	**Hot (M2) F 1, Phosphate (µmoles)**	**KOH (M2) F 2, Phosphate (µmoles)**	**Hot (M1) F 3, Phosphate (µmoles)**	**F 2 + 3 (M2), RNA (µmoles)**	**F 2 + 3 (M2), DNA (µmoles)**	**Hot (M1) F 3, RNA (µmoles)**	**Hot (M1) F 3, DNA (µmoles)**	**F 2 (M2), Total NA-P (µmoles)**	**F 2 (M2), TA-P (µmoles)**	**Glycerol teichoic content of 1 g of biomass, Teichoic acid mg.g dry weight**	**Ribitol teichoic content of 1 g of biomass, Teichoic acid mg.g dry weight**
Ferm 1, Day 4	58.26	29.06	14.20	17.45	2.04	2.49	5.64	19.49	9.58	**1.03**	**1.26**

Methods / Fractions	**Hancock (1994) method, NA-P ($\mu moles.g^{-1}$)**	**Hancock (1994) method, TA-P (C. $\mu moles.g^{-1}$) glycerol**	**Hancock (1994) method, TA-P (C. $\mu moles.g^{-1}$) ribitol**	**Glycerol teichoic content of 1 g of biomass, Teichoic acid mg.g dry weight**	**Ribitol teichoic content of 1 g of biomass, Teichoic acid mg.g dry weight**
Ferm 1, Day 4	104.02	936.17	1144.20	**11.23**	**13.73**

The fractions obtained from *S. coelicolor* 1147 biomass cultured a glucose minimal medium (Chapter 3, section 3.6.1) grown in batch culture (see Chapter 4, Fig 4.18 - 4.20)[corresponds 5.9 H & I]. The cold and hot PCA (fractions 1 and 2) extraction method 1 (Chapter 3, section 3.16.1) and fractions 2 and 3 from extraction method 2 (Chapter 3, section 3.16.2). The teichoic acid extraction was undertaken and verified in the following manner by Hancock (1994) cell wall separation protocol (Chapter 3, section 3.21) were applied in triplicate to the biomass samples. Further analysis was undertaken to quantify the RNA and DNA content of the biomass (Chapter 3, section 3.19.2 and 3.19.4). All these fractions were further subjected to phosphate determination (in triplicate; Chapter 3, section 3.22.4). In addition, the phosphate contents of the cold PCA fraction method 1 and fraction 1 method 2 were measured. These fractions were also subjected to phosphate determination (in triplicate). In addition the phosphate contents of the cold PCA fraction (Method 1) and the hot fraction were measured. The combined RNA & DNA contents of the fractions were then expressed in terms off phosphate (total NA-P). An estimation of the teichoic acid content of the fractions was obtained from the teichoic acid phosphate (TA-P). This was calculated by subtracting the nucleic acid phosphate from the total phosphate measured in the fractions. Exact quantification of carbon derived from teichoic acid was therefore not possible but estimates were calculated using the assumptions that teichoic acid in *S. coelicolor* 1147 (Table 5.23) and *S. fradiae* C373-10 (Table 5.24 and 5.25) were composed of either a glycerol backbone or a ribitol backbone. The number of carbons in one unit of teichoic acid would therefore be either 9 or 11 (teichoic acid also contains an additional group which in this case was assumed to be a sugar group).

Table 5.4 Part 1 (Part 1 & 2 companion tables) The extraction and quantification of teichoic acids by direct phosphate analysis using extraction methods 1 & 2 on *S. fradiae* C373-10 biomass samples cultured on a glucose glutamate defined medium [corresponds to Table 5.8 and 5.9A].

Methods / Fraction	Total (M2), NA-P, P.μmoles.g^{-1}	Glycerol backbone, TA-P (M2), C.μmoles.g^{-1}	Ribitol backbone, TA-P (M2), C.μmoles.g^{-1}	Glycerol backbone, percentage teichoic acid content of 1 g dry weight	Ribitol backbone, percentage teichoic acid content of 1 g dry weight
Ferm 1; Day 1	nd	nd	nd	nd	nd
Ferm 2; Day 1	nd	nd	nd	nd	nd
Ferm 3; Day 1	nd	nd	nd	nd	nd
Ferm 4; Day 1	nd	nd	nd	nd	nd
Ferm 1; Day 2	413.53	1513.82	1850.22	20.89	36.26
Ferm 2; Day 2	358.50	1167.37	1426.78	16.11	27.96
Ferm 3; Day 2	375.03	889.28	1086.90	12.27	21.30
Ferm 4; Day 2	582.62	1060.97	1296.74	14.64	25.42
Ferm 1; Day 3	799.02	3495.82	4272.67	48.24	83.74
Ferm 2; Day 3	nd	1555.31	1900.93	nd	nd
Ferm 3; Day 3	900.93	-680.73	-832.00	-9.39	-16.31
Ferm 4; Day 3	403.55	1749.21	2137.92	24.14	41.90
Ferm 1; Day 4	721.12	1580.27	1931.44	21.81	37.86
Ferm 2; Day 4	nd	2533.99	3097.11	nd	nd
Ferm 3; Day 4	nd	738.04	902.05	nd	nd
Ferm 4; Day 4	nd	942.49	1151.94	nd	nd
Ferm 1; Day 5	520.70	1857.58	2270.38	25.634	44.50
Ferm 2; Day 5	429.72	1041.51	1272.95	14.37	24.95

Ferm 3; Day 5	277.75	1130.39	1381.58	15.60	27.08
Ferm 4; Day 5	436.49	382.24	467.18	5.27	9.16
Ferm 1; Day 6	548.69	936.30	1144.37	12.92	22.43
Ferm 2; Day 6	517.03	1210.87	1479.96	16.71	29.01
Ferm 3; Day 6	703.29	322.43	394.08	4.45	7.72
Ferm 4; Day 6	341.13	1088.12	1329.92	15.02	26.07

The fractions obtained from *S. fradiae* C373-10 cultured on a glucose glutamate defined medium (Chapter 3, section 3.6.4)[corresponds Tables 5.8 & 5.9A] for the cold and hot PCA (fraction 1 and 2) extraction method 1 (Chapter 3, section 3.16.1) and fractions 2 and 3 from extraction method 2 (Chapter 3, section 3.16.2). The teichoic acid extraction was undertaken and verified in the following manner by Hancock (1994) cell wall separation protocol (Chapter 3, section 3.21) were applied in triplicate to the biomass samples (Table 5.25). Further analysis was undertaken to quantify the RNA and DNA content of the biomass (Chapter 3, section 3.19.2 and 3.19.4). All these fractions were further subjected to phosphate determination (in triplicate; Chapter 3, section 3.22.4). In addition, the phosphate contents of the cold PCA fraction method 1 and fraction 1 method 2 were measured. The combined RNA & DNA contents of the fractions were then expressed in terms off phosphate (total NA-P). An estimation of the teichoic acid content of the fractions was obtained from the teichoic acid phosphate (TA-P). This was calculated by subtracting the nucleic acid phosphate from the total phosphate measured in the fractions. Exact quantification of carbon derived from teichoic acid was therefore not possible but estimates were calculated using the assumptions that teichoic acid in *S. coelicolor* 1147 (Table 5.23) and *S. fradiae* C373-10 (Table 5.24 and 5.25) were composed of either a glycerol backbone or a ribitol backbone. The number of carbons in one unit of teichoic acid would therefore be either 9 or 11 (teichoic acid also contains an additional group which in this case was assumed to be a sugar group). The presented figures in $mg.g^{-1}$ dry weight biomass for glycerol or ribitol backbone teichoic acid content (the macromolecular composition was calculated by working out a coefficient between the wet weight [Chapter 3, section 3.11.1] and dry weight [Chapter 3, section 3.11.2] biomass determinations) and converted to the percentage composition. nd, not determined; STDEV, standard deviation. Standard deviations were given as plus minus the unit of measurement. The total mean percentage STDEV was also presented.

Table 5.24 Part 2 (Part 1 & 2 companion tables) The extraction and quantification of teichoic acids by direct phosphate analysis using extraction methods 2 of *S. fradiae* C373-10 biomass samples cultured on a glucose glutamate defined medium [corresponds to Table 5.8] and used verify the unaccountable for carbon of fraction 3 method 2 (corresponds to Table 19A Part 1 & 2).

Methods / Fraction	KOH fraction RNA content of F 3, M 2 (ppm)	Glycerol backbone teichoic acid (ppm)	Ribitol backbone teichoic acid ppm	Carbon content of F 3, M 2 KOH (ppm)	Total unaccounted for carbon not taking teichoic acid into account	Percentage unaccountable for carbon teichoic glycerol backbone	Percentage unaccountable for carbon teichoic ribitol backbone
Ferm 1; Day 1	nd	nd	nd	**nd**	**nd**	nd	nd
Ferm 2; Day 1	nd	nd	nd	**nd**	**nd**	nd	nd
Ferm 3; Day 1	nd	nd	nd	**nd**	**nd**	nd	nd
Ferm 4; Day 1	nd	nd	nd	**nd**	**nd**	nd	nd
Ferm 1; Day 2	29.13	38.42	46.96	**250.2**	**88.36**	5.52	6.04
Ferm 2; Day 2	33.76	31.43	38.41	**244.8**	**86.21**	4.25	4.66
Ferm 3; Day 2	38.63	31.39	38.37	**268.5**	**85.61**	3.25	3.56
Ferm 4; Day 2	50.15	50.46	61.67	**311.8**	**83.92**	3.8722	4.23
Ferm 1; Day 3	49.28	73.34	89.64	**455.8**	**89.19**	12.748	13.94
Ferm 2; Day 3	71.93	nd	nd	**505.2**	**85.76**	nd	nd
Ferm 3; Day 3	88.95	74.28	90.79	**611.2**	**85.45**	-1.04	-1.49
Ferm 4; Day 3	23.15	38.29	46.80	**752.1**	**96.92**	2.68	3.81
Ferm 1; Day 4	48.14	64.01	78.23	**289.6**	**83.38**	5.7622	6.30
Ferm 2; Day 4	43.91	nd	nd	**245.7**	**82.13**	nd	nd
Ferm 3; Day 4	45.74	nd	nd	**264.3**	**82.69**	nd	nd
Ferm 4; Day 4	59.35	nd	nd	**202.4**	**70.68**	nd	nd

Ferm 1; Day 5	27.21	45.61	55.74	**152.3**	**82.13**	6.77	7.41
Ferm 2; Day 5	17.98	39.09	47.78	**149.5**	**87.97**	3.80	4.15
Ferm 3; Day 5	2.7	28.23	34.50	**234.9**	**98.85**	4.13	4.51
Ferm 4; Day 5	26.16	38.42	46.96	**175.2**	**85.07**	1.39	1.53
Ferm 1; Day 6	19.15	49.09	59.99	**272.53**	**92.97**	3.41	3.73
Ferm 2; Day 6	9.44	51.21	62.60	**233.26**	**95.95**	4.41	4.83
Ferm 3; Day 6	34.57	60.21	73.59	**248.8**	**86.10**	1.17	1.29
Ferm 4; Day 6	10.38	32.07	39.20	**286.71**	**96.38**	3.98	4.34

The fractions obtained from *S. fradiae* C373-10 cultured on a glucose glutamate defined medium (Chapter 3, section 3.6.4)[corresponds Tables 5.8 & 5.9A] for the cold and hot PCA (fraction 1 and 2) extraction method 1 (Chapter 3, section 3.16.1) and fractions 2 and 3 from extraction method 2 (Chapter 3, section 3.16.2). The teichoic acid extraction was undertaken and verified in the following manner by Hancock (1994) cell wall separation protocol (Chapter 3, section 3.21) and applied in triplicate to the biomass samples (Table 5.25). Further analysis was undertaken to quantify the RNA and DNA content of the biomass (Chapter 3, section 3.19.2 and 3.19.4). All these fractions were further subjected to phosphate determination (in triplicate; Chapter 3, section 3.22.4). In addition, the phosphate contents of the cold PCA fraction method 1 and fraction 1 method 2 were measured. The combined RNA & DNA contents of the fractions were then expressed in terms off phosphate (total NA-P). An estimation of the teichoic acid content of the fractions was obtained from the teichoic acid phosphate (TA-P). This was calculated by subtracting the nucleic acid phosphate from the total phosphate measured in the fractions. Exact quantification of carbon derived from teichoic acid was therefore not possible but estimates were calculated using the assumptions that teichoic acid in *S. coelicolor* 1147 (Table 5.23) and *S. fradiae* C373-10 (Table 5.24 and 5.25) were composed of either a glycerol backbone or a ribitol backbone. The number of carbons in one unit of teichoic acid would therefore be either 9 or 11 (teichoic acid also contains an additional group which in this case was assumed to be a sugar group). The presented figures in $mg.g^{-1}$ dry weight biomass for glycerol or ribitol backbone teichoic acid content (the macromolecular composition was calculated by working out a coefficient between the wet weight [Chapter 3, section 3.11.1] and dry weight [Chapter 3, section 3.11.2] biomass determinations) and converted to the percentage composition. nd, not determined; STDEV, standard deviation. Standard deviations were given as plus minus the unit of measurement. The total mean percentage STDEV was also presented. Further analysis was also incorporated to further verify the unaccounted for carbon of the KOH fraction of method 2 (this corresponds to Tables 5.18 – 5.20) accounting for the teichoic acid content.

Table 5.25 The extraction, quantification, and estimation of teichoic acid using Hancock (1994) cell wall separation protocol with direct phosphate analysis on *S. fradiae* C373-10 biomass

Fraction glucose glutamate defined medium	Total NA-P (μmoles.g^{-1})	glycerol backbone TA-P (C.μmoles.g^{-1})	ribitol backbone TA-P (C.μmoles.g^{-1})	Glycerol backbone, mg.g^{-1} dry wt teichoic acid content	Ribitol backbone, mg.g^{-1} dry wt teichoic acid content
Ferm 1; Day 2	83.33	750	916.67	27.33	29.92
Ferm 2; Day 2	83.25	749.25	915.75	27.31	29.89
Ferm 3; Day 2	71.71	645.42	788.84	23.52	25.75
Ferm 4; Day 2	84.47	760.25	929.19	27.71	30.32
STDEV	**± 6.01**				
Ferm 1; Day 3	122.86	1105.75	1351.47	40.30	44.11
Ferm 2; Day 3	132.11	1189	1453.22	43.33	47.43
Ferm 3; Day 3	114.48	1030.33	1259.30	37.55	41.10
Ferm 4; Day 3	129.62	1166.58	1425.82	42.51	46.53
STDEV	**± 7.89**				
Ferm 1; Day 4	171.72	1545.5	1888.94	56.32	61.65
Ferm 2; Day 4	126.42	1137.75	1390.58	41.46	45.38
Ferm 3; Day 4	83.32	749.92	916.56	27.33	29.91
Ferm 4; Day 4	258.28	2324.5	2841.05	84.71	92.72
STDEV	**± 74.84**				
Ferm 1; Day 5	178.06	1602.58	1958.71	58.40	63.92
Ferm 2; Day 5	165.24	1487.13	1817.61	54.20	59.32
Ferm 3; Day 5	22.71	204.417	249.84	7.45	8.15
Ferm 4; Day 5	78.3	704.67	861.26	25.68	28.11
STDEV	**± 73.72**				
Ferm 1; Day 6	122.82	1105.42	1351.06	40.29	44.09
Ferm 2; Day 6	120.32	1082.92	1323.56	39.47	43.20

Ferm 3; Day 6	106.07	954.67	1166.82	34.79	38.08
Ferm 4; Day 6	87.52	787.67	962.70	28.71	31.42
STDEV	**± 16.22**				
Mean percentage STDEV	**± 28.36**				

S. fradiae C373-10 was cultured on a glucose glutamate defined medium (Chapter 3, section 3.6.4) fermentations (Ferm 1 – 4; corresponding to collected Table 5.4). Preparation of cell wall fractions was as Hancock (1994)[Chapter 3, section 3.21). Teichoic acids was measured as phosphate (Chapter 3, section 3.22.4) by the method of Mousdale (1997). The total phosphate contents of the cell were then expressed in terms of phosphate (total NA-P). The cell wall fraction estimation of the teichoic acid content of the fractions was obtained from the phosphate concentration (TA-P). Exact quantification of carbon derived from teichoic acid was not possible but estimates were calculated using the assumptions that teichoic acid in *S. coelicolor* C373-10 and *S. fradiae* 1147 was composed of either a glycerol backbone or a ribitol backbone. The number of carbons in one unit of teichoic acid would therefore be either 9 or 11 presented as the TA-P (C.µmoles). All measurements are as stated or $mg.g^{-1}$ dry weight biomass for glycerol or ribitol backbone teichoic acid content (the macromolecular composition was calculated by working out a coefficient between the wet weight [Chapter 3, section 3.11.1] and dry weight [Chapter 3, section 3.11.2] biomass determinations) and converted to the percentage composition. nd, not determined; STDEV, standard deviation. STDEV were given as the unit of measurement. The total mean percentage STDEV was also presented.

Table 5.26 The percentage amino acid composition of *S. fradiae* C373-10, *S. coelicolor* 1147, and *E. coli* ML308 cell wall residue fractions of method 1 (corresponds to Tables 5.4 A - J).

Carbon source / organism	Ala	Asn	Arg	Asp	Glu	Gly	His	Ile	Leu	Lys	Met	Phe	Ser	Thr	Trp	Tyr	Val
***S. fradiae* C373-10**																	
Glucose																	
Ferm 1; Day 2	22.17	1.70	20.00	4.06	14.62	16.98	0.07	0.75	0.57	nd	0.66	0.94	0.57	12.27	1.60	0.38	2.64
Ferm 2; Day 2	24.16	5.71	18.55	7.61	12.08	15.22	0.01	0.67	0.57	nd	0.66	0.95	0.57	8.56	1.62	0.38	2.67
Ferm 1; Day 7	20.97	0.98	27.23	1.62	13.44	19.21	0.28	0.14	1.90	nd	nd	0.49	0.49	11.19	0.70	nd	1.34
Ferm 2; Day 7	13.24	1.29	45.68	3.07	9.68	21.47	2.26	0.08	1.29	nd	0.16	0.32	0.16	0.65	0.65	nd	nd
Glucose / glutamate																	
Ferm 1; Day 1	16.72	2.25	25.86	4.92	12.51	19.11	2.95	0.98	4.22	0.14	0.07	0.84	0.28	3.37	1.83	0.28	3.65
Ferm 2; Day 1	19.38	2.13	21.87	5.33	7.11	22.58	1.78	1.24	5.33	0.18	0.09	1.07	0.35	4.27	2.31	0.35	4.62
Ferm 1; Day 7	0.59	2.35	37.10	3.37	18.33	27.71	4.69	0.29	2.20	nd	0.59	0.73	0.15	0.29	1.03	0.44	0.15
Ferm 2; Day 7	19.31	1.50	29.28	2.82	13.23	24.43	2.38	0.44	1.15	nd	0.35	0.79	0.35	0.18	1.41	nd	2.38
Glucose / oxo-glutarate																	
Ferm 1; Day 1	10.18	3.39	41.85	4.52	10.18	13.57	1.13	0.90	1.13	5.66	1.13	nd	0.34	2.26	2.26	1.13	0.34
Ferm 2; Day 1	12.59	3.78	34.00	5.04	11.33	15.11	1.26	1.01	1.26	6.30	1.26	nd	0.38	2.52	2.52	1.26	0.38
Ferm 3; Day 1	4.01	2.00	34.07	4.68	6.01	4.01	1.00	30.06	6.68	2.34	1.67	nd	0.33	2.67	0.33	0.13	nd
Ferm 4; Day 1	9.20	4.92	23.95	9.38	10.11	9.93	1.37	4.10	8.20	0.07	0.64	0.02	1.37	6.47	8.47	1.46	0.36
Ferm 1; Day 5	11.92	7.95	5.71	0.062	2.73	19.94	1.74	5.65	nd	1.68	3.66	0.43	1.06	13.17	16.96	5.59	1.74
Ferm 2; Day 5	7.519	2.51	48.04	5.85	7.52	5.01	1.25	4.59	8.35	2.92	2.09	nd	0.42	3.34	0.42	0.17	nd
Ferm 3; Day 5	10.47	3.70	31.83	6.98	9.51	8.01	1.03	3.08	11.22	0.05	0.48	0.01	1.03	4.86	6.36	1.09	0.27
Ferm 4; Day 5	12.65	4.45	13.25	10.44	11.90	10.68	2.20	3.61	4.54	2.15	0.047	3.61	1.59	6.88	9.65	2.34	nd
Glycerol																	
Ferm 1; Day 1	12.81	3.96	5.75	7.99	9.97	7.53	1.85	5.42	7.40	1.58	nd	15.92	2.31	11.16	3.30	3.04	nd
Ferm 2; Day 1	15.62	1.50	21.63	4.51	16.37	15.92	3.30	1.65	3.61	nd	0.45	1.35	0.45	5.56	2.85	0.09	5.11
Ferm 1; Day 7	13.21	4.79	5.08	8.12	11.40	11.40	1.64	4.79	6.55	1.40	nd	14.08	2.04	9.88	2.92	2.69	nd
Ferm 2; Day 9	17.94	2.35	23.33	5.05	12.90	20.19	2.47	1.23	2.69	nd	0.34	1.01	0.34	4.15	2.13	0.067	3.81

Fructose																	
Ferm 1; Day 1	6.90	3.07	68.25	2.30	4.60	10.74	1.53	nd	0.77	nd	nd	nd	0.69	0.77	0.38	nd	nd
Ferm 1; Day 8	11.45	3.97	11.33	9.70	10.98	9.35	3.27	3.39	9.34	3.15	0.12	12.27	1.63	5.96	2.34	1.75	nd
Oxo-glutarate																	
Ferm 1; Day 1	0.48	nd	92.23	1.21	1.46	1.21	2.43	nd	nd	nd	nd	nd	0.97	nd	nd	nd	nd
Ferm 1; Day 10	19.92	1.84	14.40	3.06	12.87	27.27	3.68	2.14	4.60	0.09	0.31	5.52	0.92	2.45	0.61	0.31	nd
Methyl oleate medium																	
Ferm 1; Day 3	17.22	2.93	23.99	6.41	13.37	16.49	2.93	1.46	5.49	0.16	nd	1.46	0.37	5.31	1.46	0.92	nd
Ferm 2; Day 3	11.48	2.58	23.10	6.06	16.00	19.87	3.10	1.55	6.19	nd	nd	1.42	0.13	5.55	1.93	1.03	nd
Ferm 1; Day 6	17.68	2.70	20.06	5.63	12.93	20.78	3.01	1.189	4.99	2.70	nd	1.27	0.32	4.52	1.59	0.63	nd
Ferm 2; Day 5	17.37	2.57	19.71	5.14	12.84	21.98	2.72	2.34	6.87	1.28	nd	1.21	0.30	4.46	0.38	0.80	nd
Ferm 1; Day 10	17.22	2.49	13.06	5.17	12.09	21.66	3.30	2.25	6.69	1.36	nd	2.22	1.20	4.86	5.87	0.54	nd
Ferm 2; Day 10	17.85	2.12	19.80	4.89	12.47	27.14	3.18	4.32	1.55	0.24	nd	0.90	0.57	3.50	0.90	0.57	nd
***S. coelicolor* 1147**																	
Glucose																	
Ferm 1, Day 4	12.52	5.42	4.91	1.28	12.87	10.59	1.03	4.78	9.05	13.39	nd	4.32	3.47	3.34	1.03	4.01	7.99
Ferm 2, Day 4	11.87	5.19	5.17	2.47	15.25	11.02	0.55	3.41	10.69	3.05	nd	3.35	9.51	1.37	0.82	3.38	12.86

S. fradiae C373-10, *S. coelicolor* 1147, and *E. coli* ML308 were cultured on a number of different medium compositions and carbon sources (corresponds to Tables 5.9 A - J). *S. fradiae* C373-10 and was cultured on glucose, fructose, glycerol, oxo-glutarate minimal media, glucose glutamate, glucose oxo-glutarate defined media (Chapter 3, section 3.6.4), and a methyl oleate medium (Chapter 3, section 3.7.2), *S. coelicolor* 1147 and *E. coli* ML308 both cultured on glucose minimal media (Chapter 3, section 3.6.1 & 3.6.3 respectively). All sampling points were taken after inoculation and at sampling point II [SP] (as Chapter 4, Fig 4.1 - 4.20) for the methyl oleate defined medium SP I, II and III was used. Previously collected biomass was washed with dH_2O and fractionated with method 1 (Chapter 3, section 3.16.1) at a concentration of 100 $mg.ml^{-1}$ (wet weight). The residue fraction (fraction 4) was subjected to acid hydrolysis (as Chapter 3, section 3.25.6) and analysed by HPLC for amino acid content (Chapter 3, section 3.25.6). Cysteine, proline, and glutamine were not determined (see Chapter 3, section 3.25). All figures were expressed in $mmoles.g^{-1}$ dry weight biomass and converted to percentage format. nd, not determined.

Table 5.27 Theoretical calculation for the peptidoglycan composition of *S. fradiae* C373-10, *S. coelicolor* 1147, and *E. coli* ML308 biomass.

Fermentation / organism	Alanine (mmoles.g^{-1} dry wt)	Glutamate (mmoles.g^{-1} dry wt)	NAG (ratio)	Alanine (ratio)	Glutamate (ratio)	NAG (mmole.g^{-1} dry wt)	Peptidoglycan content calculated from alanine ratio[percentage composition (%)]	NAG (mmole.g^{-1} dry wt)	Peptidoglycan content calculated from glutamate ratio [percentage composition (%)]
S. fradiae									
Glucose									
Ferm 2; Day 7	0.082	0.06	1.37	2	1.37	37.06	3.71	54.24	5.42
Ferm 1; Day 7	0.298	0.194	1.54	2	1.54	134.70	13.47	175.38	17.54
Glucose oxo-glutarate									
Ferm 1; Day 7	0.004	0.125	0.03	2	0.03	1.808	0.18	1130	11.3
Ferm 2; Day 7	0.219	0.15	1.46	2	1.46	98.99	9.90	135.6	13.56
Glucose Glutamate									
Ferm 1; Day 5	0.018	0.018	1	2	1	8.136	0.81	16.27	1.63
Ferm 2; Day 5	0.153	0.139	1.10	2	1.10	69.16	6.92	125.66	12.7
Ferm 3; Day 5	0.192	0.044	4.36	2	4.36	86.78	8.68	39.78	3.98
Ferm 4; Day 5	0.27	0.254	1.06	2	1.06	122.04	12.20	229.62	22.96
Glycerol									
Ferm 1; Day 7	0.226	0.195	1.16	2	1.16	102.15	10.21	176.28	17.63
Ferm 1; Day 9	0.16	0.115	1.39	2	1.39	72.32	7.23	103.96	10.40
Fructose									
Ferm 1; Day 8	0.098	0.094	1.04	2	1.04	44.30	4.43	84.976	8.50
Oxo-glutarate									

Ferm 1; Day 10	0.065	0.042	1.55	2	1.55	29.38	2.94	37.968	3.80
Methyl oleate medium									
Ferm 1; Day 3	0.094	0.073	1.29	2	1.29	42.49	4.25	65.99	6.60
Ferm 2; Day 3	0.089	0.124	0.72	2	0.72	40.228	4.02	112.10	11.21
Ferm 2; Day 5	0.23	0.17	1.35	2	1.35	103.96	10.40	153.68	15.37
Ferm 1; Day 5	0.223	0.163	1.37	2	1.37	100.80	10.08	147.35	14.73
Ferm 1; Day 10	0.443	0.311	1.42	2	1.42	200.24	20.02	281.14	28.11
Ferm 2; Day 10	0.22	0.153	1.44	2	1.44	99.44	9.94	138.31	13.83
					Mean (%)		**7.74**		**12.18**
S. coelicolor									
Ferm 1; Day 6	0.104	0.05	2.08	2	2.08	47.008	4.70	45.2	4.52
Ferm 2; Day 6	0.136	0.11	1.24	2	1.24	61.472	6.15	99.44	9.94
					Mean (%)		**5.42**		**7.23**
E. coli									
Ferm 1; Day 2	0.09	0.04	2.25	2	2.25	40.68	4.07	36.16	3.62
Ferm 2; Day 2	0.1	0.03	3.33	2	3.33	45.20	4.52	27.12	2.71
					Mean (%)		**4.29**		**3.16**

S. fradiae C373-10, *S. coelicolor* 1147, and *E. coli* ML308 were cultured on a number of different medium compositions and carbon sources (corresponds to Tables 5.9 A - J). *S. fradiae* C373-10 and was cultured on glucose, fructose, glycerol, oxo-glutarate minimal media, glucose glutamate, glucose oxo-glutarate defined media (Chapter 3, section 3.6.4), and a methyl oleate defined medium (Chapter 3, section 3.7.2), *S. coelicolor* 1147 and *E. coli* ML308 were both cultured on glucose minimal media (Chapter 3, section 3.6.1 & 3.6.3 respectively). All sampling points were taken at Sampling point (SP) II (as Chapter 4, Fig 4.1 - 4.20). Previously collected biomass was washed with dH_2O and fractionated with method 1 (Chapter 3, section 3.16.1) at a concentration of 100 $mg.ml^{-1}$ (wet weight). The residue fraction (fraction 4) was subjected to acid hydrolysis (as Chapter 3, section 3.25.6) and analysed by HPLC for amino acid content (Chapter 3, section 3.25.6). All figures are in $mmoles.g^{-1}$ dry weight biomass. nd, not determined. Theoretical calculation of the peptidoglycan composition of *S. fradiae*, *S. coelicolor*, and *E. coli* biomass (N-acetyl-glucosamine was not measured in this work therefore a rough ratio was converted from the alanine / N-acetyl-glucosamine and glutamate / N-acetyl-glucosamine concentration) and converted to mmoles of peptidoglycan (peptidoglycan has a molecular weight of 904) and converted to percentage format.

Table 5.28 Comparison of total amino acid recovery over a number of time frames with fractionation method 1 & 2 (alkali + residue) and whole biomass amino acid recovery of biomass hydrolylates of *S. fradiae* C373-10

	Method 1 Alkali + Residue fraction			Method 2 Alkali + Residue fraction			Whole biomass broth			Whole biomass hydroylates			Reconciled data
Time period of hydrolysis (hrs)	**6**	**12**	**24**	**6**	**12**	**24**	**6**	**12**	**24**	**6**	**12**	**24**	**6 - 24**
Amino acid													
Ala	0.266	0.366	0.342	0.264	0.359	0.455	0.410	0.444	0.564	0.268	0.334	0.499	0.381
Arg	0.462	0.501	0.534	0.689	0.892	0.901	0.554	0.693	0.715	0.594	0.698	0.854	0.674
Asp	nd	nd	nd	nd	nd	nd	nd	nd	nd	nd	nd	nd	nd
Asn	0.133	0.145	0.169	0.078	0.125	0.147	0.156	0.174	0.198	0.169	0.198	0.222	0.159
Cys	nd	nd	nd	nd	nd	nd	nd	nd	nd	nd	nd	nd	nd
Glu	0.178	0.202	0.214	0.255	0.399	0.442	0.212	0.459	0.412	0.301	0.333	0.356	0.314
Gln	nd	nd	nd	nd	nd	nd	nd	nd	nd	nd	nd	nd	nd
Gly	0.402	0.412	0.444	0.366	0.389	0.401	0.267	0.365	0.411	0.321	0.415	0.436	0.386
His	0.062	0.088	0.079	0.068	0.099	0.101	0.092	0.001	0.112	0.066	0.036	0.098	0.075
Ile	0.195	0.123	0.213	0.132	0.179	0.210	0.202	0.203	0.215	0.312	0.366	0.296	0.220
Leu	0.312	0.215	0.001	0.001	0.289	0.359	0.012	0.156	0.089	0.111	0.145	0.156	0.154
Lys	1.456	2.126	0.261	0.001	0.156	1.972	0.459	0.905	0.389	0.01	0.136	1.412	0.774
Met	0.010	0.012	0.060	0.002	0.187	0.002	0.033	0.003	0.089	0.008	0.009	0.012	0.035
Phe	0.036	0.096	0.045	0.099	0.111	0.127	0.125	0.196	0.144	0.213	0.096	0.112	0.117
Pro	nd	nd	nd	nd	nd	nd	nd	nd	nd	nd	nd	nd	nd
Ser	0.044	0.056	0.039	0.038	0.047	0.061	0.013	0.016	0.044	0.018	0.052	0.056	0.040
Thr	0.296	0.288	0.310	0.233	0.258	0.264	0.302	0.311	0.357	0.211	0.269	0.299	0.283
Trp	0.315	0.218	0.111	0.456	0.237	0.087	0.958	0.125	0.110	0.452	0.239	0.098	0.284

Tyr	0.312	0.356	0.383	0.218	0.399	0.354	0.344	0.314	0.368	0.222	0.356	0.333	0.330
Val	nd	nd	nd	nd	nd	nd	nd	nd	nd	nd	nd	nd	nd
Percentage carbon recovery	**60.52**	**40.12**	**80.29**	**28.56**	**36.58**	**68.36**	**90.12**	**12.36**	**40.23**	**18.52**	**47.52**	**20.69**	**43.32**

One biomass sample was obtained from a glucose glutamate defined medium culture (Chapter 3, section 3.6.4)[Ferm 1 day 5] and analysed for the individual amino acid composition. Biomass sample pellet previously fractionated with method 1 (Chapter 3, section 3.16.1; all solutions were filtered and the residue biomass washed back in to following steps) at concentration of 100 $mg.ml^{-1}$ (wet weight) and stored at -70^0 C. The alkali and residue fractions were hydrolysed with 6 M HCl for 24, 48 and 72 hours to release protein components (Chapter 3, section 3.25.2). The alkali and residue fractions of methods 1 & 2 (Chapter 3, section 3.16.1 & 3.16.2 respectively)[alkali and residue fraction added together], whole biomass and hydroyslate samples were analysed by HPLC analysis for the individual amino acids (Chapter 3, section 3.25.2). The HPLC method was as Chapter 3, section 3.25.2 for primary and secondary amino acids. Taurine was used as the internal standard. The internal standard was used to correct for sample carbon loss. All figures given in $mmoles.g^{-1}$ dry weight biomass. In addition the percentage carbon recovery calculated from the internal standard and standard taurine solution. Nd, not determined.

Table 5.29 Amino acid composition of *S. coelicolor* 1147, *E. coli* ML 308 & *S. fradiae* C373-10 expressed as the percentage of the total amino acid content and the order of biosynthetic requirement.

	***S. coelicolor* 1147**									***S. coelicolor* 1147[a]**			***S. fradiae* C373-10[b]**			***E. coli* ML308**			
Amino acids	**A#**	**B#**	**C#**	**D#**	**E#**	**F#**	**G#**	**H#**	**Ord**	**Glc (Ferm 1)#**	**Glc (Ferm 2)#**	**Ord**	**Glc (Ferm 1)#**	**Glc (Ferm 2)#**	**Ord**	**a**	**b**	**c**	**Ord**
Ala	12.2	13.5	15.5	14.8	13.4	14.7	13.5	15.6	**1**	13.8	12.8	**1**	8.7	12.9	**4**	9.4	9.6	12.7	**1**
Arg	6.6	6	6.7	6.6	6.3	6	8.6	5.8	**6**	6.4	9	**6**	31.5	14.4	**1**	5.2	5.5	5.4	**7**
Asp	4.1	5.5	5.8	5.9	4.4	6.3	7	9.8	**7**	5.8	6.9	**7**	8.1	9.43	**5**	4.2	4.5	9.9	**12**
Asn	nd	nd	nd	nd	nd	nd	nd	nd	**nd**	nd	nd	**nd**	nd	nd	**nd**	2.1	4.5	nd	**13**
Cys	nd	nd	nd	nd	nd	nd	nd	nd	**nd**	nd	nd	**nd**	nd	nd	**nd**	2.1	1.7	1.7	**17**
Glu	5.1	5.5	7.3	7.3	5.2	7.8	7.6	10.2	**5**	7.6	7.2	**5**	8.2	10.6	**3**	7.3	4.9	10.5	**5**
Gln	nd	nd	nd	nd	nd	nd	nd	nd	**nd**	nd	nd	**nd**	nd	nd	**nd**	4.2	4.9	nd	**10**
Gly	18.6	12.5	14.8	14.5	17.6	14	11.2	11.2	**2**	14.8	11.1	**2**	19.7	25.4	**2**	8.9	11.4	8	**2**
His	0.5	1.6	1.2	2.1	0.4	1.8	3	2.7	**15**	1.5	2.8	**15**	1.5	1.1	**12**	1	1.8	1	**18**
Ile	4.5	4.2	4.7	5	4.8	4.4	4.1	4.2	**12**	4.9	3.3	**12**	1.4	2.8	**10**	5.2	5.4	4.6	**8**
Leu	7	8.2	8	6.9	7.2	7.8	8.4	8.5	**4**	7.6	7.9	**4**	4.8	6.9	**6**	8.4	8.4	7.9	**3**
Lys	7.2	5.3	4.4	5.2	9.1	4.9	5	5.3	**16**	6.1	6.1	**16**	0.1	0.1	**14**	8.4	6.4	7	**4**
Met	2.2	1.4	2.1	1.6	2.9	1.7	0.2	0.05	**16**	1.1	0.2	**16**	0.1	0.1	**15**	4.2	2.9	3.4	**14**
Phe	3.5	2.6	3	3	4.4	3.5	3.1	2.8	**13**	2.8	2.8	**13**	1.6	2.3	**11**	2.3	3.5	3.3	**15**
Pro	6.8	5.4	4.4	4.9	8.9	4.8	5.7	5.6	**9**	4.9	5.1	**9**	5.3	5.5	**7**	5.2	4.1	4.6	**11**
Ser	5.1	4.2	5.1	5	5.4	4.6	4.5	3.9	**11**	4.3	4.2	**11**	0.25	1.1	**13**	6.2	4	6.1	**7**
Thr	7.1	4.6	5	4.8	6.8	5.7	6.8	4.6	**10**	4.5	5.1	**10**	3.5	3.9	**8**	5.2	4.7	4.7	**9**
Trp	nd	nd	nd	nd	nd	nd	nd	nd	**nd**	0.9	3.3	**nd**	0.1	0.1	**16**	1	1.1	1	**19**
Tyr	2.2	1.3	2.1	1.4	1.5	3.1	2	1.7	**14**	1.5	1.5	**14**	0.1	0.1	**17**	2.1	2.6	2.1	**16**
Val	7	9.3	8.4	8.5	8.6	7.4	9	8.1	**3**	9.4	8.5	**3**	3.7	1.9	**9**	6.2	7.9	5.5	**6**

The amino acid contents were expressed as the percentage (%) amino acid composition of 1 g of *S. coelicolor* 1147, *S. fradiae* C373-10 and *E. coli* ML308. Samples A to H were taken from Davidson (1992); growing on new glucose (Glc) minimal medium (Chapter 3, section 3.6.1; Hobbs *et al*. 1989). Amino acid analysis was undertaken by HPLC (Chapter 3, section 3.25). [a]Fermentation samples 1 & 2 results were obtained from this project for *S. coelicolor* 1147 cultured on a glucose minimal medium (Chapter 3, section 3.6.1)[corresponding to Tables 5.9 A - J]. [b]Fermentations 1 & 2 were results obtained from this project for *S. fradiae* C373-10 cultured on a glucose minimal medium (Chapter 3, section 3.6.4)[corresponding to Tables 5.9 A - J] Amino acid compositions of *E. coli* were expressed in the same manner and were tabulated under the columns headed a, b, & c. a, from Holms (1986); b, from Neidhardt (1987); c, from Umbarger (1977). The figures in bold denote the position of the amino acids in the order (ord) of decreasing relative proportions. Figure 5.7a – c presents the above data in a graphed format. #denotes fractions where both the alkali and residue fraction were both accounted for. nd, not determined, Glc, glucose.

Table 5.30 Amino acid composition of 1 g dry weight *S. fradiae* C373-10 biomass cultured on a number of carbon sources expressed as the percentage of the total amino acid content and the order of biosynthetic requirement.

Amino acids	Glc, day 6 (Ferm 1)#	Glc, day 6 (Ferm 2)#	Ord	Fru, day 7#	Ord	Glyc, day 8 (Ferm 1)#	Glyc, day 8 (Ferm 1)#	Ord	OGA, day 9#	Ord
Ala	8.7	12.9	**3**	9.7	**5**	29.7	17.9	**1**	14.5	**2**
Arg	31.5	14.4	**1**	17	**1**	5.7	4.4	**9**	13.3	**3**
Asp	8.1	9.43	**5**	12.2	**3**	18	11.2	**2**	7.3	**5**
Asn	nd	nd	**nd**	nd	**nd**	nd	nd	**nd**	nd	**nd**
Cys	nd	nd	**nd**	nd	**nd**	nd	nd	**nd**	nd	**nd**
Glu	8.2	10.6	**4**	9.9	**4**	10	9.9	**4**	10.8	**4**
Asn	nd	nd	**nd**	nd	**nd**	nd	nd	**nd**	nd	**nd**
Gly	19.7	25.4	**2**	14.2	**2**	15.5	9.9	**3**	22.8	**1**
His	1.5	1.1	**11**	2.5	**11**	1.9	1.4	**13**	2.5	**12**
Ile	1.4	2.8	**10**	3.3	**10**	0.93	4.1	**11**	2.9	**11**
Leu	4.8	6.9	**6**	8.4	**7**	2.1	5.7	**10**	5.9	**6**
Lys	0.1	0.1	**14**	0	**13**	0	1.2	**17**	0	**15**
Met	0.1	0.1	**15**	0	**14**	0.3	0	**18**	0	**16**
Phe	1.6	2.3	**12**	8.6	**6**	0.7	12.2	**6**	4.1	**8**
Pro	5.3	5.5	**7**	5.44	**8**	6.3	5.5	**7**	5.6	**7**
Ser	0.25	1.1	**13**	0	**15**	0.26	1.7	**16**	1	**13**
Thr	3.5	3.9	**8**	1.9	**12**	3.2	8.5	**8**	3.8	**9**
Trp	0.1	0.1	**16**	0	**16**	2.9	0	**15**	0	**17**
Tyr	0.1	0.1	**17**	0	**17**	0.05	2.3	**14**	0.7	**14**
Val	3.7	1.9	**9**	5.2	**9**	1.7	2.5	**12**	3.3	**10**

Amino acids	MO (Ferm 1) Day 2#	Ord	MO (Ferm 1) Day 4#	Ord	MO (Ferm 1) Day 8	Ord	MO (Ferm 2) Day 2#	Ord	MO (Ferm 2) Day 4#	Ord	MO (Ferm 2) Day 8#	Ord
Ala	11.1	**3**	12.4	**3**	nd	**nd**	10.2	**5**	13.9	**4**	12.3	**2**
Arg	19.2	**1**	18.1	**1**	nd	**nd**	19.3	**1**	18.2	**1**	18.4	**1**
Asp	8.2	**5**	9.5	**5**	nd	**nd**	10.5	**4**	8.6	**5**	9.6	**5**
Asn	nd	**nd**	nd	**nd**	nd	**nd**	nd	**nd**	nd	**nd**	nd	**nd**
Cys	nd	**nd**	nd	**nd**	nd	**nd**	nd	**nd**	nd	**nd**	nd	**nd**
Glu	9.6	**4**	10.4	**4**	nd	**nd**	11.3	**3**	11.1	**3**	10.3	**4**
Asn	nd	**nd**	nd	**nd**	nd	**nd**	nd	**nd**	nd	**nd**	nd	**nd**
Gly	11.6	**2**	14	**2**	nd	**nd**	11.4	**2**	16.6	**2**	12.1	**3**
His	2.4	**13**	2.3	**12**	nd	**nd**	2.3	**12**	2.4	**10**	2.2	**11**
Ile	5.4	**7**	4.7	**9**	nd	**nd**	5.6	**7**	3.7	**9**	4.6	**9**
Leu	4.9	**10**	5.5	**6**	nd	**nd**	5.5	**8**	5.8	**6**	5.4	**6**
Lys	3.9	**11**	2.9	**11**	nd	**nd**	0	**17**	2.2	**11**	0	**17**
Met	0	**17**	0.09	**16**	nd	**nd**	0.25	**15**	0	**16**	0.02	**15**
Phe	2.8	**12**	2.1	**13**	nd	**nd**	2.7	**11**	1.7	**13**	1.9	**12**
Pro	5.3	**8**	5.4	**7**	nd	**nd**	5.3	**9**	5.5	**7**	5.2	**7**
Ser	1.2	**15**	0.9	**15**	nd	**nd**	1.1	**14**	0.7	**15**	0.8	**14**
Thr	5.6	**6**	4.9	**8**	nd	**nd**	5.3	**10**	4.6	**8**	4.9	**8**
Trp	0.03	**16**	0	**17**	nd	**nd**	0.07	**16**	0	**17**	0.01	**16**
Tyr	1.6	**14**	1.3	**14**	nd	**nd**	1.5	**13**	1.1	**14**	1.2	**13**
Val	5.3	**9**	3.5	**10**	nd	**nd**	6	**6**	2.2	**12**	4.5	**10**

The amino acid contents were expressed as the percentage (%) composition of 1 g dry weight *S. fradiae* C373-10 biomass cultured on a number of different carbon sources. MO, methyl oleate defined medium (Chapter 3, section 3.7.2); Glc, glucose; Fru, fructose; Glyc, glycerol; and OGA, oxo-glutarate minimal media (Chapter 3, section 3.6.4)[samples correspond to Tables 5.9 A - J; Chapter 4, Fig 4.1 - 4.20 & Chapter 6, Tables 6.1 - 6.29]. Amino acid analysis was undertaken by HPLC (Chapter 3, section 3.25). The corresponding number fermentation (Ferm) number denotes the number of fermentations undertaken. The figures in bold denote the position of the amino acids in the order (ord) of decreasing relative proportions. Figure 5.7a - c presents the above data in graphed format. # denotes where the alkali and residue fractions were both taken into account. nd, not determined.

Table 5.31 Amino acid composition of *S. fradiae* C373-10 biomass determined throughout a glucose glutamate defined medium culture and expressed as the percentage of the total amino acid content and the order of biosynthetic requirement.

	Day 0					Day 1					Day 2				
Amino acids	**Ferm 1#**	**Ferm 2#**	**Ferm 3#**	**Ferm 4#**	**ord**	**Ferm 1#**	**Ferm 2#**	**Ferm 3**	**Ferm 4#**	**ord**	**Ferm 1**	**Ferm 2**	**Ferm 3#**	**Ferm 4#**	**ord**
Ala	7.1	7.97	9.08	8.46	**6**	13.18	9.82	nd	9.24	**1**	12.38	9.67	5.8	10.96	**4**
Arg	31.34	24.34	10.33	17.69	**1**	4.47	6.73	nd	3.07	**9**	2.73	2.86	12.71	2.15	**12**
Asp	11.75	10.62	9.44	11.92	**3**	4.46	11.64	nd	9.59	**5**	8.57	8.99	10.75	12.58	**3**
Asn	nd	nd	nd	nd	**nd**	nd	nd	nd	nd	**nd**	nd	nd	nd	nd	**nd**
Cys	nd	nd	nd	nd	**nd**	nd	nd	nd	nd	**nd**	nd	nd	nd	nd	**nd**
Glu	9.79	8.85	9.97	12.77	**4**	12.43	9.91	nd	8.97	**2**	12.12	9.22	10.91	12.78	**2**
Cys	nd	nd	nd	nd	**nd**	nd	nd	nd	nd	**nd**	nd	nd	nd	nd	**nd**
Gly	14.2	17.7	9.08	7.69	**2**	14.25	7.27	nd	6.05	**4**	14.24	10.31	9.95	1.69	**6**
His	0.98	1.33	2.31	2.31	**11**	2.86	3.09	nd	2.95	**13**	2.81	2.86	2.45	1.29	**14**
Ile	1.96	1.73	6.41	6.15	**10**	5.78	2.54	nd	2.33	**11**	0.78	7.67	7.02	8.7	**9**
Leu	7.34	6.86	11.75	10	**5**	8.04	6.73	nd	6.29	**7**	11.34	11.9	12.56	12.78	**1**
Lys	0	0	4.98	0	**14**	6.46	1.36	nd	2.02	**12**	5.24	8.9	6.12	9.24	**7**
Met	0	0	4.98	0	**15**	0	0	nd	0	**16**	0	0	0	0	**18**
Phe	1.47	2.21	0.125	1.538	**12**	3.2	0.54	nd	1.16	**15**	3.12	2.72	2.55	2.68	**13**
Pro	5.14	5.21	5.243	5.16	**7**	5.29	5.26	nd	2.99	**10**	5.26	5.18	5.2	5.21	**11**
Ser	0.78	0.31	1.17	0.92	**16**	1.73	1.18	nd	5.24	**14**	1.69	1.36	1.33	1.61	**16**
Thr	4.9	4.43	4.98	5.61	**8**	8.28	5.36	nd	1.24	**8**	7.97	6.13	2.55	7.41	**10**
Trp	0	0	0	0.23	**17**	0	0	nd	0	**17**	0	0.68	0	0	**17**
Tyr	0.78	1.33	1.6	1	**13**	2.15	13.9	nd	14.28	**3**	2.47	2.59	1.81	1.18	**15**
Val	0.59	5.3	6.77	6.69	**9**	5.71	12.91	nd	5.24	**6**	7.53	7.13	6.49	7.95	**8**

	Day 3					Day 4					Day 5				
Amino acids	**Ferm 1#**	**Ferm 2#**	**Ferm 3#**	**Ferm 4**	**ord**	**Ferm 1#**	**Ferm 2#**	**Ferm 3**	**Ferm 4#**	**ord**	**Ferm 1#**	**Ferm 2**	**Ferm 3#**	**Ferm 4#**	**ord**
Ala	9.57	9.93	12.35	nd	**2**	7.66	7.11	6.76	9.81	**6**	9.91	11.5	10.7	11.5	**3**
Arg	2.93	5.08	5.68	nd	**12**	16.45	15.46	21.17	6.76	**1**	10.06	10.12	9.99	6.9	**6**
Asp	10.58	9.35	12.25	nd	**1**	8.69	7.68	7.71	9.77	**4**	10.57	10.67	10.88	13.17	**1**
Asn	nd	nd	nd	nd	**nd**	nd	nd	nd	nd	**nd**	nd	nd	nd	nd	**nd**
Cys	nd	nd	nd	nd	**nd**	nd	nd	nd	nd	**nd**	nd	nd	nd	nd	**nd**
Glu	9.44	9.12	13.26	nd	**3**	8.69	7.92	7.71	8.23	**5**	9.14	9.24	9.33	11.16	**4**
Cys	nd	nd	nd	nd	**nd**	nd	nd	nd	nd	**nd**	nd	nd	nd	nd	**nd**
Gly	6.85	10.51	13.2	nd	**4**	6.32	5.41	5.08	5.33	**8**	7.83	7.89	8.12	9.74	**5**
His	3.12	2.83	2.95	nd	**14**	2.57	2.467	2.39	3.82	**14**	3.9	3.93	4.11	4.81	**9**
Ile	2.38	6.52	1.4	nd	**13**	6.27	5.64	5.5	4.05	**9**	3.81	3.82	3.99	1.8	**12**
Leu	6.54	11.08	4.56	nd	**7**	9.56	9.77	9.15	5.87	**3**	8.13	8.35	8.44	6.98	**7**
Lys	1.94	10.74	7.58	nd	**9**	11.98	18.36	15.61	4.05	**2**	3.99	4.01	3.89	4.47	**10**
Met	0	0	0	nd	**18**	0.035	0.04	0.036	0	**18**	0	0	0	0.19	**15**
Phe	3.24	2.48	1.12	nd	**15**	1.95	1.87	1.73	3.44	**15**	12.14	12.11	11.98	11.66	**2**
Pro	5.24	5.24	5.25	nd	**11**	5.16	5.17	0	5.25	**11**	5.26	5.12	4.99	5.31	**8**
Ser	1.36	1.44	1.75	nd	**16**	1.08	0.99	0.86	1.31	**16**	1.19	0.99	1.11	1.38	**14**
Thr	5.37	5.89	8.07	nd	**10**	5.04	4.36	4.01	5.64	**10**	5.48	5.55	5.46	6.23	**7**
Trp	0.151	0	0	nd	**17**	0	0.047	0	0	**17**	0	0	0	0	**16**
Tyr	17.53	1.84	2.74	nd	**8**	1.08	0.66	0.42	13.28	**12**	1.67	1.23	1.44	1.5	**13**
Val	11.76	6.17	6.1	nd	**5**	5.6	5.17	4.84	11.62	**7**	5.18	4.99	4.89	1.5	**11**

The amino acid contents were expressed as the percentage (%) composition of 1 g dry weight of *S. fradiae* C373-10 biomass determined throughout a glucose glutamate defined medium fermentation (Chapter 3, section 3.6.4)[samples correspond to Tables 5.9A]. The corresponding fermentation (Ferm) number denotes the number of fermentations undertaken. Amino acid analysis was undertaken by HPLC (Chapter 3, section 3.25). The figures in bold denote the position of the amino acids in the order (ord) of decreasing relative proportions. Figure 5.7a - c presents the above data in graphed format. # Denotes where the alkali and residue fraction were both taken into account. nd, not determined.

Table 5.32 Amino acid composition of *S. fradiae* C373-10 biomass determined throughout a glucose oxo-glutarate defined medium culture and expressed as the percentage of the total amino acid content and the order of biosynthetic requirement.

Amino acids	G/O (Ferm 1) Day 0	G/O (Ferm 2) Day 0#	Ord	G/O (Ferm 1) Day 1#	G/O (Ferm 2) Day 1	Ord	G/O (Ferm 1) Day 3	G/O (Ferm 2) Day 3#	Ord	G/O (Ferm 1) Day 4#	G/O (Ferm 2) Day 4#	Ord
Ala	10.7	10.09	**3**	7.31	10.47	**4**	9.28	11.18	**3**	9.55	10.64	**2**
Arg	2.87	7.2	**9**	8.11	2.78	**9**	1.32	4.79	**13**	5.11	6.23	**8**
Asp	11.98	11.8	**2**	10.94	9.14	**2**	9.34	10.6	**4**	9.52	9.99	**4**
Asn	nd	nd	**nd**	nd	nd	**nd**	nd	nd	**nd**	nd	nd	**nd**
Cys	nd	nd	**nd**	nd	nd	**nd**	nd	nd	**nd**	nd	nd	**nd**
Glu	10.4	10.09	**4**	8.21	6.52	**5**	8.4	8.06	**5**	8.85	7.55	**6**
Gln	nd	nd	**nd**	nd	nd	**nd**	nd	nd	**nd**	nd	nd	**nd**
Gly	22.63	24.43	**1**	4.24	7.25	**8**	8.4	6.71	**6**	9.99	10.12	**3**
His	1.49	1.56	**13**	3.01	1.95	**14**	2.97	1.92	**14**	2.45	1.96	**15**
Ile	4.11	3.65	**10**	5.37	4.47	**11**	5.65	4.57	**10**	4.98	4.56	**12**
Leu	10	6.71	**5**	6.42	6.76	**6**	6.26	6.68	**7**	6.51	6.74	**7**
Lys	0	0	**15**	10.47	2.22	**7**	5.16	3.41	**11**	5.84	4.13	**11**
Met	0	0	**16**	1.51	0.04	**17**	0	0	**16**	0.04	0.03	**16**
Phe	2.82	2.48	**11**	0.38	3.78	**15**	4.12	3.48	**12**	4.22	3.55	**13**
Pro	5.27	5.27	**8**	5.17	5.27	**10**	5.24	5.3	**9**	5.99	4.97	**9**
Ser	1.24	1.29	**14**	0.94	1.36	**16**	2.86	1.38	**15**	2.98	1.44	**14**
Thr	6.09	5.54	**7**	3.96	5.86	**12**	5.16	5.99	**8**	5.63	5.46	**10**
Try	0	0	**17**	0.57	0.05	**18**	0	0	**17**	0.01	0.01	**17**
Tyr	1.88	1.56	**12**	5.14	14.87	**3**	12.91	10.53	**2**	13.92	10.12	**1**
Val	6.78	6.56	**6**	16.37	15.47	**1**	11.15	13.68	**1**	4.41	12.5	**5**

Amino acids	G/O (Ferm 1) Day 5	G/O (Ferm 2) Day 5#	Ord	G/O (Ferm 1) Day 6#	G/O (Ferm 2) Day 6#	Ord	G/O (Ferm 1) Day 7#	G/O (Ferm 2) Day 7#	Ord
Ala	8.45	8.99	**4**	7.33	8.81	**5**	6.45	7.84	**6**
Arg	15.67	22.56	**1**	14.97	18.61	**2**	15.36	16.78	**2**
Asp	8.91	10.23	**3**	8.87	11.98	**3**	8.12	10.65	**3**
Asn	Nd	nd	**nd**	nd	nd	**nd**	nd	nd	**nd**
Cys	Nd	nd	**nd**	nd	nd	**nd**	nd	nd	**nd**
Glu	6.98	8.87	**5**	7.3	9.55	**4**	7.74	9.12	**4**
Gln	Nd	nd	**nd**	nd	nd	**nd**	nd	nd	**nd**
Gly	16.95	21.23	**2**	18.9	22.37	**1**	22.56	15.67	**1**
His	1.11	1.52	**13**	1.42	1.24	**13**	1.23	1.55	**14**
Ile	2.75	3.52	**11**	2.73	3.46	**10**	2.74	3.33	**11**
Leu	6.12	7.52	**7**	5.99	7.17	**7**	6.14	7.41	**7**
Lys	0.01	0.03	**16**	0	0	**16**	0.01	0.01	**16**
Met	0.22	0.512	**15**	0	0.213	**15**	3.41	0.38	**13**
Phe	2.11	2.88	**12**	2.09	2.62	**12**	2.11	2.44	**12**
Pro	6.12	3.54	**8**	5.16	1.09	**9**	5.66	4.65	**9**
Ser	0.27	0.57	**14**	0.18	0.48	**14**	0.22	0.23	**15**
Thr	4.82	3.82	**9**	4.6	0.49	**11**	3.82	4.11	**10**
Try	0.01	0.01	**17**	0	0	**17**	0	0	**17**
Tyr	8.12	0.512	**10**	8.09	0.39	**8**	6.99	6.84	**8**
Val	11.38	3.69	**6**	10.51	5.59	**6**	7.74	8.99	**5**

The amino acid contents were expressed as the percentage (%) composition of 1 g dry weight of *S. fradiae* C373-10 biomass determined throughout a glucose oxo-glutarate defined medium fermentation (Chapter 3, section 3.6.4)[samples correspond to Tables 5.7 A - J]. The corresponding number denotes the number of fermentations undertaken. Amino acid analysis was undertaken by HPLC (Chapter 3, section 3.25). The figures in bold after Ferm (fermentation) denote the position of the amino acids in the order (ord) of decreasing relative proportions. Figure 5.7a - c presents the above data graphed. # Denotes where the alkali and residue fractions were both taken into account. nd, not determined.

Table 5.33. Amino acid profile of the *S. fradiae* C373-18 industrial complex process broth samples and individual medium components.

	Inoculation					Harvest				
Amino acids	**Ferm 1, Day 0**	**Ferm 2, Day 0**	**Ferm 3, Day 0**	**STDEV**	**ord**	**Ferm 1, Harvest**	**Ferm 2, Harvest**	**Ferm 3, Harvest**	**STDEV**	**ord**
Ala	6.03	6.00	6.09	± 0.044	**5**	9.33	8.82	9.07	± 0.251	**3**
Arg	8.27	8.30	8.35	± 0.038	**3**	7.63	7.36	7.43	± 0.138	**5**
Asp	10.31	10.26	10.33	± 0.039	**2**	11.74	11.25	11.03	± 0.364	**2**
Cys	0.77	0.91	0.75	± 0.084	**18**	1.48	1.37	1.36	± 0.068	**18**
Glu	18.51	18.49	18.62	± 0.066	**1**	17.12	16.28	17.16	± 0.497	**1**
Gly	5.61	5.65	5.82	± 0.112	**7**	7.79	7.45	7.48	± 0.189	**4**
His	2.80	2.72	2.80	± 0.049	**14**	0.02	2.19	2.76	± 1.441	**16**
Ile	3.99	3.91	3.90	± 0.054	**13**	3.24	3.15	3.08	± 0.077	**13**
Leu	7.93	7.82	7.73	± 0.097	**4**	7.46	7.22	7.25	± 0.129	**6**
Lys	5.89	5.72	5.89	± 0.097	**6**	4.33	5.07	4.16	± 0.486	**10**
Met	1.89	2.16	1.92	± 0.151	**16**	1.65	1.46	1.59	± 0.095	**17**
Phe	4.98	5.03	4.93	± 0.049	**10**	3.51	3.48	3.46	± 0.025	**12**
Pro	5.12	5.30	5.20	± 0.093	**8**	4.66	4.85	4.67	± 0.103	**9**
Ser	4.63	4.67	4.65	± 0.024	**11**	4.11	4.12	4.07	± 0.028	**11**
Thr	4.21	4.18	4.26	± 0.031	**12**	5.156	5.03	5.05	± 0.069	**8**
Trp	1.26	1.19	1.09	± 0.084	**17**	2.03	1.78	1.82	± 0.134	**15**
Tyr	2.67	2.58	2.67	± 0.048	**15**	2.58	2.56	2.62	± 0.029	**14**
Val	5.12	5.09	4.99	± 0.064	**9**	6.16	6.54	5.94	± 0.305	**7**

	Corn gluten					Fish meal				
Amino acids	**Sample 1**	**Sample 2**	**Sample 3**	**STDEV**	**ord**	**Sample 1**	**Sample 2**	**Sample 3**	**STDEV**	**ord**
Ala	13	12.6	13.3	± 0.351	**3**	9.96	8.93	7.98	± 0.990	**2**
Arg	2.7	2.7	2.5	± 0.115	**13**	3.81	4.02	3.68	± 0.172	**8**
Asp	5.9	6.5	6.4	± 0.321	**5**	4.86	4.99	5.12	± 0.130	**3**
Cys	nd	nd	nd	nd	**nd**	nd	nd	nd	nd	**nd**
Glu	20.3	19.8	21.5	± 0.874	**1**	12.63	14.89	15.66	± 1.574	**1**
Gly	5.7	6.2	5.1	± 0.551	**6**	3.68	4.42	4.46	± 0.439	**7**
His	2.6	2.5	2	± 0.321	**14**	1.59	1.34	1.42	± 0.128	**16**
Ile	4.6	4.7	4.2	± 0.264	**8**	3.06	2.72	2.28	± 0.391	**10**
Leu	14.9	14.5	15.4	± 0.451	**2**	4.98	4.36	4.16	± 0.427	**6**
Lys	2.2	2.5	2	± 0.252	**15**	5.07	4.53	4.51	± 0.318	**4**
Met	1.7	1.5	1.6	± 0.100	**16**	1.95	1.68	1.63	± 0.172	**14**
Phe	4.4	4.3	4.5	± 0.100	**10**	2.75	2.28	2.21	± 0.294	**12**
Pro	1.7	1.6	1.6	± 0.058	**17**	1.53	1.96	1.57	± 0.238	**15**
Ser	6.9	7.1	7.2	± 0.153	**4**	5.70	5.63	2.89	± 1.602	**5**
Thr	4.4	4.4	4.1	± 0.173	**9**	2.82	2.57	2.46	± 0.184	**11**
Trp	3.8	3.8	3.7	± 0.058	**11**	0.78	0.67	0.49	± 0.146	**17**
Tyr	3.8	3.8	3.7	± 0.058	**12**	2.22	1.83	1.80	± 0.234	**13**
Val	5.3	5	4.9	± 0.208	**7**	3.46	3.02	2.77	± 0.349	**9**

The amino acid contents were expressed as the percentage (%) composition of 1 g dry weight of *S. fradiae* C373-10 fermentation liquor. The liquor was analysed at inoculation and harvest cultured on an industrial complex medium (Chapter 3, section 3.7.3). In addition further analysis was undertaken on individual medium components, corn gluten and fish meal was presented in the same format. The corresponding fermentation (Ferm) number denotes the number of fermentations undertaken. Amino acid analysis was undertaken by HPLC (Chapter 3, section 3.25) at Eli Lilly Ltd. The figures in bold denote the position of the amino acids in the order (ord) of decreasing relative proportions. Figure 5.7a - c presents the above data graphed. nd, not determined.

Table 5.34 Part 1 (Part 1 & 2 companion Tables) Comparison of the amino compositional order of amino acid requirement in relation to codon usage and branch point stabability.

Amino Acids	[a] *Streptomyces* codon usage (%) calculated from genomic codon usage tables	[b] *S. coelicolor* (mean) % amino content	[c] *S. fradiae* (mean) % amino content	*Streptomyces* expected codon order of requirement take from genomic codon usage tables	*S. coelicolor* 1147 codon order of requirement calculated from amino acid composition	*S. fradiae* C373-10 codon order of requirement calculated from average amino acid composition
Glucose-6-phosphate						
Phe	2.9	3.2	2.9	**12**	**13**	**11**
Tyr	2.3	1.9	3.2	**15**	**14**	**12**
Trp	1.6	nd	0.3	**17**	**nd**	**16**
3-phosphoglycerate						
Ser	5.3	4.7	0.86	**10**	**11**	**14**
Cys	0.8	nd	nd	**nd**	**nd**	**nd**
Gly	9.1	14.3	13.1	**3**	**2**	**1**
Pyruvate						
Ala	13.1	14.1	11.9	**1**	**1**	**2**
Val	7.9	8.3	5.9	**5**	**3**	**6**
Leu	9.2	7.8	5.6	**2**	**4**	**7**
Oxo-glutarate						

Glu	5.9	7.2	9.4	**8**	**5**	**5**
Gln	2.6	nd	nd	**nd**	**nd**	**nd**
Pro	5.5	5.8	5.2	**9**	**9**	**8**
Arg	8.1	6.6	20.12	**4**	**6**	**3**
Oxaloacetate						
Asp	6.4	6.1	9.5	**7**	**7**	**4**
Asn	2.5	nd	nd	**nd**	**nd**	**nd**
Met	1.6	1.5	0.12	**16**	**16**	**15**
Thr	6.8	5.7	4.7	**6**	**10**	**9**
Lys	2.4	5.8	2.9	**14**	**16**	**13**
Ile	3.3	4.5	4.3	**11**	**12**	**10**

The amino acid composition of ten *S. coelicolor* 1147[b] (present work in addition to Davidson, 1992 work) biomass samples; and forty two *S. fradiae* C373-10[c] biomass samples cultured on a number of different carbon sources (Tables 5.27 - 5.30). Amino acids were determined by HPLC analysis (Chapter 3, section 3.25). The amounts of the amino acids per gram dry weight were expressed as a percentage of the total amino acid content (Tables 5.28 - 5.32). The means of these percentages were presented above. [a]The relative use of the codons for each amino acid was calculated from the individual codon usage Tables for 63 streptomycete genes (Wright & Bibb, 1992). The codon order denotes the actual and expected positions of the amino acids in order (ord) of decreasing relative proportions (Table 5.35 Part 1) from amino acid analysis and genomic codon usage tables. nd, indicates no available data due these amino acids not being detectable with the analytical protocols used in this work.

Table 5.34 Part 2 (Part 1 & 2 companion Tables) Comparison of the amino compositional order of amino acid requirement in relation to codon usage and branch point stabability.

Amino Acid families arranged as branch points	*E. coli* ML308[a] mean order of requirement of branch points	*S. coelicolor* 1147[b] mean order of requirement of branch points	*S. fradiae* C373-10[c] mean order of requirement of branch points
Glucose-6-phosphate	5	5	5
3-phosphoglycerate	3	2	3
Pyruvate	1	1	1
Oxo-glutarate	2	3	2
Oxaloacetate	4	4	4

The amino acid composition of ten *S. coelicolor* 1147[b] (present work in addition to Davidson, 1992 work) biomass samples; and forty two *S. fradiae* C373-10[c] biomass samples cultured on a number of different carbon sources (Tables 5.27 - 5.30). Amino acids were determined by HPLC analysis (Chapter 3, section 3.25). The amounts of the amino acids per gram dry weight were expressed as a percentage of the total amino acid content (Tables 5.28 - 5.32). The means of these percentages were presented above. [a]The relative use of the codons for each amino acid was calculated from the individual codon usage Tables for 63 streptomycete genes (Wright & Bibb, 1992). The codon order denotes the actual and expected positions of the amino acids in order (ord) of decreasing relative proportions (Table 5.35 Part 1) from amino acid analysis and genomic codon usage tables. The mean order of requirement for branch point codon usage was also calculated for *E. coli* ML308, *S. coelicolor* 1147 and *S. fradiae* C373-10 (Table 5.35 Part 2). nd, indicates no available data due these amino acids not being detectable with the analytical protocols used in this work.

Table 5.35 Part 1 The analytical verification of the percentage elemental composition, of *S. fradiae* C373-10, *S. coelicolor* 1147 and *E. coli* ML308 cultured on a number of different carbon sources (corresponds to Tables 5.9 A - J).

Fermentation	C [E] (%)	C [M] (%)	TOCA (%)	C [R] (%)	N [E] (%)	N [M] (%)	TONA (%)	N [R] (%)
***S. fradiae* C373-10**								
Glucose (Ferm 1)	43.62 ± 0.06	40.84	45.62 ± 0.10	43.36 ± 2.95	8.45 ± 0.13	14.61	8.91 ± 0.35	10.66 ± 2.85
Glucose (Ferm 2)	42.68 ± 0.16	41.10	45.44 ± 0.26	43.07 ± 2.80	9.42 ± 0.16	14.13	10.90 ± 0.52	11.48 ± 1.61
Fructose	46.87 ± 0.14	44.69	46.34 ± 0.33	45.97 ± 1.14	14.76 ± 0.05	10.77	7.66 ± 0.66	11.06 ± 3.56
Glycerol (Ferm 1)	51.37 ± 0.18	45.11	49.69 ± 0.89	48.72 ± 3.24	14.05 ± 0.06	9.99	10.88 ± 0.44	11.64 ± 2.13
Glycerol (Ferm 2)	48.37 ± 0.31	42.02	46.39 ± 0.45	45.59 ± 3.25	12.73 ± 0.21	14.22	6.84 ± 0.69	11.26 ± 3.90
Oxo-glutarate	40.74 ± 0.08	40.55	43.69 ± 0.18	41.66 ± 1.76	12.72 ± 0.06	11.23	10.88 ± 0.52	11.61 ± 0.98
G / G (Ferm 1) Day 5	48.60 ± 0.07	47.94	49.26 ± 0.57	48.60 ± 0.66	12.59 ± 0.26	10.11	9.05 ± 0.23	10.58 ± 1.82
G / G (Ferm 2) Day 5	49.54 ± 0.12	50.37	49.99 ± 0.22	49.97 ± 0.41	12.82 ± 0.03	8.21	6.26 ± 0.86	9.10 ± 3.37
G / G (Ferm 3) Day 5	48.82 ± 0.08	50.27	49.62 ± 0.81	49.57 ± 0.73	12.67 ± 0.09	7.60	5.99 ± 0.33	8.75 ± 3.49
G / G (Ferm 4) Day 5	47.93 ± 0.08	48.65	48.24 ± 0.51	48.27 ± 0.36	12.49 ± 0.24	10.00	8.01 ± 0.36	10.17 ± 2.24
G / O (Ferm 1) Day 7	46.44 ± 0.09	39.19	43.52 ± 0.59	43.05 ± 3.65	11.70 ± 0.11	15.05	10.87 ± 0.65	12.54 ± 2.21
G / O (Ferm 2) Day 7	46.55 ± 0.29	40.91	45.56 ± 0.39	44.34 ± 3.01	12.19 ± 0.21	16.29	12.88 ± 0.38	13.79 ± 2.19
MO (Ferm 1) Day 3	46.29 ± 0.04	44.71	47.69 ± 0.84	46.23 ± 1.49	14.80 ± 0.06	14.72	10.89 ± 0.99	13.47 ± 2.23
MO (Ferm 1) Day 5	44.04 ± 0.05	43.33	44.67 ± 0.58	44.01 ± 0.67	12.93 ± 0.14	14.96	11.80 ± 0.56	13.23 ± 1.60
MO (Ferm 1) Day 10	45.67 ± 0.12	nd	45.86 ± 0.53	30.51 ± 0.13	12.27 ± 0.12	nd	15.88 ± 0.37	9.38 ± 2.55
MO (Ferm 2) Day 3	41.12 ± 0.16	43.99	43.22 ± 0.26	42.78 ± 1.48	13.72 ± 0.14	14.47	13.88 ± 0.68	14.02 ± 0.39
MO (Ferm 2) Day 5	43.37 ± 0.16	42.88	44.47 ± 0.57	43.57 ± 0.81	12.30 ± 0.06	14.51	13.89 ± 0.77	13.57 ± 1.13
MO (Ferm 2) Day 10	46.68 ± 0.10	43.36	46.99 ± 0.15	45.68 ± 2.01	11.95 ± 0.10	14.36	15.12 ± 0.88	13.81 ± 1.65
***E. coli* ML308**								
Glucose (Ferm 1)	49.20 ± 0.10	42.77	51.20 ± 0.57	47.72 ± 4.40	15.11 ± 0.17	11.07	14.44 ± 0.39	13.54 ± 2.16
***S. coelicolor* 1147**								
Glucose (Ferm 1)	46.68 ± 0.48	41.90	45.12 ± 0.28	44.57 ± 2.44	8.02 ± 0.11	11.89	9.99 ± 0.66	9.97 ± 1.93

Glucose (Ferm 2)	46.23 ± 0.55	41.37	46.88 ± 0.89	44.83 ± 3.01	8.44 ± 0.23	12.86	10.12 ± 0.19	10.47 ± 2.23

The elemental composition of *S. fradiae* C373-10, *S. coelicolor* 1147, and *E. coli* ML308 were cultured on a number of different medium compositions. *S. fradiae* C373-10 and was cultured on glucose, fructose, glycerol, oxo-glutarate minimal media, glucose glutamate (G/G), glucose oxo-glutarate (G/O) defined media (Chapter 3, section 3.6.4), and a methyl oleate defined medium (MO) (Chapter 3, section 3.7.2), *S. coelicolor* 1147 and *E. coli* ML308 both were cultured on a glucose minimal media (Chapter 3, section 3.6.1 & 3.6.3 respectively)[corresponds with Tables 5.9 A - J]. All sampling points were taken at sampling point II (as Chapter 4, Fig 4.1 - 4.20) and for the MO medium SP I, II, and III. E, denotes elemental analysis (analysis undertaken as Chapter 3, section 3.15) for C, H, & N; M denotes molecular elemental analysis calculated from the macromolecular composition (Tables 6.1 to 6.29, Chapter 6, where the monomeric composition was converted to the atomic composition and then the number of grams of each atom was calculated and thus converted to percentage format for C, H, N, S, & P). R denotes the reconciled data (an mean between E and M). The percentage carbon and nitrogen composition was further verified with total organic carbon analysis (TOCA) [Chapter 3, section 3.15.5] and total organic nitrogen analysis (TONA)[Kjeldal method, Chapter 3, section 3.15.6]. Numbers denoted in brackets show the number of fermentations (Ferm) undertaken this corresponds with Chapter 4 (Fig 4.1 - 4.20).

Table 5.35 Part 2 The analytical verification of the percentage elemental composition, of *S. fradiae* C373-10, *S. coelicolor* 1147 and *E. coli* ML308 cultured on a number of different carbon sources (corresponds to Tables 5.9 A - J).

Fermentation	E H%	M H%	R H%	M S%	M P%	O (E)	O (E1)	O (E2)	O (E3)	O (M)	R O%
***S. fradiae* C373-10**											
Glucose (Ferm 1)	7.12 ± 0.02	7.04	7.08 ± 0.95	0.29	2.25	33.48	33.15	27.98	23.98	34.94	32.38 ± 4.59
Glucose (Ferm 2)	7.26 ± 0.11	7.09	7.17 ± 0.87	0.36	1.00	32.83	32.5	27.33	23.33	36.31	32.24 ± 5.11
Fructose	8.24 ± 0.09	6.90	7.57 ± 0.95	0.23	3.57	30.13	29.8	24.63	20.63	33.81	29.59 ± 5.17
Glycerol (Ferm 1)	8.40 ± 0.04	7.07	7.73 ± 0.94	0.29	1.56	26.18	25.85	20.68	16.68	35.95	27.16 ± 7.24
Glycerol (Ferm 2)	8.36 ± 0.09	7.28	7.82 ± 0.76	0.37	2.06	30.54	30.21	25.04	21.04	34.03	29.95 ±5.12
Oxo-glutarate	7.26 ± 0.21	6.29	6.77 ± 0.69	0.18	6.72	39.28	38.95	33.78	29.78	34.98	36.75 ± 3.93
G / G (Ferm 1) Day 5	8.35 ± 0.06	8.12	8.23 ± 0.16	0.46	1.58	30.46	30.13	24.96	20.96	31.78	29.33 ± 4.56
G / G (Ferm 2) Day 5	8.23 ± 0.09	7.89	8.06 ± 0.24	0.24	1.62	29.41	29.08	23.91	19.91	31.65	28.51 ± 4.78
G / G (Ferm 3) Day 5	8.41 ± 0.01	7.96	8.18 ± 0.32	0.20	2.63	30.1	29.77	24.6	20.6	31.33	28.95 ± 4.54
G / G (Ferm 4) Day 5	8.32 ± 0.06	8.07	8.19 ± 0.18	0.27	1.22	31.26	30.93	25.76	21.76	31.77	29.93 ± 4.38
G / O (Ferm 1) Day 7	8.05 ± 0.05	6.57	7.31 ± 1.05	0.29	4.14	33.81	33.48	28.31	24.31	34.61	32.55 ± 4.44
G / O (Ferm 2) Day 7	7.96 ± 0.08	7.26	7.61 ± 0.49	0.41	1.38	33.3	32.97	27.8	23.8	33.71	31.94 ± 4.37
MO (Ferm 1) Day 3	7.47 ± 0.03	7.45	7.46 ± 0.01	0.35	1.58	31.44	31.11	25.94	21.94	31.15	29.91 ± 4.24
MO (Ferm 1) Day 5	7.16 ± 0.04	7.35	7.25 ± 0.13	0.39	1.07	35.87	35.54	30.37	26.37	32.87	33.66 ± 3.95
MO (Ferm 1) Day 10	7.23 ± 0.10	nd	3.61	nd	nd	34.83	34.5	29.33	25.33	nd	nd
MO (Ferm 2) Day 3	6.73 ± 0.09	7.22	6.97 ± 0.35	0.40	1.32	38.43	38.1	32.93	28.93	32.56	35.50 ± 4.54
MO (Ferm 2) Day 5	7.07 ± 0.12	7.31	7.19 ± 0.17	0.35	1.56	37.26	36.93	31.76	27.76	33.37	34.83 ± 4.04
MO (Ferm 2) Day 10	8.05 ± 0.08	7.20	7.62 ± 0.60	0.37	1.07	33.32	32.99	27.82	23.82	33.63	31.94 ± 3.93
***E. coli* ML308**											
Glucose (Ferm 1)[a]	7.94 ± 0.44	7.22	7.58 ± 0.51	1.00	2.50	27.3	nd	23.18	21.98	35.42	28.63 ± 6.08
***S. coelicolor* 1147**											
Glucose (Ferm 1)	7.23 ± 0.16	6.90	7.06 ± 0.23	0.48	4.16	38.07	36.69	35.14	28.04	34.65	36.14 ± 3.86
Glucose (Ferm 2)	7.99 ± 0.28	6.89	7.44 ± 0.78	0.61	3.66	37.34	35.96	34.41	27.31	34.58	35.57 ± 3.88

The elemental composition of *S. fradiae* C373-10, *S. coelicolor* 1147, and *E. coli* ML308 were cultured on a number of different medium compositions. *S. fradiae* C373-10 and was cultured on glucose, fructose, glycerol, oxo-glutarate minimal media, glucose glutamate (G/G), glucose oxo-glutarate (G/O) defined media (Chapter 3, section 3.6.4), and a methyl oleate defined medium (MO) (Chapter 3, section 3.7.2), *S. coelicolor* 1147 and *E. coli* ML308 both were cultured on a glucose minimal media (Chapter 3, section 3.6.1 & 3.6.3 respectively)[corresponds with Tables 5.9 A - J]. All sampling points were taken at sampling point II (as Chapter 4, Fig 4.1 - 4.20) and for the MO medium SP I, II, and III. E, denotes elemental analysis (analysis undertaken as Chapter 3, section 3.15) for C, H, & N; M denotes molecular elemental analysis calculated from the macromolecular composition (Tables 6.1 to 6.29, Chapter 6, where the monomeric composition was converted to the atomic composition and then the number of grams of each atom was calculated and thus converted to percentage format for C, H, N, S, & P). R denotes the reconciled data (an mean between E and M). The percentage carbon and nitrogen composition was further verified with total organic carbon analysis (TOCA) [Chapter 3, section 3.15.5] and total organic nitrogen analysis (TONA)[Kjeldal method, Chapter 3, section 3.15.6]. Numbers denoted in brackets show the number of fermentations (Ferm) undertaken this corresponds with Chapter 4 (Fig 4.1 - 4.20). The oxygen (O) content was calculated by subtraction of the C, H, N, S and P from 100 % this included the subtraction of the theoretical ash content where appropriate, the theoretical ash content was calculated in the following way, E, no ash content taken into account, E1 theoretical ash content taken into account, E2 non-hydrolysed ash content taken into account, and E3 hydrolysed ash content taken into account (corresponds with Table 5.38).

Table 5.36 Elemental composition of various microorganisms quoted in the literature

Micro-organism	Elemental composition	Ash content (w/w %)	Conditions
Candida utilis	$CH_{1.83}\ O_{0.46}\ N_{0.19}$	7.0	Glucose limited
	$CH_{1.87}\ O_{0.56}\ N_{0.20}$	7.0	Glucose limited
	$CH_{1.83}\ O_{0.54}\ N_{0.10}$	7.0	Ammonia limited
	$CH_{1.87}\ O_{0.56}\ N_{0.20}$	7.0	Ammonia limited
Klebsiella aerogenes	$CH_{1.75}\ O_{0.43}\ N_{0.22}$	3.6	Glycerol limited
	$CH_{1.73}\ O_{0.43}\ N_{0.24}$	3.6	Glycerol limited
	$CH_{1.75}\ O_{0.43}\ N_{0.17}$	3.6	Ammonia limited
	$CH_{1.73}\ O_{0.43}\ N_{0.24}$	3.6	Ammonia limited
Saccharomyces cerevisiae	$CH_{1.82}\ O_{0.58}\ N_{0.16}$	7.3	Glucose limited
	$CH_{1.78}\ O_{0.60}\ N_{0.19}$	9.7	Glucose limited
	$CH_{1.94}\ O_{0.52}\ N_{0.25}$	5.5	Unlimited growth
Escherichia coli	$CH_{1.77}O_{0.49}\ N_{0.22}$	5.5	Unlimited growth
	$CH_{1.96}\ O_{0.55}\ N_{0.25}$	5.5	Unlimited growth
	$CH_{1.83}\ O_{0.50}\ N_{0.22}$	5.5	Unlimited growth
	$CH_{1.96}\ O_{0.55}\ N_{0.25}$	5.5	Unlimited growth
Pseudomonas fluorescens	$CH_{1.83}\ O_{0.55}\ N_{0.26}$	5.5	Unlimited growth

Aerobacter aerogenes	$CH_{1.64}\ O_{0.52}\ N_{0.16}$	7.9	Unlimited growth
Penicillium chrysogenum	$CH_{1.70}\ O_{0.58}\ N_{0.15}$	unknown	Glucose limited
	$CH_{1.68}\ O_{0.53}\ N_{0.17}$	unknown	Glucose limited
Aspergillus niger	$CH_{1.72}\ O_{0.55}\ N_{0.17}$	7.5	Unlimited growth
S. thermonitrificans	$CH_{1.85}\ O_{0.61}\ N_{0.22}$	1.5	
S. cattleya	$CH_{1.66}\ O_{0.58}\ N_{0.17}$	theoretical	
S. coelicolor	$CH_{1.86}\ O_{0.61}\ N_{0.15}$	theoretical	Phosphate limited
Average	$CH_{1.81}\ O_{0.52}\ N_{0.21}$	6.0	

Reported elemental compositions of various microorganisms cultured on various carbon and nitrogen sources. Compositions for *P. chrysogenum* were taken from Christensen *et al*. (1995); other data was taken from Roels (1983), Burke (1991), and Davidson (1992). The experimental procedure for calculating the ash content was not always stated. nd, not determined.

Table 5.37 Part 1 (Part 1 & 2 companion Tables) Elemental analysis for *S. fradiae* C373-10, *S. coelicolor* 1147, & *E. coli* ML308 cultured on a number of different carbon sources.

Fermentation	CH	O (E)	O (E1)	O (E2)	O (E3)	N	S	P
S. fradiae								
Glucose (Ferm 1)	1.96	0.62	0.61	0.52	0.45	0.17	0.022	0.021
Glucose (Ferm 2)	2.04	0.63	0.62	0.53	0.45	0.19	0.023	0.022
Fructose	2.11	0.40	0.40	0.31	0.25	0.27	0.021	0.020
Glycerol (Ferm 1)	1.96	0.31	0.31	0.23	0.17	0.23	0.019	0.018
Glycerol (Ferm 2)	2.07	0.40	0.39	0.31	0.24	0.22	0.020	0.019
Oxo-glutarate	2.14	0.63	0.63	0.53	0.45	0.27	0.024	0.023
G/G (Ferm 1) Day 5	2.06	0.39	0.39	0.31	0.24	0.22	0.020	0.019
G/G (Ferm 2) Day 5	1.99	0.37	0.37	0.29	0.22	0.22	0.020	0.019
G/G (Ferm 3) Day 5	2.07	0.39	0.38	0.30	0.24	0.22	0.020	0.019
G/G (Ferm 4) Day 5	2.08	0.41	0.41	0.32	0.26	0.22	0.020	0.019
G/O (Ferm 1) Day 7	2.08	0.47	0.46	0.38	0.31	0.22	0.021	0.020
G/O (Ferm 2) Day 7	2.05	0.46	0.45	0.37	0.30	0.22	0.021	0.020
MO (Fem 1) Day 3	1.94	0.43	0.42	0.34	0.27	0.27	0.021	0.020
MO (Fem 1) Day 5	1.95	0.53	0.52	0.43	0.36	0.25	0.022	0.021
MO (Fem 1) Day 9	1.90	0.49	0.49	0.40	0.33	0.23	0.021	0.020
MO (Fem 2) Day 3	1.96	0.61	0.60	0.51	0.43	0.29	0.024	0.022
MO (Fem 2) Day 5	1.96	0.56	0.55	0.46	0.39	0.24	0.023	0.021
MO (Fem 2) Day 9	2.07	0.46	0.45	0.37	0.30	0.22	0.021	0.020
***E. coli* ML308**								
Glucose (Ferm 1)	1.94	0.38	nd	0.32	0.30	0.26	0.007	0.015
***S. coelicolor* 1147**								
Glucose (Ferm 1)	1.90	0.58	0.55	0.53	0.41	0.15	0.009	0.023

Glucose (Ferm 2)	1.99	0.56	0.54	0.51	0.39	0.16	0.009	0.023

The elemental composition of *S. fradiae* C373-10, *S. coelicolor* 1147, and *E. coli* ML308 were cultured on a number of different medium compositions [corresponding to Tables 5.9 A - J]. *S. fradiae* C373-10 and was cultured on glucose, fructose, glycerol, oxo-glutarate minimal media, glucose glutamate (G/G), glucose oxo-glutarate (G/O) defined media (Chapter 3, section 3.6.4), and a methyl oleate medium (MO) (Chapter 3, section 3.7.2), *S. coelicolor* 1147 and *E. coli* ML308 were both cultured on a glucose minimal media (Chapter 3, section 3.6.1 & 3.6.3 respectively). All sampling points were taken at sampling point II (as Chapter 4, Fig 4.1 - 4.20) and for the MO medium SP I, II and III. The empirical elemental composition was calculated by converting the percentage elemental composition (Table 5.34 Part 1 & 2) to the empirical formula of the biomass. This was computed by expressing each element as the number of gram atoms by dividing the percentage value of the elements by their specific atomic masses (Table 5.37 Part 1 & 2). The values were then normalised with respect to a carbon unit of 1.0 (as Chapter 5, section 5.9). The degree of reduction (γ) was calculated as Appendix D and the molecular mass calculated as Chapter 5, section 5.9. The oxygen (O) content was calculated by subtraction from 100 % of the C, H, N, S, and P this included the subtraction of the theoretical ash content where appropriate, the theoretical ash content was calculated in the following way, E, no ash content taken into account, E1 theoretical ash content taken into account, E2 non-hydrolysed ash content taken into account, and E3 hydrolysed ash content taken into account (corresponds with Table 5.38). C, carbon; N, nitrogen; O, oxygen; H, hydrogen; S, sulphur; P, phosphorus; nd, not determined

Table 5.37 Part 2 Elemental analysis for *S. fradiae* C373-10, *S. coelicolor* 1147, & *E. coli* ML308 cultured on a number of different carbon sources.

Fermentation	O (E)	O (E)	O (E1)	O (E1)	O (E2)	O (E2)	O (E3)	O (E3)
	molecular mass	Degree of reductance	molecular mass	Degree of reductance	molecular mass	Degree of reductance	molecular mass	Degree of reductance
S. fradiae								
Glucose (Ferm 1)	27.51	4.23	27.42	4.24	25.99	4.41	24.81	4.56
Glucose (Ferm 2)	28.12	4.22	28.03	4.23	26.57	4.41	25.36	4.56
Fructose	25.60	4.49	25.52	4.50	24.19	4.67	23.09	4.81
Glycerol (Ferm 1)	23.36	4.64	23.29	4.65	22.07	4.80	21.07	4.92
Glycerol (Ferm 2)	24.81	4.60	24.73	4.61	23.44	4.77	22.38	4.91
Oxo-glutarate	29.45	4.07	29.36	4.08	27.83	4.27	26.57	4.43
G/G (Ferm 1) Day 5	24.69	4.61	24.61	4.62	23.33	4.78	22.27	4.91
G/G (Ferm 2) Day 5	24.22	4.59	24.15	4.60	22.89	4.75	21.85	4.88
G/G (Ferm 3) Day 5	24.58	4.63	24.50	4.64	23.23	4.79	22.17	4.93
G/G (Ferm 4) Day 5	25.04	4.59	24.96	4.60	23.66	4.76	22.58	4.90
G/O (Ferm 1) Day 7	25.84	4.50	25.76	4.51	24.42	4.68	23.31	4.82
G/O (Ferm 2) Day 7	25.78	4.46	25.70	4.47	24.36	4.64	23.25	4.78
MO (Fem 1) Day 3	25.92	4.25	25.84	4.26	24.50	4.43	23.38	4.57
MO (Fem 1) Day 5	27.25	4.14	27.17	4.15	25.75	4.33	24.58	4.48
MO (Fem 1) Day 9	26.27	4.23	26.19	4.24	24.83	4.41	23.70	4.55
MO (Fem 2) Day 3	29.18	3.88	29.09	3.89	27.58	4.08	26.32	4.24
MO (Fem 2) Day 5	27.67	4.11	27.58	4.12	26.15	4.29	24.96	4.45
MO (Fem 2) Day 9	25.71	4.50	25.63	4.51	24.29	4.68	23.19	4.81
***E. coli* ML308**								
Glucose	24.39	4.39	nd	nd	23.38	4.51	23.09	4.55

***S. coelicolor* 1147**								
Glucose (Ferm 1)	26.34	4.28	25.86	4.34	25.54	4.38	23.62	4.62
Glucose (Ferm 2)	26.21	4.39	25.89	4.43	25.41	4.49	23.49	4.73

The elemental composition of *S. fradiae* C373-10, *S. coelicolor* 1147, and *E. coli* ML308 were cultured on a number of different medium compositions [corresponding to Tables 5.9 A - J]. *S. fradiae* C373-10 and was cultured on glucose, fructose, glycerol, oxo-glutarate minimal media, glucose glutamate (G/G), glucose oxo-glutarate (G/O) defined media (Chapter 3, section 3.6.4), and a methyl oleate medium (MO) (Chapter 3, section 3.7.2), *S. coelicolor* 1147 and *E. coli* ML308 were both cultured on a glucose minimal media (Chapter 3, section 3.6.1 & 3.6.3 respectively). All sampling points were taken at sampling point II (as Chapter 4, Fig 4.1 - 4.20) and for the MO medium SP I, II and III. The empirical elemental composition was calculated by converting the percentage elemental composition (Table 5.34 Part 1 & 2) to the empirical formula of the biomass. This was computed by expressing each element as the number of gram atoms by dividing the percentage value of the elements by their specific atomic masses (Table 5.37 Part 1 & 2). The values were then normalised with respect to a carbon unit of 1.0 (as Chapter 5, section 5.9). The degree of reduction (γ) was calculated as Appendix D and the molecular mass calculated as Chapter 5, section 5.9. The oxygen (O) content was calculated by subtraction from 100 % of the C, H, N, S, and P this included the subtraction of the theoretical ash content where appropriate, the theoretical ash content was calculated in the following way, E, no ash content taken into account, E1 theoretical ash content taken into account, E2 non-hydrolysed ash content taken into account, and E3 hydrolysed ash content taken into account (corresponds with Table 5.38). C, carbon; N, nitrogen; O, oxygen; H, hydrogen; S, sulphur; P, phosphorus; nd, not determined

Table 5.38 Determination of the ash content of *S. fradiae* C373-10, *S. coelicolor* 1147 and *E. coli* ML308 growing on various substrates.

Fermentation	Experimentally determined non-hydrolysed ash content (%)	Experimentally determined hydrolysed ash content (%)	Theoretical ash content (%)	Total mean STDEV
***S. fradiae* C373-10**				
Glucose	8.9	3.2	0.25	± 4.40
Glucose	9.2	3.7	0.65	± 4.33
Glucose	9.3	3.4	0.91	± 4.31
Standard deviation	**± 0.49**	**± 0.15**	**± 0.23**	
Glucose glutamate	9.4	3.4	nd	± 4.24
Glucose glutamate	9.5	3.3	nd	± 4.38
Glucose glutamate	9.7	3.4	nd	± 4.45
Standard deviation	**± 0.15**	**± 0.06**	**nd**	
Glucose oxo-glutarate	8.8	2.5	nd	± 4.45
Glucose oxo-glutarate	9.5	3.6	nd	± 4.17
Glucose oxo-glutarate	9.6	3.9	nd	± 4.03
Standard deviation	**± 0.44**	**± 0.74**	**nd**	
Glycerol	9.4	2.1	nd	± 5.16
Glycerol	9.5	3.1	nd	± 4.52
Glycerol	9.3	3.5	nd	± 4.10
Standard deviation	**± 0.10**	**± 0.72**	**nd**	
Fructose	9.9	3.4	nd	± 4.60
Fructose	9.6	3.4	nd	± 4.38
Fructose	9.7	3.3	nd	± 4.52
Standard deviation	**± 0.15**	**± 0.06**	**nd**	
Oxo-glutarate	9.8	3.6	nd	± 4.38
Oxo-glutarate	9.6	3.1	nd	± 4.60
Oxo-glutarate	9.8	3.6	nd	± 4.38

Standard deviation	**± 0.11**	**± 0.29**	**nd**	
Methyl oleate medium	9.7	3.5	nd	± 4.38
Methyl oleate medium	9.8	3.7	nd	± 4.31
Methyl oleate medium	9.6	2.4	nd	± 5.09
Standard deviation	**± 0.10**	**± 0.70**	**nd**	
Mean ash content	**± 9.80[a]**	**± 5.50[b]**	**0.33[c]**	
***E. coli* ML308**				
Glucose	5.62	4.23	nd	± 5.05
Glucose	5.23	4.52	nd	± 4.46
Glucose	5.11	3.62	nd	± 4.32
Standard deviation	**± 0.27**	**± 0.46**	**nd**	
Mean ash content	**± 5.32[a]**	**± 4.12[b]**		
***S. coelicolor* 1147**				
Glucose	10.6	2.8	1.12	± 0.28
Glucose	9.8	2.9	1.46	± 0.35
Glucose	9.7	3.1	1.56	± 1.41
Standard deviation	**± 0.49**	**± 0.15**	**± 0.23**	
Mean percentage STDEV	**± 10.03[a]**	**± 2.93[b]**	**1.38[c]**	

The elemental composition of *S. fradiae* C373-10, *S. coelicolor* 1147, and *E. coli* ML308 were cultured on a number of different medium compositions [corresponding to Tables 5.9 A - J]. *S. fradiae* C373-10 was cultured on glucose, fructose, glycerol, oxo-glutarate minimal media, glucose glutamate, glucose oxo-glutarate defined media (Chapter 3, section 3.6.4), and a methyl oleate medium (Chapter 3, section 3.7.2), *S. coelicolor* 1147 and *E. coli* ML308 were both cultured on a glucose minimal media (Chapter 3, section 3.6.1 & 3.6.3 respectively). Biomass was harvested at 72 hrs after inoculation. Each pellet was divided into approximately six (two sets of triplicates) samples of equal wet weight. The ash content was measured as Chapter 3, section 3.15.4 for the hydrolysed and non-hydrolysed method. The theoretical ash content was calculated as follows, phosphorous typically comprises 50 % of the total ash (Burke, 1991), then an approximation for the residue can be made (proportion for phosphorus minus that of sulphur). The theoretical measurement was only undertaken for *S. fradiae* and *S. coelicolor* growing on a glucose minimal media. All figures were expressed as a percentage of the dry weight. Standard deviations were given as plus or minus the unit of measurement. Non-hydrolysed ash content represented by E1 in Tables 5.37 - 5.39. Hydrolysed ash content represented by E2 in Tables 5.37 - 5.39. Theoretical ash content represented by E3 in Tables 5.37 - 5.39. nd, not determined; STDEV, standard deviation.

Table 5.39 A summary of the reported stoichiometric parameters of a number of microorganisms derived from the analysis of biomass composition.

Organism	Yield (g.g. glucose^{-1})	Degree of reductance (γ)	RQ	Reference
Average microorganism	0.68	4.19	1.33	Roels, 1980
Brevibacterium spp.	nd	4.25	nd	Erickson *et al*., 1979
Saccharomyces cerevisiae	0.50	4.19	1.04	Cooney *et al*., 1977 & Wang *et al*., 1977
Candida utilis	0.54	4.12	1.16	Herbert, 1976
Klebsiella aerogenes	0.66	4.20	1.38	Roels, 1980
Escherichia coli	0.69	4.07	1.1	Burke, 1991
S. cattleya	0.78	3.93	0.8	Bushell and Fryday, 1983
S. thermonitrificans	0.70	3.97[c]	1.0	Burke, 1991
Present work				
S. coelicolor[a]	0.35	6.63	nd	Davidson, 1992
S. fradiae[b]	0.19	4.45[c]	nd	Present work
S. fradiae[b]	0.17	4.42[c]	nd	Present work
S. coelicolor[b]	0.41	4.20	nd	Present work

Reported elemental compositions of various microorganisms cultured on various carbon and nitrogen sources. Compositions for *P. chrysogenum* were taken from Christensen *et al*. (1995); other data was taken from Roels (1983), Burke (1991), and Davidson (1992). Experimental means of calculating ash content was not always stated. Biomass was obtained from bioreactor vessels for *S. coelicolor* 1147 and *S. fradiae* C373-10 grown on a glucose minimal media (Chapter 3, section 3.6.1 & 3.6.4 respectively) see Chapter 4 fermentation profiles. RQ, denotes the respiratory quotient. Underlined values are those determined by calculation. [a] Results taken from Davidson (1992), [b]results from this work, [c] results calculated from the elemental composition (Table 5.37 part 1 & 2). nd, not determined.

Table 5.40 Molecular elemental composition for *S. fradiae* C373-10, *S. coelicolor* 1147 and *E. coli* ML308 calculated from the monomeric compositional tables (Chapter 6,Tables 6.1 - 6.29).

Fermentation	CH	O	N	S	P	molecular mass	Degree of reductance
***S. fradiae* C373-10**							
Glucose (Ferm 1) Day 7	2.07	0.64	0.31	0.003	0.022	29.37	3.86
Glucose (Ferm 2) Day 7	2.07	0.66	0.29	0.003	0.010	29.19	3.86
Fructose Day 8	1.85	0.57	0.21	0.002	0.032	26.84	4.10
Glycerol (Ferm 2) Day 9	1.88	0.60	0.19	0.002	0.014	26.59	4.12
Glycerol (Ferm 1) Day 9	2.08	0.61	0.29	0.003	0.020	28.55	3.99
OGA Day 10	1.86	0.65	0.24	0.002	0.066	29.58	3.85
G/Gl (Ferm 1) Day 5	2.03	0.50	0.18	0.004	0.013	25.03	4.50
G/G (Ferm 2) Day 5	1.88	0.47	0.14	0.002	0.013	23.82	4.52
G/G (Ferm 3) Day 5	1.90	0.47	0.13	0.001	0.021	23.87	4.58
G/G (Ferm 4) Day 5	1.99	0.49	0.18	0.002	0.010	24.66	4.48
G/O Day 7	2.01	0.66	0.33	0.003	0.042	30.57	3.70
G/O Day 7	2.13	0.62	0.34	0.004	0.013	29.32	3.87
MO (Ferm 1) Day 3	1.99	0.52	0.28	0.003	0.014	26.83	4.11
MO (Ferm 1) Day 5	2.03	0.57	0.30	0.003	0.010	27.69	4.01
MO (Ferm 1) Day 9	nd	nd	nd	nd	nd	nd	nd
MO (Ferm 2) Day 3	1.97	0.55	0.28	0.003	0.012	27.27	4.01
MO (Ferm 2) Day 5	2.04	0.58	0.29	0.003	0.014	27.98	4.01
MO (Ferm 2) Day 9	1.99	0.58	0.28	0.003	0.010	27.67	3.98
Mean	**1.99**	**0.57**	**0.25**	**0.003**	**0.020**	**27.34**	**4.09**
***E. coli* ML308**							
Glucose (Ferm 1)[a]	2.03	0.62	0.22	0.009	0.023	28.05	4.12
***S. coelicolor* 1147**							
Glucose (Ferm 1)	1.98	0.62	0.24	0.004	0.040	28.63	4.01
Glucose (Ferm 2)	1.99	0.63	0.27	0.005	0.035	28.99	3.94

The molecular elemental composition of *S. fradiae* C373-10, *S. coelicolor* 1147, and *E. coli* ML308 were cultured on a number of different medium compositions [corresponding to Tables 5.9 A - J]. *S. fradiae* C373-10 was cultured on glucose, fructose, glycerol, oxo-glutarate minimal media, glucose glutamate (G/G), glucose oxo-glutarate (G/O) defined media (Chapter 3, section 3.6.4), and a methyl oleate medium (MO) (Chapter 3, section 3.7.2), *S. coelicolor* 1147 and *E. coli* ML308 were both cultured on a glucose minimal media (Chapter 3, section 3.6.1 & 3.6.3 respectively). All sampling points were taken at sampling point II (as Chapter 4, Fig 4.1 - 4.20) and for the MO medium SP I, II and III. The molecular elemental analysis was calculated from the macromolecular composition Tables 6.1 to 6.29, Chapter 6, and converted to the atomic composition and then converted to the number of grams of each atom and divided by the appropriate molecular formula weight. The values were then normalised with respect to a carbon unit of 1.0 carbon (Chapter 5, section 5.9). The degree of reduction (γ) was calculated as Appendix D and the molecular mass calculated as Chapter 5, section 5.9. C, carbon; N, nitrogen; O, oxygen; H, hydrogen; S, sulphur; P, phosphorus; nd, not determined.

Table 5.41 Reconciled elemental analysis and the percentage difference between the molecular and the elemental composition of *S. fradiae* C373-10, *S. coelicolor* 1147,and *E. coli* ML308.

	Reconciled empirical formula							Percentage difference between elemental analysis and macromolecular elemental analysis							
Fermentation	**CH**	**O**	**N**	**S**	**P**	**molecular mass**	**Degree of reduction**	**CH (%)**	**O (E) [%]**	**O (E1)[%]**	**O (E2) [%]**	**O (E3) [%]**	**N (%)**	**S (%)**	**P (%)**
***S. fradiae* C373-10**															
Glucose 1 Day 7	1.96	0.58	0.21	0.013	0.022	27.56	4.16	± 0.05	± 5.63	± 4.81	± 11.46	± 29.83	± 26.87	± 44.13	± 4.03
Glucose 2 Day 7	1.99	0.59	0.23	0.013	0.010	27.44	4.13	± 2.07	± 5.75	± 4.92	± 1.41	± 29.90	± 20.79	± 43.65	± 55.05
Fructose Day 8	1.98	0.49	0.21	0.012	0.032	26.54	4.37	± 6.33	± 22.50	± 24.03	± 56.71	± 100.46	± 23.57	± 44.54	± 62.08
Glycerol / 2 Day 9	1.90	0.44	0.20	0.011	0.014	24.82	4.40	± 2.91	± 43.48	± 45.60	± 93.58	± 166.28	± 12.65	± 41.45	± 23.10
Glycerol /1 Day 9	2.06	0.51	0.21	0.012	0.020	26.33	4.41	± 0.76	± 27.54	± 29.10	± 62.42	± 106.59	± 6.13	± 39.46	± 2.65
OGA Day 10	1.95	0.59	0.24	0.013	0.066	30.13	4.05	± 8.74	± 6.56	± 5.71	± 11.26	± 30.74	± 10.74	± 47.74	± 192.27
G/G Ferm 1 Day 5	2.03	0.44	0.19	0.012	0.013	24.55	4.60	± 1.38	± 10.91	± 12.27	± 41.36	± 80.01	± 15.94	± 41.22	± 30.66
G/G Ferm 2 Day 5	1.94	0.43	0.16	0.011	0.013	23.87	4.61	± 2.90	± 15.72	± 17.20	± 49.25	± 92.96	± 29.65	± 45.89	± 31.03
G/G Ferm 3 Day 5	1.98	0.43	0.15	0.011	0.021	24.29	4.66	± 4.15	± 11.86	± 13.26	± 43.14	± 83.19	± 31.96	± 46.99	± 10.57
G/G Ferm 4 Day 5	2.04	0.45	0.18	0.011	0.010	24.57	4.59	± 2.20	± 9.76	± 11.06	± 38.74	± 74.83	± 19.18	± 45.24	± 47.97
G/O Day 7	2.04	0.55	0.25	0.013	0.042	28.54	4.19	± 2.04	± 17.72	± 18.99	± 45.41	± 78.18	± 15.62	± 40.09	± 112.38
G/O Day 7	2.06	0.51	0.27	0.013	0.013	26.89	4.24	± 0.37	± 11.58	± 12.81	± 38.41	± 70.46	± 18.73	± 39.29	± 32.02
MO Day 3	1.94	0.46	0.25	0.012	0.014	25.76	4.27	± 0.004	± 7.24	± 8.51	± 35.31	± 70.13	± 8.87	± 43.25	± 29.18
MO Day 5	1.98	0.53	0.26	0.013	0.010	26.82	4.15	± 1.39	± 0.24	± 1.25	± 21.91	± 46.71	± 2.38	± 42.52	± 52.92
MO Day 9	1.42	nd	0.26	nd	nd	nd	nd	nd	nd	nd	nd	nd	nd	nd	nd
MO Day 3	1.96	0.55	0.28	0.013	0.012	27.59	4.01	± 0.37	± 10.00	± 9.17	± 7.67	± 27.21	± 1.75	± 44.59	± 46.59
MO Day 5	1.98	0.53	0.27	0.013	0.014	27.28	4.11	± 1.22	± 4.32	± 3.40	± 15.29	± 37.29	± 9.78	± 43.58	± 31.70
MO Day 9	2.00	0.48	0.26	0.012	0.010	26.08	4.27	± 3.20	± 5.23	± 6.39	± 30.51	± 60.70	± 18.10	± 41.68	± 50.13

Mean	**1.99**	**0.50**	**0.24**	**0.012**	**0.020**	**26.41**	**4.31**	**± 2.36**	**± 7.71**	**± 7.06**	**± 35.52**	**± 69.73**	**± 16.04**	**± 43.25**	**± 47.90**
***E. coli* ML308**															
Glucose[a]	1.91	0.42	0.24	0.007	0.018	25.26	4.33	± 1.58	± 11.84	nd	± 33.96	± 42.15	± 7.62	± 8.82	± 19.37
***S. coelicolor* 1147**															
Glucose	1.99	0.59	0.20	0.007	0.028	28.06	4.20	± 4.7	± 2.61	± 8.21	± 12.30	± 45.16	± 29.83	± 23.87	± 19.99
Glucose	1.90	0.56	0.19	0.007	0.030	27.44	4.20	4.49	-0.16	-3.87	-9.98	-43.82	-18.78	26.64	-28.97

The reconciled elemental composition of *S. fradiae* C373-10, *S. coelicolor* 1147, and *E. coli* ML308 were cultured on a number of different medium compositions [corresponding to Tables 5.9 A - J]. *S. fradiae* C373-10 was cultured on glucose, fructose, glycerol, oxo-glutarate minimal media, glucose glutamate (G/G), glucose oxo-glutarate (G/O) defined media (Chapter 3, section 3.6.4), and a methyl oleate medium (MO) (Chapter 3, section 3.7.2), *S. coelicolor* 1147 and *E. coli* ML308 were both cultured on a glucose minimal media (Chapter 3, section 3.6.1 & 3.6.3 respectively). All sampling points were taken at sampling point II (as Chapter 4, Fig 4.1 - 4.20) and for the MO medium SP I, II and III. Reconciled (R) empirical formula percentage values were calculated from the mean values adapted from Tables 5.35 Part 1 & 2, & 5.38. The percentage difference between the empirical elemental formula and the molecular elemental empirical formula was also presented (differences between Tables 5.35 Part 1 & 2, 5.36 & 5.38). This gave an estimation of the percentage experimental error between the elemental and molecular elemental analytical techniques used in this work. The oxygen (O) content was calculated by subtraction of C, H, N, S and P from 100 % this included the subtraction of the theoretical ash content where appropriate, the theoretical ash content was calculated in the following way, E, no ash content taken into account, E1 theoretical ash content taken into account, E2 non-hydrolysed ash content taken into account, and E3 hydrolysed ash content taken into account (corresponds with Table 5.37 Part 1 & 2). C, carbon; N, nitrogen; O, oxygen; H, hydrogen; S, sulphur; P, phosphorus.

Table 5.42 The carbon nitrogen ratio on a elemental basis calculated for the medium composition, elemental analysis, molecular elemental analysis, and the reconciled data for *S. fradiae* C373-10, *S. coelicolor* 1147, and *E. coli* ML308 (adapted from Tables 5.37 Part 1 & 2, 5.36, and 5.38).

Fermentation	Medium composition C/N	Elemental analysis (E) C/N	Molecular elemental (M) C/N	Reconciled (R) elemental C/N	STDEV between M:E:R	Percentage difference (M-E)
***S. fradiae* C373-10**						
Glucose 1 Day 7	9.43	6.02	3.26	4.75	± 1.38	± 45.85
Glucose 2 Day 7	9.43	5.29	3.39	4.38	± 0.95	± 35.92
Fructose Day 8	9.43	3.70	4.84	4.85	± 0.66	± 30.81
Glycerol / 2 Day 9	18.86	4.26	5.27	4.88	± 0.51	± 23.71
Glycerol /1 Day 9	18.86	4.43	3.45	4.72	± 0.66	± 22.12
OGA Day 10	14.52	3.74	4.21	4.19	± 0.27	± 12.57
G/G Ferm 1 Day 5	12.95	4.50	5.53	5.36	± 0.55	± 22.89
G/G Ferm 2 Day 5	12.95	4.51	7.16	6.41	± 1.37	± 58.76
G/G Ferm 3 Day 5	12.95	4.49	7.72	6.61	± 1.64	± 71.94
G/G Ferm 4 Day 5	12.95	4.48	5.68	5.54	± 0.66	± 26.79
G/O Day 7	12.95	4.63	3.04	4.00	± 0.80	± 34.34
G/O Day 7	12.95	4.45	2.93	3.75	± 0.76	± 34.16
MO Day 3	13.02	3.65	3.54	4.00	± 0.24	± 3.01
MO Day 5	13.02	3.97	3.38	3.88	± 0.32	± 14.86
MO Day 9	13.02	4.34	nd	3.79	± 0.39	nd
MO Day 3	13.02	3.50	3.55	3.56	± 0.03	± 1.43
MO Day 5	13.02	4.11	3.45	3.75	± 0.33	± 16.06
MO Day 9	13.02	4.56	3.52	3.86	± 0.53	± 22.81
Mean	**13.13**	**4.37**	**4.35**	**4.57**	± **0.71**	**± 28.12**
***E. coli* ML308**						
Glucose[a]	2.08	3.80	4.51	4.11	± 0.35	± 18.68

***S. coelicolor* 1147**						
Glucose	6.48	6.48	4.11	4.99	± 1.20	± 36.57
Glucose	6.20	6.20	3.75	5.22	± 1.23	± 39.52

The elemental, molecular elemental and reconciled elemental composition of *S. fradiae* C373-10, *S. coelicolor* 1147, and *E. coli* ML308 were cultured on a number of different medium compositions [corresponding to Tables 5.9 A - J]. *S. fradiae* C373-10 was cultured on glucose, fructose, glycerol, oxo-glutarate minimal media, glucose glutamate (G/G), glucose oxo-glutarate (G/O) defined media (Chapter 3, section 3.6.4), and a methyl oleate medium (MO) (Chapter 3, section 3.7.2), *S. coelicolor* 1147 and *E. coli* ML308 were both cultured on a glucose minimal media (Chapter 3, section 3.6.1 & 3.6.3 respectively). All sampling points were taken at sampling point II (as Chapter 4, Fig 4.1 - 4.20) and for the MO medium SP I, II and III. Carbon nitrogen ratios (C/N) were calculated from Tables 5.35 Part 1 & 2, & 5.38 for *S. fradiae* C373-10, *S. coelicolor* 1147 and *E. coli* ML308. The theoretical medium C/N ratio was calculated from the theoretical elemental medium components (Chapter 3, section 3.6). E, denotes elemental analysis (analysis undertaken as Chapter 3, section 3.15) for C, H, & N; M denotes molecular elemental analysis calculated from the macromolecular composition (Chapter 6, Tables 6.1 to 6.29 were converted to the compositional atomic requirement and then number of grams of each atom was calculated and thus converted to percentage format for C, H, & N). The percentage elemental composition was then converted to the empirical formula by expressing each element as the number of gram atoms (calculated by dividing the percentage value of the elements by their specific atomic masses). The values were then normalised with respect to a carbon unit of 1.0 carbon (Chapter 5, section 5.9). R denotes the reconciled data (an mean between E and M; Table 5.41). Standard deviations (STDEVs) was calculated between, elemental analysis, molecular elemental analysis, and the reconciled data for *S. fradiae*, *S. coelicolor*, and *E. coli*.

Table 5.43 Standard deviation of measurements in the mean percentage (%) of values of all the analysis undertaken in this project.

Standard Deviation of measurements in % of values			
Measurement	**Between samples**	**Triplicates between extraction procedures of the same culture**	**Between cultures**
Elemental			
C	0 - 1	nd	0.01 - 0.55
H	0 - 1	nd	0.02 - 0.44
N	0 - 1	nd	0.06 - 0.20
O	0 - 1	nd	nd
P	0 - 1	nd	0.01 - 0.23
S	0 - 1	nd	0.01 - 0.23
Elemental monomeric			
C	nd	nd	< 1
H	nd	nd	< 1
N	nd	nd	< 1
O	nd	nd	< 1
TOCA			
C	4 - 12	nd	0.1 - 0.9
TONA			
N	6 - 19	nd	0.3 - 1.0
Protein assays			
Bradford	1 - 6	0.5 - 5	0.4 - 4.5
Reverse Biuret	1 - 8	2 - 9	1.29 - 10.13
BCA	5 - 13	2 - 4	1.96 - 2.89
Lowry	6	3 - 10	2.08 - 9.52
Ninhydrin	9 - 12	2 - 17	1.52 - 14.13

HPLC amino acids[a]	10 - 35	1 - 20	4 - 58
Carbohydrate assays			
Anthrone	2 -18	1 - 13	1 - 13
Phenol-sulphuric	5 - 25	2 - 7	2 - 7
Lipid			
Vanillin	42.00	1 - 6	1 - 6
Gravimetric	26.23	0 - 1	0 - 1
DNA			
Total nucleic acids	3 - 27	1 - 2	0.7 - 1
Diphenylamine	2 - 9	0.1 - 0.9	2 - 6
Hoechst	5 - 14	0 - 1	0.05 - 1
RNA			
Orcinol	3 - 21	1.8 - 9.0	0.3 - 4.6
Simple RNA extraction	4 - 13	0 - 1	1.33

The tabulated total standard deviations between samples, between triplicates between extraction procedures of the same culture and between different cultures. Microbiological techniques used throughout out this work were as follows: elemental analysis, sulphur (Chapter 3, section 3.15.1), phosphorus (Chapter 3, section 3.15.2), simultaneous determination of C, H, N (Chapter 3, section 3.15.3), total organic carbon analysis [TOCA] (Chapter 3, section 3.15.5), total organic nitrogen analysis [TONA] (Chapter 3, section 3.15.6), anthrone assay (Chapter 3, section 3.18.1), phenol-sulphuric assay (Chapter 3, section 3.18.2), total nucleic acids (Chapter 3, section 3.19.1), diphenylamine assay (Chapter 3, section 3.19.2), Hoechst assay (Chapter 3, section 3.19.3), orcinol assay (Chapter 3, section 3.19.4), simple UV method (Chapter 3, section 3.19.5), Bradford assay (Chapter 3, section 3.20.1), Lowry assay (Chapter 3, section 3.20.2), bicinchoninic acid assay [BCA] (Chapter 3, section 3.20.4), reverse biuret method (Chapter 3, section 3.20.5), ninhydrin assay (Chapter 3, section 3.20.6), vanillin assay (Chapter 3, section 3.23.1), lipid gravimetric assay (Chapter 3, section 3.23.3), total amino acids (Chapter 3, section 3.3.25.2). The monomeric elemental percentage composition was calculated as Chapter 5 (section 5.9.2). The units of measurement were converted to a percentage format. [a]mean incorporating all measured amino acids. nd, not undertaken.

Table 7.1 Bioreaction network parameters for stoichiometric models 1 & 2 with an altering NADPH/NADH balance (Appendices L & M2)

Carbon source	No. Metabolites	No. equations	Degree of freedom	Condition number
Model 1				
NADH/NADPH				
Glucose	64	56	8	97.56
Fructose	65	57	8	97.84
Glycerol	64	56	8	97.91
Average				**97.77**
NADPH/NADPH				
Glucose	64	56	8	57.76
Fructose	65	57	8	58.06
Glycerol	64	56	8	58.06
Average				**57.96**
Model 2				
NADH/NADPH				
Glucose	nd	Nd	nd	Nd
Fructose	nd	Nd	nd	Nd
Glycerol	72	62	11	408.14
NADPH/NADPH				
Glucose	nd	Nd	nd	nd
Fructose	nd	Nd	nd	nd
Glycerol	72	62	10	168.81

The analysed BRNE parameters for models 1 and 2 (Appendices L & M). No. metabolites, indicates the number of metabolites in the bioreaction network; No. equations, indicates the number of equations in the network; degree of freedom the minimum number of measured metabolites allowed. The condition number was calculated as Appendix N with the Fluxmap program. nd, no data or analysis was not undertaken.

Table 7.2 Calculated flux sensitivities with respect to changes in measured fluxes (as calculated by Daae and Isson, 1999): proposed primary metabolic reaction network for *Streptomyces fradiae* C373-10 (Appendix L, model 1).

Reaction	Glucose	PYR	MAL	OGA	Acetate	Lipid	Protein	Carbohydrate	RNA/DNA
1	0.01	0	0.03	0.02	0.03	0.01	0.01	0.03	0.01
2	0.3	0.46	0.84	0.24	0.56	2.23	0.36	0.45	2.23
3	0.02	0.3	0.15	0.2	0.33	0.64	0.25	0.29	0.64
4	0.1	0.27	0.11	0.21	0.27	0.07	0.21	0.52	0.07
5	0.19	0.28	0.03	0.28	0.3	0.06	0.62	0.45	0.06
6	0.03	0.24	0.03	0.03	0.66	0.39	0.29	0.17	0.39
7	0.09	0.26	0.32	0.15	0.87	0.23	0.18	0.05	0.23
8	0.05	0.37	0.59	0.6	0.83	0.35	0.3	0.08	0.35
9	0.07	0.24	0.58	0.33	0.5	0.15	0.08	0.15	0.15
10	0.35	0.16	0.26	0.18	0.26	0.18	0.13	0.09	0.18
11	0.38	0.12	0.18	0.11	0.21	0.18	0.1	0.13	0.18
12	0.26	0.45	0.9	0.19	0.51	2.26	0.35	0.4	2.26
13	0.24	0.44	0.94	0.17	0.49	2.27	0.34	0.37	2.27
14	0.32	0.19	0.45	0.09	0.28	1.15	0.1	0.69	1.15
15	0.31	0.14	0.71	0.03	0.22	1.67	0.12	0.75	1.67
16	0.31	0.08	0.04	0.01	0.02	0.17	0.11	0.18	0.17
17	0.18	0.08	0.08	0.04	0	0.11	0.1	0.1	0.11
18	0.07	0.06	0.02	0.01	0.01	0.04	0.03	0.03	0.04
19	0.04	0.03	0.02	0.01	0	0.02	0.02	0.02	0.02
20	1.66	0.05	0.17	0.09	0.23	0.22	0.22	0.19	0.22
21	1.16	0.01	0.14	0.07	0.15	0.11	0.12	0.09	0.11
22	0.13	0.01	0.08	0.03	0.07	0.04	0.05	0.03	0.04
23	0.11	0.06	0.02	0.02	0.05	0.04	0.04	0.03	0.04
24	0.22	0.12	0.07	0.41	0.36	0.68	0.42	0.24	0.68
25	0.08	0.1	0.04	0.06	0.12	0.1	0.01	0.13	0.1
26	0.02	0.03	0.01	0.02	0.04	0.03	0	0.04	0.03
27	0.02	0.03	0.01	0.02	0.04	0.03	0	0.04	0.03
28	0.05	0.06	0.02	0.02	0.04	0.06	0.02	0.06	0.06
29	0.06	0.01	0.21	0.05	0.05	0.07	0.1	0.03	0.07
30	0.03	0.03	0.3	0.02	0.07	0.08	0.05	0.04	0.08
31	0	0.02	0.14	0.04	0.11	0.07	0.01	0.06	0.07
32	0.18	0.08	1.39	0.3	0.21	0.43	0.72	0.38	0.43
33	0.63	0.03	0.19	0.02	0.1	0.32	0.32	0.26	0.32
34	0	0	0.04	0.02	0.04	0.04	0.02	0.02	0.04
35	0.13	0.03	0.28	0.01	0.03	0.09	0.15	0.01	0.09
36	0.31	0.07	0.78	0.13	0.01	1.66	0.66	0.32	1.66
37	0.08	0.01	0.06	0.03	0	0.05	0.09	0.02	0.05
38	0.03	0.03	0.18	0.01	0.04	0.08	0.06	0.03	0.08
39	0.02	0.02	0.04	0.01	0.01	0.96	0.03	0.02	0.04
40	0.03	0.04	0.07	0.02	0.04	0.06	0.04	0.03	0.94
41	0.01	0.03	0.05	0.01	0.04	0.05	0.01	0.03	0.05

42	0.27	0.02	0.47	0.12	0.01	0.32	2.22	0.12	0.32
43	0.03	0	0.05	0.02	0.01	0.03	0.05	0.01	0.03
44	0.16	0.01	0.07	0.01	0.02	0.06	0.07	0.03	0.06
45	0.11	0.12	0.07	0.02	0.04	0.07	0	0.1	0.07
46	0.07	0.09	0.21	0.02	0.05	0.08	0.05	0.03	0.08
47	0.02	0.03	0.09	0.04	0.06	0.03	0.02	0.02	0.03
48	0.01	0.01	0.01	0.01	0.01	0	0	0	0
49	0.04	0.94	0.01	0.03	0.03	0.02	0	0.01	0.02
50	0.02	0.01	0	0	0.01	0.01	0	0.01	0.01
51	0.01	0.05	0.06	0.01	0	0.04	0.02	0.02	0.04
52	0.01	0	0.01	0	0	0	0	0.01	0
53	0.07	0.03	0.02	0.05	0.94	0.01	0.01	0.02	0.01
54	0.01	0.01	0.03	0.03	0.04	0.01	0.01	0.02	0.01
55	0.04	0.03	0.04	0.96	0.05	0.01	0.02	0.02	0.01
56	0.04	0.02	0.04	0.03	0.03	0	0.02	0.02	0
Total	**9.19**	**6.41**	**11.75**	**5.66**	**9.5**	**18.14**	**9.33**	**7.49**	**18.1**
Total (%)	**5.98**	**4.17**	**7.65**	**3.69**	**6.19**	**11.81**	**6.08**	**4.88**	**11.79**

Sensitivity analysis undertaken for *S. fradiae* C373-10 cultured on glucose for BRNE model 1 (Appendix L). Calculations were carried out using the program Fluxmap (see Appendix N for theory) and further presented as Daae and Isson (1999). All values were presented as positives, although positive and negative values were both obtained. PYR, pyruvate; MAL, malate; OGA, oxo-glutarate.

Table 7.3 Calculated flux sensitivities with respect to changes in measured fluxes: proposed primary metabolic reaction network for *Streptomyces lividans* (taken from Daae & Isson, 1999).

Reactions	Specific growth rate	Glucose uptake	Pyruvate secretion	Oxo-glutarate secretion	Alanine uptake	O2 utilisation	CO2 evolution
2	-2.69	0.55	-0.08	-0.24	-0.47	0.62	-0.54
3	0.21	0.42	0.21	0.32	-0.3	0.16	-0.07
4	1.72	0.75	0.58	0.94	-0.51	0.1	0.11
5	1.32	0.74	0.65	1.1	-0.63	-0.05	0.26
6	1.47	0.02	0.99	0.64	-0.89	0.01	0.32
7	0.78	-0.12	-0.08	0.48	-0.03	0.29	0.07
9	2.63	0.4	0.11	0.29	0.47	-0.62	0.55
10	2.69	0.03	0.21	0.42	0.18	-0.45	0.44
11	0.02	0.33	-0.08	-0.1	0.29	-0.17	0.12
12	0.96	0.16	0.05	0.12	0.12	-0.25	0.23
13	1.05	0.1	0.08	0.17	0.12	-0.26	0.24
14	1.81	-0.17	0.19	0.34	0.06	-0.2	0.23
15	0.84	0.25	-0.14	0.77	0.17	0.02	-0.06
16	-0.18	-0.17	-0.14	0.37	-0.2	0.45	-0.08
18	-0.58	-0.21	-0.12	-0.61	-0.26	0.46	-0.09
19	-1.06	-0.39	-0.02	-0.44	-0.1	0.42	-0.03
51	3.72	-0.46	1.2	1.89	-2.08	4.05	0.47
52	1.76	0.2	0.12	0.6	0.14	1.57	0.07
53	-2.06	-0.2	-0.08	-0.54	-0.13	0.37	0
Accumulated	**37.43**	**7.03**	**6.01**	**12.12**	**10.39**	**12.35**	**5.71**

Tabulated sensitivity analysis undertaken by Daae and Isson (1999) for *S. lividans*. Accumulated values were the addition of all sensitivity data calculated as a positive value. BRNE as Appendix J. Calculation undertaken as Appendix N using Matlab program.

Table 7.4 Calculated flux sensitivities with respect to changes in measured fluxes and carbon source.

Carbon source	Glucose	PYR	MAL	OGA	Acetate	Lipid	Protein	CARB	RNA / DNA	CO2	O2
Model 1											
***S. fradiae* C373-10**											
glucose											
Total	**9.19**	**6.41**	**11.75**	**5.66**	**9.5**	**18.14**	**9.33**	**7.49**	**18.1**	**6.33**	**5.57**
Order	6	8	3	10	4	1	5	7	2	9	11
Fructose											
Total	**7.47**	**5.62**	**6.17**	**5.58**	**9.47**	**4.46**	**7.62**	**2.57**	**6.38**	**14.04**	**14.35**
Order	4	8	7	9	3	10	6	11	5	2	1
Glycerol											
Total	**13.72**	**2.62**	**18.16**	**4.68**	**9.41**	**5.23**	**6.4**	**7.53**	**7.49**	**13.86**	**4.76**
Order	3	11	1	10	4	8	7	5	6	2	9

Carbon source	ACCOA	Biomass	Butyrate	CO2	Fum	Glyc	Lac	Mal	NH4	O2	OGA	Propionate	PYR	Tylactone
Model 2														
Glycerol Order	**8.24 8**	**2.85 13**	**15.81 3**	**14.8 5**	**3.11 12**	**13.7 5**	**8.83 7**	**5.84 11**	**22.05 2**	**33.66 1**	**6.97 9**	**15.46 4**	**5.11 10**	**12.37 6**

The accumulated sensitivity analysis data for *S. fradiae* C373-10 cultured on a number of different carbon sources for bioreaction networks models 1 and 2 (Appendices L & M; stoichiometric reactions altered as appropriate). Calculations were carried out using the program Bioflux (see Appendix N for theory). All values were presented as positives, although positive and negative values were both obtained. ACCOA, acetyl-CoA; Glyc, glycerol; LAC, lactate; MAL, malate; PYR, pyruvate; MAL, malate; OGA, oxo-glutarate; CARB, carbohydrate.

Table 7.5: Percentage change in the calculated fluxes in response to a 20 % change in each of the biomass components at a standardised specific growth.

Reaction	Setting 1, *E. coli* ML308	Setting 2, *E. coli* ML308 20% increase	Setting 3, *E. coli* ML308 20% decrease	Setting 4, *S. fradiae* C373-10 average	Setting 5, *S.fradiae* Average NADPH/NADH
1	100	100	100	100	100.19
2	35.97	35.03	36.16	35.59	30.13
3	39.74	39.36	39.36	38.61	27.12
4	62.52	63.65	61.96	62.33	66.10
5	58.57	59.70	58.00	58.76	62.71
6	29.00	29.94	28.62	29.19	31.64
7	8.29	9.04	8.10	8.66	11.30
8	-16.95	-16.19	-17.33	-16.38	-10.73
9	-24.29	-23.92	-24.29	-24.10	-2.01
10	-20.34	-20.34	-20.34	-19.96	-17.14
11	-27.87	-27.87	-27.68	-27.49	-24.48
12	36.53	36.16	36.35	35.40	24.10
13	34.46	34.09	34.09	33.33	21.84
14	14.69	14.88	14.31	14.12	9.23
15	1.130	1.69	0.56	0.38	-6.03
16	10.55	9.98	11.11	10.55	9.60
17	3.39	3.01	3.58	3.39	3.01
18	0.94	0.94	1.13	1.13	0.94
19	0.75	0.75	0.75	0.75	0.75
20	5.08	4.14	5.84	4.90	3.01
21	1.51	1.13	1.88	1.51	0.38
22	0.38	0.19	0.38	0.19	-0.19
23	0.19	0.19	0.38	0.19	0.19
24	25.61	26.18	25.23	25.23	27.68
25	13.56	13.37	13.75	13.94	13.93
26	4.33	4.33	4.33	4.33	4.33
27	4.14	4.14	4.14	4.52	4.52
28	5.27	5.08	5.27	5.08	4.90
29	4.33	4.52	4.14	4.52	4.33
30	6.97	6.97	6.97	7.34	6.97
31	10.17	10.36	9.98	9.60	9.23
32	27.12	27.68	26.74	27.12	29.19
33	11.49	10.73	12.05	11.86	10.36
34	1.88	1.88	1.88	1.88	2.45
35	-0.75	-0.56	-0.94	0.94	1.32
36	16.38	16.19	16.57	15.82	19.21
37	0.94	0.94	0.753	0.56	0.38
38	3.58	3.77	3.58	2.45	3.20
39	0.94	0.94	0.94	0.56	1.32
40	2.82	2.64	2.82	2.64	3.77
41	3.20	3.20	3.20	3.20	3.95
42	2.82	2.64	2.82	2.26	1.69

43	-0.19	-0.19	-0.19	-0.19	-0.19
44	0.56	0.56	0.56	0.75	0.56
45	8.29	7.91	8.47	8.47	7.91
46	-2.26	-2.07	-2.45	-2.26	-3.39
47	11.86	11.86	11.86	11.86	12.62
48	-0.38	-0.38	-0.38	-0.38	-0.38
49	0.75	0.56	0.75	0.56	0.38
50	1.13	1.13	0.94	1.13	1.32
51	7.72	7.72	7.53	7.53	7.53
52	1.69	1.88	1.69	1.69	1.69
53	6.03	6.03	6.03	6.03	6.03
54	5.46	5.46	5.46	5.46	5.27
55	2.45	2.45	2.45	2.45	2.45
56	4.71	4.71	4.71	4.71	4.52

The percentage flux estimates for *S. fradiae* C373-10 cultured on glucose for BRNE model 1 (Appendix L). Changes were made to the BRNE to determine the effects on the overall flux. Where average *E. coli* compositional data was used (setting 1), the average *E. coli* ML308 compositional data was increased by 20 % (setting 2), the average *E. coli* compositional data was decreased by 20 % (setting 3), and average compositional data for *S. fradiae* C373-10 cultured on glucose (setting 4)[the enzymes G6PDH and 6PGDH were set to NADP-dependent]. A further analysis was undertaken to assess the effects of the reproducibility of changing co-factor dependency of the PP pathway (setting 5)[the enzymes G6PDH and 6PGDH were NADP-G6PDH and NAD-6PGDH dependent].

Table 7.6: Percentage change in the calculated fluxes in response to a 20 % change in each of the biomass components at a standardised specific growth.

Reaction	Setting 1, *E. coli* average data	Setting 2, *E. coli* 20% increase	Setting 3, *E. coli* 20% decrease	Setting 4, *S. fradiae* average	Setting 5, *S.fradiae* Average NADPH
1	100	100	100	100	100
2	49.31	49.31	49.99	49.31	115.062
3	132.64	132.19	134.24	131.04	329.66
4	59.13	58.90	58.44	59.81	26.25
5	59.81	59.59	58.90	60.49	26.94
6	45.89	45.66	44.29	45.66	13.01
7	36.98	36.76	37.90	38.13	4.11
8	0.91	0.91	0.91	1.14	0.91
9	8.22	8.22	7.99	8.67	-13.70
10	26.03	26.25	25.57	27.62	-39.95
11	25.11	25.80	24.20	27.17	-29.68
12	4.34	4.79	3.65	5.25	-39.50
13	5.02	5.25	3.88	5.71	-38.81
14	-0.91	-0.91	-0.68	-0.68	-0.91
15	2.28	2.28	-0.46	2.51	2.28
16	0.91	0.91	0.91	0.91	0.91
17	3.88	3.88	3.88	3.88	3.88
18	4.11	4.11	4.11	4.34	4.11
19	3.65	3.65	3.65	3.65	3.65
20	-0.68	-0.68	-0.68	-0.91	-0.68
21	131.50	131.04	132.87	129.67	328.52
22	131.27	130.82	132.64	129.45	328.29
23	38.81	38.58	39.27	38.58	93.60
24	72.14	71.69	72.84	71.00	181.50
25	37.90	37.67	38.35	37.44	92.69
26	52.05	51.82	52.51	51.37	128.76
27	33.10	32.87	33.56	32.42	87.89
28	37.67	37.90	37.67	36.98	37.67
29	-2.74	-3.20	-2.51	-3.20	-2.74
30	1.60	1.60	1.60	1.60	1.60
31	-2.05	-2.05	-2.05	-2.05	-2.05
32	5.02	4.79	5.02	4.11	5.02
33	11.19	11.19	11.41	9.82	11.19
34	-0.46	-0.46	0	-1.37	-0.46
35	10.73	10.73	10.50	10.73	10.73
36	5.94	6.16	5.93	6.39	5.94
37	-2.28	-2.28	-2.28	-2.28	-2.28
38	4.57	4.57	4.57	4.57	4.57
39	5.71	5.71	5.71	5.94	5.71
40	2.74	2.74	2.75	2.74	2.75
41	0.91	0.68	0.91	0.68	0.91

42	2.97	2.97	2.97	2.28	2.97
43	2.97	2.97	2.97	2.51	2.97
44	2.28	2.28	2.28	2.51	2.28
45	1.83	1.83	1.83	1.83	1.83
46	1.60	1.60	1.60	1.60	1.60
47	-2.74	-2.51	-2.74	-2.51	-2.74
48	0	0	0	-0.23	0
49	-1.83	-1.83	-1.83	-1.83	-1.83
50	0.46	0.46	0.46	0.46	0.46
51	0.68	0.68	0.68	0.46	0.68
52	11.19	11.19	11.64	11.87	11.19
53	17.35	17.35	17.35	17.35	22.83
54	32.65	32.65	32.65	32.87	27.17
55	136.29	136.52	134.47	136.98	125.34
56	2.05	1.60	2.74	1.83	2.05
57	28.08	28.08	28.08	27.17	28.08
58	4.11	4.11	4.11	4.34	4.11
59	15.98	16.21	15.98	16.44	15.98
60	9.59	9.59	9.59	9.82	9.59
61	7.08	7.31	7.08	7.31	7.08
62	11.87	11.87	11.64	12.10	11.87

The percentage flux estimates for *S. fradiae* C373-10 cultured on glucose for BRNE model 2 (Appendix M). Changes were made to the BRNE to determine the effects on the overall flux. Where average *E. coli* compositional data was used (setting 1), the average *E. coli* ML308 compositional data was increased by 20 % (setting 2), the average *E. coli* compositional data was decreased by 20 % (setting 3), and average compositional data for *S. fradiae* C373-10 cultured on glucose (setting 4)[the enzymes G6PDH and 6PGDH were set to NADP-dependent]. A further analysis was undertaken to assess the effects of the reproducibility of changing co-factor dependency of the PP pathway (setting 5)[the enzymes G6PDH and 6PGDH were NADP-G6PDH and NAD-6PGDH dependent].

Table 8.1 Metabolic costs of precursor metabolites in *E. coli* ML308

Precursor abbrev.	Energetic cost					
	Glucose		Acetate		Malate	
	~P	H	~P	H	~P	H
R5P	7	10	19	10	11	10
PRPP	9	10	21	10	13	10
E4P	5	8	11	8	7	8
PGA	4	6	4	6	3	6
PEP	2	4	3	5	2	5
PYR	2	4	3	5	2	5
AcCoA	0	4	2	5	1	4
OGA	0	2	1	4	1	2
OAA	1	4	5	7	2	5

~P and H refer to numbers of high-energy phosphate bonds carried in ATP and GTP molecules and numbers of available hydrogen atoms carried in NADH, NADPH, and $FADH_2$ molecules, respectively. Ribose-5-phosphate, R5P; Phosphoenolpyruvate, PEP; 5-phosphoribosyl pyrophosphate, PRPP; erythrose 4-phosphate, E4P; 3-phosphoglycerate, PGA; pyruvate, PYR; acetyl-CoA, AcCoA; oxo-glutarate, OGA; oxaloacetate, OAA (taken from Akashi & Gojobori, 2002).

Table 8.2 Metabolic costs for biosynthesis of the twenty amino acids in bacteria and fungi.

Amino acids	Precursors metabolites	ATP[a]	NADH	NADPH	1-C[b]	NH_3	S[c]
Alanine	1 PYR	0	0	-1	0	-1	0
Arginine	1 OGA	-7	1	-4	0	-4	0
Aspartate	1 OAA	-3	0	-1	0	-2	0
Asparagine	1 OAA	0	0	-1	0	-1	0
Cysteine[d]	1 PGA	-4	1	-5	0	-1	-1
Glutamate	1 OGA	0	0	-1	0	-1	0
Glutamine	1 OGA	-1	0	-1	1	-2	0
Glycine	1 PGA	0	1	-1	-1	-1	0
Histidine	1 PEP	-6	3	-1	0	-3	0
Isoleucine	1 OAA, 1 PYR	-2	0	-5	0	-1	0
Leucine	2 PYR, 1 ACCOA	0	1	-2	0	-1	0
Lysine (fungi)	1 OGA, 1 ACCOA	-2	2	-4	0	-2	0
Lysine	1 PYR, 1 OAA	-3	0	-4	0	-2	0
Methionine	1 OAA	-7	0	-8	-1	-1	-1
Phenylalanine	2 PEP, 1 E4P	-1	0	-2	0	-1	0
Proline	1 OGA	-1	0	-3	0	-1	0
Serine	1 PGA	0	1	-1	0	-1	0
Threonine	1 OAA	-2	0	-3	0	-1	0
Tryptophan	1 PEP, 1 E4P, 1PEP	-5	2	-3	0	-2	0
Tyrosine	2 PEP, 1 E4P	-1	1	-2	0	-1	0
Valine	2 PYR	0	0	-2	0	-1	0

[a]For those reactions where ATP is hydrolysed to AMP, it was assumed that two ATPs were used.[b]5'10-Methylene tetrahydrofolate is used as one carbon donor which is converted to tetrahydrofolate. Other forms of tetrahydrofolate used in the biosynthesis of 1-methionine and 1-histidine are converted to this basis. Erythrose-4-phosphate, E4P; 3-phosphoglycerate, PGA; pyruvate, PYR; Phosphoenolpyruvate, PEP; acetyl-CoA, AcCoA; oxo-glutarate, OGA; oxaloacetate, OAA (taken from Stephanopoulos *et al*., 1998).

Table 8.3 The Total Metabolic costs of amino acid biosynthesis in *E. coli* ML308.

Amino acid	Precursor metabolites	Energetic cost					
		Glucose		Acetate		Malate	
		~P	H	~P	H	~P	H
Ala	PYR	0	5	2	6	1	5
Cys	PGA	7	8	8	9	7	9
Asp	OAA	1	5	2	6	1	6
Glu	OGA	1	5	5	8	2	6
Phe	2 PEP, E4P	10	18	18	20	12	20
Gly	PGA	2	4	3	5	2	5
His	PPRP	15	9	27	9	19	9
Ile	PYR, OAA	3	13	6	15	4	14
Lys	OAA, CYS, -PYR	3	12	6	14	4	13
Leu	2 PYR, AcCoA	0	11	5	15	3	11
Met	OAA, E4P	9	11	11	13	9	13
Asn	OAA	3	5	4	6	3	6
Pro	OGA	2	7	6	10	3	8
Gln	OGA	2	5	6	8	3	6
Arg	OGA	9	7	13	10	10	8
Ser	PGA	2	4	3	5	2	5
Thr	OAA	3	7	4	8	3	8
Val	2 PYR	0	10	4	12	2	10
Trp	2 PEP, E4P, PRPP, -PYR	19	22	39	24	25	24
Tyr	E4P, 2 PEP	10	17	18	19	12	19

Table 8.4 shows energetic costs for the precursors employed in biosynthesis of amino acids. For growth on glucose, the production of oxaloacetate was assumed to be (for biosynthesis) through the carboxylation of phosphoenolpyruvate. The cost of OGA includes the cost of producing an oxaloacetate molecule (through the anaplerotic pathway) to replenish the tricarboxylic acid (TCA) cycle. Relative costs of precursors are similar for other substrates that enter fueling pathways as C5 or C6 units (fructose, lactose, and pentoses). For growth on acetate, a maximum energy gain through the oxidation of acetyl-CoA via the TCA cycle was assumed. The glyoxylate shunt and gluconeogenesis were assumed to operate to produce precursors. The cost of OGA includes the cost of replenishing the TCA cycle with an oxaloacetate molecule (through the glyoxylate cycle). For growth on malate, a maximum energy gain through the conversion of malate to acetyl-CoA (via pyruvate) and oxidation through the TCA cycle was assumed. Precursors were generated via malate and oxaloacetate and malate and pyruvate and subsequent gluconeogenesis. The cost of OGA includes the cost of producing an oxaloacetate molecule (directly from malate) to replenish the TCA cycle. Phosphoenolpyruvate, PEP; 5-phosphoribosyl pyrophosphate, PRPP; erythrose 4-phosphate, E4P; 3-phosphoglycerate, PGA; pyruvate, PYR; acetyl-CoA, AcCoA; oxo-glutarate, OGA; oxaloacetate, OAA (taken from Akashi & Gojobori, 2002).

Table 8.4 The calculation of the total amount of energy required for the biosynthesis of amino acids in *E. coli* ML308.

***E. coli* glucose**						
Monomer		**Monomer content**	**~P**	**~H**	**Total**	**Energy**
Alanine	PYR	0.454	1	5.33	11.67	**5.30**
Arginine	PGA	0.252	7.33	8.67	24.67	**6.22**
Aspartate	OAA	0.201	1.33	5.67	12.67	**2.55**
Asparagine	OGA	0.101	2.67	6.33	15.33	**1.55**
Cysteine	2 PEP, E4P	0.101	13.33	19.33	52.00	**5.25**
Glutamate	PG	0.353	2.33	4.67	11.67	**4.12**
Glutamine	PPRP	0.201	20.33	9.00	38.33	**7.70**
Glycine	PYR, OAA	0.403	4.33	14.00	32.33	**13.03**
Histidine	OAA, PYR	0.05	4.33	13.00	30.33	**1.52**
Isoleucine	2 PYR, AcCoA	0.252	2.67	12.33	27.33	**6.89**
Leucine	OAA, Cys, -PYR	0.403	9.67	12.33	34.33	**13.84**
Lysine	OAA	0.403	3.33	5.67	14.67	**5.91**
Methionine	OGA	0.201	3.67	8.33	20.33	**4.09**
Phenylalanine	OGA	0.151	3.67	6.33	16.33	**2.47**
Proline	OGA	0.252	10.67	8.33	27.33	**6.89**
Serine	PGA	0.302	2.33	4.67	11.67	**3.52**
Threonine	OAA	0.252	3.33	7.67	18.67	**4.70**
Tryptophan	2 PYR	0.05	2.00	10.67	23.33	**1.17**
Tyrosine	2 PEP, E4P, PRPP, -PYR	0.101	27.67	23.33	74.33	**7.51**
Valine	E4P, 2 PEP	0.302	13.33	18.33	50.00	**15.10**
Total energy						**119.31**

The calculation of the total amount of energy for amino acid biosynthesis in *E. coli*. This takes into account the cost of precursor costs from Table 8.1 and the cost of amino acid biosynthesis Table 8.2. Phosphoenolpyruvate, PEP; 5-phosphoribosyl pyrophosphate, PRPP; erythrose 4-phosphate, E4P; 3-phosphoglycerate, PGA; pyruvate, PYR; acetyl-CoA, AcCoA; oxo-glutarate, OGA; oxaloacetate, OAA (adapted from Akashi & Gojobori, 2002).

Table 8.5 Calculation of the total amount of energy used for the biosynthesis of amino acids in *E. coli* ML308, *S. coelicolor* 1147 and *S. fradiae* C373-10

Fermentation	Energy charge
***E. coli* ML308**	
Glucose	**119.31**
***S. coelicolor* 1147**	
glucose (A)	52.26
glucose (B)	44.51
glucose (C)	80.23
glucose (D)	114.39
glucose (Ferm 1)	77.71
glucose (Ferm 2)	107.6
STDEV	**± 5.92**
***S. fradiae* C373-10**	
glucose (Ferm 1)	54.16
glucose (Ferm 2)	124.93
STDEV	**± 27.94**
fructose (Ferm 1)	31.2
glycerol (Ferm 1)	24.71
glycerol (Ferm 2)	43.04
oxo-glutarate (Ferm 1)	15.09
STDEV	**± 10.29**
glucose glutamate (Ferm 1)	48.85
glucose glutamate (Ferm 2)	43.04
glucose glutamate (Ferm 3)	74.02
glucose glutamate (Ferm 4)	105.28
STDEV	**± 10.46**
glucose oxo-glutarate (Ferm 1)	95.55
glucose oxo-glutarate (Ferm 2)	78.27
STDEV	**± 7.03**
methyl oleate medium (Ferm 1)	74.28
methyl oleate medium (Ferm 2)	76.45
STDEV	**± 1.02**
***S. fradiae* C373-18**	
complex medium	57.56
Total mean percentage STDEV	**± 10.44**

Table 8.5 presents the energetic costs of amino acid biosynthesis converted to a common currency of ~P based on a proportion of two ~P per H (Akashi & Gojobori, 2002). The fueling reactions of central metabolism provide precursor metabolites for synthesis of the 20 amino acids incorporated into proteins (see appendix B). The metabolic costs of synthesising the 20 amino acids used in proteins are shown in Table 8.5. The cost of using a particular precursor metabolite is the number of high-energy phosphate bonds, ~P, carried in ATP and GTP, plus the number of available hydrogen atoms, H, carried in NADH, NADPH, and FADH2, that would have been gained if the metabolite had remained in energy-producing pathways minus the numbers of these molecules gained before diversion. For each amino acid, the energetic requirements of its biosynthetic pathway are added to the costs of its starting metabolite(s) to obtain a total metabolic cost per molecule synthesized. Amino acids that require chemical intermediates early in fueling reaction pathways (the aromatic amino acids and His) are more costly than those derived from intermediates downstream in glycolysis (the serine family) and the TCA cycle (the aspartate and glutamate families).

Compendium

Precursor Tables

Table 6.1 The amounts of precursor required for the biosynthesis of 1 g of *S. coelicolor* 1147 biomass; growth on glucose as sole carbon source (Ferm 1).

Monomer content (mmoles.g^{-1})		G6P	TP	PG	PEP	PYR	OAA	OGA	AcCoA
Alanine	0.424					0.424			
Arginine	0.198							0.198	
Aspartate	0.179						0.179		
Asparagine	nd								
Cysteine	0.059			0.059					
Glutamate	0.233							0.233	
Glutamine	nd								
Glycine	0.455			0.455					
Histidine	0.045	0.045							
Isoleucine	0.152					0.152	0.152		
Leucine	0.234					0.468			0.234
Lysine	0.188					0.188	0.188		
Methionine	0.033						0.033		
Phenylalanine	0.088	0.088			0.176				
Proline	0.152							0.152	
Serine	0.134			0.134					
Threonine	0.138						0.138		
Tryptophan	0.028	0.056			0.028				
Tyrosine	0.045	0.045			0.090				
Valine	0.288					0.576			
A	0.059	0.059		0.059					
DA	0.022	0.022		0.022					
G	0.115	0.115		0.115					
DG	0.064	0.064		0.064					
C	0.101	0.101					0.101		
DC	0.064	0.064					0.064		
U	0.078	0.078					0.078		
DT	0.022	0.022					0.022		
C16 FA	0.167					0.132	0.012		1.715
Glycerophosphate	0.064		0.064						
Carbohydrate	0.236	0.236							
Total draw of monomers to biosynthesis (mmoles.g^{-1})		**0.995**	**0.064**	**0.908**	**0.294**	**1.94**	**0.967**	**0.583**	**1.949**
Total draw of carbon to biosynthesis (C.mmoles.g^{-1})		**5.97**	**0.192**	**2.724**	**0.882**	**5.821**	**3.866**	**2.915**	**3.898**

The total demand of monomers to biosynthesis in the CMPs of *S. coelicolor* 1147 were expressed in terms of carbon flux. All values are in mmoles.g^{-1} and converted to C.mmoles.g^{-1}, i.e., the flux, from each intermediate (Total mmoles.g^{-1}) was multiplied by the number of carbon atoms present in the molecular structure of the starting precursor of the pathway (Total C.mmoles.g^{-1}). <, denotes this monomer was below the detection limits of the appropriate assay. G6P, glucose-6-phosphate; TP, triose phosphate; PG, phosphoglycerate; PEP, phosphoenolpyruvate; PYR, pyruvate; OAA, Oxaloacetate; OGA, oxo-glutarate; AcCoA, acetyl-CoA; d, deoxy; A, adenine; C, cytosine; G, guanosine; U, uracil. Tables constructed as Holms. (1986, 1996, 1997, 2001) for theory and a worked example see Chapter 1, & Appendix B. nd, not determined.

Table 6.2 The amounts of precursor required for the biosynthesis of 1 g of *S. coelicolor* 1147 biomass; growth on glucose as sole carbon source (Ferm 2).

Monomer content (mmoles.g^{-1})		G6P	TP	PG	PEP	PYR	OAA	OGA	AcCoA
Alanine	0.555					0.555			
Arginine	0.39							0.390	
Aspartate	0.299						0.299		
Asparagine	nd								
Cysteine	0.076			0.076					
Glutamate	0.311							0.311	
Glutamine	nd								
Glycine	0.483			0.483					
Histidine	0.123	0.123							
Isoleucine	0.144					0.144	0.144		
Leucine	0.344					0.688			0.344
Lysine	0.266					0.266	0.266		
Methionine	0.008						0.008		
Phenylalanine	0.122	0.122			0.244				
Proline	0.222							0.222	
Serine	0.184			0.184					
Threonine	0.222						0.222		
Tryptophan	0.144	0.288			0.144				
Tyrosine	0.066	0.066			0.132				
Valine	0.367					0.734			
A	0.09	0.09		0.09					
dA	0.022	0.022		0.022					
G	0.135	0.135		0.135					
dG	0.064	0.064		0.064					
C	0.108	0.108					0.108		
dC	0.064	0.064					0.064		
U	0.079	0.079					0.079		
dT	0.022	0.022					0.022		
C16 FA	0.167					0.132	0.012		1.715
Glycerophosphate	0.064		0.064						
Carbohydrate	0.244	0.244							
Total draw of monomers to biosynthesis (mmoles.g^{-1})		**1.427**	**0.064**	**1.054**	**0.52**	**2.519**	**1.224**	**0.923**	**2.059**
Total draw of carbon to biosynthesis (C.mmoles.g^{-1})		**8.562**	**0.192**	**3.162**	**1.56**	**7.558**	**4.894**	**4.617**	**4.118**

The total demand of monomers to biosynthesis in the CMPs of *S. coelicolor* 1147 were expressed in terms of carbon flux. All values are in mmoles.g^{-1} and converted to C.mmoles.g^{-1}, i.e., the flux, from each intermediate (Total mmoles.g^{-1}) was multiplied by the number of carbon atoms present in the molecular structure of the starting precursor of the pathway (Total C.mmoles.g^{-1}). <, denotes this monomer was below the detection limits of the appropriate assay. G6P, glucose-6-phosphate; TP, triose phosphate; PG, phosphoglycerate; PEP, phosphoenolpyruvate; PYR, pyruvate; OAA, Oxaloacetate; OGA, oxo-glutarate; AcCoA, acetyl-CoA; d, deoxy; A, adenine; C, cytosine; G, guanosine; U, uracil. Tables constructed as Holms. (1986, 1996, 1997, 2001) for theory and a worked example see Chapter 1, & Appendix B. nd not determined.

Table 6.3 The amounts of precursor required for the biosynthesis of 1 g of *S. fradiae* C373-10 biomass; growth on glucose as sole carbon source (Ferm 1).

Monomer content (mmoles.g^{-1})		G6P	TP	PG	PEP	PYR	OAA	OGA	AcCoA
Alanine	0.192					0.192			
Arginine	0.691							0.691	
Aspartate	0.177						0.177		
Asparagine	nd								
Cysteine	0.037			0.037					
Glutamate	0.181							0.181	
Glutamine	nd								
Glycine	0.432			0.432					
Histidine	0.032	0.032							
Isoleucine	0.031					0.031	0.031		
Leucine	0.104					0.209			0.104
Lysine	<0.001					0.001	0.001		
Methionine	<0.001						0.001		
Phenylalanine	0.036	0.036			0.071				
Proline	0.112							0.112	
Serine	0.006			0.006					
Threonine	0.078						0.078		
Tryptophan	<0.001	0.002			0.001				
Tyrosine	<0.001	0.001			0.002				
Valine	0.082					0.165			
A	0.044	0.044		0.044					
DA	0.007	0.007		0.007					
G	0.066	0.066		0.066					
DG	0.016	0.016		0.016					
C	0.043	0.043					0.043		
DC	0.016	0.016					0.016		
U	0.039	0.039					0.039		
DT	0.007	0.007					0.007		
C16 FA	0.135					0.086	0.008		1.115
Glycerophosphate	0.051		0.051						
Carbohydrate	0.527	0.527							
Total draw of monomers to biosynthesis (mmoles.g^{-1})		**0.832**	**0.051**	**0.607**	**0.071**	**0.682**	**0.398**	**0.984**	**1.219**
Total draw of carbon to biosynthesis (C.mmoles.g^{-1})		**4.993**	**0.153**	**1.821**	**0.213**	**2.047**	**1.59**	**4.918**	**2.439**

The total demand of monomers to biosynthesis in the CMPs of *S. fradiae* C373-10 were expressed in terms of carbon flux. All values are in mmoles.g^{-1} and converted to C.mmoles.g^{-1}, i.e., the flux, from each intermediate (Total mmoles.g^{-1}) was multiplied by the number of carbon atoms present in the molecular structure of the starting precursor of the pathway (Total C.mmoles.g^{-1}). <, denotes this monomer was below the detection limits of the appropriate assay. G6P, glucose-6-phosphate; TP, triose phosphate; PG, phosphoglycerate; PEP, phosphoenolpyruvate; PYR, pyruvate; OAA, Oxaloacetate; OGA, oxo-glutarate; AcCoA, acetyl-CoA; d, deoxy; A, adenine; C, cytosine; G, guanosine; U, uracil. Tables constructed as Holms. (1986, 1996, 1997, 2001) for theory and a worked example see Chapter 1, & Appendix B. nd, not determined.

Table 6.4 The amounts of precursor required for the biosynthesis of 1 g of *S. fradiae* C373-10 biomass; growth on glucose as sole carbon source (Ferm 2).

Monomer content (mmoles.g^{-1})		G6P	TP	PG	PEP	PYR	OAA	OGA	AcCoA
Alanine	0.679					0.679			
Arginine	0.755							0.755	
Aspartate	0.495						0.495		
Asparagine	nd								
Cysteine	0.088			0.088					
Glutamate	0.556							0.556	
Glutamine	nd								
Glycine	1.331			1.331					
Histidine	0.060	0.06							
Isoleucine	0.149					0.149	0.149		
Leucine	0.365					0.729			0.365
Lysine	<0.001					0.001	0.001		
Methionine	<0.001						0.001		
Phenylalanine	0.120	0.12			0.24				
Proline	0.284							0.284	
Serine	0.060			0.06					
Threonine	0.204						0.204		
Tryptophan	<0.001	0.002			0.001				
Tyrosine	0.007	0.007			0.013				
Valine	0.098					0.196			
A	0.029	0.029		0.029					
dA	0.012	0.012		0.012					
G	0.043	0.043		0.043					
dG	0.027	0.027		0.027					
C	0.035	0.035					0.035		
dC	0.027	0.027					0.027		
U	0.025	0.025					0.025		
dT	0.012	0.012					0.012		
C16 FA	0.175					0.112	0.01		1.448
Glycerophosphate	0.066		0.066						
Carbohydrate	0.657	0.657							
Total draw of monomers to biosynthesis (mmoles.g^{-1})		**1.051**	**0.066**	**1.589**	**0.253**	**1.865**	**0.956**	**1.595**	**1.813**

Total draw of carbon to biosynthesis (C.mmoles.g^{-1})	**6.308**	**0.198**	**4.766**	**0.758**	**5.595**	**3.822**	**7.976**	**3.625**

The total demand of monomers to biosynthesis in the CMPs of *S. fradiae* C373-10 were expressed in terms of carbon flux. All values are in mmoles.g^{-1} and converted to C.mmoles.g^{-1}, i.e., the flux, from each intermediate (Total mmoles.g^{-1}) was multiplied by the number of carbon atoms present in the molecular structure of the starting precursor of the pathway (Total C.mmoles.g^{-1}). <, denotes this monomer was below the detection limits of the appropriate assay. G6P, glucose-6-phosphate; TP, triose phosphate; PG, phosphoglycerate; PEP, phosphoenolpyruvate; PYR, pyruvate; OAA, Oxaloacetate; OGA, oxo-glutarate; AcCoA, acetyl-CoA; d, deoxy; A, adenine; C, cytosine; G, guanosine; U, uracil. Tables constructed as Holms. (1986, 1996, 1997, 2001) for theory and a worked example see Chapter 1, & Appendix B. nd, not determined.

Table 6.5 The amounts of precursor required for the biosynthesis of 1 g of *S. fradiae* C373-10 biomass; growth on fructose as sole carbon source (Ferm 1).

Monomer content (mmoles.g^{-1})		G6P	TP	PG	PEP	PYR	OAA	OGA	AcCoA
Alanine	0.127					0.127			
Arginine	0.222							0.222	
Aspartate	0.159						0.159		
Asparagine	nd								
Cysteine	0.022			0.022					
Glutamate	0.129							0.129	
Glutamine	nd								
Glycine	0.185			0.185					
Histidine	0.032	0.032							
Isoleucine	0.043					0.043	0.043		
Leucine	0.109					0.218			0.109
Lysine	<0.001					0.001	0.001		
Methionine	<0.001						0.001		
Phenylalanine	0.112	0.112			0.224				
Proline	0.067							0.067	
Serine	<0.001			0.001					
Threonine	0.026						0.026		
Tryptophan	<0.001	0.002			0.001				
Tyrosine	<0.001	0.001			0.002				
Valine	0.068					0.137			
A	0.036	0.036		0.036					
DA	0.011	0.011		0.011					
G	0.054	0.054		0.054					
DG	0.026	0.026		0.026					
C	0.043	0.043					0.043		
DC	0.026	0.026					0.026		
U	0.032	0.032					0.032		
DT	0.011	0.011					0.011		
C16 FA	0.207					0.132	0.012		1.715
Glycerophosphate	0.078		0.078						
Carbohydrate	0.309	0.309							
Total draw of monomers to biosynthesis (mmoles.g^{-1})		**0.693**	**0.078**	**0.334**	**0.224**	**0.657**	**0.351**	**0.418**	**1.824**
Total draw of carbon to biosynthesis (C.mmoles.g^{-1})		**4.157**	**0.235**	**1.003**	**0.671**	**1.972**	**1.406**	**2.089**	**3.648**

The total demand of monomers to biosynthesis in the CMPs of *S. fradiae* C373-10 were expressed in terms of carbon flux. All values are in mmoles.g^{-1} and converted to C.mmoles.g^{-1}, i.e., the flux, from each intermediate (Total mmoles.g^{-1}) was multiplied by the number of carbon atoms present in the molecular structure of the starting precursor of the pathway (Total C.mmoles.g^{-1}). <, denotes this monomer was below the detection limits of the appropriate assay. G6P, glucose-6-phosphate; TP, triose phosphate; PG, phosphoglycerate; PEP, phosphoenolpyruvate; PYR, pyruvate; OAA, Oxaloacetate; OGA, oxo-glutarate; AcCoA, acetyl-CoA; d, deoxy; A, adenine; C, cytosine; G, guanosine; U, uracil. Tables constructed as Holms. (1986, 1996, 1997, 2001) for theory and a worked example see Chapter 1, & Appendix B. nd, not determined.

Table 6.6 The amounts of precursor required for the biosynthesis of 1 g of *S. fradiae* C373-10 biomass; growth on glycerol as sole carbon source (Ferm 1).

Monomer content (mmoles.g^{-1})		G6P	TP	PG	PEP	PYR	OAA	OGA	AcCoA
Alanine	0.344					0.344			
Arginine	0.208							0.208	
Aspartate	0.066						0.066		
Asparagine	nd								
Cysteine	0.019			0.019					
Glutamate	0.115							0.115	
Glutamine	nd								
Glycine	0.180			0.18					
Histidine	0.022	0.023							
Isoleucine	0.011					0.011	0.011		
Leucine	0.024					0.049			0.025
Lysine	<0.001					0.001	0.001		
Methionine	0.003						0.003		
Phenylalanine	0.009	0.009			0.017				
Proline	0.074							0.074	
Serine	0.003			0.003					
Threonine	0.037						0.037		
Tryptophan	0.034	0.068			0.034				
Tyrosine	<0.001	0.001			0.001				
Valine	0.020					0.039			
A	0.013	0.013		0.013					
dA	0.007	0.007		0.007					
G	0.019	0.019		0.019					
dG	0.017	0.017		0.017					
C	0.015	0.015					0.015		
dC	0.017	0.017					0.017		
U	0.011	0.011					0.011		
dT	0.007	0.007					0.007		
C16 FA	0.115					0.074	0.006		0.956
Glycerophosphate	0.044		0.044						
Carbohydrate	0.097	0.097							
Total draw of monomers to biosynthesis (mmoles.g^{-1})		**0.302**	**0.044**	**0.257**	**0.052**	**0.516**	**0.174**	**0.397**	**0.981**
Total draw of carbon to biosynthesis (C.mmoles.g^{-1})		**1.811**	**0.131**	**0.772**	**0.157**	**1.548**	**0.696**	**1.984**	**1.961**

The total demand of monomers to biosynthesis in the CMPs of *S. fradiae* C373-10 were expressed in terms of carbon flux. All values are in mmoles.g^{-1} and converted to C.mmoles.g^{-1}, i.e., the flux, from each intermediate (Total mmoles.g^{-1}) was multiplied by the number of carbon atoms present in the molecular structure of the starting precursor of the pathway (Total C.mmoles.g^{-1}). <, denotes this monomer was below the detection limits of the appropriate assay. G6P, glucose-6-phosphate; TP, triose phosphate; PG, phosphoglycerate; PEP, phosphoenolpyruvate; PYR, pyruvate; OAA, Oxaloacetate; OGA, oxo-glutarate; AcCoA, acetyl-CoA; d, deoxy; A, adenine; C, cytosine; G, guanosine; U, uracil. Tables constructed as Holms. (1986, 1996, 1997, 2001) for theory and a worked example see Chapter 1, & Appendix B. nd, not determined.

Table 6.7 The amounts of precursor required for the biosynthesis of 1 g of *S. fradiae* C373-10 biomass; growth on glycerol as sole carbon source (Ferm 2).

Monomer content (mmoles.g^{-1})		G6P	TP	PG	PEP	PYR	OAA	OGA	AcCoA
Alanine	0.355					0.355			
Arginine	0.087							0.087	
Aspartate	0.221						0.221		
Asparagine	nd								
Cysteine	0.033			0.033					
Glutamate	0.195							0.195	
Glutamine	nd								
Glycine	0.195			0.195					
Histidine	0.028	0.028							
Isoleucine	0.082					0.082	0.082		
Leucine	0.113					0.225			0.113
Lysine	0.024					0.024	0.024		
Methionine	<0.001						0.001		
Phenylalanine	0.241	0.241			0.481				
Proline	0.107							0.107	
Serine	0.035			0.035					
Threonine	0.169						0.169		
Tryptophan	<0.001	0.002			0.001				
Tyrosine	0.046	0.046			0.091				
Valine	0.050					0.101			
A	0.017	0.017		0.017					
dA	0.010	0.01		0.01					
G	0.026	0.026		0.026					
dG	0.023	0.023		0.023					
C	0.021	0.021					0.021		
dC	0.029	0.029					0.029		
U	0.015	0.015					0.015		
dT	0.0107	0.01					0.01		
C16 FA	0.217					0.139	0.006		1.796
Glycerophosphate	0.082		0.082						
Carbohydrate	0.459	0.459							
Total draw of monomers to biosynthesis (mmoles.g^{-1})		**0.923**	**0.082**	**0.338**	**0.573**	**0.925**	**0.577**	**0.389**	**1.909**
Total draw of carbon to biosynthesis (C.mmoles.g^{-1})		**5.535**	**0.245**	**1.014**	**1.718**	**2.774**	**2.308**	**1.947**	**3.817**

The total demand of monomers to biosynthesis in the CMPs of *S. fradiae* C373-10 were expressed in terms of carbon flux. All values are in mmoles.g^{-1} and converted to C.mmoles.g^{-1}, i.e., the flux, from each intermediate (Total mmoles.g^{-1}) was multiplied by the number of carbon atoms present in the molecular structure of the starting precursor of the pathway (Total C.mmoles.g^{-1}). <, denotes this monomer was below the detection limits of the appropriate assay. G6P, glucose-6-phosphate; TP, triose phosphate; PG, phosphoglycerate; PEP, phosphoenolpyruvate; PYR, pyruvate; OAA, Oxaloacetate; OGA, oxo-glutarate; AcCoA, acetyl-CoA; d, deoxy; A, adenine; C, cytosine; G, guanosine; U, uracil. Tables constructed as Holms. (1986, 1996, 1997, 2001) for theory and a worked example see Chapter 1, & Appendix B. nd not determined.

Table 6.8 The amounts of precursor required for the biosynthesis of 1 g of *S. fradiae* C373-10 biomass; growth on oxo-glutarate as sole carbon source (Ferm 1).

Monomer content (mmoles.g^{-1})		G6P	TP	PG	PEP	PYR	OAA	OGA	AcCoA
Alanine	0.091					0.091			
Arginine	0.083							0.083	
Aspartate	0.046						0.046		
Asparagine	nd								
Cysteine	0.011			0.01					
Glutamate	0.068							0.068	
Glutamine	nd								
Glycine	0.143			0.143					
Histidine	0.016	0.016							
Isoleucine	0.018					0.018	0.018		
Leucine	0.037					0.074			0.037
Lysine	<0.001					0.001	0.001		
Methionine	<0.001						0.001		
Phenylalanine	0.026	0.026			0.052				
Proline	0.034							0.034	
Serine	0.006			0.006					
Threonine	0.024						0.024		
Tryptophan	<0.001	0.002			0.001				
Tyrosine	0.004	0.004			0.008				
Valine	0.020					0.041			
A	0.039	0.039		0.039					
dA	0.022	0.022		0.022					
G	0.059	0.059		0.059					
dG	0.052	0.052		0.052					
C	0.047	0.047					0.047		
dC	0.052	0.052					0.052		
U	0.035	0.035					0.035		
dT	0.022	0.022					0.022		
C16 FA	0.174						0.01		1.439
Glycerophosphate	0.066		0.066						
Carbohydrate	0.120	0.12							
Total draw of monomers to biosynthesis (mmoles.g^{-1})		**0.494**	**0.066**	**0.332**	**0.06**	**0.224**	**0.253**	**0.185**	**1.476**
Total draw of carbon to biosynthesis (C.mmoles.g^{-1})		**2.965**	**0.197**	**0.996**	**0.18**	**0.672**	**1.012**	**0.924**	**2.952**

The total demand of monomers to biosynthesis in the CMPs of *S. fradiae* C373-10 were expressed in terms of carbon flux. All values are in mmoles.g^{-1} and converted to C.mmoles.g^{-1}, i.e., the flux, from each intermediate (Total mmoles.g^{-1}) was multiplied by the number of carbon atoms present in the molecular structure of the starting precursor of the pathway (Total C.mmoles.g^{-1}). <, denotes this monomer was below the detection limits of the appropriate assay. G6P, glucose-6-phosphate; TP, triose phosphate; PG, phosphoglycerate; PEP, phosphoenolpyruvate; PYR, pyruvate; OAA, Oxaloacetate; OGA, oxo-glutarate; AcCoA, acetyl-CoA; d, deoxy; A, adenine; C, cytosine; G, guanosine; U, uracil. Tables constructed as Holms. (1986, 1996, 1997, 2001) for theory and a worked example see Chapter 1, & Appendix B. nd, not determined.

Table 6.9 The amounts of precursor required for the biosynthesis of 1 g of *S. fradiae* C373-10 biomass; growth on glucose & glutamate Day 2 (Ferm 1).

Monomer content (mmoles.g^{-1})		G6P	TP	PG	PEP	PYR	OAA	OGA	AcCoA
Alanine	0.176					0.176			
Arginine	0.169							0.169	
Aspartate	0.074						0.074		
Asparagine	nd								
Cysteine	0.027			0.027					
Glutamate	0.168							0.168	
Glutamine	nd								
Glycine	0.184			0.184					
Histidine	0.037	0.037							
Isoleucine	0.081					0.081	0.081		
Leucine	0.117					0.234			0.117
Lysine	0.086					0.086	0.086		
Methionine	<0.001						0.001		
Phenylalanine	0.039	0.039			0.077				
Proline	0.074							0.074	
Serine	0.022			0.022					
Threonine	0.146						0.146		
Tryptophan	<0.001	0.002			0.001				
Tyrosine	0.040	0.04			0.079				
Valine	0.150					0.301			
A	0.030	0.03		0.03					
dA	0.010	0.01		0.01					
G	0.046	0.046		0.046					
dG	0.025	0.025		0.025					
C	0.036	0.036					0.036		
dC	0.025	0.025					0.025		
U	0.027	0.027					0.027		
dT	0.010	0.01					0.01		
C16 FA	0.297					0.19	0.017		2.464
Glycerophosphate	0.112		0.112						
Carbohydrate	0.599	0.599							
Total draw of monomers to biosynthesis (mmoles.g^{-1})		**0.923**	**0.112**	**0.344**	**0.156**	**1.068**	**0.502**	**0.411**	**2.581**
Total draw of carbon to biosynthesis (C.mmoles.g^{-1})		**5.538**	**0.336**	**1.032**	**0.469**	**3.204**	**2.008**	**2.055**	**5.162**

The total demand of monomers to biosynthesis in the CMPs of *S. fradiae* C373-10 were expressed in terms of carbon flux. All values are in mmoles.g^{-1} and converted to C.mmoles.g^{-1}, i.e., the flux, from each intermediate (Total mmoles.g^{-1}) was multiplied by the number of carbon atoms present in the molecular structure of the starting precursor of the pathway (Total C.mmoles.g^{-1}). <, denotes this monomer was below the detection limits of the appropriate assay. G6P, glucose-6-phosphate; TP, triose phosphate; PG, phosphoglycerate; PEP, phosphoenolpyruvate; PYR, pyruvate; OAA, Oxaloacetate; OGA, oxo-glutarate; AcCoA, acetyl-CoA; d, deoxy; A, adenine; C, cytosine; G, guanosine; U, uracil. Tables constructed as Holms. (1986, 1996, 1997, 2001) for theory and a worked example see Chapter 1, & Appendix B. nd, not determined.

Table 6.10. The amounts of precursor required for the biosynthesis of 1 g of *S. fradiae* C373-10 biomass; growth on glucose & glutamate Day 2 (Ferm 2).

Monomer content (mmoles.g^{-1})		G6P	TP	PG	PEP	PYR	OAA	OGA	AcCoA
Alanine	0.111					0.111			
Arginine	0.024							0.024	
Aspartate	0.108						0.108		
Asparagine	nd								
Cysteine	0.018			0.018					
Glutamate	0.103							0.103	
Glutamine	nd								
Glycine	0.117			0.117					
Histidine	0.029	0.029							
Isoleucine	0.069					0.069	0.069		
Leucine	0.125					0.250			0.125
Lysine	0.124					0.124	0.124		
Methionine	<0.001						0.001		
Phenylalanine	0.031	0.031			0.062				
Proline	0.053							0.053	
Serine	0.014			0.014					
Threonine	0.066						0.066		
Tryptophan	0.005	0.01			0.005				
Tyrosine	<0.001	0.001			0.002				
Valine	0.064					0.128			
A	0.038	0.038		0.038					
dA	0.008	0.007		0.007					
G	0.058	0.058		0.058					
dG	0.017	0.017		0.017					
C	0.046	0.046					0.046		
dC	0.017	0.017					0.017		
U	0.034	0.034					0.034		
dT	0.008	0.007					0.007		
C16 FA	0.393					0.251	0.022		3.259
Glycerophosphate	0.148		0.148						
Carbohydrate	0.625	0.625							
Total draw of monomers to biosynthesis (mmoles.g^{-1})		**0.922**	**0.148**	**0.270**	**0.069**	**0.934**	**0.493**	**0.180**	**3.384**

Total draw of carbon to biosynthesis (C.mmoles.g^{-1})	**5.530**	**0.444**	**0.809**	**0.207**	**2.801**	**1.973**	**0.897**	**6.768**

The total demand of monomers to biosynthesis in the CMPs of *S. fradiae* C373-10 were expressed in terms of carbon flux. All values are in mmoles.g^{-1} and converted to C.mmoles.g^{-1}, i.e., the flux, from each intermediate (Total mmoles.g^{-1}) was multiplied by the number of carbon atoms present in the molecular structure of the starting precursor of the pathway (Total C.mmoles.g^{-1}). <, denotes this monomer was below the detection limits of the appropriate assay. G6P, glucose-6-phosphate; TP, triose phosphate; PG, phosphoglycerate; PEP, phosphoenolpyruvate; PYR, pyruvate; OAA, Oxaloacetate; OGA, oxo-glutarate; AcCoA, acetyl-CoA; d, deoxy; A, adenine; C, cytosine; G, guanosine; U, uracil. Tables constructed as Holms. (1986, 1996, 1997, 2001) for theory and a worked example see Chapter 1, & Appendix B. nd, not determined.

Table 6.11. The amounts of precursor required for the biosynthesis of 1 g of *S. fradiae* C373-10 biomass; growth on glucose & glutamate Day 2 (Ferm 3).

Monomer content (mmoles.g^{-1})		G6P	TP	PG	PEP	PYR	OAA	OGA	AcCoA
Alanine	0.112					0.112			
Arginine	0.042							0.042	
Aspartate	0.121						0.121		
Asparagine	nd								
Cysteine	0.020			0.02					
Glutamate	0.124							0.124	
Glutamine	nd								
Glycine	0.128			0.128					
Histidine	0.022	0.022							
Isoleucine	0.079					0.079	0.079		
Leucine	0.138					0.276			0.138
Lysine	0.103					0.103	0.103		
Methionine	<0.001						0.001		
Phenylalanine	0.029	0.029			0.058				
Proline	0.061							0.061	
Serine	0.014			0.014					
Threonine	0.052						0.052		
Tryptophan	0.023	0.046			0.023				
Tyrosine	0.080	0.08			0.16				
Valine	0.065					0.13			
A	0.050	0.05		0.05					
dA	0.011	0.011		0.011					
G	0.078	0.078		0.078					
dG	0.025	0.025		0.025					
C	0.061	0.061					0.061		
dC	0.025	0.025					0.025		
U	0.044	0.044					0.044		
dT	0.011	0.011					0.011		
C16 FA	0.572					0.366	0.032		4.742
Glycerophosphate	0.216		0.216						
Carbohydrate	0.739	0.739							
Total draw of monomers to biosynthesis (mmoles.g^{-1})		**1.22**	**0.216**	**0.326**	**0.241**	**1.066**	**0.528**	**0.227**	**4.88**
Total draw of carbon to biosynthesis (C.mmoles.g^{-1})		**7.322**	**0.648**	**0.978**	**0.723**	**3.197**	**2.11**	**1.134**	**9.76**

The total demand of monomers to biosynthesis in the CMPs of *S. fradiae* C373-10 were expressed in terms of carbon flux. All values are in mmoles.g^{-1} and converted to C.mmoles.g^{-1}, i.e., the flux, from each intermediate (Total mmoles.g^{-1}) was multiplied by the number of carbon atoms present in the molecular structure of the starting precursor of the pathway (Total C.mmoles.g^{-1}). <, denotes this monomer was below the detection limits of the appropriate assay. G6P, glucose-6-phosphate; TP, triose phosphate; PG, phosphoglycerate; PEP, phosphoenolpyruvate; PYR, pyruvate; OAA, Oxaloacetate; OGA, oxo-glutarate; AcCoA, acetyl-CoA; d, deoxy; A, adenine; C, cytosine; G, guanosine; U, uracil. Tables constructed as Holms. (1986, 1996, 1997, 2001) for theory and a worked example see Chapter 1, & Appendix B.

Table 6.12. The amounts of precursor required for the biosynthesis of 1 g of *S. fradiae* C373-10 biomass; growth on glucose & glutamate Day 2 (Ferm 4).

Monomer content (mmoles.g^{1})		G6P	TP	PG	PEP	PYR	OAA	OGA	AcCoA
Alanine	0.111					0.111			
Arginine	0.034							0.034	
Aspartate	0.061						0.061		
Asparagine	nd								
Cysteine	0.009			0.009					
Glutamate	0.063							0.063	
Glutamine	nd								
Glycine	0.063			0.063					
Histidine	<0.001	0.001							
Isoleucine	0.043					0.043	0.043		
Leucine	<0.001					0.001			0.002
Lysine	0.067					0.067	0.067		
Methionine	<0.001						0.001		
Phenylalanine	0.015	0.015			0.03				
Proline	0.031							0.031	
Serine	<0.001			0.001					
Threonine	0.022						0.022		
Tryptophan	<0.001	0.002			0.001				
Tyrosine	0.004	0.004			0.008				
Valine	0.004					0.008			
A	0.064	0.064		0.064					
dA	0.013	0.013		0.013					
G	0.097	0.097		0.097					
dG	0.031	0.031		0.031					
C	0.040	0.04					0.04		
dC	0.031	0.031					0.031		
U	0.056	0.056					0.056		
dT	0.013	0.013					0.013		
C16 FA	0.298					0.191	0.017		2.473
Glycerophosphate	0.113		0.113						
Carbohydrate	0.845	0.845							
Total draw of monomers to biosynthesis (mmoles.g^{-1})		**1.213**	**0.113**	**0.276**	**0.034**	**0.42**	**0.35**	**0.128**	**2.473**

Total draw of carbon to biosynthesis (C.mmoles.g^{-1})		**7.276**	**0.339**	**0.829**	**0.102**	**1.259**	**1.399**	**0.639**	**4.946**

The total demand of monomers to biosynthesis in the CMPs of *S. fradiae* C373-10 were expressed in terms of carbon flux. All values are in mmoles.g^{-1} and converted to C.mmoles.g^{-1}, i.e., the flux, from each intermediate (Total mmoles.g^{-1}) was multiplied by the number of carbon atoms present in the molecular structure of the starting precursor of the pathway (Total C.mmoles.g^{-1}). <, denotes this monomer was below the detection limits of the appropriate assay. G6P, glucose-6-phosphate; TP, triose phosphate; PG, phosphoglycerate; PEP, phosphoenolpyruvate; PYR, pyruvate; OAA, Oxaloacetate; OGA, oxo-glutarate; AcCoA, acetyl-CoA; d, deoxy; A, adenine; C, cytosine; G, guanosine; U, uracil. Tables constructed as Holms. (1986, 1996, 1997, 2001) for theory and a worked example see Chapter 1, & Appendix B. nd, not determined.

Table 6.13. The amounts of precursor required for the biosynthesis of 1 g of *S. fradiae* C373-10 biomass; growth on glucose & glutamate Day 5 (Ferm 1).

Monomer content (mmoles.g^{-1})		G6P	TP	PG	PEP	PYR	OAA	OGA	AcCoA
Alanine	0.342					0.342			
Arginine	0.412							0.412	
Aspartate	0.298						0.298		
Asparagine	nd								
Cysteine	0.061			0.061					
Glutamate	0.214							0.214	
Glutamine	nd								
Glycine	0.444			0.444					
Histidine	0.079	0.079							
Isoleucine	0.213					0.213	0.213		
Leucine	0.186					0.372			0.186
Lysine	0.261					0.261	0.261		
Methionine	0.059						0.059		
Phenylalanine	0.045	0.045			0.09				
Proline	0.164							0.164	
Serine	0.039			0.039					
Threonine	0.309						0.309		
Tryptophan	<0.001	0.002			0.001				
Tyrosine	0.111	0.111			0.222				
Valine	0.382					0.764			
A	0.038	0.038		0.038					
dA	0.021	0.021		0.021					
G	0.058	0.058		0.058					
dG	0.049	0.049		0.049					
C	0.046	0.046					0.046		
dC	0.049	0.049					0.049		
U	0.034	0.034					0.034		
dT	0.021	0.021					0.021		
C16 FA	1.171					0.749	0.065		9.71
Glycerophosphate	0.442		0.442						
Carbohydrate	0.485	0.485							
Total draw of monomers to biosynthesis (mmoles.g^{-1})		**1.035**	**0.442**	**0.71**	**0.312**	**2.701**	**1.355**	**0.79**	**9.896**

Total draw of carbon to biosynthesis (C.mmoles.g^{-1})	**6.212**	**1.326**	**2.13**	**0.936**	**8.104**	**5.419**	**3.952**	**19.792**

The total demand of monomers to biosynthesis in the CMPs of *S. fradiae* C373-10 were expressed in terms of carbon flux. All values are in mmoles.g^{-1} and converted to C.mmoles.g^{-1}, i.e., the flux, from each intermediate (Total mmoles.g^{-1}) was multiplied by the number of carbon atoms present in the molecular structure of the starting precursor of the pathway (Total C.mmoles.g^{-1}). <, denotes this monomer was below the detection limits of the appropriate assay. G6P, glucose-6-phosphate; TP, triose phosphate; PG, phosphoglycerate; PEP, phosphoenolpyruvate; PYR, pyruvate; OAA, Oxaloacetate; OGA, oxo-glutarate; AcCoA, acetyl-CoA; d, deoxy; A, adenine; C, cytosine; G, guanosine; U, uracil. Tables constructed as Holms. (1986, 1996, 1997, 2001) for theory and a worked example see Chapter 1, & Appendix B. nd, not determined.

Table 6.14. The amounts of precursor required for the biosynthesis of 1 g of *S. fradiae* C373-10 biomass; growth on glucose & glutamate Day 5 (Ferm 2).

Monomer content (mmoles.g^{1})		G6P	TP	PG	PEP	PYR	OAA	OGA	AcCoA
Alanine	0.342					0.342			
Arginine	0.157							0.157	
Aspartate	0.337						0.337		
Asparagine	nd								
Cysteine	0.058			0.057					
Glutamate	0.274							0.274	
Glutamine	nd								
Glycine	0.237			0.237					
Histidine	0.083	0.083							
Isoleucine	0.126					0.126	0.126		
Leucine	0.193					0.386			0.193
Lysine	0.095					0.095	0.095		
Methionine	<0.001						0.001		
Phenylalanine	0.119	0.119			0.238				
Proline	0.159							0.159	
Serine	0.005			0.005					
Threonine	0.185						0.185		
Tryptophan	0.023	0.046			0.023				
Tyrosine	0.607	0.607			1.214				
Valine	0.410	0.023				0.82			
A	0.034	0.033		0.033					
dA	0.018	0.018		0.018					
G	0.049	0.049		0.049					
dG	0.069	0.069		0.069					
C	0.040	0.04					0.04		
dC	0.069	0.069					0.069		
U	0.029	0.029					0.029		
dT	0.018	0.018					0.018		
C16 FA	1.270					0.812	0.071		10.529
Glycerophosphate	0.479		0.479						
Carbohydrate	0.510	0.510							
Total draw of monomers to biosynthesis (mmoles.g^{-1})		**1.711**	**0.479**	**0.467**	**1.475**	**2.581**	**0.968**	**0.59**	**10.722**

Total draw of carbon to biosynthesis (C.mmoles.g^{-1})	**10.26**	**1.437**	**1.401**	**4.425**	**7.744**	**3.873**	**2.949**	**21.444**

The total demand of monomers to biosynthesis in the CMPs of *S. fradiae* C373-10 were expressed in terms of carbon flux. All values are in mmoles.g^{-1} and converted to C.mmoles.g^{-1}, i.e., the flux, from each intermediate (Total mmoles.g^{-1}) was multiplied by the number of carbon atoms present in the molecular structure of the starting precursor of the pathway (Total C.mmoles.g^{-1}). <, denotes this monomer was below the detection limits of the appropriate assay. G6P, glucose-6-phosphate; TP, triose phosphate; PG, phosphoglycerate; PEP, phosphoenolpyruvate; PYR, pyruvate; OAA, Oxaloacetate; OGA, oxo-glutarate; AcCoA, acetyl-CoA; d, deoxy; A, adenine; C, cytosine; G, guanosine; U, uracil. Tables constructed as Holms. (1986, 1996, 1997, 2001) for theory and a worked example see Chapter 1, & Appendix B. nd, not determined.

Table 6.15. The amounts of precursor required for the biosynthesis of 1 g of *S. fradiae* C373-10 biomass; growth on glucose & glutamate Day 5 (Ferm 3).

Monomer content (mmoles.g^{-1})		G6P	TP	PG	PEP	PYR	OAA	OGA	AcCoA
Alanine	0.212					0.212			
Arginine	0.118							0.118	
Aspartate	0.223						0.223		
Asparagine	nd								
Cysteine	0.037			0.037					
Glutamate	0.182							0.182	
Glutamine	nd								
Glycine	0.139			0.139					
Histidine	0.048	0.048							
Isoleucine	0.089					0.089	0.089		
Leucine	0.105					0.21			0.105
Lysine	0.069					0.069	0.069		
Methionine	<0.001						0.001		
Phenylalanine	0.008	0.008			0.016				
Proline	0.097							0.097	
Serine	0.034			0.034					
Threonine	0.124						0.124		
Tryptophan	0.004	0.008			0.004				
Tyrosine	0.363	0.363			0.726				
Valine	0.324					0.648			
A	0.048	0.048		0.048					
dA	0.029	0.029		0.029					
G	0.072	0.072		0.072					
dG	0.069	0.069		0.069					
C	0.058	0.058					0.058		
dC	0.069	0.069					0.069		
U	0.042	0.042					0.042		
dT	0.029	0.029					0.029		
C16 FA	1.249					0.799	0.07		10.358
Glycerophosphate	0.472		0.472						
Carbohydrate	0.336	0.336							
Total draw of monomers to biosynthesis (mmoles.g^{-1})		**1.178**	**0.472**	**0.427**	**0.746**	**2.027**	**0.772**	**0.397**	**10.463**
Total draw of carbon to biosynthesis (C.mmoles.g^{-1})		**7.07**	**1.416**	**1.281**	**2.238**	**6.081**	**3.089**	**1.987**	**20.926**

The total demand of monomers to biosynthesis in the CMPs of *S. fradiae* C373-10 were expressed in terms of carbon flux. All values are in mmoles.g^{-1} and converted to C.mmoles.g^{-1}, i.e., the flux, from each intermediate (Total mmoles.g^{-1}) was multiplied by the number of carbon atoms present in the molecular structure of the starting precursor of the pathway (Total C.mmoles.g^{-1}). <, denotes this monomer was below the detection limits of the appropriate assay. G6P, glucose-6-phosphate; TP, triose phosphate; PG, phosphoglycerate; PEP, phosphoenolpyruvate; PYR, pyruvate; OAA, Oxaloacetate; OGA, oxo-glutarate; AcCoA, acetyl-CoA; d, deoxy; A, adenine; C, cytosine; G, guanosine; U, uracil. Tables constructed as Holms. (1986, 1996, 1997, 2001) for theory and a worked example see Chapter 1, & Appendix B. nd, not determined.

Table 6.16. The amounts of precursor required for the biosynthesis of 1 g of *S. fradiae* C373-10 biomass; growth on glucose & glutamate Day 5 (Ferm 4).

Monomer content (mmoles.g^{-1})		G6P	TP	PG	PEP	PYR	OAA	OGA	AcCoA
Alanine	0.455					0.455			
Arginine	0.526							0.526	
Aspartate	0.523						0.523		
Asparagine	nd								
Cysteine	0.070			0.070					
Glutamate	0.442							0.442	
Glutamine	nd								
Glycine	0.401			0.401					
Histidine	0.101	0.101							
Isoleucine	0.210					0.21	0.21		
Leucine	0.359					0.718			0.359
Lysine	<0.001					0.001	0.001		
Methionine	<0.002						0.002		
Phenylalanine	0.127	0.127			0.254				
Proline	0.202							0.202	
Serine	0.062			0.062					
Threonine	0.264						0.264		
Tryptophan	<0.001	0.002			0.001				
Tyrosine	0.087	0.087			0.174				
Valine	0.354					0.708			
A	0.029	0.029		0.029					
dA	0.020	0.02		0.02					
G	0.044	0.044		0.044					
dG	0.047	0.047		0.047					
C	0.035	0.035					0.035		
dC	0.047	0.047					0.047		
U	0.026	0.026					0.026		
dT	0.02	0.02					0.02		
C16 FA	1.367					0.874	0.076		11.333
Glycerophosphate	0.516		0.516						
Carbohydrate	0.356	0.356							
Total draw of monomers to biosynthesis (mmoles.g^{-1})		**0.939**	**0.516**	**0.674**	**0.428**	**2.965**	**1.203**	**1.17**	**11.692**
Total draw of carbon to biosynthesis (C.mmoles.g^{-1})		**5.635**	**1.548**	**2.021**	**1.284**	**8.896**	**4.811**	**5.852**	**23.384**

The total demand of monomers to biosynthesis in the CMPs of *S. fradiae* C373-10 were expressed in terms of carbon flux. All values are in mmoles.g^{-1} and converted to C.mmoles.g^{-1}, i.e., the flux, from each intermediate (Total mmoles.g^{-1}) was multiplied by the number of carbon atoms present in the molecular structure of the starting precursor of the pathway (Total C.mmoles.g^{-1}). <, denotes this monomer was below the detection limits of the appropriate assay. G6P, glucose-6-phosphate; TP, triose phosphate; PG, phosphoglycerate; PEP, phosphoenolpyruvate; PYR, pyruvate; OAA, Oxaloacetate; OGA, oxo-glutarate; AcCoA, acetyl-CoA; d, deoxy; A, adenine; C, cytosine; G, guanosine; U, uracil. Tables constructed as Holms. (1986, 1996, 1997, 2001) for theory and a worked example see Chapter 1, & Appendix B. nd, not determined.

Table 6.17 The amounts of precursor required for the biosynthesis of 1 g of *S. fradiae* C373-10 biomass; growth on glucose & oxo-glutamate Day 3 (Ferm 1).

Monomer content (mmoles.g^{-1})		G6P	TP	PG	PEP	PYR	OAA	OGA	AcCoA
Alanine	0.361					0.361			
Arginine	0.183							0.183	
Aspartate	0.368						0.368		
Asparagine	nd								
Cysteine	0.053			0.053					
Glutamate	0.246							0.246	
Glutamine	nd								
Glycine	0.263			0.263					
Histidine	0.085	0.085							
Isoleucine	0.344					0.344	0.344		
Leucine	0.089					0.178			0.089
Lysine	0.157					0.157	0.157		
Methionine	<0.001						0.001		
Phenylalanine	0.143	0.143			0.286				
Proline	0.148							0.148	
Serine	0.042			0.042					
Threonine	0.189						0.189		
Tryptophan	0.017	0.034			0.017				
Tyrosine	0.084	0.084			0.168				
Valine	0.396	0.017				0.792			
A	0.098	0.098		0.098					
dA	0.005	0.005		0.005					
G	0.147	0.147		0.147					
dG	0.010	0.01		0.01					
C	0.118	0.118					0.118		
dC	0.010	0.01					0.01		
U	0.086	0.086					0.086		
dT	0.005	0.005					0.005		
C16 FA	0.066					0.042	0.004		0.545
Glycerophosphate	0.025		0.025						
Carbohydrate	0.270	0.270							
Total draw of monomers to biosynthesis (mmoles.g^{-1})		**1.111**	**0.025**	**0.618**	**0.471**	**1.874**	**1.28**	**0.577**	**0.634**
Total draw of carbon to biosynthesis (C.mmoles.g^{-1})		**6.668**	**0.074**	**1.855**	**1.413**	**5.622**	**5.121**	**2.886**	**1.268**

The total demand of monomers to biosynthesis in the CMPs of *S. fradiae* C373-10 were expressed in terms of carbon flux. All values are in mmoles.g^{-1} and converted to C.mmoles.g^{-1}, i.e., the flux, from each intermediate (Total mmoles.g^{-1}) was multiplied by the number of carbon atoms present in the molecular structure of the starting precursor of the pathway (Total C.mmoles.g^{-1}). <, denotes this monomer was below the detection limits of the appropriate assay. G6P, glucose-6-phosphate; TP, triose phosphate; PG, phosphoglycerate; PEP, phosphoenolpyruvate; PYR, pyruvate; OAA, Oxaloacetate; OGA, oxo-glutarate; AcCoA, acetyl-CoA; d, deoxy; A, adenine; C, cytosine; G, guanosine; U, uracil. Tables constructed as Holms. (1986, 1996, 1997, 2001) for theory and a worked example see Chapter 1, & Appendix B. nd, not determined.

Table 6.18 The amounts of precursor required for the biosynthesis of 1 g of *S. fradiae* C373-10 biomass; growth on glucose & oxo-glutamate Day 3 (Ferm 2).

Monomer content (mmoles.g^{-1})		G6P	TP	PG	PEP	PYR	OAA	OGA	AcCoA
Alanine	0.314					0.314			
Arginine	0.088							0.088	
Aspartate	0.262						0.262		
Asparagine	nd								
Cysteine	0.051			0.051					
Glutamate	0.227							0.227	
Glutamine	nd								
Glycine	0.217			0.217					
Histidine	0.088	0.088							
Isoleucine	0.127					0.127	0.127		
Leucine	0.174					0.348			0.174
Lysine	0.100					0.100	0.100		
Methionine	<0.001						0.001		
Phenylalanine	0.110	0.110			0.220				
Proline	0.135							0.1347	
Serine	0.039			0.039					
Threonine	0.175						0.175		
Tryptophan	<0.001	0.002			0.001				
Tyrosine	0.436	0.436			0.872				
Valine	0.458					0.916			
A	0.027	0.027		0.027					
dA	0.002	0.002		0.002					
G	0.041	0.041		0.041					
dG	0.005	0.005		0.005					
C	0.033	0.033					0.033		
dC	0.005	0.005					0.005		
U	0.024	0.024					0.024		
dT	0.002	0.002					0.002		
C16 FA	0.064					0.041	0.003		0.526
Glycerophosphate	0.024		0.024						
Carbohydrate	0.521	0.521							
Total draw of monomers to biosynthesis (mmoles.g^{-1})		**1.294**	**0.024**	**0.382**	**1.092**	**1.846**	**0.7313**	**0.450**	**0.701**
Total draw of carbon to biosynthesis (C.mmoles.g^{-1})		**7.764**	**0.072**	**1.146**	**3.276**	**5.537**	**2.925**	**2.249**	**1.401**

The total demand of monomers to biosynthesis in the CMPs of *S. fradiae* C373-10 were expressed in terms of carbon flux. All values are in mmoles.g^{-1} and converted to C.mmoles.g^{-1}, i.e., the flux, from each intermediate (Total mmoles.g^{-1}) was multiplied by the number of carbon atoms present in the molecular structure of the starting precursor of the pathway (Total C.mmoles.g^{-1}). <, denotes this monomer was below the detection limits of the appropriate assay. G6P, glucose-6-phosphate; TP, triose phosphate; PG, phosphoglycerate; PEP, phosphoenolpyruvate; PYR, pyruvate; OAA, Oxaloacetate; OGA, oxo-glutarate; AcCoA, acetyl-CoA; d, deoxy; A, adenine; C, cytosine; G, guanosine; U, uracil. Tables constructed as Holms. (1986, 1996, 1997, 2001) for theory and a worked example see Chapter 1, & Appendix B. nd, not determined.

Table 6.19. The amounts of precursor required for the biosynthesis of 1 g of *S. fradiae* C373-10 biomass; growth on glucose & oxo-glutamate Day 7 (Ferm 1).

Monomer content (mmoles.g^{-1})		G6P	TP	PG	PEP	PYR	OAA	OGA	AcCoA
Alanine	0.267					0.267			
Arginine	0.791							0.791	
Aspartate	0.255						0.255		
Asparagine	nd								
Cysteine	0.060			0.06					
Glutamate	0.388							0.388	
Glutamine	nd								
Glycine	0.868			0.868					
Histidine	0.083	0.083							
Isoleucine	0.100					0.100	0.100		
Leucine	0.230					0.46			0.230
Lysine	<0.001					0.001	0.001		
Methionine	<0.001						0.001		
Phenylalanine	0.080	0.08			0.16				
Proline	0.183							0.183	
Serine	0.008			0.008					
Threonine	0.017						0.017		
Tryptophan	<0.001	0.002			0.001				
Tyrosine	0.050	0.05			0.100				
Valine	0.178					0.356			
A	0.070	0.07		0.07					
dA	0.158	0.158		0.158					
G	0.105	0.105		0.105					
dG	0.037	0.037		0.037					
C	0.084	0.084					0.084		
dC	0.037	0.037					0.037		
U	0.061	0.061					0.061		
dT	0.158	0.158					0.158		
C16 FA	0.124					0.079	0.007		1.027
Glycerophosphate	0.047		0.047						
Carbohydrate	0.360	0.360							
Total draw of monomers to biosynthesis (mmoles.g^{-1})		**1.282**	**0.047**	**1.304**	**0.26**	**1.262**	**0.719**	**1.361**	**1.257**
Total draw of carbon to biosynthesis (C.mmoles.g^{-1})		**7.693**	**0.14**	**3.913**	**0.781**	**3.786**	**2.876**	**6.806**	**2.513**

The total demand of monomers to biosynthesis in the CMPs of *S. fradiae* C373-10 were expressed in terms of carbon flux. All values are in mmoles.g^{-1} and converted to C.mmoles.g^{-1}, i.e., the flux, from each intermediate (Total mmoles.g^{-1}) was multiplied by the number of carbon atoms present in the molecular structure of the starting precursor of the pathway (Total C.mmoles.g^{-1}). <, denotes this monomer was below the detection limits of the appropriate assay. G6P, glucose-6-phosphate; TP, triose phosphate; PG, phosphoglycerate; PEP, phosphoenolpyruvate; PYR, pyruvate; OAA, Oxaloacetate; OGA, oxo-glutarate; AcCoA, acetyl-CoA; d, deoxy; A, adenine; C, cytosine; G, guanosine; U, uracil. Tables constructed as Holms. (1986, 1996, 1997, 2001) for theory and a worked example see Chapter 1, & Appendix B. nd, not determined.

Table 6.20 The amounts of precursor required for the biosynthesis of 1 g of *S. fradiae* C373-10 biomass; growth on glucose & oxo-glutamate Day 7 (Ferm 2).

Monomer content (mmoles.g^{-})		G6P	TP	PG	PEP	PYR	OAA	OGA	AcCoA
Alanine	0.397					0.397			
Arginine	0.708							0.708	
Aspartate	0.206						0.206		
Asparagine	nd								
Cysteine	0.052			0.052					
Glutamate	0.344							0.344	
Glutamine	nd								
Glycine	0.729			0.729					
Histidine	0.053	0.053							
Isoleucine	0.075					0.075	0.075		
Leucine	0.158					0.316			0.158
Lysine	<0.001					0.001	0.001		
Methionine	0.009						0.009		
Phenylalanine	0.062	0.062			0.123				
Proline	0.171							0.171	
Serine	0.026			0.026					
Threonine	0.013						0.013		
Tryptophan	<0.001	0.002			0.001				
Tyrosine	<0.001	0.001			0.002				
Valine	0.129					0.258			
A	0.025	0.025		0.025					
dA	0.008	0.008		0.008					
G	0.037	0.037		0.037					
dG	0.020	0.02		0.02					
C	0.030	0.03					0.03		
dC	0.020	0.02					0.02		
U	0.022	0.022					0.022		
dT	0.008	0.008					0.008		
C16 FA	0.125					0.08	0.007		1.036
Glycerophosphate	0.047		0.047						
Carbohydrate	0.166	0.166							
Total draw of monomers to biosynthesis (mmoles.g^{-1})		**0.45**	**0.047**	**0.897**	**0.123**	**1.127**	**0.39**	**1.222**	**1.194**
Total draw of carbon to biosynthesis (C.mmoles.g^{-1})		**2.70**	**0.142**	**2.692**	**0.370**	**3.381**	**1.559**	**6.112**	**2.388**

The total demand of monomers to biosynthesis in the CMPs of *S. fradiae* C373-10 were expressed in terms of carbon flux. All values are in mmoles.g^{-1} and converted to C.mmoles.g^{-1}, i.e., the flux, from each intermediate (Total mmoles.g^{-1}) was multiplied by the number of carbon atoms present in the molecular structure of the starting precursor of the pathway (Total C.mmoles.g^{-1}). <, denotes this monomer was below the detection limits of the appropriate assay. G6P, glucose-6-phosphate; TP, triose phosphate; PG, phosphoglycerate; PEP, phosphoenolpyruvate; PYR, pyruvate; OAA, Oxaloacetate; OGA, oxo-glutarate; AcCoA, acetyl-CoA; d, deoxy; A, adenine; C, cytosine; G, guanosine; U, uracil. Tables constructed as Holms. (1986, 1996, 1997, 2001) for theory and a worked example see Chapter 1, & Appendix B. nd, not determined.

Table 6.21 The amounts of precursor required for the biosynthesis of 1 g of *S. fradiae* C373-10 biomass; growth on Grays medium glucose, glutamate & methyl-oleate Day 3 (Ferm 1).

Monomer content (mmoles.g^{-1})		G6P	TP	PG	PEP	PYR	OAA	OGA	AcCoA
Alanine	0.203					0.203			
Arginine	0.352							0.352	
Aspartate	0.150						0.15		
Asparagine	nd								
Cysteine	0.031			0.031					
Glutamate	0.175							0.175	
Glutamine	nd								
Glycine	0.212			0.212					
Histidine	0.044	0.044							
Isoleucine	0.099					0.099	0.099		
Leucine	0.091					0.182			0.091
Lysine	0.071					0.071	0.071		
Methionine	<0.001						0.001		
Phenylalanine	0.051	0.051			0.102				
Proline	0.092							0.092	
Serine	0.023			0.023					
Threonine	0.101						0.102		
Tryptophan	<0.001	0.002			0.001				
Tyrosine	0.029	0.029			0.058				
Valine	0.098					0.195			
A	0.018	0.018		0.018					
dA	0.005	0.005		0.005					
G	0.028	0.028		0.028					
dG	0.012	0.012		0.012					
C	0.021	0.021					0.021		
dC	0.012	0.012					0.012		
U	0.016	0.016					0.016		
dT	0.005	0.005					0.005		
C16 FA	0.167					0.299	0.019		1.476
Glycerophosphate	0.064		0.064						
Carbohydrate	0.034	0.034							
Total draw of monomers to biosynthesis (mmoles.g^{-1})		**0.275**	**0.064**	**0.327**	**0.161**	**1.049**	**0.495**	**0.618**	**1.567**
Total draw of carbon to biosynthesis (C.mmoles.g^{-1})		**1.651**	**0.192**	**0.982**	**0.483**	**3.148**	**1.979**	**3.092**	**3.134**

The total demand of monomers to biosynthesis in the CMPs of *S. fradiae* C373-10 were expressed in terms of carbon flux. All values are in mmoles.g^{-1} and converted to C.mmoles.g^{-1}, i.e., the flux, from each intermediate (Total mmoles.g^{-1}) was multiplied by the number of carbon atoms present in the molecular structure of the starting precursor of the pathway (Total C.mmoles.g^{-1}). <, denotes this monomer was below the detection limits of the appropriate assay. G6P, glucose-6-phosphate; TP, triose phosphate; PG, phosphoglycerate; PEP, phosphoenolpyruvate; PYR, pyruvate; OAA, Oxaloacetate; OGA, oxo-glutarate; AcCoA, acetyl-CoA; d, deoxy; A, adenine; C, cytosine; G, guanosine; U, uracil. Tables constructed as Holms. (1986, 1996, 1997, 2001) for theory and a worked example see Chapter 1, & Appendix B. nd, not determined.

Table 6.22. The amounts of precursor required for the biosynthesis of 1 g of *S. fradiae* C373-10 biomass; growth on methyl oleate defined medium Day 5 (Ferm 1).

Monomer content (mmoles.g^{-1})		G6P	TP	PG	PEP	PYR	OAA	OGA	AcCoA
Alanine	0.39					0.39			
Arginine	0.57							0.57	
Aspartate	0.302						0.302		
Asparagine	nd								
Cysteine	0.053			0.053					
Glutamate	0.329							0.329	
Glutamine	nd								
Glycine	0.441			0.441					
Histidine	0.072	0.072							
Isoleucine	0.151					0.151	0.151		
Leucine	0.172					0.344			0.172
Lysine	0.093					0.093	0.093		
Methionine	0.003						0.003		
Phenylalanine	0.067	0.067			0.134				
Proline	0.165							0.165	
Serine	0.0292			0.029					
Threonine	0.156						0.156		
Tryptophan	<0.001	0.002			0.001				
Tyrosine	0.04	0.04			0.08				
Valine	0.111					0.222			
A	0.022	0.022		0.022					
dA	0.004	0.004		0.004					
G	0.034	0.034		0.034					
dG	0.009	0.009		0.009					
C	0.027	0.027					0.027		
dC	0.009	0.009					0.009		
U	0.020	0.02					0.02		
dT	0.004	0.004					0.004		
C16 FA	0.167					0.299	0.019		1.476
Glycerophosphate	0.064		0.064						
Carbohydrate	0.153	0.153							
Total draw of monomers to biosynthesis (mmoles.g^{-1})		**0.46**	**0.064**	**0.592**	**0.214**	**1.499**	**0.783**	**1.064**	**1.648**
Total draw of carbon to biosynthesis (C.mmoles.g^{-1})		**2.762**	**0.192**	**1.775**	**0.642**	**4.497**	**3.134**	**5.318**	**3.296**

The total demand of monomers to biosynthesis in the CMPs of *S. fradiae* C373-10 were expressed in terms of carbon flux. All values are in mmoles.g^{-1} and converted to C.mmoles.g^{-1}, i.e., the flux, from each intermediate (Total mmoles.g^{-1}) was multiplied by the number of carbon atoms present in the molecular structure of the starting precursor of the pathway (Total C.mmoles.g^{-1}). <, denotes this monomer was below the detection limits of the appropriate assay. G6P, glucose-6-phosphate; TP, triose phosphate; PG, phosphoglycerate; PEP, phosphoenolpyruvate; PYR, pyruvate; OAA, Oxaloacetate; OGA, oxo-glutarate; AcCoA, acetyl-CoA; d, deoxy; A, adenine; C, cytosine; G, guanosine; U, uracil. Tables constructed as Holms. (1986, 1996, 1997, 2001) for theory and a worked example see Chapter 1, & Appendix B. nd, not determined.

Table 6.23 The amounts of precursor required for the biosynthesis of 1 g of *S. fradiae* C373-10 biomass; growth on methyl oleate defined medium Day 3 (Ferm 2).

Monomer content (mmoles.g^{-1})		G6P	TP	PG	PEP	PYR	OAA	OGA	AcCoA
Alanine	0.274					0.274			
Arginine	0.518							0.518	
Aspartate	0.280						0.281		
Asparagine	nd								
Cysteine	0.045			0.045					
Glutamate	0.304							0.304	
Glutamine	nd								
Glycine	0.305			0.305					
Histidine	0.062	0.062							
Isoleucine	0.149					0.149	0.149		
Leucine	0.148					0.296			0.148
Lysine	<0.001					0.001	0.001		
Methionine	0.007						0.007		
Phenylalanine	0.074	0.074			0.148				
Proline	0.133							0.133	
Serine	0.029			0.029					
Threonine	0.142						0.142		
Tryptophan	0.002	0.004			0.002				
Tyrosine	0.040	0.04			0.08				
Valine	0.161					0.323			
A	0.025	0.025		0.025					
dA	0.004	0.004		0.004					
G	0.037	0.037		0.037					
dG	0.009	0.009		0.009					
C	0.03	0.03					0.03		
dC	0.009	0.009					0.009		
U	0.022	0.022					0.022		
dT	0.004	0.004					0.004		
C16 FA	0.167					0.299	0.019		1.476
Glycerophosphate	0.064		0.064						
Carbohydrate	0.149	0.149							
Total draw of monomers to biosynthesis (mMoles.g^{-1})		**0.468**	**0.064**	**0.454**	**0.229**	**1.341**	**0.661**	**0.955**	**1.624**
Total draw of carbon to biosynthesis (C.mMoles.g^{-1})		**2.805**	**0.192**	**1.361**	**0.688**	**4.022**	**2.645**	**4.776**	**3.248**

The total demand of monomers to biosynthesis in the CMPs of *S. fradiae* C373-10 were expressed in terms of carbon flux. All values are in mmoles.g^{-1} and converted to C.mmoles.g^{-1}, i.e., the flux, from each intermediate (Total mmoles.g^{-1}) was multiplied by the number of carbon atoms present in the molecular structure of the starting precursor of the pathway (Total C.mmoles.g^{-1}). <, denotes this monomer was below the detection limits of the appropriate assay. G6P, glucose-6-phosphate; TP, triose phosphate; PG, phosphoglycerate; PEP, phosphoenolpyruvate; PYR, pyruvate; OAA, Oxaloacetate; OGA, oxo-glutarate; AcCoA, acetyl-CoA; d, deoxy; A, adenine; C, cytosine; G, guanosine; U, uracil. Tables constructed as Holms. (1986, 1996, 1997, 2001) for theory and a worked example see Chapter 1, & Appendix B. nd, not determined.

Table 6.24 The amounts of precursor required for the biosynthesis of 1 g of *S. fradiae* C373-10 biomass; growth on methyl oleate defined medium Day 5 (Ferm 2).

Monomer content (mmoles.g^{-1})		G6P	TP	PG	PEP	PYR	OAA	OGA	AcCoA
Alanine	0.295					0.295			
Arginine	0.386							0.386	
Aspartate	0.183						0.183		
Asparagine	nd								
Cysteine	0.035			0.035					
Glutamate	0.234							0.234	
Glutamine	nd								
Glycine	0.352			0.352					
Histidine	0.051	0.051							
Isoleucine	0.079					0.079	0.079		
Leucine	0.124					0.248			0.124
Lysine	0.047					0.047	0.047		
Methionine	<0.001						0.001		
Phenylalanine	0.037	0.037			0.073				
Proline	0.114							0.114	
Serine	0.0141			0.014					
Threonine	0.098						0.098		
Tryptophan	<0.001	0.002			0.001				
Tyrosine	0.023	0.023			0.046				
Valine	0.048					0.096			
A	0.022	0.023		0.023					
dA	0.005	0.005		0.005					
G	0.034	0.034		0.034					
dG	0.011	0.011		0.011					
C	0.027	0.027					0.027		
dC	0.011	0.011					0.011		
U	0.020	0.02					0.02		
dT	0.005	0.005					0.005		
C16 FA	0.167					0.299	0.019		1.476
Glycerophosphate	0.064		0.064						
Carbohydrate	0.126	0.126							
Total draw of monomers to biosynthesis (mmoles.g^{-1})		**0.371**	**0.064**	**0.474**	**0.119**	**1.064**	**0.49**	**0.735**	**1.600**
Total draw of carbon to biosynthesis (C.mmoles.g^{-1})		**2.226**	**0.192**	**1.421**	**0.356**	**3.193**	**1.96**	**3.675**	**3.200**

The total demand of monomers to biosynthesis in the CMPs of *S. fradiae* C373-10 were expressed in terms of carbon flux. All values are in mmoles.g^{-1} and converted to C.mmoles.g^{-1}, i.e., the flux, from each intermediate (Total mmoles.g^{-1}) was multiplied by the number of carbon atoms present in the molecular structure of the starting precursor of the pathway (Total C.mmoles.g^{-1}). <, denotes this monomer was below the detection limits of the appropriate assay. G6P, glucose-6-phosphate; TP, triose phosphate; PG, phosphoglycerate; PEP, phosphoenolpyruvate; PYR, pyruvate; OAA, Oxaloacetate; OGA, oxo-glutarate; AcCoA, acetyl-CoA; d, deoxy; A, adenine; C, cytosine; G, guanosine; U, uracil. Tables constructed as Holms. (1986, 1996, 1997, 2001) for theory and a worked example see Chapter 1, & Appendix B. nd, not determined.

Table 6.25 The amounts of precursor required for the biosynthesis of 1 g of *S. fradiae* C373-10 biomass; growth on methyl oleate defined medium Day 9 (Ferm 2).

Monomer content (mmoles.g^{-1})		G6P	TP	PG	PEP	PYR	OAA	OGA	AcCoA
Alanine	0.413					0.413			
Arginine	0.492							0.492	
Aspartate	0.328						0.328		
Asparagine	nd								
Cysteine	0.053			0.053					
Glutamate	0.344							0.344	
Glutamine	nd								
Glycine	0.495			0.495					
Histidine	0.068	0.068							
Isoleucine	0.213					0.213	0.213		
Leucine	0.124					0.248			0.124
Lysine	<0.001					0.001	0.001		
Methionine	<0.001						0.001		
Phenylalanine	0.077	0.077			0.155				
Proline	0.165							0.165	
Serine	0.039			0.039					
Threonine	0.162						0.162		
Tryptophan	<0.001	0.002			0.001				
Tyrosine	0.042	0.042			0.084				
Valine	0.161					0.322			
A	0.019	0.019		0.019					
dA	0.007	0.007		0.007					
G	0.028	0.028		0.028					
dG	0.015	0.015		0.015					
C	0.023	0.023					0.023		
dC	0.015	0.015					0.015		
U	0.017	0.017					0.017		
dT	0.007	0.007					0.007		
C16 FA	0.167					0.299	0.019		1.476
Glycerophosphate	0.064		0.064						
Carbohydrate	0.177	0.177							
Total draw of monomers to biosynthesis (mmoles.g^{-1})		**0.494**	**0.064**	**0.657**	**0.238**	**1.496**	**0.784**	**1.000**	**1.600**
Total draw of carbon to biosynthesis (C.mmoles.g^{-1})		**2.966**	**0.192**	**1.97**	**0.715**	**4.487**	**3.136**	**5.002**	**3.200**

The total demand of monomers to biosynthesis in the CMPs of *S. fradiae* C373-10 were expressed in terms of carbon flux. All values are in mmoles.g^{-1} and converted to C.mmoles.g^{-1}, i.e., the flux, from each intermediate (Total mmoles.g^{-1}) was multiplied by the number of carbon atoms present in the molecular structure of the starting precursor of the pathway (Total C.mmoles.g^{-1}). <, denotes this monomer was below the detection limits of the appropriate assay. G6P, glucose-6-phosphate; TP, triose phosphate; PG, phosphoglycerate; PEP, phosphoenolpyruvate; PYR, pyruvate; OAA, Oxaloacetate; OGA, oxo-glutarate; AcCoA, acetyl-CoA; d, deoxy; A, adenine; C, cytosine; G, guanosine; U, uracil. Tables constructed as Holms. (1986, 1996, 1997, 2001) for theory and a worked example see Chapter 1, & Appendix B. nd, not determined.

Table 6.26 The amounts of precursor required for the biosynthesis of 1 g of *S. fradiae* C373-10 biomass; average compositional table constructed from tables 6.3 to 7.21.

Monomer content (mmoles.g^{-1})		G6P	TP	PG	PEP	PYR	OAA	OGA	AcCoA
Alanine	0.337					0.337			
Arginine	0.380							0.380	
Aspartate	0.276						0.276		
Asparagine	nd								
Cysteine	0.049			0.049					
Glutamate	0.269							0.269	
Glutamine	nd								
Glycine	0.432			0.432					
Histidine	0.061	0.061							
Isoleucine	0.123					0.123	0.123		
Leucine	0.170					0.340			0.170
Lysine	0.054					0.054	0.054		
Methionine	0.006						0.006		
Phenylalanine	0.093	0.093			0.186				
Proline	0.146							0.146	
Serine	0.027			0.027					
Threonine	0.138						0.138		
Tryptophan	0.006	0.012			0.006				
Tyrosine	0.138	0.138			0.275				
Valine	0.227					0.454			
A	0.039	0.039		0.039					
dA	0.024	0.024		0.024					
G	0.059	0.059		0.059					
dG	0.032	0.032		0.032					
C	0.046	0.046					0.046		
dC	0.032	0.032					0.032		
U	0.034	0.034					0.034		
dT	0.024	0.024					0.024		
C16 FA	0.483					0.132	0.012		1.715
Glycerophosphate	0.182		0.182						
Carbohydrate	0.388	0.389							
Total draw of monomers to biosynthesis (mmoles.g^{-1})		**0.982**	**0.182**	**0.662**	**0.468**	**1.441**	**0.745**	**0.795**	**1.88**
Total draw of carbon to biosynthesis (C.mmoles.g^{-1})		**5.89**	**0.547**	**1.986**	**1.403**	**4.322**	**2.978**	**3.977**	**3.77**

The total demand of monomers to biosynthesis in the CMPs of *S. fradiae* C373-10 were expressed in terms of carbon flux. All values are in mmoles.g^{-1} and converted to C.mmoles.g^{-1}, i.e., the flux, from each intermediate (Total mmoles.g^{-1}) was multiplied by the number of carbon atoms present in the molecular structure of the starting precursor of the pathway (Total C.mmoles.g^{-1}). <, denotes this monomer was below the detection limits of the appropriate assay. G6P, glucose-6-phosphate; TP, triose phosphate; PG, phosphoglycerate; PEP, phosphoenolpyruvate; PYR, pyruvate; OAA, Oxaloacetate; OGA, oxo-glutarate; AcCoA, acetyl-CoA; d, deoxy; A, adenine; C, cytosine; G, guanosine; U, uracil. Tables constructed as Holms. (1986, 1996, 1997, 2001) for theory and a worked example see Chapter 1, & Appendix B. nd, not determined.

Table 6.27 The amounts of precursor required for the biosynthesis of 1 g of *S. fradiae* C373-18 biomass; for the complex industrial medium (Ferm 1; Day 3)

Monomer content (mmoles.g^{-1})		G6P	TP	PG	PEP	PYR	OAA	OGA	AcCoA
Alanine	0.18					0.18			
Arginine	0.08							0.08	
Aspartate	0.257						0.257		
Asparagine	nd								
Cysteine	0.042			0.042					
Glutamate	0.267							0.267	
Glutamine	nd								
Glycine	0.215			0.215					
Histidine	0.086	0.085							
Isoleucine	0.118					0.118	0.118		
Leucine	0.291					0.582			0.291
Lysine	0.679					0.679	0.679		
Methionine	0.002						0.002		
Phenylalanine	0.059	0.058			0.117				
Proline	0.131							0.131	
Serine	0.028			0.028					
Threonine	0.096						0.096		
Tryptophan	0.112	0.223			0.111				
Tyrosine	0.029	0.029			0.059				
Valine	0.006					0.012			
A	0.027	0.026		0.027					
dA	0.006	0.006		0.006					
G	0.04	0.040		0.040					
dG	0.014	0.014		0.014					
C	0.023	0.023					0.023		
dC	0.014	0.014					0.014		
U	0.023	0.023					0.023		
DT	0.006	0.006					0.006		
C16 FA	0.167					0.299	0.019		1.476
Glycerophosphate	0.064		0.064						
Carbohydrate	0.021	0.021							
Total draw of monomers to biosynthesis (mmoles.g^{-1})		**0.574**	**0.064**	**0.372**	**0.288**	**1.869**	**1.084**	**0.478**	**1.77**
Total draw of carbon to biosynthesis (C.mmoles.g^{-1})		**3.446**	**0.192**	**1.118**	**0.865**	**5.608**	**4.338**	**2.390**	**3.534**

The total demand of monomers to biosynthesis in the CMPs of *S. fradiae* C373-18 to biosynthesis were expressed in terms of carbon flux. All values are in mmoles.g^{-1} and converted to C.mmoles.g^{-1}, i.e., the flux, from each intermediate (Total mmoles.g^{-1}) was multiplied by the number of carbon atoms present in the molecular structure of the starting precursor of the pathway (Total C.mmoles.g^{-1}). <, denotes this monomer was below the detection limits of the appropriate assay. G6P, glucose-6-phosphate; TP, triose phosphate; PG, phosphoglycerate; PEP, phosphoenolpyruvate; PYR, pyruvate; OAA, Oxaloacetate; OGA, oxo-glutarate; AcCoA, acetyl-CoA; d, deoxy; A, adenine; C, cytosine; G, guanosine; U, uracil. Tables constructed as Holms. (1986, 1996, 1997, 2001) for theory and a worked example see Chapter 1, & Appendix B. nd, not determined.

Compendium

Normalised flux diagrams

Fig 6.1. Normalised flux diagram for *S. coelicolor* 1147 growing on glucose [Ferm 1] (C.mmoles.g^{-1} dry wt biomass. h^{-1} normalised to 100 % of input).

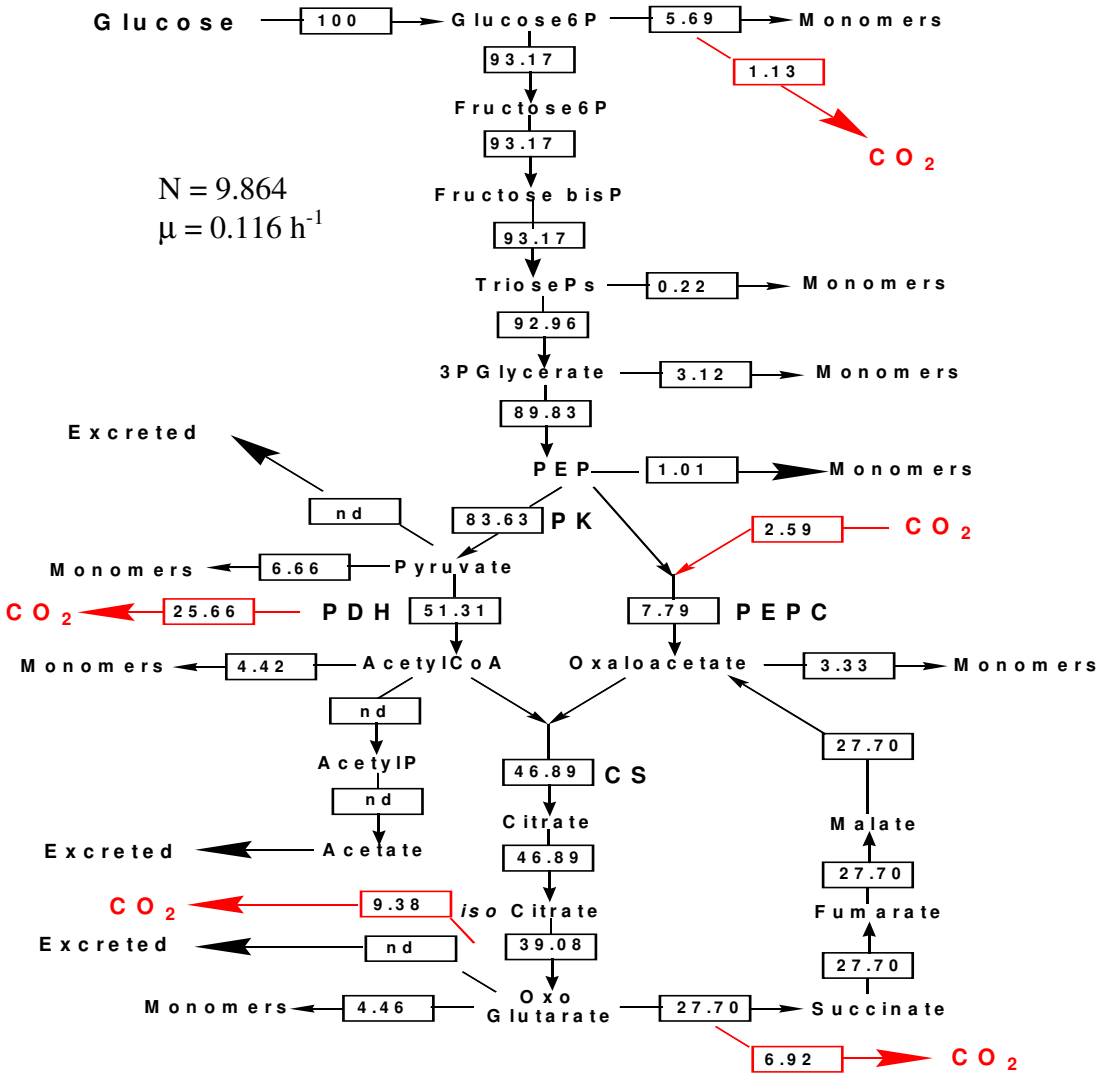

The diagram was constructed using data from Table 6.1. The values were calculated by subtracting the amount of precursors required for biosynthesis of the biomass from the input carbon source. Glucose6P, glucose-6-phosphate; PK, pyruvate kinase; TriosePs, triose phosphate; 3PGlycerate, glyceraldehyde-3-phosphate; PEP, phosphoenolpyruvate; fructose6P, fructose-6-phosphate; fructose bisP, fructose 1,6-diphosphate; acetylP, acetyl phosphate; CS, citrate synthase, CO_2, carbon dioxide. The remaining flux to CO_2 is via pyruvate dehydrogenase (PDH), isocitrate dehydrogenase, oxo-glutarate dehydrogenase, phosphoenolpyruvate carboxylase (PEPC) and enzymes of the PP pathway. Dividing the normalised fluxes by the normalising factor (N), converts the normalised units to C.mmoles.g^{-1} dry wt biomass h^{-1}. Dividing these figures by the specific growth rate (μ), converts the diagram to throughputs (C.mmoles.g^{-1}). All workings are contained in the compendium if required (Fig 6.1). The μ was taken as the reconciled value (as Chapter 4, Table 4.12). nd, not determined.

Fig 6.2. Normalised flux diagram for *S. coelicolor* 1147 growing on glucose [Ferm 2](C.mmoles.g^{-1} dry wt biomass. h^{-1} normalised to 100 % of input).

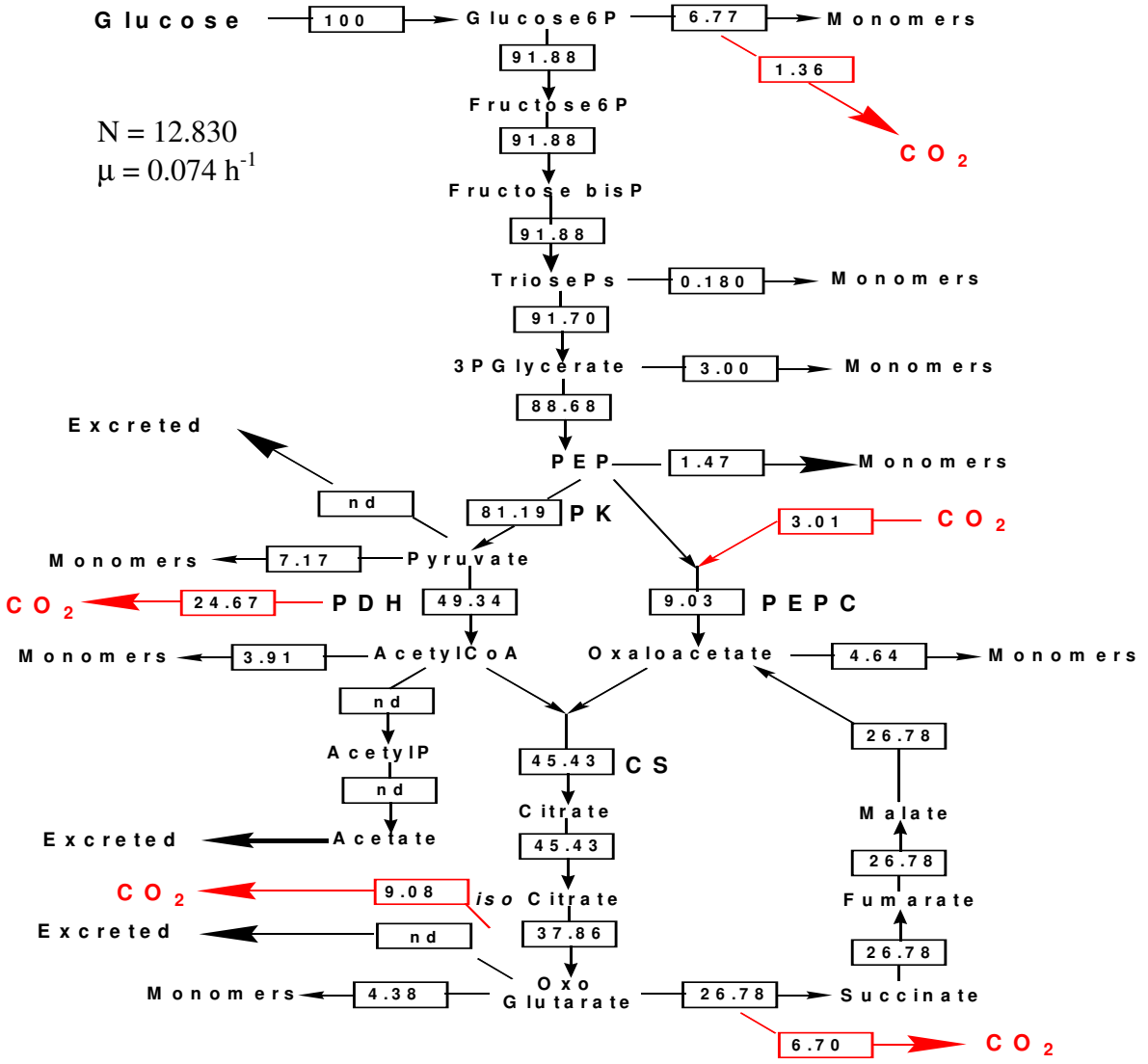

The diagram was constructed using data from Table 6.2. The values were calculated by subtracting the amount of precursors required for biosynthesis of the biomass from the input carbon source. Glucose6P, glucose-6-phosphate; PK, pyruvate kinase; TriosePs, triose phosphate; 3PGlycerate, glyceraldehyde-3-phosphate; PEP, phosphoenolpyruvate; fructose6P, fructose-6-phosphate; fructose bisP, fructose 1,6-diphosphate; acetylP, acetyl phosphate; CS, citrate synthase, CO_2, carbon dioxide. The remaining flux to CO_2 is via pyruvate dehydrogenase (PDH), isocitrate dehydrogenase, oxo-glutarate dehydrogenase, phosphoenolpyruvate carboxylase (PEPC) and enzymes of the PP pathway. Dividing the normalised fluxes by the normalising factor (N), converts the normalised units to C.mmoles.g^{-1} dry wt biomass h^{-1}. Dividing these figures by the specific growth rate (μ), converts the diagram to throughputs (C.mmoles.g^{-1}). All workings are contained in the compendium if required (Fig 6.2). The μ was taken as the reconciled value (as Chapter 4, Table 4.12). nd, not determined.

Fig 6.3. Normalised flux diagram for *S. fradiae* C373-10 growing on glucose [Ferm 1] (C.mmoles.g^{-1} dry wt biomass. h^{-1} normalised to 100 % of input).

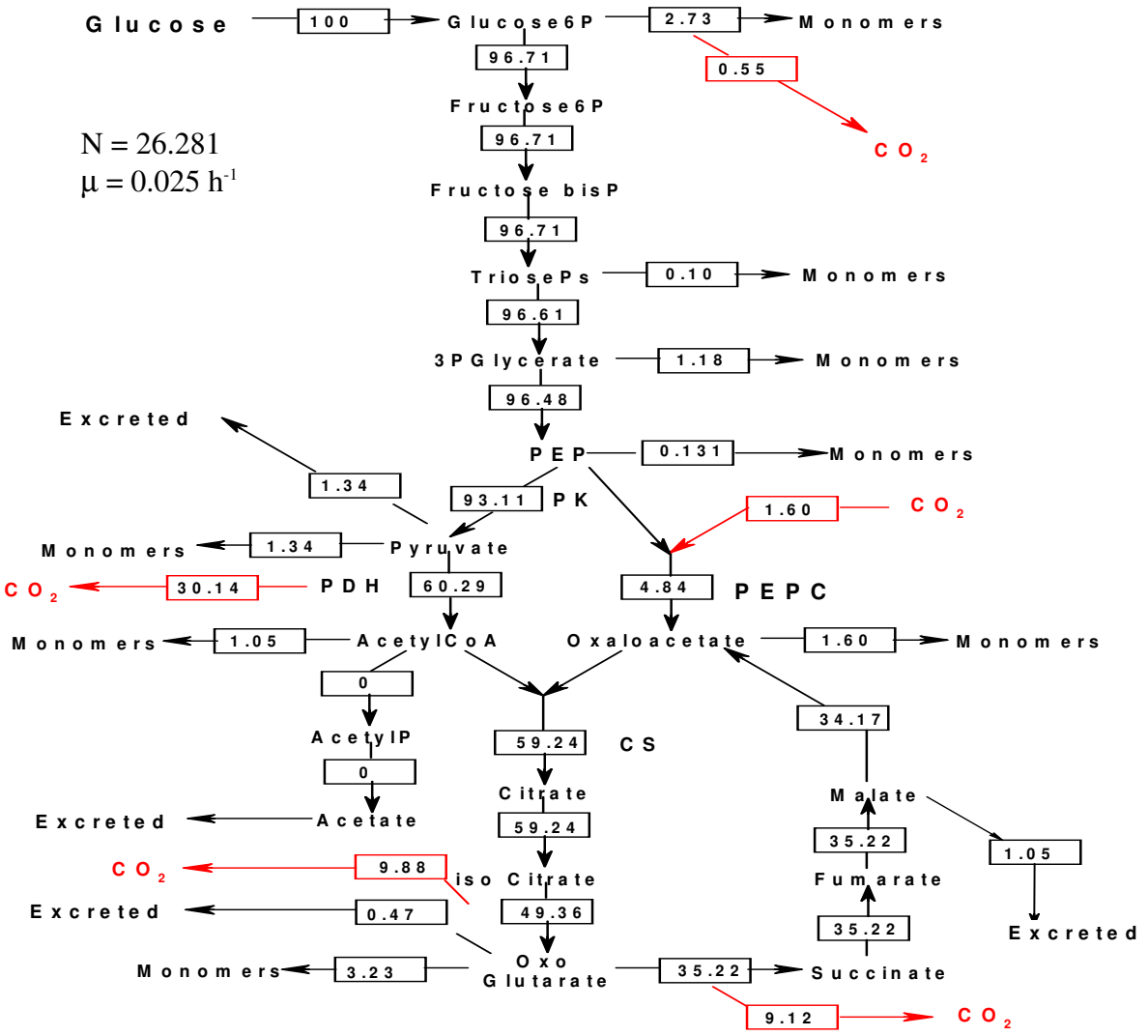

The diagram was constructed using data from Table 6.3. The values were calculated by subtracting the amount of precursors required for biosynthesis of the biomass from the input carbon source. Glucose6P, glucose-6-phosphate; PK, pyruvate kinase; TriosePs, triose phosphate; 3PGlycerate, glyceraldehyde-3-phosphate; PEP, phosphoenolpyruvate; fructose6P, fructose-6-phosphate; fructose bisP, fructose 1,6-diphosphate; acetylP, acetyl phosphate; CS, citrate synthase, CO_2, carbon dioxide. The remaining flux to CO_2 is via pyruvate dehydrogenase (PDH), isocitrate dehydrogenase, oxo-glutarate dehydrogenase, phosphoenolpyruvate carboxylase (PEPC) and enzymes of the PP pathway. Dividing the normalised fluxes by the normalising factor (N), converts the normalised units to C.mmoles.g^{-1} dry wt biomass h^{-1}. Dividing these figures by the specific growth rate (μ), converts the diagram to throughputs (C.mmoles.g^{-1}). The μ was taken as the reconciled value (as Chapter 4, Table 4.12). All workings are contained in the compendium if required (Fig 6.3).

Fig 6.4. Normalised flux diagram for *S. fradiae* C373-10 growing on glucose [Ferm 2](C.mmoles.g^{-1} dry wt biomass. h^{-1} normalised to 100 % of input).

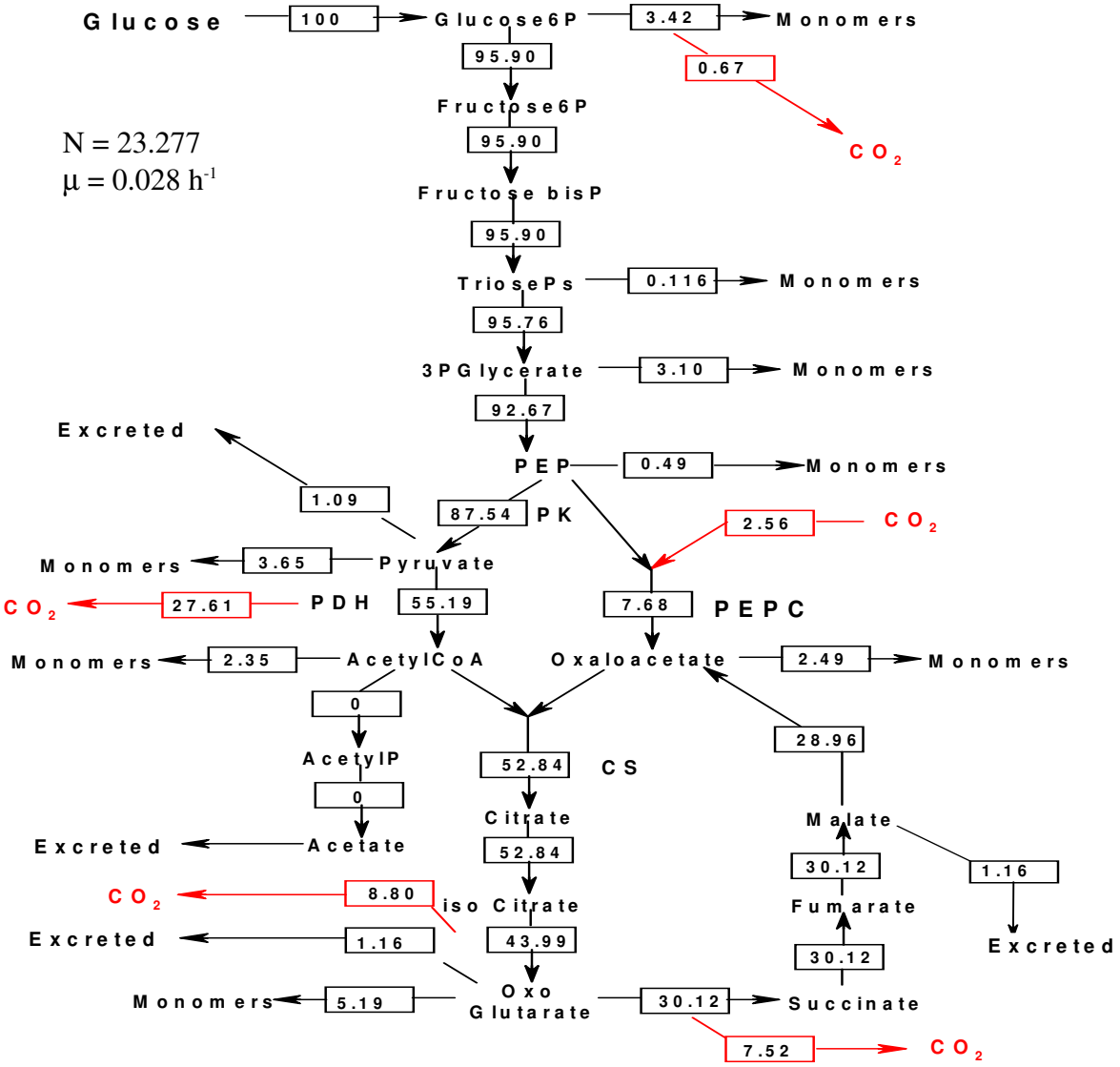

The diagram was constructed using data from Table 6.4. The values were calculated by subtracting the amount of precursors required for biosynthesis of the biomass from the input carbon source. Glucose6P, glucose-6-phosphate; PK, pyruvate kinase; TriosePs, triose phosphate; 3PGlycerate, glyceraldehyde-3-phosphate; PEP, phosphoenolpyruvate; fructose6P, fructose-6-phosphate; fructose bisP, fructose 1,6-diphosphate; acetylP, acetyl phosphate; CS, citrate synthase, CO_2, carbon dioxide. The remaining flux to CO_2 is via pyruvate dehydrogenase (PDH), isocitrate dehydrogenase, oxo-glutarate dehydrogenase, phosphoenolpyruvate carboxylase (PEPC) and enzymes of the PP pathway. Dividing the normalised fluxes by the normalising factor (N), converts the normalised units to C.mmoles.g^{-1} dry wt biomass h^{-1}. Dividing these figures by the specific growth rate (μ), converts the diagram to throughputs (C.mmoles.g^{-1}). The μ was taken as the reconciled value (as Chapter 4, Table 4.12). All workings are contained in the compendium if required (Fig 6.4).

Fig 6.5. Normalised flux diagram for *S. fradiae* C373-10 growing on fructose {Ferm 1} [without phosphotransferase system] (C.mmoles.g^{-1} dry wt biomass. h^{-1} normalised to 100 % of input).

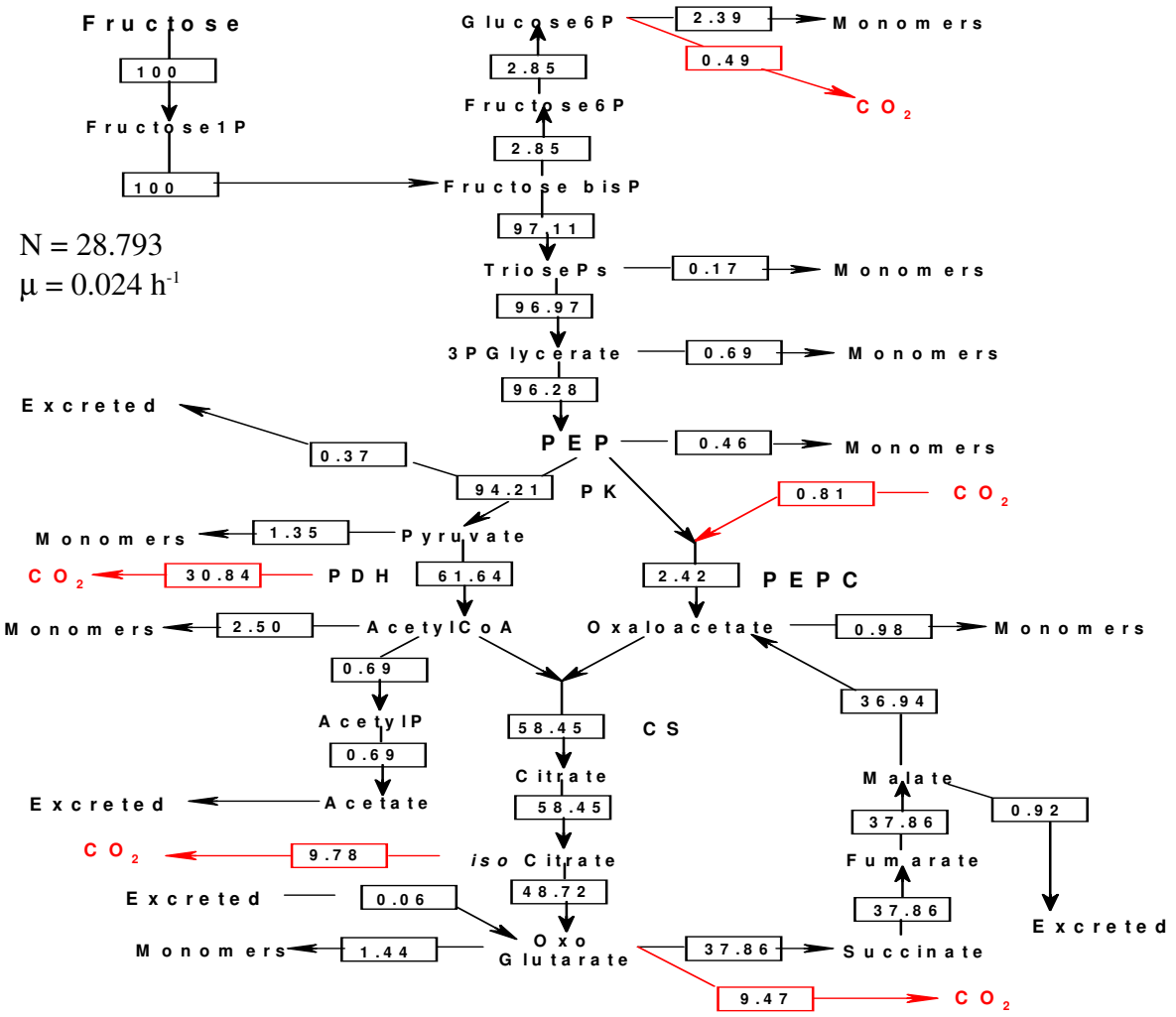

The diagram was constructed using data from Table 6.5. The values were calculated by subtracting the amount of precursors required for biosynthesis of the biomass from the input carbon source. Glucose6P, glucose-6-phosphate; PK, pyruvate kinase; TriosePs, triose phosphate; 3PGlycerate, glyceraldehyde-3-phosphate; PEP, phosphoenolpyruvate; fructose6P, fructose-6-phosphate; fructose bisP, fructose 1,6-diphosphate; acetylP, acetyl phosphate; CS, citrate synthase, CO_2, carbon dioxide. The remaining flux to CO_2 is via pyruvate dehydrogenase (PDH), isocitrate dehydrogenase, oxo-glutarate dehydrogenase, phosphoenolpyruvate carboxylase (PEPC) and enzymes of the PP pathway. Dividing the normalised fluxes by the normalising factor (N), converts the normalised units to C.mmoles.g^{-1} dry wt biomass h^{-1}. Dividing these figures by the specific growth rate (μ), converts the diagram to throughputs (C.mmoles.g^{-1}). The μ was taken as the reconciled value (as Chapter 4, Table 4.12). All workings are contained in the compendium if required (Fig 6.5).

Fig 6.6. Normalised flux diagram for *S. fradiae* C373-10 growing on fructose {Ferm 1} [with phosphotransferase system] (C.mmoles g^{-1} dry wt biomass. h^{-1} normalised to 100 % of input).

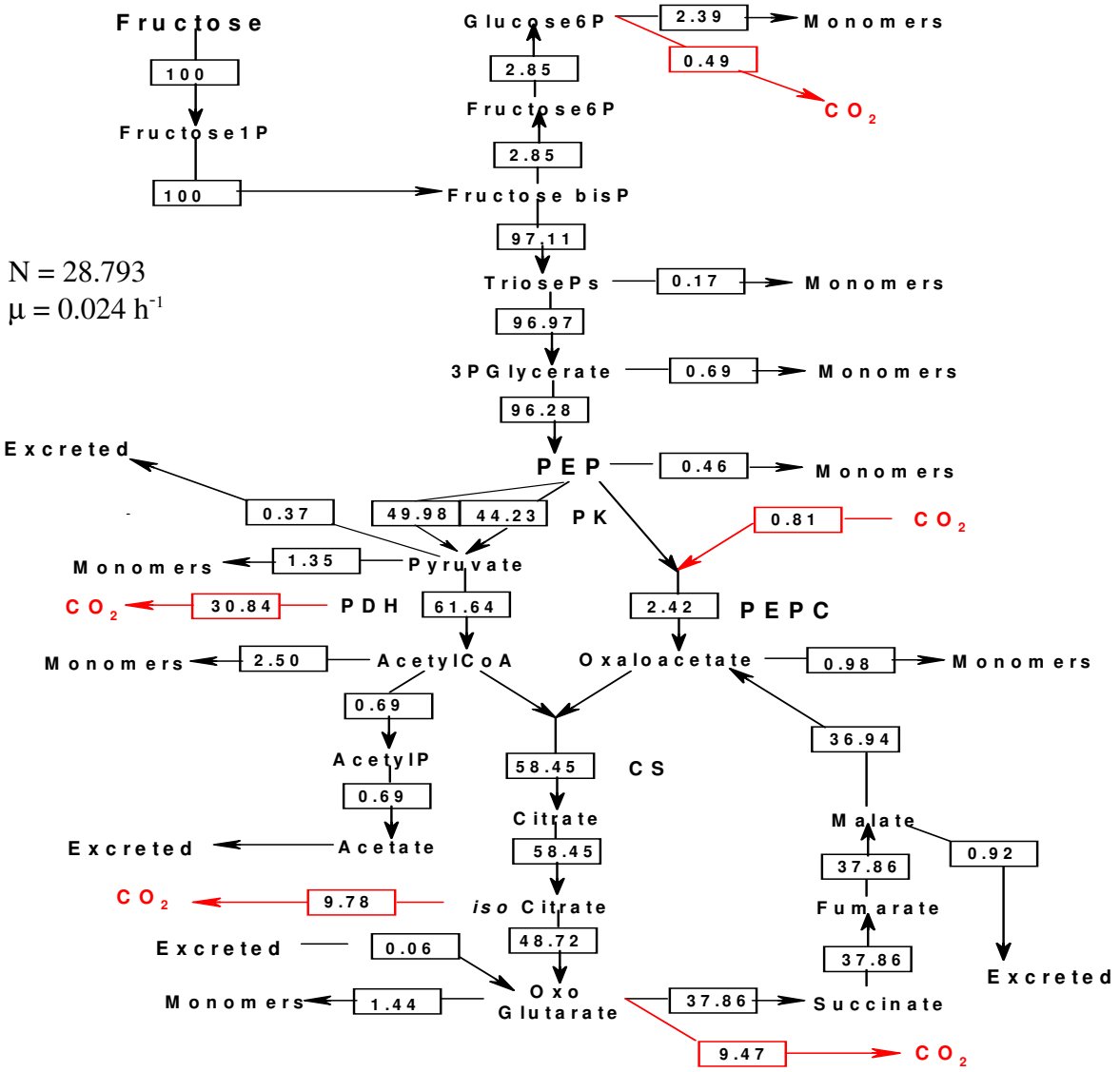

The diagram was constructed using data from Table 6.5. The values were calculated by subtracting the amount of precursors required for biosynthesis of the biomass from the input carbon source. Glucose6P, glucose-6-phosphate; PK, pyruvate kinase; TriosePs, triose phosphate; 3PGlycerate, glyceraldehyde-3-phosphate; PEP, phosphoenolpyruvate; fructose6P, fructose-6-phosphate; fructose bisP, fructose 1,6-diphosphate; acetylP, acetyl phosphate; CS, citrate synthase, CO_2, carbon dioxide. The remaining flux to CO_2 is via pyruvate dehydrogenase (PDH), isocitrate dehydrogenase, oxo-glutarate dehydrogenase, phosphoenolpyruvate carboxylase (PEPC) and enzymes of the PP pathway. Dividing the normalised fluxes by the normalising factor (N), converts the normalised units to C.mmoles.g^{-1} dry wt biomass h^{-1}. Dividing these figures by the specific growth rate (μ), converts the diagram to throughputs (C.mmoles.g^{-1}). The μ was taken as the reconciled value (as Chapter 4, Table 4.12). All workings are contained in the compendium if required (Fig 6.6).

Fig 6.7. Normalised flux diagram for *S. fradiae* C373-10 growing on glycerol [Ferm 1] (C.mmoles.g^{-1} dry wt biomass. h^{-1} normalised to 100 % of input).

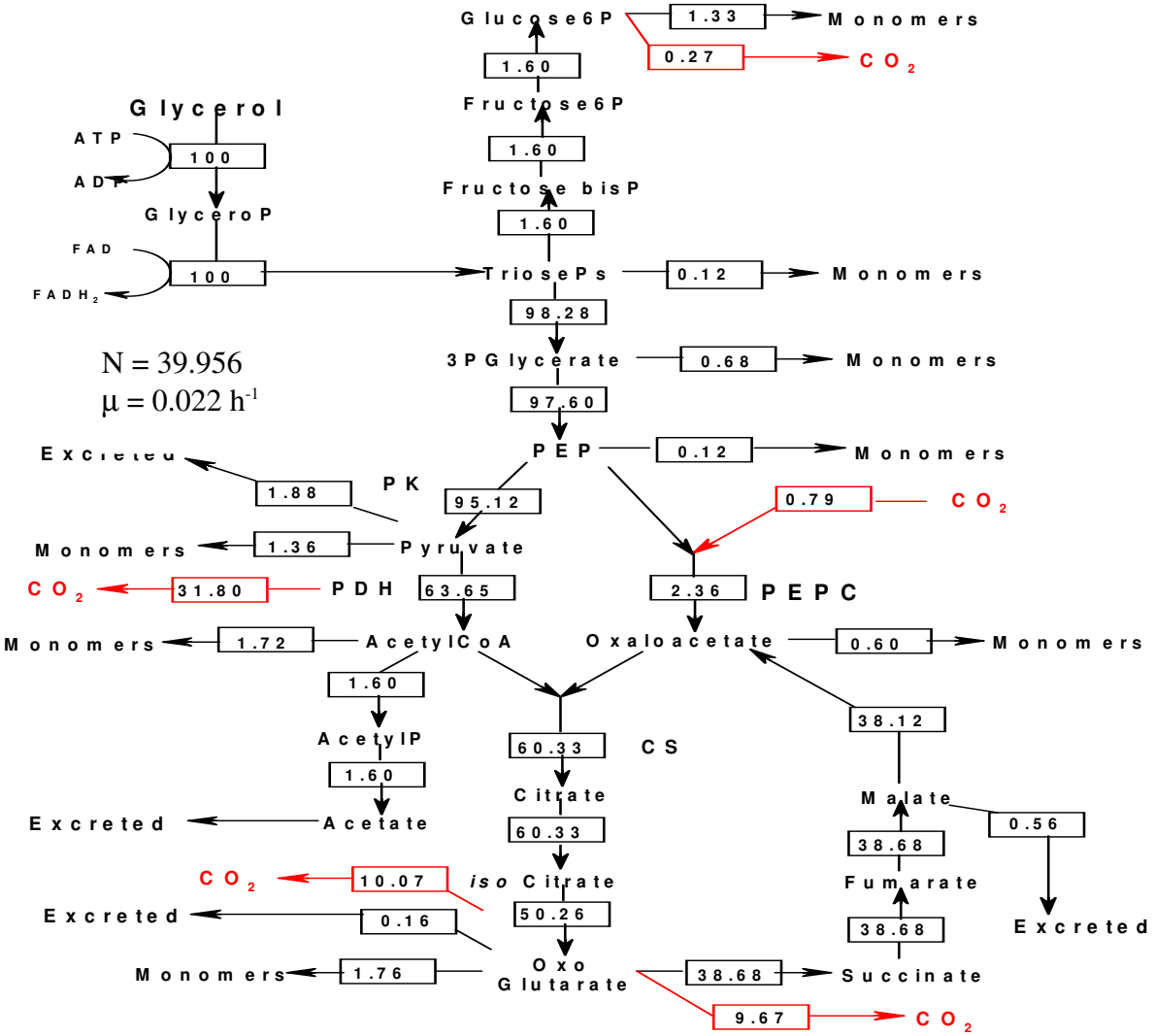

The diagram was constructed using data from Table 6.6. The values were calculated by subtracting the amount of precursors required for biosynthesis of the biomass from the input carbon source. Glucose6P, glucose-6-phosphate; PK, pyruvate kinase; TriosePs, triose phosphate; 3PGlycerate, glyceraldehyde-3-phosphate; PEP, phosphoenolpyruvate; fructose6P, fructose-6-phosphate; fructose bisP, fructose 1,6-diphosphate; acetylP, acetyl phosphate; CS, citrate synthase, CO_2, carbon dioxide. The remaining flux to CO_2 is via pyruvate dehydrogenase (PDH), isocitrate dehydrogenase, oxo-glutarate dehydrogenase, phosphoenolpyruvate carboxylase (PEPC) and enzymes of the PP pathway. Dividing the normalised fluxes by the normalising factor (N), converts the normalised units to C.mmoles.g^{-1} dry wt biomass h^{-1}. Dividing these figures by the specific growth rate (μ), converts the diagram to throughputs (C.mmoles.g^{-1}). The μ was taken as the reconciled value (as Chapter 4, Table 4.12). All workings are contained in the compendium if required (Fig 6.7).

Fig 6.8. Normalised flux diagram for *S. fradiae* C373-10 growing on glycerol [Ferm 2] (C.mmoles.g^{-1} dry wt biomass. h^{-1} normalised to 100 % of input).

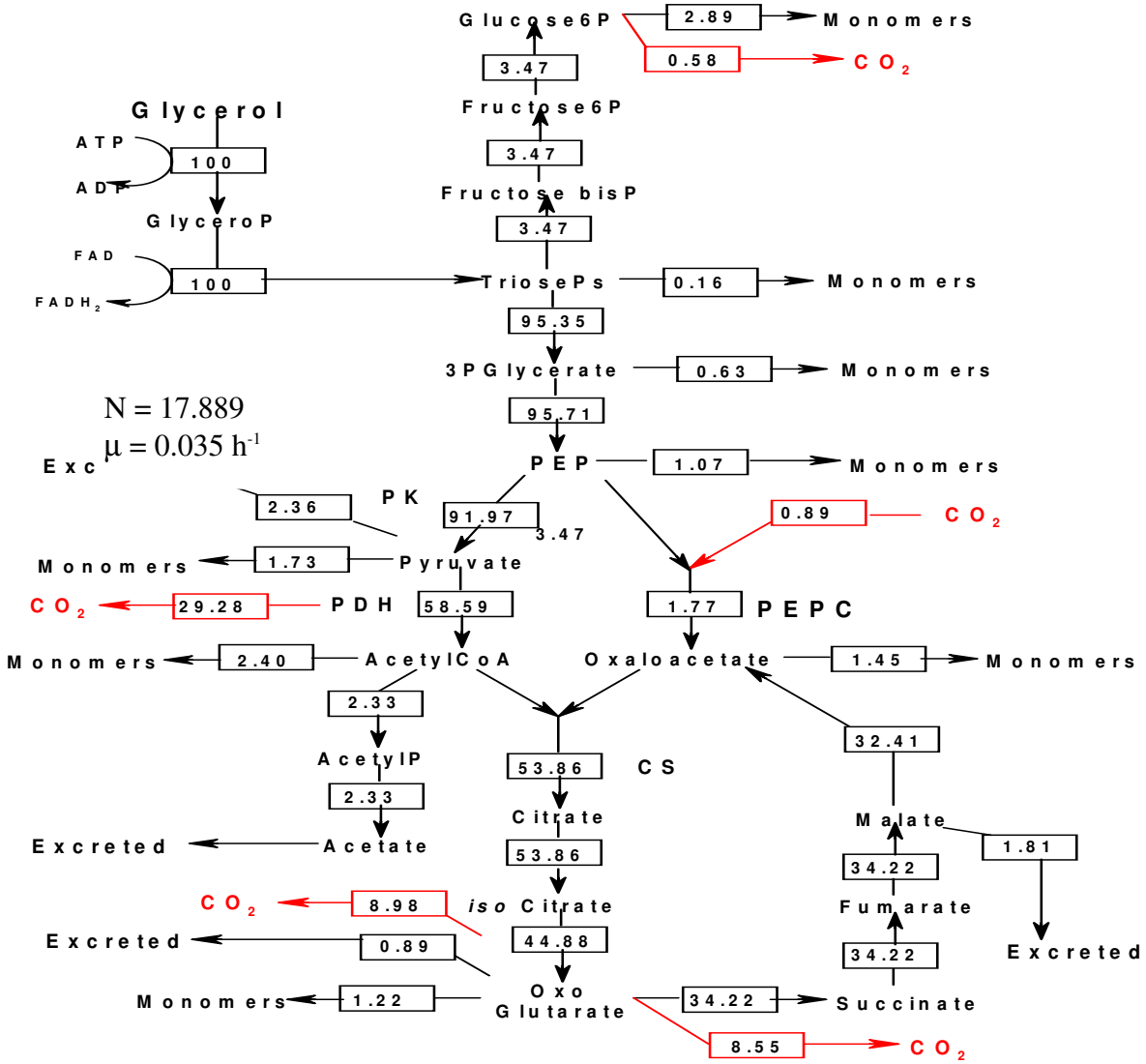

The diagram was constructed using data from Table 6.7. The values were calculated by subtracting the amount of precursors required for biosynthesis of the biomass from the input carbon source. Glucose6P, glucose-6-phosphate; PK, pyruvate kinase; TriosePs, triose phosphate; 3PGlycerate, glyceraldehyde-3-phosphate; PEP, phosphoenolpyruvate; fructose6P, fructose-6-phosphate; fructose bisP, fructose 1,6-diphosphate; acetylP, acetyl phosphate; CS, citrate synthase, CO_2, carbon dioxide. The remaining flux to CO_2 is via pyruvate dehydrogenase (PDH), isocitrate dehydrogenase, oxo-glutarate dehydrogenase, phosphoenolpyruvate carboxylase (PEPC) and enzymes of the PP pathway. Dividing the normalised fluxes by the normalising factor (N), converts the normalised units to C.mmoles.g^{-1} dry wt biomass h^{-1}. Dividing these figures by the specific growth rate (μ), converts the diagram to throughputs (C.mmoles.g^{-1}). The μ was taken as the reconciled value (as Chapter 4, Table 4.12). All workings are contained in the compendium if required (Fig 6.8).

Fig 6.9. Normalised flux diagram for *S. fradiae* C373-10 growing on glycerol [Ferm 1] (mmoles.g^{-1} dry wt biomass. h^{-1} normalised to 100 % of input).

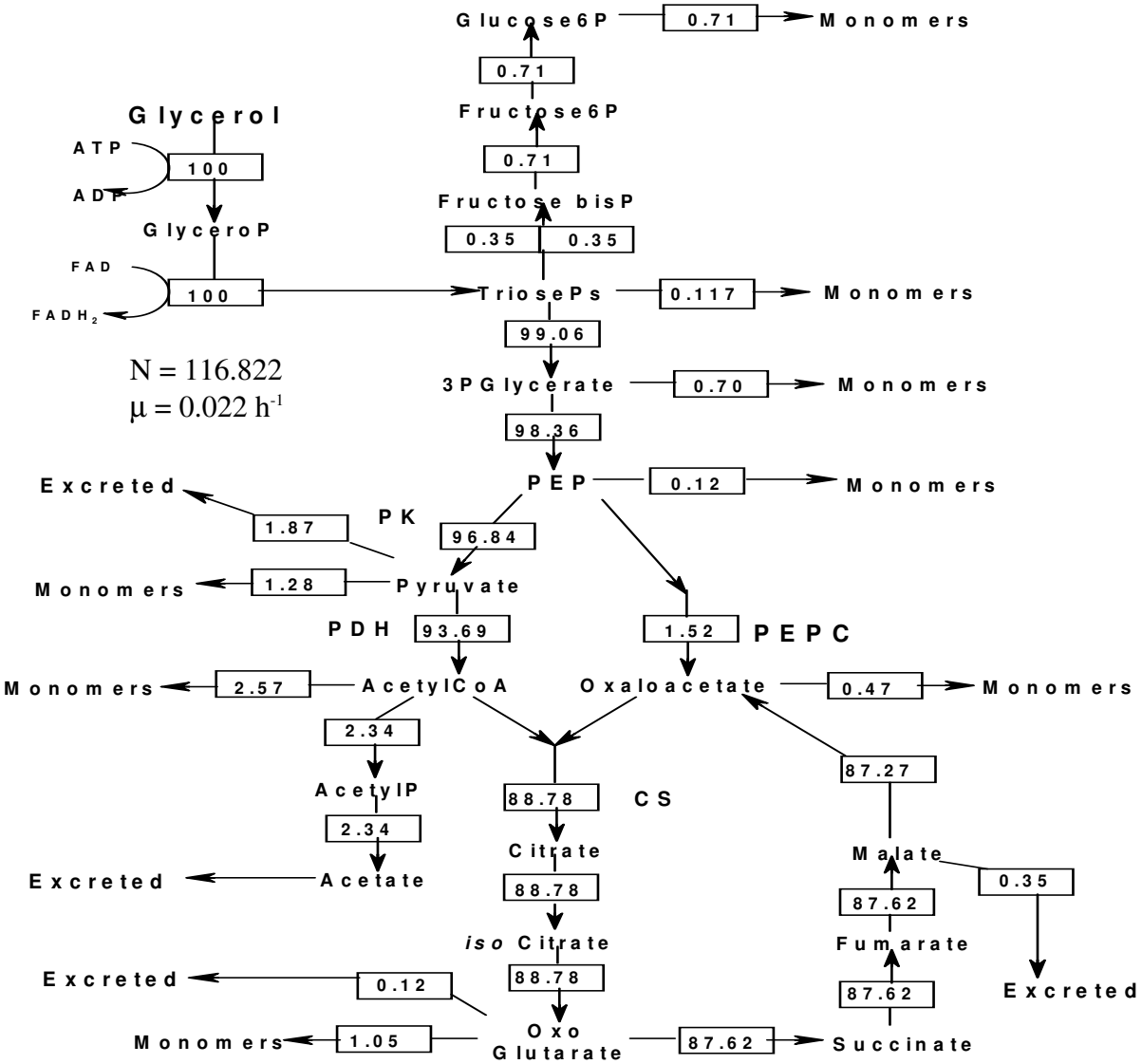

The diagram was constructed using data from Table 6.6. The values were calculated by subtracting the amount of precursors required for biosynthesis of the biomass from the input carbon source. Glucose6P, glucose-6-phosphate; PK, pyruvate kinase; TriosePs, triose phosphate; 3PGlycerate, glyceraldehyde-3-phosphate; PEP, phosphoenolpyruvate; fructose6P, fructose-6-phosphate; fructose bisP, fructose 1,6-diphosphate; acetylP, acetyl phosphate; CS, citrate synthase, CO_2, carbon dioxide. The remaining flux to CO_2 is via pyruvate dehydrogenase (PDH), isocitrate dehydrogenase, oxo-glutarate dehydrogenase, phosphoenolpyruvate carboxylase (PEPC) and enzymes of the PP pathway. Dividing the normalised fluxes by the normalising factor (N), converts the normalised units to C.mmoles.g^{-1} dry wt biomass h^{-1}. Dividing these figures by the specific growth rate (μ), converts the diagram to throughputs (C.mmoles.g^{-1}). The μ was taken as the reconciled value (as Chapter 4, Table 4.12). All workings are contained in the compendium if required (Fig 6.9).

Fig 6.10. Normalised flux diagram for *S. fradiae* C373-10 growing on glycerol [Ferm 2] (mmoles.g^{-1} dry wt biomass. h^{-1} normalised to 100 % of input).

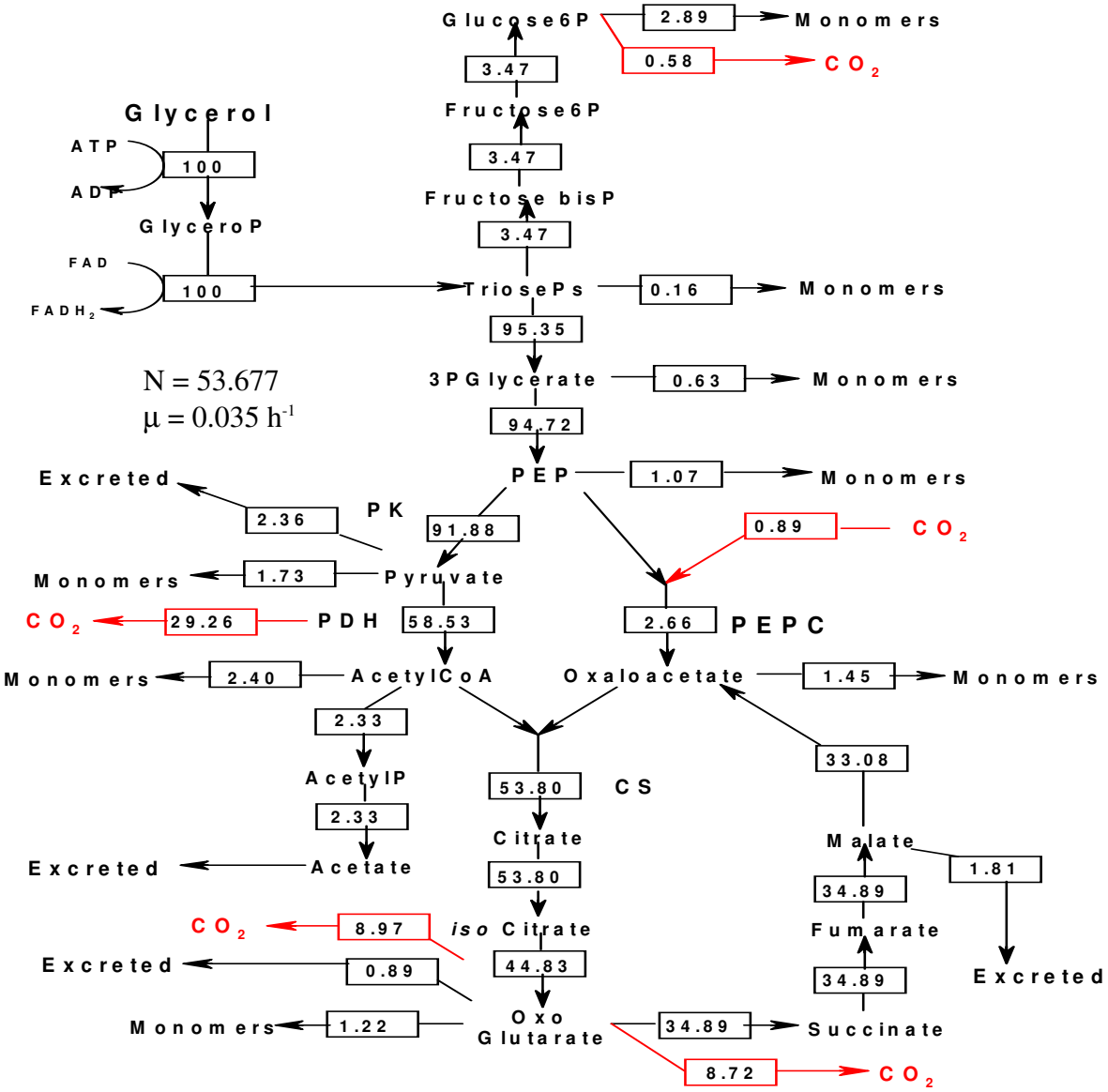

The diagram was constructed using data from Table 6.7. The values were calculated by subtracting the amount of precursors required for biosynthesis of the biomass from the input carbon source. Glucose6P, glucose-6-phosphate; PK, pyruvate kinase; TriosePs, triose phosphate; 3PGlycerate, glyceraldehyde-3-phosphate; PEP, phosphoenolpyruvate; fructose6P, fructose-6-phosphate; fructose bisP, fructose 1,6-diphosphate; acetylP, acetyl phosphate; CS, citrate synthase, CO_2, carbon dioxide. The remaining flux to CO_2 is via pyruvate dehydrogenase (PDH), isocitrate dehydrogenase, oxo-glutarate dehydrogenase, phosphoenolpyruvate carboxylase (PEPC) and enzymes of the PP pathway. Dividing the normalised fluxes by the normalising factor (N), converts the normalised units to C.mmoles.g^{-1} dry wt biomass h^{-1}. Dividing these figures by the specific growth rate (μ), converts the diagram to throughputs (C.mmoles.g^{-1}). The μ was taken as the reconciled value (as Chapter 4, Table 4.12). All workings are contained in the compendium if required (Fig 6.10).

Fig 6.11. Normalised flux diagram for *S. fradiae* C373-10 growing on oxo-glutarate (C.mmoles.g^{-1} dry wt biomass. h^{-1} normalised to 100 % of input).

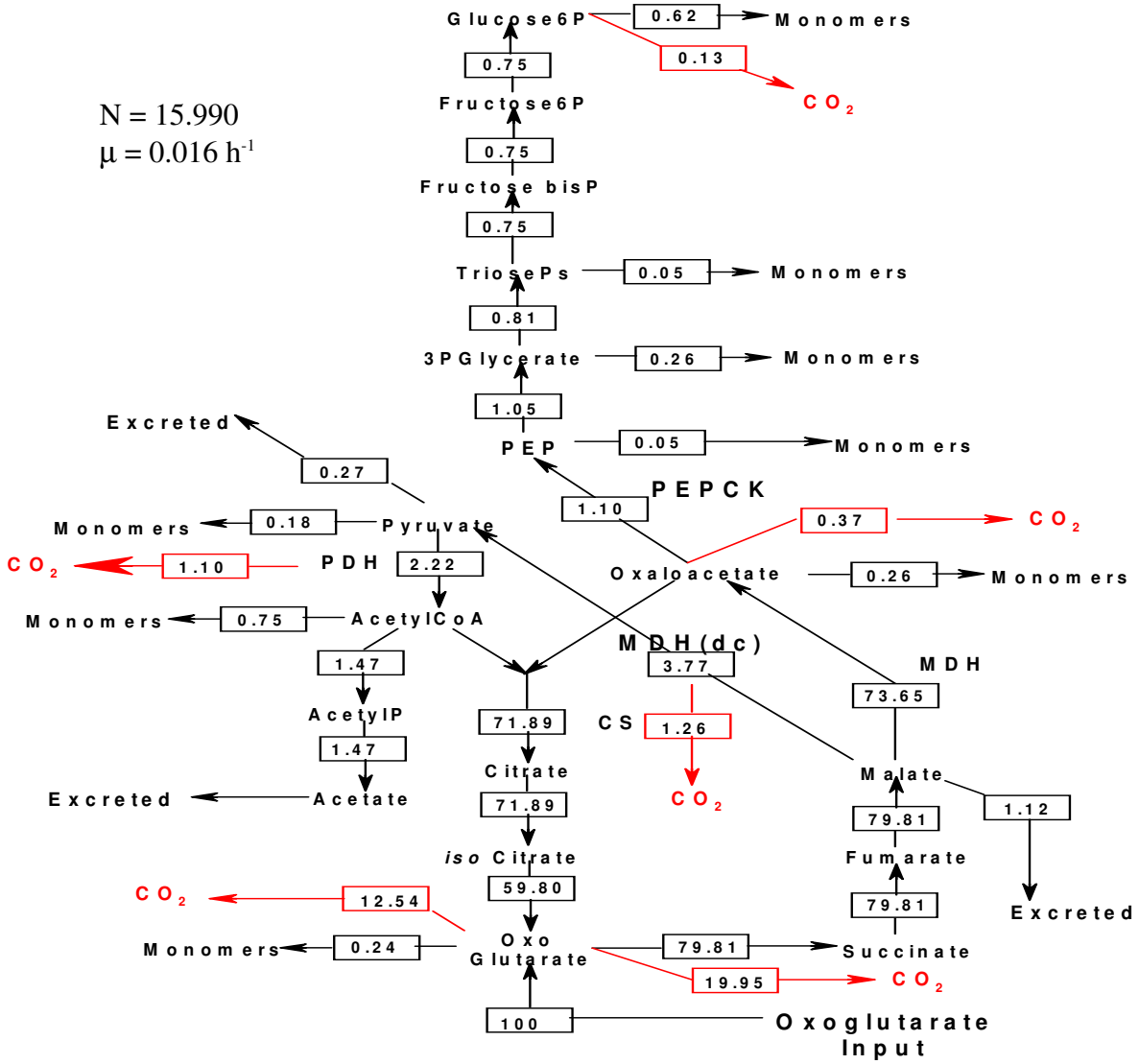

The diagram was constructed using data from Table 6.8. The values were calculated by subtracting the amount of precursors required for biosynthesis of the biomass from the input carbon source. Glucose6P, glucose-6-phosphate; malate dehydrogenase, MDH; PK, pyruvate kinase; TriosePs, triose phosphate; 3PGlycerate, glyceraldehyde-3-phosphate; PEP, phosphoenolpyruvate; fructose6P, fructose-6-phosphate; fructose bisP, fructose 1,6-diphosphate; acetylP, acetyl phosphate; CS, citrate synthase, CO_2, carbon dioxide. The remaining flux to CO_2 is via pyruvate dehydrogenase (PDH), isocitrate dehydrogenase, oxo-glutarate dehydrogenase, malate dehydrogenase decarboxylating (MDH[dc]), phosphoenolpyruvate carboxykinase (PEPCK) and enzymes of the PP pathway. Dividing the normalised fluxes by the normalising factor (N), converts the normalised units to C.mmoles.g^{-1} dry wt biomass h^{-1}. Dividing these figures by the specific growth rate (μ), converts the diagram to throughputs (C.mmoles.g^{-1}). The μ was taken as the reconciled value (as Chapter 4, Table 4.12). All workings are contained in the compendium if required (Fig 6.11).

Fig 6.12. Normalised flux diagram for *S. fradiae* C373-10 growing on glucose & glutamate [Ferm 1; Day 2] (C.mmoles.g^{-1} dry wt biomass. h^{-1} normalised to 100 % of input).

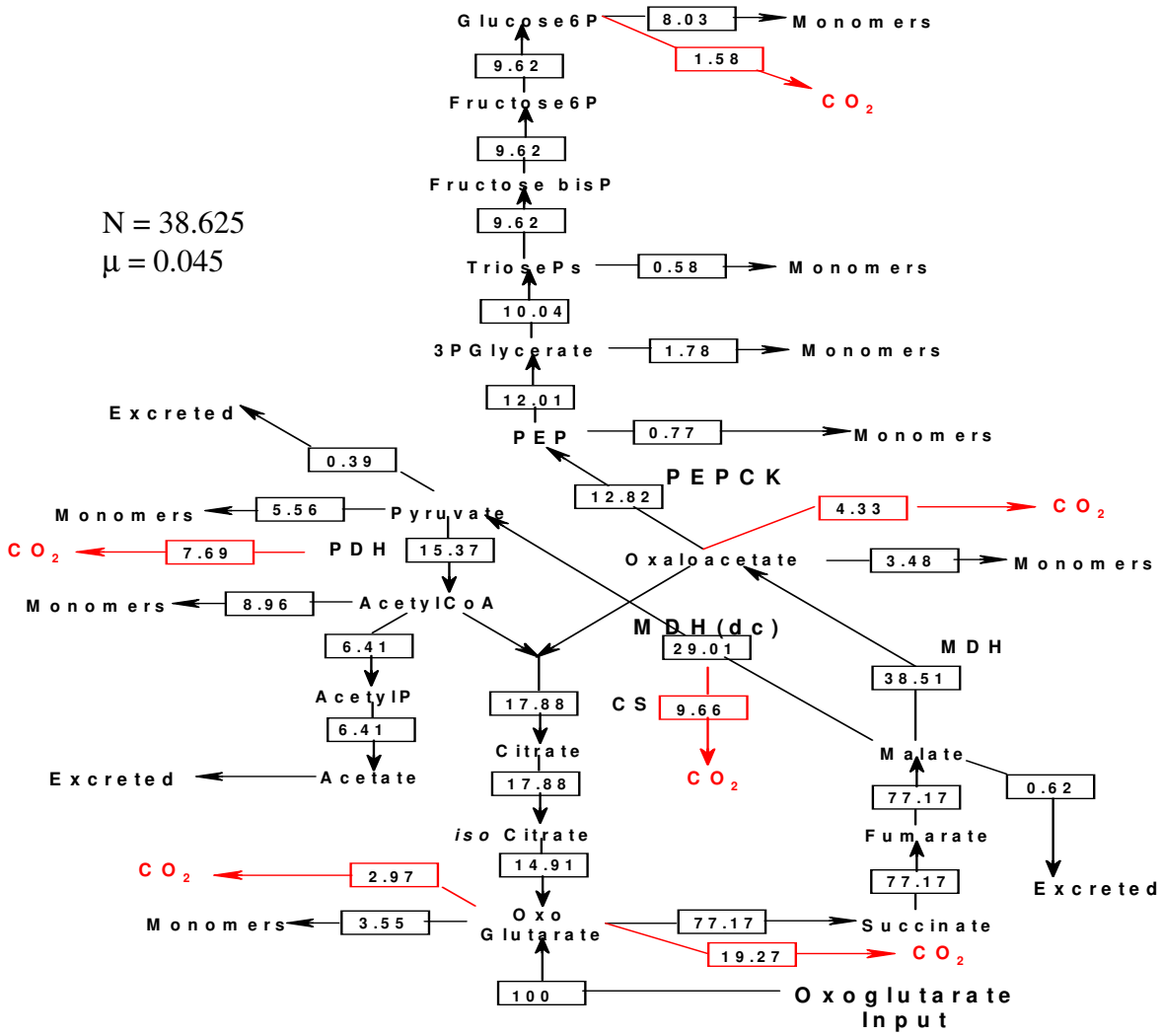

The diagram was constructed using data from Table 6.9. The values were calculated by subtracting the amount of precursors required for biosynthesis of the biomass from the input carbon source. Glucose6P, glucose-6-phosphate; malate dehydrogenase, MDH; PK, pyruvate kinase; TriosePs, triose phosphate; 3PGlycerate, glyceraldehyde-3-phosphate; PEP, phosphoenolpyruvate; fructose6P, fructose-6-phosphate; fructose bisP, fructose 1,6-diphosphate; acetylP, acetyl phosphate; CS, citrate synthase, CO_2, carbon dioxide. The remaining flux to CO_2 is via pyruvate dehydrogenase (PDH), isocitrate dehydrogenase, oxo-glutarate dehydrogenase, malate dehydrogenase decarboxylating (MDH[dc]), phosphoenolpyruvate carboxykinase (PEPCK) and enzymes of the PP pathway. Dividing the normalised fluxes by the normalising factor (N), converts the normalised units to C.mmoles.g^{-1} dry wt biomass h^{-1}. Dividing these figures by the specific growth rate (μ), converts the diagram to throughputs (C.mmoles.g^{-1}). The μ was taken as the reconciled value (as Chapter 4, Table 4.12). All workings are contained in the compendium if required (Fig 6.12).

Fig 6.13. Normalised flux diagram for *S. fradiae* C373-10 growing on glucose & glutamate [Ferm 2; Day 2] (C.mmoles.g^{-1} dry wt biomass. h^{-1} normalised to 100 % of input).

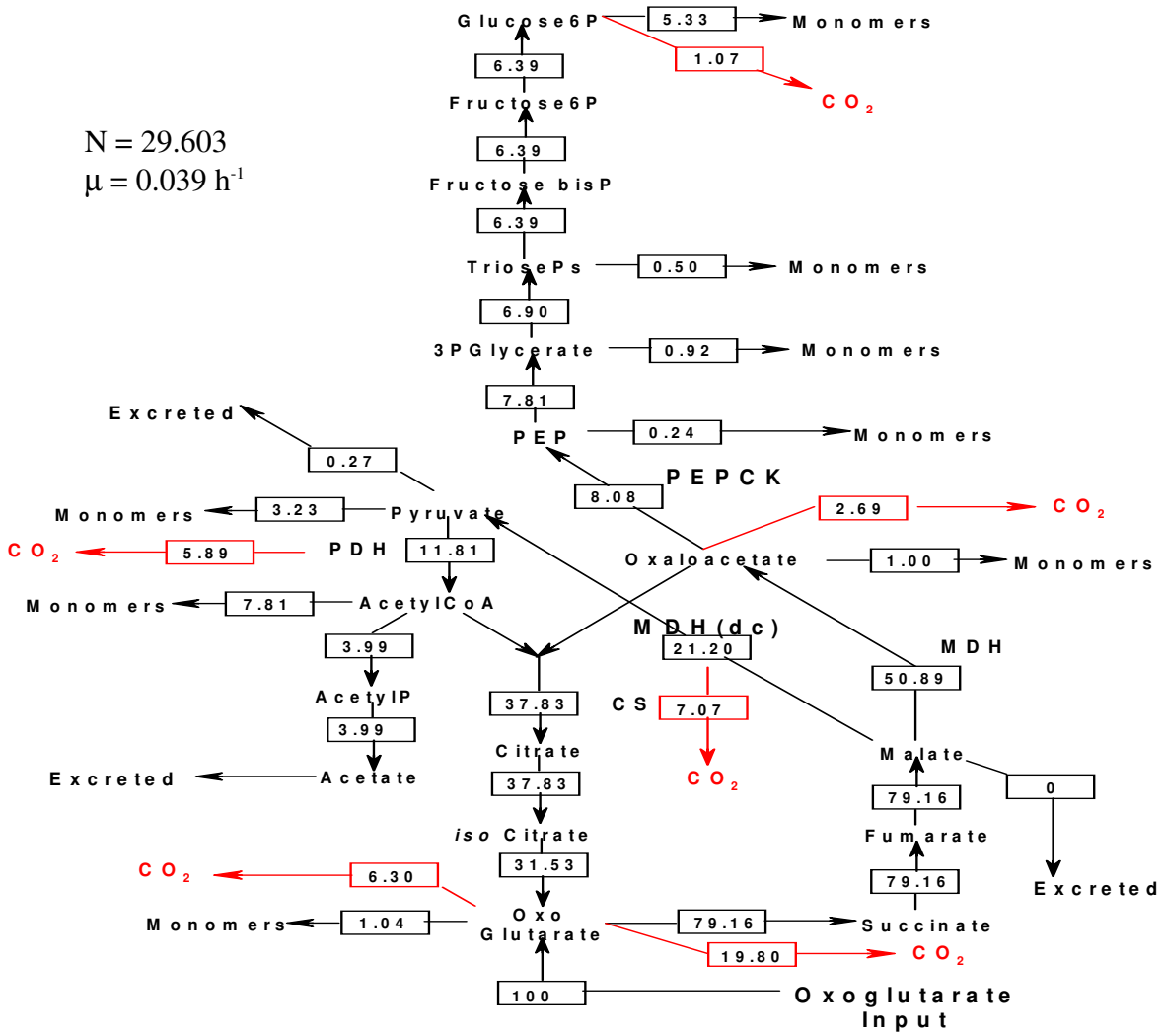

The diagram was constructed using data from Table 6.10. The values were calculated by subtracting the amount of precursors required for biosynthesis of the biomass from the input carbon source. Glucose6P, glucose-6-phosphate; malate dehydrogenase, MDH; PK, pyruvate kinase; TriosePs, triose phosphate; 3PGlycerate, glyceraldehyde-3-phosphate; PEP, phosphoenolpyruvate; fructose6P, fructose-6-phosphate; fructose bisP, fructose 1,6-diphosphate; acetylP, acetyl phosphate; CS, citrate synthase, CO_2, carbon dioxide. The remaining flux to CO_2 is via pyruvate dehydrogenase (PDH), isocitrate dehydrogenase, oxo-glutarate dehydrogenase, malate dehydrogenase decarboxylating (MDH[dc]), phosphoenolpyruvate carboxykinase (PEPCK) and enzymes of the PP pathway. Dividing the normalised fluxes by the normalising factor (N), converts the normalised units to C.mmoles.g^{-1} dry wt biomass h^{-1}. Dividing these figures by the specific growth rate (μ), converts the diagram to throughputs (C.mmoles.g^{-1}). The μ was taken as the reconciled value (as Chapter 4, Table 4.12). All workings are contained in the compendium if required (Fig 6.13).

Fig 6.14. Normalised flux diagram for *S. fradiae* C373-10 growing on glucose & glutamate [Ferm 3; Day 2] (C.mmoles.g^{-1} dry wt biomass. h^{-1} normalised to 100 % of input).

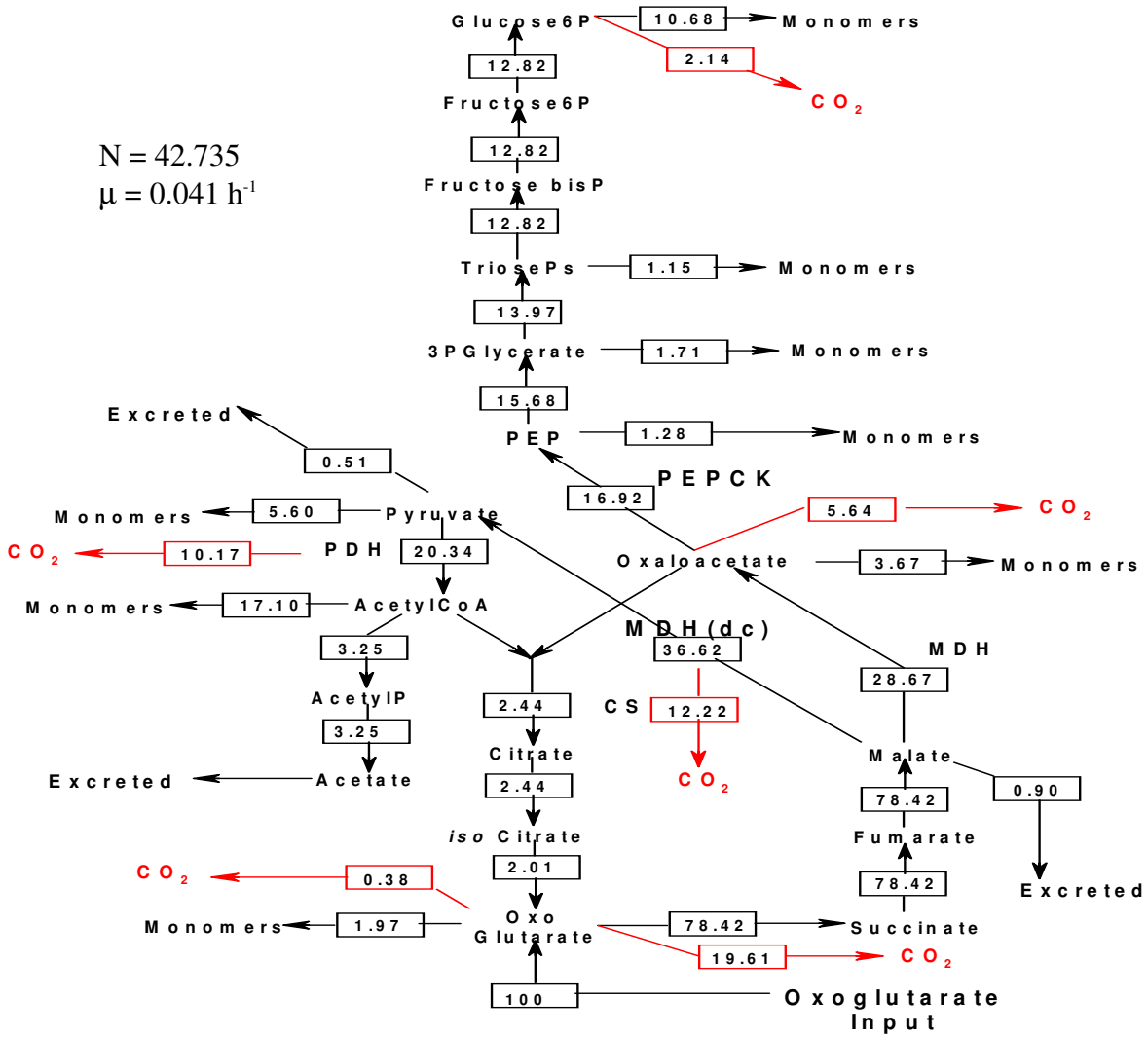

The diagram was constructed using data from Table 6.11. The values were calculated by subtracting the amount of precursors required for biosynthesis of the biomass from the input carbon source. Glucose6P, glucose-6-phosphate; malate dehydrogenase, MDH; PK, pyruvate kinase; TriosePs, triose phosphate; 3PGlycerate, Glyceraldehyde-3-phosphate; PEP, phosphoenolpyruvate; fructose6P, fructose-6-phosphate; fructose bisP, fructose 1,6-diphosphate; acetylP, acetyl phosphate; citrate synthase, CO_2, carbon dioxide. The remaining flux to CO_2 is via pyruvate dehydrogenase (PDH), isocitrate dehydrogenase, oxo-glutarate dehydrogenase, malate dehydrogenase decarboxylating (MDH[dc]), phosphoenolpyruvate carboxykinase (PEPCK) and enzymes of the PP pathway. Dividing the normalised fluxes by the normalising factor (N), converts the normalised units to C.mmoles.g^{-1} dry wt biomass h^{-1}. Dividing these figures by the specific growth rate (μ), converts the diagram to throughputs (C.mmoles.g^{-1}). The μ was taken as the reconciled value (as Chapter 4, Table 4.12). All workings are contained in the compendium if required (Fig 6.14).

Fig 6.15. Normalised flux diagram for *S. fradiae* C373-10 growing on glucose & glutamate [Ferm 4; Day 2] (C.mmoles.g^{-1} dry wt biomass. h^{-1} normalised to 100 % of input).

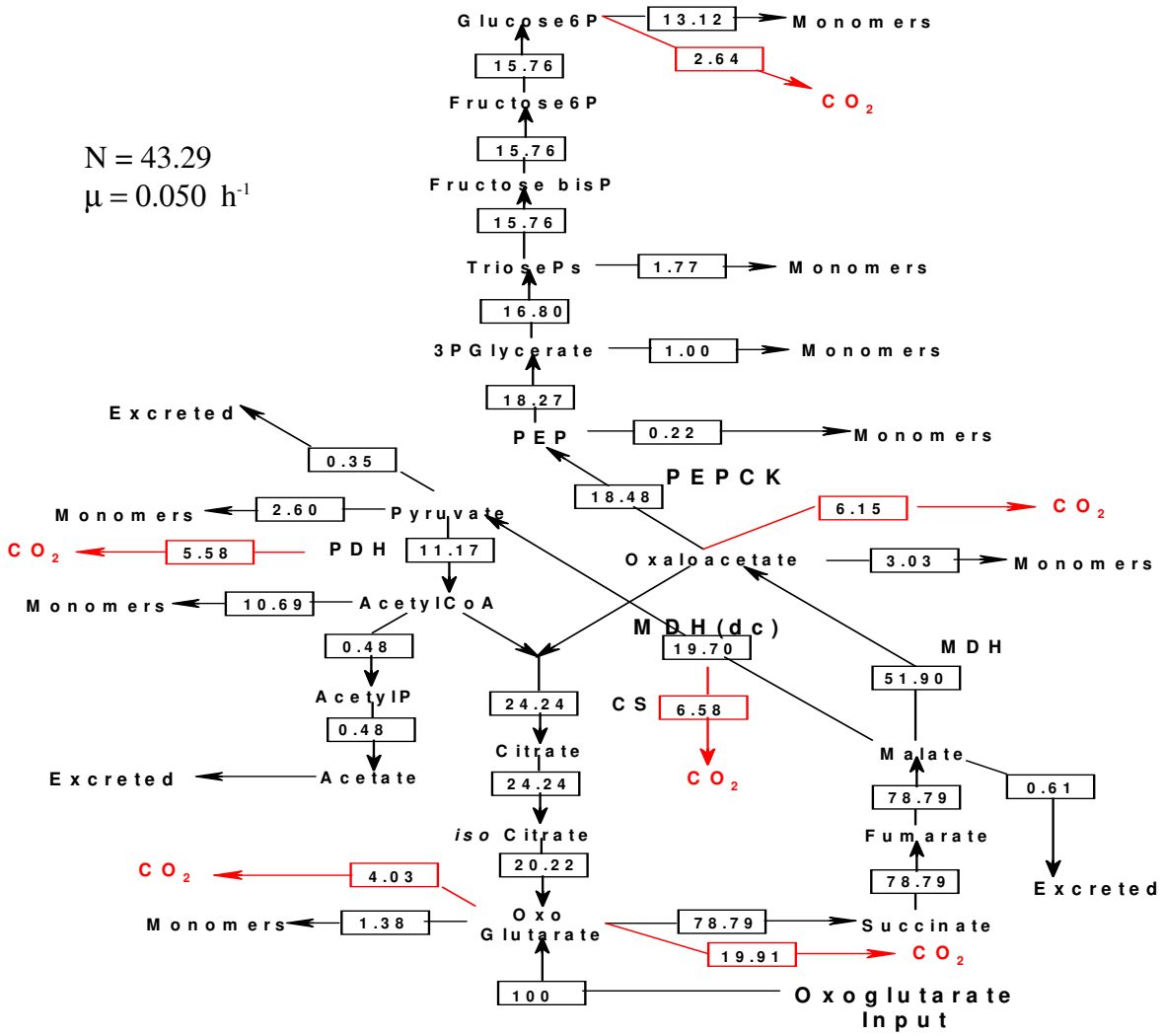

The diagram was constructed using data from Table 6.12. The values were calculated by subtracting the amount of precursors required for biosynthesis of the biomass from the input carbon source. Glucose6P, glucose-6-phosphate; malate dehydrogenase, MDH; PK, pyruvate kinase; TriosePs, triose phosphate; 3PGlycerate, Glyceraldehyde-3-phosphate; PEP, phosphoenolpyruvate; fructose6P, fructose-6-phosphate; fructose bisP, fructose 1,6-diphosphate; acetylP, acetyl phosphate; citrate synthase, CO_2, carbon dioxide. The remaining flux to CO_2 is via pyruvate dehydrogenase (PDH), isocitrate dehydrogenase, oxo-glutarate dehydrogenase, malate dehydrogenase decarboxylating (MDH[dc]), phosphoenolpyruvate carboxykinase (PEPCK) and enzymes of the PP pathway. Dividing the normalised fluxes by the normalising factor (N), converts the normalised units to C.mmoles.g^{-1} dry wt biomass h^{-1}. Dividing these figures by the specific growth rate (μ), converts the diagram to throughputs (C.mmoles.g^{-1}). The μ was taken as the reconciled value (as Chapter 4, Table 4.12). All workings are contained in the compendium if required (Fig 6.15).

Fig 6.16. Normalised flux diagram for *S. fradiae* C373-10 growing on glucose & glutamate [Ferm 1; Day 5] (C.mmoles.g^{-1} dry wt biomass. h^{-1} normalised to 100 % of input).

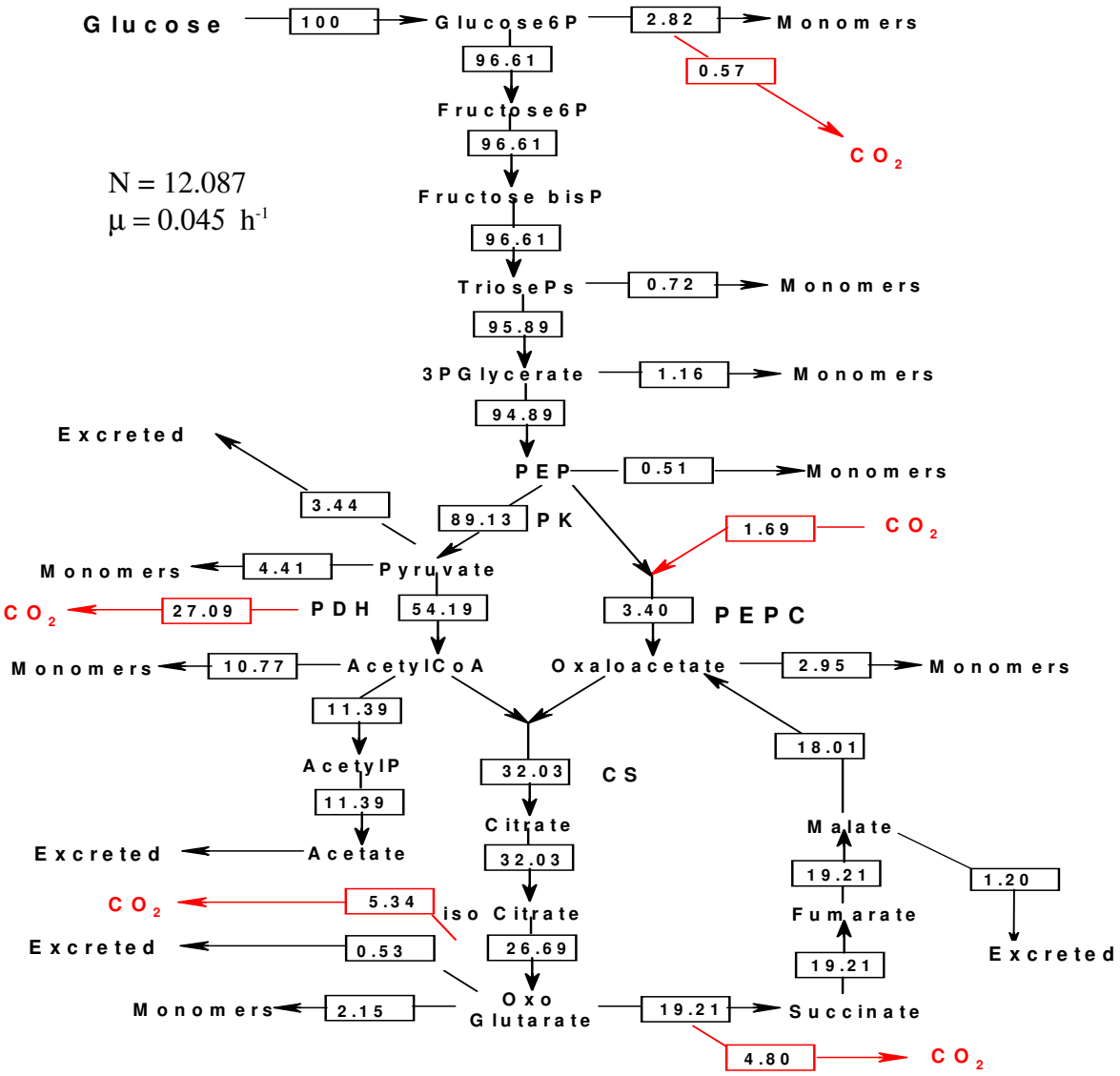

The diagram was constructed using data from Table 6.13. The values were calculated by subtracting the amount of precursors required for biosynthesis of the biomass from the input carbon source. Glucose6P, glucose-6-phosphate; malate dehydrogenase, MDH; PK, pyruvate kinase; TriosePs, triose phosphate; 3PGlycerate, Glyceraldehyde-3-phosphate; PEP, phosphoenolpyruvate; fructose6P, fructose-6-phosphate; fructose bisP, fructose 1,6-diphosphate; acetylP, acetyl phosphate; citrate synthase, CO_2, carbon dioxide. The remaining flux to CO_2 is via pyruvate dehydrogenase (PDH), isocitrate dehydrogenase, oxo-glutarate dehydrogenase, malate dehydrogenase decarboxylating (MDH[dc]), phosphoenolpyruvate carboxykinase (PEPCK) and enzymes of the PP pathway. Dividing the normalised fluxes by the normalising factor (N), converts the normalised units to C.mmoles.g^{-1} dry wt biomass h^{-1}. Dividing these figures by the specific growth rate (μ), converts the diagram to throughputs (C.mmoles.g^{-1}). All workings are contained in the compendium if required (Fig 6.16).

Fig 6.17. Normalised flux diagram for *S. fradiae* C373-10 growing on glucose & glutamate [Ferm 2; Day 5] (C.mmoles.g^{-1} dry wt biomass. h^{-1} normalised to 100 % of input).

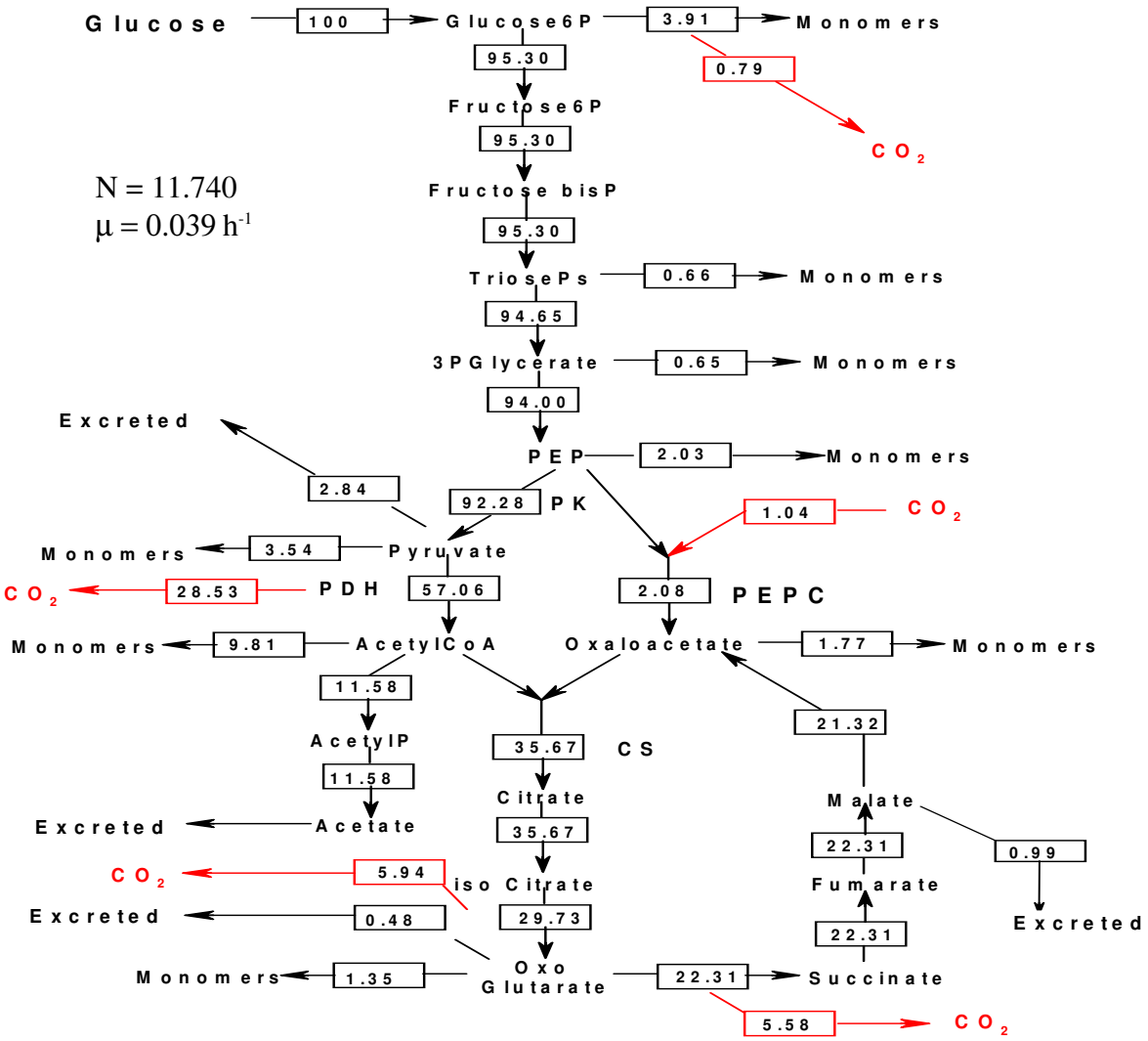

The diagram was constructed using data from Table 6.14. The values were calculated by subtracting the amount of precursors required for biosynthesis of the biomass from the input carbon source. Glucose6P, glucose-6-phosphate; malate dehydrogenase, MDH; PK, pyruvate kinase; TriosePs, triose phosphate; 3PGlycerate, glyceraldehyde-3-phosphate; PEP, phosphoenolpyruvate; fructose6P, fructose-6-phosphate; fructose bisP, fructose 1,6-diphosphate; acetylP, acetyl phosphate; CS, citrate synthase, CO_2, carbon dioxide. The remaining flux to CO_2 is via pyruvate dehydrogenase (PDH), isocitrate dehydrogenase, oxo-glutarate dehydrogenase, malate dehydrogenase decarboxylating (MDH[dc]), phosphoenolpyruvate carboxykinase (PEPCK) and enzymes of the PP pathway. Dividing the normalised fluxes by the normalising factor (N), converts the normalised units to C.mmoles.g^{-1} dry wt biomass h^{-1}. Dividing these figures by the specific growth rate (μ), converts the diagram to throughputs (C.mmoles.g^{-1}). The μ was taken as the reconciled value (as Chapter 4, Table 4.12). All workings are contained in the compendium if required (Fig 6.17).

Fig 6.18. Normalised flux diagram for *S. fradiae* C373-10 growing on glucose & glutamate [Ferm 3; Day 5] (C.mmoles.g^{-1} dry wt biomass. h^{-1} normalised to 100 % of input).

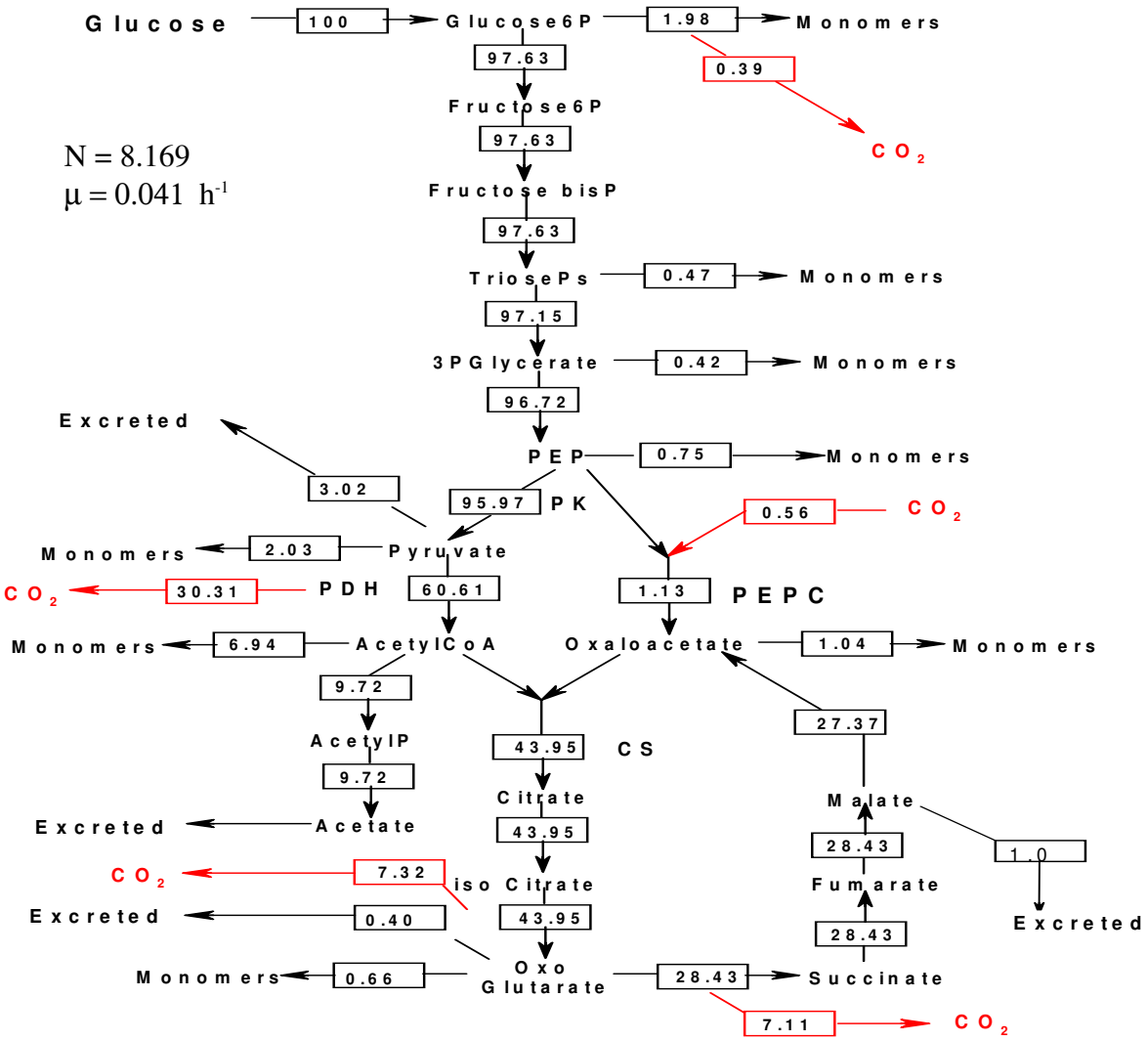

The diagram was constructed using data from Table 6.16. The values were calculated by subtracting the amount of precursors required for biosynthesis of the biomass from the input carbon source. Glucose6P, glucose-6-phosphate; malate dehydrogenase, MDH; PK, pyruvate kinase; TriosePs, triose phosphate; 3PGlycerate, glyceraldehyde-3-phosphate; PEP, phosphoenolpyruvate; fructose6P, fructose-6-phosphate; fructose bisP, fructose 1,6-diphosphate; acetylP, acetyl phosphate; CS, citrate synthase, CO_2, carbon dioxide. The remaining flux to CO_2 is via pyruvate dehydrogenase (PDH), isocitrate dehydrogenase, oxo-glutarate dehydrogenase, malate dehydrogenase decarboxylating (MDH[dc]), phosphoenolpyruvate carboxykinase (PEPCK) and enzymes of the PP pathway. Dividing the normalised fluxes by the normalising factor (N), converts the normalised units to C.mmoles.g^{-1} dry wt biomass h^{-1}. Dividing these figures by the specific growth rate (μ), converts the diagram to throughputs (C.mmoles.g^{-1}). The μ was taken as the reconciled value (as Chapter 4, Table 4.12). All workings are contained in the compendium if required (Fig 6.19).

Fig 6.19. Normalised flux diagram for *S. fradiae* C373-10 growing on glucose & glutamate [Ferm 4; Day 5] (C.mmoles.g^{-1} dry wt biomass. h^{-1} normalised to 100 % of input).

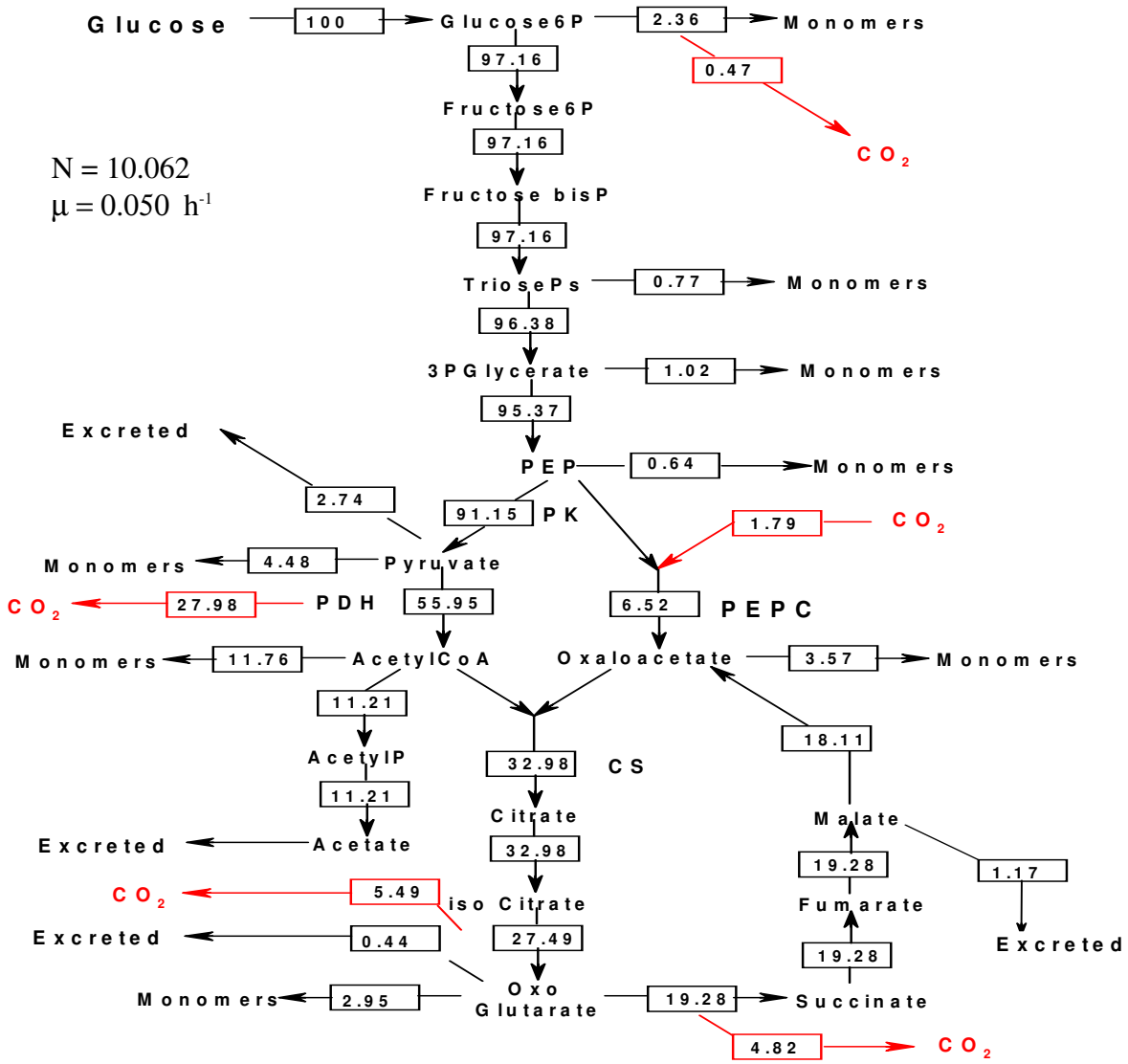

The diagram was constructed using data from Table 6.16. The values were calculated by subtracting the amount of precursors required for biosynthesis of the biomass from the input carbon source. Glucose6P, glucose-6-phosphate; malate dehydrogenase, MDH; PK, pyruvate kinase; TriosePs, triose phosphate; 3PGlycerate, Glyceraldehyde-3-phosphate; PEP, phosphoenolpyruvate; fructose6P, fructose-6-phosphate; fructose bisP, fructose 1,6-diphosphate; acetylP, acetyl phosphate; citrate synthase, CO_2, carbon dioxide. The remaining flux to CO_2 is via pyruvate dehydrogenase (PDH), isocitrate dehydrogenase, oxo-glutarate dehydrogenase, malate dehydrogenase decarboxylating (MDH[dc]), phosphoenolpyruvate carboxykinase (PEPCK) and enzymes of the PP pathway. Dividing the normalised fluxes by the normalising factor (N), converts the normalised units to C.mmoles.g^{-1} dry wt biomass h^{-1}. Dividing these figures by the specific growth rate (μ), converts the diagram to throughputs (C.mmoles.g^{-1}). The μ was taken as the reconciled value (as Chapter 4, Table 4.12). All workings are contained in the compendium if required (Fig 6.19).

Fig 6.20. Normalised flux diagram for *S. fradiae* C373-10 growing on glucose & oxo-glutamate [Ferm 1; Day 3] (C.mmoles.g^{-1} dry wt biomass. h^{-1} normalised to 100 % of input).

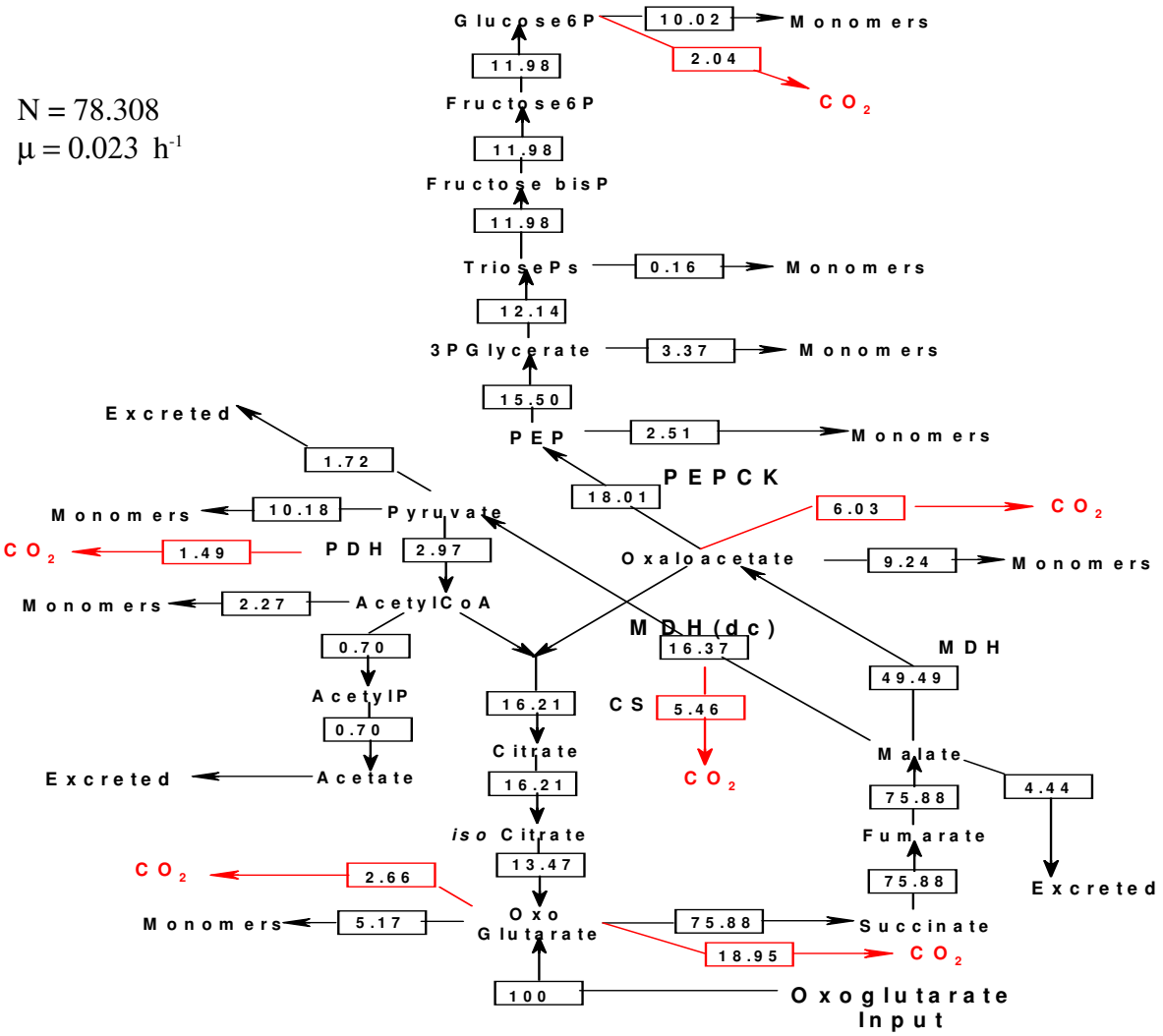

The diagram was constructed using data from Table 6.17. The values were calculated by subtracting the amount of precursors required for biosynthesis of the biomass from the input carbon source. Glucose6P, glucose-6-phosphate; malate dehydrogenase, MDH; PK, pyruvate kinase; TriosePs, triose phosphate; 3PGlycerate, glyceraldehyde-3-phosphate; PEP, phosphoenolpyruvate; fructose6P, fructose-6-phosphate; fructose bisP, fructose 1,6-diphosphate; acetylP, acetyl phosphate; CS, citrate synthase, CO_2, carbon dioxide. The remaining flux to CO_2 is via pyruvate dehydrogenase (PDH), isocitrate dehydrogenase, oxo-glutarate dehydrogenase, malate dehydrogenase decarboxylating (MDH[dc]), phosphoenolpyruvate carboxykinase (PEPCK) and enzymes of the PP pathway. Dividing the normalised fluxes by the normalising factor (N), converts the normalised units to C.mmoles.g^{-1} dry wt biomass h^{-1}. Dividing these figures by the specific growth rate (μ), converts the diagram to throughputs (C.mmoles.g^{-1}). The μ was taken as the reconciled value (as Chapter 4, Table 4.12). All workings are contained in the compendium if required (Fig 6.20).

Fig 6.21. Normalised flux diagram for *S. fradiae* C373-10 growing on glucose & oxo-glutamate [Ferm 2; Day 3] (C.mmoles.g^{-1} dry wt biomass. h^{-1} normalised to 100 % of input).

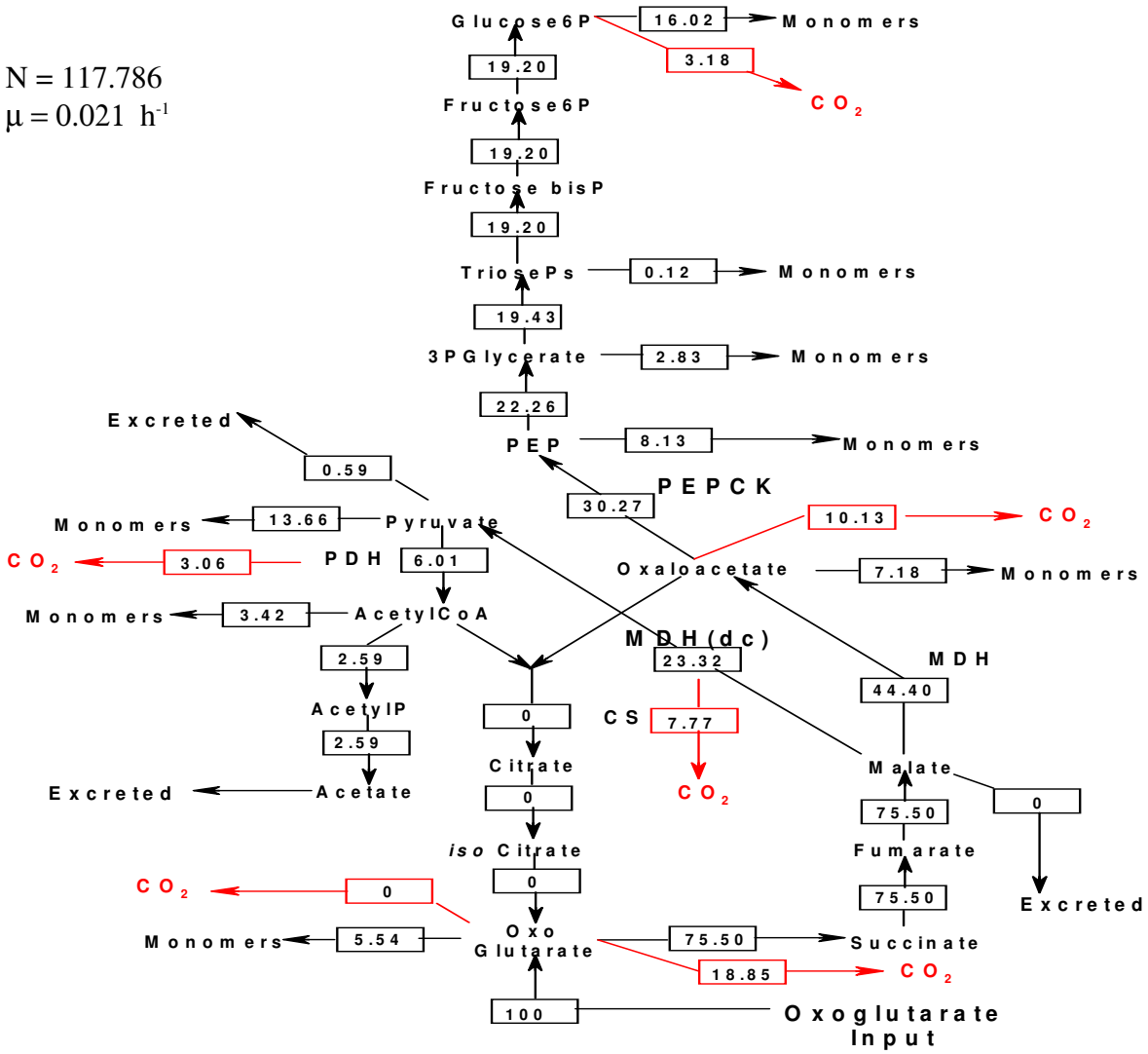

The diagram was constructed using data from Table 6.18. The values were calculated by subtracting the amount of precursors required for biosynthesis of the biomass from the input carbon source. Glucose6P, glucose-6-phosphate; malate dehydrogenase, MDH; PK, pyruvate kinase; TriosePs, triose phosphate; 3PGlycerate, Glyceraldehyde-3-phosphate; PEP, phosphoenolpyruvate; fructose6P, fructose-6-phosphate; fructose bisP, fructose 1,6-diphosphate; acetylP, acetyl phosphate; citrate synthase, CO_2, carbon dioxide. The remaining flux to CO_2 is via pyruvate dehydrogenase (PDH), isocitrate dehydrogenase, oxo-glutarate dehydrogenase, malate dehydrogenase decarboxylating (MDH[dc]), phosphoenolpyruvate carboxykinase (PEPCK) and enzymes of the PP pathway. Dividing the normalised fluxes by the normalising factor (N), converts the normalised units to C.mmoles.g^{-1} dry wt biomass h^{-1}. Dividing these figures by the specific growth rate (μ), converts the diagram to throughputs (C.mmoles.g^{-1}). The μ was taken as the reconciled value (as Chapter 4, Table 4.12). All workings are contained in the compendium if required (Fig 6.21).

Fig 6.22. Normalised flux diagram for *S. fradiae* C373-10 growing on glucose & oxo-glutamate [Ferm 1; Day 8] (C.mmoles.g^{-1} dry wt biomass. h^{-1} normalised to 100 % of input).

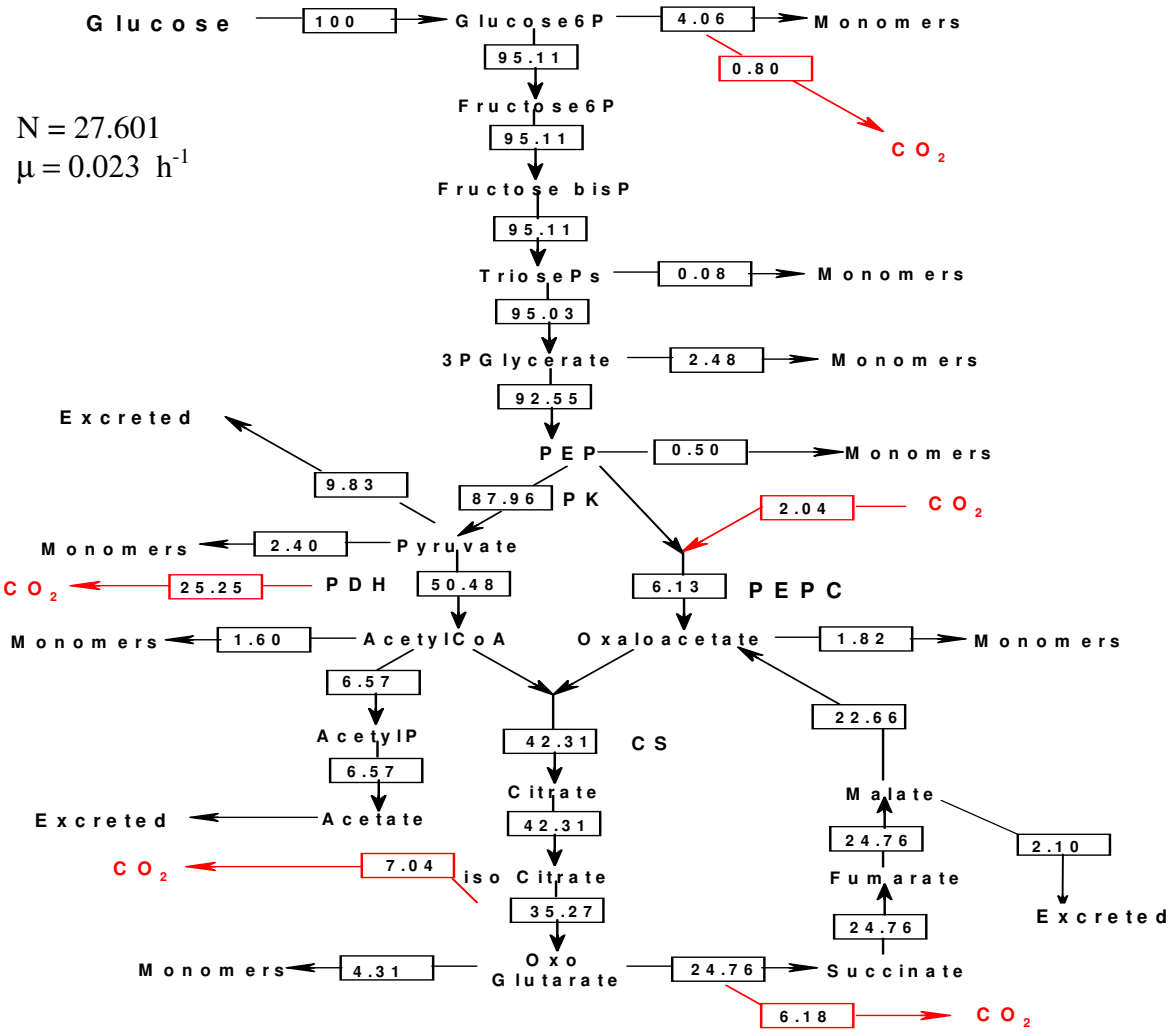

The diagram was constructed using data from Table 6.19. The values were calculated by subtracting the amount of precursors required for biosynthesis of the biomass from the input carbon source. Glucose6P, glucose-6-phosphate; malate dehydrogenase, MDH; PK, pyruvate kinase; TriosePs, triose phosphate; 3PGlycerate, glyceraldehyde-3-phosphate; PEP, phosphoenolpyruvate; fructose6P, fructose-6-phosphate; fructose bisP, fructose 1,6-diphosphate; acetylP, acetyl phosphate; CS, citrate synthase, CO_2, carbon dioxide. The remaining flux to CO_2 is via pyruvate dehydrogenase (PDH), isocitrate dehydrogenase, oxo-glutarate dehydrogenase, malate dehydrogenase decarboxylating (MDH[dc]), phosphoenolpyruvate carboxykinase (PEPCK) and enzymes of the PP pathway. Dividing the normalised fluxes by the normalising factor (N), converts the normalised units to C.mmoles.g^{-1} dry wt biomass h^{-1}. Dividing these figures by the specific growth rate (μ), converts the diagram to throughputs (C.mmoles.g^{-1}). The μ was taken as the reconciled value (as Chapter 4, Table 4.12). All workings are contained in the compendium if required (Fig 6.22).

Fig 6.23. Normalised flux diagram for *S. fradiae* C373-10 growing on glucose & oxo-glutamate [Ferm 2; Day 8] (C.mmoles.g^{-1} dry wt biomass. h^{-1} normalised to 100 % of input).

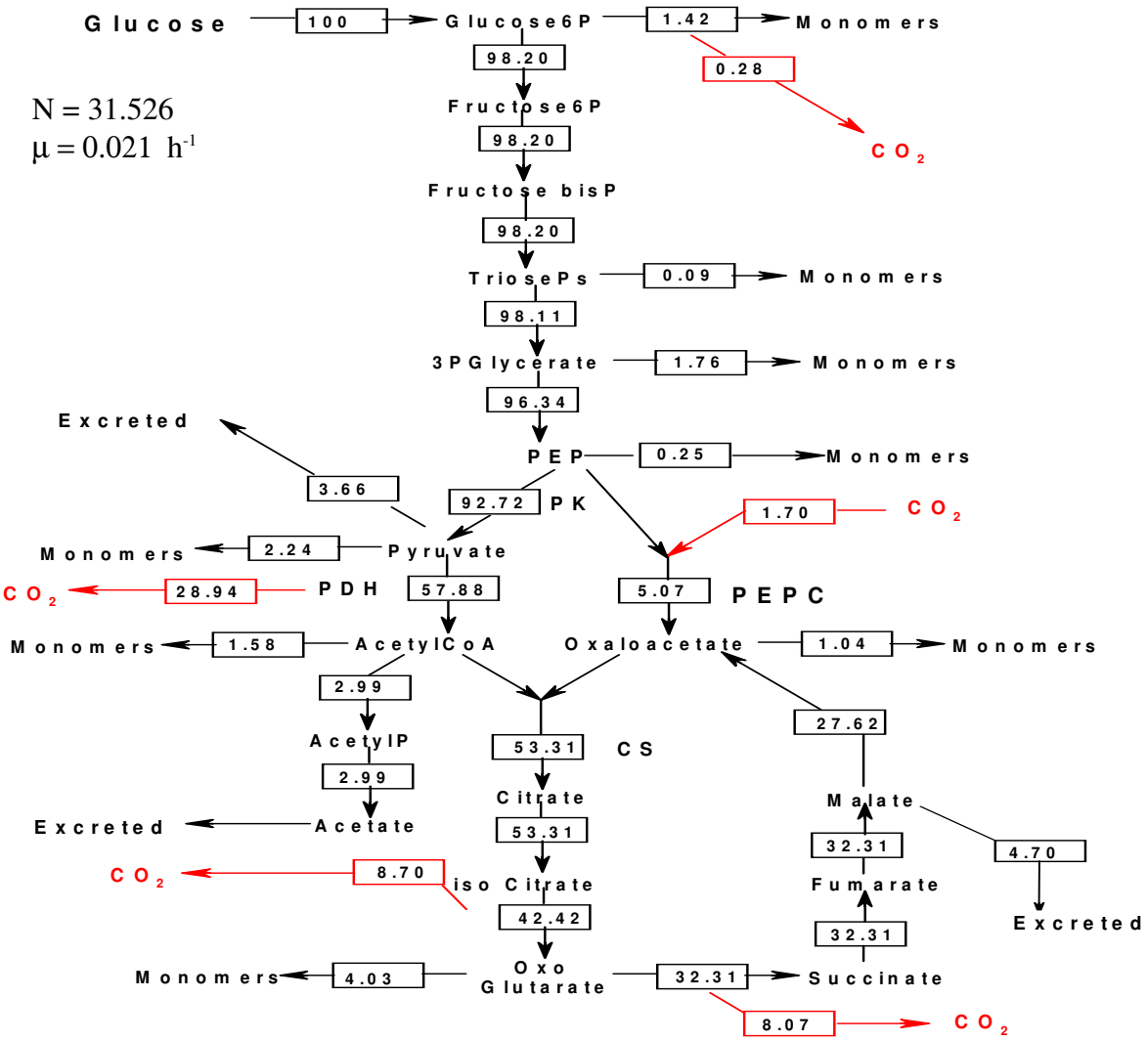

The diagram was constructed using data from Table 6.20. The values were calculated by subtracting the amount of precursors required for biosynthesis of the biomass from the input carbon source. Glucose6P, glucose-6-phosphate; malate dehydrogenase, MDH; PK, pyruvate kinase; TriosePs, triose phosphate; 3PGlycerate, glyceraldehyde-3-phosphate; PEP, phosphoenolpyruvate; fructose6P, fructose-6-phosphate; fructose bisP, fructose 1,6-diphosphate; acetylP, acetyl phosphate; CS, citrate synthase, CO_2, carbon dioxide. The remaining flux to CO_2 is via pyruvate dehydrogenase (PDH), isocitrate dehydrogenase, oxo-glutarate dehydrogenase, malate dehydrogenase decarboxylating (MDH[dc]), phosphoenolpyruvate carboxykinase (PEPCK) and enzymes of the PP pathway. Dividing the normalised fluxes by the normalising factor (N), converts the normalised units to C.mmoles.g^{-1} dry wt biomass h^{-1}. Dividing these figures by the specific growth rate (μ), converts the diagram to throughputs (C.mmoles.g^{-1}). The μ was taken as the reconciled value (as Chapter 4, Table 4.12). All workings are contained in the compendium if required (Fig 6.23).

Fig 6.24. Normalised throughput diagram for *S. fradiae* C373-10 growing on methyl-oleate, glucose & glutamate [Ferm 1; Day 3 - Day 9] (C.mmoles.g^{-1} normalised to 100 % of input).

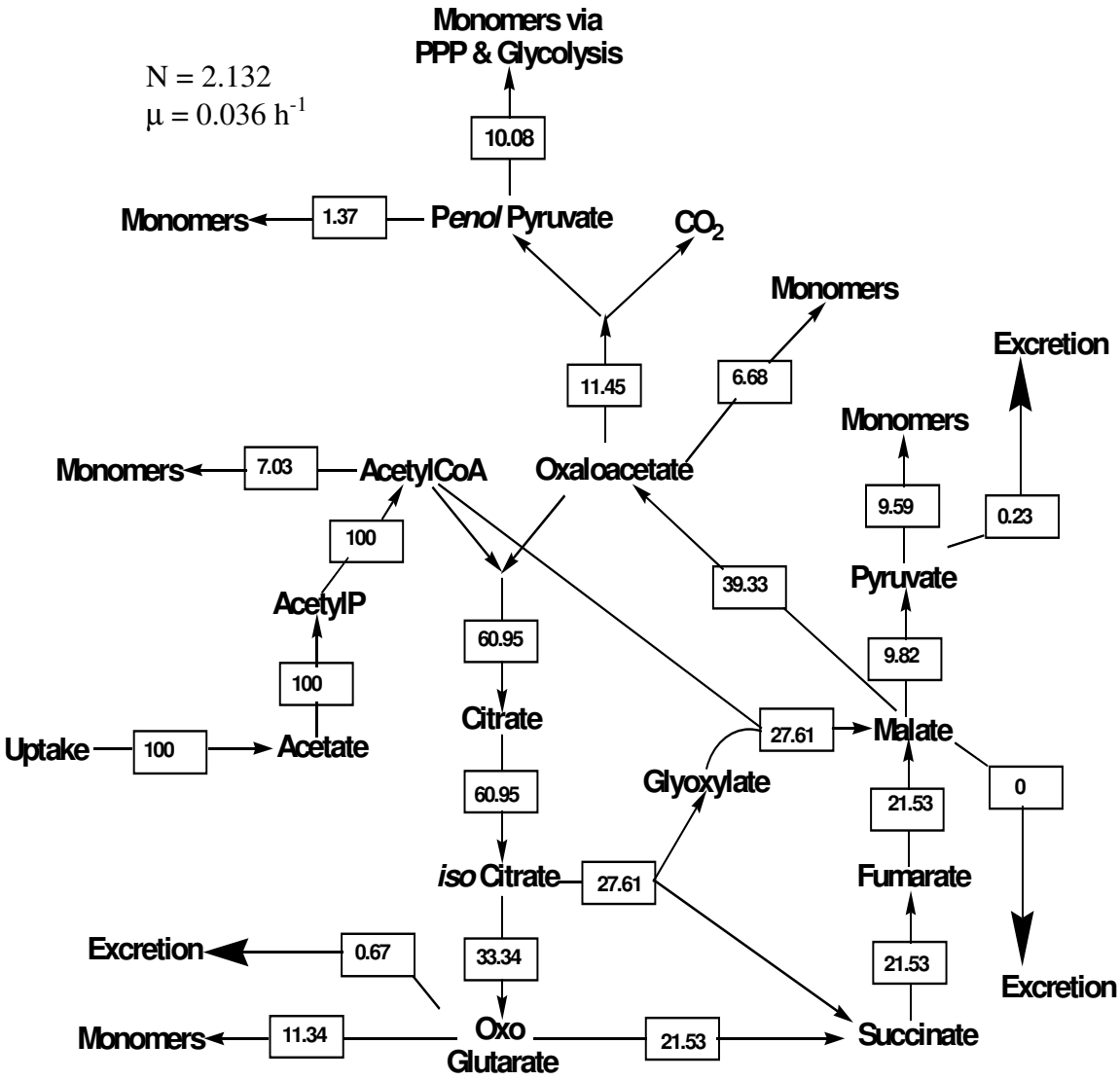

The diagram was constructed using data from Table 6.21. The values were calculated by subtracting the amount of precursors required for biosynthesis of the biomass from the input carbon source. Phenol pyruvate, phosphoenolpyruvate; acetylP, acetyl phosphate. The remaining flux to CO_2 is via pyruvate dehydrogenase, isocitrate dehydrogenase, oxo-glutarate dehydrogenase, malate dehydrogenase decarboxylating, phosphoenolpyruvate carboxykinase and enzymes of the PP pathway. Dividing the normalised fluxes by the normalising factor (N), converts the normalised units to C.mmoles.g^{-1} dry wt biomass h^{-1}. Dividing these figures by the specific growth rate (μ), converts the diagram to throughputs (C.mmoles.g^{-1}). The μ was taken as the reconciled value (as Chapter 4, Table 4.12). All workings are contained in the compendium if required (Fig 6.24).

Fig 6.25. Normalised throughput diagram for *S. fradiae* C373-10 growing on methyl-oleate, glucose & glutamate [Ferm 2; Day 3 - Day 9] (C.mmoles.g^{-1} normalised to 100 % of input).

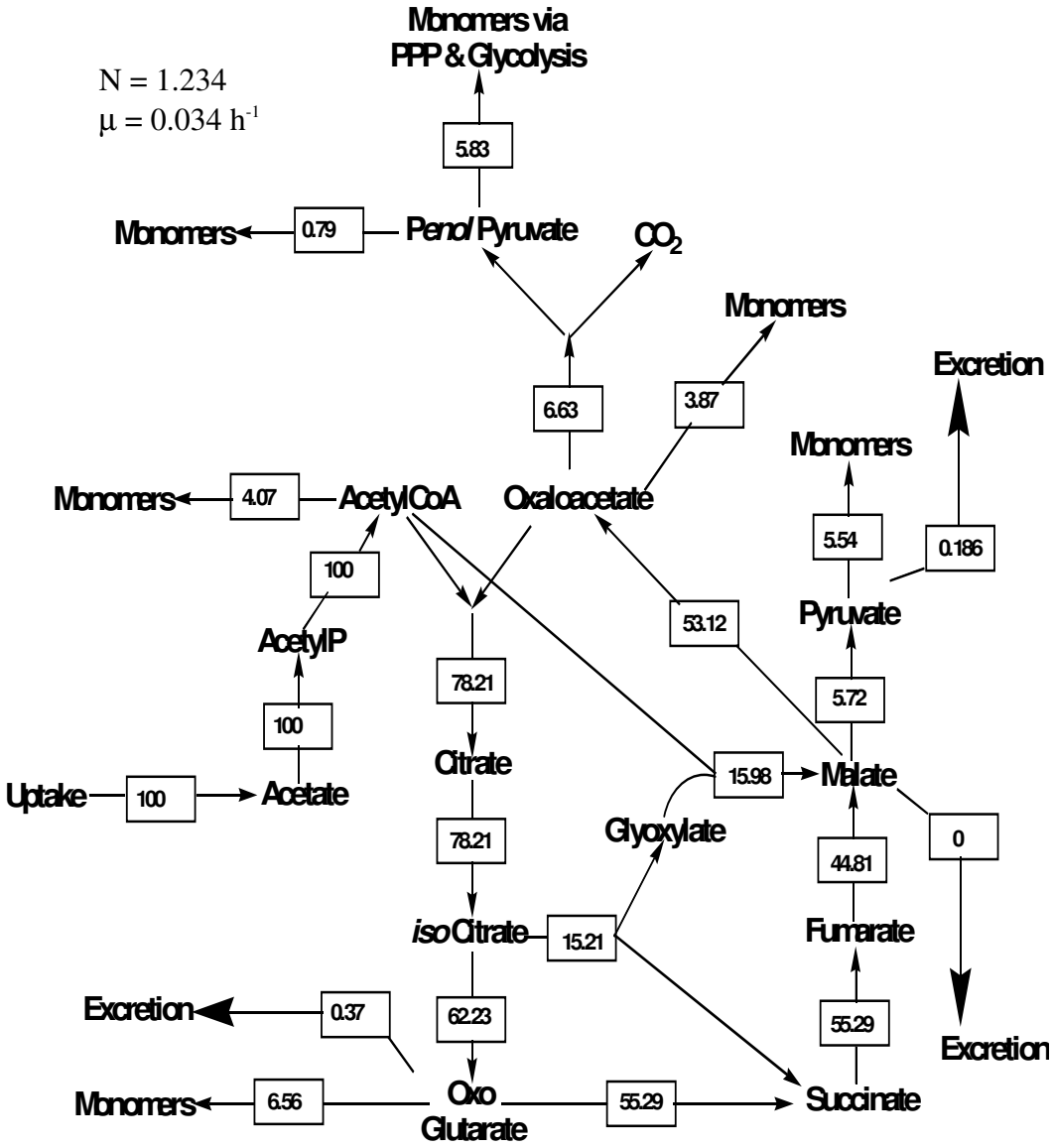

The diagram was constructed using data from Table 6.22. The values were calculated by subtracting the amount of precursors required for biosynthesis of the biomass from the input carbon source. Phenol pyruvate, phosphoenolpyruvate; acetylP, acetyl phosphate. The remaining flux to CO_2 is via pyruvate dehydrogenase, isocitrate dehydrogenase, oxo-glutarate dehydrogenase, malate dehydrogenase decarboxylating, phosphoenolpyruvate carboxykinase and enzymes of the PP pathway. Dividing the normalised fluxes by the normalising factor (N), converts the normalised units to C.mmoles.g^{-1} dry wt biomass h^{-1}. Dividing these figures by the specific growth rate (μ), converts the diagram to throughputs (C.mmoles.g^{-1}). The μ was taken as the reconciled value (as Chapter 4, Table 4.12). All workings are contained in the compendium if required (Fig 6.25).